

Ephraim Cohen
Bernard Moussian *Editors*

Extracellular Composite Matrices in Arthropods

 Springer

Extracellular Composite Matrices in Arthropods

Ephraim Cohen • Bernard Moussian
Editors

Extracellular Composite Matrices in Arthropods

 Springer

Editors

Ephraim Cohen
Department of Entomology,
The Robert H. Smith Faculty
of Agriculture, Food and Environment
The Hebrew University of Jerusalem
Rehovot, Israel

Bernard Moussian
Genetik der Tiere
Eberhard-Karls Universität Tübingen
Tübingen, Germany

ISBN 978-3-319-40738-8

ISBN 978-3-319-40740-1 (eBook)

DOI 10.1007/978-3-319-40740-1

Library of Congress Control Number: 2016952623

© Springer International Publishing Switzerland 2016

Chapter 10 is published with kind permission of the Her Majesty the Queen Right of Canada.

This work is subject to copyright. All rights are reserved by the Publisher, whether the whole or part of the material is concerned, specifically the rights of translation, reprinting, reuse of illustrations, recitation, broadcasting, reproduction on microfilms or in any other physical way, and transmission or information storage and retrieval, electronic adaptation, computer software, or by similar or dissimilar methodology now known or hereafter developed.

The use of general descriptive names, registered names, trademarks, service marks, etc. in this publication does not imply, even in the absence of a specific statement, that such names are exempt from the relevant protective laws and regulations and therefore free for general use.

The publisher, the authors and the editors are safe to assume that the advice and information in this book are believed to be true and accurate at the date of publication. Neither the publisher nor the authors or the editors give a warranty, express or implied, with respect to the material contained herein or for any errors or omissions that may have been made.

Printed on acid-free paper

This Springer imprint is published by Springer Nature
The registered company is Springer International Publishing AG Switzerland

Preface

Extracellular Composite Matrices in Arthropods

The book contains comprehensive contributions on extracellular composite matrices in arthropods. The building blocks of such matrices are formed in and secreted by single-layered epithelial cells into exterior domains where their final assembly or transformation takes place. Emphasis is placed largely on insects, due to the extensive body of published research that in part is the result of available whole genome sequences of several model species (in particular *Drosophila melanogaster*) and accessible ESTs for other species. Such advances have facilitated fundamental insights into genomic, proteomic, and molecular-based physiology. The book includes also chapters on noninsect arthropod biocomposites such as the mineralized crustacean cuticles (Chap. 5), spider silks (Chaps. 12 and 13), and salivary gland secretion of ticks (Chap. 17). However, it is appropriate to acknowledge that the book excludes arthropod toxins and venoms that merit a sizable separate volume.

The phylum Arthropoda that arose about 550–600 MYA is the biggest and most diverse in the animal kingdom. Arthropods show a remarkable and insuperable adaptation to survive, colonize, and essentially thrive, in a plethora of aquatic and terrestrial habitats. Basically, the cuticular structures have been pivotal for their successful adaptations to the external environment and thus have been conserved through eons. It is noteworthy that extracellular matrices of arthropods amount to a large inert biomass. The global organic biomass of chitin from insects and crustaceans is regarded as second only to cellulose. The first seven chapters of the book are dedicated to these highly organized and super-complex composite matrices.

The cuticular matrix has been explored from diverse viewpoints, thus providing useful perspectives related to function and biological significance. Different morphologies of external surfaces that affect appearance; various colors that may function for camouflage, recognition, heat absorption, mating, and defense; and mechanical properties such as strength, rigidity, elasticity, or plasticity are

determined by specific chitin-protein interactions and architectural assemblies, degree of protein sclerotization and hydration, or types of proteins.

One example is the pliant resilin with its characteristic amino acid sequences and intermolecular di- and tri-tyrosine cross-linking (Chap. 4). Due to its superlative energy storage efficiency and high fatigue lifetime, resilin is crucial in activities including legged locomotion, flight, jumping, attachment to substrates, and sound production (in cicadas).

The diverse composite assemblies of chitin filament systems and proteins, which form the architectural matrix of skeletal procuticles and peritrophic membranes, dictate their varied functional properties (Chaps. 1, 2, 3 and 8). Basically, the chitin-protein matrix is formed by interactions between a single aminosugar biopolymer (largely the antiparallel α -chitin allomorph) and a large number of highly diverse proteins. Furthermore, cuticular diversity may be amplified by a later intermolecular cross-linking of proteins and different stacking configurations. Nucleophilic reactions, by low molecular weight oxidation products of catecholamine derivatives, stabilize (sclerotize) the proteinaceous exocuticular layer and overall contribute strength and rigidity to the cuticle (Chap. 6). In addition to such cross-linking, the crustacean chitin-protein layers are primarily rigidified by calcification (Chap. 5).

Cuticular hydrocarbons and lipids are integral parts of the epicuticular layer where their hydrophobic nature functions as waterproofing components. It is reasonable to perceive that involvement of cuticular hydrocarbons has been essential to solve ecophysiological constraints during the transition of arthropods from aquatic to terrestrial habitats. Existing on or near the cuticle surface, volatile hydrocarbons have also evolved to serve in defense, reproduction, and communication (Chap. 7). In the context of waterproofing, eggs of oviparous insects, which normally face the major problem of desiccation, are protected by certain waterproofing chorionic layers. Moreover, the embryonic layer of serosal cuticle is paramount in protecting developing embryos from dehydration (Chap. 9).

The dynamic spatial and temporal events that accompany synthesis (and degradation) of the cuticular complex structure are comprehensively covered in chapters dealing with the integumental matrices (Chaps. 1, 2 and 3). It includes specific genes and the interplay of genes, specific structural proteins and enzymes that are involved *inter alia* in biosynthesis, and degradation of the cuticular matrix. In addition, intercalation of low molecular weight components essential for waterproofing (like hydrocarbons) or quinone-based compounds that are used as stabilizing elements (sclerotization, melanization) or as pigments are included. Colors of cuticles are varied, depending on insect species and in anatomical regions of the same species. Pigmentation/melanization also plays important roles in wound healing and encapsulation of invading parasites (Chap. 6).

The dynamic events and sequential assembly of cuticular layers as well as the secretions of enzymes and low molecular weight component are cued and synchronized by sets of hormonally regulated genes (Chaps. 1, 2, 3, 4, 5, 6 and 7).

The eggshell structural complex shares many similarities to the cuticular matrix. It is largely an organized multilayered composite structure assembled according to

an idiosyncratic spatial and temporal program (Chap. 9). The largely proteinaceous layers of eggshells are secreted by sets of monolayered follicular cells inherently equipped with a predetermined genetic plan for the complex structural design. Chorionic eggshells provide protection against desiccation and/or flooding and against predation or invasion of pathogenic microorganisms, as well as resistance to mechanical stresses or temperature fluctuations. Several eggshell chorionic layers are stabilized by intermolecular cross-linking such as disulfide bridges, di- and tri-tyrosine bonds, and quinone-based sclerotization.

Silks, which are biopolymeric composite natural fibrous materials spun from protein secretions, occur in various lepidopterans, hymenopterans, beetles, flies, thrips, lacewings, spiders, and acari. Another part of the book (Chaps. 12, 13 and 14) is limited to glandular secretions of silk moths and spiders. Spiders, for example, produce different types of fibers with remarkable properties, compositions, and morphologies that serve various functions like locomotion, signaling the presence of caught prey, web construction, wrapping pray, or creation of cases for protecting developing eggs. The cocoon silk of *Bombyx mori* (the only domesticated arthropod), which is known for over 5000 years, has been commercialized into valuable textiles.

A cluster of three Chaps. (15, 16 and 17) is dedicated to saliva which is water or oily oral secretions of mostly labial salivary glands. Its various functions include lubrication of mouthparts, predigestion and digestion of plant materials, water balance, and antimicrobial and antipredator actions as well as in host-vector interactions. Saliva of plant sap feeders plays a role in transmitting viral and protozoan pathogens. The pharmacologically active saliva of hematophagous arthropods blocks host antibleeding defense, serves as an analgesic in tick bites, and affects inflammatory and immune systems of vertebrate hosts, in addition to transmitting debilitating pathogens.

The *Drosophila* salivary glands are well known for the exocrine secretion of a glue material that attaches their puparia to the substrate (Chap. 15). Additionally, this chapter deals with apocrine secretion of salivary gland cells where they lose part of their cytoplasm into the lumen. In contrast to the exocrine glue proteins, a large number of cytoskeletal, cytosolic, mitochondrial, ribosomal, and Golgi apparatus components are released and exposed to the exterior.

Chapter 11 is dedicated to *Drosophila melanogaster* female and male secretory products of accessory glands that play critical roles in fertility and overall reproduction. It involves the complicated network of interactions of the multiple secreted components that target multiple receptors which are involved in preparation for mating, during mating, and through postmating events.

A number of Chaps. (4, 5, 12, 13 and 14) cover commercially applicative aspects related to extracellular matrices. There is a worldwide market for chitin, its deacetylated form chitosan, and for their chemical modifications. Such products are biodegradable, biocompatible, and nontoxic with a large range of useful applications in the textile and pharmaceutical industries, in agriculture, water treatment, cosmetics, food, and photography products.

Blocking chitin synthesis by commercial acylurea insecticides or inhibition of acarine chitin synthase by the acaricide etoxazole indicates the applicative value of

chitin as target in pest control. The physiologically essential processes of chitin synthesis and degradation have been regarded as useful selective targets for interference, and their potent inhibitors were subjected to further scrutiny of successful lead compounds in the hope of developing commercial pharmaceuticals and pest control agents (Chap. 10).

Genes of cuticular protein and chitin synthesis and degradation, which are expressed at transition stages, are regulated by growth hormones. Interfering juvenile hormone analogs and juvenile hormone mimetics, as well as ecdysterone agonists, were developed and commercialized as highly successful insecticides.

Natural biocomposites like crustacean mineralized cuticle, the pliant resilin, or the insect and spider silks have generated much interest and have inspired basic and applied research that yield sophisticated functional biomimetics, biomaterials, and structural hybrids. The rigid calcified crustacean cuticle stimulated development of organic/inorganic hybrid materials and motivated the use of synthetic polymer templates that generated ceramic and fiber-reinforced composites. Resilin with its outstanding elasticity, energy storage, resilience, and high fatigue lifetime has opened avenues for various polymer designs leading to potential applications for biorubbers, biosensors, and biomedical scaffolds. Spider silks, which have unique mechanical properties in terms of strength, extensibility, and toughness, offer exciting opportunities for the design of biomaterials for tailor-made applications in medicine, engineering, and defense.

Authors and coauthors are gracefully acknowledged for their joint effort in contributing state-of-the art chapters. In this regard, I like to express my genuine gratitude to the reviewers listed below who invested time and energy in carefully reading massive manuscripts and provided valuable corrections, comments, and suggestions. Their helpful input was indispensable for improving the quality of many chapters and, overall, for contributing remarkable “added value” to them:

Drs. Jasna Štrus, University of Ljubljana, Slovenia; Coby Schal, North Carolina State University, USA; Russel Jurenka, Iowa State University, USA; Anna Rising, Swedish University of Agricultural Sciences, Sweden; Heiko Vogel, Max Planck Institute for Chemical Ecology, Germany; Judith H. Willis, University of Georgia, USA; Kostas Iatrou, Institute of Bioscience and Applications, Greece; Lukas H. Margaritis, National and Kapodistrian University, Greece; Hans Merzendorfer, University of Siegen, Germany; Subbaratnam Muthukrishnan, Kansas State University, USA; Cheryl Hayashi, University of California, Riverside, USA; Bruce Chase, University of Nebraska at Omaha, USA; Mark L. Siegal, New York University, USA; and Lawrence Harshman, University of Nebraska-Lincoln, USA.

Contents

Part I Skeletal Matrices

1	Genes of Cuticular Proteins and Their Regulation.....	3
	Hideki Kawasaki	
2	Chitin Metabolic Pathways in Insects and Their Regulation	31
	Subbaratnam Muthukrishnan, Hans Merzendorfer, Yasuyuki Arakane, and Qing Yang	
3	Molecular Model of Skeletal Organization and Differentiation.....	67
	Bernard Moussian	
4	Resilin – The Pliant Protein	89
	Jan Michels, Esther Appel, and Stanislav N. Gorb	
5	The Mineralized Exoskeletons of Crustaceans.....	137
	Shmuel Bentov, Shai Abehsera, and Amir Sagi	
6	Tyrosine Metabolism for Insect Cuticle Pigmentation and Sclerotization.....	165
	Yasuyuki Arakane, Mi Young Noh, Tsunaki Asano, and Karl J. Kramer	
7	Insect Hydrocarbons: Biochemistry and Chemical Ecology.....	221
	Matthew D. Ginzl and Gary J. Blomquist	

Part II Peritrophic Membranes and Eggshell Matrices

8	Peritrophic Matrices	255
	Hans Merzendorfer, Marco Kelkenberg, and Subbaratnam Muthukrishnan	
9	Composite Eggshell Matrices: Chorionic Layers and Sub-chorionic Cuticular Envelopes	325
	Gustavo L. Rezende, Helena Carolina Martins Vargas, Bernard Moussian, and Ephraim Cohen	

Part III Skeletal Components as Targets for Interference

- 10 Targeting Cuticular Components for Pest Management**..... 369
Daniel Doucet and Arthur Retnakaran

Part IV Glandular Secretions

- 11 Nature and Functions of Glands and Ducts in the *Drosophila* Reproductive Tract**..... 411
Frank W. Avila, Javier A. Sánchez-López, Jennifer L. McGlaughon, Sukirtha Raman, Mariana F. Wolfner, and Yael Heifetz
- 12 Molecular and Structural Properties of Spider Silk**..... 445
Taylor Crawford, Caroline Williams, Ryan Hekman, Simone Dyrness, Alisa Arata, and Craig Vierra
- 13 Spider Silk: Factors Affecting Mechanical Properties and Biomimetic Applications**..... 489
Shichang Zhang and I-Min Tso
- 14 Insect Silks and Cocoons: Structural and Molecular Aspects** 515
Kenji Yukuhiro, Hideki Sezutsu, Takuya Tsubota, Yoko Takasu, Tsunenori Kameda, and Naoyuki Yonemura
- 15 The Complex Secretions of the Salivary Glands of *Drosophila melanogaster*, A Model System**..... 557
Robert Farkaš
- 16 Salivary Gland Secretions of Phytophagous Arthropods** 601
Maria P. Celorio-Mancera and John M. Labavitch
- 17 Glandular Matrices and Secretions: Blood-Feeding Arthropods**..... 625
Ben J. Mans
- Erratum** E1
- Index**..... 689

Contributors

Shai Abehsera Department of life Sciences and the National Institute for Biotechnology in the Negev, Ben Gurion University, Beer Sheva, Israel

Esther Appel Department of Functional Morphology and Biomechanics, Institute of Zoology, Christian-Albrechts-Universität zu Kiel, Kiel, Germany

Yasuyuki Arakane Department of Applied Biology, Chonnam National University, Gwangju, South Korea

Alisa Arata Department of Biological Sciences, University of the Pacific, Stockton, CA, USA

Tsunaki Asano Department of Biological Sciences, Tokyo Metropolitan University, Tokyo, Japan

Frank W. Avila Department of Molecular Biology and Genetics, Cornell University, Ithaca, NY, USA

Shmuel Bentov Department of life Sciences and the National Institute for Biotechnology in the Negev, Ben Gurion University, Beer Sheva, Israel

Gary J. Blomquist Department of Biochemistry and Molecular Biology, University of Nevada, Reno, NV, USA

Maria P. Celorio-Mancera Department of Zoology, Ecology, Stockholm University, Stockholm, Sweden

Ephraim Cohen Department of Entomology, The Robert H. Smith Faculty of Agriculture, Food and Environment, The Hebrew University of Jerusalem, Rehovot, Israel

Taylor Crawford Department of Biological Sciences, University of the Pacific, Stockton, CA, USA

Daniel Doucet Great Lakes Forestry Centre, Canadian Forest Service, Natural Resources Canada, Sault Ste Marie, ON, Canada

Simmons Dyrness Department of Biological Sciences, University of the Pacific, Stockton, CA, USA

Robert Farkaš Institute of Experimental Endocrinology, Slovak Academy of Sciences, Bratislava, Slovakia

Matthew D. Ginzel Departments of Entomology and Forestry & Natural Resources, Hardwood Tree Improvement and Regeneration Center, Purdue University, West Lafayette, IN, USA

Stanislav N. Gorb Department of Functional Morphology and Biomechanics, Institute of Zoology, Christian-Albrechts-Universität zu Kiel, Kiel, Germany

Yael Heifetz Department of Entomology, The Robert H. Smith Faculty of Agriculture, Food and Environment, the Hebrew, University of Jerusalem, Rehovot, Israel

Ryan Hekman Department of Biological Sciences, University of the Pacific, Stockton, CA, USA

Tsunenori Kameda Silk Materials Research Unit, Genetically Modified Organism Research Center, National Institute of Agrobiological Sciences, Tsukuba, Ibaraki, Japan

Hideki Kawasaki Insect Molecular Biology, Faculty of Agriculture, Utsunomiya University, Utsunomiya, Tochigi, Japan

Marco Kelkenberg Department of Chemistry and Biology – Institute of Biology, University of Siegen, Siegen, Germany

Karl J. Kramer Department of Biochemistry and Molecular Biophysics, Kansas State University, Manhattan, KS, USA

John M. Labavitch Plant Sciences Department, University of California, Davis, CA, USA

Ben J. Mans Parasites, Vectors and Vector-borne Diseases, Onderstepoort Veterinary Institute, Agricultural Research Council, Pretoria, South Africa

Jennifer L. McGlaughon Department of Molecular Biology and Genetics, Cornell University, Ithaca, NY, USA

Hans Merzendorfer Department of Chemistry and Biology – Institute of Biology, University of Siegen, Siegen, Germany

Jan Michels Department of Functional Morphology and Biomechanics, Institute of Zoology, Christian-Albrechts-Universität zu Kiel, Kiel, Germany

Bernard Moussian Genetik der Tiere, Eberhard-Karls Universität Tübingen, Tübingen, Germany

Subbaratnam Muthukrishnan Department of Biochemistry & Molecular Biophysics, Kansas State University, Manhattan, KS, USA

Mi Young Noh Department of Applied Biology, Chonnam National University, Gwangju, South Korea

Sukirtha Raman Department of Marine, Earth and Atmospheric Sciences, North Carolina State University, Raleigh, NC, USA

Arthur Retnakaran Great Lakes Forestry Centre, Canadian Forest Service, Natural Resources Canada, Sault Ste Marie, ON, Canada

Gustavo L. Rezende LQFPP, CBB, UENF, Campos dos Goytacazes, RJ, Brazil

Amir Sagi Department of life Sciences and the National Institute for Biotechnology in the Negev, Ben Gurion University, Beer Sheva, Israel

Javier A. Sánchez-López Department of Entomology, The Hebrew University of Jerusalem, Rehovot, Israel

Hideki Sezutsu Transgenic Silkworm Research Unit, Genetically Modified Organism Research Center, National Institute of Agrobiological Sciences, The University of Tokyo, Tsukuba, Ibaraki, Japan

Yoko Takasu Silk Materials Research Unit, Genetically Modified Organism Research Center, National Institute of Agrobiological Sciences, Tsukuba, Ibaraki, Japan

I-Min Tso Department of Life Science, Tunghai University, Taichung, Taiwan

Takuya Tsubota Transgenic Silkworm Research Unit, Genetically Modified Organism Research Center, National Institute of Agrobiological Sciences, Tsukuba, Ibaraki, Japan

Helena Carolina Martins Vargas LQFPP, CBB, UENF, Campos dos Goytacazes, RJ, Brazil

Craig Vierra Department of Biological Sciences, University of the Pacific, Stockton, CA, USA

Caroline Williams Department of Biological Sciences, University of the Pacific, Stockton, CA, USA

Mariana F. Wolfner Department of Molecular Biology and Genetics, Cornell University, Ithaca, NY, USA

Qing Yang School of Life Science and Biotechnology, Dalian University of Technology, Dalian, China

Naoyuki Yonemura Transgenic Silkworm Research Unit, Genetically Modified Organism Research Center, National Institute of Agrobiological Sciences, Tsukuba, Japan

Kenji Yukuhiro Transgenic Silkworm Research Unit, Genetically Modified Organism Research Center, National Institute of Agrobiological Sciences, Tsukuba, Ibaraki, Japan

Shichang Zhang Department of Life Science, Tunghai University, Taichung, Taiwan

Part I

Skeletal Matrices

Chapter 1

Genes of Cuticular Proteins and Their Regulation

Hideki Kawasaki

Abstract In this chapter, recent development of the analysis of cuticular protein (CP) genes and the regulation of their expression are covered. Genomic analysis and annotation of CP genes have elucidated the overall number and kind of CP gene. The nomenclature and structure of cuticle layers are described first. The factors that regulate CP gene expression are described next. Expression of CP genes is regulated mainly by ecdysone responsive transcription factors (ERTFs). Ecdysone activates target ERTFs through its receptor complex. ERTFs interaction determines the expression pattern of themselves, resulting in the induction of their target genes. Ecdysone is known also to trigger chromatin remodeling by recruiting chromatin-remodeling factors that act by chromatin loosening. Juvenile hormone affects the type of cuticle layers through BR-C and HR38 and determines the type of CPs. Recent genomic analysis has generated new findings for the cuticle research. Annotation enabled to specify the kinds and number of all cuticular proteins. Now we can discuss cuticular layers depending on the classical studies. Genomic, proteomic and transcriptomic analysis brought about new findings. Clustering CP genes have been identified in several insects. Overall expression, its regulation, binding site analysis, genomic structure of CP genes, regulation of larval, pupal adult CP layers were described.

1.1 Recent Classification of Cuticular Proteins and the Construction of Cuticular Layers

1.1.1 Recent Classification of Cuticular Proteins

Cuticular proteins (CPs) are classified by using distinctive names derived from their specific sequence motifs and amino acid compositions. Sequencing the genomes of several insect species resulted in the identification of a large numbers of CP genes. Over 200 CP genes have been identified in the malaria mosquito *Anopheles*

H. Kawasaki (✉)

Insect Molecular Biology, Faculty of Agriculture, Utsunomiya University,
350 Mine, Utsunomiya, Tochigi 321-8505, Japan
e-mail: kawasaki@cc.utsunomiya-u.ac.jp

gambiae (Cornman et al. 2008; Cornman and Willis 2009) and the silkworm *Bombyx mori* (Futahashi et al. 2008), and several distinct families of CPs have been established (Cornman and Willis 2009; Willis 2010). Among them are CPRs, which represents CPs having the Rebers and Riddiford Consensus. Their names are derived from the work of Rebers and Riddiford, who first identified this sequence motif. The original motif was G-(x8)-G-x(6)-Y-x(2)-A-x-E-x-G-F-x(7)-P-x-P (R&R Consensus; Rebers and Riddiford 1988) (where x represents any amino acid, the values in parentheses indicate the number of amino acid residues). Three types of CPRs have been classified: RR-1 is generally found in soft cuticle, RR-2 in hard cuticle (Andersen 1998; Willis 2010), and RR-3 group comprises a few CPs (Andersen 2000; Willis 2010). An extended version of the R&R Consensus sequence was demonstrated to bind chitin (Rebers and Willis 2001; Togawa et al. 2004), and the amino acids responsible for this binding in the R&R Consensus were identified (Rebers and Willis 2001).

The name CPF was derived from a 51 amino acid motif first identified in *Tenebrio* and *Locusta* by Andersen et al. (1997). A shorter version (42–44 amino acids) was found by Togawa et al. (2007) in several species and the name CPF retained. These authors also identified another group of proteins that had carboxyl-termini similar to the CPFs and they were given the family name CPFL.

Binding with chitin was not observed in the case of AgamCPF1 or CPF3 (Togawa et al. 2007). The CPT family, sometimes called TWDL family, is named from the mutation of body shape (TweedleD, Guan et al. 2006), CPG is named due to its high content of glycine (Zhong et al. 2006; Futahashi et al. 2008), and CPH is a group of hypothetical *Bombyx* CPs (Futahashi et al. 2008), some of which have been shown to be members of distinct families (Willis 2010). Cornman and Willis (2009) have offered new additional classification for some CPs with low complexity. CPLCG contains invariant glycine residues in the conserved domain separated by eight amino acids, but so far this group was found only in Diptera. The name CPLCW refers to an invariant tryptophan within the conserved domain, and this family was found only in mosquitoes. CPLCP is proline-rich and consists of high density of PV and PY repeats, and CPLCA is alanine-rich. These different CP genes presumably make it possible to construct different types of cuticles in different species, stages and anatomical locations. Depending on these sequences, Ioannidou et al. (2014) developed CutProtFam-Pred, an on-line tool (<http://aias.biol.uoa.gr/CutProtFam-Pred/home.php>; 2014) that allows the accurate detection and classification of putative structural cuticular proteins, from sequence alone, in proteomes. Nevertheless, the mechanisms involved in determining the specific combinations of CPs, have not been elucidated.

1.1.2 The Construction of Cuticular Layers

Expression of CP genes is related to the structure of the cuticular layers. The insect cuticle is made up of three major cuticular layers, the envelope, the epicuticle and the procuticle. The envelope, formerly called cuticulin, is sometimes covered with wax (Locke 1961; Wigglesworth 1972). Next is the epicuticle that lacks chitin and

is composed of sclerotized proteins. The procuticle is divided into two layers, the upper exocuticle and the lower endocuticle. The procuticle is secreted before and after ecdysis in response to the rise and decline of the hemolymph ecdysteroid (Wigglesworth 1972; Andersen 2000). The exo- and endo-cuticle layers consist of chitin, CPRs and other types of CPs and are suggested to construct or fill the space within the two procuticle layers (Andersen 2002).

The timing of expression defines the kind of cuticular proteins that construct the layer, and determine the nature of each cuticular layer. The upper part of the procuticle becomes sclerotized after ecdysis (Hopkins et al. 2000), as phenolic compounds are incorporated into the CPs (Andersen 2010). Since His residues in CPs are used for the sclerotization of cuticles (Schaefer et al. 1987; Hopkins et al. 2000; Andersen 2010), CPs in the exocuticle should contain high percentage of His. In contrast, acidic amino acids are involved in soft cuticle such as inter-segmental membrane (Cox and Willis 1987) or larval cuticle (Missios et al. 2000). Therefore, acidic amino acid residues are suggested to be frequently involved in CPs in the endocuticle. Mun et al. (2015) recently reported that a CP of the red flour beetle, *Tribolium castaneum*, TcCP30, having a low complexity sequence, was cross-linked with the RR-2 CPs, TcCPR18 and TcCPR27 by laccase2, but not with the RR-1 CP, TcCPR4. TcCP30, TcCPR18 and TcCPR27 contained high percentage of His residues that could bind together. RR-2 CPs contain His and Lys, and these amino acids react with sclerotizing reagents (Iconomidou et al. 2005), therefore RR-2 CPs cross-linked by CP30 are suggested to be involved in construction of the hard cuticle.

Shahin et al. (2016) speculated that the exocuticle is constructed with RR-1, RR-2 and other types of CPs, while the endocuticle is formed with RR-1 and other CPs from the expression profiles of CP genes of *B. mori*. They examined the expression profiles of 52 CP genes that are identified in wing disc ESTs during prepupal to early pupal stages. The earliest expressed group, which is composed of RR-2 CP and CPH, contains high percentage of His. It is suggested that these proteins bind via His residues to make the tanned exocuticle, as shown by Mun et al. (2015). RR-2 CPs, which are expressed at a later stage, have a lower percentage of His (Shahin et al. unpublished data), which suggests that they play a minor role in sclerotization of the cuticle. The transcription of RR-2 CP genes ceases before pupation, while that of RR-1 CP genes continue until after pupation even if the start of transcription was at the same time as that of the RR-2 CP genes (Shahin et al. 2016). This suggests that RR-1 CPs construct both layers of the exocuticle and endocuticle, while RR-2 CPs construct only exocuticle. It was also reported that CPFL, CPG, CPT and CPH constitute the exo-and endocuticle layers (Shahin et al. 2016). It is noteworthy that CPH1, CPH33, CPG11, CPG12 and CPG24, which are expressed at the prepupal stage, have high percentages of His and Lys (Shahin et al. unpublished data).

Recent analysis clarified the mechanism that determines the order of expression timing of the deposited cuticular layers (Nita et al. 2009; Wang et al. 2009a, b, 2010; Shahin et al. 2016). The expression timing of CP genes is determined by ecdysone responsive transcription factors (ERTFs). The expression timing and its regulation are described in Sect. 1.2.

1.1.3 Distinctive Function of Each Cuticular Protein

A large number of CP genes were identified in the genome of certain insects as described in Sect. 1.3. There is an issue whether all CPs have evolved separately or most of them are the result of gene duplication. Some reports suggest that each CP has a distinctive function (Guan et al. 2006; Arakane et al. 2012; Noh et al. 2014, 2015; Qiao et al. 2014).

The *TweedleD* mutation in *D. melanogaster* showed dramatic effect on the body shape, but not on viability and fertility (Guan et al. 2006). Recent analysis of *B. mori*, which revealed the binding of CTP with chitin (Tang et al. 2010), may explain the function of Tweedle and the defect of its mutant. TcCPR18 and TcCPR27, which belong to RR-2 CP, are expressed in elytra, pronotum and ventral abdomen in *T. castaneum*. RNA interference study of *TcCPR27* demonstrated unorganized laminae and pore canals as well as aberrant hind wings, while *TcCPR18* silencing showed similar but less pronounced defects (Arakane et al. 2012). The distinctive roles of TcCPR18 and TcCPR27 suggest a significant function of each insect CP (Arakane et al. 2012; Noh et al. 2014). Down-regulation of another CP gene, *TcCPR4*, which belongs to RR-1 CP group, showed abnormal shape of the pore canals that had amorphous fibers (Noh et al. 2015). Analysis of *stony*, the *B. mori* mutant, revealed the function of BmorCPR2 (Qiao et al. 2014). *Stony* mutant shows hard body, which is caused by the lack of chitin binding site of CPR2.

1.2 Factors that Affect Gene Expression of Cuticular Proteins

1.2.1 Ecdysone

Ecdysone is a major factor that controls insect embryonic development, ecdysis, metamorphosis and adult development. The ecdysone-responsive characteristics of several CP genes have been studied (Horodyski and Riddiford 1989; Apple and Fristrom 1991; Hiruma et al. 1991; Braquart et al. 1996; Devarakonda et al. 2003; Noji et al. 2003; Nita et al. 2009; Wang et al. 2009a). Most of their expressions are induced by exposure to an ecdysteroid pulse (Apple and Fristrom 1991; Hiruma et al. 1991; Zhong et al. 2006; Nita et al. 2009; Wang et al. 2009a). *LCP-14* of the tobacco hornworm, *Manduca sexta*, was induced after 12 h following exposure to the hormone and transfer of cultures to hormone-free medium. Induction of *GCPI* of the silkworm, *Bombyx mori* (Suzuki et al. 2002) was observed 16 h after hormone removal, and induction of *GRPs* of *B. mori* was observed 12 or 18 h after 20E removal (Zhong et al. 2006). Induction of *LCPI6/17* of *M. sexta* required *in vitro* exposure to low concentration of 20E (50 ng/ml) for 24 h (Horodyski and Riddiford 1989). *BMWCP10* of *B. mori* was induced *in vitro* 4 h after addition of the hormone (Noji et al. 2003; Wang et al. 2010). It can be concluded that CP genes, which have

different developmental profiles, are induced with different types of ecdysone exposure, as described in a recent review by Charles (2010).

1.2.2 Ecdysone Signaling Cascade

Ecdysone binds with the ECR/USP heterodimer and the activated complex moves to the nucleus and binds with the hormone response element of the *hsp* gene (Nieva et al. 2007). Ecdysteroid titer in the hemolymph, which increases before ecdysis, activates a large number of primary and secondary responsive genes that triggers ecdysis. Ecdysone signaling regulates insect metamorphosis through successively expressed ERTFs (Karim and Thummel 1991; Antoniewaki et al. 1993, 1994; Huet et al. 1995; Fletcher and Thummel 1995; Zhou et al. 1998; Lam et al. 1999; Charles et al. 1999; Yamada et al. 2000; Blalecki et al. 2002; Kozlova and Thummel 2003; White et al. 1997; Riddiford et al. 2003). Expression profiles of several ERTFs during insect development were reported (Sullivan and Thummel 2003; Riddiford et al. 2003; Sekimoto et al. 2006, 2007). The interaction between ERTFs determines the expression profiles of ERTF themselves (Huet et al. 1995; White et al. 1997; Lam et al. 1997; Hiruma and Riddiford 2001). Results of their interactions triggered a successive activation of metamorphosis-related genes, including CP genes.

HR3 is a key factor of ecdysone signaling cascade and was reported to be expressed for a short time during the prepupal stage in the fruit fly *Drosophila melanogaster* (Horner et al. 1995), *M. sexta* (Palli et al. 1992) and *B. mori* (Shahin et al. 2016). *HR3* is inducible by 20E *in vitro* in 2–6 h in *D. melanogaster* (Horner et al. 1995), *M. sexta* (Palli et al. 1992) *B. mori* (Sekimoto et al. 2006) and the German cockroach *Blattella germanica* (Cruz et al. 2007). In *D. melanogaster*, mutants of *HR3* failed in adult head eversion, showed disorder of muscle, trachea and wing, and reduced expression of *BR-C*, *E74*, *E75*, β *F1* and *E93* (Lam et al. 1999). Raud et al. (2010) also observed similar defects and reduction of expression of *E74A*, *E75A*, and β *F1* in the *HR3* mutant. In *Drosophila* embryos, *HR3* was expressed first, and then β *F1* followed by *E74A* and *E75A* expression (Raud et al. 2010). They suggested that *HR3* functions upstream of β *F1*, since transcripts from *E74A* and *E75A* disappeared in β *F1* mutant, and *HR3* mutant reduced the expression of β *F1*, resulting in the reduction of the expression of *E74A* and *E75A*. White et al. (1997) observed the repression of the expression of *E74A*, *E75A* and the induction β *F1* by the overexpression of *DHR3*. Lam et al. (1997) also observed the inhibition of *BR-C*, *E75A*, *E74A*, *E74b* and *E78B* by the over expression of *DHR3*. The activation of β *F1* was also observed by over expression of *DHR3* (Cáceres et al. 2011). Thus, *HR3* down-regulates the early genes and up-regulates late genes.

HR4 was induced slightly after *HR3* in *Drosophila* and *Manduca* (Charles et al. 1999; Hiruma and Riddiford 2001), and mutation of *HR4* down-regulated the expression of *EcR*, *E75A*, *E74A* and β *F1* in *Drosophila* (King-Jones et al. 2005).

β FTZ-F1 is an attractive ERTF and mediates ecdysone signaling from HR3 to other ERTFs that resulted in the continuation of ecdysone signaling at each molting, including the larval to pupal molting. β FTZ-F1 is expressed after the decline of ecdysteroid titres in the hemolymph in *B. mori* (Sun et al. 1994) and *M. sexta* (Weller et al. 2001), and its expression preceded the expression of *E74A* and *E75A* (Broadus et al. 1999). β FTZ-F1, which is different from other ERTF genes, is induced by *in vivo* ecdysone or its removal after *in vitro* exposure (Woodard et al. 1994; Sun et al. 1994; Charles et al. 1999). β FTZ-F1 mutant disrupted the pupation of *D. melanogaster* (Broadus et al. 1999) and affected the denticle or tracheal formation (Raud et al. 2010). β FTZ-F1 mutants also inhibited the expression of metamorphic genes of *D. melanogaster*, *rpr*, *ark* and *Dronc* in the salivary glands (Lee et al. 2002b). Similar to this mutation, down regulation of ERTFs by RNAi also affected metamorphosis. Heat-shock treatment also indicated the interaction of ERTFs during metamorphosis as described below. Down-regulation of β FTZ-F1 inhibited the expression of *E74A*, *E74B* and *E75A* in *D. melanogaster* (Lam et al. 1997; Lam and Thummel 2000) and *A. aegypti* (Zhu et al. 2003). β FTZ-F1 activated *E74A* and *E75A* (Broadus et al. 1999; Lam and Thummel 2000; Raud et al. 2010). Thus, β FTZ-F1 is activated by HR3 and affects early genes such as *E74A*, *E74B* and *E75A*.

E74 has two different isoforms that are expressed at different stages in *D. melanogaster* (Thummel et al. 1990), *M. sexta* (Stilwell et al. 2003) and *B. mori* (Sekimoto et al. 2007); *E74B* is expressed earlier than *E74A*, and *in vitro* experiments showed that it responded to ecdysone at a low concentration and was repressed by high concentration of the hormone (Karim and Thummel 1991; Stilwell et al. 2003; Sekimoto et al. 2007; Wang et al. 2014), while *E74A* was induced by the high concentration of ecdysone being pulse-responsive (Karim and Thummel 1991; Stilwell et al. 2003; Sekimoto et al. 2007). A mutant of *E74B* caused the earlier expression of *E75A* and *HR3* and abolished *Sgs-5* expression, while that of *E74A* abolished *L71-6* (Fletcher and Thummel 1995). Together with the experiment of over-expression, Fletcher et al. (1997) concluded that *E74B* inhibited, whereas *E74A* promoted late genes.

E75 has three different isoforms in *D. melanogaster* (Blalecki et al. 2002) and in *A. aegypti* (Pierceall et al. 1999), and these different isoforms, which were expressed at different stages in *D. melanogaster* (Huet et al. 1995), *M. sexta* (Zhou et al. 1998) and *B. mori* (Sekimoto et al. 2006), showed different juvenile hormone (JH) responsiveness; *E75A* was activated by JH (Zhou et al. 1998; Dubrovsky et al. 2004). A mutant of *E75A* died during the second and third larval instars and inhibited the expression of *E74A* and β FTZ-F1 (Blalecki et al. 2002), and down-regulation of *E75A* inhibited the adult cuticle formation in *B. germanica* (Mané-Padrós et al. 2008). It suggests that *E75A* affects insect metamorphosis and the successively expressed genes. *E75A* and *E75C* bind to the same receptor response element of HR3 upstream of the target gene, and *E75C* also interacts with HR3 by creating a complex in *B. mori* (Swevers et al. 2002). White et al. (1997) demonstrated that DHR3 function is inhibited by binding to *E75B*. Reinking et al. (2005) also observed that *E75* inhibited the HR3 function with binding both to the upstream region of

HR3 gene and to HR3 protein. Moreover, Johnston et al. (2011), using BR-C chip assay and down-regulation of E75A, demonstrated the binding activity of E75A and the inactivation of the *EcR*, *BR-C* promoters. They concluded that E75A inhibits the expression of other ERTFs, including *EcR* itself at low concentration of ecdysone. Thus, E75 triggers the ecdysone-signaling cascade by the binding to the promoters of target genes and binding with the target protein.

Ecdysone-signaling cascade starts from inducing E74 and E75 under the low concentration of the ecdysteroid, and later, HR3 and HR4 appear at high concentrations of the hormone, which triggers late genes such as β FTZ-F1 that induces again E74 and E75. These successively induced ERTFs regulate each target gene, resulting in the successive production of CPs that construct new cuticle layers. ERTFs, which have diverged during insect evolution and being integrated with ecdysone-signaling cascade, present a super-complicated and intricate phenomenon (Bonneton et al. 2008).

1.2.3 Target Genes of Ecdysone-Responsive Transcription Factors

The involvement of *EcRE* in the *Drosophila DDC* gene promoter (Chen et al. 2002) and the *Aedes vitellogenin* gene (Martin et al. 2001) was reported. *Drosophila L71-1* (Fletcher et al. 1997) and *L71-6* (Urness and Thummel 1995) were identified as target genes of E74A. Targets of β FTZ-F1 are mostly CP genes: *Drosophila EDG84A* (Murata et al. 1996), *EDG78E* (Kawasaki et al. 2002), *BmorCPR99* (Nita et al. 2009), and *BmorCPR92* (Wang et al. 2009b). Most *BR-C* genes function together with other ERTFs as reported in *Drosophila Dronc* (Cakouros et al. 2002), *BhC4-1* (Basso et al. 2006), *DDC* (Chen et al. 2002), *BmorCPR21* (Wang et al. 2009a) and *BmorCPR92* (Wang et al. 2009b). Thus, ERTFs regulate metamorphosis-related genes and *CP* genes, and *CP* genes are expressed according to their regulation by ERTFs as described by Weller et al. (2001).

1.2.4 Remodeling of Chromatin and Histone Modification

Ecdysone also plays a role in the expression of genes through chromatin remodeling. The encyclopedia of DNA elements (ENCODE) has systematically mapped regions of transcription, transcription factor association, chromatin structure and histone modification, contributed a large scale of information including follow-up research (The ENCODE Project Consortium 2012). Comparison of genome-wide histone modification was conducted among *Homo sapiens*, *D. melanogaster* and the nematode, *Caenorhabditis elegans*, and similarities and differences among these three species were described (Ho et al. 2014). Histone modifications during cell

differentiation of human stem cell (Dixon et al. 2015) and during development of *D. melanogaster* (Nègre et al. 2011) were examined, and the functional analysis of remodeling factors was implemented (Islam et al. 2011; Blanco et al. 2008; Zraly 2006). From these studies, chromatin structure and the mechanism of gene expression became clear, as well as the significance of histone modifications.

Studies of steroid hormones in vertebrates revealed how they recruit factors that generate chromatin remodeling. Progesterone receptor removes a repressive complex by the phosphorylation of H3Ser10 (Vicent et al. 2013). Estrogen recruits H3K4 methylase (Shi et al. 2011) and ER α and H3K9 demethylase (Kawazu et al. 2011). A glucocorticoid recruits chromatin-remodeling complex to the MMTV promoter (Johnson et al. 2008). CREB-binding protein (CBP) methylated by arginine methyltransferase (CARM1) is recruited to the TFF1 promoter, where ER α , CARM1, H3K18Ac and pol II bind, and after which the histone is acetylated by E2 (Ceschin et al. 2011).

Ecdysone was also reported to bring about chromatin remodeling as follows. By the addition of 20E, EcR and histone methyltransferase Trithorax-related (TRR) are bound and induces H3K4 methylation (Sedkov et al. 2003). Nucleosome remodeling factor (NURF) bind to EcR-A and EcR-B2, and mutation of NURF decreases *BR-C* and *Eig* expression (Badenhorst et al. 2005). dDEK is a co-activator of EcR that stimulates remodeling of the chromatin complex (Sawatsubashi et al. 2010). Ecdysone signaling and transcription activation by EcR is required for the binding of the *Drosophila* EcR co-factor, *cara mitad*, to chromatin, and for methylation of H3K4 by TRR and demethylation of H3K27 by demethylase (Chauhan et al. 2012). Mutation of *Ash2* decreased *E75A* and *BR-C* expression, and the decrease of the binding of H3K4me3 was observed by the chip assay of the *E75A* and *BR-C* promoter (Carbonel et al. 2013). Mutant of the histone demethylase (Kdm4) down-regulated the expression of *EcR*, *BR-C* and *E75B* in the presence of 20E, and inhibited the development of *D. melanogaster* (Tsurumi et al. 2013). They observed accumulation of H3Kme3 on the *BR-C* promoter, binding of Kdm4A and EcR on the same sites on the chromosome, and activation of Kdm4A and Kdm4B by 20E. From these observations, it was suggested that H3K4 methylase was up-regulated by ecdysone and was recruited to the promoter of the target genes.

Arginine methyltransferase 1 of *D. melanogaster* (DART1) binds with EcR in the presence of 20E (Kimura et al. 2008). Knock-out of *DART1* reduced fertility, and *DART1* silencing activated the EcRE promoter, and it was concluded that DART1 functions as co-repressor of EcR. Dominant negative mutant of BRM revealed that ecdysone induced dendrite pruning, and down-regulated *sox14* expression in the mutant revealed that *sox14* is a required factor for this function. Existence of 20E, EcR, BRM and CPB was effective in the recruitment of H3K27Ac (Kirilly et al. 2011). Ables and Drummond-Barbosa (2010) showed that ecdysone affected chromatin remodeling in the female germline stem cells of *D. melanogaster*. Ecdysone functions as a key player of the chromatin remodeling system and brings about histone modification, resulting in a change of gene expression profiles. Therefore, chromatin remodeling occurs during the change of expression of multiple genes within a short time in the presence of ecdysone during the prepupal stage (Fig. 1.1).

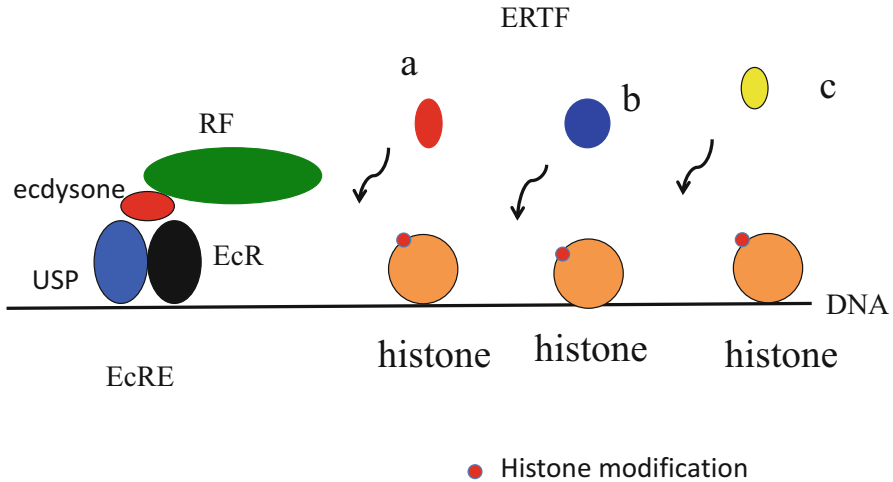


Fig. 1.1 Ecdysone and EcR complex recruit remodeling factors and make access of ERTFs easy in the wide range. *Alphabets of a, b and c* indicate different ERTFs. *RF* remodeling factors

In mutations of histone methyl transferase, the *CP* genes are down-regulated (Blanco et al. 2008). The relationships between ecdysone-inducible chromatin remodeling and the order of *CP* genes expression need to be elucidated. Shahin et al. (2016) observed five different peaks of *CP* gene expression during the prepupal stage, and suggested that they are regulated by different ERTFs. Some genes that showed peaks at different times are clustered in the same locus (Shahin et al. 2016). *BMWCP1*, *BMWCP2*, *BMWCP3*, *BMWCP4* and *BMWCP5* locate in tandem on chromosome 22 of *B. mori*, but their peak expressions were different. This suggests that the chromatin is loosened by ecdysone around the locus, and different ERTFs can access and activate different target genes (Fig. 1.1).

1.2.5 Juvenile Hormone

JH is a critical hormone that determines the type of cuticle. When its levels increase before larval ecdysis, the type of cuticle deposited is larval. In holometabolous insects, JH disappears in the early stages of the last larval instars, then again increases before pupation (Niimi and Sakurai 1997; Riddiford et al. 2003), thereby triggering complete pupal ecdysis (Riddiford et al. 2010) and a pupal type cuticle. Adult cuticle is deposited in the absence of JH during the pupal stage. HR38 of *D. melanogaster* is produced in the absence of JH bringing about the adult-type CP (Bruey-Sedano et al. 2005; Kozlova et al. 2009; Cui et al. 2009), and it is similar to the case of the pupal cuticle production by BR-C. CPs for cuticle were named previously as LCP, PCP and ACP for larva, pupa and adult, respectively. Now this division is inadequate, since some types of CPs are used for larval, pupal and adult cuticle as described in the Sect. 1.4.

BR-C has four different isoforms in *D. melanogaster* (von Kalm et al. 1994), *A. aegypti* (Zhu et al. 2007), *T. castaneum* (Suzuki et al.; 2008) and in *B. mori* (Ijiri et al. 2004), that showed different developmental or hormonal responses (Fletcher and Thummel 1995; Emery et al. 1994; Bayer et al. 1996; Tzolovsky et al. 1999; Sandstrom and Restifo 1999; Mugat et al. 2000; Zhu et al. 2007). *BR-C* is ecdysone-inducible (Bayer et al. 1996) and has EcRE in its upstream region (Nishita 2014), showing high expression during the prepupal stage. A *BR-C* mutant showed abnormality after puparium formation (Fletcher and Thummel 1995) where the expression of *rpr*, *hid* and *crq* is down-regulated, resulting in the inhibition of larval midgut destruction (Lee et al. 2002a), disordered appendages (Tzolovsky et al. 1999) and defective connections between epidermis and flight muscles (Sandstrom and Restifo 1999). RNAi experiments revealed that *BR-C* is necessary for pupal metamorphosis (Uhlirva et al. 2003; Suzuki et al. 2008). Target genes and binding sites of *BR-C* were identified (von Kalm et al. 1994). Different binding sites in promoter regions of genes for different isoforms was demonstrated (Table 1.1); *Dronc* (Cakouros et al. 2002), *sgs4* (von Kalm et al. 1994) of *D. melanogaster* and vitellogenin receptor of *A. aegypti* (Cho et al. 2006).

RNAi and chip analyses revealed that *BR-C ZI* promoter is activated by EcR and inhibited by E75A in *D. melanogaster* (Johnston et al. 2011); both EcR and E75A bind to the *BR-C* promoter region. *BR-C* family has expanded to include four isoforms during insect evolution (Erezyilmaz et al. 2006; Spokony and Restifo 2007; Suzuki et al. 2008). *BmBR-C* has a different promoter than EcRE (Nishita 2014), and it appears to be related to pupal commitment (Zhou and Riddiford 2001) in response to insulin signal in *M. sexta* (Koyama et al. 2008). *BR-C* RNAi promoted pupal program and suppressing larval and adult programs in *T. castaneum* (Parthasarathy et al. 2008). This suggests that *BR-C* has another function for the final larval instar, being apparently related to a commitment to pupal metamorphosis.

1.3 Application of Genome Information

1.3.1 Recent Genomic Research, Annotation and Analysis of Cuticular Protein Genes

Recent genomic analysis has revealed the existence of many cuticle protein genes in *D. melanogaster* (Karouzou et al. 2007), other *Drosophila* species (Cornman 2009), honey bee *Apis mellifera* (Honeybee Genome Sequencing Consortium 2006), *An. gambiae* (Cornman et al. 2008; Cornman and Willis 2009) and *B. mori* (Futahashi et al. 2008). Most of them are transcribed, and cataloged in EST databases. Over 200 CP genes were identified in *B. mori*, and 54 of them were found in *Bombyx* EST clones of wing discs (Futahashi et al. 2008). *Manduca* genome annotation identified 248 CP genes, including 207 CPR (Dittmer et al. 2015).

The R&R Consensus was found in 156 genes in the *Anopheles* genome (Cornman et al. 2008), which is 1 % of the total number of predicted genes in this species, and many RR-2 genes were in clusters having similar sequences. Karouzou et al. (2007) annotated 101 CP genes in *D. melanogaster*, and identified the chromosome band in which the gene is located. Futahashi et al. (2008) which annotated CP genes of *B. mori*, identified 220 CP genes in *Bombyx* genome and classified them into 56 RR-1, 89 RR-2, three RR-3, four Tweedle, one CPF, four CPFL, 29 GRP and 34 CPH, then compared RR-1 and RR-2 CPs with those of *D. melanogaster* and *A. mellifera*.

1.3.2 Clustering of Cuticular Protein Genes

Snyder et al. (1982), which found the cluster of CP genes in the *Drosophila* genome, identified four cuticle protein genes in a 9-kb region and speculated on their duplication and evolution. Charles et al. (1997) also reported a cluster of cuticle protein genes of *D. melanogaster*, where a 22-kb genomic DNA segment contained 12 clustered cuticle protein genes at position 65A on the third chromosome. By comparing these genes, they found two different genes duplications. Expression analysis showed different profiles for these genes (Charles et al. 1998). Dotson et al. (1998) obtained a genomic clone including three *An. gambiae* CP genes; *agcp2a*, *agcp2b* and *agcp2c*, and the latter two have 90% identity in the coding region. Recent genome wide analysis identified the clustering of cuticle protein genes in *An. gambiae* (Cornman et al. 2008; Cornman and Willis 2009). Genome wide clustering of CP genes was identified through the *Bombyx* genome research (The International Silkworm Genome Consortium 2008), where 53 RR-2 and 26 RR-1 cluster on chromosome 22. Liang et al. (2010) examined the expression profiles of CP genes clustering on Chromosome 22, and found that 26 CP genes showed co-expression during larval molting, pupal molting and for adult cuticular proteins. All of them were for proteins of larval and pupal cuticles, and half of them were expressed for the formation of the adult cuticle. Thus, insect CP genes in several insect species are the result of duplication and mutation during insect evolution, and suggests their co-regulation as being related to chromatin remodeling as described in Sect. 1.2.

1.3.3 Analysis of the Binding Sites of Transcription Factors

EcRE of ecdysone target genes have been examined (Table 1.1); *Eip28/28* (Cherbas et al. 1991; Andrew and Cherbas 1994), *hsp 22* (Rudolph et al. 1991), *Fbp1* (Laval et al. 1993), *Ddc* (Chen et al. 2002) and *Dronc* (Cakouros et al. 2004) of *D. melanogaster* and *Vg* of *A. aegypti* (Martin et al. 2001; Chen et al. 2002), and the sites of EcREs were found at proximal and distal regions. Genome wide EcRE search was conducted with a *Drosophila* cell line (Gauhar et al. 2009) where 502 sites were

Table 1.1 EcRE and ERTF binding site sequences

EcRE	AGGTCATTGACCT
	GATGGGACCCATC
	TAC GTAG
HR3	AAGTCA
	GG
HR4	AGGTC A
E75	AGGTC A
E74	AACCCGGAAGT
	T A
β FTZ-F1	TCAAGGTGG
	C CA
BR-C Z1	TAAATAACA AAT
	ATTATGC GA
	G T G
BR-C Z2	TTTACTATTT
	C AT AA
	G
BR-C Z3	TAACTAAA
	AT TATGT
	C
BR-C Z4	ATAACA
	GG G

EcRE ecdysone receptor response element, *ERTF* ecdysone-responsive transcription factor; HR3, HR4, E75, E74 are ERTFs, *β FTZ-F1* ERTF fushi tarazu, *BR-C Z1* ERTF Brord-Complex Z1 isoform

identified. Genome wide EcRE search conducted with *Drosophila* E75 (Bernardo et al. 2009) identified multiple EcREs in a distant place (over 20 kb).

Transcription factors bind to DNA and activate the RNA polymerase complex. ERTFs usually have their binding sites upstream region of their target genes. After ERTFs were identified, their binding sites were explored. Binding site of E74A (Table 1.1; Urness and Thummel 1990) and of β FTZ-F1 (Ueda and Hirose 1990) were identified. DHR3 and DHR4 are members of GGG family and have the same binding site (Table 1.1; Charles et al. 1999). Horner et al. (1995) examined the binding of several transcription factors with various nucleotide sequences, and found that EcR binds to DNA as a heterodimer with USP. EcR/USP, DHR3, and β FTZ-F1 bind with the same sequences, like E75A and DHR3 (Table 1.1). It is suggested that they have the similarity of DNA binding domain and the same origin. Thereafter, DHR3 binding sites downstream of *β FTZ-F1* were identified (Lam et al. 1997). Later, the binding of TmGRF (Mouillet et al. 1999) and BmGRF (Charles et al. 1999) to *β FTZ-F1* binding site was confirmed; recently, GRF is known as HR4. von Kalm et al. (1994) identified the binding sites of BR-C by using mutants of BR-C

Z1, Z2, Z3, Z4 isoforms and BR-C core. DNase I foot printing analysis revealed the binding sites of BR-C proteins; some of them shared the same elements (Table 1.1). The result was applied to other genes; *L71* (Crossgrove et al. 1996), *hsp 23* (Dubrovské et al. 2001), *Ddc* (Chen et al. 2002) and *Dronc* of *D. melanogaster* (Cakouros et al. 2002) and *VgR* (Cho et al. 2006) and *Vg* (Cho et al. 2007) of *A. aegypti*. Binding and effect of ERTFs on the regulatory region of CP genes were later reported. *DGE84* and *DEG78* are CP genes of *D. melanogaster*, whose promoter activity is regulated by β FTZ-F1 (Kawasaki et al. 2002; Kayashima et al. 2005). The binding analysis and following expression profiles of CP genes as well as the ecdysone and ERTF functioning through several stages of ecdysis, will be later clarified.

1.3.4 Application of Genomic Information vis-à-vis the Cuticular Protein Research

1.3.4.1 Genomic Research and Expression Profiles of Cuticular Protein Genes

Liang et al. (2010) performed microarray analysis using 6676 genes of *B. mori* and divided them into three groups based on their expression timings. Among them, 227 CP genes were detected, and CP genes of cluster A were widely expressed among 16 developmental stages. Three genes that were carefully examined showed distinctive expression; the expression of *BmorCPR53* was observed at an intermolt stage in addition to molting stages, that of *BmorCPR96* was at larval and larval to pupal molting stages, and that of *BmorCPR125* was at a mid-pupal (pharate adult) stage when adult cuticle was produced (Kawasaki et al. 1986). Three types of regulatory elements were identified upstream of 26 CP genes on chromosome 22 that showed similar expression pattern. Togawa et al. (2008) conducted RT-qPCR of 156 CPR genes in *An. gambiae* and divided them into 21 clusters with different expression patterns. They showed the similarities of expression patterns and levels of expression in the clustered genes with some exceptions. Okamoto et al. (2008) examined 6, 653 ESTs of the fourth molting-stage epidermis of *B. mori* (epM) and identified 1380 genes, including 92 CP genes. By comparing ESTs of epM with another set of ESTs of the fifth instar feeding-stage epidermis (epV3) of *B. mori*, different expression patterns between epM and epV3 were found. They revealed expression of several kinds of CP genes and a larger number of CP genes in epM, but RR-2 gene was not expressed at epV3. The results showed different expression profiles of CP genes between molting and inter-molting stages.

1.3.5 Genomic Research of the Regulatory Region of Cuticular Protein Genes

B. mori is an effective insect model for understanding development because of extensive genomic research, mass rearing and *in vitro* organ cultures are simple, ecdysone and JH titers are easy to determine, and the endocrinological conditions and timing are simple to handle. Genomic analyses in this species clarified the regulatory regions of cuticle protein genes, and ERTF binding sites, which were estimated from the genomic information, appeared to be functional as described below (Nita et al. 2009; Wang et al. 2009a, b, 2010). These regulatory sequences concerned the ecdysone responsiveness and the developmental expression patterns of CP genes. A method was devised to identify the ERTF-regulated target genes (Nita et al. 2009). Cultured wing discs were used for reporter assays *in vitro*, and gold particles with plasmids containing regulatory regions of cuticular protein genes and a luciferase reporter were introduced into wing discs. After ecdysone pulse-treatment that brought about CP gene induction that was similar to *in vivo* before pupation, high promoter activity was observed in the wing discs. Mutation of the presumed ERTF binding site reduced the promoter activity, and together with EMSA analysis, they identified the regulation of CP expression by ERTFs.

Direct regulation by EcR/USP was observed in the expression of the CP gene, *BmorCPR21* (previously named as *BMWCP10*), where BR-C functioned together with EcR/USP (Wang et al. 2010). As observed in Fig. 1.2, upstream of *BmorCPR21*, a putative EcRE was identified, and the reporter assay and electrophoretic mobility shift assay (EMSA) demonstrated the existence of EcRE and the activation of this gene by the binding to EcR (Wang et al. 2010). 20E treatment activated and mutation of putative EcRE reduced the promoter activity. Transcripts of *BmorCPR99* (*BMWCP2*) and *BmorCPR92* (*BMWCP5*) were induced by an ecdysone pulse through β FTZ-F1 that was bound to the upstream region of these CP genes and increased their promoter activity (Nita et al. 2009; Wang et al. 2009b). Thus, CP

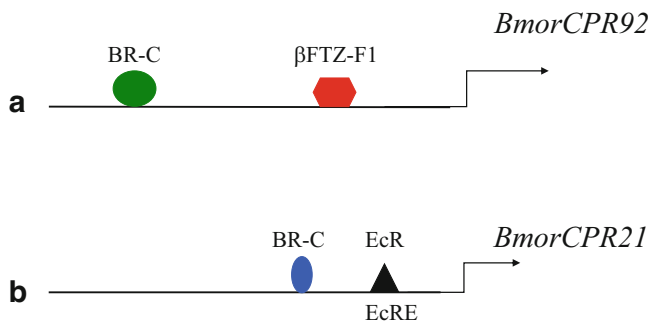


Fig. 1.2 Schematic presentation of different two CP genes that shows differ expression peaks and regulated by different ERTFs. *BmorCPR92* is regulated by β FTZ-F1 and BR-C, *BmorCPR21* is regulated by EcR and BR-C

genes, which are the downstream targets of ecdysone signaling pathway, have become key players in clarifying the mechanism of ecdysone signaling function.

In *Tribolium*, *ACP20* promoter activity required the first intron, the upstream promoter region of *ACP20* up to position -583 and the presence of 20E (Lemoine et al. 2004). The regulation of *D. melanogaster* CP gene, *ACP65A*, was also examined (Bruey-Sadano et al. 2005; Lestradet et al. 2009). The first intron of this gene was required, and the deletion of upstream region reduced the promoter activity. Both *ACP* genes required first intron for their transcriptional regulation, but the mechanism is unclear. As most *CP* genes have short first exons coding for three to four amino acids (Willis 2010), some functional mechanism in the first intron might be relevant here, and is a matter to be elucidated.

1.4 Regulation of Gene Expression of Cuticular Proteins

Recent EST analysis (Mita et al. 2003; Kawasaki et al. 2004) and genome analysis (The International Silkworm Genome Consortium 2008; Futahashi et al. 2008) of *B. mori* were essential for our insight about the construction of the cuticle via the analysis of CP genes. The section below is mainly based on the research on *B. mori* CP genes.

1.4.1 Cuticular Protein Genes in Larval Integument During Molting

Liang et al. (2010) reported that the 23 RR-2 CP genes on chromosome 22 of *B. mori* were expressed at the larval and pupal molting stages. From this report, it was concluded that RR-2 CPs are used for larval ecdysis, yet RR-1 CPs are dominant in the larval molting and intermolt stages in the epidermis of *B. mori* (Okamoto et al. 2008). Transcripts of RR-1 and RR-2 CP genes amount to 61 % and 2 % of the total ESTs of CP genes in the fourth molting stage, respectively. The above percentages of the epidermis are different from those of the wing discs of the prepupal stage. *CPG* genes, however, contain 29 % of the total ESTs of *CP* genes.

The induction of *CP* genes during larval ecdysis has been analyzed. Hiruma et al. (1991) demonstrated that the ecdysone pulse is critical for *M. sexta* epidermis, which was exposed to 2 $\mu\text{g/ml}$ 20E for 17 h before its removal, induced *LCP-14* 12 h later. Induction of *B. mori* *CPG1* was observed 16 h after hormone removal (Suzuki et al. 2002). As described in Sect. 1.2, the ERTF was reported to be induced by the ecdysone pulse was in fact $\beta\text{FTZ-F1}$ (Nita et al. 2009; Wang et al. 2009b). As described below, possible ERTFs that are the constituent the ecdysone signaling exist for the induction of *CP* genes. CP genes are induced by the ecdysone pulse in the larval molting stages in the presence of JH.

1.4.2 *Cuticular Protein Genes in the Intermolt Stage*

Reports and analyses of the expression of *CP* genes during the intermolt stage are few. *LCP16/17* of *M. sexta* was expressed 2–3 days into the final larval instar (Horodyski and Riddiford 1989); *AgLCP12.3* of mulberry longicorn beetle, *Apriona germari*, was expressed in the epidermis at the intermolt stage (Kim et al. 2003). *CP* genes, expressed during larval feeding stage in the epidermis and wing discs, have been reported (Okamoto et al. 2008; Kim et al. 2003; Gu and Willis 2003; Futahashi et al. 2008; Togawa et al. 2008). *BmorCPR46* (previously reported as *BMWCP11*) showed enhanced expression during the feeding stage and decreased after the increase of hemolymph ecdysteroid titers (Futahashi et al. 2008). Transcripts of RR-1 *CP* genes were detected but those of RR-2 genes were not observed during the feeding stage (Okamoto et al. 2008). Shahin et al. (unpublished data) observed several RR-1 but not RR-2 genes in wing discs during feeding stage of the last larval instar, which is similar to larval epidermis during the feeding stage, as Okamoto et al. (2008) reported. The location of these CPs, which were deposited in the cuticle layers, was not clarified, and the factors that induce these genes during the feeding stage were also unclear. The function and the regulatory mechanism of CPs, which are expressed during intermolt stage, have not been elucidated.

1.4.3 *Cuticular Protein Genes in the Prepupal Stage*

Thick cuticles are generated dramatically during pupation. A large number and several kinds of *CP* genes are transcribed during prepupal to early pupal stages of wing discs of *B. mori*. (Takeda et al. 2001; Kawasaki et al. 2004; Shahin et al. 2016). Fifty *CP* genes were transcribed in the prepupal to early pupal stages of *B. mori*, and the transcription of RR-2 *CP* genes stopped before pupation, while that of RR-1 genes continued until early pupal stage, even if their transcription started at the same time as RR-2 genes. They suggested that the stability of RR-1 transcripts is responsible for the difference between the exo- and endo-cuticle layers. As described above, RR-2 CPs were expressed before pupation, suggesting that transcripts expressed before pupation construct the exocuticle and those expressed after pupation build the endocuticle. The earliest CPs to be expressed code for proteins with a high percentage of His that are involved in sclerotization and creation of the hard exocuticle (Shahin et al. unpublished data). Accordingly, the content of RR-2 and RR-1 of exocuticle and endocuticle become different as described in Sect. 1.1 (Fig. 1.3).

Several kinds of *CP* genes were successively expressed during prepupal to early pupal stages. Shahin et al. (2016) observed five peaks of *CP* gene expression, and suggested that each peak is regulated by a different ERTF (Fig. 1.4). Different kinds of genes were included in each group, suggesting the function of each *CP* in each cuticle layer. It was speculated that ERTFs regulated these different peaks by comparing the developmental and ecdysone pulse expression between ERTFs and *CP* genes; the first by HR4, the second by β FTZ-F1, the third to fifth by E74A, as shown

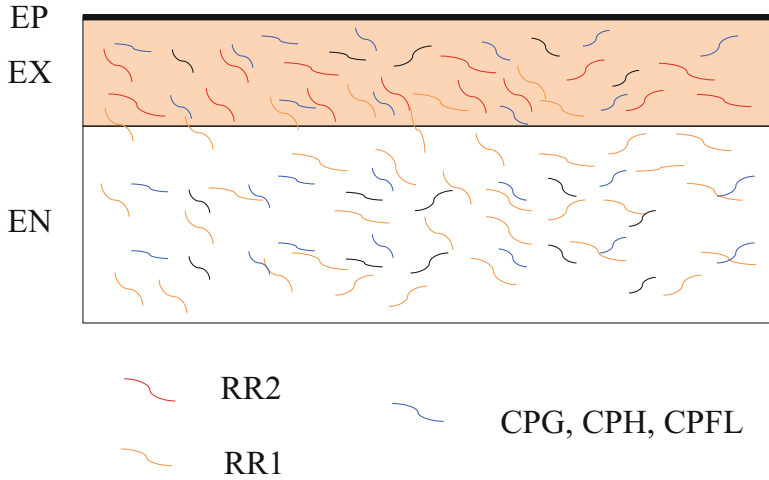


Fig. 1.3 Schematic presentation of cuticular layers of pupae. RR2 CPs are deposited in the exo-cuticular layer. RR1 CPs and other types of CPs are in the exo- and endo-cuticular layers. *EP* epicuticle, *EX* exocuticle, *EN* endocuticle

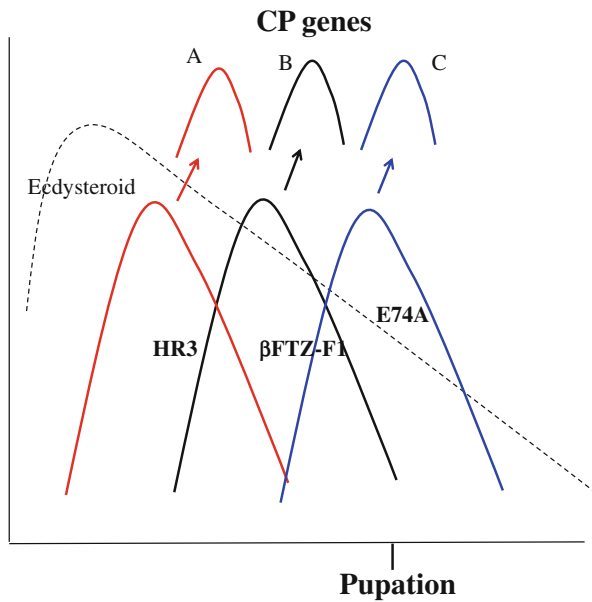


Fig. 1.4 Schematic presentation of the regulation of CP expression by different ERTFs during prepupal stage. HR3, βFTZ-F1 and E74A regulate A, B and C group CP genes, respectively

in Fig. 1.4. The regulatory mechanism governing the appearance of the second peak by ERTF was clarified by Nita et al. (2009) and Wang et al. (2009a, b). Wang et al. (2009b) demonstrated regulation of *BmorCPR92* by βFTZ-F1 and BR-C, where the

binding of ERTFs was shown on the upstream *cis*-element, and the promoter activation by the hormone pulse treatment and by abolishment of the binding site by mutation (Fig. 1.2). For these successively expressed genes, interaction of ERTFs should be required as described in Sect. 1.2. If these ERTFs have distinctive targets, the series of gene expression is determined, resulting in the construction of larval, pupal or adult cuticles.

1.4.4 *Cuticular Proteins Genes in the Adult Cuticular Layer*

Induction of adult *CP* genes needs two hormonal conditions, disappearance of JH and the ecdysone pulse similar to the larval stage. The regulatory mechanism for adult cuticle formation is similar to that of larval and pupal cuticle construction since ERTFs are expressed in all stages (Shahin et al. unpublished data). In *B. mori*, *E74A* and *E75A* showed peaks at the early pupal stage, followed by the induction of *BHR3* and *BHR4* with peaks at the mid pupal stage. The expression of *βFTZ-F1* increased from the late pupal stage (Shahin et al. unpublished data). Expression of CPs showed peaks at the mid pupal stage, and some *CP* gene transcripts increased before eclosion (Shahin et al. unpublished data). It was suggested that the expression of CPs is related to these ERTFs.

JH caused re-expression of *BR-C* in *Manduca* pupal epidermis and in pupal wings *in vitro* (Zhou and Riddiford 2002). JH application to the white puparium of *D. melanogaster* caused the induction of *BR-C* and the pupal specific gene, *EDG78E*, and the reduction of the adult specific *CP* gene, *ACP65A* (Zhou and Riddiford 2002). The induction of *BR-C* by heat–shock treatment inhibited generation of *DHR38* (Cui et al. 2009), which affected the adult *CP* gene induction (Cui et al. 2009). A mutant of *DHR38* reduced the expression of an adult specific *CP* gene *ACP65A* (Bruey-Sadano et al. 2005; Kozlova et al. 2009), and the expression of *ACP65A* required *DHR38* binding on its upstream region (Cui et al. 2009). Thus, the adult *CP* gene induction requires the disappearance of *BR-C* and appearance of *HR38*.

1.4.5 *Different Regulation at Different Stages*

Hormonal signals in larval feeding, larval molting, larval-pupal molting and mid-pupal (pharate adult) stages are different as described above. Nevertheless, several genes showed expression at each larval molting stage, larval-pupal molting stage and pupal stage as shown by the microarray analysis (Liang et al. 2010). The results were confirmed by Northern analysis; transcripts of *BmorCPR53* were observed at the fourth molting stage and feeding stage of the fifth larval instar, and those of *BmorCPR96* were observed at every larval molting stages and larval-pupal molting stages (Liang et al. 2010). Another *CP* gene that showed distinct expression was *BmorCPR21* with two different peaks. The first one was demonstrated by Wang et al. (2009a, 2010) to be regulated by EcR directly. EcR bound and activated its

transcription, and BR-C enhanced the activation. The second peak of *BmorCPR21* was observed at around pupation (Shahin et al. unpublished data); the regulation of the second peak is not clear. Some *CP* genes that showed peak expression at the prepupal stage (Shahin et al. 2016) were expressed also at the feeding stage, and another *CP* gene that showed peak expression at the prepupal stage, again showed peaks at the pupal stage (Shahin et al. unpublished data). Complexity of the regulatory region of *CP* genes has been developed during insect evolution, resulting in diverse cuticular structures.

1.4.6 Other Factors that Affect the Expression of Cuticular Protein Genes

Glycine rich proteins of the Colorado beetle *Leptinotarsa decemlineata* were induced by the exposure to an insecticide and by dry conditions (Zhang et al. 2008). Azinphosmethyl-resistant and susceptible strains were exposed to 1 μ l of 0.25 % of the organophosphorus insecticide that is equivalent to the lethal dose to the susceptible strain. Three types of glycine-rich *CP* genes were detected by cDNA dot blot hybridization; the strong signal of three GRPs, *Ld-GRP1*, *Ld-GRP2* and *Ld-GRP3* in resistant adult beetles of *L. decemlineata*, while faint signals in the susceptible strain. Adult beetles kept in the plastic box containing Dryrite showed induction of *Ld-GRP1* and *Ld-GRP2* (Zhang et al. 2008). They suggested that GRPs play a role of resistance to the insecticide by reducing cuticular penetration and reduction of water loss (Zhang et al. 2008). Two *CP* genes were upregulated by the treatment of pyrethroid insecticide in tolerant strain (Awolola et al. 2009), four adult *CP* genes were detected by microarray analysis (Vontas et al. 2007).

Another glycine-rich protein of *B. mori*, *BmSIGRP* that contains 41 % glycine, was expressed in maxilla, antenna, labrum and labium. Starvation induced *BmSIGRP* in the mouth region 5-fold compared with the usual diet (Taniai et al. 2014), and the difference of expression appeared in 3 h. Cuticular abrasion and bacterial infection also induced the expression of *CP* in *Bombyx* epidermis (Asano et al. 2013). Heat-shock induced the expression of *CP* genes in the abdominal integument of *M. sexta* (Fittinghoff-Lohmann and Riddiford 1992).

These factors induce *CP* gene expression in addition to ecdysis, which suggests that the induction of *CP* genes serves as protection against stress.

1.5 Future Prospects

Owing to recent genomic and proteomic advances, new information is expected to provide better perspectives and insights into the complex and intricate field of genes coding for cuticular proteinaceous matrices and their regulatory mechanism. The following topics will be the focus of research in the future.

1. Clarifying the regulation of successively expressed *CP* genes, and identifying the different targets of different ERTFs.
2. Elucidating the mechanism of chromosome remodeling related with *CP* gene expression and the intricate involvement of 20E.
3. Illuminating the order of expression of *CP* genes that determine the combination of CPs and consequently, the construction and nature of the cuticle and its layers.

References

- Ables ET, Drummond-Barbosa D (2010) The steroid hormone ecdysone functions with intrinsic chromatin remodeling factors to control female germline stem cells in *Drosophila*. *Cell Stem Cell* 7:581–592
- Andersen SO (1998) Amino acid sequence studies on endocuticular proteins from the desert locust, *Schistocerca gregaria*. *Insect Biochem Mol Biol* 28:421–434
- Andersen SO (2000) Studies on proteins in post-ecdysial nymphal cuticle of locust, *Locusta migratoria*, and cockroach, *Blaberus craniifer*. *Insect Biochem Mol Biol* 30:569–577
- Andersen SO (2002) Characteristic properties of proteins from pre-ecdysial cuticle of larvae and pupae of the mealworm *Tenebrio moritor*. *Insect Biochem Mol Biol* 32:1077–1087
- Andersen OS (2010) Insect cuticular sclerotization: a review. *Insect Biochem Mol Biol* 40:166–178
- Andersen SO, Rafn K, Roepstorff P (1997) Sequence studies of proteins from larval and pupal cuticle of the yellow mealworm, *Tenebrio molitor*. *Insect Biochem Mol Biol* 27:121–131
- Andrew AJ, Cherbas P (1994) Tissue-specific regulation by ecdysone: distinct patterns of Eip28/29 expression are controlled by different ecdysone response elements. *Dev Genet* 15:320–331
- Antoniewaki C, Laval M, Lepesant J-A (1993) Structural features critical to the activity of an ecdysone receptor binding site. *Insect Biochem Mol Biol* 23:105–114
- Antoniewaki C, Laval M, Dahan A, Lepesant J-A (1994) The ecdysone response enhancer of the *fbp1* gene of the *Drosophila melanogaster* is a direct target for the EcR/USP nuclear receptor. *Mol Cell Biol* 14:4465–4474
- Apple RT, Fristrom JW (1991) 20-Hydroxyecdysone is required for, and negatively regulates, transcription of *Drosophila* pupal cuticle protein genes. *Dev Biol* 146:569–582
- Arakane Y, Lomakin J, Gehrke SH, Hiromasa Y, Tomich JM, Muthukrishnan S, Beeman RW, Kramer KJ, Kanost MR (2012) Formation of rigid, non-flight forewings (elytra) of a beetle requires two major cuticular proteins. *PLoS Genet* 8:e1002682
- Asano T, Taoka M, Shinkawa T, Yamauchi Y, Isobe T, Sato D (2013) Identification of a cuticle protein with unique repeated motifs in the silkworm, *Bombyx mori*. *Insect Biochem Mol Biol* 42:344–351
- Awolola TS, Oduola OA, Strode C, Koekemoer LL, Brooke B, Ranson H (2009) Evidence of multiple pyrethroid resistance mechanisms in the malaria vector *Anopheles gambiae* sensu stricto from Nigeria. *Trans R Soc Trop Med Hyg* 103:1139–1145
- Badenhorst P, Xiao H, Cherbas L, Kwon SY, Voas M, Rebay I, Cherbas P, Wu C (2005) The *Drosophila* nucleosome remodeling factor NURF is required for ecdysteroid signaling and metamorphosis. *Genes Dev* 19:2540–2545
- Basso LR Jr, de C Neves M, Monesi N, Paçó-Larson ML (2006) Broad-Complex, E74 and E75 early genes control DNA puff BhC4-1 expression in prepupal salivary gland. *Genesis* 44:505–514
- Bayer CA, Holley B, Fristrom JW (1996) A switch in broad-complex zinc-finger isoform expression is regulated post transcriptionally during the metamorphosis of *Drosophila* imaginal discs. *Dev Biol* 177:1–14

- Bernardo TJ, Dubrovskaya VA, Jannat H, Maughan B, Dubrovsky EB (2009) Hormonal regulation of the E75 gene in *Drosophila*: identifying functional regulatory elements through computational and biological analysis. *J Mol Biol* 387:794–808
- Blalock M, Shilton A, Fichtenberg C, Seagraves WA, Thummel CS (2002) Loss of the ecdysteroid-inducible E75A orphan nuclear receptor uncouples from metamorphosis in *Drosophila*. *Dev Cell* 3:209–220
- Blanco E, Pignatelli M, Beltran S, Punset A, Pérez-Lluch S, Serras F, Guigó R, Corominas M (2008) Conserved chromosomal clustering of genes governed by chromatin regulators in *Drosophila*. *Genome Biol* 9:R134
- Bonneton F, Chaumot A, Laudet V (2008) Annotation of *Tribolium* nuclear receptors reveals an increase in evolutionary rate of a network controlling the ecdysone cascade. *Insect Biochem Mol Biol* 38:416–429
- Braquart C, Bouhin H, Quennedy A, Delachambre J (1996) Up-regulation of an adult cuticular gene by 20-hydroxyecdysone in insect metamorphosing epidermis cultured *in vitro*. *Eur J Biochem* 240:336–341
- Broadus J, McCabe JR, Endrizzi B, Thummel CS, Woodard CT (1999) The *Drosophila* β FTZ-F1 orphan nuclear receptor provides competence for stage-specific responses to the steroid hormone ecdysone. *Mol Cell* 3:143–149
- Bruey-Sedano N, Alabouvette J, Lestrade M, Hong L, Girard A, Gervasio E, Quennedy B, Charles JP (2005) The *Drosophila* ACP65A cuticle gene: deletion scanning analysis of cis-regulatory sequences and regulation by DHR38. *Genesis* 43:17–27
- Cáceres L, Necako AS, Schwartz C, Kimber S, Roberts IJH, Krause HM (2011) Nitric oxide coordinates metabolism, growth, and development via the nuclear receptor E75. *Genes Dev* 25:1476–1485
- Cakouros D, Daish T, Martin D, Baehrecke EH, Kumar S (2002) Ecdysone induced expression of the caspase DRONC during hormone dependent programmed cell death in *Drosophila* is regulated by Broad-Complex. *J Cell Biol* 157:985–995
- Cakouros D, Daish TJ, Kumar S (2004) Ecdysone receptor directly binds the promoter of the *Drosophila* caspase dronc, regulating its expression in specific tissues. *J Cell Biol* 165:631–640
- Carbonel A, Mazo A, Serras F, Corominas M (2013) Ash2 acts as an ecdysone receptor coactivator by stabilizing the histone methyltransferase Trr. *Mol Biol Cell* 24:361–372
- Ceschin DG, Walia M, Wenk SS, Duboé C, Gaudon C, Xiao Y, Fauquier L, Sankar M, Vandel L, Gronemeyer H (2011) Methylation specifies distinct estrogen-induced binding site repertoires of CBP to chromatin. *Genes Dev* 25:1132–1146
- Charles JP (2010) The regulation of expression of insect cuticle protein genes. *Insect Biochem Mol Biol* 40:205–213
- Charles J-P, Chihara C, Nejad S, Riddiford LM (1997) A cluster of cuticle protein genes of *Drosophila melanogaster* at 65A: sequence, structure and evolution. *Genetics* 147:1213–1224
- Charles J-P, Chihara C, Nejad S, Riddiford LM (1998) Identification of proteins and developmental expression of RNAs encoded by the 65A cuticle protein gene cluster in *Drosophila melanogaster*. *Insect Biochem Mol Biol* 28:131–138
- Charles JP, Shinoda T, Chinzei Y (1999) Characterization and DNA-binding properties of GRF, a novel monomeric binding orphan receptor to GCNF and β FTZ-F1. *Eur J Biochem* 266:181–190
- Chauhan C, Zraly CB, Parilla M, Diaz MO, Dingwall AK (2012) Histone recognition and nuclear receptor co-activator functions of *Drosophila* cara mitad, a homology of the N-terminal portion of mammalian MLL2 and MLL3. *Development* 139:1997–2008
- Chen L, Reece C, O’Keefe SL, Hawryluk GWL, Engstrom MM, Hodgetts RB (2002) Induction of the early-late *Ddc* gene during *Drosophila* metamorphosis by the ecdysone receptor. *Mech Dev* 114:95–107
- Cherbas L, Lee K, Cherbas P (1991) Identification of ecdysone response elements by analysis of the *Drosophila* Eip28/29 gene. *Genes Dev* 5:120–131

- Cho K-H, Cheon HM, Kokoza V, Raikhel AS (2006) Regulatory region of the vitellogenin receptor gene sufficient for high-level, germ line cell-specific ovarian expression in transgenic *Aedes aegypti* mosquitoes. *Insect Biochem Mol Biol* 36:273–281
- Cho C, Liu Y, Lehmann M (2007) Fork head controls the timing and time selectivity of steroid-induced developmental cell death. *J Cell Biol* 176:843–853
- Cornman RS (2009) Molecular evolution of *Drosophila* cuticular protein genes. *PLoS One* 4:e8345
- Cornman RS, Willis JH (2009) Annotation and analysis of low-complexity protein families of *Anopheles gambiae* that are associated with cuticle. *Insect Mol Biol* 18:607–622
- Cornman RS, Togawa T, Dunn WA, He N, Emmons AC, Willis JH (2008) Annotation and analysis of a large cuticular protein family with the R&R Consensus in *Anopheles gambiae*. *BMC Genomics* 18:9–22
- Cox DL, Willis JH (1987) Analysis of the cuticular proteins of *Hyalophora cecropia* with two dimensional electrophoresis. *Insect Biochem* 17:457–468
- Crossgrove K, Bayer CA, Fristrom JW, Guild GM (1996) The *Drosophila* Broad-Complex early gene directly regulates late gene transcription during the ecdysone-induced puffing cascade. *Dev Biol* 180:745–758
- Cruz J, Martin D, Bellés X (2007) Redundant ecdysis regulatory functions of three nuclear receptor HR3 isoforms in the direct-developing insect *Blattella germanica*. *Mech Dev* 124:180–189
- Cui HY, Lestradet M, Bruey-Sedano N, Charles JP, Riddiford LM (2009) Elucidation of the regulation of an adult cuticle gene Acp65A by the transcription factor Broad. *Insect Mol Biol* 18:421–429
- Devarakonda S, Harp JM, Kim Y, Ozyhar A, Rastinejad F (2003) Structure of the heterodimeric ecdysone receptor DNA-binding complex. *EMBO J* 22:5827–5840
- Dittmer NT, Tetreau G, Cao X, Jiang H, Wang P (2015) Annotation and expression analysis of cuticular proteins from the tobacco hornworm, *Manduca sexta*. *Insect Biochem Mol Biol* 62:100–113
- Dixon JR et al (2015) Chromatin architecture reorganization during stem cell differentiation. *Nature* 518:331–336
- Dotson EM, Cornel AJ, Willis JH, Collins FH (1998) A family of pupal-specific cuticular protein genes in the mosquito *Anopheles gambiae*. *Insect Biochem Mol Biol* 28:459–472
- Dubrovsky EB, Dubrovskaya VA, Berger EM (2001) Selective binding of *Drosophila* BR-C isoforms to a distal regulatory element in the *hsp23* promoter. *Insect Biochem Mol Biol* 31:1231–1239
- Dubrovsky EB, Dubrovskaya VA, Berger EM (2004) Hormonal regulation and functional roles of *Drosophila* E75A orphan nuclear receptor in the juvenile hormone signaling pathway. *Dev Biol* 658:258–270
- Emery IF, Bedian V, Guild GM (1994) Differential expression of Broad-Complex transcription factors may forecast tissue-specific developmental fates during *Drosophila* metamorphosis. *Development* 120:3275–3287
- Erezyilmaz DF, Riddiford LM, Truman JW (2006) The pupal specifier broad directs progressive morphogenesis in a direct developing insect. *Proc Natl Acad Sci U S A* 103:6925–6930
- Fittinghoff-Lohmann CM, Riddiford LM (1992) Synthesis and secretion of low molecular weight cuticular proteins during heat shock in the tobacco hornworm, *Manduca sexta*. *J Expl Zool* 262:374–382
- Fletcher JC, Thummel CS (1995) The *Drosophila* E74 gene is required for the proper stage- and tissue-specific transcription of ecdysone-regulated genes at the onset of metamorphosis. *Development* 121:1411–1421
- Fletcher JC, D'avino PP, Thummel CS (1997) A steroid-triggered switch in E74 transcription factor isoforms regulates the timing of secondary-response gene expression. *Proc Natl Acad Sci U S A* 94:4582–4586
- Futahashi R, Okamoto S, Kawasaki H, Zhong YS, Iwanaga M, Mita K, Fujiwara H (2008) Genome-wide identification of cuticular protein genes in the silkworm, *Bombyx mori*. *Insect Biochem Mol Biol* 38:1138–1146

- Gauhar Z, Sun LV, Hua S, Mason CE, Fuchs F, Li T-R, Boutros M, White KP (2009) Genomic mapping of binding regions for the ecdysone receptor protein complex. *Genome Res* 19:1006–1013
- Gu S, Willis JH (2003) Distribution of cuticular protein mRNAs in silk moth integument and imaginal discs. *Insect Biochem Mol Biol* 33:1177–1188
- Guan X, Middlebrooks BW, Alexander S, Wasserman SA (2006) Mutation of TweedleD, a member of an unconventional cuticle protein family, alters body shape in *Drosophila*. *Proc Natl Acad Sci U S A* 103:16794–16799
- Hiruma K, Riddiford LM (2001) Regulation of transcription factors MHR4 and β FTZ-F1 by 20-hydroxyecdysone during a larval molt in the tobacco hornworm, *Manduca sexta*. *Dev Biol* 232:265–274
- Hiruma K, Hardie J, Riddiford LM (1991) Hormonal regulation of epidermal metamorphosis *in vitro*: control of expression of a larval-specific cuticle gene. *Dev Biol* 144:369–378
- Ho JWK et al (2014) Comparative analysis of metazoan chromatin organization. *Nature* 512:449–452
- Honeybee Genome Sequencing Consortium (2006) Insights into social insects from the genome of the honeybee *Apis mellifera*. *Nature* 443:931–949
- Hopkins TL, Krchma LJ, Ahmad SA, Kramer KJ (2000) Pupal cuticle proteins of *Manduca sexta*: characterization and profiles during sclerotization. *Insect Biochem Mol Biol* 30:19–27
- Horner MA, Chen T, Thummel CS (1995) Ecdysteroid regulation and DNA binding properties of *Drosophila* nuclear hormone receptor superfamily members. *Dev Biol* 168:490–502
- Horodyski FM, Riddiford LM (1989) Expression and hormonal control of a new larval cuticular multigene family at the onset of metamorphosis of the tobacco hornworm. *Dev Biol* 132:292–303
- Huet F, Ruiz C, Richards G (1995) Sequential gene activation by ecdysone in *Drosophila melanogaster*: the hierarchical equivalence of early and early late genes. *Development* 121:1195–1204
- Iconomidou VA, Willis JH, Hamodrakas SJ (2005) Unique features of the structural model of ‘hard’ cuticle proteins: implications for chitin-protein interactions and cross-linking in cuticle. *Insect Biochem Mol Biol* 35:553–560
- Ijro T, Urakawa H, Yasukochi Y, Takeda M, Fujiwara Y (2004) cDNA cloning, gene structure, and expression of *Broad-Complex (BR-C)* genes in the silkworm, *Bombyx mori*. *Insect Biochem Mol Biol* 34:963–969
- Ioannidou ZS, Theodoropoulou MC, Papandreou NC, Willis JH, Hamodrakas SJ (2014) CutProtFam-Pred: detection and classification of putative structural cuticular proteins from sequence alone, based on profile Hidden Markov Models. *Insect Biochem Mol Biol* 52:51–59
- Islam AB, Richter WF, Lopez-Bigas N, Benevolenskaya EV (2011) Selective targeting of histone methylation. *Cell Cycle* 10:413–424
- Johnson TA, Elbi C, Parekh BS, Hager GL, John S (2008) Chromatin remodeling complexes interact dynamically with a glucocorticoid receptor-regulated promoter. *Mol Biol Cell* 19:3308–3322
- Johnston DM, Sedkov Y, Petruk S, Riley KM, Fujioka M, Jaynes JB (2011) Ecdysone- and NO-mediated gene regulation by competing EcR/Usp and E75A nuclear receptors during *Drosophila* development. *Mol Cell* 44:51–61
- Karim FD, Thummel CS (1991) Ecdysone coordinates the timing and amounts of E74A and E74B transcription in *Drosophila*. *Genes Dev* 5:1067–1079
- Karouzou MV, Spyropoulos Y, Iconomidou VA, Cornman RS, Hamodrakas SJ, Willis JH (2007) *Drosophila* cuticular proteins with the R&R Consensus: annotation and classification with a new tool for discriminating RR-1 and RR-2 sequences. *Insect Biochem Mol Biol* 37:754–760
- Kawasaki H, Kiguchi K, Agui N, Iwashita Y (1986) Ecdysteroid titer and wing development during the pupal-adult transformation of *Bombyx mori*. *Zool Sci* 30:301–304
- Kawasaki H, Hirose S, Ueda H (2002) β FTZ-F1 dependent and independent activation of *Edg78E*, a pupal cuticle gene, during the early metamorphic period in *Drosophila melanogaster*. *Develop Growth Differ* 44:419–425

- Kawasaki H, Ote M, Okano H, Shimada T, Quan G-X, Mita K (2004) Change in the expressed gene patterns of the wing disc during the metamorphosis of *Bombyx mori*. *Gene* 343:133–142
- Kawazu M, Saso K, Tong KI, McQuire T, Goto K, Son DO, Wakeham A, Miyagishi M, Mak TW, Okada H (2011) Histone demethylase JMJD2B functions as a o-factor of estrogen receptor in breast cancer proliferation and mammary gland development. *PLoS ONE* 6:e17830
- Kayashima Y, Hirose S, Ueda H (2005) Anterior epidermis-specific expression of the cuticle gene EDG84A is controlled by many *cis*-regulatory elements in *Drosophila melanogaster*. *Dev Genes Evol* 215:545–552
- Kim SR, Yoon HJ, Lee KS, Kim I, Je YH, Sohn HD, Jin BR (2003) Molecular cloning of three cDNAs encoding putative larval cuticle protein expressed differentially after larval ecdysis from the mulberry longicorn beetle, *Apriona germari*. *Comp Biochem Physiol B Biochem Mol Biol* 136:803–811
- Kimura S et al (2008) *Drosophila* arginine methyltransferase 1 (DART1) is an ecdysone receptor co-repressor. *Biochem Biophys Res Commun* 371:889–893
- King-Jones K, Charles J-P, Lam G, Thummel CS (2005) The ecdysone-induced DHR4 orphan nuclear receptor coordinates growth and maturation in *Drosophila*. *Cell* 121:773–784
- Kirilly D, Wong JLL, Lim EKH, Wang Y, Zhang H, Wang C, Liao Q, Wang H, Liou Y-C, Wang H, Yu F (2011) Intrinsic epigenetic factors cooperate with the steroid hormone ecdysone to govern dendrite pruning in *Drosophila*. *Cell* 146:86–100
- Koyama T, Syropyatova MO, Riddiford LM (2008) Insulin/IGF signaling regulates the change in commitment in imaginal discs and primordia by overriding the effect of juvenile hormone. *Dev Biol* 324:258–265
- Kozlova T, Thummel CS (2003) Essential roles for ecdysone signaling during *Drosophila* mid-embryonic development. *Science* 301:1911–1914
- Kozlova T, Lam G, Thummel CS (2009) *Drosophila* DHR38 nuclear receptor is required for adult cuticle integrity at eclosion. *Dev Dyn* 238:701–707
- Lam TG, Thummel CS (2000) Inducible expression of double-stranded RNA directs specific genetic interference in *Drosophila*. *Curr Biol* 10:957–963
- Lam TG, Jiang C, Thummel CS (1997) Coordination of larval and prepupal gene expression by DHR3 orphan receptor during *Drosophila* metamorphosis. *Development* 124:1757–1769
- Lam TG, Bonnie LH, Bender M, Thummel CS (1999) DHR3 is required for the prepupal-pupal transition and differentiation of adult structures during *Drosophila* metamorphosis. *Dev Biol* 212:204–216
- Laval M, Pourrain F, Deutsch J, Jean-Antoine L (1993) In vivo functional characterization of an ecdysone response enhancer in the proximal upstream region of the *fbp1* gene of *D. melanogaster*. *Mech Dev* 44:123–138
- Lee CY, Cooksey BA, Baehrecke EH (2002a) Steroid regulation of midgut cell death during *Drosophila* development. *Dev Biol* 250:101–111
- Lee CY, Simon CR, Woodard CT, Baehrecke EH (2002b) Genetic mechanism for the stage-specific regulation of steroid triggered programmed cell death in *Drosophila*. *Dev Biol* 252:138–148
- Lemoine A, Mathelin J, Braquart-Varnier C, Everaerts C, Delachambre J (2004) A functional analysis of ACP-20, adult specific cuticular protein gene from the beetle *Tenebrio*: role of an intronic sequence in transcriptional activation during the late metamorphic period. *Insect Mol Biol* 13:481–493
- Lestrade M, Gervasio E, Fraichard S, Dupas S, Alabouvette J, Lemoine A, Charles JP (2009) The *cis*-regulatory sequences required for expression of the *Drosophila melanogaster* adult cuticle gene ACP65A. *Insect Mol Biol* 18:431–441
- Liang J, Zhang L, Xiang Z, He N (2010) Expression profile of cuticular genes of silkworm, *Bombyx mori*. *BMC Genomics* 11:173
- Locke M (1961) Pore canals and related structures in insect. *J Biophys Biochem Cytol* 10:589–618
- Mané-Padrós D, Cruz J, Vilaplana L, Pascual N, Bullés X, Martín D (2008) The nuclear hormone receptor BgE75 links molting and developmental progression in the direct-developing insect *Blattella germanica*. *Dev Biol* 315:147–160

- Martin D, Wang S-F, Raikhel AS (2001) The vitellogenin gene of the mosquito *Aedes aegypti* is a direct target of ecdysteroid receptor. *Insect Biochem Mol Biol* 31:827–837
- Missios S, Davidson HC, Linder D, Moltimer L, Okobi AO, Doctor JS (2000) Characterization of cuticular proteins in the red flour beetle *Tribolium castaneum*. *Insect Biochem Mol Biol* 30:47–56
- Mita K, Morimyo M, Okano K, Koike Y, Nohata J, Kawasaki H, Kadono-Okuda K, Yamamoto K, Suzuki MG, Shimada T, Goldsmith MR, Maeda S (2003) The construction of an EST database for *Bombyx mori* and its application. *Proc Natl Acad Sci U S A* 100:14121–14126
- Mouillet JF, Bousquet F, Sedano N, Alabouvette J, Nicolai M, Zelus D, Laudet V, Delachambre J (1999) Cloning and characterization of new orphan nuclear receptors and their developmental profiles during *Tenebrio* metamorphosis. *Eur J Biochem* 265:972–981
- Mugat B, Brodu V, Kejzlarova-lepesant J, Antoniewski C, Bayer CA, Fristrom JW, Lepesant JA (2000) Dynamic expression of broad-complex isoforms mediates temporal control of ecdysteroid target gene at the onset of *Drosophila* metamorphosis. *Dev Biol* 227:104–117
- Mun S, Noh MY, Dittmer NT, Muthukrishnan S, Kramer KJ, Kanost MR (2015) Cuticular protein with a low complexity sequence becomes cross-linked during insect cuticle sclerotization and is required for the adult molt. *Sci Rep* 5:10484
- Murata T, Kagayama Y, Hirose S (1996) Regulation of the EDG84A gene by FTZ-F1 during metamorphosis in *Drosophila melanogaster*. *Mol Cell Biol* 16:6509–6515
- Nègre N et al (2011) *Cis*-regulatory map of the *Drosophila* genome. *Nature* 471:527–531
- Nieva C, Spindler-Barth M, Azoitei A, Spindler KD (2007) Influence of hormone on intracellular localization of the *Drosophila melanogaster* ecdysteroid receptor. *Cell Signal* 19:2582–2587
- Niimi S, Sakurai S (1997) Development changes in juvenile hormone and juvenile hormone acid titers in the hemolymph and in vitro juvenile hormone synthesis by corpora allata of the silkworm, *Bombyx mori*. *J Insect Physiol* 43:875–884
- Nishita Y (2014) Ecdysone response elements in the distal promoter of the Broad Complex gene, BmBR-C. *Insect Mol Biol* 23:341–356
- Nita M, Wang HB, Zhong YS, Mita K, Iwanaga M, Kawasaki H (2009) Analysis of ecdysone-pulse responsive region of *BMWCP2* in wing disc of *Bombyx mori*. *Comp Biochem Physiol B* 153:101–108
- Noh MY, Kramer KJ, Muthukrishnan S, kanost MR, Beeman R, Arakane Y (2014) Two major cuticular proteins are required for assembly of horizontal laminae and vertical pore canals in rigid cuticle of *Tribolium castaneum*. *Insect Biochem Mol Biol* 53:22–29
- Noh MY, Muthukrishnan S, Kramer KJ, Arakane Y (2015) *Tribolium castaneum* RR-1 cuticular protein TcCPR4 is required for formation of pore canals in rigid cuticle. *PLoS Genet* 11:e1004963. doi:10.1371/journal.pgen.1004963
- Noji T, Ote M, Takeda M, Mita K, Shimada T, Kawasaki H (2003) Isolation and comparison of different ecdysone-responsive cuticle protein genes in wing discs of *Bombyx mori*. *Insect Biochem Mol Biol* 33:671–679
- Okamoto S, Futahashi R, Kojima T, Mita K, Fujiwara H (2008) Catalogue of epidermal genes expressed in the epidermis during larval molt of the silkworm *Bombyx mori*. *BMC Genomics* 9:396
- Palli SR, Hiruma K, Riddiford LM (1992) An ecdysteroid inducible *Manduca* gene similar to the *Drosophila* DHR3 gene, a member of the steroid hormone receptor superfamily. *Dev Biol* 150:306–318
- Parthasarathy R, Tan A, Bai H, Palli SR (2008) Transcription factor broad suppresses precocious development of adult structures during larval-pupal metamorphosis in the red flour beetle, *Tribolium castaneum*. *Mech Dev* 125:299–313
- Pierceall WE, Li C, Biran A, Miura K, Raikhel AS, Segraves WA (1999) E75 expression in *A. aegypti* mosquito ovary and fat body suggests reiterative use of ecdysone-regulated hierarchies in development and reproduction. *Mol Cell Endocrinol* 150:73–89
- Qiao L, Xiong G, Wang R-x, He S-z, Chen J, Tong X-l, Hu H, Li C-l, Gai T-t, Xin Y-q, Liu X-f, Chen B, Xiang Z-h, Lu C, Dai F-y (2014) Mutation of a cuticular protein, BmorCPR2, alters larval body shape and adaptability in silkworm, *Bombyx mori*. *Genetics* 196:1103–1115

- Raud AF, Lam G, Thummel CS (2010) The *Drosophila* nuclear receptors DHR3 and bFTZ-F1 control overlapping developmental responses in late embryos. *Development* 137:123–131
- Rebers JE, Riddiford LI (1988) Structure and expression of a *Manduca sexta* larval cuticle gene homologous to *Drosophila* cuticle genes. *J Mol Biol* 203:411–423
- Rebers JE, Willis JH (2001) A conserved domain in arthropod cuticular proteins binds chitin. *Insect Biochem Mol Biol* 31:1083–1094
- Reinking J, Lam MMS, Pardee K, Sampson HM, Liu S, Yang P, Williams S, White W, Lajoie G, Edwards A, Krause HM (2005) The *Drosophila* nuclear receptor E75 contains heme and is gas responsive. *Cell* 122:195–207
- Riddiford LM, Hiruma K, Zhou X, Nelson CA (2003) Insights into the molecular basis of the hormonal control of molting and metamorphosis from *Manduca sexta* and *Drosophila melanogaster*. *Insect Biochem Mol Biol* 33:1327–1338
- Riddiford LM, Truman JW, Mirth CK, Shen YC (2010) A role for juvenile hormone in the prepupal development of *Drosophila melanogaster*. *Development* 137:1117–1126
- Rudolph K, Morganelli C, Berger EM (1991) Regulatory elements near the *Drosophila hsp 22* gene required for ecdysterone and heat shock induction. *Dev Genet* 12:212–218
- Sullivan AA, Thummel CS (2003) Temporal profiles of nuclear receptor gene expression reveal co-ordinate transcriptional responses during *Drosophila* development. *Mol Endocrinol* 17:2125–2137
- Sandstrom DJ, Restifo LL (1999) Epidermal tendon cells require broad complex function for correct attachment of the indirect flight muscles in *Drosophila melanogaster*. *J Cell Sci* 112:4051–4065
- Sawatsubashi S et al (2010) A histone chaperone, DEK transcriptionally coactivates a nuclear receptor. *Genes Dev* 24:159–170
- Schaefer J, Kramer KJ, Garbow JR, Jacob GS, Stejskal EO, Hopkins TL, Speirs RD (1987) Aromatic cross-links in insect cuticle: detection by solid-state ¹³C and ¹⁵N NMR. *Science* 235:1200–1204
- Sedkov Y, Cho E, Petruk S, Cherbas L, Smith ST, Jones RS, Cherbas P, Canaani E, Jaynes JB, Mazo A (2003) Methylation at lysine 4 of histone H3 in ecdysone-dependent development of *Drosophila*. *Nature* 426:78–83
- Sekimoto T, Iwami M, Sakurai S (2006) Coordinate responses of transcription factors to ecdysone during programmed cell death in the anterior silk gland of the silkworm, *Bombyx mori*. *Insect Mol Biol* 15:281–292
- Sekimoto T, Iwami M, Sakurai S (2007) 20-hydroxyecdysone regulation of two isoforms of the Ets transcription factor *E74* gene in programmed cell death in the silkworm anterior silk gland. *Insect Mol Biol* 16:581–590
- Shahin R, Iwanaga M, Kawasaki H (2016) Cuticular protein and transcription factor genes expressed during prepupal-pupal transition and by ecdysone pulse treatment in wing discs of *Bombyx mori*. *Insect Mol Biol* 25:138–152
- Shi L et al (2011) Histone demethylase JMJD2B coordinates H3K4/H3K9 methylation and promotes hormonally responsive breast carcinogenesis. *Proc Natl Acad Sci U S A* 108:7541–7546
- Snyder M, Hunkapiller M, Yuen D, Silvert D, Fristrom J, Davidson N (1982) Cuticle protein genes of *Drosophila*: structure, organization, and evolution of four clustered genes. *Cell* 29:1027–1040
- Spokony RF, Restifo LL (2007) Anciently duplicated Broad Complex exons have distinct temporal functions during tissue morphogenesis. *Dev Genes Evol* 217:499–513
- Stilwell GE, Nelson CA, Weler J, Cui H, Hiruma K, Truman JW, Riddiford LM (2003) *E74* exhibits stage-specific hormonal regulation in the epidermis of the tobacco hornworm, *Manduca sexta*. *Dev Biol* 258:76–90
- Sun GC, Hirose S, Ueda H (1994) Intermittent expression of BmFTZ-F1, a member of the nuclear hormone receptor superfamily during development of the silkworm *Bombyx mori*. *Dev Biol* 162:426–437

- Suzuki Y, Matsuoka T, Imura Y, Fujiwara H (2002) Ecdysteroid dependent expression of a novel cuticle protein gene *BMCPG1* in the silkworm, *Bombyx mori*. *Insect Biochem Mol Biol* 32:599–607
- Suzuki Y, Truman JW, Riddiford LM (2008) The role of Broad in the development of *Tribolium castaneum*: implications for the evolution of the holometabolous insect pupa. *Development* 135:569–577
- Swevers L, Ito K, Iatrou K (2002) The BmE75 nuclear receptors function as dominant repressors of the nuclear receptor BmHR3A. *J Biol Chem* 277:41637–41644
- Takeda M, Mita K, Quan GX, Shimada T, Okano K, Kanke E, Kawasaki H (2001) Mass isolation of cuticle protein cDNAs from wing discs of *Bombyx mori* and their characterization. *Insect Biochem Mol Biol* 31:1019–1028
- Tang L, Liang J, Zhan Z, Xiang Z, He N (2010) Identification of the chitin-binding proteins from the larval proteins of silkworm, *Bombyx mori*. *Insect Biochem Mol Biol* 40:228–234
- Taniai K, Hirayama C, Mita K, Asaoka K (2014) Starvation-responsive glycine-rich protein gene in the silkworm *Bombyx mori*. *J Comp Physiol B* 184:827–834
- The ENCODE Project Consortium (2012) An integrated encyclopedia of DNA elements in the human genome. *Nature* 489:57–74
- The International Silkworm Genome Consortium (2008) The genome of a lepidopteran model insect, the silkworm *Bombyx mori*. *Insect Biochem Mol Biol* 38:1036–1045
- Thummel CS, Burtis KC, Hogness DS (1990) Spatial and temporal patterns of E74 transcription during *Drosophila* development. *Cell* 61:101–111
- Togawa T, Natkato H, Izumi S (2004) Analysis of the chitin recognition mechanism of cuticle proteins from the soft cuticle of the silkworm, *Bombyx mori*. *Insect Biochem Mol Biol* 34:1059–1067
- Togawa T, Dunn WA, Emmons AC, Willis JH (2007) CPF and CPFL, two related gene families encoding cuticular proteins of *Anopheles gambiae* and other insects. *Insect Biochem Mol Biol* 37:675–688
- Togawa T, Dunn WA, Emmons AC, Nagao J, Willis JH (2008) Developmental expression patterns of cuticular protein genes with the R&R Consensus from *Anopheles gambiae*. *Insect Biochem Mol Biol* 38:508–519
- Tsurumi A, Dutta O, Shang R, Yan SJ, Li WX (2013) *Drosophila* Kdm4 demethylases in histone H3 lysine 9 demethylation and ecdysteroid signaling. *Sci Rep* 3:2894
- Tzolovsky G, Deng WM, Schlitt T, Bownes M (1999) The function of the broad-complex during *Drosophila melanogaster* oogenesis. *Genetics* 153:1371–1383
- Ueda H, Hirose S (1990) Identification and purification of a *Bombyx mori* homologue of FTZ-F1. *Nucleic Acids Res* 18:7229–7234
- Uhlirova M, Foy BD, Beaty BJ, Olson KE, Riddiford LM, Jindra M (2003) Use of Sindbis virus-mediated RNA interference to demonstrate a conserved role of Broad-Complex in insect metamorphosis. *Proc Natl Acad Sci U S A* 100:15607–15612
- Urness LD, Thummel CS (1990) Molecular interaction within the ecdysone regulatory hierarchy: DNA binding properties of the *Drosophila* ecdysone-inducible E74A protein. *Cell* 63:47–61
- Urness DL, Thummel SC (1995) Molecular analysis of a steroid-induced regulatory hierarchy: the *Drosophila* E74A protein directly regulates L71-6 transcription. *EMBO J* 14:6239–6246
- Vicent GP, Nacht AS, Zaurin R, Font-Mateu J, Soronellas D, Le Dily F, Reyes D, Beato M (2013) Unliganded progesterone receptor-mediated targeting of an RNA-containing repressing complex silences a subset of hormone-inducible genes. *Genes Dev* 27:1179–1197
- von Kalm L, Crossgrove K, Von Seggern D, Guild GM, Beckendorf SK (1994) The Broad-Complex directly controls a tissue-specific response to the steroid hormone ecdysone at the onset of *Drosophila* metamorphosis. *EMBO J* 13:3505–3516
- Vontas J, David JP, Nikou D, Hemingway J, Christophides GK, Louis C, Ranson H (2007) Transcriptional analysis of insecticide resistance in *Anopheles stephensi* using cross-species microarray hybridization. *Insect Mol Biol* 16:315–324

- Wang H-B, Iwanaga M, Kawasaki H (2009a) Activation of BMWCP10 promoter and regulation by BR-C Z2 in wing disc of *Bombyx mori*. *Insect Biochem Mol Biol* 39:615–623
- Wang H-B, Nita M, Iwanaga M, Kawasaki H (2009b) β FTZ-F1 and Broad-Complex positively regulate the transcription of the wing cuticle protein gene, BMWCP5, in wing discs of *Bombyx mori*. *Insect Biochem Mol Biol* 39:624–633
- Wang H-B, Moriyama M, Iwanaga M, Kawasaki H (2010) Ecdysone directly and indirectly regulates a cuticle protein gene, BMWCP10, in the wing disc of *Bombyx mori*. *Insect Biochem Mol Biol* 40:453–459
- Wang H-B, Iwanaga M, Kawasaki H (2014) Stage-specific activation of the E74B promoter by low ecdysone concentrations in the wing disc of *Bombyx mori*. *Gene* 537:322–327
- Weller J, Sun G-C, Zhou B, Lan Q, Hiruma K, Riddiford LM (2001) Isolation and developmental expression of two nuclear receptors, MHR4 and β FTZ-F1, in the tobacco hornworm, *Manduca sexta*. *Insect Biochem Mol Biol* 31:827–837
- White KP, Hurban P, Watanabe T, Hogness DS (1997) Coordination of *Drosophila* metamorphosis by two ecdysone-induced nuclear receptors. *Science* 276:114–117
- Wigglesworth VB (1972) The principles of insect physiology, 7th edn. Chapman and Hall, London
- Willis JH (2010) Structural cuticular protein from arthropods: annotation, nomenclature, and sequence characteristics in genomics era. *Insect Biochem Mol Biol* 40:189
- Woodard CT, Baehrecke EH, Thummel CS (1994) A molecular mechanism for the stage specificity of the *Drosophila* prepupal genetic response to ecdysone. *Cell* 79:607–615
- Yamada M, Murata T, Hirose S, Lavorgna G, Suzuki E, Ueda H (2000) Temporally restricted expression of transcription factor betaFTZ-F1: significance for embryogenesis, molting and metamorphosis in *Drosophila melanogaster*. *Development* 127:5083–5092
- Zhang J, Goyer C, Pelletier Y (2008) Environmental stresses induce the expression of putative glycine-rich insect cuticular protein genes in adult *Leptinotarsa decemlineata* (Say). *Insect Mol Biol* 17:209–216
- Zhong Y-S, Mita K, Shimada T, Kawasaki H (2006) Glycine-rich protein genes, which encode a major component of the cuticle protein genes in *Bombyx mori*. *Insect Biochem Mol Biol* 36:99–110
- Zhou B, Riddiford LM (2001) Hormonal regulation and patterning of the Broad-Complex in the epidermis and wing discs of the tobacco hornworm, *Manduca sexta*. *Dev Biol* 231:125–137
- Zhou X, Riddiford LM (2002) Broad specifies pupal development and mediates the “status quo” action of juvenile hormone on the pupal-adult transformation in *Drosophila* and *Manduca*. *Development* 129:2259–2269
- Zhou B, Hiruma K, Shinoda T, Riddiford LM (1998) Juvenile hormone prevents ecdysteroid-induced expression of Broad Complex RNAs in the epidermis of the tobacco hornworm, *Manduca sexta*. *Dev Biol* 203:233–244
- Zhu J, Chen L, Raikhel AS (2003) Posttranscriptional control of the competence factor bFTZ-F1 by juvenile hormone in the mosquito *Aedes aegypti*. *Proc Natl Acad Sci U S A* 100:13338–13343
- Zhu J, Chen L, Raikhel AS (2007) Distinct roles of broad isoforms in regulation of the 20-hydroxyecdysone effector gene, Vitellogenin, in the mosquito *Aedes aegypti*. *Mol Cell Endocrinol* 267:97–106
- Zraly CB (2006) Hormone-response genes are direct *in vivo* regulating targets of Brahma (SWI/SNF) complex function. *J Biol Chem* 281:35305–35315

Chapter 2

Chitin Metabolic Pathways in Insects and Their Regulation

Subbaratnam Muthukrishnan, Hans Merzendorfer, Yasuyuki Arakane, and Qing Yang

Abstract Chitin, the matrix polymer of arthropod exoskeleton, occurs in three forms that have different structural and mechanical properties. In the insect cuticle and the peritrophic matrix, individual chitin chains are further organized into higher order structures that give chitinous matrices their unique and widely differing properties such as rigidity, elasticity and waterproofing. In this chapter, we review the biochemical pathways of chitin biosynthesis, degradation and modification. In many cases, there are multiple isozymes for carrying out each step of chitin metabolism with specialization among members of families of isozymes. The gene families encoding the enzymes of chitin metabolism and their regulation are presented. The roles of chitin metabolism isoenzymes within families as revealed by gene deletion studies or RNA interference are discussed. How the association of chitin with different assortments of proteins modifies the properties of chitin matrices is briefly outlined.

S. Muthukrishnan (✉)

Department of Biochemistry & Molecular Biophysics, Kansas State University,
141 Chalmers Hall, Manhattan, KS 66506, USA
e-mail: smk@ksu.edu

H. Merzendorfer

Department of Chemistry and Biology – Institute of Biology, University of Siegen,
Adolf-Reichwein-Str. 2, 57076 Siegen, Germany
e-mail: merzendorfer@chemie-bio.uni-siegen.de

Y. Arakane

Department of Applied Biology, Chonnam National University, Gwangju 61186, South Korea
e-mail: arakane@chonnam.ac.kr

Q. Yang

School of Life Science and Biotechnology, Dalian University of Technology,
No. 2 Linggong Road, Dalian 116024, China
e-mail: qingyang@dlut.edu.cn

2.1 Introduction

Chitin, a linear, unbranched aminopolysaccharide, made up of *N*-acetylglucosamine monomers, is a structural constituent of extracellular matrices such as the cell walls of fungi and the exoskeletons of arthropods including insects (Muzzarelli 1973). In arthropods, the choice of chitin rather than cellulose as the matrix polymer seems to have been designed to increase the versatility of the cuticle in response to the need to adapt to widely different environmental stresses to which they have been subjected during hundreds of millions of years of evolution in both aquatic and terrestrial environments. The presence of the amide function in chitin polymer increases additional hydrogen-bonding opportunities and possibly confers the ability to cross-link with other functional groups in the components of the cuticle. In particular, the large and anisotropic variations in the physicochemical and mechanical properties of the insect cuticle derive from the ability of chitin to be arranged in unique ways and its potential to interact with a large assortment of proteins and possibly tanning agents during the process of cuticle deposition. In this review, we will focus mostly on the metabolic pathways leading to chitin synthesis, modification and degradation, but we will also address how chitin might interact with different proteins to alter the physicochemical properties of chitin-containing matrices. The properties of the mineralized exoskeletons of crustaceans and the hydrated peritrophic matrix will be dealt with in other chapters in this book.

2.2 Structure of Chitin

In natural materials chitin can occur in different forms including the α , β and γ forms (Lotmer and Picken 1950; Ruddal 1963). The α -form is the predominant form characterized by its strong mechanical properties and low solubility and is the form found in the exoskeletons of arthropods including insects. In crustaceans, it is heavily mineralized with calcium or magnesium salts, further increasing its strength. In the crystal structure of α -chitin, which forms orthorhombic crystals, the unit cell has two chains in an antiparallel orientation stabilized by intra-chain H-bonds (Carlstrom 1957; Minke and Blackwell 1978). More recent analysis and refinements of high resolution synchrotron X-ray diffraction data of highly crystalline α -chitin fibers have indicated that in this form, there is a three dimensional network of H-bonded sheets in which two distinct conformations of C6-O6 hydroxymethyl groups exist. These two distinctive O6 atom conformations allow the formation of a three-dimensional network of chitin sheets. This maximizes the formation of intra-chain as well as inter-chain H-bonds involving this H-atom, the carbonyl group (C7) and amino group of the side chain (Sikorski et al. 2009; Beckham and Crowley 2011) that accounts for the extraordinary stability of α -chitin compared to cellulose II (Fig. 2.1a).

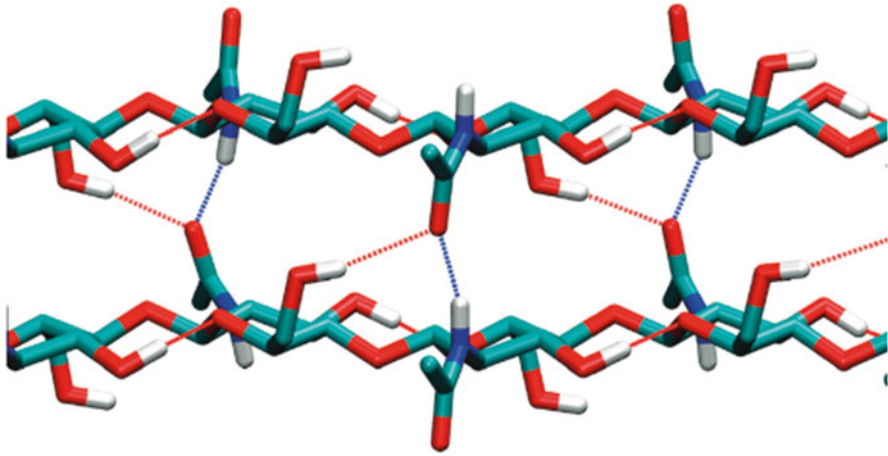


Fig. 2.1a Hydrogen bonding in α -chitin: Bifurcated hydrogen bonds (*broken red and blue lines*) are formed between the GlcNAc side chain and the O6 side chain of every two residues in a layer to the GlcNAc side chain in the layer above. The hydrogen bonds internal to a chain between O5 and O3/HO3 (*solid red lines*) are self-hydrogen bonds (From Sarkar and Perez 2015)

In β -chitin, which forms monoclinical crystals, the chains are organized in a parallel orientation as in cellulose I and forms mostly intra-chain H-bonds involving O3H and O5 except for two H-bonds in the a-axis (NH...O7 and O6H...O7). There are no H-bonds in the b-c plane (Sarkar and Perez 2015; (Fig. 2.1b)). Strong interactions between pyranose rings in adjacent chains do allow formation of stacked sheets, but due to the absence of H-bonds between chains in different planes, β -chitin can be easily hydrated unlike α -chitin. β -chitin is found in squid pens, spines of diatoms, tubes of giant tubeworms and possibly in the peritrophic matrix lining the midgut epithelial cells of insects. These linings lack the structural rigidity of cuticles and, in fact, are highly flexible and hydrated. The chitin in these structures is associated with a large number of glycoproteins with mucin domains, which increase their hydration and help forming hydrogels. γ -chitin is found in the cocoons of some beetles and consists of both β -chitin and α -chitin but its precise structure is not resolved to the same extent as the other two forms of chitin.

2.3 Higher Order Structures Involving Chitin Fibers in the Cuticle

Arthropod cuticles have, in addition to chitin, a wide assortment of proteins, quinones and minerals that contribute to and alter the physicochemical properties of the exoskeleton. The estimates of the size of the chitin molecules vary widely (from 5 to 700 kDa; ~20–3000 monomeric sugars) depending on the technique used for the preparation of chitin for these analyses (Kaya et al. 2014). The low molecular

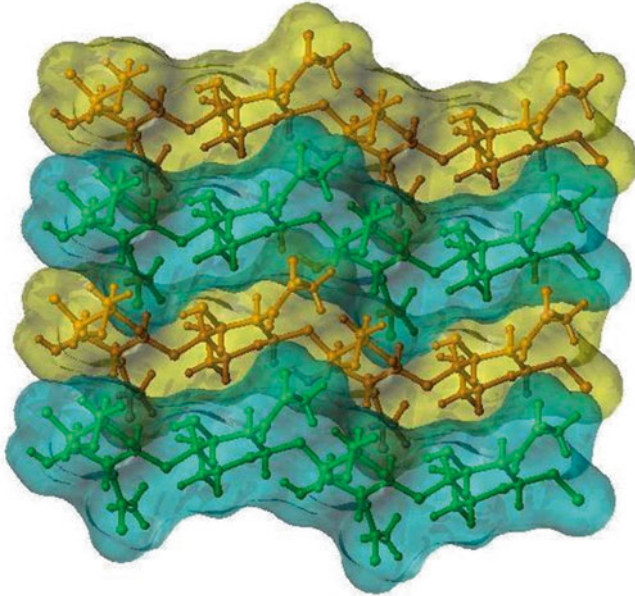


Fig. 2.1b Stacking of adjacent chains in β -chitin without involvement of hydrogen bonds (From Sarkar and Perez 2015)

weight chitins may represent degradation products occurring naturally due to the action of endogenous chitinolytic enzymes or artifacts of the isolation procedures, which require harsh conditions. It is often assumed that the average chitin nanofibers have 18–25 chitin chains that form a chitin core, which associate with various proteins to form chitin-protein composite fibers with an effective diameter of 50–250 nm and lengths of 300 nm (Fabritius et al. 2009). Since this size is significantly smaller than the width of an epidermal cell ($\sim 10 \mu\text{m}$), several chitin bundles must be attached end to end to cover the epidermal cell. These larger fibrils are arranged in parallel to form a sheet (or lamina) of chitin parallel to the apical surface of the underlying epidermal cells. Additional laminae consisting of chitin-protein complexes are added continuously to the growing cuticle from the assembly zone between the epidermis and the cuticle during intermolt periods. These laminae can be stacked on top of one another in two ways. In the first pattern, each successive layer of fibers is twisted with respect to the layers above and below by a constant angle of rotation of the lamina. This helicoidal pattern of arrangement of successive laminae is known to result in isotropic stress resistance. This helicoidal arrangement also known as Bouligand structure results in an optical illusion in oblique sections in which the chitin fibrils assume a parabolic shape corresponding to each 180° stack (Bouligand 1972). A second type of arrangement involves a “pseudo-orthogonal stack” with two stacks of multiple laminae arranged orthogonally with respect to each other with a transitional zone of helicoidal laminae between them (Fig. 2.2; Fabritius et al. 2009). This is similar to a “cross-ply” laminate used in

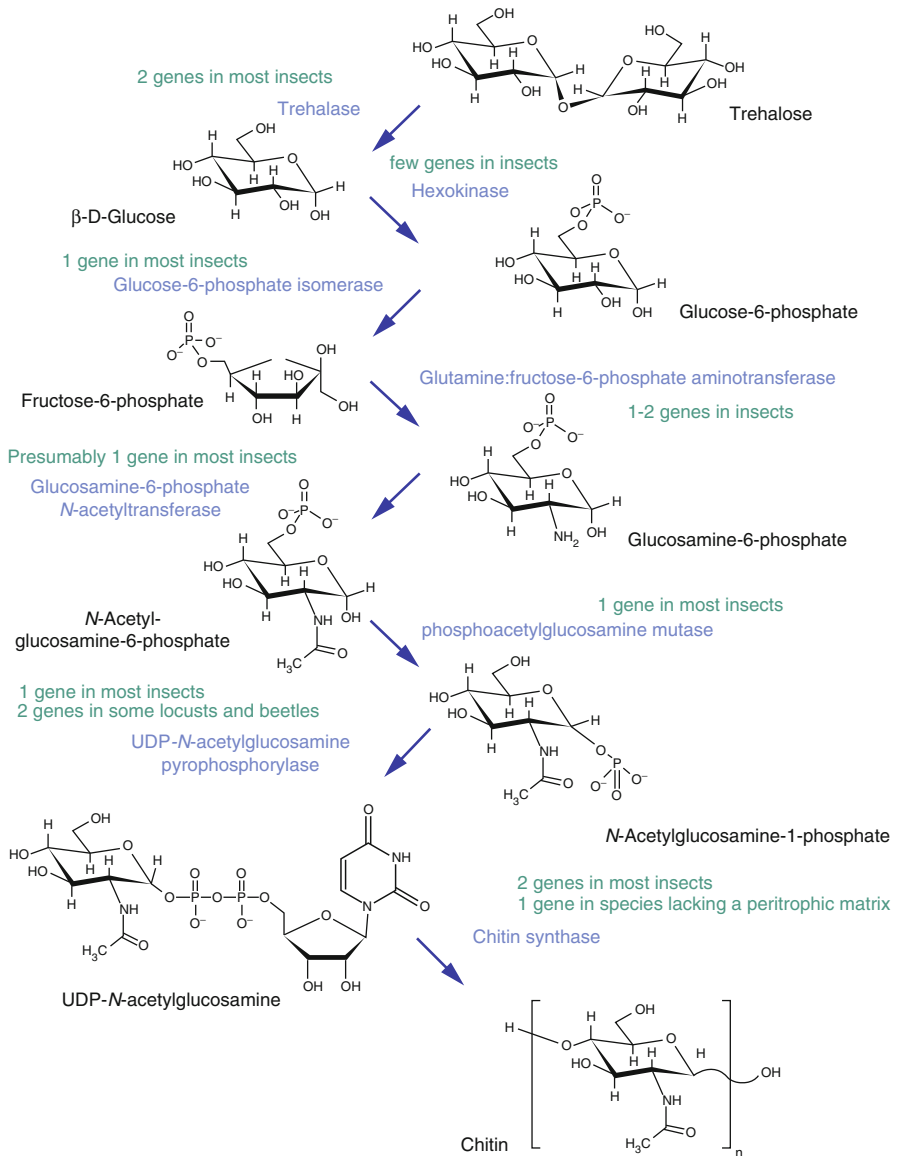


Fig. 2.2 Pathway of chitin biosynthesis in insects. Enzymes of the chitin biosynthesis pathway are depicted in *blue*, and gene numbers are given in *green* (Modified from Merzendorfer and Zimoch 2003)

constructions. In addition, the vertical stacks of laminae are further stabilized by pore canals that traverse the procuticle in a cork-screw-like arrangement. In the middle of these canals are pore canal fibers made of chitin (Fabritius et al. 2009). The composition of the outer boundary of the pore canals is unknown, but presumably is made up of proteins. Immunostaining using gold labeled secondary

antibodies indicate that the presence of cuticular proteins in these pore canals is distinct and often in unique locations (Mun et al. 2015).

2.4 Higher Order Structure in the Peritrophic Matrix

In contrast to the cuticle, the peritrophic matrix (PM)-associated chitin is well hydrated, flexible and can vary widely in thickness and number of layers (Hegedus et al. 2009; Merzendorfer et al. Chap. 8). The PM appears to emerge from the microvilli of the epithelial cells that line the midgut of several lepidopteran and coleopteran insects both in the larval and adult stages. Successive layers of PM (consisting of chitin and proteins associated with them) delaminate from the microvilli and form mesh-like tubules covering the luminal surface of the entire midgut epithelium. They do not form laminae as in the cuticle, but form loosely associated grid-like structures where the chitin-protein complexes criss-cross each other nearly orthogonally (Harper and Hopkins 1997; Harper et al. 1998). Additional proteinaceous material is added to the forming meshwork, which becomes thicker and has a reduced pore size. The structure of the PM and the nature of the proteins associated with it are discussed in more detail in the Chap. 8 by Merzendorfer and colleagues in this book.

2.5 Precursors of Chitin and Generation of Activated Substrates

While it is logical to assume that the supply of carbon for the chitin chains found in insect cuticle and PM would come ultimately from stored form of sugars such as glycogen and from the highly abundant disaccharide, trehalose, in circulating hemolymph (10–50 mM), direct proof for this is lacking for insects. However, several studies are consistent with this assumption. The enzyme trehalase that is needed to convert trehalose into glucose is widespread in species that contain chitin (Becker et al. 1996; Thompson 2002). Two isoforms have been identified in most insects, one of them a soluble form and the other a membrane-bound form that acts on the substrate found in the hemolymph. The glucose liberated by the action of trehalase is presumed to be taken up by cells for utilization in chitin synthesis. In a detailed study, the two genes encoding the beet armyworm, *Spodoptera exigua* trehalase proteins showed differences in tissue specificity of expression and were found to be highly expressed in cuticle-forming tissues and tracheae. Their transcript levels also showed developmental control with the highest levels reached during pupal stages when the rate of chitin synthesis is high (Tang et al. 2008; Chen et al. 2010). RNA interference studies using dsRNA for the trehalase resulted in molting defects and loss of chitin in the cuticle suggesting the importance of trehalose as a precursor for chitin (Chen et al. 2010).

The activated substrate for chitin biosynthesis by the membrane-bound enzyme, chitin synthase, is UDP-*N*-acetylglucosamine. Its formation requires the activity of several enzymes including trehalase, hexokinase, glucose-6-phosphate isomerase, glutamine-fructose-6-phosphate aminotransferase, glucosamine-6-phosphate *N*-acetyltransferase, phosphoglucosamine mutase and UDP-*N*-acetylglucosamine pyrophosphorylase (UAP) (Merzendorfer and Zimoch 2003; Cohen 2010; Muthukrishnan et al. 2012). These enzymes are shared by the glycolytic pathway and the pathway leading to the formation of aminosugars (Fig. 2.2). In particular, the enzyme, glutamine-fructose-6-phosphate aminotransferase (GFAT) is the first committed step in the formation of a common pathway for the biosynthesis of chitin and complex carbohydrates containing *N*-acetylglucosamine. RNAi of one of the two genes encoding this enzymes in the yellow fever mosquito, *Aedes aegypti* led to loss of chitin in the midgut and this was reversed by administration of glucosamine into the hemocoel (Kato et al. 2006). RNAi of this gene in the blood sucking cattle tick, *Haemaphysalis longicornis* resulted in less blood feeding, lower body weight gain and ultimately in death (Huang et al. 2007). GFAT is also sensitive to feedback inhibition by UDP-GlcNAc indicating the importance of this enzyme in regulating the flow of carbon into this pathway. The functional significance of the presence of two genes encoding GFAT has not been explored so far.

Another enzyme of the pathway leading to the formation of UDP-*N*-acetylglucosamine (UDPGlcNAc) has also been studied in some detail. This enzyme, named UDP-*N*-acetylglucosamine pyrophosphorylase (UAP) catalyzes the transfer of UMP moiety from UTP to *N*-acetylglucosamine to form UDPGlcNAc, the substrate for chitin synthase, and pyrophosphate, which is hydrolyzed to inorganic phosphate by the ubiquitous pyrophosphatase. The fruit fly, *Drosophila* UAP enzyme is encoded by a gene named *mummy/cystic/cabrio* and homozygous mutants of this gene show severe cuticular defects and tracheal deformities (Araujo et al. 2005; Schimmelpfeng et al. 2006; Tonning et al. 2006). RNAi of the *Uap* gene in the olive fruit fly, *Bactrocera dorsalis*, results in mortality and abnormal cuticular defects (Yang et al. 2015). There is only one copy of this gene encoding this enzyme in most insects with the exception of the red flour beetle, *Tribolium castaneum*, the migratory locust, *Locusta migratoria* and the Colorado potato beetle, *Leptinotarsa decemlineata* (Arakane et al. 2010; Liu et al. 2013; Li et al. 2015). Down-regulation of transcripts for either gene from *T. castaneum* results in lethality. However, the phenotypes were quite different. Only *TcUap1* appeared to be essential for chitin formation in both the epidermal cuticle and gut. *TcUap2* RNAi resulted in developmental arrest and shrinkage and pupal paralysis without affecting chitin content of either the cuticle or the PM (Arakane et al. 2010). It is likely that *Tribolium* UAP2 may be affecting glycosylation (addition of *N*-acetylglucosamine) of some glycoproteins or some other metabolites. RNAi of *L. migratoria* *Uap* resulted in molting defects but no phenotype was seen after RNAi for *Uap2* from this insect (Liu et al. 2013). RNAi of *L. decemlineata* *Uap1* gene reduced chitin content of integument and tracheal taenidia and affected molting. RNAi of *Uap2* gene from this insect adversely affected peritrophic matrix integrity and larval growth and led to fat body depletion (Shi et al. 2016). Thus, the role of the *Uap2* gene varies in different

insects. The presence of a single *Uap* gene in many other insects indicates that a single UAP protein contributes UDPGlcNAc needed for both chitin synthesis and glycosylation involving addition of *N*-acetylglucosamine, with *T. castaneum*, *L. migratoria* and *L. decemlineata* being exceptions in which the duplicated *Uap* genes have assumed specialized functions. It is noteworthy that the two human UAP enzymes can accept glucosamine-1-phosphate and galactosamine-1-phosphate as co-substrates, though with different kinetic constants (Peneff et al. 2001).

The pathway leading to chitin from trehalose is shown in Fig. 2.2. In the final step, the membrane-bound chitin synthase (CHS) utilizes cytosolic UDP-GlcNAc to synthesize and extrude the product chitin chains across the lipid bilayer to the extracellular matrix side. The number of genes encoding CHS in most insect species genomes is two (Tellam et al. 2000; Ibrahim et al. 2000; Gagou et al. 2002; Zhu et al. 2002; Arakane et al. 2004; Hogenkamp et al. 2005). However, several hemipteran insects that do not elaborate a PM appear to harbor only one *Chs* gene. Examples are the brown planthopper, *Nilaparvata lugens*, the soybean aphid, *Aphis glycines*, the pea aphid, *Acyrtosiphon pisum* and the kissing bug, *Rhodnius prolixus* (Wang et al. 2012; Bansal et al. 2012; Mansur et al. 2014). This is similar to the situation in nematodes, with some nematode genomes having only one *Chs* gene, whereas others have two *Chs* genes (Harris et al. 2000; Harris and Fuhrman 2002). Once again, when there is more than one *Chs* gene, there is specialization in the functions and/or tissue specificity of expression. For example, one *Chs* gene in the nematode, *Caenorhabditis elegans* is responsible for producing chitin in the pharynx, whereas the other one is involved in production of chitin in the eggshell (Veronico et al. 2001; Zhang et al. 2005).

CHS-A protein (encoded by *Chs-1* gene) is expressed in epidermal cells of insects, tracheal lining cells and embryonic serosal cells that specialize in the synthesis of cuticular chitin, whereas CHS-B protein (encoded by *Chs-2* gene) specializes in the synthesis of PM-associated chitin (Arakane et al. 2004, 2005, 2008; Bolognesi et al. 2005; Hogenkamp et al. 2005; Zimoch et al. 2005; Chen et al. 2007; Kumar et al. 2008; Rezende et al. 2008; Jacobs et al. 2015; Chaudhari et al. 2015). Membrane preparations from larval integuments or guts do exhibit chitin synthase activity that is sensitive to inhibitors of chitin synthases (Cohen and Casida 1980a, b). Maue et al. (2009) showed that this enzyme forms an oligomeric complex and there is indication that the enzyme may require proteolytic activation for gaining full activity (Broehan et al. 2007).

While the two enzymes share extensive amino acid sequence and structural similarities and have all the conserved motifs of the glycosyltransferase II family enzymes, they differ in some significant ways. The most interesting difference is the presence of alternate exons in *Chs-1* gene while they are absent in *Chs-2* genes. Depending upon the insect species, there are two sets of alternate exons in *Chs-1* gene, one near the 5' end and one close to the 3'-end. The set of two alternate exons that occurs near the 3'-end of the *Chs-1* gene encodes a 59 amino acids-long region that includes the penultimate transmembrane helix in CHS-A protein. Each of these alternate exons is of the exact same length (177 nucleotides long). The two 59 amino acids-long segments encoded by the two alternate exons of the same species have

significant sequence similarity/identity to each other. But phylogenetic analysis of this region alone from multiple insects belonging to different orders indicates that alternate exon “a”-encoded regions from all insect species are more closely related to one another than to the “b” form encoded by the second alternate exon-encoded region from the same species (Arakane et al. 2004; Ashfaq et al. 2007; Wang et al. 2012; Yang et al. 2013). Thus, the utilization of alternate exons must have occurred long before the branching of the insect orders. Furthermore, there must be an evolutionary pressure to conserve this variation in different orders of insects. Of particular interest is the finding that the relative abundances of the two alternative transcripts are developmentally controlled at least in *T. castaneum*, *Manduca sexta*, and the oriental fruit fly, *Bactrocera dorsalis* (Arakane et al. 2004; Hogenkamp et al. 2005; Zimoch et al. 2005; Zhang et al. 2010; Yang et al. 2013). The relative abundance of the transcript with the exon “a” or “b” changes during developmental stages, with the “b” exon becoming prominent in the pupal stage. In addition, the transcripts with the “b” exon seem to be enriched in tracheae of *M. sexta* and *B. dorsalis* during late pupal stages. There are two notable exceptions to this rule. The water flea, *Daphnia pulex* and the aphid, *A. pisum*, seem to have only the “b” form of this alternate exon (Wang et al. 2012). It has been suggested that the “a” form was lost in species that had no need to make a PM (Wang et al. 2012).

The fruit fly, *Drosophila melanogaster*, embryos with homozygous mutations of the *Chs-1* gene (also known as *kkv*), have a blimp phenotype and the embryos are unable to break open the egg shell (Ostrowski et al. 2002; Moussian et al. 2005a). RNA interference studies in several holometabolous insects have established that the two *Chs* genes have specialized functions. Down-regulation of transcripts for *T. castaneum Chs-1* gene results in reduction in cuticular chitin, failure to molt, mortality and failure of eggs to hatch without affecting PM-associated chitin. On the other hand, RNAi of *Chs-2* gene resulted in loss of PM-associated chitin, growth retardation, and loss of PM integrity (Arakane et al. 2005; Agrawal et al. 2014; Kelkenberg et al. 2015). RNAi at the adult stage resulted in fat body depletion and mortality and loss of chitin in the PM. Similarly, RNAi of *Chs-2* gene from *A. aegypti* led to failure to form a PM after having had a blood meal (Kato et al. 2006). Feeding of *Anopheles gambiae* with dsRNA for *Chs-1* or *Chs-2* genes along with chitosan to promote uptake of dsRNA also led to greater sensitivity to chitin inhibitors and calcofluor (Zhang et al. 2010). Tian et al. (2009) also reported that *S. exigua* larvae fed a diet containing *Escherichia coli* expressing dsRNA for *SeChs-1* gene had reduced survival rate. Mansur et al. (2014) demonstrated that injection of dsRNA for the single *Chs* gene in *R. prolixus* led to severe deformations of the cuticle. In female adults, RNAi of this *Chs* gene affected oogenesis, reduction in ovary size and a significant increase in degenerated oocytes indicating a novel role for CHS in ovary and egg development. Using the same system, Souza-Ferreira et al. (2014) also reported eclosion defects and alterations in the cuticle morphology.

DsRNAs specific for splice variants of *Chs-1* gene have also been performed. In several insects, dsRNA's for either of the two alternatively spliced transcripts resulted in molting failure and death (Arakane et al. 2005; Wang et al. 2012; Yang

et al. 2013). However, the phenotypes and timing of developmental arrest were not identical suggesting that the protein products of this *Chs* gene derived from alternatively spliced mRNAs may have distinctly different functions and/or different tissue specificity. One attractive possibility is that one of these isozymes is uniquely required for tracheal cuticle development and that it cannot be substituted by the other isozyme (Hogekamp et al. 2005; Yang et al. 2013).

Alternative splicing of an upstream exon of *Chs-1* has been described in some lepidopteran species, including the Asian corn borer, *Ostrinia furnacalis*, the silk worm, *Bombyx mori* and *M. sexta*. In well-studied *Chs-1* gene of *O. furnacalis*, there are two promoters that give rise to two proteins with different *N*-terminal sequences (Qu and Yang 2011, 2012). The shorter of the two transcripts uses a promoter located in the 2nd intron of the larger transcript and codes for a protein that is nine amino acids shorter. From the third exon, the sequences of the transcripts and the encoded proteins are identical. The promoter regions of the two transcripts differ in the presence of binding sites for the ecdysone receptor or the down-stream transcription factors elements, BR-C or FTZ, of the ecdysone-signaling pathway, suggesting differences in the control of their expression by molting hormone. Consistent with this possibility, the relative abundances of the two transcripts also differed at different developmental times, most notably during the pupal period and in different tissues. 20-hydroxyecdysone (20E)-treatment of early fifth instar larvae resulted in an earlier increase in transcripts with exon 2b and 19b indicating that the two promoters respond differently to this hormone (Qu and Yang 2012). Down-regulation of each of these two transcripts using splice isoform-specific dsRNAs resulted in molting abnormalities in a significant number of individuals, with the RNAi of the longer transcript being more likely to produce severe molting defects (Qu and Yang 2011).

More recently, alternative splicing of transcripts for a gene encoding the CHS-B protein from the corn earworm, *Helicoverpa zea* has been reported (Shirk et al. 2015). One of the two alternative spliced transcripts is predicted to result in a truncated protein and to be devoid of chitin synthase activity. The functional significance of this observation and whether similar splicing of *Chs-2* transcripts occurs in other insects remains to be explored.

2.6 Towards the Mode of Action of Insect Chitin Synthases

Chitin synthase is a member of the glycosyltransferase-2 (GT-2) class of enzymes that includes cellulose synthase and hyaluronan synthase. Insect CHS enzymes have 15–16 membrane-spanning helices in a characteristic arrangement of three sets of transmembrane helices (TMH) with 8–9 helices in the *N*-terminal domain followed by the catalytic domain in the cytosolic side, immediately followed by a second 5-TMH-domain presumed to translocate the nascent polysaccharide, and a *C*-terminal domain with two TMHs in the central catalytic domain. There are several conserved motifs characteristic of all chitin synthases as well as cellulose

synthases and hyaluronan synthases. These motifs include the CHS signature sequence motifs, EDR, QRRRW, and WGTRE (Zhu et al. 2002; Moussian et al. 2005a, b; Merzendorfer 2006) (Fig. 2.3a). Of these, the EDR and QRRRW motifs are close to the active site and are implicated in catalysis and/or binding of substrates based on mutagenic studies with yeast chitin synthases.

Even though there are no crystal structures of GT-2 enzymes from insects, crystal structure of a bacterial cellulose synthase is available. Based on this structure, a model for a chitooligosaccharide synthase encoded by the bacterial *NodC* gene has been proposed (Dorfmueller et al. 2014). These studies have led to the conclusion that the NodC protein has three membrane spanning regions that traverse the lipid bilayer in the following order: outside \rightarrow inside, inside \rightarrow outside and the last one outside \rightarrow inside with the catalytic domain inside the cytosol where it will have access to UDP-GlcNAC (Dorfmueller et al. 2014). This proposed model is consistent with the role of the conserved aspartate in the [EDR] motif acting as the base in the nucleophilic attack of the 4-OH group of the acceptor sugar. It also explains the role of the [Q(Q/R)XRW] motif as part of an α -helix that lines the active site where the W residue can stack on the GlcNac residue at subsite +2 and the R residue interacts with the negatively charged diphosphate of UDP-GlcNac (Dorfmueller et al. 2014). We have modeled an insect chitin synthase based on the crystal structures of eight GT-2 enzymes including these two bacterial structures for cellulose synthase and NodC (Fig. 2.3b). The notable difference between the NodC structure and that of the cellulose synthase and insect chitin synthase is the presence of a long tunnel at the active site, which can accommodate several sugars of the elongating chains of cellulose and chitin, whereas the NodC enzyme has a closed pocket that can accommodate only a chain with 5 sugars. The homology model further predicts a central, narrow channel formed by 6 TMH. Interestingly, one helix of the 5-TMS cluster, which was originally predicted to traverse the membrane, is not membrane-integral but is attached to the cytosolic side of the membrane (Fig. 2.3b). This helix is bent and seems to control the entry of the chitin-conducting channel. Mutations in the *Chs-1* gene of the spider mite associated with resistance for the chitin synthesis inhibitor, etoxazole, was found to locate in this helix in a bulk-segregant analysis (van Leeuwen et al. 2012; Demaeght et al. 2012).

Dorfmueller et al. (2014) proposed a reaction mechanism in which during the first synthetic step both the +1 and -1 sugars rotate, but during elongation, the sugar at +1 position rotates only once during two sugar additions as shown in Fig. 2.3. This proposal solves a vexing problem of generating β -1-4 linked sugar polymers where alternating sugars are turned 180° with respect to one another, while utilizing a α -UDP-*N*-acetylglucosamine sugar as the substrate (Fig. 2.4).

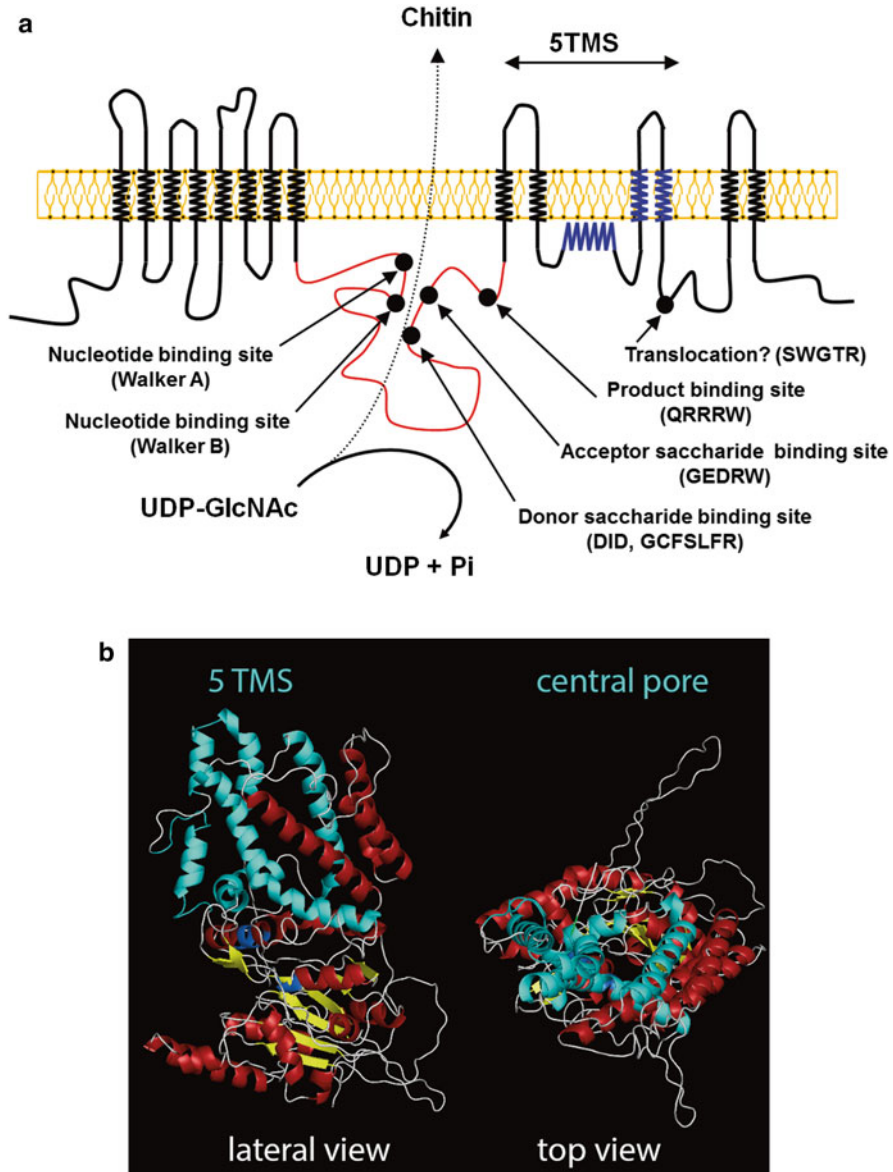


Fig. 2.3 Structural models of the tripartite domain organization of the insect CHS. **(a)** Topology of transmembrane helices (TMHs) and soluble domains. The *N*-terminal *domain A* of *Drosophila* CHS-1 contains 8 TMHs, but this number may vary, from 7 to 10 in other insects. The central *domain B*, forms the catalytic site facing the cytoplasm. *Domain C* was predicted to contain 5+2 conserved TMHs. However, homology modeling revealed that one helix does not span the membrane but is attached to the cytosolic side of the plasma membrane, resulting in an intracellular orientation of the *C*-terminus. Putative motifs involved in nucleotide, donor, acceptor, and product binding are indicated. **(b)** Partial 3D structure predictions for CHS-2 from *M. sexta* generated by PHYRE2–Homology modeling was performed using the crystal structures of eight GT2 enzymes as templates. (Left) lateral view, (right) top view. Yellow, β -strands; red, α -helices; cyan, highly conserved α -helices of the 5 TMS cluster; blue, catalytic site motifs (Structure predictions and models were made by S. Gohlke and H. Merzendorfer)

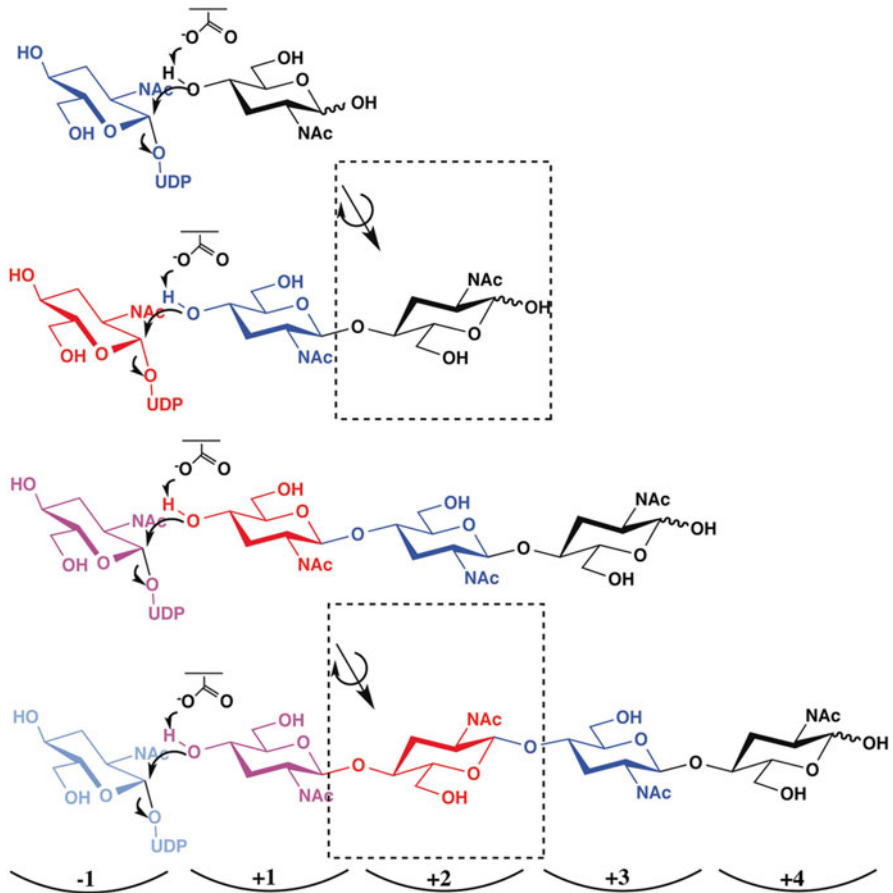


Fig. 2.4 Proposed reaction mechanism of chitin synthesis. Chemical drawing of the proposed reaction mechanism for NodC and chitin synthesis. The 1-hydroxyl group of the donor substrate UDP-GlcNAc is transferred onto the non-reducing end of the growing acceptor oligosaccharide. When the transfer reaction is completed, UDP leaves the active site. In the first synthesis step, the two terminal sugars (-1 and +1) of the growing chain would both rotate while moving into the next binding site (+1 and +2). During further elongation, the +1 sugar would only rotate every second synthesis step (*red sugar* compared with *blue sugar*). All sugars moving into the +3/+4 subsites would remain of a fixed orientation. This rotation and translocation enables the newly added non-reducing sugar to be in the same acceptor position as the previous one (From Dorfmueller et al. 2014)

2.7 Regulation of Chitin Synthesis

During every intermolt period, insects develop a multi-laminate cuticle which seems to arise from the tips of microvilli that are enriched for electron-dense “plasma membrane plaques” (Locke and Huie; 1979; Locke 2001). Presumably, these are the sources of cuticular material including cuticular proteins and chitin synthase, which synthesize and secrete chitin into the procuticle. The procuticle of

several lepidopteran and coleopteran insects is very thin in the early stage of the last instar and keeps growing to a thickness of several hundred laminae, almost until the first appearance of ecdysial droplets. However, this is the period of low ecdysone titers making it unlikely that ecdysone response elements in promoter regions of *Chs* genes regulate chitin synthesis directly (Gagou et al. 2002).

In *O. furnacalis*, the core promoter of *OfChsB* contains the binding sites of only early ecdysone-inducible elements (BR-C and E74A), but not ecdysone-response elements (EcR and USP) (Qu and Yang 2011). The consensus sequences for BR-C and E74A were also predicted to be within the promoter region of *DmeChsB* (Gagou et al. 2002). The presence of ecdysone-inducible instead of ecdysone-response elements indicates that *Chs-B* might be in an ecdysone-dependent regulatory pathway and not directly stimulated by ecdysone. On the contrary, both of the alternative promoter regions of *OfChs-A*, contain the ecdysone-response element EcR, suggesting that *OfChs-A* could be regulated by ecdysone directly (Qu and Yang 2011; Qu and Yang 2012).

2.8 Chitin Deacetylation and Possible Role in Cuticle Assembly

The role of chitin deacetylation is still shrouded in mystery. Naturally occurring chitin is partially deacetylated as revealed by Fourier transform infrared spectroscopy, chemical analysis and analysis of enzymatic digestion products by thin layer chromatography. Depending on the source of chitin, the degree of deacetylation can vary ranging from 5 to 25 %. These estimates are further complicated by the effects of the harsh extraction methods utilized for obtaining chitin free of protein and other cuticular components including lipids and quinone derivatives. But it is clear that deacetylation is vital to proper function of cuticles, which diverge widely in their physicochemical properties. Interfering with deacetylation by RNAi results in abnormal tracheal tubes, cuticle and joint defects, and molting failure and mortality. Since no enzyme is known to synthesize chitosan directly from precursors, chitosan can only arise by chemical or enzymatic deacetylation of preformed chitin. Chitin deacetylation may be coupled with chitin synthesis in the assembly zone of the procuticle because chitin deacetylase (CDA) in the epidermal cuticle is confined to the assembly zone (Arakane, unpublished data). Even the distribution of chitosan in different layers of procuticle has not been studied yet.

2.9 Chitin Deacetylases in Insects

CDAs are metalloproteins belonging to the class of carbohydrate esterase family 4 (CE4) (EC 3.5.1.41) that remove the acetyl group from chitin. They are present in all species that have chitin including fungi, nematodes, and arthropods including

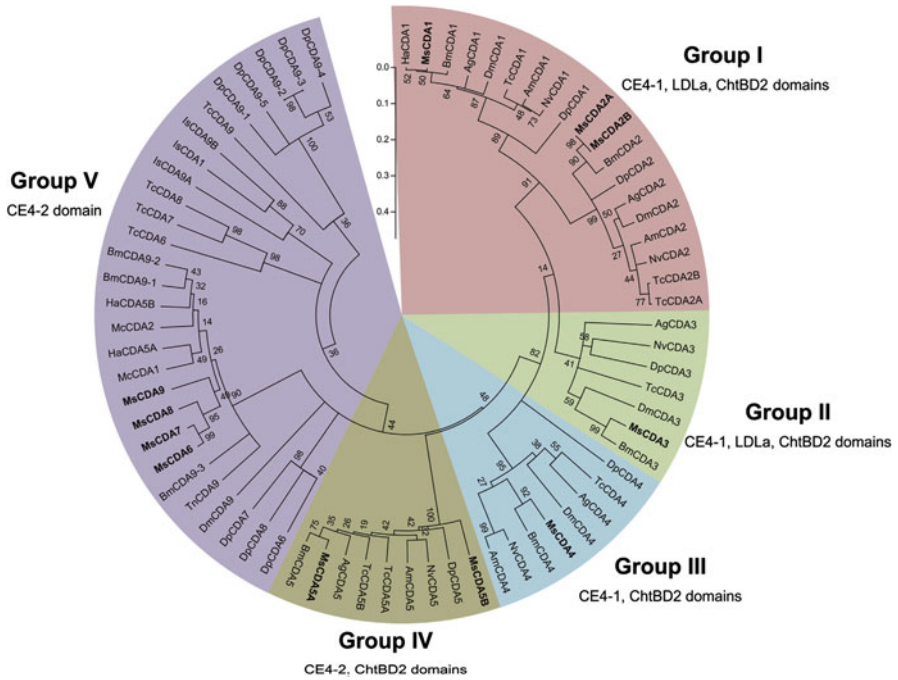


Fig. 2.5 Phylogenetic analysis of chitin deacetylases (CDA) from 12 different species: *Anopheles gambiae* (Ag), *Apis mellifera* (Am), *Bombyx mori* (Bm), *Daphnia pulex* (Dp), *Drosophila melanogaster* (Dm), *Helicoverpa armigera* (Ha), *Ixodes scapularis* (Ix), *Mamestra configurata* (Mc), *Manduca sexta* (Ms), *Nasonia vitripennis* (Nv), *Tribolium castaneum* (Tc) and *Trichoplusia ni* (Tn). A bootstrap analysis of 2000 replications was carried out on the trees inferred from the neighbor joining method and bootstrap values are shown at each branch of the tree. CDAs are divided into five different groups: group I (pink), group II (green), group III (light blue), group IV (brown) or group V (dark purple) as described in Dixit et al. (2008) (Reproduced with permission from Tetreau et al. (2015b))

insects. In insects, these proteins are encoded by a family of genes that number from 4 to 9 (Dixit et al. 2008; Campbell et al. 2008; Xi et al. 2014; Tetreau et al. 2015b). Phylogenetically, insect CDAs fall into five groups with distinct domain organizations (Fig. 2.5). While all groups have the CE-4 domain at the C-terminal part, groups I and II have two additional domains, a low density lipoprotein receptor-a (LDLa) domain and a chitin binding domain (CBD) at the N-terminal part. The group III and IV CDAs lack the LDLa domain but retain the CBD domain (see Muthukrishnan et al. 2012 for a more complete description of the five phylogenetic groups). The purpose of the additional domains besides the catalytic domain (CE4) is not established, but the conservation of representatives of all five groups in most insects (some hemipterans and anapleurans lack group II and group V CDAs) suggests that these CDAs are essential for insect survival.

Evidence for the requirement of distinct CDAs belonging to different groups comes from studies of *D. melanogaster* Cda mutants, RNAi studies in *T. castaneum*

and *N. lugens*, and studies on the suppression of specific *Cda* transcripts following baculovirus infection of *H. armigera* (Jakubowska et al. 2010). Homozygous null alleles of two group I *Cda* genes from *D. melanogaster* (*serpentine* and *vermiform*) exhibit convoluted, elongated, and wider dorsal tracheal trunks during embryonic development indicating a role for these proteins in regulating tracheal tube dimensions and rigidity. The embryos had a bloated phenotype reminiscent of *Chs* mutants indicating loss of rigidity of the cuticle as well (Luschnig et al. 2006; Wang et al. 2006). A detailed RNAi study of all 9 *Cda* genes from *T. castaneum* was carried out by Arakane et al. (2009). These studies have revealed distinct and specific functions of several CDAs and, in some cases, specific splice isoforms. Group I CDAs (TcCDA1 and TcCDA2) were both critical for molting and survival during development (but not in adult life) indicating that they performed non-redundant, but essential functions, even though both were expressed in the same tissues. The two splice isoforms of CDA2 appeared to regulate different cuticles. RNAi of *Cda2a* isoform affected movement of femoral-tibial joints and led to failure of egg hatch. On the other hand, RNAi of CDA2b did not affect these functions but led to wrinkled elytral surface. It is likely that there are differences in expression (and requirement) for specific CDAs and their isoforms in different regions of the insect anatomy. RNAi of group I CDAs does lead to reduction in chitin content and loss of laminar organization (our unpublished data).

RNAi of the CDAs belonging to the other four groups in *T. castaneum* failed to produce any visible effects and, therefore, no conclusions regarding their function could be drawn, except some speculations based on the tissue specificity and developmental patterns of expression. However, RNAi studies using a dsRNA for a group IV CDA in *N. lugens* did result in molting failure (Xi et al. 2014). The finding that several hemimetabolous insects and even mosquitoes do not have group V CDAs and the failure to see RNAi effects for this group of CDAs in insects that are expressed predominantly in the gut tissue is intriguing. This finding suggests that the group V CDA may be involved in digestion of chitinous material in the diet or some immune function rather than modification of endogenous chitin. It is interesting to note that there is wide variation in the number of proteins belonging to this group.

CDAs are proteins with leader peptides and are without membrane-spanning or obvious membrane-anchoring segments. Therefore, they are expected to be secreted from the cells in which they are made. This is consistent with their location in the lumen of tracheal tubes and in the procuticle (Luschnig et al. 2006; Wang et al. 2006; Arakane et al. 2009). However, a second tissue, namely the fat body has been shown to be a source of this protein as well (Dong et al. 2014). All CDAs except group V members have CBD or LDLa domains that have several cysteines presumably involved in the formation of disulfide bonds that stabilize the three dimensional structures of these proteins. They are thought to partially deacetylate chitin consistent with a degree of deacetylation of ~20% observed in naturally occurring chitin. Toprak et al. (2008) reported that an *M. configurata* CDA expressed in *E. coli* could deacetylate colloidal chitin using an *in gel* assay that detects formation of chitosan. Zhong et al. (2014) expressed a *B. mori* CDA in yeast and claimed

it has deacetylase activity using an assay involving conversion of p-nitroacetanilide to p-nitroaniline. Whether or not this enzyme can deacetylate native chitin remains to be proven. Three CDAs belonging to family 1, 2 and 4 were found in the molting fluid of *B. mori* (Qu et al. 2014). The recombinant products of these CDAs were catalytically inactive when assayed with the formaldehyde-fluorescamine method (Blair et al. 2005). Other attempts to demonstrate deacetylation of chitin using ^3H -chitin, colloidal chitin in gel assays, or with chitooligosaccharides as substrates using purified CDAs, expressed in a baculovirus expression system, have failed as well (Guo et al. 2005; Jakubowska et al. 2010; Arakane, Dittmer and Muthukrishnan unpublished). However, Jakubowska et al. (2010) reported increased permeability of PM incubated *in vitro* with the CDA preparation from *H. armigera*. They also reported suppression of transcripts coding for a specific CDA after baculovirus infection, which suggests a biological function for this protein. Since chitosan is present in cuticle and there is no pathway for direct synthesis of this polymer except via deacetylation of chitin, we suspect that CDA may be active only on nascent chitin and that it may require assistance from other proteins in this process.

2.10 Chitin Degradation

The pathway of chitin degradation is almost as complex as the biosynthetic pathway, because the native substrate is crystalline chitin in association with a large assortment of proteins in the cuticle, which is often sclerotized. In the gut, chitin is in association with an assortment of chitin-binding peritrophic matrix proteins, of which many have mucin-like linker domains (Tellam 1996; Wang et al. 2004; Campbell et al. 2008; Dinglasan et al. 2009; Hegedus et al. 2009; Merzendorfer et al. Chap. 8). Very little is known about the reactions that strip away the matrix-associated proteins to expose the chitin nanofibrils to chitinases. In the gut and in the molting fluid, there is a large assortment of proteases, which assists in this process. The process of matrix-associated chitin degradation must be regulated, because transcripts for the major chitinase are not detectable in the integument tissue until after cessation of the feeding period in each larval instar, and appears only just prior to pupation (Kramer et al. 1993). In addition, the transcripts encoding chitinases essentially disappear after a very short period of a day or two in the molt cycle. Likewise, transcripts for some chymotrypsin-like enzymes implicated in molting also exhibit developmental control (Broehan et al. 2008, 2010).

Just prior to molting and apolysis, dramatic changes occur at the interface between the old cuticle and the underlying epidermal cell layer. The inner unsclerotized part of the old procuticle begins to get degraded as a result of the accumulation of hydrolytic enzymes in the molting fluid, which appears in the space between the epidermal cell and the overlying cuticle. The apical plasma membrane-associated microvilli enriched in electron-dense “plasma membrane plaques” begin to degrade and disappear presumably due to endocytosis (Locke and Huie; 1979). This is followed by the appearance of new microvilli associated with epidermal

cells, which are initially devoid of these plaques but become electron-dense soon after. These authors also noted that the peak of 20E coincided precisely with the timing of disappearance of the plaques and the onset of apolysis. It is likely that ecdysteroids control the expression of genes encoding several proteins in the molting fluid either directly or indirectly. Injection of 20E into last instar *B. mori* and *M. sexta* larval abdomens isolated from the source of prothoracic hormones by a ligation results in premature appearance of chitinase activity in several insect systems (Kimura 1976; Fukamizo and Kramer 1987; Koga et al. 1992). This induction is at the level of transcription, as shown by the increase in transcripts for chitinase in the same ligated abdominal system described above (Kramer et al. 1993; Zheng et al. 2003). Similarly, Royer et al. (2002) reported that transcript levels for a larger chitinase (a class II chitinase) increased within 2–4 h after injection of 20E. This induction was unaffected in the presence of the protein synthesis inhibitor cycloheximide indicating that the effect of 20E was directly at the level of transcription and did not require continued protein synthesis. However, analysis of promoter regions of individual chitinase genes has not identified the presence of ecdysteroid responsive elements. No studies on the binding of 20E-inducible transcription factors to promoter regions of chitinase genes have been reported.

2.10.1 Chitinases Are Encoded by a Very Large Family of Genes

The initial report of the isolation and characterization of a molting fluid-associated chitinase, cloning of a full length cDNA encoding this protein and characterization of the corresponding gene by sequencing along with Southern blot analysis with probes from the chitinase cDNA, gave rise to the false impression that a single chitinase gene was responsible for the appearance of chitinolytic activity in the molting fluid and gut (Kramer et al. 1993; Choi et al. 1997; Koga et al. 1997). As whole insect genome sequences became available and functional analyses of individual chitinases were increasingly conducted, it became clear that insect chitinases belong to a large family of enzymes with different domain organizations, expression profiles, tissue specificity and function. The number of genes in insect genomes encoding chitinases or related proteins ranges from a low of seven to as many as 22 (or more) chitinases (Zhu et al. 2004, 2008a; Nakabachi et al. 2010; Zhang et al. 2011; Pan et al. 2012; Merzendorfer 2013). They have been grouped into ever increasing number of subgroups based on a combination of domain organization and/or tissue specificity of expression and phylogenetic analyses as well as functional analyses (Zhu et al. 2008c; Nakabachi et al. 2010; Zhang et al. 2011; Tetreau et al. 2015a) (Fig. 2.6).

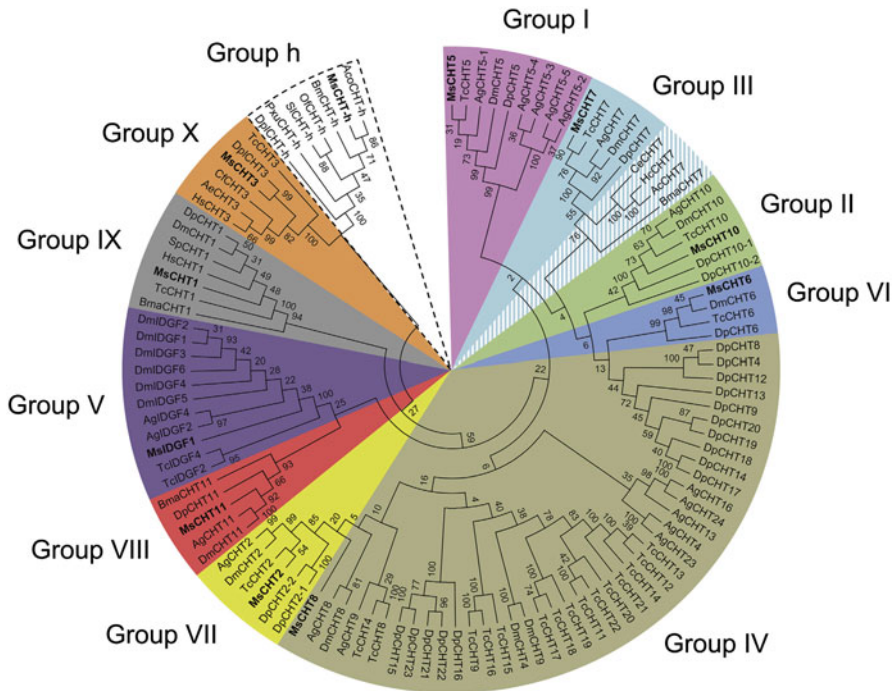


Fig. 2.6 Phylogenetic analyses of insect chitinase-like proteins: *Ancylostoma ceylanicum* (*Ac*), *Agrius convolvuli* (*Aco*), *Anopheles gambiae* (*Ag*), *Bombyx mori* (*Bm*), *Brugia malayi* (*Bma*), *Caenorhabditis elegans* (*Ce*), *Camponotus floridanus* (*Cf*), *Danaus plexippus* (*Dpl*), *Daphnia pulex* (*Dp*), *Drosophila melanogaster* (*Dm*), *Haemonchus contortus* (*Hc*), *Harpegnathos saltator* (*Hs*), *Manduca sexta* (*Ms*), *Ostrinia furnacalis* (*Of*), *Papilio xuthus* (*Pxu*), *Plutella xylostella* (*Px*), *Spodoptera litura* (*Sl*), *Strongylocentrotus purpuratus* (*Sp*) and *Tribolium castaneum* (*Tc*). A bootstrap analysis of 2000 replications was carried out on the trees inferred from the maximum likelihood method and bootstrap values are shown at each branch of the tree. CHTs are grouped into 10 different groups: group I (light purple), group II (green), group III (light blue), group IV (brown), group V (dark purple), group VI (dark blue), group VII (yellow), group VIII (red), group IX (gray), group X (orange) or group h (white and dotted lines). As CHT7 chitinases from Nematoda (*A. ceylanicum*, *B. malayi*, *C. elegans* and *H. contortus*) have a divergent domain organization from other group III chitinases they are highlighted by a hatched light blue area. CHT from *M. sexta* are indicated in bold (Figure reprinted with permission from Tetreau et al. (2015a))

2.10.2 Domain Organization and Structure of Chitinases

The individual chitinases differ in the number and assortment of catalytic domains, chitin-binding domains, serine-threonine-rich linker or mucin domains and polycystic kidney disease domains (PKD). It is clear that while there are at least seven groups of chitinases with one member in each group in all insects (the body louse, *Pediculus humanis corporis* with seven chitinases represents the minimal set), expansion of groups and duplications within groups has occurred to raise this number to ten at present (Fig. 2.7).

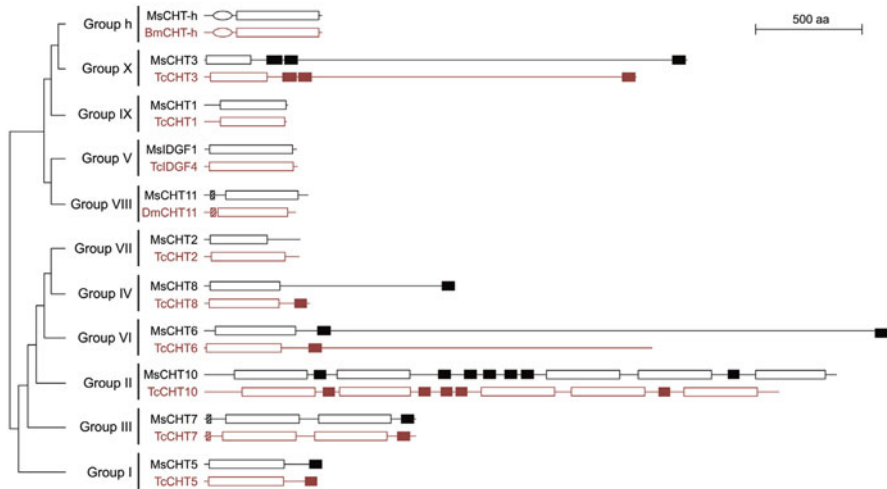


Fig. 2.7 Domain organization of chitinases (CHT) and chitinase-like (IDGF) proteins in insects. For each *M. sexta* CHT from each group, one ortholog from *T. castaneum* (groups I, II, III, IV, V, VI, VII, IX, and X), *B. mori* (group h) or *D. melanogaster* (group VIII) is represented. These orthologs are representative of the typical domain organization for each group. The domain organization was generated with the SMART tool (<http://smart.embl-heidelberg.de/>) by using the protein sequences. *M. sexta* proteins are represented in black, while proteins from other species are in red. Catalytic GH18 domains (white boxes), chitin-binding CBM14 domains (dark and red boxes), transmembrane spans (hatched boxes), polycystic kidney disease 1 (PKD1) domain (ovals), and linker regions (lines) are indicated (Figure reprinted with permission from Tetreau et al. (2015a))

The domain organization and conserved motifs of insect chitinases have been reviewed recently (Arakane and Muthukrishnan 2010; Merzendorfer 2013). The simplest and smallest chitinases have just the glycosylhydrolase 18 (GH18) domain (with a signal peptide coding region), while the largest chitinases have 5 GH18 domains, and 5–7 CBDs. Full-length cDNA clones for representative chitinases from several of these groups have been obtained (Kramer et al. 1993; Abdel-Banat et al. (2001); Royer et al. 2002; Zhu et al. 2008a; Wu et al. 2013). In some cases, they were expressed in baculovirus-insect cells or yeast expression systems and shown to have chitinolytic activities (Gopalakrishnan et al. 1995; Arakane et al. 2003; Wu et al. 2013; Zhu et al. 2008b). They differ in their pH optima, kinetic constants for chitin versus chitoooligosaccharide substrates and affinity for chitin beads. Vast majority of them have the signature motif 2 (FDGLDLDWEYP or variations thereof) that has been implicated in catalysis (Watanabe et al. 1993; Lu et al. 2002; Arakane and Muthukrishnan 2010). Notable exceptions are chitinases belonging to group V (also known as imaginal disc growth factors, or IDGF's that lack catalytic activity; Kawamura et al. 1999; Kanost et al. 1994) and have additional insertion loops (Zhu et al. 2008b). In particular, the proton donor, glutamate (E residue) that is critical for catalysis in the conserved region 2 found in all family 18 chitinases (Watanabe et al. 1993; Lu et al. 2002) is replaced with an asparagine or a glutamine residue. Unlike the plant derived family 19 chitinases with an inverting

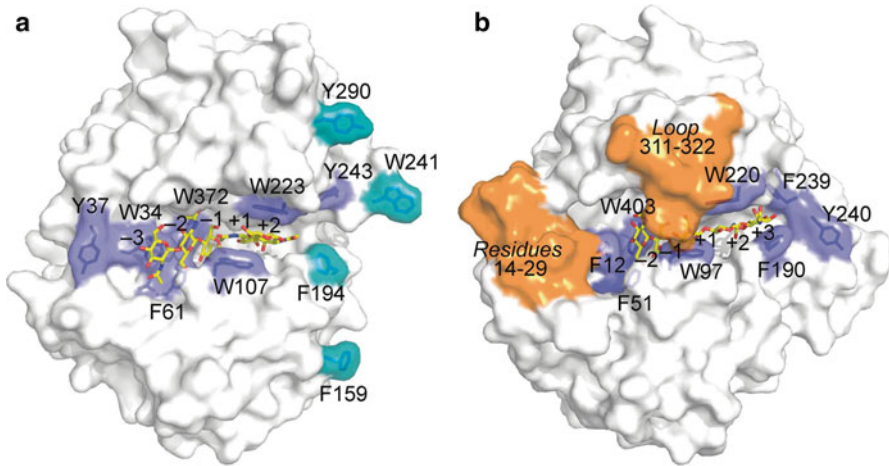


Fig. 2.8 The substrate-binding clefts of the OfChtI-CAD (**a**) and SmChiB (**b**) complexes. The carbohydrate-binding module and the linker of SmChiB are not shown. The (GlcNAc) 2/3 bound to OfChtI-CAD and the (GlcNAc) 5 bound to SmChiB (PDB entry 1e6n) are shown as sticks with yellow C atoms. The numbers indicate the subsites to which the sugar is bound. The aromatic residues in the substrate-binding clefts of OfChtI-CAD and SmChiB are labeled and are shown as blue sticks. In OfChtI-CAD, the four residues forming the hydrophobic plane are shown in cyan. In SmChiB, loop 311–322 forming the roof of the tunnel and residues 14–29 forming the blunted non-reducing end are labeled (With permission granted on behalf of IUCr)

mechanism that yields α -anomer products, insect chitinases that belong to family 18 have a retraining mechanism of action and produce β -anomers. It is also likely that the action of these enzymes involves substrate-assisted catalysis utilizing the carbonyl group of the *N*-acetylglucosamine and the formation of an oxazolium ion intermediate (Brameld et al. 1998).

The crystal structures of a family 1 chitinase from *O. furnacali* in the unbound form and in complex with substrates have been determined recently by Chen et al. (2014). This study has revealed that the substrate-binding site takes the shape of an open groove-like cleft and that the reducing sugar at the -1 site is in the energetically unfavorable boat conformation (Fig. 2.8). This is in contrast to the bacterial enzyme SmChiB from *Serratia marcescens*, which has a tunnel-like substrate-binding pocket. Further, the presence of four aromatic amino acids forming a hydrophobic plane near the catalytic site were shown to be involved in substrate anchoring, but not in catalysis using mutant forms of these enzymes in which these aromatic amino acids were substituted by other residues.

2.10.3 *Tissue Specificity and Regulation of Expression of Chitinase Families*

The timing of appearance and locations of the chitinases belonging to different groups provide some clues regarding their putative functions. Chitinases belonging to groups I and II are found in molting fluid (for examples see Koga et al. 1992; Qu et al. 2014) and are expressed only in cuticle forming tissue (notably they are absent in the gut). Group IV chitinases show the opposite specificity with strong expression in the gut during larval stages and low (or no) expression in integument (Zhu et al. 2008b; Zhang et al. 2011). Some of them were expressed in insect cells using baculoviral expression systems and were also shown to be enzymatically active (Gopalakrishnan et al. 1995; Zhu et al. 2008b). The members of group III (and the more recently discovered group VIII) chitinases have a membrane-spanning domain. Group III chitinases have also been shown to be enzymatically active (Arakane, unpublished data; Qing Yang, unpublished data) and their catalytic domains are pointing to the cuticle side and therefore are presumed to digest chitin. Group III chitinases are expressed predominantly in pupal stages in *An. gambiae* (Zhang et al. 2011; Noh and Arakane unpublished results; Qing Yang unpublished data). This group of chitinases is not required for molting *per se*, but seems to affect the ultrastructure of the cuticle.

2.10.4 *Specialization in the Functions of Families of Chitinases*

The diversification in the domain architecture of the many families of chitinases may be related to their distinctive biological functions. There are substantial variations in the tissue specificity, timing of expression and regulation of each family of chitinases. RNAi experiments have revealed that group I chitinases are critical for molting especially at the pharate adult stage. Down-regulation of transcripts for these genes resulted in molting failure and trapping of the fully developed insects inside their pupal cuticles (or cuticle from the previous instar) (Zhu et al. 2008c; Zhang et al. 2012a, b; Xi et al. 2015; Li et al. 2015). However, at earlier stages, this enzyme appears dispensable, presumably because other enzymes can fill in for this enzyme. RNAi of group II chitinases that have four or more catalytic domains affected hatching of embryos and molting at every developmental stage indicating their indispensable nature. This chitinase is also likely to be present in the molting fluid as it has a cleavable signal peptide, though this point has not been studied carefully. RNAi of group III chitinases that have two catalytic domains in tandem did not prevent adult eclosion but the insects had reduced chitin content in their procuticle, loss of laminar organization and abnormal adult cuticles (Arakane, unpublished data). RNAi of group IV chitinases from *T. castaneum* using dsRNAs for a single group IV chitinase gene or combinations of dsRNAs for three genes of this

group did not result in any visible phenotypes (Zhu et al. 2008c). However administration of dsRNA for a group IV chitinase from *O. nubilalis* resulted in an increase in chitin content of PM and reduced weight gain of larvae (Khajuria et al. 2010). RNAi of a group V chitinase-like protein from *T. castaneum*, TcIDGF4, prevented adult eclosion but had no effect at other developmental stages (Zhu et al. 2008c). Similarly in *N. lugens*, RNAi of chitinases belonging to group I, II, III and V resulted in failure of nymph-nymph molt (Xi et al. 2015) confirming that at least these four groups of chitinases are indispensable in this insect too.

The presence of chitinases with distinct domain organization and non-redundant, but essential functions suggests that they have functions besides degradation of chitin in the old cuticle. These could include providing primers for elongation of chitin and processing of mature chitin chains for higher level of organization.

2.11 Chitinolytic *N*-Acetylglucosaminidases (EC 3.2.1.52) and Their Genes

N-acetylglucosaminidases (NAGases) have been identified or purified from a variety of sources from insects including molting fluid, hemolymph, integument and gut and shown to be enzymatically active (Koga et al. 1982; Nagamatsu et al. 1995; Zen et al. 1996; Filho et al. 2002; Tomiya et al. 2006; Leonard et al. 2006; Yang et al. 2008; Kokuho et al. 2007). They belong to family 20 glycosylhydrolases and produce hexosamines (*N*-acetylglucosamine and *N*-acetylgalactosamine) by cleaving aminosugars from the non-reducing ends of chitoooligosaccharides or the terminal residues of *N*-glycans, glycoproteins and glycolipids (Intra et al. 2008; Liu et al. 2012). While some of them may be specific for degrading chitoooligosaccharides, others may be involved exclusively in the removal of hexosamines from *N*-glycans (Léonard et al. 2006; Yang et al. 2008), glycoconjugate degradation and egg-sperm recognition (Cattaneo et al. 2006; Okada et al. 2007; Liu et al. 2012). The enzymes of the former group act synergistically with endochitinases, which cleave crystalline chitin into chitoooligosaccharides. They may also alleviate the inhibition of chitinases by accumulating chitotriose and chitotetraose in the molting fluid (Fukamizo and Kramer 1985a, b).

NAGases in insects have been divided into three major groups based on phylogenetic analyses of proteins predicted from several insect genomes (Hogenkamp et al. 2008). In addition, insects have additional proteins with lower sequence similarity to these three groups and constitute another branch that includes several well-characterized mammalian hexosaminidases involved in glycan processing (Fig. 2.9).

NAGases belonging to group I are the major chitinolytic enzymes and are found in abundance in insects. They have the highest catalytic efficiency with chitoooligosaccharide substrates (Liu et al. 2012). The crystal structure of NAG-1 (Hex-1) from *O. furnacalis* was determined by Liu et al. (2012). In the crystal structure, this enzyme exists as a homodimer and has a deeper and larger substrate-binding pocket

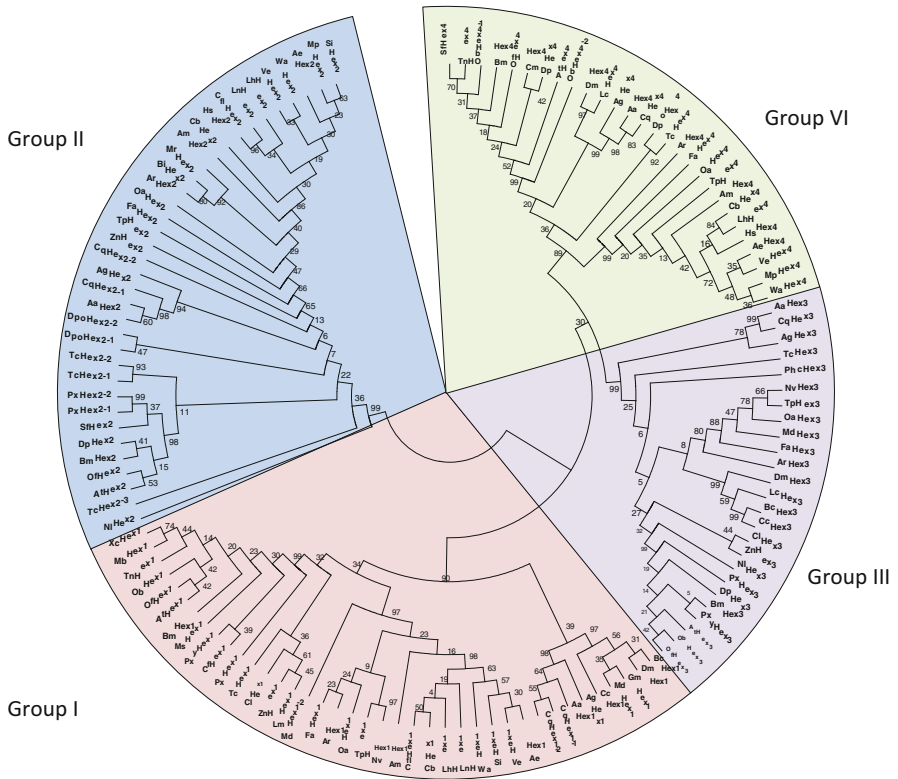


Fig. 2.9 Phylogenetic analysis of insects GH20 *N*-acetylhexosaminidases (Hex) from 48 different species; *Aedes aegypti* (Aa), *Acromyrmex echinator* (Ae), *Anopheles gambiae* (Ag), *Apis mellifera* (Am), *Athalia rosae* (Ar), *Amyeloid transitella* (At), *Bactrocera cucurbitae* (Bc), *Bombus impatiens* (Bi), *Bombyx mori* (Bm), *Cerapachys biroi* (Cb), *Ceratitidis capitata* (Cc), *Choristoneura fumiferana* (Cf), *Camponotus floridanus* (Cfl), *Cimex lectularius* (Cl), *Cnaphalocrocis medinalis* (Cm), *Culex quinquefasciatus* (Cq), *Drosophila melanogaster* (Dm), *Danaus plexippus* (Dp), *Dendroctonus ponderosae* (Dpo), *Fopius arisanus* (Fa), *Glossina morsitans morsitans* (Gm), *Harpognathos saltator* (Hs), *Lucilia cuprina* (Lc), *Linepithema humile* (Lh), *Locusta migratoria* (Lm), *Lasius niger* (Ln), *Mamestra brassicae* (Mb), *Musca domestica* (Md), *Monomorium pharaonis* (Mp), *Megachile rotundata* (Mr), *Manduca sexta* (Ms), *Nilaparvata lugens* (Nl), *Nasonia vitripennis* (Nv), *Orussus abietinus* (Oa), *Operophtera brumata* (Ob), *Ostrinia furnacalis* (Of), *Pediculus humanus corporis* (Phc), *Papilio xuthus* (Px), *Plutella xylostella* (Pxy), *Spodoptera frugiperda* (Sf), *Solenopsis invicta* (Si), *Tribolium castaneum* (Tc), *Trichoplusia ni* (Tn), *Trichogramma pretiosum* (Tp), *Vollenhovia emeryi* (Ve), *Wasmannia auropunctata* (Wa), *Xestia nigrum* (Xc), *Zootermopsis nevadensis* (Zn). A bootstrap analysis of 2000 replications was carried out on the trees inferred from the neighbor joining method and bootstrap values are shown at each branch of the tree. Hexs are divided into four different groups: group I (light red), group II (light blue), group III (light purple), group IV (light green) (Figure reprinted with permission from Tetreau et al. (2015a))

capable of binding oligosaccharides compared to the human and bacterial enzymes, which can accommodate only one sugar in their active site pockets. They are expressed at high levels in the larval carcass, and down-regulation of the transcripts for these genes has been shown to result in severe molting defects and death at the next molt in *T. castaneum* and *O. furnacalis* (Hogenkamp et al. 2008; Liu et al. 2012).

TcNag2 is expressed predominantly in the midgut in the larval stage. However, RNAi of this gene resulted in only lower mortality during larval-larval and larval-pupal molts but substantial mortality at the pharate adult stage indicating its role in molting. The tissue specificity of expression of this gene at the pupal stage has not been reported so far. The enzymatic properties of Hex2 show that it is an enzyme with broad substrate-spectrum capable of hydrolyzing *N*-acetylhexosamine from chitin oligosaccharides, *N*-glycan and glycolipids (Liu et al. 2012). But unlike human Hex A, OfHex2 could not degrade charged substrates such as ganglioside GM2 and peptidoglycan. Real-time PCR analysis demonstrated that the expression of the *O. furnacalis* Hex2 was up-regulated in larva and pupa, and mainly occurred in the carcass rather than in the midgut during the feeding stage of fifth (final) instar larva. RNAi of *Hex2* caused non-lethal but severe abnormalities of larval abdomen, pupal and adult appendages (Liu et al. 2013). Thus its properties are consistent with a more limited role in degradation of chitooligosaccharides compared to NAG1.

The third group of NAGases is called FDLs based on prior nomenclature of an orthologous gene from *D. melanogaster*, which has “fused lobes” phenotype (Leonard et al. 2006). The DmFDL was shown to release α -1,3-linked mannose of the core pentasaccharide of *N*-glycans, but does not act on chitotriose or on the GlcNAc-GlcNAc bonds in *N*-glycans. DmHex3 may be involved in sperm-egg recognition and in fertilization (Cattaneo et al. 2006). The tissue-specific expression pattern analysis indicated that OfHex3 was mostly localized in the fat body and testis. Thus the enzymes of this group are like to be involved in deglycosylation of hexosamine residues from terminal positions of *N*-glycans or glycolipids. In the molting fluid of *O. furnacalis*, an interaction between OfHex3 with OfHex1 was detected by co-immunoprecipitation (Qu et al. 2014). Enzymatic activity analysis indicates that OfHex3 is able to degrade chitooligosaccharides, but at a lower rate than that of OfHex1, and had no ability to hydrolyze other glycans from glycoproteins and glycolipids. A recent proteomic analysis proved the presence of Hex-3 (FDL) in the molting fluid of *B. mori* (Qu et al. 2014). Thus the precise function of enzymes of the FDL group remains to be resolved.

The fourth group of *N*-acetylglucosaminidases in insects is grouped along with hexosaminidases from mammalian and other sources. The enzymes of this group have a broad specificity for sugars containing either *N*-acetylglucosamine or *N*-acetylgalactosamine and there is only limited evidence for their role in chitin metabolism and will therefore be not discussed in this review.

2.12 Additional Proteins Involved in Chitin Protection and Degradation

One of the reasons that chitin in the cuticle is remarkably stable is its firm association with other proteins. In fact, the formation of chitin laminae requires the participation of CDA and Knickkopf (KNK) (our unpublished results; Moussian et al. 2005a, b; Chaudhari et al. 2011, 2015) as well as Obstructor–A (CPAP3-A) (Pesch et al. 2015). KNK, CDA as well as cuticular proteins analogous to peritrophins (CPAPs) that have one or three CBDs have been predicted or shown to bind to chitin (Jasrapuria et al. 2010, 2012; Petkau et al. 2012). Removal of these proteins from chitin-protein complexes may be an essential prerequisite for chitin degradation. The specific protease(s) involved in this turnover have not been characterized. But the finding that RNAi of some chymotrypsin-like proteins in *T. castaneum* results in molting defects similar to RNAi of chitin synthase indicates that these proteins may be important for digestion of the old cuticle (Broehan et al. 2010). The roles of PMPs that associate with chitin in the midgut will be discussed by Merzendorfer in Chap. 8.

2.13 Cuticular Proteins Analogous to Peritrophins (CPAPs)

Several cuticular proteins contain peritrophin-A type chitin binding motifs, and they have been described in all insects. These are all expressed only in cuticle forming epithelial cells and predicted to be secreted proteins. Some of them have been localized either within the cuticle or the molting fluid. They have been grouped into two families based on the number of these chitin-binding domains they contain. The family with one CBD has been named CPAP1 family and that with three CBDs was named CPAP3 family (Jasrapuria et al. 2010). The CPAP3 family members were originally named GASPs or “Obstructors” in *D. melanogaster* (Barry et al. 1999; Behr and Hoch 2005). The CPAP1 family has been subdivided into 15 subfamilies (Tetreau et al. 2015a, b) and the CPAP3 family was divided into 9 subfamilies (Behr and Hoch 2005; Jasrapuria et al. 2010). RNAi for some of the genes encoding these proteins indicated that they affect either molting, integrity, morphology or the ultrastructure of the cuticle. Some of them are essential for survival while others produce visible morphological defects in cuticles of different parts of the insect’s anatomy or joint defects (Petkau et al. 2012; Jasrapuria et al. 2012; Pesch et al. 2015). These proteins may be involved in organization of chitin into laminae or higher order structures, or the formation of pore canals or tracheal tubules or other chitin-containing structures such as denticles.

2.14 Cuticular Proteins Belonging to R & R and Other Groups

The chitin in the procuticle is also associated with several other proteins that have chitin binding domains other than the peritrophin-A domains. A large assortment of cuticular proteins with one of the three types of Rebers & Riddiford (R & R) consensus motifs have been identified and classified into multiple groups. The reader is referred to recent excellent reviews on this topic (Willis 2010; Willis et al. 2012) and to the chapter on cuticular proteins by Heideki Kawasaki (Chap. 1). Other proteins were shown to be associated with some specialized exoskeletal structures. Some insects such as locusts, fleas and click beetles use deformations of exoskeleton as a way to store energy for sudden release. The exoskeletons of these insects have, in addition to chitin, an elastic protein known as resilin, which contains di- or tri-tyrosine linkages thought to be involved in energy storage. These insects use the combination of the stored energy in the chitinous cuticle and resilin to power their sudden movements. For example, froghoppers have bow-shaped pleural arches linking the coxa to the hinge of the hindwing that contains resilin to store energy by deformation of these bow-shaped chitin-resilin composites (Burrows et al. 2008). A more extensive description of resilin and its role is described by Gorb et al. in Chap. 4 of this book.

2.15 Concluding Remarks

In the past, studies of biosynthesis, turnover, and assembly of matrices containing chitin had been hampered by the difficulties of developing soluble systems to study them biochemically and by the fact that many of these reactions occur in extracellular spaces. Advances in genomics and proteomics and applications of RNA interference and ultra-structural analyses have provided new insights into how chitin-composites are assembled and turned over. In the near future, we can expect to see several new studies that will provide more details of the dynamics of assembly and turnover of cuticle and PM. They will also reveal the roles of the numerous proteins and small molecules that participate in the overall process of how these complex extracellular structures are shaped and how they function in supporting several physiological processes that are vital for insect survival and extraordinary resilience.

References

- Abdel-Banat BM, Koga D (2001) A genomic clone for a chitinase gene from the silkworm, *Bombyx mori*: structural organization identifies functional motifs. *Insect Biochem Mol Biol* 31:497–508
- Agrawal S, Kelkenberg M, Begum K, Steinfeld L, Williams CE, Kramer KJ, Beeman RW, Park Y, Muthukrishnan S, Merzendorfer H (2014) Two essential peritrophic matrix proteins mediate matrix barrier functions in the insect midgut. *Insect Biochem Mol Biol* 49:24–34

- Arakane Y, Muthukrishnan S (2010) Insect chitinase and chitinase-like proteins. *Cell Mol Life Sci* 67:201–216
- Arakane Y, Zhu Q, Matsumiya M, Muthukrishnan S, Kramer KJ (2003) Properties of catalytic, linker and chitin-binding domains of insect chitinase. *Insect Biochem Mol Biol* 33:631–648
- Arakane Y, Hogenkamp DG, Zhu YC, Kramer KJ, Specht CA, Beeman RW, Kanost MR, Muthukrishnan S (2004) Characterization of two chitin synthase genes of the red flour beetle, *Tribolium castaneum*, and alternate exon usage in one of the genes during development. *Insect Biochem Mol Biol* 34:291–304
- Arakane Y, Muthukrishnan S, Kramer KJ, Specht CA, Tomoyasu Y, Lorenzen MD, Kanost MR, Beeman RW (2005) The *Tribolium* chitin synthase genes TcCHS1 and TcCHS2 are specialized for synthesis of epidermal cuticle and midgut peritrophic matrix. *Insect Mol Biol* 14:453–463
- Arakane Y, Specht CA, Kramer KJ, Muthukrishnan S, Beeman RW (2008) Chitin synthases are required for survival, fecundity and egg hatch in the red flour beetle, *Tribolium castaneum*. *Insect Biochem Mol Biol* 38:959–962
- Arakane Y, Dixit R, Begum K, Park Y, Specht CA, Merzendorfer H, Kramer KJ, Muthukrishnan S, Beeman RW (2009) Analysis of functions of the chitin deacetylase gene family in *Tribolium castaneum*. *Insect Biochem Mol Biol* 39:355–365
- Arakane Y, Baguion M, Jasarapuria S, Chaudhari S, Doyungan A, Kramer KJ, Muthukrishnan S, Beeman RW (2010) Two uridine-diphosphate N-acetylglucosamine pyrophosphorylases are critical for *Tribolium castaneum* molting, survival and fecundity. *Insect Biochem Mol Biol* 41:42–50
- Araújo SJ, Aslam H, Tear G, Casanova J (2005) *mummy/cystic* encodes an enzyme required for chitin and glycan synthesis, involved in trachea, embryonic cuticle and CNS development – analysis of its role in *Drosophila* tracheal morphogenesis. *Dev Biol* 288:179–193
- Ashfaq M, Sonoda S, Tsumuki H (2007) Developmental and tissue-specific expression of CHS1 from *Plutella xylostella* and its response to chlorfluazuron Pesticide. *Biochem Physiol* 89:20–30
- Bansal R, Mian MA, Mittapalli O, Michel AP (2012) Characterization of a chitin synthase encoding gene and effect of diflubenzuron in soybean aphid, *Aphis glycines*. *Int J Biol Sci* 8:1323–1334
- Barry MK, Triplett AA, Christensen AC (1999) A peritrophin-like protein expressed in the embryonic tracheae of *Drosophila melanogaster*. *Insect Biochem Mol Biol* 29:319–327
- Becker A, Schloder P, Steele JE, Wegener G (1996) The regulation of trehalose metabolism in insects. *EXS* 52:433–439
- Beckham GT, Crowley MF (2011) Examination of the α -chitin structure and decrystallization thermodynamics at the nanoscale. *J Phys Chem B* 115:4516–4522
- Behr M, Hoch M (2005) Identification of the novel evolutionary conserved obstructor multigene family in invertebrates. *FEBS Lett* 579:6827–6833
- Blair DE, Schuttelkopf AW, MacRae JI, van Aalten DMF (2005) Structure and metal-dependent mechanism of peptidoglycan deacetylase, a streptococcal virulence factor. *Proc Natl Acad Sci U S A* 102:15429–15434
- Bolognesi R, Arakane Y, Muthukrishnan S, Kramer KJ, Terra WR, Ferreira C (2005) Sequences of cDNAs and expression of genes encoding chitin synthase and chitinase in the midgut of *Spodoptera frugiperda*. *Insect Biochem Mol Biol* 35:1249–1259
- Bouligand Y (1972) Twisted fibrous arrangements in biological-materials and cholesteric mesophases. *Tissue Cell* 4:189–217
- Brameld KA, Shrader WD, Imperiali B, Goddard WA III (1998) Substrate assistance in the mechanism of family 18 chitinases: theoretical studies of potential intermediates and inhibitors. *J Mol Biol* 280:913–923
- Broehan G, Zimoch L, Wessels A, Ertas B, Merzendorfer H (2007) A chymotrypsin-like serine protease interacts with the chitin synthase from the midgut of the tobacco hornworm. *J Exp Biol* 210:3636–3643
- Broehan G, Kemper M, Driemeier D, Vogelpohl I, Merzendorfer H (2008) Cloning and expression analysis of midgut chymotrypsin-like proteinases in the tobacco hornworm. *J Insect Physiol* 54:1243–1252

- Broehan G, Arakane Y, Beeman RW, Kramer KJ, Muthukrishnan S, Merzendorfer H (2010) Chymotrypsin-like peptidases from *Tribolium castaneum*: RNA interference reveals physiological functions in molting. *Insect Biochem Mol Biol* 40:274–283
- Burrows M, Shaw SR, Sutton GP (2008) Resilin and chitinous cuticle form a composite structure for energy storage in jumping by froghopper insects. *BMC Biol* 6:41
- Campbell PM, Cao AT, Hines ER, East PD, Gordon KHJ (2008) Proteomic analysis of the peritrophic matrix from the gut of the caterpillar, *Helicoverpa armigera*. *Insect Biochem Mol Biol* 38:950–958
- Carlstrom D (1957) The crystal structure of alpha-chitin (poly-N-acetyl-D-glucosamine). *J Biophys Biochem Cytol* 3:669–683
- Cattaneo F, Pasini ME, Intra J, Matsumoto M, Briani F, Hoshi M, Perotti ME (2006) Identification and expression analysis of *Drosophila melanogaster* genes encoding β -hexosaminidases of the sperm plasma membrane. *Glycobiology* 16:786–800
- Chaudhari SS, Arakane Y, Specht CA, Moussian B, Boyle DL, Park Y, Kramer KJ, Beeman RW, Muthukrishnan S (2011) Knickkopf protein protects and organizes chitin in the newly synthesized insect exoskeleton. *Proc Natl Acad Sci U S A* 108:17028–17033
- Chaudhari SS, Noh M, Moussian M, Specht CA, Kramer KJ, Beeman RW, Arakane Y, Muthukrishnan S (2015) Knickkopf and Retroactive proteins are required for formation of laminar serosal procuticle during embryonic development of *Tribolium castaneum*. *Insect Biochem Mol Biol* 60:1–6
- Chen X, Yang X, Senthil Kumar N, Tang B, Sun X, Qui X, Hu J, Zhang W (2007) The class A chitin synthase gene of *Spodoptera exigua*: molecular cloning and expression patterns. *Insect Biochem Mol Biol* 37:409–417
- Chen J, Tang B, Chen H, Yao Q, Huang X, Chen J, Zhang D, Zhang W (2010) Different functions of the insect soluble and membrane-bound trehalase genes in chitin biosynthesis revealed by RNA interference. *PLoS One* 5:e10133
- Chen L, Liu T, Zhou Y, Chen Q, Shen X, Yang Q (2014) Structural characteristics of an insect group I chitinase, an enzyme indispensable to moulting. *Acta Crystallogr D* 70:932–942
- Choi HK, Choi KH, Kramer KJ, Muthukrishnan S (1997) Isolation and characterization of a genomic clone for the gene of an insect molting enzyme, chitinase. *Insect Biochem Mol Biol* 27:37–47
- Cohen E (2010) Chitin biochemistry: synthesis, hydrolysis and inhibition. *Adv Insect Physiol* 38:5–74
- Cohen E, Casida JE (1980a) Inhibition of *Tribolium* gut chitin synthetase. *Pestic Biochem Physiol* 13:129–136
- Cohen E, Casida JE (1980b) Properties of *Tribolium* gut chitin synthetase. *Pestic Biochem Physiol* 13:121–128
- Demaeght P, Osborne EJ, Odman-Naresh J, Grbić M, Nauen R, Merzendorfer H, Clark RM, Van Leeuwen T (2012) High resolution genetic mapping uncovers chitin synthase-I as the target-site of the structurally diverse mite growth inhibitors clofentezine, hexythiazox and etoxazole in *Tetranychus urticae*. *Insect Biochem Mol Biol* 51:52–61
- Dinglasan RR, Devenport M, Florens L, Johnson JR, McHugh CA, Donnelly-Doman M, Carucci DJ, Yates JR, Jacobs-Lorena M (2009) The *Anopheles gambiae* adult midgut peritrophic matrix proteome. *Insect Biochem Mol Biol* 39:125–134
- Dixit R, Arakane Y, Specht CA, Richard C, Kramer KJ, Beeman RW, Muthukrishnan S (2008) Domain organization and phylogenetic analysis of proteins from the chitin deacetylase gene family of *Tribolium castaneum* and three other species of insects. *Insect Biochem Mol Biol* 38:440–451
- Dong B, Miao G, Hayashi S (2014) A fat body-derived apical extracellular matrix enzyme is transported to the tracheal lumen and is required for tube morphogenesis in *Drosophila*. *Development* 141:4104–4109
- Dorfmueller HC, Ferenbach AT, Borodkin VS, van Aalten DM (2014) A structural and biochemical model of processive chitin synthesis. *J Biol Chem* 289:23020–23028

- Fabritius HO, Sachs C, Triguero PR, Raabe D (2009) Influence of structural principles on the mechanics of a biological fiber-based composite material with hierarchical organization: the Exoskeleton of the Lobster *Homarus americanus*. *Adv Mater Sci* 21:391–400
- Filho BP, Lemos FJ, Secundino NF, Pascoa V, Pereira ST, Pimenta PF (2002) Presence of chitinase and beta-N-acetylglucosaminidase in the *Aedes aegypti*: a chitinolytic system involving peritrophic matrix formation and degradation. *Insect Biochem Mol Biol* 32:1723–1729
- Fukamizo T, Kramer KJ (1985a) Mechanism of chitin hydrolysis by the binary chitinase system in insect moulting fluid. *Insect Biochem* 15:141–145
- Fukamizo T, Kramer KJ (1985b) Mechanism of chitin oligosaccharide hydrolysis by the binary enzyme chitinase system in insect moulting fluid. *Insect Biochem* 15:1–7
- Fukamizo T, Kramer KJ (1987) Effect of 20-hydroxyecdysone on chitinase and β -N-acetylglucosaminidase during the larval–pupal transformation of *Manduca sexta* (L.). *Insect Biochem* 17:547–550
- Gagou ME, Kapsetaki M, Turberg A, Kafetzopoulos D (2002) Stage-specific expression of the chitin synthase *DmeChSA* and *DmeChSB* genes during the onset of *Drosophila* metamorphosis. *Insect Biochem Mol Biol* 32:141–146
- Gopalakrishnan B, Muthukrishnan S, Kramer KJ (1995) Baculovirus-mediated expression of a *Manduca sexta* chitinase gene: properties of the recombinant protein. *Insect Biochem Mol Biol* 25:255–265
- Guo W, Li G, Pang Y, Wang P (2005) A novel chitin-binding protein identified from the peritrophic membrane of the cabbage looper, *Trichoplusia ni*. *Insect Biochem Mol Biol* 35:1224–1234
- Harper MS, Hopkins TL (1997) Peritrophic membrane structure and secretion in European corn borer larvae (*Ostrinia nubilalis*). *Tissue Cell* 29:463–475
- Harper MS, Hopkins TL, Czapl TH (1998) Effect of wheat germ agglutinin on formation and structure of the peritrophic membrane in European corn borer (*Ostrinia nubilalis*) larvae. *Tissue Cell* 30:166–176
- Harris MT, Fuhrman JA (2002) Structure and expression of chitin synthase in the parasitic nematode *Dirofilaria immitis*. *Mol Biochem Parasitol* 122:231–234
- Harris MT, Lai K, Arnold K, Martinez HF, Specht CA, Fuhrman JA (2000) Chitin synthase in the filarial parasite, *Brugia malayi*. *Mol Biochem Parasitol* 111:351–362
- Hegedus D, Erlandson M, Gillott C, Toprak U (2009) New insights into peritrophic matrix synthesis, architecture, and function. *Annu Rev Entomol* 54:285–302
- Hogenkamp DG, Arakane Y, Zimoch L, Merzendorfer H, Kramer KJ, Beeman RW, Kanost MR, Specht CA, Muthukrishnan S (2005) Chitin synthase genes in *Manduca sexta*: characterization of a gut-specific transcript and differential tissue expression of alternately spliced mRNAs during development. *Insect Biochem Mol Biol* 35:529–540
- Hogenkamp DG, Arakane Y, KKJ, Muthukrishnan S, Beeman RW (2008) Characterization and expression of the β -N-acetylhexosaminidase gene family of *Tribolium castaneum*. *Insect Biochem Mol Biol* 38:478–489
- Huang X, Tsuji N, Miyoshi T, Motobu M, Islam MK, Alim MA, Fujisaki K (2007) Characterization of glutamine: fructose-6-phosphate aminotransferase from the ixodid tick, *Haemaphysalis longicornis*, and its critical role in host blood feeding. *Int J Parasitol* 37:383–392
- Ibrahim GH, Smartt CT, Kiley LM, Christensen BM (2000) Cloning and characterization of a chitin synthase cDNA from the mosquito *Aedes aegypti*. *Insect Biochem Mol Biol* 30:1213–1222
- Intra J, Pavesi G, Horner DS (2008) Phylogenetic analyses suggest multiple changes of substrate specificity within the glycosyl hydrolase 20 family. *BMC Evol Biol* 8:214
- Jacobs CGC, Braak N, Lamers GEM, van der Zee M (2015) Elucidation of the serosal cuticle machinery in the beetle *Tribolium* by RNA sequencing and functional analysis of Knickkopf, Retroactive and laccase. *Insect Biochem Mol Biol* 60:7–12
- Jakubowska AK, Caccia S, Gordon KH, Ferre J, Herrero S (2010) Down-regulation of a chitin deacetylase-like protein in response to baculovirus infection and its application for improving baculovirus infectivity. *J Virol* 84:2547–2555

- Jasrapuria S, Arakane Y, Osman G, Kramer KJ, Beeman RW, Muthukrishnan S (2010) Genes encoding proteins with peritrophin A-type chitin-binding domains in *Tribolium castaneum* are grouped into three distinct families based on phylogeny, expression and function. *Insect Biochem Mol Biol* 40:214–227
- Jasrapuria S, Specht CA, Kramer KJ, Beeman RW, Muthukrishnan S (2012) Gene families of cuticular proteins analogous to peritrophins (CPAPs) in *Tribolium castaneum* have diverse functions. *PLoS One* 7:e49844
- Kanost MR, Zepp MK, Ladendorff NE, Andersson LA (1994) Isolation and characterization of a hemocyte aggregation inhibitor from hemolymph of *Manduca sexta* larvae. *Arch Insect Biochem Physiol* 27:123–136
- Kato N, Mueller CR, Fuchs JF, Wessely V, Lan Q, Christensen BM (2006) Regulatory mechanisms of chitin biosynthesis and roles of chitin in peritrophic matrix formation in the midgut of adult *Aedes aegypti*. *Insect Biochem Mol Biol* 36:1–9
- Kawamura K, Shibata T, Saget O, Peel D, Bryant PJ (1999) A new family of growth factors produced by the fat body and active on *Drosophila* imaginal disc cells. *Development* 126:211–219
- Kaya M, Baran T, Erdoğlan S, Menteş A, Özusağlam MA, Çakmak YS (2014) Physicochemical comparison of chitin and chitosan obtained from larvae and adult Colorado potato beetle (*Leptinotarsa decemlineata*). *Mater Sci Eng* 45:72–81
- Kelkenberg M, Odman-Naresh J, Muthukrishnan S, Merzendorfer H (2015) Chitin is a necessary component to maintain the barrier function of the peritrophic matrix in the insect midgut. *Insect Biochem Mol Biol* 56:21–28
- Khajuria C, Buschman LL, Chen MS, Muthukrishnan S, Zhu KY (2010) A gut-specific chitinase gene essential for regulation of chitin content of peritrophic matrix and growth of *Ostrinia nubilalis* larvae. *Insect Biochem Mol Biol* 40:621–629
- Kimura S (1976) Insect haemolymph exo-beta-N-acetylglucosaminidase from *Bombyx mori*. Purification and properties. *Biochim Biophys Acta* 446:399–406
- Koga D, Mai MS, Dziaidik-Turner C, Kramer KJ (1982) Kinetics and mechanism of exochitinase and β -N-acetylhexosaminidase from the tobacco hornworm, *Manduca sexta* L. (Lepidoptera: Sphingidae). *Insect Biochem* 12:493–499
- Koga D, Funakoshi T, Mizuki K, Ide A, Kramer KJ, Zen KC, Choi H, Muthukrishnan S (1992) Immunoblot analysis of chitinolytic enzymes in integument and molting fluid of the silkworm, *Bombyx mori*, and the tobacco hornworm, *Manduca sexta*. *Insect Biochem Mol Biol* 22:305–311
- Koga D, Sasaki Y, Uchiumi Y, Hirai N, Arakane Y, Nagamatsu Y (1997) Purification and characterization of *Bombyx mori* chitinases. *Insect Biochem Mol Biol* 27:757–767
- Kokuho T, Yasukochi Y, Watanabe S, Inumuru S (2007) Molecular cloning and expression of two novel β -N-acetylglucosaminidases from silkworm *Bombyx mori*. *Biosci Biotechnol Biochem* 71:1626–1635
- Kramer KJ, Corpuz L, Choi HK, Muthukrishnan S (1993) Sequence of a cDNA and expression of the gene encoding epidermal and gut chitinases of *Manduca sexta*. *Insect Biochem Mol Biol* 23:691–701
- Kumar NS, Tang B, Chen X, Tian H, Zhang W (2008) Molecular cloning, expression pattern and comparative analysis of chitin synthase gene B in *Spodoptera exigua*. *Comp Biochem Physiol B* 149:447–453
- Leonard R, Rendic D, Rabouille C, Wilson IB, Preat T, Altmann F (2006) The *Drosophila* fused lobes gene encodes an N-acetylglucosaminidase involved in N-glycan processing. *J Biol Chem* 281:4867–4875
- Li D, Zhang J, Wang Y, Liu X, Ma E, Sun Y, Li S, Zhu KY, Zhang J (2015) Two chitinase 5 genes from *Locusta migratoria*: molecular characteristics and functional differentiation. *Insect Biochem Mol Biol* 58:46–54
- Liu F, Liu T, Qu M, Yang Q (2012) Molecular and biochemical characterization of a novel β -N-acetyl-D-hexosaminidase with broad substrate-spectrum from the Asian corn borer, *Ostrinia furnacalis*. *Int J Biol Sci* 8:1085–1096

- Liu XJ, Li F, Li DQ, Ma EB, Zhang WQ, Zhu KY, Zhang JZ (2013) Molecular and functional analysis of UDP-N-acetylglucosamine pyrophosphorylases from the migratory locust, *Locusta migratoria*. *PLoS One* 8, e71970
- Locke M (2001) The Wigglesworth lecture: insects for studying fundamental problems in biology. *J Insect Physiol* 47:495–507
- Locke M, Huie P (1979) Apolysis and the turnover of plasma membrane plaques during cuticle formation in an insect. *Tissue Cell* 11:277–291
- Lotmar W, Picken LER (1950) A new crystallographic modification of chitin and its distribution. *Experientia* 6:58–59
- Lu YM, Zen KC, Muthukrishnan S, Kramer KJ (2002) Site-directed mutagenesis and functional analysis of active site acidic amino acid residues D142, D144 and E146 in *Manduca sexta* (tobacco hornworm) chitinase. *Insect Biochem Mol Biol* 32:1369–1382
- Luschnig S, Batz T, Armbruster K, Krasnow MA (2006) *Serpentine* and *vermiform* encode matrix proteins with chitin binding and deacetylation domains that limit tracheal tube length in *Drosophila*. *Curr Biol* 16:186–194
- Mansur JF, Alvarenga ES, Figueira-Mansur J, Franco TA, Ramos IB, Masuda H, Melo ACA, Moreira MF (2014) Effects of chitin synthase double-stranded RNA on molting and oogenesis in the Chagas disease vector *Rhodnius prolixus*. *Insect Biochem Mol Biol* 51:110–121
- Maue L, Meissner D, Merzendorfer H (2009) Purification of an active, oligomeric chitin synthase complex from the midgut of the tobacco hornworm. *Insect Biochem Mol Biol* 39:654–659
- Merzendorfer H (2006) Insect chitin synthases: a review. *J Comp Physiol B* 176:1–15
- Merzendorfer H (2013) Chitin synthesis inhibitors: old molecules and new developments. *Insect Sci* 20:121–138
- Merzendorfer H, Zimoch L (2003) Chitin metabolism in insects: structure, function and regulation of chitin synthases and chitinases. *J Exp Biol* 206:4393–4412
- Minke R, Blackwell J (1978) The structure of α -chitin. *J Mol Biol* 120:167–181
- Moussian B, Schwarz H, Bartoszewski S, Nüsslein-Volhard C (2005a) Involvement of chitin in exoskeleton morphogenesis in *Drosophila melanogaster*. *J Morphol* 264:117–130
- Moussian B, Tang E, Tonning A, Helms S, Schwarz H, Uv AE (2005b) *Drosophila* Knickkopf and Retroactive are needed for epithelial tube growth and cuticle differentiation through their specific requirement for chitin filament organization. *Development* 133:163–171
- Mun S, Noh MY, Dittmer NT, Muthukrishnan S, Kramer KJ, Kanost MR, Arakane Y (2015) Cuticular protein with a low complexity sequence becomes cross-linked during insect cuticle sclerotization and is required for the adult molt. *Sci Rep* 5:10484
- Muthukrishnan S, Merzendorfer H, Arakane Y, Kramer KJ (2012) Chitin metabolism in insects. In: Gilbert LI (ed) *Insect biochemistry and molecular biology*. Elsevier, San Diego, pp 193–235
- Muzzarelli RAA (1973) Chitin. In: Muzzarelli RAA (ed) *Natural chelating polymers: alginic acid, chitin, and chitosan*. Pergamon Press, New York, pp 83–252
- Nagamatsu Y, Yanagisawa I, Kimoto M, Okamoto E, Koga D (1995) Purification of a chito-oligosaccharidolytic β -N-acetylglucosaminidase from *Bombyx mori* larvae during metamorphosis and the nucleotide sequence of its cDNA. *Biosci Biotechnol Biochem* 59:219–225
- Nakabachi A, Shigenobu S, Miyagishima S (2010) Chitinase-like proteins encoded in the genome of the pea aphid, *Acyrtosiphon pisum*. *Insect Mol Biol* 19:175–185
- Ostrowski S, Dierick HA, Bejsovec A (2002) Genetic control of cuticle formation during embryonic development of *Drosophila melanogaster*. *Genetics* 161:171–182
- Okada T, Ishiyama S, Sezutsu H, Usami A, Tamura T, Mita K, Fujiyama K, Seki T (2007) Molecular cloning and expression of two novel β -N-acetylglucosaminidases from silkworm *Bombyx mori*. *Biosci Biotechnol Biochem* 71:1626–1635
- Pan Y, Lu P, Wang Y, Yin L, Ma H, Ma G, Chen K, He Y (2012) *In silico* identification of novel chitinase-like proteins in the silkworm, *Bombyx mori*, genome. *J Insect Sci* 12:150
- Peneff C, Ferrari P, Charrier V, Taburet Y, Monnier C, Zamboni V, Winter J, Harnois M, Fassy F, Bourne Y (2001) Crystal structures of two human pyrophosphorylase isoforms in complexes

- with UDPGlc(Gal)NAc: role of the alternatively spliced insert in the enzyme oligomeric assembly and active site architecture. *EMBO J* 20:6191–6202
- Pesch YY, Riedel D, Behr M (2015) Obstructor A organizes matrix assembly at the apical cell surface to promote enzymatic cuticle maturation in *Drosophila*. *J Biol Chem* 290:10071–10082
- Petkau G, Wingen C, Jussen LC, Radtke T, Behr M (2012) Obstructor-A is required for epithelial extracellular matrix dynamics, exoskeleton function, and tubulogenesis. *J Biol Chem* 287:21396–21405
- Qu M, Yang Q (2011) A novel alternative splicing site of class A chitin synthase from the insect *Ostrinia furnacalis*- Gene organization, expression pattern and physiological significance. *Insect Biochem Mol Biol* 41:923–931
- Qu M, Yang Q (2012) Physiological significance of alternatively spliced exon combinations of the single-copy gene class A chitin synthase in the insect *Ostrinia furnacalis* (Lepidoptera). *Insect Mol Biol* 21:395–404
- Qu M, Ma L, Chen P, Yang Q (2014) Proteomic analysis of insect molting fluid with a focus on enzymes involved in chitin degradation. *J Proteome Res* 13:2931–2940
- Rezende GL, Martins AJ, Gentile C, Farnesi LC, Pelajo-Machado M, Peixoto AA, Valle D (2008) Embryonic desiccation resistance in *Aedes aegypti*: presumptive role of the chitinized serosal cuticle. *BMC Dev Biol* 8:82
- Royer V, Fraichard S, Bouhin H (2002) A novel putative insect chitinase with multiple catalytic domains: hormonal regulation during metamorphosis. *Biochem J* 366:921–928
- Ruddal KM (1963) The chitin-protein complexes of insect cuticles. *Adv Insect Physiol* 1:257–313
- Sarkar A, Perez S (2015) A database of polysaccharide 3D structures. http://polysac3db.cermav.cnrs.fr/discover_chitins_chitosans.html
- Schimmelpfeng K, Strunk M, Stork T, Klambt C (2006) *Mummy* encodes an UDP-N-acetylglucosamine-diphosphorylase and is required during *Drosophila* dorsal closure and nervous system development. *Mech Dev* 123:487–499
- Senthil Kumar N, Tang B, Chen X, Tian H, Zhang W (2008) Molecular cloning, expression pattern and comparative analysis of chitin synthase gene B in *Spodoptera exigua*. *Comp Biochem Physiol Part B Biochem Mol Biol* 149:447–453
- Shi JF, Fu J, Mu LL, Guo WC, Li GQ (2016) Two *Leptinotarsa* uridine diphosphate N-acetylglucosamine pyrophosphorylases are specialized for chitin synthesis in larval epidermal cuticle and midgut peritrophic matrix. *Insect Biochem Mol Biol* 68:1–12
- Shirk PD, Perera OP, Shelby KS, Furlong RB, LoVullo ED, Popham HJR (2015) Unique synteny and alternate splicing of the chitin synthases in closely related heliothine moths. *Gene* 574:121–139
- Sikorski P, Hori R, Wada M (2009) Revisit of α -chitin crystal structure using high resolution X-ray diffraction data. *Biomacromolecules* 10:1100–1105
- Souza-Ferreira PS, Mansur JF, Berni M, Moreira MF, dos Santos RE, Araujo M, de Souza RE, Ramos E, Masuda H (2014) Chitin deposition on the embryonic cuticle of *Rhodnius prolixus*: the reduction of CHS transcripts by CHS-dsRNA injection in females affects chitin deposition and eclosion of the first instar nymph. *Insect Biochem Mol Biol* 51:101–109
- Tang B, Chen X, Liu Y, Tian H, Liu J, Hu J, Xu W, Zhang W (2008) Characterization and expression patterns of a membrane-bound trehalase from *Spodoptera exigua*. *BMC Mol Biol* 9:51
- Tellam RL (1996) The peritrophic matrix. In: Lehane ML, Billingsley PF (eds) *Biology of the insect midgut*. Chapman-Hall, Cambridge, pp 86–114
- Tellam RL, Vuocolo T, Johnson SE, Jarney J, Pearson RD (2000) Insect chitin synthase cDNA sequence, gene organization and expression. *Eur J Biochem* 267:6025–6043
- Tetreau G, Cao XL, Chen YR, Muthukrishnan S, Jiang H, Blissard GW, Kanost M, Wang P (2015a) Overview of chitin metabolism enzymes in *Manduca sexta*: identification, domain organization, phylogenetic analysis and gene expression. *Insect Biochem Mol Biol* 62:114–126

- Tetreau G, Dittmer NT, Cao X, Agrawal S, Chen YR, Muthukrishnan S, Jiang H, Blissard GR, Kanost MR, Wang P (2015b) Analysis of chitin-1 binding proteins from *Manduca sexta* provides new insights into evolution of peritrophin A type chitin-binding domains in insects. *Insect Biochem Mol Biol* 62:27–41
- Thompson SN (2002) Trehalose – the insect ‘blood’ sugar. *Adv Insect Physiol* 31:205–285
- Tian H, Peng H, Yao Q, Chen H, Xie Q, Tang B, Zhang W (2009) Developmental control of a lepidopteran pest *Spodoptera exigua* by ingestion of bacteria expressing dsRNA of a non-midgut gene. *PLoS One* 4:e6225
- Tomiya N, Narang S, Park J, Abdul-Rahman B, Choi O, Singh S, Hiratake J, Sakata K, Betenbaugh MJ, Palter KB, Lee YC (2006) Purification, characterization, and cloning of a *Spodoptera frugiperda* Sf9 β -N-acetylhexosaminidase that hydrolyzes terminal N-acetylglucosamine on the N-glycan core. *J Biol Chem* 281:19545–19560
- Tonning A, Helms S, Schwarz H, Uv AE, Moussian B (2006) Hormonal regulation of *mummy* is needed for apical extracellular matrix formation and epithelial morphogenesis in *Drosophila*. *Development* 133:331–341
- Toprak U, Baldwin D, Erlandson M, Gillott C, Hou X, Coutu C, Hegedus DD (2008) A chitin deacetylase and putative insect intestinal lipases are components of the *Mamestra configurata* (Lepidoptera: Noctuidae) peritrophic matrix. *Insect Mol Biol* 17:573–585
- Van Leeuwen T, Demaeght P, Osborne EJ, Dermauw W, Gohlke S, Nauen R, Grbic M, Tirry L, Merzendorfer H, Clark RM (2012) Population bulk segregant mapping uncovers resistance mutations and the mode of action of a chitin synthesis inhibitor in arthropods. *Proc Natl Acad Sci U S A* 109:4407–4412
- Veronico P, Gray LJ, Jones JT, Bazzicalupo P, Arbucci S, Cortese MR, Di Vito M, Giorgi C (2001) Nematode chitin synthases: gene structure, expression and function in *Caenorhabditis elegans* and the plant parasitic nematode *Meloidogyne artiellia*. *Mol Genet Genom* 266:28–34
- Wang P, Li G, Granados RR (2004) Identification of two new peritrophic membrane proteins from larval *Trichoplusia ni*: structural characteristics and their functions in the protease rich insect gut. *Insect Biochem Mol Biol* 34:215–227
- Wang S, Jayaram SA, Hemphala J, Senti KA, Tsarouhas V, Jin H, Samakovlis C (2006) Septate-junction-dependent luminal deposition of chitin deacetylases restricts tube elongation in the *Drosophila* trachea. *Curr Biol* 16:180–185
- Wang Y, Fan HW, Huang HJ, Xue J, Wu WJ, Bao YY, Xu XJ, Zhu ZR, Cheng JA, Zhang CX (2012) Chitin synthase 1 gene and its two alternative splicing variants from two sap-sucking insects, *Nilaparvata lugens* and *Laodelphax striatellus* (Hemiptera: Delphacidae). *Insect Biochem Mol Biol* 42:637–646
- Watanabe T, Kobori K, Miyashita K, Fujii T, Sakai H, Uchida M, Tanaka H (1993) Identification of glutamic acid 204 and aspartic acid 200 in chitinase A1 of *Bacillus circulans* WL-12 as essential residues for chitinase activity. *J Biol Chem* 268:18567–18572
- Willis JH (2010) Structural cuticular proteins from arthropods: annotation, nomenclature, and sequence characteristics in the genomics era. *Insect Biochem Mol Biol* 40:189–204
- Willis JH, Papandreou NC, Iconomidou VA, Hamodrakas SJ (2012) Cuticular proteins. In: Gilbert LI (ed) *Insect molecular biology and biochemistry*. Academic, Chapel Hill, pp 134–166
- Wu QY, Liu T, Yang Q (2013) Cloning, expression and biocharacterization of Cht5, the chitinase from the insect *Ostrinia furnacalis*. *Insect Sci* 20:147–157
- Xi Y, Pan PL, Ye YX, Yu B, Zhang CX (2014) Chitin deacetylase family genes in the brown planthopper, *Nilaparvata lugens* (Hemiptera: Delphacidae). *Insect Mol Biol* 23:695–705
- Xi Y, Pan PL, Ye YX, Yu B, Xu HJ, Zhang CX (2015) Chitinase-like gene family in the brown planthopper, *Nilaparvata lugens*. *Insect Biochem Mol Biol* 24:29–40
- Yang Q, Liu T, Liu FY, Qu MB, Qian XH (2008) A novel β -N-acetyl-D-hexosaminidase from the insect *Ostrinia furnacalis* (Guenée). *FEBS J* 275:5690–5702
- Yang WJ, Xu KK, Cong L, Wang JJ (2013) Identification, mRNA expression, and functional analysis of chitin synthase 1 gene and its two alternative splicing variants in oriental fruit fly, *Bactrocera dorsalis*. *Int J Biol Sci* 9:331–342

- Yang WJ, Wu YB, Chen L, Xu KK, Xie YF, Wang JJ (2015) Two chitin biosynthesis pathway genes in *Bactrocera dorsalis* (Diptera: Tephritidae): molecular characteristics, expression patterns, and roles in larval–pupal transition. *J Econ Entomol* 108:2433–2442
- Zen KC, Choi HK, Nandigama K, Muthukrishnan S, Kramer KJ (1996) Cloning, expression and hormonal regulation of an insect β -N-acetylglucosaminidase gene. *Insect Biochem Mol Biol* 26:435–444
- Zhang Y, Foster JM, Nelson LS, Ma D, Carlow CKS (2005) The chitin synthase genes *chs-1* and *chs-2* are essential for *C. elegans* development and responsible for chitin deposition in the eggshell and pharynx, respectively. *Dev Biol* 285:330–339
- Zhang J, Liu X, Li D, Sun Y, Guo Y, Ma E, Zhu KY (2010) Silencing of two alternative splicing-derived mRNA variants of chitin synthase 1 gene by RNAi is lethal to the oriental migratory locust, *Locusta migratoria manilensis* (Meyen). *Insect Biochem Mol Biol* 40:824–833
- Zhang J, Zhang X, Arakane Y, Muthukrishnan S, Kramer KJ, Ma E, Zhu KY (2011) Comparative genomic analysis of chitinase and chitinase-like genes in the African malaria mosquito (*Anopheles gambiae*). *PLoS One* 6(5):e19899
- Zhang D, Chen J, Yao Q, Pan Z, Chen J, Zhang W (2012a) Functional analysis of two chitinase genes during the pupation and eclosion stages of the beet armyworm *Spodoptera exigua* by RNA interference. *Arch Insect Biochem Physiol* 79:220–234
- Zhang X, Zhang J, Park Y, Zhu KY (2012b) Identification and characterization of two chitin synthase genes in African malaria mosquito, *Anopheles gambiae*. *Insect Biochem Mol Biol* 42:674–682
- Zheng YP, Retnakaran A, Krell PJ, Arif BM, Primavera M, Feng QL (2003) Temporal, spatial and induced expression of chitinase in the spruce budworm, *Choristoneura fumiferana*. *J Insect Physiol* 49:241–247
- Zhong XW, Wang XH, Tan X, Xia QY, Xiang ZH, Zhao P (2014) Identification and molecular characterization of a chitin deacetylase from *Bombyx mori* peritrophic membrane. *Int J Mol Sci* 15:1946–1961
- Zhu YC, Specht CA, Dittmer NT, Muthukrishnan S, Kanost MR, Kramer KJ (2002) Sequence of a cDNA and expression of the gene encoding a putative epidermal chitin synthase of *Manduca sexta*. *Insect Biochem Mol Biol* 32:1497–1506
- Zhu Q, Deng Y, Vanka P, Brown SJ, Muthukrishnan S, Kramer KJ (2004) Computational identification of novel chitinase-like proteins in the *Drosophila melanogaster* genome. *Bioinformatics* 20:161–169
- Zhu Q, Arakane Y, Banerjee D, Beeman RW, Kramer KJ, Muthukrishnan S (2008a) Domain organization and phylogenetic analysis of the chitinase-like family of proteins in three species of insects. *Insect Biochem Mol Biol* 38:452–466
- Zhu Q, Arakane Y, Beeman RW, Kramer KJ, Muthukrishnan S (2008b) Characterization of recombinant chitinase-like proteins of *Drosophila melanogaster* and *Tribolium castaneum*. *Insect Biochem Mol Biol* 38:467–477
- Zhu Q, Arakane Y, Beeman RW, Kramer KJ, Muthukrishnan S (2008c) Functional specialization among insect chitinase family genes revealed by RNA interference. *Proc Natl Acad Sci U S A* 105:6650–6655
- Zimoch L, Hogenkamp DG, Kramer KJ, Muthukrishnan S, Merzendorfer H (2005) Regulation of chitin synthesis in the larval midgut of *Manduca sexta*. *Insect Biochem Mol Biol* 35:515–527

Chapter 3

Molecular Model of Skeletal Organization and Differentiation

Bernard Moussian

Abstract The insect cuticle is an extracellular composite matrix deposited and organized by underlying epithelial cells. It protects the animal against dehydration, serves as a barrier against xenobiotics, pathogens and predators, and, as an exoskeleton, allows locomotion. To accommodate its various functions, the different components of the cuticle – the polysaccharide chitin, proteins, lipids and catecholamines – interact with each other forming a tri-dimensional structure. Despite its emergence in the Cambrium, this structure has retained its basic organization in all insect orders tested. Three horizontal layers are distinguished: the outer envelope, the middle epicuticle and the inner procuticle. The histology of the cuticle and the processes of its formation were analysed in detail especially in the kissing bug *Rhodnius prolixus* and the larger canna leafroller *Calpododes ethlius* particularly by electron microscopy. Most of the essential molecular players involved in cuticle formation were identified and characterized in the last decade using the fruit fly *Drosophila melanogaster* and the red flour beetle *Tribolium castaneum* as model insects employing genetic tools. This chapter aims at merging our histological and molecular knowledge by summarizing the central works on these four exemplar insect species.

3.1 Introduction

After a period of 13 or 17 years spent underground as larvae, a large number of adult cicadas of the genus *Magicicada* emerge and invade forests where they eat and mate (Karban et al. 2000; Karban 2014). And then end up in the stomach of a number of vertebrates including birds: Selma Lagerlöf describes impressively in her children's book "The wonderful adventures of Nils" how at the beginning of spring in Sweden awakening insect larvae populate large landscapes to boost primarily bird happiness expressed in their singing. Is this the fate of all insects, to be food for vertebrates?

B. Moussian (✉)
Genetik der Tiere, Eberhard-Karls Universität Tübingen,
Auf der Morgenstelle 28, 72076 Tübingen, Germany
e-mail: bernard.moussian@unice.fr

While indeed insects seem to be the protein source for bigger animals in many different ecological systems, at their own scale they are successful players, together assigning them as key elements of many natural environments. Especially in man-made environments they have attained doubtful fame as pests. In the up to 17 years before their eclosion, the *Magacicada* larvae live in the forest soil where they presumably contribute to soil and root ecology.

Insects are the most species-rich taxonomic class and occupy diverse terrestrial and marine ecological niches. A major defining structure of insects is their cuticle, a stratified extracellular matrix that is produced by the underlying epidermal cells. It is composed of the polysaccharide chitin, proteins and lipids, as well as small organic and inorganic molecules. The composition of the cuticle varies among body parts and species. In general, regardless of its exact composition, it is an essential coat that withstands the internal pressure of the animal thereby serving as an exoskeleton, at the same time protecting the organism against environmental harm and aggression. Numerous publications especially from the thirties to the eighties of the last century authored amongst others by Vincent Wigglesworth and Michael Locke have documented in great detail the ultrastructural architecture of the cuticle in various insects, important model insects being the kissing bug *Rhodnius prolixus* and the larger canna leafroller *Calpodes ethlius*. Following the terminology of Locke, the prototype of the cuticle consists of the three main composite layers: the outermost envelope, the middle epicuticle and the inner procuticle (Fig. 3.1) (Locke 2001). During the last decade or so, in the genomic era of insect biology, and based on genetic and molecular work in the fruit fly *Drosophila melanogaster* and the red flour beetle *Tribolium castaneum*, a detailed scheme of the molecular structure was drawn and ultimately would be merged with the histological scheme of the cuticle.

Comprehensive approaches describing the molecular model of cuticle organisation and differentiation have been published recently (Gilbert 2012; Moussian 2013). Therefore, in this chapter, I chose to take another approach and sketch this problem by summarising the main and fundamental results obtained from studies of the above-mentioned four model insects.

3.2 Cuticles of Model Insects

3.2.1 *The Cuticle of Rhodnius prolixus*

Sir Vincent Wigglesworth's seminal work on the arthropod cuticle is to a large extent based on the analyses of the kissing bug *R. prolixus*. *R. prolixus* is the vector of the protozoan *Trypanosoma cruzi* that causes Chagas fever in many subtropical and tropical regions (Abad-Franch et al. 2015). The actual reason Wigglesworth chose the kissing bug as a model insect was that staging of developmental and growth events (including cuticle formation) can easily be monitored in this animal because moulting is thoroughly controllable by blood feeding (Riddiford 2007).

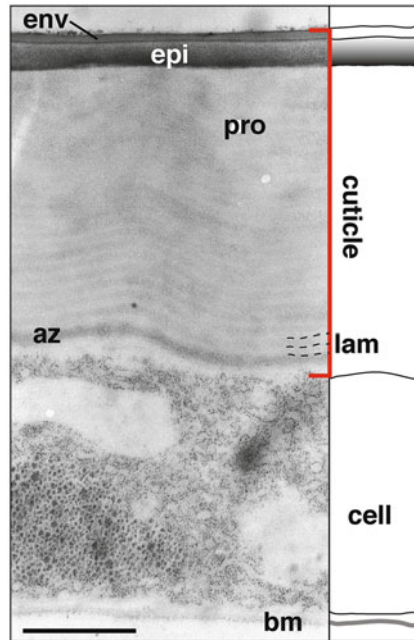


Fig. 3.1 The prototype of the insect cuticle, here the *D. melanogaster* 3rd instar larval cuticle (red bracket) by electron microscopy, is composed of three major horizontal layers at the apical site of epidermal cells that produce and organise them. The outermost layer is called envelope (env). Underneath lies the epicuticle (epi) that abuts the innermost procuticle (pro), which is laminar (lam, dashed lines). Adjacent to the apical site of the cell is the assembly zone (az, see Fig. 3.3), where cuticle material is deposited for sorting. The envelope and the epicuticle, according to Wigglesworth, constitute the outer and the inner epicuticle, respectively (see text). It is not possible to visualise free lipids at the surface of the cuticle at the ultrastructural level due to fixation protocol that involved lipid solvents. The basal site of the cell is covered by the basal membrane (bm) Scale bar 1 μm

The *R. prolixus* cuticle as described by Wigglesworth, consists of two composite layers that are subdivided in sub-layers (Fig. 3.1). The procuticle that may consist of an endo- and an exocuticle, is the chitin-bearing layer. Package of chitin laminae in the exocuticle is tighter than in the endocuticle. Moreover, the exocuticle appears to be tanned, while the endocuticle is not. The epicuticle is the outermost composite layer that is devoid of chitin. According to Wigglesworth's terminology, the epicuticle is subdivided into the outer and the inner epicuticle. The outer epicuticle corresponds to the envelope of Locke's terminology, while Wigglesworth's inner epicuticle is termed the epicuticle proper by Locke (2001). Amongst others, Wigglesworth revealed especially important features about lipid distribution in the epicuticle by sophisticated electron microscopy (Wigglesworth 1970, 1985a, b, 1988). Developing and using elaborate histological techniques, he showed that lipids are prominently present in the envelope (outer epicuticle), but also impregnate the inner epicuticle and the chitinous procuticle. This finding was confirmed in the

house cricket *Acheta domesticus* by Hendricks and Hadley (1983). Together these data suggest that cuticle lipid distribution is comparable in different insect species. In addition to the surface of the cuticle and within the epicuticle, lipids could also be detected in the chitinous exocuticle. Since *Rhodnius* (a hemipteran) and *Acheta* (an orthopteran) were separated very early in insect evolution, this suggests that lipid distribution within the cuticle may be very similar in all insects. The major lipid-containing molecule – probably in all insects – is cuticulin, a complex of proteins associated with lipids, which forms the so-called sclerotin that in turn interacts with phenolic compounds including catecholamines. The concept of cuticulin as the waterproof component of the insect cuticle was developed by Wigglesworth based on the work of Pryor (1940). The exact molecular constituents of cuticulin have not yet been determined.

Wigglesworth also speculated that cuticulin or commonly lipids might contribute to cuticle stiffness. An interesting and general issue that was investigated in *R. prolixus* is that mechanical properties of the cuticle may change depending on the physiological conditions. This aspect of cuticle plasticization in *R. prolixus* was investigated first by Bennet-Clark (1962) and then more extensively by Stuart Reynolds in Cambridge (see below). The main results of these analyses are that cuticle plasticization relies on intracuticular interaction between macromolecules and that changes of intracuticular pH values rather than of the ionic strength modulates these interactions (Reynolds 1974a, b, 1975). Cuticle plasticization is not unique to *R. prolixus* but also occurs in other insects at the time of moulting (e.g. *Calliphora* and *Manduca* (Reynolds 1985)) Possibly all insects can make use of this phenomenon at appropriate times in their lives. Another blood feeder, the completely unrelated (and non-insect) South African bont tick *Amblyomma hebraeum* also plasticizes its cuticle at the time of feeding, possibly using a similar mechanism to *R. prolixus* (Kaufman et al. 2010). This may indicate that cuticle plasticization is an evolutionarily ancient phenomenon. These findings should prove useful in understanding the mode of action of cuticle proteins that are being identified and studied in recent era of the genomic and molecular of cuticle research.

Research on the model insect *R. prolixus* has been boosted recently by the research groups around Monica Moreira and Hatisaburo Masuda at the federal university of Rio de Janeiro and the Instituto Nacional de Ciência e Tecnologia em Entomologia Molecular in Rio de Janeiro, which has published a couple of important papers on molecular and histological aspects of *R. prolixus* cuticle composition (Souza-Ferreira et al. 2014a, b). This group applied classical extraction and modern proteomic techniques to determine major components of the *R. prolixus* cuticle. By mass spectrometry, a total of 68 proteins were identified from embryonic cuticle extracts. Some of these proteins belong to families of classical insect chitin-binding cuticle proteins including CPRs, CPFs and CPAPs that have been extensively studied especially in the African malaria mosquito *Anopheles gambiae* (Cornman et al. 2008; Cornman and Willis 2009). Functional analyses of these proteins have not been carried out. Together, the classical detailed histological data on cuticle ultrastructure and recent molecular information will render the kissing bug a highly welcome and appreciated model insect to understand cuticle biology.

3.2.2 *The Cuticle of Calpodex ethlius*

The lepidopteran *C. ethlius* was the laboratory pet of Michael Locke. The architecture of the cuticle is basically the same as in *R. prolixus*. In 2001, he published a scheme of the cuticle unifying the nomenclature that we are using today and which was mentioned above. The outermost layer that was called outer epicuticle was in this scheme named, for the first time, the envelope. The layer underneath the envelope is termed the epicuticle, which in this scheme is no longer subdivided into zones. Finally, the entire chitinous layer is called procuticle that may be subdivided into the sclerotized exocuticle and the non-sclerotized endocuticle.

In two seminal works, Locke reported on the cellular mechanisms of cuticle formation in *C. ethlius* (Locke et al. 1965; Condoulis and Locke 1966; Locke and Huie 1979). In brief, actin-cored microvilli protruding at the apical plasma membrane carry electron-dense plaques at their tips where chitin is synthesised and extruded to the growing cuticle. Proteins and probably lipids are deposited in the valley between microvilli, a region he called perimicrovillar compartment (Locke 2003).

At this point, it should also be noted that the concept of pore canals as transport routes for lipids in the insect cuticle has been studied extensively in *C. ethlius*. Locke discriminated between the pore canals with a diameter of 150–200 Å that run through the entire procuticle and the so-called “wax canals” that have a diameter of 60 Å and emerge from the pore canals in the apical regions of the procuticle entering the epicuticle and contacting the envelope at the cuticle surface (Locke 1961, 1965, 1966). Wax canals are also found in non-insect arthropods such as scorpions (Filshie and Hadley 1979) underlining that they are ancient structures that evolved before the separation of chelicerates and insects. A central finding in the characterisation of pore and wax canals was the detection of an esterase in these structures (Locke 1961). Overall, however, the molecular constitution of the pore and wax canals remains enigmatic (see below).

Some molecular data are available on the *C. ethlius* cuticle. Sixteen proteins were detected in the cuticle of *C. ethlius* caterpillars using random polyclonal antibodies raised against integument and haemolymph extracts. Five proteins were detected within the procuticle, four in the pro- and one in the epicuticle, while only one was present in the epicuticle alone. Three antigens were found at the plasma membrane. Three other proteins are associated with ecdysial droplets that are supposed to digest the old cuticle during moulting. In the same work, using gold-conjugated wheat germ agglutinin (WGA) that recognises N-acetylglucosamine residues, it was confirmed that chitin is a component of the procuticle but not the epicuticle (Locke et al. 1994; Marcu and Locke 1999). What do we learn from these data? Assuming that detection was unambiguous, we can conclude that despite the distinction between the chitin containing procuticle and the chitin-less epicuticle as separate entities, some proteins are nevertheless shared by both of these layers. In summary, molecular biology of the *C. ethlius* cuticle is sparse. Unfortunately, since

the genome of *C. ethlius* has not been sequenced, identification of the main players of cuticle formation and structure remain elusive.

By contrast, the genomic sequences of other lepidopteran species such as the silkworm *Bombyx mori* and the tobacco hornworm *Manduca sexta* are available (Wang et al. 2005; Zhong et al. 2006; Dittmer et al. 2015; Tetreau et al. 2015a, b). Their cuticle, however, has been less intensively described, although a few descriptions have been published (Kawase 1961; Mitsui and Riddiford 1976; Wolfgang and Riddiford 1981; Ziese and Dorn 2003). Thus, in summary, some considerable work lies in front of us to enhance our merged understanding on the lepidopteran cuticle at the ultrastructural and molecular levels.

3.2.3 *The Cuticle of Drosophila melanogaster*

3.2.3.1 Cuticle Structure

The ultrastructure of cuticle formation in the embryo of the fruit fly *Drosophila melanogaster* was first described in 1970 by Ralph Hillman and Lorraine Heller Lesnik (1970). They reported that the layers, the epicuticle and the procuticle are deposited step-by-step. In 2006, we found that deposition of the different larval cuticle layers in the *Drosophila* embryo occurs at least partially simultaneously (Moussian et al. 2006a). First, fragments of the envelope precursor with two electron-dense sheets framing an electron-lucid one are deposited at the tips of irregular protrusions of the apical plasma membrane of epidermal cells. These fragments fuse eventually to form a continuous layer. During the maturation of the envelope to the alternating three electron-dense and two electron-lucid sheets, the epicuticle is assembled and chitin and chitin-organising proteins are deposited into the apical extracellular space forming the procuticle. These layers thicken synchronously (Fig. 3.2). This implies that the underlying molecular and cellular mechanisms are deployed in parallel in space and time without interfering with each other. The cellular mechanisms of layer construction support the cuticle model of Locke proposed in 2001: assembly of the distinct layers *envelope*, *epicuticle* and *procuticle*, occurs independently from each other suggesting specific and distinct underlying constructing mechanisms. In other words and more generally, these three composite layers are distinct building units of the cuticle prototype.

During procuticle production, the apical plasma membrane of the epidermal cells forms regular longitudinal protrusions, the so-called apical undulae. Similar to the microvillus-like structures observed in the moulting epidermis of other insects including *C. ethlius*, these corrugations carry an electron-dense plaque at their tips, where chitin is synthesised and deposited into the extracellular space. In the valley between these structures, the secretory pathway delivers cuticular materials packed in vesicles that eventually fuse with the apical plasma membrane to release their content into the growing cuticle. This repetitive arrangement at the apical plasma membrane may imply highly regulated spatial production of the cuticle. The molec-

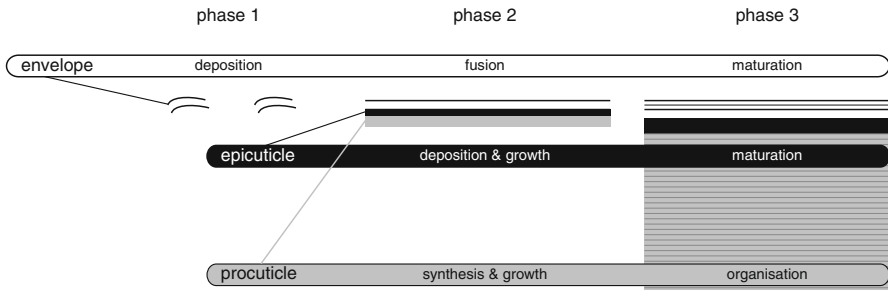


Fig. 3.2 Model for cuticle formation in insects

The prototype of the insect cuticle consists of three composite layers – the envelope, the epicuticle and the procuticle – that are formed independently and simultaneously. Conceptually, formation can be subdivided into three phases. During phase 1, fragments of the envelope are deposited in the extracellular space. During phase 2, these fragments fuse to establish a continuous layer. Concomitantly, epicuticular material accumulates underneath the immature envelope, and chitin is synthesised initiating the formation of the procuticle underneath the immature epicuticle. At phase 3, all three layers attain their final thickness and constitution. In particular, the envelope has now five layers of different electron-density, the epicuticle partitions into an electron-lucid upper part and an electron-dense lower part, and chitin microfibrils become arranged to distinct laminae

ular mechanisms establishing this subcellular architecture are absolutely enigmatic. In the simplest scenario, it might arise merely from the mutual exclusivity of the cellular processes that form chitin and other components of the cuticle. An important question regarding these membrane structures in different insect species concerns their relatedness: to what extent are microvilli-like and longitudinal protrusions alike? Both structures are stabilised by the cytoskeleton. Microvilli-like structures have an actin core, whereas apical undulae are supported by filaments of microtubules. The presence of actin in these structures has not been described but cannot be excluded. Potentially, those factors associated with conventional microvilli such as Villin and Fascin and others may also be involved in the formation of the membrane protrusions of the cuticle depositing epithelial cells (Yamashiro et al. 1998; Matova et al. 1999). Taken together, only a little is known about the molecular constitution of these structures, which therefore await detailed analyses.

3.2.3.2 Chitin Synthesis and Organisation

Who are the effective players of cuticle production? As probably in all biological systems, components of the system can be subdivided into two groups: those that drive the system (during development) but are not part of it, and those that are part of the system. The genetic approach has led to the identification of about 20 genes that are important for the formation of the cuticle in *D. melanogaster* (Table 3.1). Obviously, several proteins act in the secretory pathway. Mutations in genes coding for these proteins cause a strongly reduced cuticle. This is trivial, however, as a close inspection of the respective phenotypes teaches us that all three major layers

Table 3.1 Genes genetically characterised in *Drosophila melanogaster*

Gene	Molecular function	Cellular function
<i>ghost (gho)</i>	Sec24 of COPII vesicles	Secretion
<i>haunted (hau)</i>	Sec23 of COPII vesicles	Secretion
<i>Sar1</i>	Small GTPase of COPII vesicles	Secretion
<i>Wollknäuel (wol)</i>	UDP-glucose transfer	N-glycosylation in ER
<i>garnistan (gar)</i>	UDP-glucose transfer	N-glycosylation in ER
<i>Syntaxin1A (syx1A)</i>	SNARE complex	Secretion, vesicle fusion
<i>Sec61β</i>	Sec61 translocon complex	Secretion
<i>CrebA</i>	DNA binding	Transcription of secretion genes
<i>Krotzkopf verkehrt</i>	Glycosyltransferase	Chitin synthesis
<i>Knickkopf</i>	Unknown	Chitin organisation
<i>Retroactive</i>	Unknown	Chitin organisation
<i>Vermiform</i>	Chitin deacetylation	Chitin organisation
<i>Serpentine</i>	Chitin deacetylation	Chitin organisation
<i>grainyhead</i>	CF2-type domain DN binding	Transcription of chitin genes
<i>Expansion</i>	SMAD-domain	Localisation of Kkv
<i>Rebuf</i>	SMAD-domain	Localisation of Kkv
<i>Tubby</i>	Unknown	Body size
<i>TweedleD</i>	Unknown	Body size
<i>Dsc73c</i>	Unknown	Cuticle organisation
<i>ObstA</i>	Chitin-binding	Cuticle organisation
<i>Gasp (Obst-C)</i>	Chitin-binding	Cuticle organisation
<i>cpr72Ec</i>	Chitin-binding	Insecticide resistance
<i>Lcp-1</i>	Chitin-binding	Insecticide resistance
<i>Chitinase-2</i>	Chitin degradation	Chitin organisation

of the cuticle require material delivered by secretory vesicles. Some other factors found initially in *D. melanogaster* are implicated in procuticle production and organisation. The central enzyme of procuticle production is the membrane-inserted glycosyltransferase chitin synthase called Krotzkopf verkehrt (Kkv) in *D. melanogaster* (Moussian et al. 2005a). Mutations in the respective gene cause a chitin-less cuticle that fails to maintain the body shape of the animal, which, as expected, dies before hatching from the egg. Chitin organisation in the cuticle is not an intrinsic property of naked chitin fibres but requires specific proteins. An essential chitin organising protein is the membrane-bound dopamine-monoxygenase (DOMON) domain protein Knickkopf (Knk) (Moussian et al. 2006b; Shaik et al. 2014). The biochemical function of Knk is unknown; the DOMON domain suggests, however, that Knk might transfer electrons to yet unidentified substrates. In *knk* mutant larvae, chitin although present, is disorganised. In consequence, the larvae fail to hatch and die within the egg case. Similar to Knk, the membrane-bound snake-toxin-like protein Retroactive (Rtv) is needed for chitin organisation (Moussian et al. 2005b, 2006b).

Besides these two membrane proteins, the extracellular chitin deacetylases Vermiform and Serpentine that are predicted to randomly remove acetate moieties from the N-acetyl-glucosamine (GlcNAc) units of chitin are important chitin organising proteins (Luschnig et al. 2006). The exact significance of this reaction is not understood. On the extracellular side, close to the apical plasma membrane of epidermal cells, the interplay between Knk, Serp and Verm to assemble and organise chitin is coordinated by the chitin-binding protein Obstructor-A (ObstA) (Pesch et al. 2015). Recently, two unexpected cytosolic SMAD-domain proteins, namely Rebuf (Reb) and Expansion (Exp) were identified to be important triggers of chitin synthesis during development (Moussian et al. 2015). Indeed, the chitin synthase enzyme is not able to produce chitin in absence of these proteins. Moreover, co-expression of these factors in tissues like the salivary glands that usually do not produce chitin, results in the synthesis of chitin that is deposited into the extracellular space (Moussian et al. 2015). Thus, both chitin synthase and Reb or Exp are necessary and sufficient for chitin synthesis. The exact interaction between chitin synthase and Reb and/or Exp is not yet understood. This situation is different albeit analogous to the situation in the yeast *Saccharomyces cerevisiae*. Chs4p and Shc1p that are unrelated to Reb and Exp assist localisation of chitin synthase III to the yeast plasma membrane (Sanz et al. 2002; Reyes et al. 2007). Taken together, chitin synthesis and organisation implies intracellular membrane and extracellular molecular processes. Based on homology searches, the presence and absence of certain factors (i.e. Exp does not have counterparts outside dipterans) we conclude that the molecular mechanisms of temporal and spatial chitin synthesis and assembly may differ in different insect species, while nevertheless resulting in a comparable structure (Table 3.2).

Besides its function as a structural element of the cuticle, chitin plays also a role in cuticle pigmentation. Mutations in *kkv* affect melanisation of the ventral denticles of the larvae (Moussian et al. 2005a). This observation is supported by the finding that in adult flies hypomorphic mutations in *kkv* cause weak pigmentation (Dembeck et al. 2015). This finding nicely illustrates that different pathways or aspects of cuticle construction depend on each other.

Table 3.2 Genes genetically characterised in *Tribolium castaneum*

Gene	Molecular function	Cellular function
<i>Chitin synthase A</i>	Glycosyltransferase	Chitin synthesis
<i>Knickkopf 1-3</i>	Unknown	Chitin organisation
<i>Retroactive</i>	Unknown	Knk localisation
<i>Chitin deacetylases</i>	Chitin deacetylation	Chitin organisation
<i>Cpr4</i>	Chitin binding	Chitin organisation
<i>Cpr18</i>	Chitin binding	Chitin organisation
<i>Cpr27</i>	Chitin binding	Chitin organisation
<i>Cht5 & 10</i>	Chitin degradation	Chitin organisation

3.2.3.3 The Function of Cuticle Proteins

Cuticle proteins are major components of the cuticle defining its physical properties. In the extracellular space, chitin is bound by chitin-binding proteins that have either a chitin-binding domain 2 (CBD2, like ObstA) or the Rebers and Riddiford chitin-binding domain (R&R). The fruit fly genome harbours 102 R&R-domain proteins called CPR and 10 CBD2 proteins (Behr and Hoch 2005; Cornman 2009). To date, it is unclear whether all CPRs localise to the cuticle or whether at least some may localise to the peritrophic matrix, the chitin-containing extracellular matrix of the midgut. Tissue expression of some CBD2 protein coding genes has been monitored. Some of these proteins in fact also localise to the midgut. Interestingly, the number of proteins of these two protein families varies between even closely related insect species. In the dipteran *An. gambiae*, for instance, there are 156 CPRs (Cornman 2009). In both cases, the presence of chitin-binding domains trivially suggests that they are needed to protect chitin or to stabilise chitin organisation. In the *D. melanogaster* strain 91-R, which is less susceptible to insecticides such as DDT, the expression of *cpr72Ec* and *Lcp-1*, both coding for R&R proteins is up-regulated (Qiu et al. 2013). Exposure of *D. melanogaster* to persistent insecticides such as endosulfan induces the expression of several *cpr* genes (Sharma et al. 2011). Interestingly, *cpr72Ec* is not included in this set of genes, but *Lcp-1* is. Up-regulation of *cprs* upon environmental stress is not confined to *D. melanogaster*. In the bed bug *Cimex lectularius*, it was shown that elevated expression of several CPRs correlates with resistance to pyrethroid insecticides, possibly by preventing penetration of the poison (Koganemaru et al. 2013). These findings together suggest that the extent to which specific CPRs are present in the cuticle may define its barrier strength i.e. cuticle permeability and/or mechanics, through their interaction with chitin, depending on the stimulus. It remains to be analysed whether over-expression of these proteins is accompanied by proportional increase in chitin amounts, or whether their over-expression simply results in a higher density of protein associated with the same quantity of existing chitin microfibrils. Environmental signals have also an effect on the expression of CBD2 proteins. Along with CPRs also two CBD2 proteins are enriched in endosulfan-treated flies (Sharma et al. 2011). In addition, the function of CBD2 proteins was studied using genetic approaches. The role of Obst-A in chitin organisation was mentioned above (Petkau et al. 2012; Pesch et al. 2015). Gasp (or Obst-C) is another CBD2 protein that is needed for chitin organisation in tracheal system (Tiklova et al. 2013). Hence, while CPRs seem to have a structural role only, CBD2 proteins appear to be additionally required during cuticle construction.

Most, if not all of these factors described above are involved in procuticle formation. Only a few potentially non-procuticle proteins have been identified to date in *D. melanogaster*. Dominant mutations in two genes coding for Tweedle proteins, *tweedle D* (*twlld*) and *tubby* (*Tb*) provoke a body shape change in larvae, pupae and adult flies (Guan et al. 2006). The respective animals are shorter but thicker than wild-type animals. Interestingly, *tweedle* homozygous mutants are viable displaying the same phenotype as heterozygous siblings. Non-lethality of *tweedle* mutations

suggests that modifications in *tweedle* expression and sequence may be evolutionary mechanisms to vary body shape in insects. Indeed, it is important to note that the *tweedle* genes evolve fast. While in *D. melanogaster* there are 27, in the yellow fever mosquito *Aedes aegypti* there are 12 and in the honeybee *Apis mellifera* only two *tweedle* genes (Cornman 2009; Soares et al. 2011). At least in *A. mellifera*, it was reported that expression of *tweedle* genes depends on ecdysone signalling. This links a major insect developmental signalling pathway to the regulation of body shape, suggesting an intriguing mechanism of shape control in insects. The molecular or biochemical function of these proteins in cuticle construction has not been investigated. In one case, BmCPT1 from *B. mori*, was proposed to be a receptor for peptidoglycan on the surface of the bacterium *Escherichia coli* in the haemolymph (Soares et al. 2011; Liang et al. 2015). To what extent this finding is physiologically relevant for cuticle construction, can only be a matter of extensive speculation that I dare to omit here.

3.2.3.4 Molecular Construction Mechanisms

Obviously, in order to implement the correct cuticle architecture, cuticle components must interact with each other to form a mechanical network that is stiff and hard enough to protect the animal against environmental harm, but flexible enough to allow locomotion. Some mechanisms underlying the construction of this network occur within the cell, some at the plasma membrane and some in the extracellular space.

Sorting of cuticle components relies on the canonical secretory pathway in the cell. This simple but nevertheless seminal statement is based on several published works on *D. melanogaster*. The transcription factors CREB-A regulates the expression of an arsenal of genes that code for components of the secretory pathway (Abrams and Andrew 2005). Glycosylation of cuticle proteins in the endoplasmic reticulum involves Wollknäuel (Wol) and Garnystan (Gny) (Shaik et al. 2011). Mutations in the respective genes cause attenuation of glycosylation and a disorganised cuticle suggesting that these two enzymes are needed for coordinated construction of the cuticle. The apical plasma membrane is equipped with t-SNAREs including Syntaxin 1A (Syx1A) that mediate fusion of vesicles with different cargos (Moussian et al. 2007). Syx1A is needed for the secretion of some glycosylated cuticle proteins, whereas several chitin synthesising and organising proteins that are inserted in the plasma membrane employ another yet unknown t-SNARE for correct localisation.

Probably to stabilise cuticle structure, some proteins are covalently linked to each other in the extracellular matrix, and this is mediated either directly or indirectly by reactive small organic molecules (see more details in Chap. 6). Derivatives of dopamine including N-acetyldopamine (NADA) and N- β -alanyldopamine (NBAD) are a class of these small organic molecules. Their synthesis begins in the cytoplasm. Through a yet unknown transporter they are delivered into the extracellular space where they are further modified and cross-linked especially with proteins

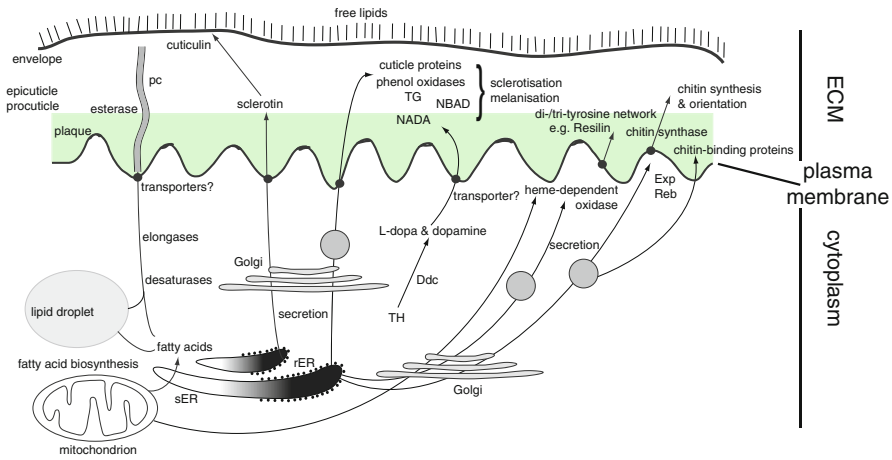


Fig. 3.3 Biochemical pathways of cuticle formation

The insect cuticle is formed through the integration of mechanisms occurring in the cytoplasm, the plasma membrane and the extracellular space (ECM) of epithelial cells. In the cytoplasm, the precursors of cuticle components are produced. Initially, lipid precursors that were produced by sub-epidermal oenocytes and fat body cells enter the cuticle forming cell at its basal site. This process is omitted here. Lipid synthesis and modification involves enzymes in the cytoplasm and located to the mitochondrion, lipid droplets and the smooth endoplasmic reticulum (sER). Lipids are subsequently transported to the cuticle by a yet unknown mechanism. It is possible that pore canals (PC) are implicated in this process. Lipids cover either the surface of the cuticle (“free lipids”) or interact with sclerotin to form cuticullin, an enigmatic immobilised form of lipids. Synthesis of reactive catecholamines (NBAD and NADA) takes place in the cytoplasm (tyrosine hydroxylase, TH and Dopamine-decarboxylase, Ddc), as well. A yet unknown transport mechanism delivers NADA and NBAD precursors to the ECM where these two molecules are formed and linked to proteins, a process called sclerotisation and melanisation. Proteins may also be cross-linked through the activity of a transglutaminase. Membrane-inserted oxidases contribute to covalent protein cross-links (e.g. dityrosines), as well. Chitin synthesis also starts in the cytoplasm, where the monomer N-acetyl-glucosamine is synthesised. The chitin synthase enzyme itself is a membrane-inserted protein that extrudes nascent chitin fibres into the ECM, where they are modified (e.g. deacetylated), recognised by chitin-binding proteins and organised. Full chitin synthase activity depends on the cytoplasmic SMAD-like proteins Exp and Reb. The *green area* in the ECM represents the assembly zone (see Fig. 3.1) where the different components are presumably assembled

by enzymes such as Yellow, a dopachrome conversion enzyme. In *D. melanogaster*, most genes coding for cytoplasmic and extracellular enzymes constituting this pathway (see Fig. 3.3) were isolated and characterised extensively (Wright 1987). Overall, they are well conserved among insects.

Correct structure of the larval cuticle also depends on one or several haem-associated enzymes that catalyse cross-linking of proteins. Mutations in the gene coding for the mitochondrial enzyme aminolevulinic acid synthase (Alas) cause breaks especially in the larval procuticle of *D. melanogaster* (Shaik et al. 2012). The target proteins that require haem to stabilise the larval cuticle remain to be identified.

A good candidate is the dual oxidase protein (Duox) that was shown to be needed for wing tanning (Anh et al. 2011). Duox activity promotes the formation of covalent di- and tri-tyrosine bridges between cuticle proteins. Concentrations of oxygen radicals are consistently reduced in wings with suppressed *duox* expression. Dominant mutations in this gene, by contrast, do not interfere with cuticle tanning but with cuticle shape (Hurd et al. 2015). These mutations called *Curly* (*Cy*) cause the exchange of a conserved glycine to a serine or cysteine, an exchange that characterises also human *duox* variants. Whether Duox function is necessary during larval cuticle formation in the embryo was not tested.

Another extracellular enzyme that creates covalent bonds between cuticle components is transglutaminase. It crosslinks glutamines with lysines in distinct cuticle proteins, including among others two Cprs, Cpr76Bd and Cpr97Eb (Shibata et al. 2010). This network has been suggested to constitute a barrier against desiccation. However, as many mutations in genes that encode cuticle components compromise its ability to prevent water-loss, more thorough and conclusive analyses of this issue are needed.

3.2.4 *The Cuticle of Tribolium castaneum*

3.2.4.1 Cuticle Structure

In *T. castaneum*, different types of cuticle were studied at different developmental stages. The larval cuticle is composed of the envelope, the epicuticle and the procuticle, which is subdivided into the exocuticle and the endocuticle. The elytral cuticle of the adult is a thick extracellular matrix consisting of the envelope, the epicuticle and the compact procuticle. The protein-chitin network is packed in brick-like units that are occasionally separated by vertical chitin-filled channels that run through the entire procuticle. In recent publications (see below), these channels are called “pore canals” although the analogy to the pore canals described by Wigglesworth and Locke is disputable. The pore canals of Wigglesworth and Locke are transport tubes, whereas the *T. castaneum* pore canals shown in these publications are rather stabilising elements of the cuticle. A distinction between exo- and endocuticle is not obvious in the elytral cuticle.

3.2.4.2 Molecular Mechanisms of Cuticle Construction

The advent of *T. castaneum* as a model insect to study cuticle formation and function was initiated at the Kansas State University. It was mainly the work of Yasuyuki Arakane working in the group of Subbaratnam Muthukrishnan and Michael Kanost and later at the Chonnam National University in South Korea that, based on genomic data and the RNA interference (RNAi) technique, characterised several essential cuticle factors. Basically, the data collected in this beetle are in agreement with

those produced in *D. melanogaster*. Down-regulation of the expression of the genes coding for the epidermal chitin synthase, *chs1* or for the chitin deacetylases 1 and 2 cause chitin deficiency and failure to moult in larvae and pupae (Arakane et al. 2005, 2009). Recently, the function of *chs1* was tested also in embryos (Arakane et al. 2008; Chaudhari et al. 2015). The procuticle of ready-to-hatch larvae with reduced Chs1 activity is thin, they are unable to hatch and die within the egg case. Of note, not only the body cuticle is affected in these animals but also the protective serosal cuticle (see more details in Chap. 10). Similarly, reduction of TcRtv and TcKnk function in embryos results in lethality presumably caused by defective body and serosal cuticles (Chaudhari et al. 2015; Jacobs et al. 2015).

The roles of TcKnk and TcRtv were analysed in detail during moulting. It was demonstrated that delivery of TcKnk to the apical plasma membrane and subsequently to the extracellular space depends on the function of TcRtv. Moreover, TcKnk is needed to prevent premature degradation of chitin by two chitinases, Cht5 and Cht10. Like TcKnk, also the paralogues TcKnk2 and TcKnk3 are essential factors that are especially needed for cuticular protrusions like denticles and tracheal taenidia (Chaudhari et al. 2014). These findings suggest functional specialisation of Knk proteins after duplication of the original *knk1* gene that has a universal role in chitin organisation. The salient question in this regard is as to whether Rtv, which does not have any paralogues, may be required for correct localisation of TcKnk2 and 3, as well.

The functions of three chitin-binding proteins of the CPR family in *T. castaneum* were investigated in detail (Arakane et al. 2012; Noh et al. 2014, 2015). TcCpr4 localises predominantly in the vertical pore canals in the procuticle of the elytra. TcCpr27 is found in both the horizontal chitin bricks of the procuticle and in the pore canals. Especially in the *TcCpr4*-reduced cuticle, the vertical chitin canals were wider, the chitin filament was less organised and did not traverse the procuticle in a straight line suggesting that TcCpr4 is needed for the compactness and integrity of these structures. In both TcCpr4- and TcCpr27-deficient elytra, tight packing of chitin bricks was lost. An important finding was that TcCpr27 is needed for TcCpr4 distribution within the procuticle without affecting the total amount of the protein, while TcCpr4 is dispensable for correct TcCpr27 localisation. Especially, TcCpr4 localisation to the pore canals depends on TcCpr27. In this view, mislocalisation of TcCpr4 in TcCpr27-deficient cuticle might be cause of disorganised chitin bricks in the respective procuticle. It is, however, unclear how TcCpr27, being expressed in both the chitin bricks and the pore canals, may restrict TcCpr4 localisation to the pore canals. The situation is even more complicated: TcCpr18 seems also be involved in this process (Noh et al. 2014); its exact role remains to be shown.

Just recently, Yasuyuki Arakane's group showed that the low-complexity cuticle protein CP30 (which does not seem to belong to any known cuticle protein family) might be cross-linked to TcCpr18 and TcCpr27 in a laccase2-dependent reaction that is necessary for elytral hardening (Mun et al. 2015). The role of Cpr proteins in defining chitin-based physical properties of the cuticle that emerges from this work on *Tribolium* is also supported by work on Cpr2 in the silkworm *B. mori* (Qiao et al. 2014). *B. mori* larvae mutant for the *cpr2* gene called *stony* have less chitin than

wild-type larvae, are smaller and their cuticle is fragile. This complex phenotype impedes, however, a clear conclusion about the role of BmCpr2 in chitin organisation and function. Overall, these data support the notion that organisation of the chitin-protein matrix along with cytoplasmic and membrane-associated processes involves molecular events occurring in the extracellular matrix. However, the exact function of Cprs in chitin organisation is yet elusive.

Molecular studies of *T. castaneum* cuticle formation have also advanced our understanding of cuticular sclerotisation and melanisation processes (Noh et al. 2015) (see more details in Chap. 6). Suppression of the expression of *yellow-e* (coding for an extracellular dopachrome conversion enzyme) by dsRNA injection results in viable adult animals that, however, do not withstand drought. These findings indicate that sclerotisation contributes to the barrier function of the cuticle.

Taken together, work in the flour beetle *T. castaneum* substantially supplemented findings in the fruit fly *D. melanogaster* and additionally yielded valuable insights into diverse aspects of insect cuticle formation and function.

3.3 Conceptual and Molecular Model of Cuticle Differentiation

3.3.1 Conceptual Model of Cuticle Differentiation

Principles of cuticle differentiation, which have been studied extensively during moulting in various insect species, were nicely reviewed by Locke (2001). Moulting, however, is not a simple process as cuticle degradation and formation occur at the same time. Therefore, analyses of cuticle differentiation during moulting may somehow yield nebulous results regarding the cellular and molecular mechanisms deployed. *De novo* cuticle differentiation during embryogenesis, by contrast, is a simple process. Comparably, only little data has been published on this matter (Hillman and Lesnik 1970; Ziese and Dorn 2003; Moussian et al. 2006a; Havemann et al. 2008). Studying cuticle differentiation in the embryo of *D. melanogaster* revealed that the establishment of the three main layers envelope, epicuticle and procuticle occurs simultaneously (Moussian et al. 2006a). A model describing the underlying events is shown in Fig. 3.2.

3.3.2 Molecular Model of Cuticle Differentiation

Most of our insight on molecular details of cuticle formation is based on work in *D. melanogaster* and *T. castaneum*. Most of our insight on histology of cuticle formation is however based on work in *R. prolixus* and *C. ethlius*. Here, I model the molecular pathways that are deployed during cuticle formation in insects merging them with histological data (Fig. 3.3).

The foundations for cuticle construction are laid within the epidermal cells when proteins (both structural ones and enzymes) are transported and processed through the canonical secretory pathway for correct modification and final localisation in the ECM or in the plasma membrane, and when monomers or precursors of non-protein cuticle components such as chitin, melanin, sclerotin and waxes, are synthesised. Some important key reactions of cuticle formation occur in the apical plasma membrane. The membrane-inserted glycosyltransferase chitin synthase uses UDP-GlcNAc monomers to synthesise chitin. The activity of this enzyme is assisted by the cytoplasmic SMAD-like proteins Reb and Exp. At the same time, several membrane-inserted and extracellular oxidases catalyse cross-linking of extracellular components including chitin, dopamine-derivatives and proteins within the procuticle (ref Schäfer). It should be noted that delivery of dopamine-derivatives and lipids into the growing cuticle is still enigmatic. Assembly of the procuticle, i.e. chitin orientation and organisation, occurs in the so-called assembly zone in the ECM adjacent to the apical plasma membrane. The extracellular, chitin-binding and modifying proteins ObstA, Verm, Serp and Knk might form a core complex in this zone. Additionally, the chitin degrading protein chitinase-2 that seems also to be involved in chitin organisation localises close to the apical plasma membrane (Pesch et al. 2016). The exact underlying molecular events occurring in this zone have not been revealed, yet. Overall, the formation of the procuticle has been addressed and studied in detail in the last decade, and we are advancing fast in our understanding of this layer. Failure to exactly identify and name the molecules that constitute the epicuticle and the envelope – proteins and lipids – has, by contrast, hampered the study of the formation of these layers at the molecular level.

3.4 Outlook

The histological and molecular analyses of cuticle formation in the four model insects presented here demonstrate that the basic underlying mechanisms are conserved among species. Of course, the cuticles of many other insect species, somewhat neglected here including those of *A. melifera* and the migratory locust *Locusta migratoria*, have also been investigated in detail (Zhang et al. 2010; Falcon et al. 2014; Wang et al. 2014). Moreover, genome information for many additional interesting and important insect species has also allowed identification and characterisation of key factors of cuticle formation and structure. Taken together, all these data lead to a relatively small number of conclusions. One is that different tissues in a given insect species, as well as differences between species, involve tissue- and species-specific factors with core domains that are evolutionary conserved such as the R&R domain in Cprs, which define the architecture of the cuticle. Hence, cuticle quality is dictated by evolved sequence differences around conserved domains rather than invention of new players. Elucidation of the function of non-conserved sequences in shared factors will contribute to our understanding of the molecular mechanisms of cuticle formation and of the molecular basis of cuticle versatility, and epicuticle and envelope assembly.

References

- Abad-Franch F, Lima MM, Sarquis O, Gurgel-Goncalves R, Sanchez-Martin M, Calzada J, Saldana A, Monteiro FA, Palomeque FS, Santos WS, Angulo VM, Esteban L, Dias FB, Diotaiuti L, Bar ME, Gottdenker NL (2015) On palms, bugs, and chagas disease in the Americas. *Acta Trop* 151:126–141
- Abrams EW, Andrew DJ (2005) CrebA regulates secretory activity in the *Drosophila* salivary gland and epidermis. *Development* 132:2743–2758
- Anh NT, Nishitani M, Harada S, Yamaguchi M, Kamei K (2011) Essential role of Duox in stabilization of *Drosophila* wing. *J Biol Chem* 286:33244–33251
- Arakane Y, Muthukrishnan S, Kramer KJ, Specht CA, Tomoyasu Y, Lorenzen MD, Kanost M, Beeman RW (2005) The *Tribolium* chitin synthase genes TcCHS1 and TcCHS2 are specialized for synthesis of epidermal cuticle and midgut peritrophic matrix. *Insect Mol Biol* 14:453–463
- Arakane Y, Specht CA, Kramer KJ, Muthukrishnan S, Beeman RW (2008) Chitin synthases are required for survival, fecundity and egg hatch in the red flour beetle, *Tribolium castaneum*. *Insect Biochem Mol Biol* 38:959–962
- Arakane Y, Dixit R, Begum K, Park Y, Specht CA, Merzendorfer H, Kramer KJ, Muthukrishnan S, Beeman RW (2009) Analysis of functions of the chitin deacetylase gene family in *Tribolium castaneum*. *Insect Biochem Mol Biol* 39:355–365
- Arakane Y, Lomakin J, Gehrke SH, Hiromasa Y, Tomich JM, Muthukrishnan S, Beeman RW, Kramer KJ, Kanost MR (2012) Formation of rigid, non-flight forewings (elytra) of a beetle requires two major cuticular proteins. *PLoS Genet* 8:e1002682
- Behr M, Hoch M (2005) Identification of the novel evolutionary conserved obstructor multigene family in invertebrates. *FEBS Lett* 579:6827–6833
- Bennet-Clark HC (1962) Active control of the mechanical properties of insect endocuticle. *J Insect Physiol* 8:627–633
- Chaudhari SS, Moussian B, Specht CA, Arakane Y, Kramer KJ, Beeman RW, Muthukrishnan S (2014) Functional specialization among members of Knickkopf family of proteins in insect cuticle organization. *PLoS Genet* 10:e1004537
- Chaudhari SS, Noh MY, Moussian B, Specht CA, Kramer KJ, Beeman RW, Arakane Y, Muthukrishnan S (2015) Knickkopf and retroactive proteins are required for formation of laminar serosal procuticle during embryonic development of *Tribolium castaneum*. *Insect Biochem Mol Biol* 60:1–6
- Condoulis W, Locke M (1966) Depositon of endocuticle in an insect *Calpodus ethlius* Stoll (Lepidoptera Hesperidae). *J Insect Physiol* 12:311
- Cornman RS (2009) Molecular evolution of *Drosophila* cuticular protein genes. *PLoS One* 4:e8345
- Cornman RS, Willis JH (2009) Annotation and analysis of low-complexity protein families of *Anopheles gambiae* that are associated with cuticle. *Insect Mol Biol* 18:607–622
- Cornman RS, Togawa T, Dunn WA, He N, Emmons AC, Willis JH (2008) Annotation and analysis of a large cuticular protein family with the R&R consensus in *Anopheles gambiae*. *BMC Genomics* 9:22
- Dembeck LM, Huang W, Magwire MM, Lawrence F, Lyman RF, Mackay TF (2015) Genetic architecture of abdominal pigmentation in *Drosophila melanogaster*. *PLoS Genet* 11:e1005163
- Dittmer NT, Tetreau G, Cao X, Jiang H, Wang P, Kanost MR (2015) Annotation and expression analysis of cuticular proteins from the tobacco hornworm, *Manduca sexta*. *Insect Biochem Mol Biol* 62:100–113
- Falcon T, Ferreira-Caliman MJ, Franco Nunes FM, Tanaka ED, do Nascimento FS, Gentile Bitondi MM (2014) Exoskeleton formation in *Apis mellifera*: cuticular hydrocarbons profiles and expression of desaturase and elongase genes during pupal and adult development. *Insect Biochem Mol Biol* 50:68–81
- Filshie BK, Hadley NF (1979) Fine structure of the cuticle of the desert scorpion, *Hadrurus arizonensis*. *Tissue Cell* 11:249–262

- Gilbert LI (ed) (2012) Insect molecular biology and biochemistry, 1st edn. Academic Press, London
- Guan X, Middlebrooks BW, Alexander S, Wasserman SA (2006) Mutation of TweedleD, a member of an unconventional cuticle protein family, alters body shape in *Drosophila*. Proc Natl Acad Sci U S A 103:16794–16799
- Havemann J, Muller U, Berger J, Schwarz H, Gerberding M, Moussian B (2008) Cuticle differentiation in the embryo of the amphipod crustacean *Parhyale hawaiiensis*. Cell Tissue Res 332:359–370
- Hendricks GM, Hadley NF (1983) Structure of the cuticle of the common house cricket with reference to the location of lipids. Tissue Cell 15:761–779
- Hillman R, Lesnik LH (1970) Cuticle formation in embryo of *Drosophila melanogaster*. J Morphol 131:383–396
- Hurd TR, Liang FX, Lehmann R (2015) Curly encodes dual oxidase, which acts with heme peroxidase Curly Su to shape the adult *Drosophila* wing. PLoS Genet 11:e1005625
- Jacobs CG, Braak N, Lamers GE, van der Zee M (2015) Elucidation of the serosal cuticle machinery in the beetle *Tribolium* by RNA sequencing and functional analysis of knickkopf1, retroactive and laccase2. Insect Biochem Mol Biol 60:7–12
- Karban R (2014) Transient habitats limit development time for periodical cicadas. Ecology 95:3–8
- Karban R, Black CA, Weinbaum SA (2000) How 17-year cicadas keep track of time. Ecol Lett 3:253–256
- Kaufman WR, Flynn PC, Reynolds SE (2010) Cuticular plasticization in the tick, *Amblyomma hebraeum* (Acari: Ixodidae): possible roles of monoamines and cuticular pH. J Exp Biol 213:2820–2831
- Kawase S (1961) Role of lipid in the hardening of the cuticle in the silkworm, *Bombyx mori*. Nature 191:279
- Koganemaru R, Miller DM, Adelman ZN (2013) Robust cuticular penetration resistance in the common bed bug (*Cimex lectularius* L.) correlates with increased steady-state transcript levels of CPR-type cuticle protein genes. Pestic Biochem Physiol 106:190–197
- Liang J, Wang T, Xiang Z, He N (2015) Tweedle cuticular protein BmCPT1 is involved in innate immunity by participating in recognition of *Escherichia coli*. Insect Biochem Mol Biol 58:76–88
- Locke M (1961) Pore canals and related structures in insect cuticle. J Biophys Biochem Cytol 10:589–618
- Locke M (1965) The hormonal control of wax secretion in an insect, *Calpodex ethlius* stoll (Lepidoptera, hesperiidae). J Insect Physiol 11:641–658
- Locke M (1966) The structure and formation of the cuticulin layer in the epicuticle of an insect, *Calpodex ethlius* (Lepidoptera, Hesperidae). J Morphol 118:461–494
- Locke M (2001) The Wigglesworth lecture: insects for studying fundamental problems in biology. J Insect Physiol 47:495–507
- Locke M (2003) Surface membranes, Golgi complexes, and vacuolar systems. Annu Rev Entomol 48:1–27
- Locke M, Huie P (1979) Apolysis and the turnover of plasma membrane plaques during cuticle formation in an insect. Tissue Cell 11:277–291
- Locke M, Condouli WV, Hurshman LF (1965) Molt and intermolt activities in epidermal cells of an insect. Science 149:437–438
- Locke M, Kiss A, Sass M (1994) The cuticular localization of integument peptides from particular routing categories. Tissue Cell 26:707–734
- Luschnig S, Batz T, Armbruster K, Krasnow MA (2006) Serpentine and vermiform encode matrix proteins with chitin binding and deacetylation domains that limit tracheal tube length in *Drosophila*. Curr Biol 16:186–194

- Marcu O, Locke M (1999) The origin, transport and cleavage of the molt-associated cuticular protein CECP22 from *Calpodex ethlius* (Lepidoptera, Hesperidae). *J Insect Physiol* 45:861–870
- Matova N, Mahajan-Miklos S, Mooseker MS, Cooley L (1999) *Drosophila* quail, a villin-related protein, bundles actin filaments in apoptotic nurse cells. *Development* 126:5645–5657
- Mitsui T, Riddiford LM (1976) Pupal cuticle formation by *Manduca sexta* epidermis *in vitro*: patterns of ecdysone sensitivity. *Dev Biol* 54:172–186
- Moussian B (2013) The arthropod cuticle. In: Minelli A, Boxshall AG, Fusco G (eds) *Arthropod biology and evolution – molecules, development, morphology*. Springer, Berlin, pp 171–196
- Moussian B, Schwarz H, Bartoszewski S, Nusslein-Volhard C (2005a) Involvement of chitin in exoskeleton morphogenesis in *Drosophila melanogaster*. *J Morphol* 264:117–130
- Moussian B, Soding J, Schwarz H, Nusslein-Volhard C (2005b) Retroactive, a membrane-anchored extracellular protein related to vertebrate snake neurotoxin-like proteins, is required for cuticle organization in the larva of *Drosophila melanogaster*. *Dev Dyn* 233:1056–1063
- Moussian B, Seifarth C, Muller U, Berger J, Schwarz H (2006a) Cuticle differentiation during *Drosophila* embryogenesis. *Arthropod Struct Dev* 35:137–152
- Moussian B, Tang E, Tønning A, Helms S, Schwarz H, Nusslein-Volhard C, Uv AE (2006b) *Drosophila* Knickkopf and retroactive are needed for epithelial tube growth and cuticle differentiation through their specific requirement for chitin filament organization. *Development* 133:163–171
- Moussian B, Veerkamp J, Muller U, Schwarz H (2007) Assembly of the *Drosophila* larval exoskeleton requires controlled secretion and shaping of the apical plasma membrane. *Matrix Biol* 26:337–347
- Moussian B, Letizia A, Martinez-Corrales G, Rotstein B, Casali A, Llimargas M (2015) Deciphering the genetic programme triggering timely and spatially-regulated chitin deposition. *PLoS Genet* 11:e1004939
- Mun S, Noh MY, Dittmer NT, Muthukrishnan S, Kramer KJ, Kanost MR, Arakane Y (2015) Cuticular protein with a low complexity sequence becomes cross-linked during insect cuticle sclerotization and is required for the adult molt. *Sci Rep* 5:10484
- Noh MY, Kramer KJ, Muthukrishnan S, Kanost MR, Beeman RW, Arakane Y (2014) Two major cuticular proteins are required for assembly of horizontal laminae and vertical pore canals in rigid cuticle of *Tribolium castaneum*. *Insect Biochem Mol Biol* 53:22–29
- Noh MY, Muthukrishnan S, Kramer KJ, Arakane Y (2015) *Tribolium castaneum* RR-1 cuticular protein TcCPR4 is required for formation of pore canals in rigid cuticle. *PLoS Genet* 11:e1004963
- Pesch YY, Riedel D, Behr M (2015) Obstructor A organizes matrix assembly at the apical cell surface to promote enzymatic cuticle maturation in *Drosophila*. *J Biol Chem* 290:10071–10082
- Pesch YY, Riedel D, Patil KR, Loch G, Behr M (2016) Chitinases and imaginal disc growth factors organize the extracellular matrix formation at barrier tissues in insects. *Sci Rep* 6:18340
- Petkau G, Wingen C, Jussen LC, Radtke T, Behr M (2012) Obstructor-A is required for epithelial extracellular matrix dynamics, exoskeleton function, and tubulogenesis. *J Biol Chem* 287:21396–21405
- Pryor MGM (1940) On the hardening of the cuticle of insects. *Proc B* 128:393–407
- Qiao L, Xiong G, Wang RX, He SZ, Chen J, Tong XL, Hu H, Li CL, Gai TT, Xin YQ, Liu XF, Chen B, Xiang ZH, Lu C, Dai FY (2014) Mutation of a cuticular protein, BmorCPR2, alters larval body shape and adaptability in silkworm, *Bombyx mori*. *Genetics* 196:1103–1115
- Qiu X, Sun W, McDonnell CM, Li-Byarlay H, Steele LD, Wu J, Xie J, Muir WM, Pittendrigh BR (2013) Genome-wide analysis of genes associated with moderate and high DDT resistance in *Drosophila melanogaster*. *Pest Manag Sci* 69:930–937
- Reyes A, Sanz M, Duran A, Roncero C (2007) Chitin synthase III requires Chs4p-dependent translocation of Chs3p into the plasma membrane. *J Cell Sci* 120:1998–2009

- Reynolds SE (1974a) Pharmacological induction of plasticization in the abdominal cuticle of *Rhodnius*. *J Exp Biol* 61:705–718
- Reynolds SE (1974b) A post-ecdysial plasticization of the abdominal cuticle in *Rhodnius*. *J Insect Physiol* 20:1957–1962
- Reynolds SE (1975) The mechanism of plasticization of the abdominal cuticle in *Rhodnius*. *J Exp Biol* 62:81–98
- Reynolds SE (1985) Hormonal control of cuticle mechanical properties. In: Kerkut GA, Gilbert LI (eds) *Comprehensive insect physiology, biochemistry and pharmacology*, vol 8. Pergamon Press, New York, pp 335–351
- Riddiford LM (2007) The control of metamorphosis in the kissing bug. *J Exp Biol* 210:3133–3134
- Sanz M, Trilla JA, Duran A, Roncero C (2002) Control of chitin synthesis through Shc1p, a functional homologue of Chs4p specifically induced during sporulation. *Mol Microbiol* 43:1183–1195
- Shaik KS, Pabst M, Schwarz H, Altmann F, Moussian B (2011) The Alg5 ortholog wollknauel is essential for correct epidermal differentiation during *Drosophila* late embryogenesis. *Glycobiology* 21:743–756
- Shaik KS, Meyer F, Vazquez AV, Flotenmeyer M, Cerdan ME, Moussian B (2012) Delta-aminolevulinic synthase is required for apical transcellular barrier formation in the skin of the *Drosophila* larva. *Eur J Cell Biol* 91:204–215
- Shaik KS, Wang Y, Aravind L, Moussian B (2014) The Knickkopf DOMON domain is essential for cuticle differentiation in *Drosophila melanogaster*. *Arch Insect Biochem Physiol* 86:100–106
- Sharma A, Mishra M, Ram KR, Kumar R, Abdin MZ, Chowdhuri DK (2011) Transcriptome analysis provides insights for understanding the adverse effects of endosulfan in *Drosophila melanogaster*. *Chemosphere* 82:370–376
- Shibata T, Aiki S, Shinzawa N, Miyaji R, Suyama H, Sako M, Inomata N, Koshiba T, Kanuka H, Kawabata S (2010) Protein crosslinking by transglutaminase controls cuticle morphogenesis in *Drosophila*. *PLoS One* 5:e13477
- Soares MP, Silva-Torres FA, Elias-Neto M, Nunes FM, Simoes ZL, Bitondi MM (2011) Ecdysteroid-dependent expression of the tweedle and peroxidase genes during adult cuticle formation in the honey bee, *Apis mellifera*. *PLoS One* 6:e20513
- Souza-Ferreira PS, Mansur JF, Berni M, Moreira MF, dos Santos RE, Araujo HM, de Souza W, Ramos IB, Masuda H (2014a) Chitin deposition on the embryonic cuticle of *Rhodnius prolixus*: the reduction of CHS transcripts by CHS-dsRNA injection in females affects chitin deposition and eclosion of the first instar nymph. *Insect Biochem Mol Biol* 51:101–109
- Souza-Ferreira PS, Moreira MF, Atella GC, Oliveira-Carvalho AL, Eizemberg R, Majerowicz D, Melo AC, Zingali RB, Masuda H (2014b) Molecular characterization of *Rhodnius prolixus*' embryonic cuticle. *Insect Biochem Mol Biol* 51:89–100
- Tetreau G, Cao X, Chen YR, Muthukrishnan S, Jiang H, Blissard GW, Kanost MR, Wang P (2015a) Overview of chitin metabolism enzymes in *Manduca sexta*: Identification, domain organization, phylogenetic analysis and gene expression. *Insect Biochem Mol Biol* 62:114–126
- Tetreau G, Dittmer NT, Cao X, Agrawal S, Chen YR, Muthukrishnan S, Haobo J, Blissard GW, Kanost MR, Wang P (2015b) Analysis of chitin-binding proteins from *Manduca sexta* provides new insights into evolution of peritrophin A-type chitin-binding domains in insects. *Insect Biochem Mol Biol* 62:127–141
- Tiklova K, Tsarouhas V, Samakovlis C (2013) Control of airway tube diameter and integrity by secreted chitin-binding proteins in *Drosophila*. *PLoS One* 8:e67415
- Wang J, Xia Q, He X, Dai M, Ruan J, Chen J, Yu G, Yuan H, Hu Y, Li R, Feng T, Ye C, Lu C, Wang J, Li S, Wong GK, Yang H, Wang J, Xiang Z, Zhou Z, Yu J (2005) SilkDB: a knowledgebase for silkworm biology and genomics. *Nucleic Acids Res* 33:D399–D402

- Wang Y, Odemer R, Rosenkranz P, Moussian B (2014) Putative orthologues of genetically identified *Drosophila melanogaster* chitin producing and organising genes in *Apis mellifera*. *Apidologie* 45:733–747
- Wigglesworth VB (1970) Structural lipids in the insect cuticle and the function of the oenocytes. *Tissue Cell* 2:155–179
- Wigglesworth VB (1985a) The transfer of lipid in insects from the epidermal cells to the cuticle. *Tissue Cell* 17:249–265
- Wigglesworth VB (1985b) Sclerotin and lipid in the waterproofing of the insect cuticle. *Tissue Cell* 17:227–248
- Wigglesworth VB (1988) The source of lipids and polyphenols for the insect cuticle: the role of fat body, oenocytes and oenocytoids. *Tissue Cell* 20:919–932
- Wolfgang WJ, Riddiford LM (1981) Cuticular morphogenesis during continuous growth of the final instar larva of a moth. *Tissue Cell* 13:757–772
- Wright TR (1987) The genetics of biogenic amine metabolism, sclerotization, and melanization in *Drosophila melanogaster*. *Adv Genet* 24:127–222
- Yamashiro S, Yamakita Y, Ono S, Matsumura F (1998) Fascin, an actin-bundling protein, induces membrane protrusions and increases cell motility of epithelial cells. *Mol Biol Cell* 9:993–1006
- Zhang J, Liu X, Zhang J, Li D, Sun Y, Guo Y, Ma E, Zhu KY (2010) Silencing of two alternative splicing-derived mRNA variants of chitin synthase 1 gene by RNAi is lethal to the oriental migratory locust, *Locusta migratoria manilensis* (Meyen). *Insect Biochem Mol Biol* 40:824–833
- Zhong YS, Mita K, Shimada T, Kawasaki H (2006) Glycine-rich protein genes, which encode a major component of the cuticle, have different developmental profiles from other cuticle protein genes in *Bombyx mori*. *Insect Biochem Mol Biol* 36:99–110
- Ziese S, Dorn A (2003) Embryonic integument and “molts” in *Manduca sexta* (Insecta, Lepidoptera). *J Morphol* 255:146–161

Chapter 4

Resilin – The Pliant Protein

Jan Michels, Esther Appel, and Stanislav N. Gorb

Abstract Resilin is an elastomeric protein typically occurring in exoskeletons of arthropods. It is composed of randomly orientated coiled polypeptide chains that are covalently cross-linked together at regular intervals by the two unusual amino acids dityrosine and trityrosine forming a stable network with a high degree of flexibility and mobility. As a result of its molecular prerequisites, resilin features exceptional rubber-like properties including a relatively low stiffness, a rather pronounced long-range deformability and a nearly perfect elastic recovery. Within the exoskeleton structures, resilin commonly forms composites together with other proteins and/or chitin fibres. In the last decades, numerous exoskeleton structures with large proportions of resilin have been described. In these structures, resilin has various functions. Today, resilin is known to be responsible for the generation of deformability and flexibility in membrane and joint systems, the storage of elastic energy in jumping and catapulting systems, the enhancement of adaptability to uneven surfaces in attachment and prey catching systems, the reduction of fatigue and damage in reproductive, folding and feeding systems and the sealing of wounds in a traumatic reproductive system. In addition, resilin is present in many compound eye lenses and is suggested to be a very suitable material for optical elements because of its transparency and amorphousness. The evolution of this remarkable functional diversity can be assumed to have only been possible because resilin exhibits a unique combination of different outstanding properties. In order to benefit from these properties in industrial and medical applications such as biosensor techniques and tissue engineering, various recombinant resilin-like polypeptides (RLPs) have been synthesised in the past few years. Due to their unusual multi-responsiveness and low toxicity and the possibility to tune their mechanical properties and to produce modular, chimeric RLPs with desired biological properties, RLPs have a wide field of potential applications and might replace many synthetic polymers in the future.

J. Michels (✉) • E. Appel • S.N. Gorb
Department of Functional Morphology and Biomechanics, Institute of Zoology,
Christian-Albrechts-Universität zu Kiel, Am Botanischen Garten 1–9,
Kiel D-24118, Germany
e-mail: jmichels@zoologie.uni-kiel.de; eappel@zoologie.uni-kiel.de;
sgorb@zoologie.uni-kiel.de

4.1 Introduction

4.1.1 *Elastomeric Proteins in Nature*

Elastomeric proteins occur in a large range of organisms and biological structures, and the spectrum of their biological functions is very broad (Shewry et al. 2004). They feature a great diversity including well-known examples such as elastin, titin and fibrillin present in vertebrate muscles and connective tissues, byssus and abductin of bivalve molluscs, gluten of wheat, spider silk proteins and resilin of arthropods (Shewry et al. 2004).

Elastomeric proteins have always attracted the attention of researchers, mainly because of their specific properties and interesting mechanical behaviours. Recently, this interest has even increased due to the idea of their potential use in the development of novel materials with a broad range of technical applications. In addition, their biological and medical significance is very high, in particular in the context of some human diseases. In the last decades, the development and improvement of micromechanical testing, confocal laser scanning microscopy (CLSM) and atomic force microscopy have facilitated detailed studies of the distribution, structure and mechanical properties of these proteins in a vast diversity of organisms and at different levels of their organisation, from the entire structure down to the level of single molecules. This chapter provides a detailed description of the elastomeric protein resilin and demonstrates this protein's broad distribution in different organisms and its functional diversity and significance in various biological structures.

4.1.2 *What Is Resilin?*

The first description of resilin, which has often been called rubber-like protein, was based on analyses of three different insect exoskeleton elements, the wing hinge and the prealar arm of the desert locust (*Schistocerca gregaria*) and the so-called elastic tendon of the pleuro-subalar muscles in dragonflies of the genus *Aeshna* (Weis-Fogh 1960). Additional insights into the characteristics of resilin, which had been gained shortly thereafter (Weis-Fogh 1961a, b), resulted in a comprehensive compilation of the then existing knowledge of resilin properties (Andersen and Weis-Fogh 1964). Resilin consists of a network of randomly orientated coiled polypeptide chains that are thermally agitated and linked together at regular intervals by stable covalent cross-links. Only the fully cross-linked protein is called resilin, whereas the not-yet cross-linked or not fully cross-linked protein is called pro-resilin (Andersen 2010). Within hydrolysates of resilin, glycine constitutes the largest proportion (30–40%) of the total amino acid residues (Bailey and Weis-Fogh 1961; Andersen 1971). Such hydrolysates also feature the two unusual amino acids dityrosine and trityrosine, which were identified to form the cross-links between the polypeptide chains (Andersen 1964). In order to allow a classification of

exoskeleton structures as resilin-containing exoskeleton according to the definition of Andersen and Weis-Fogh (1964), these structures must conform to the wing hinge, the prealar arm and the elastic tendon mentioned above with respect to their mechanical properties, strain birefringence, staining and swelling behavior and their autofluorescence (for details see the paragraph ‘Identification and Visualization of Resilin’).

The properties of resilin-containing exoskeleton material can strongly differ between structures and organisms. The reason is that in biological structures resilin seems to be rarely present in pure or nearly pure form but is known to commonly exist together with other proteins and/or chitin fibres in resilin-containing composites, which exhibit a mixture of the properties of the single components. In such composites, the resilin properties can even be ‘overlain’ by the properties of the other components making an identification of the presence of resilin in the respective structures with the criteria of Andersen and Weis-Fogh (1964) very difficult. In addition, certain exoskeleton structures feature only some of the typical characteristics of resilin-containing material but lack the others. It is then often not possible to determine whether these structures contain resilin or other proteins resembling resilin. In such cases, it is conceivable that the respective exoskeleton material consists either of a protein with properties that are similar to those of resilin or of a mixture of resilin and other proteins. For exoskeleton structures with such properties, the term ‘transitional cuticle’ was established (Andersen and Weis-Fogh 1964).

4.1.3 Occurrence of Resilin in Different Animal Lineages

Until today, resilin has been found to exist mainly in insect exoskeleton structures (Fig. 4.1a–c) where this protein has a number of different functions, which, for example, include (1) the storage of elastic energy in jumping systems (Bennet-Clark and Lucey 1967; Gorb 2004; Burrows 2010), (2) the reduction of fatigue in folding wings of beetles and dermapterans (Haas et al. 2000a, b), (3) the enhancement of the adaptability of attachment pads to uneven surfaces (Perez Goodwyn et al. 2006) and (4) the generation of flexibility of wing vein joints in dragon flies and damselflies (Gorb 1999; Appel and Gorb 2011; Donoughe et al. 2011). Besides in insect exoskeletons, resilin has been reported to be present in the exoskeletons of other arthropod taxa. The European crayfish (*Astacus astacus*), for example, bears a leg hinge operated by a flexor muscle. However, an antagonistic extensor muscle bringing the leg back to the stretched position is missing, and the returning movement is controlled by the intrinsic elasticity of resilin in the leg hinge (Andersen 2003; synonym used in the reference: *Astacus fluviatilis*). Resilin-containing exoskeleton structures have also been described for copepod crustaceans (Kannupandi 1976; Michels and Gorb 2012; Michels et al. 2012, 2015b; Fig. 4.1d), the black rock scorpion (*Palamnaeus swammerdami*) (Govindarajan and Rajulu 1974) and the centipede called Tanzanian blue ringleg (*Scolopendra morsitans*) (Sundara Rajulu 1971). In addition, resilin-like proteins that contain dityrosine and trityrosine are known to

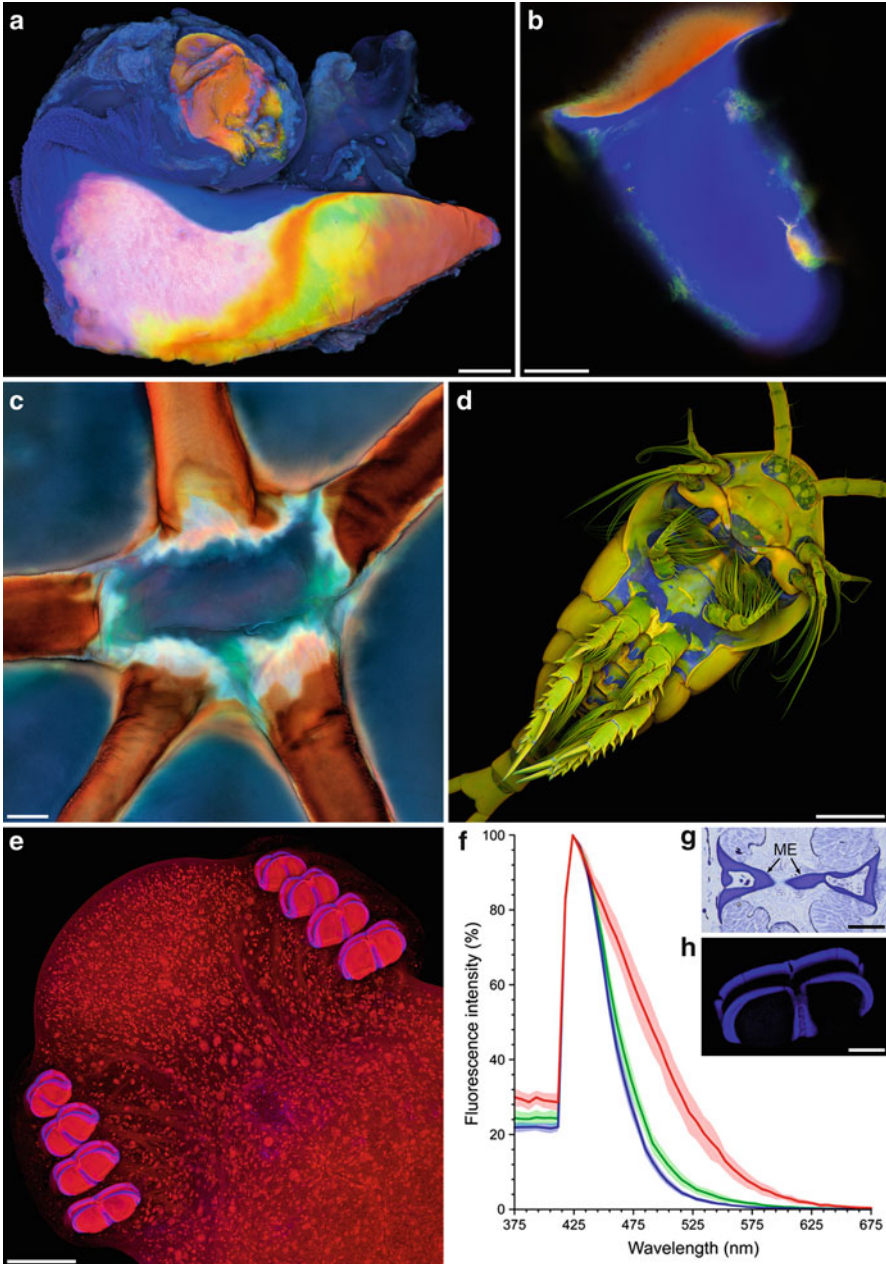


Fig. 4.1 Occurrence of resilin in insects, crustaceans and monogeneans. (a–c) Overlays of four different autofluorescences exhibited by the exoskeletons. Blue colours indicate large proportions of resilin, green structures consist mainly of non- or weakly-sclerotised chitinous material, and red structures are composed of relatively strongly sclerotised chitinous material. (a) Wing hinge and (b) prealar arm of the migratory locust (*Locusta migratoria*). (c) Wing vein joint of the

exist in several non-arthropod taxa such as nematodes (Lopez-Llorca and Fry 1989), mussels (DeVore and Gruebel 1978) and sea urchins (Foerder and Shapiro 1977). Clamp sclerites, which are part of attachment devices of monogeneans (Platyhelminthes), were reported to contain a resilin-like protein (Ramalingam 1973; Wong et al. 2013). In this context, a positive staining reaction of the clamp sclerite material and the emission of a violet/blue autofluorescence (excited with UV light) by this material were demonstrated in great detail for the monogenean *Diplozoon paradoxum*, a gill parasite of freshwater fishes (Wong et al. 2013). The emission properties of this autofluorescence are rather similar to those of the resilin autofluorescence exhibited by the wing hinge and the prealar arm of the locust *S. gregaria* (Fig. 4.1e–h). In general, the presence of resilin-like proteins in non-arthropod taxa indicates that resilin likely originated much earlier in the evolution of invertebrates than previously assumed.

4.2 Biochemistry and Molecular Biology

Elastomeric proteins show a wide structural variety. Some of them have well-defined secondary and tertiary structures (e.g. collagen), while others are structurally disordered (e.g. elastin or resilin). This structural variety is reflected by the broad spectrum of their mechanical properties. Structurally ordered proteins exhibit relatively high strength and elasticity, while highly disordered proteins have a relatively large flexibility and are more easily stretched (Rauscher and Pomès 2012). The driving force for the elastic recoil of an elastomeric protein is generally based on changes of the internal energy and the entropy. In rather stiff, structurally ordered proteins, the elastic recoil is mainly due to a change of the internal energy, meaning that after removing the applied force, the distorted molecular structure will return to the state of lowest potential energy (Rauscher and Pomès 2012). By contrast, the elastic recoil in intrinsically disordered proteins is mainly driven by a change of the



Fig. 4.1 (continued) common darter (*Sympetrum striolatum*). **(d)** Ventral view of a female copepod of the species *Temora longicornis*. Blue = autofluorescence of resilin, red = Congo red fluorescence of stained chitinous exoskeleton parts, green = mixture of autofluorescence and Congo red fluorescence of stained chitinous exoskeleton parts. **(e)** Attachment devices, featuring so-called clamp sclerites (shown in blue), of the monogenean *Diplozoon paradoxum*. **(f)** Emission spectra of the violet/blue autofluorescences exhibited by clamp sclerites of *D. paradoxum* and prealar arms and wing hinges of the desert locust (*Schistocerca gregaria*). The lines and the shaded areas represent mean values and standard deviations, respectively. **(e)** Semi-thin section through a single median clamp sclerite (*ME*) (stained with toluidine blue) of *D. paradoxum*. **(f)** Violet/blue autofluorescence (shown in blue) exhibited by a clamp sclerite of *D. paradoxum*. **(a–e, h)** Confocal laser scanning micrographs. **(a, c–e, h)** Maximum intensity projections. **(b)** Optical section. **(g)** Bright-field micrograph. Scale bars = 100 μm **(a, b)**, 20 μm **(c)**, 200 μm **(d, e)**, 25 μm **(g)**, 50 μm **(h)** ((**a–d**) Adapted with permission from Michels and Gorb (2012). (**f–h**) Adapted with permission from Wong et al. (2013))

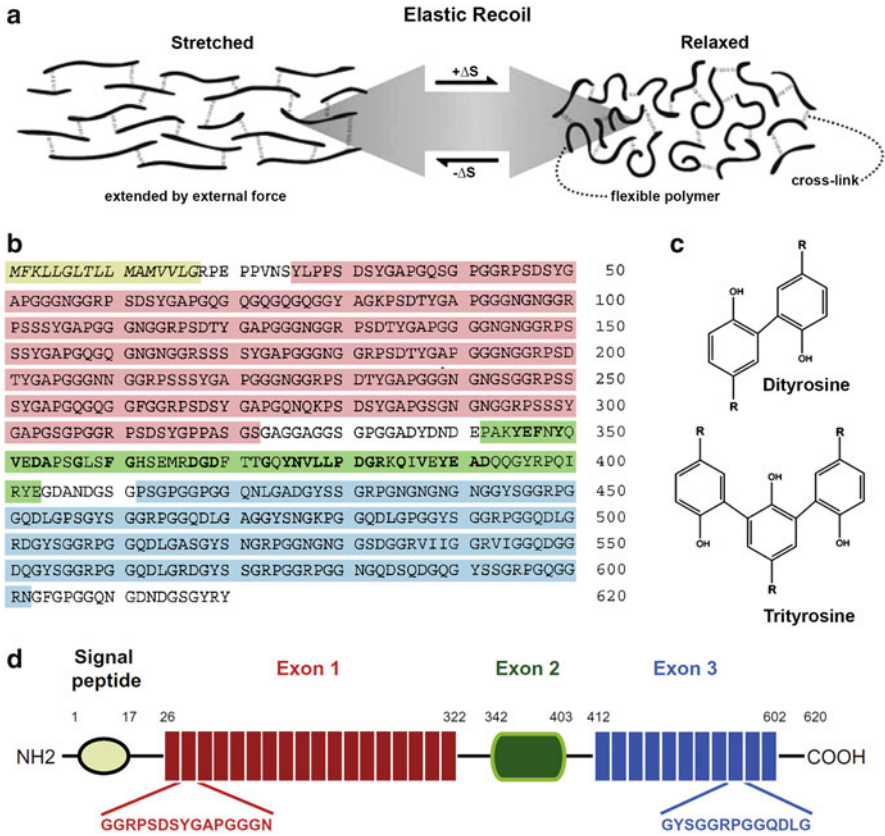


Fig. 4.2 Principle of entropy-driven elastic recoil and structure of rec1-resilin. (a) Increased entropy in the relaxed state in comparison to the stretched state leads to elastic recoil in resilin. Cross-links between polymer chains prevent that chains slide past each other during stretching. (b) Sequence of the *Drosophila melanogaster* CG15920 gene as described by Ardell and Andersen (2001), complemented with colour codes indicating the residues of the signal peptide (yellow), the exon-I-encoding peptide with A-repeat motifs (GGRPSDSYGAPGGN) (red), the chitin-binding sequence (R&R-2) (green) and the exon-III-encoding peptide with B-repeat motifs (GYSGRPGGQDLG) (blue). (c) Dityrosine and trityrosine cross-links. (d) Schema of the putative CG15290 pro-resilin sequence showing the signal peptide and the exon-I-, exon-II- and exon-III-encoding peptides ((a) Adapted with permission from Rauscher and Pomès (2012). (b) Adapted with permission from Ardell and Andersen (2001) and Andersen (2010). (c) Adapted with permission from van Eldijk et al. (2012). (d) Adapted with permission from Su et al. (2014))

entropy, as the stretching of a disordered protein decreases the sum of different ways to arrange its polymer chains (higher-ordered state), and, therefore, the protein will return to the relaxed state of increased entropy (Rauscher and Pomès 2012; Fig. 4.2a). Due to their entropy-driven elastic recoil, rubber-like proteins such as resilin exhibit an almost perfect resilience (i.e. recovery of the stored elastic energy after deformation) (Mark 1981; Mark and Erman 2007; Rauscher and Pomès 2012). With a resilience of up to 92–97% and a fatigue limit of over 300 million cycles (Lyons

et al. 2011), resilin can be called an almost perfect rubber, and its resilience is unmatched by any other elastomeric protein and the best synthetic rubbers such as the unfilled synthetic polybutadiene (Elvin et al. 2005; Rauscher and Pomès 2012). In addition, it has a low stiffness, can be stretched to more than three times its original length without permanent deformation (high extensibility) and can be compressed to one third (Weis-Fogh 1960, 1961a, b; Elvin et al. 2005).

The molecular prerequisites for such a near-perfect resilience are the following: (1) a sufficient polymer chain length and high degree of chain flexibility and mobility and (2) the presence of cross-links to join the chains into a network structure (Mark 2002, 2004; Mark and Erman 2007; Rauscher and Pomès 2012). High chain length ensures a very high deformability. This enables a large number of spatial arrangements of different extensions in the relaxed state (i.e. that the polymer system is highly disordered), but also upon stress imposition, and renders the change in internal energy, which is associated with changing the length of the sample, small (Mark and Erman 2007; Nairn et al. 2008; Rauscher and Pomès 2012). Instead, a difference in entropy between the relaxed and stretched condition is generated by allowing a large number of energetically accessible compact spatial configurations (Mark and Erman 2007; Rauscher and Pomès 2012).

In order to be able to engage in these different spatial chain arrangements, the polymer chains have to be flexible and mobile (Mark and Erman 2007). In resilin, this flexibility is based on a near-absence of any extended secondary structure (e.g. α -helices) due to a characteristic primary protein structure. As many other disordered proteins, resilin has highly repetitive low-complexity sequences with a few amino acid residues being over-represented. Amounting to around 35–40%, resilin features a remarkably high proportion of glycine residues (Ardell and Andersen 2001; Andersen 2003; Willis 2010; Fig. 4.2b). The amino acid glycine carries only a single hydrogen atom as its side chain, endowing glycine with a high conformational flexibility and enabling it to accept extreme bond angles not possible for other amino acids. Due to this high flexibility and its tendency to bend freely, glycine even deforms α -helix conformations by introducing kinks and, therefore, accounts for the absence of such conformations when it is present in a high amount. With increasing glycine content in an aqueous environment, interactions between chain segments, for example the formation of hydrogen-bonded (β -) turns, tend to be weaker than those between other segments with a lower content of glycine (Andersen 2001; Rauscher et al. 2006). Consequently, even if proline and glycine generally contribute to introducing folded β -turn conformations in peptide chains, with the amino acid motifs PG, GG and PS forming the corners of the turn, a higher abundance of glycine increases the flexibility and lability of this conformation (Andersen 2003; Rauscher et al. 2006; Tamburro et al. 2010). In other words, the higher the glycine content, the higher is the entropic cost of constraining the protein backbone in the formation of turns (or α -helix, β -sheet etc.), and, therefore, a high glycine content contributes to the formation of a disordered protein as order is entropically unfavorable (Rauscher et al. 2006; Cheng et al. 2010; Balu et al. 2015). In a non-aqueous solvent, however, the probability of intramolecular peptide-peptide hydrogen bonds is increased due to the absence of competing water molecules, which, therefore, favours more ordered structures (Rauscher et al. 2006).

Another characteristic feature of the amino acid composition of resilin is a relatively pronounced proline content of 7–10 % (Andersen 2003; Tamburro et al. 2010; Fig. 4.2b). Proline is the only amino acid featuring a side chain that is connected to the protein backbone twice, forming a heterocyclic ring. This endows proline with an exceptional conformational rigidity, locking the ϕ -backbone dihedral angle at about -75° . As a consequence, proline is unable to occupy many of the main chain conformations easily adopted by all other amino acids. For example, proline does not fit into a normal α -helix without kinks, and when evenly distributed along a chain, it can account for the absence of an α -helix. Therefore, it can be seen as a structural disruptor and, in terms of flexibility, as the opposite of glycine. In elastomeric proteins, proline contributes to maintaining the structural disorder, which avoids, for example, the formation of amyloid-like structures by reducing the ability to form peptide-peptide hydrogen bonds like hydrogen-bonded turns and β -sheets (Rauscher et al. 2006; Balu et al. 2015). In contrast, it induces a significant propensity for highly hydrated (quasi-) extended threefold poly-l-proline II helix conformations (Rauscher et al. 2006; Cheng et al. 2010; Adzhubei et al. 2013). According to Adzhubei and coworkers (2013), poly-l-proline II helices can be described as flexible structures that are not restricted by a regular pattern of intra-chain peptide-peptide hydrogen bonds and are capable of fast conformational changes within the PPII ϕ , ψ boundaries. They are markedly more flexible in comparison with the α -helix and β -sheet and correlate with increased local but decreased overall stiffness, enhanced coiling propensities and increased backbone hydration by water molecules, allowing elastomeric chain aggregates to remain amorphous and able to undergo extension and elastic recoil (Rauscher et al. 2006; Cheng et al. 2010; Adzhubei et al. 2013). Interestingly, elastomeric proteins show a dynamic equilibrium between extended conformations like the PPII helices, ‘unordered’ conformations and folded (mainly β -turn) conformations (Tamburro et al. 2005; Bochicchio et al. 2008; Adzhubei et al. 2013). The conformational proximity of the PPII and β -turn conformations can also be seen in the Ramachandran-plot, where the extended PPII conformation is very close to the type II β -turn (dihedral angles: PPII = $\phi -75^\circ$, $\psi 150^\circ$; type II β -turn = $\phi -60^\circ$, $\psi 80^\circ$ (first residue)) (Bochicchio et al. 2008). Bochicchio and coworkers (2008) suggested that stretching probably drives the equilibrium towards the extended PPII conformation, while compression drives it to the folded β -turn conformation. Tamburro and coworkers (2005) showed for tropoelastin that in aqueous solutions PPII is in equilibrium with the unordered conformation, whereas polar solvents, such as trifluorethanol, drive the conformations to an equilibrium between β -turns and the unordered conformation. Therefore, the shift of the equilibrium also depends on the microenvironment. The importance of proline as one of the major determinants for rubber-like elasticity in other elastomeric proteins can also be deduced from the comparison of ampullate silks of the garden cross spider (*Araneus diadematus*) and the golden silk orbweaver (*Nephila clavipes*) (Rauscher and Pomès 2012; also see the Chapters 12 and 13). Both of the silks have a comparably high glycine content of 40 % and 45 %, respectively (Rauscher and Pomès 2012). The significant difference, however, lies in the content of proline (*A. diadematus*: 16 %; *N. clavipes*: 3.5 %), which is therefore the main

determinant for the entropically-driven, rubber-like elasticity in *Araneus* silk and the internal-energy-driven elastic recoil in *Nephila* silk (Rauscher and Pomès 2012).

In sum, the higher content of the two amino acids glycine and proline in resilin tends (1) to increase hydration by water molecules (thereby enabling water to act as a ‘plasticiser’ by forming a solvation layer of bound water molecules around hydrophilic surface residues and having a damping effect on the attractive forces between proteins (protein chains), which increases the network mobility and decreases protein aggregation), (2) to decrease the peptide-peptide hydrogen bonding and, therefore, contribute to producing amorphous aggregates of elastomeric chains and (3) to prevent their folding into an ordered globular protein (Rauscher et al. 2006; Rauscher and Pomès 2012; Balu et al. 2015). Only when dried or dehydrated in alcohol with a concentration higher than 90 %, resilin becomes solid and glass-like. However, when rehydrated, it re-swells and becomes rubbery within seconds or minutes (Weis-Fogh 1960; Andersen 1979).

Apart from glycine and proline, the sequences of the elastic parts of resilin contain an enhanced content of hydrophilic residues like the charged residues aspartic acid, glutamic acid and arginine and the polar uncharged residues asparagine, serine and glutamine (Fig. 4.2b). As a result, the hydrophobicity index (HI) is negative (e.g. wing hinge of *S. gregaria*: $HI = -12$), indicating a classification as a soft and hydrophilic structure (Bailey and Weis-Fogh 1961; Andersen 1979; Balu et al. 2015). The elastic region of resilin lacks the sulfur-containing residues methionine and cysteine as well as hydroxyproline and contains less than 0.3 % tryptophan but a noteworthy amount of alanine (Bailey and Weis-Fogh 1961; Andersen and Weis-Fogh 1964). Unlike elastin or silk fibroin, resilin is further characterised by a low content of large, bulky hydrophobic residues like valine, isoleucine and leucine (Bailey and Weis-Fogh 1961; Ardell and Andersen 2001). This is in accordance with the results of Welinder (1976) who stated that soft cuticles were characterised by a content of hydrophilic amino acids that is significantly higher than that of sclerotised cuticles (Andersen 1979). A higher amount of hydrophilic groups decreases the protein-protein interactions and again increases the hydration, finally amounting to 50–60 % of water in resilin (at $pH = 7$) (Weis-Fogh 1960; Andersen 1979). In consequence, the lack of a sufficient amount of hydrophobic amino acids contributes to the inability of resilin to fold into a stable globular protein and supports the self-assembly (process) into a disordered protein.

Swelling experiments confirmed that resilin has an acid isoelectric point at around $pH = 4$, at which swelling is minimal (rec1-resilin, a recombinant resilin-like polypeptide produced by the cloning and expression of the first exon of the CG15920 gene of the common fruit fly (*Drosophila melanogaster*): $pH = 4.8$) (Weis-Fogh 1960; Bailey and Weis-Fogh 1961; Balu et al. 2015), which is in accordance with the results of the analysis of the amino acid composition of resilin showing that it contains more acid than base groups so that at least 4 % of the residues probably exist as free acid groups. This also conforms to the staining properties of resilin when stained with basic dyes (methylene blue and toluidine blue) (Bailey and Weis-Fogh 1961). In general, resilin swells in alkaline buffers and shrinks in acidic buffers. In case of an increase in pH , followed by an increase in hydration, the stiffness

of covalently cross-linked proteins such as resilin (see the following paragraph) increases because the cross-links prevent the proteins (protein chains) from getting away from each other (Weis-Fogh 1960; Jensen and Weis-Fogh 1962; Andersen 1979). However, resilin remains rubbery under all conditions unless it is dried or dehydrated in alcohol with a concentration higher than 90 % (Weis-Fogh 1960).

The presence of cross-links is another molecular prerequisite for the near-perfect resilience of resilin and is essential for the complete recoverability (Mark and Erman 2007; Fig. 4.2a). Immediately after secretion of the water-soluble, not yet cross-linked precursor pro-resilin from the apical surface of the epidermal cells, resilin forms its tertiary structure and becomes insoluble in water (Andersen 1964, 2010; Weis-Fogh 1970). The tertiary structure consists of stable covalent cross-links of dityrosine and trityrosine, linking the randomly coiled polypeptide chains together at regular intervals (Andersen 1964, 2010; Weis-Fogh 1970; Fig. 4.2c). In dityrosine, two tyrosine residues are linked together by means of a covalent bond between their ortho-positions, and in trityrosine, three tyrosine residues are linked together in the same way (Andersen 2004a). This cross-linking is mediated by the reaction of peroxidase and hydrogen peroxidase (shown *ex vivo*) (Aeshbach et al. 1976; van Eldijk et al. 2012). When cross-links involve tyrosine residues of the same peptide chain, a loop-structure can be formed (Andersen 2003). The covalently bonded cross-links have a high stability and even survive acid hydrolysis (Andersen 2004a). In contrast to other elastomeric proteins like elastin, where crosslinks form in more compact non-elastic domains, in resilin, the crosslinking amino acid tyrosine is distributed throughout the elastic repeat sequences (Wells 2003). It was shown that around 20–25 % of the tyrosine residues are converted into dityrosine (Andersen 1966; Elvin et al. 2005) with a spacing of 40–60 residues between the cross-links (Rauscher and Pomès 2012). Dityrosine and trityrosine cross-links can be assumed to decrease the mobility of chain segments close to the cross-link, thereby preventing the stretched polymer chains from irreversibly sliding past each other during stretching and avoiding an extended uncoiling while favoring elastic recoil (Andersen 2004a; Mark and Erman 2007; Rauscher and Pomès 2012). Considering that trityrosine cross-links tightly connect three peptide segments instead of two in the case of dityrosine, it can be assumed that resilin having a high trityrosine/dityrosine ratio is stiffer, though still elastic, than resilin with a lower trityrosine/dityrosine ratio (Andersen 2004a). The ratio of cross-linking and, therefore, the elastic properties of resilin depend on internal and external factors such as whether resilin is deposited before or after ecdysis, during the day or during the night and at constant or alternating temperature conditions (Neville 1963, 1967; Andersen 1966, 2004a).

In addition to the fluorescent di- and trityrosine (see below for the fluorescence of di- and trityrosine), small amounts of the following other fluorescent compounds have been found, for example in wing hinges and prealar arms: monochloro-dityrosine, monochloro-trityrosine and tetratyrosine (Andersen 1966, 2004a, b). Andersen (2004b) stated that it was questionable whether the chlorinated tyrosines have any function at all, considering that they might be a mere byproduct of the defence reactions (with hydrogen peroxide and hypochlorous acid). Nevertheless,

high amounts of chlorination, as, for example, found in the tibia and the femur of *S. gregaria*, can decrease the chain flexibility, resulting in a stiffer material (Andersen 2004b).

The full-length pro-resilin CG15920 from *D. melanogaster* has up to three different domains (Fig. 4.2d): (1) an N-terminal domain (exon I) of around 323 amino acids with 18 repeats of a typically 15 residues long motif (GGRPSDSYGAPGGGN), called A-repeats, (2) an extended type 2 Rebers and Riddiford chitin-binding domain (R&R-2) of 62 amino acids (exon II) and (3) a C-terminal domain (exon III) of around 235 amino acids with 11 repeats of a typically 13 residues long motif (GYSGGRPGGQDLG), called B-repeats (Ardell and Andersen 2001; Elvin et al. 2005; Qin et al. 2009; Andersen 2010). In addition, pro-resilin has an N-terminal signal peptide consisting of around 17 amino acids (MFKLLGLTLLMAxVVLG) (Ardell and Andersen 2001; Andersen 2010; Fig. 4.2d). The signal peptide allows the protein to be secreted to the apical extracellular space, but it is cleaved before the pro-resilin is secreted (Andersen 2010). Furthermore, a short sequence of 11 amino acids (RPEPPVNSYLP) can be found between the signal peptide and the first repeat-containing region (Andersen 2010). In *D. melanogaster*, both in A- and B-repeats, chain segments of zero to 15 residues with a high glycine content separate the individual repeats. In other species, like the red flour beetle (*Tribolium castaneum*), these inter-repeat regions are completely absent (Andersen 2010). Except for the R&R-2 consensus sequence, amino acid sequences differ to a more or less pronounced extent between different species of the same genus, also, for example, in the sequences of individual repeats of an A-repeat series (Andersen 2010).

Studies on the N-terminal protein domain (exon I) in the form of the rec1-resilin (the cloned and expressed exon I of the *D. melanogaster* CG15920 gene) showed that rec1-resilin exhibits a high resilience of >90% (93% when cross-linked) comparable to the one of the native resilin in dragonfly tendons, and rec1-resilin was termed the ‘soft’ segment of resilin (Elvin et al. 2005; Qin et al. 2012). Furthermore, rec1-resilin was found to have a high content of glycine and proline (glycine: 34.2%; proline: 13.8%), which are both regularly distributed (proline with around seven and glycine with zero to two amino acids between consecutive proline and glycine residues, respectively) along an overall hydrophilic sequence (Balu et al. 2015). This endows the polymer chain with overall structural disorder, high flexibility and super-elasticity, preventing the formation of tightly packed aggregates and helping to maintain sufficient hydration (Qin et al. 2012; Balu et al. 2015). Although dominated by structural disorder (approximately amounting to 60%), the repetitive motifs of exon I were also shown to exhibit a few secondary structures like PPII and β -turn conformations (see above; Charati et al. 2009; Lyons et al. 2009; van Eldijk et al. 2012; Khandaker et al. 2016). Along with that, Khandaker and coworkers (2016) showed that the repeat motif PSSSYGAPGGGNGGR of exon I shows a bend at the glycine residue between tyrosine and alanine of the SYGAP building block with only few hydrogen bonds, which results in a smaller end-to-end distance and in a lower stiffness (lower force required to pull the motif to an extended state) than in other motifs with a slightly altered sequence. Furthermore, they assumed

that the presence of serine before tyrosine (of SYGAP) can additionally favour such a bent structure by creating less steric hindrance than, for example, threonine (Khandaker et al. 2016). They finally concluded that flexible, extendable bent motifs offer increased flexibility over more linearly arranged motifs, contributing to the high elasticity of the repeat motifs of exon I (Khandaker et al. 2016).

The exon-III-encoded peptide has a resilience of around 63 % (86 % when cross-linked) and was termed the ‘hard’ segment of resilin (Qin et al. 2011, 2012). It is probably composed of several internal hydrophobic and hydrophilic domains, exhibiting a larger hydrophobic block in the middle chain, and is more prone to perform β -turn structural transitions (Qin et al. 2012). Yang and Hu (2014) further predicted the presence of β -sheet and β -turn conformations in the hydrophobic and repetitive sequences, respectively. Water-based self-assembly of this peptide is assumed to lead to the formation of micellar structures with a hydrophobic core of irregularly sized globules (Qin et al. 2012).

Qin and coworkers (2012) stated that the ‘soft’ segment alone was insufficient to store the energy required for jumping and flying insects and suggested a mechanism of elasticity requiring all segments. They assumed that the resilin network is almost devoid of β -turns in its relaxed state. Upon stress application, the super-elastic ‘soft’ segment (exon I) immediately reacts and transfers energy to the ‘hard’ segment (exon III), which thereupon transforms to a more ordered β -turn structure, thereby storing elastic energy (Qin et al. 2012). After stress removal, the ‘hard’ segment (exon III) returns to its original unstructured conformation, releasing the stored potential energy to the ‘soft’ segment (exon I), which results, for example, in different resilin-driven jumping and flying movements (Qin et al. 2012).

The R&R-2 sequence consists of a conserved motif of 35–36 amino acids (The original Rebers and Riddiford consensus sequence first recognised by Rebers and Riddiford (1988) has the sequence G-x(8)-G-x(6)-Y-x-A-x-E-x-G-Y-x(7)-P-x(2)-P (x represents any amino acid, value in parentheses indicates the number of residues.) with an N-terminal region of hydrophilic amino acids (Rebers and Willis 2001). In this type of extended Rebers and Riddiford consensus sequence, the glutamic acid and the proline residues near the C-terminus of the Rebers-Riddiford sequence are not present, and the second tyrosine is replaced by phenylalanine (Andersen et al. 1997; Andersen 1998). In addition, the N-terminal region shows considerable sequence conservation in contrast to the extended type 1 of the Rebers-Riddiford sequence (R&R-1) (Andersen 1999; Willis 1999). Interestingly, the R&R-2 consensus sequence is normally found in proteins derived from hard, sclerotised cuticle (in contrast to the R&R-1 that is normally associated with soft cuticles) and was assumed to form four β -pleated sheets, alternating with four β -turns/loops with glycine lying exactly at the maxima of the β -turns/loops (Iconomidou et al. 1999). The β -sheets have a ‘polar’ character with bulky, hydrophobic and/or aromatic residues facing to one side of the β -sheets and other, sometimes hydrophilic, residues facing the other side (Iconomidou et al. 1999). This is due to the fact that alternating residues arranged along a strand are directed towards opposite faces of the β -sheet (Iconomidou et al. 1999). In further studies, Iconomidou and coworkers showed that these β -sheets are antiparallel and fold into an antiparallel β -sheet half

barrel structure with a kind of groove containing conserved aromatic residues (mostly tyrosine and phenylalanines), which form planar hydrophobic surfaces on one ‘face’ of the structure (Iconomidou et al. 2001, 2005; Hamodrakas et al. 2002). The aromatic rings of these residues were proposed to stack against the saccharide rings of chitin (poly-N-acetylglucosamine) chains and to accommodate at least one extended chitin chain, thereby binding to chitin filaments as well as contributing to dictating the formation of their helicoidal architecture (Iconomidou et al. 1999, 2001, 2005; Hamodrakas et al. 2002). Together, the exon I, exon II, and exon III encoding peptides of resilin were suggested to build a polymer of hydrophilic-hydrophobic-hydrophilic structure and to form water-swollen assemblies with irregular sized micelles, with the hydrophobic blocks directing folding and micelle formation (Qin et al. 2012).

Alternative splicing in, for example, *D. melanogaster* can result in the formation of a pro-resilin without chitin-binding R&R-2 consensus domain (Andersen 2010). It was proposed that this variant of pro-resilin can contribute to either producing chitin-free or low-chitin resilin structures, as, for example, in dragonflies or locusts, or obtaining an optimal balance in polymer composite or increasing the probability for binding pro-resilin molecules on a low-chitin surface (Andersen 2004a, 2010; Qin et al. 2009). Furthermore, chitin-containing resilin is predominately found in structures exposed to bending and twisting forces, whereas resilin devoid of chitin is predominately exposed to stretching forces (Andersen 2010).

4.3 Identification and Visualization of Resilin

Resilin has a number of properties that, since their detailed description decades ago (Weis-Fogh 1960, 1961a, b; Andersen and Weis-Fogh 1964; Elliott et al. 1965), have commonly been used to analyse arthropod exoskeleton structures for the presence and distribution of this protein. Among these properties, some can easily be identified by means of relatively simple methods. Resilin is colourless, transparent and amorphous. These characteristics make exoskeleton parts with very large proportions of resilin look rather different from exoskeleton parts with other material compositions, in particular from those with relatively large proportions of chitin that are typically pigmented and only slightly transparent or sometimes, when the sclerotisation is very pronounced, not transparent at all. Accordingly, good indications for the presence of exoskeleton parts with large resilin proportions can be obtained by a visual inspection of arthropod exoskeletons using stereomicroscopy (with transmitted light or reflected light), bright-field microscopy and, in the case of relatively large organisms and structures, even with the naked eyes.

Simple tests of the material properties and the material behaviour can give additional indications for the presence of exoskeleton parts with large resilin proportions. When immersed in aqueous media and in many anhydrous hydrophilic liquids, resilin exhibits an isotropic swelling, which is reversible and depends on the pH. (It is least pronounced at pH values of about 4.) In its swollen state, resilin fea-

tures its typical rubbery nature, long-range deformability and complete elastic recovery. Furthermore, if swollen resilin is tensioned, it will become birefringent, and the birefringence will be positive in the direction of the extension. When resilin is completely dried, it loses its rubber-like characteristics and becomes relatively hard and brittle. Accordingly, changes of the material properties induced by hydration and drying can be a strong indication for the presence of structures with relatively large resilin proportions (e.g. Peisker et al. 2013). Besides mechanical tests, proteolytic enzymes such as pepsin or trypsin can be applied to test for the presence and distribution of resilin by digesting resilin in the respective exoskeleton structures.

Resilin has been shown to be stained by single conventional dyes. Chemical reactions with the Masson and Mallory dyes were mentioned to stain resilin red (Andersen and Weis-Fogh 1964). While these dyes have only occasionally been applied in later studies on resilin-containing exoskeleton structures, staining of resilin with aqueous solutions of methylene blue and/or toluidine blue is a common method and can provide good information about the presence and distribution of resilin (e.g. Bennet-Clark and Lucey 1967; Young and Bennet-Clark 1995; Michels et al. 2012). (When resilin is stained with one of these two dyes, it does not show metachromasia.) However, such a staining is only efficient in exoskeleton structures that are not too strongly pigmented and make a good visibility of the dyes and thereby a correct evaluation of the distribution of large resilin proportions within the structures possible.

Among the amino acids that form resilin, dityrosine and trityrosine exhibit a relatively pronounced autofluorescence (Andersen 1963, 1964; Andersen and Weis-Fogh 1964). This autofluorescence is present in natural resilin-containing structures and in isolated resilin (both before and after boiling in water) and in resilin hydrolysates. In neutral and alkaline solutions, its excitation and emission maxima are at about 320 nm and 415 nm, respectively (Andersen 1963, 1966). When wide-field fluorescence microscopy (WFM) is applied, this autofluorescence can most efficiently be visualized with a fluorescence filter set that contains an excitation filter transmitting UV light with wavelengths in the range of 300–340 nm (or shorter than about 280 nm; see Andersen 1963) and an emission filter transmitting light in the violet and/or blue sections of the light spectrum. Such filter sets are common in WFM. For example, a typical commercial filter set designed for the visualization of the fluorescence of the frequently applied fluorescence dye 4',6-diamidino-2-phenylindole (DAPI) features excitation and emission filters transmitting 321–378 nm and 420–470 nm, respectively, and is, therefore, very suitable for the visualization of the resilin autofluorescence (e.g. Michels and Gorb 2012). The obtained micrographs of the resilin autofluorescence can be overlaid on bright-field micrographs of the whole preparation in order to clearly show the distribution of the large resilin proportions within the analysed structures. This combined application of two different microscopy techniques has become one of the most commonly used methods for the visualization of resilin (e.g. Young and Bennet-Clark 1995; Burrows et al. 2008; Burrows 2009, 2010, 2011, 2014a, b; Appel and Gorb 2011; Donoughe et al. 2011; Burrows and Sutton 2012; Bayley et al. 2012; Picker et al. 2012; Burrows and Dorosenko 2014a, b; Figs. 4.4a and 4.6b).

When exoskeleton structures are supposed to contain resilin, it is recommendable to not only check them for the presence of violet/blue autofluorescence excited by UV light but also to analyse this autofluorescence in more detail. The autofluorescence properties should be compared with those of the well-known resilin autofluorescence exhibited by the prealar arm and the wing hinge of the locust *S. gregaria* and the elastic tendon of dragonflies of the genus *Aeshna*, the test specimens used to analyse and describe the properties of resilin (Weis-Fogh 1960; Andersen and Weis-Fogh 1964). This can, for example, be done with the spectral detection techniques of modern CLSM systems (Michels et al. 2012, 2015a). However, even if the spectral properties are rather similar, one has to bear in mind that some other proteins exhibit autofluorescences with comparable excitation maxima in the UV range and emission maxima in the violet and blue ranges of the light spectrum (e.g. Garcia-Castineiras et al. 1978; Fujimori 1978; Gast and Lee 1978).

The excitation spectrum of the resilin autofluorescence differs with changing pH conditions. In acid solutions, the excitation maximum of about 320 nm (mentioned above for neutral and alkaline solutions) is shifted considerably to about 285 nm, and the upper edge of the excitation peak is at about 330–340 nm (Andersen 1963, 1966). Accordingly, if resilin-containing exoskeleton structures are placed in acid solutions and visualized with WFM, nearly no resilin autofluorescence will be excited with excitation filters such as the one described above. The pH-induced changes of the excitation properties are reversible and take place rapidly (Neff et al. 2000). This can be used to get an indication of the presence of resilin by consecutively visualizing the structures of interest in neutral, acidic and alkaline solutions with WFM, a DAPI filter set (or a filter set with comparable characteristics) and identical camera exposure times and by subsequently comparing the different intensities of the excited autofluorescences (Neff et al. 2000).

In addition to resilin, other arthropod exoskeleton materials also exhibit autofluorescences, which can be efficiently visualized with fluorescence microscopy. This allows the production of overlays consisting of different micrographs that show different autofluorescences. Such overlays nicely exhibit differences in the autofluorescence composition, which are good indications for differences in the material composition and clearly reveal structures with relatively large resilin proportions within the analysed specimens (e.g. Haas et al. 2000a; Niederegger and Gorb 2003; Perez Goodwyn et al. 2006).

When thick specimens are analysed with WFM, only relatively thin layers of these specimens are in focus (because of the limited depth of field), and many out-of-focus structures are visualized. As a result, the micrographs appear blurry and do not provide much detailed information about the micromorphology of the analysed structures. In contrast, with CLSM, all structures can be visualized in great detail over the complete z-range of the specimen. Unfortunately, today not many CLSM systems are equipped with a UV laser. Therefore, an optimal excitation of the resilin autofluorescence is often not possible. However, a recent study demonstrated that resilin can also be efficiently visualized by means of a 405 nm laser, which is commonly available in a large number of CLSM systems (Michels and Gorb 2012). With the described method, four different autofluorescences are excited and detected

separately, and certain colours are allocated to each of the four visualized fluorescence signals. On the resulting overlays, exoskeleton structures with large proportions of resilin are blue, while green structures consist mainly of non- or weakly-sclerotised chitinous material, and red structures are composed of relatively strongly sclerotised chitinous material (for details see Michels and Gorb 2012; Fig. 4.1a–c). Many of the confocal laser scanning micrographs shown in this chapter were created using this method.

The described resilin identification and visualization methods are not absolutely specific. Accordingly, it is strongly advisable to apply not only one single method but a combination of several different ones to increase the reliability of the resilin analyses performed. In recent years, an antibody to *D. melanogaster* rec1-resilin was developed and has been shown to be cross-reactive and to label resilin in different insects (Elvin et al. 2005; Burrows et al. 2011; Wong et al. 2012). Until today, this immunohistochemical method has been tested for only a small number of insects and, to the best of our knowledge, only within the studies mentioned above. If it proves efficient in tests with a larger number of arthropod species, it will represent the first reliable method that specifically identifies resilin.

4.4 Mechanical Properties of Resilin

4.4.1 Elasticity, Viscoelasticity and Flexibility

The elastic tendon of the pleuro-subalar muscles of dragonflies (see above) can be stretched up to 3–4 times its relaxed length before failure. Remarkably, when the tensile force is released, the tendon snaps back to its initial state without having any residual deformations. Quantitative stress-strain relationships (Fig. 4.3a) reveal the following mechanical properties of resilin: Young's modulus (elastic modulus) = 2 MPa, strength (σ_{\max}) = 4 MPa, extensibility (ϵ_{\max}) = 1.9, toughness = 4 MJ m⁻³ and resilience = 92 % (Gosline et al. 2002, 2004). In elastic tendons of dragonflies and locust ligaments, resilin was found to have a Young's modulus of 0.6–0.7 MPa and 0.9 MPa, respectively (Jensen and Weis-Fogh 1962). When resilin is completely hydrated, it behaves close to a perfect rubber (Weis-Fogh 1961a, b; Jensen and Weis-Fogh 1962). The elastic efficiency of isolated resilin from locusts and dragonflies seems to be optimal at lower frequencies (Gosline et al. 2002). However, under low frequency loads, resilin shows viscoelastic behaviour (Fig. 4.3b). The mechanical response of resilin strongly changes with a changing degree of hydration (Fig. 4.3c; also see below).

According to the theory of rubber elasticity (Mark 1981; Mark and Erman 2007), rubber materials consist of long, randomly coiled chains that continuously change their form depending on the temperature. The interactions between chain segments are low. Only a few cross-links form stable interconnections between the chains preventing the chains from sliding under deformation. In a stretched rubber, the average distance between inter-chain links increases causing material anisotropy

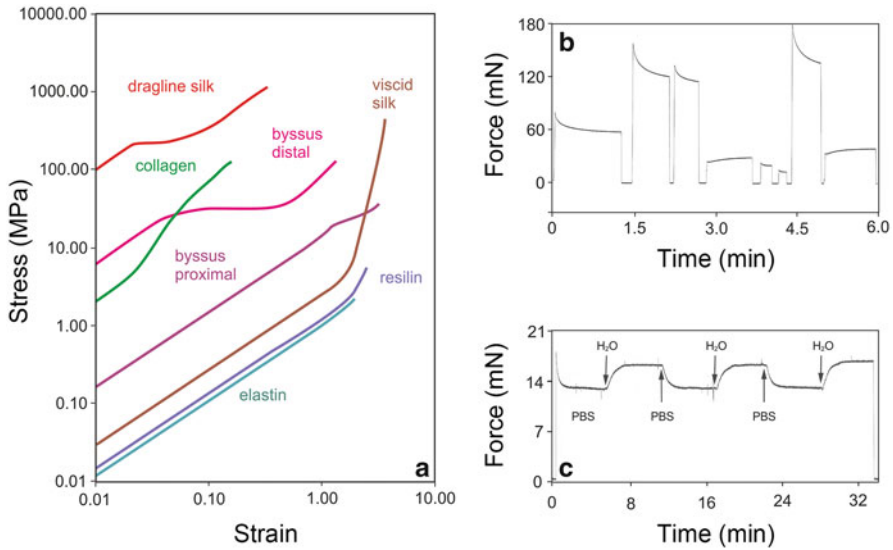


Fig. 4.3 Resilin mechanics. (a) Stress-strain curves for different elastomeric proteins. From the diagram, the following mechanical properties of resilin can be obtained: Young's modulus = 2 MPa, strength (σ_{\max}) = 4 MPa, extensibility (ϵ_{\max}) = 1.9, toughness = 4 MJ m⁻³ and resilience = 92 %. (b) Force-time curve of several load-unload cycles showing viscoelastic properties of resilin in a locust wing hinge at low frequencies. (c) Force-time curve of a loaded locust wing hinge in different aqueous environments. The experiment shows mechanical properties of resilin at different levels of hydration ((a) Adapted with permission from Gosline et al. (2004). (b, c) Adapted with permission from Jäkle (2003))

due to a partial alignment of the chains. In rubber materials, all the deformation energy remains stored, and no energy is used for changing interactions between chain segments. Resilin, with its network of polypeptide chains cross-linked by dityrosine and trityrosine, very likely behaves exactly in this way.

4.4.2 Properties of Resilin-Based Composites With Gradients of the Resilin Proportion

In biological structures, resilin usually occurs in combination with other proteins and/or chitin (Fig. 4.4f, g). Very often, gradients of the material composition with a considerably changing proportion of resilin are present in exoskeleton structures. Such resilin proportion gradients must also be reflected by gradients of the mechanical properties of the respective resilin-containing composites. Recently, the Young's moduli of adhesive tarsal setae of beetles were measured along the longitudinal axis of the setae (Fig. 4.7c). The measurements revealed that the Young's modulus of the material in the most distal section of each seta is relatively low (1.2 ± 0.3 MPa), whereas it is considerably higher at the setal base (6.8 ± 1.2 GPa). The differences in

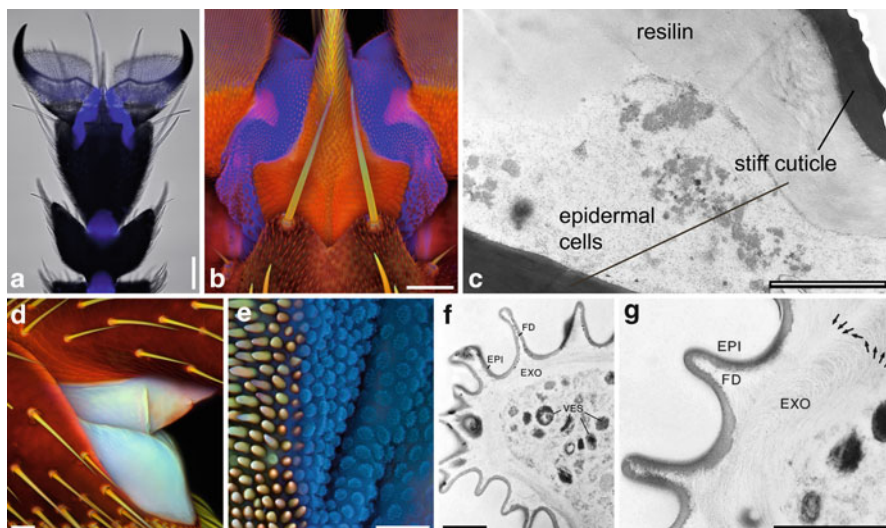


Fig. 4.4 Resilin in arthrodial membranes of insects. **(a, b)** Pretarsus of the drone fly (*Eristalis tenax*), ventral view. **(a)** Overlay of a bright-field micrograph and a wide-field fluorescence micrograph showing the presence and distribution of resilin autofluorescence (blue). **(b)** Confocal laser scanning micrograph (maximum intensity projection) revealing large proportions of resilin (shown in blue) in the membranous structures between rigid sclerites of the pretarsus. **(c)** Pretarsus of the urban bluebottle blowfly (*Calliphora vicina*). Transmission electron micrograph showing an ultra-thin section through structures comparable to those shown in blue in **(b)**. **(d)** Lateral view of the joint between the tarsomeres 1 and 2 in the third leg of the seven-spot ladybird (*Coccinella septempunctata*). **(e)** Border between the neck membrane (right side) and a postcervical sclerite (left side) of the broad-bodied chaser (*Libellula depressa*). **(f, g)** Membranous cuticle in the neck area of the blue-tailed damselfly (*Ischnura elegans*). Transmission electron micrographs showing ultra-thin sections (**EPI** epicuticle, **EXO** exocuticle, **FD** folds, **VES** vesicles. *Arrows*: preferential orientation of chitin fibres. Scale bars = 100 μm **(a)**, 50 μm **(b)**, 2 μm **(c)**, 20 μm **(d, e)**, 1 μm **(f, g)** **(a, b, d, e)** Adapted with permission from Michels and Gorb (2012). **(f, g)** Adapted with permission from Gorb (2000))

the Young's modulus between different regions correlate with the resilin proportion observed in the seta material (Peisker et al. 2013). When the setae are dehydrated, the Young's modulus of the setal tip material strongly increases from 1.2 MPa to 7.2 GPa, and it exhibits no statistically significant differences along the complete setae (Peisker et al. 2013). This is in accordance with earlier observations indicating that the material properties of resilin strongly depend on the hydration status of resilin, which is due to the fact that proteins are plasticised by water (Andersen and Weis-Fogh 1964; also see above).

In addition to the differences in the Young's modulus, the pronounced material composition differences between the tips and the bases of fresh adhesive tarsal setae are reflected by the mechanical behaviour of the respective materials. The material of the tip features only elastic deformation, whereas the base material shows both elastic and, to some extent, plastic deformations (Peisker et al. 2013). This means that the purely elastic response of the tip is due to the presence of resilin, while the partially plastic deformation at the base is mainly due to the presence of stiffer

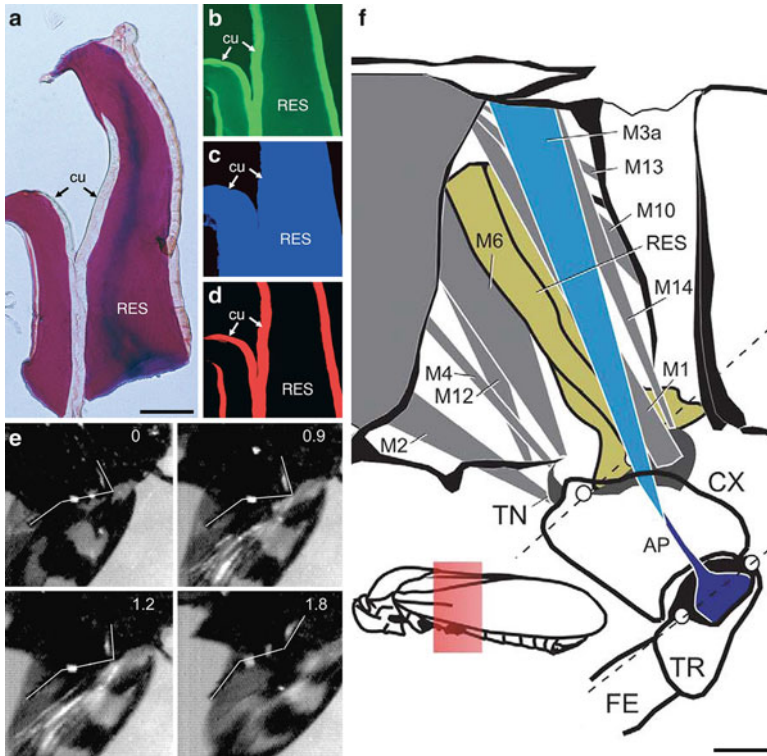


Fig. 4.5 Resilin in the jumping system of the black-and-red froghopper (*Cercopis vulnerata*). (a–d) Cuticle supplemented with resilin in the pleural area of the metathorax. Horizontal sections through the pleural seam. (a) Paraffin-embedded cuticle stained after Cason. Bright-field micrograph. (b–d) Frozen sections of the structures shown in (a). Wide-field fluorescence micrographs showing different autofluorescences exhibited by the exoskeleton. (b) Excitation: 512–546 nm; emission: 600–640 nm. (c) Excitation: 340–380 nm; emission: 420 nm. (d) Excitation: 710–775 nm; emission: 810–890 nm. *cu*, tanned cuticle; *RES*, structures containing resilin. (e) Sequence of single frames of a high-speed video recording of the cicada jump (ventral aspect). The numbers indicate the time scale in milliseconds. The approximate positions of femur, tibia and tarsus are indicated by white lines according to white marker dots on the leg. (f) Skeleton-muscle organisation of the cicada metathorax (medial aspect, right side) (*AP* apodeme of the trochanter extensor muscle *M3*, *CX* coxa, *FE* femur, *M1*, *M2*, *M4*, *M6*, *M14* subcoxal muscles, *M7*, *M9*, *M10*, *M11*, *M12*, *M13*, *M14* metathoracic muscles, *M5* trigger muscle, *M8a*, *M8b* trochanter flexor muscle, *RES* resilin, *TN* trochantine, *TR* trochanter, *white circles* condyli of the coxa and trochanter. The inset shows the position of the structures in the entire insect body. Scale bars = 100 μm (a), 250 μm (f) ((a–f) Adapted with permission from Gorb (2004))

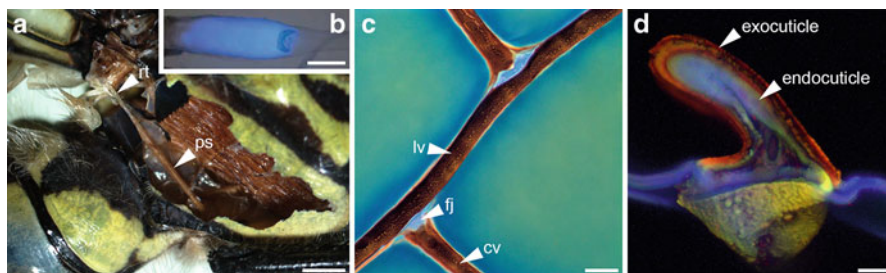


Fig. 4.6 Resilin in flight systems of dragonflies. **(a)** Stereomicrograph depicting a resilin-bearing tendon (*rt*) of a pleuro-subalar muscle (*ps*) of the southern hawkker (*Aeshna cyanea*). **(b)** Overlay of a bright-field micrograph and a wide-field fluorescence micrograph showing autofluorescence (blue) exhibited by resilin in a tendon of the genus *Zyxomma*. **(c)** Flexible wing vein joints (*fj*) joining cross veins (*cv*) to a longitudinal vein (*lv*) in a wing of the vagrant darter (*Sympetrum vulgatum*). **(d)** Cross section through a wing vein of *S. vulgatum*, revealing sclerotised exocuticle and resilin-bearing endocuticle. **(c, d)** Confocal laser scanning micrographs (maximum intensity projections) showing overlays of different autofluorescences exhibited by the exoskeletons. Structures with large proportions of resilin are shown in blue. Scale bars = 1 mm **(a)**, 100 μm **(b)**, 40 μm **(c)**, 10 μm **(d)** **(b)** Adapted with permission from Elvin et al. (2005). **(d)** Adapted with permission from Appel et al. (2015)

tanned exoskeleton. It is very likely that effects similar to those observed in beetle adhesive tarsal setae exist in other exoskeleton structures with comparable gradients of the resilin proportion.

4.5 Occurrence and Functions in Different Systems

Resilin is known from numerous arthropod exoskeletons where it is present in diverse structures and allows manifold functions, which in most cases are based on its very pronounced elasticity and its ability to completely recover after deformation. For example, resilin plays an important role in flight systems of insects, in particular in insects that use a wing beat with a low frequency (10–50 Hz) (see below). Resilin-containing exoskeleton structures have been described for various mechanical systems including leg joints (Gorb 1996; Neff et al. 2000), vein joints and membranous areas of insect wings (Gorb 1999; Haas et al. 2000a,b), the food-pump of reduviid bugs (Edwards 1983), tymbal sound production organs of cicadas (Young and Bennet-Clark 1995; Bennet-Clark 1997) and moths (Skals and Surlykke 1999), abdominal cuticle of honey ant workers (Raghu Varman 1981) and termite queens (Raghu Varman 1980), the fulcral arms of the poison apparatus of ants (Raghu Varman and Hermann 1982) and the tendons of dragonfly flight muscles and basal wing joints of locusts (as already mentioned above) (Andersen and Weis-Fogh 1964). In the following, some selected representative structures and systems with large proportions of resilin are highlighted, and their functions are described.

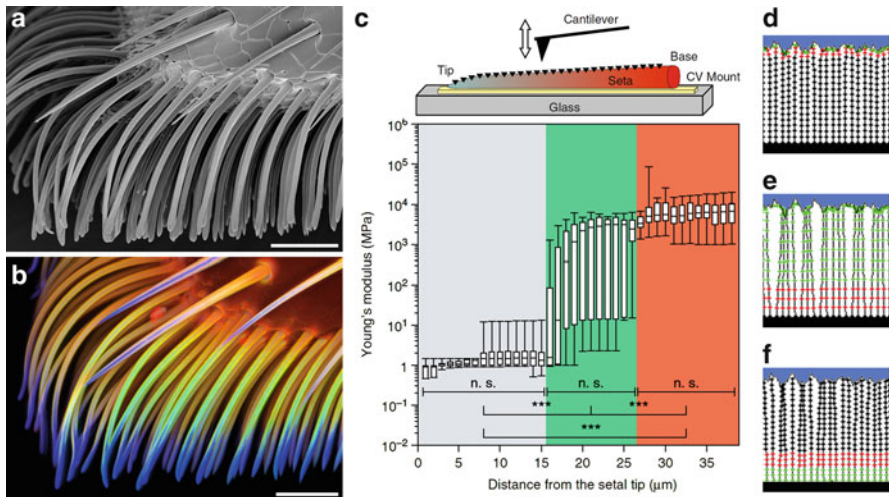


Fig. 4.7 Distribution, mechanical properties and functional significance of resilin in adhesive tarsal setae. **(a, b)** Ventral part of the second adhesive pad of a female seven-spot ladybird (*Coccinella septempunctata*), lateral view. **(a)** Scanning electron micrograph. **(b)** Confocal laser scanning micrograph (maximum intensity projection) showing an overlay of different autofluorescences exhibited by the exoskeleton. Blue colour indicates large proportions of resilin. **(c)** Box-and-whisker plots showing the median Young's modulus of fresh adhesive tarsal setae obtained by atomic force microscopy nanoindentations (see the inset above the graph) along each seta. The borders of the boxes define the 25th and 75th percentiles, the median is indicated by a horizontal line, and the error bars define the 10th and 90th percentiles (n. s. = not significant, *** = highly significant). The background colours indicate the different seta sections. **(d–f)** Numerical model showing typical configurations of a filamentary structure (setal array) attached to a stiff support (black rectangle) in adhesive contact with a random fractal surface (blue region). Three types of fibres were tested: **(d)** stiff fibres with short elastic ends, **(e)** long elastic fibres connected to the base by short stiff roots and **(f)** stiff fibres with soft elastic segments near the base. The different stiffnesses of the segments are conditionally shown by circles with different colours. Stiff, medium and soft segments are marked by black, red and green circles, respectively. Scale bars = 25 μm **(a, b)** ((a–c) Adapted with permission from Peisker et al. (2013). (d–f) Adapted with permission from Gorb and Filippov (2014))

4.5.1 Arthrodistal Membranes

Arthrodistal membranes are cuticle areas that are typically thin, non-sclerotised and very flexible. Such membranes often are multifunctional units. The soft cuticles of caterpillars, for example, have a combination of both a protective and a locomotory role, which is reflected in their ultrastructural architecture (Hepburn and Levy 1975). The main functions of arthrodistal membranes are to connect sclerotised exoskeleton elements, allow relative movement of these elements and extend whenever an increase in volume of the body is necessary (e.g. Vincent 1976; Hackman and Goldberg 1985). In addition, some membranes are armoured with miniature protuberances on their surfaces and have a defence function (Richards and Richards 1979; Hepburn 1985). For insects, two different types of membranes have previously been reported. The first type is a highly extensible membrane found in the

locust abdomen that can extend up to ten times its original length (Vincent and Wood 1972; Vincent 1975, 1981). This cuticle is highly specialised in its protein composition (Hackman and Goldberg 1987). The second type is a folding laminated membrane that is less stretchable and has been found, for example, in the abdomen of the tsetse fly *Glossina morsitans* (Hackman and Goldberg 1987) and in the bug genus *Rhodnius* (Hackman 1975; Reynolds 1975).

Membranous cuticle often contains large proportions of resilin (Fig. 4.4). Examples are membrane structures connecting claws and pulvilli to the terminal tarsomere (Gorb 1996; Niederegger and Gorb 2003). In the pretarsus of the drone fly (*Eristalis tenax*) (Diptera, Syrphidae), for example, membranous cuticle with large proportions of resilin forms a spring-like (or joint-like) element (Fig. 4.4a–c) that makes the pulvilli movable and thereby enables them to efficiently adapt to the substrate. In general, joints in legs typically feature membranes, which often contain large proportions of resilin and allow the relative movement of the joint elements (Fig. 4.4d).

The neck membrane of dragonflies is another example. This flexible cuticle connects the neck sclerites and enables an extensive mobility of the head (Gorb 2000). A recent study clearly revealed that the neck membrane material of the broad-bodied chaser (*Libellula depressa*) contains relatively large proportions of resilin, while the neighbouring sclerites are mainly composed of sclerotised chitinous material (Michels and Gorb 2012; Fig. 4.4e). Transmission electron microscopy showed that dragonfly neck membrane cuticle is rather homogenous and electron-lucent (Gorb 2000). Membranous areas of insect cuticle nearly always exhibit a relatively intensive autofluorescence similar to that of resilin. This suggests that arthrodistal membranes generally contain relatively large proportions of resilin. However, even very soft and flexible membranes such as the dragonfly neck membrane do not consist of pure resilin but rather represent resilin-chitin composites in which some reinforcement by chitin-bearing microfibrils is clearly visible (Fig. 4.4f, g).

4.5.2 Legged Locomotion

Mechanisms of fast leg movements with an acceleration that can surpass the limitations for muscle contraction have only been found in a few insect groups including fleas (Bennet-Clark and Lucey 1967; Rothschild et al. 1975), locusts (Bennet-Clark 1975) and click beetles (Evans 1973; Furth et al. 1983). The respective catapult-like devices have evolved to enhance the acceleration in relatively short legs (Gronenberg 1996). They usually contain specific types of joints that are typically supplemented with active power or latch muscles producing tractive force and trigger muscles that are responsible for releasing elastic energy from specific energy storage devices (see below).

In Auchenorrhyncha and Sternorrhyncha, the jump is performed by metathoracic muscles that are directly connected to the trochanter of the hind leg and responsible for the movements of both trochanter and coxa (Gorb 2004; Burrows 2012; Fig. 4.5f). In the jumping cicada called black-and-red froghopper (*Cercopis vulnerata*) (Cercopidae), the complete extension of the hind leg takes less than one millisecond (Gorb 2004; Fig. 4.5e). This suggests that, in addition to the muscle system, an elastic spring powers the jump. The application of fluorescence microscopy and histological staining revealed resilin-bearing structures in the pleural area of the metathorax (Fig. 4.5a–d). These structures stretch dorso-ventrally across the entire pleural area (Fig. 4.5f) and are much larger than those of fleas. Their dorsal and ventral parts are located close to the origin of the lateral portion of the power muscle and closely connected to the lateral part of the coxa, respectively. The resilin-containing structures very likely participate in the extension of both coxa and trochanter by the release of energy that is stored by deflection or twisting of their bar-like shape.

4.5.3 Flight Systems: Folds, Tendons and Micro-joints

Resilin has already been found in various elements of different insect flight apparatus, including tendons connecting muscles to pleural sclerites, wing hinge ligaments connecting the wings to the thoracic wall, prealar arms connecting pleural sclerites to the mesotergum, wing vein micro-joints connecting cross veins to longitudinal veins, regions of the wing membrane establishing a connection to the wing veins or defined patches within membrane cells, and cuticular layers within wing veins (Weis-Fogh 1960; Andersen and Weis-Fogh 1964; Haas et al. 2000a, b; Lehmann et al. 2011; Appel and Gorb 2014; Appel et al. 2015). In these structures, resilin occurs either in the form of pure or nearly pure resilin (e.g. tendons) or mixed with varying amounts of chitin fibres (e.g. prealar arm), which tend to follow distinct directions or patterns and thereby influence the material's mechanical properties (Andersen and Weis-Fogh 1964; Andersen 2003). All of these structures benefit to a more or less pronounced extent from the presence of resilin due to its low stiffness, high resilience, large and reversible extensibility, long fatigue time and ability of elastic energy storage and damping.

One of these flight system elements is a sausage-like swollen thoracic dragonfly tendon, which consists of virtually pure resilin and connects the pleuro-subalar muscle (which spans between the lower part of the pleuron and the subalar sclerite) to the subalar sclerite, which in turn connects to the axillary sclerites of the wing base (Weis-Fogh 1960; Fig. 4.6a, b). Together with the coxal muscle, it is assumed to control wing twisting (i.e. supination) during the upstroke by taking up wing movements and oscillating in length, while the attached pleuro-subalar muscle contracts slowly and tonically and keeps the tendon at a certain length and tension (Neville 1960; Andersen and Weis-Fogh 1964; King 2010). This is especially important for hovering and other refined flight manoeuvres (Andersen 1964). It

might also play a role in controlling excess wing motions during turbulent flows (King 2010). In the tendon, large reversible extensibility (e.g. over 250% in the forewing of the widow skimmer (*Libellula luctuosa*)) and a long fatigue time are of key importance for the functioning of this structure.

The wing hinge ligament of the forewing of locusts is located between the (meso-) pleural wing process and the second axillary wing sclerite (Andersen and Weis-Fogh 1964). In Odonata, Dictyoptera and Orthoptera, wing hinge ligaments exist in the form of thick, rubber-like pads (Fig. 4.1a) and, as reported for locust structures, consist of a rather tough, mainly chitinous ventral part and a soft dorsal part, which can be divided in a region of pure resilin and a region containing both chitin lamellae and resilin (Andersen and Weis-Fogh 1964). The results of several studies suggest that wing hinge ligaments take up compressive as well as tensile forces and can contribute to (1) the storage of kinetic energy at maximum wing deflection, for example during the upstroke when the wing hinge ligament is stretched, and (2) the wing acceleration during the downstroke by elastic recoil (Andersen and Weis-Fogh 1964; Weis-Fogh 1973; Andersen 2003). In other insects, such as Lepidoptera, some Coleoptera and some Hymenoptera, these ligaments are tough and inextensible, and elastic energy storage is likely provided by the rigid thoracic cuticle and the flight muscle itself (Andersen and Weis-Fogh 1964; Andersen 2003). Due to the fact that resilin has mainly been found in the flight apparatus of insects flying with synchronous flight muscles at low wing beat frequencies of <50 Hz and with inertial forces being larger than aerodynamic forces, it is assumed that its resilience might be too small at high frequencies (Jensen and Weis-Fogh 1962; Andersen and Weis-Fogh 1964; Gosline 2002; Andersen 2003). However, there is still some controversy about the frequency-dependent behaviour of resilin and chitin-resilin-composites and its function in the wing hinge ligaments of insects with high wing beat frequencies (Andersen and Weis-Fogh 1964). For example, some small wing hinge ligaments have been found between different sclerites in the genera *Calliphora*, *Bombus*, *Apis* and *Oryctes* (Andersen and Weis-Fogh 1964; Nachtigall et al. 1998). So far, only a few studies have investigated the decrease in resilience with increasing frequencies in the dragonfly tendon, locust prealar arm and cockroach tibia-tarsal joint resilin (Jensen and Weis-Fogh 1962; Andersen and Weis-Fogh 1964; Gosline et al. 2002; King 2010; Choudhury 2012). Whether the partly pronounced differences in the decrease rate of resilience between different frequency ranges are due to different measurement techniques or are actually due to differences in the material composition, still needs to be elucidated.

The prealar arm is located at the front edge of the mesotergum and establishes a connection to the first basalar sclerite of the pleural thoracic wall via a tough, flexible ligament (Andersen and Weis-Fogh 1964). The basalar sclerite in turn is connected to the humeral angle of the anterior part of the wing base. The prealar arm consists of around 23% chitin and 77% resilin and is structured by alternating layers of resilin and chitin fibrils, with the fibrils continuing into the dark, sclerotised cuticle at its base (Andersen and Weis-Fogh 1964; Fig. 4.1b). Due to the directional arrangement of chitin fibrils, the mechanical behaviour of the prealar arm is assumed to be dominated by the mechanical properties of the chitin fibrils during stretching

and by the properties of resilin during bending and compression (Jensen and Weis-Fogh 1962; Andersen and Weis-Fogh 1964). In contrast to the subalar muscle, which is involved in wing supination, the contraction of the basalar muscle causes wing pronation through the connection to the humeral angle via the basalar sclerite. During muscle contraction, the prealar arm is stretched and can be assumed to play a role in elastic energy storage.

Cross veins in wings of dragonflies and damselflies were shown to form either stiff, inflexibly fused joints or flexible resilin-bearing joints to the adjacent longitudinal veins (Newman 1982; Gorb 1999; Donoughe et al. 2011; Appel and Gorb 2011, 2014; Fig. 4.6c). The distribution pattern of different wing vein joint types on the dorsal and ventral wing sides in various species is quite diverse but was found to follow phylogenetic trends probably related to wing morphology and flight behavior (Donoughe et al. 2011; Appel and Gorb 2014). In general, flexible wing vein joints, together with the overall corrugated design of odonate wings, are assumed to feature a larger angular displacement than fused vein joints and, as a result, to provide the wing with increased chord-wise flexibility, which promotes passive wing deformations such as camber-formation during the downstroke, and thereby to improve the wing's aerodynamic and mechanical performance (Newman 1982; Gorb 1999; Donoughe et al. 2011; Appel and Gorb 2014; Rajabi et al. 2015). Moreover, resilin is important for reducing stress concentrations in vein joints (Rajabi et al. 2015). Resilin is not only present in wing vein joints but also in the wing membrane directly abutting on wing veins and internal cuticle layers of wing veins (i.e. the endocuticle) (Appel and Gorb 2014; Appel et al. 2015; Fig. 4.6d). A flexible suspension of the wing membrane is suggested to allow larger strain and thereby to help prevent its tear-off from the wing veins (Appel et al. 2015). Furthermore, the stiffness gradient in wing veins, generated by a stiff, sclerotised outer layer (exocuticle) and a soft, compliant, resilin-bearing inner layer (endocuticle) is assumed to reduce the overall vein stiffness and to improve the vein's damping properties as well as to delay Brazier ovalisation and to enhance the load-bearing capacity under large deformations (Appel et al. 2015; Rajabi et al. 2016).

By artificially stiffening single flexible, resilin-bearing vein joints in bumblebee wings through the application of micro-splints (extra-fine polyester glitter glued with cyanoacrylate), it was experimentally shown that even a single resilin-bearing joint plays an important role in overall wing flexibility and vertical aerodynamic force production (Mountcastle and Combes 2013). Ma et al. (2015) found comparable resilin joints (e.g. the 1 m-cu joint) in wings of western honey bees (*Apis mellifera*) and assumed that they might play an analogous role in increasing the chordwise wing flexibility. Based on the distribution of resilin patches, wing veins, the occurrence of a flexible hook-mediated forewing-hindwing-connection and observed wing deformations, they further suggested the existence of five flexion lines in one forewing-hindwing entity and assumed that these probably increase the chordwise flexibility and support camber formation. In addition, Mountcastle and Combes (2014) demonstrated that a resilin-bearing joint at the leading edge (the costal break) in the wings of wasps has a major role in mitigating wing wear by flexion along this joint when the wings hit an obstacle. This mechanism is espe-

cially important for wings with wing veins extending all the way to the tip because such a design endows a wing with more spanwise rigidity than, for example, bumblebee wings that lack veins at the wing tip (Mountcastle and Combes 2014).

The occurrence of resilin in several broadened vein patches as well as in membranous folding lines was described for fan-like dermapteran hind wings (Haas et al. 2000b; Deiters et al. 2016). These structures help folding the wing into a wing package being ten times smaller than the unfolded wing. This package can then be hidden under the short sclerotised forewings. The four-fold wing folding can be achieved without musculature activity and is assumed to be driven by elastic recoil of the anisotropically distributed resilin on either the ventral or the dorsal sides of broadened vein patches in intercalary and radiating veins, supported by the resilin-bearing radiating folds that influence the folding direction (Haas et al. 2000b). Unfolding of the hind wings is achieved either by wiping movements of the cerci (e.g. in the European earwig (*Forficula auricularia*) and the lesser earwig (*Labia minor*)) or by wing flapping (e.g. in the earwigs *Timomenus lugens*, which has very long cerci, and *Auchenomus* sp.) (Haas et al. 2000b, 2012). Both unfolding mechanisms are supported by several wing stiffening mechanisms such as the mid-wing mechanism and the claval flexion line, which keep the wing unfolded in all species examined (Haas et al. 2000b, 2012). These mechanisms were found to play an important role both in the static unfolded state of the wing and during flapping flight, in which they help to inhibit an unfavourable folding of the wing (Deiters et al. 2016). Furthermore, the flexible resilin-bearing folding lines were found to not only serve wing folding but also act as flexion lines at which the wing flexes during flight, thereby supporting the generation of an aerodynamically favourable cambered wing profile (Wootton 1992; Deiters et al. 2016).

In beetle wings, resilin was found to occur at the marginal joint, between veins that separate during folding, and along flexion lines in membranous areas, leading to the hypothesis that elastic energy storage by resilin can support wing unfolding also in beetle wings (Haas et al. 2000a). However, this can, if at all, only be a supportive role because wing unfolding in beetles was stated to be mainly achieved by scissor-like movements of the RA and MP1+2 veins via contraction of the *Musculus pleura alaris* and the basalar muscles, which is possibly supported by hydraulic hemolymph pressure (Haas and Beutel 2001; Sun et al. 2014). Like in dermapteran wings, in beetle wings resilin most probably delays material fatigue in highly stressed wing regions and might further play a role in wing deformation during flight (Haas et al. 2000b).

In wings of the urban bluebottle blowfly (*Calliphora vicina*), resilin is mainly present in the proximal part of the wing, predominantly in the form of resilin-bearing patches between veins (Lehmann et al. 2011). The occurrence of resilin coincides with the proximal distribution of the maximum spanwise bending stress at the beginning of each stroke cycle and suggests that the resilin patches reduce the risk of breaking near the wing hinge due to a decrease in peak stress in the rigid wing parts (Lehmann et al. 2011).

4.5.4 Attachment Systems

The contact formation of insect adhesive pads on substrates depends on the pads' ability to adapt to the surface topography. In this context, specific micro- and nano-structures can enhance the quality of the contact (Gorb 2001; Gorb and Beutel 2001; Gorb et al. 2002; Creton and Gorb 2007; Voigt et al. 2008). In the case of attachment on rough substrates, multiple contacts, being formed by some adhesive systems, provide great advantages (Hui et al. 2004). The formation of multiple contacts, which contribute to an increase of the overall length of the total peeling line, is facilitated by a hierarchical organisation of the attachment structures (Varenberg et al. 2010). It was shown that the combination of thin tape-like contact tips of hairs (setae) and applied shear force lead to the formation of a maximal real contact area without slippage within the contact (Filippov et al. 2011). This indicates that material flexibility is very important for the contact formation of adhesive pads. With a minimal normal load, flexible materials can create a large contact area between the attachment structures and the substrate. On the other hand, if elongated structures are made of too flexible materials, they will have a low mechanical stability (Borodich et al. 2010). Insect setae, for example, can buckle and collapse resulting in so-called clusterisation (or condensation) when they are too soft (Jagota and Bennison 2002; Spolenak et al. 2005). Such a clusterisation can strongly decrease the functional advantages obtained from multiple adhesive contacts (Varenberg et al. 2010). For this reason the material properties of insect adhesive setae represent an optimisation problem, which has been solved during evolution by the development of gradients of the thickness and the mechanical properties. The presence of thickness gradients, revealed by scanning electron microscopy, is well-known for various insect adhesive setae (Gorb 2001). Recently, a gradient of the material composition, present on the level of each single adhesive tarsal seta, was shown to exist in the seven-spot ladybird (*Coccinella septempunctata*) (Coleoptera) (Peisker et al. 2013; Fig. 4.7a–c). The material of the setal tip contains large proportions of resilin, while the base of the seta consists mainly of sclerotised chitinous material. Between the tip and the base, a pronounced material composition gradient was revealed by CLSM. This gradient is reflected by a pronounced gradient of the material properties: the setal tip is rather soft, whereas the setal base is relatively stiff. Both gradients were hypothesised to represent an evolutionary optimisation that increases the attachment performance of the adhesive pads when they attach to rough surfaces due to an efficient adaptation of the soft and flexible setal tips to the substrate and a simultaneous prevention of setal clusterisation by means of the stiffer setal bases (Peisker et al. 2013). Since this hypothesis is difficult to test experimentally using biological specimens, it was tested using numerical simulation (Gorb and Filippov 2014; Fig. 4.7d–f). The results indicate that setae with long soft tips and rigid bases exhibit a strong adhesion but also a pronounced clusterisation (Fig. 4.7e). Setae with rigid tips and soft bases have a low adhesion and a pronounced clusterisation (Fig. 4.7f). Only setae with short soft tips and rigid bases feature optimal adhesion properties and simultaneously a minimum of clusterisation (Fig. 4.7d), which

confirms the hypothesis. Tarsal liquids produced by beetles are assumed to contribute to the adhesion efficiency of adhesive pads in the form of capillary interactions and cleaning effects. With regard to the resilin-dominated setal tips, an additional function is conceivable. As described above, resilin is only soft and flexible when it is hydrated. Accordingly, to keep the contribution of the large resilin proportions in the setal tips to the attachment performance of the adhesive pads on a high level, the hydration of the resilin must be maintained. It is imaginable that this is achieved by slowly evaporating tarsal liquids covering the setae and thereby keeping the resilin in the setal tips hydrated (Peisker et al. 2013).

The presence of material gradients has also been demonstrated for smooth attachment devices of insects (Perez Goodwyn et al. 2006). Interestingly, the gradients revealed in smooth adhesive pads of locusts and bush crickets differ from those existing in the adhesive tarsal setae described above. The smooth pads contain a relatively soft core, which is covered by a stiffer layer. Accordingly, the direction of the material gradient is opposite to that in the adhesive tarsal setae, which can be well explained by the different pad architecture. Smooth pads consist of branching rods (fibres), which form foam-like structures and, together with fluid-filled spaces between solid structures, keep the shape of the pad. This principle is combined with the presence of a relatively stiff superficial layer terminating the fibres. The superficial layer is necessary to keep the position of the relatively long and thin fibres (and with it the distance between the fibre tips) constant (Perez Goodwyn et al. 2006; Gorb 2008). This pad architecture was studied in detail in two orthopteran species, the great green bush-cricket (*Tettigonia viridissima*) (Ensifera) and the migratory locust (*Locusta migratoria*) (Caelifera), whose adhesive pads generally have a similar structural organisation (Perez Goodwyn et al. 2006; Fig. 4.8a–d). Both pads possess a flexible resilin-containing exocuticle with fibrils that are fused into relatively large rods oriented in an angle to the surface. However, slight differences in the pad architecture exist. Adhesive pads of *L. migratoria* feature a clearly thicker superficial layer as well as a higher density of rods than those of *T. viridissima* (Fig. 4.8a–d). In addition, indentation experiments revealed a higher effective Young's modulus and a lower work of adhesion for *L. migratoria* pads (Fig. 4.8f, g). The lower adhesive properties of *L. migratoria* pads can be explained by the larger thickness of the relatively stiff superficial layer, which likely reduces the pad's adaptability to the substrate much more than the relatively thin superficial layer of the *T. viridissima* adhesive pad. The superficial layer is assumed to also protect the pad from desiccation as indicated by experiments showing that cut-off adhesive pads of *T. viridissima* (with the relatively thin superficial layer) lose water much faster than those of *L. migratoria* (Fig. 4.8e). Consequently, the material gradient provides a combination of conformability to the surface roughness of the substrate (The compliant material of the pad contributes to the efficient contact formation with the substrate.) and resistance to the dry environment. Such pad architectures likely depend on the preferred environment of each species and are the result of trade-offs between different factors such as evaporation rate, stiffness, stability and adhesion.

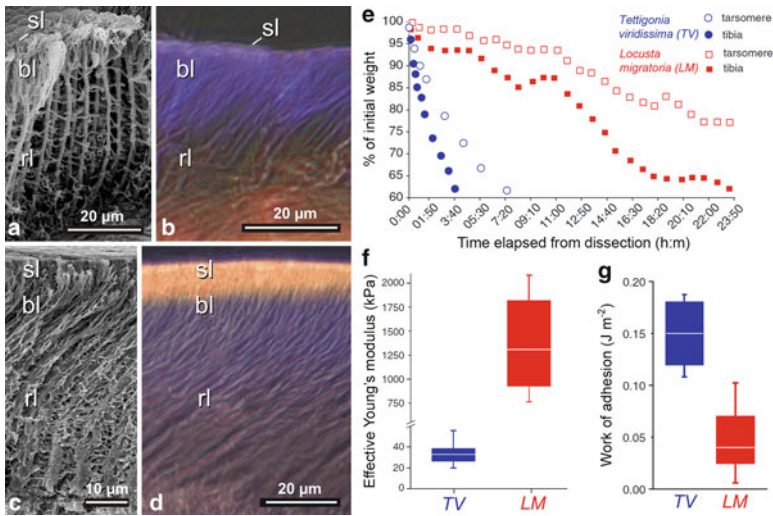


Fig. 4.8 Material structure and properties of orthopteran adhesive pads (euplantulae). **(a, b)** Great green bush-cricket (*Tettigonia viridissima*). **(c, d)** Migratory locust (*Locusta migratoria*). **(a, c)** Scanning electron micrographs showing frozen, fractured, substituted, dehydrated and critical point dried pads. **(b, d)** Wide-field fluorescence micrographs showing frozen-cut pads. Structures with large proportions of resilin are violet/blue. *sl* superficial layer, *bl* layer of branching rods, *rl* layer of primary rods. **(e)** Desiccation dynamics of tarsi and pieces of tibiae cut off the body in both species. **(f)** Effective Young's modulus of attachment pads of both species determined by means of indentation with a spherical tip radius of 250 μm . **(g)** Work of adhesion of attachment pads of both species measured by means of indentation with a sphere with a radius of 32 μm . In **(f)** and **(g)**, the ends of the boxes define the 25th and 75th percentiles, the lines indicate the medians, and the error bars define the 10th and 90th percentiles. **(a–g)** Adapted with permission from Perez Goodwyn et al. (2006)

4.5.5 Mouthparts

The first mouthpart-related structures containing resilin were already mentioned shortly after the description of resilin. In the respective studies, resilin was found in the salivary and feeding pumps of assassin bugs (Edwards 1960 (cited in Bennet-Clark 2007); Bennet-Clark 1963). Later, the findings were confirmed and complemented by additional information about the resilin distribution (Edwards 1983). In these pumps, which enable the bugs to suck relatively large amounts of blood in a short time period and to inject proteolytic enzymes into prey or assaulters or to spit on the latter, the resilin-containing structures function as elastic spring antagonists to muscles. A similar function was described for resilin-containing structures present in the maxillipeds of decapod crustaceans (Burrows 2009). The movements of

the flagella of these mouthparts influence the water flow through the gills as well as over chemoreceptors located on the head, and thereby they importantly contribute to active chemoreception and to signalling by distributing urine odours. Each of the flagella is abducted by the contraction of a single muscle. Due to this abduction, a structure that contains relatively large resilin proportions and is located in the joint between the flagellum and the exopodite of the maxilliped is bent. After relaxation of the muscle, this elastic structure recovers its original shape and moves the flagellum back to its resting position.

In general, due to its very pronounced elasticity and fatigue resistance, resilin appears to be a very suitable material for exoskeleton structures that are typically intensively deformed for a rather large number of times during the lifetime of the organisms. A butterfly proboscis, for example, is tightly and spirally coiled when it is in its resting position (e.g. Krenn 1990). For the uptake of food, hemolymph is pumped into the proboscis resulting in the generation of hydrostatic pressure that completely uncoils the proboscis (e.g. Eastham and Eassa 1955; Hepburn 1971; Krenn 1990) and strongly changes the shape of certain proboscis elements. During this process, dorsal parts of the proboscis are compressed. These parts contain relatively large proportions of resilin and act as springs that cause the recoiling of the proboscis when the hydrostatic pressure is removed (Hepburn 1971).

A remarkable resilin-containing adhesive prey-capture device, formed by the elongated labium, exists in rove beetles of the genus *Stenus* (Staphylinidae). This prey-capture apparatus can be protruded towards a prey within a few milliseconds. When sticky pads (modified paraglossae), located at the distal end of the prementum, adhere to the prey, the labium is withdrawn immediately, and thereby the prey is transported to the mouth region of the beetle where it can be seized with the mandibles (Betz et al. 2009; Koerner et al. 2012a, b). The sticky pads feature a surface that is subdivided into numerous terminally branched outgrowths. During the prey-capture, these surface structures are completely covered by an adhesive secretion that is produced in special glands located in the head capsule and makes the sticky pads a hairy, hierarchically structured and wet adhesive system. Similar to the insect tarsal adhesive pads mentioned above, softness and compliance of the pad cuticle contribute to the generation of strong adhesive forces by the pads. The cuticle material of certain parts of the sticky pads contains large proportions of resilin providing flexibility and elasticity and enabling the pads to efficiently adapt to the surface of the prey items (Koerner et al. 2012b).

Copepods are tiny crustaceans that inhabit nearly all aquatic habitats worldwide and are particularly abundant in the marine water column where they account for large proportions of the zooplankton (e.g. Longhurst 1985; Huys and Boxshall 1991). The diet of many of the marine planktonic species comprises relatively large fractions of diatoms (i.e. unicellular algae with silica-containing shells called frustules). Copepods use the gnathobases of their mandibles to grab and mince food particles. To be able to efficiently digest the diatom cells, the copepods must crack the frustules before the ingestion of the cells. The gnathobases possess tooth-like structures (called teeth in the following) at their distal ends (e.g. Michels and Schnack-Schiel 2005). In copepod species feeding on large amounts of diatoms,

these teeth are rather compact and consist of complex composites that combine diverse structures and materials with a wide range of properties. Recently, the morphology and material composition of the gnathobases of two copepod species have been analysed and described in great detail (Michels et al. 2012, 2015b). The gnathobases of the calanoid copepod *Centropages hamatus* feature two larger and relatively compact teeth (Fig. 4.9a–e). Each of these teeth possesses a chitinous socket that is covered by a cap-like structure with a large resilin proportion. On top, another cap-like structure that is composed of silica is located. All other gnathobase teeth are smaller, contain no silica, are mainly chitinous and have tips with large resilin proportions. *C. hamatus* is omnivorous and feeds on, among other organisms, diatoms and protists. It is assumed that the large silica-containing teeth are used for feeding on diatoms. The silica makes these teeth stiffer and more mechanically stable and thereby more efficient in cracking the diatom frustules. In case the diatom frustules are too stable and the pressure acting on the tips of the siliceous teeth exceeds the breaking stress level causing an increased risk of crack formation in and breakage of the teeth, the soft and elastic resilin-containing structures are supposed to function as flexible bearings that can be compressed and thereby reduce stress concentrations in the tooth material and increase the resistance of the teeth to mechanical damages. Additional structures with large resilin proportions, located in the central and proximal parts of the gnathobases, are assumed to have a damping function that makes the whole gnathobases resilient and further reduces the risk of mechanical damage of the teeth. The smaller gnathobase teeth of *C. hamatus* are likely used to grab protists. In this context, the grip of the tooth tips is suggested to be increased by the soft and elastic resilin making the grabbing process more efficient.

The gnathobases of the calanoid copepod *Rhincalanus gigas*, a species whose diet mainly consists of diatoms, are characterised by five relatively large and compact teeth that possess a combination of different materials comparable to that of the silica-containing teeth of *C. hamatus* (Fig. 4.9f, g). Each of these teeth has a silica-containing cap-like structure that is located on a chitinous socket. At the base of the socket, the gnathobase exoskeleton features large proportions of resilin. Like in the silica-containing teeth of *C. hamatus*, these resilin-containing structures very likely function as compressible supports reducing the risk of mechanical damages of the teeth during feeding on diatoms with stable frustules. In general, the complex composite systems in the gnathobase teeth are assumed to have coevolved within an evolutionary arms race together with the diatom frustules (Michels and Gorb 2015).

4.5.6 Reproductive Organs, Mechanoreceptors and Compound Eyes

The mating of bed bugs represents a famous example of sexual conflict. During every successful mating event, the cuticle of the ventral side of the female's abdomen is penetrated by the male with a cannula-like intromittent organ, and the male

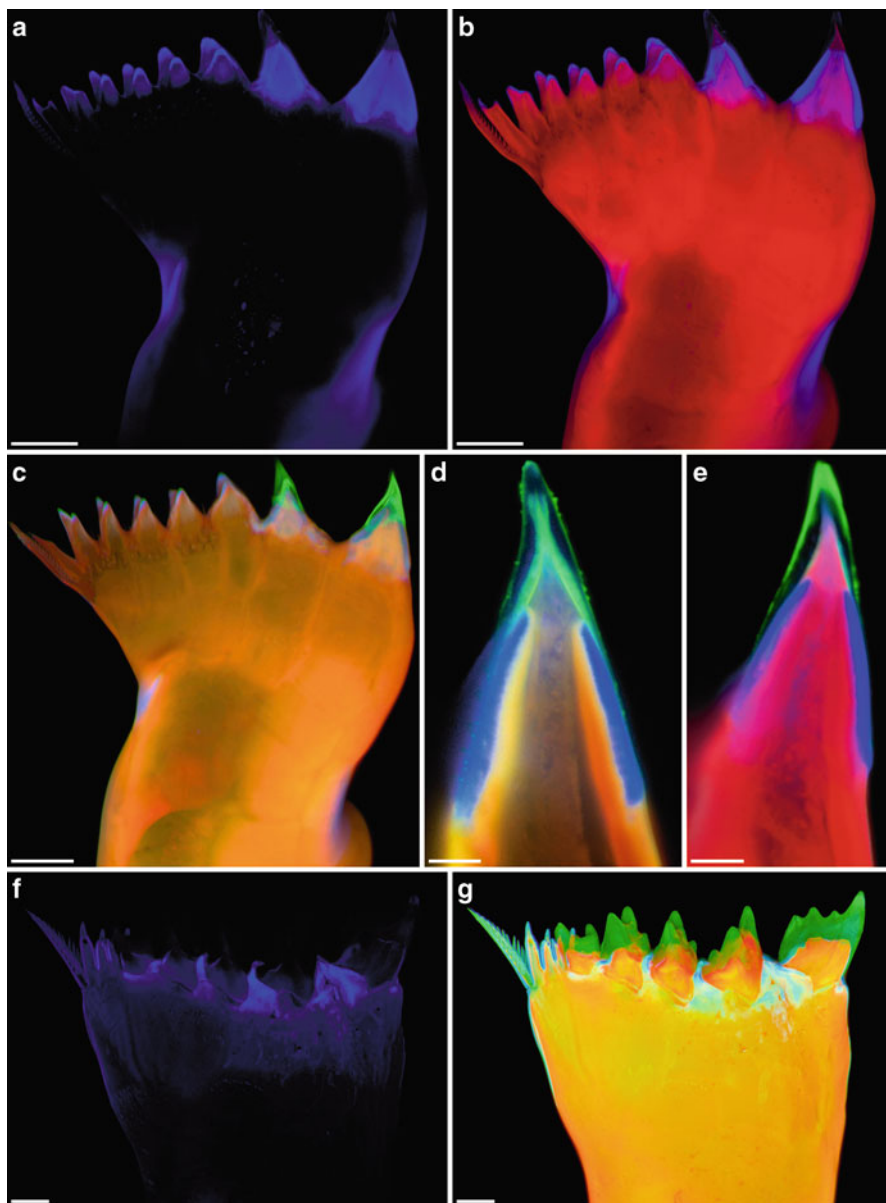


Fig. 4.9 Morphology and material composition of mandibular gnathobases of copepods. Confocal laser scanning micrographs showing gnathobase structures of (a–e) a female of the copepod species *Centropages hamatus* and (f, g) a female of the copepod species *Rhincalanus gigas*. (a–c, f, g) Maximum intensity projections. (d, e) 1- μ m-thick optical sections through the largest tooth of the gnathobase. (a, f) Distribution of resilin. (b) Chitinous exoskeleton (red) and resilin-dominated structures (blue). (c–e, g) Chitinous exoskeleton (red, orange), resilin-dominated structures (blue, light blue, turquoise) and silica-containing structures (green). Scale bars=20 μ m (a–c), 5 μ m (d, e), 25 μ m (f, g) ((a–e) Adapted with permission from Michels et al. (2012). (f, g) Adapted with permission from Michels et al. (2015b))

injects sperm and accessory gland fluids directly into the abdomen where the sperm migrate to the ovaries (Carayon 1966; Stutt and Siva-Jothy 2001). This traumatic insemination imposes survival costs on the females (e.g. Stutt and Siva-Jothy 2001) but the females cannot avoid mating (Reinhardt et al. 2009). As a result of this sexual conflict, a female organ, the so-called spermalege, has evolved. In common bed bugs (*Cimex lectularius*), this organ is located on the right side of the ventral abdomen part where it is visible as a notch-like modification of the posterior edge of the fifth segment that exposes the subjacent intersegmental membrane and cuticle of the sixth segment (Fig. 4.10a, b). A recent study revealed that the spermalege cuticle, by contrast to other cuticle sites analysed on the ventral side of the female abdomen, contains large proportions of resilin (Michels et al. 2015a; Fig. 4.10c–l). In micro-indentation tests, the penetration force necessary to pierce the resilin-rich spermalege cuticle was significantly lower than that necessary to pierce the other cuticle sites (Michels et al. 2015a; Fig. 4.10b). In addition, evidence for a significantly reduced tissue damage and hemolymph loss was obtained for piercings of the spermalege cuticle compared with piercings of the other cuticle sites (Michels et al. 2015a). The results suggest that the material composition of the spermalege cuticle has evolved as a tolerance trait that reduces the mating costs of both the female and the male: due to the softness of resilin the penetration is easier for the male and causes less wounding of the female, and after the withdrawal of the intromittent organ the elasticity of resilin causes a sealing of the puncture reducing the hemolymph loss and the risk of bacterial infection.

Hair plate sensilla and campaniform sensilla are typical mechanoreceptors that are common in insect exoskeletons (e.g. Thurm 1964; Heusslein and Gnatzy 1987; Keil 1997). These receptors possess so-called joint membranes and cap membranes that are composed of large proportions of resilin (Thurm 1964; Keil 1997; Michels and Gorb 2012). On the dorsal side of the pretarsus of *E. tenax*, for example, hair plate sensilla with rather long and relatively thick hairs are present (Fig. 4.11a–e). The base of each hair is surrounded by a joint membrane that, due to its resilin-dominated material composition, is soft and flexible and allows movement and bending of the hair shaft resulting in a stimulation of the receptor. Because the long hairs project beyond and below the pulvilli of the pretarsus, they touch the substrate shortly before the pulvilli and likely have the function to indicate the upcoming contact between the pulvilli and the substrate. The cerci of crickets feature cercal filiform hairs associated with campaniform sensilla (Heusslein and Gnatzy 1987; Heußlein et al. 2009). The latter and the bases and sockets of the filiform hairs are embedded in material that contains relatively large proportions of resilin (Michels and Gorb 2012; Fig. 4.11f) and, as mentioned above, very likely allow movement and bending of the shafts of the filiform hairs and of the campaniform sensilla, which are very sensitive strain receptors (also called flex or displacement receptors), and thereby stimulate the respective dendrite of the sensory cell.

The presence of large proportions of resilin (in part also described as ‘resilin-like protein’) in compound eye lenses has been described for different arthropods

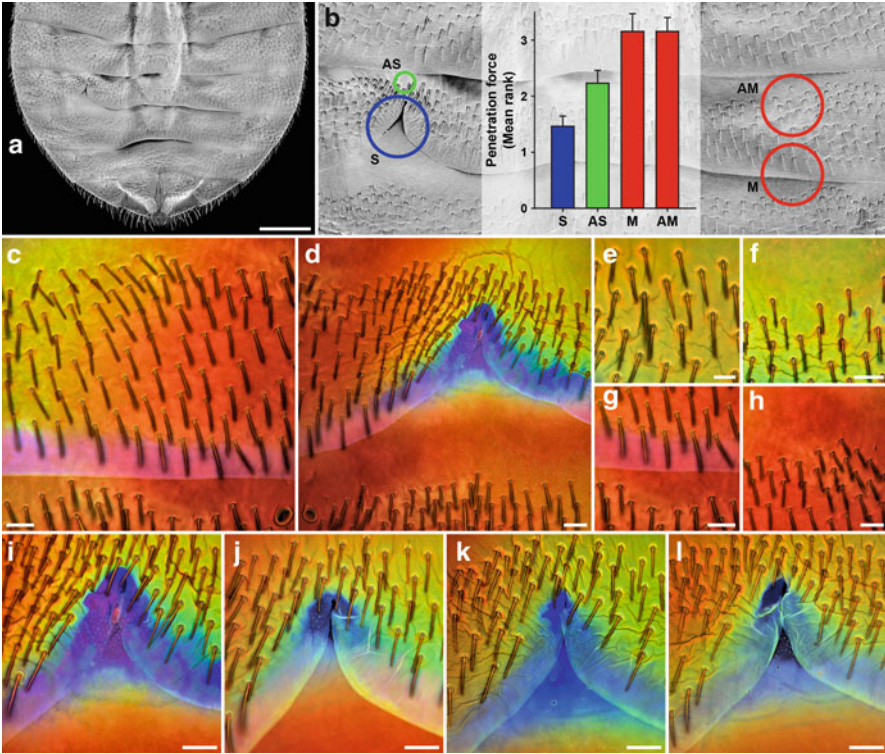


Fig. 4.10 Material composition and properties of the ventral abdominal cuticle of females of the common bed bug (*Cimex lectularius*). (a) Abdomen overview (scanning electron micrograph). (b) Section of (a) indicating the locations of the spermalege (*S*) and three other cuticle areas called AS, *M* and AM, and penetration forces (mean ranks and standard errors) determined for these four cuticle sites. (c–l) Confocal laser scanning micrographs (maximum intensity projections) showing overlays of different autofluorescences exhibited by the exoskeletons. Blue colours indicate large proportions of resilin. (c, d) Autofluorescence composition of the cuticle in the left (c) and right (d) abdomen parts. The dominance of violet/blue autofluorescence (shown in blue) is restricted to the spermalege, clearly indicating that only at this site the cuticle contains large proportions of resilin. (e–h) Autofluorescence composition of the cuticle at the sites AS (e, f), *M* (g) and AM (h). The cuticle at *M* and AM consists mainly of sclerotised chitinous material, indicated by the dominance of autofluorescence shown in red, while the presence of large proportions of autofluorescence shown in green in the cuticle at AS indicates that the respective material consists mainly of weakly or non-sclerotised chitinous material. (i–l) Autofluorescence composition of the cuticle at the spermaleges of different 1-week-old females, indicating variation of the extent of the resilin-dominated spermalege structures between females. Scale bars=500 μm (a), 50 μm (c, d, f–l), 25 μm (e) (Figure reproduced with permission from Michels et al. (2015a))

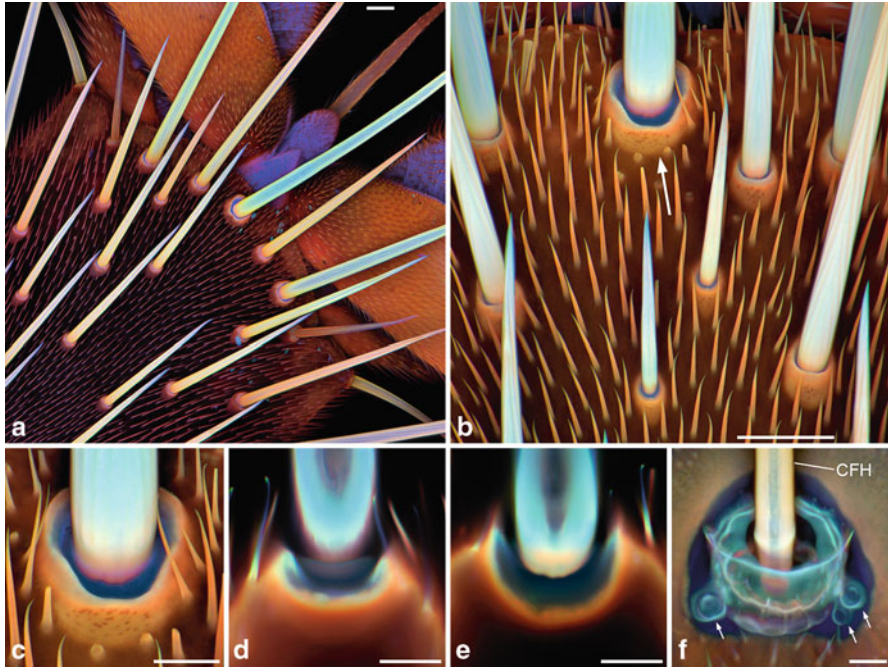


Fig. 4.11 Resilin in mechanoreceptors. (a–f) Confocal laser scanning micrographs showing overlays of different autofluorescences exhibited by the exoskeletons. Blue colours indicate large proportions of resilin. (a) Dorsal view of the pretarsus of a third leg of a female drone fly (*Eristalis tenax*). (b) Dorsal view of a section of a second leg's pretarsus of a male *E. tenax*. The arrow highlights a hair plate sensillum. (c) Larger view of the hair plate sensillum highlighted in (b). (d, e) Confocal laser scanning micrographs showing 1- μ m-thick optical sections through the hair plate sensillum shown in (c). (f) Cercal filiform hair (CFH) and associated campaniform sensilla (highlighted by small arrows) on a cercus of a female house cricket (*Acheta domestica*). (a–c, f) Maximum intensity projections. Scale bars = 25 μ m (a, b), 10 μ m (c–f) (Figure reproduced with permission from Michels and Gorb (2012))

(Sannasi 1970; Jaganathan and Sundara Rajulu 1979; Dey and Raghavarman 1983; Viswanathan and Varadaraj 1985; Michels and Gorb 2012; Fig. 4.12). While other exoskeleton components are typically micro- and nano-structured, coloured and pigmented and, therefore, not suitable as material for optical elements, the pronounced transparency, the colourlessness and the amorphousness make resilin a perfect material for the construction of optical systems.

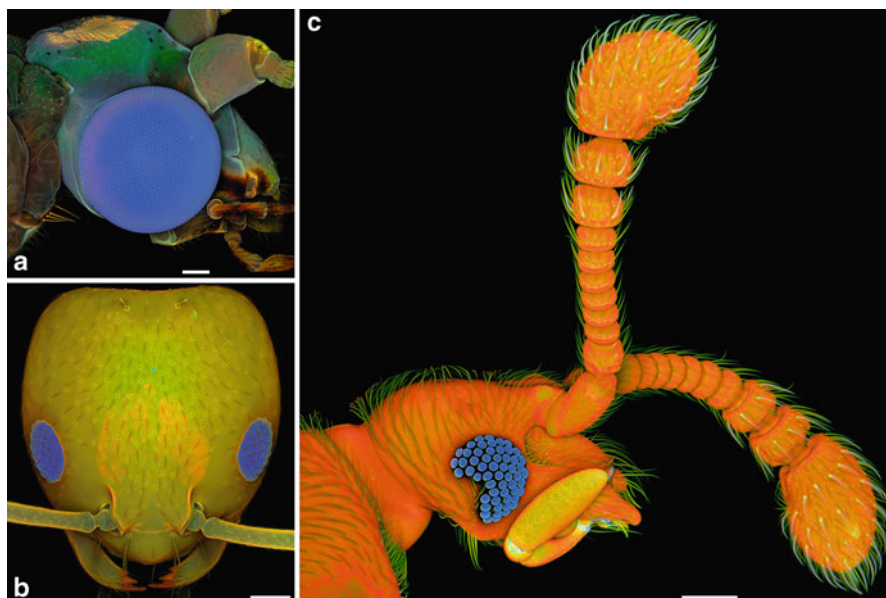


Fig. 4.12 Resilin in compound eyes. Confocal laser scanning micrographs (maximum intensity projections) depicting overlays of different autofluorescences exhibited by the exoskeletons. Blue structures contain large proportions of resilin. **(a)** Lateral view of the head of a male green lacewing (*Chrysoperla carnea*). **(b)** Frontal view of the head of a pharaoh ant (*Monomorium pharaonis*) worker. **(c)** Lateral view of the head of a beetle of the genus *Circocerus*. Scale bars = 100 μm (**a, c**), 50 μm (**b**) ((**a, b**) Adapted with permission from Michels and Gorb (2012))

4.6 Biomimetics

The outstanding combination of high extensibility, high durability, low stiffness, high solvent- and heat-stability, self-assemble ability, autofluorescence and high resilience, which is even greater than that of polybutadiene, makes resilin ideal for industrial and medical applications in a variety of different fields including tissue engineering, drug delivery, biosensor techniques and nanotechnology (Rauscher and Pomès 2012; van Eldijk et al. 2012; Su et al. 2014). In 2001, Ardell and Andersen identified the *D. melanogaster* gene product CG15920. A few years later, Elvin and coworkers (2005) reported on the first success in the cloning, expression and purification of the protein derived from the first exon of this gene in *Escherichia coli*. They produced the soluble recombinant resilin-like polypeptide rec1-resilin, which by Ru(II)-mediated photo-cross-linking can be formed into a solid, rubber-like material with physical and mechanical properties comparable to those of native resilin. Since then, a variety of different recombinant resilin-like polypeptides (RLPs) have been synthesised using more and more effective cloning and expression induction techniques to produce repetitive sequences, multimerise short sequences and increase the yield of the recombinant protein (e.g. Meyer and Chilkoti 2002; Studier 2005; Kim et al. 2007; Lyons et al. 2007, 2012; Qin et al. 2009;

Bracalello et al. 2011; McGann et al. 2013; Su et al. 2014). The increase in the yield of water soluble RLPs to concentrations higher than 20 wt% and their unique thermo-responsiveness in the form of a dual phase behaviour with lower and upper critical solution temperatures (LCST and UCST, respectively) (rec1-resilin: about 6 °C (LCST) and 70 °C (UCST)), above or below which they are completely or partially immiscible, facilitated the purification and allowed the formation of hydrogels (Elvin et al. 2005; Dutta et al. 2011; van Eldijk et al. 2012; Balu et al. 2014). Whittaker and coworkers (2015a) showed that the LCST can be tuned to lower values by inducing more ordered conformations and increasing hydrophobicity to rec1-resilin, for example by combining rec1-resilin with a hydrophobic rigid silk fibroin protein. In the future, this LCST behaviour could also be used to design a minimally invasive injectable scaffold, being, for example, soluble at room temperature but forming a fitting hydrogel scaffold at the defect site at body temperature (Li et al. 2011; Su et al. 2014).

Another useful property of RLPs is their pH responsiveness. Rec1-resilin has an isoelectric point at around pH=4.8 and shows a complex organisation with negatively charged protein residues exposed to water and positively charged residues forming the core (Dutta et al. 2011). Dutta and coworkers (2011) revealed a rapid change in the structural conformation of rec1-resilin as a function of pH and associated charge reversal, and Truong and coworkers (2010) reported on the pH-dependent behaviour of rec1-resilin at solid-liquid interfaces, forming globule to coil to extended coil conformations with varying packing densities at changing pH values, creating a ‘switchable surface’ with either a compact or a brush-like conformation (Truong et al. 2010; Balu et al. 2014). Furthermore, Dutta and coworkers (2011) found that the UCST behaviour of rec1-resilin is dependent on the pH value due to a change in hydrogen-bonding capabilities of the amino acids.

Photo-responsiveness is an additional property of native resilin and RLPs that can be influenced by the pH value. When excited with UV light, RLPs and native resilin exhibit a violet/blue autofluorescence, which can be attributed to the phenolic amino acid tyrosine. Excitation and emission wavelengths of RLPs were reported to change dramatically with increasing pH value, changing from maxima of 275 nm (absorption) and 303 nm (emission) to 293 nm and 350 nm, respectively. This shift is probably due to the ionisation (deprotonation) of the phenolic group of tyrosine at a pH value higher than its pKa (around 10.5) (Dutta et al. 2011; Balu et al. 2014).

In addition, the mechanical properties of RLPs and native resilin can be controlled through the level of hydration. Dried rec1-resilin is hard, brittle and glass-like and features a very high glass transition temperature of around 181 °C (only slightly lower than the chemical decomposition temperature of around 236 °C) due to strong intermolecular interactions between the amino acid residues (Truong et al. 2011; Balu et al. 2014). When hydrated (even when hydrated only to 10%), rec1-resilin swells and shows a dramatic decrease in the glass transition temperature, hardness and elastic modulus (Truong et al. 2011). The initial, very fast, hydration of RLPs can be ascribed to the high amount of polar amino acid residues in rec1-resilin (around 46%), with aspartic acid and glutamic acid having the highest affinity towards water molecules, which are present in the form of bound non-crystallisable

water (Truong et al. 2011). In the second stage, hydration expands by clustering/condensation around these already hydrophilic sites, followed by the third stage, in which clustering of free crystallisable water (bulk water) occurs, finally rendering the RLPs completely hydrated and soft and endowing them with high molecular chain mobility (Truong et al. 2011).

Li and coworkers (2011, 2013) also showed that mechanical properties like strength, extensibility and storage modulus of the RLPs can be easily tuned (e.g. storage modulus within a range of 500 Pa to 10 kPa) by varying the polypeptide concentration and cross-linker ratios (e.g. higher cross-linking leads to higher strength and lower extensibility; higher protein concentrations lead to higher storage modulus). Furthermore, they found that gelation times can be tuned via variations in RLPs concentration, cross-linker ratio and cross-linking temperature, suggesting possible applications in RLPs *in vivo* injection (Li et al. 2011).

Qin and coworkers (2011) demonstrated that cross-linking of the rec1-resilin via the citrate-modified photo-Fenton reaction can be used as another dityrosine mediated polymerisation and results in not only highly elastic but also adhesive materials, thereby representing a useful tool for the *in vivo* gelation of RLPs.

Dutta and coworkers (2009) further examined the adsorption of RLPs on different surfaces and reported that RLPs molecular architecture and orientation during assembly can be controlled by tuning the physical conditions at the surface (i.e. substrate surface energy). They showed the formation of mono-molecular layers on hydrophilic and of columnar structures on hydrophobic surfaces, suggesting the use of these nanoscale rec1-resilin mono/bi-layers (0.98–8.3 nm) as a template or reservoir for drug, nanoparticle or enzyme delivery and sensor applications (Dutta et al. 2009; Balu et al. 2014). Later, they used rec1-resilin to synthesise nanoclusters with a size of <2 nm, which include, for example, gold and silver (Dutta et al. 2013; Balu et al. 2014). For this purpose, they used rec1-resilin to sequester noble metal ions, entrapped those ions to the aqueous protein solution through addition of precursor salts and increased the pH to around 12 to reduce the sequestered ions (by the rec1-resilin molecules) to form particles (Dutta et al. 2013; Balu et al. 2014).

Vashi and coworkers (2013) further showed that RLPs lack cell-recognition sequences, so that cells will not bind to RLPs matrices, but that the addition of an integrin-binding motif (-RGD) to the RLPs allows cell binding. As reported by Renner and coworkers (2012), these RLP-RGD gels are not only biodegradable but in fact ensure a cell viability of 95%. In addition, Vashi and coworkers (2013) proved that the photochemical reaction for tyrosine cross-linking in RLPs is cell-compatible (*in vitro*), complementing the latter results and supporting an *in vivo* application.

All these properties together with the unusual multi-stimuli responsiveness make RLPs highly promising to be used as flexible, highly resilient scaffold or reservoir material in various applications. Furthermore, more recently, modular chimeric RLPs have been developed, conferring desired mechanical and biological properties to the resilin-based scaffold (e.g. Charati et al. 2009; Li et al. 2013; Balu et al. 2014; Su et al. 2014). For example, modules of different bioactive molecules can be incorporated into RLPs, containing several repeats of the resilin-like motif of the first exon, to mimic cellular microenvironments of the extracellular matrix. This can help engineering mechanically active tissues as blood vessels, cardiovascular tis-

sues and vocal cords (Li et al. 2011). For example, Charati and coworkers (2009) included functional domains intended to control cell adhesion, growth factor delivery and material degradation. More specifically, they used a cell-binding ligand derived from fibronectin for cell adhesion, a matrix metalloproteinase sensitive sequence to promote proteolytic degradation by respective enzymes, and a heparin-binding module for the immobilisation of heparin and the sequestration of growth factors (Charati et al. 2009; van Eldijk et al. 2012). In addition, they added lysine residues outside of the repeat motifs to have additional cross-linking sites and replaced tyrosine with phenylalanine in order to provide strategies for photochemical cross-linking (Charati et al. 2009). Such slight modifications to the amino acid sequences of the resilin-like repeat motifs, as well as the incorporation of functional domains were shown to not measurably alter the conformational and mechanical properties of the RLPs (Charati et al. 2009; Li et al. 2011). More precisely, Li and coworkers (2013) showed that the concentration of biologically active domains in a hydrogel can be uncoupled from its mechanical properties by simply mixing different RLPs constructs.

Other studies, like the one of Lv and coworkers (2010), report on the attempt to develop materials that could mimic different types of muscles. With the idea to endow the material with mechanical properties comparable to titin and resilin, they created modular RLPs consisting of mechanically resistant, folded and globular GB1 domains and resilin-like repeat domains and obtained RLPs with a stiffness comparable to that of myofibrils, a high resilience at low strain and an enhanced ability to work as shock-absorber at high strain by dissipating energy (Lv et al. 2010). In another attempt to combine the mechanical properties of elastin and resilin (high elasticity) with those of collagen (high strength), Bracalello and coworkers (2011) created a chimeric resilin-elastin-collagen like polypeptide (REC), which shows a self-assembling into higher order fibrillary structures and a Young's modulus comparable to that of elastin- or resilin-like material. Whittaker and coworkers (2015b) developed a chimeric recombinant resilin-like polypeptide by combining soft, highly elastic rec1-resilin with the mechanically strong and hard regenerated silk fibroin (RSF) and obtained a hybrid Rec1/RSF hydrogel with a higher water uptake capacity and increased storage modulus values (in the range of MPa), allowing the usage in, for example, tissue engineering applications where increased stiffness is required.

Chimeric RLPs can also be used as surfactant-like agents or bio-nanocomposite adhesives, enabling the incorporation of beneficial bio-nanocomposites into a material of different hydrophobicity and thereby enhancing its material properties (Verker et al. 2014). For example, Verker and coworkers (2014) developed an environmentally friendly method of inserting hydrophilic nano-crystalline cellulose (NCC) into a commercially available hydrophobic epoxy resin by using an RLP combined with a cellulose binding domain (CBD). Until then, incorporation of NCC into polymeric matrices or adhesives had involved unsatisfactory or environmentally unfriendly methods such as the use of waterborne epoxy resins or the use of large quantities of solvents (Capadona et al. 2007; Tang and Weder 2010; Verker et al. 2014; Xu et al. 2013). Upon mixing and sonication of RLP-CBD, NCC and epoxy resin, Verker and coworkers (2014) produced an emulsion of epoxy resin surrounding aqueous droplets of RLP-CBD bound to NCC via the CBD. Heating of the

emulsion led to a covalent reaction between the amine groups of the RLP and the epoxide groups of the epoxy resin, thereby having fixed and dispersed the NCC in the epoxy resin, and to the evaporation of water (Verker et al. 2014). After adding the commercial hardener, an epoxy resin with a higher elasticity (arising from the incorporation of the RLP) and a dramatically increased Young's modulus (arising from the incorporation of the NCC) was obtained (Verker et al. 2014).

4.7 Conclusions and Outlook

Exoskeleton structures with large proportions of resilin are common among arthropods. This book chapter demonstrates the exceptional properties of resilin and the broad range of resilin functions in various exoskeleton structures. Resilin stands out because of its low stiffness, unique resilience, large extensibility and extreme durability, and it facilitates flexibility and compliance, elastic energy storage, elastic recovery, fatigue and damage reduction, sealing and transparency and thereby makes the respective exoskeleton systems rather effective. Due to its remarkable combination of different properties, resilin is a highly efficient multi-functional protein, and this has very likely been the reason for the evolution of the large functional diversity of resilin-containing exoskeleton structures. Furthermore, the outstanding properties of resilin, especially the very pronounced resilience, the solvent- and heat-stability and the ability to self-assemble make this elastomeric protein an ideal biological material for diverse industrial and medical applications. Numerous studies have been conducted to reveal the molecular mechanism of the elasticity of resilin and to more and more tune the properties of recombinant resilin-like polypeptides, thereby paving the way for a potential extensive utilisation of this low-toxic biocompatible material as a replacement for many synthetic polymers.

Acknowledgements Joseph Parker (Columbia University and American Museum of Natural History, New York, NY, U.S.A.) provided the specimen shown in Fig. 4.12c. Peter Attermeyer, Dario Furlani and Ingo Bartholomäus (Carl Zeiss Microscopy GmbH, Jena, Germany) permitted the use of a ZEISS LSM 800 and thereby enabled the production of Fig. 4.12c. This book chapter is adapted from the publication 'Michels J, Appel E, Gorb SN (2016) Functional diversity of resilin in Arthropoda. *Beilstein J Nanotechnol* 7:1241–1259'.

References

- Adzhubei AA, Sternberg MJ, Makarov AA (2013) Polyproline-II helix in proteins: structure and function. *J Mol Biol* 425:2100–2132
- Aeshbach R, Amado R, Neukom H (1976) Formation of dityrosine cross-links in proteins by oxidation of tyrosine residues. *Biochem Biophys Acta* 439:292–301
- Andersen SO (1963) Characterization of a new type of cross-linkage in resilin, a rubber-like protein. *Biochim Biophys Acta* 69:249–262
- Andersen SO (1964) The cross-links in resilin identified as dityrosine and trityrosine. *Biochim Biophys Acta* 93:211–213

- Andersen SO (1966) Covalent cross-links in a structural protein, resilin. *Acta Physiol Scand* 66(Suppl 263):1–81
- Andersen SO (1971) Resilin. In: Florkin M, Stotz EH (eds) *Comprehensive biochemistry*, vol 26C, Extracellular and supporting structures. Elsevier, Amsterdam, pp 633–657
- Andersen SO (1979) Biochemistry of insect cuticle. *Annu Rev Entomol* 24:29–61
- Andersen SO (1998) Amino acid sequence studies on endocuticular proteins from the desert locust, *Schistocerca gregaria*. *Insect Biochem Mol Biol* 28:421–434
- Andersen SO (1999) Exoskeletal proteins from the crab, *Cancer pagurus*. *Comp Biochem Phys A* 123:203–211
- Andersen SO (2001) Matrix proteins from insect pliable cuticles: are they flexible and easily deformed? *Insect Biochem Mol Biol* 31:445–452
- Andersen SO (2003) Structure and function of resilin. In: Shewry PR, Tatham AS, Bailey AJ (eds) *Elastomeric proteins: structures, biomechanical properties, and biological roles*. Cambridge University Press, Cambridge, pp 259–278
- Andersen SO (2004a) Regional differences in degree of resilin cross-linking in the desert locust, *Schistocerca gregaria*. *Insect Biochem Mol Biol* 34:459–466
- Andersen SO (2004b) Chlorinated tyrosine derivatives in insect cuticle. *Insect Biochem Mol Biol* 34:1079–1087
- Andersen SO (2010) Studies on resilin-like gene products in insects. *Insect Biochem Mol Biol* 40:541–551
- Andersen SO, Weis-Fogh T (1964) Resilin. A rubberlike protein in arthropod cuticle. *Adv Insect Physiol* 2:1–65
- Andersen SO, Rafn K, Roepstorff P (1997) Sequence studies of proteins from larval and pupal cuticle of the yellow meal worm, *Tenebrio molitor*. *Insect Biochem Mol Biol* 27:121–131
- Appel E, Gorb SN (2011) Resilin-bearing wing vein joints in the dragonfly *Epiophlebia superstes*. *Bioinspir Biomim* 6:046006
- Appel E, Gorb SN (2014) Comparative functional morphology of vein joints in Odonata. *Zoologica* 159:1–159
- Appel E, Heepe L, Lin C-P, Gorb SN (2015) Ultrastructure of dragonfly wing veins: composite structure of fibrous material supplemented by resilin. *J Anat* 227:561–582
- Ardell DH, Andersen SO (2001) Tentative identification of a resilin gene in *Drosophila melanogaster*. *Insect Biochem Mol Biol* 31:965–970
- Bailey K, Weis-Fogh T (1961) Amino acid composition of a new rubber-like protein, resilin. *Biochim Biophys Acta* 48:452–459
- Balu R, Whittaker J, Dutta NK, Elvin CM, Choudhury NR (2014) Multi-responsive biomaterials and nanobioconjugates from resilin-like protein polymers. *J Mater Chem B* 2:5936–5947
- Balu R, Knott R, Cowieson NP, Elvin CM, Hill AJ, Choudhury NR, Dutta NK (2015) Structural ensembles reveal intrinsic disorder for the multi-stimuli responsive bio-mimetic protein Rec1-resilin. *Sci Rep* 5:10896
- Bayley TG, Sutton GP, Burrows M (2012) A buckling region in locust hindlegs contains resilin and absorbs energy when jumping or kicking goes wrong. *J Exp Biol* 215:1151–1161
- Bennet-Clark HC (1963) Negative pressures produced in the pharyngeal pump of the bloodsucking bug, *Rhodnius prolixus*. *J Exp Biol* 40:223–229
- Bennet-Clark HC (1975) The energetics of the jump of the locust *Schistocerca gregaria*. *J Exp Biol* 63:53–83
- Bennet-Clark HC (1997) Tymbal mechanics and the control of song frequency in the cicada *Cyclochila australasiae*. *J Exp Biol* 200:1681–1694
- Bennet-Clark HC (2007) The first description of resilin. *J Exp Biol* 210:3879–3881
- Bennet-Clark HC, Lucey ECA (1967) The jump of the flea: a study of the energetics and a model of the mechanism. *J Exp Biol* 47:59–76
- Betz O, Koerner L, Gorb SN (2009) An insect's tongue as the model for two-phase viscous adhesives? *Adhes Adhes Sealants* 6:32–35
- Bochicchio B, Pepe A, Tamburro AM (2008) Investigating by CD the molecular mechanism of elasticity of elastomeric proteins. *Chirality* 20:985–994

- Borodich FM, Gorb EV, Gorb SN (2010) Fracture behaviour of plant epicuticular wax crystals and its role in preventing insect attachment: a theoretical approach. *Appl Phys A* 100:63–71
- Bracalello A, Santopietro V, Vassalli M, Marletta G, Del Gaudio R, Bochicchio B, Pepe A (2011) Design and production of a chimeric resilin-, elastin-, and collagen-like engineered polypeptide. *Biomacromolecules* 12:2957–2965
- Burrows M (2009) A single muscle moves a crustacean limb joint rhythmically by acting against a spring containing resilin. *BMC Biol* 7:27
- Burrows M (2010) Energy storage and synchronisation of hind leg movements during jumping in planthopper insects (Hemiptera, Issidae). *J Exp Biol* 213:469–478
- Burrows M (2011) Jumping mechanisms and performance of snow fleas (Mecoptera, Boreidae). *J Exp Biol* 214:2362–2374
- Burrows M (2012) Jumping mechanisms in jumping plant lice (Hemiptera, Sternorrhyncha, Psyllidae). *J Exp Biol* 215:3612–3621
- Burrows M (2014a) Jumping mechanisms in dictyopharid planthoppers (Hemiptera, Dictyopharidae). *J Exp Biol* 217:402–413
- Burrows M (2014b) Jumping mechanisms in flatid planthoppers (Hemiptera, Flatidae). *J Exp Biol* 217:2590–2600
- Burrows M, Dorosenko M (2014a) Rapid swimming and escape movements in the aquatic larvae and pupae of the phantom midge *Chaoborus crystallinus*. *J Exp Biol* 217:2468–2479
- Burrows M, Dorosenko M (2014b) Jumping mechanisms in lacewings (Neuroptera, Chrysopidae and Hemerobiidae). *J Exp Biol* 217:4252–4261
- Burrows M, Sutton GP (2012) Locusts use a composite of resilin and hard cuticle as an energy store for jumping and kicking. *J Exp Biol* 215:3501–3512
- Burrows M, Shaw SR, Sutton GP (2008) Resilin and chitinous cuticle form a composite structure for energy storage in jumping by frog hopper insects. *BMC Biol* 6:41
- Burrows M, Borycz JA, Shaw SR, Elvin CM, Meinertzshagen IA (2011) Antibody labelling of resilin in energy stores for jumping in plant sucking insects. *PLoS One* 6(12):e28456
- Capadona JR, van den Berg O, Capadona LA, Schroeter M, Rowan SJ, Tyler DJ, Weder C (2007) A versatile approach for the processing of polymer nanocomposites with selfassembled nanofibre templates. *Nat Nanotechnol* 2:765–769
- Carayon J (1966) Traumatic insemination and the paragenital system. In: Usinger RL (ed) *Monograph of cimicidae (Hemiptera-Heteroptera)*. Entomological Society of America, Lanham, pp 81–166
- Charati MB, Ifkovits JL, Burdick JA, Linhardt JG, Kiick KL (2009) Hydrophilic elastomeric biomaterials based on resilin-like polypeptides. *Soft Matter* 5:3412–3416
- Cheng S, Cetinkaya M, Gräter F (2010) How sequence determines elasticity of disordered proteins. *Biophys J* 99:3863–3869
- Choudhury U (2012) Dynamic mechanical properties of cockroach (*Periplaneta americana*) resilin. Master's thesis. Virginia Polytechnic Institute and State University, Blacksburg (<https://vtechworks.lib.vt.edu/handle/10919/40869>)
- Creton C, Gorb SN (2007) Sticky feet: from animals to materials. *MRS Bull* 32:466–472
- Deiters J, Kowalczyk W, Seidl T (2016) Simultaneous optimization of earwig hindwings for flight and folding. *Biol Open* 5:638–644
- DeVore DP, Gruebel RJ (1978) Dityrosine in adhesive formed by the sea mussel, *Mytilus edulis*. *Biochem Biophys Res Commun* 80:993–999
- Dey S, Raghavarman A (1983) Occurrence of resilin in the lens-cuticle of the honey bee, *Apis cerana indica*. *Indian Zool* 7:31–34
- Donoughe S, Crall JD, Merz RA, Combes SA (2011) Resilin in dragonfly and damselfly wings and its implications for wing flexibility. *J Morphol* 272:1409–1421
- Dutta NK, Choudhury NR, Truong MY, Kim M, Elvin CM, Hill AJ (2009) Physical approaches for fabrication of organized nanostructure of resilin-mimetic elastic protein rec1-resilin. *Biomaterials* 30:4868–4876
- Dutta NK, Truong MY, Mayavan S, Choudhury NR, Elvin CM, Kim M, Knott R, Nairn KM, Hill AJ (2011) A genetically engineered protein responsive to multiple stimuli. *Angew Chem Int Ed Engl* 50:4428–4431

- Dutta NK, Choudhury NR, Balu R, Elvin CM, Hill AJ (2013) Formation of sub-nano metal particles. Aus Patent AU2013903210
- Eastham LES, Eassa YEE (1955) The feeding mechanism of the butterfly *Pieris brassicae* L. Phil Trans R Soc B 239:1–43
- Edwards JS (1960) Predation and digestion in assassin bugs (Heteroptera, Reduviidae). PhD thesis, University of Cambridge, UK
- Edwards HA (1983) Occurrence of resilin in elastic structures in the food-pump of reduviid bugs. J Exp Biol 105:407–409
- Elliott GF, Huxley AF, Weis-Fogh T (1965) On the structure of resilin. J Mol Biol 13:791–795
- Elvin CM, Carr AG, Huson MG, Maxwell JM, Pearson RD, Vuocolo T, Liyou NE, Wong DCC, Merritt DJ, Dixon NE (2005) Synthesis and properties of crosslinked recombinant pro-resilin. Nature 437:999–1002
- Evans MEG (1973) The jump of the click beetle (Coleoptera: Elateridae) – energetics and mechanics. J Zool 169:181–194
- Filippov AE, Popov VL, Gorb SN (2011) Shear induced adhesion: contact mechanics of biological spatula-like attachment devices. J Theor Biol 276:126–131
- Foerder CA, Shapiro BM (1977) Release of ovoperoxidase from sea urchin eggs hardens the fertilization membrane with tyrosine crosslinks. Proc Natl Acad Sci U S A 74:4214–4218
- Fujimori E (1978) Blue-fluorescent bovine α -crystallin. Biochim Biophys Acta 534:82–88
- Furth DG, Traub W, Harpaz I (1983) What makes *Blepharida* jump? A structural study of the metafemoral spring of a flea beetle. J Exp Zool 227:43–47
- Garcia-Castineiras S, Dillon J, Spector A (1978) Non-tryptophan fluorescence associated with human lens protein; apparent complexity and isolation of bityrosine and anthranilic acid. Exp Eye Res 26:461–476
- Gast R, Lee J (1978) Isolation of the *in vivo* emitter in bacterial bioluminescence. Proc Natl Acad Sci U S A 75:833–837
- Gorb SN (1996) Design of insect unguitactor apparatus. J Morphol 230:219–230
- Gorb SN (1999) Serial elastic elements in the damselfly wing: mobile vein joints contain resilin. Naturwissenschaften 86:552–555
- Gorb SN (2000) Ultrastructure of the neck membrane in dragonflies (Insecta, Odonata). J Zool 250:479–494
- Gorb SN (2001) Attachment devices of insect cuticle. Kluwer Academic Publishers, Dordrecht
- Gorb SN (2004) The jumping mechanism of cicada *Cercopis vulnerata* (Auchenorrhyncha, Cercopidae): skeleton-muscle organisation, frictional surfaces, and inverse-kinematic model of leg movements. Arthropod Struct Dev 33:201–220
- Gorb SN (2008) Smooth attachment devices in insects. In: Casas J, Simpson SJ (eds) Advances in insect physiology: insect mechanics and control. Elsevier, London, pp 81–116
- Gorb SN, Beutel RG (2001) Evolution of locomotory attachment pads of hexapods. Naturwissenschaften 88:530–534
- Gorb SN, Philippov AE (2014) Fibrillar adhesion with no clusterisation: functional significance of material gradient along adhesive setae of insects. Beilstein J Nanotech 5:837–846
- Gorb SN, Beutel RG, Gorb EV, Jiao Y, Kastner V, Niederegger S, Popov VL, Scherge M, Schwarz U, Vötsch W (2002) Structural design and biomechanics of friction-based releasable attachment devices in insects. Integr Comp Biol 42:1127–1139
- Gosline J, Lillie M, Carrington E, Guerette P, Ortlepp C, Savage K (2002) Elastic proteins: biological roles and mechanical properties. Phil Trans Roy Soc B 357:121–132
- Gosline J, Lillie M, Carrington E, Guerette P, Ortlepp C, Savage K (2004) Elastic proteins: biological roles and mechanical properties. In: Shewry PR, Tatham AS, Bailey AJ (eds) Elastomeric proteins: structures, biomechanical properties, and biological roles. Cambridge University Press, Cambridge, pp 15–38
- Govindarajan S, Rajulu GS (1974) Presence of resilin in a scorpion *Palamnaeus swammerdami* and its role in the food-capturing and sound-producing mechanisms. Experientia 30:908–909
- Gronenberg W (1996) Fast actions in small animals: springs and click mechanisms. J Comp Physiol A 178:727–734

- Haas F, Beutel RG (2001) Wing folding and the functional morphology of the wing base in Coleoptera. *Zoology* 104:123–141
- Haas F, Gorb S, Blickhan R (2000a) The function of resilin in beetle wings. *Proc R Soc Lond B* 267:1375–1381
- Haas F, Gorb S, Wootton RJ (2000b) Elastic joints in dermapteran hind wings: materials and wing folding. *Arthropod Struct Dev* 29:137–146
- Haas F, Hwen JTC, Tang HB (2012) New evidence on mechanics of wing unfolding in Dermaptera. *Arthropod Syst Phyl* 70:95–105
- Hackman RH (1975) Expanding abdominal cuticle in the bug *Rhodnius* and in the tick *Boophilus*. *J Insect Physiol* 21:1613–1623
- Hackman RH, Goldberg M (1985) The expanding alloscutal cuticle in adults of the argasid tick *Argas (Persicargas) robertsi* (Acari: Ixodoidea). *Int J Parasitol* 15:249–254
- Hackman RH, Goldberg M (1987) Comparative study of some expanding arthropod cuticles: the relation between composition, structure and function. *J Insect Physiol* 33:39–50
- Hamodrakas SJ, Willis JH, Iconomidou VA (2002) A structural model of the chitin-binding domain of cuticle proteins. *Insect Biochem Mol Biol* 32:1577–1583
- Hepburn HR (1971) Proboscis extension and recoil in Lepidoptera. *J Insect Physiol* 17:637–656
- Hepburn HR (1985) Structure of the integument. In: Kerkut GA, Gilbert LI (eds) *Comprehensive insect physiology, biochemistry and pharmacology*, vol 3, Integument, respiration and circulation. Pergamon Press, Oxford, pp 1–58
- Hepburn HR, Levy P (1975) Mechanical properties of some larval cuticles. *J Entomol Soc S Afr* 38:131–141
- Heusslein R, Gnatzy W (1987) Central projections of campaniform sensilla on the cerci of crickets and cockroaches. *Cell Tissue Res* 247:591–598
- Heußlein R, Gras H, Gnatzy W (2009) Functional coupling of cercal filiform hairs and campaniform sensilla in crickets. In: Gorb SN (ed) *Functional surfaces in biology 1*. Springer, Dordrecht, pp 203–233
- Hui C-Y, Glassmaker NJ, Tang T, Jagota A (2004) Design of biomimetic fibrillar interfaces: 2. Mechanics of enhanced adhesion. *J R Soc Interface* 1:35–48
- Huys R, Boxshall GA (1991) *Copepod evolution*. The Ray Society, London
- Iconomidou VA, Willis JH, Hamodrakas SJ (1999) Is beta-pleated sheet the molecular conformation which dictates formation of helicoidal cuticle? *Insect Biochem Mol Biol* 29:285–292
- Iconomidou VA, Chryssikos GD, Gionis V, Willis JH, Hamodrakas SJ (2001) “Soft”-cuticle protein secondary structure as revealed by FT-Raman, ATR FT-IR and CD spectroscopy. *Insect Biochem Mol Biol* 31:877–885
- Iconomidou VA, Willis JH, Hamodrakas SJ (2005) Unique features of the structural model of ‘hard’ cuticle proteins: implications for chitin-protein interactions and cross-linking in cuticle. *Insect Biochem Mol Biol* 35:553–560
- Jaganathan R, Sundara Rajulu G (1979) Occurrence of resilin-like protein in the eye-lens of a centipede *Scutigera longicornis*. *Indian Zool* 3:133–134
- Jagota A, Bennison S (2002) Mechanics of adhesion through a fibrillar microstructure. *J Integr Comp Biol* 42:1140–1145
- Jäkle B (2003) *Resilin in insect flight systems*. Diploma thesis. Eberhard Karls Universität, Tübingen
- Jensen M, Weis-Fogh T (1962) Biology and physics of locust flight. V. Strength and elasticity of locust cuticle. *Phil Trans R Soc B* 254:137–169
- Kannupandi T (1976) Occurrence of resilin and its significance in the cuticle of *Pennella elegans*, a copepod parasite. *Acta Histochem* 56:73–79
- Keil TA (1997) Functional morphology of insect mechanoreceptors. *Microsc Res Techniq* 39:506–531
- Khandaker MS, Dudek DM, Beers EP, Dillard DA, Bevan DR (2016) Molecular modeling of the elastomeric properties of repeating units and building blocks of resilin, a disordered elastic protein. *J Mech Behav Biomed Mater* 61:110–121
- Kim M, Elvin C, Brownlee A, Lyons R (2007) High yield expression of recombinant pro-resilin: lactose-induced fermentation in *E. coli* and facile purification. *Protein Expr Purif* 52:230–236

- King R (2010) Dynamic mechanical properties of resilin. Master's thesis. Virginia Polytechnic Institute and State University, Blacksburg (<http://vtechworks.lib.vt.edu/handle/10919/33677>)
- Koerner L, Gorb SN, Betz O (2012a) Adhesive performance of the stick-capture apparatus of rove beetles of the genus *Stenus* (Coleoptera, Staphylinidae) toward various surfaces. *J Insect Physiol* 58:155–163
- Koerner L, Gorb SN, Betz O (2012b) Functional morphology and adhesive performance of the stick-capture apparatus of the rove beetles *Stenus* spp. (Coleoptera, Staphylinidae). *Zoology* 115:117–127
- Krenn HW (1990) Functional morphology and movements of the proboscis of Lepidoptera (Insecta). *Zoomorphology* 110:105–114
- Lehmann FO, Gorb S, Nasir N, Schützner P (2011) Elastic deformation and energy loss of flapping fly wings. *J Exp Biol* 214:2949–2961
- Li L, Teller S, Clifton RJ, Jia X, Kiick KL (2011) Tunable mechanical stability and deformation response of a resilin-based elastomer. *Biomacromolecules* 12:2302–2310
- Li L, Tong Z, Jia X, Kiick KL (2013) Resilin-like polypeptide hydrogels engineered for versatile biological functions. *Soft Matter* 9:665–673
- Longhurst AR (1985) The structure and evolution of plankton communities. *Prog Oceanogr* 15:1–35
- Lopez-Llorca LV, Fry SC (1989) Dityrosine, trityrosine and tetryrosine, potential cross-links in structural proteins of plant-parasitic nematodes. *Nematologica* 35:165–179
- Lv S, Dudek DM, Cao Y, Balamurali MM, Gosline J, Li H (2010) Designed biomaterials to mimic the mechanical properties of muscles. *Nature* 465:69–73
- Lyons RE, Lesieur E, Kim M, Wong DC, Huson MG, Nairn KM, Brownlee AG, Pearson RD, Elvin CM (2007) Design and facile production of recombinant resilin-like polypeptides: gene construction and a rapid protein purification method. *Protein Eng Des Sel* 20:25–32
- Lyons RE, Nairn KM, Huson MG, Kim M, Dumsday G, Elvin CM (2009) Comparisons of recombinant resilin-like proteins: repetitive domains are sufficient to confer resilin-like properties. *Biomacromolecules* 10:3009–3014
- Lyons RE, Wong DC, Kim M, Lekieffre N, Huson MG, Vuocolo T, Merritt DJ, Nairn KM, Dudek DM, Colgrave ML, Elvin CM (2011) Molecular and functional characterisation of resilin across three insect orders. *Insect Biochem Mol Biol* 41:881–890
- Lyons RE, Elvin CM, Taylor K, Lekieffre N, Ramshaw JA (2012) Purification of recombinant protein by cold-coacervation of fusion constructs incorporating resilin-inspired polypeptides. *Biotechnol Bioeng* 109:2947–2954
- Ma Y, Ning JG, Ren HL, Zhang PF, Zhao HY (2015) The function of resilin in honeybee wings. *J Exp Biol* 218:2136–2142
- Mark JE (1981) Rubber elasticity. *J Chem Educ* 58:898–903
- Mark JE (2002) Some aspects of rubberlike elasticity useful in teaching basic concepts in physical chemistry. *J Chem Educ* 79:1437–1443
- Mark JE (2004) Physical states of polymers. In: Mark JE, Ngai K, Graessley W, Mandelkern L, Samulski E, Koenig J, Wignall G (eds) *Physical properties of polymers*. Cambridge University Press, Cambridge, pp 1–376
- Mark JE, Erman B (2007) *Rubberlike elasticity: a molecular primer*. Cambridge University Press, Cambridge
- McGann CL, Levenson EA, Kiick KL (2013) Resilin-based hybrid hydrogels for cardiovascular tissue engineering. *Macromol Chem Phys* 214:203–213
- Meyer DE, Chilkoti A (2002) Genetically encoded synthesis of protein-based polymers with precisely specified molecular weight and sequence by recursive directional ligation: examples from the elastin-like polypeptide system. *Biomacromolecules* 3:357–367
- Michels J, Gorb SN (2012) Detailed three-dimensional visualization of resilin in the exoskeleton of arthropods using confocal laser scanning microscopy. *J Microsc* 245:1–16
- Michels J, Gorb SN (2015) Mandibular gnathobases of marine planktonic copepods – feeding tools with complex micro- and nanoscale composite architectures. *Beilstein J Nanotechnol* 6:674–685

- Michels J, Schnack-Schiel SB (2005) Feeding in dominant Antarctic copepods – does the morphology of the mandibular gnathobases relate to diet? *Mar Biol* 146:483–495
- Michels J, Vogt J, Gorb SN (2012) Tools for crushing diatoms – opal teeth in copepods feature a rubber-like bearing composed of resilin. *Sci Rep* 2:465
- Michels J, Gorb SN, Reinhardt K (2015a) Reduction of female copulatory damage by resilin represents evidence for tolerance in sexual conflict. *J R Soc Interface* 12:20141107
- Michels J, Vogt J, Simon P, Gorb SN (2015b) New insights into the complex architecture of siliceous copepod teeth. *Zoology* 118:141–146
- Mountcastle AM, Combes SA (2013) Wing flexibility enhances load-lifting capacity in bumblebees. *Proc R Soc Lond B* 280:20130531
- Mountcastle AM, Combes SA (2014) Biomechanical strategies for mitigating collision damage in insect wings: structural design versus embedded elastic materials. *J Exp Biol* 217:1108–1115
- Nachtigall W, Wisser A, Eisinger D (1998) Flight of the honey bee. VIII. Functional elements and mechanics of the “flight motor” and the wing joint – one of the most complicated gear-mechanisms in the animal kingdom. *J Comp Physiol B* 168:323–344
- Nairn KM, Lyons RE, Mulder RJ, Mudie ST, Cookson DJ, Lesieur E, Kim M, Lau D, Scholes FH, Elvin CM (2008) A synthetic resilin is largely unstructured. *Biophys J* 95:3358–3365
- Neff D, Frazier SF, Quimby L, Wang R-T, Zill S (2000) Identification of resilin in the leg of cockroach, *Periplaneta americana*: confirmation by a simple method using pH dependence of UV fluorescence. *Arthropod Struct Dev* 29:75–83
- Neville AC (1960) Aspects of flight mechanics in anisopterous dragonflies. *J Exp Biol* 37:631–656
- Neville AC (1963) Daily growth layers in locust rubber-like cuticle influenced by an external rhythm. *J Insect Physiol* 9:177–186
- Neville AC (1967) Factors affecting the tertiary structure of resilin in locusts. *J Cell Sci* 2:273–280
- Newman DJS (1982) The functional wing morphology of some Odonata. PhD thesis. University of Exeter, Exeter
- Niederegger S, Gorb S (2003) Tarsal movements in flies during leg attachment and detachment on a smooth substrate. *J Insect Physiol* 49:611–620
- Peisker H, Michels J, Gorb SN (2013) Evidence for a material gradient in the adhesive tarsal setae of the ladybird beetle *Coccinella septempunctata*. *Nat Commun* 4:1661
- Perez Goodwyn P, Peressadko A, Schwarz H, Kastner V, Gorb S (2006) Material structure, stiffness, and adhesion: why attachment pads of the grasshopper (*Tettigonia viridissima*) adhere more strongly than those of the locust (*Locusta migratoria*) (Insecta: Orthoptera). *J Comp Physiol A* 192:1233–1243
- Picker M, Colville JF, Burrows M (2012) A cockroach that jumps. *Biol Lett* 8:390–392
- Qin G, Lapidot S, Numata K, Hu X, Meirovitch S, Dekel M, Podoler I, Shoseyov O, Kaplan DL (2009) Expression, cross-linking, and characterization of recombinant chitin binding resilin. *Biomacromolecules* 10:3227–3234
- Qin G, Rivkin A, Lapidot S, Hu X, Preis I, Arinus SB, Dgany O, Shoseyov O, Kaplan DL (2011) Recombinant exon-encoded resilins for elastomeric biomaterials. *Biomaterials* 32:9231–9243
- Qin G, Hu X, Cebe P, Kaplan DL (2012) Mechanism of resilin elasticity. *Nat Commun* 3:1003
- Raghu Varman A (1980) Resilin in the cuticle of physogastric queen termites. *Experientia* 36:564
- Raghu Varman A (1981) Resilin in the abdominal cuticle of workers of the honey ants, *Myrmecocystus mexicanus*. *J Ga Entomol Soc* 16:11–13
- Raghu Varman A, Hermann HR Jr (1982) Resilin in the fulcral arms of the poison apparatus of the ants, *Pogonomyrmex badius*. *J Anim Morphol Physiol* 29:284–285
- Rajabi H, Ghoroubi N, Darvizeh A, Dirks J-H, Appel E, Gorb SN (2015) A comparative study of the effects of vein-joints on the mechanical behaviour of insect wings: I. Single joints. *Bioinspiration Biomimetics* 10:056003
- Rajabi H, Shafiei A, Darvizeh A, Dirks J-H, Appel E, Gorb SN (2016) Effect of microstructure on the mechanical and damping behaviour of dragonfly wing veins. *R Soc Open Sci* 3:160006
- Ramalingam K (1973) Chemical nature of monogenean sclerites. I. Stabilization of clamp-protein by formation of dityrosine. *Parasitology* 66:1–7

- Rauscher S, Pomès R (2012) Structural disorder and protein elasticity. In: Fuxreiter M, Tompa P (eds) Fuzziness: structural disorder in protein complexes. *Adv Exp Med Biol* 725:159–183
- Rauscher S, Baud S, Miao M, Keeley FW, Pomès R (2006) Proline and glycine control protein self-organization into elastomeric or amyloid fibrils. *Structure* 14:1667–1676
- Rebers JE, Riddiford LM (1988) Structure and expression of a *Manduca sexta* larval cuticle gene homologous to *Drosophila* cuticle genes. *J Mol Biol* 203:411–423
- Rebers JE, Willis JH (2001) A conserved domain in arthropod cuticular proteins binds chitin. *Insect Biochem Mol Biol* 31:1083–1093
- Reinhardt K, Naylor R, Siva-Jothy MT (2009) Situation exploitation: higher male mating success when female resistance is reduced by feeding. *Evolution* 63:29–39
- Renner JN, Cherry KM, Su RS, Liu JC (2012) Characterization of resilin-based materials for tissue engineering applications. *Biomacromolecules* 13:3678–3685
- Reynolds SE (1975) The mechanical properties of the abdominal cuticle of *Rhodnius* larvae. *J Exp Biol* 62:69–80
- Richards AG, Richards PA (1979) The cuticular protuberances of insects. *Int J Insect Morphol Embryol* 8:143–157
- Rothschild M, Schlein Y, Parker K, Neville C, Sternberg S (1975) The jumping mechanism of *Xenopsylla cheopis*. III. Execution of the jump and activity. *Phil Trans R Soc B* 271:499–515
- Sannasi A (1970) Resilin in the lens cuticle of the firefly, *Photinus pyralis* Linnaeus. *Experientia* 26:154
- Shewry PR, Tatham AS, Bailey AJ (2004) Elastomeric proteins: structures, biomechanical properties, and biological roles. Cambridge University Press, Cambridge
- Skals N, Surlykke A (1999) Sound production by abdominal tymbal organs in two moth species: the green silver-line and the scarce silver-line (Noctuoidea: Nolidae: Chloephorinae). *J Exp Biol* 202:2937–2949
- Spolenak R, Gorb SN, Arzt E (2005) Adhesion design maps for bio-inspired attachment systems. *Acta Biomater* 1:5–13
- Studier FW (2005) Protein production by auto-induction in high-density shaking cultures. *Protein Expr Purif* 41:207–234
- Stutt AD, Siva-Jothy MT (2001) Traumatic insemination and sexual conflict in the bed bug *Cimex lectularius*. *Proc Natl Acad Sci U S A* 98:5683–5687
- Su RS, Kim Y, Liu JC (2014) Resilin: protein-based elastomeric biomaterials. *Acta Biomater* 10:1601–1611
- Sun J, Ling M, Wu W, Bhushan B, Tong J (2014) The hydraulic mechanism of the unfolding of hind wings in *Dorcus titanus platymelus* (order: Coleoptera). *Int J Mol Sci* 15:6009–6018
- Sundara Rajulu G (1971) Presence of resilin in the cuticle of the centipede *Scolopendra morsitans* L. *Indian J Exp Biol* 9:122–123
- Tamburro AM, Boichicchio B, Pepe A (2005) The dissection of human tropoelastin: from the molecular structure to the self-assembly to the elasticity mechanism. *Pathol Biol* 53:383–389
- Tamburro AM, Panariello S, Santopietro V, Bracalello A, Boichicchio B, Pepe A (2010) Molecular and supramolecular structural studies on significant repetitive sequences of resilin. *ChemBioChem* 11:83–93
- Tang LM, Weder C (2010) Cellulose whisker/epoxy resin nanocomposites. *ACS Appl Mater Interfaces* 2:1073–1080
- Thurm U (1964) Mechanoreceptors in the cuticle of the honey bee: fine structure and stimulus mechanism. *Science* 145:1063–1065
- Truong MY, Dutta NK, Choudhury NR, Kim M, Elvin CM, Hill AJ, Thierry B, Vasilev K (2010) A pH-responsive interface derived from resilin-mimetic protein *rec1-resilin*. *Biomaterials* 31:4434–4446
- Truong MY, Dutta NK, Choudhury NR, Kim M, Elvin CM, Nairn KM, Hill AJ (2011) The effect of hydration on molecular chain mobility and the viscoelastic behavior of resilin-mimetic protein-based hydrogels. *Biomaterials* 32:8462–8473
- van Eldijk MB, McGann CL, Kiick KL, van Hest JCM (2012) Elastomeric polypeptides. In: Deming T (ed) *Peptide-based materials*. *Top Curr Chem* 310:71–116

- Varenberg M, Pugno NM, Gorb SN (2010) Spatulate structures in biological fibrillar adhesion. *Soft Matter* 6:3269–3272
- Vashi AV, Ramshaw JA, Glattauer V, Elvin CM, Lyons RE, Werkmeister JA (2013) Controlled surface modification of tissue culture polystyrene for selective cell binding using resilin-inspired polypeptides. *Biofabrication* 5:035005
- Verker R, Rivkin A, Zilberman G, Shoseyov O (2014) Insertion of nano-crystalline cellulose into epoxy resin via resilin to construct a novel elastic adhesive. *Cellulose* 21:4369–4379
- Vincent JFV (1975) Locust oviposition: stress softening of the extensible intersegmental membranes. *Proc R Soc Lond B* 188:189–201
- Vincent JFV (1976) Design for living: the elastic-sided locust. In: Hepburn HR (ed) *The insect integument*. Elsevier, Amsterdam, pp 401–419
- Vincent JFV (1981) Morphology and design of the extensible intersegmental membrane of the female migratory locust. *Tissue Cell* 13:18–31
- Vincent JFV, Wood SDE (1972) Mechanism of abdominal extension during oviposition in *Locusta*. *Nature* 235:167–168
- Viswanathan S, Varadaraj G (1985) Occurrence of a resilin-like protein in the lens cuticle of the dragonfly *Mesogomphus lineatus* (Selys) (Anisoptera: Gomphidae). *Odonatologica* 14:155–157
- Voigt D, Schuppert JM, Dattinger S, Gorb SN (2008) Sexual dimorphism in the attachment ability of the Colorado potato beetle *Leptinotarsa decemlineata* (Coleoptera: Chrysomelidae) to rough substrates. *J Insect Physiol* 54:765–776
- Weis-Fogh T (1960) A rubber-like protein in insect cuticle. *J Exp Biol* 37:889–907
- Weis-Fogh T (1961a) Molecular interpretation of the elasticity of resilin, a rubber-like protein. *J Mol Biol* 3:648–667
- Weis-Fogh T (1961b) Thermodynamic properties of resilin, a rubber-like protein. *J Mol Biol* 3:520–531
- Weis-Fogh T (1970) New molecular model for long-range elasticity of elastin. *Nature* 227:718–721
- Weis-Fogh T (1973) Quick estimates of flight fitness in hovering animals, including novel mechanisms for lift production. *J Exp Biol* 59:169–230
- Welinder BS, Roepstorff P, Andersen SO (1976) The crustacean cuticle – IV. Isolation and identification of cross-links from *Cancer pagurus* cuticle. *Comp Biochem Phys B* 53:529–533
- Wells SM (2003) Mechanical design of elastic biopolymers. *Phys Can* 59:67–74
- Whittaker JL, Dutta NK, Knott R, McPhee G, Voelcker N, Elvin CM, Choudhury NR (2015a) Tuneable thermo-responsiveness of resilin via co-assembly with rigid biopolymers. *Langmuir* 31:8882–8891
- Whittaker JL, Dutta NK, Elvin CM, Choudhury NR (2015b) Fabrication of highly elastic resilin/silk fibroin based hydrogel by rapid photo-crosslinking reaction. *J Mater Chem B* 3:6576–6579
- Willis JH (1999) Cuticular proteins in insects and crustaceans. *Am Zool* 39:600–609
- Willis JH (2010) Structural cuticular proteins from arthropods: annotation, nomenclature, and sequence characteristics in the genomics era. *Insect Biochem Mol Biol* 40:189–204
- Wong DCC, Pearson RD, Elvin CM, Merritt DJ (2012) Expression of the rubber-like protein, resilin, in developing and functional insect cuticle determined using a *Drosophila* anti-rec 1 resilin antibody. *Dev Dyn* 241:333–339
- Wong WL, Michels J, Gorb SN (2013) Resilin-like protein in the clamp sclerites of the gill monogenean *Diplozoon paradoxum* Nordmann, 1832. *Parasitology* 140:95–98
- Wootton RJ (1992) Functional morphology of insect wings. *Annu Rev Entomol* 37:113–140
- Xu S, Girouard N, Schueneman G, Shofner ML, Meredith JC (2013) Mechanical and thermal properties of waterborne epoxy composites containing cellulose nanocrystals. *Polymer* 54:6589–6598
- Yang Y, Hu X (2014) Unraveling the energy transduction mechanism of resilin elasticity – a combination of computational and experimental study. *Biophys J* 106:51a
- Young D, Bennet-Clark HC (1995) The role of the tymbal in cicada sound production. *J Exp Biol* 198:1001–1019

Chapter 5

The Mineralized Exoskeletons of Crustaceans

Shmuel Bentov, Shai Abehsera, and Amir Sagi

Abstract The crustaceans constitute one of the oldest arthropod taxa, from which insects later evolved (Giribet et al., *Nature* 413:157–161, 2001; Regier et al., *Nature* 463:1079–U1098, 2010; Giribet and Edgecombe, *Annu Rev Entomol* 57:167–186, 2012). A typical feature that characterizes the Crustacea is their mineralized chitinous exoskeleton. The reinforcement of the chitinous exoskeleton with calcium salts and the formation of inorganic-organic composite materials by the crustaceans represent one of the oldest biomineralization mechanisms to have evolved in animals. The basic function of mineralization is to enhance the mechanical strength of the skeleton. When compared to other animals with mineralized skeletons, crustaceans face two distinct challenges inherent in the fact that their skeleton is external: first, the animal's locomotion abilities must not be compromised by its mineralized exoskeleton, and second, the growth mode by periodic molting requires intensive mobilization of minerals during the resorption of the old cuticle and the rapid recalcification of the new cuticle. These two demands are among the prime determinants that govern the various calcification patterns in Crustacea. This review focuses on the mineralogical aspects of the crustacean exoskeleton with emphasis on the controllable parameters of the mineral phase properties, namely, the degree of mineralization, the degree of crystallization, the phosphate/carbonate ratio, and the involvement of proteins. It also explores potential biomimetic applications inspired by the crustacean exoskeleton against the background of similarities between crustaceans and vertebrates, namely, both groups are the only groups in the animal kingdom that combine advanced locomotion with jointed mineralized skeletons. In addition, many crustaceans have the ability of calcium phosphate mineralization, like vertebrates. These similarities provide unique opportunities to compare different evolutionary solutions to similar functional challenges that, in turn, can inspire biomimetic approaches to the development of synthetic bio-composites for various skeleton-related medical applications.

S. Bentov (✉) • S. Abehsera • A. Sagi

Department of life Sciences and the National Institute for Biotechnology in the Negev,
Ben Gurion University, 84105 Beer Sheva, Israel

e-mail: bentovs@bgu.ac.il; abehsera@post.bgu.ac.il; sagia@bgu.ac.il

5.1 Introduction

The Crustacea and the Hexapoda are the two major groups of the Arthropoda. Recently, it has been shown that the Hexapoda are phylogenetically more associated with the Crustacea (and not with the Myriapoda as was previously assumed (Manton and Harding 1964; Wheeler et al. 2004)), and can actually be considered, phylogenetically, as “terrestrial crustaceans” (Regier et al. 2005). The two groups are thus now grouped into a clade known as the Pancrustacea (or the Tetraconata). The crustaceans, which inhabit marine, freshwater, and terrestrial habitats, are a highly heterogeneous group of animals in terms of morphology and living habits—from large lobsters and crabs that can exceed 1 m at maximum diameter (e.g., the Japanese spider crab) to microscopic Tantulocarida of less than 100 μm (e.g., *Stygotantulus stocki*), from agile shrimps to sessile barnacles, from benthic walkers to pelagic swimmers. A fundamental characteristic of crustaceans is their mineralized cuticle, and the heterogeneity of the crustaceans is reflected in their diverse cuticle properties, which differ not only between species but also between different body parts. The crustacean exoskeleton comprises four layers which are, from the outermost inward: epicuticle, exocuticle, endocuticle, and the membranous layer (Fig. 5.1). The outermost epicuticle is a thin layer, composed of proteins and lipids, that provides a mechanical barrier against pathogens and provides an impermeable layer (Mary and Krishnan 1974) that enable better ionic regulation. In terrestrial crustaceans (e.g. Isopoda) the epicuticle serves as a waterproofing layer (Hadley and Warburg 1986) probably with other functions (Vittori and Štrus 2014). The epicuticle is less calcified than the underlying exo/endocuticle (Dillaman et al. 2005) whereas the minerals are usually restricted to the pore canals (Hegdahl et al. 1978). The underlying exocuticle and the inner endocuticle represent the major part of the cuticle. These are the most mineralized layers and thus govern the mechanical properties of the crustacean exocuticle. On the proximal side, below the endocuticle, lies a non-mineralized “membranous layer” that overlies a single layer of epithelial cells which are primarily a secretory tissue, responsible for producing the overlying layers of the cuticle. The basic functions of the exoskeleton are to provide protection and to serve as an anchor for the muscles. In comparison with the mineralized endoskeleton of vertebrates, the exoskeleton of crustaceans provides better protection and possibly better leverage for the pull of muscles (Currey 1967; Taylor and Dirks 2012; Žnidaršič et al. 2012). Despite these advantages, the mineralized external skeleton presents two major challenges to the crustacean: First, the mineralized exoskeleton must not compromise the animal’s locomotion abilities (e.g., walking, swimming and tail-flipping), and second, the animal must facilitate the intensive mobilization of minerals associated with the growth process, which includes periodic shedding of the old cuticle through molting, followed by rapid recalcification of the new one. These two demands are among the prime determinants that govern the general calcification patterns in Crustacea.

The structural organization of the mineral – organic composites within the crustacean cuticle occurs over multiple length scales, from the nanometer to the

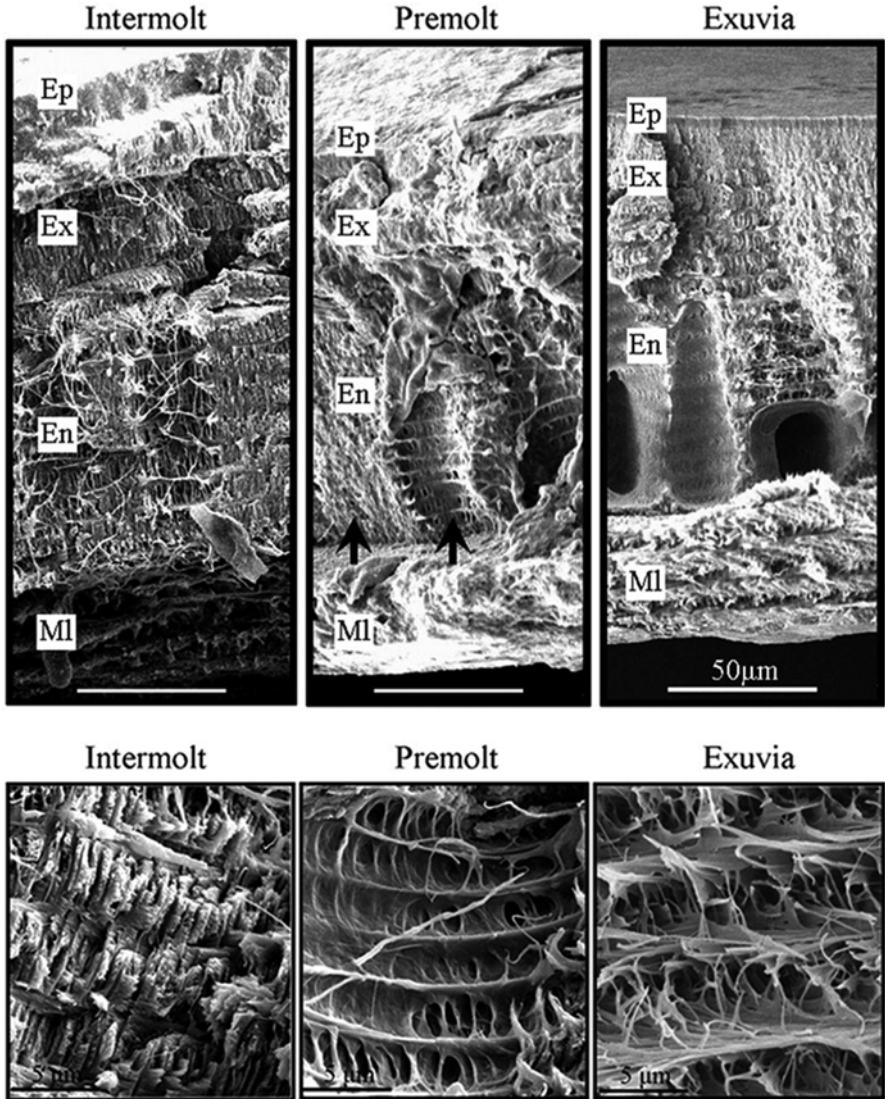


Fig. 5.1 Changes in mineralization patterns of intermolt and premolt cuticles, and of exuvia, in *Cherax quadricarinatus*. (a) Low-magnification SEM micrographs of cuticle cross sections. Ep, epicuticle; Ex, exocuticle; En, endocuticle; Ml, membranous layer. (b) High-magnification SEM micrographs of representative areas demonstrating matrix structure and mineral deposition in the cuticle during three stages of the molt cycle (Adapted from (Shechter et al. 2008a) with permission from the Marine Biological Laboratory)

millimeter scale. The building blocks of the cuticle are nanocomposite units of chitin–protein–mineral, which produce hierarchical structures with properties that are specifically tailored to carry out particular functions. Tight biological control over the properties of the mineral component of the composite is exerted via control of the degree of mineralization (from heavily mineralized to non-mineralized cuticle), the degree of crystallization (from amorphous to highly crystallized) and the nature of the mineral (ratio of calcium carbonate to calcium phosphate); this biological control over the mineral properties is probably mediated by various proteins, e.g. structural proteins, ions transporters and catalytic proteins. As discussed below, the fine biological control of the above parameters in different species and in different body parts produces various cuticular structures with different chemophysical properties.

This review focuses particularly on the mineralogical aspects of the crustacean composite exoskeleton, with emphasis on the controllable parameters of the mineral phase. Thus, we refer the interested reader to previous review papers that have been written from a more physiological perspective (Luquet 2012) or from materials science perspective (Paris et al. 2013; Grunenfelder et al. 2014), respectively.

5.2 The Advantages of Mineralization

It is currently held that most lineages with exoskeletons originally had a tough non-mineralized exoskeleton, which became mineralized later in evolution: Many arthropods and arthropod-like animals (early Panarthropoda) that appeared during the Cambrian explosion had hard skeletons of purely organic cuticles with no incorporated biominerals (Bengtson 2004; Smith and Caron 2015). Thus, biomineralization in arthropods may be regarded an impregnation of an already developed cuticle, with minerals. We note that stiffness and hardness of organic skeletons can be attained without mineralization, for example, by protein tanning (as in insect cuticles) or by the incorporation of metals, but the strongest skeletons are those that incorporate biominerals (Bengtson 2004). Accordingly, in Crustacea, the mechanical properties of the exoskeleton are attributed mainly to the mineral phase (Vincent 2002). The incorporation of minerals into the cuticle makes it less prone to deformation and tearing and less susceptible to abrasion (Lichtenegger et al. 2002). While biominerals are typically stiff and hard, they are also brittle. This drawback is overcome by combining the minerals with structural organic matrices (proteins and polysaccharides) into composite materials. The inorganic–organic composite materials possess mechanical characteristics of stiffness, toughness, and strength that are superior to those of their constituent building blocks (Nikolov et al. 2010).

An additional advantage of mineralized exoskeletons over solely organic skeletons is that reinforcement by mineralization might be cheaper, in metabolic terms, than organic sclerotization. It is assumed that the main metabolic cost of shell construction lies in the creation of the proteins and polysaccharides required for the shell's composite structure and not in the precipitation of the mineral components

(Palmer 1992; Bengtson 1994, 2004; Cohen 2005). Thus, in order to stiffen the cuticle to a certain degree, it might be cheaper to use mineral reinforcement than enhancing sclerotization. The sources of the major salt used for reinforcement of the crustacean exoskeleton, CaCO_3 , are the ocean and freshwater bodies, in most of which the mineral is present in supersaturated concentrations. Therefore, in order to deposit CaCO_3 , the animal needs to kinetically enhance a process that is frequently favored thermodynamically. Various studies showed that ocean acidification, that decreases the saturation value of CaCO_3 , and consequently increases the metabolic cost of mineralization, may have an adverse effect on growth and survival of marine crustaceans (Cameron 1985; Kurihara et al. 2008; Arnold et al. 2009; Findlay et al. 2009; Whiteley 2011). It is assumed that although the crustaceans can compensate for the acidic condition by active ionic regulation, the metabolic cost of the compensatory responses that facilitate calcification have the potential to adversely affect growth, reproduction and survival. It is noteworthy that, since the chemistry of water bodies, is not stable (on the secular level), the changing metabolic price for different minerals and their various polymorphs, probably plays a major role in the mineralogy of crustaceans.

5.2.1 Mineralization and the Adaptations to Terrestrial Environment, Hexapods and Isopods

It is now widely accepted that the Hexapoda emerged from within the Crustacea, possibly from a malacostracan-like ancestor (Andrew 2011; Strausfeld and Andrew 2011; Ma et al. 2012). Thus, it is possible that hexapods as “terrestrial crustaceans”, that successfully invaded land as insects (Glenner et al. 2006; Mallatt and Giribet 2006), lost their mineralization capabilities in favor of a lighter cuticle, as part of their adaptation to terrestrial and aerial environments. Another group of crustaceans that successfully colonized land habitats is the terrestrial isopods (Oniscidea) that retained their mineralized exoskeleton. Comparison of the two groups shows different evolutionary pathways in the adaptation to terrestrial life. Two of the main physiological challenges in arthropods adaptation to terrestrial habitat are water retention and air breathing. The exoskeleton of aquatic crustaceans is relatively water-permeable so the animal is prone to dehydration at land. In addition, the typical external gills of crustaceans enhance water loss by transpiration, and without modification they would collapse in air under their own weight. Terrestrial arthropods were thus faced with two options: adapt or innovate (Dunlop et al. 2013). Hexapods innovated and developed an entirely new tracheal respiratory system as well as a non-mineralized highly impermeable waxed integument. On the other hand, terrestrial isopods still use their traditional gills for respiration (with special adaptations such as a complex water-conducting system and protected lung-like invaginations). They also retained the typical mineralized crustaceans-cuticle probably due to their passive defense strategy. There is also evidence that increased calcification of the

exoskeleton reduces permeability and water loss in crustacea (Edney 1960). Although the cuticle of Oniscidea have improved waterproofing (Bursell 1955) they lack the highly effective impermeable epicuticular wax layer (Barnes et al. 2009). Therefore, because of the water loss associated with respiration and integumental transpiration, terrestrial isopods are usually nocturnal and are mostly restricted to cryptozoic moist niches (Edney 1960; Little 1990).

5.3 Degree of Mineralization

A major tunable parameter that is highly variable in crustaceans, both in different body parts (Fig. 5.2) and between species, is the degree of mineralization. The change in mineral density is used to control hardness vs flexibility, to form graded structures, and to control the general density of the animal as an adaptation to different environments, e.g., pelagic vs benthic habitats.

5.3.1 Degree of Mineralization in Different Body Parts

Mineral content is a dominant factor in cuticle stiffness. As mentioned above, mineralization is not uniform in the different body parts, the basic trade-off being flexibility vs hardness. The most mobile parts, such as joints, legs and arthrodistal membranes, are lightly calcified if at all (Cribb et al. 2009), whereas the carapace and claws are more heavily mineralized, and the mandibles are usually the most heavily mineralized cuticular element. A comparison of mineral contents in the carapace, claw, and finger of the American lobster *Homarus americanus* and the edible crab *Cancer pagurus* revealed a positive correlation between the degree of mineralization and hardness and a negative correlation between the degree of mineralization and elasticity (Boßelmann et al. 2007). In both species, the mineral content increases from the carapace through the claw to the finger, as is to be expected from the different requirements for hardness of these body parts: The movable finger, being an incising puncturing device, is highly mineralized and very hard. In contrast, the fixed claw, which serves as the cutting base, is less mineralized and hence softer and more elastic. Such an arrangement can be viewed as a hard sharp knife working on a stationary softer cutting board.

5.3.2 Degree of Mineralization and Graded Structures

Control over the degree of mineralization is also used to produce mechanically graded structures. As discussed above, a basic problem in mineral reinforcement is the brittleness of biominerals, which may be exploited by predators. When a

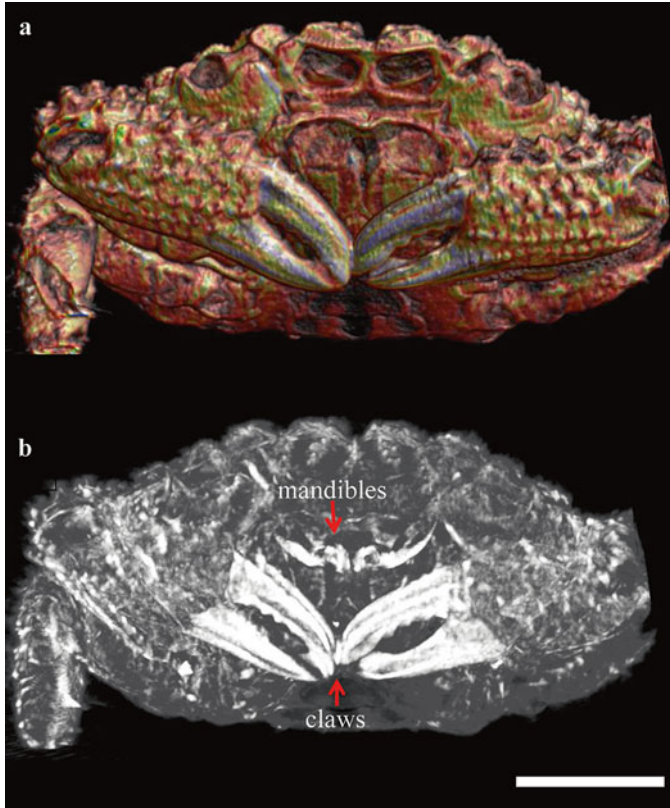


Fig. 5.2 Volume rendered micro-CT scan reconstruction of the crab *Trapezia* spp., showing high variability in the degree of mineralization. (a) 3D model surface rendering showing densitometry information for the mineral phase. The image was pseudo-colored according to an RGB palette, with low mineral density in red and high density in blue. In this setting the organic matter is transparent. (b) Maximum intensity projection (MIP) image (voxels with the highest attenuation value) show that the claws and the mandibles are the most highly mineralized parts of the exoskeleton. Scanning and volume rendering reconstructions were performed using a Skyscan1 1172 micro-CT machine and CTVOX software (Skyscan). scale bar=3 mm

predator exerts a compression force on the outer layer of the cuticle, a rigid layer would be likely to crack under the stress, exposing the underlying soft tissues. One of the solutions to this problem is the formation of a graded structure, with a hard surface layer being mounted over a more compliant layer, an arrangement that can dissipate deformation energy without the propagation of cracks (Nedin 1999). In Crustacea, the degree of mineralization plays a major role in the formation of such structures. Generally, as the degree of mineralization is increased, greater stress is required to harmfully deform the cuticle, and conversely the less mineralized the cuticle, the greater the deformation required to damage it irreversibly (Nedin 1999). Accordingly, the exocuticle layer is more mineralized and hence harder and stiffer than the endocuticle (Sachs et al. 2006). The less mineralized endocuticle is

correspondingly softer but tougher: it resists tensile stresses but is liable to failure under compression (Raabe et al. 2005; Chen et al. 2008). It is noteworthy that in many decapods, in addition to the higher mineral content, the exocuticle shows a higher stacking density of the chitin–protein layers (Raabe et al. 2005) and enhanced sclerotization when compared to the endocuticle (Neville 1975; Paris et al. 2013).

5.3.3 Mineralization and Flexibility

The degree of mineralization is usually positively correlated to hardness and elastic modulus, and negatively correlated to flexibility. Thus, more flexible crustaceans tend to have a less mineralized exoskeleton than rigid species: crabs (*Brachyura*), for example, have developed a heavily mineralized exoskeleton that provides good protection but decreased flexibility. The tradeoff between mineralization and flexibility is demonstrated in the tail flip escape mode prevalent in decapods. This mechanism allows crustaceans to escape predators through rapid abdominal flexions that produce powerful swimming strokes, thereby pushing the animal backwards and away from potential dangers. This escape behavior requires some flexibility that enables bending of the carapace. The carapace, which covers the main body, must therefore have a certain degree of elasticity to allow the movement and some bending of the animal. A study that provides a good demonstration of the tradeoff between mineralization and flexibility is the above-mentioned comparison of the mineral contents in the carapace of *H. americanus* and *C. pagurus* (Boßelmann et al. 2007). In particular, the different degrees of mineralization of the carapace of these two species are reflected in their escape behavior: the increased mineralization of the crab carapace prevents the flexural bending that is required for the tail flip, and therefore upon attack the crab clings to the ground, utilizing its highly mineralized armored exoskeleton to protect itself. In contrast, the lobster with the more elastic cuticle escapes rapidly and hides between rocks.

5.3.4 Degree of Mineralization and Habitat Zone Within the Water Column

More mineralized crustaceans are heavier. Consequently, there is a clear correlation between the degree of mineralization, on the one hand, and the habitat zone and the locomotion style, on the other hand (pelagic vs benthic and swimmers vs walkers). Benthic species tend to have a more mineralized exocuticle than pelagic species (Pütz and Buchholz 1991), a characteristic that correlates with the traditional division of the decapods into *Natantia* (comprising the families that move predominantly by swimming, such as the shrimps) and the *Reptantia* (e.g., crabs and lobsters that move chiefly by walking on the bottom of the water body).

It is noteworthy that the degree of mineralization is also associated with the general breeding and molting strategy of the different Crustacea. In highly calcified species, intermolt periods are longer than those in poorly calcified species (Aiken and Waddy 1980). A short life span and a high growth rate mean that biomineralization is relatively more costly in metabolic energy terms and therefore light calcification is advantageous. Accordingly, calcified species are associated with K-strategies (i.e., extended life span, slow maturation, brooding of young, relatively small numbers of offspring), while weakly calcified species are associated with r-strategies (short life span, rapid maturation, broadcast spawning, greater mobility, and higher population density) (Sastry 1983; Sardà et al. 1989).

5.4 Reinforcement with Stable Amorphous Phases

The Crustacea is the only major taxon in the animal kingdom that widely uses amorphous phases – amorphous calcium carbonate (ACC) and amorphous calcium phosphate (ACP) – for the structural purpose of cuticle stiffening (Addadi et al. 2003). Other species use more stable crystalline minerals, namely, calcite and aragonite in invertebrates and apatite in vertebrates. Amorphous phases are less stable than their crystalline counterparts and are usually present as a transient phase. When required permanently, such phases must therefore be stabilized by additives that inhibit crystallization. Compared to calcite, ACC has a lower hardness and a lower modulus of elasticity, but ACC has a number of potential biological advantages: (1) an isotropic structure with no preferred growth direction, which enables it to be molded into any desired shape; (2) a lack of cleavage planes, which makes it less brittle than its counterpart crystalline materials (Aizenberg et al. 2002); (3) a high solubility combined with a high surface area, which provides improved resorption potential; and (4) the ability to incorporate much higher levels of trace elements and impurities than crystalline phases (Bentov and Erez 2006).

5.4.1 Resorbability

In order to grow, crustaceans periodically shed their exoskeleton and build a new larger one. During the premolt stage, massive resorption of the ‘old’ skeleton takes place (Fig. 5.1), and ions (Ca^{2+} , CO_3^{2-} , and PO_4^{3-}) are stored in various ways, e.g., as gastroliths, hepatopancreas granules and sternal deposits (Luquet and Marin 2004); these ions are later used for calcification of the new cuticle. It is thus entirely plausible that a soluble polymorph, which enables better and faster resorption, is advantageous. It is noteworthy that in addition to thermodynamic solubility, another advantage of ACC lies in the size of the mineral spheres, usually 50–100 nm, implying a very high surface area that would further enhance efficient resorption.

Measurements of resorption yield show that up to 75 % of the cuticle can be resorbed (Skinner 1962). The resorption process is executed by the innermost epidermal layer and thus the endocuticle is frequently more resorbed, than the exocuticle (Travis 1955; Roer and Dillaman 1984). Both exocuticle and endocuticle show enhanced resorption at the “ecdysial suture” which is a region that splits to allow the animal to emerge during ecdysis (Priester et al. 2005).

5.4.2 *Mechanical Advantages*

The typically small size of the ACC spheres might also confer a mechanical advantage, as the nanometer size of the mineral particles contributes to optimum strength and maximum robustness (Gao et al. 2003). In addition, the small size enables nano-mechanical heterogeneity, which is typical of the chitin-protein-mineral nanocomposite. Such nanoscale structural heterogeneity might also enhance ductility and energy dissipation (Tai et al. 2007). Finally, as mentioned above, the lack of cleavage planes in ACC, due to its isotropic properties, probably makes it less brittle than calcite (Aizenberg et al. 2002).

5.4.3 *Phosphate Incorporation*

A factor that possibly contributes to the wide use of stable ACC for exoskeleton reinforcement is the ability of the amorphous phase to incorporate higher amounts of trace elements and impurities than crystalline phases (Bentov and Erez 2006). In Crustacea, the major co-precipitate with the bulk calcium carbonate in the exoskeleton is calcium phosphate (the possible advantages of calcium phosphate biomineralization are discussed below). Since calcite crystal lattices barely accommodate phosphate ions, this co-precipitation is restricted to amorphous phases where ACC-ACP (designated ACCP) behaves as a solid solution having various PO_4/CO_3 ratios. It is believed that the phosphate in the ACCP solid solution is used, together with other additives, for ACC stabilization (Weiner et al. 2003; Bentov et al. 2010). In addition, as discussed below, phosphate incorporation also plays a mechanical role in ACCP: It has been shown that an increased PO_4/CO_3 ratio in ACCP is associated with enhanced mechanical properties, such as improved hardness and modulus of elasticity (Figs. 5.3 and 5.4) (Currey et al. 1982; Bentov et al. 2012) and reduced solubility (Bentov et al. 2016). Importantly, as shown in Fig. 5.3, ACCP has mechanical properties (hardness and Young’s modulus) that are comparable to those of vertebrate bone. Thus, crustaceans seem to have overcome some of the limitations of ACC (e.g., solubility and low hardness) via the incorporation of phosphate.

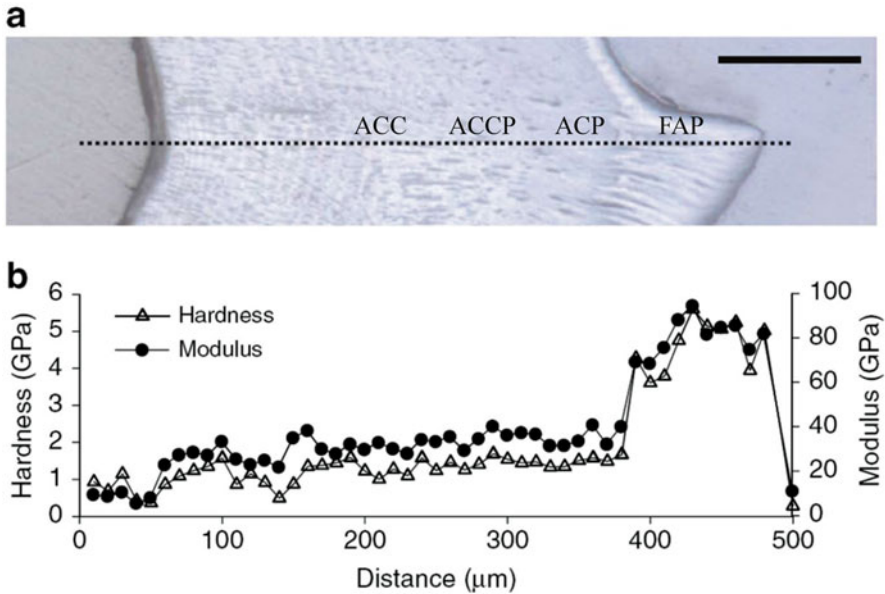


Fig. 5.3 Nanoindentation testing of the anterior crayfish molar. (a) Light micrograph of the measured region in cross-section. bar, 100 μm. (b) Hardness (*open triangles*) and reduced Young's modulus (*filled circles*) for the dotted line in a. Both properties show an increase towards the surface (ACC < ACCP < ACP) and much larger values within the fluorapatite (FAP) distal layer (Adapted from (Bentov et al. 2012) with permission from the Nature Publishing Group)

5.5 The Combination of Calcium Carbonate and Calcium Phosphate

An intriguing question in the evolution of biomineralization is why and how specific minerals were adopted by the different taxa. Mineralization with specific minerals has proved to be a conserved trait. Once a specific mineral is selected, taxa rarely switched mineralogies (Porter 2007). From the beginning of biomineralization in the major animal phyla, during the Cambrian explosion approximately 525 MYA ago, the minerals used by most animals for skeletal reinforcement were calcium salts, either calcium phosphate or calcium carbonate. Consequently, these two minerals remained the most important bioinorganic materials throughout the Phanerozoic eon (until present times), in terms of both phylogenetic distribution and biomineral quantities (Lowenstam and Weiner 1989).

According to the general scheme of biomineral distribution in animals, vertebrates adopted calcium phosphate, while invertebrates adopted calcium carbonate (Knoll 2003). However, in crustaceans the picture seems to be more complex, with various pieces of evidence suggesting that in many crustaceans controlled biomineralization of calcium phosphate takes place in addition to the formation of the bulk

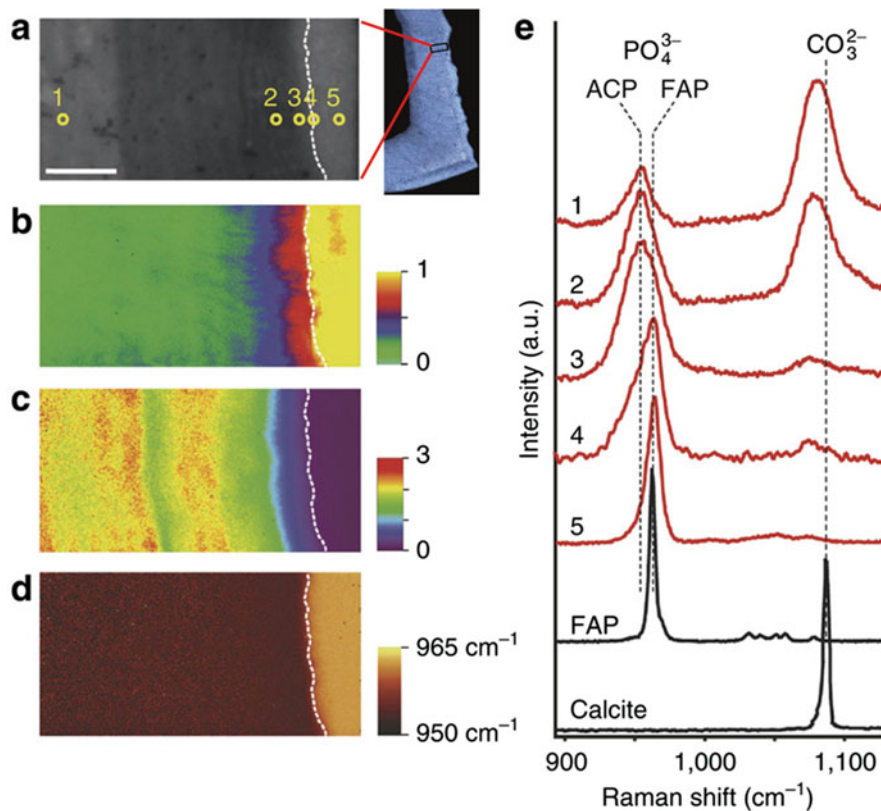


Fig. 5.4 Raman spectroscopic imaging of the *Cherax quadricarinatus* molar. (a) Light micrograph of the analyzed area. Scale bar, 20 μm . The measured area on a molar cross-section covers the transition zone between the apatite and the amorphous mineral (see inset). (b) Raman spectroscopic image of the ν_1 phosphate peak. The normalized integrated intensity ($I_{\text{PO}_4}/I_{\text{PO}_{4\text{max}}}$) shows that phosphate is found in the entire mapped region. (c) The intensity ratio ($I_{\text{CO}_3}/I_{\text{PO}_4}$) of the carbonate (ν_1) to the phosphate peak shows a pronounced gradient with superimposed fluctuations. (d) The position of the ν_1 phosphate peak shows a sharp transition from the crystalline fluorapatite (FAP) zone (*higher values*) to the amorphous regions (*lower values*). The boundary between the apatite layer and the amorphous phases is indicated by the white dashed lines in b–d. (e) Normalized single Raman spectra at positions 1, 2, 3, 4 and 5 as indicated in a, compared with synthetic reference materials, FAP and calcite. The changes in the peak intensities show the gradual decrease/increase in carbonate/phosphate contents. The broadening of the phosphate peak as well as the shift to lower wavenumbers, when passing from position 5 to position 3 across the sample, represents the transition from FAP to ACP (Adapted from (Bentov et al. 2012) with permission from Nature Publishing Group)

calcium carbonate. Unlike other invertebrates (e.g., Mollusca and Echinodermata), many crustaceans contain different amounts of phosphorous within their carbonate skeletons (Huxley 1884; Clarke and Wheeler 1922; Prenant 1927; Vinogradov 1953; Lowenstam and Weiner 1989; Bentov et al. 2010; Kunkel and Jercinovic 2013; Vatcher et al. 2015). This phenomenon was observed as long ago as the 1850s

by Darwin, who noted that crustacean calcareous shells show high variability of phosphate content, whereas molluscan shells have virtually no phosphate (Darwin 1851). As mentioned above, the presence of phosphate in crustacean skeletons has been attributed mainly to co-precipitation with ACC (Raz et al. 2002; Becker et al. 2005; Hild et al. 2009). The presence of apatite crystals in the skeletal tissues of crustaceans has long been considered to be unusual and was thought to be restricted to the barnacle group of Iblidae that contain small crystals of carbonated apatite (Lowenstam et al. 1992). However, it has recently been demonstrated that calcium phosphate mineralization is widely prevalent in crustacean mandibles and that calcium phosphate teeth are frequently formed at specified locations in the mandible in the major crustacean class, Malacostraca (which includes lobsters, crayfish, prawns and shrimps) (Bentov et al. 2016). In these structures, calcium phosphate is not merely co-precipitated with the bulk calcium carbonate but rather creates specialized structures in which a layer of calcium phosphate, frequently in the form of crystalline fluorapatite, is mounted over a calcareous “jaw.” A study of the mandible of the crayfish *Cherax quadricarinatus* showed that the molar teeth are reinforced with large oriented crystals of fluorapatite. This phosphatic cover is mounted over a carbonate basis, forming a graded structure of multi-phase composite material that produces superior mechanical properties, comparable to those of vertebrate enamel (Fig. 5.3) (Bentov et al. 2012). Another example of a particular structure that is mineralized with crystalline apatite is the raptorial appendage of the mantis shrimp (Weaver et al. 2012; Amini et al. 2014). The ability to produce sophisticated structures with superior mechanical properties suggests that many crustaceans possess two biomineralization machineries, one for calcium carbonate and the other for calcium phosphate (Bentov et al. 2016). The wide occurrence of this phenomenon further suggests that the phosphate mineralization mechanism did not evolve independently in the different groups but rather that it has older evolutionary roots.

The phosphatic “inclination” of crustaceans seems to go back to the very beginning of crustacean biomineralization. According to fossil records, calcium phosphate skeletons were more predominant than calcium carbonate skeletons during the appearance of early biomineralizing animals (Lowenstam 1972). The first arthropods frequently had a phosphatic skeleton (e.g., Bradoriida, Aglaspidida and phosphatocopines). In fact, at least until the Ordovician, arthropods exhibited the most advanced calcium phosphate skeletons, which preceded the specialization of vertebrates (Chordata) in terms of calcium phosphate mineralization (Lowenstam 1972). During the Cambrian, the relative abundance of these groups of minerals was reversed, and by the mid-Cambrian, carbonate minerals had become the most common bioinorganic constituents of skeletal elements and remain so to date (Lowenstam and Margulis 1980; Lowenstam and Weiner 1989). The reason for this shift is unclear, although it might have been associated with high phosphate concentrations in the early Cambrian oceans, as a result of the extensive phosphogenic events that took place across the Precambrian-Cambrian boundary and ended by the close of the Cambrian (Rhodes and Bloxam 1971; Cook and Shergold 1984; Cook 1992). This shift is best demonstrated within arthropods fossils, which are among the most dominant Cambrian fossils (e.g., at Burgess Shale in the Canadian Rockies).

The phylogenetic nature of this Cambrian shift from calcium phosphate to calcium carbonate is subject to dispute. According to Lowenstam (1972), the shift from phosphate to carbonate calcification represents an evolutionary adaptive change within the arthropods, namely, a change that reflects the rising metabolic cost of phosphate usage. Other authors argue that a mineralogical shift within a clade is not likely and that the “shift” merely reflects the evolutionary success of various early lineages with different mineralogies. It has further been argued that it is more likely that the apparent replacement of phosphatic minerals with carbonate was the result of secondary diagenetic (post-mortem) phosphatization of carbonate shells (Bengtson and Runnegar 1992). However, support for the option of early phosphatic arthropods may be drawn from several studies showing that fossils of Cambrian arthropods that had previously been considered to be secondarily phosphatized actually had a primary (original) phosphatic cuticle (Bachra et al. 1965; Muller 1979; Briggs and Fortey 1982; Lin et al. 2010). In addition, the above-mentioned frequent finding of dual mineralization systems in recent crustaceans demonstrates the feasibility (in evolutionary terms) of an intra-lineage mineralogical shift within the crustaceans.

The possession of dual mineralization “toolkits” for calcium carbonate and calcium phosphate has provided the crustaceans with (additional) evolutionary plasticity in designing exoskeletal properties. During evolution, the balance between the mechanical requirements of cuticular elements (e.g., the carapace and feeding tools) and the metabolic cost of phosphate and carbonate use (as derived from the animal’s environment) probably dictated the extent of phosphate distribution in the largely calcareous cuticle.

Comparing the biomineralization of calcium carbonate and calcium phosphate from a physiological perspective shows that, theoretically, these biomineralization mechanisms can share some basic features. The concentrations of calcium, carbonate, and phosphate are under tight cellular control. Calcium supply to the calcification site can be similar in both systems. It is likely that carbonate and phosphate have different transport systems, but both serve as important cellular buffers, and their global concentration is under the same cellular regulation system of pH homeostasis. In addition, in both systems, the relative concentration of the required deprotonated species, CO_3^{2-} and PO_4^{3-} , is enhanced by alkalization. The two mineralization systems also share similar crystallization inhibitors (e.g., phosphoproteins, ATP and magnesium) (Blumenthal et al. 1977; Raz et al. 2000; Bentov et al. 2010; Qi et al. 2014).

The major conflict between the two systems is their mutual inhibitory effect on the crystallization process: phosphate ions interfere with the crystallization of calcium carbonate and (to a lesser extent) carbonate ions with that of apatite. This may be one of the reasons that crustaceans frequently use fortification with non-crystallized ACC and ACP, thereby bypassing the structural lattice constraints that are not inherent in the amorphous phases. Thus, an animal can maintain these two mineralization systems utilizing, partially, the same physiological mechanisms (i.e., calcium supply, pH elevation and crystallization inhibitors), with relatively simple adaptations, such as using different matrix proteins (Tynyakov et al. 2015b).

The high variability in the phosphate/carbonate ratio suggests that many arthropods do indeed maintain two biomineralization “toolkits,” one for calcium carbonate and the other for calcium phosphate. This dual system provides an adaptable and versatile biomineralization mechanism that is able to produce separately or simultaneously all the minerals along the calcium carbonate–calcium phosphate spectrum, namely, calcite, ACC, ACP, and apatite, as demonstrated in the mandible of *C. quadricarinatus*. Calcium phosphate mineralization can be beneficial in both the amorphous and crystalline phases. In its crystallized form, apatite offers the hardest mineral option from the range of calcium carbonate/phosphate salts [on the Mohs hardness scale, apatite is 5 while calcite is 2.5–3 (Broz et al. 2006)]. Likewise, in the amorphous phase, calcium phosphate probably plays a major role in enhancing the mechanical properties and chemical resistance of the exoskeleton, in addition to its role in ACC stabilization. Mechanical analysis of the crayfish mandible (Bentov et al. 2012) and the mantis shrimp dactyl limb (Currey et al. 1982) showed that there is a positive correlation between the ACP/ACC ratio, on the one hand, and hardness and the modulus of elasticity, on the other hand (Figs. 5.3 and 5.4). In addition, ACP probably contributes to the chemical resistance of the skeletal element due to its lower solubility than ACC and calcite (Dorozhkin 2010). As mentioned above, one of the natural solutions for reinforcement of the skeletal structure with the aim of withstanding massive impact, is the formation of a mechanically graded structure, in which a hard material is mounted over a softer base that absorbs any impact and deflects potentially dangerous cracks (Currey 2005). It seems that the dual mineral system provides the animal with an efficient method of forming mechanically graded structures through a gradual change in the phosphate/carbonate ratio, as demonstrated in the mandibular structure of crustaceans (Bentov et al. 2012).

In summary, the advantage of calcium phosphate mineralization lies in improved mechanical qualities (such as hardness, stiffness, and wear resistance) and enhanced stability and acid resistance. These advantages are off-set by the higher metabolic cost of calcium phosphate (phosphorus typically present in oceans and freshwater bodies in much lower concentrations than carbonate (Smith 1984; Mackenzie et al. 1993; Urabe et al. 1997; Wu et al. 2000)), which is amplified by less efficient resorption (due to lower solubility) during the premolt stage. Therefore, at the evolutionary level, there seems to be a species-specific tradeoff between the improved mechanical and chemical resistance properties of calcium phosphate and its higher metabolic price. In many species, the balanced solution seems to be the deployment of calcium phosphate only at the wear-prone sites of the skeleton.

5.6 Involvement of Proteins and Genes

Since crustaceans are unique in their ability to rapidly mineralize and demineralize their exoskeletal matrices, they have been designated the “champions of mineral mobilization and deposition in the animal kingdom” (Lowenstam and Weiner 1989) and extensive studies have been performed on this subject (Travis and Friberg 1963;

Ueno 1980; Ueno and Mizuhira 1984; Lowenstam and Weiner 1989; Luquet and Marin 2004; Shechter et al. 2008b; Nagasawa 2012). Key players in the formation of the mineralized exoskeleton are proteins, which are involved in almost every aspect of this process, namely: chitin assembly and metabolism (Buchholz 1989; Abehsera et al. 2015); control of mineralization (Inoue et al. 2008; Bentov et al. 2010); determination of elastic and structural properties (Tynyakov et al. 2015a); and sclerotization (Kuballa and Elizur 2008). It has also been suggested that proteins are involved in mediating the interactions between the chitinous and the mineral phases and the assembly of nanocomposites during skeletogenesis (Glazer et al. 2015).

Studies on the role of proteins in cuticle formation in arthropods were originally performed on insects (Chihara et al. 1982; Snyder et al. 1982), which share cuticle similarity with crustaceans, although their cuticles are non-mineralized. Today, the field of interest has shifted to cover the entire pancrustacean clade, including decapods, as discussed in a recent review article (Roer et al. 2015b). The latter review emphasizes the high similarity across the clade in cuticular structures and content, especially in the proteins involved in cuticle formation. In the different arthropod species, the proteins related to cuticle formation have common features. An important example is the abundant chitin-binding domain found in many cuticular proteins (Ardell and Andersen 2001; Inoue et al. 2001). One such domain is the cuticle-specific chitin-binding domain known as the Rebers-Riddiford (RR) consensus sequence (Rebers and Riddiford 1988; Rebers and Willis 2001). Another chitin-binding domain found in many phyla, including the arthropods, is the type 2 cysteine-rich chitin-binding domain (cys-CBD2), which is present, for example, in the cuticular obstructor protein family (Behr and Hoch 2005). Although many proteins bind to the chitinous scaffold directly, several proteins that lack a chitin-binding domain, such as the important knickkopf protein (Chaudhari et al. 2011), bind to the scaffold through a mediator protein, such as a member of the chitin-binding Obstructor family (Chaudhari et al. 2011; Pesch et al. 2015). An example of this type of indirect scaffold binding is the key role played by protein complexes based on a single core chitin-binding protein in the formation of the gastroliths of the freshwater crayfish *C. quadricarinatus* (Glazer et al. 2015). In addition, proteins lacking a chitin-binding domain can be involved in the formation of non-chitinous cuticular matrices, such as the epicuticle (Roer and Dillaman 1984). Another important process that involves protein-protein interactions is sclerotization, the cross-linking of proteins with phenolic materials (Andersen 2010). Finally, the presence of a signal peptide is probably obligatory in most cuticle-forming proteins, due to the fact that cuticular matrices are extracellular and do not contain any living cells (Roer and Dillaman 1984). Indeed, most of the known cuticular matrix proteins do contain a signal peptide (Ardell and Andersen 2001; Takeda et al. 2001).

Up to this point we have discussed proteins that are involved in the formation of the crustacean cuticle but are not associated directly with the biomineralization process. In comparison to the extensive body of research on the role/s of proteins in biomineralization in vertebrates or echinoderms, knowledge of the protein basis of biomineralization in crustaceans is limited. There are only a few known crustacean proteins that have been shown to be involved in biomineralization, and for most of

these the mechanism of action has not been elucidated. Such proteins exhibit characteristics that are common to many biomineralization-related proteins, e.g., they are proteins having regions that are predicted to be intrinsically disordered or acidic in nature (Addadi and Weiner 1985; Evans 2012; Wojtas et al. 2012). A handful of studies have been conducted on proteins that take part in biomineralization in crustaceans. In the crayfish *Procambarus clarkii*, for example, an acidic protein was found to have an inhibitory effect on calcium carbonate precipitation (Inoue et al. 2008). Also in *P. clarkii*, the acidic gastrolith matrix protein (GAMP), which is predicted to have intrinsically disordered regions consisting of many repeats, is believed to play a key role in mineral precipitation (Ishii et al. 1996; Tsutsui et al. 1999). Similarly, several acidic proteins have been found in the gastrolith disc of the crayfish *C. quadricarinatus* and are known or suggested to be involved in the calcification of the gastroliths (Glazer and Sagi 2012). The molar tooth of *C. quadricarinatus* (see Sect. 5.5) provides a unique opportunity to study the protein basis of calcium phosphate biomineralization in crustaceans (Bentov et al. 2012). In this process, a putative chitin-binding acidic protein that was predicted to be disordered was shown to induce precipitation and mineralization of calcium phosphate *in vitro* (Tynyakov et al. 2015b).

From a genomic point of view the regulatory machinery and set of promoters during molting is poorly known in crustaceans. Since ecdysone plays a key role in regulating molting of pancrustaceans (Qu et al. 2015) the ecdysone pathways is of interest with this respect. Recently it was found in the decapod shrimp *Neocaridina denticulate* that the ecdysteroid pathways known from insects are conserved and suggested to be present in the pancrustacean common ancestor (Sin et al. 2015). Temporal expression during molting provides a powerful tool for the study and mining of molt-related genes. For example genes involved in chitin metabolism and extracellular matrices formation were found to have a molt-related pattern of expression in several studies done on crustaceans (Kuballa and Elizur 2008; Seear et al. 2010; Yudkovski et al. 2010; Rocha et al. 2012; Tynyakov et al. 2015a). Next Generation Sequencing (NGS) provides the ability to perform multigene studies based on molt-related transcriptomic libraries. Several such studies performed recently gave unique insights into the molecular mechanism of molt in crustaceans (Abehsera et al. 2015; Gao et al. 2015; Das et al. 2016). From a future perspective since designating functions in NGS studies is based on annotations, that originates mainly from insect cuticular proteins (Roer et al. 2015a), the temporal expression approach might enable mining of genes unique to crustaceans.

5.7 Potential Biomimetic Applications Inspired by the Crustacean Exoskeleton

Biomineralization in crustaceans is particularly efficient, with the few examples covered above suggesting the utility of studying the proteinaceous machinery in crustaceans. Therefore, understanding the uniqueness that makes crustaceans the

“champions of mineral mobilization and deposition” could be of great importance in biotechnological areas such as biomimetics; such an understanding could provide clues to potential bio-medical applications related to the field of regenerative bone and teeth applications.

The field of biomaterials is in the midst of a transformation in which the life sciences are being combined with materials science and engineering for the formation of bio-inspired materials (Huebsch and Mooney 2009). As part of this process, there has been renewed interest in arthropods as a guide to new biomimetic materials (Paris et al. 2013).

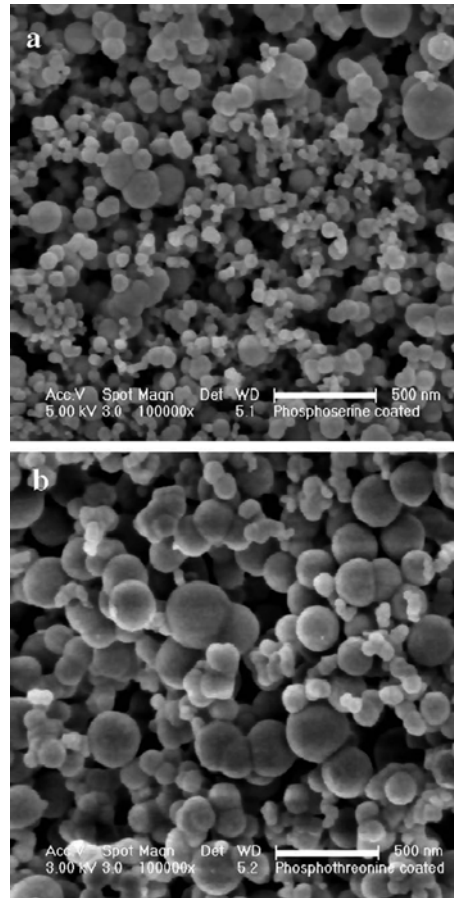
Inspiration for the development of synthetic bio-composites for various skeleton-related medical applications may be drawn by examining the differences and similarities between the crustaceans and the vertebrates, the two major groups in the animal kingdom that combine articulated mineralized skeletons with advanced locomotion. The recent findings that many crustaceans can form elaborate calcium phosphate structures with properties that are comparable to those of vertebrate bones and teeth (Bentov et al. 2016) further suggests a convergent evolution that reflects similar solutions to similar mechanical challenges. One major difference between vertebrate and crustacean skeletons is the organic scaffold that serves as a template for biomineralization: The crustacean scaffold is composed mainly of the polysaccharide α -chitin, while the vertebrate scaffold is made of collagen proteins. However, chitin and collagen are considered as universal templates in biomineralization (Ehrlich 2010). In nature, chitin was also found to serve as a template for calcium phosphate precipitation, as was shown in the chitinophosphatic skeletons of brachiopods (Williams et al. 1994). In pre-clinical and clinical studies, chitin and its deacetylated counterpart chitosan were found to be suitable biomaterials in the field of human calcified tissue engineering, showing good properties of biocompatibility, biodegradability, nontoxicity, nonimmunogenicity, osseointegration and adequate porosity (Khor and Lim 2003; Kim et al. 2008; Costa-Pinto et al. 2011).

There are several potential applications for amorphous mineral phases – stabilized ACC, stabilized ACP, and the combination of calcium carbonate and calcium phosphate mineralization as discussed below.

5.7.1 *Stabilized ACC*

The highly soluble ACC has a potential use as an available calcium supplement for bone health. However, ACC is a metastable phase that readily transforms to the more stable crystalline calcium carbonate, and therefore, understanding stabilization mechanisms is a precondition for any biotechnological application of this mineral. A study of the stabilization mechanism of ACC in the gastrolith (a calcium storage receptacle of premolt crayfish) showed that phosphorylated amino acid moieties probably play a major role as kinetic inhibitors of crystallization (Bentov et al. 2010). The elucidation of a “simplified” biogenic mechanism of ACC stabilization by phosphoamino acids (Fig. 5.5) inspired the development of synthetic stable

Fig. 5.5 Synthetic ACC produced by a biomimetic approach. **(a)** SEM micrographs of ACC comprising 20–200-nm nanospheres produced in the presence of phosphoserine (bar=500 nm). **(b)** ACC, composed of 50–300-nm nanospheres, induced by the presence of phosphothreonine (1 mM) (bar=500 nm) (Adapted from (Bentov et al. 2010) with permission from Elsevier)



ACC, which has been tested as a dietary supplement of available calcium (Bentov et al. 2014). Clinical trials showed that the stabilized ACC does indeed have improved absorption properties in humans (Meiron et al. 2011; Vaisman et al. 2014).

5.7.2 Stabilized ACP

Due to significant chemical and structural similarities with calcified mammalian tissues, as well as excellent biocompatibility and bioresorbability, ACP is a promising candidate for implementation in artificial bone grafts, bone cement, and bone fillers (Combes and Rey 2010; Dorozhkin 2010). A major challenge in bone regeneration is to adjust the degradation kinetics of the calcium phosphate bone filler with the rate of bone tissue formation. In this context, the insolubility of hydroxyapatite might be problematic, and a possible solution is to use ACP (Barrère et al. 2006).

ACP is a thermodynamically unstable compound that tends to transform spontaneously to crystalline calcium phosphates, mainly to apatite. Thus, the expertise of crustaceans in ACP formation and stabilization (Bentov et al. 2016) could be mimicked for the above applications.

5.7.3 *Combination of Calcium Phosphate with Calcium Carbonate*

As mentioned above, a basic toughening feature observed in the crustacean cuticle is the formation of different layers with different mechanical properties, e.g., the hard exocuticle that covers a more compliant endocuticle. This arrangement probably evolved to withstand compression loading and to restrict crack propagation. In addition to the macro-layering, there is a gradation of heterogeneities on the nanoscale, e.g., the gradual decrease in the PO_4/CO_3 ratio from the distal hard surface to the proximal more compliant region that is found in the crayfish mandible (Fig. 5.4) (Bentov et al. 2012) and the smashing limb of the Stomatopoda (Currey et al. 1982; Weaver et al. 2012). This gradation in mechanical properties may be attributed to the lack of long-range atomic order of the amorphous phases, which allows the formation of ACCP solid solutions with various PO_4/CO_3 ratios. A biomimetic approach could therefore be adopted for the synthesis of mechanically graded biomaterials comprising ACC and ACP, which are both biocompatible with human tissues (Tolba et al. 2016).

5.7.4 *Concluding Remarks*

Finally, an as yet unexploited biomimetic direction lies in the exoskeleton's basic building block comprising a chitin–protein–mineral nanocomposite. The intimate association of these three types of materials within the nanocomposite plays a key role in the properties of the skeleton. It is generally believed that proteins are involved in the fundamental functions of chitin binding, calcium binding, formation of nucleation sites, elastic properties, and inhibition or enhancement of crystallization. It seems therefore that elucidation of the role of proteins in the formation and functioning of the nanocomposite represents a major challenge and, once successfully addressed, could promote the development of future generations of biomaterials inspired by the crustacean exoskeleton.

Acknowledgements Writing of this chapter was supported by grants from the Israeli Science Foundation (ISF, Grant 102/09 and 613/13) and the National Institute for Biotechnology in the Negev. We would like to thank the reviewers Robert D. Roer and [Jasna Štrus](#) for their constructive and valuable comments.

References

- Abehsera S, Glazer L, Tynyakov J, Plaschkes I, Chalifa-Caspi V, Khalaila I, Aflalo ED, Sagi A (2015) Binary gene expression patterning of the molt cycle: the case of chitin metabolism. *PLoS One* 10:e0122602
- Addadi L, Weiner S (1985) Interactions between acidic proteins and crystals: stereochemical requirements in biomineralization. *Proc Natl Acad Sci U S A* 82:4110–4114
- Addadi L, Raz S, Weiner S (2003) Taking advantage of disorder: amorphous calcium carbonate and its roles in biomineralization. *Adv Mater* 15:959–970
- Aiken D, Waddy S (1980) Reproductive biology [Lobsters]. In: Cobb JS, Phillips BF (eds) *The biology and management of lobsters, vol 1, Physiology and behavior*. Academic, New York, pp 215–268
- Aizenberg J, Lambert G, Weiner S, Addadi L (2002) Factors involved in the formation of amorphous and crystalline calcium carbonate: a study of an ascidian skeleton. *J Am Chem Soc* 124:32–39
- Amini S, Masic A, Bertinetti L, Teguh JS, Herrin JS, Zhu X, Su HB, Miserez A (2014) Textured fluorapatite bonded to calcium sulphate strengthen stomatopod raptorial appendages. *Nat Commun* 5. doi:10.1038/Ncomms4187
- Andersen SO (2010) Insect cuticular sclerotization: a review. *Insect Biochem Mol Biol* 40:166–178
- Andrew DR (2011) A new view of insect–crustacean relationships II. Inferences from expressed sequence tags and comparisons with neural cladistics. *Arthropod Struct Dev* 40:289–302
- Ardell DH, Andersen SO (2001) Tentative identification of a resilin gene in *Drosophila melanogaster*. *Insect Biochem Mol Biol* 31:965–970
- Arnold K, Findlay H, Spicer J, Daniels C, Boothroyd D (2009) Effect of CO₂-related acidification on aspects of the larval development of the European lobster, *Homarus gammarus* (L.). *Biogeosciences* 6:1747–1754
- Bachra BN, Trautz OR, Simon SL (1965) Precipitation of calcium carbonates and phosphates. 3. The effect of magnesium and fluoride ions on the spontaneous precipitation of calcium carbonates and phosphates. *Arch Oral Biol* 10:731–738
- Barnes RSK, Calow PP, Olive P, Golding DW, Spicer JI (2009) *The invertebrates: a synthesis*, 3rd edn. Wiley- Blackwell, Boston
- Barrère F, van Blitterswijk CA, de Groot K (2006) Bone regeneration: molecular and cellular interactions with calcium phosphate ceramics. *Int J Nanomedicine* 1:317
- Becker A, Ziegler A, Epple M (2005) The mineral phase in the cuticles of two species of Crustacea consists of magnesium calcite, amorphous calcium carbonate, and amorphous calcium phosphate. *Dalton Trans* 10:1814–1820
- Behr M, Hoch M (2005) Identification of the novel evolutionary conserved obstructor multigene family in invertebrates. *FEBS Lett* 579:6827–6833
- Bengtson S (1994) The advent of animal skeletons. In: *Early life on earth, vol 84, Nobel symposium*. Columbia University Press, New York, pp 412–425
- Bengtson S (2004) Early skeletal fossils. *Paleontol Soc Pap* 10:67
- Bengtson S, Runnegar B (1992) Origins of biomineralization in metaphytes and metazoans. In: Schopf JW, Klein C (eds) *The proterozoic biosphere*. Cambridge University Press, Cambridge, pp 447–451
- Bentov S, Erez J (2006) Impact of biomineralization processes on the Mg content of foraminiferal shells: a biological perspective. *Geochem Geophys Geosyst* 7. doi:10.1029/2005gc001015
- Bentov S, Weil S, Glazer L, Sagi A, Berman A (2010) Stabilization of amorphous calcium carbonate by phosphate rich organic matrix proteins and by single phosphoamino acids. *J Struct Biol* 171:207–215
- Bentov S, Zaslansky P, Al-Sawalmih A, Masic A, Fratzl P, Sagi A, Berman A, Aichmayer B (2012) Enamel-like apatite crown covering amorphous mineral in a crayfish mandible. *Nat Commun* 3:839

- Bentov S, Sagi A, Berman A, Shechter A (2014) Stable amorphous calcium carbonate comprising phosphorylated amino acids. US Patent 8,802,160
- Bentov S, Aflalo ED, Tynyakov J, Glazer L, Sagi A (2016) Calcium phosphate mineralization is widely applied in crustacean mandibles. *Sci Rep* 6:22118. doi:10.1038/srep22118
- Blumenthal N, Betts F, Posner A (1977) Stabilization of amorphous calcium phosphate by Mg and ATP. *Calcif Tissue Res* 23:245–250
- Boßelmann F, Romano P, Fabritius H, Raabe D, Epple M (2007) The composition of the exoskeleton of two crustacea: the American lobster *Homarus americanus* and the edible crab *Cancer pagurus*. *Thermochim Acta* 463:65–68
- Briggs DEG, Fortey RA (1982) The cuticle of the aglaspidid arthropods, a red-herring in the early history of the vertebrates. *Lethaia* 15:25–29
- Broz ME, Cook RF, Whitney DL (2006) Microhardness, toughness, and modulus of Mohs scale minerals. *Am Mineral* 91:135–142
- Buchholz F (1989) Molt cycle and seasonal activities of chitinolytic enzymes in the integument and digestive-tract of the antarctic krill, *euphausia-superba*. *Polar Biol* 9:311–317
- Bursell E (1955) The transpiration of terrestrial isopods. *J Exp Biol* 32:238–255
- Cameron JN (1985) Post-moult calcification in the blue crab (*Callinectes sapidus*): relationships between apparent net H⁺ excretion, calcium and bicarbonate. *J Exp Biol* 119:275–285
- Chaudhari SS, Arakane Y, Specht CA, Moussian B, Boyle DL, Park Y, Kramer KJ, Beeman RW, Muthukrishnan S (2011) Knickkopf protein protects and organizes chitin in the newly synthesized insect exoskeleton. *Proc Natl Acad Sci U S A* 108:17028–17033
- Chen P-Y, Lin AY-M, McKittrick J, Meyers MA (2008) Structure and mechanical properties of crab exoskeletons. *Acta Biomater* 4:587–596
- Chihara CJ, Silvert DJ, Fristrom JW (1982) The cuticle proteins of *Drosophila melanogaster*: stage specificity. *Dev Biol* 89:379–388
- Clarke FW, Wheeler WC (1922) The inorganic constituents of marine invertebrates, vol 124. U. S Gov't. Print Off, Washington
- Cohen BL (2005) Not armour, but biomechanics, ecological opportunity and increased fecundity as keys to the origin and expansion of the mineralized benthic metazoan fauna. *Biol J Linn Soc* 85:483–490
- Combes C, Rey C (2010) Amorphous calcium phosphates: synthesis, properties and uses in biomaterials. *Acta Biomater* 6:3362–3378
- Cook PJ (1992) Phosphogenesis around the proterozoic phanerozoic transition. *J Geol Soc Lond* 149:615–620
- Cook PJ, Shergold JH (1984) Phosphorus, phosphorites and skeletal evolution at the Precambrian Cambrian boundary. *Nature* 308:231–236
- Costa-Pinto AR, Reis RL, Neves NM (2011) Scaffolds based bone tissue engineering: the role of chitosan. *Tissue Eng PT B Rev* 17:331–347
- Cribb B, Rathmell A, Charters R, Rasch R, Huang H, Tibbetts I (2009) Structure, composition and properties of naturally occurring non-calcified crustacean cuticle. *Arthropod Struct Dev* 38:173–178
- Currey J (1967) The failure of exoskeletons and endoskeletons. *J Morphol* 123:1–16
- Currey JD (2005) Materials science – Hierarchies in biomineral structures. *Science* 309:253–254
- Currey JD, Nash A, Bonfield W (1982) Calcified cuticle in the stomatopod smashing limb. *J Mater Sci* 17:1939–1944
- Darwin CR (1851) Living Cirripedia, A monograph on the sub-class Cirripedia, with figures of all the species. The Lepadidæ or pedunculated cirripedes, vol 1. The Royal Society, London
- Das S, Pitts NL, Mudron MR, Durica DS, Mykles DL (2016) Transcriptome analysis of the molting gland (Y-organ) from the blackback land crab, *Gecarcinus lateralis*. *Comp Biochem Phys D* 17:26–40
- Dillaman R, Hequembourg S, Gay M (2005) Early pattern of calcification in the dorsal carapace of the blue crab, *Callinectes sapidus*. *J Morphol* 263:356–374
- Dorozhkin SV (2010) Amorphous calcium (ortho)phosphates. *Acta Biomater* 6:4457–4475

- Dunlop JA, Scholtz G, Selden PA (2013) Water-to-land transitions. In: Minelli A, Boxshall G, Fusco G (eds) *Arthropod biology and evolution*. Springer, Berlin, pp 417–439
- Edney E (1960) Terrestrial adaptations. In: Waterman TH (ed) *The physiology of Crustacea*. I. Metabolism and growth, vol 1. Academic, New York, pp 367–393
- Ehrlich H (2010) Chitin and collagen as universal and alternative templates in biomineralization. *Int Geol Rev* 52:661–699
- Evans JS (2012) Aragonite-associated biomineralization proteins are disordered and contain interactive motifs. *Bioinformatics* 28:3182–3185
- Findlay HS, Kendall MA, Spicer JJ, Widdicombe S (2009) Future high CO₂ in the intertidal may compromise adult barnacle *Semibalanus balanoides* survival and embryonic development rate. *Mar Ecol Prog Ser* 389:193–202
- Gao H, Ji B, Jäger IL, Arzt E, Fratzl P (2003) Materials become insensitive to flaws at nanoscale: lessons from nature. *Proc Natl Acad Sci U S A* 100:5597–5600
- Gao Y, Zhang XJ, Wei JK, Sun XQ, Yuan JB, Li FH, Xiang JH (2015) Whole transcriptome analysis provides insights into molecular mechanisms for molting in *litopenaeus vannamei*. *PLoS One* 10:e0144350
- Giribet G, Edgecombe GD (2012) Reevaluating the arthropod tree of life. *Annu Rev Entomol* 57:167–186
- Giribet G, Edgecombe GD, Wheeler WC (2001) Arthropod phylogeny based on eight molecular loci and morphology. *Nature* 413:157–161
- Glazer L, Sagi A (2012) On the involvement of proteins in the assembly of the crayfish gastrolith extracellular matrix. *Invertebr Reprod Dev* 56:57–65
- Glazer L, Roth Z, Weil S, Aflalo ED, Khalaila I, Sagi A (2015) Proteomic analysis of the crayfish gastrolith chitinous extracellular matrix reveals putative protein complexes and a central role for GAP 65. *J Proteom* 128:333–343
- Glenner H, Thomsen P, Hebsgaard M, Sorensen M, Willerslev E (2006) Evolution. The origin of insects. *Science* 314:1883–1884
- Grunenfelder LK, Herrera S, Kisailus D (2014) Crustacean-derived biomimetic components and nanostructured composites. *Small* 10:3207–3232
- Hadley NF, Warburg MR (1986) Water loss in three species of xeric-adapted isopods: correlations with cuticular lipids. *Comp Biochem Phys A* 85:669–672
- Hegdahl T, Gustavsen F, Silness J (1978) The structure and mineralization of the carapace of the crab (*Cancer pagurus*) 3. the epicuticle. *Zool Scr* 6:215–220
- Hild S, Neues F, Znidarsic N, Strus J, Epple M, Marti O, Ziegler A (2009) Ultrastructure and mineral distribution in the tergal cuticle of the terrestrial isopod *Titanethes albus*. Adaptations to a karst cave biotope. *J Struct Biol* 168:426–436
- Huebsch N, Mooney DJ (2009) Inspiration and application in the evolution of biomaterials. *Nature* 462:426–432
- Huxley TH (1884) *The crayfish: an introduction to the study of zoology*, vol 28. Kegan Paul Trench, London
- Inoue H, Ozaki N, Nagasawa H (2001) Purification and structural determination of a phosphorylated peptide with anti-calcification and chitin-binding activities in the exoskeleton of the crayfish, *Procambarus clarkii*. *Biosci Biotechnol Biochem* 65:1840–1848
- Inoue H, Yuasa-Hashimoto N, Suzuki M, Nagasawa H (2008) Structural determination and functional analysis of a soluble matrix protein associated with calcification of the exoskeleton of the crayfish, *Procambarus clarkii*. *Biosci Biotechnol Biochem* 72:2697–2707
- Ishii K, Yanagisawa T, Nagasawa H (1996) Characterization of a matrix protein in the gastroliths of the crayfish *Procambarus clarkii*. *Biosci Biotechnol Biochem* 60:1479–1482
- Khor E, Lim LY (2003) Implantable applications of chitin and chitosan. *Biomaterials* 24:2339–2349
- Kim I-Y, Seo S-J, Moon H-S, Yoo M-K, Park I-Y, Kim B-C, Cho C-S (2008) Chitosan and its derivatives for tissue engineering applications. *Biotechnol Adv* 26:1–21
- Knoll AH (2003) Biomineralization and evolutionary history. *Biomineralization* 54:329–356

- Kuballa AV, Elizur A (2008) Differential expression profiling of components associated with exoskeletal hardening in crustaceans. *BMC Genomics* 9:575
- Kunkel JG, Jercinovic MJ (2013) Carbonate apatite formulation in cuticle structure adds resistance to microbial attack for American lobster. *Mar Biol Res* 9:27–34
- Kurihara H, Matsui M, Furukawa H, Hayashi M, Ishimatsu A (2008) Long-term effects of predicted future seawater CO₂ conditions on the survival and growth of the marine shrimp *Palaemon pacificus*. *J Exp Mar Biol Ecol* 367:41–46
- Lichtenegger HC, Schoberl T, Bartl MH, Waite H, Stucky GD (2002) High abrasion resistance with sparse mineralization: copper biomineral in worm jaws. *Science* 298:389–392
- Lin J, Ivantsov AY, Briggs DEG (2010) The cuticle of the enigmatic arthropod *Phytophilaspis* and biomineralization in Cambrian arthropods. *Lethaia* 44:344–349
- Little C (1990) The terrestrial invasion: an ecophysiological approach to the origins of land animals. Cambridge University Press, Cambridge
- Lowenstam HA (1972) Phosphatic hard tissues of marine invertebrates: their nature and mechanical function, and some fossil implications. *Chem Geol* 9:153–166
- Lowenstam HA, Margulis L (1980) Evolutionary prerequisites for early Phanerozoic calcareous skeletons. *Biosystems* 12:27–41
- Lowenstam HA, Weiner S (1989) On biomineralization. Oxford University Press, New York
- Lowenstam HA, Weiner S, Newman WA (1992) Carbonate apatite-containing shell plates of a barnacle (Cirripedia). In: Slavkin PA, Price PA (eds) Proceedings of the fourth international conference on the chemistry and biology of mineralized tissues. Elsevier, Leiden, pp 73–84
- Luquet G (2012) Biomineralizations: insights and prospects from crustaceans. *ZooKeys* 176:103–121
- Luquet G, Marin F (2004) Biomineralisations in crustaceans: storage strategies. *Comptes Rendus Palevol* 3:515–534
- Ma X, Hou X, Edgecombe GD, Strausfeld NJ (2012) Complex brain and optic lobes in an early Cambrian arthropod. *Nature* 490:258–261
- Mackenzie FT, Ver LM, Sabine C, Lane M, Lerman A (1993) C, N, P, S global biogeochemical cycles and modeling of global change. In: Wollast R, Mackenzie FT, Lie C (eds) Interactions of C, N, P and S biogeochemical cycles and global change. Springer, Berlin, pp 1–61
- Mallatt J, Giribet G (2006) Further use of nearly complete 28S and 18S rRNA genes to classify Ecdysozoa: 37 more arthropods and a kinorhynch. *Mol Phylogeny Evol* 40:772–794
- Manton SM, Harding J (1964) Mandibular mechanisms and the evolution of arthropods. *Philos Trans R Soc Lond Ser B Biol Sci* 247:1–183
- Mary RF, Krishnan G (1974) On the nature and role of protein constituents of the cuticle of crustaceans in relation to permeability of the cuticle. *Mar Biol* 25:299–309
- Meiron OE, Bar-David E, Afalo ED, Shechter A, Stepensky D, Berman A, Sagi A (2011) Solubility and bioavailability of stabilized amorphous calcium carbonate. *J Bone Miner Res* 26:364–372
- Muller KJ (1979) Phosphatocopine ostracodes with preserved appendages from the upper Cambrian of Sweden. *Lethaia* 12:1–27
- Nagasawa H (2012) The crustacean cuticle: structure, composition and mineralization. *Front Biosci* 4:711–720
- Nedin C (1999) Anomalocaris predation on nonmineralized and mineralized trilobites. *Geology* 27:987–990
- Neville AC (1975) Biology of the arthropod cuticle, vol 4. Springer, Berlin
- Nikolov S, Petrov M, Lymperakis L, Friák M, Sachs C, Fabritius HO, Raabe D, Neugebauer J (2010) Revealing the design principles of high-performance biological composites using Ab initio and multiscale simulations: the example of lobster cuticle. *Adv Mater* 22:519–526
- Palmer AR (1992) Calcification in marine mollusks – how costly is it. *Proc Natl Acad Sci U S A* 89:1379–1382
- Paris O, Hartmann MA, Fritz-Popovski G (2013) The mineralized crustacean cuticle: hierarchical structure and mechanical properties. In: Fratzl P, Dunlop JW, Weinkamer R (eds) Materials

- design inspired by nature: function through inner architecture. The Royal Society of Chemistry, London, pp 180–196
- Pesch Y-Y, Riedel D, Behr M (2015) Obstructor a organizes matrix assembly at the apical cell surface to promote enzymatic cuticle maturation in *Drosophila*. *J Biol Chem* 290:10071–10082
- Porter SM (2007) Seawater chemistry and early carbonate biomineralization. *Science* 316:1302–1302
- Prenant M (1927) Les formes mineralogiques du calcaire chez les etres vivants, et le probleme de leur determinisme. *Biol Rev* 2:365–393
- Priester C, Dillaman RM, Gay DM (2005) Ultrastructure, histochemistry, and mineralization patterns in the ecdysial suture of the blue crab, *Callinectes sapidus*. *Microsc Microanal* 11:479–499
- Pütz K, Buchholz F (1991) Comparative ultrastructure of the cuticle of some pelagic, nekto-benthic and benthic malacostracan crustaceans. *Mar Biol* 110:49–58
- Qi C, Zhu YJ, Lu BQ, Zhao XY, Zhao J, Chen F, Wu J (2014) Atp-stabilized amorphous calcium carbonate nanospheres and their application in protein adsorption. *Small* 10:2047–2056
- Qu Z, Kenny NJ, Lam HM, Chan TF, Chu KH, Bendena WG, Tobe SS, Hui JH (2015) How did arthropod sesquiterpenoids and ecdysteroids arise? Comparison of hormonal pathway genes in noninsect arthropod genomes. *Genome Biol Evol* 7:1951–1959
- Raabe D, Sachs C, Romano P (2005) The crustacean exoskeleton as an example of a structurally and mechanically graded biological nanocomposite material. *Acta Mater* 53:4281–4292
- Raz S, Weiner S, Addadi L (2000) Formation of high-magnesium calcites via an amorphous precursor phase: possible biological implications. *Adv Mater* 12:38–42
- Raz S, Testeniere O, Hecker A, Weiner S, Luquet G (2002) Stable amorphous calcium carbonate is the main component of the calcium storage structures of the crustacean *Orchestia cavimana*. *Biol Bull* 203:269–274
- Rebers JE, Riddiford LM (1988) Structure and expression of a *Manduca sexta* larval cuticle gene homologous to *Drosophila* cuticle genes. *J Mol Biol* 203:411–423
- Rebers JE, Willis JH (2001) A conserved domain in arthropod cuticular proteins binds chitin. *Insect Biochem Mol Biol* 31:1083–1093
- Regier JC, Shultz JW, Kambic RE (2005) Pancrustacean phylogeny: hexapods are terrestrial crustaceans and maxillopods are not monophyletic. *Proc R Soc Lond B Biol Sci* 272:395–401
- Regier JC, Shultz JW, Zwick A, Hussey A, Ball B, Wetzer R, Martin JW, Cunningham CW (2010) Arthropod relationships revealed by phylogenomic analysis of nuclear protein-coding sequences. *Nature* 463:1079–U1098
- Rhodes FHT, Bloxam TW (1971) Phosphatic organisms in the Paleozoic and their evolutionary significance. In: North American Paleontological Convention, pp 1485–1513
- Rocha J, Garcia-Carreno FL, Muhlia-Almazan A, Peregrino-Uriarte AB, Yepiz-Plascencia G, Cordova-Murueta JH (2012) Cuticular chitin synthase and chitinase mRNA of whiteleg shrimp *Litopenaeus vannamei* during the molting cycle. *Aquaculture* 330:111–115
- Roer R, Dillaman R (1984) The structure and calcification of the crustacean cuticle. *Am Zool* 24:893–909
- Roer R, Abehsera S, Sagi A (2015a) Exoskeletons across the pancrustacea: comparative morphology, physiology, biochemistry and genetics. *Integr Comp Biol* 55:771–791
- Roer R, Abehsera S, Sagi A (2015b) Exoskeletons across the Pancrustacea: comparative morphology, physiology, biochemistry and genetics. *Integr Comp Biol* 55(5):771–791. doi:10.1093/icb/icv080
- Sachs C, Fabritius H, Raabe D (2006) Hardness and elastic properties of dehydrated cuticle from the lobster *Homarus americanus* obtained by nanoindentation. *J Mater Res* 21:1987–1995
- Sardà F, Cros M, Sese B (1989) Ca balance during moulting in the prawn *Aristeus antennatus* (Risso, 1816): the role of cuticle calcification in the life cycle of decapod crustaceans. *J Exp Mar Biol Ecol* 129:161–171

- Sastry A (1983) Ecological aspects of reproduction. In: Vernberg FJ, Vernberg WB (eds) The biology of crustacea, vol 8. Academic, New York, pp 179–271
- Seear PJ, Tarling GA, Burns G, Goodall-Copestake WP, Gaten E, Ozkaya O, Rosato E (2010) Differential gene expression during the moult cycle of Antarctic krill (*Euphausia superba*). BMC Genomics 11:582
- Shechter A, Berman A, Singer A, Freiman A, Grinstein M, Erez J, Aflalo ED, Sagi A (2008a) Reciprocal changes in calcification of the gastrolith and cuticle during the molt cycle of the red claw crayfish *Cherax quadricarinatus*. Biol Bull 214:122–134
- Shechter A, Glazer L, Cheled S, Mor E, Weil S, Berman A, Bentov S, Aflalo ED, Khalaila I, Sagi A (2008b) A gastrolith protein serving a dual role in the formation of an amorphous mineral containing extracellular matrix. Proc Natl Acad Sci U S A 105:7129–7134
- Sin YW, Kenny NJ, Qu Z, Chan KW, Chan KW, Cheong SP, Leung RW, Chan TF, Bendena WG, Chu KH, Tobe SS, Hui JH (2015) Identification of putative ecdysteroid and juvenile hormone pathway genes in the shrimp *Neocaridina denticulata*. Gen Comp Endocrinol 214:167–176
- Skinner DM (1962) The structure and metabolism of a crustacean integumentary tissue during a molt cycle. Biol Bull 123(3):635–647
- Smith S (1984) Phosphorus versus nitrogen limitation in the marine environment. Limnol Oceanogr 29:1149–1160
- Smith MR, Caron JB (2015) Hallucigenia's head and the pharyngeal armature of early ecdysozoans. Nature 523:75–78
- Snyder M, Hunkapiller M, Yuen D, Silvert D, Fristrom J, Davidson N (1982) Cuticle protein genes of *Drosophila*: structure, organization and evolution of four clustered genes. Cell 29:1027–1040
- Strausfeld NJ, Andrew DR (2011) A new view of insect–crustacean relationships I. Inferences from neural cladistics and comparative neuroanatomy. Arthropod Struct Dev 40:276–288
- Tai K, Dao M, Suresh S, Palazoglu A, Ortiz C (2007) Nanoscale heterogeneity promotes energy dissipation in bone. Nat Mater 6:454–462
- Takeda M, Mita K, Quan GX, Shimada T, Okano K, Kanke E, Kawasaki H (2001) Mass isolation of cuticle protein cDNAs from wing discs of *Bombyx mori* and their characterizations. Insect Biochem Mol Biol 31:1019–1028
- Taylor D, Dirks JH (2012) Shape optimization in exoskeletons and endoskeletons: a biomechanics analysis. J R Soc Interface 9:3480–3489
- Tolba E, Müller WE, El-Hady BMA, Neufurth M, Wurm F, Wang S, Schröder HC, Wang X (2016) High biocompatibility and improved osteogenic potential of amorphous calcium carbonate/vaterite. J Mater Chem B 4:376–386
- Travis DF (1955) The molting cycle of the spiny lobster, *Panulirus argus* Latreille. II. Pre-ecdysial histological and histochemical changes in the hepatopancreas and integumental tissues. Biol Bull 108:88–112
- Travis DF, Friberg U (1963) The deposition of skeletal structures in the Crustacea: VI. Microradiographic studies of the exoskeleton of the crayfish *Orconectes virilis* Hagen. J Ultrastruct Res 9:285–301
- Tsutsui N, Ishii K, Takagi Y, Watanabe T, Nagasawa H (1999) Cloning and expression of a cDNA encoding an insoluble matrix protein in the gastroliths of a crayfish, *Procambarus clarkii*. Zool Sci 16:619–628
- Tynyakov J, Bentov S, Abehsera S, Khalaila I, Manor R, Katzir AL, Weil S, Aflalo E, Sagi A (2015a) A novel chitin binding crayfish molar tooth protein with elasticity properties. PLoS One 10:e0127871–e0127871
- Tynyakov J, Bentov S, Abehsera S, Yehezkel G, Roth Z, Khalaila I, Weil S, Berman A, Plaschkes I, Tom M, Aflalo ED, Sagi A (2015b) A crayfish molar tooth protein with putative mineralized exoskeletal chitinous matrix properties. J Exp Biol 218:3487–3498
- Ueno M (1980) Calcium transport in crayfish gastrolith disc: morphology of gastrolith disc and ultrahistochemical demonstration of calcium. J Exp Zool 213:161–171

- Ueno M, Mizuhira V (1984) Calcium transport mechanism in crayfish gastrolith epithelium correlated with the molting cycle. *Histochemistry* 80:213–217
- Urabe J, Clasen J, Sterner RW (1997) Phosphorus limitation of *Daphnia* growth: is it real? *Limnol Oceanogr* 42:1436–1443
- Vaisman N, Shaltiel G, Daniely M, Meiron OE, Shechter A, Abrams SA, Niv E, Shapira Y, Sagi A (2014) Increased calcium absorption from synthetic stable amorphous calcium carbonate: double-blind randomized crossover clinical trial in postmenopausal women. *J Bone Miner Res* 29:2203–2209
- Vatcher HE, Roer RD, Dillaman RM (2015) Structure, molting, and mineralization of the dorsal ossicle complex in the gastric mill of the blue crab, *Callinectes sapidus*. *J Morphol* 276:1358–1367
- Vincent JFV (2002) Arthropod cuticle: a natural composite shell system. *Compos Part A-Appl S* 33:1311–1315
- Vinogradov AP (1953) The elementary chemical composition of marine organisms (trans: J.K. Setlow JEA). Sears Foundation for Marine Research, Memoir no. II. Yale University, New Haven
- Vittori M, Štrus J (2014) The integument in troglobitic and epigeal woodlice (Isopoda: Oniscidea): a comparative ultrastructural study. *Zoomorphology* 133:391–403
- Weaver JC, Milliron GW, Miserez A, Evans-Lutterodt K, Herrera S, Gallana I, Mershon WJ, Swanson B, Zavattieri P, DiMasi E, Kisailus D (2012) The stomatopod dactyl club: a formidable damage-tolerant biological hammer. *Science* 336:1275–1280
- Weiner S, Levi-Kalisman Y, Raz S, Addadi L (2003) Biologically formed amorphous calcium carbonate. *Connect Tissue Res* 44:214–218
- Wheeler WC, Giribet G, Edgecombe GD (2004) Arthropod systematics. The comparative study of genomic, anatomical, and paleontological information. In: Cracraft J, Donoghue MJ (eds) *Assembling the tree of life*. Oxford University Press, New York, pp 281–295
- Whiteley N (2011) Physiological and ecological responses of crustaceans to ocean acidification. *Mar Ecol Prog Ser* 430:257–271
- Williams A, Cusack M, Mackay S (1994) Collagenous chitinophosphatic shell of the brachiopod *Lingula*. *Philos Trans R Soc Lond Ser B Biol Sci* 346:223–266
- Wojtas M, Dobryszczycki P, Ozyhar A (2012) Intrinsically disordered proteins in biomineralization. In: *Advanced topics in biomineralization*. InTech, Rijeka, pp 3–32
- Wu J, Sunda W, Boyle EA, Karl DM (2000) Phosphate depletion in the western north Atlantic ocean. *Science* 289:759–762
- Yudkovski Y, Glazer L, Shechter A, Reinhardt R, Chalifa-Caspi V, Sagi A, Tom M (2010) Multi-transcript expression patterns in the gastrolith disk and the hypodermis of the crayfish *Cherax quadricarinatus* at premolt. *Comp Biochem Phys D* 5:171–177
- Žnidaršič N, Mrak P, Tušek-Žnidarič M, Štrus J (2012) Exoskeleton anchoring to tendon cells and muscles in molting isopod crustaceans. *ZooKeys* 176:39–53

Chapter 6

Tyrosine Metabolism for Insect Cuticle Pigmentation and Sclerotization

Yasuyuki Arakane, Mi Young Noh, Tsunaki Asano, and Karl J. Kramer

Abstract Pigmentation or body color patterns in insects quite often differ not only between species but also in different stages of development and in different body regions of a single species. Body coloration plays physiologically and ecologically important roles as for instance in species recognition and communication, courtship/mate selection, mimicry, crypsis, warning, prey-predator/parasite interactions, and resistance to temperature, desiccation and absorbs or reflects harmful ultraviolet radiation. Many kinds of pigment molecules and structural colors contribute to the diversity of body coloration in insects. Recent studies have elucidated some of the genetic and molecular biological mechanisms underlying pigment biosynthesis. This chapter focuses on the pigments derived from the amino acid tyrosine. The tyrosine-mediated cuticle tanning pathway is responsible for production of melanins and other pigments derived from 3,4-dihydroxyphenylalanine (DOPA) and dopamine as well as from *N*-acyldopamines. The *N*-acylated dopamines, in addition, are oxidized by the phenoloxidase laccase 2 to form quinones and quinone methides, which then undergo cross-linking reactions with cuticular proteins (CPs) for cuticle sclerotization. We review the regulation and functional importance and also the diversity of the genes involved in this pathway. The unique localization and cross-linking of specific CPs for morphology and ultrastructure of the exoskeleton are also discussed.

Y. Arakane (✉) • M.Y. Noh
Department of Applied Biology, Chonnam National University, Gwangju 61186, South Korea
e-mail: arakane@chonnam.ac.kr; annemi@chonnam.ac.kr

T. Asano
Department of Biological Sciences, Tokyo Metropolitan University, Tokyo 192-0397, Japan
e-mail: asano-tsunaki@tmu.ac.jp

K.J. Kramer
Department of Biochemistry and Molecular Biophysics, Kansas State University,
Manhattan, KS 66506, USA
e-mail: kjkramer@k-state.edu

6.1 Introduction

6.1.1 *Insect Cuticle Composition and Morphology*

The insect exoskeleton or cuticle is composed of multiple functional layers including an outermost lipophilic waterproofing envelope, a protein-rich epicuticle and a chitin/protein-rich procuticle that makes up the major portion (see Chap. 7 in this book for details about insect hydrocarbons; Locke 2001; Moussian et al. 2006; Moussian 2010). It plays critical roles in protecting insects from various physical and environmental stresses and from pathogenic challenges. Two different structural biopolymers, cuticular proteins (CPs) and chitin (see Chap. 2 in this book for details about chitin metabolism), are the major components of the exo- and endocuticular layers that comprise the procuticle (Willis 2010). Other components include pigments, catechols, mineral salts, lipids and water. The primary focus of this review is the pigments found in insects that are derived from the amino acid tyrosine, which include melanins and papiliochromes with the former being the predominant class (Wittkopp and Beldade 2009; Shamim et al. 2014). Melanogenesis is a complex multistep production of high molecular weight melanins via hydroxylation, oxidation and polymerization of the oxidized metabolites (Singh et al. 2013). Although melanin-type pigments commonly occur in insect cuticles, their isolation and partial characterization have been carried out in only a few species (Hackman 1974, 1984; Hori et al. 1984; Kayser 1985). No definitive molecular structure has yet been delineated for these heterogeneous polymers, but they appear to be combinations of phenolic, indolic, pyrrolic and aliphatic structures that may interact covalently and noncovalently with macromolecular components such as cuticular proteins and chitin (Schaefer et al. 1987; Duff et al. 1988; Solano 2014; Chatterjee et al. 2015).

There are several other kinds of pigments such as pterins, ommochromes, anthraquinones, aphins (polycyclic quinones), terapyrroles, carotenoids and flavonoids/anthocyanins present in insect tissues, many of which have been described in earlier reviews (Cromartie 1959; Fuzeau-Braesch 1972; Takeuchi et al. 2005; Shamim et al. 2014). Ommochromes, for example, are one of the major pigments that have been found in eyes, eggs and body walls of insects. In ommochrome biosynthesis, tryptophan is converted to 3-hydroxykynurenine, which is then incorporated into pigment granules by ABC transporters (Tearle et al. 1989; Pepling and Mount 1990). In addition, another transporter, which is a member of a major facilitator superfamily, incorporates other precursor(s) into granules (Osanai-Futahashi et al. 2012b) where the pigments are synthesized via oxidative polymerization. Aphines synthesized from a presumed polyketide precursor have only been found in aphids and contribute to a variety of body colors during development and/or different species. Tsuchida et al. (2010) demonstrated that infection with an aphid endosymbiont of the genus *Rickettsiella* increases the amounts of blue-green aphins in the pea aphid, *Acyrtosiphon pisum*, resulting in a change in their body color from reddish to greenish. This body color change caused by endosymbiosis is likely to influence prey-predator/parasite interactions and natural populations of the aphid. Pterins

synthesized from guanosine triphosphate are also widely distributed in eyes, bodies and wings of insects. In addition, tetrahydrobiopterin (BH_4) serves as a cofactor for enzymes such as phenylalanine hydroxylase and tyrosine hydroxylase (TH) in tyrosine metabolism-associated cuticle pigmentation and sclerotization (Futahashi et al. 2010). For example, 6-pyruvoyl-tetrahydropterin synthase (PTS, Purple) is involved in the BH_4 biosynthesis, and a mutation in *BmPTS* gene is responsible for colorless cuticle of the albino (*al*) mutant of the silkworm, *Bombyx mori* (Fujii et al. 2013).

Insects and mammals possess fine-tuned systems of enzymes to meet their specific demands for tyrosine metabolites. In addition, more closely related enzymes involved in tyrosine metabolism appear to have emerged in many insect species (Vavricka et al. 2014). The metabolism of tyrosine plays a major role in not only the darkening of insect cuticle but also in its hardening or sclerotization as well as in innate immune responses to microbial pathogens. Coloration can vary from colorless to yellow to tan to orange to brown to black depending on the amounts and types of melanin-like pigments incorporated. The degree of sclerotization can vary from soft and flexible to hard and stiff, much of which is determined by the number of chitin-protein laminae and also the number of structural proteins' cross-links derived from tyrosine metabolism (Yang et al. 2014). The chemistry underlying insect pigmentation is rather complex. However, substantial progress has been made in recent years in understanding how tyrosine metabolism contributes to that process (Sugumaran 2009; Shamim et al. 2014).

CPs and chitin are the major components of the exo- and endocuticular layers that comprise the procuticle. The former layer is generally formed before molting, whereas the latter is mainly deposited after completion of the molting process. Transmission electron microscopic (TEM) analysis, for example, revealed that the embryonic cuticle of the fruit fly, *Drosophila melanogaster*, as well as dorsal larval body wall cuticle from the red flour beetle, *Tribolium castaneum*, are composed of an envelope, epicuticle and procuticle, the latter consisting of various numbers of horizontally oriented chitin-protein laminae parallel to the epidermal cell's apical plasma membrane (Fig. 6.1a; Moussian et al. 2006; Moussian 2010). These morphologically distinct layers are also evident in cuticle of elytra (modified forewings; Chen et al. 2015a, b) dissected from *T. castaneum* pharate adults, which become harder and darker shortly after eclosion. In the case of elytral dorsal cuticle, unlike the relatively soft and flexible elytral ventral and larval dorsal body wall cuticles, there are numerous vertically oriented columnar structures denoted as pore canal fibers (PCFs), which extend directly from the "apical plasma membrane protrusions" (APMP) of the underlying epidermal cells and penetrate a large number of horizontal laminae, reaching all the way to the epicuticle (Fig. 6.1b; Noh et al. 2014). Not only the horizontal laminae but also the vertical PCFs are likely composed of chitin as those structures bind to wheat germ agglutinin (Noh et al. 2015b). In *T. castaneum* adults, other regions with rigid cuticle such as the thoracic body wall and leg exhibit an ultrastructure very similar to that of the elytron's dorsal cuticle. On the other hand, there are fewer horizontal laminae and no vertical pore canals with PCFs in anatomical regions covered with soft, flexible and less pigmented cuticles such as those found on the dorsal abdomen, ventral elytron and

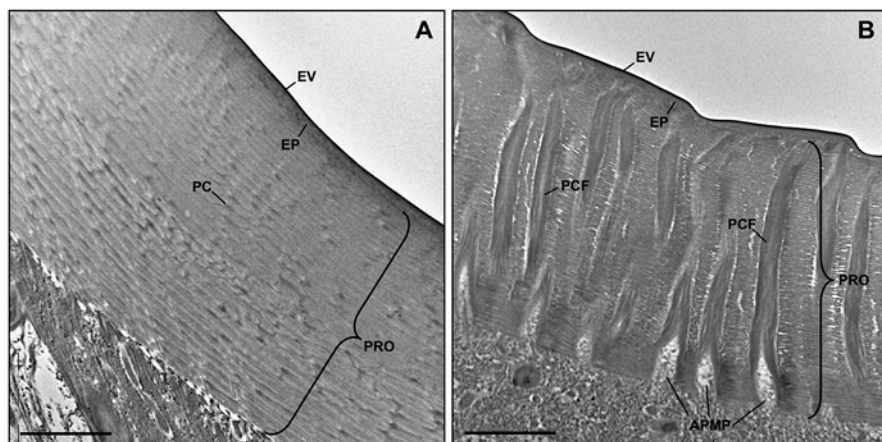


Fig. 6.1 Ultrastructure of larval (a) and adult body wall (b) cuticles in *T. castaneum*. Both larval and adult body cuticles are composed of distinct layers including the envelope, epicuticle and procuticle. The procuticle consists of a number of horizontal chitinous laminae in larval and adult body wall cuticles. In addition, there are numerous pore canals running transverse to the laminae, as well as to the apical plasma membrane. The canals extend from the apical plasma membrane to the epicuticle region and contain a core of pore canal fibers in adult body cuticle. Ultrastructure of adult body wall is similar to those of elytra and leg cuticles in *T. castaneum*, which are relatively hard cuticles (Noh et al. 2014). *EV* envelope, *EP* epicuticle, *PRO* procuticle, *PC* pore canal, *PCF* pore canal fiber, *APMP* apical plasma membrane protrusion. Scale bar = 2 μ m

hindwing (Noh et al. 2014). Similar vertical fibrillar structures or vertical fibrils have been observed not only in other insect species (Locke 1961; Delachambre 1971; Wigglesworth 1985) but also in the exoskeletons of crustaceans after removal of minerals and some proteins, including *Homarus americanus* (American lobster), *Callinectes sapidus* (Atlantic blue crab) and *Tylos europaeus* (sand-burrowing isopod) (see Chap. 5 in this book for details about exoskeletons of crustaceans; Raabe et al. 2006; Cheng et al. 2008; Seidl et al. 2011), suggesting that this unique architecture and arrangement of numerous laminae and PCFs contribute to the physical strength of rigid cuticle in arthropods. Pigments are found in cuticle and epidermis and little or no information is available as to whether they contribute to the mechanical properties of the exoskeleton.

6.1.2 Proposed Tyrosine-Mediated Cuticle Tanning Pathway

Despite a rather limited composition, cuticle has remarkably diverse mechanical properties, ranging from soft and flexible to hard and rigid. An insect must periodically replace its old cuticle with a new one by undergoing ecdysis because the mature cuticle is too restrictive to allow for continuous growth during development. Immediately after molting, the cuticle is soft and pale, but it shortly becomes

hardened (sclerotized) and often darker (pigmented) over a period of several hours or days. This vital process together with dehydration occurs during each stage of development (Kramer et al. 2001; Andersen 2005; Arakane et al. 2008; Lomakin et al. 2011).

Tanning (pigmentation and sclerotization) is a complex and important physiological event not only in cuticle formation (Andersen 2010) but also in wound healing, encapsulation during a defensive response to infection of parasites, and hardening of the egg chorion (see Chap. 9 in this book for details about chorion hardening; Li 1994; Sugumaran 2002). With tyrosine as the initial substrate, the cuticle tanning reactions include hydroxylation of tyrosine to dihydroxyphenylalanine (DOPA) and decarboxylation of DOPA to dopamine. For melanization, furthermore, oxidation of DOPA and dopamine to DOPA-quinone and dopaminequinone, conversion of these quinones to dihydroxyindole (DHI) and/or 5,6-dihydroxyindole-2-carboxylic acid (DHICA), oxidation of DHI and DHICA to DHI-chrome and DHICA-chrome (melanochromes) and finally polymerization of melanochromes to form melanins (Fig. 6.2; Arakane et al. 2009; Simon et al. 2009). For pigmentation involving acylated quinones, the reactions include *N*-acetylation of dopamine to *N*-acetyldopamine (NADA) or *N*- β -alanylation to *N*- β -alanyldopamine (NBAD), oxidation of NADA and NBAD to NADA-quinone and NBAD-quinone and their polymerization to form their corresponding pigments. These quinones, in addition, undergo isomerization to quinone methides and cross-linking reactions with CP side chains (most likely histidyl residues) for cuticle sclerotization (Fig. 6.2; Kramer et al. 2001).

Recent studies have indicated that the following enzymes are involved in the catalysis of cuticle tanning reactions: tyrosine hydroxylase (TH; Pale) converts tyrosine to DOPA; DOPA decarboxylase (DDC) converts DOPA to dopamine; dopachrome conversion enzyme (DCE, Yellow) accelerates the conversion of dopachrome to DHI; arylalkylamine *N*-acetyltransferase (NAT) converts dopamine to NADA; aspartate 1-decarboxylase (ADC) decarboxylates L-aspartic acid to β -alanine for production of NBAD; NBAD synthase (Ebony) produces NBAD and laccase 2 catalyzes the catecholic oxidation reactions in the tanning pathway (Table 6.1 and see Sect. 6.2 for details).

6.2 Functions of Key Enzymes/Proteins Involved in Tyrosine-Mediated Cuticle Tanning

6.2.1 Tyrosine Hydroxylase (TH)

The first step in the cuticle tanning pathway is the hydroxylation of tyrosine to produce DOPA (Fig. 6.2). There are two enzymes that can catalyze this hydroxylation reaction, tyrosinase (phenoloxidase, PO) and tyrosine hydroxylase (TH). Although the former enzyme has been detected in insect cuticles and is multifunctional,

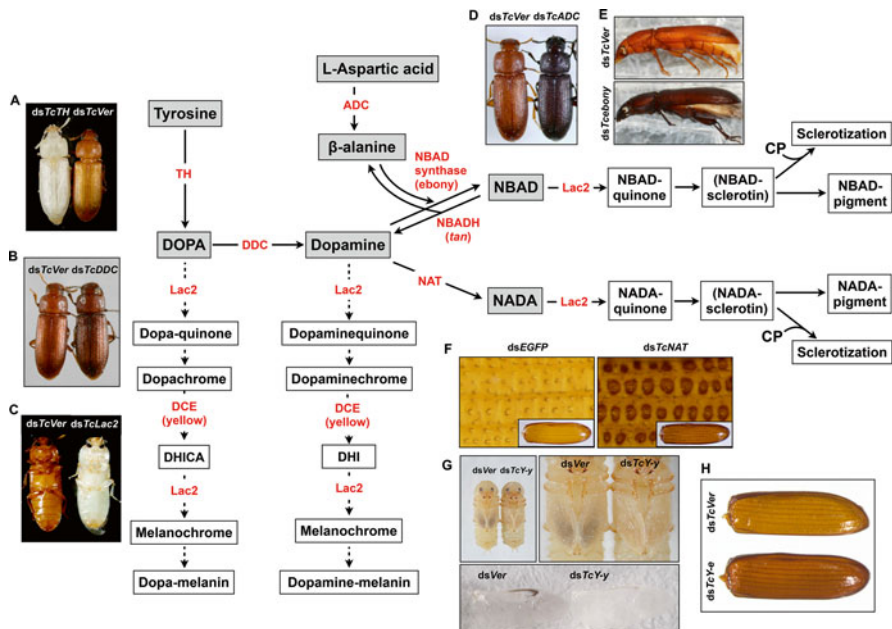


Fig. 6.2 Proposed cuticle tanning pathway in *T. castaneum*. DOPA, 3,4-dihydroxyphenylalanine; dopamine, 3,4-dihydroxyphenethylamine; NADA, *N*-acetyldopamine; NBAD, *N*-β-alanyldopamine; TH, tyrosine hydroxylase; DDC, DOPA decarboxylase; NAT, *N*-acetyltransferase; NBAD synthase (Ebony), *N*-β-alanyldopamine synthase; ADC, aspartate 1-decarboxylase; NBADH (Tan), *N*-β-alanyldopamine hydrolase; Lac2, lactase 2; DCE (Yellow), dopachrome conversion enzyme; CP, cuticle proteins. The broken and solid lines represent melanin synthesis and quinone tanning pathways, respectively. Key enzymes are indicated in red letters and body color changes are shown after RNAi for *TcTH* (a), *TcDDC* (b), *TcLac2* (c), *TcADC* (d), *Tcebony* (e), *TcNAT* (f), *TcY-y* (g) and *TcY-e* (h)

oxidizing *ortho*-diphenols as well as hydroxylating monophenols such as tyrosine (Andersen 2005; Arakane et al. 2005; Kanost and Gorman 2008), it likely plays only a role in immune-related melanization and not in cuticle tanning as suggested by several studies (Barrett 1991; Marmaras et al. 1996; Ashida and Brey 1997; Asano and Ashida 2001; Christensen et al. 2005; Kanost and Gorman 2008). In line with this notion, double-stranded RNA (dsRNA)-mediated loss of function of tyrosinase in *T. castaneum*, for instance, had no effect on larval, pupal and adult cuticle tanning (Arakane et al. 2005).

Like mammalian TH, insect TH is a pterin (BH₄)-dependent oxygenase (Liu et al. 2010; Fujii et al. 2013) that catalyzes hydroxylation of tyrosine as a homotetramer. Its activity is regulated by phosphorylation of a serine residue catalyzed by a cAMP-dependent protein kinase (Vie et al. 1999). In *D. melanogaster*, there are two alternatively spliced isoforms of *DmTH* (*pale*): the longer is expressed in the epidermis and the shorter, which lacks a highly acidic region in the N-terminus, specifically is expressed in the central nervous system (Birman et al. 1994; Friggi-Grelin

Table 6.1 Cuticle tanning-related genes and loss of function phenotypes in insects

Enzyme	Species	Accession no.	Loss of function	Phenotype	References
Tyrosine hydroxylase (TH)	<i>Tribolium castaneum</i>	EF592178	RNAi	Colorless and soft cuticle	Gorman and Arakane (2010)
	<i>Drosophila melanogaster</i>	AAF50648	Mutant (<i>pale</i>)	Unpigmented embryos/pale cuticle	Budnik and White (1987), Neckameyer and White (1993), and True et al. (1999)
	<i>Manduca sexta</i>	EF592177	–	–	Gorman et al. (2007)
	<i>Papilio xuthus</i>	AB178006	Chemical inhibition	Suppression of larval pigmentation	Futahashi and Fujiwara (2005)
	<i>Pseudaletia separata</i>	AB274834	Chemical inhibition	Diminished black pigmentation of larval stripes	Ninomiya et al. (2006)
	<i>Bombyx mori</i>	AB439286	Mutant (sch)/RNAi	Light reddish-brown neonate larval body color/delay pupal pigmentation	Liu et al. (2010) and Lee et al. (2015)
	<i>Spodoptera exigua</i>	JF795467 JF795468	Mutant (overexpression)	Dark pigmented pupal cuticle	Liu et al. (2015)
	<i>Oncopeltus fasciatus</i>	KM247780	RNAi	Loss of black pigmentation in adult cuticle	Liu et al. (2014)

(continued)

Table 6.1 (continued)

Enzyme	Species	Accession no.	Loss of function	Phenotype	References
Dopa decarboxylase (DDC)	<i>Tribolium castaneum</i>	EU019710	RNAi	Slightly darker adult cuticle	Arakane et al. (2010)
	<i>Drosophila melanogaster</i>	AAF53764	Mutant	Albino adult bristle and cuticle	True et al. (1999)
	<i>Pseudaletia separata</i>	AB072300	Chemical inhibition	Diminished black pigmentation of larval stripes	Ninomiya et al. (2006)
	<i>Papilio xuthus</i>	AB178007	Chemical inhibition	Suppression of larval pigmentation	Futahashi and Fujiwara (2005)
	<i>Bombyx mori</i>	AF372836	RNAi	Fail larval to pupal molt	Wang et al. (2013)
	<i>Papilio glaucus</i>	AF036963	Mutant (melanic female)	Yellow proximal area of adult wing alters black	Koch et al. (1998)
	<i>Spodoptera exigua</i>	SEU71404	Mutant (overexpression)	Dark pigmented pupal cuticle	Liu et al. (2015)
	<i>Oncopeltus fasciatus</i>	KM247781	RNAi	Reduction of adult black pigmentation	Liu et al. (2014)
	<i>Tribolium castaneum</i>	EU019709	RNAi/ mutant (<i>black</i> and <i>b^{or}/b^{sr}</i>)	Black body pigmentation in larva, pupa and adult	Kramer et al. (1984) and Arakane et al. (2010)
	<i>Drosophila melanogaster</i>	NM_057440	mutant (<i>black</i>)	Black/dark body pigmentation	Phillips et al. (1993, 2005)
<i>Bombyx mori</i>	KM523624	mutant (<i>bp</i>)	Black pupal cuticle	Dai et al. (2015)	
Aspartate 1-decarboxylase (ADC)					

Arylalkylamine <i>N</i> -acetyltransferase (NAT)	<i>Tribolium castaneum</i>	FJ647798	RNAi	Dark pigmented adult cuticle	Tomoyasu et al. (2009)
	<i>Bombyx mori</i>	DQ256382	RNAi/mutant (<i>mln</i>) overexpression	Darker body pigmentation Dark coloration of neonatal larvae, adult antenna and larval tracheae alters light brown	Dai et al. (2010), Zhan et al. (2010), and Qiao et al. (2012) Osanai-Futahashi et al. (2012)
NBAD synthase (Ebony)	<i>Tribolium castaneum</i>	FJ647797	RNAi	Dark pigmented adult cuticle	Tomoyasu et al. (2009)
	<i>Drosophila melanogaster</i>	AAF55870	mutant	Dark pigmented adult thorax and abdomen	Wittkopp et al. (2002a)
	<i>Papilio xuthus</i>	AB195255	–	–	Futahashi and Fujiwara (2005)
	<i>Bombyx mori</i>	AB439000	Mutant (<i>sooty</i>)	Dark body pigmentation in larva and pupa	Futahashi et al. (2008a, b)
	<i>Papilio glaucus</i>	–	Mutant (melanic female)	Black melanin replaces yellow background in wing	Koch et al. (2000)
	<i>Papilio polytes</i>	AB525746	–	–	Nishikawa et al. (2013)

(continued)

Table 6.1 (continued)

Enzyme	Species	Accession no.	Loss of function	Phenotype	References
NBAD hydrolase (Tan)	<i>Drosophila melanogaster</i>	NM_132315	Mutant	Less pigmented adult thorax and abdomen	True et al. (2005), Jeong et al. (2008), and Aust et al. (2010)
	<i>Bombyx mori</i>	AB499125	Mutant (<i>ro</i>)	Larval black marking alters light brown	Futahashi et al. (2010)
	<i>Papilio xuthus</i>	AB499122	–	–	Futahashi et al. (2010)
Laccase 2 (Lac2)	<i>Tribolium castaneum</i>	AY884061	RNAi	Colorless and soft cuticle, lethal	Arakane et al. (2005)
	<i>Monochamus alternatus</i>	EU093075	RNAi	Colorless and soft cuticle, lethal	Niu et al. (2008)
	<i>Riptortus pedestris</i>	AB586067	RNAi	Colorless and soft cuticle, lethal	Futahashi et al. (2011)
	<i>Nysius plebeius</i>	AB586069	RNAi	Less pigmentation	Futahashi et al. (2011)
	<i>Megacopta punctatissima</i>	AB586068	RNAi	Less pigmentation	Futahashi et al. (2011)
	<i>Papilio xuthus</i>	AB499123	–	–	Futahashi et al. (2010)
	<i>Oncopeltus fasciatus</i>	KM247782	RNAi	Reduction of adult black pigmentation	Liu et al. (2014)
	<i>Nilaparvata lugens</i>	KR086787	RNAi	Colorless and soft cuticle, lethal	Ye et al. (2015)

Yellow-y (Y-y)	<i>Tribolium castaneum</i>	GU111770	RNAi	Not critical for body coloration except for black pigmented pterostigma of the hindwing	Arakane et al. (2010)
	<i>Drosophila melanogaster</i>	NM_057444	mutant	Light brown/yellowish cuticle	Wittkopp et al. (2002a)
	<i>Bombyx mori</i>	AB438999	overexpression mutant (<i>ch</i>)	Black adult wing cuticle Lighter pigmented larval cuticle	Riedel et al. (2011) Futahashi et al. (2008a, b)
Yellow-e (Y-e)	<i>Papilio xuthus</i>	AB195254	–	–	Futahashi and Fujiwara (2007)
	<i>Tribolium castaneum</i>	GU111765	RNAi	Dark body color in adult body cuticle and vein of hindwing	Noh et al. (2015a)
	<i>Bombyx mori</i>	AB489224	mutant (<i>bts</i>)	White larval head and anal plates alters reddish brown	Ito et al. (2010)

et al. 2003). Similarly, long epidermal and short brain/neural isoforms of the *TH* transcript were identified in the oriental armyworm, *Pseudaletia separata* (Ninomiya and Hayakawa 2007).

Several studies have implicated a functional importance of TH in insect cuticle pigmentation. Mutation in the *DmTH* gene (*pale*) results in lethal unpigmented embryos that fail to develop into larvae, resulting in no hatching from eggs (Budnik and White 1987; Neckameyer and White 1993). Because TH is also important in the nervous system, it is possible that the embryos die before becoming fully developed because of the lack of DmTH function in this system. This embryonic lethality was rescued by expression of the epidermal form of DmTH (Friggi-Grelin et al. 2003). True et al. (1999) demonstrated by using mosaic analysis that the lack of DmTH function resulted in an adult albino cuticle phenotype, and ectopic DmTH expression caused ectopic cuticle pigmentation. In lepidopteran species such as the Asian swallowtail, *Papilio xuthus* and *P. separata*, *TH* mRNA and/or protein were detected in the epidermal cells underlying the darkly marked larval cuticle (Futahashi and Fujiwara 2005; Ninomiya and Hayakawa 2007). In the tobacco hornworm, *Manduca sexta*, the amount of TH protein in the integument of pharate pupal segments is correlated with the degree of cuticle pigmentation (Gorman et al. 2007). Treatment with a TH inhibitor such as 3-iodotyrosine inhibited pigment formation in *P. xuthus* larvae and *B. mori* adults (Futahashi and Fujiwara 2005; Lee et al. 2015) and also rescued black pupae produced by overexpressed *TH* and *DDC* genes in a pupal melanic mutation strain of the beet armyworm, *Spodoptera exigua* (Liu et al. 2015). In addition, RNAi for *BmTH* caused a delay in pupal cuticle pigmentation of *B. mori* (Lee et al. 2015), and a reduction of *BmTH* transcripts was responsible for the sex-linked chocolate (*sch*) mutant, which exhibits a light reddish-brown neonatal larval body color compared with the black color of that of the wild-type strain (Liu et al. 2010). There is differential regulation of TH during cuticular melanization and innate immunity in *B. mori* (Lee et al. 2015). *BmTH* is expressed in the epidermis during development for the purpose of pupal cuticle melanization and pigmentation in adults, and in the fat body during infection for antimicrobial activity. In the large milkweed bug, *Oncopeltus fasciatus*, RNAi for the *OfTH* gene resulted in a complete absence of black pigmentation in adult cuticles on the head, thorax, abdomen and wings (Liu et al. 2014). Similarly, in *T. castaneum*, injection of dsRNA for *TcTH* diminished the brown pigmentation in the pupal cuticle of the abdominal segments, urogomphi, bristles and gin traps as well as in the adult cuticle of the mandibles and legs, which was visible underneath the pupal cuticle, and also the dark pigmentation observed in the hindwings. The cuticle of phypomorphic ds*TcTH*-treated adults is pale (Fig. 6.2a; Gorman and Arakane 2010). Furthermore, the cuticles of both hard and dark dorsal thorax and hard and colorless eye of ds*TcTH*-treated adults are soft and flexible, indicating that TH is required for not only cuticle pigmentation but also for sclerotization in some species.

6.2.2 *Dopa Decarboxylase (DDC)*

Dopamine is a catecholamine involved in nervous systems of mammals and insects as a neurotransmitter, neuromodulator and neurohormone (Nassel 1996; Osborne 1996; Neckameyer and Leal 2002; Han et al. 2010). In insects, dopamine is also important for egg-shell hardening and the immune response as well as cuticle melanization (Hopkins et al. 1984; Nappi et al. 1992; Huang et al. 2005; Davis et al. 2008; Paskewitz and Andreev 2008; Sideri et al. 2008). In the cuticle tanning pathway, DOPA decarboxylase (DDC), which is a pyridoxal-5-phosphate (PLP)-dependent enzyme, catalyzes the decarboxylation of DOPA to yield dopamine, a major precursor in melanin/pigment production and sclerotization mediated by protein cross-linking (Hopkins et al. 1984; Hiruma et al. 1985; Kramer and Hopkins 1987; Andersen 2005; Hopkins and Kramer 1992; Riddiford et al. 2003).

The functional importance of DDC in cuticle coloration has been well studied in several lepidopteran species, which exhibit a high degree of variation in pigmentation. Like the *TH* gene, *DDC* is highly expressed in epidermal cells underlying the presumptive black markings (e.g. eyespots, V-shaped and band-markings) of larval cuticles of different swallowtail butterflies including *P. xuthus*, the common yellow swallowtail, *Papilio machaon* and the common Mormon, *Papilio polytes* (Shirataki et al. 2010). Furthermore, chemical inhibitors of DDC such as *m*-hydroxybenzylhydrazine (HBHZ) completely inhibited pigment formation of *P. xuthus* (Futahashi and Fujiwara 2005). In the eastern tiger swallowtail, *Papilio glaucus*, *DDC* expression and enzyme activity regulate the color pattern of the adult wings (Koch et al. 1998). *DDC* mRNA and activity are detected early in the presumptive yellow regions of the wings and later in the presumptive black patterns. In the melanic female of this species, early DDC activity in the central yellow region of the wing is much lower than that of wild-type females, which is later melanized concomitant with increased DDC activity. Ninomiya et al. (2006) demonstrated that DDC expression is required for the black strips in the dorsal cuticle of last instar larvae of *P. separata*. *DDC* mRNA and protein are detected in the epidermal cells underneath the black stripe, but not below the white stripe. HBHZ treatment caused the complete loss of DDC activity, a low level of dopamine, an abnormally high level of DOPA and diminished black pigmentation of the strips in the larval cuticle, indicating that DDC activity and its product dopamine are critical for melanin deposition in the black strips.

In *D. melanogaster*, the *DmDDC* gene has two alternatively spliced transcripts, of which one is expressed in the epidermis and the other in the central nervous system (Hodgetts and O'Keefe 2006). Tissue-specific expression of alternatively spliced DDC isoforms has not been reported in other species. The crystal structure and site-directed mutagenesis analysis of *DmDDC* indicate that T82 is involved in substrate binding and H192 is essential for both a substrate interaction and cofactor binding (Han et al. 2010). These amino acid residues are highly conserved among insect DDCs. Like that observed for *DmTH*, patches of epithelial cells deficient in *DmDDC* activity produce albino adult bristles and cuticle (True et al. 1999).

Similarly, loss of function of *DDC* by RNAi causes a reduction in black pigmentation of *O. fasciatus* adult cuticle (Liu et al. 2014). In *T. castaneum*, the level of DOPA increases approximately 5-fold in *dsTcDDC*-treated pharate adults (Arakane et al. 2009). However, the initial cuticle pigmentation of the resulting adults is substantially delayed, suggesting that, unlike dopamine, DOPA does not appear to be utilized to a great extent for DOPA quinone-associated melanin synthesis, probably because DOPA is a poor substrate for laccase 2 (Arakane et al. 2009). The body color of the *TcDDC*-deficient mature adults is slightly darker than that of control animals (Fig. 6.2b). This phenotype may be due to a small amount of DOPA-melanin accumulation relative to NBAD- and/or NADA-derived pigments in the adult cuticle. All of these results indicate that DDC activity is required for providing dopamine as a major precursor for melanin synthesis and also quinone-based tanning in insect cuticle.

6.2.3 Aspartate 1-Decarboxylase (ADC)

β -Alanine is involved in critical physiological events in insects. In cuticle tanning, it is conjugated with dopamine via the action of NBAD synthase (*ebony*; see Sect. 6.2.5) to produce NBAD, which is one of the major catechols serving as a cuticle tanning precursor (Hopkins et al. 1984; Kramer et al. 1984; Andersen 2007, 2010). β -Alanine is produced by decarboxylation of the α -COOH of aspartic acid, and aspartate 1-decarboxylase (ADC) catalyzes this reaction. Like DDC, ADC is a member of the pyridoxal 5-phosphate-dependent amino acid decarboxylase family, in which all members possess a conserved decarboxylase domain containing a pyridoxal phosphate-binding domain motif (Ser-X-X-Lys). Phylogenetic analysis revealed that ADCs are closely related with glutamate decarboxylases (GDCs) and distantly related with other decarboxylase family members including histidine, tyrosine and DOPA decarboxylases (Fig. 6.3; Arakane et al. 2009). Although ADCs and GDCs show a high overall amino acid sequence identity/similarity, they exhibit a rather rigorous substrate specificity probably due to small differences in the enzymes' active sites. Richardson et al. (2010) demonstrated that the recombinant ADC protein from the yellow fever mosquito, *Aedes aegypti*, produces β -alanine by decarboxylation of aspartic acid, but it is inactive toward glutamic acid. On the other hand, the recombinant GDC from the malaria mosquito, *Anopheles gambiae*, decarboxylates glutamic acid to produce γ -amino butyric acid but exhibits no activity toward aspartic acid. In addition, that research group identified Q377 to be located in the active site of *Ae. aegypti* ADC, which is a highly conserved amino acid residue among other insect ADCs and appears to be critical for selectivity of aspartic acid as the substrate (Liu et al. 2012) (Table 6.2).

In *D. melanogaster*, the *black* gene encoding ADC (DGAD2) is responsible for black/dark body color phenotype (Phillips et al. 1993, 2005). The *black* mutant had a deficiency of β -alanine (Hodgetts and Choi 1974) probably due to a significant decrease in ADC activity (Phillips et al. 2005). Similarly, black body color mutant

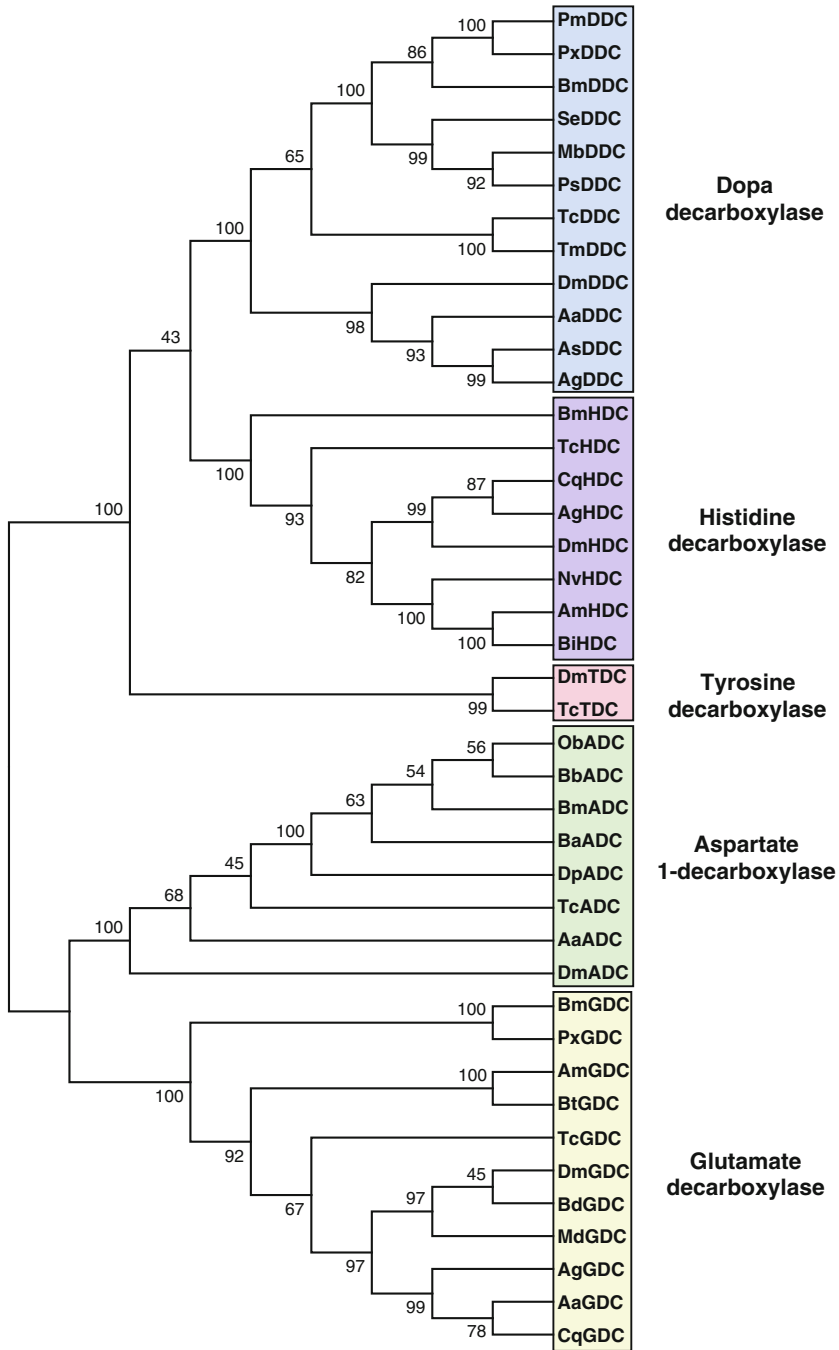


Fig. 6.3 Phylogenetic analysis of amino acid decarboxylases in insects. The amino acid sequences of DOPA decarboxylases (DDC), histidine decarboxylases (HDC), tyrosine decarboxylases (TDC), aspartate 1-decarboxylases (ADC) and glutamate decarboxylases (GDC) were obtained from GenBank. The phylogenetic tree was constructed with MEGA 6.06 software using the Neighbor-Joining method (Tamura et al. 2013). Numbers by each branch indicate results of bootstrap analysis of 5000 replications. See Table 6.2 for the accession numbers of protein sequences used in this analysis

Table 6.2 Accession numbers of insect decarboxylases used for phylogenetic analysis

Decarboxylase	Abbreviation	Species	Accession number
Dopa decarboxylase (DDC)	PmDDC	<i>Papilio machaon</i>	BAJ07588
	PxDDC	<i>Papilio xuthus</i>	NP_001299156
	BmDDC	<i>Bombyx mori</i>	NP_001037174
	SeDDC	<i>Spdoptera exigua</i>	AFG25780
	MbDDC	<i>Mamestra brassicae</i>	BAB68545
	PsDDC	<i>Pseudaletia separata</i>	BAB68549
	TcDDC	<i>Tribolium castaneum</i>	ABU25222
	TmDDC	<i>Tenebrio molitor</i>	BAA95568
	DmDDC	<i>Drosophila melanogaster</i>	NP_724164
	AaDDC	<i>Aedes aegypti</i>	AAC31639
	AsDDC	<i>Anopheles sinensis</i>	KFB39134
	AgDDC	<i>Anopheles gambiae</i>	XP_319841
Histidine decarboxylase (HDC)	BmHDC	<i>Bombyx mori</i>	XP_012551888
	TcHDC	<i>Tribolium castaneum</i>	XP_975682
	CqHDC	<i>Culex quinquefasciatus</i>	EDS34715
	AgHDC	<i>Anopheles gambiae</i>	EAA14857
	DmHDC	<i>Drosophila melanogaster</i>	CAA49989
	NvHDC	<i>Nasonia vitripennis</i>	XP_008202389
	AmHDC	<i>Apis mellifera</i>	XP_392129
BiHDC	<i>Bombus impatiens</i>	XP_012245143	
Tyrosine decarboxylase (TDC)	DmTDC	<i>Drosophila melanogaster</i>	AAM70810
	TcTDC	<i>Tribolium castaneum</i>	EFA10808
Aspartate 1-decarboxylase (ADC)	ObADC	<i>Operophtera brumata</i>	KOB74239
	BbADC	<i>Biston betularia</i>	AEP43793
	BaADC	<i>Bicyclus anynana</i>	AEQ77286
	DpADC	<i>Danaus plexippus</i>	EHJ66406
	TcADC	<i>Tribolium castaneum</i>	ABU25221
	AaADC	<i>Aedes aegypti</i>	EAT40747
	DmADC	<i>Drosophila melanogaster</i>	NP_476788
	BmADC	<i>Bombyx mori</i>	AJQ30182
Glutamate decarboxylase (GDC)	BmGDC	<i>Bombyx mori</i>	XP_004925034
	PxGDC	<i>Papilio xuthus</i>	KPI96691
	AmGDC	<i>Apis mellifera</i>	XP_391979
	BtGDC	<i>Bombus terrestris</i>	XP_012170748
	TcGDC	<i>Tribolium castaneum</i>	EFA06442
	DmGDC	<i>Drosophila melanogaster</i>	CAA53791
	BdGDC	<i>Bactrocera dorsalis</i>	XP_011201397
	MdGDC	<i>Musca domestica</i>	XP_011296520
	AgGDC	<i>Anopheles gambiae</i>	EAA11955
	AaGDC	<i>Aedes aegypti</i>	EAT35903
	CqGDC	<i>Culex quinquefasciatus</i>	EDS27073

strains of *T. castaneum* exhibit decreased concentrations of both β -alanine and NBAD as well as a higher level of dopamine when compared with those of wild-type beetles (Kramer et al. 1984). RNAi for *TcADC* resulted in a dark pigmented body color (Fig. 6.2d) and a significantly lower NBAD content compared to control animals like that seen in the *T. castaneum black* mutant strains (Arakane et al. 2009). Injection of β -alanine, the expected product of the reaction catalyzed by ADC, into the *black* mutant strains and ds*TcADC*-treated animals rescued the black body color phenotypes and restored the normal reddish-brown cuticle coloration (Kramer et al. 1984; Arakane et al. 2009). In addition, the *black* mutation affected the puncture resistance of the cuticle by delaying sclerotization (Roseland et al. 1987). Furthermore, dynamic mechanical analysis indicated less cross-linked cuticles from the black body color mutant and ds*TcADC*-treated animals (Arakane et al. 2009). These results suggested that the *black* mutants of *T. castaneum*, like the *D. melanogaster black* mutant, have a mutation(s) that causes loss of function of ADC, resulting in a depletion of β -alanine used for NBAD synthesis. Solid-state ^{13}C -nuclear magnetic resonance difference spectroscopy was used to determine the presence of melanin in the *black* mutant of *T. castaneum* (Kramer et al. 1989, 1995). It was estimated that 1–2% of the organic components in the cuticle of the *black* mutant are attributable to eumelanin. The high levels of dopamine relative to the corresponding levels in the wild-type strain led to an increased production of eumelanin when the excess dopamine was oxidized in the *black* mutant (Kramer et al. 1984; Roseland et al. 1987).

Recently, Dai et al. (2015) reported that a mutation of the *ADC* gene (*BmADC*) is responsible for the black pupal (*bp*) mutant phenotype of *B. mori*, which exhibits melanization specifically in the pupal stage. In the *bp* mutant, like that seen in the *black* mutants of *T. castaneum*, there were depleted levels of *BmADC* transcripts, β -alanine and NBAD as well as accumulation of dopamine. Injection of β -alanine into the *bp* mutant reverted the dark color pattern to the wild-type pattern. RNAi for *BmADC* in the wild-type strain, furthermore, led to a melanic pupal phenotype similar to the *bp* mutant. All of these results indicated that ADC plays a role in cuticle pigmentation and sclerotization. Loss of function of ADC results in a depletion of β -alanine used for NBAD synthesis resulting in the accumulation of abnormally high levels of dopamine, which are then used for dopamine melanin production during tanning at the expense of NBAD quinone-mediated cuticle protein cross-linking and pigmentation.

6.2.4 Arylalkylamine N-Acetyltransferase (AANAT)

Arylalkylamine N-acetyltransferases (AANATs) belong to a large Gcn5-related acetyltransferase (GNAT) superfamily, which catalyze the transacylation between acetyl-CoA and arylalkylamines (Dyda et al. 2000; Vetting et al. 2005). AANAT has been extensively studied as a key enzyme for pineal hormone melatonin synthesis, which regulates circadian rhythms in mammals (Arendt et al. 1995; Evans 1989;

Klein 2007). AANAT activity is rate-limiting and it acetylates serotonin to form *N*-acetylserotonin in the vertebrate pineal organ, which is then methylated by hydroxyindole-*o*-methyltransferase to melatonin.

In contrast to mammals, the availability of whole genome sequences from several insect species has revealed that there is a large number of genes encoding AANAT or AANAT-like proteins in their genomes (Meher et al. 2011; Han et al. 2012; Barbera et al. 2013; Hiragaki et al. 2015), suggesting a functional diversity of AANATs in insects. For example, melatonin has also been detected in insects such as *D. melanogaster*, *B. mori*, *A. pisum*, the migratory locust, *Locusta migratoria*, and the American cockroach, *Periplaneta americana* (Vivien-Roels et al. 1984; Finocchiaro et al. 1988; Hintermann et al. 1995; Itoh et al. 1995a, b; Hardie and Gao 1997). AANAT activity in melatonin synthesis was correlated with a circadian rhythm and seasonal photoperiodism (Itoh et al. 1995b; Bembenek et al. 2005; Vieira et al. 2005; Barbera et al. 2013). In mammals, several neurotransmitter arylalkylamines (e.g. octopamine, dopamine and serotonin) are inactivated by monoamine oxidase (MAO), whereas AANATs appear to metabolize arylalkylamines in insects because there is little or no MAO activity in their nervous tissues (Smith 1990; Amherd et al. 2000; Sloley 2004).

In insect cuticle tanning, AANAT apparently *N*-acetylates dopamine to form NADA, which is one of major precursors for quinone-mediated pigmentation and sclerotization (Fig. 6.2; Andersen 1974, 2005, 2010; Hopkins and Kramer 1992). Although the properties of insect AANATs including pH-activity profile, substrate specificity, kinetic parameters and site-directed mutagenesis to identify residues that participate in its catalysis have been studied (Hintermann et al. 1996; Brodbeck et al. 1998; Meher et al. 2011; Han et al. 2012; Dempsey et al. 2014), information about the functional importance of AANATs in cuticle tanning is rather limited. In *B. mori*, the *melanism* (*mln*) mutant, in which the AANAT (*Bm-iAANAT*) gene is disrupted, shows a darker body pigmentation in the head, thoracic legs, spiracle, claw hook of prolegs and anal plate of larvae as well as in the entire body of adults (Dai et al. 2010; Zhan et al. 2010). Confirmation that a mutation of the *Bm-iAANAT* was responsible for a dark color integument in the *mln* mutant was obtained by an RNAi experiment. Injection of dsRNA for *Bm-iAANAT* into wild-type pupae resulted in the adults exhibiting a darker body pigmentation similar to that of the *mln* mutant (Zhan et al. 2010). In contrast, ectopic expression of *Bm-iAANAT* altered the dark/black coloration of neonatal larvae and adult antennae as well as larval tracheae of *B. mori* to light brown (Osanai-Futahashi et al. 2012a). This coloration change was also evident in the *B. mori* black striped strain *striped*, which has a wide black stripe in each segment. The black stripes became light grey in *Bm-iAANAT*-overexpressing lines. All of these results support the hypothesis that *N*-acetylation of dopamine decreases the availability of dopamine for dopamine-melanin production.

The dopamine content in the dark pigmented tissues (e.g. head, thoracic legs and anal plate) from the *mln* mutant of *B. mori* was two times higher than that from the wild-type strain (Dai et al. 2010). More recently, the same research group reported additional information about the catecholamine content in the *mln* mutant (Qiao et al. 2012). In the head of the larvae, dopamine and NBAD levels were higher than

those of the wild-type. In the whole body of adults, dopamine content was approximately six times greater than in the wild-type, while NBAD content was nearly the same in the two strains. This may be due to significantly lower levels of *ADC* and *NBAD synthase (ebony)* present in the adult *mln* mutant. Little or no NADA was evident in both larval and adult tissues. These results suggest that a loss of function of *Bm-iAANAT* results in excess dopamine (and NBAD in larvae), which likely undergoes dopamine-melanin synthesis (and NBAD-pigment synthesis in larvae) in the *B. mori mln* mutant. Dynamic mechanical analysis revealed that elytra with abnormally high dopamine collected from the TcADC-deficient adult *T. castaneum* (*dsTcADC* knockdown and the *black* mutants) exhibited a higher elastic modulus, suggesting a less effectively cross-linked cuticle than that of control insects (Arakane et al. 2009; Lomakin et al. 2010, 2011). In contrast, the wings of the *mln* mutant showed a higher modulus, indicating that the *mln* wings are stiffer than those of the wild-type strain, probably because the CPs are abnormally cross-linked.

Similarly, in adult *T. castaneum*, depletion of TcAANAT1 function by RNAi resulted in dark pigmentation of the entire body including pronotum, ventral abdomen, elytron and veins of the hindwing (Tomoyasu et al. 2009). In addition, dark pigments surrounding the bristles located on the inter-veins of the elytron were evident (Fig. 6.2f). The elytron is a highly modified and sclerotized forewing of beetles. There are a large number of pillar-like support structures called “trabeculae”, which are located between the dorsal and ventral cuticles and contribute to the mechanical strength of the elytron (Ni et al. 2001; Chen and Wu 2013; Chen et al. 2015b; He et al. 2015; van de Kamp et al. 2015). The dark pigments in the elytra of *dsTcAANAT*-treated adults appear to be due to those pigmented trabeculae (unpublished observation), suggesting that NADA-mediated pigmentation and/or sclerotization is required for development of the trabeculae.

6.2.5 NBAD Synthase (*Ebony*)

The gene for *Ebony* encodes an enzyme catalyzing the synthesis of NBAD by conjugation of dopamine and β -alanine. The *ebony* mutant of *D. melanogaster* had already been described for its characteristic dark cuticle as early as 1923 (Bridges and Morgan 1923). Mutants in the *ebony* locus also show phenotypes of altered locomotion rhythm, vision or courtship behavior (Hotta and Benzer 1969; Kyriacou et al. 1978; Newby and Jackson 1991; Suh and Jackson 2007). *Ebony* (NBAD synthase) is closely related to non-ribosomal peptide synthases (NRPSs). Study of recombinant *Ebony* proteins of *D. melanogaster* that were expressed in an *E. coli* system revealed its biochemical properties (Richardt et al. 2003). *D. melanogaster Ebony* consists of 879 amino acids, which is divided into three domains, an activation/adenylation domain (572 aa), thiolation domain (78 aa) and amine-selecting domain (229 aa) (Hovemann et al. 1998; Richardt et al. 2003; Hartwig et al. 2014). The selectivity of amines is not very strict, and various biogenic amines, including dopamine, octopamine, histamine and serotonin, are β -alanylated (Richardt et al. 2003).

NBAD synthase can be defined with a more general name, β -alanylbiogenic amine synthase. Ebony is a novel type of NRPS-related protein that can be distinguished by its ability to rapidly conjugate the activated β -alanine and biogenic amines. The C-terminal amine selecting domain in Ebony is not homologous to any other protein with known domains, indicating a specific structural selection of the biogenic amine substrates (Hartwig et al. 2014). *ebony* is expressed in epithelial cells during cuticle sclerotization. In the visual system of *D. melanogaster*, *ebony* expression is localized in neural tissues, exclusively the neuropile and epithelial glial cells (Richardt et al. 2002, 2003). Its expression can be detected also in many regions of the brain and ventral nervous system from both larval and adult stages (Suh and Jackson 2007). In photoreception, it is thought that Ebony is regulating the neurotransmitter through the inactivation of histamine by *N*- β -alanylation (Richardt et al. 2002, 2003).

The involvement of Ebony in cuticle hardening is supported by a tradeoff relationship between the amount of NBAD and cuticle hardness, as showed in an analysis of the German cockroach, *Blattella germanica* (Czapla et al. 1990). This relationship is also demonstrated in the *black* mutant or *ADC* knockdown of *T. castaneum* such that the decreased amount of NBAD correlates with lowered levels of cross-links in the elytral cuticle (see Sect. 6.2.3; Arakane et al. 2009). A biochemical characterization of the *ebony* mutant was performed by demonstrating the incorporation of isotopically labeled β -alanine or dopamine into the pupal case or by examining the use of sources for NBAD synthesis, including β -alanine, dopamine and uracil, during cuticle formation (Jacobs 1968; Hodgetts 1972; Hodgetts and Konopka 1973; Hodgetts and Choi 1974). In both the *ebony* mutant of *D. melanogaster* and a melanotic body color mutant of the medfly, *Ceratitis capitata*, it was postulated that a defective NBAD synthase is responsible for the low level of NBAD and conversely high level of dopamine leading to a darker coloration (Wright 1987; Wappner et al. 1996). By using an *in vitro* cell free system of tissue homogenate from *C. capitata*, the enzyme activities of Ebony were directly characterized. Endogenous substrates like dopamine, norepinephrine and L-tyrosine were β -alanylated by tissue extracts from wild-type individuals, but the extract from the mutant exhibited only negligible levels of β -alanylation of these substrates (Perez et al. 2002). No *N*- β -alanyldopa was synthesized, which is consistent with the absence of *N*- β -alanyldopa in insect cuticle. It was reported in studies of *Sarcophaga* species that *N*- β -alanyl-tyrosine (Sarcophagine) and a derivative of *N*- β -alanyldopa, *N*- β -alanyl-5-S-glutathionyl-3-4-dihydroxyphenylalanine (5-S-GAD), have antibacterial activities (Leem et al. 1996; Meylaers et al. 2003). NBAD itself has an antibacterial activity comparable in strength to those of *N*- β -alanyldopa and 5-S-GAD (Schachter et al. 2007). The NBAD levels were increased in the hemolymph of the mealworm beetle, *Tenebrio molitor*, after bacterial challenges (Kim et al. 2000). Furthermore, NBAD synthase activity was detected in the integument of bacteria-injected *T. molitor* larvae (Schachter et al. 2007). In *C. capitata*, expression of *ebony* was induced in epidermal cells in response to bacterial challenges. After a bacterial challenge, an allele of the *ebony* mutant (*e¹¹*) with a cuticle deficiency (Lindsley and Grell 1968) showed susceptibility to *Serratia* infection via oral

administration (Flyg and Boman 1988). These observations imply a direct involvement of NBAD in defense reactions or probably in protection by a mechanically strong cuticle that is stabilized by protein cross-links involving NBAD.

Like other genes involved in pigmentation, insect body color pattern is associated with the pattern of *ebony* expression. NBAD is also important for production of papiliochromes that are yellowish-reddish-brownish pigments composed of NBAD and kynurenines in Papilionidae butterflies (Umebachi 1990). In larvae of *P. xuthus*, *ebony* is expressed in the epithelial cells underneath those cuticle regions that have a reddish-brown coloration (Futahashi and Fujiwara 2005). Expression of *ebony* is observed in red and yellow regions of the wings of *P. polytes* (Nishikawa et al. 2013). In Drosophilid species, high levels of *ebony* expression are linked to low levels of pigmentation in the thoracic trident or abdomen (Wittkopp et al. 2002a, 2009; Pool and Aquadro 2007; Takahashi et al. 2007). The same correlation was observed with the colors of butterfly wings (Ferguson et al. 2011b). In *B. mori sooty* mutants with a dark body color, *ebony* was identified as the responsible gene (Futahashi et al. 2008b). Recently, Ebony was utilized as a visible marker gene for genotyping of transgenic insects. Ubiquitous expression of *ebony* via the Gal4/UAS system in *B. mori* caused a light pigmentation in the larval body or adult antennae (Osanai-Futahashi et al. 2012a).

6.2.6 NBAD Hydrolase (*Tan*)

NBAD hydrolase (*Tan*) is a product of the *tan* gene and it shows high sequence similarity to fungal isopenicillin *N*-acyltransferase (IAT; True et al. 2005), which is involved in penicillin-G biosynthesis (Queener and Neuss 1982; Barredo et al. 1989). Like IAT, *Tan* appears to be expressed as a precursor protein that is activated by self-processing into two polypeptide subunits at a conserved Gly-Cys motif (e.g. Gly₁₂₁-Cys₁₂₂ in DmTan; Wagner et al. 2007; Aust et al. 2010; Perez et al. 2011). One of the essential roles of *Tan* activity is the hydrolysis of β -alanylhistamine (carcinine) in the visual system (True et al. 2005; Wagner et al. 2007; Perez et al. 2011). In *D. melanogaster*, DmTH is localized in photoreceptor cells where it hydrolyzes carcinine to histamine for neurotransmission with the former metabolite provided by NBAD synthase (Ebony) localized in the surrounding glial cells (Richardt et al. 2002).

In insect epidermal cells, *Tan* hydrolyzes NBAD to form dopamine and β -alanine, which is a reverse reaction of NABD synthesis catalyzed by Ebony (Fig. 6.2; Wittkopp et al. 2002a; Wright 1987; True et al. 2005). A functional importance of *tan* in cuticle pigmentation has been reported for a few insect species including *D. melanogaster*, *B. mori* and *P. xuthus*. Disruption of the *tan* gene by mutation or *P*-element insertion caused pigmentation defects in thoracic and abdominal cuticles in adult *D. melanogaster* (True et al. 2005; Jeong et al. 2008), and ectopic expression of *tan* rescued the pigmentation phenotypes in the *tan* mutant (True et al. 2005). In addition, Jeong et al. (2008) reported that expression of both *tan* and *dopachrome*

conversion enzyme (yellow, see Sect. 6.2.8) genes correlated with a diversity of body pigmentation patterns between *D. yakuba* and *D. santomea*. In the latter, the loss of abdominal pigmentation involves little or no *tan* and *yellow* gene expression.

In *P. xuthus* and *B. mori*, expression of *tan* along with *laccase 2* (see Sect. 6.2.7) is strongly correlated with larval black markings/pigments (Futahashi et al. 2010). For example, the *tan* transcript was clearly detected in the black region of the eyespot marking of *P. xuthus* larvae, but it was absent in the reddish-brown region of this marking. In the *B. mori rouge* (*ro*) mutant, the larval black markings are light brown. In this mutant, the *tan* cDNA lacks exon 2, resulting in a premature stop codon insertion. The predicted Tan protein is missing a large portion including a conserved self-processing site, suggesting that *tan* is responsible for the larval body color phenotype in the *ro* strain (Futahashi et al. 2010). Taken together, these results suggest that Tan plays a role in cuticle pigmentation through hydrolysis of NBAD to provide dopamine, which is a major precursor for melanin production. Tan may also be critical for the cuticle's mechanical properties because its activity influences the level of NBAD, which serves as a cuticle protein cross-linking agent. Further study is required to confirm this hypothesis.

6.2.7 Laccase (*Lac*)

Since the first description of laccase from the Japanese lacquer tree, *Rhus vernicifera* (Yoshida 1883), this enzyme has been extensively studied, and now there is a large accumulation of knowledge about its enzymatic properties, gene function and structure (Nakamura and Go 2005; Sharma et al. 2007). Proteins like laccase, ascorbate oxidase or the bacterial proteins, CueO or CumA, have a common feature in that these proteins are composed of three repeats of cupredoxin domains. They form a sub-protein group of three domain multicopper oxidases (3dMCO). In insects, laccase is regarded as one of the key enzymes for cuticle sclerotization and pigmentation. The roles of laccase are thought to be dependent on its enzyme activity to oxidize *ortho*-diphenols to the corresponding quinones. Since the first characterization of laccase-like activity in *Drosophila virilis* (Ohnishi 1954; Yamazaki 1969), laccase-like proteins were partially purified from the integument from several insect species (Yamazaki 1972; Andersen 1978; Barrett and Andersen 1981; Barrett 1987a, b; Thomas et al. 1989). Until the end of 1980s, the enzymatic properties of these proteins were characterized in some detail (Ashida and Yamazaki 1990; Barrett 1991; Dittmer and Kanost 2010). In 2004, the first cDNA sequences for laccase-like proteins from lepidopteran and dipteran species were reported (Dittmer et al. 2004). In this study, three genes, *laccase 1* and *laccase 2* from *M. sexta* (*MsLac1* and *MsLac2*) and *laccase 1* (*AgLac1*) of *An. gambiae* were identified. One characteristic of the insect laccase-like proteins is a methionine residue at the T1 copper center (Met716 of *MsLac1*, Met728 of *MsLac2* and Met948 of *AgLac1*), whereas in laccases from plants and fungi this residue position has a phenylalanine or leucine.

Other characteristics of the insect laccase-like proteins are the N-terminal extensions that include an N-terminal signal peptide and a cysteine-rich region in all three of the proteins. By using the efficient RNAi system of *T. castaneum*, loss of function phenotypes were analyzed. dsRNA for *laccase 2* (*TcLac2*) was injected into the hemocoel of individuals at various stages. After ecdysis to larva, pupa and adult, the new cuticles of the dsRNA-injected individuals were untanned. Also in the adult, a severe wing deformation was also observed (Arakane et al. 2005).

By the early 1990s, three types of phenol-oxidizing enzymes had been found in insect cuticle. They were designated as a tyrosinase-type phenoloxidase, laccase-type phenoloxidase (or laccase) and granular phenoloxidase. There had been a long discussion on the roles and classification of these cuticular enzymes (Ashida and Yamazaki 1990; Barrett 1991). Since they all have activity to oxidize *o*-diphenols, their involvement in cuticle pigmentation and hardening during development has been one of the important areas of investigation in insect cuticle physiology. It was shown that tyrosinase-type phenoloxidase is synthesized in the hemocytes, then secreted into the hemolymph, and finally transported into the cuticle (Ashida and Brey 1995; Asano and Ashida 2001). Granular-PO (GPO) was originally purified from granules in the larval cuticle of *M. sexta* by using a preparative electrophoretic gel in the presence of sodium dodecyl sulfate (see Sect. 6.4; Hiruma and Riddiford 1988). As observed in several other insect species, cuticular melanin was developed within premelanin granules deposited into the outer procuticle (Kayser-Wegmann 1976; Curtis et al. 1984). The GPO is thought to be responsible for production of melanin in such structures, but the gene for the granular enzyme has not been identified. To show the involvement of proPOs and laccase-like MCOs in cuticle formation during development, the phenotypes resulting from knockdown of these genes by RNAi were compared in *T. castaneum* (Arakane et al. 2005). dsRNAs for *proPO* genes (both of *TcTyr1* and *TcTyr2*), *laccase 1* (*TcLac1*) and *TcLac2* were injected. In contrast to the result that knockdown of *TcLac2* induced severe defects in pigmentation and abnormal adult shapes, no visible phenotypes were observed when *TcTyr1*, *TcTyr2* and *TcLac1* were knocked down. This result strongly suggests that the gene for the tyrosinase-type protein, proPO, is not involved in the process of cuticle pigmentation and hardening during development.

Since the study of *laccase 2* in *T. castaneum*, the RNAi method has been adopted for use in other species from multiple orders to study the involvement of *laccase 2* genes in cuticle formation (Niu et al. 2008; Elias-Neto et al. 2010; Futahashi et al. 2010; Ye et al. 2015). In all cases, pigmentation was suppressed. In several cases, the cuticle showed an abnormal shape and became mechanically weak (Arakane et al. 2005; Ye et al. 2015). RNAi for *TcLac2* also reduced egg hatching rates at low humidity, demonstrating that the enzyme is crucial for sclerotization of the serosal cuticle and for embryonic desiccation resistance (Jacobs et al. 2015). In the larval integument of *B. mori*, the spatial patterns of *BmLac2* expression exhibit a close correlation with those of pigmentation. The genes for substrate synthesis (*TH*, *DDC*, *tan* and *ebony* in Fig. 6.1) are also expressed strongly in the areas of black and reddish pigmentation (Futahashi and Fujiwara 2005, 2007; Futahashi et al. 2010). In the RNAi study on *TcLac2* from *T. castaneum* (Arakane et al. 2005), the authors

also described its characteristic gene structure, indicating the formation of two splice variants, A- and B-type TcLac2. The protein products from the two variants have the same N-terminal 491 amino acids, but the remaining C-terminal portion is encoded by a distinct set of exons. The C-terminal variable region includes copper-binding sites that are indispensable for oxygen binding inside the active center. It is assumed that the two isoforms have different enzymatic properties for versatility in functions. The presence of A-type and B-type isoforms is also found in *An. gambiae* (Gorman et al. 2008) and at least three variants are found in *D. melanogaster* (Flybase, <http://flybase.org/>; Asano et al. in preparation). Although it has not been proven experimentally, the gene structure of *BmLac2* implies that the A- and B-types can be produced by similar splicing patterns (Yatsu and Asano 2009). The expressions of A- and B-type variants were compared by PCR in *T. castaneum* and *An. gambiae*. In each case, the temporal peak of expression is slightly different between the two isoforms (Arakane et al. 2005; Gorman et al. 2008), indicating that each has a unique function related to a specific timing. The knockdown of each isoform in *T. castaneum* led to lethal phenotypes, but the deformation of the cuticle was more severe in the knockdown of the A-type isoform.

Amino acid sequence analysis was performed for a laccase-like enzyme that was purified from the newly ecdyzed pupae of *B. mori* (Yatsu and Asano 2009). The procedure for the purification was a modified version of the previous report by Yamazaki (1972). Like the previous study, trypsin was used for solubilization of laccase activity. Since laccase is attached to the cuticle matrix very tightly, proteases or denaturing reagents are needed to break down the cuticle structure anchoring the laccase protein. The purity was increased from three bands in the previous study to only a single band (70 kDa) by analysis with SDS-PAGE. The N-terminal sequence of the purified enzyme was NPALS that corresponds to Asn147-Ser151 of the full-length putative polypeptide deduced from the cDNA sequence of *BmLac2* (Fig. 6.4). The mass spectrometric identification of tryptic fragments from the purified enzyme (trypsin-solubilized *B. mori* laccase 2, Bm-tLac2) failed to identify peptides corresponding to 146 amino acids from the N-terminal methionine, suggesting that the purified enzyme had lost the N-terminal portion during treatment with trypsin. A similar result was reported in the analysis Lac2 from *M. sexta*. The full-length and N-terminally truncated ($\Delta 106$) recombinant proteins exhibit similar catalytic parameters when NADA is used as substrate, indicating that the presence of the N-terminal portion does not have a significant influence on the enzymatic activity (Dittmer et al. 2009). After these studies, the molecular properties of the recombinant laccase 2 proteins of *T. castaneum* and *An. gambiae* were determined (Gorman et al. 2012). They exhibit the same pattern of *K_m* values with dopamine and NADA being the more preferred substrates than DOPA and NBAD, respectively. The pH optima of enzyme activities are also weakly acidic and the A-type isoforms exhibit higher pH optima for DOPA and dopamine than the B-type isoforms. The four recombinant proteins show similar kinetic parameters, but a notable difference was seen in the case of TcLac2B with its *k_{cat}* values much larger than the values determined for TcLac2A. The variation in pH optima and substrate preference in the two isoforms may reflect the environment in which each isoform is localized.

Insect MCO proteins

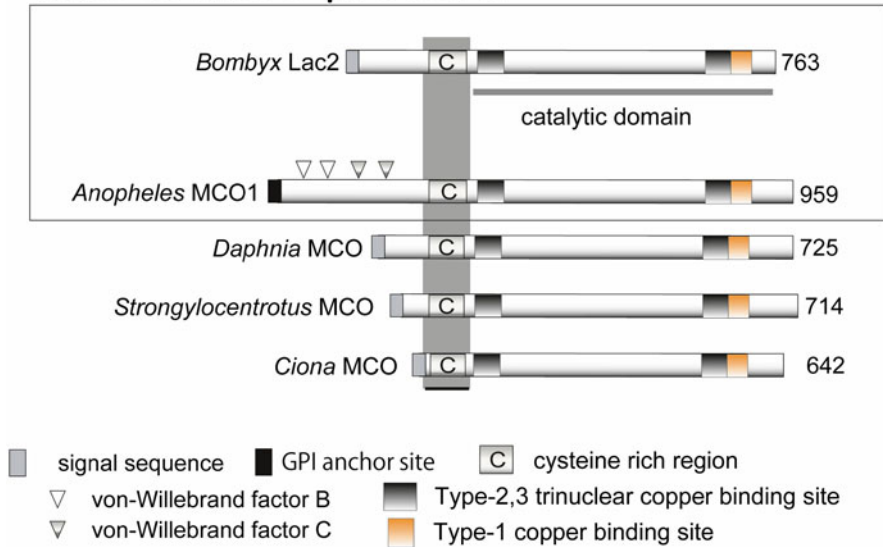


Fig. 6.4 Schematic domain structures of 3dMCOs from invertebrates. Two proteins from insects and three proteins from other invertebrate species are shown. Structural characteristics are highlighted including the signal sequence, catalytic domain, cysteine-rich region, GPI anchor site, von-Willebrand factor domains and copper-binding sites. Numbers indicate length of proteins (in numbers of amino acids)

Since the early studies, there have been observations that imply an active regulation of laccase function during the process of cuticle construction in *D. virillis* (Yamazaki 1969) and the Australian sheep blowfly, *Lucilia cuprina* (Barrett 1987b). In *B. mori*, little laccase activity was detected in the cuticle of newly ecdysed pupa, but the activity increased to a maximum at 4 h after pupal ecdysis (Yamazaki 1972). A similar result was obtained by *in situ* staining of the pupal cuticle with dopamine (Yatsu and Asano 2009). It had been suggested that laccase is synthesized as an inactive precursor and accumulates in the pupal cuticle before ecdysis. After pupal ecdysis, the precursor may be activated through processing or interactions with other molecule(s). A precursor-like protein was extracted from the cuticle of newly ecdysed pupae of *B. mori* by treatment with α -chymotrypsin. When examined by activity staining after native PAGE, only a faint activity band was detected, but after *in vitro* treatment with trypsin, an increased activity was detected (Ashida and Yamazaki 1990; Asano et al. 2014). The purified α -chymotrypsin-solubilized BmLac2 (Bm-cLac2) protein was shown to be an active enzyme, but the specific activity was increased 17-fold after treatment with trypsin. During that treatment, peptide bonds in the C-terminal region (Lys677-Gln678 and Arg674-His675) were cleaved. Although it is not an inactive precursor, Bm-cLac2 appears to preserve the character of the hypothetical inactive-precursor in that it has the potential to become

substantially more active. For the precise control of a successful completion of the entire ecdysial process, it is reasonable to utilize multiple systems to regulate laccase 2 activity. It is hypothesized that laccase 2 can become a much more active enzyme by some activating factors through proteolytic processing or other modes of interactions (Asano et al. 2014).

6.2.8 Dopachrome Conversion Enzyme (Yellow)

The *yellow* gene, which was named for a yellowish body color in a loss of function phenotype of *D. melanogaster* (Nash and Yarkin 1974), appears to be one of the most rapidly evolving gene families that generates functionally diverse paralogs. This family includes the major royal jelly proteins (MRJPs) of the honeybee, *Apis mellifera*, which are the most abundant proteins found in royal jelly (Schmitzova et al. 1998; Albert and Klaudiny 2004). The *yellow* genes encoding MRJPs and MRJP-like (MRJPL) proteins have been identified not only in honeybees but also in several other hymenopteran species. Those *MRJP* and *MRJPL* genes are generally arranged in a cluster (except for a single copy of *MRJPL* in some species) of closely linked genes, which is located between *yellow-e3* and *yellow-h* (most common gene order is *yellow-g*, *-g2*, *-e*, *-e3*, *MRJPs* or *MRJPLs*, *-h*) in their genomes (Ferguson et al. 2011a; Kupke et al. 2012; Buttstedt et al. 2014). Although the *MRJPs* or *MRJPLs* locus is highly conserved, recent studies including phylogenetic analysis suggest that the gene clades in *A. mellifera*, the jewel wasp, *Nasonia vitripennis*, and the Argentine ant, *Linepithema humile*, have independently evolved in their lineage (Fig. 6.5; Werren et al. 2010; Smith et al. 2011; Buttstedt et al. 2014). MRJP proteins were detected in a variety of tissues including brain, venom glands and larval hemolymph and in different developmental stages in *A. mellifera* (Kucharski et al. 1998; Schmitzova et al. 1998; Drapeau et al. 2006; Peiren et al. 2008; Randolt et al. 2008; Hojo et al. 2010), suggesting that MRJPs have other physiological functions in addition to a nutritional role due to their high content of essential amino acids (Table 6.3).

Yellow and *MRJP/MRJPL* comprise a gene family in insects. This gene family of the melanin pathway appears to be insect specific and deviates from the pathway common to other animals. The number of genes in insects, whose genomes are well characterized, is in the range of 10–26 in species such as *D. melanogaster* (Maleszka and Kucharski 2000; Drapeau 2001), *T. castaneum* (Arakane et al. 2010), *B. mori* (Xia et al. 2006), *P. xuthus* (Futahashi et al. 2012), *A. mellifera* (Drapeau et al. 2006) and *N. vitripennis* (Werren et al. 2010). The encoded Yellow and MRJP/MRJPL proteins have been divided into at least ten subgroups based on sequence similarity and phylogenetic analysis (Fig. 6.5; Ferguson et al. 2011a). Although a large number of *yellow* and *MRJP/MRJPL* genes has been identified in different insect species, the physiological function(s) of most of these genes has not yet been determined.

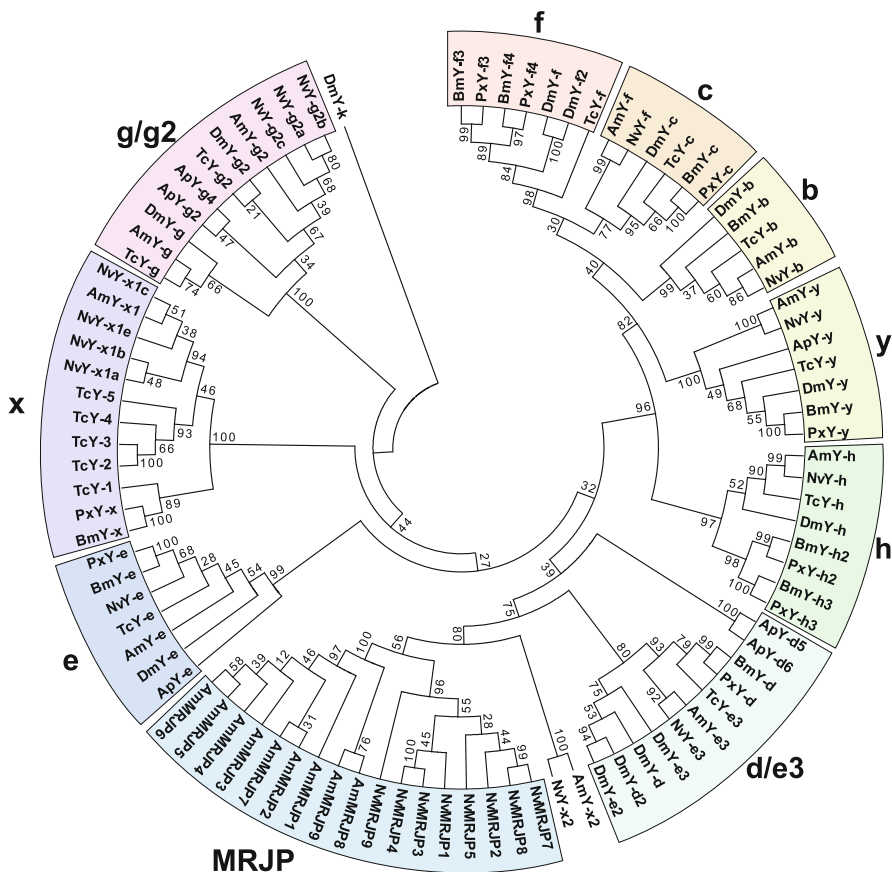


Fig. 6.5 Phylogenetic analysis of Yellow and Yellow-like proteins in insects. ClustalW software was used to perform multiple sequence alignments prior to phylogenetic tree analysis. The phylogenetic tree was constructed with MEGA 6.06 software using the Neighbor-Joining method (Tamura et al. 2013). Numbers by each branch indicate results of bootstrap analysis of 5000 replications. See Table 6.3 for the accession numbers of protein sequences used in this analysis

In the cuticle tanning pathway, a *yellow* gene encodes dopachrome conversion enzyme (DCE) that converts dopachrome and dopaminechrome to dihydroxyindole (DHI) and 5,6-dihydroxyindole-2-carboxylic acid (DHICA), respectively, during melanin biosynthesis (Fig. 6.2). DCE accelerates melanin synthesis in insects such as *D. melanogaster*, *B. mori*, *P. xuthus* and *T. castaneum* (Wittkopp et al. 2002b; Futahashi and Fujiwara 2007; Futahashi et al. 2008a; Arakane et al. 2010; Ito et al. 2010). The Yellow protein is critical for cuticle pigmentation in several species. In *D. melanogaster*, for instance, *yellow* (*DmY-y*) is required for black melanin production, because mutation of *DmY-y* leads to the light brown/yellowish cuticle and localization of *DmY-y* protein is correlated with black pigmentation patterns in adult cuticle (Wittkopp et al. 2002a, b, 2003a, 2009; Gompel et al. 2005). Riedel

Table 6.3 Accession numbers of insect Yellow and Yellow-like proteins used for phylogenetic analysis

Species	Abbreviation	Protein	Accession number
<i>Tribolium castaneum</i>	TcY-b	Yellow-b	ACY71055
	TcY-c	Yellow-c	ACY71056
	TcY-e	Yellow-e	ACY71058
	TcY-e3	Yellow-e3	ACY71057
	TcY-f	Yellow-f	ACY71059
	TcY-g	Yellow-g	ACY71060
	TcY-g2	Yellow-g2	ACY71061
	TcY-h	Yellow-h	ACY71062
	TcY-y	Yellow-y	ACY71063
	TcY-1	Yellow-1	ACY71064
	TcY-2	Yellow-2	ACY71065
	TcY-3	Yellow-3	ACY71066
	TcY-4	Yellow-4	ACY71067
TcY-5	Yellow-5	ACY71068	
<i>Drosophila melanogaster</i>	DmY-b	Yellow-b	NP_523586
	DmY-c	Yellow-c	NP_523570
	DmY-d	Yellow-d	NP_523820
	DmY-d2	Yellow-d2	NP_611788
	DmY-e2	Yellow-e2	NP_650289
	DmY-e3	Yellow-e3	NP_650288
	DmY-e	Yellow-e	NP_524344
	DmY-f	Yellow-f	NP_524335
	DmY-f2	Yellow-f2	NP_650247
	DmY-g	Yellow-g	NP_523888
	DmY-g2	Yellow-g2	NP_647710
	DmY-h	Yellow-h	NP_651912
	DmY-y	Yellow-y	NP_476792
DmY-k	Yellow-k	NP_648772	
<i>Bombyx mori</i>	BmY-b	Yellow-b	BGIBMGA014224-TA
	BmY-c	Yellow-c	ABC96696
	BmY-d	Yellow-d	ABC96694
	BmY-e	Yellow-e	BAI39592
	BmY-f3	Yellow-f3	NP_001037424
	BmY-f4	Yellow-f4	NP_001037428
	BmY-h2	Yellow-h2	BGIBMGA007255-TA
	BmY-h3	Yellow-h3	BGIBMGA007256-TA
	BmY-y	Yellow-y	BAH11146
BmY-x	Yellow-x	NP_001037430	

(continued)

Table 6.3 (continued)

Species	Abbreviation	Protein	Accession number
<i>Papilio xuthus</i>	PxY-c	Yellow-c	BAM18241
	PxY-d	Yellow-d	BAM18620
	PxY-e	Yellow-e	BAM17806
	PxY-f3	Yellow-f3	BAM18870
	PxY-f4	Yellow-f4	BAM18225
	PxY-h2	Yellow-h2	BAM17969
	PxY-h3	Yellow-h3	BAM17970
	PxY-y	Yellow-y	BAF73474
	PxY-x	Yellow-x	BAM18176
<i>Apis mellifera</i>	AmY-b	Yellow-b	XP_006569902
	AmY-e3	Yellow-e3	ABB82366
	AmY-e	Yellow-e	XP_003249426
	AmY-f	Yellow-f	NP_001011635
	AmY-g	Yellow-g	XP_396824
	AmY-g2	Yellow-g2	XP_006559006
	AmY-h	Yellow-h	ABB81847
	AmY-y	Yellow-y	NP_001091693
	AmY-x1	Yellow-x1	XP_006565008
	AmY-x2	Yellow-x2	XP_001122824
	AmMRJP1	Major Royal Jelly Protein (MRJP) 1	NP_001011579
	AmMRJP2	MRJP2	NP_001011580
	AmMRJP3	MRJP3	NP_001011601
	AmMRJP4	MRJP4	NP_001011610
	AmMRJP5	MRJP5	NP_001011599
	AmMRJP6	MRJP6	NP_001011622
	AmMRJP7	MRJP7	NP_001014429
AmMRJP8	MRJP8	NP_001011564	
AmMRJP9	MRJP9	NP_001019868	

(continued)

Table 6.3 (continued)

Species	Abbreviation	Protein	Accession number
<i>Nasonia vitripennis</i>	NvY-b	Yellow-b	NP_001154989
	NvY-e3	Yellow-e3	NP_001154982
	NvY-e	Yellow-e	NP_001154985
	NvY-f	Yellow-f	NP_001154968
	NvY-g2a	Yellow-g2a	XP_001603544
	NvY-g2b	Yellow-g2b	NP_001154986
	NvY-g2c	Yellow-g2c	XP_001603573
	NvY-h	Yellow-h	NP_001153394
	NvY-y	Yellow-y	NP_001154977
	NvY-x1a	Yellow-x1a	XP_001601771
	NvY-x1b	Yellow-x1b	NP_001155026
	NvY-x1c	Yellow-x1c	NP_001154990
	NvY-x1e	Yellow-x1e	XP_001607252
	NvY-x2	Yellow-x2	XP_001601022
	NvMRJP1	MRJP1	XP_001603404
	NvMRJP2	MRJP2	NP_001155025
	NvMRJP3	MRJP3	NP_001154981
	NvMRJP4	MRJP4	NP_001154980
	NvMRJP5	MRJP5	NP_001154979
NvMRJP7	MRJP7	NP_001154975	
NvMRJP8	MRJP8	NP_001154974	
NvMRJP9	MRJP9	NP_001154978	
<i>Acyrtosiphon pisum</i>	ApY-d5	Yellow-d5	XP_001942700
	ApY-d6	Yellow-d6	XP_001942648
	ApY-e	Yellow-e	XP_001948479
	ApY-g2	Yellow-g2	XP_001945004
	ApY-g4	Yellow-g4	XP_001944949
	ApY-y	Yellow-y	NP_001165848

et al. (2011) demonstrated that overexpression of *DmY-y* altered coloration of the adult wing cuticle from brown to black. In addition, the multi-ligand endocytic receptor Megalin (*Mgl*) plays a role in promoting internalization/endocytosis of *DmY-y*. Loss of function of *Mgl* caused excess *DmY-y*, resulting in a black pigmented wing similar to that seen in the adult in which *DmY-y* is overexpressed. This result suggests that, in addition to the spatial expression, *DmY-y* function is regulated by a cellular process such as an endocytosis for cuticle coloration of *D. melanogaster*. Further studies are needed to know whether this is the case in other insect species.

Like *DmY-y*, *Yellow* is also important for body pigmentation in lepidopteran species. Expression of *yellow* in the swallowtail species *P. xuthus* (*PxY-y*), *P. machaon* (*PmY-y*) and *P. polytes* (*PpY-y*) is correlated with black body markings of their larval cuticles (Futahashi and Fujiwara 2007; Futahashi et al. 2010; Shirataki et al. 2010). Futahashi et al. (2012) utilized microarray analysis to screen for marking-

specific genes using six markings at 11 different stages of *P. xuthus* larvae and all of the *yellow* gene family members were identified except for *yellow-b*. Interestingly, *yellow-h3* (*PxY-h3*) exhibited an expression pattern of development very similar to that of *PxY-y*. In addition, *PxY-h3* was expressed in the black pigmented markings, indicating that, like *PxY-y*, it also is involved in marking-specific melanin synthesis in *P. xuthus*. In *B. mori*, *yellow-y* (*BmY-y*) and *yellow-e* (*BmY-e*) had been characterized as genes responsible for the body color mutants, *ch* (*chocolate*) and *bts* (brown head and tail spot), respectively (Futahashi et al. 2008b; Ito et al. 2010). The larval body color of the *ch* mutant strain is a reddish brown instead of a normal black color, whereas the *bts* mutant strain exhibited a reddish brown larval head and anal plates instead of the white coloration found in the wild-type strain. These results suggested that both *BmY-y* and *BmY-e* play critical roles in larval pigmentation of *B. mori*.

In *T. castaneum*, 14 *yellow* genes have been identified and their different expression patterns indicated that *yellow* genes have diverse functions (Arakane et al. 2010). Functional importance of *yellow* in cuticle pigmentation has been identified in several insect species as described above. Interestingly, knockdown of the *yellow* (*TcY-y*) by RNAi had no effect on body pigmentation in the larva, pupa and adult except for black pigmentation in the pterostigma of the hindwing (Fig. 6.2g; Arakane et al. 2010), suggesting that *TcY-y* is not critical for *T. castaneum* body wall cuticle pigmentation. *Yellow-f* (*DmY-f*) and *-f2* (*DmY-f2*) in *D. melanogaster* showed a DCE activity required for melanin synthesis (Han et al. 2002). However, unlike *PxY-y* and *PxY-h3*, *yellow-f3* (*PxY-f3*) and *-f4* (*PxY-f4*), which are homologs of *DmY-f/-f2* in *P. xuthus*, were not up-regulated in the larval black markings (Futahashi et al. 2012). RNAi for *T. castaneum* homolog of *DmY-f/-f2* (*TcY-f*) had no effect on body pigmentation of the larva, pupa and pharate adult. The resulting pharate adults, however, were unable to shed their exuviae and died entrapped in their old pupal cuticle (Arakane et al. 2010). These results suggested that *Yellow-f*-related genes might have other functions in addition to melanin production in *P. xuthus* and *T. castaneum*.

Recently, a novel anti-dehydration function of *yellow-e* (*TcY-e*) in *T. castaneum* has been reported (Noh et al. 2015a). RNAi for *TcY-e* had no effect on larval, pupal and pharate adult cuticle pigmentation. However, the resulting adults died shortly after eclosion due to dehydration, and the lethality was prevented by high humidity. The body color of the high humidity-rescued adults, like that observed in the *B. mori* *bts* mutant, was significantly darker than that of control adults (Fig. 6.2f), suggesting that *TcY-e* plays a role not only in body pigmentation but also has a vital waterproofing function in *T. castaneum* adults. In contrast to loss of function of *yellow*, which causes a lighter body color in many insect species, depletion of *yellow-e* function results in a darker body pigmentation in both *B. mori* and *T. castaneum*. The most prominent function of the *yellow* gene is in the production of black pigment in a variety of insects. However, the function of the other members of the family is largely obscure. Further study is required to understand the function of the *yellow* paralogs across different insect species including the molecular mechanisms for the cause of the dark body pigmentation in *yellow-e* deficient insects.

6.2.9 Structural Cuticle Proteins (CPs)

In arthropods, structural cuticular proteins (CPs) play important roles in determining the diverse physical properties of the cuticle depending on developmental stages as well as different body regions as a result of interactions with other CPs and the structural biopolymer chitin (Neville 1993). Recent studies and the availability of fully sequenced and annotated genomes of several insect species such as *A. mellifera* (Honeybee Genome Sequencing Consortium. 2006), *D. melanogaster* (Karouzou et al. 2007), *T. castaneum* (Dittmer et al. 2012; *Tribolium* Genome Sequencing Consortium. 2008), *An. gambiae* (Cornman et al. 2008), *B. mori* (Futahashi et al. 2008a) and *N. vitripennis* (Werren et al. 2010) indicate that there are large numbers of genes encoding CP-like proteins in their genomes (see Chap. 1 in this book for details about CPs). Indeed, more than 200 putative CP genes have been identified in *D. melanogaster* and *An. gambiae* (Ioannidou et al. 2014), and these genes comprise ~2% of the predicted protein-coding genes in the latter species.

CPs have been classified into thirteen distinct families as defined by unique amino acid sequence motifs characteristic of each of these families (Willis 2010; Willis et al. 2012; Ioannidou et al. 2014). The largest cuticular protein family is the CPR family whose members contain a conserved amino acid sequence known as the Rebers & Riddiford (R&R) consensus motif (Rebers and Riddiford 1988). The R&R motif contains a chitin-binding domain (chitin-bind-4 domain, PF00379 in the Pfam database) that apparently helps to coordinate the interactions between chitin fibers and the proteinaceous matrix (Rebers and Willis 2001; Togawa et al. 2004, 2007; Qin et al. 2009). CPR proteins containing the RR-1 motif have been found primarily in soft and flexible cuticle, whereas the proteins containing the RR-2 motif have been found mostly in hard and rigid cuticle. The third class of CPR proteins, RR-3, has been identified in only a few insect species and is a very minor group whose distinguishable features have not yet been well defined (Andersen 2000).

During cuticle tanning, some of CPs are cross-linked by quinones and/or quinone methides produced by laccase 2-mediated oxidation of *N*-acylcatechols (Hopkins and Kramer 1992; Arakane et al. 2005; Andersen 2008; Mun et al. 2015). This vital process together with dehydration occurs during each stage of development and the expression of specific CPs appears to be required for formation of diverse cuticles in different regions of the insect's body and at different developmental stages so that an appropriate combination of physical and morphological features can provide structural support, mechanical protection and mobility. However, little is known about the functional importance of individual insect CPs in the morphogenesis and mechanical properties of the cuticle.

Four major CPs, TcCPR27, TcCPR18, TcCPR4 and TcCP30, were identified in protein extracts of elytra from *T. castaneum* adults (Arakane et al. 2012; Dittmer et al. 2012; Mun et al. 2015; Noh et al. 2015b). All of these CPs are abundant in rigid cuticles including the dorsal elytron, pronotum, ventral abdomen and leg,

while they are absent or very minor in soft and flexible cuticles such as the ventral elytron, hindwing and dorsal abdomen of the adult. TcCPR27 and TcCPR18 are members of the RR-2 group of the CPR family, and are localized in both the chitinous horizontal laminae and vertical pore canals in the procuticle of rigid adult cuticle (Noh et al. 2014). RNAi for *TcCPR27* or *TcCPR18* genes caused a disorganized laminar architecture and amorphous pore canal fibers (PCFs), which led to short, wrinkled and weakened elytra (Arakane et al. 2012; Noh et al. 2014). TcCPR4, which is more highly extractable from the elytra of TcCPR27-deficient adults than are other CPs, contains an RR-1 motif (Noh et al. 2015b). TEM immunogold labeling revealed that the TcCPR4 protein is predominantly localized in the pore canals and in the vicinity of the apical plasma membrane protrusions of the procuticle. However, depletion of TcCPR27 caused mislocalization of TcCPR4. In the TcCPR27-deficient elytra, the TcCPR4 protein was distributed over the entire procuticle including the horizontal laminae, suggesting that the presence of TcCPR27 protein is critical for the specific localization of TcCPR4 protein. Loss of function of *TcCPR4* produced by RNAi caused an abnormal shape of the pore canals with amorphous PCFs in their lumen, indicating that TcCPR4 is important for determining the morphology and ultrastructure of PCFs and pore canals in rigid cuticle.

Unlike TcCPR27, TcCPR18 and TcCPR4, the mature TcCP30 protein has a low complexity amino acid sequence with a rather unique amino acid composition (36% Glu, 21% His, 19% Arg and 16% Gly), and lacks an R&R consensus motif (Mun et al. 2015). The function of TcCP30 is critical for adult eclosion of *T. castaneum* probably because it undergoes cross-linking during cuticle maturation. Western blotting analysis of protein extracts from the elytra and pronotum revealed that TcCP30 becomes cross-linked to TcCPR27 and TcCPR18, but not to TcCPR4, by the action of laccase 2 (Mun et al. 2015). Because TcCP30, TcCPR27 and TcCPR18 have a high histidine content (10–21%), whereas TcCPR4 has a relatively low content (3%), this result appears to be consistent with the hypothesis that histidine residues of CPs most likely participate in quinone- and/or quinone methide-mediated CP cross-linking (Kramer et al. 2001). All of these results indicate that the unique localization and cross-linking of specific CPs are important for morphology and ultrastructure of the exoskeleton (Fig. 6.6). Genes encoding CPs comprise one of the largest families of insect genes so that future studies of the functional importance in cuticle morphogenesis of many other CPs, particularly ones belonging to different subfamilies, is of great interest.

6.3 Interactions and Functions of Pigments in Insect Ecology

The surfaces of insects show various types of colorations, which include structural colors and colors with versatile pigments. The structural colors are the results of optical effects by fine structures of cuticle surfaces (Seago et al. 2009). In addition, insect cuticles contain various types of substances that are responsible for

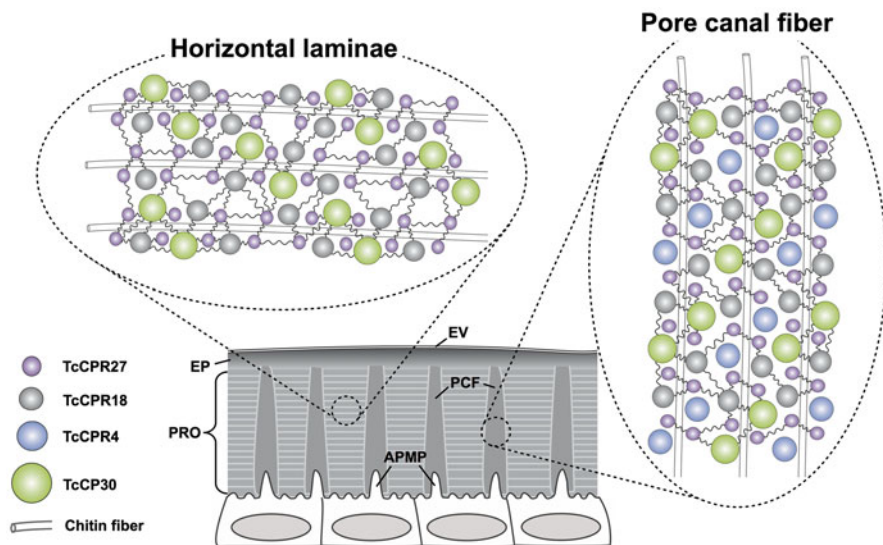


Fig. 6.6 Proposed cuticular proteins cross-linking in rigid cuticle of *T. castaneum*. Rigid adult cuticle is composed of three functional layers, envelope (EV), epicuticle (EP) and procuticle (PRO) in the 5 days-old adult of *T. castaneum*. Chitin and cuticular proteins are major components of a large number of horizontal laminae and vertical pore canal fibers in the procuticle. Major cuticular proteins, TcCPR27, TcCPR18 and TcCP30, are localized in both laminae and pore canal fibers, whereas TcCPR4 is predominantly localized in pore canal fibers (Mun et al. 2015; Noh et al. 2014, 2015b). TcCP30 undergoes cross-linking with TcCPR27 and TcCPR18, but not to TcCPR4 in rigid cuticle (Mun et al. 2015). Pigments are primarily localized in the procuticle

characteristic colors. Sometimes, there are correlations between color (pigment) patterns and the local shape of cuticle. For example, the *Junonia* butterfly wing eyespot pattern correlates with the thickness pattern of the underlying cuticle (Taira and Otaki 2016). With pigments, insects can create a variety of body color patterns that contribute to increased survival rates through camouflage, warning or mimicry and to accelerated sexual selection. The biological significance of body colors produced through tyrosine metabolism has been investigated as one major research area in many insect species. This section focuses mainly on the changes in the extent of melanization that are associated with environmental conditions.

During development, insects often change their body colors for better adaptation to the surroundings. As one example, the molecular mechanisms of body color transition are well described in *P. xuthus* (Futahashi and Fujiwara 2005, 2008). Until the fourth instar, the larvae show a pattern with white and brown colors that is thought to mimic the fecal material of birds. In contrast, during the molt to the fifth (last) instar, the pattern drastically changes to a greenish coloration that is cryptic for leaves. For this transition of body color pattern, the concentration of juvenile hormones (JH) is the critical factor (see Sect. 6.4). This transition in *P. xuthus* is an example of events that occur during the normal developmental process. Similarly, polyphenic phenotypes occur through changes in gene expressions that are regu-

lated by hormones (JH, ecdysteroid, peptidic factors) through modulations in the status of epigenetic modifications and metabolic pathways. The body color pattern is one polyphenic trait that can be modified by environmental cues. Locusts have two phases, a “solitaria phase” in low density of individuals and a “gregaria phase” under the opposite situation, each of which is characterized by a specific metabolism, behavior and body appearances. In the transition from solitary to gregarial phase, the greenish body is changed to blackish. By HPLC isolation and bioassay experiments with the albino mutant of *L. migratoria*, the peptide corazonin was identified from both *L. migratoria* and *S. gregaria* as the hormone that induces melanin synthesis (Tawfik et al. 1999; Tanaka 2000; Predel et al. 2007). Corazonin has an N-terminal pyroglutamate and C-terminal amidation, and the sequence is homologous to the human melanocyte-stimulating hormone α -MSH. Corazonins from the locust have a histidine residue at the seventh position instead of an arginine in corazonin from the cockroach, *P. americana*, and the peptide was identified as a heart-stimulating hormone in *P. americana* (Veenstra 1989, 1991). Corazonin induces not only melanogenesis, but also morphological changes (Tanaka et al. 2002; Maeno et al. 2004). It has been shown in *S. gregaria* that in a crowded situation, the signal of mechanoreception on the hind legs is transduced to the central nervous system (CNS). Then neuromodulation of the CNS leads to behavioral changes from solitary to the gregarious type. Either mechanoreception at the hind legs or a combination of sight and odor cues induce a pulse of serotonin in the metathoracic ganglion, and this is both necessary and sufficient for induction of behavioral changes for gregarization in *S. gregaria* (Simpson et al. 2011). The eggs laid by gregarious females have a tendency to be larger than those laid by solitary females and the proportion of “green hatching” from the larger eggs is lower (Tanaka and Maeno 2010).

Temperature appears to cause adaptive changes in the coloration pattern. The larval body of the five-spotted hawkmoth, *Manduca quinquemaculata*, shows two temperature-dependent phenotypes. Larvae developed at 20 °C have a blackened color, but those developed at 28 °C have a greenish color (Hudson 1966). The dark body color can be adaptive to obtain heat by absorbing sunlight in a low temperature condition, although the black coloration is thought to be in a trade-off relationship with the cryptic green color in leaves. In the related species, *M. sexta*, the *black* mutant shows similar characteristics. At normal temperature (20–28 °C) the body color is black, and low JH titer is responsible for this phenotype. In contrast, heat shock during the sensitive period in the fourth instar elevates the JH titer and suppresses *DDC* expression during the molt. The body color of the next instar is changed to green (Suzuki and Nijhout 2006). Such experiments to decipher the effect of temperature shifts have been performed since the nineteenth century. In many cases, a high-temperature shock induced phenotypes found in warm climates, and *vice versa* (Merrifield 1890, 1893). In a nymphalid butterfly, *Junonia orithya*, a cold shock during the pupal period shows polyphenic wing color patterns that are induced by a cold-shock hormone (Mahdi et al. 2010). Although such a correlation has been elusive, the cold-shocked individuals show an increase in dopamine content and a tendency to produce a darker phenotype. In *D. melanogaster*, growth

at a lower temperature induces a darker abdomen in adult females (David et al. 1990), which is associated with modulations of *TH* and *ebony* expressions (Gibert et al. 2007). This observation is consistent with the geographic distributions of darker variations (David et al. 1985; Gibert et al. 1996, 1998; Takahashi and Takano-Shimizu 2011; Telonis-Scott et al. 2011), indicating that this plasticity is an adaptive trait. The relationship between high latitudes (low temperature and weak sunlight) and darker body color has been reported in many cases (reviewed by True 2003; Rajpurohit and Nedved 2013; Takahashi 2013). The recent global warming trend has affected greatly the distribution of European insects (Zeuss et al. 2014). Based on the data obtained from a study of 473 European butterflies and dragonflies, it was found that dark and light colored insects are associated with cool and warm climates, respectively, and that the average darkness of the insects has decreased during the last century.

6.4 Hormonal Regulation of Cuticle Tanning

How does hormonal regulation lead to variations in pigmentation of the insect exoskeleton? Pigmentation development involves activating agents such as hormones that regulate the process, positioning agents that generate pigments in space and time, and the biochemical synthesis of pigments (Wittkopp and Beldade 2009). Genes in these steps are referred to as “regulating”, “patterning” and “effector” genes, respectively. Regulating genes modulate patterning genes that determine the distribution of pigments by directly or indirectly activating expression of effector genes that encode the enzymes and co-factors required for pigment biosynthesis.

There are two main classes of insect hormones, the hormones produced by epithelial glands belonging to the ecdysteroids and juvenile hormones (JH) and also the neuropeptide hormones produced by neurosecretory cells. A working hypothesis is that the pigment biochemical module is regulated primarily by ecdysteroids such as 20-hydroxyecdysone (20HE) and JH as well as transcription factors expressed in a marking-specific pattern. Neuropeptide hormones such as bursicon also play regulatory roles in pigment metabolism.

Cuticular pigmentation in *P. xuthus* is caused by exposure to ecdysteroid and its subsequent removal (Futahashi and Fujiwara 2007). For instance, the larval marking eyespot pigmentation and differences in pigmentation timing appear to be regulated by ecdysteroid-inducible transcription factors that modulate melanin-synthesis genes. In this species, stage-specific larval marking color patterns are determined by a two-phase melanin-related gene prepatterning process (Futahashi et al. 2010). Two secreted protein genes, *yellow-y* and *laccase 2*, correlated with the black markings are expressed in the middle of the molting period (phase 1). In contrast, five epidermal proteins genes, *TH*, *DDC*, *GTPCH1* (*GTP cyclohydrolase I*), *tan* and *ebony*, associated with black or reddish-brown markings are expressed in the latter half of the molting period (phase 2). In addition, topical application of ecdysteroids prevents the induction of *TH*, *DDC* and *ebony* expression as well as maintains

yellow expression in the later molting stage, suggesting that the genes expressed in phase 1 require a high ecdysteroid titer, whereas the expression of the genes in phase 2 are induced by 20HE removal. Similar spatial and temporal expression profiles of most corresponding genes are observed in two other *Papilio* species with two additional genes, *bilin-binding protein (BBP)* and a *yellow-related gene (YRG)*, whose combinations contribute larval blue, yellow and green colorations (Shirataki et al. 2010).

Two transcription factors, *spalt* and ecdysteroid signal-related *E75*, are genes expressed in the larval black eyespot markings in *Papilio* (Futahashi et al. 2012). The former expression correlated with the cryptic wing pattern (black marking) formation in several butterfly species, suggesting that it may be a positive regulator for melanin synthesis in both larvae and adult butterflies. The expression pattern of *E75* induced by ecdysteroids (Hiruma and Riddiford 2009) is correlated with the eyespot pigmentation pattern, which is similar to that of the *yellow* gene. In *M. sexta*, *DDC* expression is regulated by *E75* in response to exposure to ecdysteroids followed by its removal (Hiruma and Riddiford 1990, 2009). In *B. mori*, *tan* and *laccase 2* genes, which are also marking-specific (Futahashi et al. 2010), are apparently regulated by several ecdysteroid-inducible transcription factors including *ecdysone receptor*, *E75*, *hormone receptor 3* and *ftz transcription factor 1* (Hiruma and Riddiford 2009). These results suggested that *E75* is a strong candidate mediator of the hormone-dependent coordination of larval pigment pattern formation by regulating several black marking genes. Transcription factors such as *optomotor-blind (omb)* or *bric a brac (bab)* may also regulate patterning in insects (Wittkopp et al. 2003b). Color patterns in wings of butterflies are complex and may be the product of the co-option of developmental pathways, as exemplified by the eye development gene *optix*, which is correlated with wing patterns of *Heliconius* butterflies (Kronforst et al. 2012).

JH has been proposed to influence the expression pattern of 20HE-related genes (Riddiford 2008), and it induces the expression of genes associated with the mimetic pattern. In *P. xuthus*, a decrease in JH titer causes a switch to the cryptic pattern (Futahashi and Fujiwara 2008). Until the end of third instar larva, a high JH titer is maintained, but during the fourth instar larval stage, the titer declines. The low JH titer is the cause of the greenish cryptic pattern in the next instar, because injection of a JH analog (JH acid: JHA) at the early fourth instar larval stage suppresses the transition of body color pattern. With the injection of JHA, the spatial patterns of *TH* and *DDC* expressions in the cuticles of fourth instar larvae are maintained during the molt, and the mimicking brownish color pattern is maintained in the resulting fifth instar larvae. In addition to overall coloration, JH also regulates exoskeletal structures and pigment distribution at specific markings. In general, the hormonal condition and hormone sensitivity appear to be two of the main factors responsible for interspecific differences in larval color patterns in lepidopteran species such as the genus of *Papilio* (Shirataki et al. 2010).

The pupal color of the butterflies often shows dimorphic phenotypes, green and brown. The occurrence of the colors is dependent on the surrounding situations at the site for pupation. Optic signals from background color or tactile signals from the

surface of the pupation site (smooth or rough) have been studied as determinants for pupal colors (Hazel and West 1979; Hiraga 2005). Seasonal factors (photoperiod, temperature or humidity) can also have an influence on the pupal color determination (Hazel and West 1979, 1983; Sims and Shapiro 1984; Smith 1978, 1980). In the nymphalid butterfly, *Inachis io*, the browning of the pupa is controlled by the neuropeptide, pupal melanization-reducing factor (PMRF), that is released from the brain into hemolymph (Bückmann and Maisch 1987). In *P. xuthus*, the pupal color is controlled by pupal cuticle melanizing hormone (PCMH) and orange pupa inducing factor (OPIF; Yamanaka et al. 1999, 2004, 2006). Blackening of body color occurs in larvae of the armyworm, *P. separata*. In crowded conditions, “melanization and reddish coloration hormone” (MRCH) known for its FxPRL-amide structure at the C-terminus is released into the hemolymph to increase melanization of the cuticle. MRCH is homologous to the insulin-like growth factor (Matsumoto et al. 1981, 1986). In *P. separata* other physical stresses (cold shock or continuous mechanical stimuli) or parasitic wasp injection elevates the level of another type of peptide that shares sequence similarity with the epidermal growth factor (Hayakawa et al. 1995; Ohnishi 1954). This factor, growth-blocking peptide (GBP), is responsible for suppression of the increase in JH esterase levels after parasitization (Hayakawa 1991). GBP directly acts on epidermal cells to induce an elevation of cytoplasmic calcium ion concentration, which increases the levels of *TH* and *DDC* expression (Ninomiya and Hayakawa 2007).

At the enzyme level, the epidermal synthesis of a granular phenoloxidase (GPO) that catalyzes cuticular melanization of *M. sexta* larvae is inhibited by JH (Hiruma and Riddiford 1988). The absence of JH at the time of head capsule slippage during the last larval molt causes deposition of premelanin granules containing an inactive prophenoloxidase into the outer regions of the newly forming endocuticle. The decline of ecdysteroid titer allows activation of the proGPO and subsequent melanization (Curtis et al. 1984). Neuropeptide hormones such as MRCH, eclosion hormone, or extracts of pharate-larval subesophageal ganglia or corpora cardiaca-corpora allata complexes did not accelerate melanization. Dopamine, the precursor for melanin, is produced by the epidermis at the end of the molt, due to an increase in DOPA decarboxylase (DDC), which catalyzes dopamine production from DOPA (Hiruma and Riddiford 1993). The rise in DDC activity is controlled at the transcriptional level and dependent on the changing ecdysteroid titer during the molt as described above.

Bursicon (bur) known as “tanning hormone” is an insect heterodimeric neuropeptide hormone that is secreted from the central nervous system into the hemolymph, which initiates cuticle tanning as well as wing expansion after adult eclosion. Rickets (rk), the receptor for bur, is a member of the G protein-coupled receptor superfamily (Honegger et al. 2008; Luo et al. 2005; Mendive et al. 2005). In *D. melanogaster* larvae, Dmbur is expressed exclusively in crustacean cardioactive peptide-expressing neurons (Luan et al. 2006; Luo et al. 2005; Park et al. 2003). *D. melanogaster* mutants for *Dmbur* and the receptor mutant *Dmrk* showed deficiencies in both tanning and wing expansion (Baker and Truman 2002; Dewey et al. 2004). Eighty-seven genes in *D. melanogaster* were found to be sensitive to recombinant

bur stimulation (An et al. 2008). Thirty have no known function, but the others encode proteins with diverse functions, including cell signaling, gene transcription, DNA/RNA binding, ion trafficking, proteolysis-peptidolysis, metabolism, cytoskeleton formation, immune response and cell-adhesion. Huang et al. (2007) reported that loss of function of Bmbur caused a defect in wing expansion but no distinct tanning phenotype was observed in *B. mori* adults. Similarly, knockdown in the expression of genes coding for Tcbur and/or its receptor Tcrk in *T. castaneum* by injecting dsRNA into the pharate pupae caused a wrinkled elytra phenotype, but showed no effect on cuticle tanning. However, when Bai and Palli (2010) injected *Tcrk* dsRNA earlier in development (into young last instar larvae), pupal cuticle tanning was affected. A reduction in the expression of *laccase 2* in *Tcrk* RNAi beetles suggested that Tcrk influences pupal cuticle tanning by regulating the expression of *laccase 2* in *T. castaneum*. However, post-translational modifications such as phosphorylation may also play a role in regulation of cuticle tanning by the bursicon receptor (Honegger et al. 2008). TH is transiently activated during tanning by phosphorylation at a serine residue as a result of bursicon signaling (Davis et al. 2007). A novel bursicon-regulated gene in the housefly, *Musca domestica* (named md13379 because it is homologous with CG13379 in *D. melanogaster*), encodes a transcriptional regulator homologous to human ataxin-7-like3 and yeast sgf11, both of which encode a novel subunit of the Spt-Ada-Gcn5-acetyltransferase (An et al. 2009). Proteins related to md13379 may play a role in regulating the expression of bursicon-regulated genes involved in cuticle tanning.

6.5 Future Prospects and Concluding Remarks

Although tyrosine metabolism for insect cuticle tanning and the chemistry of pigment synthesis in general are still not well understood, past studies have demonstrated several physiologically and ecologically important roles in the tanning process. These findings suggest that the potential for development of novel control agents targeting insect cuticle tanning physiology. For example, after demonstration of specific gene down-regulation in several insect species including crop pests by orally administered dsRNA (Turner et al. 2006; Zhou et al. 2008; Tian et al. 2009; Walshe et al. 2009; Chen et al. 2010; Huvenne and Smaghe 2010; Zhang et al. 2010; Li et al. 2011; Bolognesi et al. 2012; Zhu et al. 2012; Miyata et al. 2014; Wan et al. 2014; Guo et al. 2015), RNAi based-pest management is now considered to be a promising new technology to control target pest insects with high species-specificity and environmentally friendly attributes. In addition, transgenic plants expressing dsRNAs for target insect genes impair growth and development (Baum et al. 2007; Mao et al. 2007; Pitino et al. 2011; Zha et al. 2011; Zhu et al. 2012; Kumar et al. 2013; Zhang et al. 2015). These results suggest that RNAi based-pest control could be a very useful alternative to chemical pesticides for suppression of economically damaging pest insects. Loss of function of many genes involved in the tyrosine-mediated cuticle tanning pathway caused not only alterations in color but also resulted in high mortality as described in

Sect. 6.2, indicating that the pathway is vital for insect development, growth and survival, making the genes potential targets for controlling economically important pest insects and animal/plant disease vectors.

The involvement of phenoloxidases in cuticle tanning is essential to insect survival (Dittmer and Kanost 2010) and laccases are potential phenoloxidase targets for insect control agents. One of the first compounds developed to adversely affect insect cuticle tanning is the sterically hindered phenol, 2,6-ditert-butyl-4-(2-phenylpropan-2-yl)-phenol (MON-0585, Semensi and Sugumaran 1986). In MON-0585-treated insects there was a reduced phenoloxidase activity as compared to controls as well as a significant reduction in the level of covalently bound catechols and malformations in the exoskeleton. Prasain et al. (2012) tested substituted phenolic compounds as substrates or inhibitors of laccase and also examined their effects on mosquito larval growth. Several compounds caused >90% mortalities as mosquito larvicides at nM- μ M concentrations. The treated larvae started to separate the larval cuticle, but they failed to shed it. Also there was very little synthesis of new pupal cuticle by the treated larvae. Thus, some of the laccase-active compounds affected the development of the cuticle, which is a target that is different from the neurological targets of most currently utilized insecticides. However, the exact target and mechanism of action of these modified phenolic compounds *in vivo* still remain to be determined.

In biomimetic/entomomimetic science, an area of research involves the development of novel biomimetic materials with unique physical properties similar to those of the pigmented insect exoskeleton for use in biomedical or other technological devices. For example, a pigmented cuticle structure of the highly modified and tanned forewing elytron of beetles was investigated as a biomimetic model and its application was described (Dai and Yang 2010; Lomakin et al. 2011; Chen and Wu 2013; Chen et al. 2015a, b). Unlike other pigmented and rigid cuticles in different body regions of adult beetles, the elytron composes of dual cuticular layers (dorsal and ventral cuticles) connected by a large number of pillar-like fibrous structures called trabeculae. The unique structure of the elytron, for instance, has been applied as a model to develop novel integrated honeycomb structures that are lightweight with a high mechanical strength (Chen et al. 2012, 2015b).

Although substantial progress in studies of insect cuticle tanning metabolism has occurred in the past, there remain several unanswered questions that should be addressed in future studies. What are the exact chemical structures of the insect pigments? Structural models and templates have been offered for some of the pigments including eumelanin and pheomelanin (Solano 2014), but the exact structures have not been established. How do the pigments interact with other components for assembly of the supramolecular extracellular matrix known as the exoskeleton? How do the pigments interact covalently and non-covalently with other components in the cuticle including proteins, chitin, lipids, minerals and water? What is the contribution of the pigments to the mechanical properties of exoskeletons? Substantial research designed to answer these questions remains to be conducted in the future so that we will have a more complete understanding of

the chemistry, physiology and genetics of insect cuticle pigmentation and sclerotization.

Acknowledgements This work was supported by the Basic Science Research Program through the National Research Foundation of Korea (NRF) funded by the Ministry of Science, ICT and future Planning (NRF-2015R1A2A2A01006614), Bio-industry Technology Development Program (111107011SB010), Ministry for Food, Agriculture, Forestry and Fisheries, and Basic Science Research Program through the NRF funded by the Ministry of Education (NRF-2015R1A6A3A04060323) to MYN.

References

- Albert S, Klaudiny J (2004) The MRJP/YELLOW protein family of *Apis mellifera*: identification of new members in the EST library. *J Insect Physiol* 50:51–59
- Amherd R, Hintermann E, Walz D, Affolter M, Meyer UA (2000) Purification, cloning, and characterization of a second arylalkylamine *N*-acetyltransferase from *Drosophila melanogaster*. *DNA Cell Biol* 19:697–705
- An S, Wang S, Gilbert LI, Beerntsen B, Ellersieck M, Song Q (2008) Global identification of bursicon-regulated genes in *Drosophila melanogaster*. *BMC Genomics* 9:424
- An S, Wang S, Stanley D, Song Q (2009) Identification of a novel bursicon-regulated transcriptional regulator, md13379, in the house fly *Musca domestica*. *Arch Insect Biochem Physiol* 70:106–121
- Andersen SO (1974) Evidence for two mechanisms of sclerotisation in insect cuticle. *Nature* 251:507–508
- Andersen SO (1978) Characterization of a trypsin-solubilized phenoloxidase from locust cuticle. *Insect Biochem* 8:143–148
- Andersen SO (2000) Studies on proteins in post-ecdysial nymphal cuticle of locust, *Locusta migratoria*, and cockroach, *Blaberus craniifer*. *Insect Biochem Mol Biol* 30:569–577
- Andersen SO (2005) Cuticular sclerotization and tanning. In: Gibert LI, Iatrou K, Gill SS (eds) *Comprehensive molecular insect science*, vol 4. Elsevier-Pergamon Press, Oxford, pp 145–170
- Andersen SO (2007) Involvement of tyrosine residues, N-terminal amino acids, and beta-alanine in insect cuticular sclerotization. *Insect Biochem Mol Biol* 37:969–974
- Andersen SO (2008) Quantitative determination of catecholic degradation products from insect sclerotized cuticles. *Insect Biochem Mol Biol* 38:877–882
- Andersen SO (2010) Insect cuticular sclerotization: a review. *Insect Biochem Mol Biol* 40:166–178
- Arakane Y, Muthukrishnan S, Beeman RW, Kanost MR, Kramer KJ (2005) *Laccase 2* is the phenoloxidase gene required for beetle cuticle tanning. *Proc Natl Acad Sci U S A* 102:11337–11342
- Arakane Y, Li B, Muthukrishnan S, Beeman RW, Kramer KJ, Park Y (2008) Functional analysis of four neuropeptides, EH, ETH, CCAP and bursicon, and their receptors in adult ecdysis behavior of the red flour beetle, *Tribolium castaneum*. *Mech Dev* 125:984–995
- Arakane Y, Lomakin J, Beeman RW, Muthukrishnan S, Gehrke SH, Kanost MR, Kramer KJ (2009) Molecular and functional analyses of amino acid decarboxylases involved in cuticle tanning in *Tribolium castaneum*. *J Biol Chem* 284:16584–16594
- Arakane Y, Dittmer NT, Tomoyasu Y, Kramer KJ, Muthukrishnan S, Beeman RW, Kanost MR (2010) Identification, mRNA expression and functional analysis of several *yellow* family genes in *Tribolium castaneum*. *Insect Biochem Mol Biol* 40:259–266

- Arakane Y, Lomakin J, Gehrke SH, Hiromasa Y, Tomich JM, Muthukrishnan S, Beeman RW, Kramer KJ, Kanost MR (2012) Formation of rigid, non-flight forewings (elytra) of a beetle requires two major cuticular proteins. *PLoS Genet* 8, e1002682
- Arendt J, Deacon S, English J, Hampton S, Morgan L (1995) Melatonin and adjustment to phase shift. *J Sleep Res* 4:74–79
- Asano T, Ashida M (2001) Cuticular pro-phenoloxidase of the silkworm, *Bombyx mori* Purification and demonstration of its transport from hemolymph. *J Biol Chem* 276:11100–11112
- Asano T, Taoka M, Yamauchi Y, Craig Everroad R, Seto Y, Isobe T, Kamo M, Chosa N (2014) Re-examination of a alpha-chymotrypsin-solubilized laccase in the pupal cuticle of the silkworm, *Bombyx mori*: insights into the regulation system for laccase activation during the ecdysis process. *Insect Biochem Mol Biol* 55C:61–69
- Ashida M, Brey PT (1995) Role of the integument in insect defense: pro-phenol oxidase cascade in the cuticular matrix. *Proc Natl Acad Sci U S A* 92:10698–10702
- Ashida M, Brey PT (1997) Recent advances in research on the insect prophenoloxidase cascade. In: Brey PT, Hultmark D (eds) *Molecular mechanisms of immune responses in insects*. Chapman & Hall, New York, pp 135–172
- Ashida M, Yamazaki HI (1990) Biochemistry of the phenoloxidase system in insects: with special reference to its activation. In: Ohnishi E, Ishizaki E (eds) *Molting and metamorphosis*. Japan Scientific Societies Press, Tokyo, pp 239–265
- Aust S, Brusselbach F, Putz S, Hovemann BT (2010) Alternative tasks of *Drosophila tan* in neurotransmitter recycling versus cuticle sclerotization disclosed by kinetic properties. *J Biol Chem* 285:20740–20747
- Bai H, Palli SR (2010) Functional characterization of bursicon receptor and genome-wide analysis for identification of genes affected by bursicon receptor RNAi. *Dev Biol* 344:248–258
- Baker JD, Truman JW (2002) Mutations in the *Drosophila* glycoprotein hormone receptor, rickets, eliminate neuropeptide-induced tanning and selectively block a stereotyped behavioral program. *J Exp Biol* 205:2555–2565
- Barbera M, Mengual B, Collantes-Alegre JM, Cortes T, Gonzalez A, Martinez-Torres D (2013) Identification, characterization and analysis of expression of genes encoding arylalkylamine *N*-acetyltransferases in the pea aphid *Acyrtosiphon pisum*. *Insect Mol Biol* 22:623–634
- Barredo JL, van Solingen P, Diez B, Alvarez E, Cantoral JM, Kattavilder A, Smaal EB, Groenen MA, Veenstra AE, Martin JF (1989) Cloning and characterization of the acyl-coenzyme A: 6-aminopenicillanic-acid-acyltransferase gene of *Penicillium chrysogenum*. *Gene* 83:291–300
- Barrett FM (1987a) Characterization of phenoloxidases from larval cuticle of *Sarcophaga bullata* and a comparison with cuticular enzymes from other species. *Can J Zool* 65:1158–1166
- Barrett FM (1987b) Phenoloxidases from larval cuticle of the sheep blowfly, *Lucilia cuprina*: characterization, developmental changes, and inhibition by anti-phenoloxidase antibodies. *Arch Insect Biochem Physiol* 5:99–118
- Barrett FM (1991) Phenoloxidases and the integument. In: Binnington K, Retnakaron A (eds) *Physiology of the insect epidermis*. CSIRO Publications, East Melbourne, pp 195–212
- Barrett FM, Andersen SO (1981) Phenoloxidases in larval cuticle of the blowfly, *Calliphora vicina*. *Insect Biochem* 11:17–23
- Baum JA, Bogaert T, Clinton W, Heck GR, Feldmann P, Ilagan O, Johnson S, Plaetinck G, Munyikwa T, Pleau M, Vaughn T, Roberts J (2007) Control of coleopteran insect pests through RNA interference. *Nat Biotechnol* 25:1322–1326
- Bembek J, Sehadova H, Ichihara N, Takeda M (2005) Day/night fluctuations in melatonin content, arylalkylamine *N*-acetyltransferase activity and *NAT* mRNA expression in the CNS, peripheral tissues and hemolymph of the cockroach, *Periplaneta americana*. *Comp Biochem Physiol B* 140:27–36
- Birman S, Morgan B, Anzivino M, Hirsh J (1994) A novel and major isoform of tyrosine hydroxylase in *Drosophila* is generated by alternative RNA processing. *J Biol Chem* 269:26559–26567

- Bolognesi R, Ramaseshadri P, Anderson J, Bachman P, Clinton W, Flannagan R, Ilagan O, Lawrence C, Levine S, Moar W, Mueller G, Tan J, Uffman J, Wiggins E, Heck G, Segers G (2012) Characterizing the mechanism of action of double-stranded RNA activity against western corn rootworm (*Diabrotica virgifera virgifera* LeConte). PLoS One 7, e47534
- Bridges CB, Morgan TH (1923) The third-chromosome group of mutant characters of *Drosophila melanogaster*. Carnegie Institution of Washington, Washington
- Brodbeck D, Amherd R, Callaerts P, Hintermann E, Meyer UA, Affolter M (1998) Molecular and biochemical characterization of the aaNAT1 (Dat) locus in *Drosophila melanogaster*: differential expression of two gene products. DNA Cell Biol 17:621–633
- Bückmann D, Maisch A (1987) Extraction and partial purification of the pupal melanization reducing factor (PMRF) from *Inachis io* (Lepidoptera). Insect Biochem 17:841–844
- Budnik V, White K (1987) Genetic dissection of dopamine and serotonin synthesis in the nervous system of *Drosophila melanogaster*. J Neurogenet 4:309–314
- Buttstedt A, Moritz RF, Erler S (2014) Origin and function of the major royal jelly proteins of the honeybee (*Apis mellifera*) as members of the *yellow* gene family. Biol Rev Camb Philos Soc 89:255–269
- Chatterjee S, Prados-Rosales R, Itin B, Casadevall A, Stark RE (2015) Solid-state NMR reveals the carbon-based molecular architecture of *Cryptococcus neoformans* fungal eumelanins in the cell wall. J Biol Chem 290:13779–13790
- Chen J, Wu G (2013) Beetle forewings: epitome of the optimal design for lightweight composite materials. Carbohydr Polym 91:659–665
- Chen J, Zhang D, Yao Q, Zhang J, Dong X, Tian H, Zhang W (2010) Feeding-based RNA interference of a trehalose phosphate synthase gene in the brown planthopper, *Nilaparvata lugens*. Insect Mol Biol 19:777–786
- Chen J, Xie J, Zhu H, Guan S, Wu G, Noori MN, Guo S (2012) Integrated honeycomb structure of a beetle forewing and its imitation. Mater Sci Eng C Mater Biol Appl 32:613–618
- Chen J, Xie J, Wu Z, Elbashiry EM, Lu Y (2015a) Review of beetle forewing structures and their biomimetic applications in China: (I) On the structural colors and the vertical and horizontal cross-sectional structures. Mater Sci Eng C 55:605–619
- Chen J, Zu Q, Wu G, Xie J, Tuo W (2015b) Review of beetle forewing structures and their biomimetic applications in China: (II) On the three-dimensional structure, modeling and imitation. Mater Sci Eng C 55:620–633
- Cheng L, Wang LY, Karlsson AM (2008) Image analyses of two crustacean exoskeletons and implications of the exoskeletal microstructure on the mechanical behavior. J Mater Res 23:2854–2872
- Christensen BM, Li J, Chen CC, Nappi AJ (2005) Melanization immune responses in mosquito vectors. Trends Parasitol 21:192–199
- Cornman RS, Togawa T, Dunn WA, He N, Emmons AC, Willis JH (2008) Annotation and analysis of a large cuticular protein family with the R&R Consensus in *Anopheles gambiae*. BMC Genomics 9:22
- Cromartie RIT (1959) Insect pigments. Annu Rev Entomol 4:59–76
- Curtis AT, Hori M, Green JM, Wolfgang WJ, Hiruma K, Riddiford LM (1984) Ecdysteroid regulation of the onset of cuticular melanization in allatectomized and black mutant *Manduca sexta* larvae. J Insect Physiol 30:597–606
- Czapla TH, Hopkins TL, Kramer KJ (1990) Cuticular strength and pigmentation of five strains of adult *Blattella germanica* (L.) during sclerotization: correlations with catecholamines, β -alanine and food deprivation. J Insect Physiol 6:647–654
- Dai ZD, Yang ZX (2010) Macro-/micro-structures of elytra, mechanical properties of the biomaterial and the coupling strength between elytra in beetles. J Bionic Eng 7:6–12
- Dai F, Qiao L, Tong XL, Cao C, Chen P, Chen J, Lu C, Xiang ZH (2010) Mutations of an arylalkylamine-*N*-acetyltransferase, *Bm-iAANAT*, are responsible for silkworm melanism mutant. J Biol Chem 285:19553–19560

- Dai F, Qiao L, Cao C, Liu X, Tong X, He S, Hu H, Zhang L, Wu S, Tan D, Xiang Z, Lu C (2015) Aspartate decarboxylase is required for a normal pupa pigmentation pattern in the silkworm, *Bombyx mori*. *Sci Rep* 5:10885
- David J, Capy P, Payant V, Tsakas S (1985) Thoracic trident pigmentation in *Drosophila melanogaster*: differentiation of geographical populations. *Genet Sel Evol* 17:211–224
- David JR, Capy P, Gauthier J-P (1990) Abdominal pigmentation and growth temperature in *Drosophila melanogaster*, similarities and differences in the norms of reaction of successive segments. *J Evol Biol* 3:429–445
- Davis MM, O'Keefe SL, Primrose DA, Hodgetts RB (2007) A neuropeptide hormone cascade controls the precise onset of post-eclosion cuticular tanning in *Drosophila melanogaster*. *Development* 134:4395–4404
- Davis MM, Primrose DA, Hodgetts RB (2008) A member of the p38 mitogen-activated protein kinase family is responsible for transcriptional induction of Dopa decarboxylase in the epidermis of *Drosophila melanogaster* during the innate immune response. *Mol Cell Biol* 28:4883–4895
- Delachambre J (1971) La formation des canaux cuticulaire chez l'adulte de *Tenebrio molitor* L.: Etude ultrastructurelle et remarques histochimiques. *Tissue Cell* 3:499–520
- Dempsey DR, Jeffries KA, Bond JD, Carpenter AM, Rodriguez-Ospina S, Breydo L, Caswell KK, Merkler DJ (2014) Mechanistic and structural analysis of *Drosophila melanogaster* arylalkylamine *N*-acetyltransferases. *Biochemistry* 53:7777–7793
- Dewey EM, McNabb SL, Ewer J, Kuo GR, Takanishi CL, Truman JW, Honegger HW (2004) Identification of the gene encoding bursicon, an insect neuropeptide responsible for cuticle sclerotization and wing spreading. *Curr Biol* 14:1208–1213
- Dittmer NT, Kanost MR (2010) Insect multicopper oxidases: diversity, properties, and physiological roles. *Insect Biochem Mol Biol* 40:179–188
- Dittmer NT, Suderman RJ, Jiang H, Zhu YC, Gorman MJ, Kramer KJ, Kanost MR (2004) Characterization of cDNAs encoding putative laccase-like multicopper oxidases and developmental expression in the tobacco hornworm, *Manduca sexta*, and the malaria mosquito, *Anopheles gambiae*. *Insect Biochem Mol Biol* 34:29–41
- Dittmer NT, Gorman MJ, Kanost MR (2009) Characterization of endogenous and recombinant forms of laccase-2, a multicopper oxidase from the tobacco hornworm, *Manduca sexta*. *Insect Biochem Mol Biol* 39:596–606
- Dittmer NT, Hiromasa Y, Tomich JM, Lu N, Beeman RW, Kramer KJ, Kanost MR (2012) Proteomic and transcriptomic analyses of rigid and membranous cuticles and epidermis from the elytra and hindwings of the red flour beetle, *Tribolium castaneum*. *J Proteome Res* 11:269–278
- Drapeau MD (2001) The Family of Yellow-Related *Drosophila melanogaster* Proteins. *Biochem Biophys Res Commun* 281:611–613
- Drapeau MD, Albert S, Kucharski R, Prusko C, Maleszka R (2006) Evolution of the Yellow/Major Royal Jelly Protein family and the emergence of social behavior in honey bees. *Genome Res* 16:1385–1394
- Duff GA, Roberts JE, Foster N (1988) Analysis of the structure of synthetic and natural melanins by solid-phase NMR. *Biochemistry* 27:7112–7116
- Dyda F, Klein DC, Hickman AB (2000) GCN5-related *N*-acetyltransferases: a structural overview. *Annu Rev Biophys Biomol Struct* 29:81–103
- Elias-Neto M, Soares MP, Simoes ZL, Hartfelder K, Bitondi MM (2010) Developmental characterization, function and regulation of a Laccase2 encoding gene in the honey bee, *Apis mellifera* (Hymenoptera, Apinae). *Insect Biochem Mol Biol* 40:241–251
- Evans DA (1989) *N*-acetyltransferase. *Pharmacol Ther* 42:157–234
- Ferguson LC, Green J, SurrIDGE A, Jiggins CD (2011a) Evolution of the insect *yellow* gene family. *Mol Biol Evol* 28:257–272
- Ferguson LC, Maroja L, Jiggins CD (2011b) Convergent, modular expression of *ebony* and *tan* in the mimetic wing patterns of *Heliconius* butterflies. *Dev Genes Evol* 221:297–308

- Finocchiaro L, Callebert J, Launay JM, Jallon JM (1988) Melatonin biosynthesis in *Drosophila*: its nature and its effects. *J Neurochem* 50:382–387
- Flyg C, Boman HG (1988) *Drosophila* genes *cut* and *miniature* are associated with the susceptibility to infection by *Serratia marcescens*. *Genet Res* 52:51–56
- Friggi-Grelin F, Iche M, Birman S (2003) Tissue-specific developmental requirements of *Drosophila* tyrosine hydroxylase isoforms. *Genesis* 35:260–269
- Fujii T, Abe H, Kawamoto M, Katsuma S, Banno Y, Shimada T (2013) Albino (al) is a tetrahydrobiopterin (BH4)-deficient mutant of the silkworm *Bombyx mori*. *Insect Biochem Mol Biol* 43:594–600
- Futahashi R, Fujiwara H (2005) Melanin-synthesis enzymes coregulate stage-specific larval cuticular markings in the swallowtail butterfly, *Papilio xuthus*. *Dev Genes Evol* 215:519–529
- Futahashi R, Fujiwara H (2007) Regulation of 20-hydroxyecdysone on the larval pigmentation and the expression of melanin synthesis enzymes and *yellow* gene of the swallowtail butterfly, *Papilio xuthus*. *Insect Biochem Mol Biol* 37:855–864
- Futahashi R, Fujiwara H (2008) Identification of stage-specific larval camouflage associated genes in the swallowtail butterfly, *Papilio xuthus*. *Dev Genes Evol* 218:491–504
- Futahashi R, Okamoto S, Kawasaki H, Zhong YS, Iwanaga M, Mita K, Fujiwara H (2008a) Genome-wide identification of cuticular protein genes in the silkworm, *Bombyx mori*. *Insect Biochem Mol Biol* 38:1138–1146
- Futahashi R, Sato J, Meng Y, Okamoto S, Daimon T, Yamamoto K, Suetsugu Y, Narukawa J, Takahashi H, Banno Y, Katsuma S, Shimada T, Mita K, Fujiwara H (2008b) *Yellow* and *ebony* are the responsible genes for the larval color mutants of the silkworm *Bombyx mori*. *Genetics* 180:1995–2005
- Futahashi R, Banno Y, Fujiwara H (2010) Caterpillar color patterns are determined by a two-phase melanin gene pre patterning process: new evidence from *tan* and *laccase2*. *Evol Dev* 12:157–167
- Futahashi R, Shirataki H, Narita T, Mita K, Fujiwara H (2012) Comprehensive microarray-based analysis for stage-specific larval camouflage pattern-associated genes in the swallowtail butterfly, *Papilio xuthus*. *BMC Biol* 10:46
- Futahashi R, Tanaka K, Matsuura Y, Tanahashi M, Kikuchi Y, Fukatsu T (2011) *Laccase2* is required for cuticular pigmentation in stinkbugs. *Insect Biochem Mol Biol* 41:191–196
- Fuzeau-Braesch S (1972) Pigments and color changes. *Annu Rev Entomol* 17:403–424
- Gibert P, Moreteau B, Moreteau JC, David JR (1996) Growth temperature and adult pigmentation in two *Drosophila* sibling species: an adaptive convergence of reaction norms in sympatric populations? *Evolution* 50:2346–2353
- Gibert P, Moreteau B, Moreteau JC, Parkash R, David JR (1998) Light body pigmentation in Indian *Drosophila melanogaster*: a likely adaptation to a hot and arid climate. *J Genet* 77:13–20
- Gibert JM, Peronnet F, Schlotterer C (2007) Phenotypic plasticity in *Drosophila* pigmentation caused by temperature sensitivity of a chromatin regulator network. *PLoS Genet* 3, e30
- Gompel N, Prud'homme B, Wittkopp PJ, Kassner VA, Carroll SB (2005) Chance caught on the wing: *cis*-regulatory evolution and the origin of pigment patterns in *Drosophila*. *Nature* 433:481–487
- Gorman MJ, Arakane Y (2010) Tyrosine hydroxylase is required for cuticle sclerotization and pigmentation in *Tribolium castaneum*. *Insect Biochem Mol Biol* 40:267–273
- Gorman MJ, An C, Kanost MR (2007) Characterization of tyrosine hydroxylase from *Manduca sexta*. *Insect Biochem Mol Biol* 37:1327–1337
- Gorman MJ, Dittmer NT, Marshall JL, Kanost MR (2008) Characterization of the multicopper oxidase gene family in *Anopheles gambiae*. *Insect Biochem Mol Biol* 38:817–824
- Gorman MJ, Sullivan LI, Nguyen TD, Dai H, Arakane Y, Dittmer NT, Syed LU, Li J, Hua DH, Kanost MR (2012) Kinetic properties of alternatively spliced isoforms of *laccase-2* from *Tribolium castaneum* and *Anopheles gambiae*. *Insect Biochem Mol Biol* 42:193–202

- Guo ZJ, Kang S, Zhu X, Xia JX, Wu QJ, Wang SL, Xie W, Zhang YJ (2015) The novel ABC transporter ABCH1 is a potential target for RNAi-based insect pest control and resistance management. *Sci Rep* 5:13728
- Hackman RH (1974) Chemistry of the insect cuticle. In: Rockstein M (ed) *The physiology of insects*, vol 6. Academic, New York, pp 215–270
- Hackman RH (1984) Cuticle biochemistry. In: Bereiter-Hahn J, Motolsy AG, Richards KS (eds) *Biology of the integument*, vol 1. Springer, Berlin, pp 583–610
- Han Q, Fang J, Ding H, Johnson JK, Christensen BM, Li J (2002) Identification of *Drosophila melanogaster* yellow-f and yellow-f2 proteins as dopachrome-conversion enzymes. *Biochem J* 368:333–340
- Han Q, Ding H, Robinson H, Christensen BM, Li J (2010) Crystal structure and substrate specificity of *Drosophila* 3,4-dihydroxyphenylalanine decarboxylase. *PLoS One* 5, e8826
- Han Q, Robinson H, Ding H, Christensen BM, Li J (2012) Evolution of insect arylalkylamine *N*-acetyltransferases: structural evidence from the yellow fever mosquito, *Aedes aegypti*. *Proc Natl Acad Sci U S A* 109:11669–11674
- Hardie J, Gao N (1997) Melatonin and the pea aphid, *Acyrtosiphon pisum*. *J Insect Physiol* 43:615–620
- Hartwig S, Dovengerds C, Herrmann C, Hovemann BT (2014) *Drosophila* Ebony: a novel type of nonribosomal peptide synthetase related enzyme with unusually fast peptide bond formation kinetics. *FEBS J* 281:5147–5158
- Hayakawa Y (1991) Structure of a growth-blocking peptide present in parasitized insect hemolymph. *J Biol Chem* 266:7982–7984
- Hayakawa Y, Ohnishi A, Yamanaka A, Izumi S, Tomino S (1995) Molecular cloning and characterization of cDNA for insect biogenic peptide, growth-blocking peptide. *FEBS Lett* 376:185–189
- Hazel WN, West DA (1979) Environmental control of pupal colour in swallowtail butterflies (Lepidoptera: Papilioninae): *Battus philenor* (L.) and *Papilio polyxenes* Fabr. *Ecol Entomol* 4:393–400
- Hazel WN, West DA (1983) The effect of larval photoperiod on pupal colour and diapause in swallowtail butterflies. *Ecol Entomol* 8:37–42
- He CL, Zu Q, Chen JX, Noori MN (2015) A review of the mechanical properties of beetle elytra and development of the biomimetic honeycomb plates. *J Sandw Struct Mater* 17:399–416
- Hintermann E, Jenö P, Meyer UA (1995) Isolation and characterization of an arylalkylamine *N*-acetyltransferase from *Drosophila melanogaster*. *FEBS Lett* 375:148–150
- Hintermann E, Grieder NC, Amherd R, Brodbeck D, Meyer UA (1996) Cloning of an arylalkylamine *N*-acetyltransferase (aaNAT1) from *Drosophila melanogaster* expressed in the nervous system and the gut. *Proc Natl Acad Sci U S A* 93:12315–12320
- Hiraga S (2005) Two different sensory mechanisms for the control of pupal protective coloration in butterflies. *J Insect Physiol* 51:1033–1040
- Hiragaki S, Suzuki T, Mohamed AA, Takeda M (2015) Structures and functions of insect arylalkylamine *N*-acetyltransferase (iaaNAT); a key enzyme for physiological and behavioral switch in arthropods. *Front Physiol* 6:113
- Hiruma K, Riddiford LM (1988) Granular phenoloxidase involved in cuticular melanization in the tobacco hornworm: regulation of its synthesis in the epidermis by juvenile hormone. *Dev Biol* 130:87–97
- Hiruma K, Riddiford LM (1990) Regulation of dopa decarboxylase gene expression in the larval epidermis of the tobacco hornworm by 20-hydroxyecdysone and juvenile hormone. *Dev Biol* 138:214–224
- Hiruma K, Riddiford LM (1993) Molecular mechanisms of cuticular melanization in the tobacco hornworm, *Manduca sexta* (L.) (Lepidoptera: Sphingidae). *Int J Insect Morphol Embryol* 22:103–117
- Hiruma K, Riddiford LM (2009) The molecular mechanisms of cuticular melanization: the ecdysone cascade leading to dopa decarboxylase expression in *Manduca sexta*. *Insect Biochem Mol Biol* 39:245–253

- Hiruma K, Riddiford LM, Hopkins TL, Morgan TD (1985) Roles of dopa decarboxylase and phenoloxidase in the melanization of the tobacco hornworm and their control by 20-hydroxyecdysone. *J Comp Physiol B* 155:659–669
- Hodgetts RB (1972) Biochemical characterization of mutants affecting the metabolism of β -alanine in *Drosophila*. *J Insect Physiol* 18:937–947
- Hodgetts R, Choi A (1974) Beta alanine and cuticle maturation in *Drosophila*. *Nature* 252:710–711
- Hodgetts RB, Konopka RJ (1973) Tyrosine and catecholamine metabolism in wild-type *Drosophila melanogaster* and a mutant, *ebony*. *J Insect Physiol* 19:1211–1220
- Hodgetts RB, O'Keefe SL (2006) Dopa decarboxylase: a model gene-enzyme system for studying development, behavior, and systematics. *Annu Rev Entomol* 51:259–284
- Hojo M, Kagami T, Sasaki T, Nakamura J, Sasaki M (2010) Reduced expression of *major royal jelly protein 1* gene in the mushroom bodies of worker honeybees with reduced learning ability. *Apidologie* 41:194–202
- Honegger HW, Dewey EM, Ewer J (2008) Bursicon, the tanning hormone of insects: recent advances following the discovery of its molecular identity. *J Comp Physiol A Neuroethol Sens Neural Behav Physiol* 194:989–1005
- Honeybee Genome Sequencing Consortium (2006) Insights into social insects from the genome of the honeybee *Apis mellifera*. *Nature* 443:931–949
- Hopkins TL, Kramer KJ (1992) Insect cuticle sclerotization. *Annu Rev Entomol* 37:273–302
- Hopkins TL, Morgan TD, Kramer KJ (1984) Catecholamines in haemolymph and cuticle during larval, pupal and adult development of *Manduca sexta* (L.). *Insect Biochem* 14:533–540
- Hori M, Hiruma K, Riddiford LM (1984) Cuticular melanization in the tobacco hornworm larva. *Insect Biochem* 14:267–274
- Hotta Y, Benzer S (1969) Abnormal electroretinograms in visual mutants of *Drosophila*. *Nature* 222:354–356
- Hovemann BT, Ryseck RP, Walldorf U, Stortkuhl KF, Dietzel ID, Dessen E (1998) The *Drosophila ebony* gene is closely related to microbial peptide synthetases and shows specific cuticle and nervous system expression. *Gene* 221:1–9
- Huang CY, Chou SY, Bartholomay LC, Christensen BM, Chen CC (2005) The use of gene silencing to study the role of dopa decarboxylase in mosquito melanization reactions. *Insect Mol Biol* 14:237–244
- Huang J, Zhang Y, Li M, Wang S, Liu W, Couble P, Zhao G, Huang Y (2007) RNA interference-mediated silencing of the bursicon gene induces defects in wing expansion of silkworm. *FEBS Lett* 581:697–701
- Hudson A (1966) Proteins in the haemolymph and other tissues of the developing tomato hornworm, *Protoparce quinquemaculata* Haworth. *Can J Zool* 44:541–555
- Huvenne H, Smaghe G (2010) Mechanisms of dsRNA uptake in insects and potential of RNAi for pest control: a review. *J Insect Physiol* 56:227–235
- Ioannidou ZS, Theodoropoulou MC, Papandreou NC, Willis JH, Hamodrakas SJ (2014) CutProtFam-Pred: detection and classification of putative structural cuticular proteins from sequence alone, based on profile hidden Markov models. *Insect Biochem Mol Biol* 52:51–59
- Ito K, Katsuma S, Yamamoto K, Kadono-Okuda K, Mita K, Shimada T (2010) Yellow-e determines the color pattern of larval head and tail spots of the silkworm *Bombyx mori*. *J Biol Chem* 285:5624–5629
- Itoh MT, Hattori A, Nomura T, Sumi Y, Suzuki T (1995a) Melatonin and arylalkylamine *N*-acetyltransferase activity in the silkworm, *Bombyx mori*. *Mol Cell Endocrinol* 115:59–64
- Itoh MT, Hattori A, Sumi Y, Suzuki T (1995b) Day-night changes in melatonin levels in different organs of the cricket (*Gryllus bimaculatus*). *J Pineal Res* 18:165–169
- Jacobs ME (1968) β -Alanine used by *ebony* and normal *Drosophila melanogaster* with notes on glucose, uracil, dopa, and dopamine. *Biochem Genet* 1:267–275
- Jacobs CG, Braak N, Lamers GE, van der Zee M (2015) Elucidation of the serosal cuticle machinery in the beetle *Tribolium* by RNA sequencing and functional analysis of Knickkopf1, Retroactive and Laccase 2. *Insect Biochem Mol Biol* 60:7–12

- Jeong S, Rebeiz M, Andolfatto P, Werner T, True J, Carroll SB (2008) The evolution of gene regulation underlies a morphological difference between two *Drosophila* sister species. *Cell* 132:783–793
- Kanost M, Gorman MJ (2008) Phenoloxidases in insect immunity. In: Beckage N (ed) *Insect immunology*. Academic, San Diego, pp 69–96
- Karouzou MV, Spyropoulos Y, Iconomidou VA, Cornman RS, Hamodrakas SJ, Willis JH (2007) *Drosophila* cuticular proteins with the R&R Consensus: annotation and classification with a new tool for discriminating RR-1 and RR-2 sequences. *Insect Biochem Mol Biol* 37:754–760
- Kayser H (1985) Pigments. In: Kerkut GA, Gilbert LI (eds) *Comparative insect physiology, biochemistry and pharmacology*, vol 10. Pergamon Press, New York, pp 367–415
- Kayser-Wegmann I (1976) Differences in black pigmentation in lepidopterans as revealed by light and electron microscopy. *Cell Tissue Res* 171:513–521
- Kim MH, Joo CH, Cho MY, Kwon TH, Lee KM, Natori S, Lee TH, Lee BL (2000) Bacterial-injection-induced syntheses of *N*-beta-alanyldopamine and Dopa decarboxylase in the hemolymph of coleopteran insect, *Tenebrio molitor* larvae. *Eur J Biochem* 267:2599–2608
- Klein DC (2007) Arylalkylamine *N*-acetyltransferase: “the Timezyme”. *J Biol Chem* 282:4233–4237
- Koch PB, Keys DN, Rocheleau T, Aronstein K, Blackburn M, Carroll SB, French-Constant RH (1998) Regulation of dopa decarboxylase expression during colour pattern formation in wild-type and melanic tiger swallowtail butterflies. *Development* 125:2303–2313
- Koch PB, Behnecke B, French-Constant RH (2000) The molecular basis of melanism and mimicry in a swallowtail butterfly. *Curr Biol* 10:591–594
- Kramer KJ, Hopkins TL (1987) Tyrosine metabolism for insect cuticle tanning. *Arch Insect Biochem Physiol* 6:279–301
- Kramer KJ, Morgan TD, Hopkins TL, Roseland CR, Aso Y, Beeman RW (1984) Catecholamines and β -alanine in the red flour beetle, *Tribolium castaneum*. Roles in cuticle sclerotization and melanization. *Insect Biochem* 14:293–298
- Kramer KJ, Morgan TD, Hopkins TL, Christensen AM, Schaefer J (1989) Solid-state ^{13}C -NMR and diphenol analyses of sclerotized cuticles from stored product Coleoptera. *Insect Biochem* 19:753–757
- Kramer KJ, Hopkins TL, Schaefer J (1995) Applications of solids NMR to the analysis of insect sclerotized structures. *Insect Biochem Mol Biol* 25:1067–1080
- Kramer KJ, Kanost MR, Hopkins TL, Jiang H, Zhu YC, Xu R, Kerwin JL, Turecek F (2001) Oxidative conjugation of catechols with proteins in insect skeletal systems. *Tetrahedron* 57:385–392
- Kronforst MR, Barsh GS, Kopp A, Mallet J, Monteiro A, Mullen SP, Protas M, Rosenblum EB, Schneider CJ, Hoekstra HE (2012) Unraveling the thread of nature’s tapestry: the genetics of diversity and convergence in animal pigmentation. *Pigment Cell Melanoma Res* 25:411–433
- Kucharski R, Maleszka R, Hayward DC, Ball EE (1998) A royal jelly protein is expressed in a subset of Kenyon cells in the mushroom bodies of the honey bee brain. *Naturwissenschaften* 85:343–346
- Kumar A, Wang S, Ou R, Samrakandi M, Beerntsen BT, Sayre RT (2013) Development of an RNAi based microalgal larvicide to control mosquitoes. *Malaria World J* 4:1–7
- Kupke J, Spaethe J, Mueller MJ, Rossler W, Albert S (2012) Molecular and biochemical characterization of the major royal jelly protein in bumblebees suggest a non-nutritive function. *Insect Biochem Mol Biol* 42:647–654
- Kyriacou CP, Burnet B, Connolly K (1978) Behavioral basis of overdominance in competitive mating success at the *ebony* locus of *Drosophila melanogaster*. *Anim Behav* 26:1195–1206
- Lee KS, Kim BY, Jin BR (2015) Differential regulation of tyrosine hydroxylase in cuticular melanization and innate immunity in the silkworm *Bombyx mori*. *J Asia Pac Entomol* 18:765–770
- Leem JY, Nishimura C, Kurata S, Shimada I, Kobayashi A, Natori S (1996) Purification and characterization of *N*-beta-alanyl-5-S-glutathionyl-3,4-dihydroxyphenylalanine, a novel antibacterial substance of *Sarcophaga peregrina* (flesh fly). *J Biol Chem* 271:13573–13577

- Li J (1994) Egg chorion tanning in *Aedes aegypti* mosquito. *Comp Biochem Physiol A* 109:835–843
- Li J, Chen Q, Lin Y, Jiang T, Wu G, Hua H (2011) RNA interference in *Nilaparvata lugens* (Homoptera: Delphacidae) based on dsRNA ingestion. *Pest Manag Sci* 67:852–859
- Lindsley DL, Grell EH (1968) Genetic variations of *Drosophila melanogaster*. Carnegie Institution of Washington, Washington
- Liu C, Yamamoto K, Cheng TC, Kadono-Okuda K, Narukawa J, Liu SP, Han Y, Futahashi R, Kidokoro K, Noda H, Kobayashi I, Tamura T, Ohnuma A, Banno Y, Dai FY, Xiang ZH, Goldsmith MR, Mita K, Xia QY (2010) Repression of tyrosine hydroxylase is responsible for the sex-linked chocolate mutation of the silkworm, *Bombyx mori*. *Proc Natl Acad Sci U S A* 107:12980–12985
- Liu P, Ding H, Christensen BM, Li J (2012) Cysteine sulfinic acid decarboxylase activity of *Aedes aegypti* aspartate 1-decarboxylase: the structural basis of its substrate selectivity. *Insect Biochem Mol Biol* 42:396–403
- Liu J, Lemonds TR, Popadic A (2014) The genetic control of aposomatic black pigmentation in hemimetabolous insects: insights from *Oncopeltus fasciatus*. *Evol Dev* 16:270–277
- Liu S, Wang M, Li X (2015) Overexpression of Tyrosine hydroxylase and Dopa decarboxylase associated with pupal melanization in *Spodoptera exigua*. *Sci Rep* 5:11273
- Locke M (1961) Pore canals and related structures in insect cuticle. *J Biophys Biochem Cytol* 10:589–618
- Locke M (2001) The Wigglesworth lecture: insects for studying fundamental problems in biology. *J Insect Physiol* 47:495–507
- Lomakin J, Arakane Y, Kramer KJ, Beeman RW, Kanost MR, Gehrke SH (2010) Mechanical properties of elytra from *Tribolium castaneum* wild-type and body color mutant strains. *J Insect Physiol* 56:1901–1906
- Lomakin J, Huber PA, Eichler C, Arakane Y, Kramer KJ, Beeman RW, Kanost MR, Gehrke SH (2011) Mechanical properties of the beetle elytron, a biological composite material. *Biomacromolecules* 12:321–335
- Luan H, Lemon WC, Peabody NC, Pohl JB, Zelensky PK, Wang D, Nitabach MN, Holmes TC, White BH (2006) Functional dissection of a neuronal network required for cuticle tanning and wing expansion in *Drosophila*. *J Neurosci* 26:573–584
- Luo CW, Dewey EM, Sudo S, Ewer J, Hsu SY, Honegger HW, Hsueh AJ (2005) Bursicon, the insect cuticle-hardening hormone, is a heterodimeric cystine knot protein that activates G protein-coupled receptor LGR2. *Proc Natl Acad Sci U S A* 102:2820–2825
- Maeno K, Gotoh T, Tanaka S (2004) Phase-related morphological changes induced by [His7]-corazonin in two species of locusts, *Schistocerca gregaria* and *Locusta migratoria* (Orthoptera: Acrididae). *Bull Entomol Res* 94:349–357
- Mahdi SH, Gima S, Tomita Y, Yamasaki H, Otaki JM (2010) Physiological characterization of the cold-shock-induced humoral factor for wing color-pattern changes in butterflies. *J Insect Physiol* 56:1022–1031
- Maleszka R, Kucharski R (2000) Analysis of *Drosophila yellow-B* cDNA reveals a new family of proteins related to the royal jelly proteins in the honeybee and to an orphan protein in an unusual bacterium *Deinococcus radiodurans*. *Biochem Biophys Res Commun* 270:773–776
- Mao YB, Cai WJ, Wang JW, Hong GJ, Tao XY, Wang LJ, Huang YP, Chen XY (2007) Silencing a cotton bollworm P450 monooxygenase gene by plant-mediated RNAi impairs larval tolerance of gossypol. *Nat Biotechnol* 25:1307–1313
- Marmaras VJ, Charalambidis ND, Zervas CG (1996) Immune response in insects: the role of phenoloxidase in defense reactions in relation to melanization and sclerotization. *Arch Insect Biochem Physiol* 31:119–133
- Matsumoto S, Sogai AI, Suzuki A, Ogura N, Sonobe H (1981) Purification and properties of the melanization and reddish coloration hormone (MRCH) in the armyworm, *Leucania separata* (Lepidoptera). *Insect Biochem* 11:725–733
- Matsumoto S, Isogai A, Suzuki A (1986) Isolation and amino terminal sequence of melanization and reddish coloration hormone (MRCH) from the silkworm, *Bombyx mori*. *Insect Biochem* 16:775–779

- Mehere P, Han Q, Christensen BM, Li J (2011) Identification and characterization of two arylal-kylamine *N*-acetyltransferases in the yellow fever mosquito, *Aedes aegypti*. *Insect Biochem Mol Biol* 41:707–714
- Mendive FM, Van Loy T, Claeysen S, Poels J, Williamson M, Hauser F, Grimmelikhuijzen CJ, Vassart G, Vanden Broeck J (2005) *Drosophila* molting neurohormone bursicon is a heterodimer and the natural agonist of the orphan receptor DLGR2. *FEBS Lett* 579:2171–2176
- Merrifield F (1890) Systematic temperature experiments on some Lepidoptera in all their stages. *Trans Entomol Soc Lond* 38:131–159
- Merrifield F (1893) The effects of temperature in the pupal stage on the colouring of *Pieris napi*, *Vanessa atalanta*, *Chrysophanus phloeas*, and *Ephyra punctaria*. *Trans Entomol Soc Lond* 41:55–67
- Meylaers K, Cerstiaens A, Vierstraete E, Baggerman G, Michiels CW, De Loof A, Schoofs L (2003) Antimicrobial compounds of low molecular mass are constitutively present in insects: characterisation of β -alanyl-tyrosine. *Curr Pharm Des* 9:159–174
- Miyata K, Ramaseshadri P, Zhang Y, Segers G, Bolognesi R, Tomoyasu Y (2014) Establishing an in vivo assay system to identify components involved in environmental RNA interference in the western corn rootworm. *PLoS One* 9, e101661
- Moussian B (2010) Recent advances in understanding mechanisms of insect cuticle differentiation. *Insect Biochem Mol Biol* 40:363–375
- Moussian B, Seifarth C, Muller U, Berger J, Schwarz H (2006) Cuticle differentiation during *Drosophila* embryogenesis. *Arthropod Struct Dev* 35:137–152
- Mun S, Noh MY, Dittmer NT, Muthukrishnan S, Kramer KJ, Kanost MR, Arakane Y (2015) Cuticular protein with a low complexity sequence becomes cross-linked during insect cuticle sclerotization and is required for the adult molt. *Sci Rep* 5:10484
- Nakamura K, Go N (2005) Function and molecular evolution of multicopper blue proteins. *Cell Mol Life Sci* 62:2050–2066
- Nappi AJ, Carton Y, Vass E (1992) Reduced cellular immune competence of a temperature-sensitive dopa decarboxylase mutant strain of *Drosophila melanogaster* against the parasite *Leptopilina bouvardi*. *Comp Biochem Physiol B* 101:453–460
- Nash WG, Yarkin RJ (1974) Genetic regulation and pattern formation: a study of the *yellow* locus in *Drosophila melanogaster*. *Genet Res* 24:19–26
- Nassel DR (1996) Neuropeptides, amines and amino acids in an elementary insect ganglion: functional and chemical anatomy of the unfused abdominal ganglion. *Prog Neurobiol* 48:325–420
- Neckameyer WS, Leal SM (2002) Biogenic amines as circulating hormones in insects. In: *Hormones, brain and behavior*, vol 3. Academic, San Diego, pp 141–165
- Neckameyer WS, White K (1993) *Drosophila* tyrosine hydroxylase is encoded by the pale locus. *J Neurogenet* 8:189–199
- Neville AC (1993) *Biology of fibrous composites: development beyond the cell membrane*. Cambridge University Press, New York
- Newby LM, Jackson FR (1991) *Drosophila ebony* mutants have altered circadian activity rhythms but normal eclosion rhythms. *J Neurogenet* 7:85–101
- Ni QQ, Chen JX, Iwamoto M, Kurashiki K, Saito K (2001) Interlaminar reinforcement mechanism in a beetle fore-wing. *JSME Int J C-Mech Sy* 44:1111–1116
- Ninomiya Y, Hayakawa Y (2007) Insect cytokine, growth-blocking peptide, is a primary regulator of melanin-synthesis enzymes in armyworm larval cuticle. *FEBS J* 274:1768–1777
- Ninomiya Y, Tanaka K, Hayakawa Y (2006) Mechanisms of black and white stripe pattern formation in the cuticles of insect larvae. *J Insect Physiol* 52:638–645
- Nishikawa H, Iga M, Yamaguchi J, Saito K, Kataoka H, Suzuki Y, Sugano S, Fujiwara H (2013) Molecular basis of wing coloration in a Batesian mimic butterfly, *Papilio polytes*. *Sci Rep* 3:3184
- Niu BL, Shen WF, Liu Y, Weng HB, He LH, Mu JJ, Wu ZL, Jiang P, Tao YZ, Meng ZQ (2008) Cloning and RNAi-mediated functional characterization of *MaLac2* of the pine sawyer, *Monochamus alternatus*. *Insect Mol Biol* 17:303–312

- Noh MY, Kramer KJ, Muthukrishnan S, Kanost MR, Beeman RW, Arakane Y (2014) Two major cuticular proteins are required for assembly of horizontal laminae and vertical pore canals in rigid cuticle of *Tribolium castaneum*. *Insect Biochem Mol Biol* 53C:22–29
- Noh MY, Kramer KJ, Muthukrishnan S, Beeman RW, Kanost MR, Arakane Y (2015a) Loss of function of the *yellow-e* gene causes dehydration-induced mortality of adult *Tribolium castaneum*. *Dev Biol* 399:315–324
- Noh MY, Muthukrishnan S, Kramer KJ, Arakane Y (2015b) *Tribolium castaneum* RR-1 cuticular protein TcCPR4 is required for formation of pore canals in rigid cuticle. *PLoS Genet* 11, e1004963
- Ohnishi E (1954) Tyrosinase in *Drosophila virilis*. *Annot Zool Jpn* 27:33–39
- Osanai-Futahashi M, Ohde T, Hirata J, Uchino K, Futahashi R, Tamura T, Niimi T, Sezutsu H (2012a) A visible dominant marker for insect transgenesis. *Nat Commun* 3:1295
- Osanai-Futahashi M, Tatematsu K, Yamamoto K, Narukawa J, Uchino K, Kayukawa T, Shinoda T, Banno Y, Tamura T, Sezutsu H (2012b) Identification of the *Bombyx* red egg gene reveals involvement of a novel transporter family gene in late steps of the insect ommochrome biosynthesis pathway. *J Biol Chem* 287:17706–17714
- Osborne RH (1996) Insect neurotransmission: neurotransmitters and their receptors. *Pharmacol Ther* 69:117–142
- Park JH, Schroeder AJ, Helfrich-Forster C, Jackson FR, Ewer J (2003) Targeted ablation of CCAP neuropeptide-containing neurons of *Drosophila* causes specific defects in execution and circadian timing of ecdysis behavior. *Development* 130:2645–2656
- Paskewitz SM, Andreev O (2008) Silencing the genes for dopa decarboxylase or dopachrome conversion enzyme reduces melanization of foreign targets in *Anopheles gambiae*. *Comp Biochem Physiol B* 150:403–408
- Peiren N, de Graaf DC, Vanrobaeys F, Danneels EL, Devreese B, Van Beeumen J, Jacobs FJ (2008) Proteomic analysis of the honey bee worker venom gland focusing on the mechanisms of protection against tissue damage. *Toxicol* 52:72–83
- Pepling M, Mount SM (1990) Sequence of a cDNA from the *Drosophila melanogaster white* gene. *Nucleic Acids Res* 18:1633
- Perez M, Wappner P, Quesada-Allue LA (2002) Catecholamine-beta-alanyl ligase in the medfly *Ceratitis capitata*. *Insect Biochem Mol Biol* 32:617–625
- Perez MM, Sabio G, Badaracco A, Quesada-Allue LA (2011) Constitutive expression and enzymatic activity of Tan protein in brain and epidermis of *Ceratitis capitata* and of *Drosophila melanogaster* wild-type and *tan* mutants. *Insect Biochem Mol Biol* 41:653–659
- Phillips AM, Salkoff LB, Kelly LE (1993) A neural gene from *Drosophila melanogaster* with homology to vertebrate and invertebrate glutamate decarboxylases. *J Neurochem* 61:1291–1301
- Phillips AM, Smart R, Strauss R, Brembs B, Kelly LE (2005) The *Drosophila* black enigma: the molecular and behavioural characterization of the *black1* mutant allele. *Gene* 351:131–142
- Pitino M, Coleman AD, Maffei ME, Ridout CJ, Hogenhout SA (2011) Silencing of aphid genes by dsRNA feeding from plants. *PLoS One* 6, e25709
- Pool JE, Aquadro CF (2007) The genetic basis of adaptive pigmentation variation in *Drosophila melanogaster*. *Mol Ecol* 16:2844–2851
- Prasain K, Nguyen TD, Gorman MJ, Barrigan LM, Peng Z, Kanost MR, Syed LU, Li J, Zhu KY, Hua DH (2012) Redox potentials, laccase oxidation, and antilarval activities of substituted phenols. *Bioorg Med Chem* 20:1679–1689
- Predel R, Neupert S, Russell WK, Scheibner O, Nachman RJ (2007) Corazonin in insects. *Peptides* 28:3–10
- Qiao L, Li Y, Xiong G, Liu X, He S, Tong X, Wu S, Hu H, Wang R, Hu H, Chen L, Zhang L, Wu J, Dai F, Lu C, Xiang Z (2012) Effects of altered catecholamine metabolism on pigmentation and physical properties of sclerotized regions in the silkworm melanism mutant. *PLoS One* 7, e42968
- Qin G, Lapidot S, Numata K, Hu X, Meirovitch S, Dekel M, Podoler I, Shoseyov O, Kaplan DL (2009) Expression, cross-linking, and characterization of recombinant chitin binding resilin. *Biomacromolecules* 10:3227–3234

- Queener SW, Neuss N (1982) The biosynthesis of β -lactam antibiotics. In: Morin EB, Morgan M (eds) *Beta-lactam antibiotics*, vol 3. Academic, London, pp 1–81
- Raabe D, Romano P, Sachs C, Fabritius H, Al-Sawalmih A, Yi S, Servos G, Hartwig HG (2006) Microstructure and crystallographic texture of the chitin-protein network in the biological composite material of the exoskeleton of the lobster *Homarus americanus*. *Mat Sci Eng A Struct* 421:143–153
- Rajpurohit S, Nedved O (2013) Clinal variation in fitness related traits in tropical drosophilids of the Indian subcontinent. *J Therm Biol* 38:345–354
- Randolt K, Gimple O, Geissendorfer J, Reinders J, Prusko C, Mueller MJ, Albert S, Tautz J, Beier H (2008) Immune-related proteins induced in the hemolymph after aseptic and septic injury differ in honey bee worker larvae and adults. *Arch Insect Biochem Physiol* 69:155–167
- Rebers JE, Riddiford LM (1988) Structure and expression of a *Manduca sexta* larval cuticle gene homologous to *Drosophila* cuticle genes. *J Mol Biol* 203:411–423
- Rebers JE, Willis JH (2001) A conserved domain in arthropod cuticular proteins binds chitin. *Insect Biochem Mol Biol* 31:1083–1093
- Richardson G, Ding H, Rocheleau T, Mayhew G, Reddy E, Han Q, Christensen BM, Li J (2010) An examination of aspartate decarboxylase and glutamate decarboxylase activity in mosquitoes. *Mol Biol Rep* 37:3199–3205
- Richardt A, Rybak J, Storkuhl KF, Meinertzhagen IA, Hovemann BT (2002) Ebony protein in the *Drosophila* nervous system: optic neuropile expression in glial cells. *J Comp Neurol* 452:93–102
- Richardt A, Kemme T, Wagner S, Schwarzer D, Marahiel MA, Hovemann BT (2003) Ebony, a novel nonribosomal peptide synthetase for beta-alanine conjugation with biogenic amines in *Drosophila*. *J Biol Chem* 278:41160–41166
- Riddiford LM (2008) Juvenile hormone action: A 2007 perspective. *J Insect Physiol* 54:895–901
- Riddiford LM, Hiruma K, Zhou X, Nelson CA (2003) Insights into the molecular basis of the hormonal control of molting and metamorphosis from *Manduca sexta* and *Drosophila melanogaster*. *Insect Biochem Mol Biol* 33:1327–1338
- Riedel F, Vorkel D, Eaton S (2011) Megalin-dependent yellow endocytosis restricts melanization in the *Drosophila* cuticle. *Development* 138:149–158
- Roseland CR, Kramer KJ, Hopkins TL (1987) Cuticular strength and pigmentation of rust-red and black strains of *Tribolium castaneum*: Correlation with catecholamine and β -alanine content. *Insect Biochem* 17:21–28
- Schachter J, Perez MM, Quesada-Allue LA (2007) The role of *N*- β -alanyl dopamine synthase in the innate immune response of two insects. *J Insect Physiol* 53:1188–1197
- Schaefer J, Kramer KJ, Garbow JR, Jacob GS, Stejskal EO, Hopkins TL, Speirs RD (1987) Aromatic cross-links in insect cuticle: detection by solid-state ^{13}C and ^{15}N NMR. *Science* 235:1200–1204
- Schmitzova J, Klaudiny J, Albert S, Schroder W, Schreckengost W, Hanes J, Judova J, Simuth J (1998) A family of major royal jelly proteins of the honeybee *Apis mellifera* L. *Cell Mol Life Sci* 54:1020–1030
- Seago AE, Brady P, Vigneron JP, Schultz TD (2009) Gold bugs and beyond: a review of iridescence and structural colour mechanisms in beetles (Coleoptera). *J R Soc Interface* 6(Suppl 2):S165–S184
- Seidl B, Huemer K, Neues F, Hild S, Epple M, Ziegler A (2011) Ultrastructure and mineral distribution in the tergite cuticle of the beach isopod *Tylos europaeus* Arcangeli, 1938. *J Struct Biol* 174:512–526
- Semensi V, Sugumaran M (1986) Effect of MON-0585 on sclerotization of *Aedes aegypti* cuticle. *Pestic Biochem Physiol* 26:220–230
- Shamim G, Ranjan SK, Pandey DM, Ramani R (2014) Biochemistry and biosynthesis of insect pigments. *Eur J Entomol* 111:149–164
- Sharma P, Goel R, Capalash N (2007) Bacterial laccases. *World J Microb Biot* 23:823–832
- Shirataki H, Futahashi R, Fujiwara H (2010) Species-specific coordinated gene expression and trans-regulation of larval color pattern in three swallowtail butterflies. *Evol Dev* 12:305–314

- Sideri M, Tsakas S, Markoutsas E, Lampropoulou M, Marmaras VJ (2008) Innate immunity in insects: surface-associated dopa decarboxylase-dependent pathways regulate phagocytosis, nodulation and melanization in medfly haemocytes. *Immunology* 123:528–537
- Simon JD, Peles D, Wakamatsu K, Ito S (2009) Current challenges in understanding melanogenesis: bridging chemistry, biological control, morphology, and function. *Pigment Cell Melanoma Res* 22:563–579
- Simpson SJ, Sword GA, Lo N (2011) Polyphenism in insects. *Curr Biol* 21:R738–R749
- Sims SR, Shapiro AM (1984) Pupal color dimorphism in California *Battus philenor* (L.) (Papilionidae): mortality factors and selective advantage. *J Lepid Soc* 37:236–243
- Singh S, Malhotra AG, Pandey A, Pandey KM (2013) Computational model for pathway reconstruction to unravel the evolutionary significance of melanin synthesis. *Bioinformatics* 9:94–100
- Sloley BD (2004) Metabolism of monoamines in invertebrates: the relative importance of monoamine oxidase in different phyla. *Neurotoxicology* 25:175–183
- Smith AG (1978) Environmental factors influencing pupal colour determination in Lepidoptera. I. Experiments with *Papilio polytes*, *Papilio demoleus* and *Papilio polyxenes*. *Proc R Soc B* 200:295–329
- Smith AG (1980) Environmental factors influencing pupal colour determination in Lepidoptera. II. Experiments with *Pieris rapae*, *Pieris napi* and *Pieris brassicae*. *Proc R Soc B* 207:163–186
- Smith TJ (1990) Phylogenetic distribution and function of arylalkylamine *N*-acetyltransferase. *BioEssays* 12:30–33
- Smith CD, Zimin A, Holt C, Abouheif E, Benton R, Cash E, Croset V, Currie CR, Elhaik E, Elsik CG, Fave MJ, Fernandes V, Gadau J, Gibson JD, Graur D, Grubbs KJ, Hagen DE, Helmkampf M, Holley JA, Hu H, Viniegra AS, Johnson BR, Johnson RM, Khila A, Kim JW, Laird J, Mathis KA, Moeller JA, Munoz-Torres MC, Murphy MC, Nakamura R, Nigam S, Overson RP, Placek JE, Rajakumar R, Reese JT, Robertson HM, Smith CR, Suarez AV, Suen G, Suhr EL, Tao S, Torres CW, van Wilgenburg E, Viljakainen L, Walden KK, Wild AL, Yandell M, Yorke JA, Tsutsui ND (2011) Draft genome of the globally widespread and invasive Argentine ant (*Linepithema humile*). *Proc Natl Acad Sci U S A* 108:5673–5678
- Solano F (2014) Melanins: skin pigments and much more-types, structural models, biological functions, and formation routes. *New J Sci* 2014:1–28
- Sugumaran M (2002) Comparative biochemistry of eumelanogenesis and the protective roles of phenoloxidase and melanin in insects. *Pigment Cell Res* 15:2–9
- Sugumaran M (2009) Complexities of cuticular pigmentation in insects. *Pigment Cell Melanoma Res* 22:523–525
- Suh J, Jackson FR (2007) *Drosophila* Ebony activity is required in glia for the circadian regulation of locomotor activity. *Neuron* 55:435–447
- Suzuki Y, Nijhout HF (2006) Evolution of a polyphenism by genetic accommodation. *Science* 311:650–652
- Taira W, Otaki JM (2016) Butterfly wings are three-dimensional: pupal cuticle focal spots and their associated structures in junonia butterflies. *PLoS One* 11, e0146348
- Takahashi A (2013) Pigmentation and behavior: potential association through pleiotropic genes in *Drosophila*. *Genes Genet Syst* 88:165–174
- Takahashi A, Takano-Shimizu T (2011) Divergent enhancer haplotype of *ebony* on inversion *In(3R)Payne* associated with pigmentation variation in a tropical population of *Drosophila melanogaster*. *Mol Ecol* 20:4277–4287
- Takahashi A, Takahashi K, Ueda R, Takano-Shimizu T (2007) Natural variation of *ebony* gene controlling thoracic pigmentation in *Drosophila melanogaster*. *Genetics* 177:1233–1237
- Takeuchi K, Satou Y, Yamamoto H, Satoh N (2005) A genome-wide survey of genes for enzymes involved in pigment synthesis in an ascidian, *Ciona intestinalis*. *Zool Sci* 22:723–734
- Tamura K, Stecher G, Peterson D, Filipowski A, Kumar S (2013) MEGA6: molecular evolutionary genetics analysis version 6.0. *Mol Biol Evol* 30:2725–2729

- Tanaka S (2000) The role of [His(7)]-corazonin in the control of body-color polymorphism in the migratory locust, *Locusta migratoria* (Orthoptera : Acrididae). *J Insect Physiol* 46:1169–1176
- Tanaka S, Maeno K (2010) A review of maternal and embryonic control of phase-dependent progeny characteristics in the desert locust. *J Insect Physiol* 56:911–918
- Tanaka S, Zhu DH, Hoste B, Breuer M (2002) The dark-color inducing neuropeptide, [His(7)]-corazonin, causes a shift in morphometric characteristics towards the gregarious phase in isolated-reared (solitary) *Locusta migratoria*. *J Insect Physiol* 48:1065–1074
- Tawfik AI, Tanaka S, De Loof A, Schoofs L, Baggerman G, Waelkens E, Derua R, Milner Y, Yerushalmi Y, Pener MP (1999) Identification of the gregarization-associated dark-pigmentotropin in locusts through an *albino* mutant. *Proc Natl Acad Sci U S A* 96:7083–7087
- Tearle RG, Belote JM, McKeown M, Baker BS, Howells AJ (1989) Cloning and characterization of the *scarlet* gene of *Drosophila melanogaster*. *Genetics* 122:595–606
- Telonis-Scott M, Hoffmann AA, Sgro CM (2011) The molecular genetics of clinal variation: a case study of ebony and thoracic trident pigmentation in *Drosophila melanogaster* from eastern Australia. *Mol Ecol* 20:2100–2110
- Thomas BR, Yonekura M, Morgan TD, Czaplá TH, Hopkins TL, Kramer KJ (1989) A trypsin-solubilized laccase from pharate pupal integument of the tobacco hornworm, *Manduca sexta*. *Insect Biochem* 19:611–622
- Tian H, Peng H, Yao Q, Chen H, Xie Q, Tang B, Zhang W (2009) Developmental control of a lepidopteran pest *Spodoptera exigua* by ingestion of bacteria expressing dsRNA of a non-midgut gene. *PLoS One* 4, e6225
- Togawa T, Nakato H, Izumi S (2004) Analysis of the chitin recognition mechanism of cuticle proteins from the soft cuticle of the silkworm, *Bombyx mori*. *Insect Biochem Mol Biol* 34:1059–1067
- Togawa T, Augustine Dunn W, Emmons AC, Willis JH (2007) CPF and CPFL, two related gene families encoding cuticular proteins of *Anopheles gambiae* and other insects. *Insect Biochem Mol Biol* 37:675–688
- Tomoyasu Y, Arakane Y, Kramer KJ, Denell RE (2009) Repeated co-options of exoskeleton formation during wing-to-elytron evolution in beetles. *Curr Biol* 19:2057–2065
- Tribolium Genome Sequencing Consortium (2008) The genome of the model beetle and pest *Tribolium castaneum*. *Nature* 452:949–955
- True JR (2003) Insect melanism: the molecules matter. *Trends Ecol Evol* 18:640–647
- True JR, Edwards KA, Yamamoto D, Carroll SB (1999) *Drosophila* wing melanin patterns form by vein-dependent elaboration of enzymatic prepatterns. *Curr Biol* 9:1382–1391
- True JR, Yeh SD, Hovemann BT, Kemme T, Meinertzhagen IA, Edwards TN, Liou SR, Han Q, Li J (2005) *Drosophila tan* encodes a novel hydrolase required in pigmentation and vision. *PLoS Genet* 1, e63
- Tsuchida T, Koga R, Horikawa M, Tsunoda T, Maoka T, Matsumoto S, Simon JC, Fukatsu T (2010) Symbiotic bacterium modifies aphid body color. *Science* 330:1102–1104
- Turner CT, Davy MW, MacDiarmid RM, Plummer KM, Birch NP, Newcomb RD (2006) RNA interference in the light brown apple moth, *Epiphyas postvittana* (Walker) induced by double-stranded RNA feeding. *Insect Mol Biol* 15:383–391
- Umebachi Y (1990) β -Alanine and pigmentation of insect cuticle. Molting and metamorphosis. Japan Science and Society Press, Tokyo
- van de Kamp T, Riedel A, Greven H (2015) Micromorphology of the elytral cuticle of beetles, with an emphasis on weevils (Coleoptera: Curculionoidea). *Arthropod Struct Dev*. doi:10.1016/j.asd.2015.10.002
- Vavricka CJ, Han Q, Mehere P, Ding H, Christensen BM, Li J (2014) Tyrosine metabolic enzymes from insects and mammals: a comparative perspective. *Insect Sci* 21:13–19
- Veenstra JA (1989) Isolation and structure of corazonin, a cardioactive peptide from the American cockroach. *FEBS Lett* 250:231–234
- Veenstra JA (1991) Presence of corazonin in three insect species, and isolation and identification of [His7] corazonin from *Schistocerca americana*. *Peptides* 12:1285–1289

- Vetting MW, SdC LP, Yu M, Hegde SS, Magnet S, Roderick SL, Blanchard JS (2005) Structure and functions of the GNAT superfamily of acetyltransferases. *Arch Biochem Biophys* 433:212–226
- Vie A, Cigna M, Toci R, Birman S (1999) Differential regulation of *Drosophila* tyrosine hydroxylase isoforms by dopamine binding and cAMP-dependent phosphorylation. *J Biol Chem* 274:16788–16795
- Vieira R, Miguez JM, Aldegunde M (2005) GABA modulates day-night variation in melatonin levels in the cerebral ganglia of the damselfly *Ischnura graellsii* and the grasshopper *Oedipoda caerulescens*. *Neurosci Lett* 376:111–115
- Vivien-Roels B, Pevet P, Beck O, Fevre-Montange M (1984) Identification of melatonin in the compound eyes of an insect, the locust (*Locusta migratoria*), by radioimmunoassay and gas chromatography–mass spectrometry. *Neurosci Lett* 49:153–157
- Wagner S, Heseding C, Szlachta K, True JR, Prinz H, Hovemann BT (2007) *Drosophila* photoreceptors express cysteine peptidase tan. *J Comp Neurol* 500:601–611
- Walshe DP, Lehane SM, Lehane MJ, Haines LR (2009) Prolonged gene knockdown in the tsetse fly *Glossina* by feeding double stranded RNA. *Insect Mol Biol* 18:11–19
- Wan PJ, Jia S, Li N, Fan JM, Li GQ (2014) RNA interference depletion of the Halloween gene *disembodied* implies its potential application for management of planthopper *Sogatella furcifera* and *Laodelphax striatellus*. *PLoS One* 9, e86675
- Wang MX, Cai ZZ, Lu Y, Xin HH, Chen RT, Liang S, Singh CO, Kim JN, Niu YS, Miao YG (2013) Expression and functions of dopa decarboxylase in the silkworm, *Bombyx mori* was regulated by molting hormone. *Mol Biol Rep* 40:4115–4122
- Wappner P, Kramer KJ, Manso F, Hopkins TL, Q-A LA (1996) *N*- β -alanyldopamine metabolism for puparial tanning in wild-type and mutant *niger* strains of the Mediterranean fruit fly, *Ceratitis capitata*. *Insect Biochem Mol Biol* 26:585–592
- Werren JH, Richards S, Desjardins CA, Niehuis O, Gadau J et al (2010) Functional and evolutionary insights from the genomes of three parasitoid *Nasonia* species. *Science* 327:343–348
- Wigglesworth VB (1985) The transfer of lipid in insects from the epidermal cells to the cuticle. *Tissue Cell* 17:249–265
- Willis JH (2010) Structural cuticular proteins from arthropods: annotation, nomenclature, and sequence characteristics in the genomics era. *Insect Biochem Mol Biol* 40:189–204
- Willis JH, Papandreou NC, Iconomidou VA, Hamodrakas SJ (2012) Cuticular proteins. In: Gilbert LI (ed) *Insect molecular biology and biochemistry*. Academic, San Diego, pp 134–166
- Wittkopp PJ, Beldade P (2009) Development and evolution of insect pigmentation: genetic mechanisms and the potential consequences of pleiotropy. *Semin Cell Dev Biol* 20:65–71
- Wittkopp PJ, True JR, Carroll SB (2002a) Reciprocal functions of the *Drosophila* yellow and ebony proteins in the development and evolution of pigment patterns. *Development* 129:1849–1858
- Wittkopp PJ, Vaccaro K, Carroll SB (2002b) Evolution of *yellow* gene regulation and pigmentation in *Drosophila*. *Curr Biol* 12:1547–1556
- Wittkopp PJ, Carroll SB, Kopp A (2003a) Evolution in black and white: genetic control of pigment patterns in *Drosophila*. *Trends Genet* 19:495–504
- Wittkopp PJ, Williams BL, Selegue JE, Carroll SB (2003b) *Drosophila* pigmentation evolution: divergent genotypes underlying convergent phenotypes. *Proc Natl Acad Sci U S A* 100:1808–1813
- Wittkopp PJ, Stewart EE, Arnold LL, Neidert AH, Haerum BK, Thompson EM, Akhras S, Smith-Winberry G, Shefner L (2009) Intraspecific polymorphism to interspecific divergence: genetics of pigmentation in *Drosophila*. *Science* 326:540–544
- Wright TR (1987) The genetics of biogenic amine metabolism, sclerotization, and melanization in *Drosophila melanogaster*. *Adv Genet* 24:127–222
- Xia AH, Zhou QX, Yu LL, Li WG, Yi YZ, Zhang YZ, Zhang ZF (2006) Identification and analysis of YELLOW protein family genes in the silkworm, *Bombyx mori*. *BMC Genomics* 7:195
- Yamanaka A, Endo K, Nishida H, Kawamura N, Hatase Y, Kong WH, Kataoka H, Suzuki A (1999) Extraction and partial characterization of pupal-cuticle-melanizing hormone (PCMH) in the swallowtail butterfly, *Papilio xuthus* L. (Lepidoptera, Papilionidae). *Zool Sci* 16:261–268

- Yamanaka A, Imai H, Adachi M, Komatsu M, Islam AT, Kodama I, Kitazawa C, Endo K (2004) Hormonal control of the orange coloration of diapause pupae in the swallowtail butterfly, *Papilio xuthus* L. (Lepidoptera: Papilionidae). *Zool Sci* 21:1049–1055
- Yamanaka A, Adachi M, Imai H, Uchiyama T, Inoue M, Islam AT, Kitazawa C, Endo K (2006) Properties of Orange-Pupa-Inducing Factor (OPIF) in the swallowtail butterfly, *Papilio xuthus* L. *Peptides* 27:534–538
- Yamazaki HI (1969) The cuticular phenoloxidase in *Drosophila virilis*. *J Insect Physiol* 15:2203–2211
- Yamazaki HI (1972) Cuticular phenoloxidase from the silkworm, *Bombyx mori*: properties, solubilization, and purification. *Insect Biochem* 2:431–444
- Yang J, Cohen Stuart MA, Kamperman M (2014) Jack of all trades: versatile catechol crosslinking mechanisms. *Chem Soc Rev* 43:8271–8298
- Yatsu J, Asano T (2009) Cuticle laccase of the silkworm, *Bombyx mori*: purification, gene identification and presence of its inactive precursor in the cuticle. *Insect Biochem Mol Biol* 39:254–262
- Ye YX, Pan PL, Kang D, Lu JB, Zhang CX (2015) The multicopper oxidase gene family in the brown planthopper, *Nilaparvata lugens*. *Insect Biochem Mol Biol* 63:124–132
- Yoshida H (1883) Chemistry of lacquer (urushi). *J Chem Soc* 43:472–486
- Zeuss D, Brandl R, Brandle M, Rahbek C, Brunzel S (2014) Global warming favours light-coloured insects in Europe. *Nat Commun* 5:3874
- Zha W, Peng X, Chen R, Du B, Zhu L, He G (2011) Knockdown of midgut genes by dsRNA-transgenic plant-mediated RNA interference in the hemipteran insect *Nilaparvata lugens*. *PLoS One* 6, e20504
- Zhan S, Guo Q, Li M, Li M, Li J, Miao X, Huang Y (2010) Disruption of an *N*-acetyltransferase gene in the silkworm reveals a novel role in pigmentation. *Development* 137:4083–4090
- Zhang X, Zhang J, Zhu KY (2010) Chitosan/double-stranded RNA nanoparticle-mediated RNA interference to silence chitin synthase genes through larval feeding in the African malaria mosquito (*Anopheles gambiae*). *Insect Mol Biol* 19:683–693
- Zhang J, Khan SA, Hasse C, Ruf S, Heckel DG, Bock R (2015) Pest control. Full crop protection from an insect pest by expression of long double-stranded RNAs in plastids. *Science* 347:991–994
- Zhou X, Wheeler MM, Oi FM, Scharf ME (2008) RNA interference in the termite *Reticulitermes flavipes* through ingestion of double-stranded RNA. *Insect Biochem Mol Biol* 38:805–815
- Zhu JQ, Liu S, Ma Y, Zhang JQ, Qi HS, Wei ZJ, Yao Q, Zhang WQ, Li S (2012) Improvement of pest resistance in transgenic tobacco plants expressing dsRNA of an insect-associated gene EcR. *PLoS One* 7, e38572

Chapter 7

Insect Hydrocarbons: Biochemistry and Chemical Ecology

Matthew D. Ginzel and Gary J. Blomquist

Abstract Cuticular hydrocarbons of insects often consist of complex mixtures of straight chain, unsaturated and methyl-branched components with 21 to 40+ carbons. They function to restrict water loss, to prevent a lethal rate of desiccation and serve in chemical communication in many species. This chapter describes the chemistry and chemical ecology of insect hydrocarbons with an emphasis on their role as close range or contact pheromones. Hydrocarbons are formed in oenocytes and their biosynthetic pathways are described. Recent work has begun to take advantage of the tools of molecular biology to better understand hydrocarbon formation and this information is summarized. The various methods by which insects utilize hydrocarbons as inter- and intraspecific chemical signals are also described.

7.1 Introduction

Hydrocarbons on the surface of insects are essential to prevent desiccation and death of insects and have evolved to play a number of roles in chemical communication where relatively non-volatile components are used (Howard and Blomquist 2005; Bagnères and Lorenzi 2010; Blomquist and Bagnères 2010; Ginzel 2010; Greene 2010; Liebig 2010; van Zweden and d'Ettorre 2010). They are comprised of long-chain, non-isoprenoid components of 21 to 40+ carbons. Due to their small size, insects have large surface area to volume ratios and are therefore susceptible to rapid water loss. The ability of insects to withstand desiccation was recognized in the 1930s to be due in part to the epicuticular wax layer on the cuticle. The presence

M.D. Ginzel

Departments of Entomology and Forestry & Natural Resources,
Hardwood Tree Improvement and Regeneration Center, Purdue University,
West Lafayette, IN, USA
e-mail: mginzel@purdue.edu

G.J. Blomquist (✉)

Department of Biochemistry and Molecular Biology, University of Nevada,
1664 North Virginia Street, Reno, NV 89557-0300, USA
e-mail: garyb@cabnr.unr.edu

of hydrocarbons in this wax layer was suggested by Chibnall et al. (1934) and Blount et al. (1937), and over the next few decades the importance of hydrocarbons in the cuticular wax of insects was established (Baker et al. 1963). The development and application of combined gas-liquid chromatography and mass spectrometry was key to the rapid and efficient analyses of insect hydrocarbons. In the late 1960s and during the next few decades, GC-MS analyses of insect hydrocarbons were established (Nelson and Sukkestad 1970), and since that time hydrocarbons of thousands of insect species were analyzed, first on packed columns, and then much more efficiently on capillary columns. It became recognized that for many insect species, very complex mixtures of normal (straight-chain), methyl-branched and unsaturated components exist (Howard and Blomquist 2005; Blomquist 2010a).

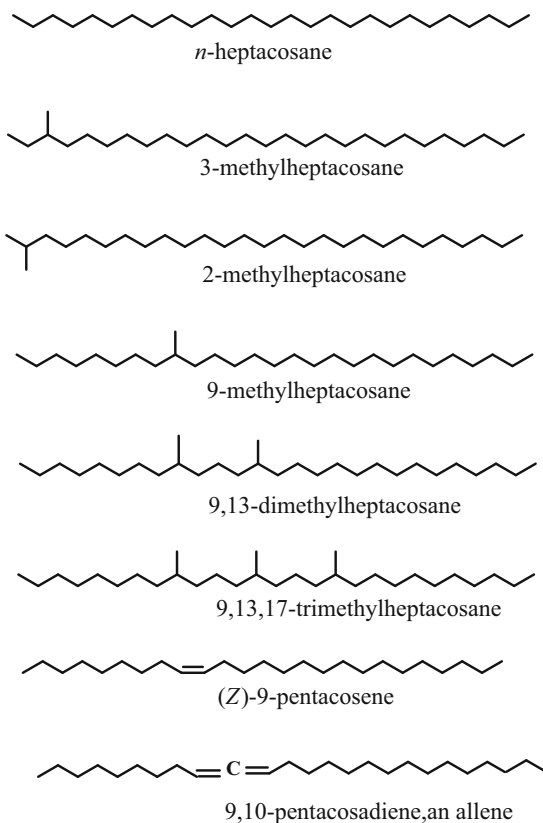
Studies on the biosynthesis of insect hydrocarbons have evolved from *in vivo* experiments in the 1970s and 1980s, in which radiolabeled and stable isotope precursors were used to establish the biochemical pathways of hydrocarbons, to recent work aimed at determining genes involved in hydrocarbon production using RNA interference and expressing and assaying key enzymes.

7.2 Chemical Composition of Insect Hydrocarbons

The hundreds of different cuticular hydrocarbon components reported in insects can be divided into three major classes: *n*-alkanes, saturated methyl-branched components and unsaturated hydrocarbons (Fig. 7.1). There are examples of other types of components including unsaturated methyl-branched components, but these are not common and often are present in small amounts. Fletcher et al. (2001, 2008) and McGrath et al. (2003) reported a novel group of allenic hydrocarbons from five species of Australian beetles, C₂₃ to C₂₇ dienes in which the double bonds are on adjacent carbons. Methyl-branched hydrocarbons have been shown to have up to four methyl branches, and the alkenes have up to four double bonds. Most of the alkenes have *cis* double bonds, and the positions of the double bonds, while often in the 9-position, can be almost anywhere on the carbon chain.

A long standing question regarding the methyl-branched alkanes was “what is their absolute stereochemistry”? In a remarkable piece of work, the Millar laboratory (Bello et al. 2015) isolated 36 monomethylalkanes from 20 species of insects representing nine orders and, using digital polarimetry with comparisons to known standards, showed all to be in the (*R*) configuration. This is consistent with the contact sex pheromone of the German cockroach, (3*S*,11*S*)-dimethylnonacosan-2-one (Eliyahou et al. 2008), which in order to have the *S*, *S* configuration in the ketone would have been derived from (3*R*, 11*S*)-dimethylnonacosane (Chase et al. 1992). Of course there was the possibility that the *R*, *S* dimethylalkane could have been enzymatically selected from a racemic mixture during hydroxylation of 3,11-dimethylnonacosane to the corresponding alcohol (Chase et al. 1992) that would then be oxidized to the ketone. The (*R*) configuration of the monomethylalkanes has interesting ramifications for the biosynthesis of methyl-branched hydro-

Fig. 7.1 Structures of representative insect cuticular hydrocarbons



carbons, indicating that the reduction of the alkene intermediate during biosynthesis is stereochemically specific. The stereochemistry of di- and trimethylalkanes has not been explored, but since they would likely be inserted by the same enzyme, the 2nd, 3rd and 4th methyl group would likely have the same orientation. Because of the assignment of the four groups on the chiral carbon, the second carbon on a dimethylalkane would likely have the (*S*) configuration. The 2-methylalkanes lack a chiral center and therefore are not *R* or *S*.

The variety of chain lengths and the number and positions of the methyl branches and double bonds provides insects that use cuticular hydrocarbons in chemical communication with a large number of possible structures, the chemical equivalent of the variably colored plumage of birds. The chain lengths of insect hydrocarbons vary from about 21 up to 40 and in some rare cases even 50 carbons. Cvačka et al. (2006) used MALDI mass spectrometry to describe a series of hydrocarbons from insect cuticles with up to 70 carbons. These very long chain components have not been verified to date. There are a number of reviews of the chemistry of cuticular hydrocarbons and the use of mass spectrometry to identify each component (Nelson and Blomquist 1995; Howard and Blomquist 2005; Blomquist 2010b; Millar 2010). Determining the Kovats index or the Equivalent Chain Length is useful in structure assignments, as the positions of the methyl group(s) decrease the retention times in

a known manner (Lockey 1985; Carlson et al. 1998a). It is difficult to determine the positions of double bonds without first derivatizing the alkene. Dimethyldisulfide derivatives are the method of choice (Francis and Veland 1981; Carlson et al. 1989) and methoxymercuration-demercuration has also been used (Blomquist et al. 1980). It is sometimes useful to consider the biosynthetic feasibility of the compound when proposing structures for cuticular hydrocarbons. Oxygenated components of cuticular lipids are also often present in small amounts associated with cuticular hydrocarbons. These include wax esters, sterols, primary and secondary alcohols, diols, ethers, epoxides, ketones and other components (Buckner 2010) and serve as semi-chemicals in some cases (see Dani et al. 2001).

7.3 Hydrocarbon Biosynthesis

7.3.1 *Oenocytes are the Site of Insect Hydrocarbon Biosynthesis*

In the fruit fly *Drosophila melanogaster*, Ferveur et al. (1997) showed that the targeted expression of *transformer* in male oenocytes resulted in the feminization of the hydrocarbon pheromone profile. In the German cockroach, Gu et al. (1995) presented evidence indicating that only the abdominal sternites and tergites synthesize hydrocarbons, which are then loaded onto hemolymph lipophorin for transport to sites of deposition. However, the mechanism of unloading and transport of hydrocarbon across the cuticle is unknown. The Schal laboratory (Fan et al. 2003) enzymatically dissociated the oenocytes of the abdominal integument of the German cockroach and separated them by Percoll gradient centrifugation. Using radiolabeled propionate, they showed that hydrocarbon synthesis was highest in the fractions most enriched in oenocytes. *D. melanogaster* *Cyp4g1*, which encodes the cytochrome P450 catalyzing the terminal step in hydrocarbon production, is expressed predominantly in oenocytes (Qiu et al. 2012), and the fatty acid synthase (FAS) that is involved in producing 2-methylalkanes is also localized to the oenocytes (Chung et al. 2014).

Different species may vary in regards to whether or not the entire hydrocarbon is formed in oenocytes. Incorporation of ^{13}C -labeled acetate into housefly alkenes showed that the hydrocarbon appeared to be equally labeled throughout the chain, indicating that the entire molecule was synthesized in oenocytes (Dillwith et al. 1982). In contrast, the American cockroach incorporated ^{13}C -acetate only into carbons 19-27 of (*Z*, *Z*)-6,9-heptacosadiene (Dwyer et al. 1981b), suggesting that it produced the linoleic acid (Blomquist et al. 1982) needed for the synthesis of the C27 diene in other tissue. Wicker-Thomas et al. (2015) and Chung et al. (2014) provided evidence that unsaturated fatty acyl and 2-methyl- fatty acyl precursors are made in oenocytes whereas some fatty acids may be imported into oenocytes for elongation and conversion to hydrocarbons.

7.3.2 Biosynthetic Pathways for Hydrocarbons

The biosynthesis of insect hydrocarbons can be divided into four steps: (1) formation of the straight chain saturated, unsaturated and methyl-branched fatty acid precursors, (2) elongation of these fatty acids to very long chain fatty acyl-CoAs, (3) conversion of the very long chain fatty acyl-CoAs to aldehydes and (4) the reductive decarbonylation of aldehydes to hydrocarbons.

7.3.2.1 Production of Fatty Acid Precursors

2-Methylalkanes arise from the elongation of the carbon skeleton of either valine (even number of carbons in the chain) or isoleucine (odd number of carbons in the chain) (Blailock et al. 1976; Fig. 7.2). The gene that forms the *n*-2-methyl branched fatty acid precursors to the 2-methylalkanes was identified in *D. melanogaster*. RNAi-mediated silencing showed that a fatty acid synthase gene (FASN^{CG3524}), one of three FASs in *D. melanogaster*, markedly decreased production of 2-methylalkanes (Chung et al. 2014) but not *n*-alkanes or alkenes. This provides strong evidence that this FAS is required for 2-methylalkane synthesis. An alternate FAS, FASN^{CG3523}, is expressed in the fat body but not the oenocytes, suggesting that all the enzymes necessary for hydrocarbon production are localized to the oenocytes, but some fatty acids are imported to oenocytes for *n*-alkane production (Wicker-Thomas et al. 2015).

The 3-methyl- and internally branched methyl-branched hydrocarbons arise from the incorporation of propionate during chain elongation (Blomquist et al. 1975; Blomquist and Kearney 1976). The labeled carbon from [1-¹³C]propionate was found exclusively in the 4-position of 3-methylpentacosane as demonstrated by

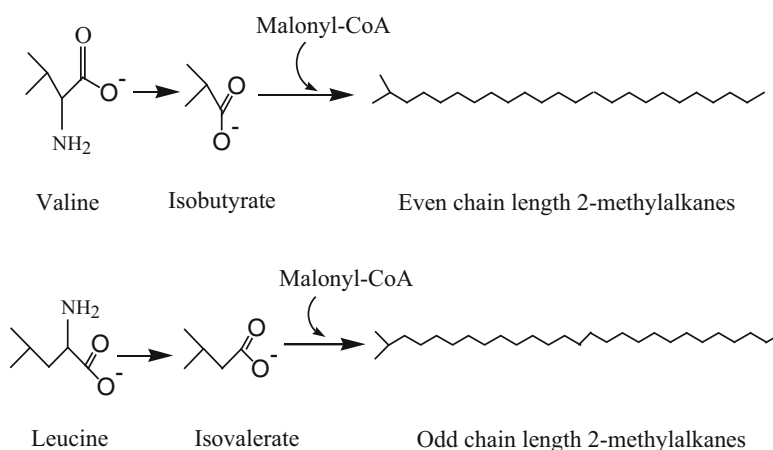


Fig. 7.2 Biosynthetic pathway for 2-methylalkanes

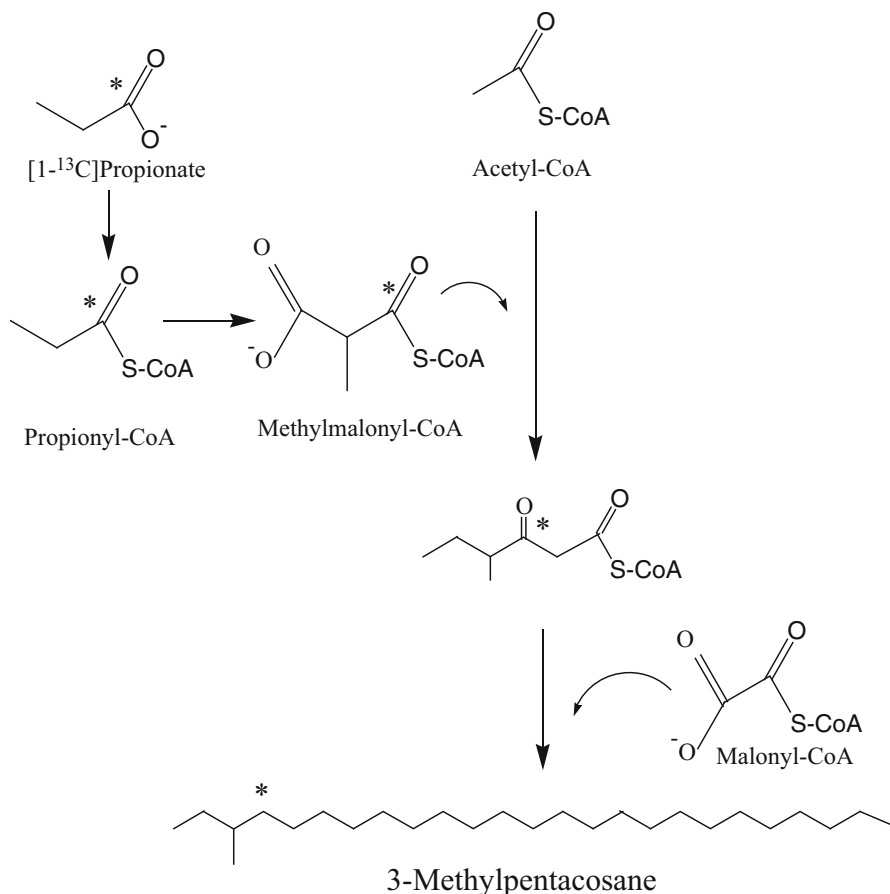


Fig. 7.3 Biosynthesis of 3-methylalkanes. The carbon from [1-¹³C]propionate labels carbon-4 of 3-methylpentacosane and not carbon-2, indicating the methyl branching group is put on as the second unit in the biosynthetic process

carbon-13 NMR in the American cockroach (Dwyer et al. 1981a), indicating that it was incorporated as methylmalonyl-CoA as the second group added to the growing chain (Fig. 7.3).

The internally branched methylalkanes also arise from the insertion of a propionate group, as a methylmalonyl-CoA, derived from valine, isoleucine or methionine (Dillwith et al. 1982) in place of a malonyl-CoA at specific points during chain elongation (Fig. 7.4). ¹³C-NMR studies (Dwyer et al. 1981a; Chase et al. 1990; Dillwith et al. 1982) were used to determine if the methyl branching group was put on early or late in hydrocarbon formation. In every case where it has been studied (Dwyer et al. 1981a; Dillwith et al. 1982; Chase et al. 1990), the methyl branch is put on early in chain synthesis by a fatty acid synthase rather than toward the end of the process by an acyl-CoA elongation enzyme. An examination of the

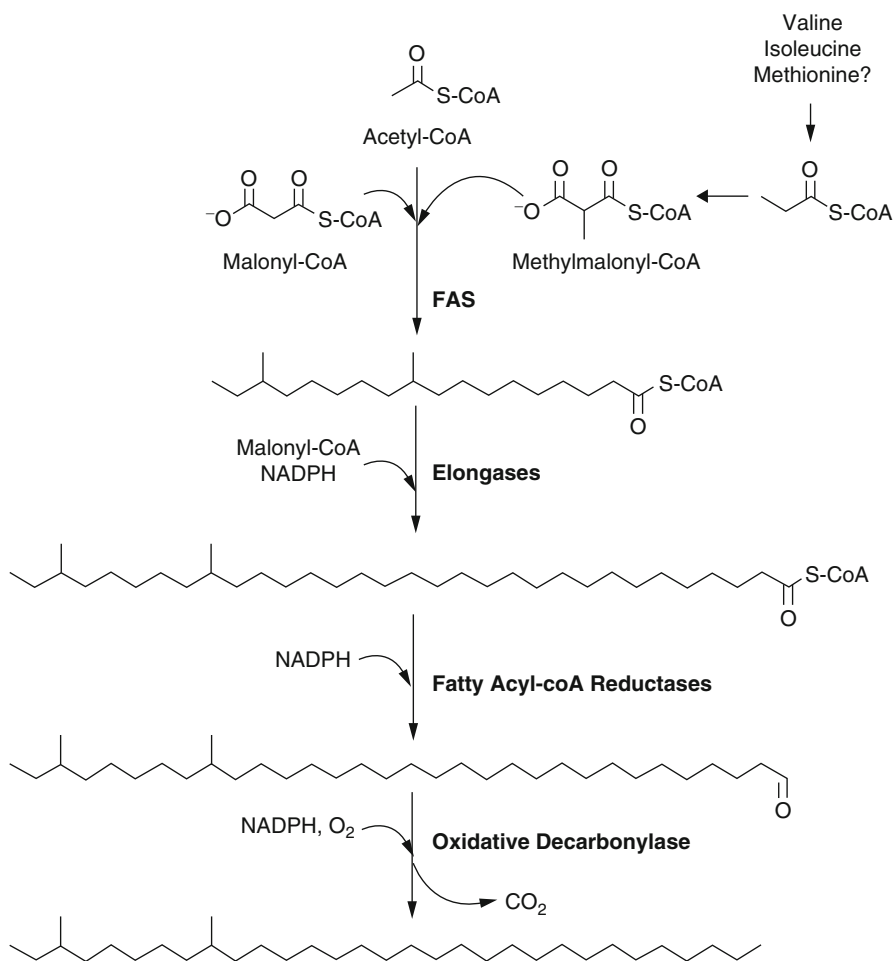


Fig. 7.4 Biosynthetic pathways for internally methyl-branched hydrocarbons in insects

methyl-branched fatty acids from the integument of the German cockroach (Juarez et al. 1992) and the housefly (Blomquist et al. 1994) showed that small amounts of fatty acids with the appropriate methyl branching to serve as precursors to hydrocarbons were present in both species. A comparison of a soluble and a microsomal FAS in the housefly (Gu et al. 1995) and the German cockroach (Juarez et al. 1992) showed that the microsomal FAS was more effective than a cytosolic FAS in incorporating methylmalonyl-CoA into a growing fatty acid chain. The presence of a unique FAS that is involved in synthesizing 2-methylalkanes in *D. melanogaster* (Chung et al. 2014) suggests that there may also be specific FASs that insert methylmalonyl-CoA at specific points during the formation of the methyl-branched fatty acid precursors to the internally branched hydrocarbons. *D. melanogaster* produces a very small amount of internally methyl-branched hydrocarbons (Dembeck et al.

2015). All insect genomes studied to date appear to have two or more FASs, lending credibility to the hypothesis of a unique FAS that produces methyl-branched fatty acid precursors to hydrocarbons.

Desaturase 1 (*desat1*) in *D. melanogaster* accepts both palmitic acid and stearic acid to form palmitoleic (Δ^9 C_{16:1}) and oleic (Δ^9 C_{18:1}) acids. This gene is expressed in both fat body and oenocytes and appears to play a role in general lipid metabolism and in hydrocarbon production (Wicker-Thomas and Chertemps 2010). A *desat2* converts myristic (C_{14:0}) to myristoleic (Δ^9 C_{14:1}, an n-5 double bond) in flies that produce a 5,9-alkadiene (Dallerac et al. 2000). A second desaturation is required for females that produce 5,9- and 7,11-diene. RNA interference was used to study this gene (Chertemps et al. 2007). This desaturase was found only in females and thus was named *desatF* (reviewed in Wicker-Thomas and Chertemps 2010).

7.3.2.2 Elongation: Chain Length Specificity and Elongases

The regulation of chain length to produce the specific blend of hydrocarbons often used in chemical communication appears to reside in the microsomal fatty acyl-CoA elongase reactions and the fatty acyl-CoA reductases. The American cockroach, *Periplaneta americana*, produces three major hydrocarbons: *n*-pentacosane, 3-methylpentacosane and (*Z*, *Z*)-9,12-heptacosadiene (Baker et al. 1963). Studies with microsomes from integument tissue showed that stearyl-CoA was elongated up to a 26 carbon acyl-CoA that could serve as the precursor to *n*-pentacosane (Fig. 7.5). In contrast, linoleoyl-CoA was readily elongated to 28 carbons (but not longer) to serve as the precursor to the 27:2 hydrocarbon (Fig. 7.5) (Vaz et al. 1988). In the housefly, the picture is even clearer, although more complicated. Laboratory-reared female houseflies produce monoenes of 27 carbons or longer for the first 2 days after adult eclosion, and then switch, at about 3 days post-eclosion, to producing (*Z*)-9-tricosene, a short range sex pheromone (Dillwith et al. 1983). Microsomes from 1 day old adult females readily elongate both 18:1-CoA and 24:1-CoA up to 28 carbons (Tillman-Wall et al. 1992). Microsomes from day-4 females elongate 18:1 to 24:1 and do not effectively elongate 24:1-CoA. In contrast, males, which produce 27 carbon and longer alkenes at all ages, readily elongate both 18:1-CoA and 24:1-CoA to 28:1-CoA. Microsomes from males, which normally do not make 23:1 hydrocarbon, readily convert 24:1-CoA to C23 alkenes (Tillman-Wall et al. 1992), so *in vivo*, elongation enzyme activity must prevail over fatty acyl-CoA reductase activity at that chain length. To further emphasize the importance of the fatty acyl-CoA elongation reactions in controlling chain length, microsomes from day-1 and day-4 females and males of both ages all convert both 28:1-CoA, 24:1-CoA and the 28:1, 24:1 and 18:1 aldehyde to hydrocarbons one carbon shorter (Reed et al. 1996).

The *D. melanogaster* genome has 19 elongases, with only two of them characterized to date (Wicker-Thomas and Chertemps 2010). Fatty acyl-CoA elongases catalyze the condensation of malonyl-CoA and a fatty acyl-CoA, and three additional steps are required to reduce the ketone to an alcohol, followed by dehydrogenation

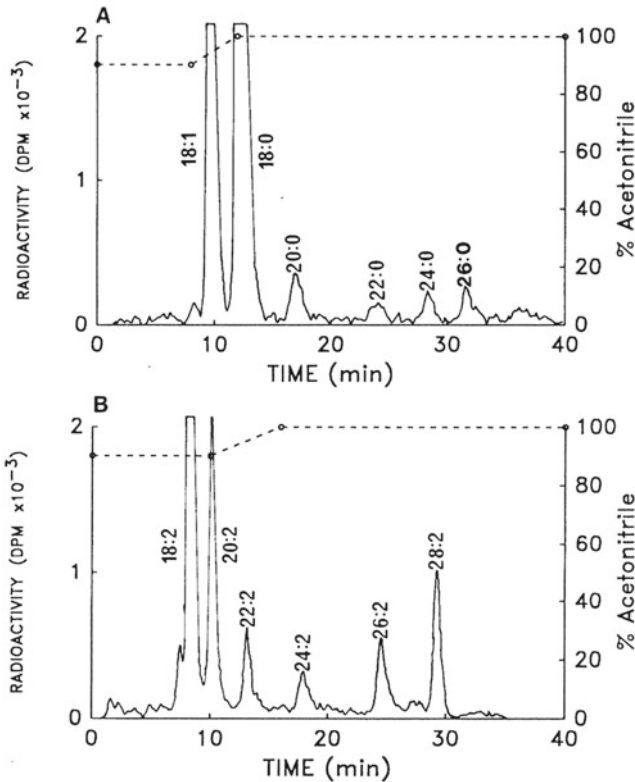


Fig. 7.5 Radio-HPLC products of the elongation of stearyl-CoA (A) and linoleyl-CoA (B) in microsomes of *P. americana*

and reduction. In other systems, the first step controls the chain length specificity (Haslam and Kunst 2013). The elongase *eloF* from *D. melanogaster* (Chertemps et al. 2007) was expressed in yeast and the results showed that *eloF* elongated both saturated and unsaturated fatty acids up to C30. A dramatic decrease in C29 dienes and an increase in C25 dienes was observed when *eloF* was knocked down by RNAi, with a concomitant decrease in courtship and mating activities. Expression of *eloF* was much higher in females than males.

7.3.2.3 Acyl-CoA Reductases

Acyl-CoA reductase activity was demonstrated in microsomes of integument enriched tissue from the housefly, and the aldehyde was trapped with hydroxylamine (Reed et al. 1994). Acyl-CoA reductases have been described in insects for the production of pheromones in Lepidoptera (Antony et al. 2009) and AmFAR1 was described in the honey bee (Teerawanichpan et al. 2010) that converts C14 to

C22 fatty acyl-CoAs to primary alcohols. Little is known about this system as it relates to hydrocarbon production in insects. All acyl-CoA reductases described in insects to date (Carot-Sans et al. 2015) reduce the acyl-CoA to the primary alcohol, and this raises the possibility that the acyl-CoA reductases in hydrocarbon production produce the alcohol which is then oxidized to the aldehyde by CYP4Gs.

7.3.2.4 Aldehyde Decarboxylases

The mechanism of long-chain fatty acid derived hydrocarbon biosynthesis is now coming into focus. It is now clear that very long chain fatty acyl-CoAs are reduced to aldehydes (Fig. 7.6) and then converted to hydrocarbons by the loss of the carbonyl carbon in insects. Plants and algae use a reductive decarbonylation of aldehydes that does not require oxygen and bacteria appear to use a variety of mechanisms for hydrocarbon biosynthesis (Bognar et al. 1984; Cheesbrough and Kolattukudy 1988; Dennis and Kolattukudy 1991; Ladygina et al. 2006; Schirmer et al. 2010; Bernard and Joubès 2013; Marsh et al. 2013; Sakuradani et al. 2013).

Insects use an aerobic mechanism for oxidative decarbonylation of aldehydes. This is consistent with plants appearing on land much earlier than insects and under oxygen levels that were much lower (Payne et al. 2009), while insects developed an aerobic mechanism for hydrocarbon production consistent with higher oxygen levels when their ancestors came to land. It is now clear that a cytochrome P450 is involved in the conversion of the aldehyde to hydrocarbon and carbon dioxide in a process that requires molecular oxygen and NADPH (Reed et al. 1994, 1995; Mpuru et al. 1996). In housefly microsomes, incubation of (Z)-15- [1- ^{14}C]- and (Z)-15- [15,16- $^3\text{H}_2$]tetracosenoyl-CoA and the corresponding aldehydes in the presence of NADPH gave equal amounts of $^{14}\text{CO}_2$ and [^3H](Z)-9-tricosene (Reed et al. 1994). The requirement for NADPH and O_2 , and inhibition by CO and antibody to cytochrome P450 reductase strongly implicated a cytochrome P450 in the reaction. Further work with microsomes from a variety of insects showed that [9,10- ^3H , 1- ^{14}C]18:0 aldehyde was converted to a C17 hydrocarbon and CO_2 in the presence of O_2 and NADPH, indicating that the pathway for hydrocarbon formation in insects

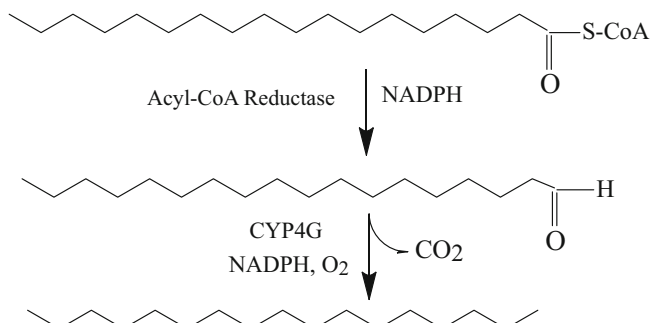


Fig. 7.6 Conversion of fatty acyl-CoAs to hydrocarbons in insects

involved the reduction of the acyl-CoA to aldehyde followed by a cytochrome P450 mediated oxidative decarbonylation (Mpuru et al. 1996). CI-GC-MS analyses of the *n*-tricosene formed by microsomal preparations from deuterated substrates showed that the deuteriums on the 2,2 and 3,3 positions of 24:1-CoA were retained on the hydrocarbon product, and that the deuterium on [1-²H]tetracosenal was transferred to the hydrocarbon product. From this and related work (Reed et al. 1995), a mechanism was proposed by which the cytochrome P450 abstracts an electron from the C=O double bond of the carbonyl group of the aldehyde. The reduced perferryl attacks the 1-carbon of the aldehyde to form a thiyl-iron-hemiacetal diradical. The latter intermediate can fragment to form an alkyl radical and a thiyl-iron-formyl radical. The alkyl radical then abstracts the formyl hydrogen to produce the hydrocarbon and CO₂ (Reed et al. 1995).

Full confirmation of the oxidative decarbonylation system proposed in insects awaited the cloning, expression and characterization of the enzymes involved. Toward this end, integument-enriched cytochrome P450 cDNAs in the housefly, *Musca domestica* (Qiu et al. 2012) were isolated. One of these, CYP4G2, has 71.7% amino acid identity and 81.8% similarity to its ortholog, CYP4G1, from *D. melanogaster*. Numerous attempts to express CYP4G2 by itself (Blomquist, Tittiger and Young, unpublished) led to inactive enzyme that did not absorb at 450 nm in the presence of carbon monoxide. The relatively high ratio of cytochrome P450 reductase (CPR) in oenocytes (Qiu et al. 2012) suggested the possibility that CPR was needed for CYP4G2 to properly fold. Expression of the CYP4G2-CPR fusion protein yielded an enzyme that in the presence of CO absorbed at 450 nm and converted long chain aldehydes to alkanes (Qiu et al. 2012). Two transgenic *D. melanogaster* lines (3972-R1 and 3972-R2) bearing CYP4G1 hairpin sequences under control of the yeast UAS promoter were obtained and crossed individually with a transgenic line carrying the Gal4 transcription factor gene under control of an oenocyte-specific promoter (Ferveur et al. 1997). Offspring from these crosses express CYP4G1 hairpin RNAs specifically in their oenocytes, thus triggering RNAi-mediated post-transcriptional gene silencing of *CYP4G1* in oenocyte cells. The amount of hydrocarbon produced by these flies was less than 100 ng/fly, as compared to about 1500 ng/fly in parental (control) insects (Qiu et al. 2012). The amount of *cis*-vaccenyl acetate was constant in experimental and control flies, indicating that fatty acid synthesis was not affected. In addition, the expressed CYP4G2 as a fusion protein with cytochrome P450 reductase converted both tritium and deuterium labeled C18 aldehyde to C17 hydrocarbon (Qiu et al. 2012). Thus, we have strong evidence that CYP4G2 and CYP4G1 are the P450s involved in hydrocarbon biosynthesis. To date, CYP4G2 (housefly, Qiu et al. 2012), CYP4G16 (The African malaria mosquito, *Anopheles gambiae*) and CYP4G55 and 56 (the mountain pine beetle, *Dendroctonus ponderosae*) but not CYP4G13 (housefly) (MacLean, Tittiger and Blomquist, unpublished) have been expressed as fusion proteins with housefly CPR and shown to be oxidative decarbonylases. All insects whose genomes are known have one or more CYP4G, and we hypothesize that one or more are involved in catalyzing the last step in hydrocarbon production.

7.4 Ecological and Behavioral Aspects

Long-chain hydrocarbons have evolved to play a plethora of roles in insects, from the essential role of restricting water loss to serving important functions in chemical communication. For chemical communication, insects have evolved to form very complicated mixture of *n*-, mono-, di-, tri- and tetramethyl branched and unsaturated components at apparently low cost, as they have modified existing components. A single component or a mixture of hydrocarbon components of the wax layer of almost all arthropods serve as the primary chemical signal to answer questions such as: “Are you a member of my species? Are you the same sex as me?” For subsocial insects, “Are you a member of my family, cohort or group?” For eusocial insects, “Are you a member of my colony? Are you a member of my nest? To which caste do you belong? Are you a queen or perhaps brood? Are you a worker trying to convey to me the need to accomplish a certain task? Are you closely related kin?” And, for many arthropods that exist asinquilines in the nest of social insects, “Can you recognize that I am alien?” (Howard and Blomquist 2005; Blomquist and Bagnères 2010).

We now recognize that hydrocarbons serve critical roles as sex pheromones, kairomones, species and sex recognition cues, nestmate recognition, dominance and fertility cues, chemical mimicry, primer pheromones, task specific cues and even as cues for maternal care of offspring (Blomquist and Bagnères 2010). The complex mixture of hydrocarbons on the surface of insects has allowed them to be used in chemotaxonomy and they are gaining importance in forensic entomology (Moore et al. 2013; Roux et al. 2008; Drijfhout 2010; Braga et al. 2013). In retrospect, the diversity of hydrocarbons and hydrocarbon blends on insect cuticles might have suggested that hydrocarbons could play important roles in chemical communication. Only after the recognition of the number and variety of roles they do play in chemical communication have we come to more fully appreciate the importance of insect hydrocarbons in chemical communication. In this section of the chapter, we will explore the many types of behaviors that are mediated by cuticular hydrocarbons.

7.4.1 *Species and Sex Recognition*

The wax layer on the insect cuticle is comprised of a complex mixture of long-chain hydrocarbons, fatty acids, alcohols, esters, aldehydes, and ketones that protects insects from desiccation (Gibbs 1998). The hydrocarbon components of the cuticular lipid layer also act as mate recognition signals in many insect species (reviewed by Nelson 1993; Howard and Blomquist 2005), and may be saturated or unsaturated, terminally branched monomethyl alkanes, or internally branched methyl alkanes (Lockey 1980; Nelson et al. 1988). The structural variability of these hydrocarbons allows for the diversity of insect pheromones, and their chemical stability and low volatility make them particularly suitable as chemical signals for species and mate recognition (Dani et al. 2001; Howard and Blomquist 2005).

In solitary insects, cuticular hydrocarbons (CHCs) mediate species recognition (Howard and Blomquist 2005) and, in such cases, may serve as a prezygotic mating isolation mechanism in closely related taxa (Ferveur 2005; Peterson et al. 2007). For example, eight species of the pine cone *Conophthorus* beetles can be easily distinguished on the basis of differences in the alkenes and mono-, di-, and trimethylalkanes. Closely related species of bark beetles in the genus *Dendroctonus* can be separated on the basis of their CHC profiles (Page et al. 1990). Also, geographically isolated populations of *D. frontalis*, each from a different host, are quantitatively very similar (Page et al. 1990), further illustrating the potential of CHCs as chemotaxonomic characters for closely related beetles. More recently, bioassays have provided a stronger link between CHCs and species recognition in insects. In *Nasonia* jewel wasps, for example, males respond to CHCs of females and multivariate analysis revealed that four species of the genus are distinguishable on the basis of CHC profiles (Buellesbach et al. 2014). Sexual isolation between two sympatric and synchronic sister species of elm beetles in the genus *Pyrrhalta* is achieved by divergence in their CHC profiles. In fact, CHC profiles are quite different between the species: methyl-branched alkanes between C29 and C35 are predominantly saturated in the elm leaf beetle, *P. maculicollis*, while shorter chain length (between C22 and C29) mono-methyl-branched alkanes are more prevalent in the CHC profiles of *P. aenescens* (Zhang et al. 2014). Moreover, males mate more readily with conspecific females or heterospecific females treated with conspecific CHCs (Zhang et al. 2014). Males of the diurnal firefly *Ellychnia corrusca* are also attracted to cuticular extracts of conspecifics over those of a diurnal heterospecific, *Lucidota atra* (South et al. 2008).

In the *D. melanogaster* subgroup, four species possess characteristic combinations of CHCs (Ferveur 2005), which may serve as species barriers between its members. Male *D. melanogaster* halt courtship with an interspecific female or a conspecific male (Billeter et al. 2009; Savarit et al. 1999). It appears that in this group, one compound, 7,11-heptacosadiene, serves as a “badge” for female *D. melanogaster* (Jallon and David 1987) and may play an important role in reproductive isolation among these closely-related species and guard against investing energy and resources in failed attempts to mate with members of different, but closely related species. In such cases, mate recognition among closely related species is typically achieved through the use of structurally similar compounds (Dani et al. 2001; Wyatt 2014). For example, the contact pheromones of congeneric long-horned beetles in the tribe Clytini (*Megacyllene caryae* and *M. robinae*) are single alkanes and chain length analogues. The contact pheromone of another clytine long-horned beetle, *Neoclytus a. acuminatus* is a blend of 7-methylheptacosane, 9-methylheptacosane and 7-methylpentacosane (Lacey et al. 2008). Interestingly, 9-methylheptacosane is also part of the cuticular profile of female *M. caryae* (Ginzel et al. 2006) and apparently a component of the contact pheromone of *Anoplophora malasiaca* (Fukaya et al. 2000), suggesting that some hydrocarbons may be common within taxonomical groups.

Due to the species-specificity of CHCs, the compounds not only serve as cues for discriminating conspecifics, but also play important roles in courtship and mate

recognition. For example, early work in Diptera established that males of the housefly, *Musca domestica*, are attracted to solvent extracts of virgin females (Silhacek et al. 1972), and the hydrocarbon, (Z)-9-tricosene, on the cuticle of the female acts as a sex pheromone for male flies (Carlson et al. 1971). Since that time, CHC contact sex pheromones are known from several insect orders including Diptera (Stoffolano et al. 1997; Carlson et al. 1998b; Wicker-Thomas 2007; Ferveur and Cobb 2010), Hymenoptera (Syvertsen et al. 1995; Steiner et al. 2006; Böröczky et al. 2009; Kühbandner et al. 2013), and Coleoptera (McGrath et al. 2003; Sugeno et al. 2006; Geiselhardt et al. 2009; Silk et al. 2009; Ginzl 2010; Ming and Lewis 2010).

7.4.1.1 Bioassays and Sampling Cuticular Hydrocarbons

Our understanding of contact chemoreception in insects has increased greatly through the use of bioassays (see Ginzl 2010). In such assays, a female insect is freeze-killed and then presented to a male in a Petri dish arena. If the male attempts to mate with the female, it demonstrates that recognition cues on the cuticle are intact. The CHCs are then stripped from the cuticle of the female by immersing her in successive aliquots of solvent. The female is then allowed to air dry before she is reintroduced to the male to test whether he will respond to her in any way. If the male does not attempt to mate with the washed female, it confirms that solvent washing removed chemical cues that mediate mate recognition. The crude CHC extract is then pipetted back onto the solvent-washed female to determine the extent to which it can restore the attractiveness of the washed female. This assay is useful for testing not only the bioactivity of the crude extract, but also fractions of the crude extract and synthetic compounds. Nevertheless, the CHC profiles of reconstituted females may not accurately reflect those on the unwashed female. In some cases, in fact, males do not respond as readily to reconstituted females, suggesting that CHCs may be stratified within the wax layer and that reapplication of crude extract scrambles their position and decreases the abundance of contact pheromones on the surface (Hughes et al. 2011).

Contact pheromones used for mate recognition are most often identified by analyzing whole-body solvent extracts using GC-MS and comparing the CHC profiles of males and females. In some cases, the CHC profiles of the sexes are qualitatively quite different, with female specific compounds serving as contact pheromones. For example, in the longhorned beetle *Megacyllene caryae* a number of aliphatic compounds are unique to the CHC profiles of females, and sex-specific compounds accounted for about half of the hydrocarbons of females and a third of those of males. The contact pheromone for this species, (Z)-9-nonacosene, is also not present in the CHC profiles of males (Ginzl et al. 2003b). Likewise, sex-based differences in the chain lengths of CHCs have been reported in other insects such as the tsetse fly (Nelson and Carlson 1986) and the bark beetle *Ips lecontei* (Page et al. 1997). However, quantitative differences in CHC profiles of the sexes may also mediate mate choice on the part of male insects. Some cuticular hydrocarbons that

serve as contact pheromones are present in extracts of the cuticles of both sexes, but are quantitatively dominant in the appropriate sex. For example, components of the female sex pheromone of the dipteran face fly *Musca autumnalis* De Geer (Z13:C₂₇, Z13:C₂₉, and Z14:C₂₉) were more abundant on females than on males (Uebel et al. 1975). Similarly, a component of the female contact sex pheromone of the cerambycid rustic borer *Xylotrechus colonus*, nC₂₅, is also present in extracts of males, but in relatively small quantities (Ginzel et al. 2003a). Moreover, only four compounds are unique to the female cuticle, and another three compounds are specific to males of this species (Ginzel et al. 2003a).

More recently solid phase microextraction (SPME) has been used as an alternative to solvent extraction to identify CHCs of insects (e.g.; Liebig et al. 2000; Sledge et al. 2000; Roux et al. 2002; Ginzel et al. 2003b, 2006), and reportedly yields samples that are qualitatively and quantitatively similar to those obtained by solvent extraction (Moneti et al. 1997; Monnin et al. 1998; Bland et al. 2001; Tentschert et al. 2002). This solvent-less sampling technique involves wiping the adsorbent SPME fiber over the surface of the cuticle and then thermally desorbing the analytes in the heated GC inlet. Because this method primarily samples only those hydrocarbons on the surface of the cuticle, it appears that SPME samples may yield a more representative profile of CHCs that are encountered by potential mates. For example, in some cerambycid beetles contact pheromones are relatively more abundant in SPME samples than solvent extracts (Ginzel et al. 2003b, 2006), suggesting that CHCs that act as semiochemicals are more abundant on the surface of the cuticle where they are more accessible to male antennae (Ginzel et al. 2003b). Another advantage of SPME over solvent extraction is that live insects can be non-destructively and repeatedly sampled and later used in bioassays – an important consideration given the large number of insects required to perform statistically robust behavioral bioassays.

7.4.2 Chirality

Many CHCs that comprise contact pheromones of insects are methyl-branched and have the potential to be chiral – existing in two or more stereoisomeric forms. Despite the important influence chirality may play in the mating systems of these insects, few studies have investigated the role of stereochemistry in contact chemoreception. Nevertheless, male of the brown spruce longhorn beetle *Tetropium fuscum* respond more strongly to solvent-washed female carcasses treated with (*S*)-11-methylheptacosane, the major contact sex pheromone component of females, than to the (*R*)-enantiomer, while males of the eastern larch borer *Tetropium cinnamopterum* require both (*S*)-11-methylheptacosane and (*Z*)-9-heptacosene to display a full mating response (Silk et al. 2011). In the parasitic wasp *Lariophagus distinguendus*, males respond to both (*R*)- and (*S*)-3-methylheptacosane when applied to male cadavers (Kühbandner et al. 2012, 2013), indicating that chirality does not play a role in mate recognition for this species. Likewise, males of the

Asiatic yellow-spotted longicorn beetle *Psacotheta hilaris* respond as strongly to both (8Z,21R)- and (8Z,21S)-21-methyl-8-pentatriacontene, demonstrating no preference for either stereoisomer (Fukaya et al. 1997). The female contact sex pheromone of the German cockroach, *Blattella germanica* (3S,11S)-3,11-dimethylnonacosan-2-one, stimulates courtship behaviors in males at very low concentrations (Eliyahu et al. 2008). Interestingly, at physiological concentrations, the natural (*S,S*)-enantiomer is the least effective of the stereoisomers at eliciting courtship behaviors. These studies demonstrate that the influence of chirality on the bioactivity of contact sex pheromones varies between species, and that a combination of cuticular hydrocarbons may be necessary to stimulate courtship and mating behaviors. As previously mentioned, a recent polarimetric analysis of 36 pure methyl-branched hydrocarbons from 20 species in nine insect orders revealed a conserved stereochemistry across all insects, with all compounds having the (*R*)-configuration – independent of methyl branch position or chain length (Bello et al. 2015). Males of the longhorned beetle *Neoclytus a. acuminatus* recognize females by a contact pheromone consisting of three chiral components: a most bioactive component, 7-methylheptacosane (7-MeC₂₇), and two minor components, 7-methylpentacosane (7-MeC₂₅) and 9-methylheptacosane (9-MeC₂₇) (Lacey et al. 2008). Through digital polarimetry, it was recently determined that the absolute configuration of 7-MeC₂₅ was (*R*) (Hughes et al. 2015). In behavioral bioassays, males responded more strongly to the blend of (*R*)-pheromone components, than to (*R*)-7-MeC₂₇ alone. Also, a blend of (*R*)-7-MeC₂₇ with the (*S*)-minor components elicited an intermediate response, suggesting that the unnatural enantiomers are not inhibitory. In light of this finding, it may be that methyl-branched hydrocarbons used as semiochemicals are biosynthesized in various stereoisomeric forms, while those used for preventing desiccation and other purposes exist only in the *R*-configuration (Bello et al. 2015). Nevertheless, it is unclear how generalizable this ability to discriminate the absolute configuration of methyl-branched CHCs may be. Future work should focus on the influence of chirality on the behavior of insects that can discriminate the absolute configuration of methyl-branched CHCs that mediate contact chemoreception.

7.4.3 Colony and Kin Recognition

The ability to recognize members and non-members of a group is essential to maintaining colony structure (van Zweden and d’Ettorre 2010), and is central to the evolution of social behavior and altruism toward kin in social insects. This behavior is almost ubiquitous among eusocial insects and a blend of CHCs on the cuticle of nestmates serves as recognition cues, and in honeybees it appears that fatty acids and esters are also involved (Breed 1998a; Châline et al. 2005; Howard and Blomquist 2005).

Nestmate recognition has been recently reviewed for ants, semi-social and social wasps, termites and bees (van Zweden and d’Ettorre 2010 and references therein). Nestmate recognition is thought to involve matching a profile of colony odor (i.e., a chemical nestmate cue) with a cognitive template, and prohibiting entry to those alien insects that do not match. In fact, insects display increased aggression toward nestmates whose CHC profile has been quantitatively altered by the topical application of hydrocarbons because they are perceived as intruders (Takahashi and Gassa 1995; Lahav et al. 1999; Dani et al. 2005). Colony size also appears to be an important factor influencing nestmate recognition abilities. In small colonies, individuals can learn the CHC profiles of nestmates, while in larger colonies it appears that individuals are accepted based on their similarity to an average or “Gestalt” odor. This average odor is learned by members of the colony and results from sharing of individual CHC profiles (Crozier 1987; Crozier and Dix 1979). In honeybees, guard bees also accept nestmates by this gestalt colony odor, which results from CHCs secreted by the bees themselves and also acquired from comb wax in the nest (Couvillon et al. 2007). Comb wax is a complex mixture of compounds that include both floral scents and compounds produced by wax glands and alkene hydrocarbons (Dani et al. 2005), as well as fatty acids secreted by mandibular glands (Breed 1998b; Breed et al. 2004). These secretions are under genetic control and, as such, different colonies have potentially quite different profiles.

In ants, nestmate recognition cues from postpharyngeal glands are shared by trophallaxis or by cuticular contact in those species that engage in colony grooming (Vander Meer and Morel 1998), thereby continuously updating that colony odor (Bos and d’Ettorre 2012). For example, in the Argentine ant *Linepithema humile*, a homogenization of CHC profiles has been linked to the erosion of colony boundaries and colony fusion (Vásquez et al. 2009). Some termites recognize castes by the relative abundances of CHCs on the cuticle (Greene 2010), while ants are able to distinguish tasks of other members of the colony by differences in the CHC profile (Wagner et al. 1998; Greene 2010).

Quantitative rather than qualitative differences in CHC profiles are used for colony recognition in many insects (Hefetz 2007; van Zweden and d’Ettorre 2010). For example, in the ant *Formica exsecta* different ratios of a set of homologous (Z)-9-alkenes, superimposed on a background of all other CHCs, are used for nestmate discrimination (Martin et al. 2008). Both genetics and the environment can influence CHC profiles used for nestmate recognition. For example, artificially induced polygyne colonies of the ant *Messor barbarus* have quantitatively different CHC profiles than natural monogynous colonies (Provost et al. 1994), providing evidence for a queen-derived influence on colony odor. Also, diet modifications in the ant *L. humile*, lead to altered CHC profiles and increased or decreased aggression between colonies (Liang and Silverman 2000; Buczkowski et al. 2005). Moreover, differences in nesting substrate of the ant *Leptothorax nylanderii* lead to qualitative dissimilarities in profiles of CHCs that serve as nestmate recognition cues and strongly affect aggressive interactions between different colonies (Heinze et al. 1996). In addition to variation between ant colonies, CHC profiles within a colony can also change over time (Nielsen et al. 1999).

7.4.4 *Task-specific Cues*

Division of labor is essential to colony survival in social insects and requires a high level of organization and integration (see Hölldobler and Wilson 1990). For example, it is well established that ants adjust the number of workers devoted to a given task in response to changes in environmental and ecological conditions. Without any central control, ants use differences in hydrocarbons to recognize tasks being performed by members of the colony and adjust their behavior accordingly. In many social insects, individuals recognize workers performing different tasks via cuticular lipids (Howard et al. 1982; Wagner et al. 1998; Sevala et al. 2000). When inactive workers within the nest of the red harvester ant, *Pogonomyrmex barbatus*, encounter an increasing rate of patrollers entering the nest, they initiate foraging trips (Gordon et al. 2007). However, an increase in the rate of foragers returning to the nest does not stimulate foraging behavior unless those ants are carrying seeds, indicating an available food resource (Wagner et al. 1998; Gordon 2002; Greene et al. 2013). Many of these compounds have methyl branches or other moieties at chiral centers. However, the absolute configuration of these compounds has not been well studied. In the honey bee, *Apis mellifera*, there is a task-specific pattern in CHCs, particularly in *n*-alkanes and alkenes with foragers having an increased abundance of *n*-alkanes relative to nurse and newly emerged bees (Kather et al. 2011). Nevertheless, the extent to which these differences are used to distinguish task groups within the colony remains unclear.

Within social colonies, CHCs also mediate the recognition of castes, including queens, workers, eggs, and brood. For example, castes of *Reticulitermes* termites differ in relative abundance of CHC components and members of the same caste share quantitatively similar hydrocarbon profiles (Howard et al. 1978, 1982; Haverty et al. 1996; Kaib et al. 2002). Similarly, castes of the Nevada termite *Zootermopsis nevadensis* have differing hydrocarbon profiles (Sevala et al. 2000). Cuticular hydrocarbons can have primer effects in social insect colonies and indicate fertility and dominance (reviewed by Le Conte and Hefetz 2008; Liebig 2010). In fact, there is a correlation between hydrocarbon profiles and fertility in many species across broad taxa of social insects (Liebig 2010). For example, there are major differences in the CHC profiles relating to reproductive status in the giant ant *Aphaenogaster cockerelli* (Smith et al. 2008). A social hierarchy exists within colonies of *Dinoponera quadriceps* and the relative concentration of one compound (9-hentriacontene) out of a profile of greater than 80 compounds is associated with top-ranking individuals (Monnin et al. 1998; Peeters et al. 1999).

7.4.5 *Chemical Mimicry*

An almost complete reliance on chemical communication for colony organization leaves many insect societies vulnerable to chemical deception by intruders (reviewed in Dettner and Liepert 1994; Lenoir et al. 2001; Bagnères and Lorenzi 2010). Once

past the gatekeepers of a colony, these invaders are afforded a rich supply of stored food and nutritious brood, as well as shelter from predators and extreme temperatures. Invaders can gain entry into a colony by being chemically insignificant – lacking the chemical cues that are recognized by the host (Bagnères and Lorenzi 2010). However, their acceptance as member of the colony largely depends on their ability to acquire or mimic CHC-based species-specific cues and colony odors. For example, queens of the parasitic wasp *Polistes semenowi* gain entrance into nests of its host, the wasp *P. dominulus*, by having a relatively low quantity of CHCs (Lorenzi et al. 2004). Within 2 weeks of host-invasion, however, the CHC profiles of the parasite-queen perfectly match those of its host (Lorenzi et al. 2004). Moreover, the CHC profiles of *P. sulcifer*, another parasite of *P. dominulus*, undergo dramatic changes to match those of the host soon after invasion (Turillazzi et al. 2000).

Inquilines may acquire CHCs responsible for the colony odor of their hosts through trophallaxis, repeated licking or stroking (e.g., Lenoir et al. 1997) or passive adsorption (Vander Meer and Wojcik 1982), thereby camouflaging them from detection (e.g., Dinter et al. 2002; Vander Meer et al. 1989). For example, the myrmecophilous salticid spider, *Cosmophasis bitaeniata*, acquires the colony odor of its tree ant host, *Oecophylla smaragdina*, through eating and handling host larvae (Elgar and Allan 2004, 2006). Alternatively, social parasites can mimic host odors by synthesizing the host specific patterns themselves. For example, the butterfly *Maculinea rebeli* is able to synthesize the compounds of its ant host, *Myrmica schencki*, before entering the nest (Akino et al. 1999). Likewise, the staphylinid beetle *Trichopsenius frosti* has the same cuticular hydrocarbons as those of its host termite *Reticulitermes flavipes* and biosynthesizes them (Howard et al. 1980). As in many inquiline species, *M. rebeli* uses a combination of strategies to gain access into and remain undetected within host nests. In fact, once inside the colony, the butterfly acquires ant CHCs to more finely tune its CHC profiles to match the colony odor (Akino et al. 1999). There are many examples of non-social inquilines of termites, ants, and the honey bee (see Bagnères and Lorenzi 2010), including colony-specific differences in CHC profiles in the ectoparasitic mite of honey bees, *Varroa destructor* (Kather et al. 2015; Le Conte et al. 2015).

Insects other than inquilines are able to mimic CHCs in order to deceive social insects. A parasitoid of the black bean aphid (*Aphis fabae*) mimics the CHC profiles of its host and thereby avoids attack by the tending ant species, *Lasius niger* (Liepert and Dettner 1996). Interestingly, another parasitoid of the black bean aphid, *Trioxys anelicae*, does not have CHCs that mimic those of its host and is readily preyed upon by honeydew-collecting ants. More recently, Endo and Itino (2013) demonstrated that the aphid, *Stomaphis yanonis*, actively produces CHCs that resemble those of the ant *Lasius fuji* that tends to them and provides protection from predators.

7.4.6 Influence of Diet, Environment and Age on CHC Profiles

One key piece of information carried in the cuticle of insects may be nutritional status – individuals that have fed on a given food source as larvae may be identified by potential mates using olfactory cues from the cuticle. For example, males of the mustard leaf beetle (*Pheadon cochleariae*) preferentially mate with females reared on the same plant species compared to those reared on a different host, suggesting hydrocarbon profiles of the beetles are host-plant specific (Geiselhardt et al. 2012). These changes in the cuticular hydrocarbons lead to assortative mating and behavioral isolation. The mechanism is thought to be either due to different precursors (e.g., plant lipids) for hydrocarbon synthesis or plant secondary metabolites that interfere with biosynthetic processes (Geiselhardt et al. 2012). Similarly, in sympatric host races of the European corn borer (*Ostrinia nubilalis*), adults that fed upon different hosts as larvae (hop-mugwort or corn) had different pheromone blends as adults, leading to complete reproductive isolation from one another (Malausà et al. 2005).

Although cuticular hydrocarbons are often the result of biosynthesis, in some cases they appear to be acquired from the environment. For example, hydrocarbons derived from the environment (e.g., honeydew, nesting material, plant lipids and walking substrate) serve as cues for nestmate recognition in ants and other social insects (see Jutsum et al. 1979; Heinze et al. 1996; Singer and Espelie 1996; Breed 1998b). Cuticular lipids can also be transferred between individuals during courtship and mating. Male tsetse flies (*Glossina* spp.) recognize females via a non-volatile contact pheromone present on their cuticle (Carlson et al. 1984). During courtship and mating, however, an unusual polymethylalkene is transferred from males to the female cuticle and acts as an anti-aphrodisiac (Carlson and Schlein 1991). As tsetse flies mate multiple times, this abstinon likely serves to reduce competition by rendering females less attractive to subsequent males they may encounter (Carlson and Schlein 1991).

Aging and development have also been demonstrated to influence CHC profiles in several insect taxa, including flies, honey bees, ants and mosquitoes (Goodrich 1970; Desena et al. 1999; Hugo et al. 2006; Ichinose and Lenoir 2009; Nunes et al. 2009; Kuo et al. 2012). For example, male *D. melanogaster* preferentially mate with younger females. Aging leads to an increase in the proportion of longer chain CHCs in both sexes (Kuo et al. 2012), suggesting that these age-related changes in CHC profiles reduce sexual attractiveness of females. Age-related changes in CHC profiles of necrophagous flies have recently found application in forensic entomology to estimate the age of fly species present on a corpse and more accurately estimate the time of death. In the callophorid fly *Aldrichina grahami*, for example, there is a change in CHC profiles as larvae age, with older larvae having longer chainlength hydrocarbons (Xu et al. 2014), and larvae of various ages can be discriminated based on hydrocarbons present on the cuticle (Xu et al. 2014). Age appears to also affect CHC profiles of adult blowflies, however other biotic factors may influence

CHC profiles and the application and utility of such changes in forensic investigations requires further exploration (Pechal et al. 2014).

7.4.7 Predator/Prey Interactions

There is a growing body of evidence suggesting that predators and parasitoids use CHCs as kairomones to identify prey. For example, females of the wasp *Cerceris fumipennis* use contact cues to discriminate their buprestid prey from other beetles based on the presence of five classes of CHCs (Rutledge et al. 2014). In fact, it appears that the wasps are deterred by CHC classes (e.g., dimethyl-branched hydrocarbons) not found in Buprestidae (Rutledge et al. 2014). The egg parasitoid *Trissolcus basalis* locates its stink bug host, *Nezara viridula*, by orienting to footprint hydrocarbons and can distinguish between male and female hosts based on the presence or absence, respectively, of one compound – *n*-nonadecane (Colazza et al. 2007). Conversely, some insects avoid predation on their progeny by detecting hydrocarbons of natural enemies and ovipositing elsewhere. The common predatory backswimmer, *Notonecta maculata*, releases two hydrocarbons, *n*-heneicosane and *n*-tricosane, that repel oviposition by the mosquito, *Culiseta longiareolata* (Silberbush et al. 2010).

7.5 Volatile Polyene Hydrocarbons

Volatile polyene hydrocarbons and related epoxides and ketones are used as pheromone components and sex attractants in the Lepidoptera (reviewed by Millar 2000; Millar 2010) and Coleoptera (reviewed by Bartelt 2010). Within Lepidoptera, pheromones can be classified into two major groups, Type I and Type II, according to their chemical structures (Ando et al. 2004). Type I is the most predominant group and comprised of straight chain acetates, aldehydes and alcohols with chain lengths of 10–18 carbons and as many as three double bonds (Millar 2000). These compounds are synthesized de novo in pheromone glands. In contrast, Type II pheromones appear to be primarily restricted to the families Arctiidae, Geometridae, Noctuidae and Lymantriidae and represent ~15% of known lepidopteran pheromones. These polyunsaturated hydrocarbons and epoxy derivatives are products of diet-derived unsaturated fatty acids (i.e., linoleic and linolenic acid), and characterized by C₁₂–C₂₅ straight chains with double bonds, all in the *Z*-configuration, located at carbon 3, 6, 9, 12, or 15 and separated by methylene groups (Millar 2010). Moreover, the chirality of many of these compounds may allow for greater opportunities for species-specific messages, including attraction and antagonism to individual enantiomers. In Coleoptera, volatile hydrocarbon pheromones can be found in the *Phyllotreta* flea beetles (Peng et al. 1999; Bartelt et al. 2001; Tóth et al. 2005), the broad-horned flour beetle *Gnatocerus cornutus* (Tebayashi et al. 1998), and the

spruce beetle *Dendroctonus rufipennis* (Gries et al. 1992). However, the most studied example of hydrocarbons as volatile pheromones is in the sap beetles (Coleoptera: Nitidulidae), with conjugated trienes and tetraenes serving as long-range pheromones in *Carpophilus* and *Colopterus* species (see Bartelt 2010). These male-specific compounds all have alkyl branches and are on alternating carbons, with double bonds in the *E*-configuration. Future work will likely uncover many examples of hydrocarbons serving as volatiles pheromones in this largest and most diverse group of insects.

7.6 Future Directions

Based on the explosion of information on the role of cuticular hydrocarbons in chemical communication that has occurred in the last four decades, it is expected that new roles for insect hydrocarbons where a relatively non-volatile signal or cue is needed will continue to be found. The recent observation that hydrocarbons serve as aggregation pheromones in the convergent lady beetle to specify overwintering sites (Wheeler and Cardé 2014) suggest that other, novel functions are yet to be discovered. The importance of chirality in chemical communication with methyl-branched hydrocarbons is just now being explored, and future work will undoubtedly address this issue in more depth. Wicker-Thomas et al. (2015) and Dembeck et al. (2015) used RNAi silencing of a number of genes in *D. melanogaster* to provide convincing evidence of the importance of a large number of suspected genes in hydrocarbon production and future work will certainly involve expressing and characterizing many of these. As more and more insect genomes are sequenced and techniques such as the use of RNA interference along with expression and cloning of key genes involved in hydrocarbon biosynthesis are employed, our understanding of these critical processes will undoubtedly increase. A major challenge facing insect scientists will be how to take advantage of this information for new and more effective insect control techniques.

References

- Akino T, Knapp JJ, Thomas JA, Elmes GW (1999) Chemical mimicry and host specificity in the butterfly *Maculinea rebeli*, a social parasite of *Myrmica* ant colonies. *Proc Roy Soc Lond B Bio* 266:1419–1426
- Ando T, Inomata SI, Yamamoto M (2004) Lepidopteran sex pheromones. *Top Curr Chem* 239:51–96
- Antony B, Fujii T, Moto K, Matsumoto S, Fukuzawa M, Nakano R, Tatsuki S, Ishikawa Y (2009) Pheromone-gland-specific fatty-acyl reductase in the adzuki bean borer, *Ostrinia scapularis* (Lepidoptera: Crambidae). *Insect Biochem Mol Biol* 39:90–95
- Bagnères A-G, Lorenzi MC (2010) Chemical deception/mimicry using cuticular hydrocarbons. In: Blomquist GJ, Bagnères A-G (eds) *Insect hydrocarbons: biology, biochemistry, and chemical ecology*. Cambridge University Press, Cambridge, pp 281–324

- Baker GL, Vroman HE, Padmore J (1963) Hydrocarbons of the American cockroach. *Biochem Biophys Res Commun* 13:360–365
- Bartelt RJ (2010) Volatile hydrocarbon pheromones of beetles. In: Blomquist GJ, Bagnères A-G (eds) *Insect hydrocarbons: biology, biochemistry, and chemical ecology*. Cambridge University Press, Cambridge, pp 448–476
- Bartelt RJ, Cossé AA, Zilkowski BW, Weisleder D, Momany FA (2001) Male-specific sesquiterpenes from *Phyllotreta* and *Aphthona* flea beetles. *J Chem Ecol* 27:2397–2423
- Bello JE, McElfresh S, Millar JG (2015) Isolation and determination of absolute configurations of insect-produced methyl-branched hydrocarbons. *Proc Natl Acad Sci U S A* 112:1077–1082
- Bernard A, Joubès J (2013) *Arabidopsis* cuticular waxes: Advances in synthesis, export and regulation. *Prog Lipid Res* 52:110–129
- Billeter JC, Atallah J, Krupp JJ, Millar JG, Levine JD (2009) Specialized cells tag sexual and species identity in *Drosophila melanogaster*. *Nature* 461:987–991
- Blailock TT, Blomquist GJ, Jackson LL (1976) Biosynthesis of 2-methylalkanes in the cricket *Nemobius fasciatus* and *Gryllus pennsylvanicus*. *Biochem Biophys Res Commun* 68:841–849
- Bland JM, Osbrink WLA, Cornelius ML, Lax AR, Vigo CB (2001) Solid-phase microextraction for the detection of termite cuticular hydrocarbons. *J Chromatogr A* 932:119–127
- Blomquist GJ (2010a) Biosynthesis of cuticular hydrocarbons. In: Blomquist GJ, Bagnères AG (eds) *Insect hydrocarbons: biology, biochemistry, and chemical ecology*. Cambridge University Press, Cambridge, pp 35–52
- Blomquist GJ (2010b) Structure and analysis of insect hydrocarbons. In: Blomquist GJ, Bagnères A-G (eds) *Insect hydrocarbons: biology, biochemistry, and chemical ecology*. Cambridge University Press, Cambridge, pp 19–34
- Blomquist GJ, Bagnères A-G (2010) Introduction: history and overview of insect hydrocarbons. In: Blomquist GJ, Bagnères AG (eds) *Insect hydrocarbons: biology, biochemistry, and chemical ecology*. Cambridge University Press, Cambridge, pp 3–18
- Blomquist GJ, Kearney GP (1976) Biosynthesis of the internally branched monomethylalkanes in the cockroach *Periplaneta fulliginosa*. *Arch Biochem Biophys* 173:546–553
- Blomquist GJ, Major MA, Lok JB (1975) Biosynthesis of 3-methylpentacosane in the cockroach *Periplaneta americana*. *Biochem Biophys Res Commun* 64:43–50
- Blomquist GJ, Howard RW, McDaniel CA, Remaley S, Dwyer LA, Nelson DR (1980) Application of methoxymercuration-demercuration followed by mass spectrometry as a convenient micro-analytical technique for double-bond location in insect-derived alkenes. *J Chem Ecol* 6:257–269
- Blomquist GJ, Dwyer LA, Chu AJ, Ryan RO, de Renobales M (1982) Biosynthesis of linoleic acid in a termite, cockroach and cricket. *Insect Biochem* 12:349–353
- Blomquist GJ, Guo L, Gu P, Blomquist C, Reitz RC, Reed JR (1994) Methyl-branched fatty acids and their biosynthesis in the housefly, *Musca domestica* L. (Diptera: Muscidae). *Insect Biochem Mol Biol* 24:803–810
- Blount BK, Chibnall AC, Mangouri EI (1937) The wax of the white pine chermes. *Biochem J* 31:1375–1378
- Bognar AL, Paliyath G, Rogers L, Kolattukudy PE (1984) Biosynthesis of alkanes by particulate and solubilized enzyme preparations from pea leaves (*Pisum sativum*). *Arch Biochem Biophys* 235:8–17
- Böröczky K, Crook DJ, Jones TH, Kenny JC, Zylstra KE, Mastro VC, Tumlinson JH (2009) Monoalkenes as contact sex pheromone components of the woodwasp *Sirex noctilio*. *J Chem Ecol* 35:1202–1211
- Bos N, d’Ettorre P (2012) Recognition of social identity in ants. *Psychology* 3:83
- Braga MV, Pinto ZT, de Carvalho Queiroz MM, Matsumoto N, Blomquist GJ (2013) Cuticular hydrocarbons as a tool for the identification of insect species: Puparial cases from Sarcophagidae. *Acta Trop* 128:479–485
- Breed MD (1998a) Recognition pheromones of the honey bee. *Bioscience* 48:463–470
- Breed MD (1998b) Chemical cues in kin recognition: criteria for identification, experimental approaches, and the honey bee as an example. In: Vander Meer RK, Breed MD, Espelie KE,

- Winston ML (eds) *Pheromone communication in social insects: ants, wasps, bees, and termites*. Westview Press, Boulder, pp 57–78
- Breed MD, Diaz PH, Lucero KD (2004) Olfactory information processing in honeybee, *Apis mellifera*, nestmate recognition. *Anim Behav* 68:921–928
- Buckner JS (2010) Oxygenated derivatives of hydrocarbons. In: Blomquist GJ, Bagnères A-G (eds) *Insect hydrocarbons: biology, biochemistry, and chemical ecology*. Cambridge University Press, Cambridge, pp 187–203
- Buczkowski G, Suib S, Kumar R, Silverman J (2005) Shared exogenous cues diminish intercolony aggression in the Argentine ant (*Linepithema humile*). *J Chem Ecol* 31:829–843
- Buellesbach J, Greim C, Raychoudhury R, Schmitt T (2014) Asymmetric assortative mating behaviour reflects incomplete pre-zygotic isolation in the *Nasonia* species complex. *Ethology* 120:834–843
- Carlson DA, Schlein Y (1991) Unusual polymethyl alkenes in tsetse flies acting as abstinon in *Glossina morsitans*. *J Chem Ecol* 17:267–284
- Carlson DA, Mayer MS, Silhacek DL, Janaes JD, Beroza M, Bierl BA (1971) Sex attractant pheromone of the house fly: Isolation, identification and synthesis. *Science* 174:76–78
- Carlson DA, Nelson DR, Langley PA, Coates TW, Davis TL, Leegwater-Van Der Linden ME (1984) Contact pheromone in the tsetse fly *Glossina pallidipes* (Austen): identification and synthesis. *J Chem Ecol* 10:429–450
- Carlson DA, Roan C-S, Yost RA (1989) Dimethyl disulfide derivatives of long chain alkenes, alkadienes, and alkatrienes for gas chromatography/mass spectrometry. *Anal Chem* 61:1564–1571
- Carlson DA, Bernier UR, Sutton BD (1998a) Elution patterns from capillary GC for methyl-branched alkanes. *J Chem Ecol* 24:1445–1465
- Carlson DA, Offor II, El-Messoussi S, Matsuyama K, Mori K, Jallon J-M (1998b) Sex pheromone of *Glossina tachinoides*: isolation, identification, and synthesis. *J Chem Ecol* 24:1563–1575
- Carot-Sans G, Munoz L, Piulachs MD, Guerrero A, Rosell G (2015) Identification and characterization of a fatty acyl reductase from a *Spodoptera littoralis* female gland involved in pheromone biosynthesis. *Insect Molec Biol* 24:82–92
- Châline N, Sandoz J-C, Martin SJ, Ratnieks FLW, Jones GR (2005) Learning and discrimination of individual cuticular hydrocarbons by honeybees (*Apis mellifera*). *Chem Senses* 30:327–335
- Chase J, Jurenka RA, Schal C, Halamkar PP, Blomquist GJ (1990) Biosynthesis of methyl branched hydrocarbons in the German cockroach *Blattella germanica* (L.) (Orthoptera, Blattellidae). *Insect Molec Biol* 20:149–156
- Chase J, Touhara K, Prestwich GD, Schal C, Blomquist GJ (1992) Biosynthesis and endocrine control of the production of the German cockroach sex pheromone, 3,11-dimethylnonacosan-2-one. *Proc Natl Acad Sci U S A* 89:6050–6054
- Cheesbrough TM, Kolattukudy PE (1988) Microsomal preparations from animal tissue catalyzes release of carbon monoxide from a fatty aldehyde to generate an alkane. *J Biol Chem* 263:2738–2742
- Chertemps T, Duportets L, Labour C, Udeda R, Takahashi K, Saigo K, Wicker-Thomas C (2007) A female-biased expressed elongase involved in long-chain hydrocarbon biosynthesis and courtship behavior in *Drosophila melanogaster*. *Proc Natl Acad Sci U S A* 104:4273–4278
- Chibnall AC, Piper SH, Pollard A, Willimas EF, Sahai PN (1934) The constitution of the primary alcohols, fatty acids and paraffins present in plant and insect waxes. *Biochem J* 28:2189–2208
- Chung H, Loehlin DW, Dufour HD, Vaccarro K, Millar JG, Carroll SB (2014) A single gene affects both ecological divergence and mate choice in *Drosophila*. *Science* 343:148–151
- Colazza S, Aquila G, De Pasquale C, Peri E, Millar J (2007) The egg parasitoid *Trissolcus basalis* uses n-nonadecane, a cuticular hydrocarbon from its stink bug host *Nezara viridula*, to discriminate between female and male hosts. *J Chem Ecol* 33:1405–1420
- Couvillon MJ, Caple JP, Endors SL, Kärcher M, Russell TE, Storey DE, Ratnieks FLW (2007) Nest-mate recognition template of guard honeybees (*Apis mellifera*) is modified by wax comb transfer. *Biol Lett* 3:228–230

- Crozier RH (1987) Genetic aspects of kin recognition: concepts, models and synthesis. In: Fletcher DJC, Michener CD (eds) Kin recognition in animals. Wiley, Chichester, pp 55–73
- Crozier RH, Dix MW (1979) Analysis of two genetic models for the innate components of colony odor in social Hymenoptera. *Behav Ecol Sociobiol* 4:217–224
- Cvačka J, Jiros P, Sobotnik J, Hanus R, Svatos A (2006) Analysis of insect cuticular hydrocarbons using matrix-assisted laser desorption/ionization mass spectrometry. *J Chem Ecol* 32:409–434
- Dallerac R, Labeur C, Jallon J-M, Knipple DC, Roelofs WL, Wicker-Thomas C (2000) A $\Delta 9$ desaturase gene with a different substrate specificity is responsible for the cuticular diene hydrocarbon polymorphism in *Drosophila melanogaster*. *Proc Natl Acad Sci U S A* 97:9449–9454
- Dani FR, Jones GR, Destri S, Spencer SH, Turillazzi S (2001) Deciphering the recognition signature within the cuticular chemical profile of paper wasps. *Anim Behav* 62:165–167
- Dani FR, Jones GR, Corsi S, Beard R, Pradella D, Turillazzi S (2005) Nestmate recognition cues in the honey bee: differential importance of cuticular alkanes and alkenes. *Chem Senses* 30:477–489
- Dembeck L, Böröczky K, Huang W, Schal C, Anholt R, Mackay T (2015) Genetic architecture of natural variation in cuticular hydrocarbon composition in *Drosophila melanogaster*. *eLife*. doi:10.7554/eLife.09861
- Dennis MW, Kolattukudy PE (1991) Alkane biosynthesis by decarbonylation of aldehyde catalyzed by a microsomal preparation from *Botryococcus brauni*. *Arch Biochem Biophys* 287:268–275
- Desena ML, Edman JD, Clark JM, Symington SB, Scott TW (1999) *Aedes aegypti* (Diptera: Culicidae) age determination by cuticular hydrocarbon analysis of female legs. *J Med Entomol* 36:824–830
- Dettner K, Liepert C (1994) Chemical mimicry and camouflage. *Ann Rev Entomol* 39:129–154
- Dillwith JW, Nelson JH, Pomonis JG, Nelson DR, Blomquist GJ (1982) A ^{13}C NMR study of methyl-branched hydrocarbon biosynthesis in the housefly. *J Biol Chem* 257:11305–11314
- Dillwith JW, Adams TS, Blomquist GJ (1983) Correlation of housefly sex pheromone production with ovarian development. *J Insect Physiol* 29:377–386
- Dinter K, Paarmann W, Peschke K, Arndt E (2002) Ecological, behavioural and chemical adaptations to ant predation in species of *Thermophilum* and *Graphipterus* (Coleoptera: Carabidae) in the Sahara desert. *J Arid Environ* 50:267–286
- Drijfhout FK (2010) Cuticular hydrocarbons: a new tool in forensic entomology? In: Amendt J, Lee Goff M, Campobasso CP, Grassberger M (eds) Current concepts in forensic entomology. Springer, New York, pp 179–203
- Dwyer LA, Blomquist GJ, Nelson JH, Pomonis JG (1981a) A ^{13}C -NMR study of the biosynthesis of 3-methylpentacosane in the American cockroach. *Biochim Biophys Acta* 663:536–544
- Dwyer LA, de Renobales M, Blomquist GJ (1981b) Biosynthesis of (Z, Z)-6,9-heptacosadiene in the American cockroach. *Lipids* 16:810–814
- Elgar MA, Allan RA (2004) Predatory spider mimics acquire colony-specific cuticular hydrocarbons from their ant model prey. *Naturwissenschaften* 91:143–147
- Elgar MA, Allan RA (2006) Chemical mimicry of the ant *Oecophylla smaragdina* by the myrmecophilous spider *Cosmophasis bitaeniata*: is it colony-specific? *J Ethol* 24:239–246
- Eliyahu D, Najima S, Mori K, Schal C (2008) New contact sex pheromone components of the German cockroach, *Blattella germanica*, predicted from the proposed biosynthetic pathway. *J Chem Ecol* 34:229–237
- Endo S, Itino T (2013) Myrmecophilous aphids produce cuticular hydrocarbons that resemble those of their tending ant. *Popul Ecol* 5:27–34
- Fan Y, Zurek L, Dykstra MJ, Schal C (2003) Hydrocarbon synthesis by enzymatically dissociated oenocytes of the abdominal integument of the German cockroach, *Blattella germanica*. *Naturwissenschaften* 90:121–126
- Ferveur J-F (2005) Cuticular hydrocarbons: their evolution and roles in *Drosophila* pheromonal communication. *Behav Genet* 35:279–295

- Ferveur J-F, Cobb M (2010) Behavioral and evolutionary roles of cuticular hydrocarbons in *Drosophila*. In: Blomquist GJ, Bagnères A-G (eds) *Insect hydrocarbons: biology, biochemistry, and chemical ecology*. Cambridge University Press, Cambridge, pp 325–343
- Ferveur J-F, Savarit F, O’Kane CJ, Sureau G, Greenspan RJ, Jallon J-M (1997) Genetic feminization of pheromones and its behavioral consequences in *Drosophila* males. *Science* 276:1555–1558
- Fletcher MT, McGrath MJ, König WA, Moore CH, Cribb BW, Allsopp PG, Kitching W (2001) A novel group of allenic hydrocarbons from five Australian (Melolonthine) beetles. *Chem Commun* 2001:885–886
- Fletcher MT, Allsopp PG, McGrath MJ, Chow S, Gallagher OP, Hull C, Cribb BW, Moore CJ, Kitching W (2008) Diverse cuticular hydrocarbons from Australian canebeetles (Coleoptera: Scarabaeidae). *Aust J Entomol* 47:153–159
- Francis GW, Veland K (1981) Alkyl thiolation for the determination of double-bond positions in linear alkenes. *J Chromatogr* 219:379–384
- Fukaya M, Wakamura S, Yasuda T, Senda S, Omata T, Fukusaki E (1997) Sex pheromonal activity of geometric and optical isomers of synthetic contact pheromone to males of the yellow-spotted longicorn beetle, *Psacotheta hilaris* (Pascoe) (Coleoptera: Cerambycidae). *Appl Entomol Zool* 32:654–656
- Fukaya M, Akino T, Yasuda T, Wakamura S, Satoda S, Senda S (2000) Hydrocarbon components in contact sex pheromone of the white-spotted longicorn beetle, *Anoplophora malasiaca* (Thomson) (Coleoptera: Cerambycidae) and pheromonal activity of synthetic hydrocarbons. *Entomol Sci* 3:211–218
- Geiselhardt S, Schmitt T, Peschke K (2009) Chemical composition and pheromonal function of the defensive secretions in the subtribe Stizopina (Coleoptera, Tenebrionidae, Opatrini). *Chemoecology* 19:1–6
- Geiselhardt S, Otte T, Hilker M (2012) Looking for a similar partner: host plants shape mating preferences of herbivorous insects by altering their contact pheromones. *Ecol Lett* 15:971–977
- Gibbs AG (1998) Water-proofing properties of cuticular lipids. *Am Zool* 38:471–482
- Ginzl MD (2010) Hydrocarbons as contact pheromones of longhorned beetles (Coleoptera: Cerambycidae). In: Blomquist GJ, Bagnères A-G (eds) *Insect hydrocarbons: biology, biochemistry, and chemical ecology*. Cambridge University Press, Cambridge, pp 375–389
- Ginzl MD, Hanks LM (2005) Role of host plant volatiles in mate location for three species of longhorned beetles. *J Chem Ecol* 31:213–217
- Ginzl MD, Blomquist GJ, Millar JG, Hanks LM (2003a) Role of contact pheromones in mate recognition in *Xylotrechus colonus*. *J Chem Ecol* 29:533–545
- Ginzl MD, Millar JG, Hanks LM (2003b) (Z)-9-pentacosene—contact sex pheromone of the locust borer, *Megacyllene robiniae*. *Chemoecology* 13:135–141
- Ginzl MD, Moreira JA, Ray AM, Millar JG, Hanks LM (2006) (Z)-9-Nonacosene—major component of the contact sex pheromone of the beetle *Megacyllene caryae*. *J Chem Ecol* 32:435–451
- Goodrich BS (1970) Cuticular lipids of adults and puparia of the Australian sheep blowfly *Lucilia cuprina* (Wied.). *J Lipid Res* 11:1–6
- Gordon DM (2002) The regulation of foraging activity in red harvester ant task decisions. *Am Nat* 159:509–518
- Gordon DM, Holmes S, Nacu S (2007) The short-term regulation of foraging in harvester ants. *Behav Ecol* 19:217–222
- Greene M (2010) Cuticular hydrocarbon cues in the formation and maintenance of insect social groups. In: Blomquist GJ, Bagnères A-G (eds) *Insect hydrocarbons: biology, biochemistry, and chemical ecology*. Cambridge University Press, Cambridge, pp 242–253
- Greene MJ, Pinter-Wollman N, Gordon DM (2013) Interactions with combined chemical cues inform harvester ant foragers’ decisions to leave the nest in search of food. *PLoS One* 8, e52219
- Gries G, Borden JH, Gries R, Lafontaine JP, Dixon EA, Wieser H, Whitehead AT (1992) 4-Methylen-6, 6-dimethylbicyclo[3.1.1]hept-2-ene (verbenene): new aggregation pheromone of the scolytid beetle *Dendroctonus rufipennis*. *Naturwissenschaften* 79:367–368

- Gu X, Quilici D, Juarez P, Blomquist GJ, Schal C (1995) Biosynthesis of hydrocarbons and contact sex pheromone and their transport by lipophorin in females of the German cockroach (*Blattella germanica*). *J Insect Physiol* 41:257–267
- Haslam TM, Kunst L (2013) Extending the story of very-long-chain fatty acid elongation. *Plant Sci* 210:93–107
- Haverty MI, Grace JK, Nelson LJ, Yamamoto RT (1996) Intercaste, intercolony, and temporal variation in cuticular hydrocarbons of *Coptotermes formosanus* Shiraki (Isoptera: Rhinotermitidae). *J Chem Ecol* 22:1813–1834
- Hefetz A (2007) The evolution of hydrocarbon pheromone parsimony in ants (Hymenoptera: Formicidae) – interplay of colony odor uniformity and odor idiosyncrasy. A review. *Myrmecological News* 10:59–68
- Heinze J, Foitzik S, Hippert A, Hölldobler B (1996) Apparent dear-enemy phenomenon and environmental based recognition cues in the ant *Leptothorax nylanderi*. *Ethology* 102:510–522
- Hölldobler B, Wilson EO (1990) The ants. Harvard University Press, Cambridge
- Howard RW, Blomquist GJ (2005) Ecological, behavioral, and biochemical aspects of insect hydrocarbons. *Annu Rev Entomol* 50:371–393
- Howard RW, McDaniel CA, Blomquist GJ (1978) Cuticular hydrocarbons of the eastern subterranean termite, *Reticulitermes flavipes* (Kollar) Isoptera:Rhinotermitidae). *J Chem Ecol* 4:233–245
- Howard RW, McDaniel CA, Blomquist GJ (1980) Chemical mimicry as an integrating mechanism: cuticular hydrocarbons of a termitophile and its host. *Science* 210:431–433
- Howard RW, McDaniel CA, Nelson DR, Blomquist GJ, Gelbaum LT, Zalkow LH (1982) Cuticular hydrocarbons of *Reticulitermes virginicus* (Banks) and their role as potential species and caste-recognition cues. *J Chem Ecol* 8:1227–1239
- Hughes GP, Spikes AE, Holland JD, Ginzel MD (2011) Evidence for the stratification of hydrocarbons in the epicuticular wax layer of female *Megacyllene robiniae* (Coleoptera: Cerambycidae). *Chemoecology* 21:99–105
- Hughes GP, Bello JE, Millar JG, Ginzel MD (2015) Determination of the absolute configuration of female-produced contact sex pheromone components of the longhorned beetle, *Neoclytus acuminatus acuminatus* (F). *J Chem Ecol*. doi:10.1007/s10886-015-0639-x
- Hugo LE, Kay BH, Eaglesham GK, Holling N, Ryan PA (2006) Investigation of cuticular hydrocarbons for determining the age and survivorship of Australasian mosquitoes. *Am J Trop Med Hyg* 74:462–474
- Ichinose K, Lenoir A (2009) Ontogeny of hydrocarbon profiles in the ant *Aphaenogaster senilis* and effects of social isolation. *C R Biol* 332:697–703
- Jallon JM, David JR (1987) Variations in cuticular hydrocarbons among the eight species of the *Drosophila melanogaster* subgroup. *Evolution* 41:294–302
- Juarez P, Chase J, Blomquist GJ (1992) A microsomal fatty acid synthetase from the integument of *Blattella germanica* synthesizes methyl-branched fatty acids, precursors to hydrocarbon and contact sex pheromone. *Arch Biochem Biophys* 293:333–341
- Jutsum AR, Saunders TS, Cherrett JM (1979) Intraspecific aggression in the leaf-cutting ant *Acromyrmex octospinosus*. *Anim Behav* 27:839–844
- Kaib M, Franke S, Francke W, Brandl R (2002) Cuticular hydrocarbons in a termite: phenotypes and a neighbour-stranger effect. *Physiol Entomol* 27:189–198
- Kather R, Drijfhout FP, Martin SJ (2011) Task group differences in cuticular lipids in the honey bee *Apis mellifera*. *J Chem Ecol* 37:205–212
- Kather R, Drijfhout FP, Shemilt S, Martin SJ (2015) Evidence for colony-specific differences in chemical mimicry in the parasitic mite *Varroa destructor*. *Chemoecology* 25:215–222
- Kühbandner S, Sperling S, Mori K, Ruther J (2012) Deciphering the signature of cuticular lipids with contact sex pheromone function in a parasitic wasp. *J Exp Biol* 215:2471–2478
- Kühbandner S, Bello JE, Mori K, Millar JG, Ruther J (2013) Elucidating structure-bioactivity relationships of methyl-branched alkanes in the contact sex pheromone of the parasitic wasp *Lariophagus distinguendus*. *Insects* 4:743–760

- Kuo TH, Yew JY, Fedina TY, Dreisewerd K, Dierick HA, Pletcher SD (2012) Aging modulates cuticular hydrocarbons and sexual attractiveness in *Drosophila melanogaster*. *J Exp Biol* 215:814–821
- Lacey ES, Ginzell MD, Millar JG, Hanks LM (2008) A major component of the contact sex pheromone of the cerambycid beetle, *Neoclytus acuminatus acuminatus* is 7-methylheptacosane. *Physiol Entomol* 33:209–216
- Ladygina N, Dedyukhina EG, Vainshtein MB (2006) A review on microbial synthesis of hydrocarbons. *Process Biochem* 41:1001–1014
- Lahav S, Soroker V, Hefetz A, Vander Meer RK (1999) Direct behavioral evidence for hydrocarbons as ant recognition discriminators. *Naturwissenschaften* 86:246–249
- Le Conte Y, Hefetz A (2008) Primer pheromones in social hymenoptera. *Annu Rev Entomol* 53:523–542
- Le Conte Y, Huang ZY, Roux M, Zeng ZJ, Christidès J-P, Bagnères A-G (2015) *Varroa destructor* changes its cuticular hydrocarbons to mimic new hosts. *Biol Lett* 11(6)
- Lenoir A, Malosse C, Yamaoka R (1997) Chemical mimicry between parasitic ants of the genus *Formicoxenus* and their host *Myrmica* (Hymenoptera, Formicidae). *Biochem Syst Ecol* 25:379–389
- Lenoir A, d’Ettorre P, Errard C, Hefetz A (2001) Chemical ecology and social parasitism in ants. *Annu Rev Entomol* 46:573–599
- Liang D, Silverman J (2000) “You are what you eat”: diet modifies cuticular hydrocarbons and nestmate recognition in the Argentine ant, *Linepithema humile*. *Naturwissenschaften* 87:412–416
- Liebig J (2010) Hydrocarbon profiles indicate fertility and dominance’s status in ant, bee, and wasp colonies. In: Blomquist GJ, Bagnères A-G (eds) *Insect hydrocarbons: biology, biochemistry, and chemical ecology*. Cambridge University Press, Cambridge, pp 254–281
- Liebig J, Peeters C, Oldham NJ, Markstadter C, Hölldobler B (2000) Are variations in cuticular hydrocarbons of queens and workers a reliable signal of fertility in the ant *Harpegnathos saltator*? *Proc Natl Acad Sci U S A* 97:4124–4131
- Liepert C, Dettner K (1996) Role of cuticular hydrocarbons of aphid parasitoids in the relationships to aphid-attending ants. *J Chem Ecol* 22:695–707
- Lockey KH (1980) Insect cuticular hydrocarbons. *Comp Biochem Physiol B* 65:457–462
- Lockey KH (1985) Insect cuticular lipids. *Comp Biochem Physiol B* 81:263–267
- Lorenzi MC, Sledge MF, Laiolo P, Sturlini E, Turillazzi S (2004) Cuticular hydrocarbon dynamics in young adult *Polistes dominulus* (Hymenoptera: Vespidae) and the role of linear hydrocarbons in nestmate recognition systems. *J Insect Physiol* 50:935–941
- Malausa T, Bethenod M, Bontemps A, Bourget D, Cornuet J, Ponsard S (2005) Assortative mating in sympatric host races of the European corn borer. *Science* 308:258–261
- Marsh E, Neil G, Waugh MW (2013) Aldehyde decarbonylases: enigmatic enzymes of hydrocarbon biosynthesis. *ACS Catal* 3:2515–2521
- Martin SJ, Vitikainen E, Helanterä H, Drijfhout FP (2008) Chemical basis of nest-mate discrimination in the ant *Formica exsecta*. *Proc R Soc B* 275:1271–1278
- McGrath MJ, Fletcher MT, König WA, Moore CJ, Cribb BW, Allsopp PG, Kitching W (2003) A suite of novel allenes from Australian melolonthine scarab beetles. Structure, synthesis and stereochemistry. *J Organic Chem* 68:3739–3748
- Millar JG (2000) Polyene hydrocarbons and epoxides: a second major class of lepidopteran sex attractant pheromones. *Annu Rev Entomol* 45:575–604
- Millar JG (2010) Polyene hydrocarbons, epoxides, and related compounds as components of lepidopteran pheromone blends. In: Blomquist GJ, Bagnères A-G (eds) *Insect hydrocarbons: biology, biochemistry, and chemical ecology*. Cambridge University Press, Cambridge, pp 390–447
- Ming QL, Lewis SM (2010) Mate-recognition & sex differences in cuticular hydrocarbons in a diurnal firefly, *Ellychnia corrusca*. *Ann Entomol Soc Am* 103:128–133

- Moneti G, Dani FR, Pieraccini G, Turillazzi S (1997) Solid-phase microextraction of insect epicuticular hydrocarbons for gas chromatographic mass spectrometric analysis. *Rapid Commun Mass Sp* 11:857–862
- Monnin T, Malosse C, Peeters C (1998) Solid-phase microextraction and cuticular hydrocarbon differences related to reproductive activity in the queenless ant *Dinoponera quadriceps*. *J Chem Ecol* 24:473–490
- Moore HE, Adam CD, Drijfhout FP (2013) Potential use of hydrocarbons for aging *Lucilia sericata* blowfly larvae to establish the postmortem interval. *J Forensic Sci* 58:404–412
- Mpuru S, Reed JR, Reitz RC, Blomquist GJ (1996) Mechanism of hydrocarbon biosynthesis from aldehyde in selected insect species: Requirement for O₂ and NADPH and carbonyl group released as CO₂. *Insect Biochem Mol Biol* 26:203–208
- Nelson DR (1993) Methyl-branched lipids in insects. In: Stanley-Samuelson DW, Nelson DR (eds) *Insect lipids: chemistry, biochemistry, and biology*. University of Nebraska Press, Lincoln, pp 271–315
- Nelson DR, Blomquist GJ (1995) Insect waxes. In: Hamilton RJ, Christie WW (eds) *Waxes: chemistry, molecular biology and functions*. The Oily Press Ltd, Dundee, pp 1–90
- Nelson DR, Carlson DA (1986) Cuticular hydrocarbons of the tsetse flies *Glossina morsitans morsitans*, *G. austeni*, and *G. pallidipes*. *Insect Biochem* 16:403–416
- Nelson DR, Sukkestad DR (1970) Normal and branched aliphatic hydrocarbons from the eggs of the tobacco hornworm. *Biochemistry* 9:4601–4616
- Nelson DR, Carlson DA, Fatland CL (1988) Cuticular hydrocarbons of the tsetse flies. II. *G. p. palpalis*, *G. p. gambiensis*, *G. fuscipes*, *G. tachinoides*, and *G. brevipalpis*. *J Chem Ecol* 14:963–987
- Nielsen J, Boomsma JJ, Oldham NJ, Petersen HC, Morgan ED (1999) Colony-level and season-specific variation in cuticular hydrocarbon profiles of individual workers in the ant *Formica truncorum*. *Insect Soc* 46:58–65
- Nunes TM, Turatti IC, Lopes NP, Zucchi R (2009) Chemical signals in the stingless bees, *Frieseomelitta varia*, indicate caste, gender, age, and reproductive status. *J Chem Ecol* 35:1172–1180
- Page M, Nelson LJ, Haverty MI, Blomquist GJ (1990) Cuticular hydrocarbons as chemotaxonomic characters for bark beetles: *Dendroctonus ponderosae*, *D. jeffreyi*, *D. brevicomis*, and *D. frontalis* (Coleoptera: Scolytidae). *Ann Entomol Soc Am* 83:892–901
- Page M, Nelson LJ, Blomquist GJ, Seybold SJ (1997) Cuticular hydrocarbons as chemosystematic characters of pine engraver beetles (*Ips* spp.) (Coleoptera: Scolytidae) in the Grandicollis subgeneric group. *J Chem Ecol* 23:1053–1099
- Payne JL, Boyer AG, Brown JH, Finnegan S, Kowalewski M, Krause RA, Lyons SK, McClain CR, McShea D, Navack-Gottshall PM (2009) Two phase increase in the maximum size of life over 3.5 billion years reflects biological innovation and environmental opportunity. *Proc Natl Acad Sci U S A* 106:24–27
- Pechal JL, Moore HE, Drijfhout F, Benbow ME (2014) Hydrocarbon profiles throughout adult Calliphoridae aging: A promising tool for forensic entomology. *Forensic Sci Int* 245:65–71
- Peeters C, Monnin T, Malosse C (1999) Cuticular hydrocarbons correlated with reproductive status in a queenless ant. *Proc R Soc Lond B* 266:1323–1327
- Peng C, Bartelt RJ, Weiss MJ (1999) Male crucifer flea beetles produce an aggregation pheromone. *Physiol Entomol* 24:98–99
- Peterson MS, Dobler S, Larson EL, Juárez D, Schlarbaum T, Monsen KJ, Francke W (2007) Profiles of cuticular hydrocarbons mediate male mate choice and sexual isolation between hybridising *Chrysochus* (Coleoptera: Chrysomelidae). *Chemecology* 17:87–96
- Provost E, Rivière G, Roux M, Bagnères A-G, Clément JL (1994) Cuticular hydrocarbons whereby *Messor barbarus* ant workers putatively discriminate between monogynous and polygynous colonies. Are workers labeled by queens? *J Chem Ecol* 20:2895–3003

- Qiu Y, Tittiger C, Wicker-Thamas C, Le Goff G, Young S, Wajnberg E, Fricaux T, Taquet N, Blomquist GJ, Feyereisen F (2012) An insect-specific P450 oxidative decarbonylase for cuticular hydrocarbon biosynthesis. *Proc Natl Acad Sci U S A* 109:14858–14863
- Reed JR, Vanderwel D, Choi S, Pomonis JG, Reitz RC, Blomquist GJ (1994) Unusual mechanism of hydrocarbon formation in the housefly: cytochrome P450 converts aldehyde to the sex pheromone component (Z)-9-tricosene and CO₂. *Proc Natl Acad Sci U S A* 91:10000–10004
- Reed JR, Quilici DR, Blomquist GJ, Reitz RC (1995) Proposed mechanism for the cytochrome P450-catalyzed conversion of aldehydes to hydrocarbons in the house fly, *Musca domestica*. *Biochemistry* 34:16221–16227
- Reed JR, Hernandez P, Blomquist GJ, Feyereisen R, Reitz RC (1996) Hydrocarbon biosynthesis in the housefly, *Musca domestica*: substrate specificity and cofactor requirement of P450hyd. *Insect Biochem Mol Biol* 26:267–276
- Roux E, Sreng L, Provost E, Roux M, Clement JL (2002) Cuticular hydrocarbon profiles of dominant versus subordinate male *Nauphoeta cinerea* cockroaches. *J Chem Ecol* 28:1221–1235
- Roux O, Gers C, Legal L (2008) Ontogenetic study of three Calliphoridae of forensic importance through cuticular hydrocarbon analysis. *Med Vet Entomol* 22:309–317
- Rutledge CE, Silk PJ, Mayo P (2014) Use of contact cues in prey discrimination by *Cerceris fumi-pennis*. *Entomol Exp Appl* 2:93–105
- Sakuradani E, Zhao L, Haslam TM, Kunst L (2013) The CER22 gene required for the synthesis cuticular wax alkanes in *Arabidopsis thaliana* is allelic to CER1. *Planta* 237:731–738
- Savarit F, Sureau G, Cobb M, Ferveur J-F (1999) Genetic elimination of known pheromones reveals the fundamental chemical bases of mating and isolation in *Drosophila*. *Proc Natl Acad Sci U S A* 96:9015–9020
- Schirmer A, Rude MA, Xuezi L, Popova E, del Cardayre SB (2010) Microbial biosynthesis of alkanes. *Science* 329:559–562
- Sevala VL, Bagnères A-G, Kuenzli M, Blomquist GJ, Schal C (2000) Cuticular hydrocarbons of the dampwood termite, *Zootermopsis nevadensis*: caste differences and role of lipophorin in transport of hydrocarbons and hydrocarbon metabolites. *J Chem Ecol* 26:765–789
- Silberbush A, Markman S, Lewinsohn E, Bar E, Cohen JE, Blaustein L (2010) Predator-released hydrocarbons repel oviposition by a mosquito. *Ecol Lett* 13:1129–1138
- Silhacek DL, Mayer MS, Carlson DA, James JD (1972) Chemical classification of a male house fly attractant. *J Insect Physiol* 18:43–51
- Silk PJ, Ryall K, Lyons DB, Sweeny J, Wu J (2009) A contact sex pheromone component of the emerald ash borer *Agrilus planipennis* Fairmaire (Coleoptera: Buprestidae). *Naturwissenschaften* 96:601–608
- Silk PJ, Sweeny J, Wu J, Sopow S, Mayom PD, Magee D (2011) Contact sex pheromones identified for two species of longhorned beetles (Coleoptera: Cerambycidae) *Tetropium fuscum* and *T. cinnamopterum* in the subfamily Spondylidinae. *Environ Entomol* 40:714–726
- Singer TL, Espelie KE (1996) Nest surface hydrocarbons facilitate nestmate recognition for the social wasp, *Polistes metricus* Say (Hymenoptera: Vespidae). *J Insect Behav* 9:857–870
- Sledge MJ, Moneti G, Pieraccini G, Turillazzi S (2000) Use of solid phase microextraction in the investigation of chemical communication in social wasps. *J Chromatogr A* 873:73–77
- Smith A, Hölldobler B, Liebig J (2008) Hydrocarbon signals explain the pattern of worker and egg policing in the ant *Aphaenogaster cockerelli*. *J Chem Ecol* 34:1275–1282
- South A, LeVan K, Leombruni L, Orians CM, Lewis AM (2008) Examining the role of cuticular hydrocarbons in firefly species recognition. *Ethology* 114:916–924
- Steiner S, Hermann N, Ruther J (2006) Characterization of a female-produced courtship pheromone in the parasitoid *Nasonia vitripennis*. *J Chem Ecol* 32:1687–1702
- Stoffolano JG, Schaubert E, Yin C, Tillman JA, Blomquist GJ (1997) Cuticular hydrocarbons and their role in copulatory behavior in *Phormia regina*. *J Insect Physiol* 43:1065–1076
- Sugeno W, Hori M, Matsuda K (2006) Identification of the contact sex pheromone of *Gastrophysa atrocyanea* (Coleoptera: Chrysomelidae). *Appl Entomol Zool* 41:269–276

- Syvertsen T, Jackson L, Blomquist GJ, Vinson S (1995) Alkadienes mediating courtship in the parasitoid *Cardiochiles nigriceps* (Hymenoptera: Braconidae). *J Chem Ecol* 21:1971–1989
- Takahashi S, Gassa A (1995) Roles of cuticular hydrocarbons in intra- and interspecific recognition behavior of two Rhinotermitidae species. *J Chem Ecol* 21:1837–1845
- Tebayashi S, Hirai N, Suzuki T, Maysuyama S, Nakakita H, Nemoto T, Nakanishi H (1998) Identification of (+)-acordiene as an aggregation pheromone for *Gnatocerus cornutus* (F). *J Stored Prod Res* 34:99–106
- Teerawanichpan P, Robertson AJ, Qiu X (2010) A fatty acyl-CoA reductase highly expressed in the head of honey bee (*Apis mellifera*) involves biosynthesis of a wide range of aliphatic fatty alcohols. *Insect Biochem Mol Biol* 40:641–649
- Tentschert J, Bestmann HJ, Heinze J (2002) Cuticular compounds of workers and queens in two *Leptothorax* ant species – a comparison of results obtained by solvent extraction, solid sampling, and SPME. *Chemoecology* 12:15–21
- Tillman-Wall JA, Vanderwel D, Kuenzli ME, Reitz RC, Blomquist GJ (1992) Regulation of sex pheromone biosynthesis in the housefly, *Musca domestica*: relative contribution of the elongation and reductive step. *Arch Biochem Biophys* 299:92–99
- Tóth M, Csonka É, Bartelt RJ, Cossé AA, Zilkowski BW, Muto S-E, Mori K (2005) Pheromonal activity of compounds identified from male *Phyllotreta cruciferae*: field tests of racemic mixtures, pure enantiomers, and combinations with allyl isothiocyanate. *J Chem Ecol* 31:2705–2720
- Turillazzi S, Sledge MF, Dani FR, Cervo R, Massolo A, Fondelli L (2000) Social hackers: integration in the host chemical recognition system by a paper wasp social parasite. *Naturwissenschaften* 87:172–176
- Uebel EC, Sonnet PE, Miller RW, Beroza M (1975) Sex pheromone of the face fly, *Musca autumnalis* De Geer (Diptera: Muscidae). *J Chem Ecol* 1:195–202
- van Zweden JS, d’Ettorre P (2010) Nestmate recognition in social insects and the role of hydrocarbons. In: Blomquist GJ, Bagnères A-G (eds) *Insect hydrocarbons: biology, biochemistry, and chemical ecology*. Cambridge University Press, Cambridge, pp 222–243
- Vander Meer RK, Morel L (1998) Nestmate recognition in ants. In: Vander Meer RK, Breed MD, Espelie KE, Winston ML (eds) *Pheromone communication in social insects: ants, wasps, bees, and termites*. Westview Press, Boulder, pp 79–103
- Vander Meer RK, Wojcik DP (1982) Chemical mimicry in the myrmecophilous beetle *Myrmecaphodius excavaticollis*. *Science* 218:806–808
- Vander Meer RK, Jouvenaz DP, Wojcik DP (1989) Chemical mimicry in a parasitoid (Hymenoptera: Eucharitidae) of fire ants (Hymenoptera: Formicidae). *J Chem Ecol* 15:2247–2261
- Vásquez GM, Schal C, Silverman J (2009) Colony fusion in Argentine ants is guided by worker and queen cuticular hydrocarbon profile similarity. *J Chem Ecol* 35:922–932
- Vaz AH, Blomquist GJ, Reitz RC (1988) Characterization of the fatty acyl elongation reactions involved in hydrocarbon biosynthesis in the housefly, *Musca domestica* L. *Insect Biochem* 18:177–184
- Wagner D, Brown MJF, Broun P, Cuevas W, Moses LE, Chao DL, Gordon DM (1998) Task related differences in the cuticular hydrocarbon composition of harvester ants, *Pogonomyrmex barbatus*. *J Chem Ecol* 24:2021–2037
- Wheeler CA, Cardé RT (2014) Following in their footprints: cuticular hydrocarbons as overwintering aggregation site markers in *Hippodamia convergens*. *J Chem Ecol* 40:418–428
- Wicker-Thomas C (2007) Pheromonal communication involved in courtship behavior in Diptera. *J Insect Physiol* 53:1089–1100
- Wicker-Thomas C, Chertemps T (2010) Molecular biology and genetics of hydrocarbon production. In: Blomquist GJ, Bagnères AG (eds) *Insect hydrocarbons: biology, biochemistry, and chemical ecology*. Cambridge University Press, Cambridge, pp 53–74
- Wicker-Thomas C, Garrido D, Bontouou G, Napal L, Mazuras N, Denis B, Rubin T, Parvy J-P, Jacques Montagne J (2015) Flexible origin of hydrocarbon/pheromone precursors in *Drosophila melanogaster*. *J Lipid Res* 56:2094–2101

- Wyatt TD (2014) Pheromones and animal behavior, 2nd edn. Cambridge University Press, Cambridge, p 419
- Xu H, Ye GY, Xu Y, Hu C, Zhu GH (2014) Age-dependent changes in cuticular hydrocarbons of larvae in *Aldrichina grahmi* (Aldrich) (Diptera: Calliphoridae). *Forensic Sci Int* 242:236–241
- Zhang B, Xue HJ, Song KQ, Liu J, Li WZ, Nie RE, Yang XK (2014) Male mate recognition via cuticular hydrocarbons facilitates sexual isolation between sympatric leaf beetle sister species. *J Insect Physiol* 70:15–21

Part II
Peritrophic Membranes and Eggshell
Matrices

Chapter 8

Peritrophic Matrices

Hans Merzendorfer, Marco Kelkenberg, and Subbaratnam Muthukrishnan

Abstract The peritrophic matrix (PM) is an invertebrate intestinal lining, which partitions the midgut lumen into separate digestive compartments, lubricates the luminal surface to protect from food abrasion, shields from invasion by pathogenic microorganisms and regulates immune responses. It is composed of chitin fibers cross-linked by chitin-binding PM proteins (PMPs) to form a three-dimensional meshwork with water-filled pores of distinct diameters. Various PMPs and other PM-associated proteins have been identified and several of them appear to be essential for maintaining the structural integrity and physiological function of the PM. The PMPs have chitin-binding domains (mostly ChtBD2) and frequently mucin-like linker domains that are more or less extensively *O*-glycosylated. The composition of PMPs largely determines the physicochemical properties of the PM, and the *O*-glycans of the mucin-like PMPs (also known as invertebrate intestinal mucins, IIMs) appear to be essential for lubrication and the control of exclusion sizes. Over the past years, much progress has been made in understanding the physiological function of the PM in digestion and innate immunity. This review aims to provide an overview on the insect PM with a particular focus on structure-function-relationships of the PM components.

8.1 Introduction

Animal nutrition requires an intestinal system, which ensures effective digestion of the ingested dietary molecules while preventing invasion of pathogens and parasites. To protect the intestinal epithelium, the majority of metazoan species, including arthropods and vertebrates, secrete non-cellular layers of a mucous material,

H. Merzendorfer (✉) • M. Kelkenberg
Department of Chemistry and Biology – Institute of Biology, University of Siegen,
Adolf-Reichwein-Str. 2, 57076 Siegen, Germany
e-mail: merzendorfer@chemie-bio.uni-siegen.de

S. Muthukrishnan
Department of Biochemistry & Molecular Biophysics, Kansas State University,
141 Chalmers Hall, Manhattan, KS 66506, USA
e-mail: smk@ksu.edu

which is rich in carbohydrates and exhibits semi-permeable properties. The first layer is the glycocalyx, which is found on the surface of most eukaryotic and even some bacterial cells. It is formed by the carbohydrate moieties of glycolipids and glycoproteins. Additional layers may be gel-like, as in case of the mucus found in the intestine of mammals, or appear membranous with more rigid properties as found in sipunculids, molluscs, annelids and arthropods (Lehane 1997). In many phylogenetic taxa such as insecta, the mucous membrane is reinforced by nanofibers, which are frequently made of chitin. Due to their fast growth rates, insects particularly depend on an effective digestive system. The gut is divided into three main regions of specialized functions: foregut, midgut and hindgut, which are all formed by mono-layered epithelia. While the epithelia of the foregut and hindgut are ectodermal, the midgut epithelium is endodermal in origin. The foregut is the anatomical structure that the food passes through. Salivary secretions are added that help to lubricate the ingested food and initiate digestion. Most of the digestion occurs in the midgut where the dietary molecules are broken down into largely monomeric units and partially absorbed. In the hindgut absorption of nutritional molecules is continued. In addition, this region is specialized in water and ion resorption. Regardless of origin and function, all of these intestinal epithelia are usually covered by extracellular secretions to protect the epithelial cells. Due to their ectodermal identities, the foregut and hindgut are covered by cuticular linings, which are regularly replaced during molting. In contrast, the midgut of most insects is lined by another type of extracellular secretion, which is called peritrophic matrix (PM). This type of lining had been noted more than 250 years ago by Pierre Lyonet in a monograph on the anatomy of the goat-moth caterpillar, *Cossus cossus* (Lyonet 1762). Similar structures were found in the nineteenth century in many insect orders and in other arthropods including species of the subphyla chelicerata, crustacea and myriapoda (Peters 1992). In most cases, the PM was described as a membranous sheath enclosing the food bolus and/or the fecal pellet. Such a PM lining the larval midgut epithelium of the red flour beetle, *Tribolium castaneum* is exemplarily shown in Fig. 8.1. Due to its appearance as a membranous sack surrounding the gut content, it was first denominated in 1890 by Édouard-Gérard Balbiani as peritrophic membrane (Balbiani 1890). This term has been successively replaced during the last decades by peritrophic matrix to avoid the misleading term “membrane”, which is reserved in biology for lipid bilayers, and emphasize that the PM is an apical extracellular matrix with surprisingly complex characteristics. In a narrower sense, the PM is a more solid lining with elastic properties, which can be grabbed with forceps (Terra 2001). In some cases, however, the secretion is highly mucous and gel-like and cannot be picked up by forceps. This type of secretion was denoted as peritrophic gel (PG). From the finding that the PG of the anterior midgut of the hide beetle, *Dermestes maculatus* cannot be stained with chitin labeling reagents it was concluded that it lacks chitin, in contrast to the chitinous PM found in the median and posterior parts of the midgut (Caldeira et al. 2007). The PGs may mainly consist of glycoproteins and are likely to be significantly more permeable than PMs, but may be more easily disrupted by rough food particles, which are often ingested by insects feeding on dry matters (Terra 2001).

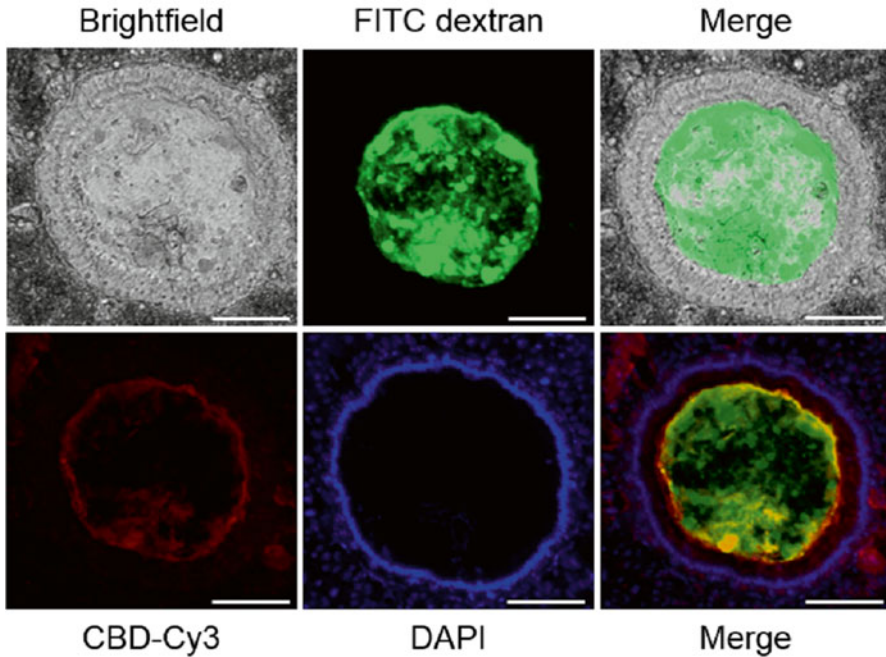


Fig. 8.1 The peritrophic matrix of *Tribolium castaneum* larvae. Over a period of 6 days, larvae were continuously fed with a wheat flour diet supplemented with fluorescent FITC-dextran possessing a mass of 2 MDa (green). Subsequent to formaldehyde-fixation, cryosections of 20 μm from the abdominal body segments A2–A5 containing the median midgut region were prepared. The samples were stained with CBD-Cy3 to label the PM (red) and with DAPI to label the nuclei of midgut epithelial cells (blue). Merged images (right panels) show a combination of images of the bright field and FITC dextran fluorescence (upper two left panels) or a combination of CBD-Cy3, FITC dextran- and DAPI fluorescence (lower two left panels and middle upper panel). Note, that the PM (red) is an efficient barrier to FITC dextran (green) as no FITC signals can be detected in the ectoperitrophic space above the midgut epithelium (nuclei stained in blue). Scale bars, 100 μm

PMs and PGs are found in most insect orders but are absent in hemipteran and thysanopteran insects, which feed on plant saps or animal blood. In these insects, the midgut epithelium is equipped with a perimicrovillar membrane (PMMs), which prevents direct contact of the microvillar membranes (MMs) with the gut content (Silva et al. 2004).

8.1.1 Perimicrovillar Membranes (PMMs)

PMMs have been originally described as a second extracellular membrane covering the MMs in the midgut of paraneopteran insects. They have been found particularly in planthoppers (infraorder Fulgoroidea) and blood-sucking bugs (suborder

heteroptera) (Marshall and Cheung 1970; Reger 1971; Burgos and Gutierrez 1976), but are absent in the psocodean orders of lice (Phthiraptera) and booklice (Psocoptera), which suggests that they may have evolved from a condylognathan ancestor (Silva et al. 2004). In addition, PMMs were reported in thrips (Thysanoptera) (Kitajima 1975; Del Bene et al. 1991). Originally, PMMs were not identified in cicadas (Cicadidae) and froghoppers (Cercopoidea) (Marshall and Cheung 1974), leafhoppers (Cicadelloidea) (Lindsay and Marshall 1980), and in aphids (Aphididae) (O'Loughlin and Chambers 1972). But closer evaluation of published data suggested that PMM-like structures do also exist in these hemipteran taxa, although in some groups such as aphids they seem to be modified to special anatomical characteristics such as the apical lamellae in the anterior midgut of aphids, where no microvilli are observed (Cristofolletti et al. 2003). PMMs have been best studied in the kissing bug, *Rhodnius prolyxus*, the triatomine vector of the Chagas parasite *Trypanosoma cruzi*. Ultrastructural analyses revealed that the outer membrane extends from the base of the microvilli into the gut lumen forming blind-ended tubes. Thereby, they generate a closed compartment named perimicrovillar space, which is located between the microvillar membrane and the PMM, and may help to partition digestive enzymes (Terra 1988). As PMMs are essentially free of intramembranous particles, they resemble myelin-sheets (Lane and Harrison 1979). Differences in the buoyant densities between microvillar membranes and PMMs allowed the separation of these membranes by density gradient centrifugation, and to identify marker enzymes for the respective membrane fractions: α -mannosidase and β -glucosidase in the MMs, and α -glucosidase in the PMM (Ferreira et al. 1988; Silva et al. 1996). Next to α -glucosidase, acidic phosphatase has also been described as a PMM marker in the sunn pest *Eurygaster integriceps* (Hemiptera: Scutelleridae) (Allahyari et al. 2010). Immunocytochemical analyses with antibodies to α -glucosidase suggest that in *Rhodnius* the PMM originates from fusions of the outer membranes of intracellular double-membrane vesicles with the MMs so that inner single-membrane vesicles are released that finally fuse with the extracellular PMM (Silva and Terra 1995). Major structural components of the PMM are phospholipids, which are synthesized and accumulated in the posterior midgut, as well as lipoproteins and glycoconjugates detectable by lectins and histochemical reagents. Glycoconjugates residing in the PMM have been suggested to function in adherence of trypanosomatids (Alves et al. 2007). Recently, chitin also has been identified as a component of the *Rhodnius* midgut and its luminal projections (Alvarenga et al. 2015). In blood-sucking bugs, PMMs have been suggested to promote heme detoxification by inducing the formation of crystalline hemozoin (Silva et al. 2007; Oliveira et al. 2007). In particular, it has been shown that α -glucosidase, which resides in the PMMs, is responsible for the nucleation of hemozoin (Mury et al. 2009; Fonseca et al. 2010). The PMM of phloem plant sap feeding hemipteran insects may have evolved in adaptation to the low content of polymeric dietary molecules which may have resulted in a loss of PM and hydrolytic enzymes associated with digestion in the gut lumen. Essential amino acids may be absorbed by potassium coupled symporters residing in the PMM that utilizes the electrochemical potassium gradient established by uncharacterized active pumps located in the MMs (Terra 1988).

Interestingly, the PM seems to be an intestinal barrier for bacteria also in the opposite direction as indicated by a study published already in 1932, in which scientists examined the intracellular parasite *Rickettsia prowazeki* in fleas that may cause epidemic typhus in humans after a flea bite (Mooser and Castaneda 1932). The authors noted that only few *Rickettsiae* were found in gut lumen, although lysing epithelial cells released the bacteria in high amounts. This finding was explained by the presence of a PMM, which covers the epithelium of the entire stomach and holds back the bacteria. This reduces the bacterial load in the feces of fleas and thus lowers the risk of flea-mediated infection of humans. In contrast, body lice appear to lack this barrier for *Rickettsiae*, as high numbers of these bacteria are found in the gut content, increasing the infectivity of lice feces.

8.1.2 Peritrophic Matrices and Gels (PMs and PGs)

In contrast to PMMs, PMs are found in most insects that have been carefully analyzed for their presence. They have been reported in many insect orders except for Hemiptera, Thysanoptera, and adult lepidopteran insects, which feed only on plant saps and blood, as well as in the coleopteran families Carabidae and Dytiscidae, which exhibit extra-intestinal digestion. In addition, PM appears to be absent in Strepsiptera, Raphidioptera and Megaloptera (Peters 1992). Some of the initial reports on the absence of a PM in particular insect species were corrected later, because either the particular stage of the insect that was inspected lacked a PM, or the PM was solubilized during fixation. In the yellow fever mosquito (*Aedes aegypti*), for instance, a PM is not detectable in pupae, in adult males or in unfed young female adults. However, shortly after female mosquitoes ingested a blood meal, a PM is formed around the blood bolus, which is different from that formed in the larval gut (Richards and Richards 1977). Since the first description of the PM and subsequent reports of its presence in many arthropods in the nineteenth century, insect physiologists have made significant progress in understanding structure and function of the PM and summarized available data in several excellent original papers and reviews. Wigglesworth (1930) collected available histological data to propose mechanisms on the formation of the PM, particularly focusing on the mid-gut of mosquito larvae but also summarizing data from other main insect orders. Next, Waterhouse (1953) analyzed the occurrence of the PM in insects based on chitin-detecting tests, and tried to figure out its possible role in digestion (Waterhouse 1957). In his text book, Werner Peters provided a comprehensive view on the structure and function of the PM based on the data available to this date (Peters 1992). Jacobs-Lorena and Oo (1996) summarized data on PM function for mosquito vectors. In his review, Lehane (1997) extended existing ideas on PM functions particularly based on PM permeability and filtration properties. Tellam et al. (1999) provided deeper insight into structure and functions of the proteins that associate with the PM. They were also the first to categorize PM-associated proteins based on their extractability, and systematically analyzed their domain

architecture. Finally, Hegedus et al. (2009) published the most recent review on PM structure and function and suggested a holistic model on the structure-function relationships in PMs.

In this review, we will focus on the physicochemical properties and the physiological functions of PMs in digestion and innate immunity. We will further discuss current hypotheses on the structure-function relationships of chitin nanofibers and PM-associated proteins.

8.2 Structural Components of the PM

Depending on the physiological context, the PM is composed of varying constituents that confer characteristic properties needed for its respective function. In addition to chitin nanofibers, which form a fibrillar meshwork, proteins and glycoproteins are structural elements of the PM (Fig. 8.3).

It is assumed that the chitin content of the PM ranges between 3 and 13 % (w/w) depending on the respective species, while the proteinaceous part accounts for 20–55 % (w/w) of the total PM mass (De Mets and Jeuniaux 1962; Ono and Kato 1968; Zimmermann et al. 1975; Becker 1980). The glycan moieties of glycoproteins and proteoglycans may represent the remaining portion of the PM. Although there are numerous approaches addressing the interplay of the different components, it still remains speculative how they exactly interact and in which way they influence one another.

8.2.1 Chitin Nanofibers

As structural components of the PM, chitin nanofibers serve as binding sites for various PM-associated proteins resulting in a chitinous meshwork embedded in a proteinaceous matrix (Fig. 8.3). The chitin fibers are thought to confer tensile strength to the PM (Dinglasan et al. 2009; Peters 1992). Single chitin chains are synthesized from UDP-*N*-acetylglucosamines to form a polymer of β -1,4-linked *N*-acetylglucosamines (GlcNAc) (Merzendorfer 2006). This reaction is catalyzed by a membrane-integral family II glycosyltransferase known as chitin synthase, which is specifically expressed in the columnar cells of the midgut epithelium (Zimoch and Merzendorfer 2002; Arakane et al. 2005; Hogenkamp et al. 2005; Zimoch et al. 2005). UDP-GlcNAc is generated from the glycolysis intermediate fructose-6-phosphate in a cascade of reactions that involves different enzymes (Merzendorfer and Zimoch 2003). The active form of the chitin synthase is supposed to form an oligomer as demonstrated for the enzyme from the tobacco hornworm, *Manduca sexta* (MsCHS2). The assembly into an oligomeric complex of several catalytic units, which simultaneously secrete chitin polymers, may be crucial during fibrillogenesis to form chitin nanofibers (Maue et al. 2009). The catalytic center of the chitin synthase faces the cytosol. Here, single GlcNAc monomers are

successively added to the non-reducing end of the elongating chitin chain. Finally, the polymer is predicted to pass through a pore formed by transmembrane domains to reach the extracellular space where it assembles with other polymers secreted by neighboring catalytic units (Merzendorfer 2006, 2013; Muthukrishnan et al. 2016, this volume). Therefore, it seems likely that polymerization, translocation and fibrillogenesis are tightly coupled processes (Merzendorfer 2013). In this way, about 20 chitin chains assemble into a nanofiber with a resulting diameter of 2–6 nm and a length of up to 500 nm or even longer (Lehane 1997). Chitin nanofibers frequently are organized into microfibrillar bundles in the PM with diameters of about 20 nm (Peters et al. 1979; Kramer et al. 1985; Peters 1992). There are three isomorphs of chitin, which differ with respect to the orientation of sugar chains relative to one another. α -Chitin, which consists of antiparallel chitin chains, appears to be present in regular PM structures and shows the highest thermodynamic stability as a consequence of the large number of hydrogen bonds formed between chitin chains (Tristram 1977, 1978; Jang et al. 2004). In β -chitin, single chitin chains are oriented in a parallel manner resulting in a more flexible structure, which may incorporate a large number of water molecules. Some insects use this form of chitin for a PM, which is designated to spin the cocoon for pupation. In this case, the PM changes from a tube to a flat yarn which emerges from the anus and is used to spin the cocoon. γ -Chitin, which is also found in the PM of some insects, is assembled of alternating α - and β -chitin variants (Rudall and Kenchington 1973; Tristram 1977; Jang et al. 2004). It should be noted that there is a lack of structural studies that would clarify which type of chitin is commonly present in the PM of insects.

8.2.2 *Proteins Loosely Associated with the PM*

The PM interacts with a large number of different proteins serving various functions. Structural proteins of the PM are firmly associated with the chitin fibers and frequently possess high affinity chitin-binding domains. Many other proteins are not permanently required to be in direct contact with the PM, and they are only loosely associated with it. Tellam et al. (1999) proposed four classes of PM-associated proteins considering their extractability using different buffers. According to this classification, class I and II proteins are only loosely associated with the PM, and they represent less than 1% and 2% of the total mass of PM-associated proteins from larvae of the Australian sheep blowfly, *Lucilia cuprina*, respectively. Class I PM-associated proteins may be simply trapped within the PM, because physiological buffers are sufficient to remove these proteins from the PM. Many digestive enzymes passing through the PM might fall into this class. The binding affinity of class II PM-associated proteins is more pronounced but still comparably weak, because these proteins can be removed with mild detergents such as SDS, which disrupt weak ionic interactions. Some digestive enzymes may also group here, as they have been shown to interact with the PM (Terra et al. 1979; Walker et al. 1980; Peters and Kalnins 1985; Ferreira et al. 1994a; Jordao et al. 1996; Rose et al. 2014).

In the fall armyworm, *Spodoptera frugiperda* the activity of PM-bound trypsin accounts for 18 % of the total enzyme activity in the midgut (Ferreira et al. 1994b). In this case, it is assumed that electrostatic interactions play a role due to the fact that positively charged trypsin was found to be associated with the negatively charged PM. Furthermore, digestive enzymes, which do not exhibit positive charges, could be immobilized by hydrogen bonds or more specific interactions (Jackson et al. 1991; Hardingham and Fosang 1992). Weak interactions were also demonstrated for enzymes involved in chitin modifications which may occur in the contexts of facilitated digestion or defense responses against ingested pathogens (Shen and Jacobs-Lorena 1997; Guo et al. 2005; Toprak et al. 2008; Rose et al. 2014). All these enzymes are only needed under feeding conditions or when pathogens are present. To date, it is unknown which types of intermolecular interactions mediate binding of proteins to the PM.

8.2.3 Proteins Tightly Associated with the PM

Most of the PM-associated proteins are firmly attached to the PM. According to the classification of Tellam et al. (1999), they belong to class III and class IV of PM-associated proteins which represent 11 % and 87 % of all larval PM-associated proteins in *L. cuprina*, respectively. The removal of class III proteins requires strong denaturants like urea, and due to their tight binding, class III proteins also have been denoted as PM proteins (PMPs). Class IV PM-associated proteins are supposed to be covalently bound, as even harsh treatments do not release them from the PM. Corresponding crosslinking reactions could involve phenoloxidases and transglutaminases, which have been detected in the midgut of insects. The multicopper oxidase-3 from the malaria transmitting mosquito, *Anopheles gambiae*, for instance, was shown to be associated with the PM, where it may crosslink toxic compounds to the PM for excretion (Lang et al. 2012). A transglutaminase has been recently shown to crosslink the drosocrystallin, a PM protein from the fruit fly, *Drosophila melanogaster*, to form a stable fiber structure on the PM (Shibata et al. 2015).

Although the number of proteins being integral components of the PM can reach up to 40 different molecules, in most species the PM possess no more than 12 PMPs with chitin binding domains (CBDs) containing 6–10 conserved cysteines (see below). Most of them have molecular masses of up to 100 kDa, and some even reach 220 kDa (Lehane 1997). Numerous PMPs possess also cysteine residues in non-CBD regions. These cysteines have been suggested to contribute to protein-protein crosslinking by forming intermolecular disulfide bridges in order to tighten the structural integrity of the PM (Hegedus et al. 2009).

Based on sequence homologies, numerous PMP-encoding genes have been identified in the genomes of various insects (see Tetreau et al. 2015 and references therein). In addition, they have been found in several PM-derived proteomes using mass spectrometry (Campbell et al. 2008; Hu et al. 2012; Toprak et al. 2015). All members of the PMP family of proteins exhibit a signal peptide for secretion. Their binding to the chitin fibrils of the PM is mediated by CBDs, which exhibit six, eight

or ten conserved cysteine residues. These domains, which belong to the carbohydrate binding module 14 family (CBM-14), are referred to as peritrophin A, B, or C domains, respectively (Tellam et al. 1999). The peritrophin-A domain (or alternatively called chitin binding domain 2, ChtBD2) is the predominant CBD in arthropods and is found in numerous proteins which associate with chitin including cuticular proteins analogous to peritrophins (CPAPs) and PMPs (Barry et al. 1999; Behr and Hoch 2005; Jasrapuria et al. 2010). A single ChtBD2 typically comprises 60 to 70 amino acids forming alternating β -sheets. It contains six cysteine residues in a motif with the conserved consensus sequence $CX_{11-30}CX_{5-6}CX_{9-24}CX_{12-17}CX_{6-12}C$ (X represents an arbitrary amino acid except cysteine) (Tetreau et al. 2015). The regions between the conserved cysteines are also highly conserved (Tellam et al. 1999; Cantarel et al. 2009). ChtBD2 forms a chitin-binding pocket, which is stabilized by three disulfide bridges formed between pairs of cysteine residues. At the core of the pocket, there are two hydrophobic and aromatic amino acids that mediate interactions with chitin chains via hydrogen bonding. Next to the binding pocket, a special ternary structure at the C-terminal end of the CBD, which is composed of two antiparallel β -sheets and a short α -helix in 3'-direction, is stabilized by a disulfide bridge (Asensio et al. 1998).

PMPs show a large variation in the number of CBDs. While some PMPs have only a single ChtBD2, others contain up to 19 of these domains. After expression and secretion into the ectoperitrophic space, some of the PMPs may be processed by tryptic cleavage resulting in smaller units with a decreased number of CBDs, because many PMPs possess trypsin cleavage sites downstream of CBDs. These fragments are believed to be integrated into the PM (Shi et al. 2004; Wang et al. 2004; Ferreira et al. 2008). In addition to structural PMPs, there are also proteins with catalytic functions with a ChtBD2 that bind to chitin. Enzymes involved in chitin metabolism such as chitinases and chitin deacetylases have been shown to belong to this group (Kramer et al. 1993; Campbell et al. 2008; Dixit et al. 2008; Zhu et al. 2008). These enzymes are assumed to modify PM properties, like porosity and permeability, according to the actual physiological requirements (Shen and Jacobs-Lorena 1997; Toprak et al. 2008).

PMPs with ChtBD2 domains can be subdivided into two large groups depending on the extent of glycosylation: non-mucin-like proteins, which may be *N*-glycosylated to some degree, and mucin-like proteins, which typically include Ser/Thr-rich linker domains that have been implicated in *O*-glycosylation generating large glycoproteins and proteoglycans. However, reliable data on glycosylation exists for only some PMPs. The vast majority of PMPs have not been analyzed for glycosylation, let alone having been examined for the degree or kind of glycosylation. Therefore, the distinction between these two classes of PMPs is uncertain.

8.2.3.1 Non Mucin-Like PMPs

Non-mucin like PMPs may constitute only a small group of PMPs, as many of the PMPs contain Ser/Thr/Pro-rich domains that are presumably glycosylated. However, it has to be emphasized that despite the fact that non-mucin like proteins lack such

Ser/Thr/Pro-rich domains, they yet may be glycosylated at Asn residues, which appears to account for many proteins secreted into the midgut lumen. Among the first PMPs described were non-mucin-like proteins, including the peritrophins 44 and 48 from *L. cuprina*, which are expressed exclusively by cardia cells of the larvae (Elvin et al. 1996; Schorderet et al. 1998). In *T. castaneum*, only two PMPs (TcPMP3 and TcPMP5-B) have marked Ser/Thr-rich linker domains with long repeats, which are extensively glycosylated and largely determine PM permeability (Agrawal et al. 2014). The nine remaining PMPs from *T. castaneum* do not possess linker domains with long unbroken Ser/Thr-rich repeats, and thus can be assumed to be *O*-glycosylated to a lower extent. While TcPMP5-B has for instance eight Ser-rich motifs with at least 9–14 consecutive serine repeats, there are no regions in TcPMP5-A that contain more than three Ser or Thr residues. As RNAi silencing of the corresponding genes for non-mucin-like PMPs did not result in nutritional deficiencies, developmental retardation or mortality, a secondary or redundant role in maintaining PM integrity may be depicted for them. In some cases, however, RNAi-mediated effects of different kinds were yet observed. Their explanation may turn out to be more subtle. For instance, after parenteral RNAi for *TcPMP1-C*, the number of eggs laid by females was significantly reduced (Agrawal et al. 2014). It is possible that this could be due to slightly impaired digestion not affecting the nutritional state of the mother but rather the development of eggs, which is more sensitive to minor changes in energy stores.

8.2.3.2 Mucin-Like PMPs

The majority of mucin-like PMPs may possess covalently attached glycans with higher molecular masses. There is a great diversity in the kind of sugar residues and their content within the glycans (Derksen and Granados 1988; Dorner and Peters 1988; Rudin and Hecker 1989; Ramos et al. 1994; Lehane et al. 1996). The first PMP with a large attached glycan was identified in the cabbage looper, *Trichoplusia ni*, and named invertebrate intestinal mucin (IIM) (Wang and Granados 1997b). This term reflects the fact that glycoproteins attract large amounts of water molecules creating a mucus-like environment in direct proximity of the PM. This resembles the glycoprotein (mucin)-containing mucus which covers digestive and respiratory epithelia in vertebrates. The IIM from *T. ni* harbors five CBDs being distributed in a specific pattern. One CBD is located at the *N*- and another at the *C*-terminal end of this protein. The three remaining CBDs form a cluster in the middle part of the protein. It is framed by Pro, Ser and Thr enriched motifs (mucin domains) with repeats of 4–27 of these amino acids acting as *O*-glycosylation sites (Wang and Granados 1997a). The overall structural organization of the mucin domains was confirmed in subsequent studies (Sarauer et al. 2003; Shi et al. 2004). A common characteristic of the mucin domains from the IIMs described so far is that more than 80% of their Ser, Thr, and Pro residues are *O*-glycosylated. Reports that the glycans contribute up to 50% to the total mass of IIMs match these findings (Wang and Granados 1997a; Shi et al. 2004; Agrawal et al. 2014). The high degree of glycosylation separates

IIMs from other glycoproteins with significantly smaller number of sugar attachments. In addition to *O*-linked glycans, there are also PMPs with long stretches of Asn residues providing the basis for large N-linked glycan moieties (Vuocolo et al. 2001; Schorderet et al. 1998). The special composition of IIM glycans is most accurately described by the term glycosaminoglycans (GAGs). At the basal core they possess two β -1,4-linked *N*-acetylglucosamine residues (Lehane 1997). At the next level, these are followed by different disaccharides branching at multiple levels. This architecture of numerous different orders enables the synthesis of widely branched and extended GAGs. One unit of the disaccharides is always a hexosamine and the remaining unit is represented by a uronic acid (D-glucuronic acid or iduronic acid) (Lehane 1997; Zhang et al. 2012). Due to their large size, the glycan moieties of IIMs occupy a significant portion of the interstitial volumes in the chitin meshwork of the PM. Thus, space filling by glycans appears to be a crucial parameter, which determines the exclusion size of the PM making glycosylated PMPs, like IIMs, important elements of the PM architecture. Experimental evidence for this hypothesis has been recently provided using RNAi to knock-down the genes for two IIM-like PMPs in *T. castaneum* larvae, which resulted in a significant increase in PM permeability for fluorescein isothiocyanate (FITC)-dextran that are completely retained in the endoperitrophic space under control conditions (Agrawal et al. 2014). The PM may be considered as a semipermeable matrix, which controls particle and molecule trafficking between the endoperitrophic and the ectoperitrophic space of the midgut. Therefore, its permeability is of enormous physiological significance for proper digestion and defense against intruding pathogens.

Due to carboxylic and sulfate side chains of the sugar residues in the GAGs, the net charge of the PM is negative (Kjellen and Lindahl 1991). Therefore, strong ionic interactions can be assumed to be present at the PM caused by the high glycan density and resulting van der Waals forces, which may chemically support the discrimination between different molecules (Hegedus et al. 2009). Accordingly, negatively-charged molecules are restricted to the endoperitrophic space due to electrostatic repulsion, while positively-charged molecules are facilitated in crossing the PM in case of close proximity as demonstrated after ingestion of calcium ions (Miller and Lehane 1993; Walski et al. 2014). The finding that a change from pH 7.3 in the anterior midgut to 6.3 in the posterior midgut of tsetse fly, *Glossinia morsitans morsitans* leads to an increase in anionic charge density within the PM provides further evidence for this relationship (Wigglesworth 1929; Lehane et al. 1996). Although alkaline phosphatase secreted by midgut cells of the tsetse fly has a net negative charge at pH 6.3, the pH gradient in the gut did not result in any alterations of the enzyme's ability to migrate through the PM. Obviously, the PM distinguishes between exo- and endogenous molecules (Miller and Lehane 1993). Electrostatic interactions may be used in this way by numerous insects showing specific gradients of pH and ionic concentrations along the midgut from anterior to posterior. This could support the adaptation of permeability conditions to different physiological requirements (Hegedus et al. 2003; Fazito do Vale et al. 2007).

Since CBDs could recognize the two β -1,4-linked GlcNAc residues at the core of GAGs, PMPs may not only be able to interact with chitin fibrils, but also directly with each other and with different glycoproteins and proteoglycans. By this means,

a network of interconnected proteins can be established (Dorner and Peters 1988; Lehane et al. 1996; Wang and Granados 1997b). The repeats of proline residues in the mucin domain may not only serve as *O*-glycosylation sites, but also enable the formation of β -turns. As a consequence, the carbohydrates are forced to face outwards due to their large size and electrostatic repulsion. Within this structure, the glycans enwrap the protein portion completely. This results in a very rigid structure protecting the whole PM not only from proteolytic but also from chitinolytic degradation, as the chitin fibers represent the innermost structure of the PM (Wang and Granados 1997b).

Serine proteases, particularly trypsin and chymotrypsin, are highly abundant in the alkaline midgut of the bertha armyworm, *Mamestra configurata*. In order to protect midgut epithelial cells from endogenous proteolytic attack, mucin domains lack amino acids that are typically present in the cleavage sites for these enzymes (Hegedus et al. 2003). In this way, the harmful impact of numerous pathogens, which release trypsin and chymotrypsin after they have invaded the digestive tract, is avoided. Additionally, glycosylated PMPs protect the organism from infections. Regarding these findings, there are two major functions of insect mucins: maintenance of PM integrity and protection of the midgut epithelium from environmental impacts. Comparable functions have been described for mucins in vertebrates (Perez-Vilar and Hill 1999).

Another group of glycosylated proteins present in insect PMs are proteoglycans. They differ from glycoproteins as their GAGs are much more extended and inflexible, and they never exhibit branched formations. The long sugar chains may form randomly coiled structures, which project far into the endoperitrophic space (Lehane 1997). Proteoglycans exhibit a strong negative charge due to the high abundance of carboxylate and sulfate groups attached to the sugar side chains. Consequently, large amounts of cations are attracted to these ionic groups followed by passive diffusion of water molecules largely accumulating in the PM. This results in a gel-like structure exhibiting a high internal turgor pressure enabling the PM to resist strong compressive forces (Jackson et al. 1991). The rigid and tensile chitin network of the PM is counteracting this pressure (Hardingham et al. 1990). This balanced interplay of structural elements and forces assures a high degree of mechanical stability of the PM. The attracted water additionally causes a solvent drag resulting in an accumulation of dissolved dietary molecules at the luminal surface of the PM (Drioli et al. 1976). This could significantly accelerate digestion, as digestive enzymes access their substrates more rapidly due to their high concentrations at the respective location. Thus, enzyme activities may be highly increased in such a situation (Lehane 1997). An additional advantage of a hygroscopic PM is an accelerated dehydration of watery diets of insects feeding on fluids, as the water is removed more effectively from the midgut while passing through the PM. The gel-like texture of the PM also serves as a lubricant for the food bolus passing through the midgut from the anterior to the posterior end, thus protecting the midgut epithelium from mechanical damage (Perez-Vilar and Hill 1999).

Due to their large dimensions, GAGs of glycoproteins and proteoglycans are crucial for PM architecture, as they are one of the main factors determining its per-

meability (Nisizawa et al. 1963; Stamm et al. 1978; Lehane et al. 1996). It is assumed that glycan attachments generate a tortuous network of water-filled channels, which take up molecules that can enter these channels being supported by hydrostatic interactions. Apparently, this provides the ability to discriminate between different molecules by size exclusion (Laurent 1964, 1970). If there is a transversal path for large molecules, they may fail to enter the narrow channels and therefore will move faster through the PM than small molecules, which laterally diffuse into the tubular network. The opposite situation occurs in a structurally less-organized PM. With increasing dimensions of the interstitial spaces, the organizational degree of the channel structure decreases and large molecules are no longer able to migrate faster through the gel matrix than smaller ones. It is conceivable that the structural organization of the PM can be modified for adaptation to actual physiological demands. Alterations of the ionic composition of the solution surrounding the PM affect the fixed charge density of GAGs. This in turn would favor small molecules to move faster through the PM, which is a consequence of a lesser hindrance by GAGs (Laurent 1964, 1970).

8.3 PM Formation and Assembly

Insect PMs exhibit great structural diversity, which likely reflects evolutionary adaptations to different food sources and other physiological and/or immunological challenges. According to the arrangement of microfibrillar textures, which can be visualized by ultrastructural microscopy, Peters (1992) proposed three structural types: orthogonal, hexagonal and random felt-like arrangements (Fig. 8.2). According to the mode of delamination, the linings were categorized as type I and type II PMs (Wigglesworth 1930). Type I PMs are produced by the entire midgut, while type II PMs are formed by a specialized zone in the anterior midgut. This is in contrast to the nomenclature used by Waterhouse (1953), who named these two types of categories in the opposite sense, but this nomenclature has not been adopted in the field. Type I delamination is considered to be the ancestral mode of PM formation and is widely distributed among insects, while type II delamination seems to be a derived mode, which is restricted to a few insect orders. Interestingly, there is no correlation between the PM types and the ultrastructural arrangement of the microfibers.

8.3.1 *General Modes of PM Assembly*

Generally, there are many variations in the mode of PM formation in insects, and sometimes the mode of PM formation falls between these two categories. In addition, it is striking that some insects produce different types of PMs at different developmental stages. For instance, mosquito larvae form a type II PM, while adults produce a type I PM in response to a blood meal (Richards and Richards 1971).

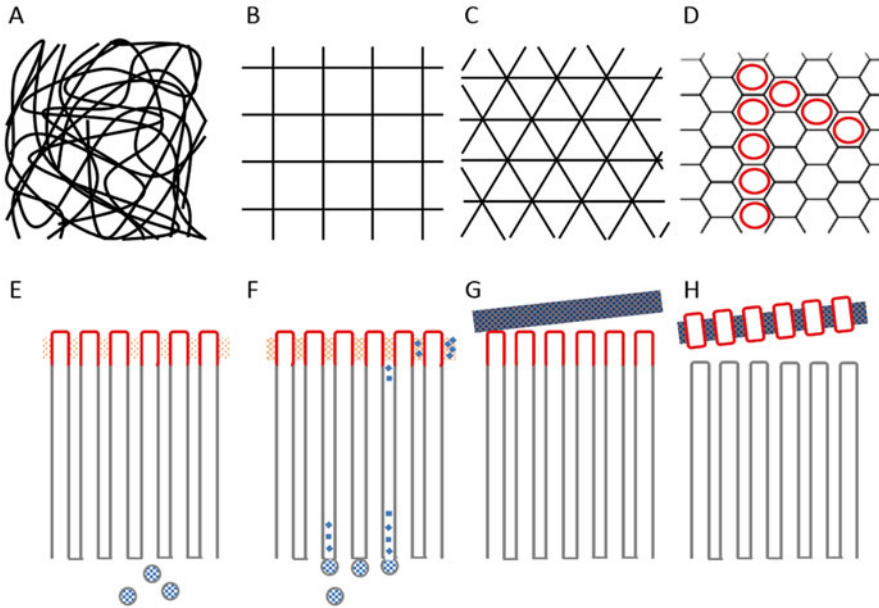


Fig. 8.2 Textures of chitin fibers found in PMs of various insects (**a–d**) and model of PM synthesis and delamination (**E–H**). Random felt-like (**a**), orthogonal (**b**), triangular (**c**), and hexagonal architectures of the chitin fibers in the PM of various insects. The diameter of microvilli is indicated by red circles within the hexagonal texture. Chitin synthesis is localized at the apical tips of microvilli of midgut columnar cells forming a chitinous meshwork between the microvilli (**e**). Secretory vesicles loaded with PMPs fuse with the plasma membrane at the base of the microvilli and release PMPs into the intermicrovillar space, where they diffuse and finally bind chitin nano-fibers and orchestrate PM assembly (**f**). The PM detaches from the microvillar array resulting in a PM with pores that correspond to the diameter of the microvilli (**g**). The PM may also delaminate in a process that resembles microapocrine secretion, as there is a small loss of cytoplasm due to the blebbing of the apical microvilli tips (**h**). In addition, apocrine secretion of PM material may occur with the formation of larger blebs with double-membranes that disintegrate to release fibrous material (not shown)

8.3.1.1 Type I PM

Type I PMs are delaminated from the surface of either the entire midgut or at least larger parts of the midgut epithelium to form concentric multi-layered sleeves. Their secretion is usually stimulated in response to feeding as observed for instance in female mosquitoes, but it can also be formed continually as in locusts. In the migratory locust, *Locusta migratoria* pulses of PM secretion occur every 15 min throughout feeding. As the PM is thought to move to the posterior part of the midgut while the next PM layer is secreted, multiple concentric layers are formed. If several individual PM layers are present, the whole structure is called peritrophic envelope. This structure can adopt the shape of a telescope as the inner PM layers continuously move posteriorly with the food bolus. As a consequence, the newest layers are missing in the more anterior regions. This kind of PM organization is well described

in the American cockroach, *Periplaneta Americana*, where the number of concentric PM layers comprises at least ten individual sheets (Lee 1968).

Type I PMs have been primarily studied in lepidopteran larvae and adult hemaphagous dipteran species. However, they are also found in many insect orders including Ephemeroptera, Odonata, Dictyoptera, Coleoptera, Orthoptera, and Hymenoptera (Waterhouse 1953; Peters 1992). In most lepidopteran species, the PM is secreted along the entire midgut, and it exhibits a felt-like structure of randomly organized fibrils. This is, for instance, the case in *M. sexta*, where the PM forms a thin multilayered lining in the anterior region of the midgut, whereas in the middle and posterior midgut multiple layers are observed (Hopkins and Harper 2001). In some lepidopteran larvae, however, different types of organization and modes of delamination were reported. In the European corn borer, *Ostrinia nubilalis*, the single-layered PM of the anterior region of the midgut fibrils forms an orthogonal network. As the food moves to the posterior region, a multi-layered PM appears with some layers particularly thicker than others (Hopkins and Harper 2001). In the tobacco budworm, *Heliothis virescens*, the PM is secreted primarily from specialized midgut epithelial cells residing at the junction of the foregut and midgut resembling the situation of type II PMs (Ryerse et al. 1992). The overall structure of the PM may also change according to different nutritional conditions. In *M. configurata*, for example, the PM of feeding larvae is comparably thin and comprised of 5–10 layers, while the PM-layers thicken during the mid-molt stage almost filling the entire gut lumen (Toprak et al. 2014). In mosquitoes, a type I PM is secreted only by females stimulated by ingestion of a blood-meal (Richards and Richards 1971). Finally, there are also reports which indicate that only the middle and posterior parts of the midgut are involved in the formation of a type I PM. This situation was observed in adult culicine mosquitoes and some lepidopterans, as well as in the ant lion (Neoptera) and in some coleopteran species producing a PM-derived cocoon (Lehane 1997).

8.3.1.2 Type II PM

Type II PMs are formed likely in a self-assembly mechanisms by the cardia (also termed proventriculus), a specialized folding of the anterior midgut and the foregut which is exceptionally resistant to mechanical stress (Wigglesworth 1930), which forms a continuous sleeve of 1–3 more highly organized layers (Peters 1992). Its occurrence is restricted to Diptera, Dermaptera, Embiodae and some families of Lepidoptera. However, some authors also consider the PMs of particular coleopteran species such as the weevils *Clionus* and *Cleopus* and the spider beetle *Ptinus* as type I PMs, because they are produced by constrained gut regions (Peters 1992).

A detailed ultrastructural study analyzed PM secretion by cardia cells in *L. cuprina* larvae. Separate components have been identified that cooperate in PM formation within the cardia: rings of secretory cells (formation zone), which secrete chitin and PM-associated proteins, and a non-secretory tissue (valvula cardiaca), which assists in PM delamination and passage (Binnington 1988).

The cardia of the of the anterior midgut epithelium from the European earwig, *Forficula auricularia*, produces a two-layered PM. Here, the cardia consists of two larger annular folds, of which the interior part of the first fold secretes the inner PM layer with an orthogonal texture structurally resembling a type I PM. The second annular fold forms a thick PM layer with random fibril orientation, which constitutes the outer peritrophic envelope. Several studies have focused on type II PM formation in mosquito larvae, where the PM forms a thin, transparent and tubular film (Wigglesworth 1930; Richards and Richards 1971; Edwards and Jacobs-Lorena 2000). The PM is continuously synthesized by a ring of cells within the cardia, and it finally lines the entire midgut epithelium. Notably, the ectoperitrophic space is separated from the gastric caeca by a caecal membrane, which seems to be similar in composition to the PM.

8.3.2 Chitin Extrusion

Chitin as a constituent component of arthropod PMs is required for PM reinforcement by providing a fibrillar meshwork. As mentioned above, the arrangement of fibrils can vary between random-felt like textures, which occurs most frequently, and orthogonal and hexagonal textures, which are found in fewer species such as *F. auricularia* and the European rhinoceros beetle, *Oryctes nasicornis*, respectively (Peters et al. 1979; Peters 1969). In the latter two cases, the microvilli may determine the spacing between the microfibers by forming a sort of a hexagonal template for the nascent PM formed between them (Mercer and Day 1952; Peters et al. 1979) (Fig. 8.2d). After delamination of the apical layers, a PM with orthogonal or hexagonal textures remains, which is presumably stabilized by certain types of PMPs that bind to the chitin nanofibers. Consequently, multiple PM layers may be delaminated from the same brush border resulting in the formation of peritrophic envelopes. As the PM is considered to lack lipids (Peters 1992), it is unlikely that microvillar membranes are included in the PM after delamination. Therefore, PM formation is unlikely due to microapocrine secretion, which would be accompanied by a loss of cell material (e.g. parts of microvilli) (Fig. 8.2h). However, the significance of this microvilli-templated mode of PM delamination has been controversial, and data have been reported that support an oppose mechanism involving random felt-like textures. In some cases, the initially ordered arrangement of fibrils may also collapse due to the lack of stabilizing proteins. However, additional more subtle mechanisms for chitin network formation must exist. These may explain, for instance, the transitions from a random felt-like structure to hexagonally arranged microfibrils in *Leptestheria dahalacensis* induced by feeding (Schlecht 1979), or the occurrence of a combination of orthogonal, hexagonal and random felt-like arrangements within relatively short distances in the single PM of the beetle *Ptinus tectus* (Rudall and Kenchington 1973). The general scenario described suggests that a chitinous mesh is generated between the tips of the microvilli of midgut epithelial cells (Fig. 8.2e–g). As chitin synthases are integral membrane proteins, they reside in the microvillar membranes of PM delaminating midgut cells, i.e. columnar cells

for type I and cardia cells for type II PMs. Indeed, immunological and biochemical studies of chitin synthase 2 (Chs2) from the midgut of *M. sexta* have shown that chitin nanofibers are formed by oligomeric Chs2 complexes residing in the membranes of columnar cell microvilli at the apical tips (Zimoch and Merzendorfer 2002; Maue et al. 2009). The single catalytic units of the oligomeric chitin synthase complex may simultaneously secrete multiple chitin chains being pre-aligned for fibrillogenesis (Merzendorfer 2013), which presumably takes place at the lateral surfaces the microvilli. If this hypothesis of PM delamination is correct, it is expected that chitin nanofibers are released into the perimicrovillar space forming a meshwork between the apical microvilli (Fig. 8.2e).

8.3.3 Secretion of PMPs

Little is known about the precise mechanism by which PM-associated proteins are delivered to the PM. It seems that in many insects this process initiates with the apocrine secretion of PM material from midgut epithelial cells. Early studies performed on the larval midgut cardia from the chironomid, *Chironomus piger*, showed two cell types, one rich in granular endoplasmic reticulum tubules (ER-cells), the other rich in mitochondria (M-cells) (Platzer-Schultz and Welsch 1969). During fixation for electron microscopy, some of the ER-cells were trapped in stages resembling cells that undergo apocrine secretion: The ER-cells cyclically formed apical blebs, which were finally released into the midgut lumen, where they disintegrated and formed fibrillar material. The remaining cells regenerated into normal epithelial cells with apical microvilli. From these findings, the author suggested that significant parts of the PM originate from granular material produced by the ER-cells. Although the larval midgut of the hide beetle, *Dermestes maculatus* is not well differentiated along the ventriculus, there is specialization as the anterior part undergoes apocrine secretion (Caldeira et al. 2007). While the ventricular cells in this region were suggested to secrete digestive enzymes, the caecal cells were supposed to produce glycosylated PM-associated proteins. Interestingly, mosquitoes respond to bacterial challenges by stimulation of apocrine secretion as a defense mechanism (Oliveira et al. 2009).

The secretion of a particular PMP by anterior midgut columnar cells from *S. frugiperda* was analyzed using monospecific, polyclonal antibodies in conjunction with confocal fluorescence and immune-gold microscopy. More specifically, this PMP was found in double membrane vesicles that bud from the microvilli of columnar cells, a process that is known as microapocrine secretion, a special form of apocrine secretion (Bolognesi et al. 2001). The screening of a midgut cDNA expression library with antibodies to isolated microapocrine vesicles from *S. frugiperda* demonstrated the presence of PMPs and various other proteins, that are released into the midgut presumably by microapocrine secretion (Silva et al. 2013). Next to various proteolytic and glycolytic enzymes that were identified by cDNA sequencing of positive clones, also some proteins that are likely involved in microapocrine

secretion were found including calmodulin, annexin, myosin 7a, and gelsolin. Similar results were previously reported thanks to the use of antibodies against cytoskeleton-depleted microvillar membranes from the larval midguts of the mealworm beetle, *Tenebrio molitor* and *S. frugiperda* (Ferreira et al. 2007).

A somewhat different secretion mechanism was reported for fly maggots. The secretion of peritrophin-15 by cardia cells from *L. cuprina* larvae was analyzed using gold-conjugated antibodies to localize the protein by immuno-electron microscopy (Eisemann et al. 2001). The cardia cells are rich in rough ER, Golgi bodies and trafficking vesicles, which were shown to be loaded with peritrophin-15. These vesicles accumulate underneath the apical plasma membrane and fuse with it to release peritrophin-15 at the base of the microvilli into the inter-microvillar space (Fig. 8.2f). Finally, peritrophin-15 binds to the fibrillar network of the PM covering the tips of the microvilli. While the cardia cells are specialized in secretion, the cells of the foregut epithelial cells of cuticle-lined valvula cardiaca are characterized by a smooth ER, and may be specialized in glycogen storage and lipid production. The foregut tissue of the valvula cardiaca contains longitudinal muscles and microtubules which appear to be involved in moving the PM through the cardia (Binnington 1988). In conclusion, depending on the insect species, different modes of PM secretion may exist, either apocrine, microapocrine or merocrine at the base of microvilli. However, it has to be noted that secretion of PM material is paralleled by other secretory processes, which may overlap in particular midgut regions. As most available data rely on ultrastructural analyses with a certain potential of fixation artefacts, an unequivocal portrayal of the mode of PM secretion is difficult.

8.3.4 Assembly of the Fibrillary Network

There is a general agreement that the PM is formed when chitin nanofibrils are crosslinked by PMPs that bind to the chitin portion. The assembly into a differentiated network may differ between type I and type II PMs. Type I PMs typically consist of several layers, which have been suggested to be formed either by the sequential secretion of PM components, by differential aggregation of PM components, or by processes that lead to different physical states of the PM such as more gel-like or solid forms (Lehane 1997). Depending on the midgut regions, properties of type I PMs such as thickness, hydration, pore size and permeability may differ widely. These structural differentiations are likely related to different functions of the PM in different gut regions (Agrawal et al. 2014). According to an immunological study on the localization of Chs2 in the midgut of *M. sexta*, which produces a type I PM, chitin synthesis and fibrillogenesis may take place at the very apical tips of midgut microvilli at least in this lepidopteran species (Zimoch and Merzendorfer 2002) (Fig. 8.2e). Subsequently, a loose meshwork of chitin fibrils may be formed between the microvilli becoming increasingly fortified by crosslinking PMPs secreted at the base of the microvilli. Depending on the nature of the secreted PMPs, this process may yield different textures, which are likely formed in a self-assembly progression. In contrast to type I PMs, the more highly organized type II PMs are

formed as a continuous single sleeve (or several concentric sleeves) by cardia cells in the region between the foregut and midgut. These cells seem to operate in a sequential manner secreting PM material that organizes into a PM in a self-assembly process ensuing frequently in multilayered sleeves, with layers being different in chemical composition (Lehane 1976). This in turn requires coordinated secretion of different PMPs that are added to the chitin network from the basal site. Orchestration of PM formation appears to be more difficult in case of apocrine secretion.

8.4 PM Properties and Structure-Function Relationships of PM Components

8.4.1 Permeability Properties of the PM

Across different insect orders, PM thickness increases from the anterior to the posterior regions in the midgut (Harper and Granados 1999; Hopkins and Harper 2001; Agrawal et al. 2014). Notably, PM thickness is inversely proportional to its permeability as evidenced by determining PM exclusion sizes for FITC-dextran particles in *T. castaneum* larvae (Agrawal et al. 2014) (Fig. 8.6). While particles exceeding a diameter of 40 nm are able to pass the PM in the anterior midgut, the cut-offs for particles in the median and posterior midgut are 8–9 nm and 1–2 nm, respectively. These large differences in PM permeabilities are supposed to be an adaptation to the requirements for partitioning digestive enzymes and their substrates in the midgut (Agrawal et al. 2014) (Fig. 8.6). An important aspect is that digestive enzymes have to be able to pass the PM in the anterior midgut in order to get access to their substrates in the endoperitrophic space. In turn, partially processed dietary molecules resulting from hydrolytic degradation in the endoperitrophic space have to pass the PM in the opposite direction for final degradation in the ectoperitrophic space by membrane-associated hydrolytic enzymes. The latter process delivers largely monomeric digestion products of dietary molecules absorbed by midgut epithelial cells of the median and posterior midgut. The PM of insects feeding on fluids or fine-structured matter typically exhibit exclusion sizes in the range of 7.5–9 nm (Terra and Ferreira 1983; Espinoza-Fuentes et al. 1984; Peters and Wiese 1986; Miller and Lehane 1990). In contrast, PMs of lepidopteran and orthopteran larvae, that feed on rough matter, exhibit exclusion sizes between 21 and 36 nm (Adang and Spence 1983; Barbehenn and Martin 1995). High PM permeabilities entail the risk of establishing infections caused by pathogens invading the ectoperitrophic space where they can get in direct contact with midgut epithelial cells. This eventually might be counteracted by an increased release of antimicrobial peptides especially in the anterior midgut, where PM permeability is highest in many insects. Another possibility to deal with this problem may be provided by the secretion of PM-active enzymes that temporally adapt PM permeability by degrading or modifying chitin and/or PMPs. After the passage of large molecules, newly formed PM components may reconstitute the original situation.

The question of how structural organization of the PM is established in different midgut regions is subject of intense discussion. As discussed earlier in this chapter, discrimination of molecules is not only based on pore size diameters but is also determined by electrostatic interactions (Lehane 1997). Indeed, there is evidence that anions pass the PM less efficiently in the presence of glycosylated proteins (Miller and Lehane 1993; Barbehenn 2001). In turn, it was demonstrated that positively charged molecules such as the fungal *Rhizoctonia solani* agglutinin preferentially permeates through the PM of *T. castaneum* (Walski et al. 2014). Its passage was significantly faster than that of the plant *Sambucus nigra* agglutinin II, which at least in the posterior midgut is negatively charged.

The amount of cations crossing the PM may additionally increase from the anterior to the posterior midgut. This assumption is based on the differential expression patterns of the PMPs in *T. castaneum* along the midgut (Jasrapuria et al. 2010). Because the pH values are known in the main midgut regions of *T. castaneum* larvae (Vinokurov et al. 2009), it was possible to estimate the degree of ionic interactions that prevent or facilitate permeation through the PM considering averaged pI values of all PMPs (Table 8.1). According to this estimate, the extent of negatively charged PMPs increases from anterior to posterior midgut regions. In parallel, the amount of positively charged molecules that become attracted is increasing in the same direction. This may constitute a mechanism allowing differential permeation through the PM along the midgut, which may improve digestion efficiency.

The PM exhibits a telescope-like shape with fewer overlapping PM layers in the anterior than in the posterior midgut, as it was found for instance in *P. americana* (Lee 1968). This implicates a longitudinal turnover of the PM, with the inner layers being excreted with the feces. However, alternative modes of turnover may occur in other insects. As shown for *T. castaneum*, the knockdown of *TcPMP3* disrupted PM integrity only in the median but not in the posterior midgut region where the gene is not expressed (Jasrapuria et al. 2010; Agrawal et al. 2014). In case of a longitudinal PM turnover, RNAi to silence *TcPMP3* (which is expressed only in the anterior and median midgut) is expected to disrupt PM permeability in the posterior midgut, because the inner PM layers, which lack *TcPMP3*, will move towards the posterior end. From these findings, a transversal mode of turnover of PM layers was proposed, in which the PM delaminates from midgut epithelial cells and is degraded from the endoperitrophic side by the action of enzymes such as chitinases, glycosidases and proteinases. Several studies demonstrated that CBDs are integral constituents of the PM presumably crosslinking chitin microfibrils, which confers

Table 8.1 pH and pI values along the midgut of *Tribolium castaneum*

Parameter	Midgut region		
	Anterior	Median	Posterior
pH ^a	5.6–6.0	6.0–7.0	7.0–7.5
Average pI of TcPMPs	4.6	4.4	5.0
pH-pI values	1.0–1.4	1.6–2.6	2.0–2.5

^aAccording to Vinokurov et al. (2009)

tensile strength (Elvin et al. 1996; Schorderet et al. 1998; Wang et al. 2004). Differential expression of PMPs along the midgut as demonstrated for *T. castaneum* may be crucial for the establishment of a PM permeability gradient. Notably, the number of CBDs present in the PMPs correlates with their site of expression in the larval midgut of *T. castaneum* (Jasrapuria et al. 2010). The more posterior the *TcPMP* is localized, the higher is the number of CBDs. PMPs with more than one CBD have been suggested to crosslink chitin polymer chains whereby a three-dimensional network is formed (Shen and Jacobs-Lorena 1998; Devenport et al. 2005). PMPs containing only few CBDs are expected to crosslink chitin fibers less efficiently than PMPs containing multiple CBDs. Therefore, the latter PMPs should be found in PMs with small pore sizes and reduced permeabilities. Indeed, transcripts for PMPs with 9 or 14 CBDs were only found in the more posterior parts of the larval midgut from *T. castaneum*, where PM permeability is very low (Jasrapuria et al. 2010; Agrawal et al. 2014). Also in *An. gambiae*, PMPs with various numbers of CBDs have been identified. Moreover, a structural model was proposed in which intersecting chitin fibrils create cross-hatch textures and form a three-dimensional structural scaffold (Dinglasan et al. 2009). In regions with PMPs containing low numbers of CBDs, the interconnection of chitin fibers may be significantly reduced, which seemingly will result in larger pore sizes. Additionally, chitin modifications such as deacetylation may prevent binding of CBDs that specifically recognize chitin. According to another suggestion, specific PMPs may contribute to PM tightening by interconnecting chitin fibers with other PMPs (Rose et al. 2014). This may lead to the densification of the PM resulting in reduced pore diameters. Structural organization of the PM as a cross-hatch meshwork of chitin fibers would confer elastic properties of the PM, which may facilitate, for instance, PM contraction in *An. gambiae* mosquitoes which occurs in the course of blood digestion (Dinglasan et al. 2009). Next to the formation of a meshwork within the plane of a single PM layer, PMPs may also mediate transversal interconnection of individual PM layers by the formation of protein bridges. Indeed in larvae of *O. nubilalis*, multiple layers of the meshwork were observed to be interconnected (Harper and Hopkins 1997). In case of a longitudinally increasing thickness of the PM like in *T. castaneum*, especially in the posterior midgut, PMPs with multiple CBDs might be required to interconnect several PM layers at once. Bridging multiple layers in this way could result in a more rigid and voluminous PM and may provide an additional explanation for the finding that PMPs with multiple CBDs are expressed in the posterior midgut region of *T. castaneum* (Agrawal et al. 2014). This type of PM organization could control the flux of molecules at an additional level by altering PM permeability through the variation of the number of PMPs interconnecting PM layers in transversal direction.

PM degrading enzymes may be considered as additional factors that contribute to the regulation of PM permeability. Although trypsin cleavage sites have been identified within CBDs of PMPs, they are presumably inaccessible upon formation of disulfide bridges (Wang et al. 2004; Rose et al. 2014). On the other hand, chitin fibrils may be protected from the action of chitinases due to their inaccessibility upon binding to PMPs. However, control of both turnover and permeability of the

PM require the regulation of enzymatic degradation. In line with this assumption, PM thickness increases drastically in larvae of *O. nubilalis* upon RNAi-mediated knockdown of a gene encoding a chitinase (Khajuria et al. 2010). Partial denaturation of PMPs could further provide access of enzymes to chitin fibrils. An analogous mechanism was described for the chitin fibers in the cuticle of *T. castaneum*, which are protected from chitinase activity by the Knickkopf protein (TcKnk) (Chaudhari et al. 2011). Thiol reducing agents and allochemicals ingested with the food can result in a significant reduction of the redox potential as demonstrated for the larval midgut of the cotton bollworm, *Helicoverpa zea* (Johnson and Felton 1996). This may lead to the decline of disulfide bridges in the CBDs of PMPs, and thus may alter PM properties.

8.4.2 Roles of PMPs in Organizing the Chitin Fibers

The functional significance of chitin in the PM has been recently demonstrated by knocking down the gene encoding the midgut specific chitin synthase in *T. castaneum* larvae (*TcCHS2*). This gene silencing led to the complete absence of chitin in the midgut and also to disruption of the PM's barrier function (Arakane et al. 2005; Kelkenberg et al. 2015). Because of the loss of the PM's capability to partition digestive enzymes and substrates, the larvae developed nutritional deficiencies resulting in a starvation phenotype with significantly reduced body weights and in fat bodies depleted of neutral lipids (Kelkenberg et al. 2015). Similar results were obtained when the larvae were fed with the general chitin synthesis inhibitor diflubenzuron (DFB). In contrast to *TcCHS2*-deficient larvae, DFB treatment only resulted in a partially reduced chitin content of the PM (Merzendorfer et al. 2012; Kelkenberg et al. 2015). In this case, PM permeability was also increased but the effect was less pronounced than in case of *TcCHS2* knockdown. Comparable effects have been observed in different insects using DFB and related chitin synthesis inhibitors that were orally administered (Clarke et al. 1977; Tellam and Eisemann 2000; Guo et al. 2007a). Thus, the chitin content may directly correlate with the exclusion size of the PM. The loss of chitin fibrils may further be accompanied by a loss the PM's protein content due to the reduced number of CBD binding sites (Clarke et al. 1977). The organization of the chitin nanofibers into a three-dimensional meshwork of chitin fibrils may be mainly controlled by PMPs containing various numbers of CBDs (see also Fig. 8.3). Table 8.2 summarizes characteristics and functions for some selected PMPs. In the following sections of this chapter the structure-function relationships of PMPs will be discussed.

8.4.2.1 PMPs with a Single CBD

PMPs as integral components of the PM largely determine its physicochemical properties, and changes in the composition of the PM lead to altered characteristics, which reflect adaptations to current physiological and immunological demands. All

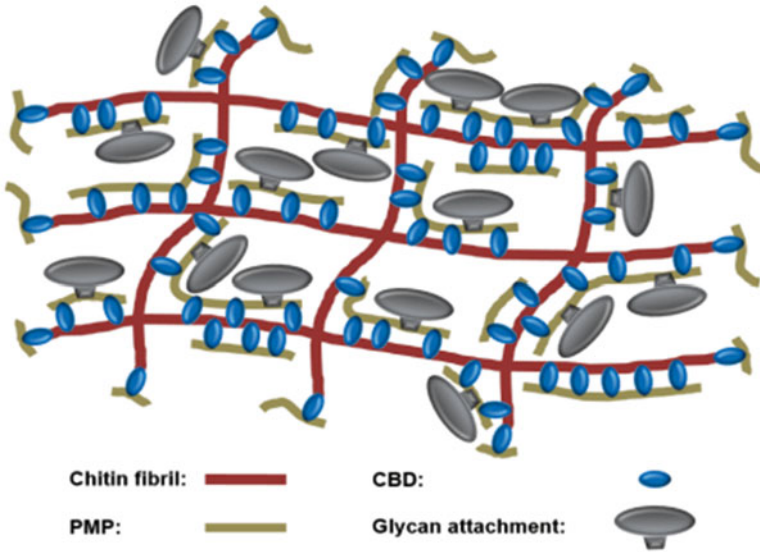


Fig. 8.3 Graphical illustration of structural elements of the PM. The basal elements of the semi-permeable PM are chitin fibrils (*red*) and PM proteins (PMPs, *brown*) containing multiple chitin binding domains (CBDs, *blue*). The cross-hatch architecture of the PM is achieved by crosslinking the chitin nanofibers by PMPs with different numbers of CBDs. Several PMPs possess large glycan moieties (*grey*) presumably projecting into the interstitial spaces between chitin fibrils narrowing the pore sizes. Therefore, glycosylated PMPs are assumed to be crucial for determination of PM permeability. Attached glycans also provide protection from degradation of the PM by shielding PM constituents from proteolytic and chitinolytic enzymes. PMPs with a single CBD may bind to the ends of chitin fibrils to prevent degradation by exo-splitting chitinases. However, they also may bind along the chitin fibers to narrow pore sizes. PMPs with multiple CBDs are thought to be involved in crosslinking the chitin nanofibers in various ways. PMPs with a high number of CBDs may be proteolytically processed into smaller units. For a better overview, chitin nanofibrils, proteins and glycans are not drawn to scale

PMPs identified from different insects so far have a varying number of CBDs, and some have additionally mucin-like domains. The chitin binding properties of PMPs have been experimentally confirmed using recombinant proteins from various sources (Elvin et al. 1996; Wang and Granados 1997b; Shen and Jacobs-Lorena 1998; Vuocolo et al. 2001; Wang et al. 2004). The number of CBDs present in the PMP appears to be crucial in organizing the 3D-meshwork of the PM (Fig. 8.3). However, the precise function of individual PMPs with different numbers of CBDs in organizing chitin fibril architecture remains speculative.

To date, many PMPs with a single CBD have been identified in insects by cDNA cloning or genome sequencing (Casu et al. 1997; Eisemann et al. 2001; Wijffels et al. 2001; Gaines et al. 2003; Venancio et al. 2009; Jasarapuria et al. 2010; Tetreau et al. 2015). It is unlikely that they contribute to the internal stability of the PM, as this would require additional CBDs to allow the formation of cross-links. They may rather protect the PM from chitinolytic degradation by exo-splitting chitinases

Table 8.2 Characteristics and assumed functions of selected PMPs

Species	Protein	Number of CBDs	Binding properties and proposed functions	Reference
<i>Aedes aegypti</i>	AeIMUC1	3	PM integral protein with a mucin-like domain; specifically binding to chitin; heme detoxification	Devenport et al. (2006); Rayms-Keller et al. (2000)
	Ae-Aper50	5	PM integral protein with mucin-like domains; specifically binding to chitin	Shao et al. (2005)
<i>Anopheles gambiae</i>	Ag-Aper1	2	PM integral protein; specifically binding to chitin; possible function in determining exclusion size; <i>N</i> -glycosylated	Shen and Jacobs-Lorena (1998)
	Ag-Aper14	1	PM integral protein, possible functions in PM assembly	Devenport et al. (2005)
<i>Drosophila melanogaster</i>	Drosocrystallin (Dcy)	1	Roles in maintaining PM structure and determining permeability; protection from bacterial infections and toxins	Kuraishi et al. (2011)
<i>Glossinia morsitans morsitans</i>	GmPro1	1	Expressed preferentially in the proventriculus; possible role in protection from invading pathogens	Hao and Aksoy (2002)
	GmPro2	1	PM integral protein as determined by immunoblots	
<i>Chrysomya bezziana</i>	Peritrophin-15	1	Specifically binding to chitin; possibly capping ends of chitin fibrils	Wijffels et al. (2001)
<i>Helicoverpa armigera</i>	HallM86	5	PM integral protein binding to chitin; mucin-like domain; target for enhancin	Zhang and Guo (2011)
<i>Lucilia cuprina</i>	Peritrophin-15	1	Specifically binding to chitin, possibly capping ends of chitin fibrils	Wijffels et al. (2001); Eisemann et al. (2001)
	Peritrophin-44	5	Specifically binding to chitin, roles in maintaining PM structure and determining permeability	Elvin et al. (1996)
	Peritrophin-48	5	Specifically binding to chitin, <i>N</i> -glycosylated	Schorderet et al. (1998)
	Peritrophin-55	1	Predicted <i>O</i> -glycosylated domain at the carboxy-terminus; tightly associated with the PM	Tellam et al. (2003)

(continued)

Table 8.2 (continued)

<i>Mamestra configurata</i>	McIIM1	7	PM integral protein; expressed in the anterior midgut of larvae	Toprak et al. (2010); Toprak et al. (2014)	
	McIIM2	2			
	McIIM3	1	PM integral proteins; expressed in the median and posterior midgut of larvae		
	McIIM4	4			
	McPM1	19	PM integral protein; expressed in the anterior midgut of larvae		Shi et al. (2004); Toprak et al. (2014)
<i>Plutella xylostella</i>	PxIIM	7	Three mucin-like domains; potentially binding to chitin	Sarauer et al. (2003)	
<i>Tribolium castaneum</i>	TcPMP3	3	PM integral proteins, differentially expressed in midgut; roles in maintaining PM structure and determining permeability; mucin-like domains, extensively <i>O</i> -glycosylated	Agrawal et al. (2014)	
	TcPMP5-B	5			
<i>Trichoplusia ni</i>	CBP1	12	PM integral proteins; proteolytically processed into smaller functional units	Wang et al. (2004)	
	CBP2	10			
	IIM14	5	Extensively <i>N</i> - and <i>O</i> -glycosylated integral PM protein, tightly associated with the PM		Harper and Granados (1999; Wang and Granados (1997a, b)
	IIM22	5	Two domains rich in threonine and proline; potentially binding to chitin		

through capping the ends of chitin fibrils, or sequester free chitin-containing molecules in the midgut (Wijffels et al. 2001; Bolognesi et al. 2005) (Fig. 8.3). For the capping function, it has to be remarked that the nature of selective binding to the terminal sites of the chitin nanofibers is uncertain. In addition, functions for single-CBD PMPs in narrowing pore size diameters have been proposed for aglycosylated proteins from *An. gambiae* such as AgAper9 and AgAper14 (Dinglasan et al. 2009). As single CBD-containing PMPs are predominantly expressed in the anterior midgut of *T. castaneum* larvae (Jasrapuria et al. 2010), chitin fibrils may be particularly well protected from chitinolytic degradation. This may be an adaptation to the overall structure (thin or gel-like) of the PM in this region, which may render the PM particularly susceptible to enzymatic degradation. As Ag-Aper14, a single CBD-containing PMP from *A. gambiae*, is found in both the PM and the microvilli, an additional function in the context of PM assembly may be assumed for this protein, though final evidence for this is missing (Devenport et al. 2005). Single CBD-containing PMPs have been further suggested to support innate immunity, since they showed increased expression levels in the tsetse fly after ingestion of trypanosomes (Hao and Aksoy 2002).

8.4.2.2 PMPs with Several CBDs

PMPs with several (2–5) CBDs are thought to be PM integral proteins that largely determine the overall structure of the PM and its physicochemical properties. They have been suggested to assemble the chitin fibrils into a wide cross-hatched matrix forming water-filled pores (Fig. 8.3). In the PM of *An. gambiae*, AgAper1 is the most abundant PMP, which is predicted to be *O*-glycosylated and exhibits two CBDs. Dinglasan et al. (2009) hypothesized that AgAper1 is associated via the CBDs to the crosshatched chitin fibers at sites forming the pores, and that the *O*-glycans project into the pores where they attract water molecules. In this way, AgAper1 may determine PM exclusion size and selectiveness. AgAper1 is also predicted to be *N*-glycosylated. As *N*-linked glycans are linked to the Asn of the polypeptide by a β -1-4-GlcNAc dimer (Kornfeld and Kornfeld 1985), they may also function in cross-linking several AgAper1 proteins within the pore, which may add a further level of control of PM permeability. PMPs with two CBDs such as AgAper1, however, may also be involved in end-to-end extension of chitin fibers. Due to the limited molecular mass, it seems unlikely that these proteins span larger distances in the chitin meshwork. In general, PMPs with 3–5 CBDs may have similar functions. However, due to their larger molecular sizes, they could also function in stabilizing interconnections between chitin fibers. Therefore, they may be particularly important in maintaining barrier function and permeability gradients of the PM along the midgut. Indeed, RNAi-mediated silencing of the gene encoding the mucin-like TcPMP3 from *T. castaneum*, which contains three CBDs and is extensively *O*-glycosylated, leads to a decreased PM thickness and a loss of PM barrier function (Agrawal et al. 2014). PMPs with four CBDs may be required to form the cross-hatch structures within the matrix by interconnecting four ends of chitin fibers (Dinglasan et al. 2009). For reasons of symmetry, 4 CBD-containing PMPs would fulfill a unique and essential function in PM assembly. However, it has to be noted that genes encoding 4 CBD PMPs are not found in all insect genomes, as *T. castaneum*, for instance, lacks this type of PMP. It is further unlikely, that a PMP with 4 CBDs is generated by proteolytic processing, because the knockdown of genes encoding putative pro-PMPs containing multiple (9 or 14) CBDs did not affect PM permeabilities or larval growth (Agrawal et al. 2014). PMPs with 5 CBDs have been identified in most insects analyzed so far. Due to the number of chitin binding motifs, they may be primarily adapted for interconnecting chitin fibers, and therefore crucial for providing tensile strength particularly under conditions of osmotic stress (Fig. 8.3). The occurrence of Pro-rich extensin-like motifs in some five CBD-containing PMPs such as AeAper50 from *A. aegypti* may support the assumption of a function in supporting the structural integrity of the PM (Wu et al. 2001). Again, many of these PMPs are found to be extensively glycosylated (Devenport et al. 2005; Dinglasan et al. 2009; Agrawal et al. 2014). The presence of sugar moieties could lubricate the surface of the PM to facilitate food passage and/or provide protection from adhesive pathogens. This hypothesis is in line with their ubiquitous occurrence in insects, and their essential function was demonstrated by the knockdown of *TcPMP5-B* transcripts in larvae of *T. castaneum* that led to a loss of PM

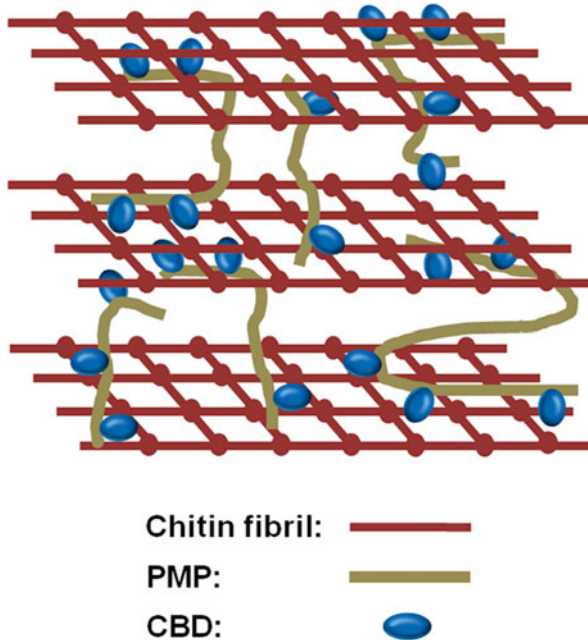


Fig. 8.4 Schematic representation of potential interconnections between single PM layers. Individual chitin layers (*red mesh works*) are assumed to be bridged by PMPs (*brown*) exhibiting different numbers of CBDs (*blue*), which leads to a three-dimensional architecture. An increasing number of CBDs has been found to be directly correlated with the tightness of chitin layer interconnections. For a better overview, chitin nanofibrils, proteins and glycans are not drawn to scale

barrier function in the midgut. In contrast, RNAi to knockdown transcripts for the second *T. castaneum* gene encoding a PMP with five CBDs (TcPMP5-A), which lacks mucin-like domains, did not result in any detectable phenotype. This further underlines the importance of *O*-glycans for proper PM function (Agrawal et al. 2014). Due to their larger size, PMPs with five CBDs are good candidates for bridging longer distances within the chitin fiber meshwork or between adjacent PM layers (Fig. 8.4).

8.4.3 PMPs with Multiple CBDs

PMPs with multiple (6–19) CBDs have been suggested to integrate into PM after being proteolytically processed into smaller fragments by midgut proteases such as trypsin (Shi et al. 2004; Wang et al. 2004) (Fig. 8.5). Trypsin cleavage sites have been identified in the linker regions downstream of the CBDs (Wang et al. 2004; Ferreira et al. 2007; Rose et al. 2014). So far, it is unknown whether proteolysis of multiple-CBD PMPs takes place before or after they have been integrated into the

structural scaffold of the PM. Multiple-CBD PMPs are assumed to contribute to the overall structure of the PM by crosslinking chitin fibrils (Fig. 8.3). Due to the higher number of CBDs that are involved in this process, they may increase the tensile strength of the PM (Zimmermann and Peters 1987). In addition, they may serve in bundling of several chitin nanofibrils by braiding the fibers, which would further strengthen the PM structure (Fig. 8.5). The presence of multiple Pro residues in regions flanking the CBDs could create hinge regions allowing the PMP to wrap around chitin fibrils, which potentially protect the fibers from chitinolytic degradation. This is particularly significant for chitin fibers of the inner PM layers, as they are exposed to the hydrolytic environment of the gut lumen. This also applies equally to the PMPs, which protect the chitin fibers from chitinolytic activities. However, the PMPs seem to be particularly protease-resistant, because potential cleavage sites are not exposed (Hegedus et al. 2009; Wang et al. 2004). Multiple-CBD PMPs may further exert tensile forces on bound chitin fibrils resulting in a condensed conformation resembling the situation of a spring. In combination with the cross-hatch fibrillary structure, this could significantly contribute to the elastic properties of the PM, which allows avoidance of mechanical stress and facilitates contraction of the midgut lumen during digestion (Dinglasan et al. 2009). Interestingly, no detectable phenotypes have been observed when the *T. castaneum* genes encoding TcPMP9 and TcPMP14 containing 9 and 14 CBDs, respectively,

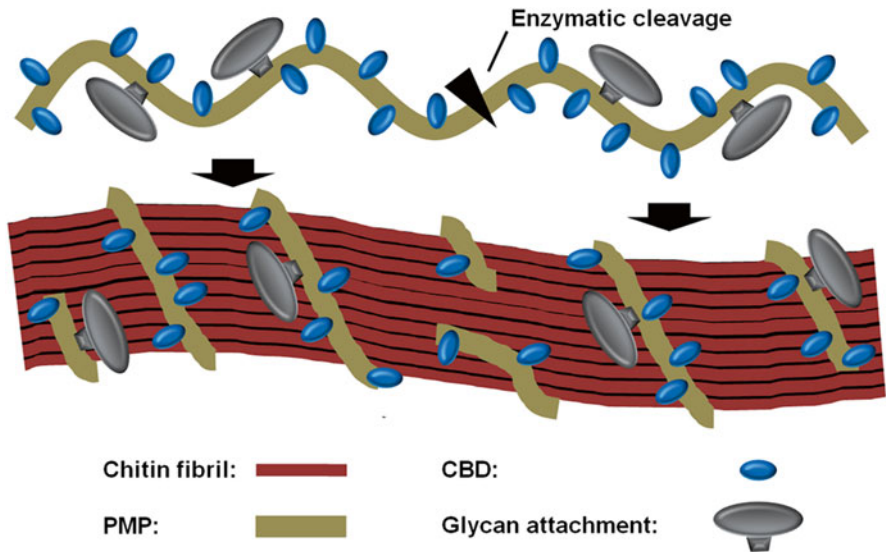


Fig. 8.5 Putative functions of multiple-CBD containing PMPs. Multiple-CBD PMPs (*brown*) which frequently carry *O*-glycans (*grey*) have been suggested to be proteolytically processed by midgut proteases resulting in functional PMP fragments that bind to chitin fibers in a way similar to PMPs that have only a single or a few CBDs (*blue*). Uncleaved multi-CBD PMPs may be involved in bundling of chitin nanofibrils (*red*) to generate thicker fibers that become interconnected by cross-linking PMPs. For a better overview, chitin nanofibrils, proteins and glycans are not drawn to scale

were knocked-down by RNAi. However, the finding that the transcript levels for other TcPMPs were found to be upregulated upon RNAi for *TcPMP9* and *TcPMP14* suggests that there is transcriptional up-regulation of *PMP* genes to compensate for the loss of multiple-CBD PMPs (Agrawal et al. 2014). This may support the idea that TcPMP9 and TcPMP14 are cleaved into smaller fragments, because PMPs with a lower number of CBDs can substitute their function (Fig. 8.5). Further studies on the structure-function relationship of PMPs are required to understand PM structure, assembly and plasticity.

8.4.4 PMPs with *O*-glycosylated Linker-Domains

The PM may be also considered as a second mucous layer, which separates from the midgut microvillar mucins in the course of PM delamination (Shen and Jacobs-Lorena 1999). The large glycan moieties of PMPs are supposed to be crucial for the maintenance of PM integrity. Additionally, the glycans may also serve in protecting PMPs from degradation by midgut proteases secreted during digestion. Extensively glycosylated PMPs have been identified in various insect species from different orders (Schorderet et al. 1998; Vuocolo et al. 2001; Shi et al. 2004; Agrawal et al. 2014). As discussed above, in feeding larvae of *T. castaneum*, RNAi-induced knock-down of the two genes encoding PMPs, TcPMP3 and TcPMP5-B, caused a drastic increase in PM permeability. While the other nine TcPMPs identified in *T. castaneum* lack apparent sites for extensive *O*-glycosylation, TcPMP3 and TcPMP5-B proteins exhibit extended mucin-like Ser/Thr-rich linker domains, which were shown to be highly *O*-glycosylated using a glycan detection assay (Agrawal et al. 2014). Thus, it is likely that glycan attachments are strongly involved in determining the PM exclusion size, presumably by occupying the interstitial spaces between chitin microfibrils narrowing pore size diameters (Fig. 8.3). In addition, the glycans may protect PM components from degradation by hydrolytic enzymes. In many cases, the sizes of the glycans could be too small to project into interstitial spaces far enough. In order to bridge longer distances, PMPs may be cross-linked by intermolecular disulfide bridges. Such binding may occur between CBDs and core chitobiose units from *N*-glycosylated PMPs, or by transglutaminases as recently shown for drosocrystallin (Shibata et al. 2015). Consequently, reduction of PM pore size diameters does not necessarily correlate with a decrease in distance between single chitin fibers within the chitin lattice. Therefore, modulating the degree of interaction of PMPs may be an even more important mechanism for the control of PM properties. However, the loss of a specific highly glycosylated and strongly interconnected PMP may not only result in a slightly increased exclusion size, but rather in a complete loss of PM integrity, as other PMPs may be not able to interconnect themselves in the absence of one of these extensively glycosylated proteins. This could potentially lead to a loss of their function as structural PM constituents in addition to the deficiency of PMPs. This scenario could explain the substantial increase in PM size exclusion in *T. castaneum* after RNAi for TcPMP3 or TcPMP5-B (Agrawal et al. 2014). Molecules that bind to the glycan portion of the PM have a critical

effect on its permeability, as it was demonstrated, for instance, by feeding PMP-binding lectins to larvae of *L. cuprina* that resulted in an artificial filling of the gaps within the PM structure. As a result of lectin binding, the PM exclusion size was significantly decreased with lethal effects for the larvae (Eisemann et al. 1994). It is tempting to speculate that larvae died from starvation due to the inability of dietary molecules to pass the PM in order to reach the ectoperitrophic space.

PGs from species such as *D. maculatus* have been suggested to lack chitin fibers and be composed mainly of glycoproteins (Terra 2001; Caldeira et al. 2007). They are frequently found in the anterior midgut where a highly permeable PM is required to allow passage of digestive enzymes secreted in this region. Since chitin is missing, only glycosylated PMPs fulfill the barrier function in this region, supporting the assumption that the presence of a chitinous scaffold is necessary to form small pore size diameters. Thus, chitin fibers may serve as a basal scaffold for the initial attachment of proteins, which in turn provide binding sites for additional PMPs whereby PM pore dimensions are reduced as described above. The special architecture of the PM provides both tensile strength and elasticity, but remodeling of the chitin meshwork to adapt to altered physiological conditions may be hindered. In contrast, remodeling of PGs seems to be much easier as the structure of a PG is supposed to be less complex. This facilitates not only digestive enzymes secreted by anterior midgut cells to enter the endoperitrophic space for digestion, but also allows antimicrobial peptides to rapidly reach those regions of the intestine challenged by pathogens.

The high glycan content of the PM attracts large amounts of water, which contributes substantially to PM thickness due to its volume, and additionally, confers a gel-like shape. These properties could rescue the midgut from dehydration when very dry food is consumed, as water molecules are highly ordered and electrostatically fixed between the glycan chains (Espinosa-Marzal et al. 2013). The extended thickness of the PM keeps the food bolus at a certain distance from the midgut epithelium. In addition, due to the presence of glycans, the surface of the PM is lubricated providing protection from mechanical damage caused by abrasive food particles. The glycan moieties of PMPs act like a shield preventing chitinolytic and proteolytic enzymes from degrading the PM (Sola and Griebenow 2009).

The sugar moieties of extremely *O*-glycosylated PMPs (IIMs) facilitate intermolecular interactions between various glycans creating a barrier which is selectively permeable (Hegedus et al. 2009). Changes in ion concentrations and/or pH result in altered charge densities and thus modified conformations of the glycans, which certainly affect the interactions that occur between them. As a consequence, the exclusion size of the PM is affected as demonstrated for the tsetse fly where the PM was significantly more permeable to alkaline phosphatase in the presence of positively charged calcium ions, which were ingested with the food (Miller and Lehane 1993). This is presumably an effect of a reduction in interconnected glycan moieties. Such a mechanism may allow rapid adjustment of molecule trafficking in response to altered physiological conditions (Lehane 1976). The midgut lumens of many insects exhibit more or less pronounced pH gradients (Dow 1992). In lepidopteran and mosquito larvae pH gradients are particularly pronounced with pH values of > 11 in the anterior and about 7–8 in the posterior midgut (Azuma et al. 1995; Boudko et al.

2001). The situation is different in coleopteran larvae, with pH values increasing from about 6 in the anterior to about 7 in the posterior midgut, as reported for *T. castaneum* larvae (Vinokurov et al. 2009). Therefore, glycan interactions are more or less prominent depending on the pH in the respective midgut region, and thus they may contribute to the decrease in PM permeability towards the posterior end (Agrawal et al. 2014). Additionally, positively charged molecules may preferentially pass the PM in the more posterior regions due to the presence of primarily negative charges resulting from the pH gradient (Miller and Lehane 1993). Because of their large and extremely hydrated glycan moieties, IIMs may be considered as integral structural PM elements, which largely contribute to solvent drag that supports molecule trafficking across the PM.

In conclusion, the PM is composed of different PMPs that are not only differentially expressed in different midgut regions, but also exhibit special characteristics to fulfill their functions in maintaining a semipermeable matrix and anti-infectious barrier under different physiological conditions. Many aspects concerning PMP function are still elusive and require more studies on the structure-function relations.

8.5 Functions of the PM

Although the current knowledge about PM function is limited, there is increasing evidence that the PM is involved in different physiological contexts. In particular, the increasing availability of genetic tools that allow manipulation of gene expression in various insects has yielded more detailed insight on the functions of the PM and particular PM components. Although we are still at the beginning of the process of providing an integrated view of the structure-function relationships, we have now sufficient data that support the notion that the PM is involved in the following processes: mechanical protection, resistance to osmotic swelling, partitioning of digestion, neutralization of toxins, physical barrier against parasites and finally regulation of innate immunity.

8.5.1 Protection from Mechanical and Osmotic Stress

As outlined in the introduction, the PM has properties resembling the mucosa of the vertebrate intestinal tract (Tse and Chadee 1991). Due to the presence of mucin-like PMPs, the PM forms a lubricant matrix, which separates the food from the midgut epithelium and facilitates the passage of the food material through the gut. Thereby, the PM is also thought to protect the midgut epithelium from abrasive particles passing through the midgut along with the ingested food. Although this is an obvious assumption, only a single study has provided evidence for this function. For freak larvae of the silkworm, *Bombyx mori* lacking a PM, Sudha and Muthu (1988) reported that closely packed leaf fragments abraded the midgut epithelium during

their passage through the gut. Abrasion caused cell damage and a loss of epithelial integrity. However, the larvae did not die from this damage, presumably due to high regeneration rates of the midgut epithelial cells. In line with the anti-abrasive function, many fluid-feeding insects lack a PM. It has been argued that due to the absence of abrasive particles in plant saps, there is no evolutionary pressure to maintain the PM.

As explained earlier in this chapter, the PM resembles a hydrogel with high resistance to compressive forces (Hardingham et al. 1990; Jackson et al. 1991), which together with the tensile strength mediated by its fibrillary components contribute to its high mechanical strength. Indeed, the PM has to withstand forces up to 5000 Pa in insect intestines generated by the Donnan effect due to incorporation of high molecular weight diets, which exert a high osmotic pressure because of the high abundance of fixed charges (Zhuzhikov 1970; Zimmermann and Mehlan 1976). Thus, it is the hydrogel characteristics of the PM, which prevents swelling and rupture of the midgut (Zhuzhikov 1964). As discussed for the mucin-like PMPs, hydrated proteoglycans are also major determinants of PM permeability, as they are the most space-consuming molecules within the matrix filling the gaps between chitin fibers.

8.5.2 *Compartmentalization of Digestion*

In separating the midgut epithelium from food material within the gut, the PM divides the midgut into three physiological compartments: the endoperitrophic space (representing the gut lumen confined by the inner surface of the PM), the ectoperitrophic space (the space between the outer surface of the PM and the glycocalyx of the midgut epithelial cells) and the intraperitrophic space (the space filled by the PM itself) ((Lehane 1997), see also Fig. 8.6). As the PM is a selective barrier, partitioning into these compartments is not rigorous as it depends on the respective solute molecules (Lehane 1997). The PM has frequently been compared with a molecular sieve, permeable for small molecules and impermeable for large molecules. However, this is an oversimplified description of PM functionality, because pore size is not the only factor that determines PM permeability. Additional factors such as electrical charge, hydrophilicity, molecular shape, and selective binding of the passing molecules are also important determinants, which lead to different permeabilities for molecules of the same size. In addition, the local environment may vary largely in different midgut regions. For instance, the pH in the anterior region of lepidopteran midguts can exceed values of 11, whereas the posterior midgut is significantly less alkaline (Dow 1992). The pH largely influences PM permeability for a particular molecule due to its effects on the molecule's net charge. In addition, PM properties depend on the ionic composition in the local environment. The sugar moieties of the proteoglycans are predicted to occupy much of the space between the matrix fibers (Fig. 8.3). Interactions between the sugar chains by van der Waals forces and ionic interactions may therefore significantly contribute to the PM's

barrier function, and these relatively weak forces are predicted to be affected by changes in pH and ion concentrations. As mentioned above, calcium ions significantly increase PM permeability to alkaline phosphatase by neutralizing anionic charges in the matrix (Miller and Lehane 1993).

Likely, the partitioning of the midgut into distinct compartments facilitates digestion as it allows spatial separation of digestive reactions (Fig. 8.6). However, it is not only spatial separation into three compartments, which is important in this context. Also the anterior-to-posterior gradient in PM permeability (with large exclusion sizes in the anterior and small exclusion sizes in the posterior midgut) plays a role in digestion. Agrawal et al. (2014) have recently demonstrated such a permeability gradient in larvae of the red flour beetle, *T. castaneum*, by feeding different-sized FITC-dextrans and analyzing their distribution in cryosections using

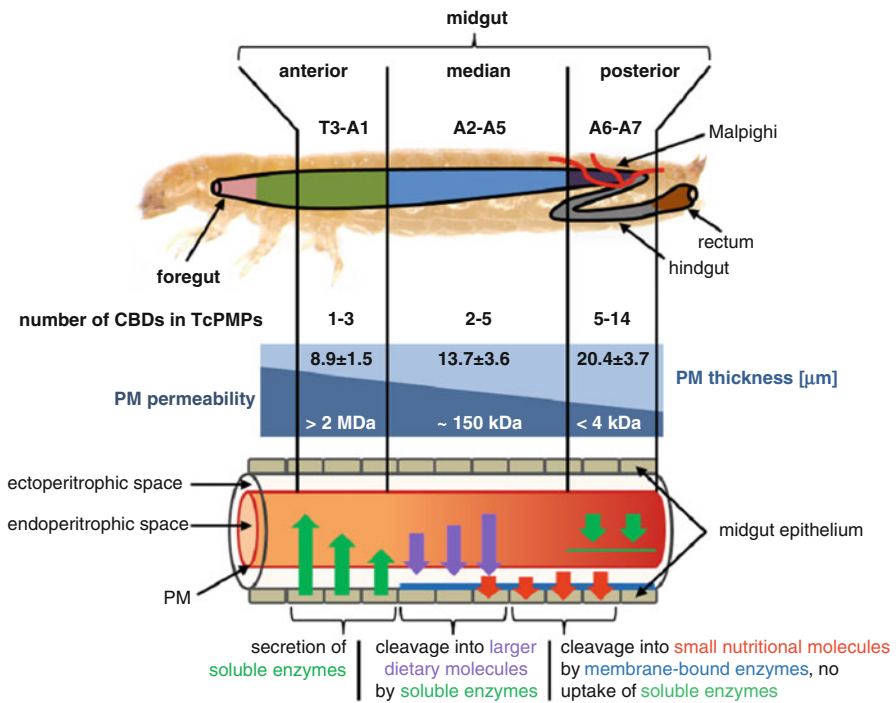


Fig. 8.6 Illustration of PM properties and the presumed effects on digestion in the midgut of *T. castaneum* larvae. PM thickness increases continuously from the anterior to the posterior midgut, whereas PM permeability is increasing in the opposite direction. In anteriorly situated midgut regions endo-cleaving digestive enzymes are secreted by midgut epithelial cells before passing through the PM. They finally reach the endoperitrophic space and degrade nutritional compounds. As a result of the exclusion size gradient, enzymes cannot be taken up again when they move towards the median midgut due to their size. Larger intermediate digestion products are taken up in this midgut region. Subsequently, they are further processed by membrane-bound exo-cleaving enzymes facing the ectoperitrophic space. The degraded nutritional constituents are small enough to pass the membrane of midgut epithelial cells in the median and posterior midgut (Modified according to (Kelkenberg et al. 2015))

a fluorescence microscope. They found that the exclusion size gradually decreases from 2 MDa molecules in the anterior midgut through 150–70 kDa in the median midgut to 4 kDa in the posterior parts. In line with this estimate on a decreasing gradient of PM permeability, the thickness of the PM increases from anterior to posterior, a finding that has been reported for many type I PM secreting insects due to the increase in the number of PM layers. Thus, a gradient in permeability may be a more general feature of type I PMs. But how does partitioning of the midgut and PM permeability gradients improve the efficiency of digestion? The anterior midgut releases digestive proenzymes by exocytosis or apocrine secretion into the midgut lumen where they are proteolytically activated (Terra et al. 2006; Caldeira et al. 2007; Neira Oviedo et al. 2008). To reach the endoperitrophic space, the enzymes have to permeate efficiently through the anterior PM, which may be supported by a high porosity of the PM in this midgut region as observed for instance in *T. castaneum* (Agrawal et al. 2014). However, other mechanisms have been also proposed including enzyme release before PM formation and the presence of selective pores which may be temporally formed (Hegedus et al. 2009). Once the enzymes have reached the endoperitrophic space in the anterior region of the midgut they start to cleave the dietary macromolecules of the ingested food, and peristaltic contractions move the food bolus towards the median midgut. In this part of the midgut, the PM exhibits a reduced exclusion size which allows permeation of the intermediate cleavage products along with solutes and water, while digestive enzymes (nucleases, lipases and proteinases) and undigested material are retained in the endoperitrophic space due to the PM permeability limits (Fig. 8.6). In the ectoperitrophic space, final processing of the intermediate cleavage products is performed by membrane-bound enzymes including α -glucosidase and amylase, trehalase, alkaline phosphatase, aminopeptidase and carboxypeptidase (Santos and Terra 1986; Takesue et al. 1989; Ferreira and Terra 1989; Jordao and Terra 1991; Jordao et al. 1999). By separating different enzymatic reactions in the way outlined above, the accumulation of cleavage products, which would impair substrate binding at the catalytic sites of the enzymes, is avoided. It also prevents unprocessed material from non-specific binding to the surface of midgut epithelial cells, which could inhibit proper final digestion or lead to damage of the epithelium (Bolognesi et al. 2008).

In line with considering the intraperitrophic space as a separate intestinal compartment, several digestive enzymes have been reported to be more or less stably associated with the PM (Terra et al. 1979; Walker et al. 1980; Peters and Kalnins 1985; Ferreira et al. 1994b; Jordao et al. 1996). Some of these enzymes may be merely trapped within the fibrillary meshwork of the PM, others may specifically bind to the PM. For instance, 5–15% of the total luminal trypsin activity is associated with the PM in the midgut of the stable fly, *Stomoxys calcitrans* (Jordao et al. 1996). In this case, binding to the PM may be mediated by electrostatic interactions, because the PM is negatively charged while trypsin is positively charged at physiological pH (Lehane 1976; Moffatt et al. 1995). Some other enzymes such as a chitin deacetylase and three intestinal lipases were shown to be integral components of the PM from *M. configurata* (Toprak et al. 2008). Immobilization of digestive enzymes within the gel-like matrix may additionally improve digestion as this pro-

cess increases enzyme activity (Selegny 1974; Drioli et al. 1976). Lateral diffusion of substrates within the matrix may increase spatial proximity and contact time with the associated enzymes (Comper and Laurent 1978; Hardingham and Fosang 1992) (Comper and Laurent 1978; Hardingham and Fosang 1992). However, the enzymes appear not to be equally distributed in the PM. Rather an anterior-to-posterior gradient of decreasing enzyme concentrations has been shown for the larval midgut of the gnat *Rhynchosciara americana* (Terra and Ferreira 1981). In comparison to their activities within the PM and the time required to pass the intestine, there is only a low rate of enzyme loss via the feces, so that some sort of enzyme recycling was assumed. In addition, dye injection experiments showed retrograde water fluxes to occur in the ectoperitrophic space (Wigglesworth 1930; Berridge 1970; Dow 1981; Terra et al. 1988). Based on these findings, Terra (1990) proposed a model for enzyme recycling in the intestinal tract of insects, which is mediated by a posterior-to-anterior flux of fluid in the ectoperitrophic space (Terra 1990). According to this model, digestive enzymes permeate the PM again when they have reached the posterior midgut and reenter the ectoperitrophic space (Cristofoletti et al. 2001; Caldeira et al. 2007; Neira Oviedo et al. 2008). Back in the ectoperitrophic space they are finally transported to the anterior region where they are recovered and reutilized (Ferreira and Terra 1989; Bolognesi et al. 2008). The retrograde flux in the ectoperitrophic space may be driven by water secretion of posterior midgut cells and water absorption by caecal cells in the anterior midgut (Caldeira et al. 2007). Species lacking caeca are also assumed to establish a countercurrent flow, as water absorption can be detected in anterior and median midgut regions while the posterior midgut secretes water (Santos et al. 1984). Nevertheless, some insects exhibit a countercurrent being restricted to the posterior midgut, a phenomenon indicating that the model of a countercurrent flow is not generally valid and probably varies strongly among different species, if it is present at all (Lehane 1976; Espinoza-Fuentes and Terra 1987; Terra et al. 1988). Although the model of enzyme recovery by a retrograde fluid flux in the ectoperitrophic space has been widely accepted, there are still some unsolved problems. One point of criticism is that many conclusions on the distribution of enzymes within the intestine were based only on measurement of enzyme activities, which complicates correct interpretation of the data because the activities may change over time (Dow 1986). Also the question of how the enzymes permeate the PM particularly in the posterior region is unclear. In the larval midgut of *T. castaneum*, the PM of the very posterior region was shown to exhibit an exclusion size of only about 4 kDa (Agrawal et al. 2014). This indicates that only small processed compounds such as oligosaccharides, peptides and fatty acids are able to permeate the PM in this region, while larger molecules such as enzymes are excluded from entering the PM.

Although we still do not know all details on the PM's function in digestion, the findings described above make it likely that partitioning of the gut lumen into different digestive compartments significantly enhances intestinal performance. This may have particularly contributed to the evolutionary success of insect species with fast-growing larval stages that need to build up energy stores for metamorphosis.

8.5.3 Neutralization of Toxic Compounds

The intestine of insects is frequently challenged by toxic compounds, which are directly ingested with the food, generated during metabolism of other compounds or produced by microorganism during intestinal infections. Plants have evolved a broad spectrum of defense strategies to combat herbivorous insects. They include the production of a broad spectrum of chemical compounds such as secondary metabolites (allelochemicals), peptides and proteins, which are taken up in larger amounts with the ingested plant material and may exert insecticidal activities. Different mechanisms have been proposed by which the PM potentially protects herbivorous insects from ingested allelochemicals: adsorption, ultrafiltration, polyanion exclusion, and the capacity of PMs to act as antioxidants (Barbehenn 2001). Tannins, for instance, are secondary metabolites synthesized by many plant species to protect from predation. The PM of many insects has been shown to be impermeable for tannic acid, one form of tannins. In lepidopterans and other insect species with a highly alkaline gut, tannic acids are known to react with proteins, lipids and polyvalent metal cations to form high molecular mass complexes that are unable to pass the PM and thus are retained in the endoperitrophic space (Barbehenn 2001). This ultrafiltration mechanism, which protects the midgut epithelium from tannins, appears also to account for lipophilic and amphiphilic allelochemical compounds such as xanthotoxins, digitoxins and saponins (Barbehenn 2001). Ingested tannic acids and many other allelochemicals are metabolized by the activity of peroxidases released in the foregut and anterior midgut. During this process hydrogen peroxide and reactive oxygen species are generated, which are partially inactivated by antioxidant enzymes (Krishnan et al. 2007). The majority of these reactive compounds becomes neutralized by the PM, which likely function as a radical-scavenging antioxidant in the insect midgut. On the one hand, this is due to the PM's ability of binding catalytically active metal ions such as iron. On the other hand, different components of the PM including carbohydrates and aromatic amino acids become oxidized themselves. By acting as a sacrificial antioxidant, the PM protects midgut epithelial cells from oxidative stress as evidenced in different lepidopteran species (Summers and Felton 1996; Barbehenn and Stannard 2004). Lectins are another group of plant-derived compounds with insecticidal activities. According to ultrastructural data for larvae of *O. nubilalis*, feeding of lectins leads to morphological alterations of the PM, which may be explained by their carbohydrate binding properties (Harper et al. 1998; Macedo et al. 2003). Due to the structural alterations of the PM, it was speculated that the insecticidal mechanism is at least partially associated with the disruption of PM function as the lectins bind to chitin or other sugar moieties of the PM. However, more recently Walski et al. (2014) performed a study in *T. castaneum* larvae, and suggest that lectin toxicity depends on its ability to permeate the PM as the lectins exhibited the greatest insecticidal activity upon reaching the ectoperitrophic space.

The PM is also involved in the elimination of xenobiotics other than the above-mentioned plant-derived allelochemicals including compounds that are used for

pest control. The xenobiotic DDT, for instance, is retained in the midgut of resistant adults of *A. aegypti* by a strongly increased PM production lowering the effective toxin concentrations in midgut epithelial cells (Abedi and Brown 1961). Similarly, a protective role of the PM has been suggested for cry- δ -endotoxins from *Bacillus thuringiensis* (*Bt*), which are used as biopesticides that exert their toxic effects by pore formation within the apical membranes of midgut epithelial cells.

Accordingly, Cry toxins have been shown to be restricted to the midgut lumen in *B. mori* larvae (Hayakawa et al. 2004). In contrast, Cry toxins are able to access the midgut epithelium of the cotton leafworm, *Spodoptera littoralis*, due to the larger exclusion size of the PM, which clearly demonstrates the functional diversity of PMs in insects (Yunovitz et al. 1986).

Binding of these toxins to PM-associated proteins may prevent the toxin from entering the ectoperitrophic space in those species, which are not susceptible to the respective variant of the δ -endotoxin (Rees et al. 2009; Perez-Hedo et al. 2012). In line with this view, it has been shown that parallel feeding of recombinant δ -endotoxins and endochitinases results in synergistically increased toxicity in larvae of *S. frugiperda*, presumably due to the perforation of the PM by the endochitinase allowing the toxin to access the midgut epithelium more easily. However, comparable effects have not been reported for calcofluor white which is known to disrupt the PM as well (Rees et al. 2009). This may result from preferential binding of the toxin to PM fragments, which are then excreted with the feces and therefore only show minor toxic effects. Recently, Chinese scientists showed that domain III of the CryIle toxin mediates the interaction with the PM from the Asian corn borer, *O. furnacalis* (Feng et al. 2015). As this domain has remarkable similarities to carbohydrate-binding domains from other proteins (de Maagd et al. 2003), it is likely that domain III interacts with the GlcNAc moieties of chitin. In insect species susceptible to specific δ -endotoxins, the toxin has to permeate through the PM in order to reach the ectoperitrophic space. The insecticidal activity of δ -endotoxins requires toxin solubilization in the midgut, processing by midgut proteases, receptor binding, toxin oligomerization, insertion into membranes of midgut epithelial cells and finally pore formation. Recently, it was shown that oligomerization is not only an important step in membrane insertion and pore formation, but it also affects PM permeability (Leetachewa et al. 2013). In case of Cry4Ba, an arginine residue at position 158 was identified to be crucial for oligomerization. Substitution of this arginine by glutamine or glutamate did not only impair oligomerization, but also led to a significant reduction in PM-permeability, suggesting that alteration of PM permeability is an important step for insecticidal activity.

The PM prevents the damaging action of pore-forming toxins derived from enteric bacteria other than *B. thuringiensis*. In the fruit fly, *D. melanogaster*, the protein drosocrystallin (Dcy) with an R&R chitin-binding domain is expressed in the gut and is required for PM formation (Kuraishi et al. 2011). A loss of function mutation in the *Dcy* gene leads to increased lethality of flies when challenged by entomopathogenic bacteria such as *Pseudomonas entomophila* and *Serratia marcescens*. This is accompanied by an increased susceptibility to the pore-forming toxin monalysin released by *entomophila*.

Blood sucking mosquitoes rely on hemoglobin as their main dietary protein source. However, its digestion causes problems, because heme released into the gut lumen during this process may be toxic through the generation of reactive oxygen species (Ryter and Tyrrell 2000). Pascoa et al. (2002) were the first who showed that the PM of adult female mosquitoes binds heme. As binding to the PM was saturable, the presence of specific binding sites within the PM was postulated. Indeed, a few years later, Devenport et al. (2006) demonstrated that the chitin-binding PMP, AeIMUC1, is capable of binding large amounts of heme *in vitro* suggesting a role in protecting the midgut epithelium from the harmful heme effects. It is worth mentioning that in blood feeding parasites such as *Plasmodium falciparum*, toxic heme released during hemoglobin degradation is converted into an insoluble crystalline form named hemozoin for detoxification. Hemozoin is also found in *R. prolixus* (Oliveira et al. 1999). Here, PMMs promote hemozoin formation presumably mediated by the PMM marker enzyme α -glucosidase, which seems to trigger hemozoin nucleation (Mury et al. 2009). Interestingly, heme aggregates that may resemble hemozoin were detected recently in *An. gambiae* females that ingested a blood meal (Magalhaes 2014). As these aggregates seem to be excluded from the PM, it is tempting to speculate that the PM in blood sucking mosquitoes functions in heme detoxification by an ultrafiltration-based mechanism that is similar to that of tannin detoxification.

8.5.4 Functions as an Anti-Infectious Barrier

Nutrients are frequently contaminated with viruses, bacteria, fungi or parasites. Thus, potential pathogens can easily invade the intestine together with the ingested food, and establish more or less devastating infections. Preventing infections is essential to insects for survival. Increasing knowledge on innate immunity has accumulated during the past decades and the mechanisms of how insects fight invading microorganisms and viruses have been partially deciphered. The PM has been recognized as an important factor in this fight, as it acts as a first-line of defense in the midgut. Indeed, protection of the midgut epithelium from pathogens ingested with the food may be one prime reason why insects produce a PM (Lehane 1997). As a physical barrier with limited pore sizes and carbohydrates acting as adhesive sites, it is effective in preventing many pathogens from getting access to the midgut epithelium (Sutherland et al. 1986; Laurent 1964; Ponnudurai et al. 1988). Accordingly, disruption of the PM's barrier function has been shown in a number of cases to promote infections and increase mortality. For instance, feeding of the mammalian galectin-1 to larvae of the diamondback moth, *Plutella xylostella*, leads to reduced survival rates as a consequence of PM disruption by this lectin, which is thought to interfere with PM structure by chitin binding and thus with the PM's barrier function against bacteria (Chen et al. 2009). Similar findings were obtained for *D. melanogaster* mutants defective in PM production due to the loss of a functional form of the drosocrystallin gene (Kuraishi et al. 2011). These mutant flies showed an increased susceptibility to oral infections with the entomopathogenic bacteria

Pseudomonas entomophila and *Serratia marcescens*. Interestingly, the PM of the tsetse fly appears not to be a physical barrier to the establishment of a bacterial infection, but it may be involved in modulating host immune detection of ingested bacteria (Weiss et al. 2014). In contrast, an intact PM reduces infection rates with the parasitic trypanosomes in tsetse's gut.

To avoid the PM barrier, some bacteria use developmental periods when the PM is naturally discontinuous to invade into the ectoperitrophic space. First-instar larvae of the bagworm moth, *Dahlica triquetrella*, for instance, stay uninfected during the larval feeding stage but become infected during ecdysis when the PM becomes permeable to bacteria in some regions (Puchta and Wille 1956).

In addition, ingested microfilarial nematodes such as the *Brugia pahangi* parasite are efficiently blocked by the PM of the mosquito *Ae. aegypti*, as they are only able to enter the hemocoel directly after a blood meal, when the PM is not yet formed completely (Perrone and Spielman 1986). Upon PM formation, the microfilariae are confined in the midgut lumen of *Ae. trivittatus* demonstrating the importance of the PM's barrier function to prevent parasitic infection (Sutherland et al. 1986). The meconial PM is a specialized PM surrounding the meconium, synthesized at the early pupal stage. Around the time of adult emergence sometimes a second meconial PM is formed. This structure allows the encapsulation of potential pathogenic microorganisms ingested during larval stages within the midgut avoiding infections during the dormant pupal stage. Subsequent extrusion of meconial PMs after adult emergence sterilizes the midgut (Moncayo et al. 2005). Next to physical retention by size exclusion, the PM also mediates immobilization of pathogens by serving as an alternative glycosylated adhesion site mimicking the surface of the glycocalyx present at midgut epithelial cells. This effectively deflects pathogens from attaching to the midgut epithelium (Mantle and Husar 1994; Smith et al. 1995).

Attachment to the PM is of special significance also for the defense against viruses, because not all insect species produce a PM with an exclusion size, which is sufficient to restrain harmful particles by size along the whole midgut (Barbehenn and Martin 1995; Edwards and Jacobs-Lorena 2000). However, the efficiency of protection from viral infections varies largely among different insect species and depends on the mode of PM formation. For instance, adult hematophagous Diptera that produce a type II PM are largely resistant to arboviral vectors and do not transmit these viruses, whereas adult Diptera with a type I PM transmit arboviral diseases. It is also worth mentioning that mosquito larvae with a type II PM are difficult to infect with these viruses (Stoltz and Summers 1971). Also the role of the PM from lepidopteran larvae that produce either a type I PM (as in the case of *T. ni*) or a type II-like PM (as in case of *H. virescens*) has been examined for its potential to protect from viral infections. Using a recombinant baculovirus containing the *lacZ* reporter gene, which allowed monitoring early viral pathogenesis and dose-mortality relationships, Washburn et al. (1995) concluded that PM provides little protection from baculoviral infections because the midgut epithelium is not permanently protected by a PM throughout development. In contrast to this report, Wang and Granados (1998) provided evidence for the presence of a PM prior to, during, and

immediately after ecdysis of *T. ni* larvae. Based on the additional finding that proteolytic degradation of the PM increased viral infectivity, these authors suggested the PM indeed serves as a partial barrier to viruses. This was further supported by the finding that treatment of *T. ni* larvae with calcofluor white, a compound known to inhibit PM formation, resulted in an increased susceptibility to baculoviral infection (Wang and Granados 2000). More direct evidence supporting a role of the PM in preventing viral infections was provided in a study comparing the velvetbean caterpillar, *Anticarsia gemmatilis* being resistant or susceptible to baculoviral infections. Here, structural preservation of the PM in resistant larvae suggested that it is involved in preventing baculoviral infections (Levy et al. 2011). Similar results suggesting that the PM is a barrier to virus transmission were reported for houseflies, *Musca domestica*, and a different virus (Boucias et al. 2015). Normally feeding flies are resistant to *per os* infections with the salivary gland hypertrophy virus MdSGHV. However, when the larvae were fed with a diet containing reducing agents such as dithiothreitol (DTT), which evidently disrupts the PM to various degrees, they showed significantly increased infection rates compared to control flies with intact PMs.

As mentioned in this paragraph, the resistance of insects to viral infections varies among different insects and viruses. As we will see in the next chapter, some viruses have developed particular strategies to overcome the PM barrier, which might explain why some viruses have a particularly high virulence in insects.

8.6 Mechanisms Developed by Pathogens and Parasites to Cross the PM Barrier

Coevolution between insects and pathogens has created mechanisms by which ingested viruses, bacteria and parasites became capable of perturbing existing defense mechanisms. Next to strategies that interfere with innate immunity, some pathogens and parasites have developed mechanisms that lead to the disruption of the PM barrier allowing them to enter the ectoperitrophic space and invade the mid-gut epithelium (Derksen and Granados 1988; Shao et al. 2001; Abraham and Jacobs-Lorena 2004). For instance, a chitinase is used by *Plasmodium falciparum* ookinetes, which disrupts PM integrity in order to reach the underlying epithelial tissue (Shahabuddin et al. 1993). In the following section, we will discuss the most prominent examples of mechanisms to interfere with the PM's barrier function.

8.6.1 Chitin Degradation

One of the first reports that pathogens or parasites actively disrupt the PM barrier originates from a study in which Huber et al. (1991) demonstrated that the ookinete of the avian malaria parasite *Plasmodium gallinaceum* secretes an chitinase to

disintegrate the chitin fibrils of the PM allowing them to cross the barrier. In line with this study, Shahabuddin et al. (1993) found that the chitinase inhibitor, allosamidin, blocked oocyte development of the parasite in the mosquito midgut, an effect that was reversed by supplementing the blood meal with exogenous chitinase, which prevented PM formation. Further studies suggested that the activities of more than one chitinolytic enzyme are required to allow the *P. gallinaceum* ookinete to pass the PM (Vinetz 2005). Subsequent studies on the human malaria parasite, however, showed that the PM of *An. tessellatus* is not an efficient barrier for the *P. vivax* ookinete whereas PM passage of the late *P. falciparum* ookinete is facilitated by chitinases (Ramasamy et al. 1997). Mammalian malarial parasites either express a smaller or larger version of the chitinase from a single gene locus. In *P. vivax* and *P. knowlesi* and some rodent parasites, a large chitinase that contains a catalytic domain and a chitin-binding domain is utilized, whereas in *P. falciparum* and *P. reichenowi* a small chitinase that lacks the chitin-binding domain is used (Li et al. 2005). In contrast, the avian parasites *P. gallinaceum* and *P. relictum* have two functional gene copies, which encode a large (CHT1) and a small (CHT2) chitinase (Li et al. 2005; Garcia-Longoria et al. 2014). Notably, PM proteoglycans serve also as recognition sites for the attachment of the ookinetes to the PM.

Other parasites disrupt the PM by means of chitinases to get access to the midgut epithelium. The *Leishmania* parasites, for instance, which are ingested with the blood meal by the sandfly *Phlebotomus papatasi*, lyse the chitin layer of the peritrophic membrane in the anterior midgut by the activities of a chitinase and an *N*-acetylglucosaminidase, which they produce and secrete (Schlein et al. 1991). Similar chitinolytic activities were detected in cell culture supernatants from other trypanosomatid species. Remarkably, the *Leishmania* parasite also benefits from the PM, as it protects the parasite from midgut hydrolytic activities at a time when they are particularly susceptible to proteolytic damage (Pimenta et al. 1997). More recently, a recombinant chitinase from *L. donovani* (LdCHT1) was expressed in *Escherichia coli*, purified and enzymatically characterized (Razek-Desouky et al. 2001). This enzyme turned out to exhibit endochitinase activity. However, not all parasites use chitinases to facilitate permeation through the PM. In tsetse flies there is some evidence that the PM is not a physical barrier to *Trypanosoma brucei rhodesiense*, and they do not express chitinolytic activities (Welburn et al. 1993).

Chitinolytic activities have also been implicated to play a role as in the pathogenesis of *Bt* in infected insects (Sampson and Gooday 1998). Two subspecies *Bt israelensis* IPS78 and *Bt aizawai* HD133 were shown to exhibit high larvicidal activities against larvae of the midge *Culicoides nubeculosus* and the caterpillars of *S. littoralis*, respectively. Both strains produce high amounts of chitinolytic activities. When the chitinases were inhibited by treatment with allosamidin, the larvicidal activities of both bacterial strains were strongly inhibited. On the other hand, when chitinase was added to the diet of the larvae, the larvicidal effects were increased. In another study, *B. thuringiensis* ssp. *kurstaki* HD-1(G) was identified as an efficient chitinase producer and its insecticidal activity was assayed in *P. xylostella* (Wiwat et al. 2000). This strain exhibited significant higher toxicity to the larvae than a *B. subtilis* ssp. *kurstaki* strain that produces no chitinase. It is tempting to speculate

that the chitinases of *B. thuringiensis* act as virulence factors, as they disrupt the PM and facilitate the cry- δ -endotoxin to cross the barrier and bind to the receptor on the apical membrane of midgut epithelial cells. Chitinases are produced widely by *B. thuringiensis*, as from 70 strains examined 38 have been tested positive for chitinolytic activity. For some of these strains further evidence has been provided that chitinase activity enhances their toxicity in larvae of the beet armyworm, *Spodoptera exigua* (Liu et al. 2002).

Finally, entomopathogenic viruses also use chitinases to enhance virulence and they seem to be involved in the terminal stage of infection of host insects (Hawtin et al. 1997; Vieira et al. 2012; D'Amico et al. 2013). Although the precise function of the chitinase still needs to be unraveled, it cannot be excluded that one function is to permeabilize the PM at a certain stage of the viral life cycle or host development (Ishimwe et al. 2015). The first such chitinase was described in the baculovirus *Autographa californica* MNPV (AcMNPV) (Hawtin et al. 1995). Later on, chitinases were identified in other baculoviruses too, and they all belong to family 18 glycohydrolases also found in mammals, bacteria, plants, and fungi (Jollès and Muzzarelli 1999). Meanwhile, it turned out that most baculoviruses, specifically those that infect lepidopteran larvae, contain chitinase genes. Interestingly, apart from baculoviruses, only Chlorella viruses were reported to produce chitinases (Hiramatsu et al. 1999). For baculoviral chitinases it has been suggested that the ancestral form may have been acquired from lepidopteran insects by horizontal gene transfer, either from an intestinal bacterium of the lepidopteran gut or from an intron-less gene encoding a lepidopteran chitinase (Kang et al. 1998; Hawtin et al. 1995; Daimon et al. 2003). Synergistic effects were observed upon infection of *S. littoralis* larvae with five isolated bacterial strains producing chitinolytic enzymes in combination with Cry toxin from *B. thuringiensis*, as lethality was increased compared to treatments with either bacteria or Cry toxin alone. This is explained by facilitated access of the toxin to epithelial membrane receptors in case of a disrupted PM (Sneh et al. 1983).

8.6.2 Proteases that Cleave PM-Associated Proteins

The pathogenesis of baculoviral infections has been extensively studied, and many factors have been identified that enhance viral infectivity. Among them were chitinases, as described above, but also viral enhancing factors that in contrast to chitinase evidently lead to changes in PM structure. One of the factors was found within the occlusion bodies of granulosis viruses from the armyworm *Pseudaletia unipuncta*, *T. ni* and the setaceous Hebrew character *Xestia c-nigrum* (Tanada 1959; Derksen and Granados 1988; Goto 1990; Granados and Corsaro 1990). Due to their enhancing effects on NPV infection, these proteases were termed “enhancers” (Corsaro et al. 1993). This factor was shown to be a metalloprotease that accounts for the degradation of specific mucin-like PMPs leading to the disruption of the PM from *T. ni* larvae (Lepore et al. 1996; Wang and Granados 1997a). This function is in

contrast to other baculoviral matrix metalloproteases that appear to share some redundant functions with viral cathepsins (Ishimwe et al. 2015). Genes encoding enhancin-like proteases were found in a number of baculoviral genomes. They are usually present as single copy genes, but sometimes also as multi-copy genes (Slavicek and Popham 2005). As components of viral occlusion bodies, enhancins are released along with the virions upon ingestion and facilitate infection by PM degradation. Evidence for this hypothesis is based on the finding that the PM treated with TnGV enhancin changes its structure and permeability (Derksen and Granados 1988; Gallo et al. 1991; Peng et al. 1999). In addition, recombinant baculoviruses, which express enhancin genes from different sources, have been shown to have increased virulence in different lepidopteran species (Derksen and Granados 1988; Gallo et al. 1991; Lepore et al. 1996; Guo et al. 2007b; Toprak et al. 2012). In contrast, mutant baculoviruses lacking a functional version of the enhancin gene showed decreased viral potency (Bischoff and Slavicek 1997; Popham et al. 2001). Interestingly, the degradation of mucin-like PMPs may depend on deglycosylation, as partially and fully deglycosylated forms of the PM protein McMUC1 were preferentially degraded in *M. configurata*, after infection of the larvae with the *M. configurata* multicapsid nucleopolyhedrovirus (McMNPV) (Shi et al. 2004). From the finding that a double enhancin deletion construct of the gypsy moth, *Lymantria dispar* MNPV was less infectious compared to wild-type LdMNPV, when it was used to infect larvae treated with calcofluor white to disrupt the PM, it may be concluded that enhancins may have additional target sites to increase viral infectivity (Hoover et al. 2010).

Enhancin-like metalloproteases were also identified in several bacterial species but with biochemical functions different from the baculoviral enhancins (Galloway et al. 2005; Hajajj-Ellouze et al. 2006). The gene product of the *bel* gene from *B. thuringiensis*, however, was found to have an activity similar to that of the viral enhancin, as Bel was shown to disrupt the PM and degrade mucin-like PMPs in the larval midgut of the cotton bollworm, *Helicoverpa armigera*, both *in vivo* and *in vitro* (Fang et al. 2009).

Notably, plants also produce proteases to weaken the PM's protective barrier function as a defense strategy. This mechanism was intensively studied in case of an insecticidal 33-kDa cysteine protease from *Zea mays*, which evidently damages the PM by degrading PM-associated proteins when ingested by larvae of *S. frugiperda* (Pechan et al. 2002; Mohan et al. 2006). In response to the action of the protease, genes encoding PM constituents and digestive enzymes were found to be upregulated presumably to compensate for the loss of PM function (Fescemyer et al. 2013). Due to its activity to increase PM permeability, the cysteine proteases synergize the toxicity of δ -endotoxins from *B. thuringiensis*. They also increase the efficacy of plant-mediated RNA interference, as transmission of the dsRNA produced by transgenic plants is facilitated (Mohan et al. 2008; Mao et al. 2013). Remarkably, herbivorous insects such as *T. ni* seem to have developed a counter-strategy to prevent the attack of plant cysteine proteases on the PM by producing inhibitors in the digestive tract (Li et al. 2009).

8.6.3 PM Disruption by Viral Spindles

Entomopoxviruses (EPVs) have been shown to promote baculoviral (NPV) infections (Mitsuhashi et al. 1998; Hukuhara et al. 1999). The genomes of many of these viruses encode a protein named fusolin that forms spindle-like structures. It was demonstrated that the spindles, but not spheroid forms which contain little or no fusolin, lead to the disintegration of the PM and increased PM permeability for the NPV virions (Mitsuhashi and Miyamoto 2003; Mitsuhashi et al. 2007). Using different EPV deletion mutants and testing them for their ability to enhance BmNPV infectivity in *B. mori* larvae, Takemoto et al. (2008) provided evidence that the *N*-terminus of fusolin is essential for its function, whereas the *C*-terminus is eliminated in the digestive juice. The *N*-terminus contains a chitin-binding domain, which is required for the disruption of the PM barrier. In addition, an *N*-glycosylation site in the *N*-terminal half was found to be important for fusolin function. Further research on the EPV spindles demonstrated that co-treatment of the cupreous chafer, *Anomala cuprea*, with both fusolin and a Bt δ -endotoxin improved insecticidal efficacy (Mitsuhashi et al. 2014). Recently, the structure of the viral spindles was solved at high resolution by X-ray micro-crystallography using crystals purified from infected insects. This study suggested that disruption of the PM by fusolin is caused by a globular domain that has the hallmarks of a lytic polysaccharide mono-oxygenase from chitinovorous bacteria capable of degrading chitin by oxidation. The monooxygenase domain is released as a result of destabilization of the protein structure in the digestive juice of the midgut.

8.7 Comparative Genomics: PMPs in Different Insect Orders

Genome sequence analysis of coleopteran and lepidopteran insects provided first insight into the evolution PMP encoding genes, particularly of their CBDs. In the *T. castaneum* genome, 11 genes were identified that encode putative PMPs with 1–14 CBDs from a set of a total of 42 CBDs (Jasrapuria et al. 2010). In contrast, *M. sexta* has 16 putative PMP genes with 1–14 CBDs from a set of a total of 67 CBDs (Tetreau et al. 2015). Phylogenetic analyses of the CBD coding sequences from both species revealed no clustering either by species or by sequence homology. However, many of the CBDs found within one particular PMP cluster together. This was also observed when additional sequences from dipteran (the southern house mosquito, *Culex quinquefasciatus*), hymenopteran (the jewel wasp, *Nasonia vitripennis*) and lepidopteran species (*B. mori*, the monarch butterfly *Danaus plexippus*, *H. armigera*, *M. configurata*, the oriental leafworm *Spodoptera litura*, and *T. ni*) were considered. Based on these findings, Tetreau et al. (2015) suggested that diversification of CBDs found in PMPs has occurred after radiation of insect species, even though the PMP domains seem to have emerged earlier. In this context, it

is also interesting to discuss whether the CBDs from PMPs have a common origin. From the finding that CBDs from PMPs and CPAP3s are in the same branches in several insect species, it was concluded that the PMP-CBDs may have originated from CPAP3 CBDs. Following gene duplication, they may have been incorporated into gut-specific genes with mucin-like domains (Tetreau et al. 2015). Most of the PMP genes from *T. castaneum* are expressed primarily in the midgut, and many of them are expressed in particular regions of the midgut (Jasrapuria et al. 2010). As mentioned earlier in this chapter, the number of CBDs present in the PMPs from *T. castaneum* correlates with the region where they are expressed in the midgut (Agrawal et al. 2014). However, currently it is not known whether this correlation does also apply to other insect species, and whether differences between the CBDs relate to different functions of the PMPs. Clearly more comparative analyses are needed to shed light onto this question.

8.8 PM as a Target for Pest Control

Because the PM is evidently crucial in many insects for nutrition and protection from enteric pathogens, it is an attractive target for pest control. There are many compounds available, which disrupt PM function by different means. On the one hand, there are available compounds that bind chitin whereby PMPs essential to maintain PM architecture are displaced, or the pore sizes in the three-dimensional meshwork are narrowed down. On the other hand, different enzymes can be employed to destroy the chitin fibrillary network or PMP function. All of these compounds and enzymes can be applied along with ingested insecticides to increase their efficiency. In addition, RNAi-based strategies tackling genes involved in PM formation may prove efficient to impair growth and development of pest insects.

8.8.1 PM Active Compounds

PM active compounds interfere with the components of the PM in a way that affects the barrier function. These compounds include chitin binding molecules such as optical brighteners and lectins, or enzymes that have chitinolytic or proteolytic properties.

8.8.1.1 Optical Brighteners

Optical brighteners such as Calcofluor white or Congo red have been demonstrated to interfere with chitin microfibril formation in unicellular algae (Herth 1980). When the PM from larvae of *T. ni* is treated with Calcofluor white, the majority of PMPs is released into the supernatant demonstrating that this compound competes

with the PMPs for binding sites on the chitin microfibrils (Wang and Granados 2000). Further experiments showed that feeding Calcofluor white to larvae leads to the disruption of the PM in five different lepidopteran species (Wang and Granados 2000). Because of PM disruption by calcofluor white treatment, the larval development was retarded and mortality increased. Thus, the mechanism of PM disruption by chitin binding agents has been suggested as one possible approach to develop novel strategies in pest management (Wang and Granados 2000). For instance, genes encoding chitin-binding domains could be used to create transgenic plants. Once they have been ingested with the plant material by herbivorous insects, the expressed CBDs would impair PM function and midgut physiology. As the larvae of *T. ni* treated with Calcofluor white became more susceptible to baculoviral infections, chitin binding domains may also be used to increase the efficiency of biological insecticides (Wang and Granados 2000). However, it is obviously not suitable to enhance the insecticidal effects of Bt Cry δ -endotoxins, because the toxin presumably binds to fragments of the disrupted PM and finally becomes excreted with the feces (Rees et al. 2009).

8.8.1.2 Lectins

A large group of biological molecules that have carbohydrate-binding properties are lectins, which bind to the PM due to the presence of chitin and glycosylated PMPs. The first lectin used to reliably label the PM of different insects for electron microscopy was gold-conjugated wheat germ agglutinin (WGA), which preferentially binds to *N*-acetylglucosamine residues in chitin and PM glycoproteins (Peters and Latka 1986). While in *An. gambiae* and *A. aegypti* only lectins specific for *N*-acetylglucosamine bind to the PM and the microvillar glycocalyx (Rudin and Hecker 1989), studies using labeled lectins identified different carbohydrate moieties in the PM of *G. morsitans morsitans* (Okolo et al. 1988). Some of these lectins such as the *Galanthus nivalis* agglutinin exhibit well-known insecticidal activities and the toxicity is thought to be mediated by binding to glycoproteins on the inner surface of the midgut (Pusztai 1991). Indeed, ultrastructural studies demonstrated that these lectins bind to the apical region of the midgut epithelium (Gatehouse et al. 1984; Powell et al. 1993; Sauvion et al. 1996; Sauvion et al. 2004). Next to the apical membranes of gut epithelial cells, different insecticidal lectins such as Concanavalin A (ConA), WGA and lentil lectin also bind to the carbohydrate moieties of the PM (Eisemann et al. 1994). The latter observation was paralleled by a reduction in PM permeability and diminished food uptake, which may indicate that the lectins block the pores of the PM. Fitches and Gatehouse (1998) showed that ConA binds to PM-associated proteins *in vitro* next to proteins present in the brush border (Fitches and Gatehouse 1998). Similar binding properties were reported for the mannose-binding lectin DB1 from *Dioscorea batatas* in larvae of *H. armigera* (Ohizumi et al. 2009). Finally, ultrastructural analysis of WGA effects in the larval midgut of the *O. nubilalis* finally provided evidence that the insecticidal lectin interferes with PM formation and integrity, which may induce the appearance of

additional PM layers, disruption of microvilli and nutritional deficiencies (Harper et al. 1998). In contrast to *O. nubilalis*, however, larvae of *M. sexta* tolerate high WGA amounts in their diet with no visible signs of PM disintegration, which was explained by differences in PM organization between both species (Hopkins and Harper 2001). Another example is labramin, a lectin-like protein from seeds of the beach apricot tree (*Labramia bojeri*), which causes insecticidal effects in the Mediterranean flour moth, *Ephestia kuehniella*, possibly by perturbing the PM's function partitioning digestive enzymes (Martinez et al. 2012). However, it has to be noted that the PM is not only a target for lectins, but also may protect midgut epithelial cells from their insecticidal activity. In *T. castaneum* for instance, differences in the insecticidal activities of *Sambucus nigra* agglutinin II (SNA II) and *Rhizoctonia solani* agglutinin (RSA) were shown to be due to different PM permeabilities for these lectins (Walski et al. 2014). While SNA II was more toxic to cultured *T. castaneum* cells than RSA, it was less toxic to whole larvae, presumably because SNA II passed less efficiently through the PM as evidenced by confocal microscopy. Thus, the insecticidal effect of lectins on gut physiology may have several interdependent causes. The finding that some lectins are also efficient in hemipteran species underlines the presence of target sites other than the PM. Nevertheless, the fact that lectins have insecticidal activities of which some are evidently related to the disruption of the PM, make them attractive molecules for pest control, particularly because their genes can be used to create transgenic plants. Several studies demonstrated insecticidal effects in transgenic plants expressing lectins. For instance, the *Galanthus nivalis* agglutinin (GNA) impairs growth and development when fed to different insect species including hemipterans, and similar effects were observed when the insects were allowed to feed on transformed plants (Down et al. 1996; Rao et al. 1998; Nagadhara et al. 2004). Using RNAi and transgenic tobacco plants, Vandenborre et al. (2010) showed the involvement of the *Nicotina tabacum* agglutinin in the defense against *S. littoralis* and *M. sexta*. Moreover, synergistic effects were reported when plant lectins were co-expressed with other insecticidal genes. For instance, the combined expression of genes for the pea lectin and cowpea trypsin inhibitor in transgenic tobacco plants resulted in a higher protection against *H. virescens* compared to plants that only expressed single genes (Boulter et al. 1990). The approach of combining a plant defense gene with a lectin gene (resulting in a single insecticidal fusion protein) enhanced protection from plant-feeding pests. Such an experiment was performed with the soya bean cysteine protease inhibitor and *Griffonia simplicifolia* lectin II. The recombinant fusion protein resulted in 100% mortality when fed to the cowpea bruchid (*Callosobruchus maculatus*), whereas the lectin or the protease inhibitor alone led only to about 50% of mortality rate (Zhu-Salzman et al. 2003). Due to the high resistance of some lectins against proteolytic degradation, some researchers came up with the idea to use these lectins as carriers for guiding protease-sensitive insecticidal compounds safely through the gut to reach the hemolymph. A proof of concept for this strategy was reported by Fitches et al. (2002) in the bright-line brown-eye moth, *Lacanobia oleracea*, using GNA as a carrier and *M. sexta* allatostatin (Manse-AS), a neuropeptide which has insecticidal activity when injected but not when fed, as it is rapidly degraded by gut

proteases (Audsley et al. 2001). When the recombinant GNA-Manse-AS fusion protein was fed to *L. oleracea* larvae, the intact neuropeptide was delivered into the hemolymph (Fitches et al. 2002). Similar studies were performed with recombinant GNA fusion proteins with the ButaIT neurotoxin from the red scorpion, *Mesobuthus tamulus*, the spider-venom peptide ω -hexatoxin-Hv1a (Hv1a), or the spider venom peptide, δ -amaurobitoxin-PI1a. All of them demonstrated oral insecticidal activities in various tested insects (Fitches et al. 2010; Fitches et al. 2012; Yang et al. 2014). Interestingly, the GNA-Hv1a fusion protein exhibited no toxicity to honey bees, *Apis mellifera*, and no adverse effects on learning and memory were observed (Nakasu et al. 2014). Recently, Tajne et al. (2014) demonstrated that a fusion protein of *Allium sativum* agglutinin (ASAL) and *Bt* Cry1Ac δ -endotoxin is significantly more toxic to larvae of the pink bollworm, *Pectinophora gossypiella*, and *H. armigera* in comparison to feeding experiment using the unfused Cry1Ac toxin. In this case, the effect was explained by increased binding of the lectin- Cry1Ac to carbohydrate-binding sites in the midgut.

8.8.1.3 Chitinases

Although chitin is absent in plants, they express chitinases in response to different biotic and abiotic stresses such as heat, cold, drought, soil salinization or harmful microorganisms and parasites (Cletus et al. 2013). Chitinase genes from plants and other sources have been used to create transgenic plants to induce resistance mainly against fungal diseases (Ceasar and Ignacimuthu 2012). However, it was also realized that chitinase have a potential to control agricultural pests and insect vectors for human diseases. For instance, heterologous expression of the poplar chitinase (which is naturally upregulated upon gypsy moth infestation) in tomato plants efficiently retards growth and development of the Colorado potato beetle, *Leptinotarsa decemlineata* (Lawrence and Novak 2006). In many cases, it has been reported that the PM is a major target for these exogenous chitinases. In addition, insect midgut chitinases, which are required for PM turnover, were identified as promising targets to interfere with the PM and thus with the life cycle of parasites that attach to the PM before penetration.

In the early 1990s chitinases secreted by different parasites including *Plasmodium* and *Leishmania* have been implicated in the invasion process of the midgut epithelium by disrupting the PM (Huber et al. 1991; Schlein et al. 1991; Shahabuddin et al. 1993). In addition, endogenous chitinases such as PpChit1 secreted by the midgut epithelium of the sandfly, *Phlebotomus papatasi* are required for PM maturation (Coutinho-Abreu et al. 2010). Accordingly, deletion of chitinase genes or RNAi-based silencing of their gene expression in the parasites results in reduced infectivity and impaired invasion of the host's midgut epithelium (Dessens et al. 2001; Tsai et al. 2001; Coutinho-Abreu et al. 2010). Moreover, antibodies have been developed to interfere with the chitinase function. A single-chain antibody against *Plasmodium* chitinases was demonstrated to reduce parasite transmission to mos-

quitoes (Li et al. 2005). In the sandfly, an antiserum to the midgut chitinase PpChit1 impaired degradation of the PM (Robles-Murguía et al. 2014).

Initially, attempts were followed to increase the insecticidal activity of Cry1C δ -endotoxin by feeding exogenous chitinases, and it has been noted that feeding the chitinase on its own disrupts the PM already at a low concentration of about 100 ng/ml (Regev et al. 1996). In line with this and other studies, the insecticidal activity of Cry1C δ -endotoxins against *S. exigua* larvae was improved when the *Bt* subsp. Aizawai strain was genetically modified to express a chitinase gene from *Bacillus licheniformis* (Thamthiankul et al. 2004).

Several studies confirmed the insecticidal effects using recombinant chitinases. When ladybird beetles were fed on tomato leaves sprayed with microbial bead suspensions containing chitinases produced by *Enterobacter cloacae*, they showed reduced feeding and egg-laying compared to controls fed on non-treated plants (Otsu et al. 2003). Also a chitinase from *L. oleracea* was cloned, expressed in the yeast *Pichia pastoris* and characterized for its insecticidal activity, which was additionally compared to the activity of a GNA-chitinase fusion protein to deliver it into the hemolymph after oral ingestion (Fitches et al. 2004). Both proteins were highly toxic to *L. oleae* larvae when injected into the hemolymph, and oral application caused decreased feeding and growth of the larvae. Interestingly, attachment of GNA did not increase the toxicity after oral administration as observed for several hormones and neurotoxins. Also a chitinase from viral sources was tested for insecticidal activity. The recombinant chitinase A (ChiA) from the *Autographa californica* multicapsid nucleopolyhedrovirus (AcMNPV), which was purified from *E. coli* cell extracts, caused a 100% mortality when fed to fifth instar larvae of *B. mori* at doses of about 1 μ g/g body weight (Rao et al. 2004). As a result of ChiA treatment, the PM structure was altered and PM permeability increased. Likewise, disruption of the PM was observed in adult Japanese pine sawyer beetle after feeding a recombinant chitinase from *B. mori* (Kabir et al. 2006). Interestingly, ultrastructural analysis revealed no indications of changes in the midgut epithelium. Also the insecticidal activity of the ChiA enzyme from the *Epinotia aporema* granulovirus was tested. For this purpose, the ChiA was over-expressed in cell culture to yield recombinant occlusion bodies that were used to feed *A. gemmatilis* larvae, and again the PM was found to be altered in structure (Salvador et al. 2014). The chitinase genes discussed so far may be good candidates for the generation of transgenic plants with resistance to insect pests.

Ding et al. (1998) were the first to generate a transgenic tobacco plant expressing an insect chitinase gene, and they showed that *H. virescens* larvae fed on these plants exhibited reduced growth rates and caused less feeding damage when compared to larvae fed on wild type plants. In addition, synergetic insecticidal effects were observed for the chitinase-expressing plants, when the leaves were coated with Bt δ -endotoxins. Also the baculoviral AcMNPV-ChiA gene was used to transform tobacco plants (Di Maro et al. 2010). The recombinant enzyme was shown to be stable at higher temperatures and at alkaline pH, which makes it particularly interesting to combat lepidopteran pests, because the pH in the gut lumen can reach high alkaline values (Dow 1992). Indeed, its expression in transgenic tobacco plants mediated resistance against agricultural pests and fungi (Di Maro et al. 2010).

8.8.1.4 Proteases

Several plants, parasites and entomopathogenic viruses have been reported to produce insecticidal proteases that disrupt the PM's barrier function. To protect from herbivorous pests, for instance, plants express defense genes that encode proteases, which confer resistance to many pest species. For instance, several maize (*Zea mays*) lines have been reported to produce a 33 kDa cysteine protease in response to caterpillar feeding damage (Pechan et al. 2002). When the gene for this cysteine protease (named *mir-1*) was used to transform black Mexican sweetcorn, the larval growth of *S. frugiperda* was significantly diminished. Ultrastructural examination of the PM of larvae fed on maize plants expressing the *mir-1* gene, revealed severe damage of the PM, which suggests that the observed growth defects are due to the loss of the PM function that facilitates digestion. When the recombinant Mir-1 protein was tested *in vitro*, complete permeabilization was observed after treating the dissected PM with the protease, and the time until complete permeabilization was inversely proportional to the protease concentration (Mohan et al. 2006). Although the protease also damaged the PMs from *H. zea*, *D. plexippus*, *O. nubilalis*, *P. americana* and *T. molitor*, the PM from *S. frugiperda* was most susceptible to Mir-1. Due to its general effects on PM permeability, Mir-1 synergizes the toxicity of sublethal concentrations of the Bt CryIIA δ -endotoxin in four different lepidopteran species (Mohan et al. 2008). Notably, treatment of the isolated PM from *S. frugiperda* with the Mir-1 protein preferentially led to the loss of mucin-like PMPs (IIMs), and larvae fed on a maize line overexpressing the *mir-1* gene (Mp798) produced feces with a comparably low IIM content (Fescemyer et al. 2013). Genomic analysis of changes in global gene expression further revealed compensatory up-regulation of genes involved in PM biosynthesis in response to feeding on Mp708 maize. Interestingly, genes encoding different hydrolytic enzymes were also found to be higher expressed in the Mp708-fed caterpillars.

Similar to the Mir-1 protease, a cysteine protease found in the latex of papaya trees (*Carica papaya*) and wild figs (*Ficus virgata*) was reported to increase mortality and reduce the larval growth of different caterpillars including the Eri silkworm (*Samia ricini*), the cabbage moth (*Mamestra brassicae*) and *S. litura* (Konno et al. 2004). Treatment of papaya or fig leaves with the cysteine protease inhibitor E-64 reversed these toxic effects completely. Furthermore, plant cysteine proteases with potential roles in interfering with the PM function were identified in genomic and proteomic studies performed in tobacco plants (*Nicotiana attenuata*) and in *Arabidopsis thaliana* (Reymond et al. 2004; Schmidt et al. 2005; Little et al. 2007).

As already discussed in Sect. 8.6.2, baculoviral genomes harbor genes that encode zinc metalloproteases that promote nuclear polyhedrosis virus (NPV) infectivity in lepidopteran larvae, and disintegrate the larval PM by cleaving mucin-like PMPs (Derksen and Granados 1988; Wang et al. 1994; Wang and Granados 1997a; Peng et al. 1999). When the baculoviral enhancin genes were used to transform tobacco or rice plants, reduced growth and high mortality were observed in different caterpillars that were fed on these transgenic plants (Cao et al. 2002; Mori et al. 2006). As in the case of chitinases and other PM degrading proteases, enhancins

were shown to promote toxicity of *Bt* Cry- δ -endotoxins (Granados et al. 2001). The finding that bacterial genomes including that of *Bt* contain homologous enhancin genes, may indicate horizontal gene transfer between these bacteria and NPVs (Ivanova et al. 2003; Read et al. 2003). However, only the *Bt* enhancin-like Bel-protein is capable of promoting oral toxicity of the Cry1Ac protein fed to *H. armigera* larvae through PM disruption by cleaving mucin-like proteins (Fang et al. 2009). As many of the bacterial enhancins do not promote baculoviral infectivity in insect cells and even exhibit more cytotoxic effects, it was suggested that viral and bacterial enhancins have developed different functions (Galloway et al. 2005). In contrast to cysteine proteases and metalloproteases such as the enhancins, serine proteases apparently are not effective in degrading dissected PM or recombinant PMPs expressed in insect cells (Wang et al. 2004; Li et al. 2009).

8.9 RNAi-Based Strategies

RNAi-based strategies of gene silencing have been proven to be highly powerful in analyzing gene functions not only in *D. melanogaster* but also in many other insect species (Belles 2010). One of the best-characterized RNAi models is *T. castaneum*, a crop pest whose genome has been sequenced and annotated (Brown et al. 2003). RNAi in *T. castaneum* is very robust and causes systemic effects, which are simply induced by injecting dsRNA into the hemocoel of larvae, pupae or adults. In this way, numerous genes have been analyzed for their function in this species, and even parental RNAi-induced phenotypes in progeny insects were described (Bucher et al. 2002). In addition to help in unraveling gene functions, they have also been used in comparative approaches for analyzing developmental gene networks in different insect taxa to probe the evolutionary context of the involved signaling cascades (Brown et al. 1999; Peel 2008). RNAi has also been increasingly exploited as a mechanism to control insect pests in a highly species-specific manner. The proof of principle for RNAi being a suitable method in pest control was first provided for the western corn rootworm, *Diabrotica virgifera virgifera*, and *H. armigera*, using dsRNA to target the genes for V-ATPase subunit A and cytochrome P450, *CYP6AE14*, respectively (Baum et al. 2007; Mao et al. 2007). In both studies, dsRNA was fed to the larvae, which is feasible under laboratory conditions but limits practical applicability of RNAi, because dsRNA simply sprayed onto plants would be exposed to environmental factors that lead to disintegration. However, expression of dsRNA by transgenic plants evidently circumvents such problems and makes RNAi an extremely promising technique in pest control. However, in lepidopteran insects large variations and inconsistent results regarding the success of RNAi-induced gene silencing were reported (Terenius et al. 2011). These difficulties may be due the extremely high pH in the midgut of lepidopteran species, which may reduce RNAi efficacy significantly, when dsRNA is orally administered. In addition, the stability of dsRNA in the hemolymph may be limited particularly in lepidopteran species because of dsRNase activity (Garbutt et al. 2013). Interestingly,

also the PM itself has been suggested to be an effective barrier for dsRNA, because cysteine proteases, which evidently increase PM permeability, enhance plant-mediated RNA interference in the bollworm (Mao et al. 2013).

For improving the efficacy of sprayed RNA in pest insects, carriers such as bacteria, viruses or nanoparticles, and the application of PM active proteases may help to protect the dsRNA from adverse environmental factors, and to facilitate PM permeation. To circumvent problems arising from RNAses present in the hemolymph of lepidopteran species, essential genes that are specifically expressed in the midgut epithelium may be used as suitable targets for RNAi. As V-type ATPases are critical for energization of nutrient uptake and alkalinization of the midgut lumen, RNAi-induced silencing of genes encoding different subunits of this multimeric enzyme complex has been reported repeatedly to be successful in orally inducing mortality in various insects including lepidopteran larvae (Whyard et al. 2009; Jin et al. 2015). As the PM is important for insect nutrition and defense against pathogens, genes involved in PM formation and its maintenance may prove useful in RNAi-mediated pest control. Such genes include those encoding enzymes involved in chitin formation such as *Gfat1* (glutamine: fructose-6-phosphate amidotransferase-1), *UAP* (UDP-*N*-acetylglucosamine pyrophosphorylase) and *CHS2* (chitin synthase 2) (Arakane et al. 2005; Kato et al. 2006; Arakane et al. 2011; Kelkenberg et al. 2015), as well as chitin modifying enzymes such as *CDAs* (chitin deacetylases) and *CHTs* (chitinases) (Khajuria et al. 2010; Quan et al. 2013). In addition, RNAi of genes encoding specific PMPs have been shown to affect PM permeability and thickness (Kuraishi et al. 2011; Agrawal et al. 2014). In all these case, dsRNA injection has been shown to affect PM formation, and as a consequence nutrition and larval growth as well. Finally, some of these genes have been shown to be down-regulated after oral administration of dsRNAs in lepidopteran larvae (Toprak et al. 2013). Future studies will show the potential of these genes as targets for insect control.

8.10 Concluding Remarks and Perspectives

Although substantial progress has been made in the past years that increased our understanding of the PM structure and function, there is still much to be learned. The fact that most insects have to produce a PM suggests that it provides important capabilities allowing them to survive and reproduce in a hostile environment. The PM serves as an effective first line of defense against viruses, bacteria and parasites. However, some entomopathogens have evolved mechanisms to disrupt the PM barrier by producing hydrolytic enzymes that disintegrate the chitinous meshwork or specifically degrade PM-associated proteins, which are usually resistant to proteases. Due to the availability of fully annotated genomes for an increasing number of insects and improved mass-spectrometric techniques, much progress has been made in identifying PM components. RNAi allowed demonstration of loss-of function phenotypes and provided some clues on *in vivo* functions of specific genes. Their precise functions in organizing the PM meshwork, however, remain elusive. The

availability of recombinant proteins expressed in bacterial and insect cells will allow the examination of their individual potential in organizing chitin nanofibers. In-depth analyses of protein-protein and protein-chitin interactions will resolve the details of PM architecture and allow addressing how PM properties may be regulated in response to physiological changes. The combination of classical biochemical and modern biophysical methods including scanning electron, super-resolution fluorescence and atomic force microscopy may provide further insights into structure-function relationships. We are currently establishing suitable techniques that allow addressing these questions to unravel the mechanism of PM formation, which presumably is a self-assembly process. As the disruption of the PM has been shown to interfere with growth, development and fitness of pest insects, the PM has gained increasing attention as a potential target for pest control. PM-active compounds have been shown to enhance the toxicity of chemical and biological insecticides that are already in commercial use in forestry, agriculture and public health. Finally, genes that are required for PM formation may prove useful to create transgenic plants that express dsRNA for gene silencing. It is foreseeable that significant progress will be made in the coming year in understanding the structure, function and regulation of the PM.

Acknowledgements This work was supported by the NSF Grant IOS-1022227 to S.M. and the DFG Grant Me2210/3-1 to H.M. M.K. was supported by a Lichtenberg fellowship by the Government of the State of Lower Saxonia, Germany.

References

- Abedi ZH, Brown AWA (1961) Peritrophic membrane as vehicle for DDT and DDE excretion in *Aedes aegypti* larvae. *Ann Entomol Soc Am* 54:539–542
- Abraham EG, Jacobs-Lorena M (2004) Mosquito midgut barriers to malaria parasite development. *Insect Biochem Mol Biol* 34:667–671
- Adang MJ, Spence KD (1983) Permeability of the peritrophic membrane of the Douglas fir tussock moth (*Orgyia pseudotsugata*). *Comp Biochem Phys A* 75:233–238
- Agrawal S, Kelkenberg M, Begum K, Steinfeld L, Williams CE, Kramer KJ, Beeman RW, Park Y, Muthukrishnan S, Merzendorfer H (2014) Two essential peritrophic matrix proteins mediate matrix barrier functions in the insect midgut. *Insect Biochem Mol Biol* 49:24–34
- Allahyari M, Bandani AR, Habibi-Rezaei M (2010) Subcellular fractionation of midgut cells of the sunn pest *Eurygaster integriceps* (Hemiptera: Scutelleridae): enzyme markers of microvillar and perimicrovillar membranes. *J Insect Physiol* 56:710–717
- Alvarenga ES, Mansur JF, Justi SA, Figueira-Mansur J, Dos Santos VM, Lopez SG, Masuda H, Lara FA, Melo AC, Moreira MF (2015) Chitin is a component of the *Rhodnius prolixus* midgut. *Insect Biochem Mol Biol*. pii: S0965-1748(15)00070-3
- Alves CR, Albuquerque-Cunha JM, Mello CB, Garcia ES, Nogueira NF, Bourguignon SC, de Souza W, Azambuja P, Gonzalez MS (2007) *Trypanosoma cruzi*: attachment to perimicrovillar membrane glycoproteins of *Rhodnius prolixus*. *Exp Parasitol* 116:44–52
- Arakane Y, Muthukrishnan S, Kramer KJ, Specht CA, Tomoyasu Y, Lorenzen MD, Kanost M, Beeman RW (2005) The *Tribolium* chitin synthase genes *TcCHS1* and *TcCHS2* are specialized for synthesis of epidermal cuticle and midgut peritrophic matrix. *Insect Mol Biol* 14:453–463

- Arakane Y, Baguion M, Jasrapuria S, Chaudhari S, Doyungan A, Kramer KJ, Muthukrishnan S, Beeman RW (2011) Two uridine-diphosphate N-acetylglucosamine pyrophosphorylases are critical for *Tribolium castaneum* molting, survival and fecundity. *Insect Biochem Mol Biol* 41:42–50
- Asensio JL, Canada FJ, Bruix M, Gonzalez C, Khiar N, Rodriguez-Romero A, Jimenez-Barbero J (1998) NMR investigations of protein-carbohydrate interactions: refined three-dimensional structure of the complex between hevein and methyl beta-chitobioside. *Glycobiology* 8:569–577
- Audsley N, Weaver RJ, Edwards JP (2001) In vivo effects of *Manduca sexta* allatostatin and allatotropin on larvae of the tomato moth, *Lacanobia oleracea*. *Physiol Entomol* 26:181–188
- Azuma M, Harvey WR, Wiczorek H (1995) Stoichiometry of K⁺/H⁺ antiport helps to explain extracellular pH 11 in a model epithelium. *FEBS Lett* 361:153–156
- Balbani EG (1890) Etudes anatomiques et histologiques sur le tube digestif des Crytops. *Arch Zool Exp Gen* 8:1–82
- Barbehenn RV (2001) Roles of peritrophic membranes in protecting herbivorous insects from ingested plant allelochemicals. *Arch Insect Biochem Physiol* 47:86–99
- Barbehenn RV, Martin MM (1995) Peritrophic envelope permeability in herbivorous insects. *J Insect Physiol* 41:303–311
- Barbehenn RV, Stannard J (2004) Antioxidant defense of the midgut epithelium by the peritrophic envelope in caterpillars. *J Insect Physiol* 50:783–790
- Barry MK, Triplett AA, Christensen AC (1999) A peritrophin-like protein expressed in the embryonic tracheae of *Drosophila melanogaster*. *Insect Biochem Mol Biol* 29:319–327
- Baum JA, Bogaert T, Clinton W, Heck GR, Feldmann P, Ilagan O, Johnson S, Plaetinck G, Munyikwa T, Pleau M, Vaughn T, Roberts J (2007) Control of coleopteran insect pests through RNA interference. *Nat Biotechnol* 25:1322–1326
- Becker B (1980) Effects of polyoxin D on in vitro synthesis of peritrophic membranes in *Calliphora erythrocephala*. *Insect Biochem* 10:101–106
- Behr M, Hoch M (2005) Identification of the novel evolutionary conserved obstructor multigene family in invertebrates. *FEBS Lett* 579:6827–6833
- Belles X (2010) Beyond *Drosophila*: RNAi in vivo and functional genomics in insects. *Annu Rev Entomol* 55:111–128
- Berridge MJ (1970) A structural analysis of intestinal absorption. *Symp R Entomol Soc Lond* 5:135–150
- Binnington KC (1988) Ultrastructure of the peritrophic membrane-secreting cells in the cardia of the blowfly, *Lucilia cuprina*. *Tissue Cell* 20:269–281
- Bischoff DS, Slavicek JM (1997) Molecular analysis of an enhancer gene in the *Lymantria dispar* nuclear polyhedrosis virus. *J Virol* 71:8133–8140
- Bolognesi R, Ribeiro AF, Terra WR, Ferreira C (2001) The peritrophic membrane of *Spodoptera frugiperda*: secretion of peritrophins and role in immobilization and recycling digestive enzymes. *Arch Insect Biochem Physiol* 47:62–75
- Bolognesi R, Arakane Y, Muthukrishnan S, Kramer KJ, Terra WR, Ferreira C (2005) Sequences of cDNAs and expression of genes encoding chitin synthase and chitinase in the midgut of *Spodoptera frugiperda*. *Insect Biochem Mol Biol* 35:1249–1259
- Bolognesi R, Terra WR, Ferreira C (2008) Peritrophic membrane role in enhancing digestive efficiency. Theoretical and experimental models. *J Insect Physiol* 54:1413–1422
- Boucias D, Baniszewski J, Prompiboon P, Lietze V, Geden C (2015) Enhancement of the *Musca domestica* hytrosavirus infection with orally delivered reducing agents. *J Invertebr Pathol* 124:35–43
- Boudko DY, Moroz LL, Harvey WR, Linser PJ (2001) Alkalinization by chloride/bicarbonate pathway in larval mosquito midgut. *Proc Natl Acad Sci U S A* 98:15354–15359
- Boulter D, Edwards GA, Gatehouse AMR, Gatehouse JA, Hilder VA (1990) Additive protective effects of different plant-derived insect resistance genes in transgenic tobacco plants. *Crop Prot* 9:351–354

- Brown SJ, Mahaffey JP, Lorenzen MD, Denell RE, Mahaffey JW (1999) Using RNAi to investigate orthologous homeotic gene function during development of distantly related insects. *Evol Dev* 1:11–15
- Brown SJ, Denell RE, Beeman RW (2003) Beetling around the genome. *Genet Res* 82:155–161
- Bucher G, Scholten J, Klingler M (2002) Parental RNAi in *Tribolium* (Coleoptera). *Curr Biol* 12:R85–R86
- Burgos MH, Gutierrez LS (1976) The intestine of *Triatoma infestans*. I Cytology of the midgut. *J Ultrastruct Res* 57:1–9
- Caldeira W, Dias AB, Terra WR, Ribeiro AF (2007) Digestive enzyme compartmentalization and recycling and sites of absorption and secretion along the midgut of *Dermestes maculatus* (Coleoptera) larvae. *Arch Insect Biochem Physiol* 64:1–18
- Campbell PM, Cao AT, Hines ER, East PD, Gordon KH (2008) Proteomic analysis of the peritrophic matrix from the gut of the caterpillar, *Helicoverpa armigera*. *Insect Biochem Mol Biol* 38:950–958
- Cantarel BL, Coutinho PM, Rancurel C, Bernard T, Lombard V, Henrissat B (2009) The Carbohydrate-Active Enzymes database (CAZy): an expert resource for glycogenomics. *Nucleic Acids Res* 37(Database issue):D233–D238
- Cao J, Ibrahim H, Garcia J, Mason H, Granados R, Earle E (2002) Transgenic tobacco plants carrying a baculovirus enhancin gene slow the development and increase the mortality of *Trichoplusia ni* larvae. *Plant Cell Rep* 21:244–250
- Casu R, Eisemann C, Pearson R, Riding G, East I, Donaldson A, Cadogan L, Tellam R (1997) Antibody-mediated inhibition of the growth of larvae from an insect causing cutaneous myiasis in a mammalian host. *Proc Natl Acad Sci U S A* 94:8939–8944
- Cesar SA, Ignacimuthu S (2012) Genetic engineering of crop plants for fungal resistance: role of antifungal genes. *Biotechnol Lett* 34:995–1002
- Chaudhari SS, Arakane Y, Specht CA, Moussian B, Boyle DL, Park Y, Kramer KJ, Beeman RW, Muthukrishnan S (2011) Knickkopf protein protects and organizes chitin in the newly synthesized insect exoskeleton. *Proc Natl Acad Sci U S A* 108:17028–17033
- Chen SJ, Chen NT, Wang SH, Hsu JC, Ding WH, Kuo-Huang LL, Huang RN (2009) Insecticidal action of mammalian galectin-1 against diamondback moth (*Plutella xylostella*). *Pest Manag Sci* 65:923–930
- Clarke L, Temple GH, Vincent JF (1977) The effects of a chitin inhibitor-dimilin- on the production of peritrophic membrane in the locust, *Locusta migratoria*. *J Insect Physiol* 23:241–246
- Cletus J, Balasubramanian V, Vashisht D, Sakthivel N (2013) Transgenic expression of plant chitinases to enhance disease resistance. *Biotechnol Lett* 35:1719–1732
- Comper WD, Laurent TC (1978) Physiological functions of connective tissue polysaccharides. *Physiol Rev* 58:255–315
- Corsaro BG, Gijzen M, Wang P, Granados RR (1993) Baculovirus enhancing proteins as determinants of viral pathogenesis. In: Beckage NE, Thompson SN, Federici BA (eds) Parasites and pathogens of insects, vol 2. Pathogens. Academic Press, New York, pp 127–145.
- Coutinho-Abreu IV, Sharma NK, Robles-Murguía M, Ramalho-Ortigao M (2010) Targeting the midgut secreted PpChit1 reduces *Leishmania major* development in its natural vector, the sand fly *Phlebotomus papatasi*. *PLoS Negl Trop Dis* 4:e901
- Cristofaletti PT, Ribeiro AF, Terra WR (2001) Apocrine secretion of amylase and exocytosis of trypsin along the midgut of *Tenebrio molitor* larvae. *J Insect Physiol* 47:143–155
- Cristofaletti PT, Ribeiro AF, Deraison C, Rahbe Y, Terra WR (2003) Midgut adaptation and digestive enzyme distribution in a phloem feeding insect, the pea aphid *Acyrtosiphon pisum*. *J Insect Physiol* 49:11–24
- D'Amico V, Slavicek J, Podgwaite JD, Webb R, Fuester R, Peiffer RA (2013) Deletion of v-chiA from a baculovirus reduces horizontal transmission in the field. *Appl Environ Microbiol* 79:4056–4064
- Daimon T, Hamada K, Mita K, Okano K, Suzuki MG, Kobayashi M, Shimada T (2003) A *Bombyx mori* gene, BmChi-h, encodes a protein homologous to bacterial and baculovirus chitinases. *Insect Biochem Mol Biol* 33:749–759

- de Maagd RA, Bravo A, Berry C, Crickmore N, Schnepf HE (2003) Structure, diversity, and evolution of protein toxins from spore-forming entomopathogenic bacteria. *Annu Rev Genet* 37:409–433
- De Mets R, Jeuniaux C (1962) Composition of peritrophic membrane. *Arch Int Physiol Biochim* 70:93–96
- Del Bene G, Dallai R, Marchini D (1991) Ultrastructure of the midgut and the adhering tubular salivary glands of *Frankliniella occidentalis* (Pergande) (Thysanoptera: Thripidae). *Int J Insect Morph Embryol* 20:15–24
- Derksen AC, Granados RR (1988) Alteration of a lepidopteran peritrophic membrane by baculoviruses and enhancement of viral infectivity. *Virology* 167:242–250
- Dessens JT, Mendoza J, Claudianos C, Vinetz JM, Khater E, Hassard S, Ranawaka GR, Sinden RE (2001) Knockout of the rodent malaria parasite chitinase pbCHT1 reduces infectivity to mosquitoes. *Infect Immun* 69:4041–4047
- Devenport M, Fujioka H, Donnelly-Doman M, Shen Z, Jacobs-Lorena M (2005) Storage and secretion of Ag-Aper14, a novel peritrophic matrix protein, and Ag-Muc1 from the mosquito *Anopheles gambiae*. *Cell Tissue Res* 320:175–185
- Devenport M, Alvarenga PH, Shao L, Fujioka H, Bianconi ML, Oliveira PL, Jacobs-Lorena M (2006) Identification of the *Aedes aegypti* peritrophic matrix protein AeIMUCI as a heme-binding protein. *Biochemistry* 45:9540–9549
- Di Maro A, Terracciano I, Sticco L, Fiandra L, Ruocco M, Corrado G, Parente A, Rao R (2010) Purification and characterization of a viral chitinase active against plant pathogens and herbivores from transgenic tobacco. *J Biotechnol* 147:1–6
- Ding X, Gopalakrishnan B, Johnson LB, White FF, Wang X, Morgan TD, Kramer KJ, Muthukrishnan S (1998) Insect resistance of transgenic tobacco expressing an insect chitinase gene. *Transgenic Res* 7:77–84
- Dinglasan RR, Devenport M, Florens L, Johnson JR, McHugh CA, Donnelly-Doman M, Carucci DJ, Yates JR 3rd, Jacobs-Lorena M (2009) The *Anopheles gambiae* adult midgut peritrophic matrix proteome. *Insect Biochem Mol Biol* 39:125–134
- Dixit R, Arakane Y, Specht CA, Richard C, Kramer KJ, Beeman RW, Muthukrishnan S (2008) Domain organization and phylogenetic analysis of proteins from the chitin deacetylase gene family of *Tribolium castaneum* and three other species of insects. *Insect Biochem Mol Biol* 38:440–451
- Dorner R, Peters W (1988) Localization of sugar components of glycoproteins in peritrophic membranes of larvae of Diptera (Culicidae, Simuliidae). *Entomol Gen* 14:11–24
- Dow JAT (1981) Countercurrent flows, water movements and nutrient absorption in the locust midgut. *J Insect Physiol* 27:579–585
- Dow JAT (1986) Insect midgut function. *Adv Insect Physiol* 19:188–328
- Dow JAT (1992) pH gradients in lepidopteran midgut. *J Exp Biol* 172(Pt 1):355–375
- Down RE, Gatehouse AMR, Hamilton WDO, Gatehouse JA (1996) Snowdrop lectin inhibits development and decreases fecundity of the Glasshouse Potato Aphid (*Aulacorthum solani*) when administered in vitro and via transgenic plants both in laboratory and glasshouse trials. *J Insect Physiol* 42:1035–1045
- Drlioli E, Gianfreda L, Palescandolo R, Scardi V (1976) The kinetic behaviour of enzymes gelified on ultrafiltration membranes. In: Thomas D, Kernevez JP (eds) Analysis and control of immobilised enzyme systems. North Holland Publications, Amsterdam
- Edwards MJ, Jacobs-Lorena M (2000) Permeability and disruption of the peritrophic matrix and caecal membrane from *Aedes aegypti* and *Anopheles gambiae* mosquito larvae. *J Insect Physiol* 46:1313–1320
- Eisemann CH, Donaldson RA, Pearson RD, Cadogan LC, Vuocolo T, Tellam RL (1994) Larvicidal activity of lectins on *Lucilia cuprina*: Mechanism of action. *Ent Exp Appl* 72:1–10
- Eisemann C, Wijffels G, Tellam RL (2001) Secretion of the type 2 peritrophic matrix protein, peritrophin-15, from the cardia. *Arch Insect Biochem Physiol* 47:76–85

- Elvin CM, Vuocolo T, Pearson RD, East IJ, Riding GA, Eisemann CH, Tellam RL (1996) Characterization of a major peritrophic membrane protein, peritrophin-44, from the larvae of *Lucilia cuprina*. cDNA and deduced amino acid sequences. *J Biol Chem* 271:8925–8935
- Espinosa-Marzal RM, Fontani G, Reusch FB, Roba M, Spencer ND, Crockett R (2013) Sugars communicate through water: oriented glycans induce water structuring. *Biophys J* 104:2686–2694
- Espinoza-Fuentes FP, Terra WR (1987) Physiological adaptations for digesting bacteria. Water fluxes and distribution of digestive enzymes in *Musca domestica* larval midgut. *Insect Biochem* 17:809–817
- Espinoza-Fuentes FP, Ferreira C, Terra WR (1984) Spatial organization of digestion in the larval and imaginal stages of the sciarid fly *Trichosia pubescens*. *Insect Biochem* 14:631–638
- Fang S, Wang L, Guo W, Zhang X, Peng D, Luo C, Yu Z, Sun M (2009) *Bacillus thuringiensis* bel protein enhances the toxicity of Cry1Ac protein to *Helicoverpa armigera* larvae by degrading insect intestinal mucin. *Appl Environ Microbiol* 75:5237–5243
- Fazito do Vale V, Pereira MH, Gontijo NF (2007) Midgut pH profile and protein digestion in the larvae of *Lutzomyia longipalpis* (Diptera: Psychodidae). *J Insect Physiol* 53:1151–1159
- Feng D, Chen Z, Wang Z, Zhang C, He K, Guo S (2015) Domain III of *Bacillus thuringiensis* CryIIe ioxin plays an important role in binding to peritrophic membrane of Asian corn borer. *PLoS One* 10:e0136430
- Ferreira C, Terra WR (1989) Spatial organization of digestion, secretory mechanisms and digestive enzyme properties in *Pheropsophus aequinoctialis* (Coleoptera: Carabidae). *Insect Biochem* 19:383–391
- Ferreira C, Ribeiro AF, Garcia ES, Terra WR (1988) Digestive enzymes trapped between and associated with the double plasma membranes of *Rhodnius prolixus* posterior midgut cells. *Insect Biochem* 18:521–530
- Ferreira C, Capella AN, Sitnik R, Terra WR (1994a) Digestive enzymes in midgut cells, endo- and ectoperitrophic contents, and peritrophic membranes of *Spodoptera frugiperda* (Lepidoptera) larvae. *Arch Insect Biochem Physiol* 26:299–313
- Ferreira C, Capella AN, Sitnik R, Terra WR (1994b) Properties of the digestive enzymes and the permeability of the peritrophic membrane of *Spodoptera frugiperda* (Lepidoptera) larvae. *Comp Biochem Physiol* 107A:631–640
- Ferreira AH, Cristofoletti PT, Lorenzini DM, Guerra LO, Paiva PB, Briones MR, Terra WR, Ferreira C (2007) Identification of midgut microvillar proteins from *Tenebrio molitor* and *Spodoptera frugiperda* by cDNA library screenings with antibodies. *J Insect Physiol* 53:1112–1124
- Ferreira AH, Cristofoletti PT, Pimenta DC, Ribeiro AF, Terra WR, Ferreira C (2008) Structure, processing and midgut secretion of putative peritrophic membrane ancillary protein (PMAP) from *Tenebrio molitor* larvae. *Insect Biochem Mol Biol* 38:233–243
- Fescemyer HW, Sandoya GV, Gill TA, Ozkan S, Marden JH, Luthe DS (2013) Maize toxin degrades peritrophic matrix proteins and stimulates compensatory transcriptome responses in fall armyworm midgut. *Insect Biochem Mol Biol* 43:280–291
- Fitches E, Gatehouse JA (1998) A comparison of the short and long term effects of insecticidal lectins on the activities of soluble and brush border enzymes of tomato moth larvae (*Lacanobia oleracea*). *J Insect Physiol* 44:1213–1224
- Fitches E, Audsley N, Gatehouse JA, Edwards JP (2002) Fusion proteins containing neuropeptides as novel insect control agents: snowdrop lectin delivers fused allatostatin to insect haemolymph following oral ingestion. *Insect Biochem Mol Biol* 32:1653–1661
- Fitches E, Wilkinson H, Bell H, Bown DP, Gatehouse JA, Edwards JP (2004) Cloning, expression and functional characterisation of chitinase from larvae of tomato moth (*Lacanobia oleracea*): a demonstration of the insecticidal activity of insect chitinase. *Insect Biochem Mol Biol* 34:1037–1050
- Fitches EC, Bell HA, Powell ME, Back E, Sargiotti C, Weaver RJ, Gatehouse JA (2010) Insecticidal activity of scorpion toxin (ButaIT) and snowdrop lectin (GNA) containing fusion proteins towards pest species of different orders. *Pest Manag Sci* 66:74–83

- Fitches EC, Pyati P, King GF, Gatehouse JA (2012) Fusion to snowdrop lectin magnifies the oral activity of insecticidal omega-Hexatoxin-Hv1a peptide by enabling its delivery to the central nervous system. *PLoS One* 7:e39389
- Fonseca FV, Silva JR, Samuels RI, DaMatta RA, Terra WR, Silva CP (2010) Purification and partial characterization of a midgut membrane-bound alpha-glucosidase from *Quesada gigas* (Hemiptera: Cicadidae). *Comp Biochem Phys B* 155:20–25
- Gaines PJ, Walmsley SJ, Wisniewski N (2003) Cloning and characterization of five cDNAs encoding peritrophin-A domains from the cat flea, *Ctenocephalides felis*. *Insect Biochem Mol Biol* 33:1061–1073
- Gallo LG, Corsaro BG, Hughes PR, Granados RR (1991) In vivo enhancement of baculovirus infections by the viral enhancing factor of a granulosis virus of the cabbage looper, *Trichoplusia ni* (Lepidoptera: Noctuidae). *J Invertebr Pathol* 58:203–210
- Galloway CS, Wang P, Winstanley D, Jones IM (2005) Comparison of the bacterial Enhancin-like proteins from *Yersinia* and *Bacillus* spp. with a baculovirus Enhancin. *J Invertebr Pathol* 90:134–137
- Garbutt JS, Belles X, Richards EH, Reynolds SE (2013) Persistence of double-stranded RNA in insect hemolymph as a potential determiner of RNA interference success: evidence from *Manduca sexta* and *Blattella germanica*. *J Insect Physiol* 59:171–178
- Garcia-Longoria L, Hellgren O, Bensch S (2014) Molecular identification of the chitinase genes in *Plasmodium relictum*. *Malar J* 13:239
- Gatehouse AMR, Dewey FM, Dove J, Fenton KA, Pusztai A (1984) Effect of seed lectin from *Phaeolus vulgaris* on the development of larvae of *Callosobruchus maculatus*; mechanism of toxicity. *J Sci Food Agric* 35:373–380
- Goto C (1990) Enhancement of a nuclear polyhedrosis virus (NPV) infection by a granulosis virus (GV) isolated from the spotted cutworm, *Xestia c-nigrum* L. (Lepidoptera: Noctuidae). *Appl Entomol Zool* 25:135–137
- Granados RR, Corsaro BG (1990) Baculovirus enhancing proteins and their implication for insect control. In: Proceedings of the 5th international colloquium invertebrate pathology and microbial control, Adelaide, Australia, pp 174–178
- Granados RR, Fu Y, Corsaro B, Hughes PR (2001) Enhancement of *Bacillus thuringiensis* Toxicity to Lepidopterous Species with the Enhancin from *Trichoplusia ni* Granulovirus. *Biol Control* 20:153–159
- Guo W, Li G, Pang Y, Wang P (2005) A novel chitin-binding protein identified from the peritrophic membrane of the cabbage looper, *Trichoplusia ni*. *Insect Biochem Mol Biol* 35:1224–1234
- Guo HF, Fang JC, Liu BS, Wang JP, Zhong WF, Wan FH (2007a) Enhancement of the biological activity of nucleopolyhedrovirus through disruption of the peritrophic matrix of insect larvae by chlorfluazuron. *Pest Manag Sci* 63:68–74
- Guo HF, Fang JC, Wang JP, Zhong WF, Liu BS (2007b) Interaction of *Xestia c-nigrum* granulovirus with peritrophic matrix and *Spodoptera litura* nucleopolyhedrovirus in *Spodoptera litura*. *J Econ Entomol* 100:20–25
- Hajajj-Ellouze M, Fedhila S, Lereclus D, Nielsen-LeRoux C (2006) The enhancin-like metalloprotease from the *Bacillus cereus* group is regulated by the pleiotropic transcriptional activator PlcR but is not essential for larvicidal activity. *FEMS Microbiol Lett* 260:9–16
- Hao S, Aksoy S (2002) Proventriculus-specific cDNAs characterized from the tsetse, *Glossina morsitans morsitans*. *Insect Biochem Mol Biol* 32:1663–1671
- Hardingham TE, Fosang AJ (1992) Proteoglycans: many forms and many functions. *FASEB J* 6:861–870
- Hardingham TE, Fosang AJ, Dudhia J (1990) Domain structure in aggregating proteoglycans from cartilage. *Biochem Soc Trans* 18:794–796
- Harper MS, Granados RR (1999) Peritrophic membrane structure and formation of larval *Trichoplusia ni* with an investigation on the secretion patterns of a PM mucin. *Tissue Cell* 31:202–211

- Harper MS, Hopkins TL (1997) Peritrophic membrane structure and secretion in European corn borer larvae (*Ostrinia nubilalis*). *Tissue Cell* 29:463–475
- Harper MS, Hopkins TL, Czaplá TH (1998) Effect of wheat germ agglutinin on formation and structure of the peritrophic membrane in European corn borer (*Ostrinia nubilalis*) larvae. *Tissue Cell* 30:166–176
- Hawtin RE, Arnold K, Ayres MD, Zanotto PM, Howard SC, Gooday GW, Chappell LH, Kitts PA, King LA, Possee RD (1995) Identification and preliminary characterization of a chitinase gene in the *Autographa californica* nuclear polyhedrosis virus genome. *Virology* 212:673–685
- Hawtin RE, Zarkowska T, Arnold K, Thomas CJ, Gooday GW, King LA, Kuzio JA, Possee RD (1997) Liquefaction of *Autographa californica* nucleopolyhedrovirus-infected insects is dependent on the integrity of virus-encoded chitinase and cathepsin genes. *Virology* 238:243–253
- Hayakawa T, Shitomi Y, Miyamoto K, Hori H (2004) GalNAc pretreatment inhibits trapping of *Bacillus thuringiensis* Cry1Ac on the peritrophic membrane of *Bombyx mori*. *FEBS Lett* 576:331–335
- Hegedus D, Baldwin D, O’Grady M, Braun L, Gleddie S, Sharpe A, Lydiat D, Erlandson M (2003) Midgut proteases from *Mamestra configurata* (Lepidoptera: Noctuidae) larvae: characterization, cDNA cloning, and expressed sequence tag analysis. *Arch Insect Biochem Physiol* 53:30–47
- Hegedus D, Erlandson M, Gillott C, Toprak U (2009) New insights into peritrophic matrix synthesis, architecture, and function. *Annu Rev Entomol* 54:285–302
- Herth W (1980) Calcofluor white and Congo red inhibit chitin microfibril assembly of *Poteroiochromonas*: evidence for a gap between polymerization and microfibril formation. *J Cell Biol* 87:442–450
- Hiramatsu S, Ishihara M, Fujie M, Usami S, Yamada T (1999) Expression of a chitinase gene and lysis of the host cell wall during *Chlorella* virus CVK2 infection. *Virology* 260:308–315
- Hogenkamp DG, Arakane Y, Zimoch L, Merzendorfer H, Kramer KJ, Beeman RW, Kanost MR, Specht CA, Muthukrishnan S (2005) Chitin synthase genes in *Manduca sexta*: characterization of a gut-specific transcript and differential tissue expression of alternately spliced mRNAs during development. *Insect Biochem Mol Biol* 35:529–540
- Hoover K, Humphries MA, Gendron AR, Slavicek JM (2010) Impact of viral enhancer genes on potency of *Lymantria dispar* multiple nucleopolyhedrovirus in *L. dispar* following disruption of the peritrophic matrix. *J Invertebr Pathol* 104:150–152
- Hopkins TL, Harper MS (2001) Lepidopteran peritrophic membranes and effects of dietary wheat germ agglutinin on their formation and structure. *Arch Insect Biochem Physiol* 47:100–109
- Hu X, Chen L, Xiang X, Yang R, Yu S, Wu X (2012) Proteomic analysis of peritrophic membrane (PM) from the midgut of fifth-instar larvae, *Bombyx mori*. *Mol Biol Rep* 39:3427–3434
- Huber M, Cabib E, Miller LH (1991) Malaria parasite chitinase and penetration of the mosquito peritrophic membrane. *Proc Natl Acad Sci U S A* 88:2807–2810
- Hukuhara T, Hayakawa T, Wijonarko A (1999) Increased baculovirus susceptibility of armyworm larvae feeding on transgenic rice plants expressing an entomopoxvirus gene. *Nat Biotechnol* 17:1122–1124
- Ishimwe E, Hodgson JJ, Passarelli AL (2015) Expression of the *Cydia pomonella* granulovirus matrix metalloprotease enhances *Autographa californica* multiple nucleopolyhedrovirus virulence and can partially substitute for viral cathepsin. *Virology* 481:166–178
- Ivanova N, Sorokin A, Anderson I, Galleron N, Candelon B, Kapatral V, Bhattacharyya A, Reznik G, Mikhailova N, Lapidus A, Chu L, Mazur M, Goltsman E, Larsen N, D’Souza M, Walunas T, Grechkin Y, Pusch G, Haselkorn R, Fonstein M, Ehrlich SD, Overbeek R, Kyrpides N (2003) Genome sequence of *Bacillus cereus* and comparative analysis with *Bacillus anthracis*. *Nature* 423(6935):87–91
- Jackson RL, Busch SJ, Cardin AD (1991) Glycosaminoglycans: molecular properties, protein interactions, and role in physiological processes. *Physiol Rev* 71:481–539

- Jacobs-Lorena M, Oo M-M (1996) The peritrophic matrix of insects. In: Beaty BJ, Marquardt WC (eds) *The biology of disease vectors*. University Press of Colorado, Niwot, pp 318–332
- Jang M-K, Kong B-G, Jeong Y-I, Lee CH, Nah JW (2004) Physicochemical characterization of α -chitin, β -chitin, and γ -chitin separated from natural resources. *J Polym Sci A1*(42):3423–3432
- Jasrapuria S, Arakane Y, Osman G, Kramer KJ, Beeman RW, Muthukrishnan S (2010) Genes encoding proteins with peritrophin A-type chitin-binding domains in *Tribolium castaneum* are grouped into three distinct families based on phylogeny, expression and function. *Insect Biochem Mol Biol* 40:214–227
- Jin S, Singh ND, Li L, Zhang X, Daniell H (2015) Engineered chloroplast dsRNA silences cytochrome p450 monooxygenase, V-ATPase and chitin synthase genes in the insect gut and disrupts *Helicoverpa armigera* larval development and pupation. *Plant Biotechnol J* 13:435–446
- Johnson KS, Felton GW (1996) Physiological and dietary influences on midgut redox conditions in generalist lepidopteran larvae. *J Insect Physiol* 42:191–198
- Jollès P, Muzzarelli RAA (1999) *Chitin and Chitinases*. Birkhauser Verlag, Basel
- Jordao BP, Terra WR (1991) Regional distribution and substrate specificity of digestive enzymes involved in terminal digestion in *Musca domestica* hind-midguts. *Arch Insect Biochem Physiol* 17:157–168
- Jordao BP, Lehane MJ, Terra WR, Ribeiro AF, Ferreira C (1996) An immunocytochemical investigation of trypsin secretion in the midgut of the stablefly, *Stomoxys calcitrans*. *Insect Biochem Mol Biol* 26:445–453
- Jordao BP, Capella AN, Terra WR, Ribeiro AF, Ferreira C (1999) Nature of the anchors of membrane-bound aminopeptidase, amylase, and trypsin and secretory mechanisms in *Spodoptera frugiperda* (Lepidoptera) midgut cells. *J Insect Physiol* 45:29–37
- Kabir KE, Sugimoto H, Tado H, Endo K, Yamanaka A, Tanaka S, Koga D (2006) Effect of *Bombyx mori* chitinase against Japanese pine sawyer (*Monochamus alternatus*) adults as a biopesticide. *Biosci Biotechnol Biochem* 70:219–229
- Kang W, Tristram M, Maeda S, Crook NE, O'Reilly DR (1998) Identification and characterization of the *Cydia pomonella* granulovirus cathepsin and chitinase genes. *J Gen Virol* 79:2283–2292
- Kato N, Mueller CR, Fuchs JF, Wessely V, Lan Q, Christensen BM (2006) Regulatory mechanisms of chitin biosynthesis and roles of chitin in peritrophic matrix formation in the midgut of adult *Aedes aegypti*. *Insect Biochem Mol Biol* 36:1–9
- Kelkenberg M, Odman-Naresh J, Muthukrishnan S, Merzendorfer H (2015) Chitin is a necessary component to maintain the barrier function of the peritrophic matrix in the insect midgut. *Insect Biochem Mol Biol* 56:21–28
- Khajuria C, Buschman LL, Chen M-S, Muthukrishnan S, Zhu KY (2010) A gut-specific chitinase gene essential for regulation of chitin content of peritrophic matrix and growth of *Ostrinia nubilalis* larvae. *Insect Biochem Mol Biol* 40:621–629
- Kitajima EW (1975) A peculiar type of glycocalyx on the microvilli of the midgut epithelial cells of the thrips *Frankliniella* sp. (Thysanoptera: Thripidae). *Cytobiologie* 11:299–303
- Kjellen L, Lindahl U (1991) Proteoglycans: structures and interactions. *Annu Rev Biochem* 60:443–475
- Konno K, Hirayama C, Nakamura M, Tateishi K, Tamura Y, Hattori M, Kohno K (2004) Papain protects papaya trees from herbivorous insects: role of cysteine proteases in latex. *Plant J* 37:370–378
- Kornfeld R, Kornfeld S (1985) Assembly of asparagine-linked oligosaccharides. *Annu Rev Biochem* 54:631–664
- Kramer KJ, Dziadik-Turner C, Koga D (1985) Chitin metabolism in insects. In: Kerkut GA, Gilbert LI (eds) *Comprehensive insect physiology, biochemistry, and pharmacology*, vol 3. Pergamon Press, Oxford, pp 75–115
- Kramer KJ, Corpuz L, Choi HK, Muthukrishnan S (1993) Sequence of a cDNA and expression of the gene encoding epidermal and gut chitinases of *Manduca sexta*. *Insect Biochem Mol Biol* 23:691–701

- Krishnan N, Kodrik D, Turanli F, Sehna F (2007) Stage-specific distribution of oxidative radicals and antioxidant enzymes in the midgut of *Leptinotarsa decemlineata*. *J Insect Physiol* 53:67–74
- Kuraishi T, Binggeli O, Opota O, Buchon N, Lemaitre B (2011) Genetic evidence for a protective role of the peritrophic matrix against intestinal bacterial infection in *Drosophila melanogaster*. *Proc Natl Acad Sci U S A* 108:15966–15971
- Lane NJ, Harrison JB (1979) An unusual cell surface modification: a double plasma membrane. *J Cell Sci* 39:355–372
- Lang M, Kanost MR, Gorman MJ (2012) Multicopper oxidase-3 is a laccase associated with the peritrophic matrix of *Anopheles gambiae*. *PLoS One* 7:e33985
- Laurent TC (1964) The interaction between polysaccharides and other macromolecules. 9. The exclusion of molecules from hyaluronic acid gels and solutions. *Biochem J* 93:106–112
- Laurent TC (1970) The structure and function of intercellular polysaccharides in connective tissue. In: Crone C, Lassen NA (eds) *Capillary permeability*. Copenhagen, p 681
- Lawrence SD, Novak NG (2006) Expression of poplar chitinase in tomato leads to inhibition of development in Colorado potato beetle. *Biotechnol Lett* 28:593–599
- Lee RF (1968) The histology and histochemistry of the anterior midgut of *Periplaneta americana* (Dictyoptera: Blattellidae) with reference to the formation of the peritrophic membrane. *Proc R Entomol Soc Lond Ser* 43A:122–134
- Leetachewa S, Moonsong S, Chaisri U, Khomkhum N, Yoonim N, Wang P, Angsuthanasombat C (2013) Functional characterizations of residues Arg-158 and Tyr-170 of the mosquito-larvicidal toxic *Bacillus thuringiensis* Cry4Ba. *BMB Rep* 47(10):546–551
- Lehane MJ (1976) Formation and histochemical structure of the peritrophic membrane in the stablefly, *Stomoxys calcitrans*. *J Insect Physiol* 22:1551–1557
- Lehane MJ (1997) Peritrophic matrix structure and function. *Annu Rev Entomol* 42:525–550
- Lehane MJ, Allingham PG, Weglicki P (1996) Composition of the peritrophic matrix of the tsetse fly, *Glossina morsitans morsitans*. *Cell Tissue Res* 283:375–384
- Lepore LS, Roelvink PR, Granados RR (1996) Enhancin, the granulosis virus protein that facilitates nucleopolyhedrovirus (NPV) infections, is a metalloprotease. *J Invertebr Pathol* 68:131–140
- Levy SM, Falleiros AM, Moscardi F, Gregorio EA (2011) The role of peritrophic membrane in the resistance of *Anticarsia gemmatilis* larvae (Lepidoptera: Noctuidae) during the infection by its nucleopolyhedrovirus (AgMNPV). *Arthropod Struct Dev* 40:429–434
- Li F, Patra KP, Vinetz JM (2005) An anti-Chitinase malaria transmission-blocking single-chain antibody as an effector molecule for creating a *Plasmodium falciparum*-refractory mosquito. *J Infect Dis* 192:878–887
- Li C, Song X, Li G, Wang P (2009) Midgut cysteine protease-inhibiting activity in *Trichoplusia ni* protects the peritrophic membrane from degradation by plant cysteine proteases. *Insect Biochem Mol Biol* 39:726–734
- Lindsay KC, Marshall AT (1980) Ultrastructure of the filter chamber complex in the alimentary canal of *Eurymela distincta* Signoret (Homoptera: Eurymelyidae). *Int J Insect Morphol Embryol* 15:211–224
- Little D, Gouhier-Darimont C, Bruessow F, Reymond P (2007) Oviposition by pierid butterflies triggers defense responses in *Arabidopsis*. *Plant Physiol* 143:784–800
- Liu M, Cai QX, Liu HZ, Zhang BH, Yan JP, Yuan ZM (2002) Chitinolytic activities in *Bacillus thuringiensis* and their synergistic effects on larvicidal activity. *J Appl Microbiol* 93:374–379
- Lyonet P (1762) *Traité Anatomique de la Chenille qui ronge le bois de Saule*. La Haye, Holland
- Macedo MLR, Damico DCS, Freire MDGM, Toyama MH, Marangoni S et al (2003) Purification and characterization of an N-acetylglucosamine-binding lectin from *Koelerutera paniculata* seeds and its effect on the larval development of *Callosobruchus maculatus* (Coleoptera: Bruchidae) and *Anagasta kuehniella* (Lepidoptera: Pyralidae). *J Agric Food Chem* 51:2980–2986

- Magalhaes T (2014) What is the association of heme aggregates with the peritrophic matrix of adult female mosquitoes? *Parasit Vectors* 7:362
- Mantle M, Husar SD (1994) Binding of *Yersinia enterocolitica* to purified, native small intestinal mucins from rabbits and humans involves interactions with the mucin carbohydrate moiety. *Infect Immun* 62:1219–1227
- Mao YB, Cai WJ, Wang JW, Hong GJ, Tao XY, Wang LJ, Huang YP, Chen XY (2007) Silencing a cotton bollworm P450 monooxygenase gene by plant-mediated RNAi impairs larval tolerance of gossypol. *Nat Biotechnol* 25:1307–1313
- Mao YB, Xue XY, Tao XY, Yang CQ, Wang LJ, Chen XY (2013) Cysteine protease enhances plant-mediated bollworm RNA interference. *Plant Mol Biol* 83:119–129
- Marshall AT, Cheung WW (1970) Ultrastructure and cytochemistry of an extensive plexiform surface coat on the midgut cells of a fulgorid insect. *J Ultrastruct Res* 33:161–172
- Marshall AT, Cheung WW (1974) Studies on water and ion transport in homopteran insects: ultrastructure and cytochemistry of the cicadoid and cercopoid Malpighian tubules and filter chamber. *Tissue Cell* 6:153–171
- Martinez DS, Freire M, Mazzafera P, Araujo-Junior RT, Bueno RD, Macedo ML (2012) Insecticidal effect of labramin, a lectin-like protein isolated from seeds of the beach apricot tree, *Labramia bojeri*, on the Mediterranean flour moth, *Ephestia kuehniella*. *J Insect Sci* 12:62
- Maue L, Meissner D, Merzendorfer H (2009) Purification of an active, oligomeric chitin synthase complex from the midgut of the tobacco hornworm. *Insect Biochem Mol Biol* 39:654–659
- Mercer EH, Day MF (1952) The fine structure of the peritrophic membrane of certain insects. *Biol Bull* 103:384–394
- Merzendorfer H (2006) Insect chitin synthases: a review. *J Comp Physiol* 176B:1–15
- Merzendorfer H (2013) Chitin synthesis inhibitors: old molecules and new developments. *Insect Sci* 20:121–138
- Merzendorfer H, Zimoch L (2003) Chitin metabolism in insects: structure, function and regulation of chitin synthases and chitinases. *J Exp Biol* 206:4393–4412
- Merzendorfer H, Kim HS, Chaudhari SS, Kumari M, Specht CA, Butcher S, Brown SJ, Robert Manak J, Beeman RW, Kramer KJ, Muthukrishnan S (2012) Genomic and proteomic studies on the effects of the insect growth regulator diflubenzuron in the model beetle species *Tribolium castaneum*. *Insect Biochem Mol Biol* 42:264–276
- Miller N, Lehane MJ (1990) In vitro perfusion studies on the peritrophic membrane of the tsetse fly *Glossina morsitans morsitans* (Diptera, Glossinidae). *J Insect Physiol* 36:813–818
- Miller N, Lehane MJ (1993) Ionic environment and the permeability properties of the peritrophic membrane of *Glossina morsitans morsitans*. *J Insect Physiol* 63:139–144
- Mitsuhashi W, Miyamoto K (2003) Disintegration of the peritrophic membrane of silkworm larvae due to spindles of an entomopoxvirus. *J Invertebr Pathol* 82:34–40
- Mitsuhashi W, Furuta Y, Sato M (1998) The spindles of an entomopoxvirus of coleoptera (*Anomala cuprea*) strongly enhance the infectivity of a nucleopolyhedrovirus in lepidoptera. *J Invertebr Pathol* 71:186–188
- Mitsuhashi W, Kawakita H, Murakami R, Takemoto Y, Saiki T, Miyamoto K, Wada S (2007) Spindles of an entomopoxvirus facilitate its infection of the host insect by disrupting the peritrophic membrane. *J Virol* 81:4235–4243
- Mitsuhashi W, Asano S, Miyamoto K, Wada S (2014) Further research on the biological function of inclusion bodies of *Anomala cuprea* entomopoxvirus, with special reference to the effect on the insecticidal activity of a *Bacillus thuringiensis* formulation. *Pest Manag Sci* 70:46–54
- Moffatt MR, Blakemore D, Lehane MJ (1995) Studies on the synthesis and secretion of digestive trypsin in *Stomoxys calcitrans* (Insects, Diptera). *Comp Biochem Physiol* 110B:291–300
- Mohan S, Ma PW, Pechan T, Bassford ER, Williams WP, Luthe DS (2006) Degradation of the *S. frugiperda* peritrophic matrix by an inducible maize cysteine protease. *J Insect Physiol* 52:21–28
- Mohan S, Ma PW, Williams WP, Luthe DS (2008) A naturally occurring plant cysteine protease possesses remarkable toxicity against insect pests and synergizes *Bacillus thuringiensis* toxin. *PLoS One* 3:e1786

- Moncayo AC, Lerdthusnee K, Leon R, Robich RM, Romoser WS (2005) Meconial peritrophic matrix structure, formation, and meconial degeneration in mosquito pupae/pharate adults: histological and ultrastructural aspects. *J Med Entomol* 42:939–944
- Mooser H, Castaneda MR (1932) The multiplication of the virus of Mexican typhus fever in fleas. *J Exp Med* 55:307–323
- Mori M, Kitamura H, Kondo A, Dohi K, Mori M, Kaido M, Mise K, Shimojyo E, Hashimoto Y (2006) Expression of an enhancer gene from the *Trichoplusia ni* granulosis virus confers resistance to lepidopteran insect pests to rice. *Plant Biotechnol* 23:55–61
- Mury FB, da Silva JR, Ferreira LS, dos Santos FB, de Souza-Filho GA, de Souza-Neto JA, Ribolla PE, Silva CP, de Nascimento VV, Machado OL, Berbert-Molina MA, Dansa-Petretski M (2009) Alpha-glucosidase promotes hemozoin formation in a blood-sucking bug: an evolutionary history. *PLoS One* 4:e6966
- Nagadhara D, Ramesh S, Pasalu IC, Rao YK, Sarma NP, Reddy VD, Rao KV (2004) Transgenic rice plants expressing the snowdrop lectin gene (gna) exhibit high-level resistance to the white-backed planthopper (*Sogatella furcifera*). *Theor Appl Genet* 109:1399–1405
- Nakasu EY, Williamson SM, Edwards MG, Fitches EC, Gatehouse JA, Wright GA, Gatehouse AM (2014) Novel biopesticide based on a spider venom peptide shows no adverse effects on honeybees. *Proc Biol Sci* 281(1787):20140619
- Neira Oviedo M, Vanekeris L, Corena-McLeod MD, Linser PJ (2008) A microarray-based analysis of transcriptional compartmentalization in the alimentary canal of *Anopheles gambiae* (Diptera: Culicidae) larvae. *Insect Mol Biol* 17:61–72
- Nisizawa K, Yamaguchi T, Handa N, Maeda M, Yamazaki H (1963) Chemical nature of a uronic acid-containing polysaccharide in the peritrophic membrane of the silkworm. *J Biochem* 54:419–426
- O’Loughlin GT, Chambers TC (1972) Extracellular microtubules in the aphid gut. *J Cell Biol* 53:575–578
- Ohizumi Y, Gaidamashvili M, Ohwada S, Matsuda K, Kominami J, Nakamura-Tsuruta S, Hirabayashi J, Naganuma T, Ogawa T, Muramoto K (2009) Mannose-binding lectin from yam (*Dioscorea batatas*) tubers with insecticidal properties against *Helicoverpa armigera* (Lepidoptera: Noctuidae). *J Agric Food Chem* 57:2896–2902
- Okolo CJ, Molyneux DH, Wallbanks KR, Maudlin I (1988) Fluorescein conjugated lectins identify different carbohydrate residues on *Glossina* peritrophic membranes. *Trop Med Parasitol* 39:208–210
- Oliveira MF, Silva JR, Dansa-Petretski M, de Souza W, Lins U, Braga CM, Masuda H, Oliveira PL (1999) Haem detoxification by an insect. *Nature* 400:517–518
- Oliveira MF, Gandara AC, Braga CM, Silva JR, Mury FB, Dansa-Petretski M, Menezes D, Vannier-Santos MA, Oliveira PL (2007) Heme crystallization in the midgut of triatomine insects. *Comp Biochem Physiol* 146:168–174
- Oliveira CD, Tadei WP, Abdalla FC (2009) Occurrence of apocrine secretion in the larval gut epithelial cells of *Aedes aegypti* L., *Anopheles albitalis* Lynch-Arribalzaga and *Culex quinquefasciatus* say (Diptera: Culicidae): a defense strategy against infection by *Bacillus sphaericus* Neide? *Neotrop Entomol* 38:624–631
- Ono M, Kato S (1968) Amino acid composition of the peritrophic membrane in the silkworm, *Bombyx mori* L. *Bull Sericult Exp Stn Jpn* 23:1–8
- Otsu Y, Mori H, Komuta K, Shimizu H, Nogawa S, Matsuda Y, Nonomura T, Sakuratani Y, Tosa Y, Mayama S, Toyoda H (2003) Suppression of leaf feeding and oviposition of phytophagous ladybird beetles (Coleoptera: Coccinellidae) by chitinase gene-transformed phyloplane bacteria and their specific bacteriophages entrapped in alginate gel beads. *J Econ Entomol* 96:555–563
- Pascoa V, Oliveira PL, Dansa-Petretski M, Silva JR, Alvarenga PH, Jacobs-Lorena M, Lemos FJ (2002) *Aedes aegypti* peritrophic matrix and its interaction with heme during blood digestion. *Insect Biochem Mol Biol* 32:517–523
- Pechan T, Cohen A, Williams WP, Luthe DS (2002) Insect feeding mobilizes a unique plant defense protease that disrupts the peritrophic matrix of caterpillars. *Proc Natl Acad Sci U S A* 99:13319–13323

- Peel AD (2008) The evolution of developmental gene networks: lessons from comparative studies on holometabolous insects. *Philos Trans R Soc Lond B Biol Sci* 363:1539–1547
- Peng J, Zhong J, Granados RR (1999) A baculovirus enhancer alters the permeability of a mucosal midgut peritrophic matrix from lepidopteran larvae. *J Insect Physiol* 45:159–166
- Perez-Hedo M, Lopez C, Albajes R, Eizaguirre M (2012) Low susceptibility of non-target Lepidopteran maize pests to the Bt protein Cry1Ab. *Bull Entomol Res* 102:737–743
- Perez-Vilar J, Hill RL (1999) The structure and assembly of secreted mucins. *J Biol Chem* 274:31751–31754
- Perrone JB, Spielman A (1986) Microfilarial perforation of the midgut of a mosquito. *J Parasitol* 72:723–727
- Peters W (1969) Vergleichende Untersuchungen der Feinstruktur peritrophischer Membranen von Insekten. *Z Morphol Okol Tiere* 64:21–58
- Peters W (1992) Peritrophic membranes. vol 30. *Zoophysiology*. Springer, Berlin
- Peters W, Kalnins M (1985) Aminopeptidases as immobilized enzymes on the peritrophic membranes of insects. *Entomol Gener* 11:25–32
- Peters W, Latka I (1986) Electron microscopic localization of chitin using colloidal gold labelled with wheat germ agglutinin. *Histochemistry* 84:155–160
- Peters W, Wiese B (1986) Permeability of the peritrophic membranes of some Diptera to labelled dextrans. *J Insect Physiol* 32:43–49
- Peters W, Heitmann S, D'Haese J (1979) Formation and fine structure of peritrophic membranes in the earwig, *Forficula auricularia*. *Entomol Gen* 5:241–254
- Pimenta PF, Modi GB, Pereira ST, Shahabuddin M, Sacks DL (1997) A novel role for the peritrophic matrix in protecting *Leishmania* from the hydrolytic activities of the sand fly midgut. *Parasitology* 115:359–369
- Platzer-Schultz I, Welsch U (1969) Zur Entstehung und Feinstruktur der peritrophischen Membran der Larven von *Chironomus strenzkei* Fittkau (Diptera). *Z Zellforsch Mikrosk Anat* 100:594–605
- Ponnudurai T, Billingsley PF, Rudin W (1988) Differential infectivity of *Plasmodium* for mosquitoes. *Parasitol Today* 4:319–321
- Popham HJ, Bischoff DS, Slavicek JM (2001) Both *Lymantria dispar* nucleopolyhedrovirus enhancer genes contribute to viral potency. *J Virol* 75:8639–8648
- Powell KS, Gatehouse AMR, Hilder VA, Gatehouse JA (1993) Antimetabolic effects of plant lectins and fungal enzymes on the nymphal stages of two important rice pests, *Nilaparvata lugens* and *Nephotettix cinciteps*. *Entomol Exp Appl* 66:119–126
- Puchta O, Wille H (1956) A parasitic bacterium in the mid-intestine of *Solenobia triquetrella*. *Zeitschrift für Parasitenkunde* 17:400–418
- Pusztai A (1991) Plant lectins. Chemistry and pharmacology of natural products. Cambridge University Press, Cambridge
- Quan G, Ladd T, Duan J, Wen F, Doucet D, Cusson M, Krell PJ (2013) Characterization of a spruce budworm chitin deacetylase gene: stage- and tissue-specific expression, and inhibition using RNA interference. *Insect Biochem Mol Biol* 43:683–691
- Ramasamy MS, Kulasekera R, Wanniarachchi IC, Srikrishnaraj KA, Ramasamy R (1997) Interactions of human malaria parasites, *Plasmodium vivax* and *P.falciparum*, with the midgut of *Anopheles* mosquitoes. *Med Vet Entomol* 11:290–296
- Ramos A, Mahowald A, Jacobs-Lorena M (1994) Peritrophic matrix of the black fly *Simulium vittatum*: formation, structure, and analysis of its protein components. *J Exp Zool* 268:269–281
- Rao KV, Rathore KS, Hodges TK, Fu X, Stoger E, Sudhakar D, Williams S, Christou P, Bharathi M, Bown DP, Powell KS, Spence J, Gatehouse AM, Gatehouse JA (1998) Expression of snow-drop lectin (GNA) in transgenic rice plants confers resistance to rice brown planthopper. *Plant J* 15:469–477
- Rao R, Fiandra L, Giordana B, de Eguileor M, Congiu T, Burlini N, Arciello S, Corrado G, Pennacchio F (2004) AcMNPV ChiA protein disrupts the peritrophic membrane and alters midgut physiology of *Bombyx mori* larvae. *Insect Biochem Mol Biol* 34:1205–1213

- Rayms-Keller A, McGaw M, Oray C, Carlson JO, Beaty BJ (2000) Molecular cloning and characterization of a metal responsive *Aedes aegypti* intestinal mucin cDNA. *Insect Mol Biol* 9:419–426
- Razek-Desouky A, Specht CA, Soong L, Vinetz JM (2001) *Leishmania donovani*: expression and characterization of *Escherichia coli*-expressed recombinant chitinase LdCHT1. *Exp Parasitol* 99:220–225
- Read TD, Peterson SN, Tourasse N, Baillie LW, Paulsen IT, Nelson KE, Tettelin H, Fouts DE, Eisen JA, Gill SR, Holtzapple EK, Okstad OA, Helgason E, Rilstone J, Wu M, Kolonay JF, Beanan MJ, Dodson RJ, Brinkac LM, Gwinn M, DeBoy RT, Madpu R, Daugherty SC, Durkin AS, Haft DH, Nelson WC, Peterson JD, Pop M, Khouri HM, Radune D, Benton JL, Mahamoud Y, Jiang L, Hance IR, Weidman JF, Berry KJ, Plaut RD, Wolf AM, Watkins KL, Nierman WC, Hazen A, Cline R, Redmond C, Thwaite JE, White O, Salzberg SL, Thomason B, Friedlander AM, Koehler TM, Hanna PC, Kolsto AB, Fraser CM (2003) The genome sequence of *Bacillus anthracis* Ames and comparison to closely related bacteria. *Nature* 423(6935):81–86
- Rees JS, Jarrett P, Ellar DJ (2009) Peritrophic membrane contribution to Bt Cry delta-endotoxin susceptibility in Lepidoptera and the effect of Calcofluor. *J Invertebr Pathol* 100:139–146
- Reger JF (1971) Fine structure of the surface coat of midgut epithelial cells in the homopteran *Phyllosclis atra* (Fulgorid). *J Submicrosc Cytol* 3:353–358
- Regev A, Keller M, Strizhov N, Sneh B, Prudovsky E, Chet I, Ginzberg I, Koncz-Kalman Z, Koncz C, Schell J, Zilberstein A (1996) Synergistic activity of a *Bacillus thuringiensis* delta-endotoxin and a bacterial endochitinase against *Spodoptera littoralis* larvae. *Appl Environ Microbiol* 62:3581–3586
- Reymond P, Bodenhausen N, Van Poecke RM, Krishnamurthy V, Dicke M, Farmer EE (2004) A conserved transcript pattern in response to a specialist and a generalist herbivore. *Plant Cell* 16:3132–3147
- Richards AG, Richards PA (1971) Origin and composition of the peritrophic membrane of the mosquito, *Aedes aegypti*. *J Insect Physiol* 17:2253–2275
- Richards AG, Richards PA (1977) The peritrophic membranes of insects. *Annu Rev Entomol* 22:219–240
- Robles-Murguía M, Bloedow N, Murray L, Ramalho-Ortigao M (2014) Effect of mouse antisera targeting the *Phlebotomus papatasi* midgut chitinase PpChit1 on sandfly physiology and fitness. *Mem Inst Oswaldo Cruz* 109:1064–1069
- Rose C, Belmonte R, Armstrong SD, Molyneux G, Haines LR, Lehane MJ, Wastling J, Acosta-Serrano A (2014) An investigation into the protein composition of the teneral *Glossina morsitans morsitans* peritrophic matrix. *PLoS Negl Trop Dis* 8:e2691
- Rudall KM, Kenchington W (1973) The chitin system. *Biol Rev* 48:597–636
- Rudin W, Hecker H (1989) Lectin-binding sites in the midgut of the mosquitoes *Anopheles stephensi* Liston and *Aedes aegypti* L. (Diptera: Culicidae). *Parasitol Res* 75:268–279
- Ryerse JS, Purcell JP, Sammons RD, Lavrik PB (1992) Peritrophic membrane structure and formation in the larva of a moth, *Heliothis*. *Tissue Cell* 24:751–771
- Ryter SW, Tyrrell RM (2000) The heme synthesis and degradation pathways: role in oxidant sensitivity. Heme oxygenase has both pro- and antioxidant properties. *Free Radic Biol Med* 28:289–309
- Salvador R, Ferrelli ML, Sciocco-Cap A, Romanowski V (2014) Analysis of a chitinase from EpapGV, a fast killing betabaculovirus. *Virus Genes* 48:406–409
- Sampson MN, Gooday GW (1998) Involvement of chitinases of *Bacillus thuringiensis* during pathogenesis in insects. *Microbiology* 144:2189–2194
- Santos C, Terra WR (1986) Distribution and characterization of oligomeric digestive enzymes from *Erinnyis ello* larvae and inferences concerning secretory mechanisms and the permeability of the peritrophic membrane. *Insect Biochem* 16:691–700
- Santos CD, Ribeiro AF, Ferreira C, Terra WR (1984) The larval midgut of the cassava hornworm (*Erinnyis ello*). *Cell Tissue Res* 237:565–574

- Sarauer BL, Gillott C, Hegedus D (2003) Characterization of an intestinal mucin from the peritrophic matrix of the diamondback moth, *Plutella xylostella*. *Insect Mol Biol* 12:333–343
- Sauvion N, Rahbé Y, Peumans WJ, Van Damme EJM, Gatehouse JA, Gatehouse AMR (1996) Effects of GNA and other mannose binding lectins on development and fecundity of the peach-potato aphid *Myzus persicae*. *Entomol Exp Appl* 79:285–293
- Sauvion N, Nardon C, Febvay G, Gatehouse AM, Rahbe Y (2004) Binding of the insecticidal lectin Concanavalin A in pea aphid, *Acyrtosiphon pisum* (Harris) and induced effects on the structure of midgut epithelial cells. *J Insect Physiol* 50:1137–1150
- Schlecht F (1979) Elektronenoptische Untersuchungen des Darmtraktes und der peritrophischen Membran von Cladoceren und Conchostracen (Phyllozoa, Crustacea). *Zoomorphologie* 92:161–181
- Schlein Y, Jacobson RL, Shlomai J (1991) Chitinase secreted by *Leishmania* functions in the sandfly vector. *Proc Biol Sci* 245:121–126
- Schmidt DD, Voelckel C, Hartl M, Schmidt S, Baldwin IT (2005) Specificity in ecological interactions: attack from the same lepidopteran herbivore results in species-specific transcriptional responses in two solanaceous host plants. *Plant Physiol* 138:1763–1773
- Schorderet S, Pearson RD, Vuocolo T, Eisemann C, Riding GA, Tellam RL (1998) cDNA and deduced amino acid sequences of a peritrophic membrane glycoprotein, 'peritrophin-48', from the larvae of *Lucilia cuprina*. *Insect Biochem Mol Biol* 28:99–111
- Selegny E (1974) Some systems coupling enzymic reactions and other phenomena: energy conversions. In: Selegny E (ed) *Polyelectrolytes*. Reidel Publ, Dordrecht, p 533
- Shahabuddin M, Toyoshima T, Aikawa M, Kaslow DC (1993) Transmission-blocking activity of a chitinase inhibitor and activation of malarial parasite chitinase by mosquito protease. *Proc Natl Acad Sci U S A* 90:4266–4270
- Shao L, Devenport M, Jacobs-Lorena M (2001) The peritrophic matrix of hematophagous insects. *Arch Insect Biochem Physiol* 47:119–125
- Shao L, Devenport M, Fujioka H, Ghosh A, Jacobs-Lorena M (2005) Identification and characterization of a novel peritrophic matrix protein, Ae-Aper50, and the microvillar membrane protein, AEG12, from the mosquito, *Aedes aegypti*. *Insect Biochem Mol Biol* 35:947–959
- Shen Z, Jacobs-Lorena M (1997) Characterization of a novel gut-specific chitinase gene from the human malaria vector *Anopheles gambiae*. *J Biol Chem* 272:28895–28900
- Shen Z, Jacobs-Lorena M (1998) A type I peritrophic matrix protein from the malaria vector *Anopheles gambiae* binds to chitin. Cloning, expression, and characterization. *J Biol Chem* 273:17665–17670
- Shen Z, Jacobs-Lorena M (1999) Evolution of chitin-binding proteins in invertebrates. *J Mol Evol* 48:341–347
- Shi X, Chamankhah M, Visal-Shah S, Hemmingsen SM, Erlandson M, Braun L, Altling-Mees M, Khachatourians GG, O'Grady M, Hegedus DD (2004) Modeling the structure of the type I peritrophic matrix: characterization of a *Mamestra configurata* intestinal mucin and a novel peritrophin containing 19 chitin binding domains. *Insect Biochem Mol Biol* 34:1101–1115
- Shibata T, Maki K, Hadano J, Fujikawa T, Kitazaki K, Koshihara T, Kawabata S (2015) Crosslinking of a peritrophic matrix protein protects gut epithelia from bacterial exotoxins. *PLoS Pathog* 11:e1005244
- Silva CP, Terra WR (1995) An α -glucosidase from perimicrovillar membranes of *Dysdercus peruvianus* (Hemiptera: Pyrrhocoridae) midgut cells. Purification and properties. *Insect Biochem Mol Biol* 25:487–494
- Silva CP, Ribeiro AF, Terra WR (1996) Enzyme markers and isolation of the microvillar and perimicrovillar membranes of *Dysdercus peruvianus* (Hemiptera: Pyrrhocoridae) midgut cells. *Insect Biochem Mol Biol* 26:1011–1018
- Silva CP, Silva JR, Vasconcelos FF, Petretski MD, Damatta RA, Ribeiro AF, Terra WR (2004) Occurrence of midgut perimicrovillar membranes in paraneopteran insect orders with comments on their function and evolutionary significance. *Arthropod Struct Develop* 33:139–148
- Silva JR, Mury FB, Oliveira MF, Oliveira PL, Silva CP, Dansa-Petretski M (2007) Perimicrovillar membranes promote hemozoin formation into *Rhodnius prolixus* midgut. *Insect Biochem Mol Biol* 37:523–531

- Silva W, Cardoso C, Ribeiro AF, Terra WR, Ferreira C (2013) Midgut proteins released by microapocrine secretion in *Spodoptera frugiperda*. *J Insect Physiol* 59:70–80
- Slavicek JM, Popham HJ (2005) The *Lymantria dispar* nucleopolyhedrovirus enhancins are components of occlusion-derived virus. *J Virol* 79:10578–10588
- Smith CJ, Kaper JB, Mack DR (1995) Intestinal mucin inhibits adhesion of human enteropathogenic *Escherichia coli* to HEP-2 cells. *J Pediatr Gastroenterol Nutr* 21:269–276
- Sneh B, Schuster S, Gross S (1983) Improvement of the insecticidal activity of *Bacillus thuringiensis* var. *entomocidus* on larvae of *Spodoptera littoralis* (Lepidoptera, Noctuidae) by addition of chitinolytic bacteria, a phagostimulant and a UV-protectant. *Z Angew Entomol* 96:77–83
- Sola RJ, Griebenow K (2009) Effects of glycosylation on the stability of protein pharmaceuticals. *J Pharm Sci* 98:1223–1245
- Stamm B, D'Haese J, Peters W (1978) SDS gel electrophoresis of proteins and glycoproteins from peritrophic membranes of some Diptera. *J Insect Physiol* 24:1–8
- Stoltz DB, Summers MD (1971) Pathway of infection of mosquito iridescent virus. I. Preliminary observations on the fate of ingested virus. *J Virol* 8:900–909
- Sudha PM, Muthu SP (1988) Damage to the midgut epithelium caused by food in the absence of peritrophic membrane. *Curr Sci* 57:624–625
- Summers CB, Felton GW (1996) Peritrophic envelope as a functional antioxidant. *Arch Insect Biochem Physiol* 32:131–142
- Sutherland DR, Christensen BM, Lasee BA (1986) Midgut barrier as a possible factor in filarial worm vector competency in *Aedes trivittatus*. *J Invertebr Pathol* 47:1–7
- Tajne S, Boddupally D, Sadumpati V, Vudem DR, Khareedu VR (2014) Synthetic fusion-protein containing domains of Bt Cry1Ac and *Allium sativum* lectin (ASAL) conferred enhanced insecticidal activity against major lepidopteran pests. *J Biotechnol* 171:71–75
- Takemoto Y, Mitsuhashi W, Murakami R, Konishi H, Miyamoto K (2008) The N-terminal region of an entomopoxvirus fusolin is essential for the enhancement of peroral infection, whereas the C-terminal region is eliminated in digestive juice. *J Virol* 82:12406–12415
- Takesue Y, Yokota K, Miyajima S, Taguchi R, Ikezawa H (1989) Membrane anchors of alkaline phosphatase and trehalase associated with the plasma membrane of larval midgut epithelial cells of the silkworm, *Bombyx mori*. *J Biochem* 105:998–1001
- Tanada Y (1959) Synergism between two viruses of the armyworm *Pseudaletia unipuncta* (Haworth) (Lepidoptera, Noctuidae). *J Insect Pathol*:215–231
- Tellam RL, Eisemann C (2000) Chitin is only a minor component of the peritrophic matrix from larvae of *Lucilia cuprina*. *Insect Biochem Mol Biol* 30:1189–1201
- Tellam RL, Wijffels G, Willadsen P (1999) Peritrophic matrix proteins. *Insect Biochem Mol Biol* 29:87–101
- Tellam RL, Vuocolo T, Eisemann C, Briscoe S, Riding G, Elvin C, Pearson R (2003) Identification of an immuno-protective mucin-like protein, peritrophin-55, from the peritrophic matrix of *Lucilia cuprina* larvae. *Insect Biochem Mol Biol* 33:239–252
- Terenius O, Papanicolaou A, Garbutt JS, Eleftherianos I, Huvenne H, Kanginakudru S, Albrechtsen M, An C, Aymeric JL, Barthel A, Bebas P, Bitra K, Bravo A, Chevalier F, Collinge DP, Crava CM, de Maagd RA, Duvic B, Erlandson M, Faye I, Felfoldi G, Fujiwara H, Futahashi R, Gandhe AS, Gatehouse HS, Gatehouse LN, Giebultowicz JM, Gomez I, Grimmelikhuijzen CJ, Groot AT, Hauser F, Heckel DG, Hegedus DD, Hrycaj S, Huang L, Hull JJ, Iatrou K, Iga M, Kanost MR, Kotwica J, Li C, Li J, Liu J, Lundmark M, Matsumoto S, Meyering-Vos M, Milllichap PJ, Monteiro A, Mrinal N, Niimi T, Nowara D, Ohnishi A, Oostra V, Ozaki K, Papakonstantinou M, Popadic A, Rajam MV, Saenko S, Simpson RM, Soberon M, Strand MR, Tomita S, Toprak U, Wang P, Wee CW, Whyard S, Zhang W, Nagaraju J, Ffrench-Constant RH, Herrero S, Gordon K, Swevers L, Smaghe G (2011) RNA interference in Lepidoptera: an overview of successful and unsuccessful studies and implications for experimental design. *J Insect Physiol* 57:231–245
- Terra WR (1988) Physiology and biochemistry of insect digestion: an evolutionary perspective. *Braz J Med Biol Res* 21:675–734

- Terra WR (1990) Evolution of digestive systems of insects. *Annu Rev Entomol* 35:181–200
- Terra WR (2001) The origin and functions of the insect peritrophic membrane and peritrophic gel. *Arch Insect Biochem Physiol* 47:47–61
- Terra WR, Ferreira C (1981) The physiological role of the peritrophic membrane and trehalase: Digestive enzymes in the midgut and excreta of starved larvae of *Rhynchosciara*. *J Insect Physiol* 27:325–331
- Terra WR, Ferreira C (1983) Further evidence that enzymes involved in the final stages of digestion by *Rhynchosciara* do not enter the endoperitrophic space. *Insect Biochem* 13:143–150
- Terra WR, Ferreira C, De Bianchi AG (1979) Distribution of digestive enzymes among the endo- and ectoperitrophic spaces and midgut cells of *Rhynchosciara* and its physiological significance. *J Insect Physiol* 25:487–494
- Terra WR, Espinoza-Fuentes FP, Ribeiro AF, Ferreira C (1988) The larval midgut of the housefly (*Musca domestica*): Ultrastructure, fluid fluxes and ion secretion in relation to the organization of digestion. *J Insect Physiol* 34:463–472
- Terra WR, Costa RH, Ferreira C (2006) Plasma membranes from insect midgut cells. *An Acad Bras Cienc* 78:255–269
- Tetreau G, Dittmer NT, Cao X, Agrawal S, Chen YR, Muthukrishnan S, Haobo J, Blissard GW, Kanost MR, Wang P (2015) Analysis of chitin-binding proteins from *Manduca sexta* provides new insights into evolution of peritrophin A-type chitin-binding domains in insects. *Insect Biochem Mol Biol* 62:127–141
- Thamthiankul S, Moar WJ, Miller ME, Panbangred W (2004) Improving the insecticidal activity of *Bacillus thuringiensis* subsp. *aizawai* against *Spodoptera exigua* by chromosomal expression of a chitinase gene. *Appl Microbiol Biotechnol* 65:183–192
- Toprak U, Baldwin D, Erlandson M, Gillott C, Hou X, Coutu C, Hegedus DD (2008) A chitin deacetylase and putative insect intestinal lipases are components of the *Mamestra configurata* (Lepidoptera: Noctuidae) peritrophic matrix. *Insect Mol Biol* 17:573–585
- Toprak U, Baldwin D, Erlandson M, Gillott C, Hegedus DD (2010) Insect intestinal mucins and serine proteases associated with the peritrophic matrix from feeding, starved and moulting *Mamestra configurata* larvae. *Insect Mol Biol* 19:163–175
- Toprak U, Harris S, Baldwin D, Theilmann D, Gillott C, Hegedus DD, Erlandson MA (2012) Role of enhancin in *Mamestra configurata* nucleopolyhedrovirus virulence: selective degradation of host peritrophic matrix proteins. *J Gen Virol* 93:744–753
- Toprak U, Baldwin D, Erlandson M, Gillott C, Harris S, Hegedus DD (2013) In vitro and in vivo application of RNA interference for targeting genes involved in peritrophic matrix synthesis in a lepidopteran system. *Insect Sci* 20:92–100
- Toprak U, Hegedus DD, Baldwin D, Coutu C, Erlandson M (2014) Spatial and temporal synthesis of *Mamestra configurata* peritrophic matrix through a larval stadium. *Insect Biochem Mol Biol* 54:89–97
- Toprak U, Erlandson M, Baldwin D, Karcz S, Wan L, Coutu C, Gillott C, Hegedus DD (2015) Identification of the *Mamestra configurata* (Lepidoptera: Noctuidae) peritrophic matrix proteins and enzymes involved in peritrophic matrix chitin metabolism. *Insect Sci*. doi:10.1111/1744-7917.12225
- Tristram JN (1977) Normal and cocoon-forming peritrophic membrane in larvae of the beetle *Gibbium psylloides*. *J Insect Physiol* 23:79–87
- Tristram JN (1978) The peritrophic membrane and cocoon ribbons in larvae of *Cionus scrophulariae*. *J Insect Physiol* 24:391–398
- Tsai YL, Hayward RE, Langer RC, Fidock DA, Vinetz JM (2001) Disruption of *Plasmodium falciparum* chitinase markedly impairs parasite invasion of mosquito midgut. *Infect Immun* 69:4048–4054
- Tse SK, Chadee K (1991) The interaction between intestinal mucus glycoproteins and enteric infections. *Parasitol Today* 7:163–172
- Vandenborre G, Groten K, Smaghe G, Lannoo N, Baldwin IT, Van Damme EJ (2010) *Nicotiana tabacum* agglutinin is active against Lepidopteran pest insects. *J Exp Bot* 61:1003–1014

- Venancio TM, Cristofolletti PT, Ferreira C, Verjovski-Almeida S, Terra WR (2009) The *Aedes aegypti* larval transcriptome: a comparative perspective with emphasis on trypsins and the domain structure of peritrophins. *Insect Mol Biol* 18:33–44
- Vieira CM, Tuelher ES, Valicente FH, Wolff JL (2012) Characterization of a *Spodoptera frugiperda* multiple nucleopolyhedrovirus isolate that does not liquefy the integument of infected larvae. *J Invertebr Pathol* 111:189–192
- Vinetz JM (2005) Plasmodium ookinete invasion of the mosquito midgut. *Curr Top Microbiol Immunol* 295:357–382
- Vinokurov KS, Elpidina EN, Zhuzhikov DP, Oppert B, Kodrik D, Sehnan F (2009) Digestive proteolysis organization in two closely related Tenebrionid beetles: red flour beetle (*Tribolium castaneum*) and confused flour beetle (*Tribolium confusum*). *Arch Insect Biochem Physiol* 70:254–279
- Vuocolo T, Eisemann CH, Pearson RD, Willadsen P, Tellam RL (2001) Identification and molecular characterisation of a peritrophin gene, peritrophin-48, from the myiasis fly *Chrysomya bez-ziana*. *Insect Biochem Mol Biol* 31:919–932
- Walker VK, Geer W, Williamson JH (1980) Dietary modulation and histochemical localisation of leucine aminopeptidase activity in *Drosophila melanogaster*. *Insect Biochem* 10:543–548
- Walski T, Van Damme EJ, Smaghe G (2014) Penetration through the peritrophic matrix is a key to lectin toxicity against *Tribolium castaneum*. *J Insect Physiol* 70:94–101
- Wang P, Granados RR (1997a) An intestinal mucin is the target substrate for a baculovirus enhancer. *Proc Natl Acad Sci U S A* 94:6977–6982
- Wang P, Granados RR (1997b) Molecular cloning and sequencing of a novel invertebrate intestinal mucin cDNA. *J Biol Chem* 272:16663–16669
- Wang P, Granados RR (1998) Observations on the presence of the peritrophic membrane in larval *Trichoplusia ni* and its role in limiting baculovirus infection. *J Invertebr Pathol* 72:57–62
- Wang P, Granados RR (2000) Calcofluor disrupts the midgut defense system in insects. *Insect Biochem Mol Biol* 30:135–143
- Wang P, Hammer DA, Granados RR (1994) Interaction of *Trichoplusia ni* granulosis virus-encoded enhancer with the midgut epithelium and peritrophic membrane of four lepidopteran insects. *J Gen Virol* 75:1961–1967
- Wang P, Li G, Granados RR (2004) Identification of two new peritrophic membrane proteins from larval *Trichoplusia ni*: structural characteristics and their functions in the protease rich insect gut. *Insect Biochem Mol Biol* 34:215–227
- Washburn JO, Kirkpatrick BA, Volkman LE (1995) Comparative pathogenesis of *Autographa californica* nuclear polyhedrosis virus in larvae of *Trichoplusia ni* and *Heliothis virescens*. *Virology* 209:561–568
- Waterhouse DF (1953) Occurrence and endodermal origin of the peritrophic membrane in some insects. *Nature* 172(4380):676–677
- Waterhouse DF (1957) Digestion in insects. *Annu Rev Entomol* 2:1–18
- Weiss BL, Savage AF, Griffith BC, Wu Y, Aksoy S (2014) The peritrophic matrix mediates differential infection outcomes in the tsetse fly gut following challenge with commensal, pathogenic, and parasitic microbes. *J Immunol* 193:773–782
- Welburn SC, Arnold K, Maudlin I, Gooday GW (1993) *Rickettsia*-like organisms and chitinase production in relation to transmission of trypanosomes by tsetse flies. *Parasitology* 107:141–145
- Whyard S, Singh AD, Wong S (2009) Ingested double-stranded RNAs can act as species-specific insecticides. *Insect Biochem Mol Biol* 39:824–832
- Wigglesworth VB (1929) Digestion in the tsetse-fly: a study of structure and function. *Parasitology* 21:288–321
- Wigglesworth VB (1930) The formation of the peritrophic membrane in insects, with special reference to the larvae of mosquitoes. *Q J Microsc Sci* 73:593–616
- Wijffels G, Eisemann C, Riding G, Pearson R, Jones A, Willadsen P, Tellam R (2001) A novel family of chitin-binding proteins from insect type 2 peritrophic matrix. cDNA sequences, chitin binding activity, and cellular localization. *J Biol Chem* 276:15527–15536

- Wiwat C, Thaithanun S, Pantuwatana S, Bhumiratana A (2000) Toxicity of chitinase-producing *Bacillus thuringiensis* ssp. *kurstaki* HD-1 toward *Plutella xylostella*. *J Invertebr Pathol* 76:270–277
- Wu H, de Graaf B, Mariani C, Cheung AY (2001) Hydroxyproline-rich glycoproteins in plant reproductive tissues: structure, functions and regulation. *Cell Mol Life Sci* 58:1418–1429
- Yang S, Pyati P, Fitches E, Gatehouse JA (2014) A recombinant fusion protein containing a spider toxin specific for the insect voltage-gated sodium ion channel shows oral toxicity towards insects of different orders. *Insect Biochem Mol Biol* 47:1–11
- Yunovitz H, Sneh B, Schuster S, Oron U, Broza M, Yawetz A (1986) A new sensitive method for determining the toxicity of a highly purified fraction from δ -endotoxin produced by *Bacillus thuringiensis* var. *entomocidus* on isolated larval midgut of *Spodoptera littoralis* (Lepidoptera, Noctuidae). *J Invertebr Pathol* 48:223–231
- Zhang X, Guo W (2011) Isolation and identification of insect intestinal mucin HaIM86—the new target for *Helicoverpa armigera* biocontrol. *Int J Biol Sci* 7:286–296
- Zhang S, Sherwood RW, Yang Y, Fish T, Chen W, McCardle JA, Jones RM, Yusibov V, May ER, Rose JK, Thannhauser TW (2012) Comparative characterization of the glycosylation profiles of an influenza hemagglutinin produced in plant and insect hosts. *Proteomics* 12:1269–1288
- Zhu Q, Arakane Y, Banerjee D, Beeman RW, Kramer KJ, Muthukrishnan S (2008) Domain organization and phylogenetic analysis of the chitinase-like family of proteins in three species of insects. *Insect Biochem Mol Biol* 38:452–466
- Zhu-Salzman K, Koiwa H, Salzman RA, Shade RE, Ahn JE (2003) Cowpea bruchid *Callosobruchus maculatus* uses a three-component strategy to overcome a plant defensive cysteine protease inhibitor. *Insect Mol Biol* 12:135–145
- Zhuzhikov DP (1964) Function of the peritrophic membrane in *Musca domestica* L. and *Calliphora erythrocephala* Meig. *J Insect Physiol* 10:273–278
- Zhuzhikov DP (1970) Permeability of the peritrophic membrane in the larvae of *Aedes aegypti*. *J Insect Physiol* 16:1193–1202
- Zimmermann U, Mehlan D (1976) Water transport across peritrophic membranes of *Calliphora erythrocephala*. *Comp Biochem Physiol* 55A:119–126
- Zimmermann D, Peters W (1987) Fine structure and permeability of peritrophic membranes of *Calliphora erythrocephala* (Meigen) (Insecta: Diptera) after inhibition of chitin and protein synthesis. *Comp Biochem Physiol* 86B:353–360
- Zimmermann U, Mehlan D, Peters W (1975) Investigations on the transport function and structure of peritrophic membranes; V – Amino acid analysis and electron microscopic investigations of the peritrophic membranes of the blowfly *Calliphora erythrocephala* Mg. *Comp Biochem Physiol* 51B:181–186
- Zimoch L, Merzendorfer H (2002) Immunolocalization of chitin synthase in the tobacco hornworm. *Cell Tissue Res* 308:287–297
- Zimoch L, Hogenkamp DG, Kramer KJ, Muthukrishnan S, Merzendorfer H (2005) Regulation of chitin synthesis in the larval midgut of *Manduca sexta*. *Insect Biochem Mol Biol* 35:515–527

Chapter 9

Composite Eggshell Matrices: Chorionic Layers and Sub-chorionic Cuticular Envelopes

Gustavo L. Rezende, Helena Carolina Martins Vargas, Bernard Moussian, and Ephraim Cohen

Abstract Many arthropods and the majority of insects lay their eggs without parental care. These immobile stages of life must rely on the various eggshell layers deposited upon the developing embryo to survive biotic and abiotic stresses such as desiccation, flooding, predators and pathogens. At the same time, these protective layers must allow sperm entry and gas exchanges. During insect oogenesis most of these layers are deposited by the follicle cells: vitelline membrane, wax layer, innermost chorionic layer, endochorion and exochorion. Follicle cells will also produce some regions with chorionic complexities such as micropyles, aeropyles and the operculum. After fertilization and egg deposition, the developing egg of insects and other arthropods produces a blastodermal or serosal cuticle, which is located below the vitelline membrane and serves as an additional protective extracellular structure. Through a literature survey comprising more than 40 species this chapter is dedicated to the description of the formation, structure and physiology of these multilayered and multiregional composite structures as well as the cellular and molecular mechanisms underlying it.

G.L. Rezende (✉) • H.C.M. Vargas
LQFPP, CBB, UENF, Campos dos Goytacazes, RJ, Brazil
e-mail: guslrezende@gmail.com; helenacvargas@gmail.com

B. Moussian
Genetik der Tiere, Eberhard-Karls Universität Tübingen,
Auf der Morgenstelle 28, 72076 Tübingen, Germany
e-mail: bernard.moussian@unice.fr

E. Cohen
Department of Entomology, The Robert H. Smith Faculty of Agriculture, Food and
Environment, The Hebrew University of Jerusalem, Rehovot 76 100, Israel
e-mail: ephraim.cohen@mail.huji.ac.il

9.1 Introduction

Arthropod eggs are laid in extremely wide niches of habitats and microhabitats, and are exposed to various physical and biological challenges. Development of the eggshell is an elaborate and essential physiological adaptation in the evolutionary transition of insects and other arthropods from marine to terrestrial environments. The eggshell is the only protection for those species that lack parental care. Further evolution of species-specific eggshell composition, organization and morphology was likely been driven by the different ecological niches and ovipositional substrates (Zeh et al. 1989). The eggshell is a boundary between the external environment and the developing embryo, and as such, provides protection against desiccation or flooding, predation and invasion of pathogenic microorganisms as well as providing resistance to mechanical stressors or temperature fluctuations. At the same time it participates in embryo patterning and provides access to penetrating sperms, regulates gas exchange of oxygen supply and discharge of carbon dioxide, and allows hatching (Margaritis 1985a). During embryogenesis a cuticular egg envelope is produced in many species. These cuticles will supplement or, in some cases, replace the protection granted by the maternal eggshell layers.

The first part of this chapter deals with maternal eggshell layers in insects while the second part deals with the cuticular egg envelopes (blastodermal or serosal cuticles) that are produced post-zygotically in arthropods. In both parts how these layers are produced, their morphology, the genes and proteins associated with their formation and their physiological role are discussed.

9.2 Maternal Eggshell Layers

9.2.1 Eggshell Structure

Eggshell of oviparous insects is largely a highly organized proteinaceous multilayered multiregional composite structure. Due to its massively organized structural complexity, as well as because of the distinctive spatial and temporal programs, eggshell formation (mainly in the fruit fly *Drosophila melanogaster*) has been used as a model system in developmental biology for the assemblage of complex extracellular matrices (Margaritis et al. 1980; Margaritis 1985a, 1986; Trougakos and Margaritis 2002; Waring 2000; Papantonis et al. 2015). It has been suggested that adaptation to diversified ecological niches drives the evolutionary patterns of insect eggshell layers (Jagadeeshan and Singh 1997). Basically, the eggshell consists of a vitelline membrane close to the oocyte and the chorionic layers of the endochorion and a sculptured outer surface layer, the exochorion. The general morphology and anatomy of such layers has been conserved as described in a rare fossil eggshell about 145 MYA (Fisher and Watson 2015).

Model insects for the fundamental and comprehensive studies on the morphological, histochemical, physiological, biochemical, molecular and genetic aspects of eggshell layers and choriogenesis have largely been restricted to dipteran species like *D. melanogaster*, the olive fly *Dacus oleae*, the cherry fly, *Rhagoletis cerasi*, and the yellow fever mosquito *Aedes aegypti*, or to lepidopteran organisms such as the silkworm *Bombyx mori*, the polyphemus moth *Antheraea polyphemus*, or the tobacco hornworm, *Manduca sexta*. Diagnostic research tools employed in these studies include scanning and transmission electron microscopy (SEM and TEM), laser scanning microscopy (LSM) and freeze-fracturing that provided 3-dimensional images of eggshell surface, internal radial layers and regional structures (Margaritis et al. 1980; Mouzaki and Margaritis 1991a, b; Mouzaki et al. 1991; Orfanidou et al. 1992). Morphogenesis and assembly studies were carried out by immunogold electron microscopy and immunoblot analyses, by pulse-chase autoradiography to follow protein intercalation events and by use of selected mutants defective in eggshell assembly. More recently, proteomic, transcriptome and gene silencing techniques are expanding the findings obtained in the field.

9.2.1.1 Radial Organization of Eggshell Layers

The apposition of the composite egg layers is depicted in the schematic presentation in Fig. 9.1. The number of layers is based on a variety of publications mainly describing eggshell morphology and ultrastructure of dipterans (*D. melanogaster*,

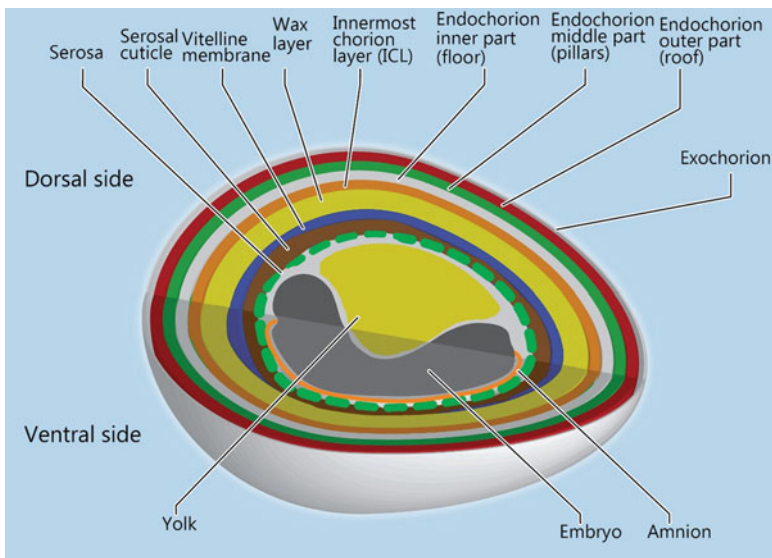


Fig. 9.1 A schematic presentation of the radial complexity of a holometabolous insect egg layers. Size of layers is out of scale. Anterior is to the left. The amnion is produced from the margin of the embryo and it covers only the ventral side of the developing embryo. Embryo position related to the yolk varies in hemimetabolous insects

A. aegypti, *Anopheles gambiae*), lepidopterans (*B. mori*, *A. polyphemus*) or of a variety of odonate and coleopteran species. Insect species though may lack certain layers like for instance the wax layer described in higher dipterans that is absent in some lepidopteran and mosquitoes (Monnerat et al. 1999).

Eggshell vitelline membrane and chorionic layers (wax layer, innermost chorionic layer, endochorion and exochorion) are the secretory products of the ovarian follicular epithelial cells that produce these layers at the last stages of oogenesis (Sect. 9.2.2). Subpopulations of follicle cells are accountable for secretion and assembly of the various radial layers of the chorion as well as for its specialized regional constructs (Sect. 9.2.5). Two unicellular membranes cover the developing embryo: the amnion that covers the embryo ventrally and the serosa that covers the amnion, the entire embryo and the yolk. Both membranes are composed of extraembryonic cells produced at early embryogenesis (Panfilio 2008). The serosa secretes the serosal cuticle, the last eggshell matrix that will be produced and localized beneath the vitelline membrane (Sect. 9.3).

9.2.2 Dynamics of Eggshell Formation During Oogenesis

The insect eggshell is a composite matrix synthesized at late oogenesis by the follicular cells that surround the oocyte. This intricate structure is composed of different layers (Margaritis 1985a; Chapman 2013), and its complexity is linked to a rich protein composition and also to an elaborate genetic process that coordinates their synthesis and deposition (Kafatos 1975; Chapman 2013). The process of vitelline membrane and other eggshell layers are well described during *D. melanogaster* oogenesis and will be used to illustrate this process (Hinton 1981; Margaritis 1985a) along with punctual comparisons with other species.

9.2.2.1 Eggshell Formation in *Drosophila melanogaster*

The oogenesis of *D. melanogaster* is divided in 14 consecutive stages. The vitelline membrane (VM) is the first eggshell layer to be synthesized at the end of the vitellogenesis period. While genes of vitelline membrane proteins begin to be transcribed between stages 8–10 of oogenesis (Margaritis 1985a; Pascucci et al. 1996), the first signs of its formation arise at stage 9A as small secreted vesicle proteins, the vitelline bodies (Fig. 9.2a) (Klowden 2007; Chapman 2013). Vitelline bodies are also described for *A. aegypti* and the German cockroach *Blattella germanica* (Mathew and Rai 1975; Belles et al. 1993). At stage 10B of *D. melanogaster* the vitelline bodies fuse and form a continuous and functional vitelline membrane (Fig. 9.2a) (Margaritis 1985a). In other insects, VM is secreted directly as a continuous layer as is the case of *B. mori*, *A. polyphemus* and others lepidopterans (Margaritis 1985a). In some species, the oocyte contributes to the synthesis of this structure (Chapman 2013).

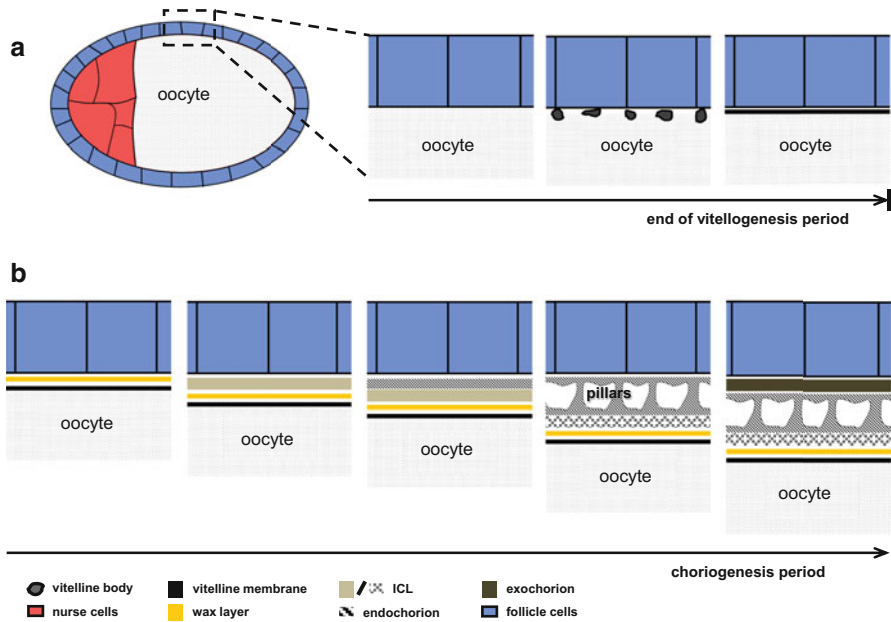


Fig. 9.2 Scheme of eggshell synthesis in the fruit fly *D. melanogaster*. (a) End of the vitellogenesis period, associated with vitelline membrane formation. Initially, the vitelline membrane is secreted as vitelline bodies at stage 9A and becomes a continuous layer at stage 10B. (b) Choriogenesis period occurs between stages 11 and 14, when all other eggshell layers are produced in the following order: wax layer, innermost chorionic layer (ICL), endochorion and exochorion. During choriogenesis, the innermost chorionic layer crystallizes and pillars are formed within the endochorion. The oocyte is the topological reference: the innermost and outermost layers are the vitelline membrane and the exochorion, respectively

In *D. melanogaster* choriogenesis is initiated at the end of oogenesis stage 11A with the formation of the wax layer, located above the VM (Fig. 9.2b). After this step, the formation of both innermost chorionic layer (ICL) and endochorion commences at stage 11B. Between stages 12C to 14A, the formation of pillars occurs within the endochorion. At these stages ICL crystallization takes place and the endochorion is fully formed. The formation of the last, outermost eggshell layer, the exochorion occurs at stage 14A (Fig. 9.2b) (Margaritis 1986). In *B. mori* and other lepidopterans, the choriogenesis is initiated by formation of the trabecular layer (endochorion) (Hinton 1981; Margaritis 1985a).

9.2.2.2 Proteins Necessary for the Coordinated Secretion of Eggshell Material

In the fruit fly, the polarity of the follicular epithelium cells depends on the function of canonical polarity determinants like Crumbs (Crb) and Stardust (Sdt) (Fletcher et al. 2012; Sherrard and Fehon 2015). The apical plasma membrane of follicle cells forms a dense array of microvilli that involve the function of Cad99C and Myosin

VIIA (Myo7A) (Schlichting et al. 2006; Glowinski et al. 2014). The microvilli are key structures in the assembly of the vitelline membrane. Emanating from the follicle cells and the oocyte they segregate precursor vitelline bodies. These proteins aggregate, fuse together when the microvilli are retracted suggesting that microvilli play an active role in vitelline membrane construction. In follicle cells lacking Cad99C the function of the precursor vitelline bodies are malformed, and the vitelline membrane is aberrant. The mature vitelline membrane has been postulated to serve as a substrate for chorion assembly (Pascucci et al. 1996).

9.2.3 Inner Eggshell Barriers to Water Permeability and Gas Exchange

The three layers closest to the oocyte, the VM, wax layer and the ICL are believed to serve as waterproofing barriers and provide resistance to ambient air influx. At the same time, they function also by regulating rates of air influx and carbon dioxide efflux (Margaritis et al. 1983, 1991; Woods et al. 2005).

9.2.3.1 Vitelline Membrane (VM)

VM is a homogenous cross-linked robust and flexible layer that varies in thickness among insect species and at different parts of a specific egg. This first eggshell layer in *D. melanogaster* is synthesized by the follicle cells but eventually, it was shown that also the germline contributes components to the VM biogenesis (Ventura et al. 2010). Still, the intricate biochemical and biophysical events taking place in the biogenesis of VM are ill-understood. The discontinuous layer of vitelline bodies is separated by scaffolding microvilli extended from both the oocyte and the follicular cells (D'Alterio et al. 2005; Schlichting et al. 2006). Eventually, the microvilli degenerate or retract thus creating a uniformly continuous layer that thins in later stages of oogenesis. In *D. melanogaster* for example, the identified four major VM proteins, undergo modifications that involve specific proteolytic processes and intermolecular disulfide bridges during oogenesis (Sect. 9.2.6.1). Later, at post-ovulation, the layer undergoes protein stabilization by di- and tri-tyrosine crosslinking (Sect. 9.2.8) (Trougakos and Margaritis 1998a; Heifetz et al. 2001)

The *D. melanogaster* and *A. aegypti* VMs serve as a reservoir for pro-proteins which later, by post-translational modification are processed to smaller components that move into other chorionic layers (Pascucci et al. 1996; Mauzy-Melitz and Waring 2003; Marinotti et al. 2014). The waterproof role of the VM may be indicated by presence of *n*-alkanes and methyl-branched alkanes at the surface of dechorionated eggs of several dipteran species (Nelson and Leopold 2003).

Aside from the role of an eggshell barrier, the VM participates *inter alia* as a spatial determinant signal for both dorso-ventral and terminal pattern formation pathways of the enclosed embryo (Zhang et al. 2009; Stein and Stevens 2014).

9.2.3.2 Wax Layer

The wax layer, which is formed by secretion of lipid vesicles by the follicle cells that accumulate on the VM surface, is sandwiched between the VM and the ICL. This hydrophobic layer in *D. melanogaster*, which is initially created by 3–4 overlapping plaques, are later compressed and thinned between the VM that increases in volume due to water uptake and by the rigid non-expandable ICL (Papassideri and Margaritis 1986; Papassideri et al. 1991; 1993). The eggshell wax is apparently similar to cuticular wax, but there are no recent studies identifying its chemical composition. However, genes related with lipid metabolism were recently identified in follicle cells during eggshell formation (Tootle et al. 2011). The hydrocarbons extracted from dechorionated eggs of flies (Nelson and Leopold 2003) might be components of both VM and wax layers. As the wax layer is structurally conserved in drosophilids, it most likely implies its important waterproof function in this taxonomic group (Papassideri et al. 1991). It should be mentioned that some insect species like the cat flea, *Ctenocephalides felis* (Marchiondo et al. 1999) or the tarnished plant bug *Lygus lineolaris* (Ma et al. 2002) lack a wax layer.

9.2.3.3 Innermost Chorion Layer (ICL)

ICL (first reported by Margaritis et al. 1979 and Hamodrakas et al. 1982) which is a bridge between the VM plus wax layers and the adjacent endochorionic layer (sometimes called floor) is composed of proteinaceous components synthesized by the follicle cells prior to the other chorionic proteins. Initially, the electron-dense ICL is closely attached to the apposed endochorion. But later, at the end of chorionogenesis, detachment occurs as the ICL gradually assumes a unique multilayered structure characterized as a three-dimensional crystal configuration (Fig. 9.2b) (Papassideri and Margaritis 1996). Thus, the final step of protein self-assembly that forms the crystal lattices takes place between two existing eggshell layers (Akey et al. 1987). The ICL is composed of up to four discrete sublayers in several drosophilids with a basic structural unit of crystals that consist of octamers made up of four heterodimers. Parallel to crystallization, stabilization of ICL crystallized structure by intermolecular crosslinking occurs via disulfide bridges and di- and tri-tyrosine bonds (Sect. 9.2.8). Eggshell peroxidase was cytochemically identified as a structural component in ICL of *Drosophila virilis* (Trougakos and Margaritis 1998a).

In addition of functioning as a barrier to water permeability, the ICL facilitates hatching of larvae that get free by shedding the inner eggshell layers.

9.2.4 Outer Chorionic Barriers

9.2.4.1 Endochorion

The endochorion (Figs. 9.1 and 9.2b) is largely a tripartite structure that consists of a thin inner part (floor), an intermediate region of vertical pillars and pillar cavities, and a solid outer part (roof). The cavities facilitate gas exchange and the roof displays ridges that are the borders of the follicular cell imprints (Waring 2000). The temporal formation of the endochorion involves major early proteins that are detected in all endochorion sublayers. They create the final morphology of the endochorion and provide the scaffold for middle and late proteins that diffuse and intercalate to associate extracellularly with the existing early proteins and shape the final functional endochorionic configuration of *D. virilis* (Trougakos and Margaritis 1998b). Migration and intercalating processes were demonstrated with VM32E protein, which is initially uniformly distributed in *D. melanogaster* VM, and is partially released and trafficked into the endochorionic layer (Andrenacci et al. 2001). It was suggested that a derivative of a proprotein (fc177) cleaved within the VM in *D. melanogaster* prevents the coalescence of the endochorionic tripartite substructures (Mauzy-Melitz and Waring 2003).

Three major endochorionic proteins undergo disulfide bond crosslinking prior to oviposition in *A. aegypti*. Further crosslinking after oviposition occurs via di- and tri-tyrosine bonds mediated by chorion peroxidase activity that involves hydrogen peroxide in addition to quinone crosslinking reaction mediated by phenoloxidase (Sect. 9.2.8) (Li and Li 2006). Peroxidase, which was immunolocalized in ICL and endochorion of *D. melanogaster* and *D. virilis*, is a chorionic component with enzymatic activity (Keramaris et al. 1991; Trougakos and Margaritis 1998a; Konstandi et al. 2005).

9.2.4.2 Exochorion

The last secreted layer is the exochorion featuring a sculptured outer surface of the eggshell. It is composed of two lamellar layers in mosquitos (Monnerat et al. 1999) and flies (Mouzaki and Margaritis 1991a, b; Zarani and Margaritis 1994). The architectural patterns of egg chorions that include its specialized regions, depend on imprints of the follicular cells. The sculptured patterns portray reticulated polygonal network design, ridges, protruding tubercles, domes or threads of various shapes and sizes. However, eggs of several stored products coleopterans (Gautam et al. 2015) lack distinct chorionic patterns and are devoid of regional complexities like micropyles and aeropyles. As the sculptured morphological patterns are species-specific they have served for ootaxonomical purpose and may indicate evolutionary adaptation related to oviposition sites (Fausto et al. 1992; Mazzini et al. 1992; Guglielmino et al. 1997; Kumar et al. 2007).

In mosquitoes exochorion sculpture may vary within a single species at different seasons or according to abiotic influences (Clements 1992). Moreover, some species possess an exquisite sculpturing, such as the exochorion of *Anopheles shannoni*, striking in its singularity and complexity, when compared to the exochorion of others mosquitoes (Lounibos et al. 1997; Clements 1992). Exochorion formation is governed by the genetic processes that occur within the follicle cells, such as the dorsal-ventral patterning system (Chasan and Anderson 1993). In this regard, it would be interesting to analyze the genetic process that induces the exochorionic sculpturing differences observed within and between species.

9.2.5 Regional Chorionic Complexities

The eggshell chorion is comprised of stripes or flat regions as well as specialized areas like micropyles and micropylar apparatus that facilitates penetration of sperms; aeropyles and respiratory appendages that mediate gas exchange and operculum that enables larval hatching. Distinct subpopulations of cells of the follicular epithelium are responsible for the temporal and spatial creation of these particular regional areas (Waring 2000).

9.2.5.1 Micropyles and Micropylar Apparatuses

The micropyle is an aperture surrounded by a distinct architectural area that facilitates access of sperms into the oocyte via the micropylar canal that terminate at the VM (as described in the cherry fly *Rhagoletis cerasi* by Zarani and Margaritis 1991). The micropyle appears as a protrusion or a depression in eggshells of Diptera and Lepidoptera, respectively. In lepidopteran species the micropylar pore is surrounded by a rosette of follicle cell imprints (Kumar and Kamble 2008) (Fig. 9.3a). The micropylar canal, which passes through the eggshell, is formed of microvillar extensions of the follicular cells that eventually degenerate (Mouzaki et al. 1991). Morphological patterns of such areas depend on the imprints of the previously overlying follicle cells (Kumar and Kamble 2008; Kumar et al. 2007). The micropyle is located at the anterior pole in dipteran, lepidopteran and neuropterid species (Mouzaki and Margaritis 1991a; Andrew and Tembhare 1992; Kubrakiewicz et al. 2005), or in the mid-ventral region in the two-spotted cricket *Gryllus bimaculatus* (Sarashina et al. 2005), whereas the location of the micropylar appendage in the almond seed wasp *Eurytoma amygdali* or in the beetle *Adalia bipunctata* is at the posterior end (Zarani and Margaritis 1994). It should be noted that although micropyles are functionally entities, many stored products insects (Kučerová and Stejskal 2008; Osawa and Yoshinaga 2009) as well as certain scale insect eggs (Vogelgesang and Szklarzewicz 2001) lack such structures. In such cases there is still an intriguing question regarding penetrations of sperms to fertilize the ovum. Perceptively, viable

eggs like in the subsocial burrower bug, *Adomerus triguttulus*, or the stingless bee *Tetragonisca angustula* have micropyles, whereas their trophic eggs are by and large devoid of such structures (Kudo et al. 2006).

9.2.5.2 Aeropyles and Appendages – Respiratory Mechanism

Aeropyles are microscopic apertures (Fig. 9.3c) that either scatter all over the entire chorionic surface or are confined to specific areas on the egg. They can be positioned on protrusions (or crowns, Fig. 9.3d) over entire egg surfaces or arranged in distinct bands or rings (Hatzopoulos and Regier 1987; Regier et al. 2005). Aeropyles are connected via chorion traversing canals to the interior of the egg either directly or to gas-filled meshwork in the inner chorionic layers. Such a meshwork or the trabecular layer was described in *C. felis* (Marchiondo et al. 1999). Functionally, they facilitate air passage and gas exchange for respiration of the metabolically active embryos. The number and surface arrangement of aeropyles varies across insect species. Moreover, they can undergo change in size as was reported for maturing eggs of the Ailanthus silkmoth *Samia ricini* (Renthlei et al. 2010). Aeropyles in lepidopteran species, for example, range in number from a few up to 400 per egg. (Kumar and Kamble 2008). Aeropyles were not detected in eggs of the scale insect *Orthezia urticae* (Vogelgesang and Szklarzewicz 2001), in many aquatic insects or in eggs of certain stored products coleopterans like the stored grain borer *Rhyzopertha dominica* or the red flour beetle *Tribolium castaneum*, where it was suggested that their relatively permeable chorions facilitate gas exchange (Kučerová and Stejskal 2008; Gautam et al. 2015). Diversity of eggshell chorionic structures and characteristics could explain differential tolerance of stored products insects to fumigants (Gautam et al. 2015).

Some eggs of insect species living in aquatic environments develop a structural modification described as a plastron network that traps air film and serve as physical gills that establish an extensive air-water interface when submerged under water (Hinton 1968; Goforth and Smith 2011). A wide and extended plastron was

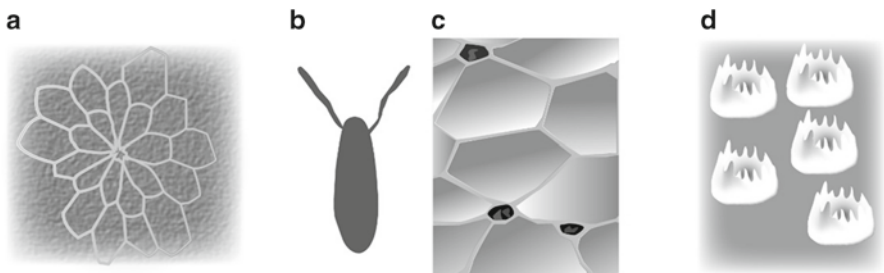


Fig. 9.3 Regional structures of insect eggshell. (a) A micropyle surrounded by a rosette pattern of polygonal imprints of follicle cells (*Manduca sexta*). (b) Dorsal respiratory appendages (*Drosophila melanogaster*). (c) Aeropylar apertures (*Abedus herberti*). (d) Aeropylar crown (*Antheraea polyphemus*). Schemes are not in scale

described in eggshells of non-aquatic insect species, like in the blowflies *Chrysomya nigripes* and *Lucilia cuprina* (Sukontason et al. 2004, 2007). Although plastron-like configuration was described, their function has not been unequivocally demonstrated. A different structure is the water-impermeable hydrophobic respiratory horns (Fig. 9.3b) at the anterior end of *D. melanogaster* eggs that obtains oxygen from ambient water. The three-dimensional morphogenesis of *D. melanogaster* respiratory projecting tubes was described by Osterfield et al (2013). It is noteworthy, that compared to *D. melanogaster*, the respiratory appendages of the Hawaiian *Drosophila grimshawi* are four, much longer with a wider surface area that functions as plastron for underwater respiration (Margaritis et al. 1983).

9.2.5.3 Operculum

In many species the operculum is a sculptured chorionic region at the anterior pole of the egg that is encircled by hatching lines built into the eggshell to ease larval hatching. Areas of the operculum may harbor aeropyles (Burkhart et al. 1999) and micropyles (Zawadzka et al. 1997; Ma et al. 2002). It was shown that follicular subpopulation of anteriorly migrating cells in *D. melanogaster* form the operculum (Kleve et al. 2006) and the hatching line called collar (Margaritis 1985a). However, hatching lines were not observed in lepidopterans like *S. ricini* as the larva chews its way out of the chorionic egg layers (Renthlei et al. 2010).

9.2.6 Genes and Proteins Required for Eggshell Formation

Compared to other protective extracellular matrices such as the cuticle (Chap. 3), the molecular and cellular processes of eggshell protein synthesis and assembly are well studied, including regulation by hormones, gene amplification and *cis* and *trans*-regulatory elements (Turner and Mahowald 1976; Margaritis et al. 1980; Regier and Kafatos 1985; Swevers et al. 2005; Papantonis et al. 2015; Chen et al. 2015a). We therefore rather aim at drawing a general scheme of vitelline membrane and chorion formation rather than a detailed survey of the literature. An arsenal of eggshell genes and proteins have been isolated or described in recent years using modern large-scale proteomic and genomic techniques (e.g. Chen et al. 2015a). These findings complement earlier reports on eggshell genes and proteins.

Description of eggshell proteins, genes and the regulation of their expression are well known largely for *D. melanogaster* and *B. mori* and, to some extent, mosquito vectors of parasites. All of these insects are holometabolous species with polytrophic meroistic ovaries. Recently, the genetic process of eggshell production has been studied in *B. germanica*, a hemimetabolous insect with panoistic ovaries (Chapman 1998; Irles et al. 2009a). Further comparison among these species will shed light on relevant information related to the evolution of the maternal matrices that surround developing insect embryos.

9.2.6.1 *Drosophila melanogaster*

In the fruit fly the central proteins of the VM are sV17, sV23, VM32E and VM34C. Many vitelline membrane proteins (VMPs) are rich in proline and alanine and contain a highly conserved hydrophobic domain of 38 residues, the so-called VM domain (Scherer et al. 1988; Wu et al. 2010). A similar domain with conserved amino acids is present in the mosquito *A. aegypti* VMPs (Sect. 9.2.6.3). Another conserved motif of 10 amino acids is present in *D. melanogaster* VM32E and VM34C. VM proteins are embedded in protein networks by different types of cross-linking including disulfide bonds and inter-peptide di-tyrosines. In *D. melanogaster* along with *A. aegypti*, many VM proteins have three precisely spaced cysteines, suggesting disulfide bridge formation (Wu et al. 2010). VM32E contains seven tyrosine residues that may form di-tyrosine crosslinking structures catalyzed by extracellular peroxidases and, apart from being an integral constituent of the VM, are important for the formation of other eggshell layers (Andrenacci et al. 2001).

A mutant allele of sV23 in *D. melanogaster* was analyzed in detail (Savant and Waring 1989; Wu et al. 2010). The exchange of an evolutionary conserved cysteine in the VM domain to serine leads to a collapse of the eggshell and unfertilized eggs. Besides this motif, the hydrophobic N-terminal prodomain of sV23 is also essential for eggshell construction and it is proposed to be crucial for the alignment of matrix proteins during vitelline membrane maturation (Manogaran and Waring 2004).

Three other VMPs, Closca (Clos), Nasrat (fs(1)N) and Polehole (fs(1)ph), which may be grouped as a separate class of integral VMPs were reported to be essential for VM formation (Ventura et al. 2010). Fs(1)N and Fs(1)ph have been shown to be needed for non-disulfide crosslinking of the vitelline protein sVM23 (Cernilogar et al. 2001; Jiménez et al. 2002). Another integral component of the VM is Torsolike that is needed for terminal pattern formation in *D. melanogaster* (Stevens et al. 2003). The VM of eggs derived from homozygous mutant for either of these genes is fragile and brittle. Taken together, these data underline that some components of the VM besides being incorporated in the inert barrier, also serve as signaling factors regulating early embryo development.

The function of the VM constituent Palisade was also studied in detail (Elalayli et al. 2008). Palisade was initially found in the mass spectrometry screen for eggshell matrix proteins reported by Fakhouri et al. (2006) (see below). Down regulation of Palisade function by RNA interference (RNAi) causes mislocalisation of VMPs such as sV17 and its crosslinking. Ultimately, this results in morphological defects of the palisade-like vitelline bodies.

While some genes required for VM production are transcribed during the early period of its formation (e.g., *VM26.A.1*, *VM34C* and *VM26A.2*) other genes such as *VM32E* are expressed later, at the end of this period (Swevers et al. 2005).

The chorion harbors a class of proteins with the chorion-3 superfamily domain including s36 and s38 (Pascucci et al. 1996). Initially, s36 is localized in the VM, but during chorion formation, s36 relocates to the chorion. Interestingly, s36 and related proteins are found only in a sub-group of dipterans excluding mosquitoes. This suggests rapid evolution of chorion composition and assembly in insects.

Regarding gene expression, while *s36*, *s38* and *femcoat* are expressed when the inner chorionic layer and endochorion are being produced, the genes *s15*, *s16*, *s18*, *s19* are expressed later, when the exochorion is secreted (Parks and Spradling 1987; Kim et al 2002). Some of those genes are clustered on chromosomes X and 3 and high levels of their expression are ensured by a process of gene amplification through local DNA replication (Swevers et al. 2005; Cavaliere et al. 2008).

One of the first genetically identified factors needed for chorion assembly involve the defective chorion-1 (*Dec-1*) (Hawley and Waring 1988; Waring et al. 1990). Mutations in *dec-1* gene in the fruit fly cause female sterility. The *Dec-1* locus codes for three alternatively spliced proproteins, c106, fc125, and fc177, that are processed in the extracellular space giving rise to five distinct proteins (Noguerón and Waring 1995; Noguerón et al. 2000). These proteins display a complex localization behavior. Some localize to the VM before they gradually penetrate into the chorion. Some others end up in the endochorionic spaces or enter the oocyte. The isoform fc177 was shown to affect the correct spatial localization of endochorionic proteins during assembly thereby controlling eggshell morphology. The domain structure of fc177 suggests that it is involved in formation of cavities in the tripartite endochorion (Mauzy-Melitz and Waring 2003). The function of Dec-1 is conserved within the *Drosophila* genus (Badciong et al. 2001). It is noteworthy that Dec-1 proteins were identified in mollusks of the genus *Aplysia* indicating that they are conserved among invertebrates (Cummins and Nagle 2005).

Eggs silenced for *femcoat* through dsRNA present a malformed endochorion where the pillars are absent or are sparse (Kim et al. 2002). There are other known genes coding for minor proteins required for eggshell formation (Swevers et al. 2005; Papantonis et al. 2015), as new putative genes associated with choriogenesis were recently described.

Further information regarding *D. melanogaster* eggshell proteins and genes was obtained through proteomic and transcriptome analysis. By mass spectrometry, Fakhouri et al. (2006) isolated 46 proteins in eggshell matrix preparations. Together with previously known eggshell factors and proteins (e.g., Dec-1, s36, s38, VM32E and VM34C) some new and unknown proteins were found. Moreover, microarray experiments with follicle cells during eggshell production identified 150 genes expressed specifically in this tissue (Tootle et al. 2011). Thirty of these genes code for known eggshell proteins such as Dec-1, s36 and VM34C, while another 19 are putative chorion genes. The remaining 100 genes were proposed to be involved in eggshell maturation. To evaluate the significance of these genes, their expression profiles were determined in wild-type and *peroxinectin-like* (*pxt*) mutant flies. In *pxt* ovaries, most of these genes were expressed prematurely. The authors conclude that Pxt, a cyclooxygenase, synchronizes egg maturation and eggshell production. These data, thus, indicate that the eggshell communicates with follicle cells thereby controlling its own production. The data obtained with the proteome and transcriptome analyses partially overlap, underlining the robustness of these approaches.

9.2.6.2 *Bombyx mori*

In *B. mori*, only two genes coding for VM proteins are described. The genes *BmVMP30* and *BmVMP90* are expressed at late vitellogenesis and early choriogenesis stages (when the VM is being produced) and their silencing by antisense oligoDNA affects the integrity of the follicular epithelium. Both proteins are localized specifically in the VM. *BmVMP90* shares only minor similarity to the *D. melanogaster* VM proteins *sV17* and *sV23* (Kendirgi et al. 2002; Sdralia et al. 2012). A third gene was putatively associated with VM formation: *BmEP80* is expressed in follicle cells at late vitellogenesis and early choriogenesis stages. RNAi for this gene resulted in eggs that collapsed during early embryogenesis and the hatching rate was affected when the eggs were kept at low relative humidity conditions (Xu et al. 2011). The proteins *BmEP80* and *BmVMP90* share 97.4% identity and they might be the same gene with strain polymorphisms (Sdralia et al. 2012). Another hypothesis is that these genes duplicated recently; the fact that both genes have a slightly different period of expression (Xu et al. 2011; Sdralia et al. 2012) favors this hypothesis.

The genes that are known to be involved in choriogenesis are classically located in two clusters in chromosome 2: Ch1-Ch2 and Ch3. These genes belong to the same superfamily of chorion genes that is subdivided in two branches, coding for A-type or B-type proteins (also named α and β branches). The A-type branch is composed of the gene families *ErA*, *A* and *HcA*, and the B-type branch is composed of the gene families *ErB*, *B* and *HcB*. It is believed that all six gene families originated from a single common ancestor since their proteins have a conserved central domain. Many of these chorion genes occur in pairs within the chromosome: each *ErA* gene is paired with an *ErB* gene (*ErA/ErB*) and the same pattern occurs for *A/B* and *HcA/HcB* genes. Genes of a couplet are located in opposite strands with a common bidirectional promoter region of approximately 300 base pairs. The two genes in each pair are transcribed coordinately. Moreover, *ErA/ErB* genes are expressed during early choriogenesis while *A/B* and *HcA/HcB* genes are expressed during middle and late choriogenesis, respectively (Regier and Kafatos 1985; Lecanidou et al. 1986; Spoerel et al. 1989; Goldsmith 1989; Swevers et al. 2005; Papantonis et al. 2015; Chen et al. 2015a).

In a recent publication, the chorion locus of chromosome 2 was re-analyzed and 127 chorion genes were annotated (Chen et al. 2015b). These genes code for low-molecular weight proteins that are expressed during early (36 genes), mid (46 genes) and late (45 genes) stages of choriogenesis. They are arranged in clusters probably sharing distinct regulatory sequences. The late chorion proteins, which are particularly rich in cysteines (such as *HcA/HcB*), are needed for maturation of the chorion by crosslinking. Like in *D. melanogaster* (see above), the genes of this locus are expressed sequentially, and after expression of VM genes such as *BmVM30*.

9.2.6.3 Mosquitoes

In *A. aegypti* the following genes coding for vitelline membrane proteins were described: VMP 15-a1, 15a2, 15a3, AAEL006670, AAEL017471 and AAEL0017501, all of which contain the conserved hydrophobic domain common to members of the VMP family. While AAEL017471 is expressed with 48 h after blood meal (period related with exochorion formation) all the other genes are transcribed earlier, within 24–36 h after the blood meal, when the VM and endochorion are secreted (Clements 1992; Edwards et al. 1998; Marinotti et al. 2014). Since AAEL017471 is the only gene with late expression, it was postulated to have a similar function to *VM32* in *D. melanogaster*. In addition, putative cysteine rich chorion proteins (CRPs) that share distinct sequence signatures, odorant and chitin binding proteins (OBPs, CBPs) were isolated. CBPs suggest that chitin may play a role in the construction of the eggshell matrix (Sect. 9.2.9); OBPs are proposed to function as transporters of crosslinking substrates. Several enzymes previously suspected or characterized as eggshell factors including peroxidases, phenoloxidases, laccases, dopachrome conversion enzymes, and transglutaminases were also detected (Marinotti et al. 2014). In the African malaria mosquito *Anopheles gambiae*, only two putative vitelline membrane genes are transcribed, AGAP002134-RA and AGAP008696-RA, at 24 h after blood meal (Amenya et al. 2010).

9.2.6.4 *Blattella germanica*

In *B. germanica* a suppression subtractive hybridization cDNA library found 34 sequences, with 15 homologs of known genes in other insects and 19 sequences without homology. Some of these 15 genes are putatively related with chorion formation, such as *yellow-g*, associated with VM crosslinking (Irles et al. 2009a). Two of the novel predicted genes, *Brownie* and *Citrus*, were further studied and found to be specifically transcribed between middle and late choriogenesis (Irles et al. 2009b; Irles and Piulachs 2011). *Brownie* is expressed in the whole follicular epithelium with a more concentrated expression in follicle cells located at the anterior pole. RNAi for this gene impairs the formation of the sponge-like body of the eggshell and the keel of the ootheca, structures with aeropyle and micropyle-associated functions. *Brownie* is also necessary for ootheca tanning: while control oothecae darken in 5–6 h, those silenced for *Brownie* takes 6–7 days to darken (Irles et al. 2009b). The *Citrus* protein is composed of a motif repeated 33 times that is rich in glycine, tyrosine, proline and glutamic acid residues but lacks cysteines. Females silenced for *Citrus* did not produce ootheca, the eggs are fragile, and while the eggshell has all layers both the endochorion and exochorion structures are compromised: endochorion pillars are taller while the external layers (outer endochorion with exochorion) are thinner when compared to normal eggs. A relation of *Citrus* with egg impermeability is also suggested (Irles and Piulachs 2011). Interestingly there are no sequences similar to *Citrus* deposited in public databases, suggesting that it might be confined to insect species with panoistic ovaries.

9.2.7 Regulation of Eggshell Gene Expression

Formation of the eggshell requires coordinated gene expression since the whole process takes place in a relatively short period and, as cited above, distinct genes are necessary for different eggshell layers. While the VM is produced at the end of the vitellogenesis stage, the other eggshell components are subsequently produced at the choriogenesis stage. This vitellogenesis to choriogenesis transition is regulated by changes in levels of ecdysteroids (Swevers et al. 2005; Papantonis et al. 2015). The formation of the VM is dependent upon 20-hydroxyecdysone signaling, as was demonstrated in *in vitro* assays with *B. germanica* and *A. aegypti* (Raikhel and Lea 1991; Belles et al. 1993). However, in the tobacco budworm, *Heliothis virescens*, *in vitro* assays showed that only juvenile hormone is needed to trigger the formation of the VM and other eggshell layers (Ramaswamy et al. 1990).

In *B. mori*, some *cis*-regulatory elements and transcription factors involved with chorion genes expression are known (Papantonis et al. 2015; Chen et al. 2015a). They regulate the temporal expression of chorion genes by repressing or activating the expression according to the choriogenesis stage. In the silkworm, CCAAT/enhancer binding proteins (C/EBPs), which belong to b-ZIP (basic leucine zipper) transcription factor superfamily, regulates early and middle chorion gene expression while transcription factors of the GATA β family are responsible for late chorion gene expression. Both C/EBPs and GATA transcription factors also regulates *D. melanogaster* chorion gene expression. (Sourmeli et al. 2005; Swevers et al. 2005; Papantonis et al. 2008, 2015). Despite such accumulated knowledge related to the regulation of chorion gene expression at the level of gene pair, however, our understanding of the global regulation of the chorion locus at the level of the chromosome remains elementary.

In *B. germanica*, chorion formation is related with epigenetic regulation. The trimethylation of histone 3 lysine 9 (H3K9me3) is mediated by the product of the gene *Windei*. RNAi for *Windei*, which appears to reduce H3K9me3 in the DNA of follicular cells, inhibits *Brownie*, *Citrus* and *Yellow-g* expression and prevents eggshell formation (Herraiz et al. 2014).

9.2.8 Stabilization, Sclerotization and Melanization of Eggshell Layers

Eggshell proteins are integrated into networks requiring enzymes that assist covalent protein association (i.e, crosslinking). These proteinaceous components are essentially stabilized by three crosslinking intermolecular phenomena: disulfide bridges, di- and tri-tyrosine covalent bonds, and quinone-based sclerotization. In eggs of certain insects like *A. aegypti*, tyrosine-based melanization occurs, a process that is partially similar to the sclerotization pathway (Chap. 6). While in some species such as *D. melanogaster* and the kissing bug *Rhodnius prolixus* these

crosslinking occurs before oviposition when eggs are still in the ovary, in other species such as mosquitoes this process occurs within 2 h after the eggs are laid, concomitantly with chorion melanization (Christophers 1960; Mindrinos et al. 1980; Margaritis 1985a). In addition to these covalent proteins associations, some eggshell proteins such as Dec-1 and the VM proteins are modified post-translationally and these modifications are necessary for eggshell stabilization.

9.2.8.1 Crosslinking via Disulfide Bonds

Crosslinking via disulfide bonds is common in stabilizing chorionic proteins that are relatively rich in cysteine residues (Kafatos et al. 1977). Stabilization of chorionic proteins in odonates, lepidopterans and coleopterans occurs mainly by disulfide bonds (Margaritis 1985a; Regier and Wong 1988). The reversible disulfide bonding by reductive enzymatic activity, which involves the evolutionary conserved cysteines in *D. melanogaster* VM proteins, suggests its role in retaining flexibility to ease mechanical pressures during oviposition (Wu et al. 2010).

9.2.8.2 Hardening via Di- and Tri-Tyrosine Crosslinking

A major class of enzymes related with eggshell stabilization are peroxidases. These enzymes catalyze oxidation of tyrosine residues that form di- and tri tyrosine bridges between extracellular chorion proteins leading to eggshell hardening. Hydrogen peroxide (H_2O_2) is essential to trigger and carry out such crosslinking via interaction of tyrosine radicals formed by one electron oxidation of neighboring tyrosine residues on proteins (Chapman 2013).

Peroxidase activity was detected in *D. melanogaster* chorions (Mindrinos et al. 1980; Keramaris et al. 1991). The peroxidase Pxt is localized specifically in the ICL and the floor of the endochorion (Margaritis 1985b; Konstandi et al. 2005). Hydrogen peroxide is produced and secreted by follicular cells at the final stage of oogenesis and Pxt enzymatic activity is proposed to be important for di- and tri-tyrosine formation that occurs during chorion hardening (Margaritis 1985b; Margaritis and Keramaris 1991).

Di and tri-tyrosine were detected in chorion hydrolysates of *A. aegypti*, and peroxidase, which was released from chorion layers, was analyzed using tyrosine and hydrogen peroxide (Li et al. 1996). *A. aegypti* chorion peroxidase was isolated, purified and characterized as a heme protein (Han et al. 2000a; 2000b), and its partial peptide sequence was determined (Li et al. 2004). Crosslinking mediated by chorionic peroxidase in the mosquito occurs after oviposition (Li and Li 2006). Recently, three chorion peroxidases were identified in this mosquito (Marinotti et al. 2014).

In *R. prolixus*, the *Dual oxidase (Duox)* gene encodes a membrane-bound enzyme present in the follicle cells that contains both peroxidase and NADPH oxidase domains. Duox is responsible for generating hydrogen peroxide (H_2O_2) that

enables eggshell hardening through protein crosslinking by di-tyrosines. *RpDuoX*-silenced eggs did not produce H_2O_2 resulting in a decrease of eggshell hardening that lead to egg dehydration in low relative humidity conditions (Dias et al. 2013).

In the olive fruit fly *Bactrocera oleae* immunolocalization assays showed the presence of a chorion peroxidase in the VM and other eggshell structures in late choriogenesis (Konstandi et al. 2006). Peroxidase activity was also histochemically or cytochemically detected in chorions of *D. virilis* (Trogakos and Margaritis 1998a), *E. amygdali* (Mouzaki and Margaritis 1994) and *An. gambiae* (Amenya et al. 2010).

9.2.8.3 Sclerotization

Egg chorion sclerotization was extensively studied in *A. aegypti* (Li 1994). Hardening of mature eggs, which takes place immediately after oviposition, involves a catecholamine cascade pathway (the sclerotization process is detailed in Chap. 6). A fully sclerotized chorion of *A. aegypti* eggs is important to confer physical protection for the developing embryo (Li et al. 2004). Tyrosine is hydroxylated to dopa and dopa is decarboxylated through the action of dopa decarboxylase forming dopamine. Dopamine can be acetylated by two distinct enzymes forming *N*-acetyldopamine (NADA) and *N*- β -alanyldopamine (NBAD). NADA and NBAD can be further oxidized giving rise to reactive quinones that interact with nucleophilic groups to crosslink structural chorionic proteins (Hopkins and Kramer 1992). The presence of dopa decarboxylase required for eggshell sclerotization in another mosquito species, *Anopheles albitarsis*, was shown by Monnerat et al. (1999). This process of hardening that involves dopa decarboxylase is induced by ingestion a blood meal (Li 1994). Additionally to the above enzymes, laccase2 as one of phenoloxidase enzymes is highly expressed in the common house mosquito *Culex pipiens* eggs (Pan et al. 2009) and it is induced in the Asian tiger mosquito *Aedes albopictus* females after blood ingestion (Wu et al. 2013). Laccase2 is fundamental for both chorion melanization and sclerotization in *Aedes albopictus* (Wu et al. 2013).

9.2.8.4 Melanization

Melanization process of *A. aegypti* eggs, which initiates a dramatic change of colors from white to almost black within 90 min after oviposition (Li and Li 2006), is mediated by an alternative biochemical route. Both dopa and dopamine can be oxidized by phenoloxidase to dopaquinone and dopaminequinone, respectively. Dopaquinone and dopaminequinone are cyclized to form dopachrome and dopaminechrome on the long and complex pathway to form polymeric melanin (Li 1994). In the pathway of catecholamine metabolism, dopa decarboxylase is required for both sclerotization and melanization (see Chap. 6 for more details). As described above, dopa, which is the phenoloxidase-catalyzed hydroxylation product of

tyrosine, is decarboxylated to dopamine by dopa decarboxylase (Schlaeger and Fuchs 1974; Ferdig et al. 1996; Margaritis 1985a). Based on genome and transcriptome sequencing, enzymes such as peroxidase, phenoloxidase, laccase and dopachrome conversion enzymes were detected in *An. gambiae* (Amenya et al. 2010). These same catalytic proteins, which are known to be involved in sclerotization and melanization, were recently identified in eggshell chorion layers of *A. aegypti* (Marinotti et al. 2014).

9.2.8.5 Post-translational Modification

The enzymes Pipe and Nudel that play an essential role in *D. melanogaster* dorso-ventral patterning, are also important for eggshell assembly (LeMosy and Hashimoto 2000; Zhang et al. 2009). VM32E and Palisade depend on the sulfotransferase activity of Pipe (Zhang et al. 2009). Proteolytic processing of sV17 and sV23 depends on the protease activity of Nudel (LeMosy and Hashimoto 2000) that was also identified in the proteomics approach by Fakhouri et al. (2006). The proteases processing other proteins such as Dec-1 await identification.

9.2.9 Is There Chitin in the Eggshell?

Chitin is a major and essential component of invertebrate cuticular or peritrophic membrane matrices. In Chaps. 2, 3 and 8, the role of chitin in these structures is extensively described. In the crustacean *Daphnia magna* resting eggs, chitin was claimed to be detected suggesting that it may be a common component of arthropod eggshells (Kaya et al. 2013). A protein similar of peritrophins that binds to midgut chitin fibers was identified during oocyte development in the marine shrimp *Penaeus semisulcatus* (Khayat et al. 2001). In insects, genes expressing chitin-binding proteins were identified in the follicle cells of *R. prolixus* (Medeiros et al. 2011) and *A. aegypti*. In this mosquito species, proteins with chitin binding domains or chitinase domains were found as constituents of the eggshell (Sect. 9.2.6.3) (Marinotti et al. 2014). These data allow a speculation that chitin is an important scaffold material in eggshells like it is in the cuticle. The eggshell of *A. aegypti* was reported to contain a chitin-like polysaccharide (Moreira et al. 2007). However, the authors do not exclude the possibility that the detected chitin is from the serosal cuticle in *A. aegypti*, as this mosquito as well as others have chitin in their serosal cuticle (Sect. 9.3.5) (Rezende et al. 2008; Goltsev et al. 2009; Farnesi et al. 2015). Essentially however, a direct and biochemical evidence for eggshell chitin is lacking.

9.3 Cuticular Egg Envelopes of Arthropods

As stated on Sect. 9.1, after being laid, eggs of arthropods must deal with a myriad of biotic and abiotic challenges that can be stressful or lethal, such as pathogen attack or temperature variations. For those species without parental care, their eggs must rely on the protection conferred solely by the eggshell maternal layers. However, during early embryogenesis a cuticular egg envelope (a composite extracellular matrix named blastodermal cuticle or serosal cuticle) is produced in many species. Blastodermal or serosal cuticles will enhance or, sometimes substitute the protection conferred by the maternal eggshell layers.

The formation of these extracellular matrices is tightly associated with the early stages of arthropod embryogenesis. After fertilization the newly formed zygote nuclei divides and, depending on the species, such divisions can be followed by total (holoblastic), partial (meroblastic) or no cleavage of the cytoplasm (when energids are formed). In all cases, a uniform cellular blastoderm is eventually formed. Subsequently the blastoderm differentiates giving rise to two anlagen: the extraembryonic and the embryonic regions. The extraembryonic region in insects is named serosa and a second extraembryonic tissue arises from the embryonic margin of this group of animals: the amnion (Fig. 9.1). While the blastodermal cuticle is produced by either the uniform or the differentiated blastoderm, the serosal cuticle is solely produced by serosal cells. Further information related to arthropod embryogenesis and extraembryonic membranes can be found elsewhere (e.g., Jura 1972; Anderson 1973; Gilbert and Raunio 1997; Chapman 1998; Machida and Ando 1998; Panfilio 2008).

During late embryogenesis some species produce embryonic cuticles, (i.e. cuticles secreted by the proper embryo) (Tiegs 1940; Dorn 1976; Konopová and Zrzavý 2005). These cuticles are shed prior to the synthesis of the nymphal/larval cuticle, which are addressed in Chap. 3.

9.3.1 Phylogenetic Relationships Among Arthropods

For a proper explanation of arthropod cuticular egg envelopes, a brief phylogenetic description is necessary. Arthropoda is a monophyletic clade comprised of four living groups: Chelicerata, Myriapoda, Crustacea and Hexapoda. Current views indicate that crustaceans are a sister group of hexapods and both constitute the clade Tetraconata (= Pancrustacea). Myriapods are the sister group of Tetraconata and both are named Mandibulata and accordingly, Chelicerates are the sister group of Mandibulata (Fig. 9.4a). The hexapods are constituted of the paraphyletic Entognatha, comprised of Collembola, Protura and Diplura, and the monophyletic Insecta (= Ectognatha) (Budd and Telford 2009; Regier et al. 2010; Giribet and Edgecombe 2012; Misof et al. 2014). Within insects, Archaeognatha is the sister

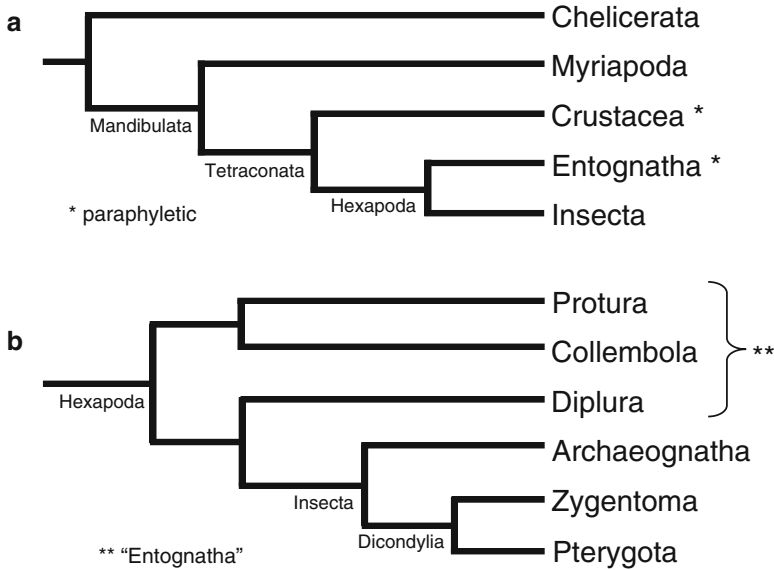


Fig. 9.4 Arthropod phylogeny. Current scheme of phylogenetic relationships among (a) arthropods and (b) hexapods. Based on Regier et al. 2010; Giribet and Edgecombe 2012; Misof et al. 2014. Crustaceans and entognathans are considered as paraphyletic taxa

group of Dicondylia while in Dicondylia the wingless Zygentoma is the sister group of all winged insects (Pterygota) (Misof et al. 2014) (Fig. 9.4a, b).

9.3.2 Blastodermal Cuticle in Non-insect Arthropods

In arthropods belonging to the Chelicerata, Myriapoda, Crustacea and Entognatha groups, the presence of a blastodermal (also blastoderm or blastodermic) cuticle is described. While in some species the blastodermal cuticle is produced by the uniform blastoderm (Fig. 9.5a), in other species this cuticle is produced by the differentiated blastoderm (extraembryonic tissue+embryo) (Fig. 9.5b) (Jura 1972; Machida 2006). There are few descriptions of blastodermal cuticles in chelicerates, myriapods and crustaceans. Identification of this structure in some cases (especially in crustaceans) is difficult due to lack of nomenclature standardization (Anderson 1973; Machida et al. 2002).

In chelicerates a blastodermal cuticle was described in a Xiphosura horse-shoe crab (Sekiguchi 1960 quoted in Anderson 1973). In myriapods from the classes diplopods, symphyla and pauropods the blastodermal cuticle is described as “thin but highly resistant” and “is a major barrier to the penetration of reagents into the egg during histological treatment” (Anderson 1973). Tiegs (1940) states that the blastodermal cuticle of *Hanseniella agilis* is “impermeable to watery stains” and the

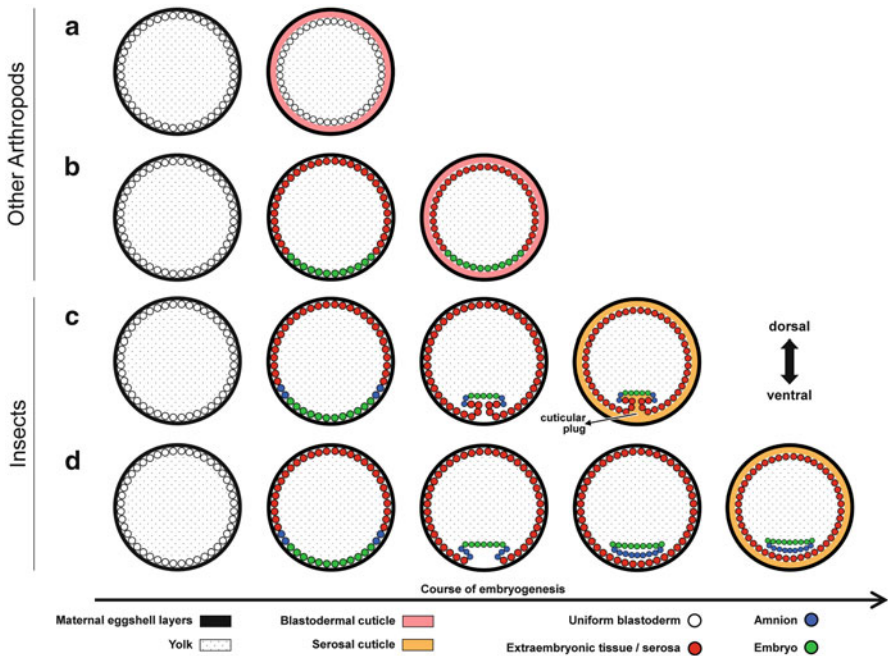


Fig. 9.5 Dynamics of cuticular egg envelope formation during early embryogenesis in arthropods. Schematic drawing of embryonic cross-sections. (a) In Chelicerata, Myriapoda, Crustacea and Entognatha a blastodermal cuticle is produced by the cells of the uniform blastoderm or (b) cells of the differentiated blastoderm, comprising the embryo and the extraembryonic region (named serosa by some authors). (c) In Archeognatha and occasionally in Zygentoma after blastoderm differentiation the embryo sinks into the yolk but the serosa does not fuse ventrally. In this case, a serosal cuticle with a cuticular plug is produced. (d) In Pterygota and often in Zygentoma, after the embryo sinks into the yolk the serosa fuses ventrally and a uniform serosal cuticle is secreted. For the sake of simplicity, the primary dorsal organ is not depicted. Inspired in schemes presented by van der Zee et al. 2005 and Machida 2006

one from *Pauropus silvaticus* (Tiegs 1947) is “a very thin and perfectly smooth membrane, without any surface-sculpture. Unlike the chorion, it resists boiling with caustic soda” suggesting the presence of chitin (Campbell 1929). There is also the description of a blastodermal cuticle in chilopods (Knoll 1974, quoted in Machida and Ando 1998) and in crustaceans, a blastodermal cuticle was described in some species (Machida et al. 2002), including the parasitic pentastomid *Raillietiella sp.* (Stender-Seidel and Thomas 1997).

Regarding entognathans (Collembola, Protura and Diplura), the blastodermal cuticle is better described in collembolans. Jura (1972) and Anderson (1973) mention the existence of a blastodermal cuticle in a vast number of collembolan species. In some species, a second, or even third or fourth blastodermal cuticles are produced and, in many species, the chorion ruptures after blastodermal cuticle formation (Jura 1972). In the giant springtail *Tetradontophora bielansensis*, the first blastodermal cuticle is relatively thin and smooth, while the second blastodermal cuticle is

wrinkled. After formation of both cuticles the chorion ruptures, and then, the vitelline membrane becomes the outermost eggshell layer (Jura et al. 1987). In *Tomocerus ishibashii* the smooth chorion is ruptured by the formation of a highly sculptured first cuticle (with four spines at the dorsal side of the egg and the occurrence of many button, cone and seta-like projections throughout the majority of its surface). Later, a smooth and thinner second cuticle is also formed (Uemiya and Ando 1987). Description of embryonic aspects in Protura, however, are very scarce (Jura 1972), and a single investigation depicts *Baculentulus densus* (Fukui and Machida 2006; Machida 2006) in which the secretion of the blastodermal cuticle is described occurring right after blastoderm differentiation. Regarding diplurans, Tieggs (1942) describes the presence of a blastodermal cuticle in *Campodea fragilis* but does not mention its formation process. A detailed account of blastodermal cuticle formation in the two-pronged bristletail *Lepidocampa weberi* is given by Ikeda and Machida (2001) where this cuticle has diverse alternating regions with differing electron density that resembles the insect serosal cuticle structure (Sect. 9.3.4).

9.3.3 Presence and Formation of Serosal Cuticle in Insects

Given that species from all non-insect arthropod clades produce a blastodermal cuticle, the production of a cuticle solely by the extraembryonic serosa is considered an insect innovation (apomorphy). This could have occurred due to the loss of capacity to secrete a cuticle by undifferentiated blastoderm cells or embryonic cells of the differentiated blastoderm (Machida and Ando 1998). Therefore it is necessary that serosal cells envelop the embryo in order to synthesize its cuticle (see below).

Serosal cuticle descriptions were reported in species of the following insect orders: Archaeognatha (Machida et al. 1994), Zygentoma (Masumoto and Machida 2006), Ephemeroptera (Tojo and Machida 1997), Zoraptera (Mashimo et al. 2014), Dermaptera (Chauvin et al. 1991) Plecoptera (e.g., Miller 1939, 1940), Orthoptera (e.g., Slifer 1937), Grylloblattodea (Uchifune and Machida 2005), Embioptera (Kershaw 1914), Phasmatodea (Jintsu et al. 2010), Isoptera (Striebel 1960 quoted in Anderson 1973), Thysanoptera (Heming 1979; Haga 1985), Hemiptera (e.g., Miura et al. 2003), Psocodea (Hinton 1977), Coleoptera (e.g., Lincoln 1961), Lepidoptera (e.g., Chauvin and Barbier 1979) and Diptera (e.g., Beckel 1958).

After blastoderm differentiation, the embryo rudiment sinks into the yolk and the serosa completely wraps the embryo, and forms its cuticle. However, in Archaeognata the serosa does not fuse beneath the embryo and a cuticular plug is produced (Machida et al. 1994) (Fig. 9.5c). With the exception of Zygentoma, the serosa in all other dicondylian insects (i.e. the pterygotes, see Fig. 9.4b) becomes a continuous sheet that secretes a uniform cuticle (e.g., Machida 2006) (Fig. 9.5d). In the silverfish *Lepisma saccharina* (Zygentoma) an interesting feature was described: while in 68% of analyzed embryos a continuous cuticle is present (Fig. 9.5d), in 32% of

them the serosa does not fuse ventrally and then a cuticular plug is present, as in Archaeognatha (Fig. 9.5c) (Masumoto and Machida 2006).

Although serosal cuticle presence occurs throughout insect taxons, some species lack this structure. The most conspicuous example is *D. melanogaster*, which does not possess serosa and amnion but rather a derived amnioserosa and no serosal cuticle (Panfilio 2008). The amnioserosa (and lack of serosal cuticle) evolved in the higher Cyclorrhapha (Schizophora) lineage (Schmidt-Ott 2000; Rafiqi et al. 2008). Exceptions also occur in hemipteran species like the milkweed bug *Oncopeltus fasciatus* that despite having serosa and amnion, does not produce a serosal cuticle (Dorn 1976). The sexually-produced eggs of the pea aphid *Acyrtosiphon pisum* have a serosal cuticle, whereas the parthenogenetic embryos, which develop within the ovarioles of the mother, have a reduced serosa and lack a serosal cuticle (Miura et al. 2003).

In the tobacco hornworm *Manduca sexta*, the serosa produces another extracellular matrix, the serosal membrane, after the serosal cuticle secretion is completed (Lamer and Dorn 2001). The authors describe this membrane as possessing uncommon physical characteristics being “tough, rubbery” and “extremely elastic, tear-proof and somewhat gluey”.

9.3.4 Serosal Cuticle Structure

Contrary to the extensive description of serosal cuticle existence throughout the class Insecta, a detailed characterization of its structure can be found in species confined to few orders: Archaeognatha, Dermaptera, Orthoptera, Coleoptera and Lepidoptera.

According to Machida and Ando (1985) and Machida et al. (1994), the serosal cuticle of the archeognathan *Pedetontus unimaculatus* is a three-layered structure. It is important to mention that in the Machida and Ando communication, these serosal cuticle layers are misnamed ‘blastodermic cuticles’. The first layer is 2–4 μm thick and is deposited facing the chorion. It is initially light brown and darkens, changing the egg color from orange to dark brown probably due to melanization (Sects. 9.2.8.4 and 9.3.5, Chap. 6). The apical surface has polygonal structures with pointed processes at the center of each polygon. A hyaline sheet named coating layer is deposited at the apical surface of this first layer. Subsequently, the electron-lucent homogeneous second layer of 4–8 μm thickness is deposited below, followed by a 5–10 μm thick third layer. The third layer has a laminar organization similar to the one found in the serosal endocuticle of other insects (see below). The cuticular plug is comprised of the second and third layers of the serosal cuticle (Machida and Ando 1985; Machida et al. 1994).

In most pterygotes, the serosal cuticle is comprised of a thin outermost epicuticle with a thickness of about 1 μm and a thick lamellate and fibrous endocuticle (also named procuticle), synthesized after epicuticle formation (Fig. 9.6), with thickness ranging from 1.6 to 22 μm , depending on the species. It is worth mentioning that

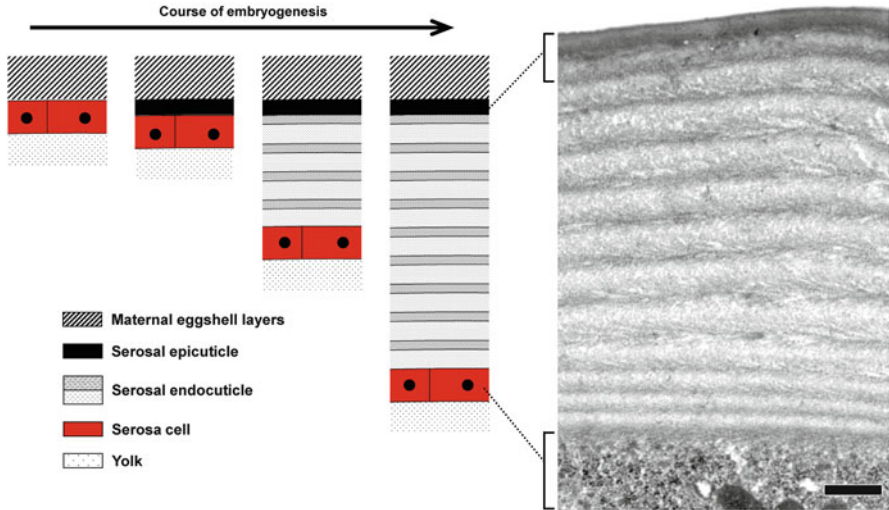


Fig. 9.6 Structure and dynamics of serosal cuticle deposition in pterygote insects. *Left*: Cartoons depicting the stepwise secretion of serosal cuticle layers. A thin epicuticle is produced below the maternal eggshell layers produced during oogenesis. Subsequently, a thick endocuticle composed of various lamellae is gradually deposited. *Right*: Transmission electron micrograph of a serosal cuticle from *Tribolium castaneum* composed of 12 endocuticle sheets (courtesy of M. van der Zee). Other endocuticle lamellae will be further added as embryogenesis progresses. Scale bar=0.5 μm

Eleanor Slifer, in her seminal communication from 1937, named the serosal epicuticle and endocuticle, respectively, ‘yellow cuticle’ and ‘white cuticle’. The serosal epicuticle and endocuticle resemble the epicuticle and procuticle layers of post-embryonic integuments of insects (Chap. 3) (Chapman 1998). Apart from these similarities, the epicuticle structure varies among species, as well as the thickness of both serosal epicuticle and endocuticle (Table 9.1). In all cases observed, the endocuticle is comprised of a stratified, lamellate structure with regions of alternating electron densities. Number of lamellae varies between 7 and 90, and layer thickness may differ in a single species, depending on the methodology of sample preparation and analysis (see the case with the house cricket *Acheta domesticus*, Table 9.1).

In *R. prolixus* a thin layer of less than 1 μm thick is produced by the serosa (Beament 1949). The author names it the “epembryonic membrane” but its description falls within serosal epicuticle depictions reported in other species. The endocuticle is the only serosal cuticle layer that contains chitin (see below), and it seems that this bug lacks this layer: an analysis of chitin presence or formation through dye labeling, gene expression and gene silencing indicates that the first chitin-containing cuticle produced during *R. prolixus* embryogenesis is an embryonic cuticle (Souza-Ferreira et al. 2014). The presence of a two-layered serosal cuticle has not been described in mosquitoes, although preliminary results indicate that this is indeed the case (Beckel 1954; Farnesi, personal communication).

Table 9.1 Physical features of serosal cuticle layers from pterygote insects

Order	Species	Epicuticle		Endocuticle		Reference
		Thickness (µm)	Details	Thickness (µm)	Lamellae number	
Dermoptera	<i>Forficula auricularia</i>	0.02	–	2	–	Chauvin et al. (1991)
Orthoptera	<i>Melanoplus differentialis</i>	1	Two regions, innermost very thin (0.02 µm) and very electron dense	15–20	≥14	Slifer (1937); Slifer and Sekhon (1963)
	<i>Acheta domesticus</i> ^a	0.4	–	8–10	–	McFarlane (1960)
	<i>Acheta domesticus</i> ^b	0.1	Five regions, alternating electron lucent and electron dense zones	22	30–40	Furneaux et al. (1969)
Lepidoptera	<i>Manduca sexta</i>	0.3	An outer electron dense region and an inner electron lucent region	2	7–9	Lamer and Dorn (2001)
Coleoptera	<i>Listronotus oregonensis</i>	n.m.	–	10–13	90	Nenon et al. (1995)
	<i>Tribolium castaneum</i>	0.4	An outer electron dense region and an inner electron lucent region	1.6	14	Chaudhari et al. (2015)

^aObserved through frozen sections and light microscopy

^bObserved through electron microscopy

n.m. not mentioned

9.3.5 Serosal Cuticle Biochemical Constitution

The serosal epicuticle contains protein and is generally believed to be also composed of lipids and waxes, whereas the serosal endocuticle is made of chitin and proteins. Most likely, sclerotization-related substances are also present in both layers. There is little definitive evidence regarding serosal cuticle composition, although recent genetic evidences corroborate earlier descriptions.

The serosal epicuticle of *A. domesticus* is considered as a ‘lipoid layer’, since it is hydrophobic, stains with Sudan dyes and is intensely osmiophilic (McFarlane 1960; Furneaux et al. 1969). It contains proteins that after hydrolysis yield all aminoacids except methionine, hydroxyproline and tryptophan. It is noteworthy that “readily available” amounts of phenylalanine and tyrosine are observed (McFarlane 1962), whereas these are precursors of both melanization and sclerotization pathways (Chap. 6, Hopkins and Kramer 1992). The serosal epicuticle of *R. prolixus* (epembryonic membrane, see above) is described as being “probably proteinaceous with tanning substances” and impregnated with a wax-like substance (Beament 1949). Indirect evidence suggests that *A. aegypti* serosal cuticle contains a wax layer (Harwood and Horsfall 1959).

The serosal endocuticle of *A. domesticus* contains proteins with amino acid composition similar to the one observed for its epicuticle (McFarlane 1962). Chitin presence in the serosal endocuticle has been described in two orthopteran species, the differential grasshopper *Melanoplus differentialis* and *A. domesticus*, through chemical procedures that reacted positive to chitin (Campbell 1929; Jahn 1935; McFarlane 1960). However, due to inconsistency among different methods, Jahn raises the issue about chitin specificity of these methods (Jahn 1935). In any case, gene silencing experiments confirmed chitin presence in *T. castaneum* serosal endocuticle (see below) (Jacobs et al. 2013). Although not being localized specifically to its endocuticle, chitin presence in the serosal cuticle is mentioned in zygentoman species (Jura 1972) and detected in mosquitoes of the genera *Aedes*, *Culex* and *Anopheles* through chemical methods or lectin labeling (Beckel 1958; Rezende et al. 2008; Goltsev et al. 2009; Farnesi et al. 2015).

In the orthopterans *A. domesticus* and the two-striped grasshopper *Melanoplus bivittatus* the molecules dopa, dopamine and NADA, related with both melanization and sclerotization pathways (Sects. 9.2.8.3 and 9.2.8.4, Chap. 6) (Hopkins and Kramer 1992) are exclusively found in the serosal cells and the serosal cuticle. However, their specific presence in either serosal epicuticle or endocuticle was not investigated (Furneaux and McFarlane 1965a, b). The serosa and serosal cuticle of *A. domesticus* also possess an enzyme that can melanize both structures, when stimulated (McFarlane 1960). Since the serosa and serosal cuticle of this cricket do not darken, this enzyme might physiologically participate in the sclerotization pathway.

Finally, gene expression analyses in *An. gambiae* and *T. castaneum* also point to the presence of chitin, wax-like and tanning agents in serosal cuticle composition (see below).

9.3.6 *Hormonal and Genetic Processes Related with Serosal Cuticle Formation*

Ecdysteroids are involved in serosal cuticle formation, similarly to their involvement in post-embryonic cuticle synthesis (Chapman 1998). Follicle cells of the migratory locust *Locusta migratoria* produce ecdysteroids during ovarian

development. These are introduced into the oocyte as inactive conjugated polar compounds (Lagueux et al. 1977). At the onset of serosal cuticle formation, there is a peak of expression of ecdysone (an active form of ecdysteroid) in serosal cells (Lagueux et al. 1979). Most likely, ecdysone autocrinally triggers cuticle production in serosal cells (Goltsev et al. 2009). Descriptions of effector genes expression in the serosa are few and recent (see below). In a broad sense, the molecular evidence corroborates previous biochemical findings that the serosal cuticle is composed of lipids or wax, chitin, proteins and sclerotization-related molecules. However, structural evidence exists only for the presence of chitin.

The first report of a gene putatively associated with serosal cuticle formation is *Chitin synthase 1* (also named *Chitin synthase A*) in the mosquito *A. aegypti*. This gene is related to chitin production (Moussian et al. 2005a) and has two alternative splicing forms: *Chs1a* and *Chs1b*. While both splice forms are expressed at late embryogenesis for larval cuticle synthesis, only *Chs1a* is expressed in eggs at the moment of serosal cuticle formation (Rezende et al. 2008). Beyond that, information regarding genes associated with serosal cuticle production comes from studies carried out in *An. gambiae* and *T. castaneum*.

During early *An. gambiae* embryogenesis, prior to the secretion of its cuticle, the serosa gets intimately associated with the endochorion. After egg fixation the eggshell-associated serosa is manually separable from the embryo. A microarray gene expression profile comparison of these two isolated samples (embryo and serosa), identified 359 candidate transcripts as being “serosa-specific” (Goltsev et al. 2009). In the same study, *in situ* hybridizations confirmed serosal expression of the following genes: *Chs1*, *serpentine* – related with chitin microfibrils organization (Luschning et al. 2006), *Dopa decarboxylase* and *Tyrosine hydroxylase* – related both with sclerotization and melanization pathways (Hopkins and Kramer 1992), and *Elovl1*, presumably related with wax production (Vasireddy et al. 2007). The expression of *knickopf* (*knk*), necessary for proper chitin deposition (Moussian et al. 2006), was evaluated throughout *An. gambiae* embryogenesis (Goltsev et al. 2009). It was suggested that *knk* is expressed in the serosa of this mosquito, and later, this was confirmed in *T. castaneum* (see below). Most of the cuticle genes detected in *An. gambiae* serosa present a biphasic expression: at early embryogenesis, related with serosal cuticle formation and at late embryogenesis, associated with larval cuticle synthesis. The existence of a cuticle gene battery employed for the production of both cuticles during embryogenesis was suggested. This gene battery would also be used for post-embryonic cuticle production (Goltsev et al. 2009).

It is possible to silence *T. castaneum* genes in the egg through dsRNA-mediated RNAi targeted against the desired transcript (van der Zee et al. 2005). With this approach the following cuticle-related genes were silenced in the egg: *Chs1*, *Knk1*, *retroactive* (*rtv*), important for the correct organization of chitin filaments (Moussian et al. 2005b) and *Laccase2* (*Lac2*), related with melanization and sclerotization (Arakane et al. 2005). Absence of *Chs1* affects the inner serosal cuticle layer: instead of the organized lamellate structure, the serosal endocuticle becomes an amorphous layer, most likely composed solely of structural proteins (see below). Absence of *Knk1* and *Rtv* shows a similar pattern but in these cases the amorphous

serosal endocuticle might also contain disorganized chitin molecules. In all cases the serosal epicuticle remains intact (Jacobs et al. 2013, 2015; Chaudhari et al. 2015). *Lac2* silencing does not affect neither serosal epicuticle nor endocuticle structures although it interferes with the serosal cuticle physiological role (see below) (Jacobs et al. 2015).

It is feasible to generate *T. castaneum* eggs without a serosa through RNAi aiming the transcription factor *zerknüllt 1* (*Zen1*) (van der Zee et al. 2005). These serosa-less eggs do not produce a cuticular egg envelope but develops normally and are viable under standard conditions (Jacobs et al. 2013). A comparison between the transcriptome profile of late embryos with and without serosa was performed (Jacobs et al. 2015). Twelve genes coding cuticular proteins that are putatively associated with serosal cuticle formation were identified: three proteins annotated as “cuticle protein-like”, seven proteins containing peritrophin domains and two new uncharacterized proteins containing chitin binding motifs.

9.3.7 Physiological Role of the Serosal Cuticle

Serosal cuticle formation is related to water balance alterations in insect eggs. There are differences regarding how the dynamics of egg water flow occurs among species, one of the aspects being if extra water is required for egg development after it is laid (Wigglesworth 1972; Hinton 1981). In any case, the general perspective is the same: complete serosal cuticle formation leads to a decrease in egg water permeability.

Eggs of some species are laid in moist environments, but during early embryogenesis they do not absorb water. In crickets and grasshoppers the egg commences to uptake water and increases in length, width, volume and weight only after the serosa surrounds the developing embryo (McFarlane and Kennard 1960; Chapman 1998; Donoughe and Extavour 2015). The rate of water loss increases considerably during this period if eggs are transferred to desiccating conditions. The period associated with water uptake is concomitant with serosal cuticle generation: serosal endocuticle complete formation and serosal cuticle sclerotization coincide with the finalization of the egg water absorption phase and the decrease of water loss rate under desiccating conditions (McFarlane 1960; Hinton 1981; Chapman 1998). In some insect species, egg expansion causes the chorion to crack and the vitelline membrane becomes the outermost egg envelope (Wigglesworth 1972; Hartley 1962; Hinton 1981), similar to the chorion rupture that occurs with some collembolans (see Sect. 9.3.2). With respect to lepidopteran species, a similar pattern was described in the fairy moth *Nemophora albiantennella* (Kobayashi 1998): commencement and finalization of egg water uptake are correlated with serosal envelopment of the embryo and complete formation of the serosal cuticle, respectively.

Eggs of other insect species are laid in moist environments and water uptake starts way before the serosa surrounds the embryo. Water uptake in eggs of the Devil’s coach-horse beetle *Ocyptus olens* commences shortly after they are laid. The

water uptake period ceases with serosal cuticle formation and, under desiccating conditions, this cuticle diminishes egg water loss (Lincoln 1961). Mosquito eggs commence to uptake water promptly after being laid (Kliewer 1961). If during this period eggs are transferred into a dry environment, they shrink in few minutes and the embryo dies (Valencia et al. 1996; Rezende et al. 2008; Goltsev et al. 2009). After serosal cuticle production, water no longer enters the egg and water loss susceptibility decreases considerably (Kliewer 1961). Serosal cuticle formation in mosquitoes is associated with the egg capacity to survive under dry conditions (Rezende et al. 2008; Goltsev et al. 2009). However, the degree of egg viability outside water varies among species, from few hours to months (Vargas et al. 2014, Farnesi et al. manuscript in preparation). Higher chitin content in mosquito serosal cuticle seems to be correlated with higher egg viability under desiccating conditions, yet other factors might also play a role in viability differences (see below) (Farnesi et al. 2015).

The serosal cuticle also increases the resistance to desiccation in species that lay eggs in relatively dry environments. In these cases, analyses are performed under artificial conditions such as (i) submitting eggs to temperatures above 40 °C to evaluate the critical temperature when wax layers (a major component limiting water loss) melts, or (ii) keeping eggs at extreme desiccating conditions, such as a 5% relative humidity (Hadley 1994; Chapman 1998). In *R. prolixus* the desiccating critical temperature raises from 42.5 °C to 68 °C after the wax-impregnated serosal epicuticle (epembryonic membrane) is formed (Beament 1949).

While all the above reports present circumstantial evidences suggesting the physiological role of serosal cuticles in increasing egg resistance to desiccation, none present functional proofs. Recently, however, RNAi experiments in *T. castaneum* paved the way to carefully confirm serosal cuticle function and the genes related with it. Silencing of *Zen1*, *Chs1*, *Knk1* and *Rtv* leads to distinct levels of serosal cuticle disruption and egg viability. When *Zen1* and *Chs1* RNAi eggs are kept at 5% relative humidity, the respective viability is 5% and 30% while about 67% viability was recorded in *Knk1*- and *Rtv*-silenced eggs kept at the same humidity. Control eggs present 80-90% viability (Jacobs et al. 2013, 2015). These differences are probably associated with the role of each gene: without *Zen1* there is neither serosa nor serosal cuticle; in eggs lacking *Chs1* both serosa and serosal cuticle exists, but are devoid of chitin; without *Knk1* and *Rtv*, serosa and serosal cuticle occurs, but most likely with disorganized chitin fibrils. The viability difference found between *Zen1* and *Chs1* RNAi eggs might be due to the presence of the serosal cells, that may have an active role in water balance, or to other serosal cuticle constituents, such as the proteins of the endocuticle or the components of the serosal epicuticle, that are not affected (Jacobs et al. 2013). Silencing of *Lac2* under desiccating conditions also led to an egg viability of about 70% (Jacobs et al. 2015). Although the sclerotization driven by Laccase2 might be relevant for serosal cuticle formation and role against desiccation, its relevance in chorion formation; or both chorion and cuticle, should also be considered.

Apart from water balance, the serosal cuticle seems to be involved in egg protection against predators. While freshly laid embryos of *M. sexta* are predated by the slit bug *Jalysus spinosus*, later ones become sheltered from this attack. Formation of

the serosal cuticle and the serosal membrane (Sect. 9.3.3) coincides with the inability of *J. spinosus* to predate the egg (Elsey 1972).

9.4 Concluding Remarks

This chapter attempted to combine classical information regarding the eggshell of insects with recent findings, embracing genetic, structural and physiological aspects. We hope to contribute with relevant information for those interested in insect eggs and eggshells, as other literature revisions have done in the past (Hinton 1981; Margaritis 1985a; Regier and Kafatos 1985; Trougakos and Margaritis 2002; Swevers et al. 2005). The increase in the number of insect species amenable to be used in the laboratory, as well as the advent of gene silencing and editing techniques allow us to predict that the genetic understanding regarding insect eggshells will flourish in the near future. In addition, the epigenetic regulation of eggshell formation is poorly understood and should also be aimed. It is of interest to understand the commonalities present throughout the insect taxa as well as the evolutionary processes related with specific taxon or species. How are specific (epi)genetic features related with the ecology of each egg? e.g., if the egg is parasitized by other insects or by microorganisms; if eggs are laid in litter, under bark, within animals or plants, in aquatic or semiaquatic habitats or other environments (Zeh et al. 1989). In addition only one species with panoistic ovaries has its (epi)genetic process of eggshell formation studied with some depth: the German cockroach *Blattella germanica* (Sects. 9.2.2.1, 9.2.6, 9.2.7). The eggs of this cockroach are encased within an ootheca that poses distinct challenges for the egg. How similar or different is the production of an egg originated from a panoistic ovary without ootheca?

This is the first time that blastodermal and serosal cuticle egg envelopes have been reviewed. While their genetics and physiology are reasonably well described in insects, nearly null information regarding these aspects exists in non-insect arthropods. In addition, to understand how the ancestral blastodermal cuticle originated the derived serosal cuticle (Sect. 9.3.3) is an interesting theme for the fields of developmental biology and evolution. This can be tackled employing species whose genes can be silenced or edited such as some spiders, crustaceans, collembolans, crickets, grasshoppers, moths and beetles.

Finally, one of the themes deserving attention is the genetics of production of lipids (or waxes) present in structures such as the chorion wax layer and the serosal epicuticle. The relevance of lipids or its derivatives for the production of waterproofing layers is well acknowledged (Hadley 1994; Chapman 1998) but there are few studies in insects showing the genetics behind it (Qiu et al. 2012) and none at the egg stage. Transcriptome analyses, such as the ones employed in *D. melanogaster* follicle cells (Tootle et al. 2011) and *An. gambiae* serosal cells (Goltsev et al. 2009), when properly followed by functional studies, might fill this gap.

References

- Akey CW, Crepeau RH, Edelstein SJ (1987) The innermost chorionic layer of *Drosophila* II. Three-dimensional structure determination of the 90° crystal form by electron microscopy. *J Mol Biol* 193:685–692
- Amenya DA, Chou W, Li J, Yan G, Gershon PD, James AD, Marinotti O (2010) Proteomics reveals novel components of the *Anopheles gambiae* eggshell. *J Insect Physiol* 56:1414–1419
- Anderson DT (1973) Embryology and phylogeny in annelids and arthropods. Pergamon Press, Oxford
- Andrenacci D, Cemilogar FM, Taddei C, Rotoli D, Cavaliere V, Graziani F, Gargiulo G (2001) Specific domains drive VM32E protein distribution and integration in *Drosophila* eggshell layers. *J Cell Sci* 114:2819–2829
- Andrew RJ, Tembhare DB (1992) Surface ultrastructure of the egg chorion in the dragonfly, *Ictinogomphus rapax* (Rambur) (Odonata, Gomphidae). *Int J Insect Morphol Embryol* 21:347–350
- Arakane Y, Muthukrishnan S, Beeman RW, Kanost MR, Kramer KJ (2005) Laccase 2 is the phenoloxidase gene required for beetle cuticle tanning. *Proc Natl Acad Sci U S A* 102:11337–11342
- Badciong JC, Otto JM, Waring GL (2001) The functions of the multiproduct and rapidly evolving *dec-1* eggshell gene are conserved between evolutionarily distant species of *Drosophila*. *Genetics* 159:1089–1102
- Beament JWL (1949) The Penetration of Insect Egg-Shells. 2. The properties and permeability of sub-chorial membranes during development of *Rhodnius prolixus* Stål. *Bull Entomol Res* 9:467–488
- Beckel WE (1954) Studies the biology of the *Aedes* of northern Canada (Culicidae). I. Preliminary investigation of development in the egg. Defence research northern laboratory technical paper no. 6. Defence Research Board, Ottawa
- Beckel WE (1958) Investigation of permeability, diapause, and hatching in the eggs of the mosquito *Aedes hexodontus* Dyar. *Can J Zool* 36:541–554
- Belles X, Cassier P, Cerda X, Pascual N, Andre M, Rosso Y, Piulachs MD (1993) Induction of choriogenesis by 20-hydroxyecdysone in the German cockroach. *Tissue Cell* 25:195–204
- Budd GE, Telford MJ (2009) The origin and evolution of arthropods. *Nature* 457:812–817
- Burkhart CN, Arbogast J, Smythe P, Butkhart CG (1999) Histochemical analysis of the nit of *Pediculus humanus capitis* (Anoplura: Pediculidae). *J Med Entomol* 30:530–532
- Campbell FL (1929) The detection and estimation of insect chitin; and the irrelation of “chitinization” to hardness and pigmentation of the cuticula of the American cockroach, *Periplaneta americana*. *L. Ann Entomol Soc Am* 22:401–426
- Cavaliere V, Bernardi F, Romani P, Duchi S, Gargiulo G (2008) Building up the *Drosophila* eggshell: first of all the eggshell genes must be transcribed. *Dev Dyn* 237:2061–2072
- Cernilogar FM, Fabbri F, Andrenacci D, Taddei C, Gargiulo G (2001) *Drosophila* vitelline membrane cross-linking requires the *fs(1)Nasrat*, *fs(1)polehole* and chorion genes activities. *Dev Genes Evol* 211:573–580
- Chapman RF (1998) The insects – structure and function, 4th edn. Cambridge University Press, Cambridge
- Chapman RF (2013) The insects – structure and function, 5th edn. Cambridge University Press, Cambridge
- Chasan R, Anderson KV (1993) Maternal control of dorsal-ventral polarity and pattern in the embryo. In: Bate M, Martinez-Arias A (eds) The development of *Drosophila melanogaster*, vol 1. Cold Spring Harbor Laboratory Press, New York, pp 387–424
- Chaudhari SS, Noh MY, Moussian B, Specht CA, Kramer KJ, Beeman RW, Arakane Y, Muthukrishnan S (2015) Knickkopf and retroactive proteins are required for formation of laminar serosal procuticle during embryonic development of *Tribolium castaneum*. *Insect Biochem Mol Biol* 60:1–6

- Chauvin G, Barbier R (1979) Morphogenese de l'enveloppe vitelline, ultrastructure du chorion et de la cuticule serosale chez *Korscheltellus lupulinus* L. (Lepidoptera:Hepialidae). *Int J Insect Morphol Embryol* 8:375–386
- Chauvin G, Hamon C, Vancassel M, Vannier G (1991) The eggs of *Forficula auricularia* L. (Dermaptera, Forficulidae): ultrastructure and resistance to low and high temperatures. *Can J Zool* 69:2873–2878
- Chen Z, Nohata J, Guo H, Li S, Liu J, Guo Y, Yamamoto K, Kadono-Okuda K, Liu C, Arunkumar KP, Nagaraju J, Zhang Y, Liu S, Labropoulou V, Swevers L, Tsitoura P, Iatrou K, Gopinathan KP, Goldsmith MR, Xia Q, Mita K (2015a) A comprehensive analysis of the chorion locus in silkworm. *Sci Rep* 5:16424
- Chen Z, Nohata J, Guo H, Li S, Liu J, Guo Y, Yamamoto K, Kadono-Okuda K, Liu C, Arunkumar KP, Nagaraju J, Zhang Y, Liu S, Labropoulou V, Swevers L, Tsitoura P, Iatrou K, Gopinathan KP, Goldsmith MR, Xia Q, Mita K (2015b) Construction, complete sequence, and annotation of a BAC contig covering the silkworm chorion locus. *Sci Data* 2:150062
- Christophers SR (1960) *Aedes aegypti* (L) the yellow fever mosquito. Its life history, bionomics and structure. Cambridge University Press, Cambridge
- Clements AN (1992) The biology of mosquitoes: development, nutrition and reproduction, vol 1. Chapman and Hall, London
- Cummins SF, Nagle GT (2005) *Aplysia* capsulin is localized to egg capsules and egg cordon sheaths and shares sequence homology with *Drosophila dec-1* gene products. *Peptides* 26:589–596
- D'Alterio C, Tran DDD, Yeung MWYA, Hwang MS, Li MA, Arana CJ, Mulligan VK, Kubesh M, Sharma P, Chase M, Tepass U, Godt D (2005) *Drosophila melanogaster* Cad99C, the orthologue of human Usher cadherin CDH15, regulates the length of microvilli. *J Cell Biol* 171:549–558
- Dias FA, Gandara AC, Queiroz-Barros FG, Oliveira RL, Sorgine MH, Braz GR, Oliveira PL (2013) Ovarian dual oxidase (Duox) activity is essential for insect eggshell hardening and waterproofing. *J Biol Chem* 288:35058–35067
- Donoughe S, Extavour CG (2015) Embryonic development of the cricket *Gryllus bimaculatus*. *Dev Biol*. doi:10.1016/j.ydbio.2015.04.009
- Dorn A (1976) Ultrastructure of embryonic envelopes and integument of *Oncopeltus fasciatus* Dallas (Insecta, Heteroptera). I. Chorion, amnion, serosa, integument. *Zoomorphologie* 85:111–131
- Edwards MJ, Severson DW, Hagedorn HH (1998) Vitelline envelope genes of the yellow fever mosquito, *Aedes aegypti*. *Insect Biochem Mol Biol* 28:915–925
- Elalayli M, Hall JD, Fakhouri M, Neiswender H, Ellison TT, Han Z, Roon P, LeMosy EK (2008) Palisade is required in the *Drosophila* ovary for assembly and function of the protective vitelline membrane. *Dev Biol* 319:359–369
- Elsey KD (1972) Defenses of eggs of *Manduca sexta* against predation by *Jalysus spinosus*. *Ann Entomol Soc Am* 65:896–897
- Fakhouri M, Elalayli M, Sherling D, Hall JD, Miller E, Sun X, Wells L, LeMosy EK (2006) Minor proteins and enzymes of the *Drosophila* eggshell matrix. *Dev Biol* 293:127–141
- Farnesi LC, Menna-Barreto RF, Martins AJ, Valle D, Rezende GL (2015) Physical features and chitin content of eggs from the mosquito vectors *Aedes aegypti*, *Anopheles aquasalis* and *Culex quinquefasciatus*: connection with distinct levels of resistance to desiccation. *J Insect Physiol* 83:43–52
- Fausto AM, Maroli M, Mazzini M (1992) Ootaxonomy and eggshell ultrastructure of *Phlebotomus* sandflies. *Med Vet Entomol* 6:201–208
- Ferdig MT, Li J, Steverson DW, Christensen BM (1996) Mosquito dopa decarboxylase cDNA characterization and blood-meal-induced ovarian expression. *Insect Mol Biol* 5:119–126
- Fisher HL, Watson J (2015) A fossil insect egg on an early cretaceous conifer shoot from the Wealden of Germany. *Cretac Res* 53:38–47

- Fletcher GC, Lucas EP, Brain R, Tournier A, Thompson BJ (2012) Positive feedback and mutual antagonism combine to polarize Crumbs in the *Drosophila* follicle cell epithelium. *Curr Biol* 22:1116–1122
- Fukui M, Machida R (2006) Embryonic development of *Baculentulus densus* (Imadaté): an outline (Hexapoda: Protura, Acerentomidae). *Proc Arthropod Embryol Soc Jpn* 41:21–28
- Furneaux PJ, Mcfarlane JE (1965a) Identification, estimation, and localization of catecholamines in eggs of the house cricket, *Acheta domesticus* L. *J Insect Physiol* 11:591–600
- Furneaux PJ, Mcfarlane JE (1965b) A possible relationship between the occurrence of catecholamines and water absorption in insect eggs. *J Insect Physiol* 11:631–635
- Furneaux PJ, James CR, Potter S (1969) The egg shell of the house cricket (*Acheta domesticus*): an electronmicroscope study. *J Cell Sci* 5:227–249
- Gautam SG, Opit GP, Margosan D, Hoffmann JS, Tebbets SW (2015) Comparative egg morphology and chorionic ultrastructure of key stored-product insect pests. *Ann Entomol Soc Am* 108:43–56
- Gilbert SF, Raunio AM (1997) Embryology: constructing the organism. Sinauer Associates, Sunderland
- Giribet G, Edgecombe GD (2012) Reevaluating the arthropod tree of life. *Annu Rev Entomol* 57:167–186
- Glowinski C, Liu RH, Chen X, Darabie A, Godt D (2014) Myosin VIIA regulates microvillus morphogenesis and interacts with cadherin Cad99C in *Drosophila* oogenesis. *J Cell Sci* 127:4821–4832
- Goforth CL, Smith RL (2011) Respiratory morphology of the *Abedus herberti* Hidalgo egg chorion (Hemiptera: Belostomatidae). *J Morphol* 272:796–801
- Goldsmith MR (1989) Organization and developmental timing of the *Bombyx mori* chorion gene clusters in strain C108. *Dev Genet* 10:16–23
- Goltsev Y, Rezende GL, Vranizan K, Lanzaro G, Valle D, Levine M (2009) Developmental and evolutionary basis for drought tolerance of the *Anopheles gambiae* embryo. *Dev Biol* 330:462–470
- Guglielmino A, Taddei AR, Carcupino M (1997) Fine structure of the eggshell of *Ommatissus binotatus* Fieber (Homoptera, Auchenorrhyncha, Tropiduchidae). *Int J Insect Morphol Embryol* 26:85–89
- Hadley NF (1994) Water relations of terrestrial arthropods. Academic Press, California, p 356
- Haga K (1985) Oogenesis and embryogenesis of the idolothripine thrips, *Bactrothrips brevitubus* (Thysanoptera, Phlaeothripidae). In: Ando H, Miya K (eds) Recent advances in insect embryology in Japan. ISEBU Co. Ltd., Tsukuba, pp 45–106
- Hamodrakas SJ, Margaritis LH, Nixon PE (1982) Crystalline layer in *Drosophila melanogaster* egg-shell: arrangement of components as revealed by negative staining and reconstruction. *Int J Biol Macromol* 4:25–31
- Han Q, Li G, Li J (2000a) Chorion peroxidase-mediated NADH/O₂ oxidoreduction cooperated by chorion malate dehydrogenase-catalyzed NADH production: a feasible pathway leading to H₂O₂ formation during chorion hardening in *Aedes aegypti* mosquitoes. *Biochim Biophys Acta* 1523:246–253
- Han Q, Li G, Li J (2000b) Purification and characterization of chorion peroxidase from *Aedes aegypti* eggs. *Arch Biochem Biophys* 378:107–115
- Hartley JC (1962) The egg of *Tetrix* (Tetrigidae, Orthoptera), with a discussion on the probable significance of the anterior horn. *Q J Microsc Sci* 103:253–259
- Harwood RF, Horsfall WR (1959) Development, structure, and function of coverings of eggs of floodwater mosquitoes. III. Functions of coverings. *Ann Entomol Soc Am* 52:113–116
- Hatzopoulos AK, Regier JC (1987) Evolutionary changes in the developmental expression of silkworm chorion genes and their morphological consequences. *Proc Natl Acad Sci U S A* 84:479–483
- Hawley RJ, Waring GL (1988) Cloning and analysis of the *dec-1* female-sterile locus, a gene required for proper assembly of the *Drosophila* eggshell. *Genes Dev* 2:341–349

- Heifetz Y, Yu J, Wolfner MF (2001) Ovulation triggers activation of *Drosophila* oocytes. *Dev Biol* 234:416–424
- Heming BS (1979) Origin and fate of germ cells in male and female embryos of *Haplothrips verbasci* (Osborn) (Insecta, Thysanoptera, Phlaeothripidae). *J Morph* 160:323–344
- Herraiz A, Belles X, Piulachs MD (2014) Chorion formation in panoistic ovaries requires Wende and trimethylation of histone 3 lysine 9. *Exp Cell Res* 220:46–53
- Hinton HE (1968) Structure and protective devices of the egg of the mosquito *Culex pipiens*. *J Insect Physiol* 14:145–161
- Hinton HE (1977) Function of shell structures of pig louse and how egg maintains a low equilibrium temperature in direct sunlight. *J Insect Physiol* 23:785–800
- Hinton HE (1981) *Biology of insect eggs*, vols I-III. Pergamon Press, Oxford
- Hopkins TL, Kramer KJ (1992) Insect cuticle sclerotization. *Annu Rev Entomol* 37:273–302
- Ikeda Y, Machida R (2001) Embryogenesis of the dipluran *Lepidocampa weberi* Oudemans (Hexapoda: Diplura, Campodeidae): formation of dorsal organ and related phenomena. *J Morphol* 249:242–251
- Irls P, Piulachs MD (2011) Citrus, a key insect eggshell protein. *Insect Biochem Mol Biol* 41:101–108
- Irls P, Bellés X, Piulachs MD (2009a) Identifying genes related to choriogenesis in insect panoistic ovaries by suppression subtractive hybridization. *BMC Genomics* 10:206
- Irls P, Bellés X, Piulachs MD (2009b) Brownie, a gene involved in building complex respiratory devices in insect eggshells. *PLoS One* 4(12):e8353
- Jacobs CG, Rezende GL, Lamers GE, van der Zee M (2013) The extraembryonic serosa protects the insect egg against desiccation. *Proc Biol Sci* 280:20131082
- Jacobs CG, Braak N, Lamers GE, van der Zee M (2015) Elucidation of the serosal cuticle machinery in the beetle *Tribolium* by RNA sequencing and functional analysis of Knickkopf1, Retroactive and Laccase2. *Insect Biochem Mol Biol* 60:7–12
- Jagadeeshan S, Singh RS (1997) Rapid evolution of outer egg membrane proteins in the *Drosophila melanogaster* subgroup: a case of ecologically driven evolution of female reproductive traits. *Mol Biol Evol* 24:929–938
- Jahn TL (1935) Nature and permeability of grasshopper egg membranes. II. Chemical composition of membranes. *Proc Soc Exp Biol Med* 33:159–163
- Jiménez G, González-Reyes A, Casanova J (2002) Cell surface proteins Nasrat and Polehole stabilize the Torso-like extracellular determinant in *Drosophila* oogenesis. *Genes Dev* 16:913–918
- Jintsu Y, Uchifune T, Machida R (2010) Structural features of eggs of the basal phasmatodean *Timema monikensis* Vickery & Sandoval, (Insecta: Phasmatodea: Timematidae). *Arthropod Syst Phylogeny* 68:71–78
- Jura C (1972) Development of apterygote insects. In: Counce SJ, Waddington CH (eds) *Developmental systems: insects*. Academic Press, London, pp 49–94
- Jura C, Krzysztofowicz A, Kisiel E (1987) Embryonic development of *Tetradontophora bielensis* (Collembola): descriptive, with scanning electron micrographs. In: Ando H, Jura C (eds) *Recent advances in insect embryology in Japan and Poland*. Arthropod Embryol Soc Jpn ISEBU Co. Ltd., Tsukuba
- Kafatos FC (1975) The insect chorion: programmed expression of specific genes. *Adv Exp Med Biol* 62:103–121
- Kafatos FC, Regier JC, Mazur GD, Nadel MR, Blau HM, Petri WH, Wyman AR, Gelinas RE, Moore PB, Paul M, Efstratiadis A, Vournakis JN, Goldsmith MR, Hunsley JR, Baker B, Nardi J, Koehler M (1977) The eggshell of insects: differentiation-specific proteins and the control of their synthesis and accumulation during development. *Results Probl Cell Differ* 8:45–145
- Kaya M, Sargin I, Tozak KÖ (2013) Chitin extraction and characterization from *Daphnia magna* resting eggs. *Int J Biol Macromol* 61:459–464
- Kendirgi F, Swevers L, Iatrou K (2002) An ovarian follicular epithelium protein of the silkworm (*Bombyx mori*) that associates with the vitelline membrane and contributes to the structural integrity of the follicle. *FEBS Lett* 524:59–68

- Keramaris KE, Stravopodis D, Margaritis LH (1991) A structural protein that plays an enzymatic role in the eggshell of *Drosophila melanogaster*. *Cell Biol Int Rep* 15:151–159
- Kershaw JC (1914) Development of an embiid. *J R Microsc Soc* 34:24–27
- Khayat M, Babin PJ, Funkenstein B, Sammar M, Nagasawa H, Tietz A, Lubzens E (2001) Molecular characterization and high expression during oocyte development of a shrimp ovarian cortical rod protein homologous to insect intestinal peritrophins. *Biol Reprod* 64:1090–1099
- Kim C, Han K, Kim J, Yi JS, Kim C, Yim J, Kim YJ, Kim-Ha J (2002) *Femcoat*, a novel eggshell protein in *Drosophila*: functional analysis by double stranded RNA interference. *Mech Dev* 110:61–70
- Kleve CD, Siler DA, Syed SK, Eldon ED (2006) Expression of *18-wheeler* in the follicle cell epithelium affects cell migration and egg morphology in *Drosophila*. *Dev Dyn* 235:1953–1961
- Kliewer JW (1961) Weight and hatchability of *Aedes aegypti* eggs. *Ann Entomol Soc Am* 54:912–917
- Klowden MJ (2007) *Physiological systems in insects*. Academic Press, Burlington
- Knoll HJ (1974) Untersuchungen zur entwicklungsgeschichte von *Scutigera coleoptrata* L. (Chilopoda). *Zool Jb Anat* 92:47–132
- Kobayashi Y (1998) Embryogenesis of the fairy moth *Nemophora albiantennella* Issiki (Lepidoptera, Adelidae) with special emphasis on its phylogenetic implications. *Int J Insect Morphol Embryol* 27:157–166
- Konopová B, Zrzavý J (2005) Ultrastructure, development, and homology of insect embryonic cuticles. *J Morphol* 264:339–362
- Konstandi OA, Papassideri IS, Stravopodis DJ, Kenoutis CA, Hasan Z, Katsorchis T, Wever R, Margaritis LH (2005) The enzymatic component of *Drosophila melanogaster* chorion is the Pxd peroxidase. *Insect Biochem Mol Biol* 35:1043–1057
- Konstandi OA, Papassideri IS, Stravopodis DJ, Antonelou MH, Kenoutis CA, Stefanidou DC, Margaritis LH (2006) The dual role of chorion peroxidase in *Bactrocera oleae* chorion assembly. *Int J Dev Biol* 50:543–552
- Kubrakiewicz J, Jedrzejowka I, Szymańska B, Biliński SM (2005) Micropyle in neuropterid insects. Structure and late stages of morphogenesis. *Arthropod Struct Dev* 34:179–188
- Kučerová Z, Stejskal V (2008) Differences in egg morphology of the stored-grain pests *Rhyzopertha dominica* and *Prostephanus truncates* (Coleoptera, Bostrichidae). *J Stored Prod Res* 44:103–105
- Kudo S-I, Nakahira T, Saito Y (2006) Morphology of trophic eggs and ovarian dynamics in the subsocial bug *Adomerus triguttulus* (Heteroptera, Cydnidae). *Can J Zool* 84:723–728
- Kumar V, Kamble CK (2008) Scanning electron microscope study on the egg chorion of silkworm, *Antheraea assamensis* Helf. (Lepidoptera, Saturniidae). *Anim Biol* 58:235–244
- Kumar V, Kariappa BK, Babu AM, Dandin SB (2007) Surface ultrastructure of the egg chorion of Eri silkworm, *Samia ricini* Donovan (Lepidoptera, Saturniidae). *J Entomol* 4:68–81
- Lagueux M, Hirn M, Hoffmann JA (1977) Ecdysone during ovarian development in *Locusta migratoria*. *J Insect Physiol* 23:109–119
- Lagueux M, Hetru C, Goltzene F, Kappler C, Hoffmann JA (1979) Ecdysone titre and metabolism in relation to cuticulogenesis in embryos of *Locusta migratoria*. *J Insect Physiol* 25:709–723
- Lamer A, Dorn A (2001) The serosa of *Manduca sexta* (Insecta, Lepidoptera): ontogeny, secretory activity, structural changes, and functional considerations. *Tissue Cell* 33:580–595
- Lecanidou R, Rodakis GC, Eickbush TH, Kafatos FC (1986) Evolution of the silk moth chorion gene superfamily: gene families CA and CB. *Proc Natl Acad Sci U S A* 83:6514–6518
- LeMosy EK, Hashimoto C (2000) The nudel protease of *Drosophila* is required for eggshell biogenesis in addition to embryonic patterning. *Dev Biol* 217:352–361
- Li J (1994) Egg chorion tanning in *Aedes aegypti* mosquito. *Comp Biochem Physiol* 109:835–843
- Li JS, Li J (2006) Major chorion proteins and their crosslinking during chorion hardening in *Aedes aegypti* mosquitoes. *Insect Biochem Mol Biol* 6:954–964

- Li J, Hodgeman BA, Christensen BM (1996) Involvement of peroxidase in chorion hardening in *Aedes aegypti*. *Insect Biochem Mol Biol* 26:309–317
- Li J, Kim SR, Li J (2004) Molecular characterization of a novel peroxidase involved in *Aedes aegypti* chorion protein crosslinking. *Insect Biochem Mol Biol* 34:1195–1203
- Lincoln DCR (1961) The oxygen and water requirements of the egg of *Ocyptus olens* Muller (Staphylinidae, Coleoptera). *J Insect Physiol* 7:265–272
- Lounibos LP, Duzak D, Linley JR, Lourenço-de-Oliveira R (1997) Egg structures of *Anopheles fluminensis* and *Anopheles shannoni*. *Mem Inst Oswaldo Cruz* 92:221–232
- Luschnig S, Bätz T, Armbruster K, Krasnow MA (2006) Serpentine and vermiform encode matrix proteins with chitin binding and deacetylation domains that limit tracheal tube length in *Drosophila*. *Curr Biol* 16:186–194
- Ma PWK, Baird S, Ramaswamy SB (2002) Morphology and formation of the eggshell in the tarnished plant bug, *Lygus lineolaris* (Palisot de Beauvois) (Hemiptera, Miridae). *Arthropod Struct Dev* 31:131–146
- Machida R (2006) Evidence from embryology for reconstructing the relationships of hexapod basal clades. *Arthropod Syst Phylogeny* 64:95–104
- Machida R, Ando H (1985) Blastodermic cuticles of the jumping bristletail, *Pedetontus unimaculatus* (Microcoryphia, Machilidae). In: Ando H, Miya K (eds) Recent advances in insect embryology in Japan. ISEBU Co. Ltd., Tsukuba, pp 131–137
- Machida R, Ando H (1998) Evolutionary changes in developmental potentials of the embryo proper and embryonic membranes along with the derivative structures in atelocerata, with special reference to hexapoda (Arthropoda). *Proc Arthropod Embryol Soc Jpn* 33:1–13
- Machida R, Nagashima T, Ando H (1994) Embryonic development of the jumping bristletail *Pedetontus unimaculatus* Machida, with special reference to embryonic membranes (Hexapoda: Microcoryphia, Machilidae). *J Morphol* 220:147–165
- Machida R, Ikeda Y, Tojo K (2002) Evolutionary changes in developmental potentials of the embryo proper and embryonic membranes in Hexapoda: a synthesis revised. *Proc Arthropod Embryol Soc Jpn* 37:1–11
- Manogaran A, Waring GL (2004) The N-terminal prodomain of sV23 is essential for the assembly of a functional vitelline membrane network in *Drosophila*. *Dev Biol* 270:261–271
- Marchiondo AA, Meola SM, Palma KG, Slusser JH, Meola RW (1999) Chorion formation and ultrastructure of the egg of the cat flea (Siphonaptera: Pulicidae). *J Med Entomol* 36:149–157
- Margaritis LH (1985a) Structure and physiology of the eggshell. In: Kerkut GA, Gilbert LL (eds) *Comprehensive insect physiology, biochemistry and pharmacology*, vol 1. Pergamon Press, Oxford, pp 153–230
- Margaritis LH (1985b) The egg-shell of *Drosophila melanogaster* III. Covalent crosslinking of the chorion proteins involves endogenous hydrogen peroxide. *Tissue Cell* 17:553–559
- Margaritis LH (1986) The eggshell of *Drosophila melanogaster*. II. New staging characteristics and fine structural analysis of choriogenesis. *Can J Zool* 64:2152–2175
- Margaritis LH, Keramaris KE (1991) Immunolocalization of a peroxidase in the eggshell of *D. melanogaster*: evidence for its participation in the hardening process. *Micron Microsc Acta* 22:247–248
- Margaritis LH, Petri WH, Wyman AR (1979) Structural and image analysis of a crystalline layer from the dipteran egg-shell. *Cell Biol Int Rep* 3:61–66
- Margaritis LH, Kafatos FC, Petri WH (1980) The eggshell of *Drosophila melanogaster*. I. Fine structure of the layers and regions of the wild-type eggshell. *J Cell Sci* 43:1–35
- Margaritis LH, Dellas K, Kalantzi MCh, Kambysellis MP (1983) The eggshell of Hawaiian *Drosophila*: structure and biochemical studies in *D. grimshawi* and comparison to *D. melanogaster*. *Roux Arch Dev Biol* 192:303–316
- Margaritis LH, Hamodrakas SJ, Papassideri I, Arad T, Leonard KR (1991) Three-dimensional reconstruction of innermost chorion layer of *Drosophila grimshawi* and *Drosophila melanogaster* eggshell mutant *fs(1)384*. *Int J Biol Macromol* 191:247–253

- Marinotti O, Ngo T, Kojin BB, Chou SP, Nguyen B, Juhn J, Carballar-Lejarazú R, Marinotti PN, Jiang X, Walter MF, Tu Z, Gershon PD, James AA (2014) Integrated proteomic and transcriptomic analysis of the *Aedes aegypti* eggshell. *BMC Dev Biol* 14:15
- Mashimo Y, Beutel RG, Dallai R, Lee CY, Machida R (2014) Embryonic development of Zoraptera with special reference to external morphology, and its phylogenetic implications (Insecta). *J Morphol* 275:295–312
- Masumoto M, Machida R (2006) Development of embryonic membranes in the silverfish *Lepisma saccharina* Linnaeus (insecta: Zygentoma, Lepismatidae). *Tissue Cell* 38:159–169
- Mathew G, Rai KS (1975) Structure and formation of egg membranes in *Aedes aegypti* (L.) (Diptera: Culicidae). *Int J Insect Morphol Embryol* 4:369–380
- Mauzy-Melitz D, Waring GL (2003) fc177, a minor dec-1 proprotein, is necessary to prevent ectopic aggregation of the endochorion during eggshell assembly in *Drosophila*. *Dev Biol* 255:193–205
- Mazzini M, Carcupino M, Santini L (1992) Eggshell fine structure of fungus-gnats *Neoempheria lineola* (Meig.) and *N. striata* (Meig.) (Diptera mycetophilidae, Mycomyinae). *Redia*, LXXV, 179–188
- McFarlane JE (1960) Structure and function of the egg shell as related to water absorption by the eggs of *Acheta domesticus* (L.). *Can J Zool* 38:231–241
- McFarlane JE (1962) The cuticles of the egg of the house cricket. *Can J Zool* 40:13–21
- McFarlane JE, Kennard CP (1960) Further observations on water absorption by the eggs of *Acheta domesticus* (L.). *Can J Zool* 38:77–85
- Medeiros MN, Logullo R, Ramos IB (2011) Transcriptome and gene expression profile of ovarian follicle tissue of the triatomine bug *Rhodnius prolixus*. *Insect Biochem Mol Biol* 41:823–831
- Miller A (1939) The egg and early development of the stonefly, *Pteronarcys proteus* Newman (Plecoptera). *J Morphol* 64:555–609
- Miller A (1940) Embryonic membranes, yolk cells, and morphogenesis of the stonefly *Pteronarcys proteus* Newman (Plecoptera: Pteronarcidae). *Ann Entomol Soc Am* 33:437–477
- Mindrinis MN, Petri WH, Galanopoulos VK, Lombard MF, Margaritis LH (1980) Crosslinking of the *Drosophila* chorion involves a peroxidase. *Roux Arch Dev Biol* 189:187–196
- Misof B, Liu S, Meusemann K, Peters RS, Donath A, Mayer C, Frandsen PB, Ware J, Flouri T, Beutel RG, Niehuis O, Petersen M, Izquierdo-Carrasco F, Wappler T, Rust J, Aberer AJ, Aspöck U, Aspöck H, Bartel D, Blanke A, Berger S, Böhm A, Buckley TR, Calcott B, Chen J, Friedrich F, Fukui M, Fujita M, Greve C, Grobe P, Gu S, Huang Y, Jermin LS, Kawahara AY, Krogmann L, Kubiak M, Lanfear R, Letsch H, Li Y, Li Z, Li J, Lu H, Machida R, Mashimo Y, Kapli P, McKenna DD, Meng G, Nakagaki Y, Navarrete-Heredia JL, Ott M, Ou Y, Pass G, Podsiadlowski L, Pohl H, von Reumont BM, Schütte K, Sekiya K, Shimizu S, Slipinski A, Stamatakis A, Song W, Su X, Szucsich NU, Tan M, Tan X, Tang M, Tang J, Timelthaler G, Tomizuka S, Trautwein M, Tong X, Uchifune T, Walz MG, Wiegmann BM, Wilbrandt J, Wipfler B, Wong TK, Wu Q, Wu G, Xie Y, Yang S, Yang Q, Yeates DK, Yoshizawa K, Zhang Q, Zhang R, Zhang W, Zhang Y, Zhao J, Zhou C, Zhou L, Ziesmann T, Zou S, Li Y, Xu X, Zhang Y, Yang H, Wang J, Wang J, Kjer KM, Zhou X (2014) Phylogenomics resolves the timing and pattern of insect evolution. *Science* 346:763–767
- Miura T, Braendle C, Shingleton A, Sisk G, Kambhampati S, Stern DL (2003) A comparison of parthenogenetic and sexual embryogenesis of the pea aphid *Acyrtosiphon pisum* (Hemiptera: Aphidoidea). *J Exp Zool Part B* 295:59–81
- Monnerat AT, Soares MJ, Lima JBP, Rosa-Freitas MG, Valle D (1999) *Anopheles albitarsis* eggs: ultrastructural analysis of chorion layers after permeabilization. *J Insect Physiol* 45:915–922
- Moreira MF, Dos Santos AS, Marotta HR (2007) A chitin-like component in *Aedes aegypti* eggshells, eggs and ovaries. *Insect Biochem Mol Biol* 37:1249–1261
- Moussian B, Schwarz H, Bartoszewski S, Nüsslein-Volhard C (2005a) Involvement of chitin in exoskeleton morphogenesis in *Drosophila melanogaster*. *J Morphol* 264:117–130
- Moussian B, Söding J, Schwarz H, Nüsslein-Volhard C (2005b) Retroactive, a membrane-anchored extracellular protein related to vertebrate snake neurotoxin-like proteins, is required for cuticle organization in the larva of *Drosophila melanogaster*. *Dev Dyn* 233:1056–1063

- Moussian B, Tång E, Tonning A, Helms S, Schwarz H, Nüsslein-Volhard C, Uv AE (2006) *Drosophila* Knickkopf and retroactive are needed for epithelial tube growth and cuticle differentiation through their specific requirement for chitin filament organization. *Development* 133:163–171
- Mouzaki DG, Margaritis LH (1991a) Choriogenesis in the medfly *Ceratitis capitata* (Wiedermann) (Diptera: Tephritidae). *Int J Insect Morphol Embryol* 20:51–68
- Mouzaki DG, Margaritis LH (1991b) The eggshell of the cherry fly *Rhagoletis cerasi*. *Tissue Cell* 23:745–754
- Mouzaki DG, Margaritis LH (1994) The eggshell of the almond wasp *Eurytoma amygdali* (Hymenoptera, Eurytomidae) – 1. Morphogenesis and fine structure of the eggshell layers. *Tissue Cell* 26:559–568
- Mouzaki DG, Zarani FE, Margaritis LH (1991) Structure and morphogenesis of the eggshell and micropylar apparatus in the olive fly, *Dacus oleae* (Diptera: Tephritidae). *J Morphol* 209:39–52
- Nelson DR, Leopold RA (2003) Composition of the surface hydrocarbons from the vitelline membranes of dipteran embryos. *Comp Biochem Physiol* 136:295–308
- Nonon JP, Boivin G, Allo MR (1995) Fine-structure of the egg envelopes in *Listronotus oregonensis* (Leconte) (Coleoptera, Curculionidae) and morphological adaptations to oviposition sites. *Int J Insect Morphol Embryol* 24:333–342
- Noguerón MI, Waring GL (1995) Regulated processing of dec-1 eggshell proteins in *Drosophila*. *Dev Biol* 172:272–279
- Noguerón MI, Mauzy-Melitz D, Waring GL (2000) *Drosophila* dec-1 eggshell proteins are differentially distributed via a multistep extracellular processing and localization pathway. *Dev Biol* 225:459–470
- Orfanidou CC, Hamodrakas SJ, Margaritis LH, Galanopoulos K, Dedieu JC, Gulik-Krzywick T (1992) Fine structure of the chorion of *Manduca sexta* and *Sesamia nonagrioides* as revealed by scanning electron microscopy and freeze-fracturing. *Tissue Cell* 24:735–744
- Osawa N, Yoshinaga A (2009) The presence of micropyles in the shells of developing and undeveloped eggs of the ladybird beetle *Harmonia axyridis* (Coleoptera: Coccinellidae). *Eur J Entomol* 106:607–610
- Osterfield M, Du XX, Schüpbach T, Wieschaus E, Shvartsman SY (2013) Three-dimensional morphogenesis in the developing *Drosophila* egg. *Dev Cell* 24:400–410
- Pan C, Zhou Y, Mo J (2009) The clone of laccase gene and its potential function in cuticular penetration resistance of *Culex pipiens pallens* to fenvalerate. *Pestic Biochem Physiol* 93:105–111
- Panfilio KA (2008) Extraembryonic development in insects and the acrobatics of blastokinesis. *Dev Biol* 313:471–491
- Papantonis A, Sourmeli S, Lecanidou R (2008) Chorion gene activation and repression is dependent on BmC/EBP expression and binding to cognate *cis*-elements. *Biochem Biophys Res Commun* 369:905–909
- Papantonis A, Swevers L, Iatrou K (2015) Chorion genes: a landscape of their evolution, structure, and regulation. *Annu Rev Entomol* 60:177–194
- Papassideri IS, Margaritis L (1986) Specific secretion of wax by the follicular cells of *Drosophila melanogaster*. *Cell Biol Int Rep* 10:963–968
- Papassideri IS, Margaritis LH (1996) The eggshell of *Drosophila melanogaster*. IX. Synthesis and morphogenesis of the innermost chorionic layer. *Tissue Cell* 28:401–409
- Papassideri IS, Margaritis LH, Gulik-Krzywicki T (1991) The egg-shell of *Drosophila melanogaster* VI, structural analysis of the wax layer in laid eggs. *Tissue Cell* 23:567–575
- Papassideri IS, Margaritis LH, Gulik-Krzywicki T (1993) The eggshell of *Drosophila melanogaster*. VIII. Morphogenesis of the wax layer during oogenesis. *Tissue Cell* 25:929–936
- Parks S, Spradling A (1987) Spatially regulated expression of chorion genes during *Drosophila* oogenesis. *Genes Dev* 1:497–509

- Pascucci T, Perrino J, Mahowald AP, Waring GL (1996) Eggshell assembly in *Drosophila*: processing and localization of vitelline membrane and chorion proteins. *Dev Biol* 177:590–598
- Qiu Y, Tittiger C, Wicker-Thomas C, Le Goff G, Young S, Wajnberg E, Fricaux T, Taquet N, Blomquist GJ, Feyereisen R (2012) An insect-specific P450 oxidative decarbonylase for cuticular hydrocarbon biosynthesis. *Proc Natl Acad Sci U S A* 109:14858–14863
- Rafiqi AM, Lemke S, Ferguson S, Stauber M, Schmidt-Ott U (2008) Evolutionary origin of the amnioserosa in cyclorrhaphan flies correlates with spatial and temporal expression changes of zen. *Proc Natl Acad Sci U S A* 105:234–239
- Raikhel AS, Lea AO (1991) Control of follicular epithelium development and vitelline envelope formation in the mosquito; role of juvenile hormone and 20-hydroxyecdysone. *Tissue Cell* 23:577–591
- Ramaswamy SB, Mbata GN, Cohen NE (1990) Necessity of juvenile-hormone for choriogenesis in the moth, *Heliothis virescens* (Noctuidae). *Invertebr Reprod Dev* 17:57–63
- Regier JC, Kafatos FC (1985) Molecular aspects of chorion formation. In: Kerkut GA, Gilber LI (eds) *Comprehensive insect physiology biochemistry and pharmacology*. Pergamon Press, Oxford, pp 113–151
- Regier JC, Wong JR (1988) Assembly of silkmoth chorion proteins: *In vivo* patterns of disulfide bond formation. *Insect Biochem* 18:471–482
- Regier JC, Paukstadt U, Paukstadt LH, Mitter C, Peigler RS (2005) Phylogenetic of eggshell morphogenesis in *Antheraea* (Lepidoptera: Saturniidae): unique origin and repeated reduction of aeropyle crown. *Syst Biol* 54:254–267
- Regier JC, Shultz JW, Zwick A, Hussey A, Ball B, Wetzer R, Martin JW, Cunningham CW (2010) Arthropod relationships revealed by phylogenomic analysis of nuclear protein-coding sequences. *Nature* 463:1079–1083
- Renthleil CZ, Raghuvaraman A, Kharbuli B, Dey S (2010) Progressive chorion morphology during egg development in *Samia ricini* (Donovan). *Microsc Res Tech* 73:234–239
- Rezende GL, Martins AJ, Gentile C, Farnesi LC, Pelajo-Machado M, Peixoto AA, Valle D (2008) Embryonic desiccation resistance in *Aedes aegypti*: presumptive role of the chitinized serosal cuticle. *BMC Dev Biol* 8:82
- Sarashina I, Mito T, Saito M, Uneme H, Miyawaki K, Shinmyo Y, Ohuchi H, Noji S (2005) Location of micropyles and early embryonic development of the two-spotted cricket *Gryllus bimaculatus* (Insecta, Orthoptera). *Dev Growth Differ* 47:99–108
- Savant SS, Waring GL (1989) Molecular analysis and rescue of a vitelline membrane mutant in *Drosophila*. *Dev Biol* 135:43–52
- Scherer LJ, Harris DH, Petri WH (1988) *Drosophila* vitelline membrane genes contain a 114 base pair region of highly conserved coding sequence. *Dev Biol* 130:786–788
- Schlaeger DA, Fuchs MS (1974) Effect of dopa-decarboxylase inhibition on *Aedes aegypti* eggs: evidence for sclerotization. *J Insect Physiol* 20:349–357
- Schlichting K, Wilsch-Brauninger M, Demontis F, Dahmann C (2006) Cadherin Cad99C is required for normal microvilli morphology in *Drosophila* follicle cells. *J Cell Sci* 119:1184–1195
- Schmidt-Ott U (2000) The amnioserosa is an apomorphic character of cyclorrhaphan flies. *Dev Genes Evol* 210:373–376
- Sdralia N, Swevers L, Iatrou K (2012) BmVMP90, a large vitelline membrane protein of the domesticated silkmoth *Bombyx mori*, is an essential component of the developing ovarian follicle. *Insect Biochem Mol Biol* 42:717–727
- Sekiguchi K (1960) Embryonic development of the horse-shoe crab studied by vital staining. *Bull Mari Sta Asamushi, Tohoku Univ* 10:161–164
- Sherrard KM, Fehon RG (2015) The transmembrane protein Crumbs displays complex dynamics during follicular morphogenesis and is regulated competitively by Moesin and aPKC. *Development* 142:1869–1878
- Slifer EH (1937) The origin and fate of the membranes surrounding the grasshopper egg, together with some experiments on the source of the hatching enzyme. *Q J Microsc Sci* 79:493–509

- Slifer EH, Sekhon SS (1963) The fine structure of the membranes which cover the egg of the grasshopper, *Melanoplus differentialis*, with special reference to the hypopyle. *Q J Microsc Sci* 104:321–334
- Sourmeli S, Papantonis A, Lecanidou R (2005) A novel role for the *Bombyx* Slbo homologue, BmC/EBP, in insect choriogenesis. *Biochem Biophys Res Commun* 337:713–719
- Souza-Ferreira PS, Mansur JF, Berni M, Moreira MF, dos Santos RE, Araújo HM, de Souza W, Ramos IB, Masuda H (2014) Chitin deposition on the embryonic cuticle of *Rhodnius prolixus*: the reduction of CHS transcripts by CHS-dsRNA injection in females affects chitin deposition and eclosion of the first instar nymph. *Insect Biochem Mol Biol* 51:101–109
- Spoerel NA, Nguyen HT, Eickbush TH, Kafatos FC (1989) Gene evolution and regulation in the chorion complex of *Bombyx mori*: hybridization and sequence analysis of multiple developmentally middle A/B chorion gene pairs. *J Mol Biol* 209:1–19
- Stein DS, Stevens LM (2014) Maternal control of the *Drosophila* dorsal-ventral body axis. *WIREs Dev Biol* 3:301–330
- Stender-Seidel S, Thomas G (1997) Investigation of different ontogenetic stages of *Raillietiella* sp. (Pentastomida:Cephalobaenida): the embryonic gland – glandula embryonalis – or dorsalar-gan. *Parasitol Res* 83:157–162
- Stevens LM, Beuchle D, Jurcsak J (2003) The *Drosophila* embryonic patterning determinant torso-like is a component of the eggshell. *Curr Biol* 13:1058–1063
- Striebel H (1960) Zur Embryonalentwicklung der Termiten. *Acta Trop* 1:193–260
- Sukontason K, Sukontason KL, Boonchu N, Chaiwong T, Piangjai S (2004) Ultrastructure of eggshell of *Chrysomya nigripes* Aubertin (Diptera: Calliphoridae). *Parasitol Res* 93:151–154
- Sukontason KL, Bunchu N, Chaiwong T, Kuntalue B, Sukontason K (2007) Fine structure of the eggshell of the blow fly, *Lucilia cuprina*. *J Insect Sci* 7:1–9
- Swevers BL, Raikhel AS, Sappington TW, Shirk P, Iatrou K (2005) Vitellogenesis and post-vitellogenic maturation of the insect ovarian follicle. In: Gilbert LI, Iatrou K, Gill SS (eds) *Comprehensive molecular insect science*. Elsevier, Boston, pp 87–155
- Tiegs OW (1940) The embryology and affinities of the symphylas based on a study of *Hanseniella agilis*. *Q J Microsc Sci* 82:1–225
- Tiegs OW (1942) The ‘dorsal organ’ of the embryo of *Campodea*. *Q J Microsc Sci* 84:35–48
- Tiegs OW (1947) The development and affinities of the Pauropoda, based on a study of *Pauropus sylvaticus*. *Q J Microsc Sci* 88:165–271
- Tojo K, Machida R (1997) Embryogenesis of the mayfly *Ephemera japonica* McLachlan (Insecta:Ephemeroptera, Ephemeridae), with special reference to abdominal formation. *J Morphol* 234:97–107
- Tootle TL, Williams D, Hubb A (2011) *Drosophila* eggshell production: identification of new genes and coordination by Pxt. *PLoS One* 6:e19943
- Trougakos IP, Margaritis LH (1998a) The formation of the functional chorion structure of *Drosophila virilis* involves interaction of the “middle” and “late” major chorion proteins into scaffold formed by the “early” chorion proteins: a general model for chorion assembly in Drosophilidae. *J Struct Biol* 123:97–110
- Trougakos IP, Margaritis LH (1998b) Immunolocalization of the temporally “early” secreted major structural chorion proteins, Dvs38 and Dvs36, in the eggshell layers and regions of *Drosophila virilis*. *J Struct Biol* 123:111–123
- Trougakos IP, Margaritis LH (2002) Novel morphological and physiological aspects of insect eggs. In: Hilker M, Meiners T (eds) *Chemoecology of Insect Eggs and Egg Deposition*. Blackwell Wissenschaftsverlag, Berlin, pp 3–36
- Turner FR, Mahowald AP (1976) Scanning electron microscopy of *Drosophila* embryogenesis. 1. The structure of the egg envelopes and the formation of the cellular blastoderm. *Dev Biol* 50:95–108
- Uchifune T, Machida R (2005) Embryonic development of *Galloisiana yuasai* Asahina, with special reference to external morphology (Insecta: Grylloblattodea). *J Morphol* 266:182–207
- Uemiyama H, Ando H (1987) Blastodermic cuticles of a springtail, *Tomocerus ishibashii* Yosii (Collembola, Tomoceridae). *Int J Insect Morphol Embryol* 16:5–6

- Valencia MD, Miller LH, Mazur P (1996) Permeability of intact and dechorionated eggs of the *Anopheles* mosquito to water vapor and liquid water: a comparison with *Drosophila*. *Cryobiology* 33:142–148
- van der Zee M, Berns N, Roth S (2005) Distinct functions of the *Tribolium* zerknüllt genes in serosa specification and dorsal closure. *Curr Biol* 15:624–636
- Vargas HC, Farnesi LC, Martins AJ, Valle D, Rezende GL (2014) Serosal cuticle formation and distinct degrees of desiccation resistance in embryos of the mosquito vectors *Aedes aegypti*, *Anopheles aquasalis* and *Culex quinquefasciatus*. *J Insect Physiol* 62:54–60
- Vasireddy V, Uchida Y, Salem N Jr, Kim SY, Mandal MN, Reddy GB, Bodepudi R, Alderson NL, Brown JC, Hama H, Dlugosz A, Elias PM, Holleran WM, Ayyagari R (2007) Loss of functional ELOVL4 depletes very long-chain fatty acids (\geq C28) and the unique omega-O-acylceramides in skin leading to neonatal death. *Hum Mol Genet* 16:471–482
- Ventura G, Furriols M, Martín N, Barbosa V, Casanova J (2010) *clasca*, a new gene required for both Torso RTK activation and vitelline membrane integrity. Germline proteins contribute to *Drosophila* eggshell composition. *Dev Biol* 334:224–232
- Vogelgesang M, Szklarzewicz T (2001) Formation and structure of egg capsules in scale insects (Hemiptera, Coccidae) I, Orthoziidae. *Arthropod Struct Dev* 30:63–68
- Waring GL (2000) Morphogenesis of the eggshell in *Drosophila*. *Int Rev Cytol* 198:67–108
- Waring GL, Hawley RJ, Schoenfeld T (1990) Multiple proteins are produced from the dec-1 eggshell gene in *Drosophila* by alternative RNA splicing and proteolytic cleavage events. *Dev Biol* 142:1–12
- Wigglesworth VB (1972) The principles of insect physiology. Chapman and Hall Limited, Cambridge
- Woods AH, Bonnacaze RY, Zrubek B (2005) Oxygen and water flux across eggshells of *Manduca sexta*. *J Exp Biol* 208:1297–1308
- Wu T, Manogaran AL, Beauchamp JM, Waring GL (2010) *Drosophila* vitelline membrane assembly: a critical role for an evolutionarily conserved cysteine in the “VM domain” of sV23. *Dev Biol* 347:360–368
- Wu X, Zhan X, Gan M, Zhang D, Zhang M, Zheng X, Wu Y, Li Z, He A (2013) Laccase2 is required for sclerotization and pigmentation of *Aedes albopictus* eggshell. *Parasitol Res* 112:1929–1934
- Xu Y, Fu Q, Li S, He N (2011) Silkworm egg proteins at the germ-band formation stage and a functional analysis of BmEP80 protein. *Insect Biochem Mol Biol* 41:572–581
- Zarani FE, Margaritis LH (1991) Ultrastructural features and formation of the micropylar apparatus in the cherry fly *Rhagoletis cerasi*. *J Morphol* 208:205–214
- Zarani FE, Margaritis LH (1994) The eggshell of the almond wasp *Eurytoma amygdali* (Hymenoptera, Eurytomidae) -2. The micropylar appendage. *Tissue Cell* 26:569–577
- Zawadzka M, Jankowska W, Biliński SM (1997) Egg shell of mallophagans and anoplurans (Insecta: Phthiraptera): morphogenesis of specialized regions and the relation to F-actin cytoskeleton of follicular cells. *Tissue Cell* 29:665–673
- Zeh DW, Zeh JA, Smith RL (1989) Ovipositors, amnions and eggshell architecture in the diversification of terrestrial arthropods. *Q Rev Biol* 64:147–168
- Zhang Z, Stevens LM, Stein D (2009) Sulfation of eggshell components by Pipe defines dorsal-ventral polarity in the *Drosophila* embryo. *Curr Biol* 19:1200–1205

Part III
Skeletal Components as Targets
for Interference

Chapter 10

Targeting Cuticular Components for Pest Management

Daniel Doucet and Arthur Retnakaran

Abstract The insect exoskeleton is present as a rigid structure above a monolayer of epidermal cells and together both form the integument. The cuticle is composed of an outer, multilayered epicuticle and an inner procuticle containing the chitinous exo- and endo- cuticle. The non-living cuticle is replaced during each instar to accommodate growth and development by sequentially degrading the old cuticle and replacing it with a new one. The entire molting cycle and the shedding of the old cuticle are precisely regulated by a series of endocrine and neuroendocrine cues. This chapter addresses the various cuticular components, cuticular metabolism and cuticular biogenesis regulatory systems that have been targeted for pest management. Major classes of synthetic compounds, including benzoylphenyl ureas, benzoyl hydrazines and etoxazole that target chitin synthesis and the molting cycle are presented. In addition, we focus on recent developments toward the targeting of additional components of the cuticle or processes of cuticle biogenesis that may find future applications in pest management.

10.1 Introduction

Insects and humans compete for the same resources such as food crops and lumber as well as many of them serve as vectors of human diseases like malaria. This age old conflict has been the impetus that led to the development of ways and means of controlling insects. As early as 2500 BC the Sumerians used sulfur compounds to control insects (Perry et al. 1998). The development of chlorinated hydrocarbons such as DDT (dichlorodiphenyltrichlorethane) revolutionized insect control by efficient performance against agricultural pests as well as saving thousands of lives from malaria. The indiscriminate and large scale use of DDT led to collateral damage on non-target species and was highlighted by Rachel Carson in her epic book “Silent Spring”, in 1962. This singular event has been a major catalyst for the

D. Doucet (✉) • A. Retnakaran
Great Lakes Forestry Centre, Canadian Forest Service, Natural Resources Canada,
1219 Queen St. East, Sault Ste Marie, ON P6A 2E5, Canada
e-mail: dan.doucet@NRCan.gc.ca; aretnakaran@gmail.com

development of successive generations of insecticides that are less harmful to the environment (Berry-Caban 2011).

Insects have various cells, tissues and organ systems that are either unique or that exhibit differences with those of other taxa in terms of their ontology or metabolism. These differences, even if subtle, can offer opportunities for pest management. One defining structure of insects is the exoskeleton which they share with other arthropods. The exoskeleton acts as a defensive shield against predators, parasites and microbial infections, forms a watertight barrier against desiccation and maintains sensory interaction with the outside world. It also provides sites for anchoring the muscles necessary for locomotion (Vincent and Wegst 2004). Several pest management strategies, which have been developed either by design or serendipitously to target the different components of the cuticle, will be the subject of this chapter.

10.2 Structure of the Integument

The exoskeleton of insects is made up of a non-living cuticle secreted by an underlying epidermis and together both form the integument (Fig. 10.1). As insects grow they molt by shedding the old cuticle and replacing it with a new one. In preparation for the molt, the epidermal cells proliferate and separate from the cuticle above, a process called apolysis. The subcuticular space is filled with a molting fluid containing a cocktail of cuticle-degrading enzymes (proteases and chitinases) secreted by

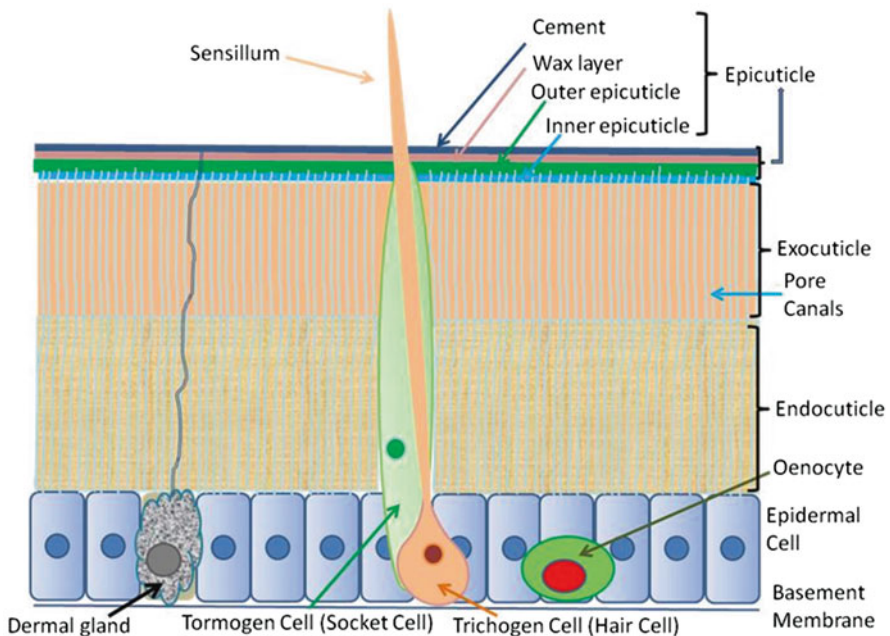


Fig. 10.1 Scheme of a generalized insect integument (with the kind permission of Elsevier Ltd.)

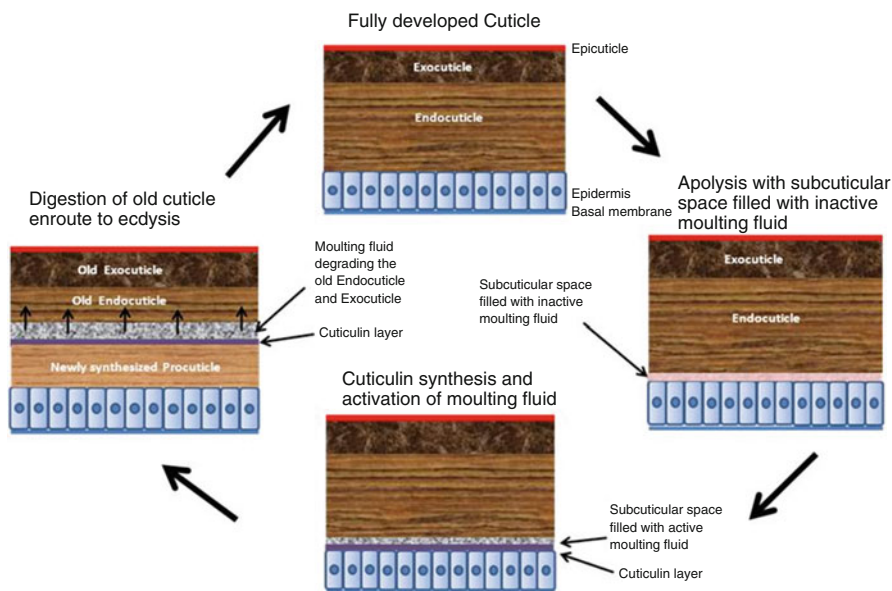


Fig. 10.2 The molting cycle (See text for details, with the kind permission of John Wiley and Sons.)

the epidermis in the form of a gel. The zymogenic proteases require activation once the protective cuticulin layer (outer epicuticle) is secreted, while chitinases appear to be constitutively active (Chaudhari et al. 2011). The enzymatically active molting fluid progressively degrades the procuticle in a baso-apical direction up to the exocuticular layer, while concomitantly the epidermis secretes the procuticle under the new cuticulin layer. At this stage, the insect undergoes ecdysis resulting in the shedding of the remnants of the old cuticle (exocuticle and epicuticle). The proliferated epidermal cells stretch and the procuticle expands into the endo- and exocuticle layers with the latter undergoing sclerotization and in certain cases melanization (Fig. 10.2).

10.3 The Epicuticle

The formation of the epicuticle begins with the onset of secretion of the cuticulin layer on the surface of the epidermis covered by a thin lipoprotein envelope and heralds the beginning of the molting cycle. The smooth surface of the epidermal cell transforms into microvilli at the apices of which epicentres of cuticulin are secreted. These epicentres become confluent to form a thin layer covering the surface of the cell (Fristrom et al. 1986; Locke 1991; Payre 2004; Moussian 2010). The cuticulin is made of lipids and proteins and protects the epidermis from the molting fluid.

The cuticulin layer becomes the outer epicuticle and an inner epicuticle is secreted as the cuticle is progressively elaborated.

The epicuticle contains various types of hydrocarbons that act among other things as antidesiccants. The cement layer and the wax layer probably originate from the dermal glands and are deposited on the surface to augment the antidesiccation process (Villaverde et al. 2009). Oenocytes, which are specialized cells found in many anatomical locations, including the epidermis, are involved in lipid processing and deposition on the surface of the exoskeleton (Martins and Ramalho-Ortiago 2012; Makki et al. 2014). The bevy of hydrocarbons and lipids present in the epicuticle waterproof its surface, but also have a variety of chemosensory and pheromonal functions (Neville 1975; Chap. 7 in this book). Two types of control products that affect the physico-chemical integrity of the epicuticle are in use against insects, one inorganic (diatomaceous earth), the other a class of biological agent (entomofungi).

10.3.1 *Diatomaceous Earths and Dessicants*

Diatomaceous earths (DE) are silica based fossilized remains of diatoms and are used against many insect pests as a desiccant (Cook et al. 2008; Blomquist and Bagnères 2010). They were originally considered as abrasive agents physically damaging the epicuticle, but this appears to be a minor effect. DEs adsorb the lipids in the epicuticle layer, thereby removing the waterproofing effect of the exoskeleton and allowing rapid desiccation of the insect. In the flour mite *Acarus siro*, GC-MS analysis of epicuticle solvent washes indicated the presence of C₁₃ – C₂₆ hydrocarbons, with *n*-tridecane being a major component. When treated with DEs for 72 h, little or no hydrocarbons including *n*-tridecane were left on the mites, but surprisingly scanning electron microscopy revealed very little sign of abrasion (Cook et al. 2008). DEs are very effective in controlling adults of the lesser grain borer, *Rhyzopertha dominica*, the rice weevil, *Sitophilus oryzae* and the confused flour beetle, *Tribolium confusum* (Kavallieratos et al. 2015).

10.3.2 *Entomopathogenic Fungi*

Entomopathogenic fungi (EFs) are parasites of insects that penetrate the body, and ramify inside and sporulate on the surface, leading to lethality. EFs belong to as many as 52 genera distributed across nine higher taxonomic ranks of fungi, the common feature being pathogenicity to insects (Samson et al. 1988). One of the best characterized EF, *Beauveria bassiana*, leads a saprophytic existence in the soil and asexually produces conidiospores from special hyphae, the conidiophores. When conidiospores land on an insect they stick to the cuticle with a gel containing adhesive molecules, hydrophobins (water repelling proteins) and Mad adhesins (anchor

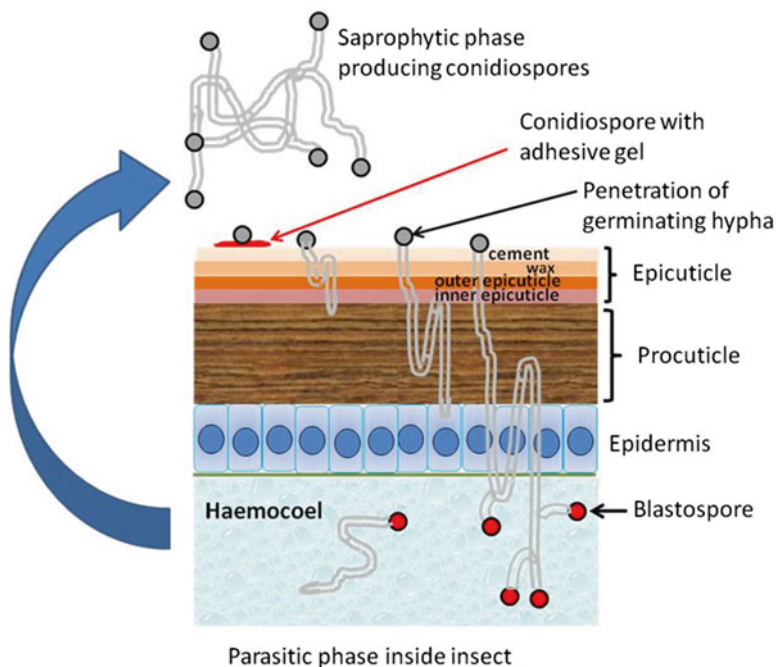


Fig. 10.3 Cuticle penetration by entomopathogenic fungus (with the kind permission of Elsevier Ltd.)

sites) (Fig. 10.3). The various fatty acids and hydrocarbons on the surface of the insect cuticle have differential effects on conidiospores, some stimulating and others inhibiting adhesion. EFs have been shown to survive on insect-like hydrocarbons as the sole source by hydroxylating the substrate with a cytochrome P450 monooxygenase followed by β -oxidation (Huarte-Bonnet et al. 2015). The insect cuticle is the first line of defence against invasion by parasites and microbes and has *inter alia* antimicrobial peptides, quinones, terpenes, β -1,3-glucanases, proteinases and chitinase inhibitors which the fungus has to overcome in order to enter the insect. Upon adhesion, the conidiospore germinates and enters the epicuticle utilizing panoply of enzymes and anti-immune compounds. EFs secrete hydrolases, lipases, esterases, chitinases and proteases as well as penetrant tubes called appressoria that aid in the penetration into the cuticle (Bai et al. 2012; Ortiz-Urquiza and Keyhani 2013). Hyphae infiltrate and reach the haemocoel and bud spores, the blastospores which invade the various organ systems and upon the death of the insect the spores spread in the soil and start the saprophytic cycle. In terms of their field application, *Beauveria bassiana*, *Metarhizium anisopliae* and *Isaria fumosorosea* are EFs that have been well developed for commercial use, but many others are in the process of being tested (Gabarty et al. 2014).

As DE and EFs display distinct effects on the insect cuticle, their combined application should in principle enhance insecticidal activity. This assumption may not hold for all pest control settings, and research within the last two decades has

shown that the effect of the co-application of both products is highly species- and stage-specific. DE potently synergises *B. bassiana* treatment in adults of *R. dominica* and of the sawtoothed grain beetle *Oryzaephilus surinamensis*, but a positive interaction against adults of the rusty grain beetle *Cryptolestes ferrugineus* is only observed at moderate doses of conidia (Lord 2001). Likewise, DE reduces the LC₅₀ of *B. bassiana* against *T. castaneum* larvae up to 17-fold, but doesn't increase mortality against adults (Akbar et al. 2004). In addition to host-dependent factors, temperature and humidity are strong determinants of the efficacy of DE and EFs. DE and *B. bassiana* co-treatment was found to be more effective against *R. dominica* under low (43%) than high (75%) relative humidities which is counter intuitive since fungi are maximally effective under elevated ambient moisture. Low humidity may be stressful to the insects, making them more vulnerable to the fungal infection process (Lord 2005). For stored grain pests, the type of conidial preparation (aqueous versus dry), the type of commodity (flour, wheat, maize) and exposure intervals were also shown to be important (Kavallieratos et al. 2006; Athanassiou et al. 2008). Apart from pests of stored commodities, the efficacy of DE+EF treatment was tested for control of the poultry red mite (*Dermanyssus gallinae*) and the Chagas disease vector *Triatoma infestans*, where synergism was demonstrated in these cases (Luz et al. 2012; Steenberg and Kilpinen 2014).

10.3.3 *The Cuticular Hydrocarbons*

Cuticular hydrocarbons are covered in detail in Chap. 7, but a brief mention of volatile hydrocarbons and their importance in pest management is warranted here. Insects depend on an array of volatile hydrocarbons produced in the integument and released from the epicuticle for chemical communication. Besides protection, these cuticular hydrocarbons are used by insects as chemical signals to send and receive various types of information crucial to their survival. All these signaling hydrocarbons are grouped together as semiochemicals. They can be either intraspecific (pheromone) or interspecific (allomones, kairomones) (Ingleby 2015). Semiochemicals of both types have been utilized for pest management. Sex pheromones have been used in traps for monitoring pest population levels and have also been applied for mating disruption using aerial dispersal or with special ground-based dispensers (Touhara 2013).

10.4 The Endocuticle

The endocuticle, which is a major component of the cuticle, is characterized by chito-protein lamellae (Locke 1991). Chitin is an amino polysaccharide made up of N-acetyl glucosamine units and is the second most abundant naturally-occurring polymer behind cellulose. It forms an integral part of the exoskeleton of insects and

is degraded and resynthesized during each molt. Such processes are meticulously managed by several hormones acting in concert with a panoply of transcription factors (Nijhout 1981; Hiruma and Kaneko 2013; Chaudhari et al. 2015; Cheong et al. 2015). Chitin synthesis in the endocuticle has been successfully targeted for pest management by a collection compounds usually referred to as insect growth regulators (IGRs).

10.4.1 *Chitin as Target*

Chitin is synthesized, cross-linked with cuticular proteins to form cuticular structures and subsequently is degraded and resorbed during each molting cycle. Three targets within chitin metabolism, which are amenable for pest control, have been exploited. First, chitin synthesis can be blocked, resulting in an incomplete and deformed molt that consequently led to lethality. Benzoylphenyl ureas cause such molt deformities and many compounds of this family have been commercialized. Second, the hormonal regulation of chitin formation can be adversely interfered with, resulting in aberrant molting. Benzoyl hydrazines are non-steroidal ecdysone agonists that cause such defects and some have been developed as insecticides. Third, the targeting of chitin dissolution via chitinases can be attempted. The latter strategy is still largely in development, using transgenic organisms expressing chitinases.

10.4.2 *Benzoylphenyl Ureas*

Benzoylphenylureas (BPUs) were developed in the early 1970s from a serendipitous discovery made at Philips-Duphar in Holland during a routine assay of newly synthesized compounds *inter alia* for insecticidal activity. Larvae treated with a BPU left on the bench showed delayed molting deformities resulting in mortality. This discovery led to the development of the first commercially viable new class of insecticide, diflubenzuron or by its commercial name Dimilin (Maas et al. 1981). This compound has to be ingested to be effective and manifests its effects at the time of molt where various degrees of deformities become apparent. Since the introduction of diflubenzuron, a host of new IGRs that interfere with chitin synthesis have been developed by several agrochemical companies around the world. BPUs have a relatively narrow spectrum of activity affecting only species that have a chitinous exoskeleton and the material needs to be ingested to manifest its effects. This class of compounds has been extensively reviewed and in this chapter we will update the status of BPU development (Retnakaran et al. 1985; Cohen 1987; Wright and Retnakaran 1987; Dhadialla et al. 2005; Cohen 2010; Dhadialla et al. 2010; Matsumura 2010; Doucet and Retnakaran 2012; Sun et al. 2015).

10.4.2.1 Benzoylphenyl Urea Structures

BPU consist of a urea bridge flanked by a benzoyl group on one side and a phenyl group on the other. The two side groups have been modified with diverse substituents resulting in an array of BPUs that show differential activity towards various species of insects (Doucet and Retnakaran 2012; Sun et al. 2015). A representative list of BPUs that have been commercialized is shown in Table 10.1.

10.4.2.2 Physiological and Morphological Effects of Benzoylphenyl Ureas

BPU adversely interfere with chitin synthesis in the insect cuticle and manifest their effects at the time of the molt. Molt deformities in the ultimate larval instar extend from being arrested at the onset of being mostly larval, to being almost pupal in appearance (Sundaramurthy and Santhanakrishnan 1979) (Fig. 10.4). The window of sensitivity to BPUs occurs in the early part of the stadium, but since these compounds are known for their persistence, this is therefore of little consequence. BPU treatment causes the appearance of an outer zone of normal lamellae located over a fibrous layer, with a transitional layer in between. BPUs also cause the progressive loss of apical plasma membrane microvilli through which the chitin fibrils are extruded. These microvilli are replaced by a smooth membrane (Retnakaran et al. 1989).

10.4.2.3 Resistance to Benzoylphenylureas

Resistance can be manifested in many forms from behavioral avoidance, lack of penetration to metabolic resistance and target insensitivity, the latter two being more common. Lack of cuticular penetration is common for BPUs since they have to be ingested in order to be effective. Metabolic resistance is caused by the ability of the insect to metabolise the insecticide, notably by over expressing enzymes that can neutralize the compound. A diflubenzuron-modifying hydrolase is over-expressed in the resistant forms of the red flour beetle, *Tribolium castaneum* and the Egyptian cotton leaf worm, *Spodoptera littoralis* (Ishaaya 1993). In some cases, resistance is caused when the insecticide binds to an off-target receptor and is rendered ineffective or detoxified. Some evidence for the involvement of membrane-bound ATP binding cassette transporters or ABC transporters (also called permeability glycoprotein or PGP or Multi Drug Resistance) in the elimination of benzoylphenyl ureas has been presented (Li et al. 2013). The Australian sheep blowfly, *Lucilia cuprina* developed resistance to diflubenzuron after repeated use to control fly strikes and concomitantly, developed cross-resistance to cyromazine which is an unrelated chitin inhibitor (Levot and Sales 2004).

Table 1 Representative selection of commercially important benzoylphenyl ureas

Name	Year introduced	Manufacturer	Comments
Diflubenzuron	1972	Philips-Duphar	Effective on numerous Lepidopteran larvae but its effects on the Gypsy moth, <i>Lymantria dispar</i> and the Forest tent caterpillar, <i>Malacosoma disstria</i> are truly spectacular providing near complete control (Granett and Dunbar 1974; Retnakaran et al. 1976).
Flufenoxuron	1987	Shell International	Successfully used against many insects of public health concern and Lepidopteran larvae on fruits, vegetables and grains. It has been very effective on the mushroom sciarid fly, <i>Lycoriella ingenua</i> (Erler et al. 2011).
Bistrifluron	2000	Dongbu Hannong Chemical	Primarily used as a termiticide. Target species include the Formosan subterranean termite (<i>Coptotermes formosanus</i>) (Kubota et al. 2006), and the mound building termite, <i>Nasutitermes exitosus</i> in south eastern Australia (Webb and McClintock 2015).
Chlorfluazuron	1982	Ishihara Sangyo Kaisha	Chlorfluazuron has been successfully tested on a wide variety of insect species including for termite baiting (Evans and Iqbal 2015). Found to be very active against the spruce budworm, <i>Choristoneura fumiferana</i> (Retnakaran 1982).
Lufenuron	1977	Lufenuron	The commercial formulation of Lufenuron, Match, has been tested on a variety of insect orders with good activity. It was tested on the fall armyworm, <i>Spodoptera frugiperda</i> along with entomopathogenic nematodes. It was found to be compatible with both <i>Heterorhabditis</i> and <i>Steinernema</i> species (Negrisoli et al. 2010).
Triflumuron	1982	Bayer	Extensively tested on hemipteran, dipteran, coleopteran and lepidopteran pests. Prophylactic mosquito control with Triflumuron against <i>Aedes aegypti</i> , to prevent the establishment of Dengue fever in Australia has been successful (Jacups et al. 2014).
Fluazuron	1990	Novartis	Used in controlling the cattle tick, <i>Rhipicephalus microplus</i> either by itself or with a combination with Ivermectin (Gomes et al. 2015). Useful in dusky footed wood rat baits for the control ticks and fleas (Slowik et al. 2001).

(continued)

Table 10.1 (continued)

Name	Year introduced	Manufacturer	Comments
Teflubenzuron	1982	Celamerck GmBh	Successfully used for controlling trichodinid parasites (fish lice) and other parasites of fish in fish farms, e.g. Tilapia (<i>Oreochromis niloticus</i>), and Pacu (<i>Piaractus mesopotamicus</i>) (Ikefuti et al. 2015). The copepod parasite <i>Lepeophtheirus salmonis</i> affecting salmon farms can also be effectively controlled with teflubenzuron (Branson et al. 2000).
Hexaflumuron	1984	Dow Elanco	Originally used for the control of the western subterranean termite, <i>Reticulitermes hesperus</i> (Haagsma and Rust 2005). Also used for controlling many Lepidopteran pests, notably the cotton bollworm, <i>Helicoverpa armigera</i> (Darvishzadeh et al. 2014).
Novaluron	1990	Makkhteshim Agan Industries	Useful in controlling mosquitoes such as <i>Anopheles albimanus</i> , <i>Anopheles pseudopunctipennis</i> , <i>Aedes aegypti</i> , <i>Aedes albopictus</i> and <i>Culex quinquefasciatus</i> (Arredondo-Jiménez and Valdez-Delgado 2006). Excellent control of subterranean termites in Texas (Keefer et al. 2015).

10.4.2.4 Environmental Effects

Two of the major environmental problems with BPUs are their persistence and non-target collateral damage. Persistence can be both an insecticidal boon and an environmental problem. Non-target crustaceans that have a chitinous exoskeleton, not surprisingly, are sensitive to BPUs, but two factors mitigate their adverse effects, namely low solubility in water and rapid microbial degradation. Lufenuron displayed various degrees of effects on crustaceans in mesocosm ditches, affecting more severely the bivoltine and multivoltine species than the univoltine species (Brock et al. 2009). Novaluron had similar effects on non-target organisms but with judicious use regarding time and application the off-target effects can be minimised (Cutler and Scott-Dupree 2007).

10.4.2.5 Mode of Action of Benzoylphenyl Ureas

Chitin synthesis can be demonstrated by employing various techniques such as tracking the incorporation of ^{14}C or ^3H N-acetyl glucosamine precursors into the polymer, or by staining with fluorescein-labelled wheat germ agglutinin that specifically binds with chitin (Retnakaran 1995). Using autoradiographic and histological methods it was established that BPUs inhibit chitin synthesis. However, the exact

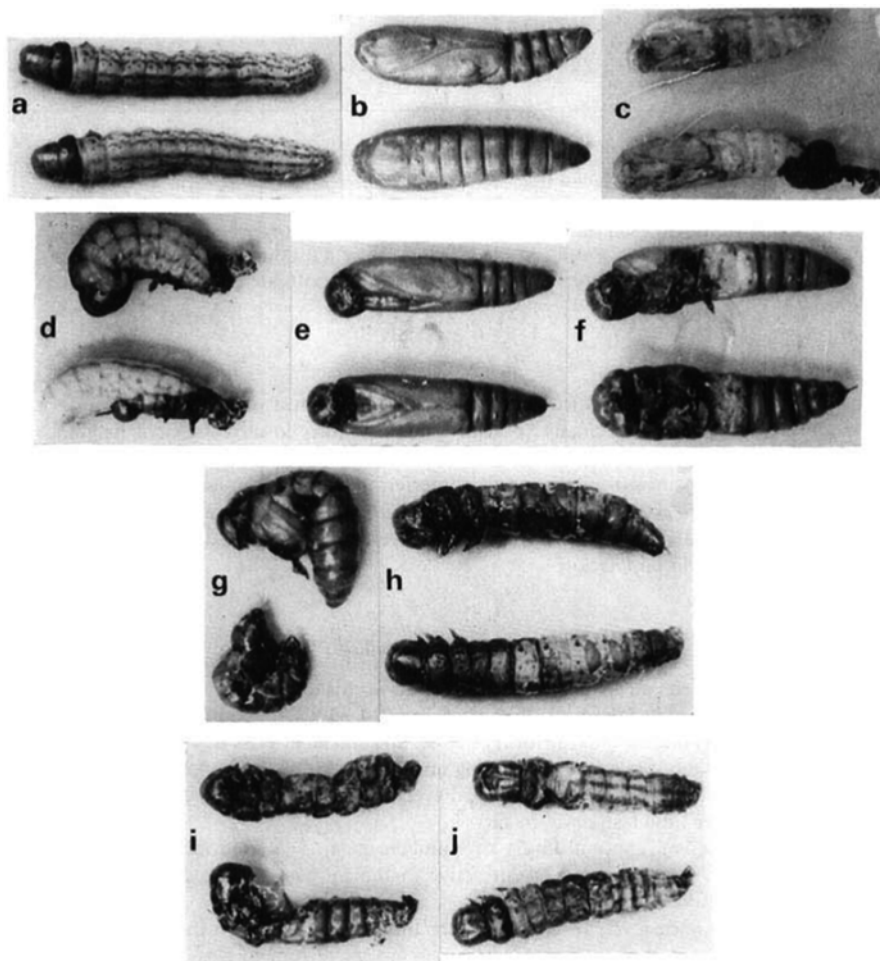


Fig. 10.4 Morphogenetic effects of diflubenzuron on the coconut black-headed caterpillar, *Nephantis serinopa* fed with treated coconut leaflets. (a) Normal 6th instar larvae; (b) Normal pupae; (c), White pupae with degenerate proboscis; (d) Malformed pupae; (e) Pupae with larval heads; (f) Pupae with larval abdominal patch; (g) Abnormal pupae with extended wings; (h, i, j) Progressively worsening larval pupal intermediates (Sundaramurthy and Santhanakrishnan 1979, with the kind permission of John Wiley and Sons.)

biochemical lesion where this happens has not been resolved unequivocally. One theory claims that polymerisation of N-acetyl glucosamine is catalysed by the epidermal chitin synthase which is packaged in vesicles that harbor sulfonylurea receptors (SUR). SUR is an atypical member of a large group of ABC transporters that are ubiquitous and involved *inter alia* in transporting proteins across membranes (Burke et al. 2008). A classic role of SUR is in the exocytosis of insulin stored in vesicles inside β cells in the pancreas of mammals (Fig. 10.5). Upon entry of glucose with the aid of the glucose transporter into the β cells, the ATP/ADP levels increase which shuts the K_{ATP} channel. Reduced K^+ levels leads to the

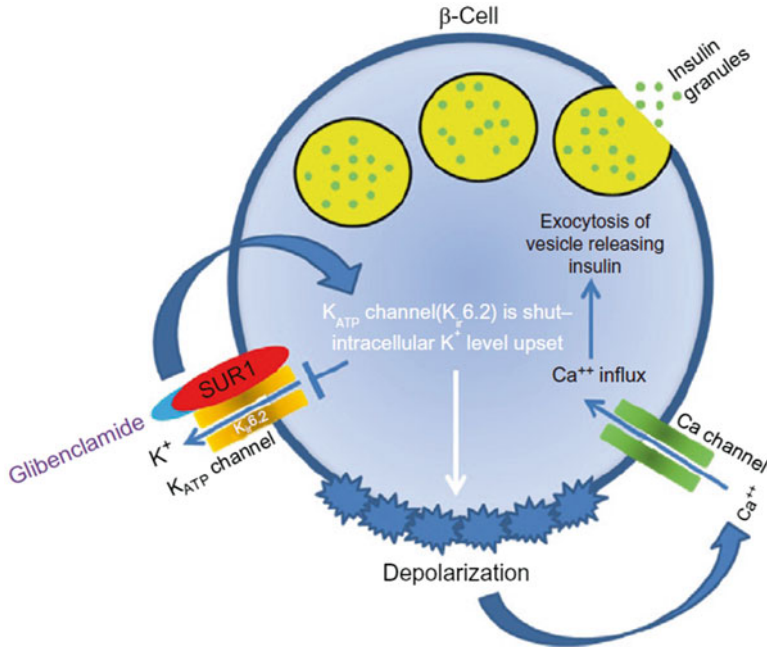


Fig. 10.5 Glibenclamide, a sulfonylurea, upon binding to the sulfonylurea receptor (SUR1) results on the closure of the K_{ATP} channel ($K_{i6.2}$) which depolarises the membrane and allows the influx of Ca^{2+} into the β cell resulting in the exocytosis of the vesicle releasing the insulin granules (Doucet and Retnakaran 2012, with the kind permission of John Wiley and Sons.)

depolarization of cell membrane and opening the Ca^{2+} channel allowing the influx of Ca^{2+} ions into the β cell which facilitates the exocytosis of the vesicle releasing the insulin granules. When a person suffers from diabetes, among other things, the vesicles in the β cell are unable to exocytose to release insulin. However, if an anti-diabetic drug such as the sulfonylurea glibenclamide is administered, it binds with the receptor, SUR, leading to the closure of the K^+ ion channel, followed by membrane depolarization, Ca^{2+} influx and exocytosis of the vesicles leading to the release of insulin. When this drug was administered to nymphs of the German cockroach, *Blattella germanica*, it blocked chitin synthesis and induced molt deformities similar to diflubenzuron. Furthermore, in a competitive binding assay 3H glibenclamide was found to bind to a SUR preparation, and could be displaced with diflubenzuron, leading to the suggestion that the target of BPUs is likely SUR (Abo-Elghar et al. 2004; Matsumura 2010; Li et al. 2013). When a *Drosophila melanogaster* fruit fly lacking in SUR was generated, it did not show any chitin deformity indicating that it is not essential for normal integumental chitin deposition (Meyer et al. 2013). In addition, RNAi-mediated knockdown of SURs in *T. castaneum* did not reveal altered phenotypes when compared to control insects (Broehan et al. 2013), suggesting that SURs may be not involved in BPU-mediated inhibition of chitin synthesis (though BPUs may nonetheless bind to SURs). Clarifying the role(s) of SURs

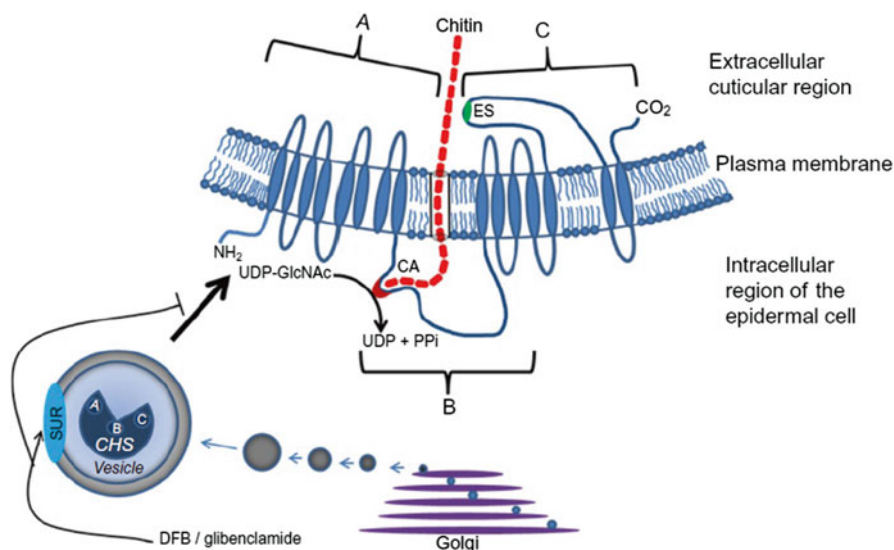


Fig. 10.6 Hypothetical mode of action of diflubenzuron (DFB) through the ABC transporter, sulfonylurea receptor (SUR), by interfering with the exocytosis of chitin synthase (CHS) of *Drosophila*. Normally the CHS vesicle binds with the plasma membrane where it initiates chitin synthesis and SUR which includes the K_{ATP} channel and maintains energy homeostasis within the cell. A, B, C, – the three main domains of CHS, B being the catalytic domain and the other two are transmembrane domains. CA, Catalytic area with the Walker motifs; ES, consensus sequence for chitin extrusion; Other consensus sequences are not shown (Based on Matsumura (2010); Merzendorfer (2006); Moussian (2010)) (From Doucet and Retnakaran (2012), with the kind permission of John Wiley and Sons.)

BPU metabolism can only be resolved with a better understanding of their functions in insects. (Fig. 10.6) (Doucet and Retnakaran 2012).

10.4.3 Benzoyl Hydrazines (Non-Steroidal Ecdysone Agonists)

Chitin synthesis and deposition take place at the onset of the molting process and continue until the appearance of the ecdysteroid peak, at which time the larva stops the synthetic process indicating that ecdysone either directly or indirectly down regulates chitin synthesis. The regulation of epidermal chitin synthase by 20-hydroxyecdysone (20E) may not be direct but through other transcription factors although it is clear that chitin is synthesized during the absence of the molting hormone and is not synthesized during its presence (Zhuo et al. 2014). Larvae treated with 20E at the beginning of a stadium exhibit chitin synthesis inhibition (Palli and Retnakaran 1999). In 1988 Wing et al. reported that a substituted benzoyl hydrazine developed by Rohm and Haas Company mimicked the effects of ecdysone and

induced a precocious, albeit deformed, molt in the tobacco hornworm, *Manduca sexta*.

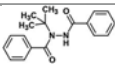
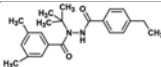
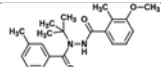
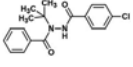
10.4.3.1 Benzoyl Hydrazine Structures

Benzoyl hydrazines, which are characterized by 2 moieties, a benzoyl group and a hydrazine group, have been extensively reviewed (Nakagawa 2005; Dhadialla et al. 2005, 2010; Smagghe et al. 2012). There are at present 5 benzoyl hydrazines of commercial importance and a 6th one that may be developed (Table 10.2). Although there have been attempts to synthesize other non-steroidal ecdysone agonists, only tetrahydroquinoline-substituted compounds were found to have insecticidal potential. Although their activity against the tobacco budworm, *Heliothis virescens* was relatively weak, they were all quite active against the yellow fever mosquito *Aedes aegypti* (Palli et al. 2005). Interestingly enough, in a cell-based receptor transactivation assay, one such substituent, RG 120768, worked only with the *A. aegypti* ecdysone receptor (AaEcR) indicating that it is mosquito-specific. Some new diacyl hydrazines and acyl hydrazones with high ecdysone agonist activity have been reported recently and are being actively studied to evaluate their control potential (Sun and Zhou 2015).

10.4.3.2 Physiological and Morphological Effects of Benzoyl Hydrazines

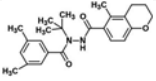
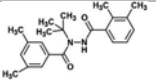
Ingestion of a benzoyl hydrazine ecdysone agonist by a larva induces a precocious incomplete molt and lethality. The newly formed cuticle is membranous and unsclerotized. The old cuticle is separated from the new one and appears as a loose shroud (Fig. 10.7) (Wing et al. 1988; Retnakaran et al. 2001; 2003). Upon ingestion of the ecdysone agonist the larva stops feeding and enters into the molting phase that is incomplete. The larva remains in a moribund state and eventually dies of starvation and desiccation. The newly-synthesized cuticle is wrinkled and the head capsule is buckled with the mandibles misaligned (Fig. 10.8) (Retnakaran et al. 1997a). Chitin synthesis occurs during the early part of the larval stadium prior to the appearance of the ecdysone peak (Fig. 10.9). When an ecdysone agonist is provided during the early part of the stadium, chitin synthesis is turned off, but the molting process is initiated as seen in the morphological changes illustrated in Fig. 10.10. Apolysis is followed by secretion of ecdysial droplets and dissolution of the cuticle, but the new cuticle lacks the characteristic lamellate structure (Retnakaran et al. 1997a).

Table 10.2 Non-steroidal benzoylhydrazines ecdysone agonists used in pest control

Structure	Name	Manufacturer	Comments
	RH-5849	Rohm & Haas	First benzoylhydrazone for which the ecdysone-mimicking activity was characterized. RH-5849 caused changes in the morphology and biochemistry of a <i>Drosophila</i> cell line with the formation of cellular processes and the induction of acetyl cholinesterase. The compound also competed with ^3H -ponasterone for the receptor binding sites (Wing 1988).
	Tebufenozide	Rohm & Haas	Particularly effective on lepidopteran larvae (Retnakaran et al. 1997a; Smagghe and Degheele 1994; Smagghe et al. 2012). The formulated product Mimic® has been used to control forest insect pests. Another formulation, Confirm®, has been used successfully on cotton insects such as the beet army worm, <i>Spodoptera exigua</i> (Walton et al. 1995).
	Methoxyfenozide	Rohm & Haas	Several times more active than tebufenozide especially on lepidopteran larvae (Carlson et al. 2001; Ishaaya et al. 1995). It is very effective against the cotton bollworm, <i>Helicoverpa armigera</i> and the Oriental leaf worm, <i>Spodoptera litura</i> (Saber et al. 2013; Rehan and Freed 2015).
	Halofenozide	Rohm & Haas	Active on various insects, but has a propensity to be more effective on coleopterans (Soin et al. 2009). It has been particularly successful in controlling turf insects such as the Japanese beetle, <i>Popillia japonica</i> (Cowles and Villani 1996). Studies on the Colorado potato beetle, <i>Leptinotarsa decemlineata</i> suggests that one of the reasons for the success of halofenozide on coleopterans could be because of retention of the compound due to low excretion (Farinós et al. 1999).

(continued)

Table 10.2 (continued)

Structure	Name	Manufacturer	Comments
	Chromafenozide	Nippon Kayaku Co and Sankyo Co	Potent control agent against lepidopteran pests and almost non-toxic to non-lepidopterans (Yanagi et al. 2006). It is just as active on lepidopterans as the other strong contender, methoxyfenozide (Mosallanejad et al. 2008).
	KU-106	N/A	Identified in a <i>Bombyx mori</i> cell line based screening system of ecdysone agonists. Displayed activity against the malarial mosquito, <i>Anopheles gambiae</i> (Morou et al. 2013).

10.4.3.3 Mode of Action of Benzoyl Hydrazines

The mode of action of benzoyl hydrazines has been well characterized and studied in detail in the tobacco hornworm *Manduca sexta*. Ingestion of tebufenozide by a larva is followed by its binding to the cytosolic 20E receptors EcR and USP. After transfer into the nucleus, the complex of benzoyl hydrazine and EcR/USP heterodimer attaches itself to ecdysone response elements (ERE) located upstream of molting genes, activating a sequence of transcription factors in a pattern initially undistinguishable from the natural hormone. The transcription factors involved in molting include FTZ-F1, which is expressed at the end of the ecdysteroid peak and induced by HR3, which in turn is induced by the ecdysteroid (Cruz et al. 2008; Mane-Padros et al. 2012). The difference between the action of 20E and benzoyl hydrazine agonists becomes readily apparent during the second phase of the ecdysteroid peak, when levels of the hormone are dropping. Chitin synthesis occurs at a rapid pace as soon as the insect ecdyses into the next instar and is completed at the appearance of the ecdysteroid peak (Fig. 10.9).

When three well-characterized genes from *M. sexta* were used to study the effect of tebufenozide, the molecular mode of action became apparent. Each gene is differentially regulated by 20E. *MHR3* (*Manduca* hormone receptor 3) is expressed in the epidermis when exposed to 20E, *LCP14* (Larval cuticular protein 14 kD) is expressed in the absence of 20E and finally *DDC* (dopa decarboxylase) is expressed after exposure followed by removal of 20E (transient exposure). When exposed to tebufenozide, *MHR3* is expressed, but both *LCP14* and *DDC* are repressed, in contrast to events following exposure to 20E. Attempts to rinse the integument preparations and remove the tebufenozide failed to restore normal expression patterns, indicating that it was tightly bound to the receptor. Treatment with tebufenozide, therefore, initiates the molting process, but does not allow it to continue to its logi-

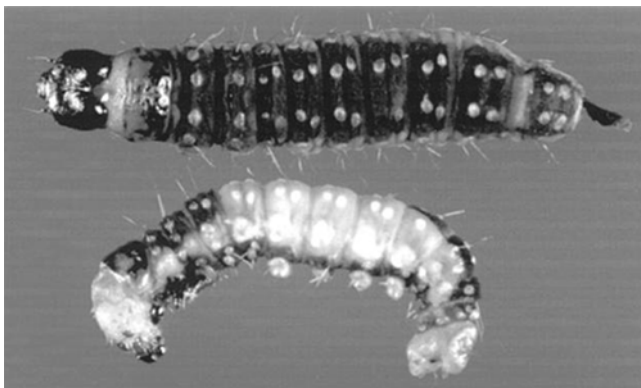


Fig. 10.7 Phenotypic effects 48 h after feeding on 100 ng of RH-5992 (tebufenozide) to a 5th instar spruce budworm (*Choristoneura fumiferana*) along with an untreated control (larva on top). The loose head capsule was removed to reveal the untanned head capsule. Apolysis and digestion of the old cuticle has resulted in the separation of the old cuticle and the larva appears pharate with the old cuticular shell enclosing the larva with a new cuticle. The untreated control (larva on top) has molted into a normal 6th instar (Retnakaran et al. 2003)

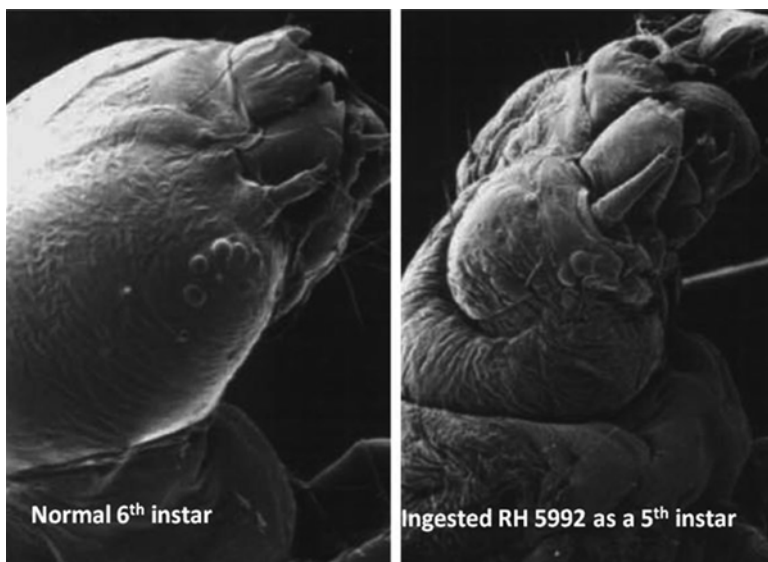


Fig. 10.8 Scanning electron micrograph of the lateral view of the head capsules of untreated and RH-5992 (tebufenozide) treated spruce budworm (*Choristoneura fumiferana*) larvae. The untreated 5th instar has molted into a normal 6th instar whereas the treated 5th instar went through an incomplete molt and the loose head capsule was removed to show the malformed new head capsule which is membranous and buckled. The mandibles are lopsided and non-functional (Retnakaran et al. 1997b)

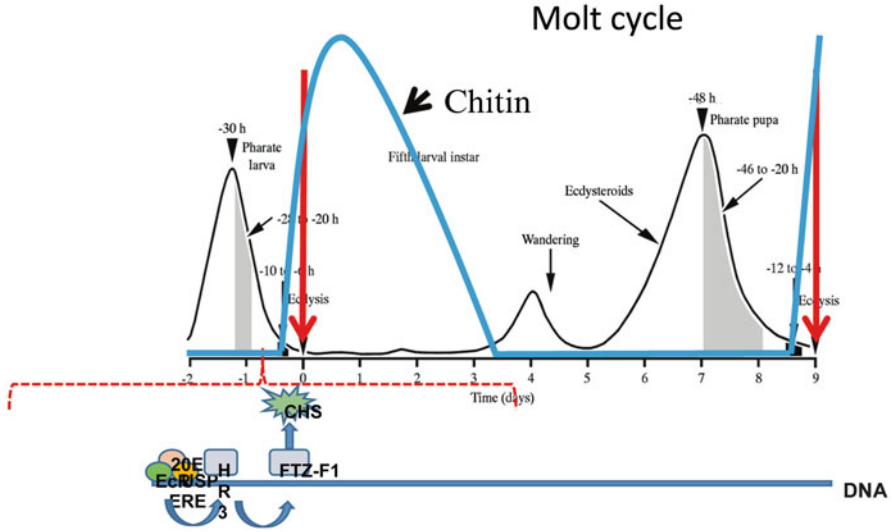


Fig. 10.9 Chitin synthesis profile (blue) superimposed on the ecdysone titer during the molting cycle in *Manduca sexta*. 20E, 20 hydroxy ecdysone; *CHS* chitin synthase, *ECR* ecdysone receptor, *ERE* ecdysone response element, *FTZ-F1* Fushi tarazu transcription factor1, *HR3* hormone receptor3; *USP* ultraspiracle (Based on Bollenbacher et al. (1981); Cruz et al. (2008); Li et al. (2015); Mame-Padros (2012); Retnakaran et al. (1989); Riddiford et al. (2003)). With the kind permission of Elsevier Ltd. See text for details

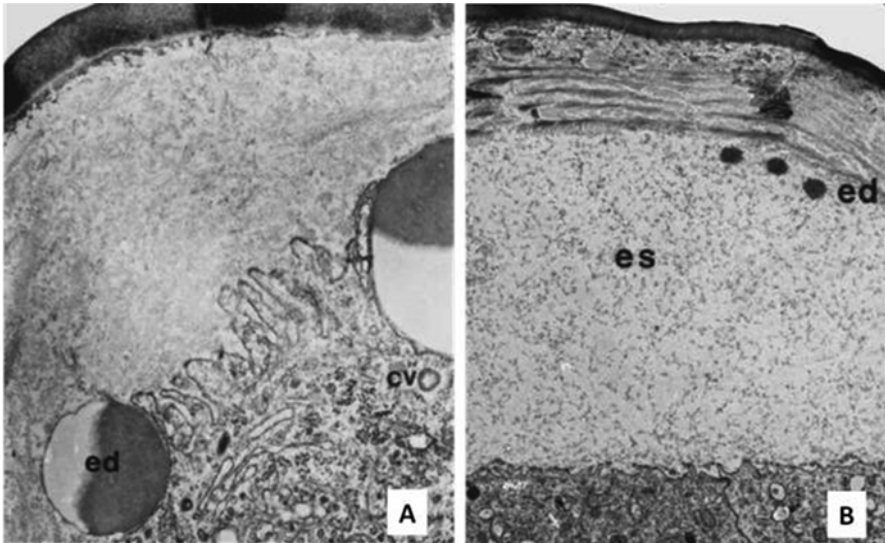


Fig. 10.10 Transmission electron micrographs of RH-5992 (tebufenozide) treated 6th instar larvae of the spruce budworm, *Choristoneura fumiferana*. (a) 4 h post treatment showing putative ecdysial droplets; (b) 16 h post treatment showing separation of old cuticle with ecdysial space filled with fibrous material instead of chitinous endocuticular lamellae. *cv* coated vesicle, *ed* ecdysial droplets, *es* ecdysial space (Retnakaran et al. 1997b)

cal conclusion and instead molting comes to a halt. This mechanism of action is consistent with the carryover effects from one instar to the next as documented in the eastern spruce budworm, *Choristoneura fumiferana* (Kothapalli et al. 1995; Palli et al. 1995; Retnakaran et al. 1995, 2007b, 2001; Cadogan et al. 2002; Retnakaran et al. 2003). The binding affinities of the different ecdysone agonists to the EcR/USP receptor largely determine their biological activities (Minakuchi et al. 2003).

10.4.4 Etoxazole, Hexythiazox and Clofentazine

Etoxazole belongs to the family of 2,4-diphenyl-1,3-oxazoline compounds. Launched commercially in 1998, it represented the culmination of efforts by Yashima Chemical Industry to develop new acaricidal and insecticidal chemistries based on heterocyclic structures containing endocyclic oxygen and nitrogen atoms, compounds known in nature as highly bioactive (Suzuki et al. 2002). Among the series of substituted compounds from this study, 1-[2-(2,6-difluorophenyl)-1,3-oxazolin-4-yl]-2-ethoxy-4-tert-butylbenzene (etoxazole, Fig. 10.11a) behaved both as an excellent acaricide against two-spotted spider mite (*Tetranychus urticae*) eggs, larvae and nymphs, and as a promising insecticide for controlling green rice leafhoppers, diamondback moth (*Plutella xylostella*) larvae and green peach aphids (*Myzus persicae*).

The discoverers of etoxazole noted early on that its acaricidal and insecticidal activity was reminiscent of benzoylphenylureas by preventing molting. Later, *in vivo* experiments using fall armyworm (*Spodoptera frugiperda*) larvae confirmed that it inhibited chitin synthesis. Fifth instar larvae treated with etoxazole displayed incomplete ecdysis as evidenced by double head-capsules, and treated sixth-instar larvae showed lower integumental chitin content compared to controls (Nauen and Smaghe 2006). Incorporation of radiolabeled N-acetylglucosamine into chitin chains during cuticle formation was likewise decreased in a dose-dependent fashion, although etoxazole potency in this regard was much lower (40X) than the BPU triflumuron.

The exact target site of etoxazole remained elusive until a recent breakthrough was achieved by genetically mapping etoxazole resistance found in certain populations of *T. urticae*. Using bulk segregant analysis (BSA) and Illumina genome sequencing, Van Leeuwen et al. (2012) were able to map the resistance to a single DNA lesion affecting the chitin synthase 1 locus (*CHS1*). The *CHS1* allele conferring resistance presents an isoleucine-to-phenylalanine substitution at position 1017, toward the C-terminus of the protein. The change in amino acid residue affects the fifth transmembrane domain of a 5-transmembrane segment (called 5TMS), a region highly conserved between insect and mite chitin synthases which is thought to be involved in pore formation and the extrusion of nascent chitin fibers. The exact mechanism by which this mutation confers etoxazole resistance in *T. urticae* is still a matter of conjecture, but the bulkiness of the phenylalanine residue

may block access to etoxazole without affecting CHS1 catalytic activity (Merzendorfer 2013).

The market need for oxazoline compounds with higher potency against insects, and the desire to address resistance in spider mites have fostered the development of several new etoxazole-based leads. The engineering of these new variants was inspired in part from the interpretation of quantitative structure activity relationship (QSAR) data accumulated on BPU's over the years. BPU's, like etoxazole, possess a difluorophenyl moiety which is key for activity. Thus, the most promising oxazoline candidates also all share the same 2,6-difluorophenyl at the 2-phenyl moieties, as modification of this structure is deleterious to miticidal activity. In contrast, the 4-phenyl moiety was found to be more amenable to modification and several derivatives have been generated recently (Fig. 10.11b–d). The presence of electron-withdrawing groups in this moiety was shown initially by Suzuki et al. (2006) to favor ovicidal and acaricidal activity. Liu et al. (2013) produced a suite of 4-phenyl variants, combining a phenoxy- or alkoxy- group at the *para* position along with with Cl-, methyl- or ethoxy- groups at the *meta*- and/or *ortho*-position. The compound in Fig. 10.11b was retained as a the best candidate among 25, with activities against spider mites and insects equivalent to etoxazole (100% mortality at doses of 2.5 mg/L against *T. cinnabarinus*, and 65 and 93% mortality at 12.5 mg/L when tested on beet armyworm and diamondback moth). Inspired by these results, the

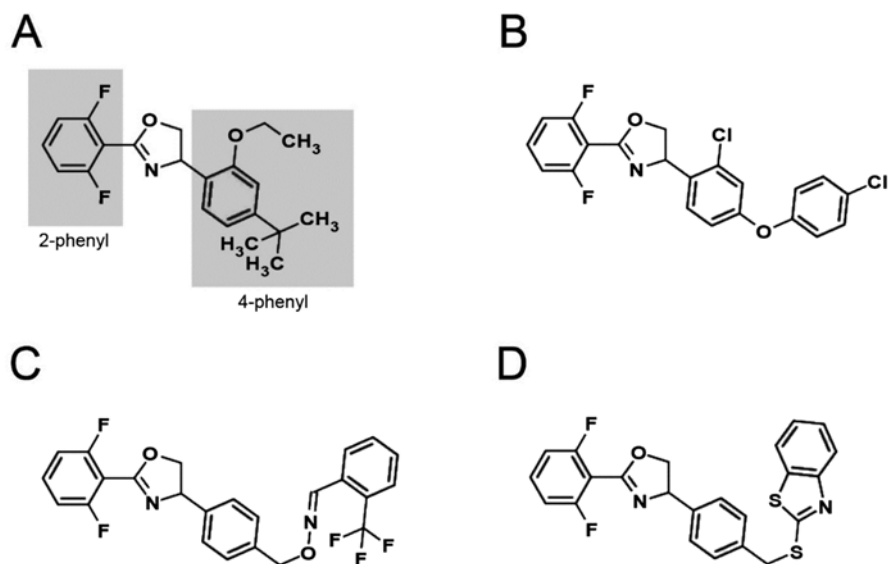


Fig. 10.11 Chemical structure of etoxazole (1-[2-(2,6-difluorophenyl)-1,3-oxazolin-4-yl]-2-ethoxy-4-*tert*-butylbenzene) (a) and three novel analogs. The 2-phenyl and 4-phenyl moieties of etoxazole are shaded; (b) 2-(2,6-difluorophenyl)-4-(2-Cl-4-(4-Cl-phenoxy) phenyl)-1,3-oxazoline (Liu et al. 2013); (c) 2-(trifluoromethyl)benzaldehyde O-(4-(2-(2,6-difluorophenyl)-4,5-dihydrooxazol-4-yl) benzyl) oxime (Li et al. 2014); (d) 4-(4-((Benzo[d]thiazol-2-ylthio) methyl) phenyl)-2-(2,6-difluorophenyl)-4,5-dihydrooxazole (Yu et al. 2015)

same team designed further variants containing 4-phenyl oxime ether substituents based on the presence of a similar oxime ether group present in the BPU flucycloxonon (Li et al. 2014). The best compound of this category (Fig. 10.11c) surpassed etoxazole in toxicity, being able to kill 100% of the Carmine mite, *T. cinnabarinus* eggs and larvae at the lowest concentration tested (0.0001 mg/L) while etoxazole itself was ineffective at the same dose. Field trials conducted in 2013 in various regions in China have confirmed its potential as an etoxazole alternative for the control of the citrus red mite *Panonychus citri* or *Tetranychus cinnabarinus*. Lastly, oxazolines bearing sulfur ether moieties localized at the *para*- position of the 4-phenyl group were synthesized by Yu et al. (2015). Among 23 compounds, the one represented in Fig. 10.11d displayed excellent acaricidal activity in the lab (*T. cinnabarinus* egg LC₅₀ 0.0003±0.0001 vs. 0.0089±0.0028 for etoxazole), but showed less activity than etoxazole against mosquitoes and the rice ear-cutting caterpillar *Mythimna separata*. Field trials of this new compound against the Broad mite, *Polyphagotarsonemus latus* and *T. cinnabarinus* on eggplant revealed that it performed better than etoxazole, when used at 22 kg/ha, and might prove useful in mite management on multiple other crops.

Hexythiazox is an acaricide of the thiazolidinone family of compounds. Developed in the early 1980s by Nippon Soda, it was found to inhibit larval mite growth and is also active against eggs and nymphs. It has seen widespread use against several species of spider mites infesting fruit and vegetable crops (Sheets et al. 2012). Hexythiazox is long-lasting in the field and is also compatible with integrated pest management due to its low impact on non-targets such as predatory mites (Bower 1990; Blümel and Gross 2001; Kaplan et al. 2012). Subsequent efforts at developing novel hexythiazox derivatives failed to improve on the miticidal activity of the original compound (Novak et al. 1997).

Clofentezine and diflovidazin are tetrazine compounds that inhibit mite growth. Clofentezine chemical structure presents symmetrical phenyl groups (3,6-bis(2-Chlorophenyl)-1,2,4,5-tetrazine), while diflovidazine is an asymmetrical derivative (3-(2-Chlorophenyl)-6-(2,6-difluorophenyl)-1,2,4,5-tetrazine). Clofentezine displays much of the same properties as hexythiazox in the field with long-lasting miticidal effects after application and negligible impact on non-target arthropods (Sheets et al. 2012; Merzendorfer 2013).

Resistance to both hexythiazox and clofentezine was reported a few years after their introduction, and the existence of cross-resistance between the two compounds was observed in *P. ulmi* and *T. urticae* (Thwaite 1991; Herron et al. 1993; Pree et al. 2002). Recently, Demaeght et al. (2014) were able to pinpoint the genetic basis of hexythiazox and clofentezine resistance in a strain of *T. urticae* (HexR) that is also resistant to etoxazole. Strikingly, HexR exhibits the same I1017F amino acid substitution mentioned above, that is present in four other etoxazole-resistant *T. urticae* collected in geographically diverse locations. These results provide evidence that despite their structural differences, etoxazole, hexythiazox and clofentezine share the same mode of action.

10.4.5 Other Synthetic Chitin Synthesis Inhibitors

Compounds based on the thiadiazine heterocyclic scaffold have seen applications as antifungal and antiparasitic drugs, but buprofezin is the only member of that class that has been commercialized as an insecticide (Rodríguez et al. 2012; Merzendorfer 2013). Buprofezin is effective against plant sucking insect pests such as planthoppers (Delphacidae e.g. the brown planthopper *Nilaparvata lugens*, the white-backed planthopper *Sogatella furcifera*), leafhoppers (Cicadellidae e.g. the green rice leafhopper *Nephotettix virescens*), whiteflies (Aleyrodidae e.g. the sweet potato whitefly *Bemisia tabaci*) and mealybugs (Pseudococcidae e.g., *Pseudococcus* sp.) (Heinrichs et al. 1984; Darvas 1997; Sheets et al. 2012). The target site of buprofezin remains unknown. Izawa et al. (1985) demonstrated that it prevents the polymerisation of N-acetyl-D-[1-³H] glucosamine monomers into chitin in the brown planthopper *N. lugens*. Later, De Cock and Degheele (1991; 1993) performed detailed observations on the cuticular structure of the greenhouse whitefly *Trialeurodes vaporariorum* treated with buprofezin. Buprofezin treatment of larvae caused thinner pharate procuticle and its impact appears limited to post-apolysial cuticle. Interestingly, ultrastructural effects on the epidermal cells themselves were observed after buprofezin treatment (e.g. hypertrophied mitochondria) which led the authors to conclude that the compound may have pleiotropic effects on the epidermal tissue.

Multiple instances of resistance to buprofezin have been recorded, particularly in *S. furcifera* and *B. tabaci* (Arthropod Pesticide Resistance Database, <http://www.pesticideresistance.org>, accessed Jan. 2016). In the small brown planthopper *Laodelphax striatellus*, buprofezin resistance exhibited by the YN-BPF strain is dependent in part on detoxification by the cytochrome P450 gene *CYP6CW1*. Furthermore, reduction of NADPH-cytochrome P450 reductase (CPR) transcript levels by RNAi-mediated knockdown triggers a much more elevated mortality by buprofezin in the resistant strain than in the susceptible strain, confirming the key role of the P450-mediated detoxification system against this compound (Zhang et al. 2012, 2016).

Captan is a thiophthalamide that is widely used as a broad-spectrum fungicide. It is chiefly a non-specific compound that reacts with cellular thiols groups, but it is also able to inhibit the activity of insect chitin synthase in cell-free systems (Cohen and Casida 1982; Merzendorfer 2013).

10.4.6 Chitin Synthesis Inhibitors from Natural Sources

Compounds interfering with chitin synthesis have been isolated from natural sources. Polyoxins and nikkomycins are peptidyl nucleosides that display good chitin synthase inhibition *in vitro*, particularly against those of fungi. Polyoxins were purified in the 1960s from the fungus *Streptomyces cacaoi* var. *asoensis*, while

nikkomycin was isolated from *Streptomyces tendae* (Jackson et al. 2013). These molecules bear a structural resemblance to UDP-GlcNAc and therefore act as competitive inhibitors in the synthesis of the chitin polymer. However, due to their charged nature and their poor transport across cell membrane, very few have been developed as agriculturally relevant fungicides and none are used against insects or mites (Merzendorfer 2013). Polyoxins A, B and D have received some attention in terms of their chitin-synthesis inhibition properties in insects. Polyoxin A inhibits cuticle deposition in grasshopper nymphs (Vardanis 1978). A similar effect was observed with polyoxin D in sheep blowfly larvae (Binnington 1985), and Cohen and Casida (1980) reported that polyoxin D can inhibit chitin synthase activity from cell-free larval guts of *Tribolium castaneum*. Arakawa et al. (2008) tested the insecticidal activity of polyoxin AL, a fungicide with a high content of polyoxin B. Ingestion of polyoxin AL was toxic to larvae of the Oriental leafworm *Spodoptera litura*, *Mythimna separata*, and the cabbage moth *Mamestra brassicae*, but larvae of the silkworm *B. mori* were unaffected. The basis for this selective effect is unknown, but could be interesting to study further for controlling lepidopteran pests affecting sericulture. Nikkomycin Z has been widely used to study chitin synthase activity and chitin metabolism in model insect systems (Gangishetti et al. 2009; Chaudhari et al. 2011). However, it has not been developed commercially to control pest species.

10.5 Interfering with Chitin Formation and Degradation

As mentioned before, chitin is synthesized during the first half of the larval stadium prior to the ecdysone peak and degradation starts once ecdysone is secreted. The polymerising enzyme, chitin synthase 1 is secreted in the epidermis and chitin synthase 2 is involved in the synthesis of chitin in the peritrophic membrane by the midgut (Merzendorfer 2006; Shirk et al. 2015). We have so far examined the inhibition of various matrices of the cuticle by interfering with the biosynthetic process at the receptor or gene expression level. We will now examine the possibility of directly interfering with either chitin synthase or chitinase.

10.5.1 Inhibition of Chitin Synthase A in the Epidermis

RNAi (RNA interference) is a recent development where a naturally occurring gene silencing process used for inactivating deleterious DNA sequences arising from virus infections or transposons or during development, has been developed for sequence specific gene silencing (Kola et al. 2015). RNAi against chitin synthase is exemplified by experiments performed by Chen et al. (2008) on the chitin synthase gene (*SeCHSA*) from the beet armyworm (*Spodoptera exigua*). Injecting larvae with 18–25 bp siRNA fragments specific to *SeCHSA* resulted in either failure to molt or

molting into small larvae that failed to pupate. When larvae of *T. castaneum*, were injected with dsRNAs specific to *TcCHS1*, chitin synthase transcripts were successfully silenced. *TcCHS1* has two splice variants, 8a and 8b, the former being required for both larval-pupal and pupal-adult molts, whereas the latter is required only for the pupal-adult molt (Arakane et al. 2005). In order to utilize dsRNA molecules for control, they must be appropriately formulated to resist environmental degradation, and must enter the insect either by topical application or oral administration. In *A. aegypti*, dsRNA specific to the chitin synthase 1 gene were shown to enter the larvae by soaking them in water containing the dsRNA. Gene silencing was achieved, as larvae show molt deformities (Singh et al. 2013). The obvious major advantage of the RNAi approach is in the development of highly pest-specific control with little or no collateral damage. Oral delivery of dsRNA and siRNAs was also elegantly demonstrated in the potato psyllid, *Bactericera cockerelli* (Wuriyangan et al. 2011).

10.5.2 Chitinases and Inhibition of Chitin Degradation

Chitinolytic enzymes are responsible for the depolymerisation of chitin and are widespread in nature (Patil et al. 2000). They have been recruited in many instances of the coevolutionary arms race between insects and their pathogenic microorganisms, to allow penetration of the insect chitin barrier. Plants also synthesize chitinases, mainly to combat fungal infection, but some are known to be produced in response to insect damage (Kolosova et al. 2014).

The degradation of insect chitin in an untimely fashion or in the wrong organ or structure has long been thought as a viable strategy for insect control. Chitin present in the peritrophic membrane (PM) appears the most vulnerable to attack, and chitinase-expressing transgenic organisms have been developed for this purpose. Transgenic plants expressing fungal chitinases, alone or in “stacked” configuration with other insecticidal proteins have been engineered, with varying effects on insect herbivory (Amian et al. 2011; Vihervuori et al. 2013; Chen et al. 2014). Chitinases from insect baculoviruses serve largely to rupture the epidermal cuticle for the release of occlusion bodies after host liquefaction. However, the chitinase A protein from *Autographa californica* multicapsid nucleopolyhedrovirus (AcMNPV) has gut permeating activity in the tobacco budworm *Heliothis virescens* PM, which makes possible its use to synergize the activity of other ingested biopesticides (Fiandra et al. 2010). Several bacterial entomopathogens are also producers of chitinases, and must likewise be ingested to produce insecticidal effects (Aggarwal et al. 2015). However, the Gram-negative bacteria *Aeromonas dhkanesis* 3K1C15 appears to be an exception, in that it secretes a cocktail of chitinases that is able to directly degrade chitin present in the eggs of chironomid flies (Laviad et al. 2016).

Fungal pathogens of arthropods for their part routinely bypass the oral route to successfully infect their hosts. They are therefore equipped with a battery of hydrolases, including powerful chitinases that can breach the thick and challenging exo-

skeleton (St Leger and Wang 2010; Agrawal et al. 2015). The entomofungal pathogen *Metharizhium anisopliae* encodes 24 genes of the glycosyl hydrolase 18 family, of which chitinases are members (Junges et al. 2014). Two of these chitinases (ChiMaB1 and ChiMaB2) are associated with host colonisation, as their genetic deletion affects virulence toward insect hosts (Boldo et al. 2009; Staats et al. 2013).

Attempts to increase the virulence of fungal entomopathogens by altering chitinase expression have been made, particularly with *B. bassiana*. The *B. bassiana* chitinase Bbchit1 has a catalytic domain, but lacks a chitin-binding domain. The addition of a chitin-binding domain from the *B. mori* chitinase to Bbchit1 was found to increase the virulence of *B. bassiana* expressing the fusion construct (Fan et al. 2007). Constitutive expression in *B. bassiana* of a fusion transgene combining Bbchit1 with the cuticle-degrading protease virulence factor CDEP1 resulted in even better insecticidal properties compared to wild-type or to transgenic fungi overexpressing Bbchit1 (Fang et al. 2009).

The inhibition of insect chitinase activity with chemical compounds has been attempted. The compounds tested include allosamidin, argadin, argifin, psammaplin and pentoxifyllin. The best characterized chemical remains allosamidin, a pseudo trisaccharide isolated from *Streptomyces* sp. and which structure consists of 2-acetamido-2-deoxy-D-allose (N-acetyl-D-allosamine) and an allosamizoline (Sakuda et al. 1986). Allosamidin was found to inhibit larval-larval ecdysis when injected in the moth *B. mori* and *M. separata*. In the latter species, allosamidin was also effective at blocking larval pupal ecdysis (Sakuda et al. 1987). Blattner et al. (1997) synthesized eight allosamidin analogs, and established that the spatial configuration of the cyclitol unit attached to the disaccharide is key for activity.

Argadin and Argifin are cyclic pentapeptides isolated from cultures of the soil fungi *Clonostachys* sp. FO-7314 and *Gliocladium* sp. FTD-0668, respectively. Both compounds were found to be ca. 9 times less active than allosamidin in a *L. cuprina* chitinase inhibition assay conducted at 20 °C (Hirose et al. 2010). Both compounds were also active *in vivo* when injected into American cockroach nymphs. Injection of 20 µg of either compound resulted in 60% (argadin) or 73% (argifin) mortality, with nymphs displaying a new cuticle, but unable to shed the old one. These results are consistent with an inhibition of chitinases at a critical juncture of the molting cycle.

Psammaplin A is a brominated tyrosine derivative isolated during an antibiotic screening program, and later shown to have anti-chitinolytic activity in assays of crude *Bacillus* chitinase extracts (Tabudravu et al. 2002). Like allosamidin, psammaplin A interacts with the chitinase active site. Psammaplin A has been tested via ingestion and found to be toxic to the eastern subterranean termite *Reticulitermes flavipes*, and *M. persicae* (Saguez et al. 2006; Husen and Kamble 2013).

Pentoxifyllin is a 1,3-dimethylxanthine that was identified in a screen of *Aspergillus fumigatus* chitinase inhibitors (Rao et al. 2005). Pentoxifyllin is a competitive inhibitor, and has shown activity against *R. flavipes*, but acts more slowly on this species than other chitin synthesis insecticides such as benzoylphenylureas (Husen and Kamble 2013).

The activity of insect chitinases can also be reduced *in vivo* by knocking down their transcripts with double-stranded RNA molecules. The injection of sequence specific dsRNAs was used by Zhu et al. (2008) to tease apart the functions of 10 out of 23 chitinase genes present in *T. castaneum*. Only two of the tested gene targets, *TcCHT10* and *TcCHT5* were inferred to have a role in the catabolism of cuticular chitin, with *TcCHT10* required for all molts (larval, pupal and adult) while *TcCHT5* was only critical for adult eclosion. The dsRNA tested on the other chitinases provoked localized effects or did not lead to visible phenotypes.

The translation of RNAi technology from the bench to the field to control pest species is an active area of research, in part because of the implied superior environmental safety of dsRNA compared to conventional chemical pesticides. The concepts and technical considerations surrounding the use of RNAi in pest control have been addressed elsewhere (Scott et al. 2013; Yu et al. 2013; Kim et al. 2015), but published data on the targeting of chitinases is so far limited. Expression of the European corn borer *Ostrinia nubilalis* larval gut chitinase gene *Oncht* was targeted by including *Oncht*-specific dsRNAs in the artificial diet. Hatchlings fed this dsRNA reached a lower weight than control larvae and presented higher peritrophic membrane chitin content, implying that *Oncht* plays a crucial role in PM chitin degradation (Khajuria et al. 2010). More recently, Mamta et al. (2016) engineered transgenic tobacco and tomato plants expressing a dsRNA hairpin encoding 144 bp of the cotton bollworm, *Helicoverpa armigera* chitinase I gene (*HaCHI*). Some of the transformed lines caused a significant reduction in *H. armigera* larvae survival, longer larval development time and lower larval weight up to 16 days of continuous feeding. A high percentage of larvae feeding on lines expressing elevated *HaCHI*-dsRNA could not complete development and were arrested as pupal-adult intermediates. These results strongly suggest that chitin content of the epidermis is affected by *HaCHI*-dsRNA.

10.6 The Exocuticle

The exocuticle is the outer layer of the procuticle which under electron microscopy appears darker than the inner endocuticle, and also exhibits a distinct lamellar structure (Moussian 2010). The electron-dense appearance of the exocuticle is due to its higher degree of sclerotization, the process by which chitin and cuticular proteins become covalently cross-linked by their reaction with phenolic compounds. Sclerotization is often accompanied by melanisation (darkening) and both processes were reviewed by Andersen (2010, 2012) and are comprehensively reviewed in Chap. 6 of this book. Briefly, sclerotization begins with the synthesis of the catechols *N*-acetyldopamine (NADA) and *N*- β -alanyldopamine (NBAD) in epidermal cells. Both NADA and NBAD are generated first by the conversion of tyrosine into dopa by the enzyme tyrosine hydroxylase. Dopa is further converted to dopamine by the dopa-decarboxylase enzyme. Dopamine can then be converted into NADA by *N*-acetylation, or into NBAD by *N*- β -alanylation (Andersen 2010). NADA and

NBAD are actively trafficked from the epidermal cells to the cuticle, and through the successive action of multiple enzymes (i.e. laccase, ortho-quinone isomerase, quinone methide tautomerase) the cross-linking of cuticular matrices via nucleophilic reactions is facilitated.

As an essential step of the molting cycle, sclerotization is conceptually an attractive process to misregulate to ultimately kill insects. However, no active ingredient currently in use specifically targets sclerotization enzymes or the transport of precursors from epidermal cells. Cyromazine (*N*-Cyclopropyl-1,3,5-triazine-2,4,6-triamine) is a triazine compound that was hypothesised early on to target sclerotization due to its phenotypic effects on dipteran and lepidopteran pupae, which become elongated in shape after treatment (Binnington 1985; Reynolds and Blakey 1989). *M. sexta* larvae treated with cyromazine exhibit weaker extensibility (more rigidity) of the body wall cuticle, resulting in internal pressure buildup and rupturing of the cuticle (Reynolds and Blakey 1989). Cyromazine neither affect chitin synthesis, nor does it change the electrophoretic pattern of cuticular proteins or tyrosine pools, indicating that the essential building blocks of the exocuticle are unaffected (Kotze and Reynolds 1991; Bel et al. 2000). Working with *D. melanogaster*, where under certain exposure regimes cyromazine shortened the time to adult emergence, Van De Wouw et al. (2006) proposed that the compound interferes with 20E. A more solid identification of the target was accomplished by the positional cloning of a cyromazine resistance gene in *D. melanogaster* (Chen et al. 2006). The gene encodes a phosphatidylinositol 3-kinase-related kinase (PIKKs), which could be involved in DNA metabolism. Treatment of flies with a dsRNA engineered against this gene caused the flies to become resistant to cyromazine, thus recapitulating the phenotype of the mutated locus. Cyromazine may therefore affect a fundamental DNA metabolism process in insects, of which cuticle aberrations constitute the most overt phenotype.

Dicyclanil (4,6-diamino-2-(cyclopropylamino)pyrimidine-5-carbonitrile) is an IGR which is structurally close to cyromazine. Its effect on cuticle and the occurrence of cross-resistance with cyromazine indicate that both compounds share a similar mode of action (Magoc et al. 2005). Dicyclanil is used in the prevention of blowfly strike in sheep (Bowen et al. 1999).

10.7 The Ecdysis Cascade

The molting cycle extends from ecdysis or shedding of the old cuticle at the end of a stadium to ecdysis at the subsequent stadium. Ecdysis occurs at the tail end of the molting cycle after the nascent cuticle has been synthesized and the old cuticle has been incompletely digested. The ecdysis sequence consists of three stages, preecdysis, ecdysis and postecdysis. The symphony of events that occur under the control of a group of neuroendocrine hormones and peptides has been reviewed by White and Ewer (2014). As the insect prepares to shed the old cuticle, several muscles have to be stimulated to enable the insect to wriggle out of the old cuticle, fill itself

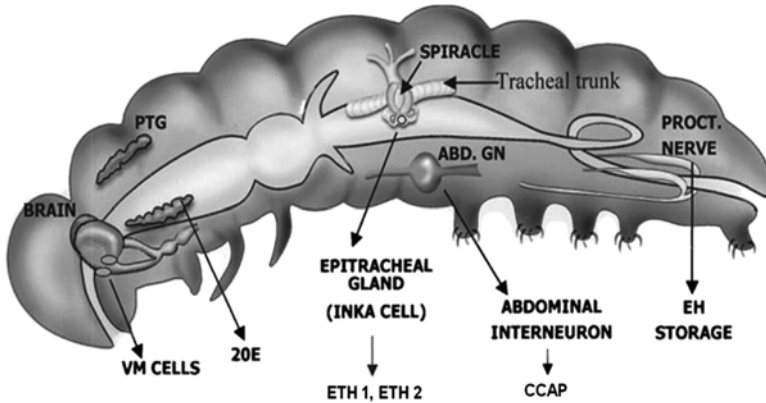


Fig. 10.12 The ecdysis cascade begins with the ventro-medial neurosecretory cells (VM cells) secreting the eclosion hormone (EH) in the presence of 20-hydroxy ecdysone (20E) and stored in the proctodeal nerve (proct.nerve) and is released in the absence of 20E stimulated by ETH. The EH acts on the Inka cells in the epitrichal gland and releases ETH and PETH. There appears to be a reciprocal stimulation. EH and ETH initiate tracheal response, start contractions and induce the release of crustacean cardioactive peptide (CCAP) which completes the ecdysis together with contributions from neuropeptides, corazonin and bursicon. For details see text (Retnakaran et al. 2003)

with air and harden the exoskeleton. It accomplishes all these steps with a set of neurohormones that interact with their corresponding receptors located in strategic motor neurons that stimulate muscle contractions that result in ecdysis. These neuropeptides include ETH (ecdysis triggering hormone), PETH (preecdysis triggering hormone), EH (eclosion hormone), the crustacean cardioactive peptide (CCAP), Corazonin and Bursicon (Zitnan and Adams 2000; Mesce and Fahrbach 2002; Zitnan et al. 2003; Clark et al. 2004; Truman 2005) (Fig. 10.12).

Given that the ecdysis cascade is regulated by several neuropeptides with built-in redundancies and fail safe mechanisms, it would appear that targeting the neurohormones for pest management may not be very successful. But using RNAi against many of them has resulted in derailing the ecdysis cascade (Arakane et al. 2008). Palli and Cusson (2007) discussed ways and means of targeting the neuropeptides for pest control. Each neuropeptide has its corresponding receptor which can also be targeted. Overexpressing EH by infecting the insect with an engineered baculovirus carrying the EH gene was ineffective (Eldridge et al. 1992). The kissing bug, *Rhodnius prolixus* is a vector that transmits the protozoan *Trypanosoma cruzi* which causes Chagas disease. The *R. prolixus* G-protein receptor for CCAP was cloned (RhoprCCAPR) and a knockdown with RNAi had a deleterious effect on the insect (Lee et al. 2013). The receptor for bursicon, a GPCR called rickets in *D. melanogaster*, may also be targetable with antagonists. The ubiquitous knockdown of rickets with dsRNA blocks larval ecdysis (Loveall and Deitcher 2010).

10.8 Identifying Other Possible Targets During Cuticle Genesis

Many of the cuticular matrices that have been successfully targeted for control have been the result of serendipitous discoveries that saw BPUs and benzoyl hydrazines deployed commercially. Molting is by far the most vulnerable state of an insect's life history. This feature complicates the search for targets of cuticular genesis because insects often die during molting regardless of the insecticide used or its mode of action. Recent interest in botanicals has resulted in the isolation of several plant metabolites that may act adversely on cuticle formation (Isman 2015). One problem with botanicals is that they have collective effects on multiple components including cuticular compartments. Azadirachtin is a well-known botanical that has several effects including interference with the molting process (growth regulator effect) and quite possibly with the eclosion cascade (El-Wakeil 2013; Senthil-Nathan 2013). Certain triterpenes (Ceanothane and oleanane) from the shrub, *Talguenea quinquenervia* were found to interfere with sclerotization and molting against the codling moth *Cydia pomonella*, the mealworm, *Tenebrio molitor* and *D. melanogaster* (Quiroz et al. 2015).

With the increased use of combinatorial chemistry and *in silico* screening one could envisage development of insecticides with enhanced environmental safety and target specificity against many of the neuropeptides and their receptors involved in the molting process. Use of RNAi against many of these targets has demonstrated that it is indeed feasible (Palli and Cusson 2007; Arakane et al. 2008).

10.9 Conclusions

Target specificity with little or no collateral damage and environmental safety without sacrificing efficacy are the two guiding principles that should form the driving force in developing new pest control agents. As our understanding of the molting sequence and the synthesis and degradation of various cuticular matrices increases with the use of molecular techniques such as selective gene editing and inhibition, we should be able to develop better control agents with increased specificity. The dynamic status of the cuticle that undergoes dramatic changes during the molting cycle and the eclosion cascade affords ample opportunities to interfere with several components at various stages of formation, dissolution and rebuilding.

References

- Abo-Elghar GE, Fujiyoshi P, Matsumura F (2004) Significance of the sulfonylurea receptor (SUR) as the target of diflubenzuron in chitin synthesis inhibition in *Drosophila melanogaster* and *Blattella germanica*. *Insect Biochem Mol Biol* 34:743–752
- Aggarwal C, Paul S, Tripathi V, Paul B, Khan MA (2015) Chitinolytic activity in *Serratia marcescens* (strain SEN) and potency against different larval instars of *Spodoptera litura* with effect of sublethal doses on insect development. *BioControl* 60:631–640
- Agrawal Y, Khatri I, Subramanian S, Shenoy BD (2015) Genome sequence, comparative analysis, and evolutionary insights into chitinases of entomopathogenic fungus *Hirsutella thompsonii*. *Genome Biol Evol* 7:916–930
- Akbar W, Lord JC, Nechols JR, Howard RW (2004) Diatomaceous earth increases the efficacy of *Beauveria bassiana* against *Tribolium castaneum* larvae and increases conidia attachment. *J Econ Entomol* 97:273–280
- Amian AA, Papenbrock J, Jacobsen HJ, Hassan F (2011) Enhancing transgenic pea (*Pisum sativum* L.) resistance against fungal diseases through stacking of two antifungal genes (chitinase and glucanase). *GM Crops* 2:104–109
- Andersen SO (2010) Insect cuticular sclerotization: a review. *Insect Biochem Mol Biol* 40:166–178
- Andersen SO (2012) Cuticular sclerotization and tanning. In: Gilbert LI, Iatrou K, Gill SS (eds) *Comprehensive molecular insect science*, vol 4. Elsevier, New York, pp 167–192
- Arakane Y, Muthukrishnan S, Kramer KJ, Specht CA, Tomoyasu Y, Lorenzen MD, Kanost M, Beeman RW (2005) The *Tribolium* chitin synthase genes *TcCHS1* and *TcCHS2* are specialized for synthesis of epidermal cuticle and mid gut peritrophic matrix. *Insect Mol Biol* 14:453–463
- Arakane Y, Li B, Muthukrishnan S, Beeman RW, Kramer KJ, Park Y (2008) Functional analysis of four neuropeptides, EH, ETH, CCAP and bursicon, and their receptors in adult ecdysis behavior of the red flour beetle, *Tribolium castaneum*. *Mech Dev* 125:984–995
- Arakawa T, Yukuhiro F, Noda H (2008) Insecticidal effect of a fungicide containing polyoxin B on the larvae of *Bombyx mori* (Lepidoptera: Bombycidae), *Mamestra brassicae*, *Mythimna separata*, and *Spodoptera litura* (Lepidoptera: Noctuidae). *Appl Entomol Zool* 43:173–181
- Arredondo-Jiménez JI, Valdez-Delgado KM (2006) Effect of Novaluron (Rimon 10 EC) on the mosquitoes *Anopheles albimanus*, *Anopheles pseudopunctipennis*, *Aedes aegypti*, *Aedes albopictus* and *Culex quinquefasciatus* from Chiapas, Mexico. *Med Vet Entomol* 20:377–387
- Athanassiou CG, Kavallieratos NG, Vayias BJ, Tsakiri JB, Mikeli NH, Meletsis CM, Tomanović Z (2008) Persistence and efficacy of *Metarhizium anisopliae* (Metschnikoff) Sorokin (Deuteromycotina: Hyphomycetes) and diatomaceous earth against *Sitophilus oryzae* (L.) (Coleoptera: Curculionidae) and *Rhyzopertha dominica* (F.) (Coleoptera: Bostrychidae) on wheat and maize. *Crop Prot* 27:1303–1311
- Bai NS, Remadevi OK, Sasidharan TO, Balachander M, Dharmarajan P (2012) Cuticle degrading enzyme production by some isolates of the entomopathogenic fungus, *Metarhizium anisopliae* (metsch.). *J Biol Sci* 20:25–32
- Bel Y, Wiesner P, Kayser H (2000) Candidate target mechanisms of the growth inhibitor cyromazine: studies of phenylalanine hydroxylase, puparial amino acids, and dihydrofolate reductase in dipteran insects. *Arch Insect Biochem Physiol* 45:69–78
- Berry-Caban CS (2011) DDT and silent spring: fifty years after. *J Mil Veterans Health* 19:19–24
- Binnington KC (1985) Ultrastructural changes in the cuticle of the sheep blowfly, *Lucilia*, induced by certain insecticides and biological inhibitors. *Tissue Cell* 17:131–140
- Blattner R, Gerard PJ, Spindler-Barth M (1997) Synthesis and biological activity of allosamidin and allosamidin analogues. *Pestic Sci* 50:312–318
- Blomquist GJ, Bagnères A-G (2010) History and overview of insect hydrocarbons. In: Blomquist GJ, Bagnères A-G (eds) *Insect hydrocarbons: biology, biochemistry and chemical ecology*. Cambridge University Press, Cambridge, pp 1–18

- Blümel S, Gross M (2001) Effect of pesticide mixtures on the predatory mite *Phytoseiulus persimilis* A.H. (Acarina, Phytoseiidae) in the laboratory. *J Appl Entomol* 125:201–205
- Boldo JT, Junges A, Do Amaral KB, Staats CC, Vainstein MH, Schrank A (2009) Endochitinase CH2 of the biocontrol fungus *Metarhizium anisopliae* affects its virulence toward the cotton stainer bug *Dysdercus peruvianus*. *Curr Genet* 55:551–560
- Bollenbacher WE, Smith SL, Goodman W, Gilbert LI (1981) Ecdysone titer during larval-pupal-adult development of the tobacco hornworm, *Manduca sexta*. *Gen Comp Endocrinol* 44:302–306
- Bowen FL, Fisara P, Junquera P, Keevers DT, Mahoney RH, Schmid HR (1999) Long-lasting prevention against blowfly strike using the insect growth regulator dicyclanil. *Aust Vet J* 77:454–460
- Bower CC (1990) Comparison of clofentezine and hyxythiazox with cyhexatin for integrated control of European red mite, *Panonychus ulmi* (Koch). *Crop Prot* 9:463–468
- Branson EJ, Ronsberg SS, Ritchie G (2000) Efficacy of teflubenzuron (Calicide) for the treatment of sea lice, *Lepeophtheirus salmonis* (Kroyer 1838), infestations of farmed Atlantic salmon (*Salmo salar* L.). *Aquacult Res* 31:861–867
- Brock TCM, Roessink I, Belgers JDM, Bransen F, Maund SJ (2009) Impact of a benzoyl urea insecticide on aquatic macroinvertebrates in ditch mesocosms with and without non-sprayed sections. *Environ Toxicol Chem* 28:2191–2205
- Broehan G, Kroeger T, Lorenzen M, Merzendorfer H (2013) Functional analysis of the ATP-binding cassette (ABC) transporter gene family of *Tribolium castaneum*. *BMC Genomics* 14:6
- Burke MA, Mutharasan RK, Ardehali H (2008) The sulfonylurea receptor, an atypical ATP-binding cassette protein, and its regulation of the KATP channel. *Circ Res* 102:164–176
- Cadogan BL, Scharbach RD, Krause RE, Knowles KR (2002) Evaluation of tebufenozide carry-over and residual effects on *Spruce Budworm* (Lepidoptera: Tortricidae). *J Econ Entomol* 95:578–586
- Carlson GR, Dhadialla TS, Hunter R, Jansson RK, Jany CS, Lidert Z, Slaweki RA (2001) The chemical and biological properties of methoxyfenozide, a new insecticidal ecdysteroid agonist. *Pest Manag Sci* 57:115–119
- Chaudhari SS, Arakane Y, Specht CA, Moussian B, Boyle DL, Park Y, Kramer KJ, Beeman RW, Muthukrishnan S (2011) Knickkopf protein protects and organizes chitin in the newly synthesized insect exoskeleton. *Proc Natl Acad Sci U S A* 108:17028–17033
- Chaudhari SS, Noh MY, Moussian B, Specht CA, Kramer KJ, Beeman RW, Arakane Y, Muthukrishnan S (2015) Knickkopf and retroactive proteins are required for formation of laminar serosal procuticle during embryonic development of *Tribolium castaneum*. *Insect Biochem Mol Biol* 60:1–6
- Chen Z, Robin C, Damiano J, Lydall J, Lumb C, Smith K, Blasetti A, Daborn PJ, Heckel D, McKenzie JA, Batterham P (2006) Positional cloning of a cyromazine resistance gene in *Drosophila melanogaster*. *Insect Mol Biol* 15:181–186
- Chen X, Tian H, Zou L, Tang B, Hu J, Zhang W (2008) Disruption of *Spodoptera exigua* larval development by silencing chitin synthase gene A with RNA interference. *Bull Entomol Res* 98:613–619
- Chen P-J, Senthilkumar R, Jane W-N, He Y, Tian Z, Yeh K-W (2014) Transplastomic *Nicotiana benthamiana* plants expressing multiple defence genes encoding protease inhibitors and chitinase display broad-spectrum resistance against insects, pathogens and abiotic stresses. *Plant Biotech J* 12:503–515
- Cheong SP, Huang J, Bendena WG, Tobe SS, Hui JH (2015) Evolution of ecdysis and metamorphosis in arthropods: the rise of regulation of juvenile hormone. *Integr Comp Biol* 55:878–890
- Clark AC, del Campo ML, Ewer J (2004) Neuroendocrine control of larval ecdysis behavior in *Drosophila*: complex regulation by partially redundant neuropeptides. *J Neurosci* 24:4283–4292
- Cohen E (1987) Chitin biochemistry: synthesis and inhibition. *Annu Rev Entomol* 32:71–93

- Cohen E (2010) Chitin biochemistry: synthesis, hydrolysis and inhibition. *Adv Insect Physiol* 38:5–74
- Cohen E, Casida JE (1980) Inhibition of *Tribolium* gut chitin synthetase. *Pestic Biochem Physiol* 13:129–136
- Cohen E, Casida JE (1982) Properties and inhibition of insect integumental chitin synthetase. *Pestic Biochem Physiol* 17:301–306
- Cook DA, Wakefield ME, Bryning GP (2008) The physical action of three diatomaceous earths against the cuticle of the flour mite *Acarus siro* L. (Acari: Acaridae). *Pest Manag Sci* 64:141–146
- Cowles RS, Villani MG (1996) Susceptibility of Japanese beetle, oriental beetle and European chafer (Coleoptera:Scarabaeidae) to halofenozide, an insect growth regulator. *J Econ Entomol* 89:1556–1565
- Cruz J, Nieva C, Mané-Padrós D, Martín D, Bellés X (2008) Nuclear receptor BgFTZ-F1 regulates molting and the timing of ecdysteroid production during nymphal development in the hemimetabolous insect *Blattella germanica*. *Dev Dyn* 237:3179–3191
- Cutler GC, Scott-Dupree CD (2007) Novaluron: prospects and limitations in insect pest management. *Pest Tech* 1:38–46
- Darvas B (1997) Chapter 3.2 Control. 3.2.1 Insect development and reproduction disrupters. In: Ben-Dov Y, Hodgson CJ (eds) *World crop pests, soft scale insects their biology, natural enemies and control*, vol 7 (Part B). Elsevier, New York, pp 165–182
- Darvishzadeh A, Salimian-Rizi S, Katoulinezhad A (2014) Effect of Biolep®, permethrin and hexaflumuron on mortality of cotton bollworm, *Helicoverpa armigera* (Noctuidae: Lepidoptera). *Arthropods* 3:161–165
- De Cock A, Degheele D (1991) Effects of buprofezin on the ultrastructure of the third instar cuticle of the insect *Trialeurodes vaporariorum*. *Tissue Cell* 23:755–762
- De Cock A, Degheele D (1993) Cytochemical demonstration of chitin incorporation in the cuticle of *Trialeurodes vaporariorum* (Westwood) (Homoptera: Aleyrodidae) after buprofezin treatment. *Int J Insect Morphol Embryol* 22:119–125
- Demaeght P, Osborne EJ, Odman-Naresh J, Grbić M, Nauen R, Merzendorfer H, Clark RM, Van Leeuwen T (2014) High resolution genetic mapping uncovers chitin synthase-1 as the target-site of the structurally diverse mite growth inhibitors clofentezine, hexythiazox and etoxazole in *Tetranychus urticae*. *Insect Biochem Mol Biol* 51:52–61
- Dhadialla TS, Retnakaran A, Smagghe G (2005) Insect growth and developmental-disturbing insecticides. In: Gilbert LI, Iatrou K, Gill SS (eds) *Comprehensive molecular insect science*, vol 6. Elsevier, Oxford, pp 55–116
- Dhadialla TS, Retnakaran A, Smagghe G (2010) Insect growth and development disrupting insecticides. In: Gilbert LI, Gill SS (eds) *Insect control: biological and synthetic agents*. Academic, New York, pp 121–184, p. 451
- Doucet D, Retnakaran A (2012) Insect chitin: metabolism, genomics and pest management. *Adv Insect Physiol* 43:438–511
- Eldridge R, O'Reilly DR, Miller LK (1992) Efficacy of a baculovirus pesticide expressing an eclosion hormone gene. *Biol Control* 2:104–110
- El-Wakeil NE (2013) Botanical pesticides and their mode of action. *Gesunde Pflanzen* 65:125–149
- Erler F, Polat E, Demir H, Catal M, Tuna G (2011) Control of mushroom sciarid fly *Lycoriella ingenua* populations with insect growth regulators applied by soil drench. *J Econ Entomol* 104:839–844
- Evans TA, Iqbal N (2015) Termite (order Blattodea, infraorder Isoptera) baiting 20 years after commercial release. *Pest Manag Sci* 71:897–906
- Fan Y, Fang W, Guo S, Pei X, Zhang Y, Xiao Y, Li D, Jin K, Bidochka MJ, Pei Y (2007) Increased insect virulence in *Beauveria bassiana* strains overexpressing an engineered chitinase. *Appl Environ Microbiol* 73:295–302

- Fang W, Feng J, Fan Y, Zhang Y, Bidochka MJ, St Leger RJS, Pei Y (2009) Expressing a fusion protein with protease and chitinase activities increases the virulence of the insect pathogen *Beauveria bassiana*. *J Invertebr Pathol* 102:155–159
- Farinós GP, Smaghe G, Tirry L, Castañera P (1999) Action and pharmacokinetics of a novel insect growth regulator, halofenozide, in adult beetles of *Aubeonimus mariaefranciscae* and *Leptinotarsa decemlineata*. *Arch Insect Biochem Physiol* 41:201–213
- Fiandra L, Terracciano I, Fanti P, Garonna A, Ferracane L, Fogliano V, Casartelli M, Giordana B, Rao R, Pennacchio F (2010) A viral chitinase enhances oral activity of TMOF. *Insect Biochem Mol Biol* 40:533–540
- Fristrom D, Doctor J, Fristrom JW (1986) Procuticle proteins and chitin-like material in the inner epicuticle of the *Drosophila* pupal cuticle. *Tissue Cell* 18:531–543
- Gabarty A, Salem HM, Fouda MA, Abas AA, Ibrahim AA (2014) Pathogenicity induced by the entomopathogenic fungi *Beauveria bassiana* and *Metarhizium anisopliae* in *Agrotis ipsilon* (Hufn.). *J Rad Res Appl Sci* 7:95–100
- Gangishetti U, Breitenbach S, Zander M, Saheb SK, Müller U, Schwarz H, Moussian B (2009) Effects of benzoylphenylurea on chitin synthesis and orientation in the cuticle of the *Drosophila* larva. *Eur J Cell Biol* 88:167–180
- Gomes LVC, Lopes WDC, Cruz BC, Teixeira WB, Felipelli G, Maciel WG, Bichuette MA, Ruivo MA, Colli MHA, Cravalho RS, Martinez AC, Soares VE, Costa AJD (2015) Acaricidal effects of fluazuron (2.5 mg/kg) and a combination of fluazuron (1.6mg/kg) + ivermectin (0.63mg/kg), administered at different routes, against *Rhipicephalus (Boophilus) microplus* parasitizing cattle. *Exp Parasitol* 153:22–28
- Granett J, Dunbar DJ (1974) TH 6040: laboratory and field trials for control of gypsy moths. *J Econ Entomol* 68:99–102
- Haagsma KA, Rust MK (2005) Effect of hexaflumuron on mortality of the Western subterranean termite (Isoptera: Rhinotermitidae) during and following exposure and movement of hexaflumuron in termite groups. *Pest Manag Sci* 61:517–531
- Heinrichs EA, Basilio RP, Valencia SL (1984) Buprofezin, a selective insecticide for the management of rice planthoppers (Homoptera: Delphacidae) and leafhoppers (Homoptera: Cicadellidae). *Environ Entomol* 13:515–521
- Herron G, Edge V, Rophail J (1993) Clofentezine and hexythiazox resistance in *Tetranychus urticae* Koch in Australia. *Exp Appl Acarol* 17:433–440
- Hirose T, Sunazuka T, Omura S (2010) Recent development of two chitinase inhibitors, argifin and argadin, produced by soil microorganisms. *Proc Jpn Acad Ser B Phys Biol Sci* 86:85–102
- Hiruma K, Kaneko Y (2013) Hormonal regulation of insect metamorphosis with special reference to juvenile hormone biosynthesis. *Curr Top Dev Biol* 103:73–100
- Huarte-Bonnet C, Juárez MP, Pedrini N (2015) Oxidative stress in entomopathogenic fungi grown on insect-like hydrocarbons. *Curr Genet* 61:289–297
- Husen TJ, Kamble ST (2013) Delayed toxicity of two chitinolytic enzyme inhibitors (Psammaphin A and Pentoxifylline) against eastern subterranean termites (Isoptera: Rhinotermitidae). *J Econ Entomol* 106:1788–1793
- Ikefuti CV, Carraschi SP, Barbuio R, da Cruz C, de Pádua SB, Onaka EM, Ranzani-Paiva MJ (2015) Teflubenzuron as a tool for control of trichodinids in freshwater fish: acute toxicity and *in vivo* efficacy. *Exp Parasitol* 154:108–112
- Ingleby FC (2015) Insect cuticular hydrocarbons as dynamic traits in sexual communication. *Insects* 6:732–742
- Ishaaya I (1993) Insect detoxifying enzymes: their importance in pesticide synergism and resistance. *Arch Insect Biochem Physiol* 22:263–276
- Ishaaya I, Yablonski S, Horowitz AR (1995) Comparative toxicity of two ecdysteroid agonists, RH-2485 and RH-5992, on susceptible and pyrethroid-resistant strains of the Egyptian cotton leafworm, *Spodoptera littoralis*. *Phytoparasitica* 23:139–145
- Isman MB (2015) A renaissance for botanical insecticides? *Pest Manag Sci* 71:587–590

- Izawa Y, Uchida M, Sugimoto T, Asai T (1985) Inhibition of chitin biosynthesis by buprofezin analogs in relation to their activity controlling *Nilaparvata lugens* Stål. *Pestic Biochem Physiol* 24:343–347
- Jackson KE, Pogula PK, Patterson SE (2013) Polyoxin and nikkomycin analogs: recent design and synthesis of novel peptidyl nucleosides. *Heterocycl Commun* 19:375–386
- Jacups SP, Paton CJ, Ritchie SA (2014) Residual and pre-treatment application of starycide insect growth regulator (triflumuron) to control *Aedes aegypti* in containers. *Pest Manag Sci* 70:572–575
- Junges Â, Boldo JT, Souza BK, Guedes RLM, Sbaraini N, Kmetzsch L, Thompson CE, Staats CC, de Almeida LGP, de Vasconcelos ATR, Vainstein MH (2014) Genomic analyses and transcriptional profiles of the glycoside hydrolase family 18 genes of the entomopathogenic fungus *Metarhizium anisopliae*. *PLoS One* 9:e107864
- Kaplan P, Yorulmaz S, Ay R (2012) Toxicity of insecticides and acaricides to the predatory mite *Neoseiulus californicus* (McGregor) (Acari: Phytoseiidae). *Int J Acarol* 38:699–705
- Kavallieratos NG, Athanassiou CG, Michalaki MP, Batta YA, Rigatos HA, Pashalidou FG, Balotis GN, Tomanović Z, Vayias BJ (2006) Effect of the combined use of *Metarhizium anisopliae* (Metschnikoff) Sorokin and diatomaceous earth for the control of three stored-product beetle species. *Crop Prot* 25:1087–1094
- Kavallieratos NK, Athanassiou CG, Korunic Z, Mikeli NH (2015) Evaluation of three novel diatomaceous earths against three stored-grain beetle species on wheat and maize. *Crop Prot* 75:132–138
- Keefer TC, Puckett RT, Brown KS, Gold RE (2015) Field trials with 0.5% novaluron insecticide applied as a bait to control subterranean termites (*Reticulitermes* sp. and *Coptotermes formosanus* [Isoptera: Rhinotermitidae]) on structures. *J Econ Entomol* 108:2407–2413
- Khajuria C, Buschman LL, Chen M-S, Muthukrishnan S, Zhu KY (2010) A gut-specific chitinase gene essential for regulation of chitin content of peritrophic matrix and growth of *Ostrinia nubilalis* larvae. *Insect Biochem Mol Biol* 40:621–629
- Kim YH, Soumaila Issa M, Cooper AMW, Zhu KY (2015) RNA interference: applications and advances in insect toxicology and insect pest management. *Pestic Biochem Physiol* 120:109–117
- Kola VS, Renuka P, Madhav MS, Mangrauthia SK (2015) Key enzymes and proteins of crop insects as candidate for RNAi based gene silencing. *Front Physiol* 6:art 119
- Kolosova N, Breuil C, Bohlmann J (2014) Cloning and characterization of chitinases from interior spruce and lodgepole pine. *Phytochemistry* 101:32–39
- Kothapalli R, Palli SR, Ladd TR, Sohi SS, Cress D, Dhadialla TS, Tzertzinis G, Retnakaran A (1995) Cloning and developmental expression of the ecdysone receptor gene from the spruce budworm, *Choristoneura fumiferana*. *Dev Genet* 17:319–330
- Kotze AC, Reynolds SE (1991) An examination of cuticle chitin and protein in cyromazine-affected *Manduca sexta* larvae. *Pestic Biochem Physiol* 41:14–20
- Kubota S, Shono Y, Matsunaga T, Tsunoda K (2006) Laboratory evaluation of bistrifluron, a benzoylphenylurea compound, as a bait toxicant against *Coptotermes formosanus* (Isoptera: Rhinotermitidae). *J Econ Entomol* 99:1363–1368
- Laviad S, Golan A, Shaked T, Vaizel-Ohayon D, Halpern M, Pick E (2016) *Aeromonas* chitinase degrades chironomid egg masses. *Environ Microbiol Rep* 8:30–37
- Lee D, Vanden Broeck J, Lange AB (2013) Identification and expression of the CCAP receptor in the Chagas' disease vector, *Rhodnius prolixus*, and its involvement in cardiac control. *PLoS One* 8, e68897
- Levot G, Sales N (2004) Insect growth regulator cross-resistance studies in field and laboratory selected strains of the Australian sheep blowfly, *Lucilia cuprina* (Wiedemann) (Diptera:Calliphoridae). *Aust J Entomol* 43:374–377
- Li Y, Qin Y, Yang N, Sun Y, Yang X, Sun R, Wang Q, Ling Y (2013) Studies on insecticidal activities and action mechanism of novel benzoylphenylurea candidate NK-17. *PLoS One* 8, e66251

- Li Y, Li C, Zheng Y, Wei X, Ma Q, Wei P, Liu Y, Qin Y, Yang N, Sun Y, Ling Y, Yang X, Wang Q (2014) Design, synthesis, acaricidal activity, and mechanism of oxazoline derivatives containing an oxime ether moiety. *J Agric Food Chem* 62:3064–3072
- Li KL, Wan PJ, Wang WX, Lai FX, Fu Q (2015) Ran involved in the development and reproduction is a potential target for RNA-interference-based pest management in *Nilaparvata lugens*. *PLoS One* 10, e0142142
- Liu Y-X, Wei X-C, Li Y-Q, Yang N, Wang Q-M (2013) Design, synthesis and acaricidal/insecticidal activities of etoxazole analogues. *New J Chem* 37:1803–1810
- Locke M (1991) Insect epidermal cells. In: Binnington K, Retnakaran A (eds) *Physiology of the insect epidermis*. CSIRO, Melbourne, pp 1–22
- Lord JC (2001) Desiccant dusts synergize the effect of *Beauveria bassiana* (hyphomycetes: moniliales) on stored-grain beetles. *J Econ Entomol* 94:367–372
- Lord JC (2005) Low humidity, moderate temperature, and desiccant dust favor efficacy of *Beauveria bassiana* (Hyphomycetes: Moniliales) for the lesser grain borer, *Rhyzopertha dominica* (Coleoptera: Bruchidae). *Biol Control* 34:180–186
- Loveall BJ, Deitcher DL (2010) The essential role of bursicon during *Drosophila* development. *BMC Dev Biol* 10:92
- Luz C, Rodrigues J, Rocha LFN (2012) Diatomaceous earth and oil enhance effectiveness of *Metarhizium anisopliae* against *Triatoma infestans*. *Acta Trop* 122:29–35
- Maas W, Van Hes R, Grosscurt AC, Deul DH (1981) Benzoylphenyl urea insecticides. In: Wegler R (ed) *Chemie der Pflanzenschutzund Schadlingsbekämpfungsmittel*, vol 6. Springer, Heidelberg, pp 423–470
- Magoc L, Yen JL, Hill-Williams A, McKenzie JA, Batterham P, Daborn PJ (2005) Cross-resistance to dicyclanil in cyromazine-resistant mutants of *Drosophila melanogaster* and *Lucilia cuprina*. *Pestic Biochem Physiol* 81:129–135
- Makki R, Cinnamon E, Gould AP (2014) The development and functions of oenocytes. *Annu Rev Entomol* 59:405–425
- Mamta, Reddy KR, Rajam MV (2016) Targeting chitinase gene of *Helicoverpa armigera* by host-induced RNA interference confers insect resistance in tobacco and tomato. *Plant Mol Biol* 90:281–292
- Mane-Padros D, Cruz J, Cheng A, Raikhel AS (2012) A critical role of the nuclear receptor HR3 in regulation of gonadotrophic cycles of the mosquito *Aedes aegypti*. *PLoS One* 7, e45019
- Martins GF, Ramalho-Ortiago JM (2012) Oenocytes in insects. *Inverteb Surviv J* 9:139–152
- Matsumura F (2010) Studies on the action mechanism of benzoylurea insecticides to inhibit the process of chitin synthesis in insects: a review on the status of research activities in the past, the present and the future prospects. *Pestic Biochem Physiol* 97:133–139
- Merzendorfer H (2006) Insect chitin synthases: a review. *J Comp Physiol B* 176:1–15
- Merzendorfer H (2013) Chitin synthesis inhibitors: old molecules and new developments. *Insect Sci* 20:121–138
- Mesce KA, Fahrbach SE (2002) Integration of endocrine signals that regulate insect ecdysis. *Front Neuroendocrinol* 23:179–199
- Meyer F, Flötenmeyer M, Moussian B (2013) The sulfonylurea receptor Sur is dispensable for chitin synthesis in *Drosophila melanogaster* embryos. *Pest Manag Sci* 69:1136–1140
- Minakuchi C, Nakagawa Y, Kamimura M, Miyagawa H (2003) Binding affinity of nonsteroidal ecdysone agonists against the ecdysone receptor complex determines the strength of their molting hormonal activity. *Eur J Biochem* 270:4095–4104
- Morou E, Lirakis M, Pavlidi N, Zotti M, Nakagawa Y, Smagghe G, Vontas J, Swevers L (2013) A new dibenzoylhydrazine with insecticidal activity against *Anopheles mosquito* larvae. *Pest Manag Sci* 69:827–833
- Mosallanejad H, Soin T, Swevers L, Iatrou K, Nakagawa Y, Smagghe G (2008) Non-steroidal ecdysteroid agonist chromafenozide: gene induction activity, cell proliferation inhibition and larvicidal activity. *Pestic Biochem Physiol* 92:70–76

- Moussian B (2010) Recent advances in understanding mechanisms of insect cuticle differentiation. *Insect Biochem Mol Biol* 40:363–375
- Nakagawa Y (2005) Nonsteroidal ecdysone agonists. *Vitam Horm* 73:131–173
- Nauen R, Smaghe G (2006) Rapid report: mode of action of etoxazole. *Pest Manag Sci* 62:379–382
- Negrisoni AS, Garcia MS, Negrisoni CRCB (2010) Compatibility of entomopathogenic nematodes (Nematoda: Rhabditida) with registered insecticides for *Spodoptera frugiperda* (Smith, 1797) (Lepidoptera: Noctuidae) under laboratory conditions. *Crop Prot* 29:545–549
- Neville AC (1975) Biology of the arthropod cuticle. Springer, Berlin, p 446
- Nijhout HF (1981) Physiological control of molting in insects. *Am Zool* 21:631–664
- Novak L, Hornyanszky G, Rohaly J, Kolonits P, Szantay C (1997) Preparation of novel hexythiazox analogues. *Pestic Sci* 49:85–89
- Ortiz-Urquiza A, Keyhani NO (2013) Action on the surface: entomopathogenic fungi versus the insect cuticle. *Insects* 4:357–374
- Palli SR, Cusson M (2007) Future insecticides targeting genes involved in the regulation of molting and metamorphosis. In: Ishaaya I, Nauen R, Horowitz RA (eds) *Insecticides design using advanced technologies*. Springer, Berlin, pp 105–126, p. 314
- Palli SR, Retnakaran A (1999) Molecular and biochemical aspects of chitin synthesis inhibition. *EXS* 87:85–98
- Palli SR, Primavera M, Lambert D, Retnakaran A (1995) Age specific effects of RH-5992: a non-steroidal ecdysone agonist, RH-5992, on the spruce budworm, *Choristoneura fumiferana* (Lepidoptera: Tortricidae). *Eur J Entomol* 92:325–332
- Palli SR, Tice CM, Margam VM, Clark AM (2005) Biochemical mode of action and differential activity of new ecdysone agonists against mosquitoes and moths. *Arch Insect Biochem Physiol* 58:234–242
- Patil RS, Ghormade V, Deshpande MV (2000) Chitinolytic enzymes: an exploration. *Enzym Microb Technol* 26:473–483
- Payre F (2004) Genetic control of epidermis differentiation in *Drosophila*. *Int J Dev Biol* 48:207–215
- Perry AS, Yamamoto I, Ishaaya I, Perry R (1998) Introduction. In: *Insecticides in agriculture and environment*. Springer, Berlin, pp 1–3, p 261
- Pree DJ, Bittner LA, Whitty KJ (2002) Characterization of resistance to clofentezine in populations of European red mite from orchards in Ontario. *Exp Appl Acarol* 27:181–193
- Quiroz S, Cespedes CL, Alderete JB, Alarcon J (2015) Ceanothane and oleanane-type triterpenes from *Talguenea quinquenervia* have insecticidal activity against *Cydia pomonella*, *Tenebrio molitor* and *Drosophila melanogaster*. *Ind Crop Prod* 74:759–766
- Rao FV, Andersen OA, Vora KA, DeMartino JA, Van Aalten DM (2005) Methylxanthine drugs are chitinase inhibitors: investigation of inhibition and binding modes. *Chem Biol* 12:973–980
- Rehan A, Freed S (2015) Fitness cost of methoxyfenozide and the effects of its sublethal doses on development, reproduction and survival of *Spodoptera litura* (Fabricius) (Lepidoptera: Noctuidae). *Neotrop Entomol* 44:513–520
- Retnakaran A (1982) Laboratory and field evaluation of a fast-acting insect growth regulator against the spruce budworm, *Choristoneura fumiferana* (Lepidoptera:Tortricidae). *Can Entomol* 114:523–530
- Retnakaran A (1995) Chitin formation in the spruce budworm, *Choristoneura fumiferana* Clem. (Lepidoptera: Tortricidae). In: Zakaria MB, Muda WMW (eds) *Chitin and chitosan—the environmentally friendly modern materials*. University of Malaysia Press, Bangi, pp 1–10
- Retnakaran A, Smith L, Tomkins B (1976) Applications of Dimlin effectively controls forest tent caterpillar populations and affords foliage protection. *Can For Serv Bi-mon Res Notes* 32:26–27
- Retnakaran A, Granett J, Ennis T (1985) Insect growth regulators. In: Kerkut JA, Gilbert LI (eds) *Comprehensive insect physiology, biochemistry and pharmacology*, vol 12. Pergamon Press, Oxford, pp 529–601

- Retnakaran A, MacDonald A, Nicholson D, Percy-Cunningham J (1989) Ultrastructural and autoradiographic investigations of the interference of chlorfluazuron with cuticle differentiation in the spruce budworm, *Choristoneura fumiferana*. *Pestic Biochem Physiol* 35:172–184
- Retnakaran A, Hiruma K, Palli SR, Riddiford LM (1995) Molecular analysis of the mode of action of RH 5992, a lepidopteran-specific, non-steroidal ecdysteroid agonist. *Insect Biochem Mol Biol* 25:109–117
- Retnakaran A, Smith LFR, Tomkins WL, Primavera MJ, Palli SR, Payne N, Jobin L (1997a) Effect of RH-5992, a nonsteroidal ecdysone agonist, on the spruce budworm, *Choristoneura fumiferana* (Lepidoptera: Tortricidae): laboratory, greenhouse, and ground spray trials. *Can Entomol* 129:871–885
- Retnakaran A, Brownwright AJ, Davis CN, Tomkins WL, MacDonald A, Palli SR (1997b) Ultrastructural effects of a non-steroidal ecdysone agonist, RH-5992, on the sixth instar larva of the spruce budworm, *Choristoneura fumiferana*. *J Insect Physiol* 43:55–68
- Retnakaran A, Gelbic I, Sundaram M, Tomkins W, Ladd T, Primavera M, Feng Q, Arif B, Palli R, Krell P (2001) Mode of action of the ecdysone agonist tebufenozide (RH-5992), and an exclusion mechanism to explain resistance to it. *Pest Manag Sci* 57:951–957
- Retnakaran A, Krell P, Feng Q, Arif B (2003) Ecdysone agonists: mechanism and importance in controlling insect pests of agriculture and forestry. *Arch Insect Biochem Physiol* 54:187–199
- Reynolds SE, Blakey JK (1989) Cyromazine causes decreased cuticle extensibility in larvae of the tobacco hornworm, *Manduca sexta*. *Pestic Biochem Physiol* 35:251–258
- Riddiford LM, Hiruma K, Zhou X, Nelson CA (2003) Insights into the molecular basis of the hormonal control of molting and metamorphosis from *Manduca sexta* and *Drosophila melanogaster*. *Insect Biochem Mol Biol* 33:1327–1338
- Rodríguez H, Suárez M, Albericio F (2012) Thiadiazines, N, N-heterocycles of biological relevance. *Molecules* 17:7612–7628
- Saber M, Parsaeyan E, Vojoudi S, Bagheri M, Mehrvar A, Kamita SG (2013) Acute toxicity and sublethal effects of methoxyfenozide and thiodicarb on survival, development and reproduction of *Helicoverpa armigera* (Lepidoptera:Noctuidae). *Crop Prot* 43:14–17
- Saguez J, Dubois F, Vincent C, Laberche J-C, Sangwan-Norreeel BS, Giordanengo P (2006) Differential aphicidal effects of chitinase inhibitors on the polyphagous homopteran *Myzus persicae* (Sulzer). *Pest Manag Sci* 62:1150–1154
- Sakuda S, Isogai A, Matsumoto S, Suzuki A, Koseki K (1986) The structure of allosamidin, a novel insect chitinase inhibitor, produced by *Streptomyces* Sp. *Tetrahedron Lett* 27:2475–2478
- Sakuda S, Isogai A, Matsumoto S, Suzuki A (1987) Search for microbial insect growth regulators. II Allosamidin, a novel insect chitinase inhibitor. *J Antibiot (Tokyo)* 40:296–300
- Samson RA, Evans HC, Latgé JP (1988) Atlas of entomopathogenic fungi. Springer, New York
- Scott JG, Michel K, Bartholomay LC, Siegfried BD, Hunter WB, Smaghe G, Zhu KY, Douglas AE (2013) Towards the elements of successful insect RNAi. *J Insect Physiol* 59:1212–1221
- Senthil-Nathan S (2013) Physiological and biochemical effect of neem and other Meliaceae plants secondary metabolites against Lepidopteran insects. *Front Physiol* 4:359
- Sheets JJ, Bretschneider T, Nauen R (2012) Chitin synthesis. In: Krämer W, Schirmer U, Jeschke P, Witschel M (eds) Modern crop protection compounds, 2nd edn. Wiley-VCH Verlag GmbH & Co. KGaA, Weinheim, pp 999–1027
- Shirk PD, Perera OP, Shelby KS, Furlong RB, LoVullo ED, Popham HJ (2015) Unique synteny and alternate splicing of the chitin synthases in closely related heliothine moths. *Gene* 574:121–139
- Singh AD, Wong S, Ryan CP, Whyard S (2013) Oral delivery of double-stranded RNA in larvae of the yellow fever mosquito, *Aedes aegypti*: implications for pest mosquito control. *J Insect Sci* 13:art 69
- Slowik TJ, Lane RS, Davis RM (2001) Field trial of systemically delivered arthropod development-inhibitor (fluazuron) used to control woodrat fleas (Siphonaptera: Ceratophyllidae) and ticks (Acari: Ixodidae). *J Med Entomol* 38:75–84

- Smaghe G, Degheele D (1994) Action of novel nonsteroidal ecdysteroid mimic, tebufenozide (RH-5992), on insects of different orders. *Pestic Sci* 42:85–92
- Smaghe G, Gomez LE, Dhadialla S (2012) Bisacylhydrazine insecticides for selective pest control. *Adv Insect Physiol* 43:163–250
- Soin T, Iga M, Swevers L, Rougé P, Janssen CR, Smaghe G (2009) Towards Coleoptera-specific high-throughput screening systems for compounds with ecdysone activity: development of EcR reporter assays using weevil (*Anthonomus grandis*)-derived cell lines and *in silico* analysis of ligand binding to *A. grandis* EcR ligand-binding pocket. *Insect Biochem Mol Biol* 39:523–534
- St Leger RJS, Wang C (2010) Genetic engineering of fungal biocontrol agents to achieve greater efficacy against insect pests. *Appl Microbiol Biotechnol* 85:901–907
- Staats CC, Kmetzsch L, Lubeck I, Junges A, Vainstein MH, Schrank A (2013) *Metarhizium anisopliae* chitinase CHIT30 is involved in heat-shock stress and contributes to virulence against *Dysdercus peruvianus*. *Fungal Biol* 117:137–144
- Steenberg T, Kilpinen O (2014) Synergistic interaction between the fungus *Beauveria bassiana* and desiccant dusts applied against poultry red mites (*Dermanyssus gallinae*). *Exp Appl Acarol* 62:511–524
- Sun J, Zhou Y (2015) Design, synthesis, and insecticidal activity of some novel diacylhydrazine and acylhydrazone derivatives. *Molecules* 20:5625–5637
- Sun R, Liu C, Zhang H, Wang Q (2015) Benzoylurea chitin synthesis inhibitors. *J Agric Food Chem* 63:6847–6865
- Sundaramurthy VT, Santhanakrishnan K (1979) Morphogenetic effects of diflubenzuron, an inhibitor of chitin deposition, on the coconut black-headed caterpillar (*Nepantis serinopa* Myer.). *Pestic Sci* 10:147–150
- Suzuki J, Ishida T, Kikuchi Y, Ito Y, Morikawa C, Tsukidate Y, Tanji I, Ota Y, Toda K (2002) Synthesis and activity of novel acaricidal/insecticidal 2,4-diphenyl-1,3-oxazolines. *J Pestic Sci* 27:1–8
- Suzuki J, Tanji I, Ota Y, Toda K, Nakagawa Y (2006) QSAR of 2,4-diphenyl-1,3-oxazolines for ovicidal activity against the two-spotted spider mite *Tetranychus urticae*. *J Pestic Sci* 31:409–416
- Tabudravu JN, Eijssink VGH, Gooday GW, Jaspars M, Komander D, Legg M, Synstad B, Van Aalten DMF (2002) Psammaplin A, a chitinase inhibitor isolated from the Fijian marine sponge *Aplysinella rhax*. *Bioorg Med Chem* 10:1123–1128
- Thwaite WG (1991) Resistance to clofentezine and hexythiazox in *Panonychus ulmi* from apples in Australia. *Exp Appl Acarol* 11:73–80
- Touhara K (ed) (2013) Pheromone signaling: methods and protocols. *Methods in molecular biology*, vol 1068. Springer, New York, p 396
- Truman JW (2005) Hormonal control of insect ecdysis: endocrine cascades for coordinating behavior with physiology. *Vitam Horm* 73:1–30
- Van De Wouw AP, Batterham P, Daborn PJ (2006) The insect growth regulator insecticide cyromazine causes earlier emergence in *Drosophila melanogaster*. *Arch Insect Biochem Physiol* 63:101–109
- Van Leeuwen T, Demaeght P, Osborne EJ, Dermauw W, Gohlke S, Nauen R, Grbić M, Tirry L, Merzendorfer H, Clark RM (2012) Population bulk segregant mapping uncovers resistance mutations and the mode of action of a chitin synthesis inhibitor in arthropods. *Proc Natl Acad Sci U S A* 109:4407–4412
- Vardanis A (1978) Polyoxin fungicides: demonstration of insecticidal activity due to inhibition of chitin synthesis. *EXP* 34:228–229
- Vihervuori L, Lyytikäinen-Saarenmaa P, Lu J, Pasonen HL (2013) Effects on lepidopteran herbivores of feeding on leaves of transgenic birch (*Betula pendula*) expressing the sugar beet chitinase IV gene. *Eur J Entomol* 110:253–262

- Villaverde ML, Girotti JR, Mijailovsky SJ, Pedrini N, Juárez MP (2009) Volatile secretions and epicuticular hydrocarbons of the beetle *Ulomoides dermestoides*. *Comp Biochem Phys B* 154:381–386
- Vincent JF, Wegst UG (2004) Design and mechanical properties of insect cuticle. *Arthropod Struct Dev* 33:187–199
- Walton L, Long JW, Spivey JA (1995) Use of confirm insecticide for control of beet armyworm in cotton under section 18 in MS and AL. *Proc Beltville Cotton Conf* 2:46–47
- Webb GA, McClintock C (2015) Elimination of the mound-building termite *Nasutitermes exitiosus* (Isoptera: Termitidae) in south-eastern Australia using bistrifluron bait. *J Econ Entomol* 108:2702–2710
- White BH, Ewer J (2014) Neural and hormonal control of postecdysial behaviors in insects. *Annu Rev Entomol* 59:363–381
- Wing KD (1988) RH 5849, a nonsteroidal ecdysone agonist: effects on a *Drosophila* cell line. *Science* 241:467–469
- Wing KD, Slawewicki RA, Carlson GR (1988) RH 5849, a nonsteroidal ecdysone agonist: effects on larval lepidoptera. *Science* 241:470–472
- Wright JE, Retnakaran A (eds) (1987) Chitin and benzoylphenyl ureas. W Junk Publishers, Amsterdam, p 309
- Wuriyangan H, Rosa C, Falk BW (2011) Oral delivery of double-stranded RNAs and siRNAs induces RNAi effects in the potato/tomato psyllid, *Bactericerca cockerelli*. *PLoS One* 6, e27736
- Yanagi M, Tsukamoto Y, Watanabe T, Kawagishi A (2006) Development of a novel lepidopteran insect control agent, chromafenozide. *J Pestic Sci* 31:163–164
- Yu N, Christiaens O, Liu J, Niu J, Cappelle K, Caccia S, Huvenne H, Smagghe G (2013) Delivery of dsRNA for RNAi in insects: an overview and future directions. *Insect Sci* 20:4–14
- Yu X, Liu Y, Li Y, Wang Q (2015) Design, synthesis, and acaricidal/insecticidal activities of oxazoline derivatives containing a sulfur ether moiety. *J Agric Food Chem* 63:9690–9695
- Zhang Y, Guo H, Yang Q, Li S, Wang L, Zhang G, Fang J (2012) Overexpression of a P450 gene (CYP6CW1) in buprofezin-resistant *Laodelphax striatellus* (Fallén). *Pestic Biochem Physiol* 104:277–282
- Zhang Y, Wang Y, Wang L, Yao J, Guo H, Fang J (2016) Knockdown of NADPH-cytochrome P450 reductase results in reduced resistance to buprofezin in the small brown planthopper, *Laodelphax striatellus* (fallén). *Pestic Biochem Physiol* 127:21–27
- Zhu Q, Arakane Y, Beeman RW, Kramer KJ, Muthukrishnan S (2008) Functional specialization among insect chitinase family genes revealed by RNA interference. *Proc Natl Acad Sci U S A* 105:6650–6655
- Zhuo W, Fang Y, Kong L, Li X, Sima Y, Xu S (2014) Chitin synthase A: a novel epidermal development regulation gene in the larvae of *Bombyx mori*. *Mol Biol Rep* 41:4177–4186
- Zitnan D, Adams ME (2000) Excitatory and inhibitory roles of central ganglia in initiation of the insect ecdysis behavioural sequence. *J Exp Biol* 203:1329–1340
- Zitnan D, Zitnanová I, Spalovská I, Takác P, Park Y, Adams ME (2003) Conservation of ecdysis-triggering hormone signalling in insects. *J Exp Biol* 206:1275–1289

Part IV
Glandular Secretions

Chapter 11

Nature and Functions of Glands and Ducts in the *Drosophila* Reproductive Tract

Frank W. Avila, Javier A. Sánchez-López, Jennifer L. McGlaughon,
Sukirtha Raman, Mariana F. Wolfner, and Yael Heifetz

Abstract Successful reproduction requires interactions between males and females at many levels: the organisms, their cells (the gametes), and their molecules. Among the latter, secreted products of male and female reproductive glands are especially important. These molecules are particularly well understood in *Drosophila melanogaster*, because of this insect's excellent molecular genetic tools. Here, we discuss the biology of *Drosophila* reproductive glands, including their development, structure, and secreted products. These glands include important secretory centers, tissues that play roles in gamete maintenance and perhaps in modification, and organs that mediate dynamic transfer of gametes and molecules, and gamete support and/or discharge. Components of seminal fluid produced by male reproductive glands enter the female during mating. There, they interact with female proteins, neurons, and pathways to convert the female from a "poised" pre-mated state to an active post-mating state. This mated state is characterized by high levels of egg production, by sperm storage, and by post-mating behaviors related to re-mating, activity, and feeding. Female reproductive gland secretions include additional molecules important for sperm survival or egg transit. The interplay and coordination between male- and female-derived molecules is an area of intense study. Its conclusions are relevant to understanding reproduction in insects and, more broadly, in all animals, and as well as to questions about chemical communication, hormone biology and evolution.

F.W. Avila • J.L. McGlaughon • M.F. Wolfner (✉)
Department of Molecular Biology and Genetics, Cornell University, Ithaca, NY 14853, USA
e-mail: fwa5@cornell.edu; jla254@cornell.edu; mariana.wolfner@cornell.edu

J.A. Sánchez-López
Department of Entomology, The Hebrew University of Jerusalem, 76100 Rehovot, Israel
e-mail: javier.sanchezlo@mail.huji.ac.il

S. Raman
Department of Marine, Earth and Atmospheric Sciences,
North Carolina State University, Raleigh, NC, USA
e-mail: sukirtharaman@gmail.com

Y. Heifetz (✉)
Department of Entomology, The Robert H. Smith Faculty of Agriculture,
Food and Environment, the Hebrew University of Jerusalem, Rehovot, Israel
e-mail: yael.heifetz@mail.huji.ac.il

11.1 Introduction

Reproduction involves not simply an interaction between individuals, but also an interaction between cells and molecules belonging to those two different organisms of the same species. Both individuals ultimately benefit from a successful reproductive interaction, because it will transmit their genes to the next generation. Although the gametes contributed by each individual will ultimately fuse to form the embryo for the next generation, production and function of these gametes is facilitated by actions and products made by tissues in the male and female reproductive tract. Much is known about those tissues and their products in the genetic model system, the fruit fly *Drosophila melanogaster*, which is the focus of this chapter. Male and female reproductive tracts secrete components that contribute to a complex milieu that regulates and supports essential reproductive processes such as oocyte and sperm transport, maturation and activation, fertilization, embryo development and embryo transport (Leese 1988; Hunter 1998; Bloch Qazi et al. 2003; Avila et al. 2010; Aviles et al. 2010; Heifetz and Rivlin 2010; Schnakenberg et al. 2012). Male secreted components in animal seminal plasma include proteins and peptides, lipids, hormones, sugars, small-molecules, immune regulators, and vesicles derived from male reproductive tissues (Poiani 2006; Avila et al. 2011; Aalberts et al. 2014; Corrigan et al. 2014; Suarez and Wolfner 2016). Interestingly, although the specific molecules and extracellular vesicles that are present in seminal plasma differ across organisms, and even within genus *Drosophila*, there are commonalities in their types. Female animals' reproductive tract secretions include molecules in similar classes to the male ones just mentioned (i.e. proteins and peptide, lipids, hormones, sugars) and also include components of the innate immune response (e.g. antimicrobial peptides) that form the first line of defense against pathogenic invasion (Leese 1988; Wira et al. 2011; Mondejar et al. 2012). Sites and/or organs that store sperm provide molecules that support sperm maintenance and may enable sperm modification (maturation and activation) to facilitate fertilization. In this chapter we review what reproductive tissues and their secretions do, and why their products are so important for reproduction. Genetic tools in *D. melanogaster* have allowed a deep understanding of these molecules' and tissues' functions.

11.2 Setting the Context

Before we discuss the details of reproductive tissues and molecules, we would like to place their actions into a broader context, as we believe that this will help frame the question of why male and female contributions are important individually and in combination. Although both sexes benefit from successful reproduction, the strategies that promote reproductive success differ between males and females. In the simplest terms, the male, who produces large quantities of "lower cost" (and usually small) gametes, benefits by mating with as many females as possible. Further,

a male will stimulate the female's reproductive capacity as much as possible and expend energy in defending his reproductive investment from possible competitors. The female, in contrast, generally produces a smaller number of eggs, each of which requires a significant investment. Females are thought to benefit by being "chooser" so that the best male's sperm fertilize her eggs. These differences in strategies and in reproductive physiology/needs result in both beneficial and apparent antagonistic interactions between male secretions and the female. We review these beneficial and antagonistic interactions, briefly, here.

11.2.1 Beneficial Interactions

The mated female insect is quite different from her unmated (virgin) self, both physiologically and behaviorally. Perhaps most dramatic, a mated female produces and lays eggs at a much higher rate than a comparable unmated female (~50 eggs/day instead of ~2/day in our lab-strain of *D. melanogaster*, respectively); in some insects unmated females lay no eggs at all (Avila et al. 2011). This increase in egg production, and provisioning all those eggs, requires resources that the female must obtain not only by eating more, but also by extracting maximal nutrition from the food she consumes (Carvalho et al. 2006; Apper-McGlaughon and Wolfner 2013; Reiff et al. 2015). Such resource allocation for egg production potentially detracts from resources needed for the female's viability and health (Rose and Bradley 1998; Stearns 2000; Schwenke et al. 2016). The mated female must also find places to oviposit her eggs, requiring movement, searching, and less sleep (Isaac et al. 2010). Oviposition thus also potentially makes the female more vulnerable to predators. One could imagine that it would be advantageous for a *D. melanogaster* female to use the substances that males transfer during mating as a "switch", changing her from a virgin state of metabolism to the revved up state needed for egg production. In other words, in this model, the unmated female's physiology is poised to shift to what is needed for high levels of egg production, but remains as a soma-focused physiology until a signal from the male indicates to her that she contains sperm. At this point it is advantageous for her to switch to a higher level of egg production so that her eggs and the sperm she received can rapidly produce large numbers of progeny. While in physiological terms, this seems most beneficial to the female, it is also to the male's benefit to provide a signal that turns up egg production in females. Mating-induced egg production means that the male's progeny numbers are not limited by the female's basal (virgin) level of egg production. In parallel, male-induction of egg production insures females will not have exhausted resources on egg production prior to mating and are thus able to produce large numbers of progeny after each mating.

There are several examples of the male acting as a switch to turn on a pre-existing pathway in the female. Initial evidence came from transcriptomics: transcriptome changes shortly after mating were very small in magnitude, suggesting that many gene products needed in the first few hours after mating had already been expressed

in virgin females (McGraw et al. 2004, 2008). Consistent with this view of the “poised” female are data on vesicle release and reuptake; the virgin female already contains vesicles with peptides in them, ready-for-release upon mating (Heifetz and Wolfner 2004). Later work (Heifetz et al. 2014) showed that mating changes neuro-modulator levels and release, at characteristic times in each part of the female’s reproductive tract (providing a way to coordinate post-mating physiology along the tract). Finally, recent micro-CT scanning studies have shown that mating results in movements and shape changes of reproductive organs *in situ* that initiate the coordinated release and passage of oocytes (Mattei et al. 2015).

A major class of chemical signals that the male provides are proteins/peptides in his seminal fluid. As the action of specific seminal fluid proteins (SFPs) is becoming understood, we are beginning to see how males change the female’s physiological state. For example, the SFP sex peptide (SP) increases the production of juvenile hormone (JH) in females (Moshitzky et al. 1996; Bontonou et al. 2015). This hormone is essential for the post-mating increase in oogenesis (Dubrovsky et al. 2002). Since unmated females already have begun oogenesis, JH likely facilitates further maturation of these oocytes (Soller et al. 1999), as well initiating the production of new ones. Increased JH levels also cause a remodeling of the female’s gut (Reiff et al. 2015), presumably facilitating better digestion and nutrient absorption. In another example, the SFP Acp36DE is necessary for the conformational changes in the uterus of the mated female (Adams and Wolfner 2007; Avila and Wolfner 2009; Mattei et al. 2015). These changes are necessary for sperm to move into storage and for exerting tension on the oviduct to facilitate ovulation (Mattei et al. 2015). Another SFP, ovulin, increases octopaminergic signaling by increasing the number of synapses between neurons that innervate the oviduct and the associated oviduct musculature, allowing for the relaxation of the oviduct and the opening of its lumen to permit ovulation (Rubinstein and Wolfner 2013). Extending beyond octopamine, SFP receipt (and mating) alters the production and/or release of different neuro-modulators at different places and times along the female reproductive tract (Heifetz et al. 2014), resulting in unique combinations of neuromodulators that may help coordinate the various reproductive tract functions. Here too, the pathways are poised in the female but are turned on by the male – thus saving the female from having to run these pathways at a high level until she has mated, benefitting both her and her mate by allowing the pathways to turn up very quickly upon mating – as though a switch has been flipped on.

11.2.2 *Antagonistic Interactions*

As previously mentioned, mating is not purely a cooperative venture between the sexes at the molecular (or other) levels. Males generally produce large numbers of lower-cost gametes and thus benefit most from mating as many times as possible. But within a population, multiple mating with different males introduces the likelihood of sperm competition for fertilization opportunities. For females, with fewer costlier

gametes, multiple mating is less beneficial; females benefit more by devoting their resources to the production of progeny from better males (although they can sometimes receive beneficial resources during mating (Markow et al. 2001)). These differences in strategies can result in situations where the interests of the sexes differ, causing antagonistic effects on females from male molecules or organs. The simplest way to imagine this is to consider egg production. As noted above, it is advantageous for both the male and female that SFPs increase egg production in females. However one could imagine that a level of egg production ideal for the male's rapid progeny production might be disadvantageous for the female, requiring her to devote more resources to egg production than might be beneficial for her survival. Thus there is a constant tension between the needs and strategies of the two sexes. This in turn can drive an evolutionary "arms race" (e.g. see Rice 1996). If a male produces a molecule that exerts an effect beneficial for him, it will be selected for. However, if the effects of this molecule are not beneficial for the female, females will be selected that resist the molecule's effects. [For example, if the JH induction caused by SP is at a level that is disadvantageous for females, one could imagine that selection would then favor females whose circulatory system contained higher proteolytic activity against the SP (for example by having greater amounts of specific proteases, or proteases with higher catalytic activity or stability)]. Or, female receptors could evolve that bind a given SFP less strongly; more below. This in turn will select for males with forms of this SFP (or other molecules) that can overcome the female's resistance mechanisms.

Several examples suggest the likelihood of such a conflict between the interests of male and female *D. melanogaster*. One example is that some SFPs decrease female lifespan (Chapman et al. 1995; Lung et al. 2002; Wigby and Chapman 2005). The effect has likely been tuned in ways like those suggested above, as it takes multiple matings to see a small effect. The SP is essential for this effect on females; perhaps its effect can be understood in terms of its altering the egg production, immunity, food ingestion, and hormone balance in the female. Like SP (Wigby and Chapman 2005), several other SFPs have been shown to be toxic to flies when ectopic amounts are present in their hemolymph (Lung et al. 2002; Mueller et al. 2007), suggesting that there may be additional contributors to the decreased longevity.

In another example, the male's aedeagus punctures the vaginal intima of the female (Kamimura 2010; Mattei et al. 2015), potentially providing a rapid way to introduce his SFPs into her circulation (Lung and Wolfner 1999), but also causing wounding of the female (Mattei et al. 2015). Such injury also has the potential to introduce microbes into the female. This might be a reason why female flies induce expression of antimicrobial peptide genes after mating (Peng et al. 2005a; Domanitskaya et al. 2007), although their systemic immunity does not increase after mating (Fedorka et al. 2007; Short et al. 2012), perhaps as a consequence of a resource-allocation tradeoff between immunity and reproduction (see Schwenke et al. 2016 for further discussion).

In a third example of potentially antagonistic interactions, a male's SP reduces his mate's receptivity to remating (Chapman et al. 2003; Liu and Kubli 2003),

perhaps as part of his evolved arsenal against sperm competition. Therefore, a mated female is less likely to remate, and the male's sperm are thus less likely to encounter sperm competition. While this is advantageous for the male, it is arguably less so for the female. Although decreased re-mating could potentially protect the female from longevity-decreasing effects of mating/SFPs, there are some negative consequences for her: by reducing her re-mating-receptivity, the male is decreasing the diversity of male genetic contributions to the female's progeny. Females benefit by some ability to re-mate so that they can "choose" the best male. By decreasing her receptivity to re-mating, a male's SFPs decrease this potentially beneficial female behavior. This conflict between interests of the male and female may also contribute to the arms race described above.

Finally, sequence examination of SFPs has shown that a remarkably large percent of them (~20 %) show features of rapid evolution, consistent with the arms race described above (Swanson et al. 2001; Wagstaff and Begun 2007; Wong et al. 2008a). Interestingly, although the primary amino acid sequences appear to be evolving rapidly, the classes of SFP that are present are highly conserved – suggesting that the same functions are needed, but that different molecules with those activities are co-opted as females become resistant or other needs drive it. It would be useful to see if the female receptors/interactors of SFPs also evolve rapidly – in step with their ligands. However at present, only one SFP receptor is known (SPR, the receptor for SP) (Yapici et al. 2008) and this receptor has conserved non-reproductive ligands (MIPs) (Kim et al. 2010; Poels et al. 2010) that may constrain its evolution. An SFP-specific receptor is needed to answer this question.

11.3 Reproductive Tract Development and Overview

Given the interesting parallels in the functions of adult male and female reproductive glands and ducts (see below, and Fig. 11.1), it is interesting to note that the organs in the two sexes actually derive largely from different precursors. *D. melanogaster* genitalia are specified during larval life and differentiate into both the genitalia and analia during metamorphosis (Chatterjee et al. 2011). The genitalia are derived from the genital imaginal disc; cells from abdominal segments A8, A9 and A10 will ultimately contribute to these structures (Nothiger et al. 1977; Schupbach et al. 1978). Female genitalia are primarily derived from cells of the A8 primordium while male genitalia are primarily derived from cells of the A9 primordium (Estrada et al. 2003). However, in addition to these contributions, mesodermal cells are also recruited and contribute to the formation of the male reproductive tract (Ahmad and Baker 2002).

As is the case with the development of other imaginal discs, the *decapentaplegic* (TGF- β), *hedgehog* and *wingless* (Wnt) signaling cascades give positional information to the genital imaginal disc cells (Brook et al. 1996; Lawrence and Struhl 1996). Hox genes are required to differentiate between the genitalia, analia and the

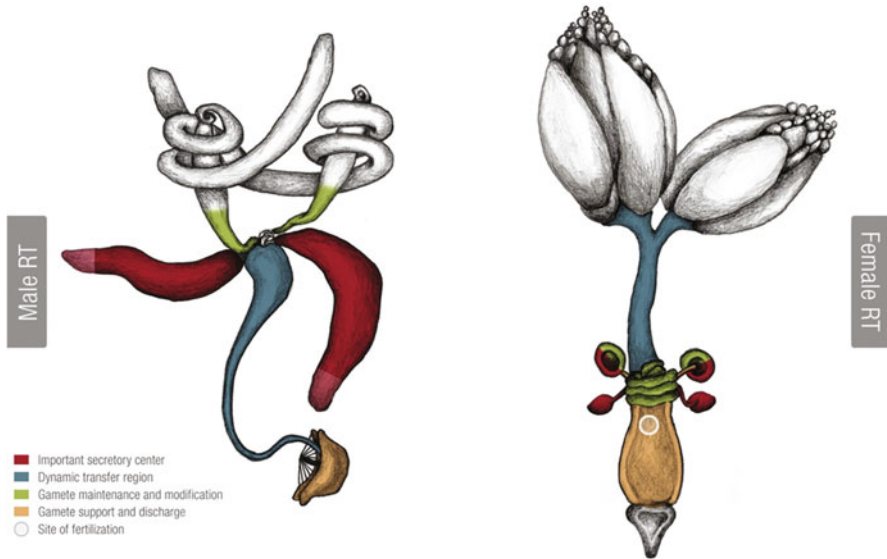


Fig. 11.1 Male and female reproductive tracts of *Drosophila melanogaster*

Reproductive tract organs are color-coded with respect to function. Gonads are not colored, nor is the female's vagina (*at the bottom of the drawing*)

In the male: sperm from the testes are stored and maintained in the seminal vesicles (*green*). The male's accessory glands (*red*) are major sites of synthesis of seminal proteins. The distal tip of the gland (*paler red*) contains both main and secondary secretory cells; the rest of each gland lobe contains only main secretory cells. Sperm and accessory gland secretions (and secretions from the testis and seminal vesicles) then transit through the ejaculatory duct (*blue*), which contributes additional secretions. Sperm and seminal fluid then pass through the ejaculatory bulb (*tan*) which contributes its own secretions (which will be part of the coagulum that forms the mating plug inside the female) before discharging the ejaculate into the female

In the female: during mating, the ejaculate is deposited into the uterus (*tan*) and the sperm move from there into the sperm storage organs (*green*; spermathecae are the two mushroom-shaped organs part-colored *green*; seminal receptacle is the coiled *green organ* at the *top* of the uterus), where they will be maintained until released for fertilization. Secretions from spermathecal secretory cells, and from the female accessory glands (parovaria) (*red*) are thought to help maintain the sperm and may facilitate egg movement as well. Mating stimulates ovulation, the process in which an oocyte from the ovary moves into a lateral oviduct and then transits into and through the common oviduct; the oviducts' (*blue*) secretions comprise an oviductal fluid that may assist with this transit. The egg then moves into the uterus (*tan*), with its anterior end up. That end of the egg contains the micropyle, and thus this site of sperm entry is positioned next to the opening of the sperm-storage organs. Sperm released from storage will enter the egg and fertilize it (*white circle*). The uterus contracts to discharge the egg from the female

more anterior segments of the fly abdomen. Finally, the downstream components of the sex-determination pathway, most notably the sex-specific isoforms of RNA and protein encoded by the *doublesex* gene, control the sexual differentiation of these tissues (Christiansen et al. 2002). Active transcription of *doublesex* initiates at the onset of metamorphosis in the genital disc (Robinett et al. 2010). *doublesex* mRNAs are alternatively spliced to produce sex-specific transcription factors thought to

coordinate the development of the genital disc. However, few direct targets of *doublesex* have been described, with *doublesex* appearing to function in genitalia development by coordinating the activity of broadly expressed transcription factors in a sex-specific manner (Chatterjee et al. 2011).

On the male side, the structures that we will focus on here are the paired accessory glands (also called paragonia), the most extensively studied organ of the male reproductive tract, and the ejaculatory duct and ejaculatory bulb (see Fig. 11.1). For the purpose of this review, we cannot say much about secretions of testes and seminal vesicles as the proteins secreted by these organs most likely interact directly with sperm and are currently difficult to distinguish from the sperm proteome. However, it is likely that the products of these tissues secrete important products, as their analogs do in mammals (Suarez 2016).

The female reproductive tract (RT) structures that will be discussed include the oviduct, the uterus, the parovaria (also called the female accessory glands), and the two types of female sperm storage organs – the single seminal receptacle and paired spermathecae, which include large secretory cells located outside the spermathecal cap (see Fig. 11.1). These spermathecal secretory cells (SSC) play a major and unique role in reproductive function. As in the testis, proteins secreted by the ovary most likely interact directly with oocytes, but probably affect other parts of the female reproductive tract. However, since little is known about such molecules we do not discuss them further in this article.

There are remarkable formal parallels in the functions of male vs. female organs (see Fig. 11.1). The male and female accessory glands, and the female's spermathecal secretory cells are major secretory centers – sources of important secretions that affect other organs (even organs in another animal in the case of the male accessory gland). The male's seminal vesicles and the female's sperm-storage organs are, in addition to secretory organs, sites that maintain sperm in a viable stored state. The male's ejaculatory duct and the female's oviducts are, in addition to secretory organs, conduits that mediate the dynamic movement of gametes. Finally, in addition to their secretory roles, the male's ejaculatory bulb and the female's uterus are organs that discharge gametes (and secretions) from the fly. As we discuss the details of each organ and its products below, it is useful to keep these parallels in mind.

11.4 The Male Reproductive Tract

11.4.1 Male Accessory Gland

The accessory gland of the *Drosophila* male reproductive tract produces the majority of studied seminal fluid proteins transferred to females during mating. These proteins elicit most of the behavioral and physical changes in mated female that have been described – increases in egg-laying, ovulation and feeding behavior,

decreases in receptivity to re-mating, in siesta sleep and in the rate of intestinal transit, as well as formation of a mating plug, induction of immune responses, and regulation of sperm storage and sperm competition (Gillott 2003; Avila et al. 2011). The accessory gland plays a crucial role in the fertility of *Drosophila* males given that ablation of the tissue results in sterility (Xue and Noll 2000; Chow et al. 2015).

The accessory gland (see Fig. 11.1) is a two-lobed structure that branches from the anterior ejaculatory duct. Late in development, mesodermal cells that express the fibroblast growth factor (FGF) receptor, *Breathless* (*Btl*), in the male genital disc will become epithelial cells that develop into the accessory gland (Ahmad and Baker 2002). The homeodomain transcription factor, *Paired* (*prd*), is required to promote the proliferation of the cells (Xue and Noll 2002). Each lobe of the accessory gland is made up of ~1000 secretory cells arranged in a monolayer epithelium. There are two types of secretory cells: “main cells” and “secondary cells” (Bairati 1968; Bertram et al. 1992; Gligorov et al. 2013). Flat, hexagonally-shaped main cells make up approximately 96% of the accessory gland. Secondary cells, which are large, spherical and filled with vacuoles, make up the remaining 4%; they are found at the distal tip of the accessory gland lobes, distributed among the main cells. Both main cells and secondary cells of the accessory gland are binucleate, a result of progressing through mitosis without cytokinesis. This is regulated by the *Drosophila* microtubule binding protein, *Mud* (Taniguchi et al. 2014).

Proteins are secreted from the monolayer of secretory cells into the lumen of the accessory gland. The monolayer of secretory cells is further encased in a muscle sheath that likely constricts, facilitating the movement of the secreted proteins into the ejaculatory duct where they mix with secreted proteins from the ejaculatory duct and sperm, and are subsequently transferred to the female during copulation (Norville et al. 2010). In addition to its role in early cell proliferation of the accessory gland, *prd* is also required later in development for the differentiation and maturation of the accessory gland (Xue and Noll 2002).

It was suggested that the main cells of the *Drosophila* accessory gland use merocrine secretion, whereas secondary cells secrete by holocrine mechanisms (Perotti 1971; Chen 1984; see Chap. 15 by Farkaš, for related discussion of secretion mechanisms in salivary glands). Merocrine secretion occurs when a cell uses exocytosis to release its secreted products via secretory vesicles, whereas holocrine secretion involves the rupture of the plasma membrane and the release of the secreted product, destroying the cell. It is unclear whether secondary cells destroyed in this process are replenished by the conversion of a main cell or by proliferation of other secondary cells. A study by Rylett et al. (2007) provides possible evidence for the holocrine secretion of secondary cells. The authors demonstrated by *in situ* hybridization that the RNA of angiotensin I-converting enzyme (ANCE), a secondary cell secreted protein, was found not only in the secondary cells but also abundant in the accessory gland lumen. Moreover, the appearance of vesicles transferred from accessory glands, and of apparent secondary cells delaminated and transferred during mating (Leiblich et al. 2012; Corrigan et al. 2014), also supports the idea of holocrine secretion by those cells.

Given that the main cells make up 96% of the accessory gland, the products of these cells have been more extensively studied. Genetic disruption of the accessory gland main cells determined that these cells are responsible for the post-mating response (Kalb et al. 1993). About ~200 proteins and peptides have been reported in *D. melanogaster* seminal fluid, most of which are derived from accessory glands (Findlay et al. 2008, 2014; Yamamoto and Takemori 2010). One class of such molecules are peptide hormones or proteins that appear to act as precursors to peptide hormones. The best known among these is the 36 amino acid “sex peptide” (SP; Aigaki et al. 1991) and the 264 amino acid peptide ovulin (Monsma and Wolfner 1988). Both of these are found in *D. melanogaster* and closely related *Drosophila* species, but neither is detectable outside the genus *Drosophila*. SP has been shown to mediate multiple post-mating events in females: the decreases in sexual receptivity (Chapman et al. 2003), siesta sleep (Isaac et al. 2010) and longevity (Wigby and Chapman 2005), the increases in feeding (Carvalho et al. 2006), egg production (Chapman et al. 2003) and juvenile hormone levels (Moshitzky et al. 1996), the observed digestive changes (Cognigni et al. 2011; Apger-McGlaughon and Wolfner 2013), a requirement for sperm release from storage (Avila et al. 2010), and the induction of antimicrobial peptide genes (Peng et al. 2005a; Domanitskaya et al. 2007). SP’s effects on behavior, egg production and sperm release are due to SP’s C-terminal region acting through a G-protein coupled receptor (SPR, Yapici et al. 2008) in a subset of neurons innervating the female reproductive tract that co-express *fruitless*, *doublesex*, and *pickpocket* (Yapici et al. 2008; Hasemeyer et al. 2009; Yang et al. 2009; Avila et al. 2015a). To mediate the release of sperm from storage, SP acts through SPR in *pickpocket* neurons and the spermathecal secretory cells (Avila et al. 2015a). The sex peptide’s effects persist long after mating, because once inside the female SP is bound to, and retained on stored sperm (Peng et al. 2005b); a network of seminal proteins is necessary to catalyze this binding (Ravi Ram and Wolfner 2009; LaFlamme et al. 2012). The active C-terminal region of the SP is slowly cleaved from sperm, releasing this active region with time. The effects of SP on JH levels are transient, and involve its N-terminal region (Peng et al. 2005b).

Ovulin is a prohormone that upon transfer to the female stimulates a short-term (<24 h) increase in ovulation (Herndon and Wolfner 1995; Heifetz et al. 2000, 2005). Ovulin acts to increase ovulation by increasing octopaminergic signaling in the reproductive tract (Rubinstein and Wolfner 2013). The increased octopaminergic signaling is thought to relax the muscles that surround the oviduct, unlooping this duct (Mattei et al. 2015) and opening its lumen to accept the ovulated egg. Interestingly, although ovulin itself is only detectable for a few hours in the female, its effects include increasing the number of synaptic boutons made by octopaminergic neurons on the muscles around the oviduct. This may allow the oviduct musculature to remain relaxed long after ovulin is gone, a feature that may contribute to the mechanical regulation of subsequent ovulation by the female (Mattei et al. 2015), as described below. Ovulin’s site of action in the female is currently unknown. The majority of transferred ovulin localizes to the upper oviduct and base of the ovaries; there it undergoes proteolytic cleavage that is thought to activate it (Monsma and Wolfner 1988; Herndon and Wolfner 1995; Park and Wolfner 1995; Heifetz et al.

2005). Approximately 10% of the transferred ovulin enters the female's hemolymph where it remains uncleaved; from this location it could be in position to indirectly stimulate ovulation via the neuroendocrine system (Lung and Wolfner 1999).

Several other SFPs made in the accessory gland have been associated with functions in the mated female. Accessory gland SFPs, in aggregate, induce a series of morphological changes of the mated female uterus. In virgin females, the uterus exists in a tightly closed conformation. During mating, a series of morphological changes 'open' the uterus (Adams and Wolfner 2007; Mattei et al. 2015). These changes have been hypothesized to move the sperm mass towards the female sperm storage organs (Adams and Wolfner 2007). The accessory gland SFP, Acp36DE, is required for the completion of these changes: the uteri of females that do not receive Acp36DE only partially open (Avila and Wolfner 2009; Mattei et al. 2015) resulting in a significant reduction of sperm being stored by the female (Neubaum and Wolfner 1999; Bloch Qazi and Wolfner 2003; Avila and Wolfner 2009). *D. melanogaster* females will sometimes store sperm even in the absence of accessory gland SFPs, albeit in significantly reduced numbers (Xue and Noll 2000). However, these sperm will not be used to fertilize eggs (Xue and Noll 2000), highlighting the importance of accessory gland proteins in female sperm management. The predicted lectin, Acp29AB, which functions in sperm competition is also required for proper sperm storage, as females that do not receive this SFP during mating cannot maintain sperm in storage, leading to a reduction in fertility (Wong et al. 2008b). Finally, the previously mentioned network of SFPs that bind SP to sperm are required for sperm storage parameters—removal of any of the proteins of this network (two proteases, a cysteine-rich secretory protein (CRISP), and two C-type lectins) results in the inability of females to release sperm from storage, a similar effect to not receiving SP itself (Ravi Ram and Wolfner 2007, 2009; Avila et al. 2010; LaFlamme et al. 2012).

Seminal fluid is also rich in proteases and their regulators. Multiple classes of proteases are found in *D. melanogaster* seminal fluid, including serine proteases and metalloproteases (LaFlamme and Wolfner 2013). Several of these proteases have been shown to act in proteolytic cascades to regulate the cleavage of other seminal proteins (such as ovulin and Acp36DE, LaFlamme et al. 2014). Proteolysis can liberate active regions of proteins, or can regulate the stability of a protein; to date the specific roles of most proteolytic events in *D. melanogaster* seminal proteins are unclear. The female reproductive tract also produces proteases and protease inhibitors (Allen and Spradling 2008; Prokupek et al. 2009, 2010), suggesting molecules that could potentially mediate the sort of interplay described in above under "Setting the context". Unfortunately, the large number of proteases and protease inhibitors found in seminal fluid has made genetic dissection of their activities difficult, due to redundancy: effects of mutation or knockdown of one can be masked by the presence of another protease with similar activity. It is intriguing to think that such redundancy (and the use of proteins with similar activity but from different ancestral genes) could be the consequence of the arms race noted earlier in this article. In mammals, proteases and their inhibitors in seminal fluid play roles in the coagulation of semen. Although *D. melanogaster* seminal fluid does contain mole-

cules that form a mating plug within the female, to date the roles of male or female proteases or protease inhibitors in this process have not been tested.

Other classes of protein in seminal fluid include lectins, which bind to carbohydrates. Carbohydrate-binding proteins are necessary for fertility and aspects of sperm storage in flies (Ravi Ram and Wolfner 2007, 2009; Wong et al. 2008b) as well as in mammals (e.g. Demott et al. 1995; Teclé and Gagneux 2015) as are another class of protein in seminal fluid, the CRISPs (cysteine-rich secretory proteins; Da Ros et al. 2015). Another class of proteins in *Drosophila* seminal fluid is odorant binding proteins (Findlay et al. 2008). Roles in seminal fluid for such proteins have not been reported, but a possibility is that they may serve to bind small molecules from the male and present them to targets or receptors in the female. Small molecules in seminal fluid are also not known in *Drosophila*, but they are inferred to be present and similar in function to small molecules present in other taxa. These molecules could include hormones such as ecdysterone (*Anopheles*, Pondeville et al. 2008), juvenile hormone (*Aedes*, Clifton et al. 2014) and prostaglandins (mammals, Robertson 2007) all of which affect female physiology. It will be interesting to test for such molecules in *D. melanogaster* seminal fluid. Finally, in addition to proteins and other molecules, seminal fluid in *Drosophila* includes small vesicles or exosomes that are reported to be derived from the male's accessory gland's secondary cells. These exosomes are transferred to females during mating. Although their contents are as yet unknown, the vesicles have been suggested to affect the mating behavior of female *Drosophila* (Corrigan et al. 2014). In mammals, such vesicles have been associated with transfer of small regulatory RNAs (e.g. Valadi et al. 2007; Belleannée et al. 2013; Vojtech et al. 2014) and possibly other molecules that can then affect gene expression or other traits in the female reproductive tract.

While the main cells and their secreted proteins (such as SP, ovulin and Acp36DE) have been extensively researched, much less is known about the role of the secondary cell secretions. However, several recent studies have shown that secondary cells are critical for a normal post-mating response. Minami et al. (2012) reported that the accessory glands of males mutant for the homeodomain transcriptional repressor *Defective proventriculus* (*Dve*) were small, lacked secondary cells, and had mononucleate main cells. These mutants had low fecundity and were unable to increase post-mating egg laying and to reduce post-mating receptivity – two responses that are elicited by the main cell accessory gland protein SP (Chapman et al. 2003), yet interestingly, *dve* mutants transferred normal amounts of SP to their mates. Gligorov et al. (2013) reported that loss of the homeotic transcription factor, *Abd-B*, in secondary cells caused those cells to develop abnormally, and resulted in defects in the long-term post mating responses in the mates of mutant males: without secondary cell function, the male's SP was unable to be bound to sperm and to be retained in the female. Additionally, this study provided evidence for interactions between the products of the two cell types: expression of *Abd-B* in the secondary cells is required for glycosylation of at least three main cell secreted proteins: ovulin (Acp26Aa), which is responsible for a short-term (<24 h) increase in egg laying after mating (Chapman et al. 2003), and CG1652 and CG1656, a pair of lectins that are part of the network of proteins that binds SP to sperm (Ravi Ram and Wolfner 2007, 2009). Recently, Sitnik et al. (2016) identified several secondary cell-expressed genes that

are necessary for the binding of SP to sperm, and the consequent persistence of the post-mating responses elicited by SP. Finally, Corrigan et al. (2014) showed that these cells are the source of vesicles that are transferred to females during mating, and are needed for her post-mating changes in remating behavior.

11.4.2 Ejaculatory Bulb (EB)

The EB derives from cells of the A9 primordium during metamorphosis (Estrada et al. 2003). Although it has not been studied to the level of detail as the male accessory gland, the EB has been shown to synthesize and transfer products—pheromones and proteins—to females that directly affect female fertility and behavior.

Secreted proteins of the EB are integral in forming the *D. melanogaster* mating plug—a coagulation of seminal proteins that forms in the posterior uterus quickly after their transfer during mating (Avila et al. 2015b; Chow et al. 2015; Mattei et al. 2015) – although accessory gland proteins also contribute to the mating plug in *Drosophila* (Avila et al. 2015c), as well as in *Anopheles gambiae* mosquitoes (Rogers et al. 2009). Two *D. melanogaster* EB proteins have been identified as important in the mating plug: Protein of the EB in melanogaster (PEBme; Ludwig et al. 1991; Lung and Wolfner 2001) and PEBII (Bretman et al. 2010). RNAi knockdown of PEBII reduces mating plug size in mated females and increases female willingness to re-mate in the immediately hours after mating has ended. However, female fertility is not impacted after *PEBII* is targeted for RNAi knockdown (Bretman et al. 2010).

In contrast, RNAi knockdown of *PEBme* in males, severely reduces or completely ablates mating plug formation in mated females. This causes significant reductions in female post-mating egg-laying and progeny production and in the likelihood of rejection of remating by females (Avila et al. 2015c). The lack of a normal post-mating response in females that had mated to PEBme knockdown males is due to the inability of these females to retain the ejaculate within their reproductive tract when mating pairs uncouple at the end of mating (Avila et al. 2015c). As the ejaculate is typically expelled by *D. melanogaster* females several hours after mating ends (Lee et al. 2015), one function of the mating plug in this species appears to be to prevent premature ejaculate expulsion by females, thus ensuring that sperm are stored in optimal numbers and that necessary SFPs are retained in mated females (Avila et al. 2015c).

While the presence of PEBme in the seminal fluid is required for mating plug formation and the maintenance of the ejaculate in the female reproductive tract, the EB is also a primary site of pheromone synthesis (Guiraudie-Capraz et al. 2007; Chin et al. 2014; Ng et al. 2015). However, there exist large variations in the EB-derived synthesis of pheromones across closely related *Drosophila* species (Chin et al. 2014; Ng et al. 2015).

In *D. melanogaster*, two sex-specific sex pheromones are synthesized in the ejaculatory bulb: 11-*cis*-vaccenyl acetate (cVA) and (3*R*,11*Z*,19*Z*)-3-acetoxy-11,19-octacosadien-1-ol (CH503). These pheromones are secreted by the ejaculatory bulb and localize to the male anogenital region. Further, these molecules are transferred

to females during mating (Yew et al. 2009). cVA has been shown to have numerous functions in this species, including inhibiting male courtship (Zawistowski and Richmond 1985; Ejima et al. 2007), acting as an aggregation factor (Kurtovic et al. 2007) and promoting male aggression (Wang and Anderson 2010; Wang et al. 2011).

CH503 also acts to inhibit male courtship, but has a longer lasting affect than cVA, being capable of remaining on the female cuticle for up to 10 days after a mating (Yew et al. 2009). Further, mutation to the enzyme required for the synthesis of CH503, the very-long-chain fatty acid elongase *bond*, is required for optimal male fertility (Ng et al. 2015). *bond* mRNA and protein are also expressed in the ejaculatory bulbs of *D. simulans* and *D. yakuba*, both species shown to produce CH503 (Yew et al. 2009).

In desert *Drosophila* species (the *repleta* group), triacylglycerides (TAGs)—a novel class of pheromones—are synthesized in the ejaculatory bulb in a sex-specific fashion (Chin et al. 2014). Chin et al. (2014) reported that 13 different triacylglycerides are broadly expressed across 11 species. Further, examining *D. arizonae* and *D. mojavensis*, male-secreted TAGs were found on mated females (but not on virgin females), with female attractiveness increasing with the decrease in detection of TAGs.

11.4.3 Ejaculatory Duct

Like the EB, ejaculatory duct cells derive from cells of the A9 primordium during metamorphosis (Estrada et al. 2003). Proteins with antimicrobial activity are produced and secreted from the ejaculatory duct (Lung et al. 2001) including the sex-specifically expressed andropin (Samakovlis et al. 1991) and cecropin, a broadly expressed antimicrobial peptide (Junell et al. 2010). The class III POU-domain transcription factor Drifter/Ventral veinless is required for the expression of cecropin, having been suggested that Drifter/Ventral veinless may act in combination with other factors to regulate the expression of antimicrobial peptides in a tissue-specific manner (Junell et al. 2010).

In addition to antimicrobial peptides, the ejaculatory duct synthesizes and secretes a peptide that can elicit some female post-mating responses. This peptide, DUP99B, has homology to the previously mentioned SP in its C-terminus, suggesting that it evolved by gene duplication (Saudan et al. 2002). When injected into virgin females, DUP99B induces sexual refractoriness and egg-laying, similar to SP (Saudan et al. 2002). Further, DUP99B has affinity for nervous system tissue (Ottiger et al. 2000; Ding et al. 2003), however, SP binds its targets with higher affinity than DUP99B while also having molecularly distinct targets (Ding et al. 2003). Finally, unlike SP, DUP99B does not bind to sperm in the female reproductive tract (Liu and Kubli 2003; Peng et al. 2005b), suggesting that its effects on mated females are short lived compared to SP. The ejaculatory duct also produces

glucose dehydrogenase, which plays an important role in the storage of sperm by mated females (Iida and Cavener 2004).

11.5 Fates of Male Secretions in Mated Females

The majority of the proteins secreted from the *D. melanogaster* male reproductive tract tissues that are transferred to females at copulation are only detectable within the female for ~4–6 h after mating ends (Ravi Ram et al. 2005). During this time, seminal proteins have been found within the mating plug (Neubaum and Wolfner 1999; Lung and Wolfner 2001; Ravi Ram et al. 2005), the sperm mass (Neubaum and Wolfner 1999; Lung and Wolfner 2001), the tissues of the female reproductive tract, including the sperm storage organs (Ravi Ram et al. 2005), the oviduct (Neubaum and Wolfner 1999) and the base of the ovary (Ravi Ram et al. 2005). Some SFPs, including ovulin and the SP, enter the hemolymph (Monsma et al. 1990; Pilpel et al. 2008) through a permeable part of the lower uterus (Lung and Wolfner 1999) and/or through a puncture made by the male genitalia (Kamimura 2007; Mattei et al. 2015). This gives these SFPs access to targets outside the female reproductive tract. The mechanism(s) that allows some SFPs to enter the female circulation but prevents others is currently unknown. The example of an SFP that persists longer than a few hours in the mated female is the SP. Its binding to sperm allows it to remain within the female for >5d post-mating (Peng et al. 2005b), where it continues to “dose” her, changing her behavior and physiology as long as she contains stored sperm.

11.6 The Female Reproductive Tract

11.6.1 Oviducts

The oviducts (see Fig. 11.1) are secretory tubes surrounded by muscle and nerves that connect the base of the ovary to the top of the uterus. Proper oviduct function is essential for successful reproduction. Contraction of the oviduct facilitates gamete movement from the ovaries to the site of fertilization. Secretions from the oviduct epithelia create an optimal environment for the final maturation of the female gametes, and for transport of the egg to the uterus (Gillott 1988; Bloch Qazi et al. 2003). In insects, the oviduct environment supports activation of the oocyte during its transit towards the uterus (Heifetz et al. 2001; Bloch Qazi et al. 2003).

The *Drosophila* oviduct begins with two short tubes (lateral oviducts), each arising from one ovary. These tubes then unite medially to form the common oviduct. Lateral and common oviducts are ectodermal in origin. The oviductal wall consists of a single-layered epithelium lined with a chitinous intima and surrounded by cir-

cular muscles (Miller 1950; Heifetz and Wolfner 2004; Middleton et al. 2006). The oviduct epithelium shows intracellular membranous folding and extensive microvilli at the apical membrane, indicating their secretory function (Middleton et al. 2006; Kapelnikov et al. 2008). The epithelium along the oviduct is covered by an electron dense apical extracellular matrix (AECM) and a thin layer of cuticle. Different regions of the oviduct (i.e. lateral oviduct, upper common oviduct, lower common oviduct) display different apical membrane morphology (i.e. microvilli or pleats). In mated females, the AECM and cuticle have increased surface area, and electron dense granules are observed in both the AECM and cell cytoplasm. Kapelnikov et al. (2008) suggested that these granules participate in the secretion and deposition of the AECM. They further indicated that the lower common oviduct is a site of active apical secretion in both mated and unmated females. However, little is known about the secretory nature of the oviduct.

Oviductal fluid is not yet characterized in *Drosophila*. However, hints to its likely composition can be taken from what is known in other organisms, in which oviducts contain a complex mixture of secretions from epithelial cells and from blood plasma. In those animals, the fluid contains metabolic components such as glucose, lactate, pyruvate and amino acids, at concentrations that often differ from those in the uterus or plasma (Hunter 1998; Aviles et al. 2010). In other insects, such as the stick insect (*Baculum thairi*), histochemical analyses of oviduct showed that the epithelial cells' secretions are rich in proteins and in acidic mucus substances (Viscuso et al. 1996). Oviductal secretions of the American migratory grasshopper (*Melanoplus sanguinipes*) contain proteins, and the oviducts of the blister beetle (*Lytta nuttali*) produce a carbohydrate-protein substance. The cytoplasm of the oviduct epithelial cells in the migratory locust (*Locusta migratoria*) and other Acridoidea are rich in RNA and proteins (Gillott 1988).

The transcriptomes and proteomes of *Drosophila* have been compared in unmated females and in females at 3 h after mating (Kapelnikov et al. 2008). These studies identified proteins and transcripts that are involved in the terminal differentiation of the oviduct. Although these analyses were done at an early post-mating time point, they also potentially highlight mating-responsive proteins and transcripts that are secreted into the lumen and thus contribute to the oviduct environment post-mating. Gene ontology analysis of oviduct-expressed proteins revealed that proteins related to cytoskeleton, developmental process, and muscle contraction, were significantly overrepresented. Mating-responsive proteins were classified as either muscle-specific or involved in epithelial cell morphogenesis, which may indicate regulatory changes affecting epithelial and muscle activity and/or structural properties that would lead to functional changes in the oviduct environment after mating (Kapelnikov et al. 2008). Transcriptome analysis of the oviduct at 3 h post-mating identified antimicrobial peptides (Kapelnikov et al. 2008). Constitutive production of antimicrobial peptides is observed along the reproductive tract of *Drosophila* to protect it from infections and guarantee a safe environment for the reproductive events (Tzou et al. 2000). In addition, mating induces a high expression of the antimicrobial peptides *cecropin* (*cec*) A1 and A2, *attacin* (*att*) A and B and CG9080 within the oviducts (Kapelnikov et al. 2008). These components of the

humoral immune responses of the fly are secreted and protect the oviducts and the laid eggs from environmental challenges.

11.6.2 Uterus

The uterus receives activated eggs (Heifetz et al. 2001) from the oviducts, and is the site of fertilization. The *Drosophila* uterus also supports the early stages of embryogenesis, and causes deposition of the fertilized egg onto the substratum where the embryo will finish its development. The uterus also orchestrates processes essential at the early post-mating stages, when sperm are introduced into the female reproductive tract, allowing sperm movement into the oviduct or the sperm storage organs (Miller 1950; Heifetz et al. 2000; Carney and Taylor 2003; Mack et al. 2006; Schnakenberg et al. 2012; Avila et al. 2015c).

The uterus (or bursa) of *Drosophila* is an elongated muscular pouch surrounded by several layers of circular musculature (Miller 1950). The uterine epithelium is composed of small cuboidal cells with a chitinous intima. Overall, the epithelial layer shows a convoluted intracellular membranous structure and extensive microvilli on the apical surface, which is consistent with their secretory activity and is similar to what is seen in the oviduct. Muscular fibers extending postero-laterally and ventrally from the uterus to the abdominal tergite and sternite enable greater expansion of lumen when the egg is passing through. The ducts of the paired parovaria and the sperm storage organs, the spermathecae and seminal receptacle, extend from the anterior part of the uterus (Miller 1950; Heifetz and Rivlin 2010).

The uterus of an unmated *Drosophila* female is contracted, with a thin lumen. Soon after mating (± 30 min) the uterus distends in stages to expose a large lumen (± 480 μm long and ± 200 μm in diameter), where initially the male ejaculate and sperm are contained (Adams and Wolfner 2007; Mattei et al. 2015). The distention also extends the oviduct, facilitating the release of one egg from the ovary. The egg is released posterior-end first, so that when it comes to rest within the uterus (which clamps down to hold it Mattei et al. 2015) its micropyle (the site for sperm entry) is positioned adjacent to the opening of the sperm storage organs. Sperm released from storage then enter the micropyle and penetrate the egg's oolema (Nonidez 1920; Sonnenblick 1950). The initial events leading to fertilization are poorly understood in *Drosophila* and we know little about any secretions potentially produced by the uterus.

In *Drosophila*, the parovaria and spermathecal secretory cells (SSC) that secrete material into the uterine lumen regulate/mediate processes essential for successful fertilization. Knockdown of both glands' secretory cells (i.e. SSC and parovaria) early during pupal stage leads to female sterility (Allen and Spradling 2008). Furthermore, ablation of the SSC before mating, reduced female egg-laying rate and delayed embryo release from the uterus up to a very late developmental stage (Schnakenberg et al. 2011). The importance of SSC and parovarial products for female fertility leads to the hypothesis that the uterine lumen may contain a combi-

nation of secreted products derived from these glands and products produced in the uterine secretory epithelia. Together, such products create the right environment for sperm to fertilize eggs and for eggs subsequently to be laid.

11.6.3 Sperm Storage Organs

Many animal species are able to store sperm effectively allowing progeny production at times when mating can no longer occur, and/or coordinating reproductive physiology for prolonged egg laying. It is therefore likely that an important function of the female secretions is to maintain the viability of the stored sperm (Bloch Qazi et al. 2003; Heifetz and Rivlin 2010; Schnakenberg et al. 2012). Indeed, such a role is supported by *in vitro* studies in *Hymenoptera* (den Boer et al. 2010), where female secretions have been shown to dampen negative effect on sperm viability caused by seminal fluid from other males.

Female *D. melanogaster* have three storage organs. These organs, which store about 1/3 to 1/4 of the sperm received during a mating, are connected to the anterior of the uterus. One organ is the long coiled tubular seminal receptacle; the others are a pair of spermathecae. The seminal receptacle generally holds ~60% of stored sperm, and the spermathecal cap stores the remainder (Avila et al. 2012). It is thought that the sperm from the seminal receptacles are used first, and that the spermathecae provide longer-term storage of sperm.

11.6.3.1 Seminal Receptacle

The seminal receptacle is a coiled and narrow blind-ended long tube that stores sperm initially, and for the shorter term (Miller 1950; Pitnick et al. 1999; Miller et al. 2001; Pattarini et al. 2006). Although the seminal receptacle was originally thought to be simply a container for sperm, recent studies suggest that it may play an active secretory role to establish an optimal environment for sperm storage and fertility (Prokupek et al. 2009, 2010; Heifetz and Rivlin 2010).

The length of the seminal receptacle varies from 1.6 to 3.5 mm (Miller et al. 2001; Miller and Pitnick 2003). Although it can influence the number of sperm stored, larger size is not proportional to a higher sperm-storage efficiency. Females with very long seminal receptacles sometimes exhibited deficient fertilization and lower hatching rates (Miller and Pitnick 2003). The proximal portion has a slit-like narrow lumen and connects to the anterior end of the uterus below the common oviduct. The distal portion of the seminal receptacle ensures wide space for sperm storage (Miller 1950; Hihara and Hihara 1993; Heifetz and Rivlin 2010). The lumen of the seminal receptacle is lined with a thin cuticle and is surrounded by a layer of secretory cells, a basement membrane, and a helically coiled layer of muscle (Blaney 1970). In unmated females, the receptacle is filled with liquid, which appears as a coagulum; in mated females the lumen is filled with active swimming spermatozoa (Manier et al. 2010).

Electron microscopy of the seminal receptacle of 3-day-old unmated and mated *Drosophila* females suggests that the proximal and distal regions of the seminal receptacle differ in their mechanism of secretion (Heifetz and Rivlin 2010). The proximal epithelium has densely packed, long microvilli covered by a thick extracellular matrix that contains electron-dense filamentous material. The distal epithelium, in contrast, has highly arranged brush border microvilli, covered by a thin extracellular matrix. Electron-dense material and numerous vacuoles can be observed in the apical cytoplasm of the cells, indicating that this epithelium is also secretory (Heifetz and Rivlin 2010).

Although we know little about the exact nature of the seminal receptacle secretions, the results of evolutionary EST studies of seminal receptacles of unmated and mated females give us an idea about this organ's functionality (Prokupek et al. 2009, 2010). Gene expression at 3 h after the start of mating showed that 29 % of the transcripts that are uniquely expressed in the seminal receptacle encode proteins that possess a secretion signal. These include molecules with odorant-related functions, such as odorant binding (Obp57a, CG1124 and CG13027) that could be involved in guiding sperm to the seminal receptacle. Lipid and carbohydrate metabolism genes are the largest functional class in the seminal receptacle. For example, CG17323 and CG11289 encode glycosyltransferases that hydrolyze terminal sugar residues in different glycoconjugates and were predicted to have a role in sperm-egg interactions (Tulsiani et al. 1998; Zitta et al. 2006; Allen and Spradling 2008; Prokupek et al. 2010). Lipid and carbohydrate metabolism enzymes can also break down complex energy sources for use by sperm in storage. Genes encoding protease inhibitors are over-expressed in the seminal receptacle. Their products could potentially regulate proteolysis and/or coagulation of seminal fluid or might regulate/interact with female molecules inside or outside the seminal receptacle. In addition, 7% of the genes up-regulated in the seminal receptacle at 3- and 6 h after the start of mating are involved in immune response (e.g. drosomycin, defensin, relish, the Toll receptor) (Prokupek et al. 2008, 2010). Other transcripts whose expression changed at 6 h after the start of mating are suggested to play roles in nerve impulse transmission and chemosensory sensing (probing male secretions), ion transport and protein kinase regulation which some are mediators of the secretory machinery (Prokupek et al. 2009). The suite of transcripts up-regulated in the seminal receptacle at different times after the start of mating suggests the possibility that this tissue's secretions keep sperm viable, but also may have roles beyond the storage of sperm. Those roles could, in theory, include sensing of molecular cues brought with the sperm from the male that could in turn affect the secretions made by the seminal receptacle.

11.6.3.2 Spermathecae

The spermathecae are a pair of mushroom-shaped organs that in addition to holding sperm for long periods (long term sperm storage) appear to maintain and release sperm, thereby potentially facilitating sperm competency for fertilization and regulating egg laying rate (Neubauer and Wolfner 1999; Pitnick et al. 1999; Heifetz and

Rivlin 2010; Schnakenberg et al. 2011; Sun and Spradling 2013). Although the number and sizes of spermathecae varies among fly species, all spermathecae consist of a dark chitinous capsule in which the sperm are stored and that is connected to the anterior end of the uterus by a duct (Miller 1950; Bloch Qazi et al. 2003; Heifetz and Rivlin 2010). The capsule is surrounded by a thin layer of epithelial cells, a layer of cuboidal secretory glandular cells, and a thick layer of fat body cells. Thus, two types of secretion, a glandular and a fat body-derived, may be produced by the spermathecae (Lazareva et al. 2007; Heifetz and Rivlin 2010). Each spermathecal gland cell (SSC) represents a single secretory unit and contains a cup-shaped, inner cavity (i.e. end apparatus) lined by extensive microvilli, connected via a small duct to the lumen of the capsule. This lumen is filled with spermatozoa early after mating (Miller 1950; Filosi and Perotti 1975; Gillott 1988).

Several studies indicate that *Drosophila* spermathecae secrete factors that maintain sperm viability in both the spermathecae and seminal receptacle. Filosi and Perotti (1975) report that the SSCs produce a laminar secretion that increases in volume after mating. Based on histochemical staining, they suggest that this secretion is composed of glycoproteins or lipoproteins, and that it may play a nutritive role in maintaining sperm for prolonged periods (Clements and Potter 1967; Filosi and Perotti 1975). Simultaneous disruption of spermathecal and parovarial development using *lozenge* (*Lz*) and *hormone receptor-like 39* (*Hr39*) mutants resulted in female sterility (Allen and Spradling 2008). In both mutants, one or both spermathecae were absent, nevertheless, normal amounts of sperm appeared to be stored in the seminal receptacle. One interpretation of these data is that the spermathecae (and or parovaria) plays a crucial role in sperm support and release. In less severe *Hr39* mutants with generally normal spermathecae and parovaria, laminar secretion and fertility are reduced (Allen and Spradling 2008). The role of spermathecal secretory cells in particular was initially dissected by Schnakenberg et al. (2011). These authors identified transcriptional regulatory regions for two genes [*Spermathecal endopeptidase 1* (*Send1*) and *Send2*] that are specifically expressed in SSC. They used these regulatory regions to drive genetic ablation of the SCC pre- and post-mating. The results of those experiments showed that SSC are required to recruit sperm to the spermathecae, and to mediate sperm motility in the seminal receptacle and egg-laying. Interestingly, SSC ablation pre-mating resulted in retention and internal development of embryos in the female's uterus (Schnakenberg et al. 2011). Further information about the roles of the spermathecal secretory cells was obtained by Sun and Spradling (2013). Using modulation of the secretory cell development through *Hr39*, they demonstrated that at least 80 secretory cells are required for normal reproductive function. Furthermore, two mechanisms of secretion were suggested. The first is the canonical mechanism that involves transit of secretory products via the endoplasmic reticulum – Golgi – plasma membrane network). Function of this mechanism in SSCs is necessary for normal sperm storage. The second secretion mechanism is different from the canonical one, and is mediated by *Hr39*. When it is inhibited in SSCs, ovulation is slowed and egg-laying is reduced by 50% (Sun and Spradling 2013). Thus, the secretory products of the

spermatheca can impact the competence of the sperm in the spermathecae, and the functionality of the seminal receptacle and the ovaries.

We know little about the molecular identity of the SSC secretions. Transcriptome and evolutionary EST analysis of *Drosophila* spermathecae in unmated and mated females (Allen and Spradling 2008; Prokupek et al. 2008, 2009) gives us an idea about likely protein classes found in these secretions. Of the 42 genes examined in the evolutionary EST analysis, 23 (55%) are predicted to have signal peptides. Transcripts encoding serine proteases with secretion-signal peptides were highly enriched in the spermatheca (Prokupek et al. 2008). The expression level of serine proteases *CG9897* and *CG17239* in spermathecae of unmated and mated females, respectively (3- and 6 h after the start of mating) was the highest (Prokupek et al. 2009). *CG17239* remains the highest expressed gene in spermatheca at 3 days after mating (Allen and Spradling 2008), suggesting that its product plays an important role in proteolytic processes inside, and possibly outside, the spermatheca. The importance of serine proteases comes from the fact that these enzymes can potentially interact with seminal proteins and assist, for example, in the maturation of sperm or in the release of SP's C-terminal active fragment from sperm. The proteases could play roles antagonistic to male "interests", such as by degrading seminal proteins, or that are cooperative with the male's interests, such as by regulating the cleavage of seminal proteins to their active forms (Lawniczak and Begun 2004; McGraw et al. 2004; Heifetz et al. 2005; Peng et al. 2005b; Prokupek et al. 2010). Prokupek et al. (2009) further compared the transcriptomes of sperm storage organs from unmated and mated females. Among over-represented categories of mating-responsive genes, were genes involved in metabolism (i.e. lipid, monosaccharide) and electron transport, particularly in spermathecae. At 3 h after the start of mating, transcript categories upregulated in spermathecae included biosynthesis of macromolecules and protein targeting; later at 6 h after the start of mating, metabolism (carboxylic acid, lipid, monosaccharide, coenzyme), biosynthesis, heme-binding and peptidase activity were up-regulated. Prokupek et al. (2009) suggested that the induction of metabolism-related genes in spermathecae are associated with storing motile sperm for long periods.

11.6.4 Female Accessory Glands (Parovaria)

The parovaria are pair of small secretory organs that connect to the uterus by a delicate duct close to the spermatheca (Miller 1950). The gland is composed of a monolayer of secretory cells, each of which has a large vacuole with acidophilic granules that are polarized towards the gland lumen. The lumen, which is lined by a thick intima, contains fine granular secretions. Similar-looking secretions are also embedded in the fat body that surrounds the parovaria and the spermathecae (Miller 1950).

The parovaria are highly specialized and their function varies among insects. Studies conducted in insects indicate that parovarial secretions are important for female reproductive success. In Diptera, parovaria produce antimicrobial peptides

(medfly, *Ceratitis capitata*, Manetti et al. 1997), oviposition-stimulating or -inhibiting pheromones (sand fly, *Lutzomyia longipalpis*, Dougherty et al. 1992), secretions that induce contraction of the oviducts during oviposition (house fly, *Musca domestica*, Wagner et al. 1993) and components that contribute to the fertilization process which modify the micropyle cap of the egg and take part in the acrosomal reaction (*M. domestica*, Degrugillier 1985).

Few reports have highlighted the secretory potential of the parovaria because of the minute size of the organs; this presents a challenge for their study. The involvement of parovarial secretions in sperm maintenance, release and fertility was shown when both spermathecae and parovaria were ablated by mutation of *Hr39* (Allen and Spradling 2008). Sun and Spradling (2013) targeted gland secretory cells (spermatheca and parovaria) by knocking down *hnt* expression during pupal development using *lz-Gal4* driver. They found that secretory cell-deficient females have defects in ovulation and deposit significantly fewer eggs than controls. Defects in ovulation were also observed when the authors used *dpr5-Gal4* (specific for the secretory lineage of the reproductive tract) to knock down *hnt* and other genes. Disabling the function of secretory cells from both glands also produced defects in sperm storage, sperm motility and fertility (Sun and Spradling 2013). Identification of a driver specific to the secretory cells of parovaria will enable us to delineate the role of the gland secretory cells and the interaction between the SSC and parovaria that possibly, together with fat body secreted products determine the reproductive success of a given female.

11.7 Taking Control – Female Secretions Shape Later Reproductive Functionality

Once male secretions have started the “poised” female reproductive machinery, the female reproductive tract takes over to orchestrate a signaling network that will control and coordinate ovulation, sperm release, fertilization, and egg laying (Heifetz et al. 2014; Mattei et al. 2015; Carmel et al. 2016). The players in this intricate coordination are both chemical and mechanical. The former comprises a diverse set of molecules, including those with hormone-like or neuromodulator activities, as well as those that can modify the acidity or ionic environment of the reproductive tract. In some cases, it is known that mating alters the presence, amount, or distribution of these molecules; in other cases, this has not yet been investigated.

Studies of oviduct innervation in *Drosophila* reveal that the female oviduct receives aminergic, peptidergic (type II) and glutamatergic (type I) input (Monastirioti 2003; Heifetz and Wolfner 2004; Cole et al. 2005; Middleton et al. 2006; Yang et al. 2008). Interestingly, mating induces a significant increase in type II innervation along the reproductive tract (Kapelnikov et al. 2008; Rubinstein and Wolfner 2013), suggesting changes in ability to produce the neuromodulators. Heifetz et al. (2014) used whole-mount immunocytochemistry to examine the pres-

ence, locations and levels of signaling molecules (i.e. octopamine, serotonin, and dromyosuppressin (DMS); also known as neuromodulators) in the reproductive tracts of unmated and mated females. They showed that each region of the unmated *Drosophila* female reproductive tract has a unique region-specific combination of signaling molecules and that each aspect of mating (sperm, seminal fluid proteins, physical/mechanical stimuli) affected the distribution patterns and levels of particular signaling molecules (Heifetz and Wolfner 2004; Heifetz et al. 2014). The characteristic combination of signaling molecules at each region could potentially modulate specific downstream cascade/s essential for the environment and function of that region, which are then altered in response to mating. Male components could alter the combination of signaling molecules by acting directly on cells in the female reproductive tract or indirectly by affecting the female's central nervous system (Arthur et al. 1998; Yang et al. 2009; Rezaval et al. 2012; Haussmann et al. 2013). For example, the seminal protein ovulin triggers an increase in the number of synaptic sites by octopamine neurons on the reproductive tract after mating, leading to the stimulation of ovulation after the start of mating (Rubinstein and Wolfner 2013).

The coordinated changes in the level of neuromodulators with time after mating could affect the environment and could coordinate different functions needed along the reproductive tract. This could occur at the mechanical level (by affecting muscle contraction, organ shape changes, etc.) and potentially at the chemical level by affecting gene expression. However, we know little about what happens to the neuromodulation once female takes control (i.e. 24 h after the start of mating; Carmel et al. 2016), nor whether the profile of signaling molecules is stable as long as there are sperm in storage.

The pH of the reproductive tract environment is critical for gamete function. The pH of each region of the female reproductive tract should be optimized to facilitate the movement of gametes or to provide the ideal environment for their maintenance and functionality. In organisms where this has been studied, it has been shown that arrival of seminal fluid after mating induce changes in the pH of the reproductive tract (e.g. Liu et al. 2012; Atikuzzaman et al. 2015; Suarez 2016). Although it is not known whether pH differs at different regions of the *D. melanogaster* reproductive tract, a hint that it might be regulated differentially comes from the expression of the *Esp* (*epidermal stripes and patches*) transporter, a molecule that mediates exchange of intracellular sulphate. *Esp* is expressed in both types of sperm storage organ of *Drosophila* (Chintapalli et al. 2007; Prokupek et al. 2010) and its RNA levels are significantly lower in the spermatheca than in the seminal receptacle before and after mating (Prokupek et al. 2009). It has been hypothesized that *Esp* activity could reduce the anionic environment in the lumen of these storage organs to facilitate SP release from the sperm membrane (Findlay et al. 2014).

Differences in osmolarity or in the ionic environment of the lumen of reproductive tract regions could also modulate gamete functionality. Several genes essential in regulating fluid homeostasis and osmolarity of the environment, such as putative Aquaporins (AQPs), are expressed in the female *D. melanogaster* reproductive tract. In humans, 11 different AQP isoforms are expressed in the female reproductive tract. He et al. (2006) suggested that their expression in the oviduct could affect

the production of oviductal fluid by epithelial cells, in order to provide the right physiological environment for fertilization and early embryonic development. In the *Drosophila* oviduct, the RNA levels of one of these AQPs, *Drosophila* Integral Protein (Drip), increased post-mating (Kapelnikov et al. 2008). It is possible that mating-regulated changes in AQP transcript activity in the *Drosophila* female reproductive tract may regulate fluid homeostasis to provide a favorable environment for egg activation, sperm survival and other essential processes leading to successful reproduction. Consistent with this, oocytes swell within the oviducts and uterus, suggesting that they are taking up water from the surrounding environment. Ionic environments within the female reproductive tract also play roles in gamete function, likely in context of osmolarity differences. For example, the wave of calcium that is associated with “activation” of oocytes to be competent to begin embryo development requires influx of calcium (Kaneuchi et al. 2015; York-Andersen et al. 2015). This occurs as the oocytes enter the oviducts, and thus likely involves calcium from the oviductal environment.

In addition to chemical differences between different parts of the reproductive tract, at least some of which are regulated by mating, mechanical events in the reproductive tract of mated females may control reproductive efficiency after most seminal proteins have been degraded. Again here the female “takes over control” after the male has initiated the process. An example is the coordination of ovulation and egg-laying. Normally, there is rarely more than one egg is present in the oviducts and lower reproductive tract of a mated female, even during the peak of egg-laying. How does the female regulate the rate of ovulation to achieve this? Mattei et al.'s (2015) micro-CT scans of female reproductive tracts before, during, and after mating suggest that mechanical controls are important in this regulation. In an unmated female, the upper oviduct contains a loop that likely impedes egg movement from the ovary. Mating relaxes this loop, through induced octopaminergic signaling caused by ovulin and a tilt of the uterus that pulls the oviduct straight. This allows release of an oocyte by the ovary; the egg then transits to the uterus. When it enters the uterus, the latter un-tilts, releasing the tension on the oviduct and allowing it to re-loop. This stops the next egg from ovulating. When the uterine egg is laid the uterus re-tilts, again exerting a pull on the oviduct, stretching the latter and allowing the next egg to be released. Continuation of this cycle coordinates ovulation and egg laying.

Thus far, we do not fully understand the interplay between chemical and mechanical cues, nor the extent to which they drive female reproductive success. Studies directed at exploring how mechanical signals are converted into changes in intracellular biochemistry and gene expression, or at further understanding how chemical signals control mechanical signals, will allow better understanding of these mechanochemical control mechanisms and might increase our chances of enhancing male and female fertility.

11.8 Concluding Remarks

Creating an optimal environment suitable for maintaining gametes, supporting their union, and moving fertilized egg to its next stage requires tight regulation of the tissues, secretions, and microenvironments in the female reproductive tract. Both males and females contribute important components to this regulation. Seminal fluid components from a variety of male reproductive glands modulate the physiology of the female reproductive tract, often moving it from a “poised” state to a state that actively supports gamete viability, movement, and fertilization and, in insects, egg-laying. The male’s contributions can be hormonal, elemental/nutritive, and through molecules that change gene expression, neuromodulation, or physical conformation of regions of the reproductive tract. These changes are coordinated by their initiation by a single event – the act of mating. In all internally-mating animals, these changes can improve the likelihood of sperm and egg meeting, and can support the next steps. In insects such as *Drosophila melanogaster* these next steps include timely laying of the egg on a substratum, but in organisms like mammals where embryo development occurs internally, the changes create an environment that results in optimal progeny development and physiology (Bromfield et al. 2014). Interestingly, at least in insects like *Drosophila*, once the male has initiated these pro-reproductive changes, the female takes over, prolonging efficient reproduction through her own chemical and physical signaling that was induced by mating. An important area for future research will be to determine at the precise molecular level how male and female interact to accomplish these changes. The genetic tools available in the *Drosophila* model system make this the ideal system for such investigation. For example, these tools have already identified a receptor for one seminal protein (SPR, the receptor for SP; Yapici et al. 2008), allowing study of how these work together, and evolutionary rate co-variation studies have identified at least three female genes (*Esp*, *hadley* and *fra mauro*; Findlay et al. 2014) that are needed to further transduce the action of the SP to the female. In another example, genetic studies have shown that the seminal protein ovulin induces the females’ octopaminergic signaling (Rubinstein and Wolfner 2013), to stimulate ovulation. Identifying the molecular basis of how males and females interact molecularly to regulate the latter’s reproductive tract microenvironments and their composition will provide important insights into mechanisms for successful reproduction and the production of healthy offspring.

Acknowledgements We are very grateful to Dr. Ephraim Cohen for the invitation to write this chapter, and for his patience during its gestation. We thank Dr. Jessica Sitnik for helpful suggestions about how to organize the chapter and of topics to include, Zohar Nir-Amitin for drawing the figure, and Drs. M. Siegal and L. Harshman for helpful comments. We thank NIH grants (HD-R01-038921 and HD-R01-059060 to MFW, and to MFW and AG Clark, respectively) and Chief Scientist Ministry of Agriculture (872-0055-10 to YH) and US-Israel Binational Science Foundation grant (2009270 to YH and Mark Siegal).

References

- Aalberts M, Stout TAE, Stoorvogel W (2014) Prostatosomes: extracellular vesicles from the prostate. *Reproduction* 147:R1–R14
- Adams EM, Wolfner MF (2007) Seminal proteins but not sperm induce morphological changes in the *Drosophila melanogaster* female reproductive tract during sperm storage. *J Insect Physiol* 53:319–331
- Ahmad SM, Baker BS (2002) Sex-specific deployment of FGF signaling in *Drosophila* recruits mesodermal cells into the male genital imaginal disc. *Cell* 109:651–661
- Aigaki T, Fleischmann I, Chen PS, Kubli E (1991) Ectopic expression of sex peptide alters reproductive-behavior of female *Drosophila melanogaster*. *Neuron* 7:557–563
- Allen AK, Spradling AC (2008) The *Sf1*-related nuclear hormone receptor *Hr39* regulates *Drosophila* female reproductive tract development and function. *Development* 135:311–321
- Apger-McGlaughon J, Wolfner MF (2013) Post-mating change in excretion by mated *Drosophila melanogaster* females is a long-term response that depends on sex peptide and sperm. *J Insect Physiol* 59:1024–1030
- Arthur BI, Hauschteck-Jungen E, Nothiger R, Ward PI (1998) A female nervous system is necessary for normal sperm storage in *Drosophila melanogaster*: a masculinized nervous system is as good as none. *Proc Roy Soc B Biol Sci* 265:1749–1753
- Atikuzzaman M, Bhai RM, Fogelholm J, Wright D, Rodriguez-Martinez H (2015) Mating induces the expression of immune- and pH-regulatory genes in the utero-vaginal junction containing mucosal sperm-storage tubuli of hens. *Reproduction* 150:473–483
- Avila FW, Wolfner MF (2009) Acp36DE is required for uterine conformational changes in mated *Drosophila* females. *Proc Natl Acad Sci U S A* 106:15796–15800
- Avila FW, Ram KR, Qazi MCB, Wolfner MF (2010) Sex peptide is required for the efficient release of stored sperm in mated *Drosophila* females. *Genetics* 186:595–600
- Avila FW, Sirot LK, LaFlamme BA, Rubinstein CD, Wolfner MF (2011) Insect seminal fluid proteins: identification and function. *Annu Rev Entomol* 56:21–40
- Avila FW, Bloch Qazi MC, Rubinstein CD, Wolfner MF (2012) A requirement for the neuromodulators octopamine and tyramine in *Drosophila melanogaster* female sperm storage. *Proc Natl Acad Sci U S A* 109:4562–4567
- Avila FW, Mattei AL, Wolfner MF (2015a) Sex peptide peptide receptor is required for the release of stored sperm by mated *Drosophila melanogaster* females. *J Insect Physiol* 76:1–6
- Avila FW, Wong A, Sitnik JL, Wolfner MF (2015b) Don't pull the plug! The *Drosophila* mating plug preserves fertility. *Fly* 9:62–67
- Avila FW, Cohen AB, Ameerudeen FS, Duneau D, Suresh S, Mattei AL, Wolfner MF (2015c) Retention of ejaculate by *Drosophila melanogaster* females requires the male-derived mating plug protein PEBme. *Genetics* 200:1171–1179
- Aviles M, Gutierrez-Adan A, Coy P (2010) Oviductal secretions: will they be key factors for the future arts? *Mol Hum Reprod* 16:896–906
- Bairati A (1968) Structure and ultrastructure of the male reproductive system in *Drosophila melanogaster* Meig. *Ital J Zool* 2:105–182
- Belleannee C, Calvo E, Caballero J, Sullivan R (2013) Epididymosomes convey different repertoires of microRNAs throughout the bovine epididymis. *Biol Reprod* 89:30
- Bertram MJ, Akerkar GA, Ard RL, Gonzalez C, Wolfner MF (1992) Cell type-specific gene-expression in the *Drosophila melanogaster* male accessory-gland. *Mech Dev* 38:33–40
- Blaney WM (1970) Some observations on the sperm tail of *Drosophila melanogaster*. *Drosoph Inf Serv* 45:125–127
- Bloch Qazi MC, Wolfner MF (2003) An early role for the *Drosophila melanogaster* male seminal protein Acp36DE in female sperm storage. *J Exp Biol* 206:3521–3528
- Bloch Qazi MC, Heifetz Y, Wolfner MF (2003) The developments between gametogenesis and fertilization: ovulation and female sperm storage in *Drosophila melanogaster*. *Dev Biol* 256:195–211

- Bontonou G, Shaik HA, Denis B, Wicker-Thomas C (2015) Acp70A regulates *Drosophila* pheromones through juvenile hormone induction. *Insect Biochem Mol Biol* 56:36–49
- Bretman A, Lawniczak MKN, Boone J, Chapman T (2010) A mating plug protein reduces early female remating in *Drosophila melanogaster*. *J Insect Physiol* 56:107–113
- Bromfield JJ, Schjenken JE, Chin PY, Care AS, Jasper MJ, Robertson SA (2014) Maternal tract factors contribute to paternal seminal fluid impact on metabolic phenotype in offspring. *Proc Natl Acad Sci U S A* 111:2200–2205
- Brook WJ, DiazBenjumea FJ, Cohen SM (1996) Organizing spatial pattern in limb development. *Annu Rev Cell Dev Biol* 12:161–180
- Carmel I, Tram U, Heifetz Y (2016) Mating induces developmental changes in the insect female reproductive tract. *Curr Opin Insect Sci* 13:106–113
- Carney GE, Taylor BJ (2003) *logjam* encodes a predicted EMP24/GP25 protein that is required for *Drosophila* oviposition behavior. *Genetics* 164:173–186
- Carvalho GB, Kapahi P, Anderson DJ, Benzer S (2006) Allocrine modulation of feeding behavior by the sex peptide of *Drosophila*. *Curr Biol* 16:692–696
- Chapman T, Liddle LF, Kalb JM, Wolfner MF, Partridge L (1995) Cost of mating in *Drosophila melanogaster* females is mediated by male accessory gland products. *Nature* 373:241–244
- Chapman T, Bangham J, Vinti G, Seifried B, Lung O, Wolfner MF, Smith HK, Partridge L (2003) The sex peptide of *Drosophila melanogaster*: female post-mating responses analyzed by using RNA interference. *Proc Natl Acad Sci U S A* 100:9923–9928
- Chatterjee SS, Uppendahl LD, Chowdhury MA, Ip PL, Siegal ML (2011) The female-specific *doublesex* isoform regulates pleiotropic transcription factors to pattern genital development in *Drosophila*. *Development* 138:1099–1109
- Chen PS (1984) The functional morphology and biochemistry of insect male accessory glands and their secretions. *Annu Rev Entomol* 29:233–255
- Chin JSR, Ellis SR, Pham HT, Blanksby SJ, Mori K, Koh QL, Etges WJ, Yew JY (2014) Sex-specific triacylglycerides are widely conserved in *Drosophila* and mediate mating behavior. *eLife* 3:e01751
- Chintapalli VR, Wang J, Dow JA (2007) Using flyatlas to identify better *Drosophila melanogaster* models of human disease. *Nat Genet* 39:715–720
- Chow CY, Avila FW, Clark AG, Wolfner MF (2015) Induction of excessive endoplasmic reticulum stress in the *Drosophila* male accessory gland results in infertility. *PLoS One* 10:e0119386
- Christiansen AE, Keisman EL, Ahmad SM, Baker BS (2002) Sex comes in from the cold: the integration of sex and pattern. *Trends Genet* 18:510–516
- Clements AN, Potter SA (1967) Fine structure of spermathecae and their ducts in mosquito *Aedes aegypti*. *J Insect Physiol* 13:1825–1836
- Clifton ME, Correa S, Rivera-Perez C, Nouzova M, Noriega FG (2014) Male *Aedes aegypti* mosquitoes use JH III transferred during copulation to influence previtellogenic ovary physiology and affect the reproductive output of female mosquitoes. *J Insect Physiol* 64:40–47
- Cognigni P, Bailey AP, Miguel-Aliaga I (2011) Enteric neurons and systemic signals couple nutritional and reproductive status with intestinal homeostasis. *Cell Metab* 13:92–104
- Cole SH, Carney GE, McClung CA, Willard SS, Taylor BJ, Hirsh J (2005) Two functional but noncomplementing *Drosophila* tyrosine decarboxylase genes: distinct roles for neural tyramine and octopamine in female fertility. *J Biol Chem* 280:14948–14955
- Corrigan L, Redhai S, Leiblich A, Fan SJ, Perera SM, Patel R, Gandy C, Wainwright SM, Morris JF, Hamdy F, Goberdhan DC, Wilson C (2014) BMP-regulated exosomes from *Drosophila* male reproductive glands reprogram female behavior. *J Cell Biol* 206:671–688
- Da Ros VG, Munoz MW, Battistone MA, Brukman NG, Carvajal G, Curci L, Gomez-Elias MD, Cohen DJ, Cuasnicu PS (2015) From the epididymis to the egg: participation of crisp proteins in mammalian fertilization. *Asian J Androl* 17:711–715
- Degrugillier ME (1985) In vitro release of house fly, *Musca domestica* L. (diptera: Muscidae), acrosomal material after treatments with secretion of female accessory gland and micropyle cap substance. *Int J Insect Morphol Embryol* 14:381–391

- Demott RP, Lefebvre R, Suarez SS (1995) Carbohydrates mediate the adherence of hamster sperm to oviductal epithelium. *Biol Reprod* 52:1395–1403
- den Boer SP, Baer B, Boomsma JJ (2010) Seminal fluid mediates ejaculate competition in social insects. *Science* 327:1506–1509
- Ding ZB, Haussmann I, Ottiger M, Kubli E (2003) Sex-peptides bind to two molecularly different targets in *Drosophila melanogaster* females. *J Neurobiol* 55:372–384
- Domanitskaya EV, Liu HF, Chen SJ, Kubli E (2007) The hydroxyproline motif of male sex peptide elicits the innate immune response in *Drosophila* females. *FEBS J* 274:5659–5668
- Dougherty MJ, Ward RD, Hamilton G (1992) Evidence for the accessory glands as the site of production of the oviposition attractant and or stimulant of *Lutzomyia longipalpis* (diptera, psychodidae). *J Chem Ecol* 18:1165–1175
- Dubrovsky EB, Dubrovskaya VA, Berger EM (2002) Juvenile hormone signaling during oogenesis in *Drosophila melanogaster*. *Insect Biochem Mol Biol* 32:1555–1565
- Ejima A, Smith BPC, Lucas C, Van Naters WV, Miller CJ, Carlson JR, Levine JD, Griffith LC (2007) Generalization of courtship learning in *Drosophila* is mediated by cis-vaccenyl acetate. *Curr Biol* 17:599–605
- Estrada B, Casares F, Sanchez-Herrero E (2003) Development of the genitalia in *Drosophila melanogaster*. *Differentiation* 71:299–310
- Fedorka KM, Linder JE, Winterhalter W, Promislow D (2007) Post-mating disparity between potential and realized immune response in *Drosophila melanogaster*. *Proc Roy Soc B-Biol Sci* 274:1211–1217
- Filosi M, Perotti ME (1975) Fine structure of the spermatheca of *Drosophila melanogaster* Meig. *J Submicr Cytol Path* 7:259–270
- Findlay GD, Yi XH, MacCoss MJ, Swanson WJ (2008) Proteomics reveals novel *Drosophila* seminal fluid proteins transferred at mating. *PLoS Biol* 6:1417–1426
- Findlay GD, Sitnik JL, Wang W, Aquadro CF, Clark NL, Wolfner MF (2014) Evolutionary rate covariation identifies new members of a protein network required for *Drosophila melanogaster* female post-mating responses. *PLoS Genet* 10:e1004108
- Gillott C (1988) Arthropoda-Insecta. In: Adiyodi KG, Adiyodi RG (eds) *Reproductive biology of invertebrates*. Wiley, New York, pp 319–417
- Gillott C (2003) Male accessory gland secretions: modulators of female reproductive physiology and behavior. *Annu Rev Entomol* 48:163–184
- Glgorov D, Sitnik JL, Maeda RK, Wolfner MF, Karch F (2013) A novel function for the Hox gene *Abd-B* in the male accessory gland regulates the long-term female post-mating response in *Drosophila*. *PLoS Genet* 9:e1003395
- Guiraudie-Capraz G, Pho DB, Jallon JM (2007) Role of the ejaculatory bulb in biosynthesis of the male pheromone cis-vaccenyl acetate in *Drosophila melanogaster*. *Integr Zool* 2:89–99
- Hasemeyer M, Yapici N, Heberlein U, Dickson BJ (2009) Sensory neurons in the *Drosophila* genital tract regulate female reproductive behavior. *Neuron* 61:511–518
- Haussmann IU, Hemani Y, Wijesekera T, Dauwalder B, Soller M (2013) Multiple pathways mediate the sex-peptide-regulated switch in female *Drosophila* reproductive behaviours. *Proc Roy Soc B-Biol Sci* 280:20131938
- He RH, Sheng JZ, Luo Q, Jin F, Wang B, Qian YL, Zhou CY, Sheng X, Huang HF (2006) Aquaporin-2 expression in human endometrium correlates with serum ovarian steroid hormones. *Life Sci* 79:423–429
- Heifetz Y, Rivlin PK (2010) Beyond the mouse model: using *Drosophila* as a model for sperm interaction with the female reproductive tract. *Theriogenology* 73:723–739
- Heifetz Y, Wolfner MF (2004) Mating, seminal fluid components, and sperm cause changes in vesicle release in the *Drosophila* female reproductive tract. *Proc Natl Acad Sci U S A* 101:6261–6266
- Heifetz Y, Lung O, Frongillo EA, Wolfner MF (2000) The *Drosophila* seminal fluid protein Acp26Aa stimulates release of oocytes by the ovary. *Curr Biol* 10:99–102
- Heifetz Y, Yu J, Wolfner MF (2001) Ovulation triggers activation of *Drosophila* oocytes. *Dev Biol* 234:416–424

- Heifetz Y, Vandenberg LN, Cohn HI, Wolfner MF (2005) Two cleavage products of the *Drosophila* accessory gland protein ovulin can independently induce ovulation. *Proc Natl Acad Sci U S A* 102:743–748
- Heifetz Y, Lindner M, Garini Y, Wolfner MF (2014) Mating regulates neuromodulator ensembles at nerve termini innervating the *Drosophila* reproductive tract. *Curr Biol* 24:731–737
- Herndon LA, Wolfner MF (1995) A *Drosophila* seminal fluid protein, Acp26Aa, stimulates egg-laying in females for 1 day after mating. *Proc Natl Acad Sci U S A* 92:10114–10118
- Hihara F, Hihara Y (1993) Electron dense particles appeared in the microvilli zone of the cuboidal cells of the ventral receptacle in *Drosophila melanogaster* mated female. *Zool Sci* 10:953–961
- Hunter RH (1998) Have the fallopian tubes a vital role in promoting fertility? *Acta Obstet Gynecol Scand* 77:475–486
- Iida K, Cavener DR (2004) Glucose dehydrogenase is required for normal sperm storage and utilization in female *Drosophila melanogaster*. *J Exp Biol* 207:675–681
- Isaac RE, Li CX, Leedale AE, Shirras AD (2010) *Drosophila* male sex peptide inhibits siesta sleep and promotes locomotor activity in the post-mated female. *Proc Roy Soc B Biol Sci* 277:65–70
- Junell A, Uvell H, Davis MM, Edlundh-Rose E, Antonsson A, Pick L, Engstrom Y (2010) The POU transcription factor drifter/ventral veinless regulates expression of *Drosophila* immune defense genes. *Mol Cell Biol* 30:3672–3684
- Kalb JM, Dibenedetto AJ, Wolfner MF (1993) Probing the function of *Drosophila melanogaster* accessory glands by directed cell ablation. *Proc Natl Acad Sci U S A* 90:8093–8097
- Kamimura Y (2007) Twin intromittent organs of *Drosophila* for traumatic insemination. *Biol Lett* 3:401–404
- Kamimura Y (2010) Copulation anatomy of *Drosophila melanogaster* (diptera: Drosophilidae): wound-making organs and their possible roles. *Zoomorphology* 129:163–174
- Kaneuchi T, Sartain CV, Takeo S, Horner VL, Buehner NA, Aigaki T, Wolfner MF (2015) Calcium waves occur as *Drosophila* oocytes activate. *Proc Natl Acad Sci U S A* 112:791–796
- Kapelnikov A, Rivlin PK, Hoy RR, Heifetz Y (2008) Tissue remodeling: a mating-induced differentiation program for the *Drosophila* oviduct. *BMC Dev Biol* 8:114
- Kim YJ, Bartalska K, Audsley N, Yamanaka N, Yapici N, Lee JY, Kim YC, Markovic M, Isaac E, Tanaka Y, Dickson BJ (2010) MIPs are ancestral ligands for the sex peptide receptor. *Proc Natl Acad Sci U S A* 107:6520–6525
- Kurtovic A, Widmer A, Dickson BJ (2007) A single class of olfactory neurons mediates behavioural responses to a *Drosophila* sex pheromone. *Nature* 446:542–546
- LaFlamme BA, Wolfner MF (2013) Identification and function of proteolysis regulators in seminal fluid. *Mol Reprod Dev* 80:80–101
- LaFlamme BA, Ram KR, Wolfner MF (2012) The *Drosophila melanogaster* seminal fluid protease “Seminase” Regulates proteolytic and post-mating reproductive processes. *PLoS Genet* 8:e1002435
- LaFlamme BA, Avila FW, Michalski K, Wolfner MF (2014) A *Drosophila* protease cascade member, Seminal Metalloprotease-1, is activated stepwise by male factors and requires female factors for full activity. *Genetics* 196:1117–1129
- Lawniczak MKN, Begun DJ (2004) A genome-wide analysis of courting and mating responses in *Drosophila melanogaster* females. *Genome* 47:900–910
- Lawrence PA, Struhl G (1996) Morphogens, compartments, and pattern: lessons from *Drosophila*? *Cell* 85:951–961
- Lazareva AA, Roman G, Mattox W, Hardin PE, Dauwalder B (2007) A role for the adult fat body in *Drosophila* male courtship behavior. *PLoS Genet* 3:e16
- Lee KM, Dauberova I, Isaac RE, Zhang C, Choi S, Chung J, Kim YJ (2015) A neuronal pathway that controls sperm ejection and storage in female *Drosophila*. *Curr Biol* 25:790–797
- Leese HJ (1988) The formation and function of oviduct fluid. *J Reprod Fertil* 82:843–856
- Leiblich A, Marsden L, Gandy C, Corrigan L, Jenkins R, Hamdy F, Wilson C (2012) Bone morphogenetic protein- and mating-dependent secretory cell growth and migration in the *Drosophila* accessory gland. *Proc Natl Acad Sci U S A* 109:19292–19297

- Liu HF, Kubli E (2003) Sex peptide is the molecular basis of the sperm effect in *Drosophila melanogaster*. Proc Natl Acad Sci U S A 100:9929–9933
- Liu Y, Wang DK, Chen LM (2012) The physiology of bicarbonate transporters in mammalian reproduction. Biol Reprod 86(99):1–13
- Ludwig MZ, Uspensky II, Ivanov AI, Kopantseva MR, Dianov CM, Tamarina NA, Korochkin LI (1991) Genetic-control and expression of the major ejaculatory bulb protein (PEB-me) in *Drosophila melanogaster*. Biochem Genet 29:215–239
- Lung O, Wolfner MF (1999) *Drosophila* seminal fluid proteins enter the circulatory system of the mated female fly by crossing the posterior vaginal wall. Insect Biochem Mol Biol 29:1043–1052
- Lung O, Wolfner MF (2001) Identification and characterization of the major *Drosophila melanogaster* mating plug protein (vol 31, pg 543, 2001). Insect Biochem Mol Biol 32:109–109
- Lung O, Kuo L, Wolfner MF (2001) *Drosophila* males transfer antibacterial proteins from their accessory gland and ejaculatory duct to their mates. J Insect Physiol 47:617–622
- Lung O, Tram U, Finnerty CM, Eipper-Mains MA, Kalb JM, Wolfner MF (2002) The *Drosophila melanogaster* seminal fluid protein Acp62F is a protease inhibitor that is toxic upon ectopic expression. Genetics 160:211–224
- Mack PD, Kapelnikov A, Heifetz Y, Bender M (2006) Mating-responsive genes in reproductive tissues of female *Drosophila melanogaster*. Proc Natl Acad Sci U S A 103:10358–10363
- Manetti AGO, Rosetto M, de Filippis T, Marchini D, Baldari CT, Dallai R (1997) Juvenile hormone regulates the expression of the gene encoding ceratotoxin a, an antibacterial peptide from the female reproductive accessory glands of the medfly *Ceratitis capitata*. J Insect Physiol 43:1161–1167
- Manier MK, Belote JM, Berben KS, Novikov D, Stuart WT, Pitnick S (2010) Resolving mechanisms of competitive fertilization success in *Drosophila melanogaster*. Science 328:354–357
- Markow TA, Coppola A, Watts TD (2001) How *Drosophila* males make eggs: it is elemental. Proc Roy Soc B Biol Sci 268:1527–1532
- Mattei AL, Riccio ML, Avila FW, Wolfner MF (2015) Integrated 3D view of post-mating responses by the *Drosophila melanogaster* female reproductive tract, obtained by micro-computed tomography scanning. Proc Natl Acad Sci U S A 112:8475–8480
- McGraw LA, Gibson G, Clark AG, Wolfner MF (2004) Genes regulated by mating, sperm, or seminal proteins in mated female *Drosophila melanogaster*. Curr Biol 14:1509–1514
- McGraw LA, Clark AG, Wolfner MF (2008) Post-mating gene expression profiles of female *Drosophila melanogaster* in response to time and to four male accessory gland proteins. Genetics 179:1395–1408
- Middleton CA, Nongthomba U, Parry K, Sweeney ST, Sparrow JC, Elliott CJ (2006) Neuromuscular organization and aminergic modulation of contractions in the *Drosophila* ovary. BMC Biol 4:17
- Miller A (1950) The internal anatomy and histology of the imago of *Drosophila melanogaster*. In: Demerec M (ed) Biology of *Drosophila*. Wiley, New York, pp 420–534
- Miller GT, Pitnick S (2003) Functional significance of seminal receptacle length in *Drosophila melanogaster*. J Evol Biol 16:114–126
- Miller GT, Starmer WT, Pitnick S (2001) Quantitative genetics of seminal receptacle length in *Drosophila melanogaster*. Heredity 87:25–32
- Minami R, Wakabayashi M, Sugimori S, Taniguchi K, Kokuryo A, Imano T, Adachi-Yamada T, Watanabe N, Nakagoshi H (2012) The homeodomain protein defective proventriculus is essential for male accessory gland development to enhance fecundity in *Drosophila*. PLoS One 7:e32302
- Monastirioti M (2003) Distinct octopamine cell population residing in the CNS abdominal ganglion controls ovulation in *Drosophila melanogaster*. Dev Biol 264:38–49
- Mondejar I, Acuna OS, Izquierdo-Rico MJ, Coy P, Aviles M (2012) The oviduct: functional genomic and proteomic approach. Reprod Domest Anim 47:22–29
- Monsma SA, Wolfner MF (1988) Structure and expression of a *Drosophila* male accessory-gland gene whose product resembles a peptide pheromone precursor. Genes Dev 2:1063–1073

- Monsma SA, Harada HA, Wolfner MF (1990) Synthesis of two *Drosophila* male accessory gland proteins and their fate after transfer to the female during mating. *Dev Biol* 142:465–475
- Moshitzky P, Fleischmann I, Chaimov N, Saudan P, Klausner S, Kubli E, Applebaum SW (1996) Sex-peptide activates juvenile hormone biosynthesis in the *Drosophila melanogaster* corpus allatum. *Arch Insect Biochem* 32:363–374
- Mueller JL, Page JL, Wolfner MF (2007) An ectopic expression screen reveals the protective and toxic effects of *Drosophila* seminal fluid proteins. *Genetics* 175:777–783
- Neubaum DM, Wolfner MF (1999) Mated *Drosophila melanogaster* females require a seminal fluid protein, Acp36DE, to store sperm efficiently. *Genetics* 153:845–857
- Ng WC, Chin JSR, Tan KJ, Yew JY (2015) The fatty acid elongase Bond is essential for *Drosophila* sex pheromone synthesis and male fertility. *Nat Commun* 6:8263
- Nonidez J (1920) The internal phenomena of reproduction in *Drosophila*. *Biol Bull* 39: 207–230
- Norville K, Sweeney ST, Elliott CJH (2010) Post-mating change in physiology of male *Drosophila* mediated by serotonin (5-HT). *J Neurogenet* 24:27–32
- Nothiger R, Dubendorfer A, Epper F (1977) Gynandromorphs reveal two separate primordia for male and female genitalia in *Drosophila melanogaster*. *Roux Arch Dev Biol* 181:367–373
- Ottiger M, Soller M, Stocker RF, Kubli E (2000) Binding sites of *Drosophila melanogaster* sex peptide pheromones. *J Neurobiol* 44:57–71
- Park M, Wolfner MF (1995) Male and female cooperate in the prohormone-like processing of a *Drosophila melanogaster* seminal fluid protein. *Dev Biol* 171:694–702
- Pattarini JA, Starmer WT, Bjork A, Pitnick S (2006) Mechanisms underlying the sperm quality advantage in *Drosophila melanogaster*. *Evolution* 60:2064–2080
- Peng J, Zipperlen P, Kubli E (2005a) *Drosophila* sex peptide stimulates female innate immune system after mating via the Toll and Imd pathways. *Curr Biol* 15:1690–1694
- Peng J, Chen S, Busser S, Liu HF, Honegger T, Kubli E (2005b) Gradual release of sperm bound sex peptide controls female post-mating behavior in *Drosophila*. *Curr Biol* 15:207–213
- Perotti ME (1971) Microtubules as components of *Drosophila* male paragonia secretion. An electron microscopic study, with enzymatic tests. *J Submicrosc Cytol* 3:255–282
- Pilpel N, Nezer I, Applebaum SW, Heifetz Y (2008) Mating increases trypsin in female *Drosophila* hemolymph. *Insect Biochem Mol Biol* 38:320–330
- Pitnick S, Markow T, Spicer GS (1999) Evolution of multiple kinds of female sperm storage organs in *Drosophila*. *Evolution* 53:1804–1822
- Poels J, Van Loy T, Vandersmissen HP, Van Hiel B, Van Soest S, Nachman RJ, Vanden Broeck J (2010) Myoinhibiting peptides are the ancestral ligands of the promiscuous *Drosophila* sex peptide receptor. *Cell Mol Life Sci* 67:3511–3522
- Poiani A (2006) Complexity of seminal fluid: a review. *Behav Ecol Sociobiol* 60:289–310
- Pondeville E, Maria A, Jacques JC, Bourgoïn C, Dauphin-Villemant C (2008) *Anopheles gambiae* males produce and transfer the vitellogenic steroid hormone 20-hydroxyecdysone to females during mating. *Proc Natl Acad Sci U S A* 105:19631–19636
- Prokupek A, Hoffmann F, Eyun SI, Moriyama E, Zhou M, Harshman L (2008) An evolutionary expressed sequence tag analysis of *Drosophila* spermatheca genes. *Evolution* 62:2936–2947
- Prokupek AM, Kachman SD, Ladunga I, Harshman LG (2009) Transcriptional profiling of the sperm storage organs of *Drosophila melanogaster*. *Insect Mol Biol* 18:465–475
- Prokupek AM, Eyun SI, Ko L, Moriyama EN, Harshman LG (2010) Molecular evolutionary analysis of seminal receptacle sperm storage organ genes of *Drosophila melanogaster*. *J Evol Biol* 23:1386–1398
- Ravi Ram K, Wolfner MF (2007) Sustained post-mating response in *Drosophila melanogaster* requires multiple seminal fluid proteins. *PLoS Genet* 3:2428–2438
- Ravi Ram K, Wolfner MF (2009) A network of interactions among seminal proteins underlies the long-term post-mating response in *Drosophila*. *Proc Natl Acad Sci U S A* 106:15384–15389
- Ravi Ram K, Ji S, Wolfner MF (2005) Fates and targets of male accessory gland proteins in mated female *Drosophila melanogaster*. *Insect Biochem Mol Biol* 35:1059–1071
- Reiff T, Jacobson J, Cognigni P, Antonello Z, Ballesta E, Tan KJ, Yew JY, Dominguez M, Miguel-Aliaga I (2015) Endocrine remodelling of the adult intestine sustains reproduction in *Drosophila*. *eLife* 4:e06930

- Rezaval C, Pavlou HJ, Dornan AJ, Chan YB, Kravitz EA, Goodwin SF (2012) Neural circuitry underlying *Drosophila* female post-mating behavioral responses. *Curr Biol* 22:1155–1165
- Rice WR (1996) Sexually antagonistic male adaptation triggered by experimental arrest of female evolution. *Nature* 381:232–234
- Robertson SA (2007) Seminal fluid signaling in the female reproductive tract: lessons from rodents and pigs. *J Anim Sci* 85:E36–E44
- Robinet CC, Vaughan AG, Knapp JM, Baker BS (2010) Sex and the single cell. II. There is a time and place for sex. *PLoS Biol* 8:e1000365
- Rogers DW, Baldini F, Battaglia F, Panico M, Dell A, Morris HR, Catteruccia F (2009) Transglutaminase-mediated semen coagulation controls sperm storage in the malaria mosquito. *PLoS Biol* 7:e1000272
- Rose MR, Bradley TJ (1998) Evolutionary physiology of the cost of reproduction. *Oikos* 83:443–451
- Rubinstein CD, Wolfner MF (2013) *Drosophila* seminal protein ovulin mediates ovulation through female octopamine neuronal signaling. *Proc Natl Acad Sci U S A* 110:17420–17425
- Rylett CM, Walker MJ, Howell GJ, Shirras AD, Isaac RE (2007) Male accessory glands of *Drosophila melanogaster* make a secreted angiotensin I-converting enzyme (ANCE), suggesting a role for the peptide-processing enzyme in seminal fluid. *J Exp Biol* 210:3601–3606
- Samakovlis C, Kylsten P, Kimbrell DA, Engstrom A, Hultmark D (1991) The andropin gene and its product, a male-specific antibacterial peptide in *Drosophila melanogaster*. *EMBO J* 10:163–169
- Saudan P, Hauck K, Soller M, Choffat Y, Ottiger M, Sporri M, Ding ZB, Hess D, Gehrig PM, Klauser S, Hunziker P, Kubli E (2002) Ductus ejaculatorius peptide 99B (DUP99B), a novel *Drosophila melanogaster* sex-peptide pheromone. *Eur J Biochem* 269:989–997
- Schnakenberg SL, Matias WR, Siegal ML (2011) Sperm-storage defects and live birth in *Drosophila* females lacking spermathecal secretory cells. *PLoS Biol* 9:e1001192
- Schnakenberg SL, Siegal ML, Bloch Qazi MC (2012) Oh, the places they'll go: female sperm storage and sperm precedence in *Drosophila melanogaster*. *Spermatogenesis* 2:224–235
- Schupbach T, Wieschaus E, Nothiger R (1978) Embryonic organization of the genital disk studied in genetic mosaics of *Drosophila melanogaster*. *Roux Arch Dev Biol* 185:249–270
- Schwenke RA, Lazzaro BP, Wolfner MF (2016) Reproduction-immunity trade-offs in insects. *Annu Rev Entomol* 61:239–256
- Short SM, Wolfner MF, Lazzaro BP (2012) Female *Drosophila melanogaster* suffer reduced defense against infection due to seminal fluid components. *J Insect Physiol* 58:1192–1201
- Sitnik JL, Gligorov D, Maeda RK, Karch F, Wolfner MF (2016) The female post-mating response requires genes expressed in the secondary cells of the male accessory gland in *Drosophila melanogaster*. *Genetics* 202:1029–1041
- Soller M, Bownes M, Kubli E (1999) Control of oocyte maturation in sexually mature *Drosophila* females. *Dev Biol* 208:337–351
- Sonnenblick BP (1950) The early embryology of *Drosophila melanogaster*. In: Demerec M (ed) *Biology of Drosophila*. Wiley, New York, pp 62–167
- Stearns SC (2000) Life history evolution: successes, limitations, and prospects. *Naturwissenschaften* 87:476–486
- Suarez SS (2016) Mammalian sperm interactions with the female reproductive tract. *Cell Tissue Res* 363:185–194
- Suarez SS, Wolfner M (2016) Seminal plasma. In: De Jonge C, Barratt C (eds) *The sperm cell: production, maturation, fertilization, regeneration*. Cambridge University Press, Cambridge
- Sun J, Spradling AC (2013) Ovulation in *Drosophila* is controlled by secretory cells of the female reproductive tract. *eLife* 2:e00415
- Swanson WJ, Clark AG, Waldrip-Dail HM, Wolfner MF, Aquadro CF (2001) Evolutionary EST analysis identifies rapidly evolving male reproductive proteins in *Drosophila*. *Proc Natl Acad Sci U S A* 98:7375–7379
- Taniguchi K, Kokuryo A, Imano T, Minami R, Nakagoshi H, Adachi-Yamada T (2014) Isoform-specific functions of Mud/NuMA mediate binucleation of *Drosophila* male accessory gland cells. *BMC Dev Biol* 14:46

- Teclé E, Gagneux P (2015) Sugar-coated sperm: unraveling the functions of the mammalian sperm glycocalyx. *Mol Reprod Dev* 82:635–650
- Tulsiani DR, Orgebin-Crist MC, Skudlarek MD (1998) Role of luminal fluid glycosyltransferases and glycosidases in the modification of rat sperm plasma membrane glycoproteins during epididymal maturation. *J Reprod Fertil* 53:85–97
- Tzou P, Ohresser S, Ferrandon D, Capovilla M, Reichhart JM, Lemaître B, Hoffmann JA, Imler JL (2000) Tissue-specific inducible expression of antimicrobial peptide genes in *Drosophila* surface epithelia. *Immunity* 13:737–748
- Valadi H, Ekström K, Bossios A, Sjöstrand M, Lee JJ, Lotvall JO (2007) Exosome-mediated transfer of mRNAs and microRNAs is a novel mechanism of genetic exchange between cells. *Nat Cell Biol* 9:654–U672
- Viscuso R, Sottile L, Narcisi L (1996) Ultrastructural and histochemical characteristics of the lateral oviducts of *Baculum thairi* Haus (Phasm). *Eur J Morphol* 34:271–283
- Vojtech L, Woo S, Hughes S, Levy C, Ballweber L, Sauteraud RP, Strobl J, Westerberg K, Gottardo R, Tewari M, Hladik F (2014) Exosomes in human semen carry a distinctive repertoire of small non-coding RNAs with potential regulatory functions. *Nucleic Acids Res* 42:7290–7304
- Wagner RM, Woods CW, Hayes JA, Kochansky JP, Hill JC, Fraser BA (1993) Isolation and identification of a novel peptide from the accessory sex gland of the female house fly, *Musca domestica*. *Biochem Biophys Res Commun* 194:1336–1343
- Wagstaff BJ, Begun DJ (2007) Adaptive evolution of recently duplicated accessory gland protein genes in desert *Drosophila*. *Genetics* 177:1023–1030
- Wang LM, Anderson DJ (2010) Identification of an aggression-promoting pheromone and its receptor neurons in *Drosophila*. *Nature* 463:227–U114
- Wang LM, Han XQ, Mehren J, Hiroi M, Billeter JC, Miyamoto T, Amrein H, Levine JD, Anderson DJ (2011) Hierarchical chemosensory regulation of male-male social interactions in *Drosophila*. *Nat Neurosci* 14:757–U392
- Wigby S, Chapman T (2005) Sex peptide causes mating costs in female *Drosophila melanogaster*. *Curr Biol* 15:316–321
- Wira CR, Ghosh M, Smith JM, Shen L, Connor RI, Sundstrom P, Frechette GM, Hill ET, Fahey JV (2011) Epithelial cell secretions from the human female reproductive tract inhibit sexually transmitted pathogens and *Candida albicans* but not lactobacillus. *Mucosal Immunol* 4:335–342
- Wong A, Turchin MC, Wolfner MF, Aquadro CF (2008a) Evidence for positive selection on *Drosophila melanogaster* seminal fluid protease homologs. *Mol Biol Evol* 25:497–506
- Wong A, Albright SN, Giebel JD, Ram KR, Ji SQ, Fiumera AC, Wolfner MF (2008b) A role for Acp29AB, a predicted seminal fluid lectin, in female sperm storage in *Drosophila melanogaster*. *Genetics* 180:921–931
- Xue L, Noll M (2000) *Drosophila* female sexual behavior induced by sterile males showing copulation complementation. *Proc Natl Acad Sci U S A* 97:3272–3275
- Xue L, Noll M (2002) Dual role of the pax gene *paired* in accessory gland development of *Drosophila*. *Development* 129:339–346
- Yamamoto MT, Takemori N (2010) Proteome profiling reveals tissue-specific protein expression in the male reproductive system of *Drosophila melanogaster*. *Fly* 4:36–39
- Yang CH, Belawat P, Hafén E, Jan LY, Jan YN (2008) *Drosophila* egg laying site selection as a system to study simple decision-making processes. *Science* 319:1679–1683
- Yang CH, Rumpf S, Xiang Y, Gordon MD, Song W, Jan LY, Jan YN (2009) Control of the post-mating behavioral switch in *Drosophila* females by internal sensory neurons. *Neuron* 61:519–526
- Yapici N, Kim YJ, Ribeiro C, Dickson BJ (2008) A receptor that mediates the post-mating switch in *Drosophila* reproductive behaviour. *Nature* 451:33–37
- Yew JY, Dreisewerd K, Luftmann H, Muthing J, Pohlentz G, Kravitz EA (2009) A new male sex pheromone and novel cuticular cues for chemical communication in *Drosophila*. *Curr Biol* 19:1245–1254

- York-Andersen AH, Parton RM, Bi CJ, Bromley CL, Davis I, Weil TT (2015) A single and rapid calcium wave at egg activation in *Drosophila*. *Biol Open* 4:553–560
- Zawistowski S, Richmond RC (1985) Experience-mediated courtship reduction and competition for mates by male *Drosophila melanogaster*. *Behav Genet* 15:561–569
- Zitta K, Wertheimer EV, Miranda PV (2006) Sperm N-acetylglucosaminidase is involved in primary binding to the zona pellucida. *Mol Hum Reprod* 12:557–563

Chapter 12

Molecular and Structural Properties of Spider Silk

Taylor Crawford, Caroline Williams, Ryan Hekman, Simone Dyrness, Alisa Arata, and Craig Vierra

Abstract Spider silk has extraordinary mechanical properties, outperforming some of the best-known man-made and natural materials in the world. Over the past 300 million years, spiders have evolved to produce high performance fibers that are uniquely designed to encompass high-tensile strength and toughness. As scientists have pursued a deeper understanding of the biochemical properties of silk, investigators have discovered that spiders are capable of spinning multiple fiber types that exhibit diverse mechanical properties. These differences are largely attributed to unique combinations of silk proteins spun into the fibers and the primary, secondary, and tertiary structure of the silk proteins in the fibers. Because of the outstanding properties of spider silk and its potential to serve as a next generation biomaterial, researchers have been racing to replicate synthetic spider silk. In this book chapter, we summarize the molecular and chemical properties of different silk types in spiders, their biological functions, and mechanisms of silk extrusion, assembly, and post-spin draw. We also discuss strategies that are being implemented for large-scale production of recombinant silk proteins using a variety of heterologous expression systems, explore purification protocols, and review the different spinning methodologies that are being applied for synthetic silk production.

12.1 Introduction

Over the past three decades, the number of reviews, books, and scientific research articles highlighting the material properties of spider silk has been increasing at a rapid rate. More than 45,000 species of spiders (class Arachnida, order Araneae) and a large number of aquatic and terrestrial insects, notably in the order Lepidoptera, have evolved the ability to spin silk. Silks are defined as fibrous material that is extruded into the environment, largely being comprised of proteinaceous

T. Crawford • C. Williams • R. Hekman • S. Dyrness • A. Arata • C. Vierra (✉)
Department of Biological Sciences, University of the Pacific, Stockton, CA 95211, USA
e-mail: taylor.rabara@gmail.com; cwilliams2@pacific.edu; rhekman@pacific.edu;
simmonedyrness@gmail.com; aarata@u.pacific.edu; cvierra@pacific.edu

substances. Perhaps, one of the best-characterized fibers represented is cocoon silk, which is derived from the domesticated silkworm, *Bombyx mori*. Cocoon silks are composed of two core silk proteins along with an outer adhesive protein known as sericin. Scientists can obtain 300–1200 m of usable fiber from a single silkworm cocoon after alkaline and heat treatment to remove the sericin layer. As the development of new biomaterials is becoming a pressing need for humanity, the scientific community has focused on exploring potential uses of natural materials that offer a broad range of diverse mechanical properties. Spider silk has outstanding material properties and certain threads, such as dragline silk, outperform Nylon, Kevlar, and high-tensile steel with respect to strength and toughness (Gosline et al. 1999). Spiders spin a plethora of different silk types with unique mechanical properties, having evolved specialized abdominal biofactories or silk-producing glands to synthesize structural proteins known as fibroins. New methodologies are emerging for large-scale production of recombinant fibroins, processing, and extrusion of fibers via mimicking conditions that resemble natural fiber synthesis, setting the stage for scientists to develop novel biomaterials. Throughout history, spider silk has served as materials for gill and dip nets, fishing lures, and ceremonial dresses. In fact, ancient Australian aborigines and natives of New Guinea have utilized spider silk as fishing lines, head gear, and bags (Lewis 1996). Spider silk has also been used for crosshairs in a number of different optical devices, including microscopes, telescopes and guns due to its small diameters (Lewis 1996; Gerritsen 2002). Additionally, in medieval and Roman times, people have used cob-webs as bandages to wrap wounds and promote wound healing, a property largely due to the unique biochemical characteristics of spider silks (Bon 1710). These properties include biocompatibility, slow degradability, and high tensile strength. More recently, spider silk has been utilized as artificial supports for nerve generation (Allmeling et al. 2006). Although the Chinese have harvested cocoon silk from silkworms for over 5000 years, spider silks are not readily attainable through conventional farming practices. Spiders are cannibalistic in nature, venomous, and “milking” these organisms to collect fibers on large-scale formats is impractical. Because of these barriers, scientists have turned to the utilization of recombinant DNA methodologies to clone spider silk genes for expression in a wide range of different organisms. The black widow spider, *Latrodectus hesperus*, a cob-weaver, is rapidly becoming a model organism of arachnids for the study of spider silk synthesis and extrusion. The long-term goal for scientists is to manufacture large quantities of artificial spider silk fibers for a variety of diverse applications, including medicine, engineering, and defense. In this book chapter, we will explore the diversity of spider silks and fibroins, their natural extrusion process, the systems that have been used for heterologous expression of recombinant spider silk proteins, and synthetic spinning techniques.

12.2 Diversity of Spider Silk

12.2.1 Different Spider Silk Glands

Over 300 million years of natural selection, spiders have evolved different silk-producing glands that have become quite specialized in synthesizing different fibroins or spidroins (a contraction of the words *spider* and *fibroin*). These spidroins can be spun into fibers that exhibit diverse mechanical properties, providing important biological functions that are critical for survival in the environment. Each gland is equipped to produce fibers with specialized functions and the resultant fibers serve important and distinct roles including locomotion (dragline silk), prey wrapping (aciniform silk), protection of eggs (tubuliform and aciniform silks), prey capture (dragline and aggregate glue silk) and web construction (dragline and attachment disc silks; Table 12.1). Based upon ecological and histochemical studies, the primary roles of the silk-producing glands are (1) synthesis of spidroins and glue components; (2) transport of silk proteins out of the cells; (3) production of proteins that prevent spidroin and glue component degradation while stored in the storage component; (4) assembly and extrusion of the materials.

Through microdissections and histological studies, the scientific research community has advanced its knowledge of the morphological features of the silk-producing glands, revealing that these structures have quite distinct physical appearances. Anatomical studies support that black widow spiders contain 7 distinct silk-producing glands, including the major and minor ampullate glands (MA and MI), tubuliform (TB), aciniform (AC), pyriform (PY), flagelliform (FL) and aggregate glands (AG; Fig. 12.1). Each gland has its own tubing or “hose-like” structures that allow the liquid spinning dope to be extruded as materials exit from the spinneret. Thus, an individual spider can extrude multiple silk types simultaneously, allowing the spider to produce a host of different composite materials.

Table 12.1 Different silk-producing glands and biological functions of the extruded fiber types from orb- and cob-weavers

Silk type and biological function	
Silk type	Function
Major ampullate	Locomotion, web frame, scaffolding fibers, gumfoot lines
Minor ampullate	Prey wrapping, temporary spiral capture silk
Flagelliform	Secretion of materials to prevent web degradation, major constituent of capture spiral
Aciniform	Prey wrapping, protection of eggs
Tubuliform	Protection of eggs
Aggregate	Adhesive droplets on gumfoot lines
Pyriform	Fastening dragline silk and joining scaffolding fibers

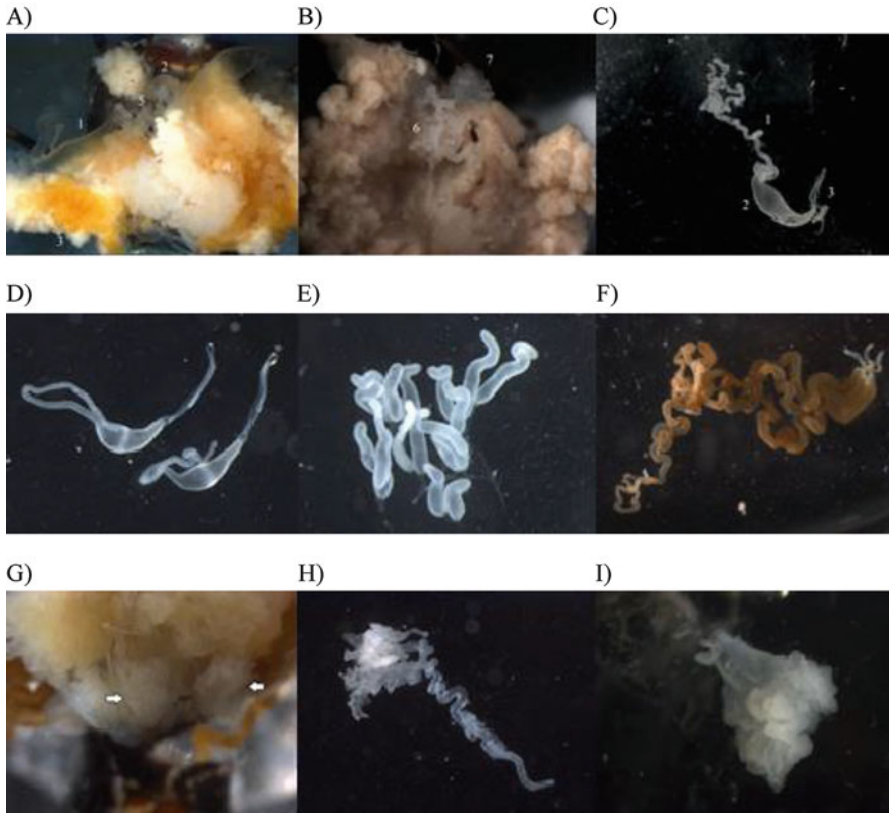


Fig. 12.1 Different silk-producing glands from a female black widow spider after microdissection. (a) Five of the seven silk-producing glands are shown; glands are 1=MA; 2=MI; 3=TB; 4=AG; 5=FL; (b) Two of the seven silk-producing glands; glands are 6=AC; 7=PY; (c) MA gland; (d) MI gland; (e) AC gland; (f) TB gland; (g) PY gland; (h) FL gland; (i) AG gland

12.2.2 Morphological Features of the Silk-Producing Glands

Most research to date has been conducted on the major ampullate (MA) gland, largely because its characteristic ampulla shape and enormous size relative to other silk-producing glands make it easy to identify during dissections. Anatomical studies reveal the MA gland consists of three regions: a tail, ampulla, and spinning duct (Fig. 12.1c). Specialized epithelial cells are found in the tail region, functioning to manufacture and secrete vast quantities of dragline silk proteins. These spidroin proteins are then stored as a spinning dope in the ampulla, a bulb-like structure. The concentration of the spinning dope can approach 30% weight/volume (w/v) in the ampulla. As the liquid is pushed into the spinning duct, which is a long S-shaped structure, it undergoes a phase transition into a solid material.

The minor ampullate (MI) gland resembles the morphology of the major ampullate gland, but it is smaller in appearance (Fig. 12.1a). Both MA and MI glands are whitish in color and found in pairs within an individual spider (Fig. 12.1c–d). Tubuliform glands, which are often pigmented, such as an orangish coloration in *L. hesperus* female species, are present as two sets of three (6 tubules) and are long cylindrical structures (Fig. 12.1f). Aciniform glands resemble small “hot-dog” shaped structures and are found in clusters, also displaying a whitish appearance (Fig. 12.1e). The flagelliform and aggregate glands are often intertwined in the abdomen of the spider, and share somewhat similar morphological features and transparent coloration (Fig. 12.1h–i). Lastly, the pyriform gland, which is pear-shaped and whitish in color, is one of the most difficult glands to remove as an intact structure due to its multiple lobules (Fig. 12.1b, g) (Jeffery et al. 2011). Histochemical analysis reveals that the pyriform gland has two distinct parts called the excretory duct and the secretory sac, which contains two unique secretory cell types (Kovoor and Zylberberg 1980; Kovoor and Zylberberg 1982). Dissection of the pyriform gland followed by isolation of intact RNA has been a challenging task for many labs across the globe. Aside from the major and minor ampullate glands, the other five silk-producing glands have distinct morphological characteristics (Fig. 12.1).

12.2.3 Different Silk Types and Biological Functions

Dragline silk has been extensively studied at the molecular and mechanical level. It is commonly known as a “safety line” for spiders because this fiber type is extruded when they fall from their webs, serving as the principle fiber type for locomotion. Spiders drop from webs by extruding dragline silk, which is cemented to the web by secretion of pyriform silk (Fig. 12.2a). Pyriform silk, which forms attachment discs, is comprised of small diameter fibers that are extruded in an adhesive substance that dries quickly and fastens dragline silk to web fibers, concrete, wood, glass, plant materials, and other abiotic and biotic materials (Blasingame et al. 2009; Geurts et al. 2010a). Black widow spiders also utilize dragline silk for web construction in three different locations: the web frame, scaffolding, and gumfoot lines. Scaffolding fibers constitute the majority of the web and are interconnected in a three-dimensional manner (Fig. 12.2b). Gumfoot lines are threads that run in a vertical fashion. These fibers are attached to the scaffolding of the web and the ground and are coated with glue droplets (Fig. 12.2c). Constituents of the glue droplets are likely derived from the aggregate gland, serving to enhance prey capture (Blackledge et al. 2005).

The precise biological function of minor ampullate silk is unknown in cobweavers. One study, however, has reported crickets being wrapped with MI silk suggesting that it plays a role in prey wrapping similar to aciniform silk (La Mattina et al. 2008). In addition to prey wrapping, aciniform silk appears to be involved in the protection of eggs, being spun and interwoven with tubuliform silk to form egg sacs (Fig. 12.2e) (Hayashi et al. 2004; Hu et al. 2005b; Vasanthavada et al. 2007).

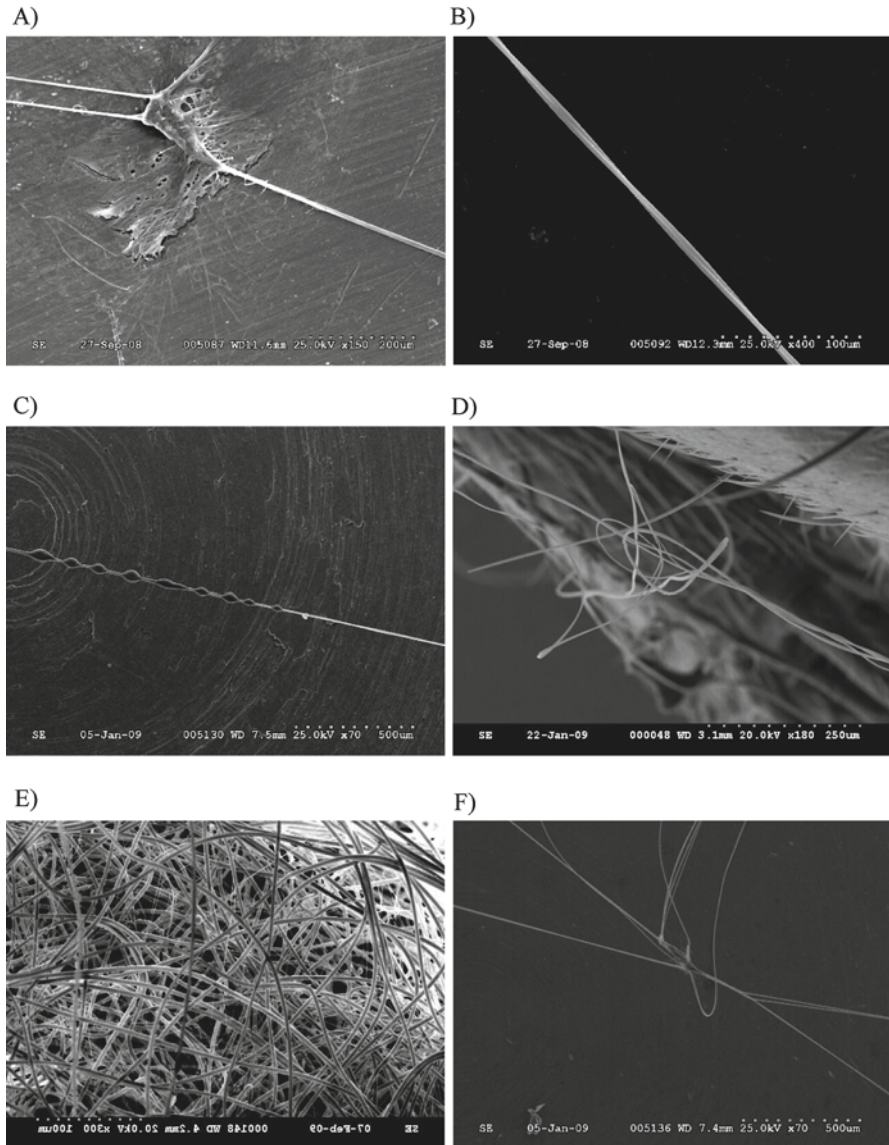


Fig. 12.2 SEM images of different fiber types spun by the black widow spider. (a) Pyriform silk in attachment discs; (b) Scaffolding silk; (c) Glue droplets on a gumfoot thread; (d) Wrapping silk on a cricket; (e) Egg sac (tubuliform and aciniform); and (f) Connection joints

Aciniform fibers have diameter sizes that are approximately 500 nm, while tubuliform threads are an order of magnitude larger, having diameter sizes of 5 μm (Vasanthavada et al. 2007). Egg sacs represent the easiest silk type to collect from female spiders; egg sacs are largely comprised of tubuliform silk (Fig. 12.2e). In orb-weavers, the flagelliform gland has been shown to extrude spiral capture silk.

Since the webs of black widow spiders lack spiral capture threads, this fiber type appears to be absent, raising the question regarding the function of the flagelliform gland in cob-weavers. As data continues to surface, it appears that the flagelliform glands function in black widow spiders to extrude peptides that coat scaffolding fibers, egg cases, attachment discs, and gumfoot lines to function as antimicrobial agents, likely slowing down web degradation in the natural environment.

12.2.4 Genes and Spidroins

In the past few years, full-length gene sequences have been reported for a number of spidroin family members, including the major ampullate spidroins (MaSp1 and MaSp2), minor ampullate spidroin (MiSp), aciniform spidroin (AcSp1), and tubuliform spidroin (TuSp1) (Table 12.2) (Ayoub et al. 2007, 2013, Chen et al. 2012). Partial cDNA sequences coding for pyriform spidroins (PySps) and other proteins identified in the different silk types have been reported as well (Blasingame et al. 2009; Perry et al. 2010). Similar to other structural proteins that are found in nature, the basic spidroin architecture can be summarized as consisting of internal block repeat modules that are flanked by non-repetitive N- and C-terminal domains (NTD and CTD). For example, the central domains of MaSp1 and MaSp2 are composed of approximately 100 tandem copies of internal block repeats that are 25–35 amino acids in length and are flanked by highly conserved non-repetitive N- and C-terminal domains (Table 12.3) (Ayoub et al. 2007). Spidroin family members are distinguished by having differences in their internal block repeat modules. These differences include having variable lengths and different amino acid compositions specific to each spidroin member. The NTD and CTD, which are both approximately 100 amino acids long, are highly conserved at the amino acid level between spidroin family members, suggesting these domains serve important biological functions during the spider silk assembly pathway (Fig. 12.3a–b). The NTD includes a secretion signal that is removed in the processed, secreted spidroin (Fig. 12.3a). NMR studies of recombinant NTD and CTDs expressed and purified from bacteria

Table 12.2 Different silk-producing glands and spidroins and other silk proteins extruded from the glands

Different silk glands and spidroins	
Silk gland	Fiber proteins
Major ampullate	MaSp1, MaSp2, AcSp1, CRPs
Minor ampullate	MiSp1
Flagelliform	SCP-1, SCP-2
Aciniform	AcSp1
Tubuliform	TuSp1, ECP-1, ECP-2
Aggregate	AgSF1, AgSF2, ASG2
Pyriform	PySp1

Table 12.3 Comparison of the ensemble repeats and core units in *L. hesperus* spidroin family members

Silk	Ensemble Repeats	Core Units	Size (aa)
MaSp1	GGAGQGGQGGYGRGGYGGGGAGQGGGAAAAAAAA (Type 1) GGAGQGGQGGYGGQGGYGGGGAGQGGGAAAAAAAA (Type 2) GGAGQGGYGRGGAGQGGGAAAAAAAA (Type 3) GAGQGGYGGQAGQGGGAAAAAAAA (Type 4)	GGX (A) _n ; n = 7	25-35
MaSp2	GGAGPGRQQAYGPPGAGAAAAAAAA (Type 1) GPGPSGYGPGAAGPSGLAGAAAAAAAA (Type 2) GGSPGGYQGPGSGYGPSGPGQQGYGPGGSGAAAAAAAA (Type 3) GGPGYGGQQGYGPPGAGAAAAAAAA (Type 4)	GGX (A) _n ; n = 7 GPGXX QQ	24-41
MiSp1	GAGGYGQGGAGGYGQQGGAGAGAGAGAGA	(GA) _n	23
AcSp1	QLASGIVLGVSTTAPQFGVDLSSINVNLDISNVARNMQASIQGGPAPITA EGPDFGAGYGGAPTDLSGLDMGAPSDGSRGGDATAKLLQALVLPALLK SDVFRAYIKRGRKQVVQYVNTSALQQAASSLGLDASTISLQTKATQ ALSSVSADSDSTAYAKAFGLAIAQVLGTSGQVNDANVNVQIGAKLATGIL RGSSAVAPRLGIDLSGINVDSDIGSVTSLILSGSTLQMTIPAAGDDLSGGY PGGFPAGAQPSGGAPVDFGGPSAGGDVAAKLARSLASTLASSGVFRAA FNSRVSTPVAVQLTDALVQKIASNLGLDYATASKLRKASQAVSKVRMG SDTNAYALAISSALAEVLSSSGKVADANINQIAP	GGX (S) _n (A) _n ; n = 2	376
TuSp1	GVGASPFQYANAVSNFAGQLLGGQGILTQENAAGLASSVSSGSSAAASS VAAQAAASAAQSSAFASQAAAQAFSQAAASRSASQSAQAQSSSTSTTT TTSQAASQAASQSSSSSSAAASQAFSQASSSALASSSSAFSSASSAS AVGQVGYQIGLNAQTLLGISNAPALADAVSQAVRTV	(S) _n (A) _n ; n = 2	184
PySp1	AAAQAQAEARAEAVARAQAQAEARVRAEAAAARAQAQAEAAAARQ AQAEAAAARAQAQAEAAAARAQAQAEAAAARAQAQAEAAAARAQAQAE AARAQSQSEAAAARAQAQAEAAAARAQAQVEAAAARAQAQAEAAAARAQ QAEARAKAEAAVRAQAQVEAAAARAQAQVEAAAARAQAQAEAAAARAQ AQAEARAKAEAAAARAQAQAEARAKAEATARAKAQAEAAAARAQAQAE ARAIAEAAAARAQAQAEARAKAEAAAARAQAQAIARAEAAAARAQAQAEAE RAYAEALARVQAEAAARAQAQTSRTQAVTHSHAHSSASHASSQASSET YAEASTAHTATETHEHTSSHSQTASHSQAAASHSKAKAHTAEDTYSQAQS AAHTI	RAQAQAE (A) _n ; n = 3	376

reveal three-dimensional structures that are similar, having a five-helix bundled structure (Hagn et al. 2010; Parnham et al. 2011). In MaSp1 and MaSp2, the CTD forms a parallel-oriented dimeric five-helix bundle and is stabilized through the formation of an intermolecular disulfide bond between a conserved cysteine residue that resides within helix 4 of the monomer (Hagn et al. 2010). SDS-PAGE analysis of recombinantly expressed proteins in bacteria has shown that dimeric complexes are present under oxidizing (non-reducing) conditions, supporting the importance of the cysteine residue in protein dimerization and spidroin aggregation. Site-directed mutagenesis of the cysteine to a serine within the MaSp1 CTD was also shown to eliminate dimerization and affect fiber formation, further supporting the critical role of the cysteine residue and the assembly process (Fig. 12.3b) (Ittah et al. 2007). The stability of the NTD and CTDs and solubility is regulated by the formation of protons and CO₂ generated by carbonic anhydrase (Andersson et al. 2014).



Fig. 12.3 Alignment of the conserved non-repetitive domains of *L. hesperus* spidroin family members. **(a)** N-terminal domain (NTD); **(b)** C-terminal domain (CTD). Asterisk represent identical residues; single and double dots represent amino acids with similar properties. N-terminal section signals or conserved Cysteine residues are shown in bold text

12.2.5 *Transcriptomic Analysis of the MA Gland and Proteomic Analysis of Dragline Silk*

MA silk is the silk type most thoroughly characterized and studied silk type by the scientific community. During the early 1990s, scientists started to unravel the molecular constituents of MA silk from the golden orb weaver spider, *Nephila clavipes*. By solubilizing MA silk followed by proteolytic digestion, and then sequencing of the peptide fragments using the Edman degradation procedure, investigators were able to obtain MA spider silk gene sequences. These peptide sequences were used to generate DNA probes to screen a cDNA library prepared from MA tissue. This led to the identification of partial cDNA sequences for MaSp1 and MaSp2, the two main protein constituents of MA fibers (Xu and Lewis 1990; Hinman and Lewis 1992). Subsequent studies have led to the retrieval of these full-length genomic DNA sequences and their regulatory sequences from *L. hesperus* (Ayoub et al. 2007). Each gene consists of a single enormous exon (>9000 base pairs), coding for polypeptides that are highly repetitive and masses that exceed 250-kDa. Glycine and alanine residues represent more than 64% of the amino acids in the spider protein sequences (Fig. 12.4a–b). Both glycine and alanine codons are GC-rich, consisting of GGN and GCN triplets, respectively. At the wobble position of the codons there is a biased nature for adenine (A), which likely serves an important role to reduce GC-rich secondary structure in the large MaSp1 and MaSp2 mRNA transcripts, which can exceed 10 kilo-bases.

Chromosome mapping of dragline silk genes using fluorescent *in situ* hybridization has revealed 3 copies of the MaSp1 gene and a single copy of the MaSp2 gene in the spider genome of *L. hesperus* (Zhao et al. 2010). Analysis of the primary sequences of the spider proteins has shown that they are highly modular in their architecture. MaSp1 and MaSp2 contain internal block repeats that consist of poly-alanine domains [poly-(A)/GA] and glycine-rich domains, and in the case of MaSp2, it also contains Gly-Pro-Gly (GPG) motifs. These GPG motifs have been proposed to form type II beta-turns, playing an important role in the extensibility of dragline silk. The internal block repeats are about 24–41 amino acids in length (Table 12.3). Sequence comparisons of MaSps from other species revealed the poly-alanine regions consist of 4–7 alanine residues and the X position is commonly occupied by Q, Y, or L in the GGX segments (Ayoub et al. 2007). The complete genetic blueprints for MaSp1 (one of the three loci) and MaSp2 were published for *L. hesperus* (Ayoub et al. 2007). Similar to *N. clavipes*, these blueprints showed that MaSp1 and MaSp2 also consist of one large exon that translates into a highly repetitive polypeptide. The 5' and 3' ends of the exon code for the non-repetitive conserved N- and C-terminal domains, respectively. MaSp1 was demonstrated to contain four types of ensemble repeat units that can be iterated up to 20 times, with each one consisting of a glycine-rich region followed by a poly-A region (Table 12.3; sizes are 25–35 amino acids). The repetitive region of MaSp2 has also been characterized to consist of four types of ensemble repeat units, but these repeat units show more variability relative to

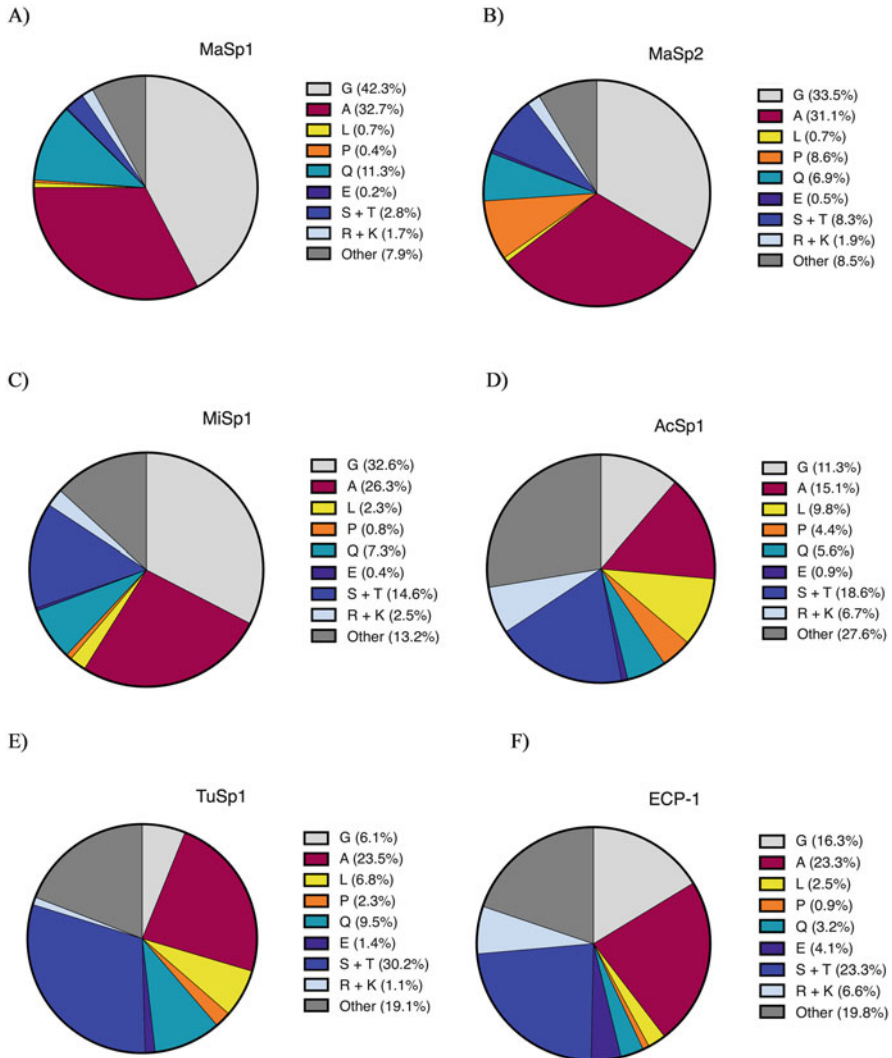


Fig. 12.4 Predicted amino acid composition of spidroins and ECP-1 from *L. hesperus*. (a) MaSp1; (b) MaSp2; (c) MiSp1-like; (d) AcSp1; (e) TuSp1; and (f) ECP-1. Amino acid percentages (e.g. G, A, L etc.) can be read in a *clockwise* fashion

MaSp1 (Table 12.3). In addition, the ensemble repeats for MaSp2 are not always strung together in the same order.

Transcriptome studies from *L. hesperus* have identified 647 silk gland-specific transcripts (SSTs), including mRNAs coding for silk fiber components, as well as proteins involved in oxidation-reduction, protein degradation, and somewhat paradoxically, inhibition of protein degradation (Clarke et al. 2014). Seventy-five percent of the SSTs were not able to be assigned a functional annotation by an

association with a Gene Ontology (GO) term. Twenty-five percent of the GOs assigned to the SSTs reveal enrichments for proteins involved in oxygen-related functions, including oxidoreductases, oxidation-reduction, monooxygenase, iron ion binding, heme binding, and choline dehydrogenase. There were also elevated SST levels for peptidase inhibitors and peptidases. The presence of peptidase inhibitors could serve to protect the spidroins against protein degradation, while the proteases could be used to degrade all non-exported or improperly synthesized spidroins. Included in the transcriptome list were families for aggregate gland silk factor 2 (AgSF2), aggregate spider glue 2 (AgSG2), ECP-1, and glycine-rich proteins that have no well-defined annotation. Potential orthologs of the capture spiral protein, Flag, which has not been discovered in black widow fibers, were also discovered in the multi-tissue transcriptome analysis (Clarke et al. 2014).

Interestingly, in a different study using massively parallel signature sequencing (MPSS) to profile mRNA expression patterns of the MA gland and cephalothorax (fused head-body) of *L. hesperus*, elevated TuSp1 transcripts were unexpectedly detected in the MA gland. However, no studies have shown that the translated products are spun into MA fibers, suggesting that TuSp1 transcripts are subject to negative translational regulation in the MA glandular tissue (Lane et al. 2013). All three MaSp1 loci are transcriptionally active and detailed analysis of the 3' UTRs reveal that these molecules undergo alternative polyadenylation. When comparing MaSp1 loci transcript levels, loci 2 was approximately 4 times more abundant relative to loci 1 and 3, supporting that loci 2 is responsible for the dominant product in female black widow spiders. When quantifying MaSp1 and MaSp2 levels, MPSS studies have revealed 3:1 ratios of MaSp1 to MaSp2, which is consistent with the amino acid composition profiles of dragline silk from *L. hesperus* (Casem et al. 1999; Ayoub et al. 2007). Somewhat surprisingly, among the most highly expressed genes in the MA gland that could be annotated were predictions for fasciclin, elongation factor 1-alpha, and lectin (Lane et al. 2013). In addition, at least two different genes encoding transcription factors were also shown to have elevated expression in the MA gland. One of these products was previously identified and shown to belong to the basic helix-loop-helix (bHLH) family of transcription factors. This factor was dubbed Silk Gland Subset Factor (SGSF) based upon its expression pattern in a subset of the silk-producing glands in cob-weavers (Kohler et al. 2005). Members of this family are known to regulate important processes such as cellular proliferation, differentiation, and neurogenesis. The biological function of SGSF in spiders is currently unknown, but electrophoretic mobility shift assays (EMSA) have shown that SGSF is capable of binding to the consensus sequence CANNTG (N=any nucleotide), also known as an E-box site, when it dimerizes with class I bHLH members, such as Daughterless (Kohler et al. 2005). Because DNA sequence analysis of the MaSp1 and MaSp2 promoter regions reveals the presence of conserved E-boxes, it is intriguing to speculate that SGSF, given its elevated expression pattern in the MA gland, could participate in the transcriptional regulation of the dragline silk genes (Ayoub et al. 2007).

MS/MS studies performed on solubilized dragline silk subject to in-solution tryptic digestion have confirmed the presence of MaSp1 and MaSp2 in the fibers of

L. hesperus. At the same time, these have failed to detect peptides derived from TuSp1 (Pham et al. 2014). Collectively, these studies support the TuSp1 transcript detected by the transcriptome analysis of the MA gland is subjected to translational regulation. During this same analysis, a new family of low molecular weight cysteine-rich proteins (CRPs) were also shown to be major constituents of the fibers (Pham et al. 2014). In addition, a more recent proteomic analysis of the major and minor ampullate glands, along with the tubuliform gland from *L. hesperus* was reported (Chaw et al. 2015). These studies have confirmed the presence of the CRPs in the spinning dope of the MA gland and, somewhat surprisingly, the presence of a previously characterized spidroin from the aciniform gland, AcSp1. At this point in time, it is unclear of the role of AcSp1 in dragline silk which warrants further investigation. Several other proteins were also identified in the MA gland, including aggregate spider glue 2 (AgSG2), alpha-2 macroglobulin (A2M), carboxylic ester hydrolase (CEH), dimethylaniline monooxygenase (FMO3), and a putative triacylglycerol lipase (PTL) (Chaw et al. 2015). Although the precise role of these other constituents is unclear, it would appear they play an important role in the silk assembly pathway.

12.2.6 Minor (MI) Ampullate Silk

In contrast to MA silk proteins, solution state conformational studies using Fourier transform infrared spectroscopy (FTIR) with deuterated-labeled MI silk proteins reveal a significant fraction of α -helical structure and reduced beta-sheet structure (Dicko et al. 2004a). Moreover, solid-state NMR studies performed on MI fibers support that the conformation of alanine residues are more heterogeneous when compared to alanine residues in MA silk, displaying a larger fraction of alanine residues in a non-beta sheet conformation (Liivak et al. 1997). Several research groups have characterized the mechanical behavior and microstructure of orb-weaver MI silk. Despite over 100 million years of divergence, different species show similarities in their mechanical properties of MI silk. Tensile tests demonstrate that MI fibers exhibit similar breaking stress values relative to MA fibers. However, when these fibers are submerged in water, dried, and subjected to mechanical testing, MA and MI fibers behave differently. The plasticizing effect of water on MA fibers is much stronger, showing a three order of magnitude reduction in the initial elastic modulus after exposure to water (Guinea et al. 2012). In this manner, MI silk does not show a supercontraction effect and its behavior in water is more similar to *B. mori* silk. Because MI silk does not exhibit supercontraction when placed in water, it has advantages over MA silk for biomedical applications or processes that cannot tolerate structural changes due to humidity or increased aqueous environments. SEM analyses of fibers collected from *Nephila inaurata* and *Argiope trifasciata* reveal mean diameter sizes of 1.8 μm (Guinea et al. 2012), which is smaller relative to diameter sizes of MA fibers.

By using a multidimensional PCR approach, the full-length gene sequence of MiSp1 from the orb-weaver *Araneus ventricosus* was shown to consist of two exons and a single intron (Chen et al. 2012). The predicted transcript length is 5440 bases, encoding a protein that contains 1766 amino acid residues. Similar to other spideroin family members, the architecture of MiSp1 is organized into non-repetitive N- and C-terminal domains and a predominantly repetitive region composed mainly of glycine and alanine (Fig. 12.4c). *A. ventricosus* MiSp1 contains more sequence and length variation within its internal block repeats (repetitive regions) than *L. hesperus* MaSp1. The repetitive region of MiSp1 is comprised of three distinct regions; these regions are referred to as region I, II, and III. The poly-Ala (A) motif occurs frequently within region I, but it is the most frequent in region III (the longest region), where it appears 8 times. These repetitive regions consist of 4 types of motifs: GX (X=A, Q, I, V, E, S, and D), GGX (X=A, S, V, E, and Y), GGGX and short poly-A repeats. Although the poly-A repeats are longer and more abundant in MaSp1 primary sequences, (GA)_n motifs are more highly represented in MI spideroins. It has been hypothesized that the (GA)_n iterations, similar to poly-A blocks, form beta-sheet structures in the silk (Hayashi et al. 1999). Region I and II, as well as region II and III, are interrupted by two spacer regions that are serine-rich. The spacer regions are predicted to form alpha-helical structures. Kyte and Doolittle hydrophathy profiles predict an alternating profile of hydrophobicity (poly-A motifs) and hydrophilicity (glycine-rich regions) for *A. ventricosus* MiSp1 over its entire sequence (Chen et al. 2012). Somewhat surprising, despite the close evolutionary relationship, the *A. ventricosus* MiSp1 repetitive region is different from sequences reported from translated partial cDNAs from MiSp1 and MiSp2 of *N. clavipes* (Colgin and Lewis 1998). Several other labs have published partial cDNA sequences for MiSps or MiSp1-like molecules, including nucleic acid sequences from cobweaver spiders (Table 12.3) (Gatesey et al. 2001; La Mattina et al. 2008). In orbweavers, MiSp1 is spun into temporary spiral capture silk, whereas in cobweavers, it has been shown to be present within silk collected from wrapped crickets (La Mattina et al. 2008).

Analysis of the N-terminal domain of *A. ventricosus* predicts five alpha helices, which is similar to the solution-state conformation determined by NMR using the NTD of recombinant MaSp1 (Parnham et al. 2011). There are two cysteine residues that reside within helix 1 and 4 of the *A. ventricosus* MiSp1 NTD that are well conserved in the NTDs of TuSp1, CySp1, MaSp2 and MiSp1, suggesting that these residues participate in the formation of an intradisulfide linkage. When analyzing the C-terminal domain of *A. ventricosus*, glycine, alanine, serine and valine represented 64%. In contrast to most other domains, cysteine was absent in the *A. ventricosus* MiSp1 C-terminal domain.

12.2.7 *Aciniform Silk*

Spiders use this silk type for wrapping prey, building sperm webs, producing web decorations, and for constructing egg sacs (Hu et al. 2006b). Thus far, biochemical studies support that aciniform silk consists of a single protein, aciniform spidroin 1 (AcSp1) (Hayashi et al. 2004; Vasanthavada et al. 2007). Full-length and partial cDNAs coding for AcSp1 or AcSp1-like molecules have been reported in the scientific literature. Analysis of the full-length cDNA sequence from *Argiope trifasciata* reveals 14 copies of internal block repeat modules that are highly homogenous. AcSp1 internal block repeats have lengths that are approximately 200 amino acids, which are considerably longer relative to ensemble repeats found within the protein chains of MaSp1 and MaSp2. However, in *L. hesperus* these block repeats are 376 amino acids (Table 12.3). Non-repetitive N- and C-terminal domains are present within the AcSp1 primary sequence. However, using the protein sequence of the AcSp1 CTD, phylogenetic analysis supports it is more evolutionary divergent relative to major and minor ampullate and flagelliform silk proteins (Hayashi et al. 2004). Moreover, translation of the AcSp1 cDNA sequence shows that the amino acid composition is substantially lower in glycine and alanine content relative to the dragline silk fibroins (Fig. 12.4d). Despite the lower levels of glycine and alanine, mechanical testing on aciniform silk reveals these fibers display higher toughness values (ability to absorb more energy per unit volume without failing) relative to major and minor ampullate silk (Hayashi et al. 2004).

Raman spectra of the luminal content from aciniform glands reveal that *N. clavipes* AcSp1 adopts a 50% alpha-helical state in solution, but during extrusion the protein chain undergoes a conformational transition. After extrusion, the secondary structure of AcSp1 displays 24% alpha-helical and 30% beta-sheet structures in the solid fibers (Lefevre et al. 2011). Solution-state NMR spectroscopy has been used to investigate the atomic-level structure of the internal block repeat recombinant AcSp1 from *A. trifasciata*. In these studies, a 199 residue repeat unit (called W_1 ; lacks CTD) was demonstrated to have a well-folded, tightly packed ellipsoidally-shaped helical core in solution from amino acid residues 12–149, flanked by unstructured N- and C-terminal tails (Tremblay et al. 2015). The tightly packed ellipsoidally-shaped helical core consists of a 5-helix bundle structure. This structure was shown to have high thermal stability and can undergo reversible denaturation at 71 °C. Under near-physiological conditions it can also form self-assembled nanoparticles (Xu et al. 2013).

12.2.8 *Tubuliform Silk*

Female spiders manufacture tubuliform silk and use it to construct egg sacs to help protect their offspring during development. It is typically manufactured during the reproductive season. Partial cDNA sequences coding for the main constituent of

tubuliform silk, tubuliform spidroin 1 (TuSp1), have been reported from orb-weavers *Argiope aurantia*, *Araneus gemmoides* and *Nephila clavipes* (Tian and Lewis 2005). In addition, partial cDNAs coding for TuSp1 in the cob-weaver, *L. hesperus*, has been isolated by cDNA library screens (Hu et al. 2005b). Analysis of the primary amino acid sequences of TuSp1 reveals that it lacks common silk modules that are present within major and minor ampullate fibroins (e.g. GGX, GPGXX, poly-A, and spacer regions). Instead, it shows a complex architecture with distinct motifs embedded within 184 ensemble block repeat segments, including S_n , $(SQ)_n$ and GX (X represents Q, N, I, L, A, V, Y, F or D) (Table 12.3) (Hu et al. 2005b; Tian and Lewis 2005). Relative to MaSp1 and MaSp2, TuSp1 has lower amounts of Gly and Ala, but higher levels of Ser and Thr (Fig. 12.4e). Somewhat unexpectedly, the MaSp1 and MaSp2 transcripts have been detected in tubuliform glands of *L. hesperus*, but no MaSp1 or MaSp2 protein constituents have been reported within egg sacs. Full-length cDNA sequences for TuSp1 have been reported for the orthologs CySp1 and CySp2, two silk proteins that are manufactured by the cylindrical (tubuliform) glands of the wasp spider, *Argiope bruennichi* (Zhao et al. 2006). The C-terminal domain of TuSp1 has been shown to have little, if any, similarity to other silk fibroin family members, suggesting this fibroin represents an evolutionarily ancient silk protein that is spun into tubuliform silk (Garb and Hayashi 2005; Tian and Lewis 2006). Cylindrical and tubuliform glands are identical structures, but in the scientific community the terms are often used interchangeably. Despite the absence of poly-A block repeats in the TuSp1 protein architecture, TuSp1 is still capable of adopting nanocrystallite beta-sheet structures in fibers; the motifs AASQAA, AAQAA, and AAQAASAA have been shown to be responsible for beta-sheet formation (Table 12.3) (Tian and Lewis 2006).

Although TuSp1 is a major constituent of tubuliform silk, two other proteins, Egg Case Protein-1 and 2 (ECP-1 and ECP-2), have been identified by MS/MS analysis of peptide fragments derived from egg cases; these molecules were discovered by solubilizing egg sacs from *L. hesperus* with chaotropic agents, followed by in-solution tryptic digestion (Hu et al. 2005a, 2006a). Similar to MaSp1 and MaSp2, the ECPs contain large amounts of Gly and Ala (Fig. 12.4f). ECP-1 and ECP-2 lack well-defined internal block repeat modules as well as the conserved, non-repetitive NTD and CTDs that are hallmark features of traditional spidroin family members. Additionally, these proteins have lower molecular weights relative to spidroins, with predicted masses of approximately 80-kDa instead of >200-kDa masses that are commonly reported for spidroins. ECP-1 and ECP-2 have highly conserved N-termini, sharing 16 Cys residues found within the first 153 amino acids (Hu et al. 2006a). These N-termini are markedly divergent from the NTD of other spidroin family members. Using recombinant ECP-2 proteins purified from bacteria, synthetic silk fibers were produced by wet-spinning methodologies, supporting these molecules have properties that are fibroin-like. These fibers show comparable mechanical properties relative to synthetic silk fibers produced from recombinant MaSp1 molecules (Gnesa et al. 2012).

12.2.9 Pyriform Silk

Pyriform silk was the last fiber type to be characterized at the biochemical level. This fiber type, which is also referred to as piriform silk, is spun from a pear-shaped structure located in the abdomen that exits a short duct opening into a nozzle-like spigot (Kovoor and Zylberberg 1982). Numerous spigots on the spinneret serve to extrude fibers that form a mesh-like structure (Wolff et al. 2015). Pyriform silk serves to fasten dragline fibers to surfaces with a minimum of material consumption, providing a function that is central to spider locomotion. Pyriform silk is secreted into a liquid material that polymerizes rapidly (less than a second) under ambient conditions, forming a structure referred to as an attachment disc. Attachment discs are highly stable structures, capable of surviving in the natural environment for years. Similar to other spider silk types, these structures are biodegradable, biocompatible, and extremely versatile. SEM and biochemical analyses of attachment discs show these structures are coated with a glue-like cement containing nanofibrils enclosed in a presumptive lipid-based material which creates a meshwork organization that facilitates stress distribution and crack arrestment when placed under a load (Geurts et al. 2010b; Wolff et al. 2015). The macroscopic structure of attachment discs is the product of a highly conserved behavioral program that involves precise movement of the abdomen, which generates countless parallel loops of crossing silk threads (Eberhard 2010). It has been reported that an attachment disc from a golden orb-weaver, *Nephila senegalensis*, can hold 4–6 times its body weight when fixed to a glass surface (Wolff et al. 2015). Given the unique design of these biomaterials, the elucidation of the intrinsic composite structure of attachment discs from different spider species has tremendous value for the development and engineering of new nanocomposites that are light-weight in nature.

The proteins that comprise pyriform silk were first reported from the cob-weaver, *L. hesperus* (Blasingame et al. 2009). The major protein constituent was named pyriform spidroin 1 (PySp1) (Blasingame et al. 2009). Shortly following the identification of PySp1 from cob-weavers, a protein with similar biological function was identified from orb-weavers – this molecule was dubbed pyriform spidroin 2 (PySp2) or PiSp1 (Geurts et al. 2010b; Perry et al. 2010). To date, no full-length gene sequences have been published for pyriform spidroins (*PySps*=*PySp1* and *PySp2*), only partial cDNAs are available in the public DNA databases. Translation of the *PySp* cDNAs reveal conventional internal block repeats that are 376 amino acids and a non-repetitive C-terminal domain (Table 12.3). Theoretical amino acid composition analyses of the translated cDNAs, demonstrate these spidroin family members contain the highest quantity of hydrophilic residue content relative to other family members. The high content of polar and charged amino acids likely functions to provide strong interactions between the secretion film and substrate. Undoubtedly, these polar and charged residues within the primary sequences of *PySps* enhance water-solubility, but also likely serve to direct self-assembly of the fibers. Analysis of the protein sequence of *PySp2* demonstrates that the internal

block repeat element has two components: one is classified as a SGA-rich element and the other is proline-rich (P-rich) (Geurts et al. 2010a).

12.2.10 *Flagelliform Silk*

The major constituent of capture spiral silk in orb-weavers is referred to as the flagelliform (Flag) protein. Capture spiral silk plays a central role to entrap flying prey, serving as an aerial net. Flagelliform fibers are coated with glue material that is extruded from the aggregate gland, a process that facilitates prey capture (Choresch et al. 2009). The aqueous glue provides hydration, which aids in the extensibility of the fibers (Vollrath and Edmonds 1989). From a mechanical perspective the capture spiral represents one of the most elastic materials known and is capable of effectively dissipating the kinetic energy delivered by a prey strike during a collision of an aerial insect. To elucidate how the extensibility of capture silk is related to secondary structure in Flag proteins, translated Flag cDNA sequences have been examined for specific patterns embedded within its protein sequence. Interestingly, Flag proteins are characterized as lacking poly-A motifs, which is a prominent module that contributes to the high tensile strength of MA silk. Despite the absence of poly-A modules, the motifs in the core of the Flag protein sequence include: (1) GPGGX; (2) GGX; and (3) spacer regions (Hayashi and Lewis 1998). In some instances, 63 copies of GPGGX motifs can be found in tandem repeats within the primary sequence of Flag. Iterations of this sequence were proposed to form a β -spiral structure that functions like a nanospring, contributing, in part, to the elastic nature of flagelliform silk. Thus, the molecular mechanism of elasticity is governed by iterations of the GPGGX motifs that form a series of type II β -turns that are linked together in the polypeptide chain. Insight into the biological function of GGX motifs has come from stress-strain studies performed with synthetic fibers spun from purified recombinant proteins. Synthetic fibers spun from recombinant proteins engineered to carry different Flag modules support the GGX motif contributes to extensibility, whereas the spacer region plays a role in the strength of the recombinant fibers (Adrianos et al. 2013).

The role of the flagelliform gland in cob-weavers is controversial, but it appears to have evolved a different ecological function relative to orb-weavers. In the three-dimensional architecture of cob-webs, capture spiral threads are completely absent. Two peptides that are extruded from the flagelliform gland of *L. hesperus* were identified and characterized at the biochemical level. These products were named spider coating peptide 1 and 2 (SCP-1 and SCP-2) (Hu et al. 2007). SCP-1 was shown to have intrinsic metal-binding activity and can be purified from crude protein lysates prepared from flagelliform glands using nickel metal-ion chromatography (unpublished data). Proteomic analyses performed with materials collected from different silk types have revealed the presence of SCPs within attachment discs, egg sacs, scaffolding fibers and gumfoot lines (Hu et al. 2007). Data is emerging to support that SCPs function as anti-microbial agents, helping to protect the

web from degradation. Consistent with this hypothesis is the observation that many microbes require metal ions for survival and proliferation. The ability of SCP-1 to sequester metal ions could attenuate microbial growth and slow web degradation. Collectively, the evolution of compounds that prevent web degradation is consistent with the observation that cob-weavers cast webs and leave them in the environment for prolonged periods of time.

12.2.11 Aggregate (Glue) Silk

Biological adhesives, such as glues, are used by a wide-range of different organisms in the world. Spiders also coat fibers with glue-like substances. In orb-weavers, two glycoproteins were identified in the aqueous glue-like substance that forms the droplets coated on flagelliform silk in *N. clavipes* (Choresh et al. 2009). These proteins have been reported to have unique 110 amino acid repetitive domains that are encoded by opposite strands of the same DNA sequence, but this has not been substantiated by genomic DNA sequencing. Other constituents were discovered in the aqueous solution, revealing its complex chemical composition. In addition to the two glycoproteins, ASG1 and ASG2 (predicted molecular masses are 38- and 65-kDa, respectively), high concentrations of water-soluble organic materials that include free amino acids, small peptides, neurotransmitter-related molecules, as well as low concentrations of inorganic salts were shown to be extruded into the droplets (Vollrath et al. 1990; Tillinghast et al. 1991; Townley et al. 2012). Since cob-weavers lack capture spiral silk, the question arises whether these species produce glue droplets for their webs. Analysis of the three-dimensional webs of *L. hesperus* has revealed the presence of glue droplets at the base of gumfoot lines, which are vertical lines that function as a spring-loaded trap that pulls walking insects into the web (Fig. 12.2c) (Argintean et al. 2006). The adhesion of the droplets serves to immobilize the prey, facilitating the capture of prey. Chemical analyses demonstrate that glue droplets on gumfoot lines from *L. hesperus* are composed of hygroscopic organic salts and glycoproteins, similar to viscid silks (Jain et al. 2015). Although the underlying assumption is that the aggregate gland is responsible for the secretion of this material, a direct linkage of the substances manufactured by the aggregate gland and their extrusion into these droplets remains to be established.

In cob-weavers the aggregate gland was shown to extrude molecules that are constituents of connection joints (Vasanthavada et al. 2012). Connection joints are structures that interconnect more than one fiber (Fig. 12.2f). These structures serve as a structural hub to join scaffolding threads together in the web; these hubs also function to interlock wrapping silk during prey capture. MS/MS analysis of solubilized connection joints led to the discovery of two proteins dubbed aggregate gland silk factor 1 (AgSF1) and aggregate gland silk factor 2 (AgSF2). Western blot anal-

yses also further confirmed the co-localization of the AgSFs to connection joints (Vasanthavada et al. 2012). Inspection of the primary sequences of AgSF1 and AgSF2 reveals different protein architectures compared to traditional spidroin family members. Interestingly, AgSF1 has iterations of the pentameric QPGSF motif, which is an element similar to mammalian elastin. In the case of AgSF2, it has repetitive elements that have the consensus sequence NVNVN. These sequences are embedded in a glycine-rich matrix. More extensive biochemical studies will need to be performed to elucidate the precise interactions and functions of AgSF1 and AgSF2 in the connection joints.

12.3 Natural Silk Extrusion Pathway

12.3.1 Fiber Extrusion from the MA Gland

Our understanding of spider silk synthesis, fiber assembly, and the extrusion pathway has been largely derived from studies of the MA gland of the genus *Nephila*. In the abdomen of *N. clavipes*, which has bilateral symmetry typical of orb- and cob-weavers, there are two MA glands that are dedicated for dragline silk production. MA glands have been characterized as having four different zones: the tail region (responsible for synthesis and secretion of the spidroins), the lumen (storage of spidroins), the spinning duct (responsible for the alignment of silk proteins), and the spigot (the nozzle that controls fiber extrusion) (Vollrath and Knight 2001).

The ampulla of the MA gland represents a storage vessel for soluble silk proteins that are manufactured in specialized columnar epithelial cells that reside in the tail region. Using the secretion signal on the N-terminal region of the spidroins, these epithelial cells secrete the spidroins into the lumen. The spidroins are stored in the lumen in a highly concentrated liquid crystalline solution that can approach 30–50 % (w/v) or 300–500 g/L (Vollrath and Knight 2001). Histological studies describe the tail region and ampulla as having two zones, which are named the A-zone and B-zone. Zone A contains a highly elongated and diverging region that consists of tall columnar secretory cells, while zone B represents a converging region characterized by more osmiophilic granules and higher peroxidase concentration (Vollrath and Knight 1999). Following the ampulla is the spinning duct (S-shaped) which has been described as having three limbs (limbs 1, 2 and 3). During the natural spinning process, the spidroins move from the tail region through the spinning duct, where these molecules experience biochemical and physical environmental changes. These changes are accompanied by a liquid-liquid phase separation that is followed by a liquid-solid phase transition that leads to the production of a preliminary silk fiber that further experiences some evaporation of water during the drawdown process of the last limb (limb 3).

12.3.2 Models of Spider Silk Extrusion

The natural spider silk assembly pathway has been described by two different models - the liquid crystalline and micelle-coalescence based theories (Vollrath and Knight 2001; Jin and Kaplan 2003). In the liquid-crystalline theory, the newly synthesized proteins, which are unfolded and rod-shaped, adopt a nematic (thread-like) liquid-crystalline phase. In this phase, the spidroin protein chains are packed in a parallel fashion to each other, but they are perpendicular to the long axis of the tall columnar secretory cells (Vollrath and Knight 2001). As the dope moves through the ampulla, the long axis flips until the packaged structures become parallel with the lining of the epithelial walls. This nematic orientation is maintained until reaching the second limb (limb 2) of the spinning duct, where they are organized into bilayered disks. As the elongational flow and shear forces accelerate in the third limb (limb 3), it leads to the elongation and alignment of the disc-like structures (Vollrath and Knight 1999). During this step, the protein chains undergo a conformational change, transitioning from random coil and polyproline-II helix-like structures to protein folds that have large β -sheet content. Spidroin conformational transitions have also been proposed to be associated with pH changes that occur between the ampulla and spinning duct. The pH was shown to drop from 7.2 to 6.3, triggering spidroins to undergo conformational changes that promote fiber assembly (Dicko et al. 2004b). This conformational change has been proposed to result from the neutralization of a conserved Asp (D) in the NTD of MaSp1, which functions as a pH sensor to control protein assembly (Gaines et al. 2010). Through the combined actions of the chemical and physical events, the spinning dope becomes gelatinous in the distal part of the spinning duct, resulting in increased viscosity. Lastly, in the third limb, the epithelial cells with apical microvilli function to reabsorb water molecules, helping to produce the final fiber product.

In contrast to the liquid-crystalline theory, the micelle theory was largely conceived from the observation that fractured natural silk fibers contain globular structures within their internal core. In order to build a model consistent with the presence of the globular structures and to add clarity to the silk assembly mechanism, synthetic fibers were generated *in vitro* utilizing aqueous solutions of reconstituted silkworm silk fibroins as a spinning dope (Jin and Kaplan 2003). This model of silk assembly proposes that spidroin sequences are amphiphilic in nature. The spidroin molecules contain short alternating hydrophobic and hydrophilic amino acid stretches that are flanked by larger hydrophilic terminal regions that make the proteins surfactant-like, allowing the protein chains to form micelles within the spinning dope material. In these *in vitro* studies, it was shown that by increasing the concentrations of the spidroins, the micelles could coalesce into larger globular structures (Jin and Kaplan 2003). Furthermore, during extrusion, it was proposed that the elongational flow and shear force placed on the liquid due to the ductal wall results in elongation of the globular structures, giving rise to fibrillar morphologies that represent the precursor of the spider silk fiber (van Beek et al. 2002).

For both theories, the proteins passing through the spinning duct experience remarkable changes in the environment of the solvent, resulting in salting-out effects that are associated with the formation of the silk structure. Potassium and phosphate ion concentrations both increase, while there is a decrease in sodium and chloride ion concentration, removal of water, and slight drop in the hydrogen ion concentration (Vollrath et al. 1998; Vollrath and Knight 1999; Knight and Vollrath 2001; Rammensee et al. 2008). Through the eloquent usage of these different chemical and physical processes during extrusion, spiders are capable of spinning a wide-range of diverse threads that are classified as high performance materials. Natural MA silk is renowned for its outstanding material properties. Relative to the tensile strength of steel, the breaking stress of MA silk is comparable, but it is considerably more extensible, leading to a material that is 30 times tougher than steel (Table 12.4) (Gosline et al. 1999). MA silk is also three times tougher than Kevlar, a synthetic fiber that is manufactured in vast quantities by many militaries across the globe during the production of body armor (Table 12.4). In the case of dragline silk, these threads have been shown to have breaking stress and strain values that are approximately 1 GPa and 31 % (Table 12.4) (Hu et al. 2006b). Furthermore, stress-strain curve analyses of different spider silk types reveal a diverse range of mechanical properties that perform well relative to bone, elastin, and carbon fiber (Table 12.4). In the scientific literature, different species of spiders have shown variability with respect to the mechanical properties of their MA silk. Biophysical studies have revealed that MA silk contains a hierarchical architecture where highly organized, hydrogen-bonded β -sheet nanocrystals from the poly-A blocks are arranged within a semiamorphous matrix that consists of 3_1 -helices and β -turn structures (Kummerlen et al. 1996; van Beek et al. 2002; Lefevre et al. 2007).

Table 12.4 Mechanical properties of spider silk fibers and other man-made and natural materials

Mechanical properties of different materials			
Fiber	Tensile strength (MPa)	Toughness (MJ/m ³)	Extensibility (%)
<i>Araneus</i> dragline	1100	160	27
<i>Latrodectus</i> dragline	996	nd	31.1
<i>Latrodectus</i> Minor ampullate	346	nd	30
<i>Latrodectus</i> Tubuliform	629	nd	71.7
<i>Latrodectus</i> Aciniform	700	290	80
<i>Araneus</i> Flagelliform	500	nd	270
Nylon fiber	950	80	18
Kevlar 49 fiber	3600	50	2.7
High-tensile steel	1500	6	0.8
Bone	160	4	3
Elastin	2	2	150
Carbon fiber	4000	25	1.3

nd no data for sample

12.4 Expression Systems for Recombinant Silk Production

12.4.1 Isolation of Spider Silk Genes

Although the Chinese have been harvesting cocoons from silkworms for thousands of years, farming spiders for large-scale fiber collection is impractical for a variety of reasons. Firstly, spiders are cannibalistic, territorial and venomous – all properties that make them undesirable for domestication. Secondly, the process of “milking” spiders is more challenging and arduous relative to milking cows, making this collection procedure unrealistic, too time consuming, and economically unfeasible. To circumvent the inability to domesticate and farm spiders, researchers have focused on the biotechnological production of recombinant spider silk proteins as alternative strategies. Since silk is largely composed of protein, molecular biologists and protein chemists have embarked on the development of various gene cloning strategies and heterologous expression systems to manufacture enormous amounts of recombinant silk proteins. Because manufacturing spider silk materials requires vast quantities of recombinant spider silk protein for the spinning process, new creative methods to replicate and express spider silk genes in other organisms are being pursued by many companies and research labs across the globe.

For investigators to produce recombinant silk proteins in other organisms, nucleic acid sequences coding for the spidroin family members must be isolated by molecular biological approaches, or alternatively, synthetic pieces of nucleic acids must be designed and assembled into DNA constructs. When the first members of the spidroin family were discovered, labs focused on retrieving spider gene sequences by screening cDNA libraries prepared from silk-producing glands of orb- or cob-weavers by conventional nucleic acid-nucleic acid hybridization (Hinman and Lewis 1992; Guerette et al. 1996; Hayashi and Lewis 2000). Although these library screens were successful, a limitation of the screens was that most of the clones retrieved represented partial cDNA sequences. Moreover, due to the construction of the libraries, most of the partial cDNAs lacked the NTD of the spidroin family members (Gatesey et al. 2001). Despite the availability of other methodologies to clone genes, such as polymerase chain reaction (PCR), the utilization of these techniques was further limited and hampered by the intrinsic properties found within the gene sequences of spidroin family members, which included the presence of repetitive block repeats, their high GC content (Gly and Ala codons), and their incredibly long lengths (>9 kb) (Xu and Lewis 1990; Hinman and Lewis 1992). Collectively, these chemical properties have challenged the reliability and robust nature of PCR to amplify repetitive modules in the fibroin family members as a single intact product. This has forced investigators to screen libraries by conventional methodologies to retrieve cDNAs that have suitable lengths for expression studies. However, as investigators have isolated longer cDNAs from conventional library screens, challenges have surfaced involving basic cloning manipulations of these genes when placed into prokaryotic or eukaryotic backgrounds, including fundamental processes, such as DNA replication and translation. With technology advancing rapidly and the

decreasing costs associated with oligonucleotide synthesis, many research groups and companies are pursuing the synthesis of codon-optimized pieces of single-stranded DNA molecules. These molecules can be annealed and multimerized by seamless cloning strategies to produce artificial spider silk genes that closely resemble natural cDNA sequences (Rabotyagova et al. 2009; Teule et al. 2009).

12.4.2 Expression Systems of MA Recombinant Proteins

Expression studies of recombinant spidroins in prokaryotic and eukaryotic systems have explored a variety of different strategies and approaches, including the utilization of natural spider silk cDNAs, the design of synthetic spider silk genes that are codon-optimized for expression, the implementation of spider gene sequences that are a combination of synthetic and natural cDNA sequences, and the incorporation of cysteine codons into block repeat modules to facilitate disulfide bond formation and crosslinking of recombinant silk protein chains (Table 12.5) (Prince et al. 1995; Grip et al. 2009; Teule et al. 2009). The majority of the expression studies have investigated the production of recombinant silk proteins that represent dragline silk constituents using bacterial expression systems (Table 12.5). In these reports, investigators have induced and purified MaSp1 and MaSp2 molecules, but a large number of these proteins have been truncated recombinant silk proteins. These truncated spidroins have molecular weights that range from 10 to 163-kDa, which is much smaller in mass relative to the native sized spidroin. Additionally, these studies have predominantly centered on the expression of internal block repeat regions, ignoring the incorporation of the highly conserved non-repetitive NTD and CTDs into the recombinant silk proteins. Thus, the synthesis of native-sized spidroins in expression systems has been a challenging barrier to overcome, forcing most investigators to synthesize truncated versions of the silk proteins. One strategy that has led to the production of recombinant silk proteins that approach native-sized spidroins has been achieved using synthetic genes that were expressed in a metabolically engineered strain of *Escherichia coli* designed to manufacture elevated levels of the glycyl-tRNA pool (Xia et al. 2010).

Because amplification of spider silk genes by PCR is difficult due to the repetitive nature of the internal block repeats, new cloning strategies have emerged to synthesize artificial DNA modules. Artificial DNA modules have been constructed from short oligonucleotide repeats that are codon-optimized for high level expression. Multimerization of the oligonucleotide repeats has allowed for fine control over the recombinant protein size. Expression of truncated spidroins, specifically MaSps, has been performed in a variety of different heterologous expression systems, including plants (tobacco and potatoes), yeast (*Pichia pastoris*), and bacteria (*E. coli* and *Salmonella*) (Prince et al. 1995; Lewis et al. 1996; Fahnestock and Bedzyk 1997; Fahnestock and Irwin 1997; Arcidiacono et al. 1998; Fukushima 1998; Winkler et al. 1999; Scheller et al. 2001; Lazaris et al. 2002; Xia et al. 2010). Synthetic genes coding for recombinant proteins ranging from 15 to 250-kDa have

Table 12.5 Different expression systems, types of spidroin genes expressed, predicted molecular mass, and amount of recombinant protein yielded after purification

Group	Gene	Protein	Expression system	Size (kDa)	(mg/L) ^b
<i>Bacteria</i>					
Prince et al. (1995)	Synthetic	MaSp1	<i>E. coli</i> SG13009pREP4	14–41	15
	Synthetic	MaSp2			
Lewis et al. (1996)	Synthetic	MaSp2	<i>E. coli</i> BL21 (DE3)	31/58/112	5
Fahnestock and Irwin (1997)	Synthetic	MaSp1	<i>E. coli</i> BL21 (DE3)	65–163	300 ^c
	Synthetic	MaSp2			
Fahnestock and Bedzyk (1997)	Synthetic	MaSp1	<i>P. pastoris</i> YFP5029	65–163	1000 ^c
Arcidiacono et al. (1998)	cDNA	MaSp1	<i>E. coli</i> BL21 (DE3)	43	4
Fukushima (1998)	Synthetic	MaSp1	<i>E. coli</i> JM109	10–20	5
Winkler et al. (2000)	Synthetic	MaSp1	<i>E. coli</i> BLR (DE3)	25	20
Szela et al. (2000)	Synthetic	MaSp1	<i>E. coli</i> BLR (DE3)	25	10
Xia et al. (2010)	Synthetic	MaSp1	<i>E. coli</i> BL21 (DE3) ^a	100–285	500–2700
Lin et al. (2013)	Synthetic	TuSp1 + CTD	<i>E. coli</i> BL21 (DE3)	189	40
Xu et al. (2012)	Synthetic	AcSp1	<i>E. coli</i> BL21 (DE3)	19–76	22–80
<i>Yeast</i>					
Fahnestock and Bedzyk (1997)	Synthetic	MaSp1	<i>P. pastoris</i> YFP5029	65–163	1000 ^c
<i>Mammalian cells</i>					
Lazaris et al. (2002)	cDNA	MaSp1 MaSp3	Baby hamster kidney	63–140	25–50
<i>Plants</i>					
Scheller et al. (2001)	Synthetic	MaSp1	Tobacco (<i>Nicotiana</i> sp.) Potato (<i>Solanum</i> sp.)	100	0.1 g/5 g leaf
Hauptmann et al. (2013)	Synthetic	FLAG	Tobacco (<i>Nicotiana</i> sp.)	47–250	1.8 mg/50 g leaf

Ibr internal block repeat

^aGenetically modified

^bPurity >90 %

^cProtein titer before purification

been reported for expression studies (Table 12.5). Unfortunately, the expression levels for the synthetic genes have been low, with the majority of the cases of the recombinant protein only representing 5% of the total cellular protein. One of the most robust production levels have approached 1000 mg for 1 L of saturated *Pichia pastoris* cultures (Fahnestock and Bedzyk 1997). However, for most prokaryotic expression systems, the typical protein yields have been in the range of 10–50 mg/L after purification (>90% purity) (Table 12.5).

Microorganisms have been the preferred choice as hosts for heterologous protein expression systems for spider silk proteins. Utilization of *E. coli* as a host system offers many benefits, including its fast replication time and low cost associated with culturing vast quantities of cells. Because *E. coli* has been heavily used by molecular biologists for cloning purposes, it also provides some of the best genetic tools available for regulating protein induction, methods for rapid purification of proteins, and techniques to circumvent recombinant proteins that display toxic effects when expressed in a prokaryotic background. Using *E. coli*, growth conditions can also be easily translated into an industrial scale format. The pharmaceutical industry has successfully used this system for large-scale protein production for numerous recombinant proteins for medicinal applications. Although chemists have developed strategies to form polymers from organic materials, it has been challenging to control the polymerization process using different building blocks, especially when attempting to design complex polymeric compounds with new biological functions. However, through the use of recombinant DNA approaches, scientists can more readily control the assembly of different DNA pieces to create protein polymers with programmed sequences, secondary structures, molecular weights and even enhance recombinant protein solubilities. In this process, scientists follow three basic steps: (i) design and assembly of synthetic silk-like segments, (ii) selection of a prokaryotic expression vector, followed by insertion and multimerization of synthetic silk-like DNA segments, and (iii) transformation, expression and purification of recombinant silk proteins from different bacterial clones. In some cases, the initial step (i) can be substituted by using different lengths of the natural spider silk cDNA sequences. Or, alternatively, a combination of synthetic silk-like genes can be coupled with pieces of the natural spider silk cDNAs.

12.4.3 *Seamless Cloning Strategy to Produce Synthetic Spider Silk Genes*

We have employed a seamless cloning strategy with oligonucleotides that were codon-optimized for expression of *L. hesperus* MaSp1 block repeats in *E. coli* (Scior et al. 2011). Because the block repeat of MaSp1 is 25–35 amino acids, it would typically require the synthesis and annealing of two complementary oligonucleotides with lengths of approximately 120 nucleotides. However, because the upper limit on the synthesis of oligonucleotides is around 100 nucleotides, we

constructed the MaSp1 block repeat segment using two steps. First, two oligonucleotides were designed to span the 40 amino acids block repeat of MaSp1. For this design, we created two oligonucleotides that were perfectly complementary at their 3' ends, but had singled-stranded 5' ends that could be filled in by a heat-stable DNA polymerase after annealing to make double-stranded molecules (Fig. 12.5a). Once the synthetic block module for MaSp1 was generated, it was amplified with gene-specific primers and three different restriction sites were added to the ends of the internal block repeat (Fig. 12.5a). The forward primer was engineered to add the restriction sites *ScaI*, *NdeI*, and *BsaI*. The incorporation of the *ScaI* site provided extra nucleotides on one end of the synthetic MaSp1 module to facilitate restriction digestion efficiency, while *NdeI* and *BsaI* sites served to simplify insertion and seamless cloning in the prokaryotic expression vector pET-24a, respectively. The reverse primer was designed to add *SpeI*, *SacI*, and *BsmBI* restriction sites, with *BsmBI* and *SacI* being used for seamless cloning and *SacI* also functioning to ligate the monomer MaSp1 internal block repeat into pET-24a. After insertion of the monomeric MaSp1 repeat (MaSp1 1X) into the *NdeI* and *SacI* site of pET-24a to create pET-24a MaSp1 1X, this vector was used for expansion of the monomeric unit into dimeric (MaSp1 2X), tetrameric (MaSp1 4X), etc. repeats. For this to be accomplished the pET-24a MaSp1 1X vector was digested with *BsaI* and *SacI* to release the monomeric block repeat and ligated into the pET-24a MaSp1 1X plasmid after it was doubly digested with *BsmBI* and *ScaI* (Fig. 12.5b). This allows for the multimerization of the MaSp1 1X block repeat without the creation of internal restriction sites during the doubling process, which would normally introduce two codons at the fusion junction specifying two amino acids (6-bp restriction site) that were not naturally found within the MaSp1 protein chain. Several rounds of cloning can be used to expand the repetitive block repeats to obtain sizes that approach the protein masses of native sized MaSp1 from spiders. After the conclusion of the block repeat expansion, amplification and insertion of natural cDNAs coding for the NTD and CTD can be readily inserted into the pET-24a vector *e.g.* pET-24a MaSp1 8X to form vectors that code for minifibroins or fibroins that approach the properties of native fibroins. This system also allows for the integration of adding 6 consecutive histidine residues (6x His tag) to the C-terminal region of the recombinant protein. The synthetic or hybrid silk genes inserted into the pET-24a vector are placed under the transcriptional control of the T7 promoter and require the addition of the inducer isopropyl- β -D-1-thiogalactopyranoside to initiate protein expression. However, it is worth noting that even with implementation of these creative strategies, there are still current barriers and challenges, largely due to the highly repetitive core sequences of the synthetic gene. This results in undesired homologous recombination of block repeats during replication in bacteria, transcriptional errors, unwanted translational pausing, and accumulation of vast quantities of recombinant proteins in inclusion bodies – all leading to lower yields of recombinant silk proteins.

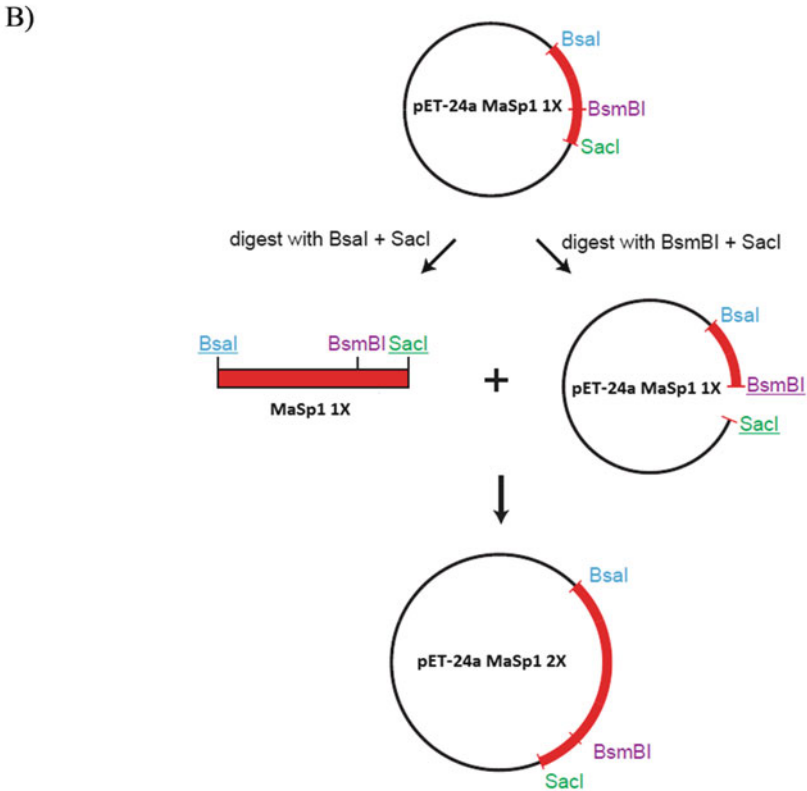
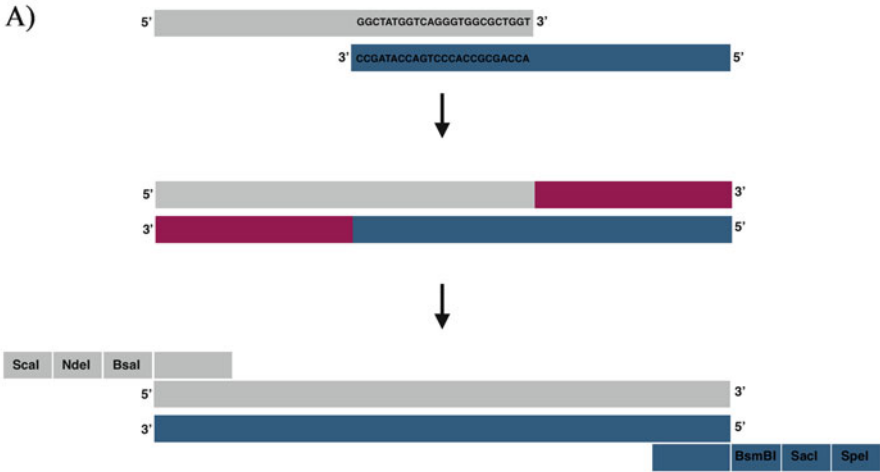


Fig. 12.5 Molecular approach using oligonucleotides to build a single block repeat that can be multimerized by a seamless cloning strategy for expression studies. In this approach, the codons are optimized for the host organism used for expression. (a) Design of single block repeat; (b) Seamless cloning strategy used for expansion of single block repeat

12.4.4 *Expression of Other Spidroin Family Members and Purification Methodologies*

Although the main emphasis has involved optimization of MaSp-like recombinant protein expression in bacteria, reports involving synthesis of other spidroin family members, such as TuSp1, have been shown to be successful. In these studies, synthetic pieces of nucleic acids were codon-optimized and multimerized, to produce 11 copies of the internal block repeat units of *N. antipodiana* TuSp1 (Lin et al. 2013). In addition, the construct was designed to contain the CTD of MiSp1, forming a hybrid recombinant protein with a predicted molecular mass of 189-kDa. The rationale for fusing the MiSp1 CTD to the block repeats of TuSp1 (constructed named 11RPC), instead of using the MaSp1 or TuSp1 CTDs, resides in its differential solubility. The MiSp1 CTD shows much higher solubility in water, resulting in a lower propensity for premature aggregation during protein purification. To increase recombinant TuSp1 protein size, a serine residue within the MiSp1 CTD was mutated to a cysteine. This resulted in the 189-kDa monomeric unit that formed a 378-kDa dimeric unit through thiol oxidation by oxygen dissolved in solution. Although this construct is considerably larger than MaSp-based recombinant constructs, it also suffered from low expression levels, yielding only about 40 mg/L in shake flasks. Fibers spun from the purified recombinant proteins were shown to have higher breaking stress, but lower extensibility relative to natural tubuliform silk fibers (Lin et al. 2013).

Several different strategies have been explored to purify recombinant silk proteins from crude bacterial lysates. The vast majority of these approaches have focused on the utilization of N- or C-terminal His-tags, which allows for rapid purification of recombinant silk proteins in a single step by immobilized metal ion affinity chromatography (IMAC). However, affinity purification on a large-scale format is costly, time consuming, and a labor intensive endeavor. Currently, it is unclear whether the presence of the His-tag influences the secondary structure of the recombinant silk proteins and whether this additional sequence impacts spidroin assembly during the *in vitro* spinning process. Further studies will be required to determine whether the His-tag compromises the mechanical properties of synthetic fibers. Alternative strategies to purify recombinant silk proteins without the implementation of His-tags and metal ion affinity chromatography have been explored, including protocols that take advantage of the thermal stability and resistance of spider silk proteins to organic acids (Dams-Kozłowska et al. 2013).

Attempts to produce tougher spider silk fibers have led scientists to become quite industrious with their approaches. For example, researchers have created transgenic silkworms that encode chimeric silkworm/spider silk proteins. These transgenic silkworms can synthesize and secrete spider silk fibers into cocoons (Teule et al. 2012). These cocoons contain endogenous silk proteins from silkworms mixed with synthetic spider silk-like products resulting in composite fibers. These composites have mechanical properties that are, on average, tougher relative to parental silkworm silk fibers and as tough as natural dragline silk (Teule et al. 2012). Breaking

stress values for the composite fibers were about half of the tensile strength for natural dragline silk. In these studies, investigators manufactured synthetic composite fibers by expression of a fusion protein consisting of a 78-kDa synthetic spider silk protein linked to the enhanced green fluorescence protein (EGFP). Expression of the spider silk-EGFP fusion protein was targeted to the posterior silk gland by using a piggyBac vector containing the *B. mori* fibroin heavy chain promoter. Immunoblot analysis using lysate from the posterior silk gland region and an anti-GFP antibody for detection confirmed the expression of the fusion protein, which migrated at a molecular mass of approximately 116-kDa (Teule et al. 2012). Despite these promising results, one caveat of the study revealed that the mechanical properties of the composite silks from the transgenic animals displayed more variability relative to parental fibers. Moreover, different transgenic lines also produced composite silks that displayed varying tensile strengths, suggesting the lines express different silkworm/spider silk protein ratios and perhaps the localization of the proteins in the fibers is dissimilar. Whether the addition of GFP, which has a molecular mass of approximately 27 kDa, produced any adverse effects on the performance of the fibers is unclear, but the transgenic animals were capable of fiber formation with GFP attached to the synthetic spider silk protein. Other studies have generated transgenic silkworms that can express an 83-kDa MaSp1 recombinant protein lacking GFP; these transgenic silkworms were also capable of secreting MaSp1 into the fibers and the mechanical properties (breaking stress and strain) were shown to outperform the parental silkworm silk fibers (Wen et al. 2010).

12.5 Biomimicry of the Spinning Process, Applications and Products

12.5.1 Artificial Silk Fibers by Biomimicry

Many studies have been exploring the production of artificial silk fibers. However, to date, no company or laboratory has reported a spinning process that produces synthetic fibers that mimic the mechanical properties of natural spider silk. In the scientific literature there have been a number of distinct protocols published that describe the formation of artificial silk fibers based upon the use of a spinning dope with purified recombinant silk proteins (Lazaris et al. 2002; Teule et al. 2009; Hsia et al. 2012). Most of these fibers have been produced using wet spinning through a coagulation bath, electrospinning, or approaches that incorporate microfluidic devices. Many of these spinning methods have relied on the use of harsh organic solvents to dissolve the recombinant silk proteins, including lithium bromide (LiBr) and 1,1,1,3,3,3-hexafluoro-2-propanol (HFIP) (Liivak et al. 1998; Min et al. 2004; Teule et al. 2009). Collectively, it is a challenging task to mimic the natural spinning process, which involves complex combinations of extrusion and drawing processes (Vollrath et al. 1998). The effective integration of these processes

distinguishes it from other methods of synthetic polymeric fiber production. Advances are being made through the use of microfluidic devices to understand the sequences of events and kinetics of silk assembly. However, the long-term goal is to integrate the knowledge obtained from the microfluidic device studies and transition it into the development of a large-scale biomimetic spinning process. Several independent labs are currently investigating this transition. In order to have success, there are many factors that will influence the drawing process, including the removal of water, the behavior of the spin-dope fluidity, and other environmental parameters e.g. temperature, humidity, and draw rate.

12.5.2 *Spinning Dope*

While several steps are involved in the production of artificial spider silk, the first step requires preparation of the spinning dope, which is a liquid solution that contains the dissolved spidroins. Organic solvents are most commonly utilized to dissolve the purified recombinant spidroins that have been subject to lyophilization, providing strong hydrogen bonding properties to ensure effective solvent-protein interactions. Many organic solvents are efficient at solubilizing spidroins, but these solvents have many drawbacks or disadvantages. For example, the toxic effects associated with the molecules pose health concerns for biomedical applications. Despite this shortcoming, most scientists have turned to dissolving spidroin powder in HFIP, which allows spidroin concentrations in the range of 10–30% (w/v), with the highest spidroin concentration being reported at 45–60% (w/v) (Brooks et al. 2008; Hsia et al. 2012; Adrianos et al. 2013; Albertson et al. 2014). One advantage of using HFIP to dissolve the spidroins is its volatility, allowing investigators to dissolve the spidroin powder in larger volumes, followed by solvent evaporation and concentration of the dope for the spinning process. In addition, some labs have preferred to use formic acid as the solvent for the spinning dope (Peng et al. 2009). Although the use of organic solvents has allowed for the synthesis of artificial spider silk fibers, these solvents are too toxic for medical applications, carrying formidable health risks for patients. In addition, vast quantities of these solvents will undoubtedly result in higher production costs associated with organic waste disposal during large-scale synthesis. In order to circumvent the toxic effects of the organic solvents, several different approaches have been reported that focus on spinning artificial silk fibers from concentrated aqueous spidroin solutions. Strategies to produce highly concentrated spidroin solutions through aqueous buffer systems are being vigorously pursued by scientists, representing one of the most active research areas in the silk community (Stark et al. 2007; Grip et al. 2009; Heidebrecht et al. 2015). One approach has involved resuspending lyophilized recombinant spidroin pellets in 6 M guanidinium isothiocyanate (GdmSCN), followed by dialysis (molecular weight cut-off 6000–8000 Da) against buffers containing 50 mM Tris-HCl [pH=8.0] and 100 mM NaCl (Heidebrecht et al. 2015). The addition of the NaCl functions to prevent unspecific protein aggregation. After

this step, the solution can be further dialyzed against a 20% (w/v) polyethylene glycol (PEG; 35-kDa) solution, serving to remove water from the recombinant protein solution, leading to spinning dope concentrations ranging from 10 to 17% (w/v) (Heidebrecht et al. 2015). One weakness of this methodology, however, is that spidroins are forced into a highly concentrated solution, hindering spidroin self-assembly into micellar-like particles that resemble *in vivo* complexes in spiders. Moreover, these spinning dopes appear to be less stable and more prone to aggregation relative to self-assembled spinning dopes. Self-assembled spinning dopes can be achieved by following the identical steps described above except of performing dialysis against PEG, the solution can be subject to dialysis against a phosphate-containing buffer (30–50 mM sodium phosphate pH=7.2), which induces a liquid-liquid phase separation of the spidroin solution into a low density and high-density phase. The high-density micellar phase contains self-assembled spidroins; this approach yielded “biomimetic” spinning dope concentrations ranging between 9 and 11% (w/v) (Heidebrecht et al. 2015). Other strategies to produce high spidroin concentrations have included dialyzing elutions obtained from affinity chromatography against urea, sodium chloride, and sodium phosphate or Tris buffers, followed by high-speed centrifugation, and then concentration of spidroins by ultrafiltration (Arcidiacono et al. 2002). Lastly, other approaches have described methods to solvate traditionally insoluble recombinant spidroins using a quick, single step process, leading to nearly 100% solvation and recovery of these proteins without degradation (Jones et al. 2015). In all cases, scientists have been able to use these aqueous spidroin solutions to produce synthetic silk fibers.

12.5.3 *Wet-Spinning and Post-spin Draw*

One common method to produce synthetic spider silk fibers is through a wet-spinning process, where spidroin dopes are extruded into dehydrating agents. A variety of different alcohols have been investigated to initiate fiber formation, including ethanol, methanol, and isopropanol. In some cases, water was added to the coagulation bath, slowing the coagulation rate of spidroins and serving as a plasticizing agent. This led to fibers that are less brittle. These processes have led to fibers that have diameter sizes in the micrometer range, with many of them ranging from 10 to 80 micrometers (Teule et al. 2009; Gnesa et al. 2012). This technique allows for slow fiber formation, which facilitates the alignment of spidroins during the extrusion step. During the wet-spinning protocol, the extrusion of the dope through the needle of the syringe is advantageous over other methods such as electrospinning, resulting in shear forces that mimic the natural extrusion pathway. This facilitates the alignment of spidroins into a structural hierarchy that is necessary to achieve outstanding material properties in fibers. Overall, this methodology, as outlined above, allows investigators to create spinning dopes formulated in organic or aqueous solvents and to spin fibers in a diverse range of coagulation baths that permits tunable mechanical properties. One weakness of wet-spinning protocols,

however, is that molecules from the organic solvent or coagulation bath can become trapped within synthetic silk fibers during polymer formation, requiring extensive soaking in water to remove contaminants. This can be an expensive and time-consuming process, especially if artificial fiber production is being carried out on a large-scale manufacturing format.

Spiders also intrinsically subjugate extruded fibers to post-spin draw, a process that leads to the production of threads with improved mechanical properties. Experiments have demonstrated that the rate of post-spin draw can have a profound impact on the quality of fibers (Carmichael et al. 1999; Albertson et al. 2014). ^{13}C NMR spectroscopy studies have shown that the fraction of alanine residues in β -sheet conformation increases as the reeling speed increases, which correlates to an enhancement of the mechanical properties (Liivak et al. 1997). Consistent with these observations, molecular modeling has shown that by tuning the size of the β -sheet nanocrystals, the strength and the toughness of the material can be modulated by reeling speed conditions (Nova et al. 2010). Moreover, depending upon the protein sequences and humidity conditions used for the spinning process, scientists may be able to control the supercontraction properties of the spun fibers. Thus, it will be important for material scientists to integrate post-spin draw procedures that are integrated into spinning processes in order to manufacture high-performance threads. Different solvents have been employed for spinning fibers and performing post-spin draw to explore their impact on fiber performance. Spinning spider dragline silk spun in an aqueous bath followed by post-spin draw resulted in stronger fibers (higher breaking stress, yield stress and Young's modulus), but these fibers have had lower extensibility (decrease in breaking strain) (Liu et al. 2005). The increased strength is attributed to the fact that spinning the fibers in water, as opposed to LiBr or HFIP, gives rise to increased molecular orientation of the protein chains, thus improving the mechanical properties. Thus, important aspects that mimic the natural spinning process will be designing artificial spinning ducts that resemble and function like normal ducts as well as engineering devices to recapitulate the influence of the post-spin draw.

12.5.4 Electrospinning and Microfluidic Devices

Another technique that scientists have explored to produce artificial spider silk fibers has involved electrospinning, which creates fibers by exposing liquid droplets of recombinant spidroin spinning dopes to high voltage. In this process, polymer nanofibers are generated by the formation and elongation of an electrified fluid jet (Reneker and Yarin 2008). When the solution is exposed to high voltage, the body of the liquid becomes charged and electrostatic repulsion counteracts the surface tension, resulting in nanofibers that are deposited on a grounded collector as the droplets experience stretching during the procedure. This process does not rely on the chemistry of coagulation that is required by wet-spinning methodologies. For artificial spider silk fibers, electric fields of 4–30 kV with electrode distances of 2–25 cm have

been used for electrospinning protocols (Bini et al. 2006; Peng et al. 2009; Yu et al. 2013). In particular, this procedure can give rise to the formation of non-woven mats. Several different parameters are important for the formation of non-woven mats, including the viscosity of the dope, the concentration of the recombinant spidroins, the electrical conductivity and permeability of the solvent, and the nanofiber surface free energy (Greiner and Wendorff 2007). One advantage of electrospinning is that lower spidroin concentrations can be used to form fibers, but higher concentrations in the range of 10–30 % (w/v) are more effective for fiber formation (Zarkoob et al. 2004; Bini et al. 2006; Zhou et al. 2008). Low β -sheet content was reported from non-woven mats electrospun from spinning dopes dissolved in HFIP (Lang et al. 2013). Interaction of the electromagnetic field with spidroin molecules inhibits β -sheet formation, but stabilizes α -helical structures via hydrogen bond dipoles (Stephens et al. 2005). Although nanofibers can be deposited on a solid container, nanofibers can be collected in coagulation baths containing organic or aqueous-based solvents. When the nanofibers are collected employing coagulation baths (fiber diameter sizes of approximately 80–1000 nm), posttreatment of the electrospun fibers with alcohols or organic solvents is necessary to induce formation of water resistance and stable β -sheet structure (Lang et al. 2013). Exposure of nanofibers to alcohol vapors has proven more effective than immersing the fibers in alcohol baths because submersion of the nanofibers can alter fiber morphology, resulting in more flattened and partially fused threads at the intersection of multiple fibers (Bini et al. 2006; Lang et al. 2013). The mechanical properties of electrospun fibers have inferior properties relative to natural fibers; however, the non-woven meshes can be used for other products, including filter or biomedical applications, where natural silk mechanical properties are not a requirement (Bogush et al. 2009).

In addition to wet spinning and electrospinning, synthetic spider silk fibers have been produced by microfluidic devices using dilute recombinant spidroin mixtures (Rammensee et al. 2008). The use of microfluidic devices has been demonstrated to lead to artificial spider silk fibers, but higher flow rates were necessary to induce fiber assembly using low or medium concentrations of protein solutions (Rammensee et al. 2008). Fiber production using microfluidic devices have many advantages over the other two spinning methods, in that, such devices can be designed and engineered to mimic aspects of the natural extrusion process of spider silk. These aspects include being able to precisely control or adjust changes in pH, ion concentrations, and elongational flow conditions.

12.5.5 Applications and Products

12.5.5.1 Fibers and Films

Although much attention has been placed on the development of artificial spider silk fibers for uses in ropes, cords, body armor and other engineering materials that are fiber-based, recombinant spider silk proteins can be processed into films, foams,

hydrogels, and nanoparticles for drug delivery. Recombinant spider silk protein films have potential for diverse applications, in particular for the medical community due to its biocompatibility (Allmeling et al. 2006). Biodegradable biomaterials that are implantable are attractive for devices that control the delivery of drugs in animals. Possible uses of films include materials for controlled release of substances at specific sites in the human body and cell supporting scaffolds (Sofia et al. 2001; Hardy et al. 2013). These films experience partial degradation in the presence of proteases associated with the wound healing process within 2 weeks, which is consistent with the timing of the normal tissue repair response (Muller-Hermann and Scheibel 2015). Micro-particles engineered to carry cargo, such as pharmaceutical drugs, could also be designed to allow for delayed drug release by coating particles with a layer of recombinant spider silk protein. Research has shown that recombinant spider silk protein films are chemically stable and transparent materials under ambient conditions (Huemmerich et al. 2006). The properties of the films are determined by the secondary structure of the protein chains, the intermolecular interactions of the chains, and the connections of the materials interface with the environment (Spiess et al. 2010). During the creation of films, recombinant spider silk proteins have been demonstrated to undergo structural transitions from either random coil or α -helical conformations to β -sheet-rich structures (Huemmerich et al. 2006). Treatment of the recombinant spider silk proteins with alcohol or kosmotropic salts was shown to lead to films that are β -sheet-rich, chemically stable and water insoluble. The stability of the films is directly linked to the β -sheet content, with increasing levels leading to films with higher strength and elastic modulus, but lower extensibility. The addition of the NTD or CTD on the recombinant spider silk construct, although important in the fiber spinning process, appear to have no substantial influence on the β -sheet formation, which is being controlled by the amino acid sequences of the internal block repeat modules. However, the presence of the NTD or CTDs have been shown to increase the chemical stability of the films (Slotta et al. 2006).

12.5.5.2 Spider Silk Particles

Recombinant spider silk proteins are also suitable for construction of particles that can be utilized for a host of applications. These particles can be assembled and designed to carry low molecular weight molecules for drug delivery (Hardy et al. 2013). Diameter particle size can be adjustable by varying the recombinant protein concentration or mixing vigorously with the reagents used for salting out (Elsner et al. 2015). The intrinsic properties of spider silk proteins, which include slow biodegradability, poor immunogenicity, and low toxicity, make them highly suitable candidates to serve as particles that can carry a broad range of different organic molecules. Packaging of the drug can be facilitated by diffusion or co-precipitation of the recombinant spidroins. When loading the drug, it cannot display electrostatic repulsion with the recombinant spidroins. Therefore, depending upon the charge on the drug, spidroins can be designed with charges that are opposite of the drug to

facilitate packaging. Moreover, silk particles have been shown to retain their molecular properties in the human body for a period of time before degradation occurs (Muller-Hermann and Scheibel 2015). Experiments designed to investigate the uptake of the particles made of recombinant spider silk proteins have shown that mammalian cells uptake particles with a positive charge more efficiently than negatively-charged particles. Incorporation of cell penetrating peptides (*e.g.* RGD-functionalized spidroins) have been shown to increase the number of particles transported into HeLa cells (Elsner et al. 2015).

12.6 Summary and Future Challenges

Over the past three decades there has been substantial progress in understanding the protein sequences of the spidroin family members. This has been accelerated by scientific advances in gene cloning, DNA sequencing, transcriptomics, and proteomics. With each passing month, scientists are replacing partial cDNA sequences that code for spidroin family members with complete genomic DNA sequences. Currently, two major challenges exist in the spider silk community. The first involves development of methodologies that allow for expression of full-length recombinant spider silk proteins in high quantities, while the second challenge involves engineering a highly concentrated aqueous spinning dope that gives rise to high performance fibers. As more chemical details regarding the natural extrusion process of spider silk emerge, scientists are incorporating these concepts into the spinning process to mimic fiber synthesis. Many different spinning methods continue to be explored, including wet-spinning and electrospinning. Through the development of creative genetic engineering strategies, strides to manufacture recombinant proteins that approach native size spidroins are becoming more feasible, providing much excitement and promise for developing a wave of next generation biomaterials. Because spiders spin a host of different fiber types with distinct mechanical properties, scientists are eager to capitalize on the production of recombinant spider silk proteins for a wide range of diverse applications, including sutures for microsurgery, silk particles for drug delivery, scaffolds for tissue engineering, body armor, and construction of a vast array of novel engineering products. For example, as proof-of-concept the successful synthesis and purification of recombinant silk proteins resembling native size MaSp1 molecules via heterologous expression systems demonstrate that the first challenge can be solved. In addition, strategies to generate recombinant spidroin mixtures that resemble natural spinning dope properties are accelerating at a fast rate. Through the development of different chemical treatments, scientists are generating recombinant spidroins with secondary and tertiary structures that more accurately reflect the folded states of natural spidroins in spinning dopes. Thus, advances in expression of longer protein chain lengths, combined with improvements of recombinant spidroin processing to form more native-like spinning dopes, are putting the field in a position to spin higher performance fibers. Although the majority of research teams have focused on

expression of recombinant silk proteins and spinning of artificial fibers from dragline fiber components, little is known whether other members of the spidroin family may have other advantageous features, including improved expression, solubility, purification, and easier processing into final products. Additional studies will need to be performed to address these issues. In closing, it is an exciting moment in the history of spider silk biology and its uses of recombinant spider silk proteins.

Acknowledgements We thank Tiffany-Blasingame Tuton, Felicia Jeffery, Coby La Mattina, Albert Lin and Tyler Chuang for their contributions with the spider microdissection images from black widow spiders. In addition, we are grateful for contributions from Yang Hsia, Eric Gnesa, Thanh Pham, and Connie Liu.

References

- Adrianos SL, Teule F, Hinman MB, Jones JA, Weber WS, Yarger JL, Lewis RV (2013) *Nephila clavipes* flagelliform silk-like GGX motifs contribute to extensibility and spacer motifs contribute to strength in synthetic spider silk fibers. *Biomacromolecules* 14:1751–1760
- Albertson AE, Teule F, Weber W, Yarger JL, Lewis RV (2014) Effects of different post-spin stretching conditions on the mechanical properties of synthetic spider silk fibers. *J Mech Behav Biomed Mater* 29:225–234
- Allmeling C, Jokuszies A, Reimers K, Kall S, Vogt PM (2006) Use of spider silk fibres as an innovative material in a biocompatible artificial nerve conduit. *J Cell Mol Med* 10:770–777
- Andersson M, Chen G, Oতিকovs M, Landreh M, Nordling K, Kronqvist N, Westermarck P, Jornvall H, Knight S, Ridderstrale Y, Holm L, Meng Q, Jaudzems K, Chesler M, Johansson J, Rising A (2014) Carbonic anhydrase generates CO₂ and H⁺ that drive spider silk formation via opposite effects on the terminal domains. *PLoS Biol* 12:e1001921
- Arcidiacono S, Mello C, Kaplan D, Cheley S, Bayley H (1998) Purification and characterization of recombinant spider silk expressed in *Escherichia coli*. *Appl Microbiol Biotechnol* 49:31–38
- Arcidiacono S, Mello CM, Butler M, Welsh E, Soares JW, Allen A, Ziegler D, Laue T, Chase S (2002) Aqueous processing and fiber spinning of recombinant spider silks. *Macromolecules* 35:1262–1266
- Argintean S, Chen J, Kim M, Moore AMF (2006) Resilient silk captures prey in black widow cobwebs. *Appl Phys A Mater Sci Process* 82:235–241
- Ayoub NA, Garb JE, Tinghitella RM, Collin MA, Hayashi CY (2007) Blueprint for a high-performance biomaterial: full-length spider dragline silk genes. *PLoS One* 2:e514
- Ayoub NA, Garb JE, Kuelbs A, Hayashi CY (2013) Ancient properties of spider silks revealed by the complete gene sequence of the prey-wrapping silk protein (AcSp1). *Mol Biol Evol* 30:589–601
- Bini E, Foo CW, Huang J, Karageorgiou V, Kitchel B, Kaplan DL (2006) RGD-functionalized bioengineered spider dragline silk biomaterial. *Biomacromolecules* 7:3139–3145
- Blackledge TA, Summers AP, Hayashi CY (2005) Gumfooted lines in black widow cobwebs and the mechanical properties of spider capture silk. *Zoology (Jena)* 108:41–46
- Blasingame E, Tuton-Blasingame T, Larkin L, Falick AM, Zhao L, Fong J, Vaidyanathan V, Visperas A, Geurts P, Hu X, La Mattina C, Vierra C (2009) Pyriform spidroin 1, a novel member of the silk gene family that anchors dragline silk fibers in attachment discs of the black widow spider, *Latrodectus hesperus*. *J Biol Chem* 284:29097–29108
- Bogush VG, Sokolova OS, Davydova LI, Klinov DV, Sidoruk KV, Esipova NG, Neretina TV, Orchanskyi IA, Makeev VY, Tumanyan VG, Shaitan KV, Debabov VG, Kirpichnikov MP

- (2009) A novel model system for design of biomaterials based on recombinant analogs of spider silk proteins. *J Neuroimmune Pharmacol* 4:17–27
- Bon M (1710) A discourse upon the usefulness of the silk of spiders. *Philos Trans* 27:2–16
- Brooks AE, Stricker SM, Joshi SB, Kamerzell TJ, Middaugh CR, Lewis RV (2008) Properties of synthetic spider silk fibers based on *Argiope aurantia* MaSp2. *Biomacromolecules* 9:1506–1510
- Carmichael S, Barghout JY, Viney C (1999) The effect of post-spin drawing on spider silk microstructure: a birefringence model. *Int J Biol Macromol* 24:219–226
- Casem ML, Turner D, Houchin K (1999) Protein and amino acid composition of silks from the cob weaver, *Latrodectus hesperus* (black widow). *Int J Biol Macromol* 24:103–108
- Chaw RC, Correa-Garhwal SM, Clarke TH, Ayoub NA, Hayashi CY (2015) Proteomic evidence for components of spider silk synthesis from black widow silk glands and fibers. *J Proteome Res* 14:4223–4231
- Chen G, Liu X, Zhang Y, Lin S, Yang Z, Johansson J, Rising A, Meng Q (2012) Full-length minor ampullate spidroin gene sequence. *PLoS One* 7:e52293
- Choresh O, Bayarmagnai B, Lewis RV (2009) Spider web glue: two proteins expressed from opposite strands of the same DNA sequence. *Biomacromolecules* 10:2852–2856
- Clarke TH, Garb JE, Hayashi CY, Haney RA, Lancaster AK, Corbett S, Ayoub NA (2014) Multi-tissue transcriptomics of the black widow spider reveals expansions, co-options, and functional processes of the silk gland gene toolkit. *BMC Genomics* 15:365
- Colgin MA, Lewis RV (1998) Spider minor ampullate silk proteins contain new repetitive sequences and highly conserved non-silk-like “spacer regions”. *Protein Sci* 7:667–672
- Dams-Kozłowska H, Majer A, Tomaszewicz P, Lozinska J, Kaplan DL, Mackiewicz A (2013) Purification and cytotoxicity of tag-free bioengineered spider silk proteins. *J Biomed Mater Res A* 101:456–464
- Dicko C, Knight D, Kenney JM, Vollrath F (2004a) Secondary structures and conformational changes in flagelliform, cylindrical, major, and minor ampullate silk proteins. Temperature and concentration effects. *Biomacromolecules* 5:2105–2115
- Dicko C, Vollrath F, Kenney JM (2004b) Spider silk protein refolding is controlled by changing pH. *Biomacromolecules* 5:704–710
- Eberhard WG (2010) Possible functional significance of spigot placement on the spinnerets of spiders. *J Arachnol* 38:407–414
- Elsner MB, Herold HM, Müller-Herrmann S, Bargel H, Scheibel T (2015) Enhanced cellular uptake of engineered spider silk particles. *Biomater Sci* 3:543–551
- Fahnestock SR, Bedzyk LA (1997) Production of synthetic spider dragline silk protein in *Pichia pastoris*. *Appl Microbiol Biotechnol* 47:33–39
- Fahnestock SR, Irwin SL (1997) Synthetic spider dragline silk proteins and their production in *Escherichia coli*. *Appl Microbiol Biotechnol* 47:23–32
- Fukushima Y (1998) Genetically engineered syntheses of tandem repetitive polypeptides consisting of glycine-rich sequence of spider dragline silk. *Biopolymers* 45:269–279
- Gaines WA, Sehorn MG, Marcotte WR (2010) Spidroin N-terminal domain promotes a pH-dependent association of silk proteins during self-assembly. *J Biol Chem* 285:40745–40753
- Garb JE, Hayashi CY (2005) Modular evolution of egg case silk genes across orb-weaving spider superfamilies. *Proc Natl Acad Sci U S A* 102:11379–11384
- Gatesey J, Hayashi C, Motriuk D, Woods J, Lewis R (2001) Extreme diversity, conservation, and convergence of spider silk fibroin sequences. *Science* 291:2603–2605
- Gerritsen VB (2002) The tiptoe of an airbus. *Protein Spotlight Swiss Prot* 24:1–2
- Geurts P, Zhao L, Hsia Y, Gnesa E, Tang S, Jeffery F, La Mattina C, Franz A, Larkin L, Vierra C (2010a) Synthetic spider silk fibers spun from Pyriform Spidroin 2, a glue silk protein discovered in orb-weaving spider attachment discs. *Biomacromolecules* 11:3495–3503
- Geurts P, Zhao L, Hsia Y, Gnesa E, Tang S, Jeffery F, Mattina CL, Franz A, Larkin L, Vierra C (2010b) Synthetic spider silk fibers spun from pyriform spidroin 2, a glue silk protein discovered in orb-weaving spider attachment discs. *Biomacromolecules* 11:3495–3503

- Gnesa E, Hsia Y, Yarger JL, Weber W, Lin-Cereghino J, Lin-Cereghino G, Tang S, Agari K, Vierra C (2012) Conserved C-terminal domain of spider tubuliform spidroin 1 contributes to extensibility in synthetic fibers. *Biomacromolecules* 13:304–312
- Gosline JM, Guerrette PA, Ortlepp CS, Savage KN (1999) The mechanical design of spider silks: from fibroin sequence to mechanical function. *J Exp Biol* 202:3295–3303
- Greiner A, Wendorff JH (2007) Electrospinning: a fascinating method for the preparation of ultrathin fibers. *Angew Chem Int Ed* 46:5670–5703
- Grip S, Johansson J, Hedhammar M (2009) Engineered disulfides improve mechanical properties of recombinant spider silk. *Protein Sci* 18:1012–1022
- Guerrette PA, Ginzinger DG, Weber BH, Gosline JM (1996) Silk properties determined by gland-specific expression of a spider fibroin gene family. *Science* 272:112–115
- Guinea GV, Elices M, Plaza GR, Perea GB, Daza R, Riekkel C, Agullo-Rueda F, Hayashi C, Zhao Y, Perez-Rigueiro J (2012) Minor ampullate silks from *Nephila* and *Argiope* spiders: tensile properties and microstructural characterization. *Biomacromolecules* 13:2087–2098
- Hagn F, Eisoldt L, Hardy JG, Vendrely C, Coles M, Scheibel T, Kessler H (2010) A conserved spider silk domain acts as a molecular switch that controls fibre assembly. *Nature* 465:239–242
- Hardy JG, Leal-Egana A, Scheibel TR (2013) Engineered spider silk protein-based composites for drug delivery. *Macromol Biosci* 13:1431–1437
- Hauptmann V, Weichert N, Menzel M, Knoch D, Paegle N, Scheller J, Spohn U, Conrad U, Gils M (2013) Native-sized spider silk proteins synthesized in planta via intein-based multimerization. *Transgenic Res* 22:369–377
- Hayashi C, Lewis RV (1998) Evidence from flagelliform silk cDNA for the structural basis of elasticity and modular nature of spider silks. *J Mol Biol* 275:773–784
- Hayashi CY, Lewis RV (2000) Molecular architecture and evolution of a modular spider silk protein gene. *Science* 287:1477–1479
- Hayashi CY, Shipley NH, Lewis RV (1999) Hypotheses that correlate the sequence, structure, and mechanical properties of spider silk proteins. *Int J Biol Macromol* 24:271–275
- Hayashi CY, Blackledge TA, Lewis RV (2004) Molecular and mechanical characterization of aciniform silk: uniformity of iterated sequence modules in a novel member of the spider silk fibroin gene family. *Mol Biol Evol* 21:1950–1959
- Heidebrecht A, Eisoldt L, Diehl J, Schmidt A, Geffers M, Lang G, Scheibel T (2015) Biomimetic fibers made of recombinant spidroins with the same toughness as natural spider silk. *Adv Mater* 27:2189–2194
- Hinman MB, Lewis RV (1992) Isolation of a clone encoding a second dragline silk fibroin. *Nephila clavipes* dragline silk is a two-protein fiber. *J Biol Chem* 267:19320–19324
- Hsia Y, Gnesa E, Pacheco R, Kohler K, Jeffery F, Vierra C (2012) Synthetic spider silk production on a laboratory scale. *J Vis Exp* 2012:e4191
- Hu X, Kohler K, Falick AM, Moore AM, Jones PR, Sparkman OD, Vierra C (2005a) Egg case protein-1. A new class of silk proteins with fibroin-like properties from the spider *Latrodectus hesperus*. *J Biol Chem* 280:21220–21230
- Hu X, Lawrence B, Kohler K, Falick AM, Moore AM, McMullen E, Jones PR, Vierra C (2005b) Araneoid egg case silk: a fibroin with novel ensemble repeat units from the black widow spider, *Latrodectus hesperus*. *Biochemistry* 44:10020–10027
- Hu X, Kohler K, Falick AM, Moore AM, Jones PR, Vierra C (2006a) Spider egg case core fibers: trimeric complexes assembled from TuSp1, ECP-1, and ECP-2. *Biochemistry* 45:3506–3516
- Hu X, Vasanthavada K, Kohler K, McNary S, Moore AM, Vierra CA (2006b) Molecular mechanisms of spider silk. *Cell Mol Life Sci* 63:1986–1999
- Hu X, Yuan J, Wang X, Vasanthavada K, Falick AM, Jones PR, La Mattina C, Vierra CA (2007) Analysis of aqueous glue coating proteins on the silk fibers of the cob weaver, *Latrodectus hesperus*. *Biochemistry* 46:3294–3303
- Huemmerich D, Slotta U, Scheibel T (2006) Processing and modification of films made from recombinant spider silk proteins. *Appl Phys A* 82:219–222

- Ittah S, Michaeli A, Goldblum A, Gat U (2007) A model for the structure of the C-terminal domain of dragline spider silk and the role of its conserved cysteine. *Biomacromolecules* 8:2768–2773
- Jain D, Zhang C, Cool LR, Blackledge TA, Wesdemiotis C, Miyoshi T, Dhinojwala A (2015) Composition and function of spider glues maintained during the evolution of cobwebs. *Biomacromolecules* 16:3373–3380
- Jeffery F, La Mattina C, Tuton-Blasingame T, Hsia Y, Gnesa E, Zhao L, Franz A, Vierra C (2011) Microdissection of black widow spider silk-producing glands. *J Vis Exp* 47:2382. doi:10.3791/2382
- Jin HJ, Kaplan DL (2003) Mechanism of silk processing in insects and spiders. *Nature* 424:1057–1061
- Jones JA, Harris TI, Tucker CL, Berg KR, Christy SY, Day BA, Gaztambide DA, Needham NJ, Ruben AL, Oliveira PF, Decker RE, Lewis RV (2015) More than just fibers: an aqueous method for the production of innovative recombinant spider silk protein materials. *Biomacromolecules* 16:1418–1425
- Knight DP, Vollrath F (2001) Changes in element composition along the spinning duct in a *Nephila* spider. *Naturwissenschaften* 88:179–182
- Kohler K, Thayer W, Le T, Sembhi A, Vasanthavada K, Moore AM, Vierra C (2005) Characterization of a novel class II bHLH transcription factor from the black widow spider, *Latrodectus hesperus*, with silk-gland restricted patterns of expression. *DNA Cell Biol* 24:371–380
- Kovoor J, Zylberberg L (1980) Fine structural aspects of silk secretion in a spider (*Araneus diadematus*). I. Elaboration in the pyriform glands. *Tissue Cell* 12:547–556
- Kovoor J, Zylberberg L (1982) Fine structural aspects of silk secretion in a spider. II. Conduction in the pyriform glands. *Tissue Cell* 14:519–530
- Kummerlen J, Van Beek JD, Vollrath F, Meier B (1996) Local structure in spider dragline silk investigated by two-dimensional spin-diffusion nuclear magnetic resonance. *Macromolecules* 29:2920–2928
- La Mattina C, Reza R, Hu X, Falick AM, Vasanthavada K, McNary S, Yee R, Vierra C (2008) Spider minor ampullate silk proteins are constituents of prey wrapping silk in the cob weaver *Latrodectus hesperus*. *Biochemistry* 47:4692–4700
- Lane AK, Hayashi CY, Whitworth GB, Ayoub NA (2013) Complex gene expression in the dragline silk producing glands of the Western black widow (*Latrodectus hesperus*). *BMC Genomics* 14:846
- Lang G, Jokisch S, Scheibel T (2013) Air filter devices including nonwoven meshes of electrospun recombinant spider silk proteins. *J Vis Exp* 2013:e50492
- Lazaris A, Arcidiacono S, Huang Y, Zhou JF, Duguay F, Chretien N, Welsh EA, Soares JW, Karzas CN (2002) Spider silk fibers spun from soluble recombinant silk produced in mammalian cells. *Science* 295:472–476
- Lefevre T, Rousseau ME, Pezolet M (2007) Protein secondary structure and orientation in silk as revealed by Raman spectromicroscopy. *Biophys J* 92:2885–2895
- Lefevre T, Boudreault S, Cloutier C, Pezolet M (2011) Diversity of molecular transformations involved in the formation of spider silks. *J Mol Biol* 405:238–253
- Lewis R (1996) Unraveling the weave of spider silk. *Bioscience* 46:636–638
- Lewis RV, Hinman M, Kothakota S, Fournier MJ (1996) Expression and purification of a spider silk protein: a new strategy for producing repetitive proteins. *Protein Expr Purif* 7:400–406
- Liivak O, Flores A, Lewis L, Jelinski LW (1997) Conformation of the polyalanine repeats in minor ampullate gland silk of the spider *Nephila clavipes*. *Macromolecules* 30:7127–7130
- Liivak O, Blye A, Shah N, Jelinski LW (1998) A microfabricated wet-spinning apparatus to spin fibers of silk proteins. Structure-property correlations. *Macromolecules* 31:2927–2951
- Lin Z, Deng Q, Liu XY, Yang D (2013) Engineered large spider eggcase silk protein for strong artificial fibers. *Adv Mater* 25:1216–1220
- Liu Y, Shao Z, Vollrath F (2005) Extended wet-spinning can modify spider silk properties. *Chem Commun* 19:2489–2491

- Min BM, Lee G, Kim SH, Nam YS, Lee TS, Park WH (2004) Electrospinning of silk fibroin nanofibers and its effect on the adhesion and spreading of normal human keratinocytes and fibroblasts *in vitro*. *Biomaterials* 25:1289–1297
- Muller-Hermann S, Scheibel T (2015) Enzymatic degradation of films, particles, and nonwoven meshes made of a recombinant spider silk protein. *ACS Biomater Sci Eng* 1:247–259
- Nova A, Keten S, Pugno NM, Redaelli A, Buehler MJ (2010) Molecular and nanostructural mechanisms of deformation, strength and toughness of spider silk fibrils. *Nano Lett* 10:2626–2634
- Parnham S, Gaines WA, Duggan BM, Marcotte WR, Hennig M (2011) NMR assignments of the N-terminal domain of *Nephila clavipes* spidroin 1. *Biomol NMR Assign* 5:131–133
- Peng H, Zhou S, Jiang J, Guo T, Zheng X, Yu X (2009) Pressure-induced crystal memory effect of spider silk proteins. *J Phys Chem B* 113:4636–4641
- Perry DJ, Bittencourt D, Siltberg-Liberles J, Rech EL, Lewis RV (2010) Piriform spider silk sequences reveal unique repetitive elements. *Biomacromolecules* 11:3000–3006
- Pham T, Chuang T, Lin A, Joo H, Tsai J, Crawford T, Zhao L, Hsia Y, Williams C, Vierra CA (2014) Dragline silk: a fiber assembled with low-molecular-weight cysteine-rich proteins. *Biomacromolecules* 15:4073–4081
- Prince JT, Mcgrath KP, Digirolamo CM, Kaplan DL (1995) Construction, cloning, and expression of synthetic genes encoding spider dragline silk. *Biochemistry* 34:10879–10885
- Rabotyagova OS, Cebe P, Kaplan DL (2009) Self-assembly of genetically engineered spider silk block copolymers. *Biomacromolecules* 10:229–236
- Rammensee S, Slotta U, Scheibel T, Bausch AR (2008) Assembly mechanism of recombinant spider silk proteins. *Proc Natl Acad Sci U S A* 105:6590–6595
- Reneker DH, Yarin AL (2008) Electrospinning jets and polymer nanofibers. *Polymer* 49:2387–2425
- Scheller J, Guhrs KH, Grosse F, Conrad U (2001) Production of spider silk proteins in tobacco and potato. *Nat Biotechnol* 19:573–577
- Scior A, Preissler S, Koch M, Deuerling E (2011) Directed PCR-free engineering of highly repetitive DNA sequences. *BMC Biotechnol* 11:87
- Slotta U, Tammer M, Kremer F, Koelsch P, Scheibel T (2006) Structural analysis of spider silk films. *Supramol Chem* 18:465–471
- Sofia S, Mccarthy MB, Gronowicz G, Kaplan DL (2001) Functionalized silk-based biomaterials for bone formation. *J Biomed Mater Res* 54:139–148
- Spieß L, Wohlrab S, Scheibel T (2010) Structural characterization and functionalization of engineered spider silk films. *Soft Matter* 6:4168–4174
- Stark M, Grip S, Rising A, Hedhammar M, Engstrom W, Hjalm G, Johansson J (2007) Macroscopic fibers self-assembled from recombinant miniature spider silk proteins. *Biomacromolecules* 8:1695–1701
- Stephens JS, Fahnestock SR, Farmer RS, Kiick KL, Chase DB, Rabolt JF (2005) Effects of electrospinning and solution casting protocols on the secondary structure of a genetically engineered dragline spider silk analogue investigated via Fourier transform Raman spectroscopy. *Biomacromolecules* 6:1405–1413
- Szela S, Avtges P, Valluzzi R, Winkler S, Wilson D, Kirschner D, Kaplan DL (2000) Reduction-oxidation control of beta-sheet assembly in genetically engineered silk. *Biomacromolecules* 1:534–542
- Teule F, Cooper AR, Furin WA, Bittencourt D, Rech EL, Brooks A, Lewis RV (2009) A protocol for the production of recombinant spider silk-like proteins for artificial fiber spinning. *Nat Protoc* 4:341–355
- Teule F, Miao YG, Sohn BH, Kim YS, Hull JJ, Fraser MJ Jr, Lewis RV, Jarvis DL (2012) Silkworms transformed with chimeric silkworm/spider silk genes spin composite silk fibers with improved mechanical properties. *Proc Natl Acad Sci U S A* 109:923–928
- Tian M, Lewis RV (2005) Molecular characterization and evolutionary study of spider tubuliform (eggcase) silk protein. *Biochemistry* 44:8006–8012

- Tian M, Lewis RV (2006) Tubuliform silk protein: a protein with unique molecular characteristics and mechanical properties in the spider silk fibroin family. *Appl Phys A* 82:265–273
- Tillinghast EK, Townley MA, Bernstein DT, Gallagher KS (1991) Comparative study of orb web hygroscopicity and adhesive spiral composition in three araneid spiders. *J Exp Zool* 259:154–165
- Townley MA, Pu Q, Zercher CK, Neefus CD, Tillinghast EK (2012) Small organic solutes in sticky droplets from orb webs of the spider *Zygiella atrica* (Araneae: Araneidae): beta-alaninamide is a novel and abundant component. *Chem Biodivers* 9:2159–2174
- Tremblay ML, Xu L, Lefevre T, Sarker M, Orrell KE, Leclerc J, Meng Q, Pezolet M, Auger M, Liu XQ, Rainey JK (2015) Spider wrapping silk fibre architecture arising from its modular soluble protein precursor. *Sci Rep* 5:11502
- Van Beek JD, Hess S, Vollrath F, Meier BH (2002) The molecular structure of spider dragline silk: folding and orientation of the protein backbone. *Proc Natl Acad Sci U S A* 99:10266–10271
- Vasanthavada K, Hu X, Falick AM, La Mattina C, Moore AM, Jones PR, Yee R, Reza R, Tuton T, Vierra C (2007) Aciniform spidroin, a constituent of egg case sacs and wrapping silk fibers from the black widow spider *Latrodectus hesperus*. *J Biol Chem* 282:35088–35097
- Vasanthavada K, Hu X, Tuton-Blasingame T, Hsia Y, Sampath S, Pacheco R, Freeark J, Falick AM, Tang S, Fong J, Kohler K, La Mattina-Hawkins C, Vierra C (2012) Spider glue proteins have distinct architectures compared with traditional spidroin family members. *J Biol Chem* 287:35986–35999
- Vollrath F, Edmonds DT (1989) Modulation of the mechanical properties of spider silk by coating with water. *Nature* 340:305–307
- Vollrath F, Knight DP (1999) Structure and function of the silk production pathway in the spider *Nephila edulis*. *Int J Biol Macromol* 24:243–249
- Vollrath F, Knight DP (2001) Liquid crystalline spinning of spider silk. *Nature* 410:541–548
- Vollrath F, Fairbrother WJ, Williams RJP, Tillinghast EK, Bernstein DT, Gallagher KS, Townley MA (1990) Compounds in the droplets of the orb spider's viscid spiral. *Nature* 345:526–528
- Vollrath F, Wen Hu X, Knight DP (1998) Silk production in a spider involves acid bath treatment. *Proc R Soc B* 263:817–820
- Wen H, Lan X, Zhang Y, Zhao T, Wang Y, Kajiura Z, Nakagaki M (2010) Transgenic silkworms (*Bombyx mori*) produce recombinant spider dragline silk in cocoons. *Mol Biol Rep* 37:1815–1821
- Winkler S, Szela S, Avtges P, Valluzzi R, Kirschner DA, Kaplan D (1999) Designing recombinant spider silk proteins to control assembly. *Int J Biol Macromol* 24:265–270
- Winkler S, Wilson D, Kaplan DL (2000) Controlling beta-sheet assembly in genetically engineered silk by enzymatic phosphorylation/dephosphorylation. *Biochemistry* 39:12739–12746
- Wolff JO, Grawe I, Wirth M, Karstedt A, Gorb SN (2015) Spider's super-glue: thread anchors are composite adhesives with synergistic hierarchical organization. *Soft Matter* 11:2394–2403
- Xia XX, Qian ZG, Ki CS, Park YH, Kaplan DL, Lee SY (2010) Native-sized recombinant spider silk protein produced in metabolically engineered *Escherichia coli* results in a strong fiber. *Proc Natl Acad Sci U S A* 107:14059–14063
- Xu M, Lewis RV (1990) Structure of a protein superfiber: spider dragline silk. *Proc Natl Acad Sci U S A* 87:7120–7124
- Xu L, Rainey JK, Meng Q, Liu XQ (2012) Recombinant minimalist spider wrapping silk proteins capable of native-like fiber formation. *PLoS One* 7:e50227
- Xu L, Tremblay ML, Orrell KE, Leclerc J, Meng Q, Liu XQ, Rainey JK (2013) Nanoparticle self-assembly by a highly stable recombinant spider wrapping silk protein subunit. *FEBS Lett* 587:3273–3280
- Yu Q, Xu S, Zhang H, Gu L, Xu Y, Ko F (2013) Structure-property relationship of regenerated spider silk protein nano/microfibrillar scaffold fabricated by electrospinning. *J Biomed Mater Res A* 102:3828–3837
- Zarkoob S, Eby RK, Reneker DH, Hudson SD, Ertley D, Adams WW (2004) Structure and morphology of electrospun silk nanofibers. *Polymer* 45:3973–3977

- Zhao AC, Zhao TF, Nakagaki K, Zhang YS, Sima YH, Miao YG, Shiomi K, Kajiura Z, Nagata Y, Takadera M, Nakagaki M (2006) Novel molecular and mechanical properties of egg case silk from wasp spider, *Argiope bruennichi*. *Biochemistry* 45:3348–3356
- Zhao Y, Ayoub NA, Hayashi CY (2010) Chromosome mapping of dragline silk genes in the genomes of widow spiders (Araneae, Theridiidae). *PLoS One* 5:e12804
- Zhou S, Peng H, Yu X, Zheng X, Cui W, Zhang Z, Li X, Wang J, Weng J, Jia W, Li F (2008) Preparation and characterization of a novel electrospun spider silk fibroin/poly(D, L-lactide) composite fiber. *J Phys Chem B* 112:11209–11216

Chapter 13

Spider Silk: Factors Affecting Mechanical Properties and Biomimetic Applications

Shichang Zhang and I-Min Tso

Abstract Spiders are using different silks to achieve a variety of tasks. Spider silks might be the toughest natural material, and therefore they serve as model polymers for the development of biomimetic fibers with extraordinary mechanical performance. Spider silks with pliable mechanical properties are indispensable for designing and manufacturing biomimetic fibers for specific applications, notably for biomedical purposes. This chapter summarizes natural factors that are known to affect the physical properties of spider silks such as the drawing speed, ambient environmental conditions and nutrient intake. Such factors induce changes in protein composition, and in the structural alignment and organization of molecules in the silks, which consequently affect silk properties. In addition, we also present the latest findings regarding the spinning processes of the silk, as well as prospects and challenges in spider silk research.

13.1 Introduction

Spiders are well-known for their silk-using skills. More than 40,000 species of spiders have been identified (Platnick 2013), most of which catch prey by using silks. They have evolved to be able to produce a variety of task-specific silks for activities such as catching prey, escaping from predators, and protecting egg sacs (Foelix 2011). Due to their fascinating characteristics, spider silks have attracted the attention of researchers for a long time, especially in biomaterial science due to their intriguing characteristics. For example, the dragline silk is the strongest natural fiber (Blackledge and Hayashi 2006), which can be more than three times tougher than the manmade fiber, Kevlar (Gosline et al. 1999; Vollrath and Knight 2001). Spider silks' potential to be applied in fields ranging from high performance textiles to medical devices has motivated scientists to keep exploring the underlying mechanisms of their remarkable mechanical properties. In contrast to silkworms, it is impossible to have large scale farming of spiders due to their cannibalistic nature

S. Zhang • I.-M. Tso (✉)

Department of Life Science, Tunghai University, Taichung 40704, Taiwan

e-mail: frankzsc@gmail.com; spider@thu.edu.tw

(Hardy and Scheibel 2009), nor is it feasible to harvest threads directly from spider webs because of small yield (Spiess et al. 2010; Lintz and Scheibel 2013). In order to harvest large quantities of spider silks, efforts have been invested in expressing spider-silk proteins via other host organisms using genetic engineering technologies and in the synthesis of spider silk by mimicking the process of silk production in spiders. Nevertheless, to achieve such goal, a full comprehension of the factors that can affect the mechanical properties of the silk is therefore necessary.

13.2 Biology of Spider Silk

Silk protein, the spidroins, is stored in silk glands before being spun into silk fibers. Spiders produce as many as seven or eight different types of silks by various glands that are distinguished morphologically and histologically as: ampullate glands, piriform glands, aciniform glands, tubuliform glands, aggregate glands, and flagelliform glands (Foelix 2011).

Each type of gland secretes a unique kind of silk with its own specific characteristic via discrete spigots, and each type of silk gland differs from the others in size, location and morphology (Moon and An 2006; Foelix 2011). Specifically, web building spiders can produce six types of silks each exhibiting different function (Moon and An 2006) (Fig. 13.1). Ampullate glands produce fibers that are used in dragline, frame and radii thread; piriform glands produce fibers used in attachment disks; aciniform glands produce fibers used in swathing silk, silk decorations, male sperm web and soft inner layer of the egg sac; tubuliform glands produce fibers used in egg sac silk; aggregate glands produce the glue of sticky spirals; flagelliform glands produce the axial thread of sticky spiral fibers (Craig 2003; Foelix 2011). Aciniform silk is remarkable for its extreme toughness, and the dragline silk (i.e. major ampullate silk) is the strongest fiber (Blackledge and Hayashi 2006) (Fig. 13.1).

A typical silk gland consists of a tail, sac, and duct. The tail secretes most of the silk proteins, an aqueous liquid of hydrated silk molecules, from the columnar epithelial cells. These silk molecules are stored as an extremely concentrated liquid crystalline solution in the lumen of the sac (Knight and Vollrath 1999a, b; Lewis 2006). From the sac, the feedstock flows into the duct, typically tapered and of substantial length, allowing silk proteins to flow in patterns that resemble liquid crystalline flow and resulting in dehydration, aggregation, and precipitation into nanofibrillar structures (Vollrath et al. 2013). The duct is folded in a way similar to an elongated 'S' to give three limbs, which progressively narrow to form a hyperbolic die (Fig. 13.2). The narrowing of the duct diameter leads to the production of shear force that results in the alignment of the silk proteins into a fiber (Römer and Scheibel 2008). The duct terminates in a structure often termed the 'valve' (Wilson 1962a, b) or 'ratchet' (Vollrath et al. 1998), which squeezes the silk and provides shear stress. Finally, before exiting the spider the thread is stripped of its bathing and coating liquid by a tight cuticular lip at the spigot (Vollrath et al. 1998, 2013; Vollrath 2000).

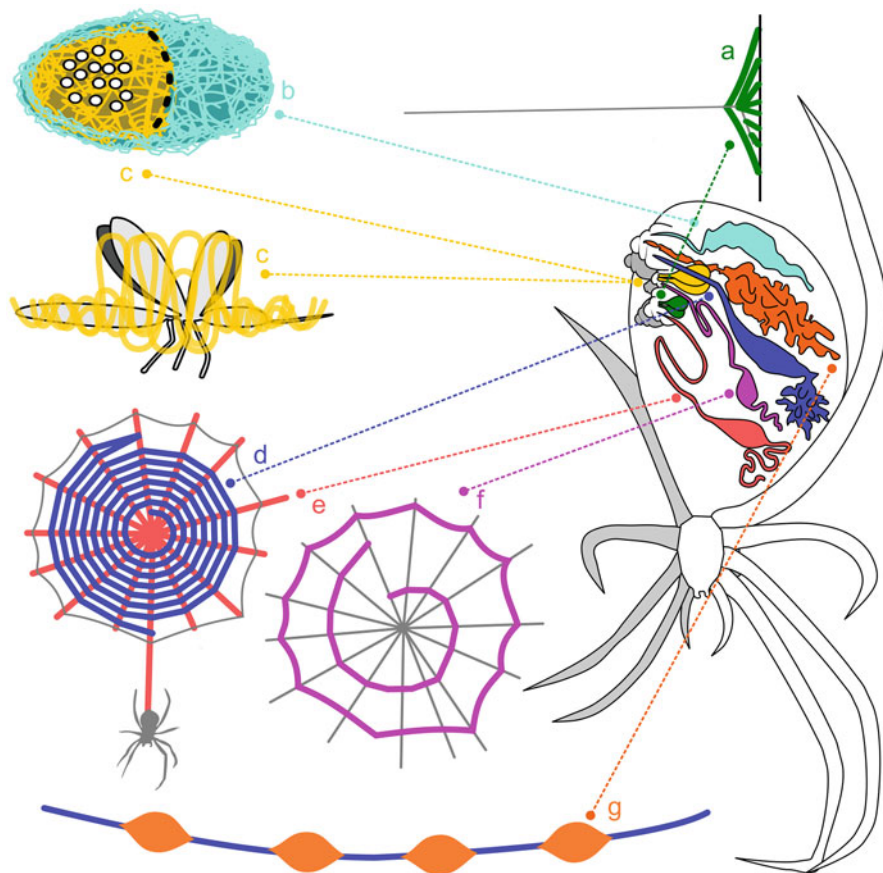


Fig. 13.1 Illustration of a typical orb-web spider's silk glands, different silks produced and their applications. (a) Piriform silk is used for the cement of joints and attachments; (b) Tubuliform silk is used in the outer layer of egg sac; (c) Aciniform silk is used in the inner layer of egg sac and prey wrapping; (d) Flagelliform silk is used as sticky capture spiral silk; (e) Major ampullate silk is used as dragline and structural silk; (f) Minor ampullate silk is used as auxiliary spiral silk; (g) Aggregate aqueous silk is produced in the aggregate gland

The relationship between mechanical properties and silk structures has been intensively studied by a great variety of experimental techniques, including X-ray diffraction (Grubb and Jelinski 1997; Parkhe et al. 1997), nuclear magnetic resonance (NMR) (Holland et al. 2008a, b), mechanical measurements (Thiel and Viney 1997; Blackledge et al. 2012), Raman spectroscopy (Sirichaisit et al. 2003; Rousseau et al. 2004), polarized Fourier transform infrared (FTIR) spectroscopy (Papadopoulos et al. 2007), scanning transmission X-ray microscopy (STXM) (Rousseau et al. 2007), and scanning electron microscopy and atomic force microscopy (Schäfer et al. 2008). The results showed that the mechanical properties of spider silk were largely dependent on their secondary structures, which were determined by the

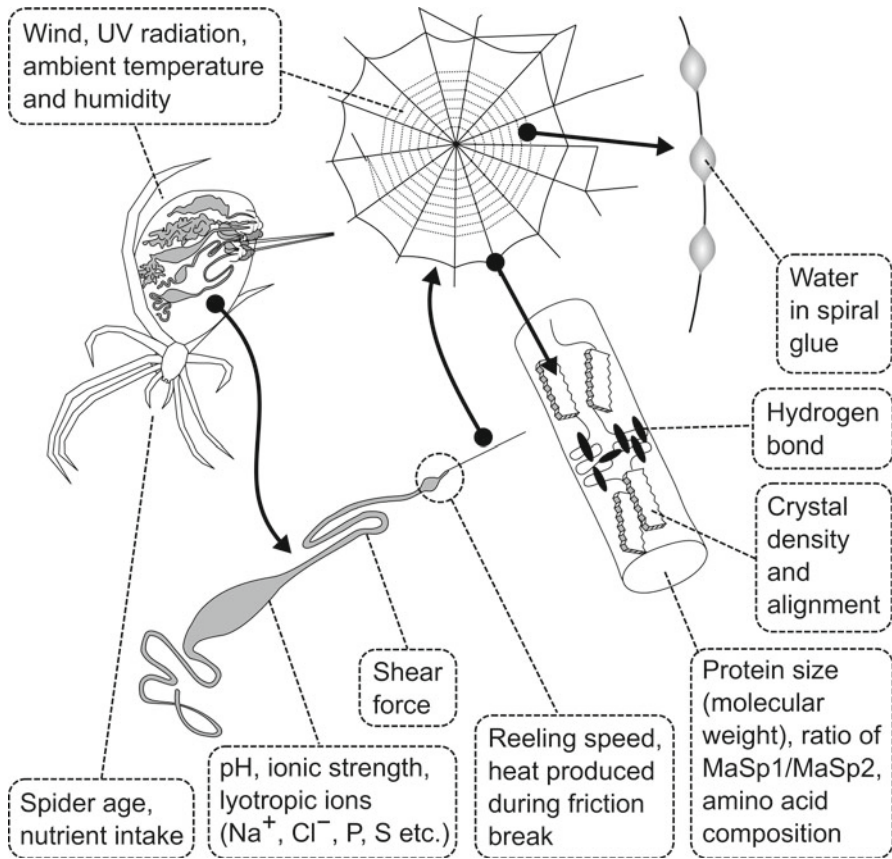


Fig. 13.2 Summary of the major factors influencing the mechanical properties of spider silk

intermolecular organization of the proteins (Rising et al. 2005). The secondary structures of silks include the highly oriented crystalline (the β -crystallites) and amorphous noncrystalline domains containing random coils, β -helices, and β -sheets (Simmons et al. 1996; Asakura et al. 2013), both of which are essential for the mechanical performance of the spider silks (Papadopoulos et al. 2007) (Fig. 13.3).

It is clear that both external and internal conditions of spiders affect silk production, and thus ultimately, the mechanical properties of the finished thread (Vollrath 2000). We disentangle various factors that may affect the mechanical properties of spider silks. A better understanding of these factors is needed in order to generate fibers for specific industrial applications, such as designing materials targeted for ultra and smart performance, or designing and fabricating new advanced materials with applications in kinetic energy buffering and absorption (Du et al. 2011). Major ampullate or dragline silk is one of the best studied silk type, so we mainly focus on dragline silk in this review.

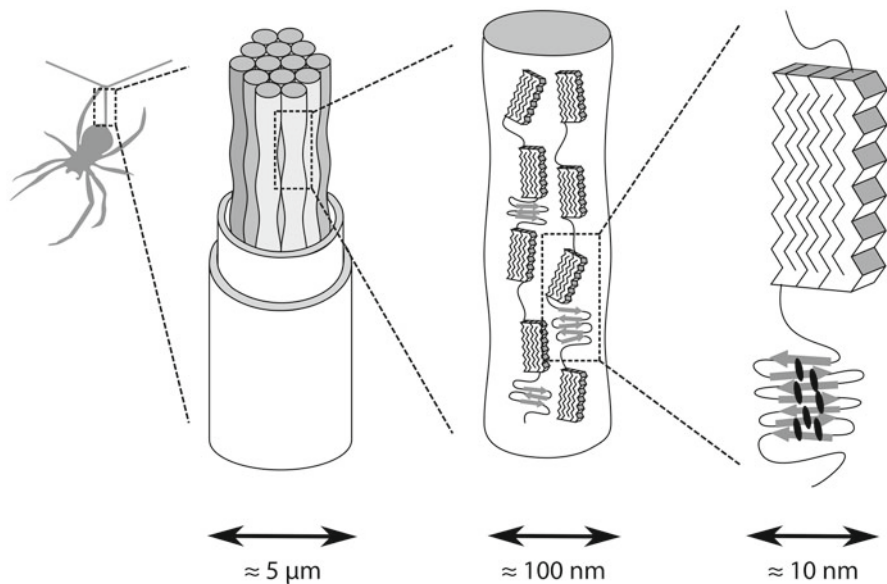


Fig. 13.3 Schematic diagram of the micro-structures of a spider's dragline silk. A single thread consists of multiple fibrils. The fibrils consist of a mix of highly crystalline domains (*rectangles*) interconnected by an amorphous matrix (canted sheet-like structures). The crystalline domains are highly oriented alanine-rich crystals of β -sheet, and the amorphous matrix is rich in glycine, containing all kinds of combinations of random coils, 3_1 helices, β -helices and β -turn or β -spiral conformations. The amorphous chains are connected by hydrogen bonds (*black oval spots*)

13.3 Factors Affecting Silk Mechanical Properties

13.3.1 Internal Factors

Environmental conditions such as reeling speed can affect silk properties (Madsen et al. 1999; Riekel et al. 1999). In forced silking experiments, higher reeling speeds led to silks with higher Young's modulus, breaking stress and lower breaking elongation (Madsen et al. 1999; Vollrath et al. 2001; Liu et al. 2005; Pérez-Rigueiro et al. 2005). It is probably because with increased reeling speeds the molecules and liquid crystals of the silk precursor proteins become more and more orientated. The increased orientation causes the silk to be stiffer and stronger but less extensible (Thiel and Viney 1997; Madsen et al. 1999; Knight et al. 2000; Vollrath et al. 2001; Liu et al. 2005). Du et al. (2006) found that the protein polypeptide chain network structure of spider dragline silks changes substantially with reeling speed. Wu et al. (2009) reported that the β -crystallites exhibit a better alignment at higher reeling speed, implying that the protein macromolecules in amorphous state are better aligned under higher reeling speed, and are more efficient in resisting external stress. After quantitatively examining the correlation between the content of the intramolecular β -sheets and the strain-hardening behavior of the *Nephila pilipes*

(Nephilidae) dragline silk at different reeling speed, Du et al. (2011) found that at higher reeling speeds, the spider is able to produce dragline fibers with higher amount of intramolecular β -sheets in the silk fibrils. Therefore, although the occurrence of intramolecular β -sheets is determined by the genetic makeup of silk, their quantity in silk fibrils can be varied by the reeling conditions, such as the reeling speeds of silk fibers. In the case of naturally spun dragline silk, there is considerable variability in mechanical properties both within a species and between threads from a single individual. Thus, it is possible that spiders are able to tailor the tensile behavior of the silk to match certain specific purpose by varying the fiber diameter and/or microstructures (Madsen et al. 1999). In fact, spiders can regulate the rate of spinning, as they possess muscular control of their spinnerets (Lewis 2006) and also use this as well as their legs as a friction brake to change the speed of spinning (Ortlepp and Gosline 2004). The upper limit to the forced silking speed might be determined by the temperature rise in the friction brake and surrounding tissues. The heat produced during the friction brake may affect the structure and mechanical properties of the dragline silk, because it may enhance the formation of β -sheet crystals and increase the axial alignment of these crystals when the silk is pulled out from the spigot in the final stages of silk production (Ortlepp and Gosline 2004). In addition, the structure of the thin layer of protein chains that coat on the surface of the spider silk can also vary with the reeling speed (Rousseau et al. 2007). The slowpull fiber contains a larger fraction of highly unoriented domains, while the protein chains are more homogeneously oriented in the fastpull fiber. The heat produced close to the spinnerets during the spinning, the protein dehydration or pH may also be involved (Rousseau et al. 2007). The biological meaning of the difference of mechanical silk property under different spinning speed is that fast spinning speed leads to a stiffer fiber that can better support the spider body weight when it attempts a fast vertical descent in response to conditions such as predator attack. On the other end, under slow spinning speeds the high density of the unoriented domains homogeneously disperses in the fiber core providing an interdigitated network that ensures good energy dissipation in the web structure.

During the passage of the spinning dope from the lumen through the spinning duct to the spigot, the dope is exposed to shear forces as it moves through a tube with small diameter. Such process has been considered to play important roles in the phase transition of the silk protein (Knight and Vollrath 1999b; Pérez-Rigueiro et al. 2001; Casem et al. 2002; Römer and Scheibel 2008). As the water is absorbed from the dope during its passage along the spinning duct (Tillinghast et al. 1984; Kojic et al. 2004), the concentration of proteins is increased with a consequent rise in the shear force between the proteins in the dope due to strengthened hydrophobic interactions (Eisoldt et al. 2010). In the spinning duct, the shear stress leads to increased aggregation of the glandular proteins which most likely triggers the assembly process (Eisoldt et al. 2010; Hagn et al. 2010). The shear force may affect the mechanical properties of the silk by determining the molecular orientation of the silk proteins just before they were pulled out and turned into fibers (Knight and Vollrath 1999b). It has been reported that during silk pulling out, the conformational transition of the glandular silk proteins from random-coil and polyproline-II

helix-like conformations to mainly β -sheet-rich structures is promoted (Vollrath and Knight 2001; Heim et al. 2009; Keten et al. 2010; Giesa et al. 2011). However, it is not clear how shear force affects phase conversion of the glandular proteins. After examining the elastic stiffness of the concentrated viscous protein solution of the dehydrated *N. clavipes* major ampullate gland by Brillouin light scattering, Koski et al. (2012) demonstrated that a simple static shear can induce rigidity to the spider silk. Future studies may explore how shear force affects the silk protein assemblies on a nano scale.

13.3.2 Environmental Factors

Spider major ampullate (MA) silks vary in mechanical properties in response to various environmental stimuli, such as humidity, ambient temperature, wind, and solar radiation (Blamires et al. 2012a) (Fig. 13.2).

13.3.2.1 Windy Condition

Environmental factors such as wind pose great challenges to the structure and functioning of spider webs, such as the web geometry and prey capture efficiency (Vollrath et al. 1997; Liao et al. 2009; Turner et al. 2011; Cranford et al. 2012; Wu et al. 2013). Webs that are exposed to strong wind must be composed of MA silk of particularly high strength to withstand wind drag and high extensibility to optimally capture prey without tearing (Liao et al. 2009; Cranford et al. 2012). It was reported that under windy condition, the garden cross spider *Araneus diadematus* (Araneidae) built smaller and rounder webs, laying down fewer capture spirals while increasing the distance between capture-spiral meshes (Vollrath et al. 1997). The persistent wind disturbances can cause the seashore-dwelling spider *Cyclosa mulmeinensis* (Araneidae) to build smaller webs composed of fewer but stronger MA silks (Liao et al. 2009). Compared to the MA silks produced by the forest dwelling *C. ginnaga*, those of *C. mulmeinensis* contained higher glycine and lower glutamine percentages, that may ultimately lead to higher tension and breaking energy (Liao et al. 2009; Wu et al. 2013). However, after comprehensively examining the amino acid composition, tensile mechanics, and crystalline structures of the *C. mulmeinensis* MA silk spun under windy and control conditions, Blamires et al. (2013) demonstrated that wind had affected the density and alignment of the crystalline β -sheets but not the composition of amino acids. The ultimate tensile strength of silk is controlled by the size and density of β -sheet nanocrystals. Nova et al. (2010) showed that the toughness of silks will increase when β -sheet nanocrystal size or density decreased. Wind, therefore, may induce *C. mulmeinensis* to tune the size of β -sheet nanocrystals or even the degree of alignment of the crystalline β -sheets (Blamires et al. 2013). However, so far it is unknown whether wind can exert influence on the protein alignment within the amorphous region, which in turn influence the

mechanical properties of the MA silk. In addition, wind may also affect the frictional stress at the spigot valve and may result in an increased shear force on the silk during pulling, which may promote greater alignment in the amorphous region and further strengthen the fibers (Blamires et al. 2013). These hypotheses are waiting to be tested in the future, and fully understanding of the impacts of the wind on the mechanics of the silk will inspire researchers and engineers interested in synthesizable and adaptable biomimetics (Cranford and Buehler 2010).

13.3.2.2 Ambient Temperature

Ambient temperature may also affect the mechanical properties of spider silk. Temperature is considered to influence a variety of behaviors because of the potential connection between metabolism and behavior (Careau et al. 2008; Houston 2010). In addition, the body temperature of ectothermic animals usually affects the speed of movement (Heinrich 1979). Hence, a spider's natural speed of web building (or drawing out of silk) is very much dictated by the ambient temperature (Vollrath and Knight 2001; Vollrath and Porter 2006a). Vollrath et al. (2001) showed that compared to *N. edulis* that were silked under cool condition, those silked under rising temperature produced silks with similar strength but with higher toughness and smaller diameter. Using the same species, Yang et al. (2005) showed that the tensile strength decreased with increasing temperature, and the elongation at break decreased with increasing temperature. Interestingly, the MA silk of *N. edulis* exhibited remarkable toughness at very low temperature ($-60\text{ }^{\circ}\text{C}$ to $0\text{ }^{\circ}\text{C}$), and they showed excellent heat resistance (up to $371\text{ }^{\circ}\text{C}$). This may be attributed to the thermal tolerance ability of the intermolecular hydrogen bonds (Yang et al. 2005). Cunniff et al. (1994) suggested that the lattice of hydrogen bonds holding together the β -sheet crystalline component of spider silk broke down at about $200\text{ }^{\circ}\text{C}$. Therefore, unlike most types of polymeric materials, spider silk is more ductile and tougher. The mechanical failure at low temperatures, however, has not been intensively studied. In addition, ambient temperature can also affect the viscosity of the capture spiral. When ambient temperature is low the glycoproteins (proteins that contain oligosaccharide chains covalently attached to polypeptide side-chains) will be stiffened, while the viscosity will be reduced when ambient temperature increases (Stellwagen et al. 2014). The impact of ambient temperature on the mechanical properties of the spider silk has significant consequences on the dispersal behaviors of spiders. Bonte et al. (2008) studied the dispersal behavior of *Erigone atra* (Linyphiidae) spiderlings, and found that long-distance ballooning occurred more frequently under cooler, spring-like conditions and short-distance rappelling was more likely to occur under warmer, summer-like conditions. They concluded that the thermal conditions experienced by the juvenile spiders during development may determine their dispersal tactics (Bonte et al. 2008). So far, however the underlying mechanism is still not clear. We hypothesize that spiders' dispersal tactics may be influenced by the mechanical properties of the silk, which in turn are affected by ambient temperatures. Appropriate temperature is also crucial during spinning

process because the transition from initiated stage to a final β -sheet-rich structure fiber is also affected by temperature (Kenney et al. 2002; Dicko et al. 2004b, 2006).

13.3.2.3 Humidity

Humidity is another important factor that affects the mechanical properties of spider silk. Dew and rain will lead spider dragline fibers to shrink significantly (up to 50 % of its initial length) and restrained silk generates stresses in excess of 50 MPa (Work 1981; Bell et al. 2002; Pérez-Rigueiro et al. 2003; Boutry and Blackledge 2010). This process is known as supercontraction (Work 1977a, 1981). Hydrogen-bonding is primarily responsible for the secondary and tertiary structuring of proteins, for it maintains the alignment of the amorphous regions of spidroins along the axis of major ampullate silk fibers (Asakura et al. 2013). Therefore, the molecular orientation is highly responsive to the environmental humidity (Vollrath and Porter 2006b; Holland et al. 2008b; Savage and Gosline 2008b; Creager et al. 2010). Water can disrupt hydrogen bonding, thereby mobilizing the spidroins and allowing them to assume a more disordered state (Jelinski et al. 1999; Yang et al. 2000; Eles and Michal 2004). The cyclic swelling and contraction under high humidity condition may inspire applications. For instance, the powerful cyclic contractions may trigger spider silk to act as a high performance mimic of biological muscles, which could potentially be applied in industry and biomedical sciences (Agnarsson et al. 2009). Supercontraction can maintain tension in webs and does not limit the ability of the web to maintain its mechanical integrity under wet conditions (Savage et al. 2004). However, there is growing evidence showing that supercontraction is a central feature of spinning process (Guinea et al. 2005), which provides spiders with a mechanism to control the overall alignment of molecules within the silk during the spinning process (Guinea et al. 2005; Liu et al. 2005). In addition, relative humidity also affects the glycoprotein of capture spiral (Opell et al. 2011; Sahni et al. 2011). The water contained in the aqueous glue that coats the sticky capture silk largely determines the thread characteristics, because it is essential for maintaining the elastic mobility of capture silk proteins (Vollrath and Edmonds 1989). After comparing the tensile properties of flagelliform fibers (i.e. axial fibers without the adhesive coating) at different relative humidity, Guinea et al. (2010) found that that water content can influence the tensile properties of flagelliform silk. Such finding was further confirmed by Perea et al. (2013), who reported that the properties of axial fibers of sticky spirals were dependent on both the alignment of the protein chains and the local relative humidity to which the fiber was subjected. However, supercontraction is regarded as a constraint of spider silk instead of an evolved feature, because it is the result of compromise between strength and extensibility (Liu et al. 2005). In addition, not all kinds of spider silks exhibit supercontraction. It was reported that this phenomenon is absent in the minor ampullate gland silk (miS) of two orb-web species, *Argiope trifasciata* (Araneidae) and *N. inaurata* (Guinea et al. 2012). The mechanisms underlying the aforementioned difference in supercontraction performance, such as the microstructural information, need to be clarified in the future.

13.3.2.4 Ultraviolet Radiation

Furthermore, environmental condition such as the ultraviolet (UV) radiation can also affect the mechanical properties of the native spider silks. For example, exposure to UV induces the draglines and capture threads of *N. clavata* to degrade. The UV irradiation may cause the scission of intermolecular bonds in a large proportion of the fibers (Kitagawa and Kitayama 1997). This may explain why some spiders need to renew their webs daily in response to exposure to solar energy. Yanagi et al. (2000) found that under γ -ray exposure, the silk decomposed in the amorphous region and the amino acid composition also changed.

13.3.3 Aging

Spider silks undergo physical and mechanical change with aging that also affect their mechanical properties (Agnarsson et al. 2008). At the initial stage of aging, the mechanical performance of silk fibers is even improved. Compared with fresh silks, aged silks are stiffer, have higher stress at yield, and the breaking force, elasticity and toughness are either improved or unaffected, which may due to an increase in structural alignment and organization of protein molecules. As the age extends, the mechanical properties deteriorate slowly, which may due to the breakdown of amino acids (Agnarsson et al. 2008). In addition, acid rain also affects the mechanical properties of the native silk, but only when the acidity is higher than pH 4 (Kitagawa and Kitayama 1997).

13.3.4 Composition of the Silk Proteins

Silk's extraordinary properties on the macroscopic scale ultimately stem from the balance of strength and extensibility at the molecular scale, as has been revealed extensively in the last decades in synthetic fibers. The general structure of most spidroins consists primarily of a central region of repetitive modules, with 10–100 of these modules making up the core region, and flanking N (amino) and C (carboxyl)-termini that are 100–200 amino acids in length (Ayoub et al. 2007). The repetitive modules are composed of hundreds of tandem repeats of different amino acid motifs, which are hypothesized to fold into various secondary structures, and contribute specific mechanical properties to natural as well as artificial silk fibers (Guerette et al. 1996; Hayashi and Lewis 1998; Hayashi et al. 1999; Hu et al. 2006; Teulé et al. 2007). Major ampullate silk is made up of two proteins: MaSp1 and MaSp2 (Hinman and Lewis 1992; Gatesy et al. 2001). MaSp1 consists of alanine (A_n) and glycine (GGX-) ($X=L, Y, Q,$ and A) repetitive motifs. MaSp2 includes a proline-containing motif (GPGXX) ($X=G, Q,$ and Y), in addition to the alanine (A_n) and glycine motifs (Parkhe et al. 1997; Jelinski et al. 1999; Gührs et al. 2000;

Rathore and Sogah 2001; Guehrs et al. 2008). These motifs are repeated several dozen times within a single spidroin core domain. Therefore, the relative quantity of MaSp1 and MaSp2 in a sample of MA silk are based on the relative amounts of alanine, glycine, and proline (Liu et al. 2007; Savage and Gosline 2008a, b). The $(GA)_n$ and $(A)_n$ motifs have been shown to create β -sheets which align parallel to the fiber's axis and bestow tensile strength and toughness in the fiber (Jelinski et al. 1999; Rathore and Sogah 2001). The GX motif forms a Gly II helix (van Beek et al. 2002; Holland et al. 2008a) and the GPGXX motif forms a spring-like type II β -turn, both are regarded to be responsible for elasticity of the fiber (Hinman and Lewis 1992; Hayashi and Lewis 1998; Jenkins et al. 2010). The mechanical properties of MA silk are the consequence of the ratio of MaSp1 and MaSp2 molecules (Creager et al. 2010; An et al. 2012). Hydrogen bonding is the primary interaction responsible for the secondary and tertiary structures of proteins and for the mechanical properties of the fiber (Keten et al. 2010; Asakura et al. 2013). Most orb web spiders have MA silks high in MaSp2 (Craig 2003). For example, in the MA silk of *N. clavipes* the percentage of proline can be more than 4% (Spohner et al. 2005). The principal reason is probably associated with the β -spiral molecular arrangement of the MaSp2 spidroin as it endows the silk with a combination of strength and extensibility (Hayashi et al. 1999; Liu et al. 2007). Amino acid composition of the spider silks is predicted to influence silks' mechanical properties because certain combination of amino acids may facilitate the production of silk proteins with determinable secondary and tertiary structures and properties (Hayashi et al. 1999; Rising et al. 2005). Brooks et al. (2008) showed that engineering the amino acid sequence can alter the mechanical properties of a synthetic silk fiber. The non-repetitive terminal motifs which flank the core domain have an α -helical secondary structure arranged in a five-helix bundle. These domains play roles in either high concentration spidroins storage in the spinning duct, or in fiber assembly (Heidebrecht et al. 2015). C-terminal non-repetitive domain is a constitutive dimer (Hagn et al. 2010), while the N-terminal domain dimerizes in response to a lowered pH (Jaudzems et al. 2012; Landreh et al. 2012). There is growing evidence showing that they have indirect influence on the mechanical properties of the fiber (Hagn et al. 2010; Heidebrecht et al. 2015). The N- and C- terminals are strongly conserved across different types of silks, both within and among species (Gatesy et al. 2001; Garb et al. 2010; Hagn et al. 2010). Future studies may investigate whether and how these conserved termini has contributed to the mechanical performance of the silk. In addition, the maximal mechanical properties of the silk fiber seem to strongly depend on the non-crystal region (Albertson et al. 2014; Hinman et al. 2014). Studies in such area may provide new perspective for understanding the relationship between silk proteins and their mechanical properties.

Studies of synthetic silk found that protein size also plays a key role in determining certain mechanical performance of silk fibers (Xia et al. 2010). A higher silk protein molecular weight is reported to associate with improved mechanical properties such as breaking strain, tenacity and Young's modulus (ratio of stress to strain) (Xia et al. 2010). It may be because fibers with larger protein molecules have more intermolecular interactions and fewer protein chain ends (An et al. 2011). Xia et al.

(2010) produced recombinant spider silk fibers with different protein size, and found that those with native-sized proteins have mechanical properties comparable to native silk, while those with lower molecular weight proteins did not yield similar properties. An et al. (2011) expressed two synthetic silk proteins based on *N. clavipes* major ampullate spidroin 1 (MaSp1) sequence, and found that fibers spun from the higher molecular weight protein had overall better mechanical properties.

13.3.5 Effects of Nutrient Intake

Nutrient intake, especially protein, can influence silk synthesis and expression, and consequently influence the mechanical performance of the silk (Blamires et al. 2012b; Blamires and Tso 2013). It has been shown that silk break elongation decreases with starvation (Madsen et al. 1999). Malnutrition may significantly affect the expression of the spider MA silk. For example, spiders express less MaSp2 in its MA silk under starvation stress (Zax et al. 2004; Guehrs et al. 2008). Prey variation can induce spiders to produce silks of different protein composition, that consequently may affect the mechanical properties of spider silk (Tso et al. 2005, 2007; Boutry and Blackledge 2008; Blamires et al. 2010). After feeding *N. pilipes* with different prey source, Tso et al. (2005) found that dragline of spiders fed with orthopteran prey contained significantly higher glutamine but lower alanine residues. Using the same species, Blamires et al. (2010) found that the MA silks from spiders fed with live crickets had greater percentages of glutamine, serine, alanine and glycine than those from spiders feeding on live flies. Proline composition of the silks, however, was unaffected by feeding regimen. They concluded that spiders can genetically alter their silk chemical compositions, and consequently, the mechanical properties upon exposure to different prey types (Blamires et al. 2010). Their later nutrient manipulation study with three spider species (*A. aetherea*, *Cyrtophora moluccensis* and *Leucauge blanda*) showed that protein concentration could influence the composition of glutamine, proline and alanine in silk, which in turn induced variation in silk extensibility and stiffness (Blamires et al. 2012b). However, it is unknown whether the expression of specific silk genes was altered upon different diet. Some silk amino acids, such as proline, are energetically costly or impossible for spiders to synthesize (Craig 2003). Therefore, the acquisition of such crucial component mainly relies on the silks being consumed and their compounds recycled into successive webs (Townley and Tillinghast 1988; Vollrath and Knight 2001; Craig 2003). So, spiders may partition digested protein between somatic processes and silk. Such protein allocation tradeoffs may partly explain why spiders receiving diets of low or no protein significantly alter the amino acid compositions of their silks (Blamires et al. 2012b). The silks of *N. pilipes* fed with protein-rich solution were stronger, stiffer and more extensible than those of spiders deprived of protein (Blamires et al. 2015). Results of amino acid analyses showed that the protein-deprived spiders down-regulated their MaSp2 expression, producing MA silks with lower percentage of glutamine, glycine, and proline (Blamires et al.

2015). This result suggested that that MaSp1 was preferentially expressed when spiders were under nutritional stress (Craig et al. 1999; Guehrs et al. 2008; Blamires et al. 2012b). Besides the influence on the MAS silks, nutrient intake can also affect the aggregate glues in the sticky spirals (Higgins and Rankin 1999; Townley et al. 2006). Blamires et al. (2014) found that when the orb web spider *N. clavipes* and the cobweb spider *Latrodectus hesperus* (Theridiidae) were deprived of protein intake, the gluey silks of both species turned stickier. Protein deprivation induced glue property variations, which might be attributed to the change of its biochemical composition. Ultimately, the impact of protein availability on the silks would impose an integral influence on web architecture and foraging strategies of web-building spiders (Vollrath and Samu 1997; Blamires and Tso 2013). For instance, cobweb spiders adjusted thread diameter when fed 'high' versus 'low' energy prey (Boutry and Blackledge 2008). In orb-web spiders *A. aemula* and *C. mulmeinensis*, the number of radii increased when fed high protein solutions (Blamires and Tso 2013). As mentioned previously, spiders may fine-tune the silk to improve their mechanical performance. However, there is growing evidence that spiders may alter a web's performance through structural changes in silk lines, such as nonlinear response of silk threads to strain and their geometrical arrangement in a web (Cranford et al. 2012; Cranford 2013; Meyer et al. 2014). Future studies may investigate whether there is a tradeoff between structural and material properties of spider silks.

13.3.6 Ions and pH in Silk Glands

The liquid–solid transition of silk proteins occurs in the spinning duct of the silk glands (Work 1977b). During the phase transition, soluble proteins with mainly helical and unordered random-coil structures convert into insoluble polymers dominated by β -sheet (Hijirida et al. 1996;). This process can be affected by a variety of parameters such as pH, ionic strength, and the concentration of lyotropic ions (Jin and Kaplan 2003; Chen et al. 2006; Landreh et al. 2010; Andersson et al. 2014; Kronqvist et al. 2014). During this process, intensive ion exchanges occur. When the spinning dope passes through the tapered S-shaped spinning duct, Na^+ and Cl^- composition decreased while K^+ , P and S increased (Knight and Vollrath 2001; Papadopoulos et al. 2007). During the spinning process, concentration of Na^+ is higher in the silk gland and is lower in the silk fiber, while the concentration of K^+ follows an opposite pattern (Chen et al. 2006). These ions play important roles during the phase transition of the silk proteins. Fourier transform infrared spectroscopy (FTIR), Raman and CD measurements demonstrate that Na^+ and K^+ can separately as well as jointly induce the conformation of spidroin from random coil and/or α -helix into β -sheet (Chen et al. 2002; Dicko et al. 2004a; Peng et al. 2005). Jin and Kaplan (2003) reported that the high concentration of NaCl in the silk gland can completely inhibit silk oligomer formation required for thread assembly because the hydrophilic interactions of the silk protein with the solvent dominate. As the spidroins are rapidly converted into a solid fiber in the spinning duct, the concentrations

of NaCl decrease and silk oligomerization is then enabled (Rising et al. 2005; Exler et al. 2007). Kurut et al. (2015) stated that high salt concentration reduced the thermodynamic dimerization of N-terminal (NT) domain of silk protein. Otkovs et al. (2015) also suggested that decreasing salt concentration was required in the dimerization of NT domain.

pH values also changed significantly during the processing of silks (Vollrath et al. 1998; Dicko et al. 2004c; Rammensee et al. 2008; Askarieh et al. 2010). The value decreases from above 7 in the spidroins storage sac to 5.7 in the middle of the spinning duct (Andersson et al. 2014). The MaSp1 NT domain is highly sensitive to changes in pH, which is proposed to function as a pH-regulated relay with a dual function: conferring solubility at high pH and facilitating fiber formation at low pH (Askarieh et al. 2010; Gaines et al. 2010; Hagn et al. 2011). When pH value is around 6, NT is a homodimer, whereas at high salt concentration and neutral pH, it is a monomeric five-helix bundle (Hagn et al. 2010, 2011; Jaudzems et al. 2012; Wallace and Shen 2012; Schwarze et al. 2013). Andersson et al. (2014) revealed that spidroin aggregation is prevented under more neutral pH conditions. However, under more acidic pH conditions, NT dimers firmly interconnect the spidroins and the C-terminal (CT) unfolds into β -sheet nuclei that can trigger rapid polymerization of the spidroins. Comparatively, the impact of pH on CT has not been intensively examined. Askarieh et al. (2010) pointed out that CT is indifferent to pH changes. However, Gauthier et al. (2014) stated that MaSp1 CT structure of *N. clavipes* is very sensitive to pH changes. Andersson et al. (2014) found that pH had opposite effects on the two domains' stability to temperature and urea. The NT dimerized at pH 6 in the beginning of the duct, and became increasingly stable as the pH dropped along the duct. In contrast, the C-terminal domain destabilized as the pH dropped, gradually unfolding until it formed the β -sheet at pH value of 5.5. The change of the pH value in the spinning duct has a close relationship with the concentration of CO₂, which is generated by carbonic anhydrase in the silk gland. The pH decreases along the gland, but the concentrations of both HCO₃⁻ and CO₂ increase (Andersson et al. 2014). Therefore, CO₂ in the silk gland may also affect the mechanical properties of the silk since it plays crucial roles in silk formation.

13.3.7 Biominerals and Polar Chemical Compounds in the Silk

Artificial biomaterial research has shown that supplementing low concentrations of biominerals, such as Zn-, Mn-, Ca-, or Cu- based minerals, can enhance the mechanical properties of tissues (Lichtenegger et al. 2002; Pontin et al. 2007; Cribb et al. 2008). Earlier studies showed that protein stability could be improved by chelation to metal ions or nanominerals due to the strengthening of the protein matrix (Kellis et al. 1991; Arnold and Zhang 1994). The technology of incorporating metal nanocomposites into spider silk to generate chimeric fusion proteins has been

mainly applied in medicines. For example, silk fabrics treated with silver hydrosol showed great antimicrobial activity (Kang et al. 2007; Gulrajani et al. 2008). However, few studies have explored the application potential of this technique to the synthesis of artificial silk fibers with desired mechanical properties. Foo et al. (2006) successfully introduced silica into MaSp1 protein of *N. clavipes* to obtain a novel family of chimeric proteins. They demonstrated that the nanocomposite morphology and structure could be regulated by controlling the processing conditions to produce films and fibers with different mechanical properties. Porter and Vollrath (2009) predicted that materials using the folded nanostructure of silk as a template for mineral-organic nanocomposites may achieve even higher strength and toughness than natural silks. Lee et al. (2009) incorporated zinc oxide (ZnO), titanium dioxide (TiO₂), and aluminum oxide (Al₂O₃) combined with water into the inner protein structures of the spider dragline silks by the multiple pulsed vapor-phase infiltration process, and they found the toughness of such silks to be greatly improved. After compositing regenerated silk fibroin (RSF) with nanoanatase TiO₂, Pan et al. (2014) found that the toughness of the artificial silk was greatly improved and exceeded that of silkworm silk. The RSF–TiO₂ fibers exhibited more α -helix/random coils, fewer β -sheets, smaller crystallites and lower crystallinity than the original RSF fiber. It is probably because the nanoanatase interacts strongly with the fibroin matrix through coordination complexes (Ti–protein) and hydrogen bonds, which prevent the conformation transition from random coil/ α -helix to β -sheet, and the crystallization is confined (Pan et al. 2014). Although the exact infiltration mechanisms and intermolecular bonding states between proteins and metals have not been determined (Lee et al. 2009), improving mechanical properties by incorporating minerals to change the structure of the fiber may be a promising direction for producing ultrastrong fibers.

In addition, treating silks with polar solvents or vapor always greatly reduces the stiffness and improves the breaking strain significantly (Shao and Vollrath 1999; Vehoff et al. 2007; Schäfer et al. 2008). Compared with polar solvents with larger molecules, those with smaller molecules can influence the mechanical properties of silks more intensively, as they penetrate the silk more easily and interact more strongly with polar groups of polypeptide chains inside the silk (Shao et al. 1999).

13.4 Current and Potential Biomimetic Applications

The primary motivation of spider silk research is to create fibers with desired mechanical properties. However, studies conducted with natural spider silk or recombinant spider silk protein analogues by experts from various disciplines using advanced technologies (Lewis 2006) inspired applications in various biomedical fields such as tissue engineering (Rising et al. 2011). The plasticity of spider silks renders them as ideal scaffolds that mimic the mechanical properties of the targeted tissue and could serve as matrix for adhesion, growth, migration, and differentiation of endogenous and/or implanted cells (Johansson and Rising 2014). For example, it

has been reported that spider silk fibers are viable graft and guiding material in promoting nerve regeneration (Allmeling et al. 2008; Radtke et al. 2011; Huang et al. 2012). Additionally, spider silks have also been successfully applied in fields such as skin replacement and regeneration (Wendt et al. 2011), cell adhesion and proliferation (Widhe et al. 2010, 2013; Wohlrab et al. 2012), artificial blood vessels (Xiang et al. 2011), wound suture (Lu et al. 2010; Kuhbier et al. 2011), drug encapsulation and delivery (Slota et al. 2008; Lammel et al. 2011; Wenk et al. 2011) and bone regeneration (Polo-Corrales et al. 2014). Recent studies showed that spider silks may also target the environment of the intermediate states that are formed during tissue repair (Polo-Corrales et al. 2014). Therefore, spider silks' application may expand to more fields in the future. As spider silks may support the growth of mammalian cells *in vitro* (Lintz and Scheibel 2013), they could be engineered as biocompatible implants with low risk of rejection (Rising et al. 2011). In addition, other applications have also been inspired by the special characteristics of spider silks. For example, the powerful cyclic contractions of spider dragline silks may allow it to act as a high performance mimic of biological muscles (Agnarsson et al. 2009). The water-collecting ability of capture silk of the cribellate spider *Uloborus walckenaerius* (Uloboridae) motivated scientists to design materials for collecting water from the air in arid areas (Zheng et al. 2010).

13.5 Summary and Future Expectations

Spider silk belongs to a unique family of biopolymers that can provide a valuable biomimetic reference point for biological and synthetic structural polymers (Porter and Vollrath 2009). We reviewed various factors that have been known to influence spider silks' mechanical properties. They include internal factors, such as the pulling/reeling speed of the silk, and environmental factors, such as humidity, ambient temperature, wind, solar radiation and nutrient intake. These factors affect silk properties by changing the structural alignment and organization of molecules, or the composition of proteins in the fiber. Studies of the spinning process revealed that factors such as shear force, ions and pH value in silk glands can also greatly influence the mechanical properties of the final product. Other factors such as silk age, silk protein size and crystal density and alignment can also influence its mechanical property. In addition, incorporating certain biominerals into the silk during synthesis to generate chimeric fusion proteins can adjust its mechanical properties to meet the needs of industry. A comprehensive understanding of these factors is essential for mass production and application. By outlining those factors here, we believe that it would be a useful reference for researchers who are interested in designing silk fibers for specific applications. Recently, certain important advances have been made towards generating spider silk mimics, such as characterization of full-length spidroins (Chen et al. 2012) and sequencing of spider genomes (Sanggaard et al. 2014). However, there are also challenges needing to overcome, such as how to keep recombinant spidroins soluble at high concentrations without the use of harsh

solvents, and how to control the effect of CO₂ on the spidroins during spinning. We believe that the technological progresses obtained so far, when integrated with our understanding of mechanisms occurred during natural spinning process of spider silk, would enable researchers to produce biomimetics for various purposes in the near future.

References

- Agnarsson I, Boutry C, Blackledge TA (2008) Spider silk aging: initial improvement in a high performance material followed by slow degradation. *J Exp Zool A* 309A:494–504
- Agnarsson I, Dhinojwala A, Sahni V, Blackledge TA (2009) Spider silk as a novel high performance biomimetic muscle driven by humidity. *J Exp Biol* 212:1989–1993
- Albertson AE, Teulé F, Weber W, Yarger JL, Lewis RV (2014) Effects of different post-spin stretching conditions on the mechanical properties of synthetic spider silk fibers. *J Mech Behav Biomed* 29:225–234
- Allmeling C, Jokuszies A, Reimers K, Kall S, Choi CY, Brandes G, Kasper C, Scheper T, Guggenheim M, Vogt PM (2008) Spider silk fibres in artificial nerve constructs promote peripheral nerve regeneration. *Cell Prolif* 41:408–420
- An B, Hinman MB, Holland GP, Yarger JL, Lewis RV (2011) Inducing β -sheets formation in synthetic spider silk fibers by aqueous post-spin stretching. *Biomacromolecules* 12:2375–2381
- An B, Jenkins JE, Sampath S, Holland GP, Hinman M, Yarger JL, Lewis R (2012) Reproducing natural spider silks' copolymer behavior in synthetic silk mimics. *Biomacromolecules* 13:3938–3948
- Andersson M, Chen G, Otikovs M, Landreh M, Nordling K, Kronqvist N, Westermarck P, Jörnvall H, Knight S, Ridderstråle Y, Holm L, Meng Q, Jaudzems K, Chesler M, Johansson J, Rising A (2014) Carbonic anhydrase generates CO₂ and H⁺ that drive spider silk formation via opposite effects on the terminal domains. *PLoS Biol* 12:e1001921
- Arnold FH, Zhang JH (1994) Metal-mediated protein stabilization. *Trends Biotechnol* 12:189–192
- Asakura T, Suzuki Y, Nakazawa Y, Holland GP, Yarger JL (2013) Elucidating silk structure using solid-state NMR. *Soft Matter* 9:11440–11450
- Askarieh G, Hedhammar M, Nordling K, Saenz A, Casals C, Rising A, Johansson J, Knight SD (2010) Self-assembly of spider silk proteins is controlled by a pH-sensitive relay. *Nature* 465:236–238
- Ayoub NA, Garb JE, Tinghitella RM, Collin MA, Hayashi CY (2007) Blueprint for a high-performance biomaterial: full-length spider dragline silk genes. *PLoS One* 2:e514
- Bell FI, McEwen IJ, Viney C (2002) Fibre science: supercontraction stress in wet spider dragline. *Nature* 416:37
- Blackledge TA, Hayashi CY (2006) Silken toolkits: biomechanics of silk fibers spun by the orb web spider *Argiope argentata* (Fabricius 1775). *J Exp Biol* 209:2452–2461
- Blackledge TA, Pérez-Rigueiro J, Plaza GR, Perea B, Navarro A, Guinea GV, Elices M (2012) Sequential origin in the high performance properties of orb spider dragline silk. *Sci Rep* 2:782
- Blamires SJ, Tso IM (2013) Nutrient-mediated architectural plasticity of a predatory trap. *PLoS One* 8:e54558
- Blamires SJ, Chao IC, Tso IM (2010) Prey type, vibrations and handling interactively influence spider silk expression. *J Exp Biol* 213:3906–3910
- Blamires SJ, Wu CL, Blackledge TA, Tso IM (2012a) Environmentally induced post-spin property changes in spider silks: influences of web type, spidroin composition and ecology. *Biol J Linn Soc* 106:580–588

- Blamires SJ, Wu CL, Tso IM (2012b) Variation in protein intake induces variation in spider silk expression. *PLoS One* 7:e31626
- Blamires SJ, Wu CC, Wu CL, Sheu HS, Tso IM (2013) Uncovering spider silk nanocrystalline variations that facilitate wind-induced mechanical property changes. *Biomacromolecules* 14:3484–3490
- Blamires SJ, Sahni V, Dhinojwala A, Blackledge TA, Tso IM (2014) Nutrient deprivation induces property variations in spider gluey silk. *PLoS One* 9:e88487
- Blamires SJ, Liao CP, Chang CK, Chuang YC, Wu CL, Blackledge TA, Sheu HS, Tso IM (2015) Mechanical performance of spider silk is robust to nutrient-mediated changes in protein composition. *Biomacromolecules* 16:1218–1225
- Bonte D, Travis JMJ, De Clercq N, Zwertvaegher I, Lens L (2008) Thermal conditions during juvenile development affect adult dispersal in a spider. *Proc Natl Acad Sci U S A* 105:17000–17005
- Boutry C, Blackledge TA (2008) The common house spider alters the material and mechanical properties of cobweb silk in response to different prey. *J Exp Zool A* 309A:542–552
- Boutry C, Blackledge TA (2010) Evolution of supercontraction in spider silk: structure–function relationship from tarantulas to orb-weavers. *J Exp Biol* 213:3505–3514
- Brooks AE, Stricker SM, Joshi SB, Kamerzell TJ, Middaugh CR, Lewis RV (2008) Properties of synthetic spider silk fibers based on *Argiope aurantia* MaSp2. *Biomacromolecules* 9:1506–1510
- Careau V, Thomas D, Humphries MM, Réale D (2008) Energy metabolism and animal personality. *Oikos* 117:641–653
- Casem ML, Tran LPP, Moore AMF (2002) Ultrastructure of the major ampullate gland of the black widow spider, *Latrodectus hesperus*. *Tissue Cell* 34:427–436
- Chen X, Knight DP, Shao ZZ, Vollrath F (2002) Conformation transition in silk protein films monitored by time-resolved Fourier transform infrared spectroscopy: effect of potassium ions on *Nephila* spidroin films. *Biochemistry* 41:14944–14950
- Chen X, Shao ZZ, Vollrath F (2006) The spinning processes for spider silk. *Soft Matter* 2:448–451
- Chen G, Liu X, Zhang Y, Lin S, Yang Z, Johansson J, Rising A, Meng Q (2012) Full-length minor ampullate spidroin gene sequence. *PLoS One* 7:e52293
- Craig CL (2003) Spiderwebs and silk: tracing evolution from molecules to genes to phenotypes. Oxford University Press, Oxford
- Craig CL, Hsu M, Kaplan D, Pierce NE (1999) A comparison of the composition of silk proteins produced by spiders and insects. *Int J Biol Macromol* 24:109–118
- Cranford SW (2013) Increasing silk fibre strength through heterogeneity of bundled fibrils. *J R Soc Interface* 10:20130148
- Cranford SW, Buehler MJ (2010) Materiomics: biological protein materials, from nano to macro. *Nanotechnol Sci Appl* 3:127–148
- Cranford SW, Tarakanova A, Pugno NM, Buehler MJ (2012) Nonlinear material behaviour of spider silk yields robust webs. *Nature* 482:72–76
- Creager MS, Jenkins JE, Thagard-Yeaman LA, Brooks AE, Jones JA, Lewis RV, Holland GP, Yarger JL (2010) Solid-state NMR comparison of various spiders' dragline silk fiber. *Biomacromolecules* 11:2039–2043
- Cribb BW, Stewart A, Huang H, Truss R, Noller B, Rasch R, Zalucki MP (2008) Insect mandibles—comparative mechanical properties and links with metal incorporation. *Naturwissenschaften* 95:17–23
- Cunniff PM, Fossey SA, Auerbach MA, Song JW, Kaplan DL, Adams WW, Eby RK, Mahoney D, Vezie DL (1994) Mechanical and thermal properties of dragline silk from the spider *Nephila clavipes*. *Polym Adv Technol* 5:401–410
- Dicko C, Kenney JM, Knight D, Vollrath F (2004a) Transition to a β -sheet-rich structure in spidroin in vitro: the effects of pH and cations. *Biochemistry* 43:14080–14087

- Dicko C, Knight D, Kenney JM, Vollrath F (2004b) Secondary structures and conformational changes in flagelliform, cylindrical, major, and minor ampullate silk proteins. Temperature and concentration effects. *Biomacromolecules* 5:2105–2115
- Dicko C, Vollrath F, Kenney JM (2004c) Spider silk protein refolding is controlled by changing pH. *Biomacromolecules* 5:704–710
- Dicko C, Kenney JM, Vollrath F (2006) β -silks: enhancing and controlling aggregation. In: *Advances in protein chemistry*. Academic Press, New York, pp 17–53
- Du N, Liu XY, Narayanan J, Li L, Lim MLM, Li D (2006) Design of superior spider silk: from nanostructure to mechanical properties. *Biophys J* 91:4528–4535
- Du N, Yang Z, Liu XY, Li Y, Xu HY (2011) Structural origin of the strain-hardening of spider silk. *Adv Funct Mater* 21:772–778
- Eisoldt L, Hardy JG, Heim M, Scheibel TR (2010) The role of salt and shear on the storage and assembly of spider silk proteins. *J Struct Biol* 170:413–419
- Eles PT, Michal CA (2004) Strain dependent local phase transitions observed during controlled supercontraction reveal mechanisms in spider silk. *Macromolecules* 37:1342–1345
- Exler JH, Hümmerich D, Scheibel T (2007) The amphiphilic properties of spider silks are important for spinning. *Angew Chem Int Ed* 46:3559–3562
- Foelix RF (2011) *Biology of spiders*, 3rd edn. Oxford University Press, Oxford
- Foo CWP, Patwardhan SV, Belton DJ, Kitchel B, Anastasiades D, Huang J, Naik RR, Perry CC, Kaplan DL (2006) Novel nanocomposites from spider silk–silica fusion (chimeric) proteins. *Proc Natl Acad Sci U S A* 103:9428–9433
- Gaines WA, Sehorn MG, Marcotte WR (2010) Spidroin N-terminal domain promotes a pH-dependent association of silk proteins during self-assembly. *J Biol Chem* 285:40745–40753
- Garb J, Ayoub N, Hayashi C (2010) Untangling spider silk evolution with spidroin terminal domains. *BMC Evol Biol* 10:243
- Gatesy J, Hayashi C, Motriuk D, Woods J, Lewis R (2001) Extreme diversity, conservation, and convergence of spider silk fibroin sequences. *Science* 291:2603–2605
- Gauthier M, Leclerc J, Lefèvre T, Gagné SM, Auger M (2014) Effect of pH on the structure of the recombinant C-terminal domain of *Nephila clavipes* dragline silk protein. *Biomacromolecules* 15:4447–4454
- Giesa T, Arslan M, Pugno NM, Buehler MJ (2011) Nanoconfinement of spider silk fibrils begets superior strength, extensibility, and toughness. *Nano Lett* 11:5038–5046
- Gosline JM, Guerette PA, Ortlepp CS, Savage KN (1999) The mechanical design of spider silks: from fibroin sequence to mechanical function. *J Exp Biol* 202:3295–3303
- Grubb DT, Jelinski LW (1997) Fiber morphology of spider silk: the effects of tensile deformation. *Macromolecules* 30:2860–2867
- Guehrs KH, Schlott B, Grosse F, Weisshart K (2008) Environmental conditions impinge on dragline silk protein composition. *Insect Mol Biol* 17:553–564
- Guerette PA, Ginzinger DG, Weber BHF, Gosline JM (1996) Silk properties determined by gland-specific expression of a spider fibroin gene family. *Science* 272:112–115
- Gühns KH, Weisshart K, Grosse F (2000) Lessons from nature — protein fibers. *Rev Mol Biotechnol* 74:121–134
- Guinea GV, Elices M, Pérez-Rigueiro J, Plaza GR (2005) Stretching of supercontracted fibers: a link between spinning and the variability of spider silk. *J Exp Biol* 208:25–30
- Guinea GV, Cerdeira M, Plaza GR, Elices M, Pérez-Rigueiro J (2010) Recovery in viscid line fibers. *Biomacromolecules* 11:1174–1179
- Guinea GV, Elices M, Plaza GR, Perea GB, Daza R, Riekel C, Agulló-Rueda F, Hayashi C, Zhao Y, Pérez-Rigueiro J (2012) Minor ampullate silks from *Nephila* and *Argiope* spiders: tensile properties and microstructural characterization. *Biomacromolecules* 13:2087–2098
- Gulrajani ML, Gupta D, Periyasamy S, Muthu SG (2008) Preparation and application of silver nanoparticles on silk for imparting antimicrobial properties. *J Appl Polym Sci* 108:614–623
- Hagn F, Eisoldt L, Hardy JG, Vendrely C, Coles M, Scheibel T, Kessler H (2010) A conserved spider silk domain acts as a molecular switch that controls fibre assembly. *Nature* 465:239–242

- Hagn F, Thamm C, Scheibel T, Kessler H (2011) pH-dependent dimerization and salt-dependent stabilization of the N-terminal domain of spider dragline silk-implications for fiber formation. *Angew Chem Int Ed* 50:310–313
- Hardy JG, Scheibel TR (2009) Production and processing of spider silk proteins. *J Polym Sci A1* 47:3957–3963
- Hayashi CY, Lewis RV (1998) Evidence from flagelliform silk cDNA for the structural basis of elasticity and modular nature of spider silks. *J Mol Biol* 275:773–784
- Hayashi CY, Shipley NH, Lewis RV (1999) Hypotheses that correlate the sequence, structure, and mechanical properties of spider silk proteins. *Int J Biol Macromol* 24:271–275
- Heidebrecht A, Eisoldt L, Diehl J, Schmidt A, Geffers M, Lang G, Scheibel T (2015) Biomimetic fibers made of recombinant spidroins with the same toughness as natural spider silk. *Adv Mater* 27:2189–2194
- Heim M, Keerl D, Scheibel T (2009) Spider silk: from soluble protein to extraordinary fiber. *Angew Chem Int Ed* 48:3584–3596
- Heinrich B (1979) Keeping a cool head: honeybee thermoregulation. *Science* 205:1269–1271
- Higgins L, Rankin MA (1999) Nutritional requirements for web synthesis in the tetragnathid spider *Nephila clavipes*. *Physiol Entomol* 24:263–270
- Hijirida DH, Do KG, Michal C, Wong S, Zax D, Jelinski LW (1996) ¹³C NMR of *Nephila clavipes* major ampullate silk gland. *Biophys J* 71:3442
- Hinman MB, Lewis RV (1992) Isolation of a clone encoding a second dragline silk fibroin. *Nephila clavipes* dragline silk is a two-protein fiber. *J Biol Chem* 267:19320–19324
- Hinman MB, Teulé F, Perry D, An B, Adrianos S, Albertson A, Lewis R (2014) Modular spider silk fibers: defining new modules and optimizing fiber properties. In: *Biotechnology of silk*. Springer, New York, pp 137–164
- Holland GP, Creager MS, Jenkins JE, Lewis RV, Yarger JL (2008a) Determining secondary structure in spider dragline silk by carbon-carbon correlation solid-state NMR spectroscopy. *J Am Chem Soc* 130:9871–9877
- Holland GP, Jenkins JE, Creager MS, Lewis RV, Yarger JL (2008b) Solid-state NMR investigation of major and minor ampullate spider silk in the native and hydrated states. *Biomacromolecules* 9:651–657
- Houston AI (2010) Evolutionary models of metabolism, behaviour and personality. *Philos Trans R Soc Lond Ser B Biol Sci* 365:3969–3975
- Hu X, Vasanthavada K, Kohler K, McNary S, Moore A, Vierra C (2006) Molecular mechanisms of spider silk. *Cell Mol Life Sci* 63:1986–1999
- Huang W, Begum R, Barber T, Ibba V, Tee NCH, Hussain M, Arastoo M, Yang Q, Robson LG, Lesage S, Gheysens T, Skaer NJV, Knight DP, Priestley JV (2012) Regenerative potential of silk conduits in repair of peripheral nerve injury in adult rats. *Biomaterials* 33:59–71
- Jaudzems K, Askarieh G, Landreh M, Nordling K, Hedhammar M, Jörnvall H, Rising A, Knight SD, Johansson J (2012) pH-dependent dimerization of spider silk N-terminal domain requires relocation of a wedged tryptophan side chain. *J Mol Biol* 422:477–487
- Jelinski LW, Blye A, Liivak O, Michal C, LaVerde G, Seidel A, Shah N, Yang Z (1999) Orientation, structure, wet-spinning, and molecular basis for supercontraction of spider dragline silk. *Int J Biol Macromol* 24:197–201
- Jenkins JE, Creager MS, Butler EB, Lewis RV, Yarger JL, Holland GP (2010) Solid-state NMR evidence for elastin-like β -turn structure in spider dragline silk. *Chem Commun* 46:6714–6716
- Jin HJ, Kaplan DL (2003) Mechanism of silk processing in insects and spiders. *Nature* 424:1057–1061
- Johansson J, Rising A (2014) Evaluation of functionalized spider silk matrices: choice of cell types and controls are important for detecting specific effects. *Front Bioeng Biotechnol* 2:50
- Kang M, Jung R, Kim HS, Youk JH, Jin HJ (2007) Silver nanoparticles incorporated electrospun silk fibers. *J Nanosci Nanotechnol* 7:3888–3891

- Kellis JT, Todd RJ, Arnold FH (1991) Protein stabilization by engineered metal chelation. *Nat Biotechnol* 9:994–995
- Kenny JM, Knight D, Wise MJ, Vollrath F (2002) Amyloidogenic nature of spider silk. *Eur J Biochem* 269:4159–4163
- Keten S, Xu Z, Ihle B, Buehler MJ (2010) Nanoconfinement controls stiffness, strength and mechanical toughness of β -sheet crystals in silk. *Nat Mater* 9:359–367
- Kitagawa M, Kitayama T (1997) Mechanical properties of dragline and capture thread for the spider *Nephila clavata*. *J Mater Sci* 32:2005–2012
- Knight D, Vollrath F (1999a) Hexagonal columnar liquid crystal in the cells secreting spider silk. *Tissue Cell* 31:617–620
- Knight DP, Vollrath F (1999b) Liquid crystals and flow elongation in a spider's silk production line. *Proc R Soc B* 266:519–523
- Knight DP, Vollrath F (2001) Changes in element composition along the spinning duct in a *Nephila* spider. *Naturwissenschaften* 88:179–182
- Knight DP, Knight MM, Vollrath F (2000) Beta transition and stress-induced phase separation in the spinning of spider dragline silk. *Int J Biol Macromol* 27:205–210
- Kojic N, Kojic M, Gudlavalleti S, McKinley G (2004) Solvent removal during synthetic and *Nephila* fiber spinning. *Biomacromolecules* 5:1698–1707
- Koski KJ, McKiernan K, Akhenblit P, Yarger JL (2012) Shear-induced rigidity in spider silk glands. *Appl Phys Lett* 101:103701
- Kronqvist N, Otikovs M, Chmyrov V, Chen G, Andersson M, Nordling K, Landreh M, Sarr M, Jörnvall H, Wennmalm S, Widengren J, Meng Q, Rising A, Otzen D, Knight SD, Jaudzems K, Johansson J (2014) Sequential pH-driven dimerization and stabilization of the N-terminal domain enables rapid spider silk formation. *Nat Commun* 5:3254
- Kuhbier JW, Reimers K, Kasper C, Allmeling C, Hillmer A, Menger B, Vogt PM, Radtke C (2011) First investigation of spider silk as a braided microsurgical suture. *J Biomed Mater Res A* 97B:381–387
- Kurut A, Dicko C, Lund M (2015) Dimerization of terminal domains in spiders silk proteins is controlled by electrostatic anisotropy and modulated by hydrophobic patches. *ACS Biomater Sci Eng* 1:363–371
- Lammel A, Schwab M, Hofer M, Winter G, Scheibel T (2011) Recombinant spider silk particles as drug delivery vehicles. *Biomaterials* 32:2233–2240
- Landreh M, Askarieh G, Nordling K, Hedhammar M, Rising A, Casals C, Astorga-Wells J, Alvelius G, Knight SD, Johansson J, Jörnvall H, Bergman T (2010) A pH-dependent dimer lock in spider silk protein. *J Mol Biol* 404:328–336
- Landreh M, Johansson J, Rising A, Presto J, Jörnvall H (2012) Control of amyloid assembly by autoregulation. *Biochem J* 447:185–192
- Lee SM, Pippel E, Gösele U, Dresbach C, Qin Y, Chandran CV, Bräuniger T, Hause G, Knez M (2009) Greatly increased toughness of infiltrated spider silk. *Science* 324:488–492
- Lewis RV (2006) Spider silk: ancient ideas for new biomaterials. *Chem Rev* 106:3762–3774
- Liao CP, Chi KJ, Tso IM (2009) The effects of wind on trap structural and material properties of a sit-and-wait predator. *Behav Ecol* 20:1194–1203
- Lichtenegger HC, Schöberl T, Bartl MH, Waite H, Stucky GD (2002) High abrasion resistance with sparse mineralization: copper biomineral in worm jaws. *Science* 298:389–392
- Lintz ES, Scheibel TR (2013) Dragline, egg stalk and byssus: a comparison of outstanding protein fibers and their potential for developing new materials. *Adv Funct Mater* 23:4467–4482
- Liu Y, Shao ZZ, Vollrath F (2005) Relationships between supercontraction and mechanical properties of spider silk. *Nat Mater* 4:901–905
- Liu Y, Spöner A, Porter D, Vollrath F (2007) Proline and processing of spider silks. *Biomacromolecules* 9:116–121
- Lu B, Zheng J, Chen D, Li M (2010) Evaluation of a new type of wound dressing made from recombinant spider silk protein using rat models. *Burns* 36:891–896

- Madsen B, Shao ZZ, Vollrath F (1999) Variability in the mechanical properties of spider silks on three levels: interspecific, intraspecific and intraindividual. *Int J Biol Macromol* 24:301–306
- Meyer A, Pugno NM, Cranford SW (2014) Compliant threads maximize spider silk connection strength and toughness. *J R Soc Interface* 11:20140561
- Moon MJ, An JS (2006) Microstructure of the silk apparatus of the comb-footed spider, *Achaearanea tepidariorum* (Araneae: Theridiidae). *Entomol Res* 36:56–63
- Nova A, Keten S, Pugno NM, Redaelli A, Buehler MJ (2010) Molecular and nanostructural mechanisms of deformation, strength and toughness of spider silk fibrils. *Nano Lett* 10:2626–2634
- Opell BD, Karinshak SE, Sigler MA (2011) Humidity affects the extensibility of an orb-weaving spider's viscous thread droplets. *J Exp Biol* 214:2988–2993
- Ortlepp CS, Gosline JM (2004) Consequences of forced silking. *Biomacromolecules* 5:727–731
- Otikovs M, Chen G, Nordling K, Landreh M, Meng Q, Jörnvall H, Kronqvist N, Rising A, Johansson J, Jaudzems K (2015) Diversified structural basis of a conserved molecular mechanism for pH-dependent dimerization in spider silk N-terminal domains. *ChemBioChem* 16:1720–1724
- Pan H, Zhang Y, Shao H, Hu X, Li X, Tian F, Wang J (2014) Nanoconfined crystallites toughen artificial silk. *J Mater Chem* 2:1408–1414
- Papadopoulos P, Sölter J, Kremer F (2007) Structure-property relationships in major ampullate spider silk as deduced from polarized FTIR spectroscopy. *Eur Phys J E* 24:193–199
- Parkhe AD, Seeley SK, Gardner K, Thompson L, Lewis RV (1997) Structural studies of spider silk proteins in the fiber. *J Mol Recognit* 10:1–6
- Peng XN, Shao ZZ, Chen X, Knight DP, Wu PY, Vollrath F (2005) Further investigation on potassium-induced conformation transition of *Nephila* spidroin film with two-dimensional infrared correlation spectroscopy. *Biomacromolecules* 6:302–308
- Perea GB, Plaza GR, Guinea GV, Elices M, Velasco B, Pérez-Rigueiro J (2013) The variability and interdependence of spider viscid line tensile properties. *J Exp Biol* 216:4722–4728
- Pérez-Rigueiro J, Elices M, Llorca J, Viney C (2001) Tensile properties of *Attacus atlas* silk submerged in liquid media. *J Appl Polym Sci* 82:53–62
- Pérez-Rigueiro J, Elices M, Guinea GV (2003) Controlled supercontraction tailors the tensile behaviour of spider silk. *Polymer* 44:3733–3736
- Pérez-Rigueiro J, Elices M, Plaza G, Real JJ, Guinea GV (2005) The effect of spinning forces on spider silk properties. *J Exp Biol* 208:2633–2639
- Platnick NI (2013) The world spider catalog, version 14.0. American Museum of Natural History
- Polo-Corrales L, Latorre-Estevés M, Ramirez-Vick JE (2014) Scaffold design for bone regeneration. *J Nanosci Nanotechnol* 14:15–56
- Pontin MG, Moses DN, Waite JH, Zok FW (2007) A nonmineralized approach to abrasion-resistant biomaterials. *Proc Natl Acad Sci U S A* 104:13559–13564
- Porter D, Vollrath F (2009) Silk as a biomimetic ideal for structural polymers. *Adv Mater* 21:487–492
- Radtke C, Allmeling C, Waldmann KH, Reimers K, Thies K, Schenk HC, Hillmer A, Guggenheim M, Brandes G, Vogt PM (2011) Spider silk constructs enhance axonal regeneration and remyelination in long nerve defects in sheep. *PLoS One* 6:e16990
- Rammensee S, Slotta U, Scheibel T, Bausch AR (2008) Assembly mechanism of recombinant spider silk proteins. *Proc Natl Acad Sci U S A* 105:6590–6595
- Rathore O, Sogah DY (2001) Self-assembly of β -sheets into nanostructures by poly (alanine) segments incorporated in multiblock copolymers inspired by spider silk. *J Am Chem Soc* 123:5231–5239
- Riekel C, Muller M, Vollrath F (1999) In situ X-ray diffraction during forced silking of spider silk. *Macromolecules* 32:4464–4466
- Rising A, Nimmervoll H, Grip S, Fernandez-Arias A, Storckenfeldt E, Knight DP, Vollrath F, Engstrom W (2005) Spider silk proteins – mechanical property and gene sequence. *Zool Sci* 22:273–281

- Rising A, Widhe M, Johansson J, Hedhammar M (2011) Spider silk proteins: recent advances in recombinant production, structure–function relationships and biomedical applications. *Cell Mol Life Sci* 68:169–184
- Römer L, Scheibel T (2008) The elaborate structure of spider silk. *Prion* 2:154–161
- Rousseau ME, Lefèvre T, Beaulieu L, Asakura T, Pézolet M (2004) Study of protein conformation and orientation in silkworm and spider silk fibers using Raman microspectroscopy. *Biomacromolecules* 5:2247–2257
- Rousseau ME, Hernández Cruz D, West MM, Hitchcock AP, Pézolet M (2007) *Nephila clavipes* spider dragline silk microstructure studied by scanning transmission X-ray microscopy. *J Am Chem Soc* 129:3897–3905
- Sahni V, Blackledge TA, Dhinojwala A (2011) Changes in the adhesive properties of spider aggregate glue during the evolution of cobwebs. *Sci Rep* 1:41
- Sanggaard KW, Bechsgaard JS, Fang X, Duan J, Dyrhlund TF, Gupta V, Jiang X, Cheng L, Fan D, Feng Y, Han L, Huang Z, Wu Z, Liao L, Settepani V, Thøgersen IB, Vanthournout B, Wang T, Zhu Y, Funch P, Enghild JJ, Schauser L, Andersen SU, Villesen P, Schierup MH, Bilde T, Wang J (2014) Spider genomes provide insight into composition and evolution of venom and silk. *Nat Commun* 5:3765
- Savage KN, Gosline JM (2008a) The effect of proline on the network structure of major ampullate silks as inferred from their mechanical and optical properties. *J Exp Biol* 211:1937–1947
- Savage KN, Gosline JM (2008b) The role of proline in the elastic mechanism of hydrated spider silks. *J Exp Biol* 211:1948–1957
- Savage KN, Guerette PA, Gosline JM (2004) Supercontraction stress in spider webs. *Biomacromolecules* 5:675–679
- Schäfer A, Vehoff T, Glišović A, Salditt T (2008) Spider silk softening by water uptake: an AFM study. *Eur Biophys J* 37:197–204
- Schwarze S, Zwettler FU, Johnson CM, Neuweiler H (2013) The N-terminal domains of spider silk proteins assemble ultrafast and protected from charge screening. *Nat Commun* 4:2815
- Shao ZZ, Vollrath F (1999) The effect of solvents on the contraction and mechanical properties of spider silk. *Polymer* 40:1799–1806
- Shao ZZ, Young RJ, Vollrath F (1999) The effect of solvents on spider silk studied by mechanical testing and single-fibre Raman spectroscopy. *Int J Biol Macromol* 24:295–300
- Simmons AH, Michal CA, Jelinski LW (1996) Molecular orientation and two-component nature of the crystalline fraction of spider dragline silk. *Science* 271:84–87
- Sirichaisit J, Brookes VL, Young RJ, Vollrath F (2003) Analysis of structure/property relationships in silkworm (*Bombyx mori*) and spider dragline (*Nephila edulis*) silks using Raman spectroscopy. *Biomacromolecules* 4:387–394
- Slotta UK, Rammensee S, Gorb S, Scheibel T (2008) An engineered spider silk protein forms microspheres. *Angew Chem Int Ed* 47:4592–4594
- Spieß K, Lammel A, Scheibel T (2010) Recombinant spider silk proteins for applications in biomaterials. *Macromol Biosci* 10:998–1007
- Sponner A, Unger E, Grosse F, Weisshart K (2005) Differential polymerization of the two main protein components of dragline silk during fibre spinning. *Nat Mater* 4:772–775
- Stellwagen SD, Opell BD, Short KG (2014) Temperature mediates the effect of humidity on the viscoelasticity of glycoprotein glue within the droplets of an orb-weaving spider's prey capture threads. *J Exp Biol* 217:1563–1569
- Teulé F, Furin W, Cooper A, Duncan J, Lewis R (2007) Modifications of spider silk sequences in an attempt to control the mechanical properties of the synthetic fibers. *J Mater Sci* 42:8974–8985
- Thiel BL, Viney C (1997) Spider major ampullate silk (drag line): smart composite processing based on imperfect crystals. *J Microsc* 185:179–187
- Tillinghast EK, Chase SF, Townley MA (1984) Water extraction by the major ampullate duct during silk formation in the spider, *Argiope aurantia* Lucas. *J Insect Physiol* 30:591–596

- Townley MA, Tillinghast EK (1988) Orb web recycling in *Araneus cavaticus* (Araneae, Araneidae) with an emphasis on the adhesive spiral component, GABamide. *J Arachnol* 16:303–319
- Townley MA, Tillinghast EK, Neefus CD (2006) Changes in composition of spider orb web sticky droplets with starvation and web removal, and synthesis of sticky droplet compounds. *J Exp Biol* 209:1463–1486
- Tso IM, Wu HC, Hwang IR (2005) Giant wood spider *Nephila pilipes* alters silk protein in response to prey variation. *J Exp Biol* 208:1053–1061
- Tso IM, Chiang SY, Blackledge TA (2007) Does the giant wood spider *Nephila pilipes* respond to prey variation by altering web or silk properties? *Ethology* 113:324–333
- Turner J, Vollrath F, Hesselberg T (2011) Wind speed affects prey-catching behaviour in an orb web spider. *Naturwissenschaften* 98:1063–1067
- van Beek JD, Hess S, Vollrath F, Meier BH (2002) The molecular structure of spider dragline silk: folding and orientation of the protein backbone. *Proc Natl Acad Sci U S A* 99:10266–10271
- Vehoff T, Glišović A, Schollmeyer H, Zippelius A, Salditt T (2007) Mechanical properties of spider dragline silk: humidity, hysteresis, and relaxation. *Biophys J* 93:4425–4432
- Vollrath F (2000) Strength and structure of spiders' silks. *Rev Mol Biotechnol* 74:67–83
- Vollrath F, Edmonds DT (1989) Modulation of the mechanical properties of spider silk by coating with water. *Nature* 340:305–307
- Vollrath F, Knight DP (2001) Liquid crystalline spinning of spider silk. *Nature* 410:541–548
- Vollrath F, Porter D (2006a) Spider silk as a model biomaterial. *Appl Phys A* 82:205–212
- Vollrath F, Porter D (2006b) Spider silk as archetypal protein elastomer. *Soft Matter* 2:377–385
- Vollrath F, Samu F (1997) The effect of starvation on web geometry in an orb-weaving spider. *Bull Br Arachnol Soc* 10:295–298
- Vollrath F, Downes M, Krackow S (1997) Design variability in web geometry of an orb-weaving spider. *Physiol Behav* 62:735–743
- Vollrath F, Knight DP, Hu XW (1998) Silk production in a spider involves acid bath treatment. *Proc R Soc B* 265:817–820
- Vollrath F, Madsen B, Shao ZZ (2001) The effect of spinning conditions on the mechanics of a spider's dragline silk. *Proc R Soc B* 268:2339–2346
- Vollrath F, Porter D, Holland C (2013) The science of silks. *MRS Bull* 38:73–80
- Wallace JA, Shen JK (2012) Unraveling a trap-and-trigger mechanism in the pH-sensitive self-assembly of spider silk proteins. *J Phys Chem Lett* 3:658–662
- Wendt H, Hillmer A, Reimers K, Kuhbier JW, Schäfer-Nolte F, Allmeling C, Kasper C, Vogt PM (2011) Artificial skin- culturing of different skin cell lines for generating an artificial skin substitute on cross-weaved spider silk fibres. *PLoS One* 6:e21833
- Wenk E, Merkle HP, Meinel L (2011) Silk fibroin as a vehicle for drug delivery applications. *J Control Release* 150:128–141
- Widhe M, Bysell H, Nystedt S, Schenning I, Malmsten M, Johansson J, Rising A, Hedhammar M (2010) Recombinant spider silk as matrices for cell culture. *Biomaterials* 31:9575–9585
- Widhe M, Johansson U, Hillerdahl CO, Hedhammar M (2013) Recombinant spider silk with cell binding motifs for specific adherence of cells. *Biomaterials* 34:8223–8234
- Wilson R (1962a) The control of dragline spinning in the garden spider. *Q J Microsc Sci* 3:557–571
- Wilson R (1962b) The structure of the dragline control valves in the garden spider. *Q J Microsc Sci* 3:549–555
- Wohlrab S, Müller S, Schmidt A, Neubauer S, Kessler H, Leal-Egaña A, Scheibel T (2012) Cell adhesion and proliferation on RGD-modified recombinant spider silk proteins. *Biomaterials* 33:6650–6659
- Work RW (1977a) Dimensions, birefringences, and force-elongation behavior of major and minor ampullate silk fibers from orb-web-spinning spiders—the effects of wetting on these properties. *Text Res J* 47:650–662
- Work RW (1977b) Mechanisms of major ampullate silk fiber formation by orb-web-spinning spiders. *Trans Am Microsc Soc* 96:170–189

- Work RW (1981) A comparative study of the supercontraction of major ampullate silk fibers of orb-web-building spiders (Araneae). *J Arachnol* 9:299–308
- Wu X, Liu XY, Du N, Xu G, Li B (2009) Unraveled mechanism in silk engineering: fast reeling induced silk toughening. *Appl Phys Lett* 95:093703
- Wu CC, Blamires SJ, Wu CL, Tso IM (2013) Wind induces variations in spider web geometry and sticky spiral droplet volume. *J Exp Biol* 216:3342–3349
- Xia XX, Qian ZG, Ki CS, Park YH, Kaplan DL, Lee SY (2010) Native-sized recombinant spider silk protein produced in metabolically engineered *Escherichia coli* results in a strong fiber. *Proc Natl Acad Sci U S A* 107:14059–14063
- Xiang P, Li M, Zhang CY, Chen DL, Zhou ZH (2011) Cytocompatibility of electrospun nanofiber tubular scaffolds for small diameter tissue engineering blood vessels. *Int J Biol Macromol* 49:281–288
- Yanagi Y, Kondo Y, Hirabayashi K (2000) Deterioration of silk fabrics and their crystallinity. *Text Res J* 70:871–875
- Yang Z, Liivak O, Seidel A, LaVerde G, Zax DB, Jelinski LW (2000) Supercontraction and backbone dynamics in spider silk: ^{13}C and ^2H NMR studies. *J Am Chem Soc* 122:9019–9025
- Yang Y, Chen X, Shao ZZ, Zhou P, Porter D, Knight DP, Vollrath F (2005) Toughness of spider silk at high and low temperatures. *Adv Mater* 17:84–88
- Zax DB, Armanios DE, Horak S, Malowniak C, Yang Z (2004) Variation of mechanical properties with amino acid content in the silk of *Nephila Clavipes*. *Biomacromolecules* 5:732–738
- Zheng YM, Bai H, Huang ZB, Tian XL, Nie FQ, Zhao Y, Zhai J, Jiang L (2010) Directional water collection on wetted spider silk. *Nature* 463:640–643

Chapter 14

Insect Silks and Cocoons: Structural and Molecular Aspects

Kenji Yukuhiro, Hideki Sezutsu, Takuya Tsubota, Yoko Takasu, Tsunenori Kameda, and Naoyuki Yonemura

Abstract In this chapter, we extensively describe insect-secreting silk proteins. Silk proteins are produced in the labial glands (functioning as silk glands), from which they are then secreted, which is a characteristic feature of the orders Trichoptera, Lepidoptera, and some other Holometabola insects. We first describe lepidopteran silk formation and describe how the two types of fibroin (fibroin heavy chain: H-fibroin and fibroin light chain: L-fibroin) observed in non-saturniid moths, represented by *Bombyx mori*. Specifically, we present how the two types of fibroins, which are linked by disulfide bonds, and P25 or fibrohexamerin as a chaperone) contribute to silk fiber organization. Saturniidae moths, which produce only one type of fibroin, are also discussed here about their silk formation. Following the description of lepidopteran silk fiber proteins, we present recent progress in the study of sericin proteins of *B. mori* and other lepidopteran. Sericins wrap silk fibers to seal two silk filaments together like glue. We also present the differences in expression patterns and gene regulation observed in the silk glands of *B. mori* and *Samia ricini*. Then, we comprehensively summarize the features of hornet and trichopteran silks different from lepidopterans. According to the current understanding, these species produce no sericin-like proteins. The principal molec-

The original version of this chapter was revised. An erratum to this chapter can be found at DOI [10.1007/978-3-319-40740-1_18](https://doi.org/10.1007/978-3-319-40740-1_18)

K. Yukuhiro (✉) • T. Tsubota • N. Yonemura
Transgenic Silkworm Research Unit, Genetically Modified Organism Research Center,
National Institute of Agrobiological Sciences, Tsukuba, Ibaraki, Japan
e-mail: kygnis@affrc.go.jp; tsubota@affrc.go.jp; yonemura@affrc.go.jp

H. Sezutsu
Transgenic Silkworm Research Unit, Genetically Modified Organism Research Center,
National Institute of Agrobiological Sciences, The University of Tokyo,
Tsukuba, Ibaraki, Japan
e-mail: hsezutsu@affrc.go.jp

Y. Takasu • T. Kameda
Silk Materials Research Unit, Genetically Modified Organism Research Center, National
Institute of Agrobiological Sciences, Tsukuba, Ibaraki, Japan
e-mail: takasu@affrc.go.jp; kamedat@affrc.go.jp

ular structure of hornet silk is α -helices, frequently in a coiled-coil conformation, a molecular structure distinct from the β -sheet structures that dominate the silks of lepidopterans. Finally, we describe the present status of transgenic technology that is being used to modify fibroins in order to add features that are lacking in the host.

14.1 Introduction

Silks are externally spun fibrous, proteinaceous materials that are insoluble in water and have excellent mechanical properties (Kenchington 1984). Many distantly related insect species from orders Trichoptera, Lepidoptera, Hymenoptera, Embioptera, Neuroptera, Coleoptera, Thysanura, and Prosoptera use fibrous proteins (silk) for various purposes. Silk proteins produced by lepidopteran, trichopteran, and hymenopteran larvae are secreted by silk glands. Such silks are often used to spin cocoons for the protection of the pupae.

Cocoon formation in the silkworm *Bombyx mori* aroused human interest more than 4000 years ago, when it was discovered that the protein fibers could be unwound from the cocoon and used for manufacturing strong and unique fabrics. Caterpillars of only a handful of species are exploited commercially by mulberry and non-mulberry sericulture; these include *B. mori* and a few wild silkworm species from the family Saturniidae. Currently, there is an increased interest in biomaterials that has promoted research on other silk proteins with outstanding mechanical and biochemical properties.

The lepidopteran silk is composed of two major classes of proteins—fibroins and sericins. Fibroins are synthesized in the posterior region of the silk gland and form threads or fibrous cores responsible for the mechanical strength of the silk fibers, whereas sericins are synthesized in the middle part of the silk glands and form a sticky cover of the silk fibers (Okamoto et al. 1982; Couble et al. 1987; Michaille et al. 1990).

Trichoptera (caddisflies) are a sister group of Lepidoptera and their silk composition, at least the fibroin fraction, appears quite similar to the lepidopteran silk. Caddisfly larvae live mostly under water and their silk seems to have unique mechanical properties. Sericins have not yet been detected in caddisfly silk, suggesting differences between the lepidopteran and the trichopteran silk structures.

Members of both hymenopteran sister superfamilies Apoidea (bees) and Vespoidea (ants/hornets) produce silks in which the principal molecular structure is an α -helix. In contrast, the lepidopteran fibroins are dominated by a β -sheet structure. Four types of relatively low molecular weight fibroins have been found in the hornet silk and three others in aculeate hymenopterans (Kameda et al. 2014).

The first biomaterials from regenerated and recombinant portions of spider and silkworm β -sheet-forming silk proteins have been produced and used in cell culture, tissue regeneration scaffolds, or as drug delivery vehicles and biosensors. A wider use of recombinant DNA technology in the production of modified silks in transgenic insects will greatly increase our ability to produce silk-based biomaterials in the future.

14.2 Silk Gland Morphology

The adaptation of the labial salivary glands to silk production has been noted in several insect orders, including Lepidoptera, Trichoptera, Hymenoptera, Siphonaptera, and Diptera. The salivary gland is a paired organ typically consisting of polyploid cells, and its structure varies with the species, from simple tubes to lobulated sacs (Sehna and Akai 1990).

The lepidopteran silk glands can be divided into three morphologically distinct regions: posterior, middle, and anterior silk glands (Machida 1926). The posterior silk gland produces fibroin, which forms the fibrous core. Liquid fibroin is released into the lumen of the posterior silk gland and then transported to the middle silk gland. The middle part of the silk glands synthesizes and secretes a series of sericins that coat the surface of the liquid fibroin, acting as an adhesive. The sericin-coated fibroins then move through the lumen to the anterior silk gland, which merely acts as a duct, and are released from a pair of spinnerets in the form of silk fiber. The spinnerets of *B. mori*, for example, open into the apical portion of the labium (Akai 1976). The structures of the silk glands differ markedly between the families Bombycidae and Saturniidae, although they are classified into the same order Bombycoidea (Fig. 14.1a–d).

The trichopteran silk glands are similar to those of Lepidoptera (Sehna and Sutherland 2008). Caddisworms (Trichoptera larvae) possess additional glands suspected of playing a role in spinning. These are called Gilson's glands and reside on the prothorax (Zaretschnaya 1965). In Hymenoptera, the labial glands first function as salivary glands and then change to silk production just before pupation. Each of the paired glands is composed of a thin-walled canal to which a large number of secretory cells are attached through short ducts (Kenchington 1972).

14.3 Cocoons Produced by Lepidopteran Larvae

The cocoons are the major silk products of Lepidoptera and other insect larvae, designed to protect pupae during metamorphosis. The cocoons vary widely in weight, shape, strength, and color, even among closely related species. For example, although the Chinese oak silkworm, *Antheraea pernyi*, and the Japanese oak silkworm, *Antheraea yamamai*, are closely related, their cocoons differ in both color and shape. Likewise, the closely related *Samia pryeri* and the Eri silkworm, *Samia ricini* also differ markedly in cocoon shape and softness. Some of the variation in cocoon shape and color is shown in Fig. 14.2. The figure shows 22 cocoons of 20 Saturniidae species. This is only a representation of the existing cocoon diversity and further studies are needed to explain it.

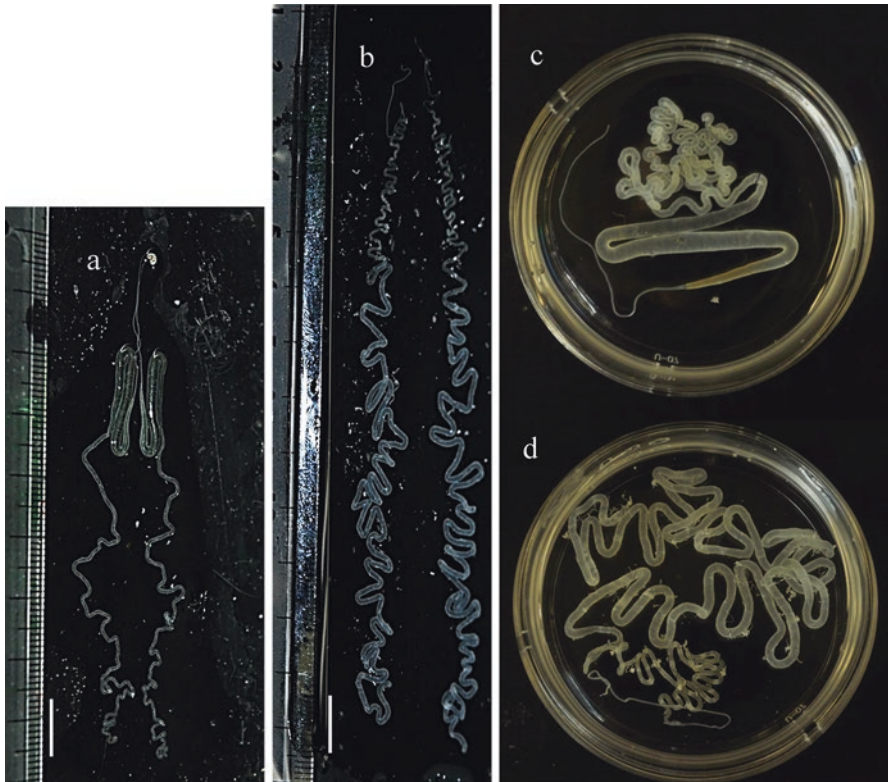


Fig. 14.1 Silk glands of *Bombyx mori* and *Samia ricini*. (a) and (c) *Bombyx mori*. (b) and (d) *Samia ricini*

14.4 Fibroins in Lepidopteran Silks

The structure of fibroins was first studied using X-ray analysis. Based on the X-ray diagrams, the lepidopteran fibroins were classified into three types all containing a parallel- β -pleated sheet structure (Lucas and Rudall 1968). Warwicker (1960) classified silk into several groups, on the basis of X-ray analysis of silk crystallites: Group 1 silks, represented by *B. mori* silk, are characterized by an intersheet packing distance of 9.3 Å; Group 2 silks, represented by *Anaphe moloneyi*, have an intersheet packing distance of 10.0 Å; and Group 3 silks, represented by the tropical tasar silkworm, *Antheraea mylitta*, have an intersheet packing of 10.6 Å (Warwicker 1960; Craig 1997). Thus, the groups defined by Warwicker (1960) are distinguished by increasing spacing between the peptides of adjacent chains, which may be the result of increasing amounts of alanine (Ala) and decreasing amounts of glycine (Gly) (Simmons et al. 1994).

Subsequent studies examined the protein composition of the fibroin core. Most of the lepidopteran species' silks were found to consist of three components: fibroin

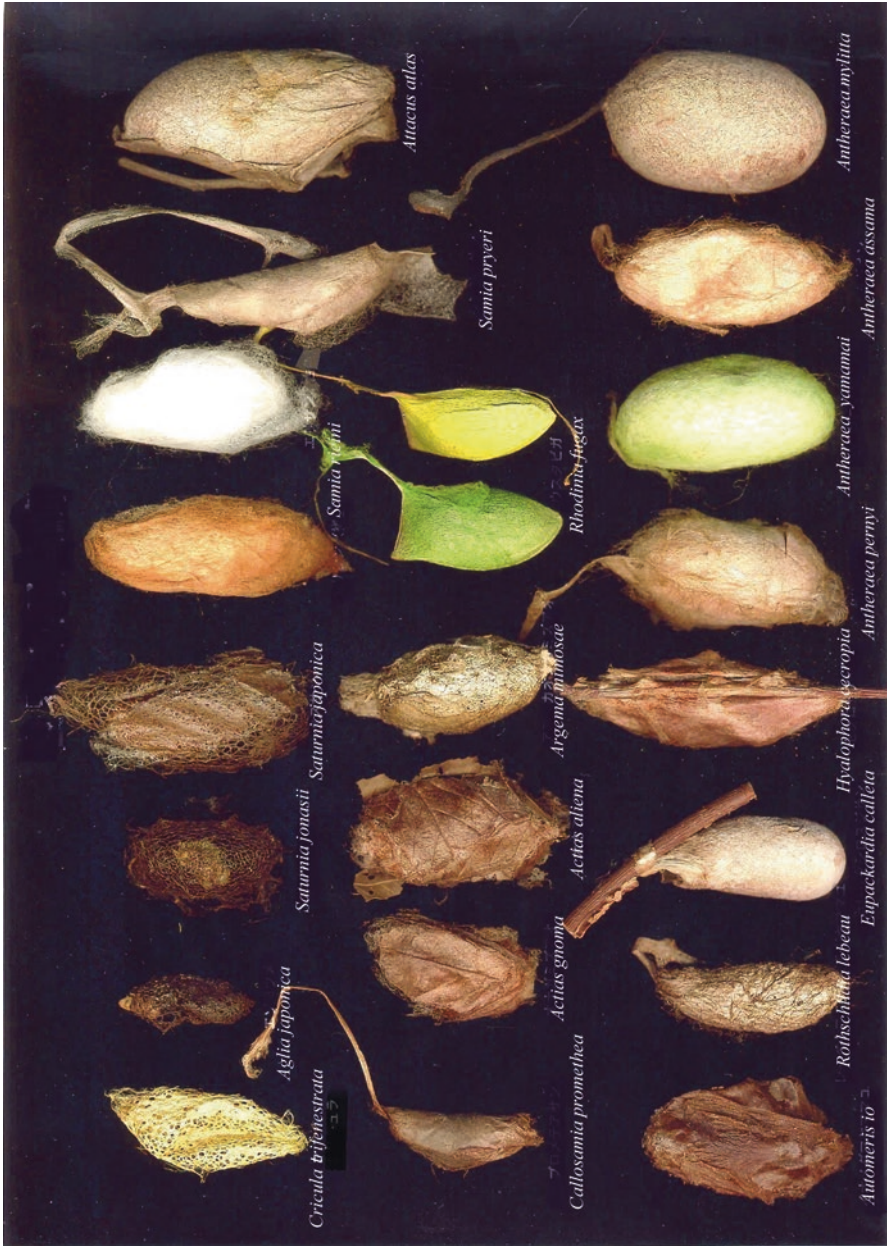


Fig. 14.2 Cocoons of 20 saturniid moths. A cocoon from each species excluding *Samia ricini* and *Rhodinia fugax* is shown in this figure. Two cocoons with different colors are depicted for *S. ricini* as well as *R. fugax*. Photo by Hitoshi Saitou

heavy chain (H-fibroin), fibroin light chain (L-fibroin), and fibrohexamerin (P25). This arrangement has been best characterized in the domestic silkmoth, *B. mori* (Inoue et al. 2000). Fibroins of other bombycoid species belonging to family Saturniidae are composed of only H-fibroin, which most probably forms homodimers (reviewed by Chevillard et al. 1986; Kikuchi et al. 1992; Inoue et al. 2000). The P-25 fibroin component appears to be absent in some primitive lepidopterans, including the lupine ghost moth, *Phymatopus californicus*. Such fibroins probably contain only H- and L-fibroin dimers (Collin et al. 2010).

14.4.1 Fibroin Heavy Chain (H-Fibroin)

The *H-fibroin* gene was one of the first genes to be studied in detail. Its DNA sequence, including the promoter and most of the coding region, has been cloned and partially sequenced (Ohshima and Suzuki 1977; Tsujimoto and Suzuki 1979; Mita et al. 1994). The complete structure of *B. mori* H-fibroin was determined by Zhou et al. (2000). The *B. mori* *H-fibroin* gene consists of a short first exon (67 bp), an intron (1 kb), and a long second exon (ca. 16 kb) (Fig. 14.3a). The whole gene encodes 5263 amino acid residues and about 90% of the second exon consists of highly repetitive arrays (Fig. 14.3b) (Zhou et al. 2000). Three amino acids, Gly, Ala, and Ser, are extremely abundant in the H-fibroin (Gly: 46%, Ala: 30%, and Ser: 12%). Two types of submotifs, each consisting of six amino acid residues, GAGAGS and GAGAGY appear frequently and their concatenations make up larger repetitive units (Fig. 14.3c) that are separated by 11 amorphous domains (Fig. 14.3d) (Zhou et al. 2000).

The partial H-fibroin gene sequence from *A. yamamai* was isolated in 1987 (Tamura et al. 1987). Later, the entire sequence (*Ay-H-fibroin*) gene was independently determined by Hwang et al. (2001) and Sezutsu et al. (2010). Sequences of six other *H-fibroin* genes have been partially or entirely determined in other species, including the wild silkmoth, *Bombyx mandarina* (Kusuda et al. 1986); *A. pernyi* (Sezutsu and Yukuhiro 2000); the greater wax moth, *Galleria mellonella* (Žurovec and Sehnal 2002); the Mediterranean flour moth, *Anagasta kuehniella* and the Indian mealmoth, *Plodia interpunctella* (Fedič et al. 2003); *P. californicus* (Collin et al. 2010); and *S. ricini* (Sezutsu and Yukuhiro 2014).

The H-fibroin sequences are highly species specific (Yukuhiro et al. 2014). To the best of our knowledge, multiple repetitions of the GX unit have so far only been found in *Bombyx* H-fibroin. The high Gly content in this molecule is responsible for the tight packing of the crystallite intersheets, as suggested for Warwicker Group 1 fibroins (Warwicker 1960). Many other fibroins contain clusters of Ala or Ala-Ser residues, which characteristic for Group 3 silks (including *A. yamamai*, *A. pernyi*, and *G. mellonella*). Unequal crossover is probably the cause of length polymorphisms, as shown, for example, by Southern blot analysis of the *Bombyx H-fibroin* gene (Maning and Gage 1980).

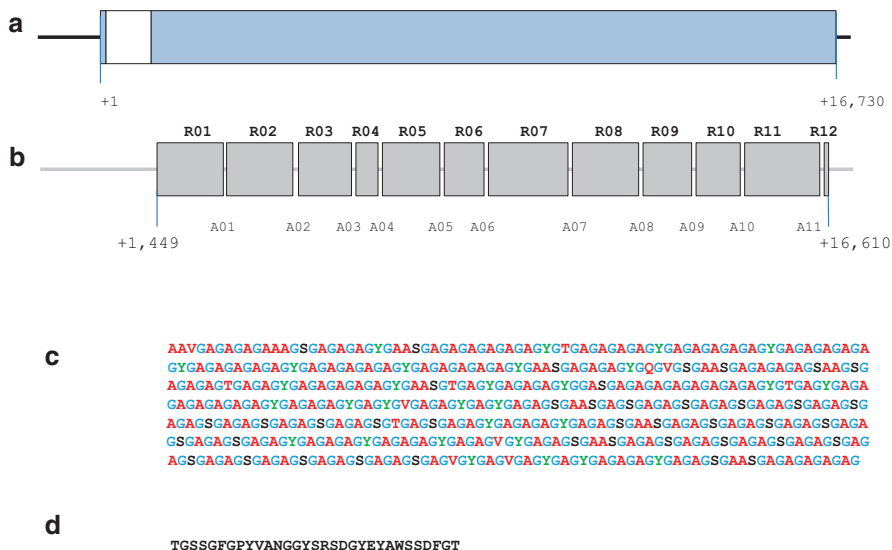


Fig. 14.3 *Bombyx mori* H-fibroin gene. **(a)** The *Bombyx mori* H-fibroin gene consists of two exons interrupted by the insertion of 971-bp intron. *Closed boxes* show exons while an *open box* represents an intron. **(b)** The central region of exon2 comprises of 12 repetitive domains (R01–R12) separated by 11 amorphous domains (A01–A11). **(c)** The amino acid sequence encoded by R01 domain. **(d)** The amino acid sequence encoded by A01 domain. These figures were prepared based on Zhou et al. (2000)

14.4.2 Fibroin Light Chain (L-Fibroin) and Fibrohexamerin (P25)

The two lower molecular weight fibroin components were discovered in *B. mori*. The first one is the fibroin light chain (L-fibroin), which consists of 262 amino acid residues (Kikuchi et al. 1992). A heterodimer of the L- and H-fibroins is formed via disulfide bonds (Tanaka et al. 1999b). There is little sequence similarity between the H- and L-fibroins and the *L-fibroin* exon-intron structure, which consists of seven exons and six introns, is quite different from the *H-fibroin* gene.

The second of the low molecular weight fibroin subunits is fibrohexamerin (P25). It is encoded by a gene with five exons and the putative protein consists of 220 amino acid residues (Chevallard et al. 1986). The fibrohexamerin protein shows no similarities to either H- or L-fibroin. Inoue et al. (2000) reported that the fibrohexamerin molecule generates hydrogen bridges with six H-fibroin–L-fibroin heterodimers, thereby prompting the formation of fibroin complexes that may assemble into filaments.

Both the L-fibroin and fibrohexamerin were later detected in another lepidopteran species, *G. mellonella*, belonging to a distantly related family Pyraloidea (Žurovec et al. 1995, 1998; Fedič et al. 2003). Later, these components were also detected in

the pine moth, *Dendrolimus spectabilis* and the Asian swallowtail, *Papilio xuthus* (Tanaka and Mizuno 2001). Interestingly, while the two lower molecular weight fibroins have been detected in several lepidopteran species and L-fibroin, in Trichoptera, they have not been found in any of the examined saturniids. This suggests that the fibroins in Saturniidae differ from those of other Lepidoptera (Figs. 14.4 and 14.5) (see Yukuhiro et al. 2014). The trichopteran L-fibroin sequences are quite similar to those of non-saturniid lepidopterans (Fig. 14.4) (Yukuhiro et al. 2014).

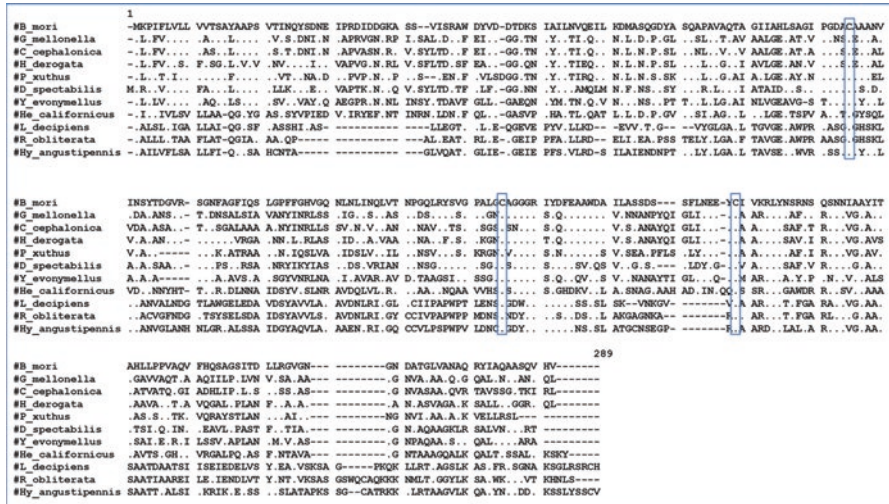


Fig. 14.4 Sequence alignment of L-fibroin sequences. The three conserved cysteine residues are boxed

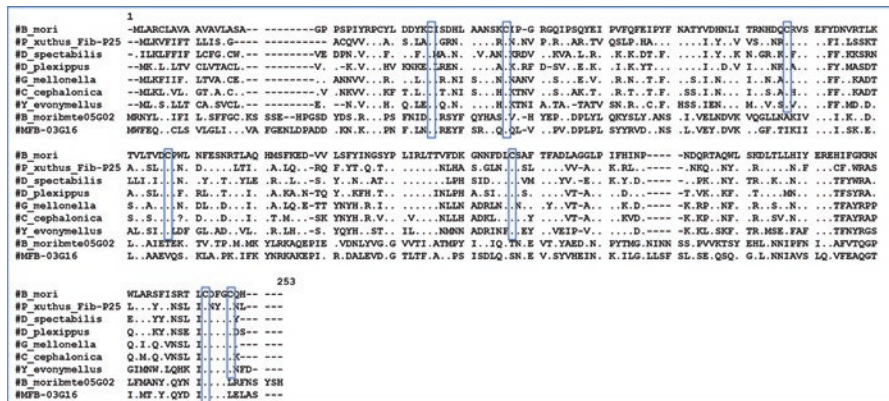


Fig. 14.5 Sequence alignment of fibrohexamerin (P25) sequences and those of 2 *Bombyx* paralogs. The conserved Cys residues were boxed

14.4.3 Fibroins in Saturniidae

Tamura et al. (1987) predicted that two *A. yamamai* H-fibroin molecules are linked by disulfide bonds and form a homodimer, which makes the composition of this type of fibroin considerably different from that found in *B. mori*. This linkage between the H-fibroin molecules was later confirmed (Tanaka et al. 1999b).

Sezutsu and Yukuhiro (2000) identified the *A. pernyi* H-fibroin (Ap-H-fibroin) gene and deduced the amino acid sequence (2639 amino acids) encoded by it (Figs. 14.6 and 14.7). *A. pernyi* is a close relative of *A. yamamai*, and the Ap-H-fibroin does resemble the known fibroin N-terminal region in *A. yamamai* (Tamura et al. 1987). As shown in Fig. 14.6, Ap-H-fibroin contains a large middle region of

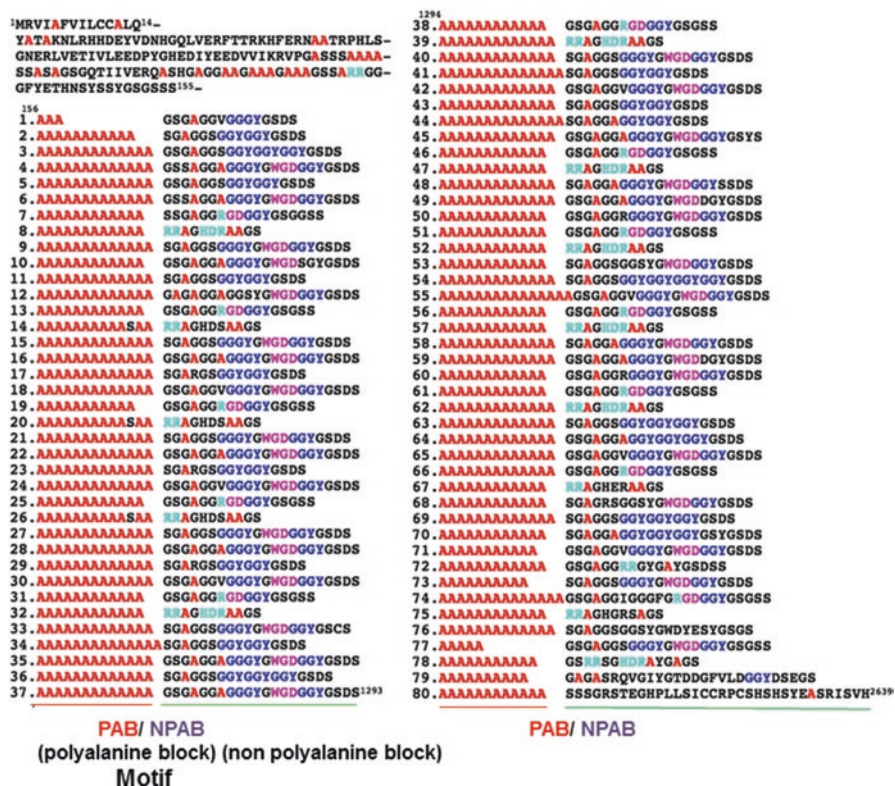


Fig. 14.6 Deduced amino acid sequence of *Antheraea pernyi* (Ap-) H-fibroin. The repeated unit (motif) is a polyalanine block (PAB)/nonpolyalanine block (NPAB) pair. PABs were marked by red letters. Type1 NPAB sequence is highlighted by tryptophan, glycine and aspartic acid (WGD) triplets marked by magenta letters. Type2 NPAB sequence is represented by glycine, glycine and tyrosine (GGY) triplets marked by deep blue letters. Type 3 NPAB sequence has an arginine (R) marked by a pale blue letter linked to a magenta GD. Type4 NPAB sequences are marked by pale blue Rs and histidine, aspartic acid and arginine (HDR) triplets. 80 motifs were found in this sequence. Numbers on the left of PABs designate the order of motifs from the N-terminal

repetitive arrays, with a polyalanine block (PAB)/non-polyalanine block (NPAB) pair as repeat unit. Hereafter, we refer to the PAB/NPAB pair as a motif. A total of 78 of 80 repeat motifs in the Ap-*H-fibroin* coding sequence were classified into four different types of motifs based on differences in the NPAB amino acid sequence (Fig. 14.7).

The Ay-*H-fibroin* genes were independently isolated and examined by Hwang et al. (2001) and Sezutsu et al. (2010). The two sequences are almost identical, except for a minor difference in the number of repeat motifs. In addition, Ap- and Ay-H-fibroin are also almost identical in terms of sharing four types of motifs (Fig. 14.7) as well as both terminal sequences (Figs. 14.8a and 14.9a).

Recently, the *H-fibroin* gene from the third *Antheraea* species, the muga silkworm (*A. assama*), was characterized (Gupta et al. 2015). As expected, it also contained four types of repeat motifs (Fig. 14.7). Among these motifs, the following similarities and differences were observed in the repeat region: (1) their type-R non-polyalanine motifs correspond to NPAB of type-4 motifs in the Ap- and Ay-H-fibroins. (2) None of their non-polyalanine motifs were found to correspond to NPAB of the Ap- and Ay-H-fibroin type-2 motifs that show variable repetition of GGY triplets. (3) Their type-Gc non-polyalanine motifs occurred only four times, although the NPABs of type-3 motifs, as possible Ap- and Ay-H-fibroin counterparts, were common. In contrast, the N-terminal non-repetitive region showed quite high sequence similarity. A similar conservation was observed in the C-terminal regions (data not shown).

As shown in Fig. 14.10, the *H-fibroin* gene structures in all three species are similar: the first exons are short, encoding for only 14 amino acid residues. These are then followed by a 120–150-bp intron, being somewhat shorter than that of the *B. mori H-fibroin* gene. As mentioned above, the second exons encode repetitive motifs.

Partial *H-fibroin* sequences (except for the 3' end) were identified in two other saturniids, the squeaking silkworm *Rhodinia fugax* and the Japanese giant silkworm, *Saturnia japonica* (Sezutsu et al. 2008a, b). These species are somewhat more distantly related to the genus *Antheraea*. These two novel H-fibroins contain a relatively high number of Leu residues (Fig. 14.7), which are almost absent in the repetitive regions of the three *Antheraea* H-fibroins. Despite the similarity in Leu residue frequency, considerable differences in the NPAB sequences were confirmed between *R. fugax* and *S. japonica* H-fibroins (Fig. 14.7). All five identified saturniid H-fibroin sequences contain a type of NPAB that carries fewer Gly residues compared to the other three types of NPABs: these are type-4 of *A. pernyi* and *A. yama-mai*, type-R of *A. assama*, type-3 of *R. fugax*, and type-2 of *S. japonica* (Fig. 14.7). These are hydrophilic relative to the other three types of NPABs. A recent analysis further confirmed that Leu residues are present in the H-fibroin of *R. newara* as well as that of the Indian moon moth, *Actias selene* (Dong et al. 2015).

To date, the only Attacini species with known H-fibroin primary structure in *S. ricini* (Sr-H-fibroin) (Fig. 14.11) (Sezutsu and Yukuhiro 2014). Its putative amino acid sequence shows common features with those of the *Antheraea* H-fibroins

<i>Antheraea pernyi</i> & <i>A. yamamami</i>	Type1	GSGAGGAGGGYGWGDGGYGSDS
	Type2	-SGAGGS (GGY) _{1~3} GGYGSDS
	Type3	GSGAGG-----RGDGGYGS GSS
	Type4	-RRAGHDRAAGS
<i>A. assama</i>	TypeG _b	GGSG ^{AG} _G ^Y _G ^D _G GGYGWGDGGYGS ^D _S GR S G E G
	TypeG _c	GSGAGG ^R _V GGGY ^R _L GDGGYGS GSS
	TypeGa	GSGAGGAGDGGYGS GSSG E
	TypeR	RRAGHDRAAGS
<i>Rhodinia fugax</i>	Type1	GSGSRGLGGYGYKDG LLLDGEYGS GS
	Type2	GSGSRGLGGYYG-DG--LLDGGYGS GS
	Type3	GSSSDYTVYESSRRGSSSS
	Type4	GSSGVGYGRRYGS DS
<i>Saturnia japonica</i>	Type1LH	GSGAGGLGGHYGLHGGVYGS DS
	Type1LHL	GSGAGGLGGLYGLHGGVYGS SSSRRDSSSASS
	Type1W	GSSSRRVGGHYGWGDGGVYGS DS
	Type2	GSSAASSERVYESES
<i>Samia ricini</i>	motif 1	GGAGSGYGGGAR ^R _G GYGHGYGSDGG
	motif 2	GGAGSGYGGGSWH ^G _S YGSDS ^G _S
	motif 3	GG ^G _S (GGYG) ^A _{1~3} DGG
	motif 4	GGAG ^G _D DYGAGS

Fig. 14.7 H-Fibroin NPAB sequences detected in six species of saturniids. Ap- and Ay-H-fibroins share four motif types, so they represent a common characteristic. The subscripts 1–3 represent the number of repetition of GGY triplet in Type 2 NPABs. *Antheraea assama* motif sequences were drawn according to Gupta et al. (2015). Excluding *S. ricini*, Gly-poor NPAB name is indicated by green letters. Gly residues in this type of NPABs are also marked by a green letter. The subscripts 1–3 in Sr-motif3 also represent the number of repetition of GGYG quartet

(Fig. 14.7). The similarities include a high abundance of the amino acid residues Ala, Gly, and Ser and that most of the protein sequences consists of four different types of PAB/NPAB motifs (Fig. 14.7).

A remarkable difference between the Sr-H-fibroin and the other H-fibroins is that all four Sr-H-fibroin NPAB sequences are Gly-rich (Fig. 14.7). Furthermore, about 80% of its amino acid residues are hydrophobic, which approaches the level of hydrophobicity encountered in *B. mori* H-fibroin. It is also worth noting that the dimerization with L-fibroin seems to result in a decreased level of hydrophobicity in the *B. mori* fibroin complex (Sehnal and Žurovec 2004).

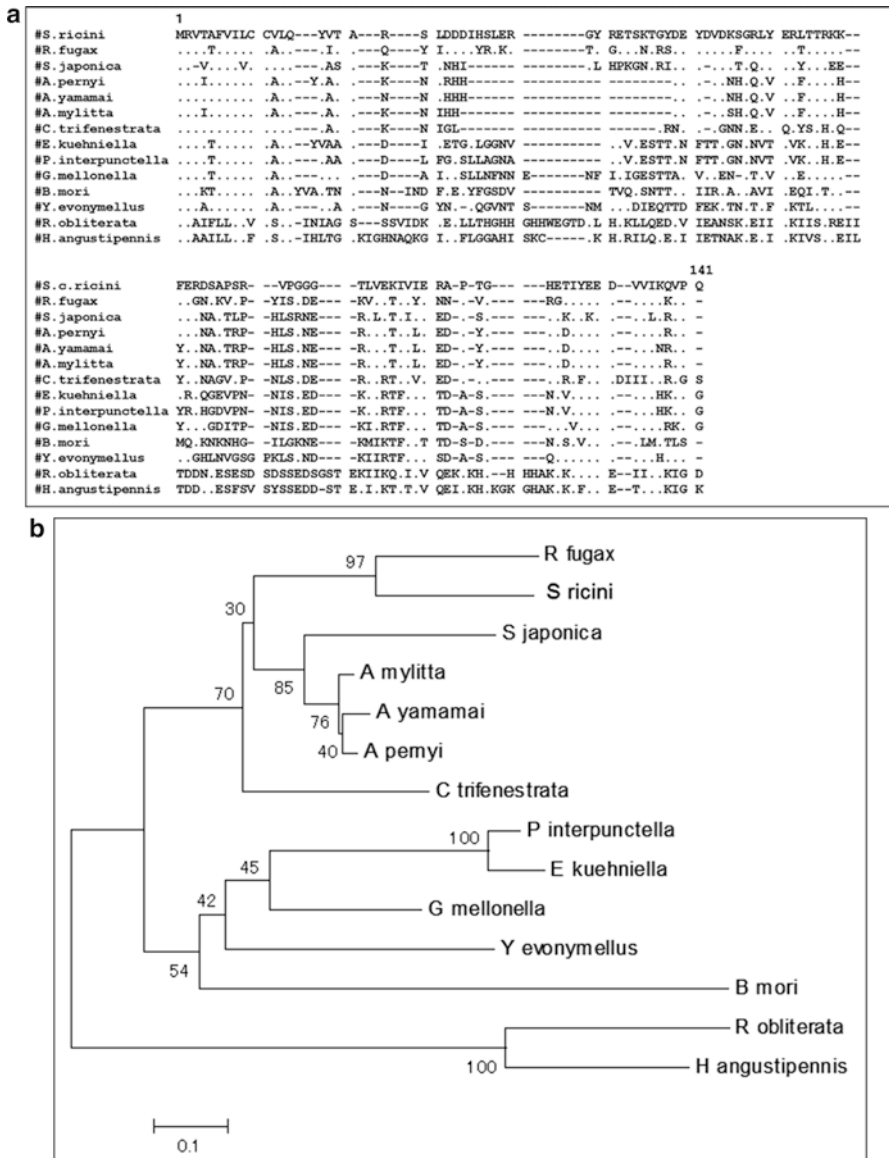


Fig. 14.8 Amino acid sequences encoded by the first exons and proximal regions of the second exons in H-fibroin genes of eleven lepidopteran species and two trichopteran species, and their phylogenetic relationship. (a) Aligned amino acids sequences. (b) Phylogenetic relationship. The sources of these sequences are as follows: *Rhodinia fugax*: AB437258; *Satunia japonica*: AB439802; *Antheraea pernyi*: AF083334; *Antheraea yamamai*: AB542805; *Antheraea mylitta*: AY136274; *Cricula trifenestrata*: JF264729; *Ephestia kuehniella*: AY253534; *Plodia interpunctella*: AY253533; *Galleria mellonella*: AF095239; *Bombyx mori*: AF226688; *Yponomeuta evonymella*: AB195979; *Rhyacophila obliterata*: AB354690; *Hydropsyche angustipennis*: AB354593

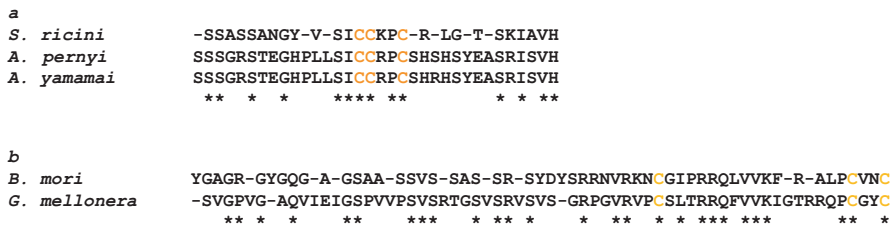


Fig. 14.9 C-terminal sequences as non-repetitive regions of five types of H-fibroin. (a) Aligned C-terminal sequences of *Samia ricini*, *Antheraea pernyi*, and *Antheraea yamamai* H-fibroins. Cys residues were marked by orange letters. (b) Aligned C-terminal sequences of *Bombyx mori* and *Galleria mellonella* H-fibroin. Cys residues were marked by orange letters. In the both figures, conserved amino acid positions are marked by asterisks

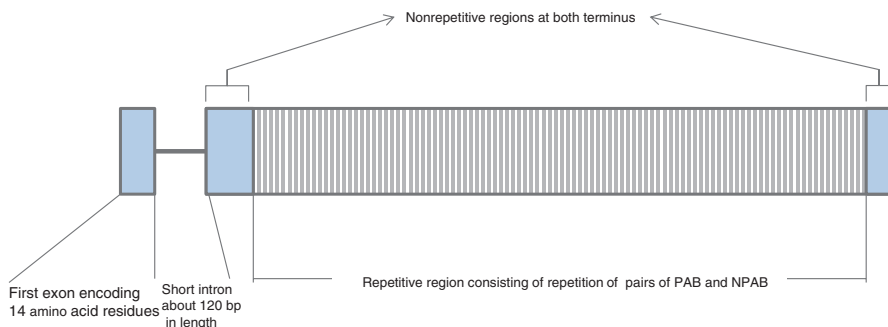


Fig. 14.10 A common gene structure that was found in four saturniid H-fibroin genes

14.4.4 Terminal Amino Acid Sequences of H-Fibroins

The sequences of the 14 amino acids encoded by the first exon are highly conserved among the saturniid *H-fibroin* genes, including those from *A. pernyi* (Sezutsu and Yukuhiro 2000), *A. yamamai* (Hwang et al. 2001; Sezutsu et al. 2010), *R. fugax* (Sezutsu et al. 2008a), and *S. ricini* (Sezutsu and Yukuhiro 2014) (Fig. 14.8a). The first exon of the *S. japonica* H-fibroin gene (Sezutsu et al. 2008b) encodes a similar sequence, except for the deletion of a single amino acid residue (Fig. 14.8a). These amino acid sequences share two conserved Cys residues at identical positions (Fig. 14.8a). However, the two conserved Cys residues (Fig. 14.8a) are removed together with the signal peptide, which suggests little functional significance for the silk fiber (Sezutsu and Yukuhiro 2014). Note that this region seems to be conserved also compared with the H-fibroins from the non-saturniid moths (Fig. 14.8a).

In addition, even the first exons of *H-fibroin* genes from the two trichopterans encode similar sequences, with the exception of an amino acid substitution in one of the two conserved Cys residues (Fig. 14.8a; Yonemura et al. 2006; Sehnal and Sutherland 2008; Yonemura et al. 2009). Since Trichoptera is a sister taxon of

```

14MRVTA14FVILCCVLQ14-
15YV15TARSLDDDIHSLERGYRETSKTYGDEYDVKSGRLYERLT-
TRK16KFERDSAPFSRV17PGG18TV19EKI20VIERAPTGHETIYEEDV21-
IK22QV23PGG24ASSA25SSAS26AGSG27GAP28TI29VERGS30AGSG31SR32H-
GAG33SA34G35
1. 145AAAAAAAAAAAAAGG146AG147GGGG148GGY149GR150GH151GT152AGS
2. AAAAAAAAAAAAAAS153EGS154AG155GY156W157Q158YGS159SDSS
3. AAAAAAAAAAAAAA160CS161AG162SG163SDS164AE
4. AAAAAAAAAAAAAA165GT166AG167GG168SG169GGY170GD171GG
5. AAAAAAAAAAAAAAS172G173AG174SG175Y176GG177AR178GGY179GH180YGS181SDGG
6. AAAAAAAAAAAAAAG182AG183RG184Y185GAGS
7. AAAAAAAAAAAAAA186G187SG188GGY189GD190GG
8. AAAAAAAAAAAAAAS191G192AG193SG194Y195GG196AR197GGY198GH199YGS200SDGG
9. AAAAAAAAAAAAAAG201AG202GGY203GGY204GGY205GD206GG
10. AAAAAAAAAAAAAAG207AG208SG209Y210GG211SW212H213YGS214SDG
11. AAAAAAAAAAAAAAG215SG216SG217GGY218GD219GG
12. AAAAAAAAAAAAAAG220SG221SG222GGY223GD224GG
13. AAAAAAAAAAAAAAG225AG226CD227GY228GAGS
14. AAAAAAAAAAAAAA229GA230GGY231GD232GG
15. AAAAAAAAAAAAAAG233AG234SG235Y236GG237AR238GGY239GH240YGS241SDGG
16. AAAAAAAAAAAAAAG242SG243SG244GGY245GD246GG
17. AAAAAAAAAAAAAAG247AG248SG249Y250GG251AR252GGY253GH254YGS255SDGG
18. AAAAAAAAAAAAAAG256SG257SG258GGY259GD260GG
19. AAAAAAAAAAAAAAG261AG262SG263Y264GG265AR266GGY267GH268YGS269SDGG
20. AAAAAAAAAAAAAAG270SG271SG272GGY273GD274GG
21. AAAAAAAAAAAAAAG275AG276GGY277GD278GG
22. AAAAAAAAAAAAAAG279AG280GD281GY282GAGS
23. AAAAAAAAAAAAAA283GA284GGY285GD286GG
24. AAAAAAAAAAAAAAG287AG288SG289Y290GG291AR292GGY293GH294YGS295SDGG
25. AAAAAAAAAAAAAAG296SG297SG298GGY299GD300GG
26. AAAAAAAAAAAAAAG301AG302SG303Y304GG305AR306GGY307GH308YGS309SDGG
27. AAAAAAAAAAAAAAG310SA311ESS312Y313GG314SW315YGS316SDSS
28. AAAAAAAAAAAA317GA318GGY319GD320GG
29. AAAAAAAAAAAAAA321G322SG323GGY324GD325GG
30. AAAAAAAAAAAAAAG326AG327GGY328GGY329GD330GG
31. AAAAAAAAAAAAAAG331GS332RS333Y334GG335SW336H337YGS338SDSG
32. AAAAAAAAAAAAAAG339AG340CD341GY342PG343PS
33. AAAAAAAAAAAAAA344GA345GGY346GD347GG
34. AAAAAAAAAAAAAAG348AG349SG350Y351GG352AR353GGY354GH355YGS356SDGG
35. AAAAAAAAAAAAAAG357SG358SG359GGY360GD361GG
36. AAAAAAAAAAAAAA362GA363SG364Y365GG366SW367H368YGS369SDSS
37. AAAAAAAAAAAAAAG370AG371GG372Y373GAGS
38. AAAAAAAAAAAAAA374GA375GGY376GD377GG
39. AAAAAAAAAAAAAAG378AG379GGY380GGY381GD382GG
40. AAAAAAAAAAAAAAG383GS384RS385Y386GG387SW388H389YGS390SDSG
41. AAAAAAAAAAAAAAG391AG392CD393GY394GAGS
42. AAAAAAAAAAAAAA395GA396GGY397GD398GG
43. AAAAAAAAAAAAAAG399AG400SG401Y402GG403AR404GGY405GH406YGS407SDGG
44. AAAAAAAAAAAAAAG408SG409SG410GGY411GD412GG1409
45. 1410AAAAAAAAAAAAAG1411AG1412SG1413Y1414GG1415SW1416H1417YGS1418SDSS
46. AAAAAAAAAAAAAAG1419AG1420GGY1421GAGS
47. AAAAAAAAAAAAAAG1422AG1423GGY1424GD1425GG
48. AAAAAAAAAAAAAAG1426AG1427SG1428Y1429GGY1430GH1431YGS1432SDGG
49. AAAAAAAAAAAAAAG1433AG1434GGY1435GAGS
50. AAAAAAAAAAAAAAG1436AG1437GGY1438GD1439GG
51. AAAAAAAAAAAAAAG1440AG1441SG1442Y1443GGY1444GH1445YGS1446SDGG
52. AAAAAAAAAAAAAAG1447AG1448GGY1449GD1450GG
53. AAAAAAAAAAAAAAG1451AG1452SG1453Y1454GG1455AR1456GGY1457GH1458YGS1459SDGG
54. AAAAAAAAAAAAAAG1460SG1461SG1462GGY1463GD1464GG
55. AAAAAAAAAAAAAAG1465AG1466GGY1467GD1468GG
56. AAAAAAAAAAAAAAG1469AG1470SG1471Y1472GGY1473GH1474YGS1475SDGG
57. AAAAAAAAAAAAAAG1476AG1477GGY1478GD1479GG
58. AAAAAAAAAAAAAAG1480AG1481SG1482Y1483GG1484AR1485GGY1486GH1487YGS1488SDGG
59. AAAAAAAAAAAAAAG1489AG1490SG1491Y1492GG1493SW1494YGS1495SDSG
60. AAAAAAAAAAAAAAG1496AG1497GD1498Y1499GAGS
61. AAAAAAAAAAAAAAG1500AG1501GGY1502GD1503GG
62. AAAAAAAAAAAAAAG1504AG1505SG1506Y1507GG1508AR1509GGY1510GH1511YGS1512SDGG
63. AAAAAAAAAAAAAAG1513SG1514SG1515GGY1516GD1517GG
64. AAAAAAAAAAAAAAG1518AG1519SG1520Y1521GG1522SW1523H1524YGS1525SDSG
65. AAAAAAAAAAAAAAG1526AG1527GGY1528GAGS
66. AAAAAAAAAAAAAAG1529AG1530GGY1531GD1532GG
67. AAAAAAAAAAAAAAG1533AG1534SG1535Y1536GG1537AR1538GGY1539GH1540YGS1541SDGG
68. AAAAAAAAAAAAAAG1542AG1543SG1544Y1545GG1546SW1547H1548YGS1549SDSG
69. AAAAAAAAAAAAAAG1550AG1551E1552GGY1553GAGS
70. AAAAAAAAAAAAAAG1554AG1555GGY1556GD1557GG
71. AAAAAAAAAAAAAA1558GS1559GGY1560GD1561GG
72. AAAAAAAAAAAAAAG1562AG1563SG1564Y1565GG1566AR1567GGY1568GH1569YGS1570SDGG
73. AAAAAAAAAAAAAAG1571SG1572SG1573GGY1574GD1575GG
74. AAAAAAAAAAAAAAG1576AG1577SG1578Y1579GG1580SW1581H1582YGS1583SDSG
75. AAAAAAAAAAAAAAG1584AG1585GGY1586GAGS
76. AAAAAAAAAAAAAAG1587AG1588GGY1589GD1590GG
77. AAAAAAAAAAAAAAG1591AG1592SG1593Y1594GG1595AR1596GGY1597GH1598YGS1599SDGG
78. AAAAAAAAAAAAAAG1600AG1601SG1602Y1603GG1604SW1605H1606YGS1607SDSG
79. AAAAAAAAAAAAAAG1608SG1609AG1610SG1611GG1612SW1613H1614YGS1615SDSG
80. AAAAAAAAAAAAAAG1616AG1617GGY1618GAGS
81. AAAAAAAAAAAAAAG1619AG1620GGY1621GR1622DDGG
82. AAAAAAAAAAAAAAG1623AG1624SG1625Y1626GG1627AR1628GGY1629GH1630YGS1631SDGG
83. AAAAAAAAAAAAAAG1632AG1633GGY1634GGY1635GD1636GG
84. AAAAAAAAAAAAAAG1637AG1638SG1639Y1640GG1641SW1642H1643YGS1644SDSG
85. AAAAAAAAAAAAAAG1645AG1646SG1647Y1648GG1649SW1650H1651YGS1652SDGG
86. AAAAAAAAAAAAAAG1653AG1654GGY1655GGY1656GD1657GG
87. AAAAAAAAAAAAAAG1658SG1659SG1660Y1661GG1662SW1663H1664YGS1665SDSG
88. AAAAAAAAAAAAAAG1666AG1667SG1668Y1669GG1670W1671Q1672YGS1673NSG
89. AAAAAAAAAAAAAAG1674AG1675SG1676Y1677GG1678AR1679GGY1680GH1681YGS1682SDS
90. AAAAAAAAAAAAAAG1683AG1684GG1685AR1686GAT1687GGY1688GGY1689SDN
91. AAAAAAAAAAAAAAG1690AG1691GGY1692Y1693GR1694ARS
92. AAAAAAAAAAAAAAG1695SG1696AR1697GV1698IV1699ET1700CD1701GF1702LR1703GD1704YGS1705SDSS
93. AAAAAAAAAAAAAAS1706SA1707SS1708ANG1709Y1710V1711CK1712PK1713RL1714TS1715K1716IA1717VH17182880

```

PAB/ NPAB
 (polyalanine block) (non polyalanine block)
 Motif

PAB/ NPAB

Fig. 14.11 Deduced amino acid sequence of *Samia ricini* (Sr-) H-fibroin. Each motif (PAB/ NPAB) is numbered based on the position relative to the N-terminus. We used red letters for A residues to highlight PABs. Motif-specific amino acid residues are marked with different colors; R in motif 1 is marked by a pale blue letter; W in motif 2 and H in motifs 1 and 2 are marked by magenta letters. The submotif, S/G G/H G Y/S in motif 3 is represented by blue letters

Lepidoptera, the *H-fibroin* gene prototype was likely present in a common ancestor of these two taxa.

The proximal region of the second exon of the lepidopteran and trichopteran H-fibroin gene contains a non-repetitive sequence. This sequence is quite conserved among Lepidoptera and it has been suggested that it has an important function in silk assembly (He et al. 2012). Fig. 14.8a shows the alignment of the N-terminal H-fibroin amino acid sequences from eight saturniid species and five non-saturniid species. Using this alignment, Sezutsu and Yukuhiro (2014) constructed a phylogenetic tree using the neighbor joining method (Saitou and Nei 1987) (Fig. 14.8b).

Based on this tree, *S. ricini* is separated from the five other saturniid species (except *R. fugax*) at the early stages of evolution in Saturniidae. This result is consistent with those of Friedlander et al. (1998) and Sima et al. (2013).

The C-terminal sequences of saturniid H-fibroins were first determined in *A. pernyi* and *A. yamamai*. However, since the two *Antheraea* species are closely related, the detected sequences were nearly identical (Fig. 14.9a). As expected, the Sr-H-fibroin C-terminal sequence was more distant (Fig. 14.9a) although the three Cys residues were found to be conserved among all three species. Therefore, the three conserved Cys residues in the C-terminal region ought to play an essential role in forming the disulfide bonds between the two molecules of H-fibroin to form homodimers.

The alignment of *B. mori* (Zhou et al. 2000) and *G. mellonella* H-fibroins (Žurovec and Sehnal 2002) indicates similarities in the C-terminal regions (Fig. 14.9a) of the two species, but differences from the saturniid H-fibroins sequences (Fig. 14.9a, b). This is expected since *B. mori* and *G. mellonella* H-fibroins form heterodimers with L-fibroins. Hence, this functional divergence might have induced extreme diversification between the C-terminal H-fibroin sequences of Saturniidae and other Lepidoptera.

14.5 Sericins as Glue Proteins

14.5.1 *Bombyx mori* Sericins

Sericins are glue proteins found on the surface of silk fibers. Sericins have been studied since the nineteenth century; the amino acid, serine (Ser), was first extracted from sericins and it was named after the proteins (Cramer 1865). Sericin proteins are produced by the secretory epithelium in the MSG and coat the jelly-like fibroin solution that moves through the gland lumen from the PSG. Sericins move together with fibroin and remain on the surface of fibroin during and after fibrilization at the spinneret.

It was previously predicted that the sericin fraction contains several proteins, since acid fuchsin staining of the anterior MSG lumen revealed three distinct layers (Yamanouchi 1922). To elucidate the molecular components of the sericin fraction, separation and characterization of sericin proteins were attempted with various methods; the most successful were ultracentrifugation and electrophoresis (Tashiro and Otsuki 1970; Gamo 1973; Sprague 1975). Interestingly, sericin protein mobility in SDS-PAGE was considerably smaller than later predictions from their molecular masses based on their elucidated sequences (Takasu et al. 2007). This discrepancy is explained by the abundance of Ser residues that reduce SDS binding to the protein (Hayashi and Nagai 1980). In spite of this problem SDS-PAGE was useful to separate major sericin proteins, which were designated as sericins A, M, and P since they were secreted in the anterior, middle, and posterior MSG, respectively (Tsutsui

et al. 1979; Takasu et al. 2002). Protein polymorphisms detected as different electrophoretic mobilities of sericin proteins allowed genetic linkage analysis and suggested the existence of two sericin-encoding genes on chromosome 11 (Shonozaki et al. 1980; Gamo 1982). Subsequent analyses of MSG mRNAs and the silkworm genome database resulted in the identification of three sericin-encoding genes located relatively close together in a 2.83 Mb region of chromosome 11 (Okamoto et al. 1982; Michaille et al. 1990; Takasu et al. 2007; The international silkworm genome consortium 2008). Now we can describe an overview of sericin proteins with the correspondences of the sericin genes to the sericins detected by protein analyses.

14.5.2 Three Bombyx Sericin Genes and Protein Products

Okamoto et al. (1982) isolated mRNAs and reported the partial genomic sequence encoding the serine-rich repetitive motif transcribed in MSG cells. The corresponding gene was designated as *sericin*, afterward *sericin-1* (*ser1*). Garel et al. (1997) showed that the *ser1* gene is approximately 23-kb long and comprises 9 exons. In addition, some of the recently discovered ESTs indicate the existence of another small exon between exons 5 and 6 (for example, the sequence with GenBank accession number BB986619) (Fig. 14.12). Exons 6 and 8 encode a serine-rich 38-amino acid-repetitive motif. At least five proteins, Ser1A, Ser1A', Ser1B, Ser1C, and Ser1D, are predicted to be the products of the *ser1* gene by alternative splicing, which is controlled developmentally and regionally (Ishikawa and Suzuki 1985; Couble et al. 1987; Garel et al. 1997. See also 14.6.2). The most abundant cocoon

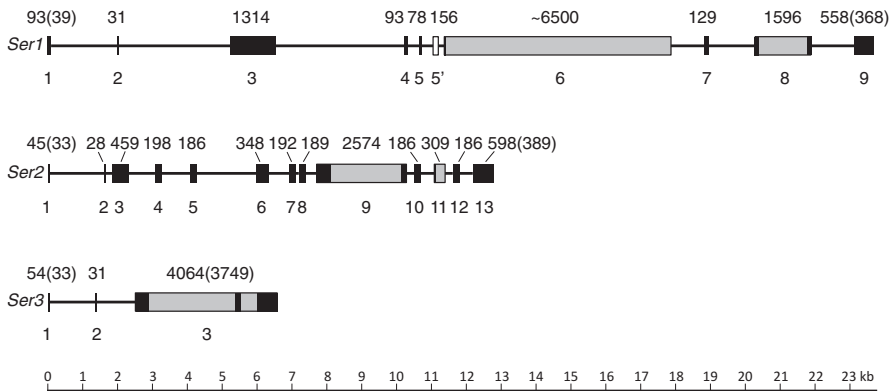


Fig. 14.12 Gene structures of *Bombyx* sericin genes. Boxes are exons and horizontal lines are introns. The sizes of exons and the exon numbers are indicated *above* and *below* the boxes, respectively. The sizes of ORFs of the first and last exons are indicated in parentheses. The white box in *ser1* (numbered 5') is the putative novel exon deduced from the EST database. The gray parts of the exons indicate the regions encoding repetitive motifs

Gene	Exons	Protein	Molecular mass
<i>Ser1</i>	1 2 3 4 5 6 7 8 9	Ser1C/Sericin M	330,767 (>400 kDa)
	1 2 - - 5 6 7 8 9	Ser1D/Sericin M	283,617 (>400 kDa)
	1 2 3 4 5 - 7 8 9	Ser1B	119,478
	1 2 - 4 5 - 7 8 9	Ser1A	76,032
	1 2 - - - 7 8 9	Ser1A'/Sericin P	69,946 (150 kDa)
<i>Ser2</i>	1 2 3 4 5 6 7 8 9 10 11 12 13	Ser2-large	198,647 (230 kDa)
	1 2 3 4 5 6 7 8 - 10 11 12 13	Ser2-small	102,432 (120 kDa)
<i>Ser3</i>	1 2 3	Ser3/Sericin A	123,282 (250 kDa)

Fig. 14.13 Constitutional profiles of sericin proteins. The *ser1* and *ser2* genes produce transcript variants by skipping one or more exon(s) indicated by “-.” The molecular masses of Ser1C and Ser1D were estimated by Garel et al. (1997), and the others were calculated from the putative sequences obtained from GenBank including signal peptides. The molecular masses estimated by SDS-PAGE are also shown in parentheses (Takasu et al. 2002; Kludkiewicz et al. 2009)

sericin component (sericin M) that migrates slower than the fibroin heavy chain in SDS-PAGE, is possibly a mixture of Ser1C and Ser1D proteins by the size and partial sequences of fragmented sericin M (Takasu et al. 2005). Another major sericin component (sericin P) that is estimated to be approximately 150-kDa by SDS-PAGE was identified as the Ser1A' protein (Fig. 14.13) (Watanabe et al. 2007). The repetitive motif encoding a high percentage of Ser codons is responsible for the high proportion (30 mol%) of Ser in Ser1 protein products. The serine-rich repeats were implicated in the structural changes leading to silk insolubility connected with the formation of β -sheet structures (Fig. 14.14a) (Takasu et al. 2006).

The second sericin encoding gene *sericin-2* (*ser2*) was identified based on the mRNA specifically transcribed in the anterior part of MSG (Michaille et al. 1990). The *ser2* gene encodes a 15-amino acid-repetitive motif with a relatively low Ser content (Fig. 14.14b). The whole gene spans over 12-kb, and 2 of 13 exons encode the repetitive sequences (Kludkiewicz et al. 2009) (Fig. 14.12). Two mRNA variants are transcribed by alternative splicing, and both are expressed throughout the larval stages except for the late fifth instar (Fig. 14.13). The Ser2 products were also detected as 230- and 120-kDa proteins in the silk spun by fourth instar larvae and in the MSG lumens of early fifth instar larvae. This supports that the Ser2 proteins are the major glue components of non-cocoon silk spun by larvae of feeding stages, whereas they represent only minor components of the cocoon silk (Kludkiewicz et al. 2009; Takasu et al. 2010; Dong et al. 2013). The similarity of the Ser2 repetitive motif with that of the adhesive protein of mussel byssus indicates the convergent evolution of both proteins due to the selective pressure on glue strength. The Ser2 proteins function as strong adhesives fixing the silk threads to surrounding substances (Kludkiewicz et al. 2009).

While the separated cocoon sericin components P and M were identified as *ser1* gene products, the last major component, sericin A, estimated to be about 250-kDa

a

B.mor_ser1, 38

GSRTSGGTSTYGYSSSHRGGVSSTGSSSNTDSSSTKNA
 GSSTSGGTSTYGYSSSHRGGVSSTGSSSNTDSSSTKSA
 GSSTSGGTSTYGYSSRRHRGGVSSTGSSSNTDSSSTKNA
 GSRTSGGTSTYGYSSSHRGGVSSTGSSSNTDSSSTKNA
 GSRTSGGTSTYGYSSSHRGGVSSTGSSSNTDSSSTKNA

A.ass_Unigene1892, 38

GGSSDTYGRHGRSHSGSYGDI2TSANSRYGTTSNSNTYT
 GGSSYTHGRHGHYSYSGTYGSDTDSGNSDGTTSNSNTH
 GGSSATYGRHGHYSYSGTYGNDDTSGNSEDGTTNSNTH
 GGSSATYGRHGHYSYSGYDGT2TSANSRYGTTSNSNTYT
 GGSSYTHGRHGHYSYSGTYGSDTDSGNSDGTTSNTH

R.new_Unigene3473, 37

GSSTTTGSSSTTGSSTTGSSTTKSYPGSQYGSQSYQ
 GSPTTTGRSSTTGSSTTGSSTTKSHPGSQYGSQSYQ
 GSPTTTGSSTTGSSTTDSSTTKSYPGSQYGSQSYQ
 GSHTTTGSSTTGSSSATGSTTTKSYPGSQYGSQSYQ
 GSSTTTGSSTTGSSTTGSSTTKSHPGSQYGSQSYQ

S.ric_Unigene3618, 54,58

SHHGSGHYPTTSTGSSTAGSTTTSSSGTSTSGSTSTSGSSHPGSHSGPG
 SHHGSGHYPTTSTGSSTAGSTTTSSSGTSTSGSTSTSGSSSTGSHSGPG
 SHHGPGHYPTTSTGSSTAGSNTSSSGTSTSGSTSTSGSSSTGSHSGPG
 SHHGPGHYPTTSTGSSTAGSNTSSSGTSTSGSTSTSGSSSTGTHPGHSGPG
 THHGPGHYPTTSTGSSTAGSTTTSSSGTSTSGSTSTSGRSSTGSHPESHHGPG

A.per_Unigene13275, 83-84

DDSTTSSSSSSSSSSSSSSSSSSDYSTSTDSSTSSNTDSTSTDSNSTASSDSSATDSSSNSSGNNTTTDSETTSTNSD
 SSSTTDSSTTDSSSSTSSSSSSSSSSSEYSTSTDSSTSSNTDSTSTDSNSTASSDSSATDSSSNSSGNNTTTDSETTTSSD
 SSSTTDSNSTASSDSSATDSSSNSSGNNTTTDSETTSTNSD
 SSSTTDSSSSTTDSSSSTSSSSSSSSSSSNYSSTDSSTSSNTDSTSTDSNSTASSDSSATDSSSNSSGNNTTTDSETTSTNSD

A.sel_Unigene3639, 21

GTTSFDTTSESNSTSTETSS
 GTTSSDNTSESSNTNADTSS
 GNTSSDATSESNSTSTDTSS
 GTTSSDNTSESNSTSTETLS
 GTTSSDNTSESNSTSTDTSS

G.mel MG-1

NNGSSGSSGSSGSSGSS
 NNGSSGSSGSS
 NNGSSGSSGSS
 NNGSSGSSGSSGSSGSS
 NNGSSGSSGSS

G.mel MG-2

NNASSGSSSS
 NNSSGSSSS
 NNSSGSSSS
 NNSSGSS
 NNSSGSSSS

G.mel MG-3

NSESSGSSGSSSS
 NNGS
 NGSSGSSSS
 NGSSSSGSSSS
 NDSSS

A.per_Unigene3413, 38

GGSSDTYGRHGRSHSGSYGDTSTNGNSRYGTTSNSNTYT
 GGSSNTHGRHGHYSYSGTYGSDTDSGNSDGTTSNSNTYT
 GGSSDTYGRHGRSHSGSYGDTSTNGNSRYGTTSNSNTYT
 GGSSNTHGRHGHYSYSGTYGSDTDSGNSDGTTSNSNTYT
 GGSSDTYGRHGRSHSGSYGDTSTNGNSRYGTTSNSNTYT

R.new_Unigene12767, 38

GGSSDTRGRKNGQSESGSYGETST2SANSNKGTYSYSDTAV
 GSSSTTRGRKNGQSESGSYGETST2SANSNKGTYSYSDTAV
 GSSSTTRGRKNGQSESGSYGETST2SANSNKGTYSYSDTAV
 GSSSTTRGRKNGQSESGSYGETST2SANSNKGTYSYSDTAV
 GSSSTTRGRKNGQSESGSYGETST2SANSNKGTYSYSDTAV

S.ric_Contig37, Unigene2067, 36

DSYTGGSNSYTSGGFDQSQSYGSSTSANNGHGSQAQ
 NSYSGSSSTSDGFGYSQTYGSSSTANNGHGSQAQ
 NSYAGSSSTSDGFGYSQTYGSSASANNGHGSQAQ
 NSYAGSSSTSDGYDYSQSYGSSASAYNGYGSSTNS
 NSNSAGSSANNGEYYSQTYGSSSTANNGHGSQAQ

Fig. 14.14 Repetitive motifs in sericins and putative sericin proteins of Lepidoptera. Each motif is classified into one of the three groups based on the predicted secondary structure. (a) The motifs with a strong tendency to form β -sheet structure. (b) The motifs with predominant α -helix. (c) The motifs with a relatively weak tendency to form β -sheet structure. The resource species and the encoding gene or nucleotide name(s) were described above each motif connected with “_”. “Unigenes” and “contigs” are the putative sericin-encoding nucleotides reported by Dong et al. (2015) and Tsubota et al. (unpublished information), respectively. The number of amino acids composing a repeat unit is shown on the right separated by a comma. B. mor: *Bombyx mori*, A. per: *Antheraea pernyi*, A. yam: *A. yamamai*, A. ass: *A. assama*, A. sel: *Actias selene*, R. new: *Rhodinia newara*, S. ric: *Samia ricini*, G. mel: *Galleria mellonella*

by SDS-PAGE turned out to be a product of a different gene. The fragmentation of sericin A by peptidases and N-terminal sequencing yielded several short amino acid sequences, which were used as queries for BLAST searches in the silkworm genome database. A novel gene was identified and designated as *sericin-3* (*ser3*) (Takasu et al. 2007). The *ser3* gene has a simpler structure and expression pattern than the other sericin genes; it spans about 6.6 kb and consists of three exons transcribed into one mRNA encoding a single protein (Figs. 14.12 and 14.13). The solubility of the Ser3 protein in hot water is higher than Ser1 proteins, probably because the serine-

b

B.mor_ser2, 15 RSPSHKDEKAKPND RSPSKDKTEKAKPND SSPSHKDEKAKHND RSPSKDKTEKAKPND RSPSHKDEKVKPND	A.per Unigene25306, 29 WRPGERAPVKKPEDNLKPEGDFERRRPDE WSPGDRAPVRRQDNLKPEGDFEKRKPDE WRPGDRAPVRRKPEDNLKPEGEFERRQPED WRPGDREPTRRRPKDNLKPEGEFTTPEKET WRPAERQRPKKPEDNLKPEGDFETRRKPDE	A.sel Unigene3674, 29 WRPAERPQKKPKDNLKPEGEFEDRKPEE WRPAERPQKKPKDNLKPEGEFEDRQPAE WRPAERPQKKPKDNLKPEGEFEDRKPEE WRPAERPQKKPKDNLKPEGEFESPKPEE
A.yam Unigenel1042, 10 RRKRTPTEPEY RRKRSPPSY RKKKSPTSEY RRKRSLSVDS QRRKRSPPSQEN	R.new Unigene27222, 36 QGEVKDRTPKDKDSPKSHPDGEPSPTKYGSYDRKHP HDEVKDRTPEKEDTSKSHPDREPSPTKYGTDRKHP HDEVKDRTPKDKDSPKSHPDREPSPTKYGTDRKHP HDEVKDRTPKDKDSPKSYPDREPSPTKYGTDRKHP QGEFKDRTPKDKDSPKSHPDREPSPTKYGSYDKKHP	S.ric Unigene21589, 5 KVDPA KGDPA KGDPA KGDPA KVDPA

c

B.mor_ser3, 86
SDDSSGATKGNSSKSSSSSQGQASSSSSDEKSSQSSSNSSNNSKSSSSQSSSSQNSSGSKGSGSEESSNGGSGSRGTSAGGTDED
SDDSSGATKGNSSKSSSSSQGQASSSSSDENSSQSSSNSSNNSKSSSSQSSSSQNSSGSKGSGSEESSNGGSGSRGNSVGGTDED
SDDSSGATKGNSSKSSSSSQGQASSSSSDEKSSQSSSNSSNNSKSSSSQSSSSQNSSGSKGSGSEESSNGGSGSRGNSAGGTDED
SDDSSGATKGNSSKSSSSSQGQASSSSSDEKSSQSSSNSSNNSKSSSSQSSSSQNSSGSKGSGSEESSNGGSGSRGNSAGGTDED
SDDSSGATKGNSSKSSSSSQGQASSSSSDEKSSQSSSNSSNNSKSSSSQSSSSQNSSGSKGSGSEESSNGGSGSRGTSAGGTDED

S.ric Contig37, Unigene2067, 77
GGSSSSGGGKSDSSSYGESNANSNENETTRNSNRAGSSSSNNSKKHSENHSSSESSSESSANSRKGSSSSNSNS
GGSSSSGGGKSDSSSYGESNANSNENETTRNSNRAGSSSSNNSKKHSENHSSSESSSESSANSRKGSSSSNSNS
GGSSSSGGGKSDSSSYGESNANSNENETTRNSNRAGSSSSNNSKKHSENHSSSESSSESSANSRKGSSSSNSNS
GGSSSSGGGKSDSSSYGESNANSNENETTRNSNRAGSSSSNNSKKHSENHSSSESSSESSANSRKGSSSSNSNS
GGSSSSGGGKSDSSSYGESNANSNENETTRNSNRAGSSSSNNSKKHSENHSSSESSSESSANSRKGSSSSNSNS

S.ric Unigenel738, 49
SSTSEEDSNASPAQAAAKTASETSASRASSSTKSKSQTTSDTTASSAT
SSTSSQAHSNASSEQTANTTSTKTSASGASSSTKSTSQTTSGTTSSAT
SSTSSQADSNVSSAQATKTAASETSASGASSSTKSTSQTTSDTTASSAT
SSTSSQADSNASSEQTANTTSETASGASSSTKSTSQRTSHTTSSGTT
SSSSSEADSNASSAQATKTAASETSASSATSYTKSTSKTSSGSI

S.ric Contig35, 55
SSSSSNKNSELYDSSSNFASHNTGNSNGYPGEHLDLGIASNEQGESYQRQSSSAT
SSSSSNESELYDSSSNFASHNTGNSNGYKGEHLDLGIASNEQGESYQRQSSIAE
SSSSSNKNSELYDSSSNFASHNTGNSNGYPGEHLDLGIASNEQGESYQRQSSIAE
SSSSSNKNSELYDSSSNFASHNTGNSNGYKGEHLDLGIASNEQGESYQRQSSIAE
SSSSSNESELYDSSSNFASHNTGNSNGYKGEHLDLGIASNEQGESYQRQSSVAE

Fig. 14.14 (continued)

rich motifs found in Ser3 form fewer β -sheet structures than that of Ser1 proteins (Figs. 14.14b, c) (Takasu et al. 2006). The relatively soft texture of Ser3 might support the fibrilization at the spinnerets where sericins are exposed to a high shear rate.

It is possible that there are other genes encoding less abundant sericin proteins. For example, the proteomic analysis of silk by Dong et al. (2013) identified some serine-rich components (BGIBMGA001820, BGIBMGA005301, and BGIBMGA011896 in the silkworm database), though their functions are unclear.

14.5.3 Sericins of Saturniidae

The sericin characterization of other Lepidoptera was performed for comparison with *Bombyx* sericins to clarify the evolution of silk encoding genes.

Recently, Dong et al. (2015) identified 22 putative sericin candidates by transcriptome analyses of silk glands from six Saturniidae silkworms (superfamily Bombycoidea), including *A. yamamai*, *A. pernyi*, *A. assama*, the Indian moon moth,

A. selene, *R. newara*, and *S. ricini*. Tsubota et al. also identified 5 contigs encoding serine-rich proteins by analyzing the EST library of *S. ricini* MSG (Tsubota et al. unpublished information). Most of the transcripts encode repetitive motifs with relatively low sequence similarities to the repeats in *Bombyx* sericins. They can be classified into three groups based on the predicted secondary structure of their putative protein products (Garnier et al. 1978; Qian et al. 1988; Prevelige and Fasman 1989). The first group members strongly tended to form β -sheet structures such as *Bombyx* Ser1 (Fig. 14.14a), the second group proteins strongly tended to form α -helix structures such as *Bombyx* Ser2 (Fig. 14.14b), and the third group showed intermediate features, reminiscent of *Bombyx* Ser3 (Fig. 14.14c). The identification of the corresponding proteins in secreted silk and detailed sequence and expression analyses are required to confirm the function of each candidate sericin gene.

14.5.4 Sericins of *Galleria mellonella*

Three sericin encoding genes, *MG-1*, *MG-2*, and *MG-3*, were identified in *G. mellonella*, a moth of the superfamily Pyraloidea, family Pyralidae. They are similar to one another and are reminiscent of the *Bombyx* sericin genes by the structure of their N-termini, including the sizes and sequences of their first two exons (Zurovec et al. 2013). *MG-1*, *MG-2*, and *MG-3* are expressed in the MSG in different developmental stages and at least one of them produces more transcripts by alternative splicing. The amino acid sequences encoded by the three genes, are different from the sequences of *Bombyx* sericins, and contain very short repeats consisting mostly of Ser (more than 50%), asparagine (Asn) (11.1–17.8%), and Gly (8.9–23.6%). The repetitive motifs of all three known *Galleria* sericins can be classified into the first sericin group since they have a strong tendency to form β -sheet structures (Fig. 14.14a).

14.6 Differences in Shape and Function of Silk Glands Between Insects

14.6.1 Gene Expression in Different Parts of Silk Glands

Specific genes or genes strongly expressed in a particular part of the silk gland were identified by several recent analyses. *B. mori* silk gland can be divided into three morphologically distinct regions (ASG, MSG and PSG), in which MSG, containing 300 secretory cells, functions for sericin production and PSG with 500 cells synthesizes fibroins (Prudhomme et al. 1985). Serial analysis of gene expression (SAGE) is a valid approach to analyzing a large number of genes expressed in a tissue of interest. SAGE was applied to the MSG and PSG of *Bombyx* (Royer et al. 2011). Approximately 18 genes were found to be specifically expressed in the MSG, in addition to *sericins*. Among them, the most annotated genes were those of enzymes.

In contrast to the MSG, just one novel protein coding gene, a storage protein, was specifically expressed in the PSG. A genome-wide microarray analysis was also utilized for gene expression analysis in multiple larval tissues (Xia et al. 2007). This study identified 412 genes that are up-regulated in the A/MSG and 109 in the PSG, respectively (Xia et al. 2007). The former included genes encoding proteases, protease inhibitors, dehydrogenases and protein kinases, and the latter encodes transcription factors or structural proteins. The protease inhibitors in the MSG might protect fibroin proteins in the silk gland lumen against proteases expressed in this region. A transcription factor up-regulated in the PSG contains a basic helix-loop-helix domain. Interestingly, Bmsage, a member of this family, was recently found to be able to bind to the *H-fibroin* promoter and activate its expression (Zhao et al. 2014).

The MSG of *B. mori* can be further divided into three subsections, MSG-A, MSG-M and MSG-P. Previous studies revealed that the *sericin* genes show region-specific expression; *ser1* is expressed only in MSG-M and MSG-P, and *ser2/ser3* in MSG-A (Matsunami et al. 1998; Takasu et al. 2007; Takasu et al. 2010). Genes showing such a region-specific expression were further explored via shotgun proteomic analysis (Li et al. 2015). This analysis revealed that 55 proteins are specifically expressed in MSG-A, 14 in MSG-M, and 173 in MSG-P, respectively. The proteins expressed in MSG-A are likely to be involved in multiple processes, such as silk gland development and silk protein protection. Proteins with abundant expression in MSG-M are involved in the ribosome pathway. On the other hand, the MSG-P proteins are mainly involved in oxidative phosphorylation and citrate cycle pathways. Protein expressions were also compared between the MSG and PSG, and it was found that 237 proteins were expressed only in the MSG and 98 had stronger expression in this region. Many of these proteins are involved in protein biosynthesis, suggesting that translation-related pathways are activated in the MSG for efficient synthesis of silk proteins. The expression of mRNA for MSG proteins was also investigated and it was found that proteins expressed abundantly in the MSG-A were regulated primarily at the transcriptional level. In contrast, there was an inconsistency between the transcription and translation levels for genes whose protein products are abundant in the MSG-M and/or MSG-P. Nevertheless, the results obtained here strongly supported the hypothesis that each MSG sub-region has distinct biological functions.

RNA-sequencing is a novel technology for high-throughput screening of gene expression. This technique was utilized to study the gene expression of the *B. mori* silk gland (Chang et al. 2015). In this study, gene expression was mainly investigated in the ASG, and it was found that 282 genes were upregulated in this region. The gene ontology and pathway analysis suggested that ion transportation, energy metabolism, protease inhibitors and cuticle proteins play essential roles in the process of silk formation and spinning. This study also clarified that a number of genes showed a different expression level between males and females. These genes might be associated with the differences in the quality of the silk fibers between sexes. As described below, RNA-sequencing has now been utilized for the transcriptomic analysis of a number of wild silkmoth species and this is potentially a very powerful approach for the elucidation of the mechanisms of silk production. Genes, gene ontologies or pathways activated in each silk gland subpart are summarized in Table 14.1.

Table 14.1 Summary of genes, gene ontologies or pathways activated in *B. mori* silk gland

ASG	MSG-A	MSG-M	MSG-P	PSG	References
	18 genes including enzymes			Storage protein	Royer et al. (2011)
	Proteases, protease inhibitors, dehydrogenases, protein kinases			Transcriptional factors, structural proteins	Xia et al. (2007)
	Silk gland development, silk protein protection	Ribosome pathway	Oxidative phosphorylation, citrate cycle pathway		Li et al. (2015)
Ion transportation, energy metabolism, protease inhibitors, cuticle proteins					Chang et al. (2015)

ASG anterior silk gland, MSG-A anterior part of the silk gland, MSG-M middle part of the silk gland, MSG-P posterior part of the silk gland, PSG posterior silk gland

14.6.2 Regulation Mechanisms for Sericin and Fibroin Genes

Recently, there has been an advance in the study of the transcriptional regulation mechanisms for *sericin* and *fibroin* genes. Expression of *ser1* is confined to the MSG-M and MSG-P. The spatial restriction is mediated by the input of several transcriptional factors, including activator(s) and repressor(s). Forkhead (Fkh) is a transcription factor with a fork head domain that binds around -90 of the *ser1* promoter sequence (Mach et al. 1995). Removal of this sequence decreased the transcriptional activity, suggesting that Fkh functions as a putative *ser1* activator. Fkh also regulates *fibroin heavy chain (H-fibroin)* expression. Another regulator of *ser1* is the MSG-intermolt-specific complex (MIC), a tissue- and stage-specific factor complex that is intrinsic for *ser1* expression (Takiya et al. 2011). The MIC binds to several *ser1* promoter sequences with ATTA-core elements. Analysis of this complex clarified that this includes a Hox transcriptional factor, Antennapedia (*Antp*), and its cofactors, Extradenticle (*Exd*) and Homothorax (*Hth*) (Kimoto et al. 2014). Among them, just *Antp* is specifically expressed in the MSG. In addition, it has been suggested that *Antp* is responsible for region-specific *ser1* expression. This was further supported by the result that *Antp*-misexpression in the PSG using transgenic techniques could significantly induce *ser1* expression in that region.

POU-M1 is another *ser1*-regulator with a class III POU domain. POU-M1 binds to approximately -200 of the *ser1* promoter sequence (Fukuta et al. 1993). Initially, this transcription factor was considered to be a *ser1* activator because the removal of this sequence decreased *ser1* promoter activity *in vitro*. However, examination of

the spatiotemporal expression revealed that *POU-M1* is expressed in a complementary pattern to that of *ser1* in various developmental stages (Kokubo et al. 1997; Matsunami et al. 1998; Kimoto et al. 2012). In addition, POU-M1 could repress *ser1* promoter activity when introduced into the silk gland via a particle gun (Kimoto et al. 2012). Competition of POU-M1 with MIC for binding to the -70 region of the *ser1* promoter sequence was also revealed (Kimoto et al. 2012). All of these results suggested that POU-M1 acts as a negative regulator of *ser1* expression.

In the PSG, the fibroin component genes [*H-fibroin*, *fibroin light chain (L-fibroin)* and *fibrohexamerin (fhx)*] are abundantly expressed and regulation of *H-fibroin* transcription has been well studied. Fkh binds to the upstream proximal region of *H-fibroin* (Takiya et al. 1997) and this region is required for transcriptional activation *in vitro* (Suzuki et al. 1986). Fibroin modulator-binding protein-1 (FMBP-1) also binds to the *H-fibroin* promoter but its function has yet to be determined (Takiya et al. 1997; 2005). Silk gland factor-2 (SGF-2), a tissue-specific *H-fibroin* regulator complex, was recently purified and its components were determined. SGF-2 mainly consists of the LIM-homeodomain transcription factor Arrowhead (Awh), LIM domain-binding protein (Ldb) and a sequence-specific single-stranded DNA-binding protein (Lcaf) (Ohno et al. 2013). Awh is a region-specific activator specifically expressed in the PSG. Also, induction of *H-fibroin* expression was confirmed when *Awh* was misexpressed in the MSG (Ohno et al. 2013; Kimoto et al. 2015). This misexpression accompanied *L-fibroin* and *fhx* expression suggesting that Awh is a key regulator for all of the silk component genes (Kimoto et al. 2015). SGF-2 could bind to the promoter region of these genes (Kimoto et al. 2015); therefore, it was suggested that Awh is regulating them directly. Recently, a basic helix-loop-helix transcription factor, Bmsage, was found to stimulate *H-fibroin* expression by interacting with Fkh (Zhao et al. 2014). The currently understood transcriptional regulation of silk genes is pictured in Fig. 14.15.

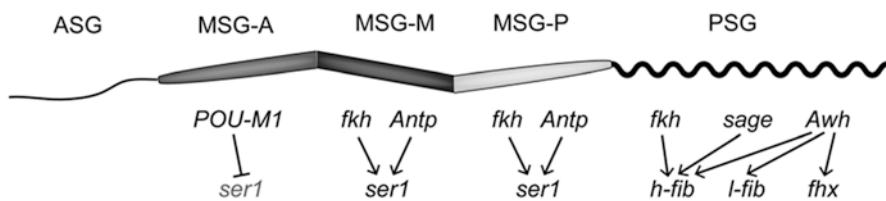


Fig. 14.15 A scheme of the transcriptional regulation for silk genes. The subregion of the silk gland is shown above the drawing of the silk gland and the transcriptional regulation is depicted below. *Abbreviations:* ASG anterior silk gland; MSG-A anterior part of the silk gland, MSG-M middle part of the silk gland, MSG-P, posterior part of the silk gland, PSG, posterior silk gland; *fkh*, *forkhead*; *Antp*, *Antennapedia*; *Awh*, *Arrowhead*; *ser1*, *sericin-1*; *h-fib*, *h-fibroin*; *l-fib*, *l-fibroin*; *fhx*, *fibrohexamerin*. POU-M1 represses *ser1* and other transcriptional factors activate expressions of silk genes, including *ser1*

14.6.3 Quantitative Differences in Gene Transcription Profiles Between *Bombyx mori* and Other Wild Silkmoths

A number of wild silkmoth species can produce various types of cocoons and gene expressions have also been extensively studied in the silk gland of these species. We will describe several recent studies concerning this topic.

B. mandarina is a wild relative of *B. mori* and this species has been selected for cocoon yield for more than 5000 years. Comparison of silk gland gene expression between *B. mori* and *B. mandarina* has helped elucidate the genetic mechanism that underlies this process. The expression analysis revealed that 16 genes were upregulated in the *B. mori* silk gland and 16 in *B. mandarina*, respectively (Fang et al. 2015). The former included genes related to tissue development, secretion of proteins and metabolism (Table 14.2). These genes may be involved in the highly efficient biosynthesis and secretion of silk proteins. The latter included genes involved in the immune response (Table 14.2) and they may be involved in responding to pathogens and environmental conditions. Gene expression in the *B. mandarina* silk gland was also analyzed by another group that focused on genes that might have undergone positive selection during domestication (Cheng et al. 2015). Using the nonsynonymous site/synonymous site (Ka/Ks) analysis, it became apparent that 400 genes might have experienced or will experience artificial selection. These genes included components of insulin or the mTOR pathway; therefore, it is possible

Table 14.2 Comparison of gene expression between *B. mori* and wild silkmoths

Species compared with <i>B. mori</i>	Genes upregulated in <i>B. mori</i>	Genes upregulated in the wild silkmoth	Genes showing conserved expression	References
<i>B. mandarina</i> (Lepidoptera; Bombycidae)	Related to tissue development, secretion of proteins, metabolism	Related to immune response		Fang et al. (2015)
<i>S. ricini</i> (Lepidoptera; Saturniidae)			Glucose dehydrogenase	Tsubota et al., unpublished information
<i>A. pernyi</i> , <i>A. yamamai</i> , <i>A. assama</i> , <i>S. ricini</i> , <i>A. selene</i> , <i>R. newara</i> (Lepidoptera; Saturniidae)		Related to binding, enzyme regulator		Dong et al. (2015)
<i>S. derogate</i> (Lepidoptera; Pyralidae)			<i>FMBP-1</i> , juvenile hormone esterase, ecdysone oxidase	Su et al. (2015)

FMBP-1 – fibroin modulator-binding protein 1 gene

that they are molecular targets of artificial selection. The genomic analysis of 29 *B. mori* strains and 11 *B. mandarina* populations also succeeded in the identification of 4 candidate genes for the domestication (Xia et al. 2009).

The lepidopteran Saturniidae family of insects produces a wide variety of cocoons with unique characteristics. The Saturniidae and Bombycidae family, including *B. mori* and *B. mandarina*, belong to the same superfamily, Bombycoidea, but the characteristics of the cocoon are largely diversified between these two families. The morphology of the silk gland is also clearly different between these families (Fig. 14.1; Sehnaal and Akai 1990). Silk gland gene expression was examined in *S. ricini*, which belongs to the saturniid species (Tsubota et al., unpublished information). Analysis of the EST library revealed that genes encoding L-fibroin or Fhx proteins are absent. This is in agreement with a previous report that these proteins are lacking in the fibroin complex of Saturniidae (Tamura and Kubota 1989; Tanaka and Mizuno 2001). The comparison of gene expression between *S. ricini* and *B. mori* revealed that several genes, including glucose dehydrogenase, showed conservation of expression, while others were differentially expressed (Table 14.2). The latter genes might be involved in the diversification of silk characteristics between Saturniidae and Bombycidae.

RNA-sequencing was also used for gene expression analysis in six saturniid species, namely, *A. pernyi*, *A. yamamai*, *A. assama*, *S. ricini*, *A. selene* and *R. newara* (Dong et al. 2015). Gene annotation and gene family analysis was carried out using the genetic information of *B. mori* and these six saturniids, and it was found that a total of 17,357 families exist within these seven species. Among the identified families, 929 are Saturniidae-specific, 181 are *Antheraea*-specific and 65–207 are species-specific. The Saturniidae-specific genes are enriched in binding and enzyme regulator activities that would primarily be involved in growth progression (Table 14.2). It is possible that these genes are contributing to the distinct morphologies of the silk gland between Bombycidae and Saturniidae. Among the analyzed species, *A. yamamai*, *A. assama* and *R. newara* produce stably colored cocoons. Comparison of gene expression between these and other species revealed that transferase, oxidoreductase and molecular transducer genes are increased or specifically expressed in the species with colored cocoons. These genes might be potential targets to manipulate cocoon color in the future.

The cotton leaf roller *Sylepta derogate*, a family of Pyralidae, also produces silk to stabilize the rolled leaf and to balloon from used to new leaves. Gene expression analysis in this species revealed that silk component genes, such as *H-fibroin* and *L-fibroin*, are strongly expressed in the silk gland, which is similar to the other families (Su et al. 2015). FMBP-1, a putative *H-fibroin* regulator, was significantly expressed in the silk gland (Table 14.2). Research into elucidating if there is a conserved mechanism for silk gene regulation across the family would be interesting. The juvenile hormone esterase and the ecdysone oxidase genes showed high levels of expression and these proteins have been shown to exhibit strong expression in the MSG of *B. mori* (Li et al. 2015). The temporal expression change was also analyzed showing that a number of genes have distinct expression levels among three different stages, namely, the fifth instar larva, prepupa and pupa.

In summary, a number of silk or silk-related genes were identified in various silk-producing species using techniques such as RNA-sequencing. The comparison of gene expression was also conducted and genes showing distinct expression levels among species were identified. RNA-sequencing could potentially be a promising method for the extensive analysis of silk gland gene expression. This technology can contribute to the elucidation of the molecular mechanisms that underlie the diversification of cocoon characteristics. Such a study would facilitate our understanding of the evolutionary biology of these organisms. In addition, it would be helpful to promote the practical use of silk to various projects including fabric production, tissue engineering and others.

14.7 Different Features Seen in Silks of Non-lepidopteran Insects

Lepidopteran silks, especially those from species of the Bombycoidea superfamily are widely known because of extensive studies on silk proteins and genes for many decades, but there are other types of insect silk with different characteristics. Silks that are spun under water by caddisfly larvae are considered orthologs of silks produced by Lepidoptera. On the other hand, coiled-coil silks of hornets or some other clades of Insecta are thought to have evolved convergently. The above silks are described in detail in this section.

14.7.1 *Trichopteran Silk Fibroins*

Trichoptera (caddisflies) is one of insect orders representing the land-water habitat. Larval and pupal stages of almost all trichopteran species stay in fresh water, and only a few marine or terrestrial species are known. Approximately 12,000 caddisfly species have already been discovered around the world. Caddisfly species are categorized into 3 suborders: Annulipalpia, Integripalpia, and Spicipalpia; the first 2 suborders in the list are monophyletic (Kjer et al. 2002). Caddisfly larvae produce silk in a pair of silk glands and spin silk under water. The use of their silk varies and is dependent on species, e.g., construction of portable cases, retreats, catching nets for prey, and cocoons. The silk glands of a caddisfly look similar in appearance to those of *Bombyx* larvae; the latter glands have a thicker middle part followed by a relatively thinner part. Similar morphology of their glands led to the supposition about similar assembly of the main product, silk.

14.7.2 Identification of Silk Fibroin Genes in Trichoptera

The silk fibroin genes of Trichoptera have been identified by expressed sequence tag (EST) analysis of silk gland-specific cDNA libraries from species that represent 3 suborders (*Hydropsyche angustipennis*: Annulipalpia, *Limnephilus decipiens*: Integripalpia, and *Rhyacophila obliterata*: Spicipalpia) (Yonemura et al. 2006). The most abundant cluster of ESTs in each cDNA library contains a 5'-truncated open reading frame (ORF) that shares similarity with lepidopteran H-fibroin genes. A full-length ORF similar to the lepidopteran L-fibroin gene was also found in another abundant cluster in each library. Nonetheless, the cluster containing the fibroin P25 gene sequence was not found.

After further research (Yonemura et al. 2009; Wang et al. 2010), trichopteran fibroin genes were characterized as follows: H-fibroin has

1. A long and dominant gene transcript; northern blot analysis showed that the entire length of H-fibroin gene transcripts can be >10 kbp if they are produced in the posterior part of silk glands of *H. angustipennis*.
2. A molecular structure similar to that of Lepidoptera. Although the entire sequence of the H-fibroin gene has not been determined, rapid amplification of 5' cDNA ends (5'RACE) and EST analysis showed that it consists of a repetitive central part flanked by nonrepetitive terminal parts. As in Lepidoptera, the deduced amino acid sequences encoded by the H-fibroin gene are highly species specific among the 3 trichopteran species. The terminal non-repetitive sequences show high similarity with the N or C terminus of lepidopteran H-fibroin.
3. A strongly conserved 1st exon and the exon/intron boundary.

On the other hand, L-fibroin has

1. High similarity of the deduced amino acid sequence to the lepidopteran counterpart.
2. The gene consisting of 6 exons. Exon/intron boundaries of the gene are highly conserved between the 2 orders, with separation of the 5th exon of Trichoptera into 2 (5th and 6th) exons in Lepidoptera.

Therefore, trichopteran *H*- and *L*-fibroin genes are considered orthologs of lepidopteran fibroins. Ancestral silk before the separation of Trichoptera and Lepidoptera might have consisted of only heterodimers of H- and L-fibroins due to a lack of the P25 gene in Trichoptera. Interaction between H-fibroin and P25 proteins involves sugar side chains (Tanaka et al. 1999a), and lepidopteran H-fibroin genes have 1 or several glycosylation signals in the 5' region (the saturniid type is an exception). Nevertheless, no glycosylation signal has been found in the 5' region of any trichopteran H-fibroin gene. EST analysis of silk glands of *P. californicus* also seems to support this finding: no cluster representing a P25 gene transcript was found (Collin et al. 2010). During evolution, assembly of P25 with fibroin heterodimers might have occurred sometime between the appearance of Hepialoidea and Yponomeutoidea.

14.7.3 Protein Analysis of Underwater Silk

Unique characteristics such as toughness and adhesiveness of underwater silk are some of its attractive features for development of new materials. Data on physical properties of trichopteran silks are accumulating and revealing the secrets of underwater silk.

Deduced amino acid sequences of trichopteran species showed that underwater silk has amino acid composition that is different from that of terrestrial lepidopteran silks. Alanine, which is dominant in lepidopteran silks (e.g., 30% in *B. mori* and 40% in *A. yamamai*), is low, while proline (Pro), which is scarce in lepidopteran silk, is abundant in trichopteran silk. These findings point to a lack of the Ala based β -sheet construct in trichopteran silk. Stewart and Wang (2010) performed proteomic analysis of *Brachycentrus echo* silk and detected abundant phosphorylated Ser residues (pSer) in this silk. They hypothesized that a construct based on pSer-rich SXXSX motifs, which are common throughout the suborders of Trichoptera, provides the physical strength of alanine free β -sheet. Those authors also suggested that pSer contributes to adhesiveness of the silk.

Transcriptomic and proteomic analyses of *Hysperophylax occidentalis* showed that there are no proteins similar to *Bombyx* sericins, but revealed peroxinectin and a superoxide dismutase that are active in the peripheral region of this silk. A model was proposed (peroxinectin-catalyzed dityrosine cross-linking occurs post-draw by means of H_2O_2 generated within the silk fiber by superoxide dismutase 3) to explain the origin of adhesiveness (Wang et al. 2014, 2015).

It is believed that underwater protein polymers are almost indissoluble after the polymerization. Some researchers attempted to isolate silk components, and 4 major silk constituents, Smsp-1 to Smsp-4, were successfully purified from the lumen silk dope of *Stenophyche marmorata*. Partial sequence of Smsp-1 3' terminus was determined, deduced amino acid sequence of which matched C-terminal sequence of *S. marmorata* H-fibroin (Ohkawa et al. 2012; 2013). While the authors speculated that the molecular weight of Smsp-1 is 380 kDa, the accurate molecular weight of Smsp-1 would be more informative and could be more precisely estimated by SDS-PAGE with use of proper size markers that contain a protein standard around 500 kDa e.g. HiMark series standards (Thermofisher Scientific). Smsp-3 (~20 kDa) has been recently identified as L-fibroin of *S. marmorata* (Bai et al. 2015).

14.7.4 Coiled Coil Silks

The coiled coil is one of structural motifs found in proteins: it results from the propensity of 2 or more right-handed helices to wind around one another. As for the silk produced by insects, aculeate insects (Apocrita, Hymenoptera), sawflies (Symphyta, Hymenoptera), fleas (Siphonaptera), lacewings (Neuroptera), and mantises (Mantodea) are reported to produce silks that contain coiled coil structure. Many

aculeate species produce cocoons during pupation. Hornet larvae build cocoons within individual cells of the hornet hive to shield themselves during pupation. Adult weaver ants manipulate silk-producing larvae to bind plant leaves together to form a nest in which the larvae pupate without a cocoon (Kirshboim and Ishay 2000).

14.7.5 *Characteristics of Genes and Proteins of Coiled Coil Silks*

Coiled coil silk proteins from 5 aculeate species were identified in the silk gland cDNA: in honeybee, weaver ant, and Australian bulldog ant by Sutherland et al. (2006, 2007) and in the hornet by Sezutsu et al. (2007). The coiled coil proteins from 3 mantis species and 1 lacewing species were also described (Weisman et al. 2008; Sutherland et al. 2013). The sequence-structure relation of coiled coils is one of the best understood among any protein domains: coiled coils are formed in proteins with repeating heptad motifs of the structure (abcdefg)ⁿ, where the 1st (a) and 4th (d) positions are occupied by residues more hydrophobic than the other positions. In the helical conformation, the (a) and (d) residues form a hydrophobic stripe down 1 side of the helix, and individual helices associate to sequester these residues from the solvent, leading to a hydrophobic interaction and close packing (of the “knobs-into-holes” type) of the side chains, thus resulting in the left-handed supercoiling (coiled coil). The coiled coil structure is dependent on amino acid characteristics rather than on identity; this flexibility of coiled coil sequences may be the reason for the divergence of primary sequences and low homology among taxa.

A coiled coil generally contains a core rich in the hydrophobic residues, e.g., Leu, isoleucine (Ile), valine (Val), and methionine (Met). In contrast, the core of the coiled coil found in silk proteins contains a high proportion of Ala residues. Theoretically, Ala is not suitable for the core of coiled coils due to its smaller and less hydrophobic side chain in comparison with other hydrophobic residues found in the core. On the other hand, Ala is commonly found in the core of natural proteins, such as tropomyosin, that have long coiled coil domains. Ala has higher helix propensity than any other amino acids do. Accumulation of weaker hydrophobic interactions created by numerous Ala residues is sufficient to stabilize coiled coil folding. An Ala residue is expected to be highly suitable for the coiled coil silk proteins that have much longer coiled coil domains: up to 30 consecutive heptads (Kameda et al. 2014).

Four paralogous genes of proteins from coiled coil silk have been found in all of the aculeate species investigated (Sutherland et al. 2006; Sezutsu et al. 2007; Sutherland et al. 2007; Shi et al. 2008). The 4 proteins of the honeybee and hornet were named AmelF1–AmelF4 [the honey bee, *Apis mellifera* fibroin 1–4 (Sutherland et al. 2006)] and Vssilk 1–4 [the Japanese yellow hornet, *Vespa similima* silk 1–4 (Sezutsu et al. 2007)], respectively. Among the 4 proteins, the primary

sequences have diverged considerably, but other features are strongly conserved, including low molecular weight; high abundance of Ala, Glu (glutamine), Lys (lysine), and Ser; and a triblocklike architecture with an extensive central coiled coil domain together with end domains of less easily predictable secondary structure.

Pioneering work on helix-type structures in the silk of Hymenoptera was done by 2 research groups (Atkins 1967; Lucas and Rudall 1968). Besides X-ray scattering at wide and small angles, cryoelectron diffraction and microscopy were utilized to demonstrate the presence and detailed structure of an α -helical coiled coil in the silk of the giant hornet *Vespa mandarinia japonica* (Kameda et al. 2014). As described above, the coiled coil structure consists of 2 or more right-handed α -helices that wind around one another. Extensive studies on the structure of aculeate silks have revealed filaments consisting of a 4-strand α -helical coiled coil rather than the more usual 2-strand coiled coil, for example, in α -keratin and myosin. The heterotetrameric arrangement of the 4 proteins into the coiled coil possibly facilitates spatial organization of the proteins or their accumulation up to high concentrations in the silk gland prior to silk fabrication.

14.7.6 Molecular Size, Cross-Linking, and Solubility of Coiled Coil Proteins

Proteins of coiled coil silk have molecular weight ranging from 29 to 50 kDa. The average, 38 kDa, is much smaller than the molecular weight of the H-fibroin protein of silkworms (ca. 400 kDa). All of the coiled coil silks that have been analyzed so far contain a central domain flanked by N and C termini. This kind of 3-domain configuration is the same as that of lepidopteran and trichopteran H-fibroins. The central domain forms a coiled coil structure, which is effectively predicted by algorithms such as MARCOIL. Among the 280 proteins analyzed (published data), the size of the coiled coil domain (17–25 kDa) is much smaller than that of H-fibroins, e.g., in *B. mori* ca. 370 kDa and in *A. yamamai* ca. 200 kDa. On the other hand, the sizes of N and C termini of coiled coil silks (from 3 to 18 kDa [average 15 kDa] and from 2 to 18 kDa [average 16 kDa], respectively) have diverged considerably in the course of evolution, while those of lepidopteran and trichopteran silks are remarkably conserved.

Individual silk protein molecules must form intermolecular (hydrophobic, polar, ionic, or covalent) bonds to produce cohesive solid materials. Obviously, the key interaction is initial formation of the coiled coil that links 4 proteins in aculeate silks and 2 proteins in mantis silks to generate protein units of ~120 kDa (aculeate silks) or 80 kDa (mantis oothecae).

Aculeate and sawfly silks contain a significant proportion of the β -sheet structure; therefore, β -sheet-based hydrogen bonding between coiled coil units is likely to contribute to the final properties of the material. It was reported that sawfly silks contain the highest proportion of β -sheet structure (Lucas and Rudall 1968), and in

hornets, this proportion is higher than in bees and ants. In contrast, much less β -sheet structure is observed in mantis oothecae or lacewing cocoons (Weisman et al. 2008).

Covalent cross-links may also contribute to intermolecular bonds in some coiled coil silk proteins (Campbell et al. 2014). Cysteines are absent in all the other aculeate silk proteins, but ant silk proteins (weaver ant, Australian bulldog ant, and Indian jumping ant) contain conserved cysteine residues at the (e) position of the 3rd heptad in the AmelF4 homolog and at the (a) position of the 25th heptad in the AmelF2 homolog. This finding is suggestive of an important role of cysteine residues. The silk protein of the lacewing cocoon and some mantis silk proteins contain cysteine residues, but no conserved positions of cysteine residues are found in the mantis silk proteins. These cysteine residues may take part in disulfide bonding, but the above observations suggest that disulfide bonds are not necessary for fiber formation.

Some proteins of coiled coil silk are also covalently linked without disulfide bridges. Honeybee silk proteins isolated from glands were analyzed by SDS-PAGE, and both multimers and monomers were identified (Sutherland et al. 2006), indicating that the proteins are at least partially cross-linked in the gland before being spun out. Spun out silks of the honeybee and ant and oothecae of mantises cannot be dissolved by the chaotropic agent lithium bromide or other protein denaturants; this observation is consistent with characteristics of mature silk proteins that form a covalent network of protein molecules (Campbell et al. 2014). In contrast to these silks, hornet silk can be dissolved in an aqueous solution of lithium bromide or calcium chloride, or in some halogenated organic solvents, such as hexafluoroisopropyl alcohol (HFIP) and dichloroacetic acid (DCA) (Kameda and Zhang 2014). Good solubility of hornet silk is due to the small number of covalent links in the protein network; this characteristic is an advantage for use in artificial materials, as described below.

14.7.7 Artificial Materials Made from Coiled Coil Silks

Silk proteins have been extensively used as templates for biomaterials. In particular, biomaterials made from regenerated and recombinant portions of the β -sheet-forming silk proteins from spiders and silkworms have been used for cell culture and as drug delivery vehicles, tissue regeneration scaffolds, and biosensors. It is possible to design coiled coil materials on the basis of naturally occurring coiled coil fibrous proteins such as silks produced by aculeates.

Pioneering work on artificial materials based on coiled coil silk was performed on the silk produced by the hornet (Kameda et al. 2005). Transparent films of hornet silk can be prepared by casting reconstituted hornet silk in HFIP (Kameda et al. 2005) or an aqueous solution of ammonia (Kameda 2015). The film of hornet silk is transparent in the wet state, has mechanical properties that allow this material to withstand surgical handling, and is flexible; therefore, hornet silk holds promise as a biomaterial for cornea engineering (Hattori et al. 2011). Transparent films can also be generated from hydrogels that are formed after lithium bromide is removed from

reconstituted hornet silk (Kameda et al. 2010). The molecular structure of these films is similar to that of native hornet silk, containing both α -helical coiled coils and β -sheets. Drawing can influence orientation of the coiled coil units. The maximal draw ratio (DR) that has been achieved during drawing is 2.0; this is the ratio of the lengths of the film after and before drawing. The maximal tensile strength and tensile modulus of the films are 170 MPa and 5.5 GPa, respectively; these values are greater than those of films prepared from silkworm silks. Hornet silk hydrogels can also be molded into tubes (Kameda and Aratani 2011).

14.8 Gene Modification in Silk Glands Using Transgenic Technology for Industrial Use

During the last two decades of the twentieth century, transposon-mediated germline transformation using a P element was established in the fruit fly, *Drosophila melanogaster* (Rubin and Spradling 1982), and played crucial roles in biological studies. Studies in *D. melanogaster* were dramatically expanded from genetic and cytogenetic investigations to those in a broad range of fields of biological research, including neurobiology and developmental biology. Nevertheless, the use of this approach has been limited to *D. melanogaster* and closely related species because P element transposition occurs only in these species.

In 1993, the *piggyBac* transposon was found to be inserted into baculoviruses from a lepidopteran host (Wang and Fraser 1993). Further work indicated the less host-dependent transposition of this transposable element, so it was applied to develop a non-P element transgenic system with a broad host range.

At the end of the twentieth century, germline transformation using a *piggyBac* transposon-derived vector was established in the domestic silkworm, *B. mori* (Tamura et al. 2000). It was the first successful procedure involving the transgenesis of lepidopteran insects. Since then, various approaches have been applied in the silkworm to clarify its biological functions as well as to develop industrial applications.

In industry, transgenic silkworms have mostly been used for producing new high-performance silk or useful recombinant proteins in the silk glands. As *fibroin* and *sericin* are genes that are highly expressed in the silk glands, they are attractive target genes for modification. Here, we briefly describe the procedures involved in this conversion.

The methods for gene modification in the posterior silk gland were developed using vectors originally containing the *L-fibroin* or *H-fibroin* gene. In these vectors, the transgene was fused with the *L-fibroin* gene (Tomita et al. 2003) or the *H-fibroin* gene (Kojima et al. 2007a).

Transgenic silk has been generated using the *H-fibroin* fusion vector. For example, colored fluorescent silk was developed using vectors in which genes encoding fluorescent proteins were fused with the N- and C-terminal sequences of the

H-fibroin gene (Iizuka et al. 2013). By this approach, transgenic silkworms and fabric products for the mass production of fluorescent silk with three colors (green, red, or orange) were successfully generated (Iizuka et al. 2013).

Some research groups have also attempted to produce transgenic silkworms expressing spider silk in order to develop high-toughness silk (e.g. Kojima et al. 2007b; Teulé et al. 2012). Recently, Kuwana et al. (2014) generated high-toughness silk that was produced by a transgenic silkworm expressing spider (*Araneus ventricosus*) dragline silk protein. This transgenic silkworm yielded a fusion protein of H-fibroin and spider dragline protein in cocoon silk. Despite the relatively low protein content, ranging from 0.37 % to 0.61 % w/w (1.4–2.4 mol%), of native silkworm fibroin, the toughness of the raw silk was improved by 53 % after the introduction of the spider silk protein. Fabric products made using this silk demonstrated its commercial feasibility for machine reeling, weaving, and sewing.

Other successful uses of genetically modified *H-fibroin* include the introduction of vascular endothelial growth factor (VEGF) or the fibronectin-derived cell-adhesive sequence (RGD) to improve revascularization properties (Saotome et al. 2015). By these approaches, improved cellularization was confirmed for transgenic fibroin samples (VEGF and RGD) compared to native fibroin.

For the production of useful recombinant proteins, Tomita et al. (2003) were the first to successfully produce a human type III procollagen mini-chain by fusion with L-fibroin. Kurihara et al. (2007) subsequently constructed an H-fibroin expression system to produce feline interferon (FeIFN) by fusion with H-fibroin. Active FeIFN was derived from protease treatment to eliminate H-fibroin N- and C-terminal sequences.

Middle silk glands effectively yield large amounts of sericin protein and are suitable for the production of useful recombinant proteins, because sericin is water-soluble and it is easy to purify the recombinant proteins. To produce recombinant proteins in the sericin layer, binary expression systems (HR3/IE1 and GAL4/UAS) using the *sericin-1* gene promoter were developed (Tomita et al. 2007; Tatematsu et al. 2010).

One of the most successful cases of the production of recombinant proteins involved the use of monoclonal antibodies (mAbs) (Iizuka et al. 2009; Tada et al. 2015). Anti-CD20 mAb produced in a transgenic silkworm showed similar antigen-binding affinity, but stronger antibody-dependent cell-mediated cytotoxicity (ADCC) compared with the antibody produced by Chinese hamster ovary (CHO) cells (Tada et al. 2015). Post-translational modification analysis showed a significant difference in N-glycosylation between the CHO- and silkworm-derived mAbs.

The procedure for N-glycosylation is simpler in silkworms than in mammals. To increase the utility of systems to produce recombinant proteins in silkworms, many studies have been conducted to understand and modify the N-glycosylation pathway. Recently, Mabashi-Asazuma et al. (2015) demonstrated that the N-glycosylation pathway in the silk gland can be glycoengineered by introducing mammalian glycosyltransferases.

In place of transposon-mediated germline transformation, genome editing, which is genome engineering using programmable nucleases, has been rapidly developed (Kim and Kim 2014). It is an innovative method that enables the disruption and/or

replacement of any target gene. In the transposon-mediated transgenic system in the silk glands, the transgenes are expressed in addition to the native *fibroin* or *sericin* gene, but the expression level of the former is usually lower than that of the latter, mainly because of the lack of genomic enhancer sequences in the vector.

If we can disrupt and/or replace the native *fibroin* or *sericin* gene, the amount of transgenic silk or recombinant proteins produced will be greatly improved. Ma et al. (2014) successfully performed gene knockout and removal of the endogenous *H-fibroin* gene. In addition, an efficient method for gene knockin in the silkworm was developed using microhomology-mediated end-joining-dependent integration of donor DNA (Nakade et al. 2014). In the near future, gene modification by genome editing in the silk glands should greatly expand the utility of silkworms for industrial use.

14.9 Conclusion

We presented in this chapter specific features of fibroins including two distinctive compositions of lepidopteran fibroins. Furthermore, lepidopteran sericins and other components expressed in the silk glands of *B. mori* and *S. ricini* were also described.

Silk proteins, produced by various insects, are extremely variable in terms of their architectures and properties, e.g. biased use of specific amino acid residues, recurrent appearance of β -sheet structure derived from repetition of specific amino acid sequence motifs, etc. Their evolutions are likely driven by adaptive selection pressure. Only limited knowledge is available for understanding how silk proteins adapt to their living environments. Therefore, we need to elucidate primary, secondary and higher order of protein structures and clarify their variation among species to understand the evolutionary machinery of silk proteins. Furthermore, it is necessary to know roles of silk proteins in cocoons to increase the insect fitness, as for example to know how effectively such cocoon protects and preserves the pupa from environmental stresses (e.g. Jin et al. 2014).

As their variety in terms of their architectures and properties, silk proteins are likely to be useful biomaterials applicable to multiple useful purposes. Furthermore, the transgenic and genome editing techniques established in *B. mori* confer the ability to generate fusion genes that hold promise for adding new functions to silk proteins. Thus, the combination of silk proteins with gene modification techniques for generating genetically modified organisms, should provide silk proteins with an extended range of properties for use as biomaterials in various fields such as the textile industry and the biomedical arena.

Acknowledgements We thank Hitoshi Saitou for his permitting us to use his photograph showing 22 Saturniidae cocoons. We would like to thank Editage (www.editage.jp) for English language editing.

References

- Akai H (1976) Surface structure of insects. University of Tokyo Press, Tokyo (Japanese with English explanation of figures)
- Atkins EDT (1967) A four-strand coiled-coil model for some insect fibrous proteins. *J Mol Biol* 24:139–141
- Bai X, Sakaguchi M, Yamaguchi Y, Ishihara S, Tsukada M, Hirabayashi K, Ohkawa K, Nomura T, Arai R (2015) Molecular cloning, gene expression analysis, and recombinant protein expression of novel silk proteins from larvae of a retreat-maker caddisfly, *Stenopsyche marmorata*. *Biochem Biophys Res Commun* 464:814–819
- Campbell PM, Trueman HE, Zhang Q, Kojima K, Kameda T, Sutherland TD (2014) Cross-linking in the silks of bees, ants and hornets. *Insect Biochem Mol Biol* 48:40–45
- Chang H, Cheng T, Wu Y, Hu W, Long R, Liu C, Zhao P, Xia Q (2015) Transcriptomic analysis of the anterior silk gland in the domestic silkworm (*Bombyx mori*) – insight into the mechanism of silk formation and spinning. *PLoS One* 10:e0139424
- Cheng T, Fu B, Wu Y, Long R, Liu C, Xia Q (2015) Transcriptome sequencing and positive selected genes analysis of *Bombyx mandarina*. *PLoS One* 10:e0122837
- Chevillard M, Couble P, Prudhomme JC (1986) Complete nucleotide sequence of the gene encoding the *Bombyx mori* silkprotein P25 and predicted amino acid sequence of the protein. *Nucleic Acids Res* 14:6341–6342
- Collin MA, Mita K, Sehna F, Hayashi CY (2010) Molecular evolution of lepidopteran silk proteins: insights from the ghost moth, *Hepialus californicus*. *J Mol Evol* 70:519–529
- Couple P, Michaille JJ, Garel A, Couble ML, Prudhomme JC (1987) Developmental switches of sericin mRNA splicing in individual cells of *Bombyx mori* silkgland. *Dev Biol* 124:431–440
- Craig CL (1997) Evolution of arthropod silks. *Annu Rev Entomol* 42:231–267
- Cramer E (1865) Über die bestandtheile der seide. *J Prakt Chem* 96:76–98
- Dong Z, Zhao P, Wang C, Zhang Y, Chen J, Wang X, Lin Y, Xia Q (2013) Comparative proteomics reveal diverse functions and dynamic changes of *Bombyx mori* silk proteins spun from different development stages. *J Proteome Res* 12:5213–5222
- Dong Y, Dai F, Ren Y, Liu H, Chen L, Yang P, Liu Y, Li X, Wang W, Xiang H (2015) Comparative transcriptome analyses on silk glands of six silkmoths imply the genetic basis of silk structure and coloration. *BMC Genomics* 16:203
- Fang SM, Hu BL, Zhou QZ, Yu QY, Zhang Z (2015) Comparative analysis of the silk gland transcriptomes between the domestic and wild silkworms. *BMC Genomics* 16:60
- Fedič R, Zurovec M, Sehna F (2003) Correlation between fibroin amino acid sequence and physical silk properties. *J Biol Chem* 278:35255–35264
- Friedlander TP, Horst KR, Regier JC, Mitter C, Peigler RS, Fang QQ (1998) Two nuclear genes yield concordant relationships within Attacini (Lepidoptera: Saturniidae). *Mol Phylogenet Evol* 9:131–140
- Fukuta M, Matsuno K, Hui C, Nagata T, Takiya S, Xu PX, Ueno K, Suzuki Y (1993) Molecular cloning of a POU domain-containing factor involved in the regulation of the *Bombyx* sericin-1 gene. *J Biol Chem* 268:19471–19475
- Gamo T (1973) Genetically different components of fibroin and sericin in the mutants, Nd and Nd-s of the silkworm *Bombyx mori*. *Jpn J Genet* 48:99–104
- Gamo T (1982) Genetic variants of the *Bombyx mori* silkworm encoding sericin proteins of different lengths. *Biochem Genet* 20:165–177
- Garel A, Deleage G, Prudhomme JC (1997) Structure and organization of the *Bombyx mori* sericin 1 gene and of the sericins 1 deduced from the sequence of the Ser 1B cDNA. *Insect Biochem Mol Biol* 27:469–477
- Garnier J, Osguthorpe DJ, Robson B (1978) Analysis of the accuracy and implications of simple methods for predicting the secondary structure of globular proteins. *J Mol Biol* 120:97–120
- Gupta AK, Mita K, Arunkumar KP, Nagaraju J (2015) Molecular architecture of silkfibroin of Indian golden silkworm, *Antheraea assama*. *Sci Rep* 5:12706. doi:10.1038/srep12706

- Hattori S, Terada D, Bintang A, Honda T, Yoshikawa C, Teramoto H, Kameda T, Tamada Y, Kobayashi H (2011) Influence of sterilisations on silk protein-based materials. *Bioins Biomim Nan* 1:195–199
- Hayashi T, Nagai Y (1980) The anomalous behavior of collagen peptides on sodium dodecyl sulfate-polyacrylamide gel electrophoresis is due to the low content of hydrophobic amino acid residues. *J Biochem* 87:803–808
- He YX, Zhang NN, Li WF, Jia N, Chen BY, Zhou K, Zhang J, Chen Y, Zhou CZ (2012) N-Terminal domain of *Bombyx mori* fibroin mediates the assembly of silk in response to pH decrease. *J Mol Biol* 418:197–207
- Hwang J, Lee J, Goo T, Yun E, Lee K, Kim Y, Jin B, Lee S, Kim K, Kang S, Suh D (2001) Cloning of the fibroin gene from the oak silkworm, *Antheraea yamamai* and its complete sequence. *Biotechnol Lett* 23:1321–1326
- Iizuka M, Ogawa S, Takeuchi A, Nakakita S, Kubo Y, Miyawaki Y, Hirabayashi J, Tomita M (2009) Production of a recombinant mouse monoclonal antibody in transgenic silkworm cocoons. *FEBS J* 276:5806–5820
- Iizuka T, Sezutsu H, Tatematsu KI, Kobayashi I, Yonemura N, Uchino K, Nakajima K, Kojima K, Takabayashi C, Machii H, Yamada K, Kurihara H, Asakura T, Nakazawa Y, Miyawaki A, Karasawa S, Kobayashi H, Yamaguchi J, Kuwabara N, Nakamura T, Yoshii K, Tamura T (2013) Colored fluorescent silk made by transgenic silkworms. *Adv Funct Mater* 23:5232–5239
- Inoue S, Tanaka K, Arisaka F, Kimura S, Ohtomo K, Mizuno S (2000) Silk fibroin of *Bombyx mori* is secreted, assembling a high molecular mass elementary unit consisting of H-chain, L-chain, and P25, with a 6:6:1 molar ratio. *J Biol Chem* 275:40517–40528
- Ishikawa E, Suzuki Y (1985) Tissue- and stage-specific expression of sericin genes in the middle silk gland of *Bombyx mori*. *Dev Growth Differ* 27:73–82
- Jin X, Zhang J, Gao W, Li J, Wang X (2014) Cocoon of the silkworm *Antheraea pernyi* as an example of a thermally insulating biological interface. *Biointerphases* 9:031013
- Kameda T (2015) Influence of pH, temperature, and concentration on stabilization of aqueous hornet silk solution and fabrication of salt-free. *Biopolymers* 103:41–52
- Kameda T, Aratani E (2011) Production and characterizations of tubes from hornet (*Vespa*) silk. *J Insect Biotech Seric* 80:109–116
- Kameda T, Zhang Q (2014) Dissolution of hornet silk in aqueous solution of calcium chloride. *J Silk Sci Tech Jpn* 22:109–116
- Kameda T, Kojima K, Miyazawa M, Fujiwara S (2005) Film formation and structural characterization of silk of the hornet *Vespa simillima* xanthoptera Cameron. *Z Naturforsch C J Biosci* 60:906–914
- Kameda T, Kojima K, Togawa E, Sezutsu H, Zhang Q, Teramoto H, Tamada Y (2010) Drawing-induced changes in morphology and mechanical properties of hornet silk gel films. *Biomacromolecules* 11:1009–1018
- Kameda T, Walker AA, Sutherland TD (2014) Evolution and application of coiled silks from insects. In: Asakura T, Miller T (eds) *Biotechnology of silk*, vol 5. Springer, Dordrecht, pp 87–106
- Kenchington W (1972) Variations in silk gland morphology among sawfly larvae (Hymenoptera: Symphyta). *J Entomol Ser A Gen Entomol* 46(2):111–116
- Kenchington W (1984) Biological and chemical aspects of silks and silk-like materials produced by arthropods. *S Pac J Nat Sci* 5:10–45
- Kikuchi Y, Mori K, Suzuki S, Yamaguchi K, Mizuno S (1992) Structure of the *Bombyx mori* fibroin light-chain-encoding gene: upstream sequence elements common to the light and heavy chain. *Gene* 110:151–158
- Kim H, Kim JS (2014) A guide to genome engineering with programmable nucleases. *Nat Rev Genet* 15:321–334
- Kimoto M, Kitagawa T, Kobayashi I, Nakata T, Kuroiwa A, Takiya S (2012) Inhibition of the binding of MSG-intermolt-specific complex, MIC, to the *sericin-1* gene promoter and *sericin-1* gene expression by POU-M1/SGF-3. *Dev Genes Evol* 222:351–359

- Kimoto M, Tsubota T, Uchino K, Sezutsu H, Takiya S (2014) Hox transcription factor Antp regulates *sericin-1* gene expression in the terminal differentiated silk gland of *Bombyx mori*. *Dev Biol* 386:64–71
- Kimoto M, Tsubota T, Uchino K, Sezutsu H, Takiya S (2015) LIM-hoeodomain transcription factor Awh is a key component activating all three fibroin genes, *fibH*, *fibL* and *fhx*, in the silk gland of the silkworm, *Bombyx mori*. *Insect Biochem Mol Biol* 56:29–35
- Kirshboim S, Ishay JS (2000) Silk produced by hornets: thermophotovoltaic properties – A review. *Comp Biochem Phys A* 127:1–20
- Kjer KM, Blahnik RJ, Holzenthal RW (2002) Phylogeny of caddisflies (Insecta, Trichoptera). *Zool Scr* 31:83–91
- Kludkiewicz B, Takasu Y, Fedic R, Tamura T, Sehnal F, Žurovec M (2009) Structure and expression of the silk adhesive protein Ser2 in *Bombyx mori*. *Insect Biochem Mol Biol* 39:938–946
- Kojima K, Kuwano Y, Sezutsu H, Kobayashi I, Uchino K, Tamura T, Tamada Y (2007a) A new method for the modification of fibroin heavy chain protein in the transgenic silkworm. *Biosci Biotechnol Biochem* 71:2943–2951
- Kojima K, Kuwana Y, Sezutsu H (2007b) NMR analysis of silk produced by transgenic silkworm which expresses spider fiber protein in silk. *Kobunshi Ronbunshu* 64:817–819
- Kokubo H, Xu PX, Xu X, Matsunami K, Suzuki Y (1997) Spatial and temporal expression pattern of POU-M1/SGF-3 in *Bombyx mori* embryogenesis. *Dev Genes Evol* 206:494–502
- Kurihara H, Sezutsu H, Tamura T, Yamada K (2007) Production of an active feline interferon in the cocoon of transgenic silkworms using the fibroin H-chain expression system. *Biochem Biophys Res Commun* 355:976–980
- Kusuda J, Tazima Y, Onimaru K, Ninaki O, Suzuki Y (1986) The sequence around the 5' end of the fibroin gene from the wild silkworm, *Bombyx mandarina*, and comparison with that of the domesticated species, *B. mori*. *Mol Gen Genet* 203:359–364
- Kuwana Y, Sezutsu H, Nakajima K, Tamada Y, Kojima K (2014) High-toughness silk produced by a transgenic silkworm expressing spider (*Araneus ventricosus*) dragline silk protein. *PLoS One* 9:e105325
- Li J, Ye L, Che J, Song J, You Z, Yun K, Wang S, Zhong B (2015) Comparative proteomic analysis of the silkworm middle silk gland reveals the importance of ribosome biogenesis in silk protein production. *J Proteomics* 126:109–120
- Lucas F, Rudall KM (1968) Extracellular fibrous proteins: the silks. In: Florkin M, Stotz EH (eds) *Comprehensive biochemistry*. Elsevier, Amsterdam, pp 475–558
- Ma S, Shi R, Wang X, Liu Y, Chang J, Gao J, Lu W, Zhang J, Zhao P, Xia Q (2014) Genome editing of BmFib-H gene provides an empty *Bombyx mori* silk gland for a highly efficient bioreactor. *Sci Rep* 4:6867
- Mabashi-Asazuma H, Sohn BH, Kim YS, Kuo CW, Khoo KH, Kucharski CA, Fraser MJ Jr, Jarvis DL (2015) Targeted glycoengineering extends the protein N-glycosylation pathway in the silkworm silk gland. *Insect Biochem Mol Biol* 65:20–27
- Mach V, Takiya S, Ohno K, Handa H, Imai T, Suzuki Y (1995) Silk gland factor-1 involved in the regulation of *Bombyx sericin-1* gene contains fork head motif. *J Biol Chem* 270:9340–9346
- Machida J (1926) Studies on the silk substances secreted by *Bombyx mori*. *Bull Sericult Exp Stn* 7:241–262 (Japanese with English summary)
- Maning RF, Gage LP (1980) Internal structure of the silk fibroin gene of *Bombyx mori* II Remarkable polymorphism of the organization of crystalline and amorphous coding sequences. *J Biol Chem* 255:9451–9457
- Matsunami K, Kokubo H, Ohno K, Suzuki Y (1998) Expression pattern analysis of SGF-3/POU-M1 in relation to sericin-1 gene expression in the silk gland. *Dev Growth Differ* 40:591–597
- Michaille JJ, Garel A, Prudhomme JC (1990) Cloning and characterization of the highly polymorphic *Ser2* gene of *Bombyx mori*. *Gene* 86:177–184
- Mita K, Ichimura S, James TC (1994) Highly repetitive structure and its organization of the silk fibroin gene. *J Mol Evol* 38:583–592

- Nakade S, Tsubota T, Sakane Y, Kume S, Sakamoto N, Obara M, Daimon T, Sezutsu H, Yamamoto T, Sakuma T, Suzuki KT (2014) Microhomology-mediated end-joining-dependent integration of donor DNA in cells and animals using TALENs and CRISPR/Cas9. *Nat Commun* 5:5560
- Ohkawa K, Miura Y, Nomura T, Arai R, Abe K, Tsukada M, Hirabayashi K (2012) Isolation of silk proteins from a caddisfly larva, *Stenopsyche marmorata*. *J Fiber Bioeng Inform* 5:125–137
- Ohkawa K, Miura Y, Nomura T, Arai R, Abe K, Tsukada M, Hirabayashi K (2013) Long-range periodic sequence of the cement/silk protein of *Stenopsyche marmorata*: purification and biochemical characterization. *Biofouling* 29:357–367
- Ohno K, Sawada J, Takiya S, Kimoto M, Matsumoto A, Tsubota T, Uchino K, Hui C, Sezutsu H, Handa H, Suzuki Y (2013) Silk gland factor-2, involved in fibroin gene transcription, consists of LIM homeodomain, LIM-interacting, and single-stranded DNA-binding proteins. *J Biol Chem* 288:31581–31591
- Ohshima Y, Suzuki Y (1977) Cloning of the silk fibroin gene and its flanking sequences. *Proc Natl Acad Sci U S A* 74:5363–5367
- Okamoto H, Ishikawa E, Suzuki Y (1982) Structural analysis of sericin genes. *J Biol Chem* 257:15192–15199
- Prevelige PJ, Fasman GD (1989) Chou-Fasman Prediction of the secondary structure of proteins: The Chou-Fasman-Prevelige algorithm. In: Fasman GD (ed) *Prediction of Protein Structure and the Principles of Protein Conformation*. Plenum, New York, pp 391–416
- Prudhomme JC, Couble P, Garel JP, Daillie J (1985) Silk synthesis. In: Kerkut GA, Gilbert LI (eds) *Comprehensive insect physiology biochemistry and pharmacology*, vol 10. Pergamon, Oxford, pp 571–594
- Qian N, Sejnowski TJ (1988) Predicting the secondary structure of globular proteins using neural network models. *J Mol Biol* 202:865–884
- Royer C, Briolay J, Garel A, Brouilly P, Sasanuma S, Sasanuma M, Shimomura M, Keime C, Gandrillon O, Huang Y, Chavancy G, Mita K, Couble P (2011) Novel genes differentially expressed between posterior and median silk gland identified by SAGE-aided transcriptome analysis. *Insect Biochem Mol Biol* 41:118–124
- Rubin GM, Spradling AC (1982) Genetic transformation of *Drosophila* with transposable element vectors. *Science* 218:348–353
- Saitou N, Nei M (1987) The neighbor-joining method: a new method for reconstructing phylogenetic trees. *Mol Biol Evol* 4:406–425
- Saotome T, Hayashi H, Tanaka R, Kinugasa A, Uesugi S, Tatematsu KI, Sezutsu H, Kuwabara N, Asakura T (2015) Introduction of VEGF or RGD sequences improves revascularization properties of *Bombyx mori* silk fibroin produced by transgenic silkworm. *J Mater Chem B* 3:7109–7116
- Sehnal F, Akai H (1990) Insect silk glands: their types, development and function, and effects of environmental factors and morphogenetic, hormones on them. *Int. J Wild Silkworm Silk* 7:25–30
- Sehnal F, Sutherland TD (2008) Silks produced by insect labial glands. *Prion* 2:145–153
- Sehnal F, Žurovec M (2004) Construction of silk fiber core in Lepidoptera. *Biomacromolecules* 497:666–667
- Sezutsu H, Yukuhiro K (2000) Dynamic rearrangement within the *Antheraea pernyi* silk fibroin gene is associated with four types of repetitive units. *J Mol Evol* 51:329–338
- Sezutsu H, Yukuhiro K (2014) The complete nucleotide sequence of the Eri-silkworm (*Samia cynthia ricini*) fibroin gene. *J Insect Biotec Sericol* 83:59–70
- Sezutsu H, Kajiwara H, Kojima K, Mita K, Tamura T, Tamada Y, Kameda T (2007) Identification of four major hornet silk genes with a complex of alanine-rich and serine-rich sequences in *Vespa simillima xanthoptera* Cameron. *Biosci Biotechnol Biochem* 71:2725–2734
- Sezutsu H, Tamura T, Yukuhiro K (2008a) Leucine-rich fibroin gene of the Japanese wild silkworm, *Rhodinia fugax* Lepidoptera (Saturniidae). *Eur J Entomol* 105:561–566
- Sezutsu H, Tamura T, Yukuhiro K (2008b) Uniform size of leucine-rich repeats in a wild silk moth *Saturnia japonica* (Lepidoptera Saturniidae) fibroin. *Int J Wild Silkworm Silk* 13:53–60

- Sezutsu H, Uchino K, Kobayashi I, Tamura T, Yukuhiro K (2010) Extensive sequence rearrangements and length polymorphism in fibroin genes in the wild silkworm, *Antheraea yamamai* (Lepidoptera, Saturniidae). *Int J Wild Silkworm Silk* 15:35–50
- Shi J, Lua S, Du N, Liu X, Song J (2008) Identification, recombinant production and structural characterization of four silk proteins from the Asiatic honeybee *Apis cerana*. *Biomaterials* 29:2820–2828
- Shonozaki N, Machida Y, Nakayama M, Doira H, Watanabe T (1980) Linkage analyses of sericins. *Kyushusanshi* 11:62
- Sima Y, Chen M, Yao R, Li Y LT, Jin X, Wang L, Su J, Li X, Liu Y (2013) The complete mitochondrial genome of the Ailanthus silkworm, *Samia cynthia cynthia* (Lepidoptera: Saturniidae). *Gene* 526:309–317
- Simmons A, Ray E, Jelinski LW (1994) Solid-state ^{13}C NMR of *Nephila clavipes* dragline silk establishes structure and identity of crystalline regions. *Macromolecules* 27:5235–5237
- Sprague KU (1975) The *Bombyx mori* silk proteins: characterization of large polypeptides. *Biochemistry* 14:925–931
- Stewart RJ, Wang CS (2010) Adaptation of caddisfly larval silks to aquatic habitats by phosphorylation of H-fibroin serines. *Biomacromolecules* 11:969–974
- Su H, Cheng Y, Wang Z, Li Z, Stanley D, Yang Y (2015) Silk gland gene expression during larval-pupal transition in the cotton leaf roller *Sylepta derogata* (Lepidoptera: Pyralidae). *PLoS One* 10:e0136868
- Sutherland TD, Campbell PM, Weisman S, Trueman HE, Sriskantha A, Wanjura WJ, Haritos VS (2006) A highly divergent gene cluster in honey bees encodes a novel silk family. *Genome Res* 16:1414–1421
- Sutherland TD, Weisman S, Trueman HE, Sriskantha A, Trueman JWH, Haritos VS (2007) Conservation of essential design features in coiled coil silks. *Mol Biol Evol* 24:2424–2432
- Sutherland TD, Peng YY, Trueman HE, Weisman S, Okada S, Walker AA, Sriskantha A, White JF, Huson MG, Werkmeister JA, Glattauer V, Stoichevska V, Mudie ST, Haritos VS, Ramshaw JAM (2013) A new class of animal collagen masquerading as an insect silk. *Sci Rep* 3:2864. doi:10.1038/srep02864
- Suzuki Y, Tsuda M, Takiya S, Hirose S, Suzuki E, Kameda M, Ninaki O (1986) Tissue-specific transcription enhancement of the fibroin gene characterized by cell-free systems. *Proc Natl Acad Sci U S A* 83:9522–9526
- Tada M, Tatematsu KI, Ishii-Watabe A, Harazono A, Takakura D, Hashii N, Sezutsu H, Kawasaki N (2015) Characterization of anti-CD20 monoclonal antibody produced by transgenic silkworms (*Bombyx mori*). *Mabs* 7:1138–1150
- Takasu Y, Yamada H, Tsubouchi K (2002) Isolation of three main sericin components from the cocoon of the silkworm, *Bombyx mori*. *Biosci Biotechnol Biochem* 66:2715–2718
- Takasu Y, Yamada H, Saito H, Tsubouchi K (2005) Characterization of *Bombyx mori* sericins by the partial amino acid sequences. *J Insect Biotec Seric* 74:103–109
- Takasu Y, Yamada H, Tsubouchi K (2006) The silk sericin component with low crystallinity. *Sanshi-Konchu Biotec* 75:133–139
- Takasu Y, Yamada H, Tamura T, Sezutsu H, Mita K, Tsubouchi K (2007) Identification and characterization of a novel sericin gene expressed in the anterior middle silk gland of the silkworm *Bombyx mori*. *Insect Biochem Mol Biol* 37:1234–1240
- Takasu Y, Hata T, Uchino K, Zhang Q (2010) Identification of Ser2 proteins as major sericin components in the non-cocoon silk of *Bombyx mori*. *Insect Biochem Mol Biol* 40:339–344
- Takiya S, Kokubo H, Suzuki Y (1997) Transcriptional regulatory elements in the upstream and intron of the fibroin gene bind three specific factors POU-M1, Bm Fkh and FMBP-1. *Biochem J* 321:645–653
- Takiya S, Ishikawa T, Ohtsuka K, Nishita Y, Suzuki Y (2005) Fibroin-modulator-binding protein-1 (FMBP-1) contains a novel DNA-binding domain, repeats of the score and three amino acid peptide (STP), conserved from *Caenorhabditis elegans* to humans. *Nucleic Acid Res* 33:786–795

- Takiya S, Inoue H, Kimoto M (2011) Novel enhancer and promoter elements indispensable for the tissue-specific expression of the *sericin-1* gene of the silkworm *Bombyx mori*. *Insect Biochem Mol Biol* 41:592–601
- Tamura T, Kubota T (1989) A determination of molecular weight of fibroin polypeptides in the saturniid silkworms, *Antheraea yamamai*, *Antheraea pernyi* and *Philosamia cynthia ricini* by SDS PAGE. In: Akai H, Wu ZS (eds) Wild silkworm '88. International Society for Wild Silkworms, Tokyo, pp 67–72
- Tamura T, Inoue H, Suzuki Y (1987) The fibroin genes of the *Antheraea yamamai* and *Bombyx mori* are different in the core regions but reveal a striking sequences similarity in their 5'-ends and 5'-flanking regions. *Mol Gen Genet* 206:189–195
- Tamura T, Thibert C, Royer C, Kanda T, Abraham E, Kamba M, Komoto N, Thomas JL, Mauchamp B, Chavancy G, Shirk P, Fraser M, Prudhomme JC, Couble P (2000) Germline transformation of the silkworm *Bombyx mori* L. using a piggyBac transposon-derived vector. *Nat Biotechnol* 18:81–84
- Tanaka K, Mizuno S (2001) Homologues of fibroin L-chain and P25 of *Bombyx mori* are present in *Dendrolimus spectabilis* and *Papilio xuthus* but not detectable in *Antheraea yamamai*. *Insect Biochem Mol Biol* 31:665–667
- Tanaka K, Inoue S, Mizuno S (1999a) Hydrophobic interaction of P25, containing Asn-linked oligosaccharide chains, with the H–L complex of silk fibroin produced by *Bombyx mori*. *Insect Biochem Mol Biol* 29:269–276
- Tanaka K, Kajiyama N, Ishikura K, Waga S, Kikuchi A, Ohtomo K, Takagi T, Mizuno S (1999b) Determination of the site of disulfide linkage between heavy and light chains of silk fibroin produced by *Bombyx mori*. *Biochim Biophys Acta* 1432:92–103
- Tashiro Y, Otsuki E (1970) Studies on the posterior silk gland of the silkworm *Bombyx mori* IV. Ultracentrifugal analyses of native silk proteins, especially fibroin extracted from the middle silk gland of the mature silkworm. *J Cell Biol* 46:1–16
- Tatematsu KI, Kobayashi I, Uchino K, Sezutsu H, Iizuka T, Yonemura N, Tamura T (2010) Construction of a binary transgenic gene expression system for recombinant protein production in the middle silk gland of the silkworm *Bombyx mori*. *Transgenic Res* 19:473–487
- Teulé F, Miao YG, Sohn BH, Kim YS, Hull JJ, Fraser MJ Jr, Lewis RV, Jarvis DL (2012) Silkworms transformed with chimeric silkworm/spider silk genes spin composite silk fibers with improved mechanical properties. *Proc Natl Acad Sci U S A* 109:923–928
- The International silkworm genome consortium (2008) The genome of a lepidopteran model insect, the silkworm *Bombyx mori*. *Insect Biochem Mol Biol* 38:1036–1045
- Tomita M, Munetsuna H, Sato T, Adachi T, Hino R, Hayashi M, Shimizu K, Nakamura N, Tamura T, Yoshizato K (2003) Transgenic silkworms produce recombinant human type III procollagen in cocoons. *Nat Biotechnol* 21:52–56
- Tomita M, Hino R, Ogawa S, Iizuka M, Adachi T, Shimizu K, Sotoshiro H, Yoshizato K (2007) A germline transgenic silkworm that secretes recombinant proteins in the sericin layer of cocoon. *Transgenic Res* 16:449–465
- Tsujimoto Y, Suzuki Y (1979) The DNA sequence of *Bombyx mori* fibroin gene including the 5' flanking, mRNA coding, entire intervening and fibroin protein coding regions. *Cell* 18:591–600
- Tsutsui R, Shonozaki N, Machida Y, Watanabe T (1979) Separation of sericins. *Kyushusanshi* 10:65
- Wang HG, Fraser MJ (1993) TTA serves as the target site for TFP3 lepidopteran transposon insertions in both nuclear polyhedrosis virus and *Trichoplusia ni* genomes. *Insect Mol Biol* 1:109–116
- Wang Y, Sanai T, Wen H, Zao T, Nakagaki M (2010) Characterization of unique heavy chain fibroin filaments spun underwater by the caddisfly *Stenopsyche marmorata* (Trichoptera: Stenopsychidae). *Mol Biol Rep* 37:2885–2892
- Wang CS, Ashton NN, Weiss RB, Stewart RJ (2014) Peroxinectin catalyzed dityrosine crosslinking in the adhesive underwater silk of a casemaker caddisfly larvae, *Hesperophylax occidentalis*. *Insect Biochem Mol Biol* 54:69–79

- Wang CS, Pan H, Weerasekare GM, Stewart RJ (2015) Peroxidase-catalysed interfacial adhesion of aquatic caddisworm silk. *J R Soc Interface* 12(112). doi:10.1098/rsif.2015.0710
- Warwicker JO (1960) Comparative studies of fibroins II. The crystal structures of various fibroins. *J Mol Biol* 2:350–362
- Watanabe M, Kamei K, Sumida M (2007) Sericin digestion by fibroinase, a cathepsin L-like cysteine proteinase, of *Bombyx mori* silk gland. *J Insect Biotech Seric* 76:9–15
- Weisman S, Trueman HE, Mudie ST, Church JS, Sutherland TD, Haritos VS (2008) An unlikely silk: The composite material of green lacewing cocoons. *Biomacromolecules* 9:3065–3306
- Xia Q, Cheng D, Duan J, Wang G, Cheng T, Zha X, Liu C, Zhao P, Dai F, Zhang Z, He N, Zhang L, Xiang Z (2007) Microarray-based gene expression profiles in multiple tissues of the domesticated silkworm, *Bombyx mori*. *Genome Biol* 8:R162
- Xia Q, Guo Y, Zhang Z, Li D, Xuan Z, Li Z, Dai F, Li Y, Cheng D, Li R, Cheng T, Jiang T, Becquet C, Xu X, Liu C, Zha X, Fan W, Lin Y, Shen Y, Jiang L, Jensen J, Hellmann I, Tang S, Zhao P, Xu H, Yu C, Zhang G, Li J, Cao J, Liu S, He N, Zhou Y, Liu H, Zhao J, Ye C, Du Z, Pan G, Zhao A, Shao H, Zeng W, Wu P, Li C, Pan M, Li J, Yin X, Li D, Wang J, Zheng H, Wang W, Zhang X, Li S, Yang H, Lu C, Nielsen R, Zhou Z, Wang J, Xiang Z, Wang J (2009) Complete resequencing of 40 genomes reveals domestication events and genes in silkworm (*Bombyx*). *Science* 326:433–436
- Yamanouchi M (1922) Morphologische Beobachtung über die Seidensekretion bei der Seidenraupe. *J Coll Agric Hokkaido Imp Univ* 10:1–50
- Yonemura N, Sehnal F, Mita K, Tamura T (2006) Protein composition of silk filaments spun under water by caddisfly larvae. *Biomacromolecules* 7:3370–3378
- Yonemura N, Mita K, Tamura T, Sehnal F (2009) Conservation of silk genes in Trichoptera and Lepidoptera. *J Mol Evol* 68:641–653
- Yukuhiro K, Sezutsu H, Yonemura N (2014) Evolutionary divergence of lepidopteran and trichopteran fibroins. In: Asakura T, Miller T (eds) *Biotechnology of silk*, vol 5. Springer, Dordrecht, pp 25–48
- Zaretschnaya SN (1965) Glands of caddisworms. III. Spinning glands. Plankton and benthos of inland water reservoirs. *Proc Acad Sci USSR* 12:293–303
- Zhao XM, Liu C, Li QY, Hu WB, Zhou MT, Nie HY, Zhang YX, Peng ZC, Zhao P, Xia QY (2014) Basic helix-loop-helix transcription factor Bmsage is involved in regulation of *fibroin H-chain* gene via interaction with SGF1 in *Bombyx mori*. *PLoS One* 9:e94091
- Zhou C, Confalonieri F, Medina N, Zivanovic Y, Esnault C, Yang T, Jacquet M, Janin J, Duguet M, Perasso R, Li Z (2000) Fine organization of *Bombyx mori* fibroin heavy chain gene. *Nucleic Acid Res* 28:2413–2419
- Žurovec M, Sehnal F (2002) Unique molecular architecture of silkfibroin in the waxmoth, *Galleria mellonella*. *J Biol Chem* 277:22639–22647
- Žurovec M, Vasková M, Kodrík D, Sehnal F, Kumaran AK (1995) Light-chain fibroin of *Galleria mellonella* L. *Mol Gen Genet* 247:1–6
- Žurovec M, Kodrík D, Yang C, Sehnal F, Scheller K (1998) The P25 component of *Galleria* silk. *Mol Gen Genet* 257:264–270
- Žurovec M, Kludkiewicz B, Fedic R, Sulitkova J, Mach V, Kucerova L, Sehnal F (2013) Functional conservation and structural diversification of silk sericins in two moth species. *Biomacromolecules* 14:1859–1866

Chapter 15

The Complex Secretions of the Salivary Glands of *Drosophila melanogaster*, A Model System

Robert Farkaš

Abstract The *Drosophila* salivary glands (SGs) are historically well known for their polytene chromosomes and became a tissue of choice to study sequential gene activation by the steroid hormone ecdysone. The widely accepted and most well documented function of the *Drosophila* salivary gland is the production of a secretory glue released during pupariation to fix the freshly formed puparia to a substrate. Besides fulfilling this function, which is tightly associated with the enormous production and exocytosis of a small group of secretory glycoproteins (Sgs proteins), the same SGs display also massive apocrine secretion 8–10 h after puparium formation (APF). A detailed analysis of the apocrine activity provided compelling evidence that this is non-vesicular transport and secretory mechanism which substantially differs from canonical exocytosis taking place 14–16 h prior to apocrine release. From the point of view of *Drosophila* fast development, this is significant time gap between two different cellular activities. This system offers a unique opportunity to dissect the molecular mechanistic aspects of the apocrine transport and secretory machinery using specific genetic tools available in the fruitfly. Although these obviously different cellular activities serve two very different purposes, in both cases the SG behaves as a distinct and also typical exocrine organ capable of two independent and separated functions, one in the late larva, the second in the late prepupa. A comparison of the secretory material and its properties from the exocytotic Sgs proteins and the apocrine secretion reveals the unexpected capabilities of this organ in reprogramming its function for two deeply different roles.

R. Farkaš (✉)

Institute of Experimental Endocrinology, Slovak Academy of Sciences,

Dúbravská cesta 9, 845 05, Slovakia

e-mail: ueenfark@savba.sk

15.1 Introduction

The larval salivary glands (SGs) of the fruit fly *Drosophila* are a single layer of unbranched, tubular epithelial tissue of ectodermal origin. The SG is the largest secretory organ in *Drosophila*, and is composed of just two principal cell types: duct cells and secretory cells. During embryogenesis, the future larval salivary glands arise from a contiguous primordia on the ventral ectodermal surface of parasegment 2 (Skaer 1993; Andrew et al. 1994; Campos-Ortega and Hartenstein 1997; Henderson and Andrew 2000; Bradley et al. 2001; Myat 2005; Vining et al. 2005; Kerman et al. 2006). Once specified, salivary gland cells do not undergo further rounds of cell division or cell death, with each lobe having approximately 130–145 large polarized epithelial cells specialized for secretion (Poulson 1937; Makino 1938; Sonnenblick 1940, 1950; Skaer 1993; Campos-Ortega and Hartenstein 1997). The absence of mitotic activity after the formation of the lateroventral ectodermal placodes suggests that the cells participating in the formation of these plates, have already been determined to become salivary gland cells. Despite the absence of cell divisions, the glands continue to grow, initially during the embryonic stage and mainly during larval development due to an increase in cell volume. This is accompanied by chromosomal replication without subsequent separation of the homologues (endoreduplication), and, as a consequence, the chromosomes become multistranded (polytene). Within individuals the gland lobes usually have an asymmetric cell number. Although the most frequently cited average number of gland cells per lobe is 128 (Grob 1952; Schnitter 1961; Hadorn and Faulhaber 1962; Gloor 1962; Berendes and Ashburner 1978; Ashburner et al. 2005), our own replicate observations have shown that the number of secretory gland is distributed about a mode of 134 cells. Only the few cells located at the junction between the duct and the start of the gland's cells start to divide during the second instar; these will form the ring of the prospective imaginal gland cells. The larval duct is composed of about 55 cuboidal epithelial cells that form simple tubes which connect the secretory cells to the larval mouth by a Y-shaped tubular conduit (Berendes and Ashburner 1978; Abrams et al. 2003). Despite fact that all of the gland's secretory cells appear to be identical during nearly all of the larvae's life, three structurally different secretory cell subtypes - corpuscular, transitional and columnar – can be recognized in the late 3rd larval instar (von Gaudecker 1972; Lane et al. 1972; Farkaš and Šut'áková 1998).

At about 4–6 h after the appearance of the ectodermal placodes the embryonic SGs display signs of secretory activity. The lumen of the gland contains a substance that readily absorbs hematoxylin and stains metachromatically with toluidine blue (Poulson 1950; Sonnenblick 1950). Myat and Andrew (2002) observed that this secretory activity of embryonic SGs is controlled by the *crb* and *hkb* genes. This embryonic secretion appears to be cyclic and there is good reason to believe that it provides for repeated excretion of luminal proteins that are required for the assembly of the extracellular matrix on the apical surface during tube expansion in manner similar to the tube expansion in the embryonic tracheal system (Tsarouhas et al. 2007; Jayaram et al. 2008; Wang et al. 2009; Armbruster and Luschnig 2012; Burgess et al. 2012).

In the first instar larva, the salivary glands are located on either side of the body, with both gland lobes usually confined to the first two thoracic segments just below the muscles of the body wall. The gland cells are uniform in size (Fig. 15.1). During the second instar the glands continue to grow until their lobes extend into to first abdominal segment. The cells remain uniform in size but their shape in cross section becomes more conical. At the beginning of the third instar there develops an anterior-posterior gradient in cell size, which is accompanied by a differential increase in nuclear volume, probably reflecting a differential increase in the level of polyteny of the chromosomes (Bodenstein 1950; Berendes 1965; Berendes and Ashburner 1978). During larval growth, SGs are thought to produce digestive enzymes released into the alimentary tract (Hsu 1948; Gregg et al. 1990); however, for unknown reasons there has been very little attention paid to their identity and characteristic. Thus, the only major and unambiguously documented function of the

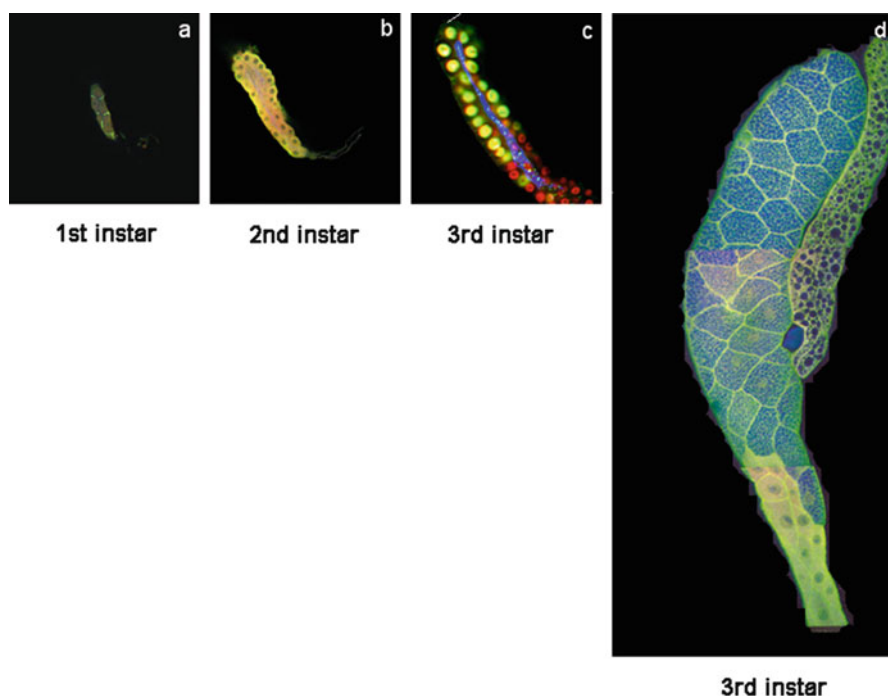


Fig. 15.1 Laser confocal microscope image of paraformaldehyde-fixed SG. The 1st (a), 2nd (b), early 3rd (c) and late 3rd (d) instar larva showing the antibody-detected distribution of two cytosolic and cytoskeletal proteins: p127^{l(2)gl} tumor suppressor (*green*) and non-muscle myosin II heavy chain (*red*) in (a), (b) and (d). In the early 3rd (c) instar the expression of two ecdysone-regulated proteins is shown: ecdysone receptor (*green*) and Broad-Complex (*red*). Blue indicates filamentous actin which concentrates predominantly on the apical membrane of the lumen. In corpuscular and transitional cells (d), the p127^{l(2)gl} and myosin II proteins form a reticular network with numerous black vacuoles that correspond to secretory granules. The cytoplasm of the columnar cells show smooth and evenly distributed pattern for the proteins. Magnification of all confocal images 400×

larval salivary glands is to produce a large amount of mucinous glue-containing secretory granules during the second half of the last instar that, when released during pupariation, serves to affix the freshly formed puparia to a substrate in an upright position (Fraenkel 1952; Fraenkel and Brookes 1953). In anticipation of this function, at about the middle of the third instar globular, highly refractile granules appear in the cytoplasm of the posterior gland cells (Ross 1939; Painter 1945; Bodenstein 1950; Berendes 1965). The cytoplasm which was strongly basophilic during the first and second instars, loses its basophilia when the granules appear (Leshner 1951a, b, 1952). These granules, the number of which gradually increases in a posterior to anterior direction, display a strong periodic acid-Schiff (PAS) positive reaction (Leshner 1952; Berendes 1965; Poels 1970; von Gaudecker and Schmale 1974; Kolesnikov and Zhimulev 1975). These glue secretory granules (Fig. 15.2) are produced mainly by posterior corpuscular cells, and to a lesser extent by transitional cells; only the few most anteriorly positioned columnar cells do not normally produce any of the glue secretion (Lane et al. 1972; von Gaudecker 1972; Berendes and Ashburner 1978; Farkaš and Šuťáková 1999). However, even these most anterior columnar cells will produce such granules if the growth of the gland is allowed to continue e.g. by its transplantation into an adult host (Berendes and Holt 1965). Towards the end of the last larval instar, the steroid hormone ecdysone is released into circulation and induces a complex response that leads to the initiation of metamorphosis. In the salivary glands, this is accompanied by a series of polytene chromosome puffs that reflect a cascade of transcriptional regulation, and the secretion of the glue by exocytosis (Boyd and Ashburner 1977; Berendes and Ashburner 1978).

15.1.1 *Drosophila* Salivary Glands as a Model Tissue

In the history of genetics, the *Drosophila* salivary glands are famous for their polytene chromosomes (Painter 1933). Their analyses has led to many conceptual advances, including establishing the first highly detailed cytogenetical maps (Bridges 1935, 1938, 1942; Bridges and Bridges 1939; Lindsley and Grell 1968; Lefevre 1976; Sorsa 1989; Lindsley and Zimm 1992), the elaboration of the elegant chromomere theory (Painter 1934; Pelling 1966; Beermann 1972), and correlating specific reversible changes in chromosomal structure (puffs) with the transcriptional activity of genes (Beermann 1952; Ashburner 1970; Pelling 1970).

Furthermore, studies using the *Drosophila* salivary glands have been at the forefront of research on the genetic and physiological responses to heat shock and stress (Ritossa 1962, 1963; Ashburner and Bonner 1979; Pardue et al. 1989) and glue gene regulation (Korge 1975; Giangrande et al. 1987, 1989; Lehmann 1996; Biyasheva et al. 2001). Detailed studies of how puffing patterns change during sequential gene activation in polytene chromosomes (Becker 1959; Ashburner 1972; Ashburner et al. 1974; Ashburner and Berendes 1978) and the molecular characterization of the puff-forming genes established a paradigm for understanding the mechanisms

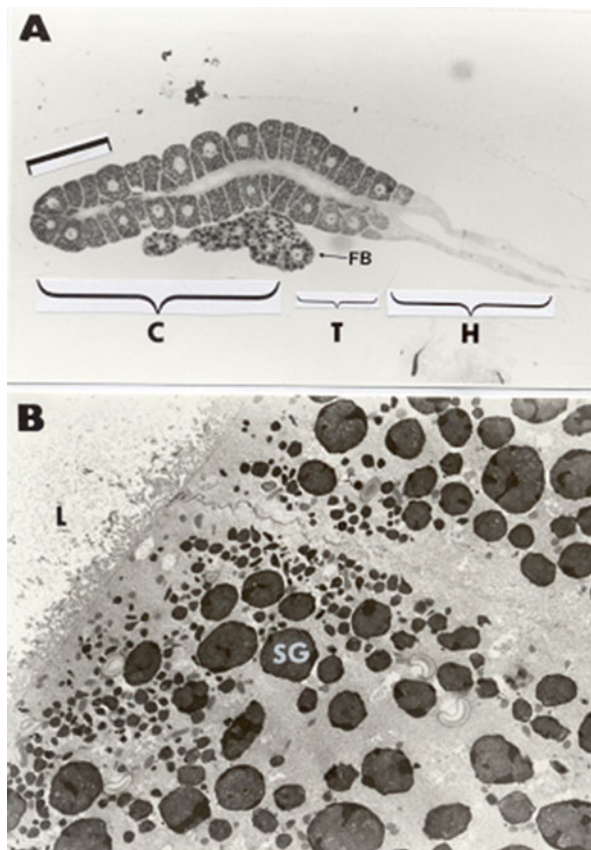


Fig. 15.2 (a) Light micrograph of a semithick section (0.5 μm) of a salivary gland. The organ was Araldite-embedded and glutaraldehyde-osmium fixed and a segment of adhering fat body (*FB*) from late 3rd instar larva, stained with toluidine blue-O in borax. The cytoplasm of corpuscular (*C*) and transitional (*T*) cells is filled with numerous (2500–3000 per cell) secretory granules of variable size (0.2–4 μm). The most anterior columnar cells (*H* – from German Halszellen) are devoid of any secretory vesicles. Magnification 250 \times . (b) Transmission electron micrograph of a glutaraldehyde-osmium fixed salivary gland from late 3rd instar larva at puff stage PS2 to PS4 showing numerous Golgi-derived electron-dense secretory granules (*SG*) filling the cytoplasm of corpuscular cells. *L*=indicates empty lumen of the gland. Magnification 2500 \times

underlying temporal and tissue-specific transcriptional control (Burtis et al. 1990; Segraves and Hogness 1990; Thummel 1996, 2002). Because the larval salivary glands become obsolete early in the hormonally triggered metamorphosis of the larvae to the adult, they are also widely used as a model system to study hormone-regulated programmed cell death (PCD).

With regard to PCD, the *Drosophila* salivary glands undergo close-to-synchronous histolysis of the entire organ about 16 h after pupariation (APF) in response to an endogenous pulse of ecdysone occurring about 6 h earlier (Jiang et al. 1997, 2000;

Farkaš and Šuťáková 1998; Farkaš and Mechler 2000; Baehrecke 2003). Only a few of the cellular events that occur in the prepupal salivary glands prior to PCD have been elucidated. Jochova et al. (1997) and later Martin and Baehrecke (2004) described changes in the clumping and redistribution of actin and tubulin cytoskeleton in the prepupal salivary glands, emphasizing that the larval and various prepupal stages show differences due to the exocytosis of glue granules in the late third instar larva. However, more comprehensive laser confocal microscopy clearly revealed that there are multiple, dynamic changes in the salivary glands during the prepupal period, including changes in the distribution of vacuoles, the arrangement of non-actin and non-tubulin cytoskeletons, and the occurrence of noncanonical protein extrusion (Farkaš and Mechler 2000).

Recently, two novel and unexpected processes were described in the prepupal salivary glands. Immediately after pupariation up to about 6/7 h APF, the *Drosophila* salivary glands undergo a very intense vacuolation that is associated with complex endosomal trafficking. This is followed by the recently discovered apocrine secretion about 8–10 h APF (Farkaš et al. 2014, 2015). To understand the function of this intense vacuolization and the apocrine secretion that follows it, and to gain additional insight into the overall metabolism of this tissue, SG respiration was measured during precisely staged late larval and prepupal and very early pupal animals. This revealed that changes to the animal's basal metabolism are correlated with feeding, postfeeding larval activity, the period of pupariation, and increased anabolic demands during the massive endosomal recycling in the early-to-mid prepupal period. There is a slow and gradual decline in respiration as the animal approaches pupation. Salivary glands stop their respiratory activity abruptly by completing histolysis 16 h after pupariation (Farkaš and Sláma 2015).

The *Drosophila* salivary glands provide a superb model to consider issues relevant to the main topics of this volume. This chapter will be devoted to two major and now clearly documented excretory functions of *Drosophila* larval SGs: (i) the production and release of a small and unique group of so-called glue proteins (Sgs-proteins), which accumulate in numerous vesicles at the end of the larval stage and are secreted by classical exocytosis, and (ii) the remarkable and massive apocrine secretion of almost all types of cellular proteins in late prepupae. In both cases, the secretory products of SG cells are delivered to the external environment. However, the secretory products are released by two mutually exclusive mechanisms, and serve functional roles that are also quite different in principle.

15.2 Larval Exocytotic Activity of *Drosophila* Salivary Glands

15.2.1 Production, Composition and Secretion of Sgs Proteins

As indicated above by about the middle of the third larval instar globular and highly refractile granules appear in the cytoplasm of the gland's posteriormost cells. These granules constitute the components of the salivary glue secretion (Sgs). The Sgs

represents a highly special and unique extracellular composite glue matrix that has not been identified so far outside of Cyclorrhaphous Dipterans; the majority of information on the composition of the Sgs that we have today comes from studies of it in *Drosophila melanogaster*.

As early as in (1948) Kodani found that the glue can be conveniently isolated after its secretion into the lumen by first fixing the glands in ethanol or an acetic acid-ethanol mixture, and then dissecting and removing the gland cells from the solid plug of precipitated glue. It was anticipated that the Sgs secretion would consist of mucinous glycoproteins (Korge 1975, 1977a; Beckendorf and Kafatos 1976). These electrophoretically separate into six to eight bands. Besides the PAS-positive histochemical reaction seen in the granules, the presence of glycomoieties was deduced from noticing that radioactively labelled ^{14}C -glucose was incorporated into some of these bands (Beckendorf and Kafatos 1976; Korge 1977b; Kress 1979; Engoher and Kress 1980). The genes corresponding to these proteins have been named *Sgs-1* to *Sgs-8* according to the mobility of the proteins (*salivary gland secretion genes 1–8*; Korge 1975, 1981). Interestingly, the electrophoretic mobility of the secreted proteins varies between different strains of *D. melanogaster*. This variation is not only due to differences in glycosylation but also to allelic variation, that was used to genetically map the genes (Korge 1975). Moreover, the activity of a small group of interecdyssal chromosomal puffs at the time of Sgs synthesis independently provided a guide for linking these proteins to their corresponding genetic loci (Korge 1977a, b; Ashburner and Berendes 1978; Velissariou and Ashburner 1980, 1981). These studies were shortly followed by the cloning of genes associated with each set of puffs: Cytological band 68C encodes the *Sgs-3*, *Sgs-7* and *Sgs-8* genes (Meyerowitz and Hogness 1982; Crowley et al. 1983, 1984; Crowley and Meyerowitz 1984; Crosby and Meyerowitz 1986), 3C encodes *Sgs-4* (Muskavitch and Hogness 1980, 1982; Chen et al. 1987), 95B encodes *Sgs-5* (Guild 1984; Guild and Shore 1984), and 25B2-3 encodes *Sgs-1* (Roth et al. 1999). The origin of *Sgs-2* and *Sgs-6* remains unclear. Some authors claim that *Sgs-2* and *Sgs-6* fractions might be a cell-debris contamination associated with the secretion isolated from salivary gland lumens (Lindsley and Zimm 1992); there are no additional *Sgs*-related genes in the *Drosophila* genome (Adams et al. 2000, 2003). Sequence analysis has revealed unique features of *Sgs*-encoded proteins not previously found among known proteins in databases. These features have been ascribed to their secretory and glue-forming nature. Although strong glycosylation was expected in most of the *Sgs* proteins even before their amino-acid sequence was known, only *Sgs-3* initially showed motifs that conclusively supported the contention that it is heavily glycosylated (Garfinkel et al. 1983). Later, detailed sequence analysis of *Sgs-4* and *Sgs-1* supported the view that they too are glycosylated (Furia et al. 1992; Roth et al. 1999). At the time of maximum synthesis, these *Sgs* proteins comprise for 25–30 % of the total protein content of the salivary glands (Zhimulev and Kolesnikov 1975), with each salivary gland cell containing 2500–3000 individual secretory granules ranging from 0.2 to 2.5 μm in diameter (Farkaš and Šuťáková 1999). These characteristics make the larval SGs of *Drosophila* an ideal and easily accessible model system to study various aspects of regulated exocytosis in metazoans.

The *Sgs* genes are coordinately activated: all of the cloned *Sgs* genes are heavily transcribed during the second half of the third larval instar only in the salivary glands (reviewed in Lehmann 1996) leading to the formation of dramatic puffs at their genes. These regress when the titre of the steroid hormone ecdysone increases at the end of the third larval instar (Becker 1959; Ashburner 1972; Richards 1981). Thus, this group of genes has provided an excellent opportunity to analyze the mechanisms that control tissue-specific and temporarily restricted gene expression. Presumably, the expression of all *Sgs* genes is controlled by the same *trans*-acting factors, possibly by the ecdysone receptor and auxiliary proteins (Lehmann and Korge 1995).

15.2.2 The Fate of *Sgs*-Secretory Granules

The *Sgs* proteins synthesized inside the salivary gland cells tend to form Golgi-derived electron-dense secretory vesicles that then fuse into larger granules (Farkaš and Štuřáková 1998, 1999). Several authors have studied secretory granules in *D. melanogaster* (von Gaudecker 1972; Lane et al. 1972; Farkaš and Štuřáková 1998), *D. pseudoobscura* (Harrod and Kastriasis 1972a, b; Pasteur and Kastriasis 1973) and *D. hydei* (Berendes 1965; Poels et al. 1971) and have described several different infrastructural elements within the granules: a foamy component, a paracrystalline component, and a fine particulate or electron-opaque component (Fig. 15.3). It is reasonable to assume that these infrastructural elements represent different states of granule maturation and reflect a level of densification that may be due to the gradual

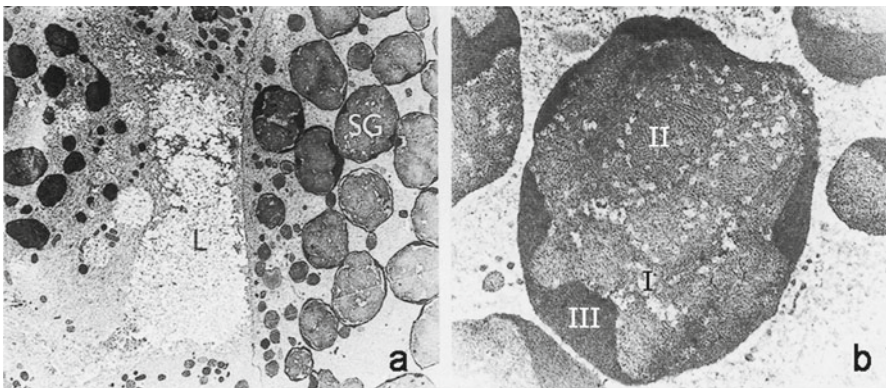


Fig. 15.3 (a) Transverse section through the interecdysially active salivary gland with a centrally located lumen (*L*). Note the large number of electron-dense *Sgs*-secretory granules (*SG*) at the apical pole displaying three different infrastructures. Magnification 3000 \times . (b) Detailed view of three different infrastructural elements (densities) inside of the granule: *I*. foamy component, *II*. paracrystalline component, and *III*. fine particulate or electron-opaque component. Magnification 18,000 \times . (Reprinted with the permission of the publisher)

dehydration of granule contents. Detailed ultrastructural analysis of the Sgs-secretory granules indicates that densification is a continuous and permanent process inherent to the granules or Sgs-proteins, because when two highly dense electron-opaque granules fuse, they form local patches of foamy or paracrystalline infrastructure at the fusion sites, often close to the vesicle membrane (von Gaudecker 1972; Lane et al. 1972; Farkaš and Šuťáková 1998). That these observations are possible over relatively long periods of time make the *Drosophila* SGs an excellent model to study the basis of regulated exocytosis. Its secretory products are first synthesized and then stored for a long period (16–20 h) prior to their singular release, and so this model provides enough time to observe and investigate the molecular regulation of the process underlying their gradual maturation and release.

Through precise counting of the number and size of granules in late 3rd instar larval SGs of *Drosophila*, Farkaš and Šuťáková (1999) obtained clear evidence that the growth and maturation of Sgs-granules occurs as a continuous process through the gradual fusion of smaller granules. Niemeyer and Schwarz (2000) found that SNAP-24, a t-SNARE (soluble NSF (*N*-ethylmaleimide-sensitive fusion protein)-attachment receptor) homologue is present on the membrane of Sgs-granules, and that it acts to mediate granule-granule fusion. It is putatively involved also in exocytosis, *i.e.*, mediating contact between the granule and the apical cell membranes. Additional key molecules in this process have also been identified. During the formation of Sgs-granules at the *trans*-Golgi network (TGN), newly synthesized glue proteins colocalize with clathrin and the clathrin adaptor protein complex subunit γ (AP1 γ) at the TGN membranes (Burgess et al. 2011). Indeed, mutations affecting AP1 or its localization have dramatic effects. Mutations in *API γ* lead to a profound block in secretory granule formation or maturation. The localization of the AP1 γ subunit to the TGN in salivary glands seems to require *Gartenzweg* (*Garz*), the *Drosophila* ortholog of mammalian guanine nucleotide exchange factor GBF1, which is essential for Golgi complex biogenesis and surface delivery of proteins involved in cell-cell and cell-matrix interactions. The loss of *Garz* function, in addition to collapsing the Sgs-secretory pathway, inhibits trafficking of two adhesion molecules, DE-cadherin with the associated α - and β -catenins and Flamingo, to the cell surface, and disrupts the localization of the tumor suppressor Discs large, involved in the determination of polarity via the formation of septate junctions. By these mechanisms, the loss of *Garz* function leads to a dramatic disorganization of the morphology of the salivary glands (Szul et al. 2011). *Drosophila* SGs mutant for *garz* also display dysfunctional Arf1-COPI machinery (Wang et al. 2012). Arf1 (ADP-ribosylation factor 1), through assembly of a COPI coating onto membranes, is likely to promote the formation and maturation of Golgi elements including secretory vesicles, and thus likely to regulate anterograde transport of the secretory granules that are targeted for exocytosis (Wu et al. 2004; Munro 2005).

The classical approach to monitoring the release of Sgs-glue is to view the lumen of *in vitro* cultured SGs in a drop of diluted Grace's or Schneider's medium under a stereomicroscope or using phase contrast imaging under low magnification (Boyd and Ashburner 1977). Alternatively, PAS-positive histochemical staining of the whole-mount SGs can be employed (Berendes 1965; Poels 1970; von Gaudecker

and Schmale 1974; Kolesnikov and Zhimulev 1975). We have routinely also used semi-thick sections of acrylate-resin embedded SGs metachromatically stained with Toluidine Blue O which strongly binds Sgs-glue (Farkaš and Sláma 1999). Currently, an easy method to view the process of granule secretion is to monitor it using a transgenic strain expressing GFP- or dsRED- fused to the Sgs-3 protein (Biyasheva et al. 2001). In these strains, the strongly fluorescent granules inside a cell's cytoplasm are gradually released into the SG lumen with a corresponding rapid loss of cell volume (Fig. 15.4). After the contents of the granules are released into the lumen by exocytosis, the lumen becomes amorphous and rehydrated. After the complete or near-complete exocytosis of Sgs-granules which takes place over a period of about 2 h (Boyd and Ashburner 1977; Farkaš and Šučáková 1998; Biyasheva et al. 2001), the lumen grows in volume by taking up the solute, most probably by active water transport from the haemolymph (Farkaš et al. 2015), to support the dilution of the glue in order to facilitate its later expectoration via the larval mouth. Indeed, the freshly formed puparium will become quickly cemented to the surface of a substrate after the evaporation of the water from the glue.

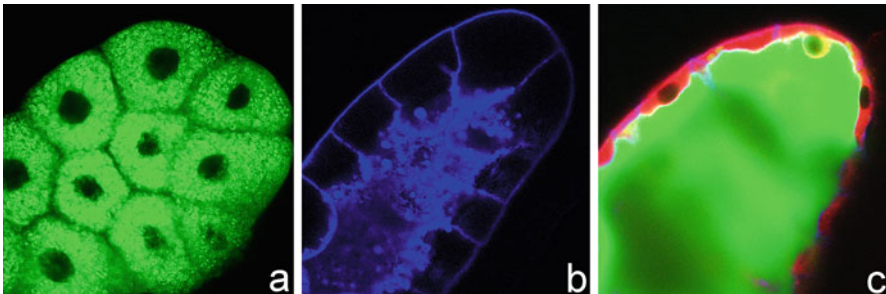


Fig. 15.4 Exocytosis of Sgs-glue proteins. They were monitored using the *GFP-SgsΔ3* strain. This strain was constructed by inserting 1.8 kb of the *Sgs3* regulatory region and the N-terminal portion of the *Sgs3* protein fused to enhanced GFP, into the pCaSpeR-4 transformation vector (Biyasheva et al. 2001). (a) Laser confocal image of most posterior region of the late 3rd instar larval salivary gland (during puff stages PS2 to PS4 corresponding to 1–3 h prior to glue exocytosis) with cells filled with numerous Sgs-granules containing GFP-fused Sgs-3 protein. (b) During PS5, when exocytosis is initiated by the elevated titre of ecdysteroids, glue granules containing Sgs proteins are transported towards the lumen where they become docked to the apical cell membrane via the actin cytoskeleton, highlighted by AlexaFluor₄₈₈-conjugated phalloidin (blue). (c) The same region of the salivary gland with GFP-glue (green) released into the lumen (PS7 to PS8). Previously large and hexagonal salivary gland cells shrink upon massive glue exocytosis into the thin rim (red) around the lumen filled with secreted glue. To show this, Rab11 was detected in the cytoplasm of the SG cells using an anti-Rab11 polyclonal antibody and a Cy3-conjugated goat anti-rabbit secondary antibody

15.2.3 Physico-Chemical Properties of Sgs Proteins

Despite the initial interest in Sgs proteins during 1970s and 1980s, due to their striking characteristics as puff-encoded products, we do not have much published information about their properties. For example, we do not know if they are present in an equimolar ratio inside of the secretory granules and inside the expectorated secretory glue, so we cannot evaluate how their relative molar ratios are related to their overall function. We do not know the role of each individual protein in granule formation and maturation/densification, or in the subsequent hydration of the glue after it is exocytosed into the lumen. Since all of the *Sgs* genes have been molecularly characterized, some information can be gleaned from extensive *in silico* analysis of amino acid sequences.

The Sgs-1 protein is cornifin-related and adhesin-like, and potentially a chitin-binding protein, with a predicted molecular weight of 134.9 kDa and an isoelectric point of 12.1. It has 1286 amino acids and consists 109 tandemly arranged TTTTPRS repeats forming the core of the polypeptide chain. Overall, it contains 600 threonines representing 46.7 mole% of its total amino acid composition (for more details see Table 15.1). Remarkably, over 70 % of these threonines are predicted by several different methods to be *O*-glycosylated. Such a dense level of glycosylation has not been described so far for any other protein. At the same time, the majority of the tandem repeats are predicted by both the Garnier-Osguthorpe-Robson and the Chou-Fasman methods as being highly hydrophilic (Fig. 15.5a) which may reflect the distribution of hydroxyl- or polar amino acids. Except for a signal peptide in the N-terminal region and two stretches of a few amino acid residues at the C-terminal end, the majority of the Sgs-1 protein is predicted to be strongly disordered, most probably forming a coil (Fig. 15.7a). Only the more ordered N- and C-terminal regions are consistently predicted to form α -helices or β -sheets (Fig. 15.6a). The Sgs-1 protein displays 57 predicted disulfide bonds, with 40 of them having a very high score (between 0.8 and 1.0, where 1.0 means the highest degree of confidence).

The Sgs-3 protein, with a predicted molecular weight of 34.8 kDa and an isoelectric point of 10.5, has 307 amino acids and consists of 20 tandemly arranged TTTKX repeats (where the most frequent X is a P) that form the core of the polypeptide chain. As for Sgs-1, threonine residues are the most abundant amino acid (130 residues, 46.7 mole%) and at least 45 % of them are predicted to be *O*-glycosylated. Also as seen in Sgs-1, the tandem repeats in the Sgs-3 protein are predicted by both the Garnier-Osguthorpe-Robson and the Chou-Fasman methods to be very hydrophilic (Fig. 15.5b), and by PONDR to be strongly disordered, forming a coil as predicted by PsiPred, Predator and other algorithms (Figs. 15.6b and 15.7b). The entire Sgs-3 protein is predicted to have 28 disulfide bonds with only two having a score under 0.8. Over 12 of the disulfide bonds, however, are predicted within the signal peptide, and therefore these cannot contribute to the protein's secondary structure and function (for more details see Table 15.1).

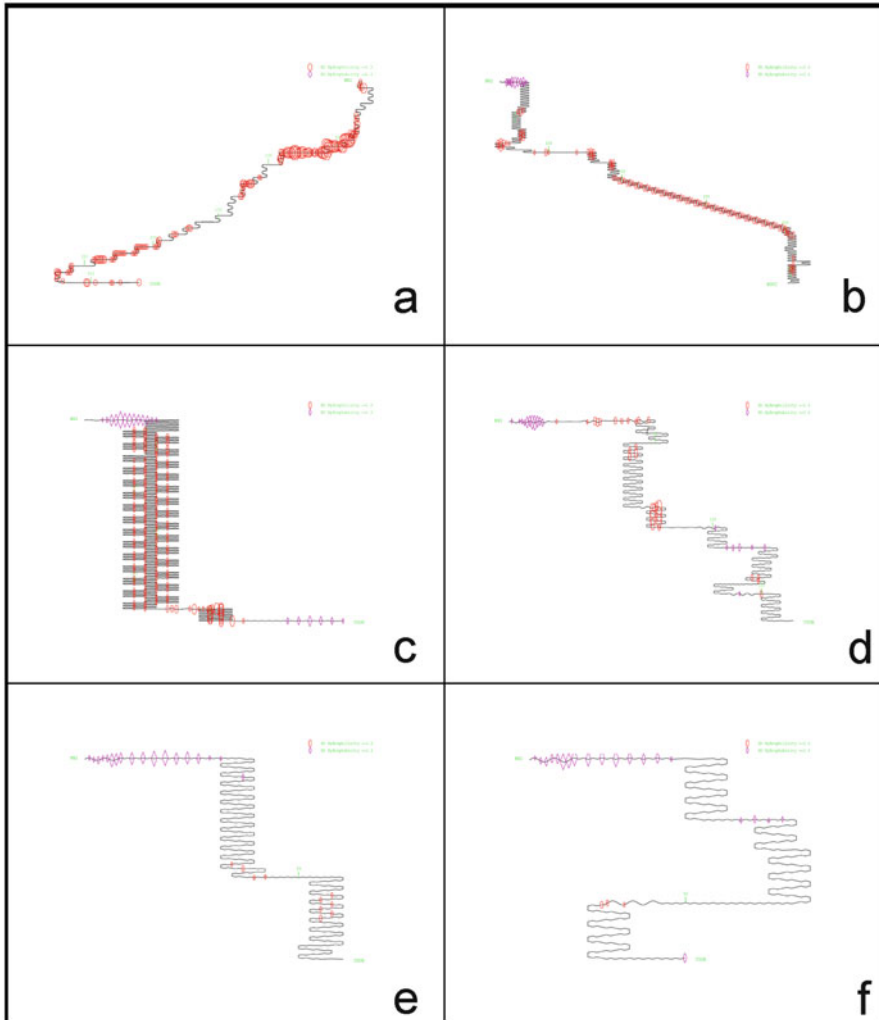


Fig. 15.5 Predictions of hydrophobicity, hydrophilicity and secondary structure of individual Sgs proteins. The Bayesian type Chou-Fasman and Garnier-Osguthorpe-Robson (*GOR*) methods were used. These methods are based on probability parameters derived from empirical studies of known protein tertiary structures solved by X-ray crystallography. In addition, the *GOR* algorithm takes into account not only the propensities of individual amino acids to form particular secondary structures, but also the conditional probability of the amino acid to form a secondary structure given that its immediate neighbors have already formed that structure. (a) Sgs-1, (b) Sgs-3, (c) Sgs-4, (d) Sgs-5, (e) Sgs-7, and (f) Sgs-8

The Sgs-4 protein, with a predicted molecular weight 32.3 kDa and an isoelectric point of 9.1, has 297 amino acids. Structural parallels with Sgs-1 and Sgs-3 are readily apparent: 24 tandemly arranged TEPP or TKPP repeats encompass more than 80 % of the length of the polypeptide chain. Again, threonine is the most abundant amino acid ($n=53$; 17.8 mole%) with at least 73 % of the threonines predicted

Table 15.1 Composition and properties of amino acid groups as revealed from *in silico* analysis of individual Sgs proteins

Property	Sgs-1		Sgs-3		Sgs-4		Sgs-5		Sgs-7		Sgs-8			
	No.	Mole%	No.	Mole%	No.	Mole%	No.	Mole%	No.	Mole%	No.	Mole%		
Molecular weight (kDa)	135.0		32.2		32.3		18.7		7.9		7.9			
Average residue weight	104.9		104.9		108.8		115.7		107.0		106.0			
Isoelectric point	12.1		10.5		9.1		7.8		7.9		4.9			
Residues	1286		307		297		161		74		74			
Charge	102.5		35		27		2		2		-1			
Residues	No.	Mole%	Residues	No.	Mole%	Residues	No.	Mole%	Residues	No.	Mole%	Residues	No.	Mole%
Small	A+B+C+D+G+N +P+S+T+V	1077	83.7	A+G	21	6.8	A+G	21	7.1	12	7.5	A+G	13	17.6
Hydroxyl	S+T	-	-	D+E	135	43.9	D+E	67	22.6	20	12.4	D+E	4	5.4
Acidic	B+D+E+Z	26	2.0	D+E+N+Q	6	1.9	D+E	32	10.8	17	10.6	D+E	5	6.7
Acid/Amide	D+E+N+Q	-	-	H+K+R	24	7.8	H+K+R	38	12.8	31	19.2	H+K+R	13	17.6
Basic	H+K+R	129	10.0	B+D+E+H+K+R+Z	41	13.4	B+D+E+H+K+R	64	21.6	22	13.6	B+D+E+H+K+R	7	9.5
Charged	B+D+E+H+K+R+Z	155	12.1	I+L+M+V	47	15.3	I+L+M+V	96	32.3	39	24.2	I+L+M+V	12	16.2
Smallphob	I+L+M+V	-	-	F+W+Y	21	6.8	F+W+Y	18	6.1	34	21.1	F+W+Y	21	28.4
Aromatic	F+H+W+Y	24	1.9	A+C+G+S+T	1	0.3	A+C+G+S+T	1	0.3	20	12.4	A+C+G+S+T	2	2.7
Tiny	A+C+G+S+T	856	66.6	A+I+L+V	50	3.9	A+I+L+V	-	-	-	-	A+I+L+V	-	-
Aliphatic	A+I+L+V	50	3.9	A+C+F+G+I+L +M+P+V+W+Y	332	25.8	A+C+F+G+I+L +M+P+V+W+Y	-	-	-	-	A+C+F+G+I+L +M+P+V+W+Y	-	-
Non-polar	A+C+F+G+I+L +M+P+V+W+Y	332	25.8	D+E+H+K+N+Q +R+S+T+Z	954	74.2	D+E+H+K+N+Q +R+S+T+Z	-	-	-	-	D+E+H+K+N+Q +R+S+T+Z	-	-
Polar	D+E+H+K+N+Q +R+S+T+Z	954	74.2											

Sgs: salivary glue secretion

to be *O*-glycosylated. Interestingly, Sgs-4 has also three *N*-glycosylable asparagines. As for Sgs-1 and Sgs-3, the tandem repeats of the Sgs-4 protein are predicted by both the Garnier-Osguthorpe-Robson and the Chou-Fasman methods to be very hydrophilic (Fig. 15.5c). In contrast to those proteins, however, Sgs-4 is less intrinsically disordered, containing two centrally and two C-terminally located short ordered regions (Fig. 15.7c). Out of 22 cysteines, at least eight are predicted to form disulfide bonds. Except for the signal peptide, there are no predicted α -helices or β -sheets (Fig. 15.6c). For more details see Table 15.1.

In contrast to Sgs-1, -2, -3, and -4, the Sgs-5 protein, with 161 amino acids, a predicted molecular weight of 18.6 kDa and an isoelectric point of 7.8, lacks any clearly identifiable tandem repeats. Threonine is far less abundant than in the previously discussed Sgs proteins (3.1 mol%). By contrast, Sgs-5 is rich in glutamic acid, leucine and serine (for more details see Table 15.1). The Garnier-Osguthorpe-Robson and the Chou-Fasman algorithms predict only a few hydrophilic and a few hydrophobic regions (Fig. 15.5d) and there appears to be just single *N*-glycosylation and a single *O*-glycosylation sites. Except for two regions, between amino acids 30 and 45, and between amino acids 75 and 95, which are intrinsically disordered, the majority of the Sgs-5 protein is highly ordered, containing five α -helices and four β -sheets (Figs. 15.6d and 15.7d). The Sgs-5 protein displays 12 predicted disulfide bonds, with eight of them having a very high score (between 0.8 and 1.0).

The Sgs-7 protein, with 74 amino acids, a predicted molecular weight of 7.9 kDa and an isoelectric point of 7.9, is also unlike Sgs-1, -2, -3, and -4 nonglycosylated and lacks their typical tandem repeats. The most abundant amino acids are cysteine, isoleucine, leucine and glutamine (for more details see Table 15.1). The Garnier-Osguthorpe-Robson and the Chou-Fasman algorithms predict only a few hydrophilic sites inside the core region and a few hydrophobic sites, the majority of which overlap with the N-terminal signal peptide (Fig. 15.5e). It lacks expected glycosylation sites, and surprisingly no disulfide bonds are predicted despite the presence of numerous cysteines. However, the potential for an unusual pattern of disulfide bonding deserves more investigation. The entire Sgs-7 protein is predicted to be strongly ordered with two long α -helices flanking a single β -sheet (Figs. 15.6e and 15.7e).

The Sgs-8 protein is highly related to Sgs-7, with a predicted molecular weight of 7.8 kDa and an acidic isoelectric point of 4.8. It has 74 amino acids without any typical tandem repeats. The most abundant amino acids are cysteine, glycine, valine and leucine (for more details see Table 15.1). The Garnier-Osguthorpe-Robson and the Chou-Fasman algorithms predict only few hydrophilic sites inside the core region and a few hydrophobic sites, the majority of which overlap with the N-terminal signal peptide (Fig. 15.5f). There are no glycosylation sites. In contrast to Sgs-7, however, the Sgs-8 protein is predicted with high confidence to have eight disulfide forming cysteines. Similar to Sgs-7, the Sgs-8 protein is strongly ordered harboring two long α -helices (Figs. 15.6f and 15.7f).

Posttranslational modification of individual Sgs proteins may have substantial effects on their properties and function. Different levels of glycosylation can have a significant effect on the final molecular weight and pI of a protein, and thus, its electrophoretic mobility may be quite different from that predicted, and several

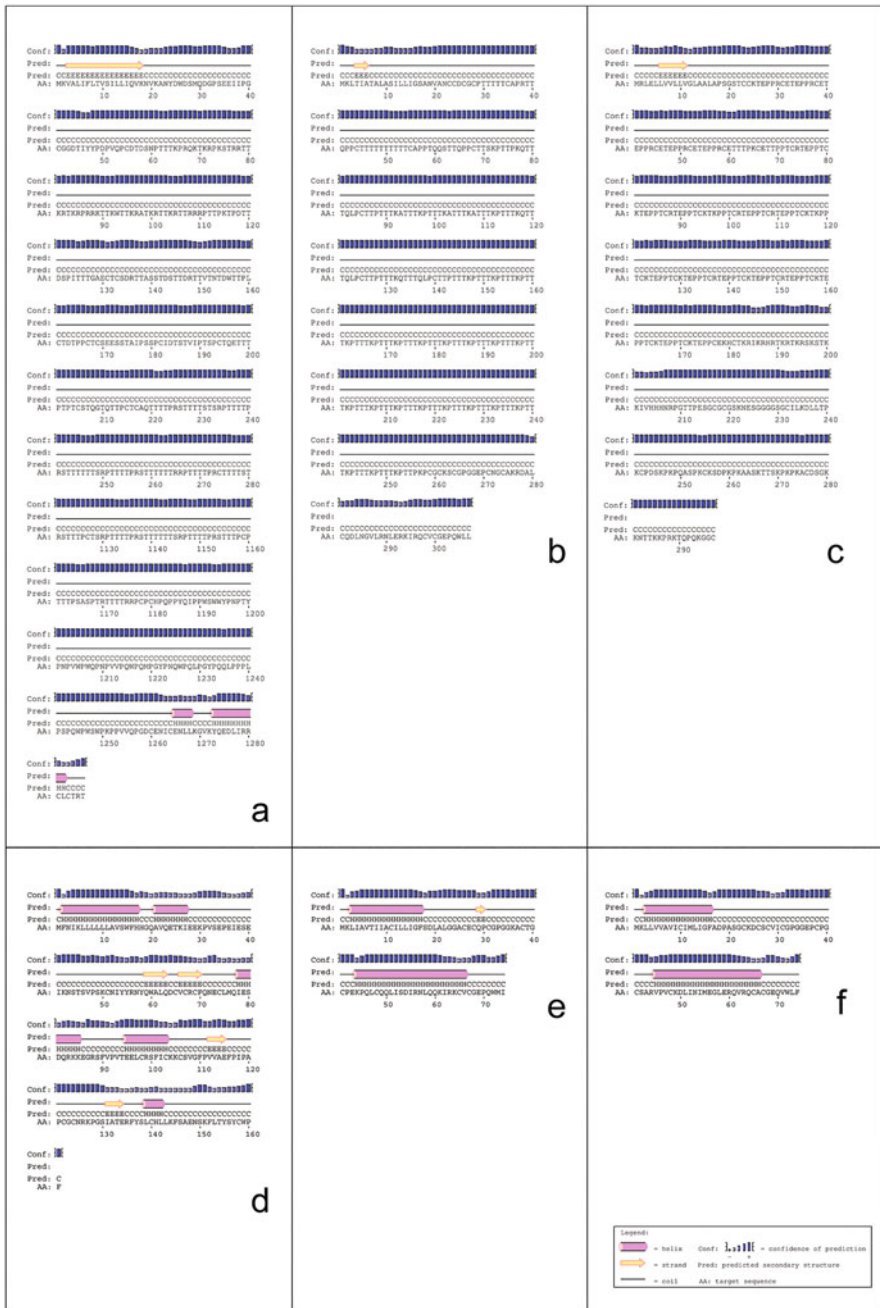


Fig. 15.6 Secondary structure of Sgs proteins predicted by PsiPred algorithm employing neural network and machine learning methods which use the information of the evolutionarily related proteins (McGuffin et al. 2000). (a) Sgs-1, (b) Sgs-3, (c) Sgs-4, (d) Sgs-5, (e) Sgs-7, and (f) Sgs-8. For clarity, in the case of Sgs-1 (a) only the N-terminal and C-terminal portions of the entire sequence are shown because the central core region contain 109 tandemly repeated stretches of TTTPRS that fail to form either α -helices or β -sheets. Legend: *magenta cylinder* = α -helix, *yellow arrow* = β -sheet, *black line* = coil, *blue oblonger bars* above secondary structures represents confidence of prediction

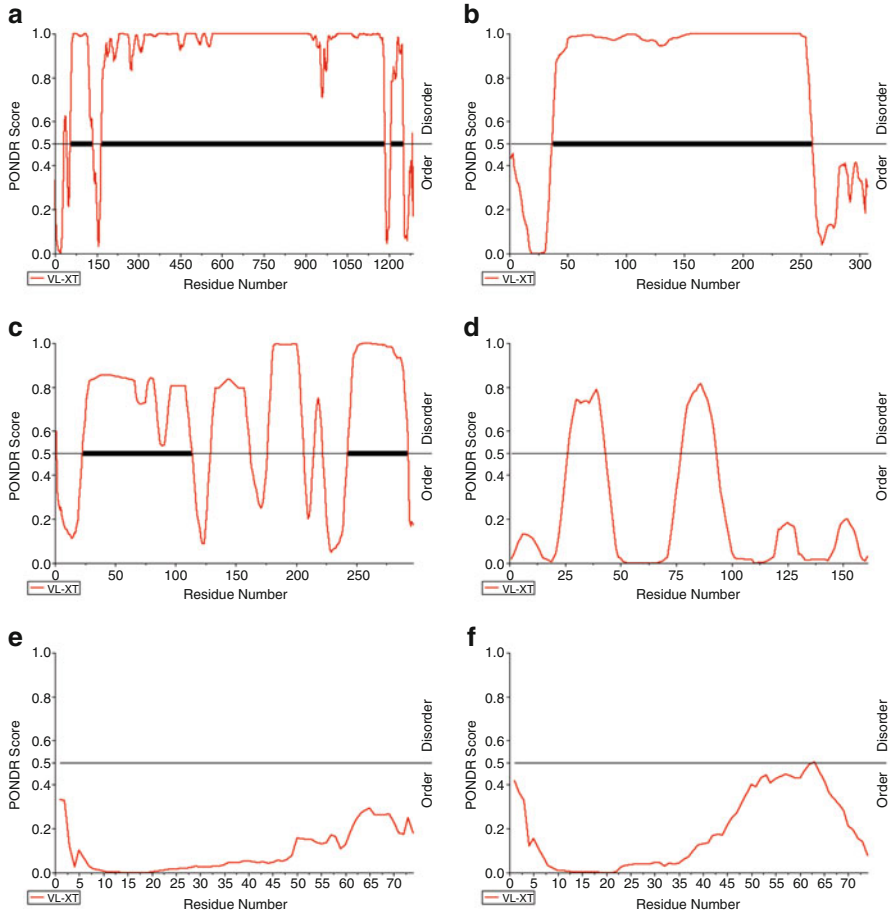


Fig. 15.7 Analysis of ordered/disordered regions in the Sgs proteins by the PONDR protocol which utilizes feedforward neural networks that use sequence information from windows of 21 amino acids (Romero et al. 1997, 2001). If a residue value exceeds a threshold of 0.5, the residue is considered disordered. (a) Sgs-1, (b) Sgs-3, (c) Sgs-4, (d) Sgs-5, (e) Sgs-7, and (f) Sgs-8

variants may be displayed. This issue deserves to be explored experimentally in more detail in the future. It will provide substantial insight into how individual Sgs proteins function as well as how the entire complex achieves its sticky properties. Currently, we can hypothesize that the glycosylated amino acid residues are likely to serve in at least three different functions: [1] Glycomoieties aid in protein folding and maturation; the nascent unmodified Sgs polypeptide would otherwise prefer a strongly disordered structure [2] Glycomoieties serve in hydration; they can be more easily dehydrated during granule densification than residues on a native protein, and vice versa, they can be more easily rehydrated after exocytosis. [3] Glycomoieties serve functional roles subsequent to exocytosis; a high level of glycosylation will serve to lubricate proteins allowing for more efficient transport via

the gland lumen and mouth and so facilitate expectoration, and perhaps also facilitate adhesion to both the surface of the chitinous puparium and the attached substrate.

15.2.4 *Speculation on the Role of Sgs Proteins*

From the predictions of various aspects of their secondary structures it is clear that the smaller and inherently ordered Sgs proteins are either not glycosylated or considerably less glycosylated than the larger and structurally disordered Sgs proteins that are quite heavily glycosylated. This identifies a specific paradox concerning the Sgs-proteins: the degree of order and disorder in the polypeptide chain is related to how much it is glycosylated. In addition, it appears that the structurally disordered, larger Sgs proteins also have more cysteines predicted to form disulfide bonds. We hypothesize that the higher level of glycosylation and disulfide bonding aids in reducing the inherently disordered state of the larger Sgs proteins since they lack α -helices and β -sheets, and that this may be required for secretory granule maturation and potentially, for fulfilling their function as glue proteins. In this context it seems logical to propose that the small nonglycosylated Sgs proteins like Sgs-7 and Sgs-8 or Sgs-5 have a higher likelihood to stably maintain their secondary structures as they proceed through the different conditions associated with granule formation, fusion, maturation, exocytosis, rehydration, and finally, expectoration. If this is the case, the higher ratio of α -helices and β -sheets in each of the small Sgs proteins, when compared to the highly glycosylated Sgs-1, Sgs-3 and Sgs-4 proteins, might allow them to serve as pivotal initiators or promoters of the densification process. On the other hand, the larger and highly glycosylated Sgs proteins are more likely to facilitate rehydration after exocytosis and the maintenance of lubrication during the process of expectoration and the cementing of the prepupa to the substrate.

It is not a rule of thumb that intrinsically disordered regions are typically involved in regulation, signaling and control pathways in which interactions with multiple partners and high-specificity/low-affinity interactions are expected (Dyson and Wright 2005; Bardwell and Jakob 2012; Mittal et al. 2013). It should be noted, however, that intrinsically disordered proteins or regions exist as dynamic ensembles in which the atom positions and the backbone Ramachandran angles vary significantly over time with no specific equilibrium values and typically involve non-cooperative conformational changes (Gunasekaran et al. 2004; Uversky et al. 2008). Such disorder may serve to provide a functional advantage by enhancing binding plasticity or allosteric coupling. Several studies showed that the conformational entropy conferred by disordered regions decreases the propensity of proteins to self-aggregate (Dyson and Wright 2005; Japrun et al. 2013). Thus, mutual interactions that can be anticipated between the inherently ordered and disordered Sgs-proteins can serve to prevent an unwanted aggregation process within the densely packed secretory granules or even after exocytosis before the glue is programmed

to solidify. Presumably, the mutual interactions between the two fundamentally different types of Sgs proteins may serve in regulating when the glue will set.

15.2.5 Evolution of Sgs Proteins

Applying both of the BLAST and FASTA algorithms to *D. melanogaster* Sgs protein sequences revealed that these proteins are not present in the genomes of all *Drosophila* species sequenced to date (Adams et al. 2000; Misra et al. 2002; Kaminker et al. 2002; Celniker and Rubin 2003; Stark et al. 2007; Pfeiffer et al. 2010). Moreover, there are also species-specific differences in the distribution or occurrence of individual Sgs proteins. The Sgs-1 protein which is responsible for interecdyal puff 25 AC in *D. melanogaster* was unambiguously found only in *D. sechelia*. The most widespread Sgs proteins found among other *Drosophila* species are proteins related to those produced by the *Sgs-5* and *Sgs-7* genes which were found in the same nine non-*melanogaster* species (*D. simulans*, *D. sechelia*, *D. yakuba*, *D. ananassae*, *D. persimilis*, *D. pseudoobscura*, *D. erecta*, *D. virilis*, *D. mojavensis*). The orthologues of *Sgs-8* were found in eight non-*melanogaster* species (*D. simulans*, *D. sechelia*, *D. yakuba*, *D. erecta*, *D. ananassae*, *D. virilis*, *D. persimilis*, and *D. pseudoobscura*), the orthologues of *Sgs-3* were found in six species (*D. simulans*, *D. yakuba*, *D. ananassae*, *D. pseudoobscura*, *D. sechelia*, *D. erecta*), and finally, the orthologues of *Sgs-4* were found in five non-*melanogaster* species (*D. simulans*, *D. yakuba*, *D. erecta*, *D. mojavensis*, and *D. virilis*). Thus, only *D. sechelia* has all six of the Sgs proteins found in *D. melanogaster*, while *D. simulans* has 5 of them (all except Sgs-1). Present in *D. mojavensis* are only *Sgs-4*, *Sgs-5* and the nonglycosylated *Sgs-7*. In summary, only those species belonging to *melanogaster* subgroup (*D. simulans*, *D. sechelia*, *D. yakuba*, *D. erecta*, and *D. melanogaster*) have all six or at least five Sgs proteins, whereas *D. ananassae* (*melanogaster* group), *D. pseudoobscura* (*obscura* group), and *D. virilis*, (*virilis* group) have four Sgs proteins. Finally, *D. persimilis* (*obscura* group) and *D. mojavensis* (*repleta* group) have only three Sgs proteins; Sgs-1 and Sgs-3 are absent in both, while Sgs-4 and Sgs-8 are missing in *D. persimilis* and *D. mojavensis*, respectively

In other species, the sequence data is either missing, or if it is available, neither BLAST nor FASTA searches, unless done under low stringency, identify positive hits. The majority of false positives are clearly not orthologues but sequences having only partial similarity (under 40%) or identity (under 30%). Nonetheless, we have made some experimental observations on morphological features found in the late larval salivary glands in few additional species. From these unpublished data, it is clear that species such as *D. willistoni*, *D. atripex*, *D. mauritiana* and *D. parabipectinata* show a reticulate network of cytoskeletal components indicating the presence of Sgs-like granules in the cytoplasm of SGs of late 3rd instar feeding and wandering larvae (Farkaš et al. unpublished observations). This indicates the potential presence of Sgs orthologues in these additional species. Detection of Sgs-like secre-

tory granules in some species, for example, *D. willistoni* and *D. mauritiana* is surprising because under obligatory or natural conditions, the larvae prefer to pupariate on the surface of or inside their food. It is notwithstanding that after small pieces of leprello or accordion-folded filter paper were inserted into the food, more than 70% of the larvae choose to climb out of the food and pupariate on the filter paper. Thus, these species are able to display a shift from sitter to rover larval behaviour (Farkaš et al., unpublished observations). It may be that in these species the use of a Sgs-based glue is facultative and not obligatory, so that its production depends on the surrounding habitat or type of material provided inside the culture. Interestingly, also we observed a similar facultative pupariation behaviour in *D. simulans*, a very close relative of *D. melanogaster*, in which five out of six Sgs proteins were identified (all except Sgs-1). Thus, we were surprised that BLAST and FASTA searches failed to identify any orthologue in *D. willistoni*. It may be that the evolutionary distance of 35–37 MYA that separates between *D. melanogaster* and *D. willistoni* (Garfinkel et al. 1983; Meyerowitz and Martin 1984; Parsons 1978, 1981, 1994; Barker et al. 1990; Korol et al. 2006) is sufficient for the Sgs genes to acquire a level of sequence divergence which prevents the identification of orthologues.

Certainly, there are several alternative explanations for these data. Still, one conclusion that can currently be made is that evolutionary older species such as *D. mojavensis* and *D. persimilis* have fewer Sgs genes, primarily Sgs-5 and Sgs-7, while more recently-evolved species such as representatives of *melanogaster* subgroup (*D. simulans*, *D. sechelia*, *D. yakuba*, *D. erecta*, and *D. melanogaster*) have five or six Sgs genes. Thus, those Sgs proteins that are more structurally ordered are either not or less glycosylated, such as Sgs-5, Sgs-7 and Sgs-8 appear to be older, while those genes encoding unordered but heavily glycosylated proteins like Sgs-1 or Sgs-3, were acquired during evolution more recently. Currently, it would be very speculative to state which of the genes are ancestral for the less ordered and heavily glycosylated Sgs proteins. The high number of short tandem repeats, however, indicates that their internal disordered structure could evolve relatively quickly by repeated duplication of a simple tandem motif. Although the information presented thus far does not let us draw a clear or unambiguous conclusion about the evolutionary or habitat-prone adaptation associated with the function and expression of each particular Sgs protein, it is evident that as a group of excretory products with a highly specified function (glue), they appear to be flexible in their adaptation to environmental and habitat factors. The evolution of the Sgs proteins will therefore serve as a very useful model to study the evolution of *Drosophila* species in the context of habitat adaptation. Further investigations along these lines in more species from more diverse habitats will be necessary to gain deeper insights about the role of environment and evolution in the composition of the Sgs-glue, as well as the expression and the sequence variability of individual Sgs proteins.

According to many classical papers, the Sgs-glue proteins were considered to be mucins (Korge 1975, 1977a, b; Beckendorf and Kafatos 1976; Kress 1979; Engoher and Kress 1980). According to currently accepted criteria, however, mucins are characterized by poorly conserved repeated sequences that are rich in prolines and

potentially glycosylated threonines and serines (PTS). If among the Sgs proteins in *D. melanogaster*, only Sgs-1 and Sgs-3 meet these stipulations (Syed et al. 2008), thus only about a third of glue proteins are true mucins. In the light of this conclusion the *Drosophila* glue system provides a challenging opportunity to understand the coevolution of proteins having considerably different structural features that nonetheless interact to form components of the same extracellular matrix.

15.3 Apocrine Secretion by *Drosophila* SGs

Drosophila SGs have been a model organ for many genetic, cytological and developmental studies, including those mentioned above. However, for a long period of time, their only well-characterized and consequently the major function associated with them was the production of the Sgs glue during the second half of the last larval instar. When released by exocytosis during pupariation, this serves to affix the freshly formed puparia to a substrate (Fraenkel and Brookes 1953). Because of their large cell size and otherwise excellent suitability to study processes underlying programmed cell death (PCD), the SGs have become also the tissue of choice for investigating developmentally-linked and hormonally-triggered PCD. Indeed, it was during a set of experiments on PCD in *Drosophila* in our laboratory that we discovered that the doomed larval salivary glands release additional proteins, distinct from and well after their secretion of Sgs-glue, by an unusual extrusion process during the late prepupal period (Farkaš and Mechler 2000). Later we showed that this hitherto neglected protein extrusion process, which takes place just 6–4 h prior to the execution of PCD, occurs via a typical apocrine mechanism (Farkaš et al. 2014). Not only it was the first description of apocrine secretion in *Drosophila*, but the rich array of methods and molecular-genetic tools available in the fruitfly offer an outstanding opportunity to dissect the mechanism of this process and identify the genes regulating it. Below, are summarized the complex light and electron microscopical evidence for the apocrine process in the prepupal salivary glands, with a description of its dynamics and characterization of the secreted proteins that provide a foundation on which to achieve this long-term goal.

The main significance of finding an apocrine process in the SGs, especially late in their life and after their glue has been secreted, lies in the fact that the only type of widespread and well-known secretory process is exocytosis. This intensely studied mechanism has identified many dozens of factors and their encoding genes (Jahn 2004; Südhof 2004; Chieriegatti and Meldolesi 2005; Südhof and Rothman 2009; Blank 2011; Porat-Shliom et al. 2013). Exocytosis or merocrine secretion is the process regulating the specific membrane contact, priming and fusion events required for the selective release of compartmentalized compounds such as signaling molecules (antibodies, neurotransmitters, cytokines, morphogens, growth factors, chemokines, hormones, etc.). It became widely accepted that the initial phase of the exocytotic secretory pathway involves the formation of vesicles in the *trans*-Golgi, then targeted translocation of these vesicles to specific sites on the plasma

membrane, the preparation of these docked vesicles for full fusion competence (priming), and the subsequent triggered fusion of these membranes, resulting in their coalescence and the release of vesicular contents to the extracellular space. A complex composed of the three major membrane proteins, NSF, SNAP, and SNARE, each representing a small protein family conserved from yeast to humans, has emerged as key player in exocytosis (Malsam et al. 2008; Saraste et al. 2009; Walter et al. 2010). The role of the hexameric ATPase NSF (*N*-ethylmaleimide-sensitive fusion protein) is to put energy into the system. Members of the SNAP (soluble NSF-attachment protein) family appear to function as adaptors between NSF and the third type of protein in the complex, the SNAREs (SNAP receptors). SNARE proteins are found on both the target membrane (t-SNAREs) and the secretory vesicle (v-SNAREs), and are therefore assumed to be the major “targeting” components of the process (Shen et al. 2007; Maximov et al. 2009; Kasai et al. 2012).

In addition to exocytosis, which takes place by targeted fusion of secretory vesicles with the plasma membrane, there exist two additional types of noncanonical secretion: apocrine and holocrine secretion. During these processes, entire portions of the cell are released and homotypic membrane fusion is not required. In the apocrine mechanism, a glandular cell loses a portion of its cytoplasm and is then completely or partially renewed. In the case of holocrine secretion, the material is released into the gland lumen upon cell death and the dissolution of the cellular structure. In contrast to exocytosis, no protein components, factors or genes affecting apocrine and/or holocrine secretion have yet been identified, and thus the mechanisms underlying these processes remain enigmatic. However, finding that apocrine secretion occurs in the *Drosophila* salivary glands, several hours after the exocytosis of Sgs glue is completed, provides a mean to reappraise our understanding of apocrine secretion. Insights made using of this wonderful molecular genetic model organism, provide a glimmer of hope for elucidating the mechanistic aspects of this fundamental, and so far, almost uncharacterized process.

15.3.1 Identification of Apocrine Secretion in the Prepupal SGs

As we described more fully elsewhere (Farkaš et al. 2014, 2015), during the first hours after pupariation and glue expectoration, the salivary gland cells become vacuolized by enormous amounts of endocytosis (Fig. 15.8a). Within 6–7 h after puparium formation (APF), the vacuoles are consolidated by continued endosomal trafficking towards the ER and Golgi (Fig. 15.8b). Surprisingly however, many different types of proteins detectable using specific antibodies, are released into the centrally located gland lumen during the 8th hour of prepupal development, a process that continues for the next ~2 h (Fig. 15.8c). Using a panel of antibodies indicates that there is a differential release of different proteins over time, depending on the phase of the secretion and the type of protein secreted. For example, even though

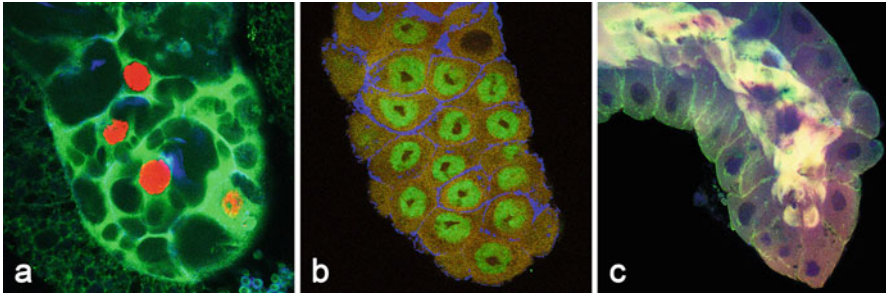


Fig. 15.8 The time course of the major developmental events in the prepupal salivary glands. They are illustrated by staining with antibodies to highlight appropriate structures. **(a)** About +2 h APF, the salivary gland cells become highly vacuolized by membrane recycling due to massive endocytosis, a consequence of exocytosis; BR-C (*red*), p127^{1(2)gl} (*green*) and filamentous actin (*blue*). **(b)** The process of vacuolization and membrane recycling is consolidated by +7 h APF, shortly prior to the next secretion; BR-C (*green*), p127^{1(2)gl} (*red*) and filamentous actin (*blue*). **(c)** At +8 h APF, the salivary glands are showing an early phase of release of myosin II, p127^{1(2)gl} and filamentous actin into the centrally located lumen. *fb* piece of adherent fat body. All confocal images 400 \times . (Reprinted with the permission of the publisher)

non-muscle myosin II and β -tubulin are being released into the lumen during the first hour of the secretory process, there is a strong accumulation of unsecreted filamentous actin at the apical membrane. Similarly, proteins such as cytoplasmic α -catenin and nuclear Smrter, the EcR-coupled transcriptional corepressor, are released almost completely during the first hour of secretion, but the transcription factor BR-C remains localized in nuclei during this time. When the lumen is at its widest during the more advanced phase of the protein extrusion (9th h APF), the lumen becomes filled with ecdysone-regulated transcription factor BR-C while cytosolic Rop is still retained in the cytoplasm. By this time, the nuclear histone deacetylase Rpd3 along with myosin II are both present in the lumen. During the tenth hour APF, any remaining nuclear receptor EcR and the ribosomal protein P21 as well as filamentous actin are all released into lumen. As a consequence of this massive extrusion by the end of the tenth hour APF, the signal of many intracellular proteins, as detected by antibodies, becomes weaker or undetectable. However, at 11 h APF some of the proteins once again can be detected, at least in modest amounts, at their original sites. This indicates either that the entire pool of cell proteinaceous components is not released, or alternatively, that at least some proteins are quickly replaced by new protein synthesis. In summary, this massive protein secretion corresponds with the relocation of measurable fluorescence signal from the salivary gland cells to the extracellular gland lumen.

Since light microscopy found no indication for the involvement of secretory vesicles in this secretion, and there were no fluorescently-detectable increases in Golgi zone areas or other exocytosis-associated activity, transmission electron microscopy (TEM) was used to verify that this massive protein extrusion was not being achieved by exocytosis. Not only did the TEM images of the extrusion pro-

cess in 8–10 h old prepupal glands confirm that proteins are not released by exocytosis during this period, but they also revealed typical attributes of apocrine secretion, which entails the loss of part of the cytoplasm. TEM images revealed also apical protrusions and cytoplasmic fragments inside the lumen of the glands. These cytoplasmic fragments contain various types of electron-dense material, including small pieces of membranes, free ribosomes, mitochondria, endoplasmic reticulum, and a plethora of amorphous structures (Fig. 15.9a–d). At the very earliest phase of apocrine secretion, during the eighth hour APF, the salivary gland cells show prominent and numerous microvilli and their lumen is filled with an “uncertain” whorling membranous-like (Fig. 15.9d) or electron-lucent filament-like material (Fig. 15.9e). Slightly later, while the apical surface of the cells still contains plenty of microvilli, the material inside the lumen becomes electron dense and almost evenly distributed, consisting of many small pieces of the cytoplasm (Fig. 15.9f). At the mid phase of apocrine secretion (9 h APF), microvilli are still present though less abundant, while larger pieces of more electron dense and compacted material start to appear in the lumen (Fig. 15.9g). At the later stages of secretion, the microvilli are almost absent and the luminal material becomes flocculent. It is electron-dense, irregularly scattered in the lumen in the form of larger pieces, some of which clearly contains structured cytoplasmic materials including ER, Golgi or mitochondria, etc. (Fig. 15.9h). Because the process of pinching-off, constriction and decapitation of the stalk of the apical protrusions was not clearly recognizable in 8–10 h prepupal salivary glands using TEM, we assessed this possibility using scanning electron microscopy (SEM). The presence of numerous aposome-like structures on the apical membrane surface of the gland lumen was identified. Some of these aposome-like structures displayed constrictions and features consistent with the decapitation of the stalk of an aposome (Fig. 15.10a, b). Thus, a combination of light, TEM and SEM methods certify that the massive protein secretion in 8–10 h prepupal SGs of *Drosophila* occurs via an apocrine process.

15.3.2 Further Characteristics of Apocrine Secretion in *Drosophila* SGs

Our initial observations indicated that prepupal salivary gland undergoing apocrine secretion release various kinds of proteins, and therefore, a fundamental question rose as to what kind or categories of proteins the glands release and whether the secreted material contains any specific proteins that could help shed light on the process’ physiological significance. To address this question, we used two different approaches to characterize the protein composition of the secretion: immunohistochemical detection at the light microscope level and top-down proteomic identification of components present in the secretion. For the former, a panel of antibodies available in our laboratory or antibodies that were readily available from colleagues was used. We also randomly selected several LacZ- and GFP-protein trap transgenic fly stocks available in *Drosophila* research community, known to be expressed either

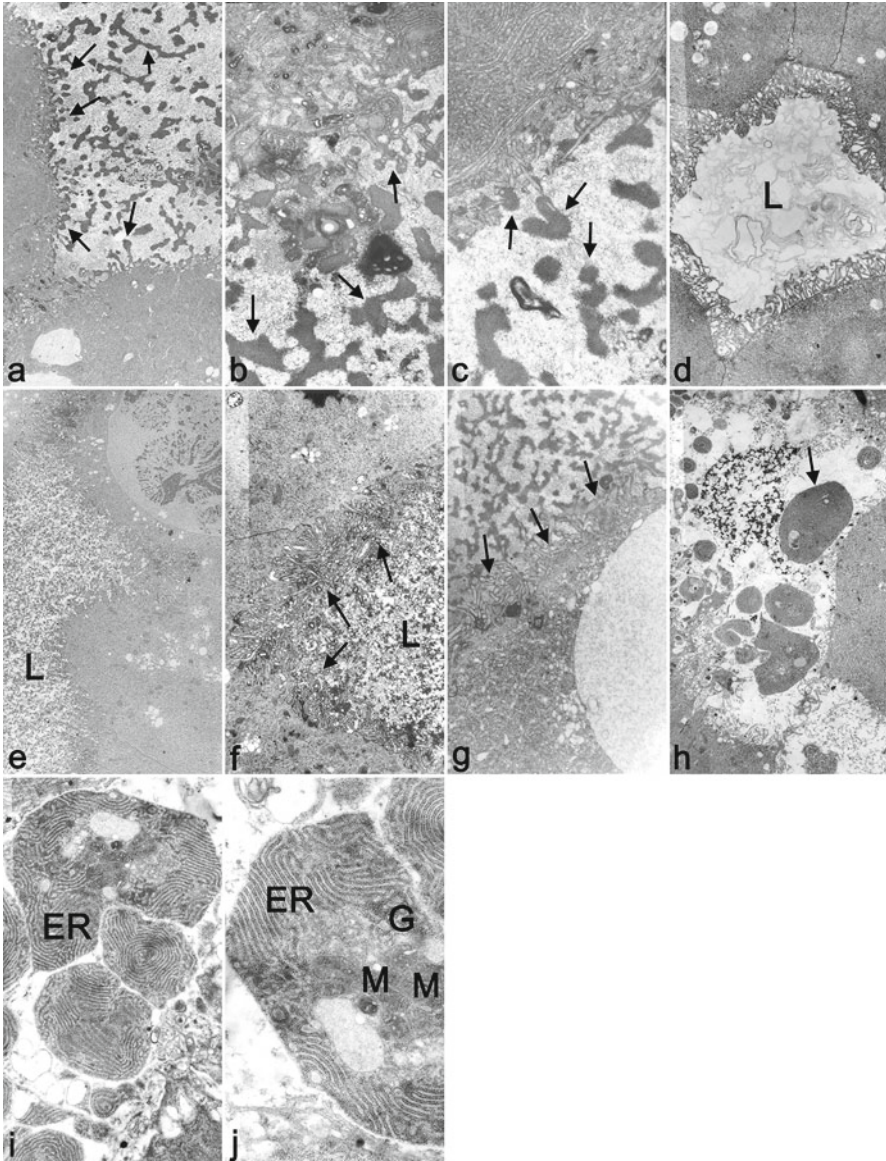


Fig. 15.9 Transmission electron microscopy of an apocrine process in 8–10 h old prepupal SGs. (a) *Prima vista* evidence of apocrine secretion is documented by apical protrusions (*arrows*) and numerous cytoplasmic fragments (*arrowheads*) inside the lumen of the salivary glands from a +9 h APF animal; 2700 \times . Higher magnification views (**b** and **c**) of the apocrine process showing details of electron-dense material (*arrows*) released from the apical surface (*arrowheads*) of 9-h old prepupal SG cells; 8000 \times and 10,000 \times , respectively. However, at the very early phases of apocrine secretion, +8 h APF, the SG cells show prominent and numerous microvilli (*m*) and the lumen is filled with “uncertain” whorled membraneous-like (*arrows*) (**d**) or electron-translucent filament-like material (**e**); both 2700 \times . Slightly later (+8.5 h APF), the apical surface of the cells still contains

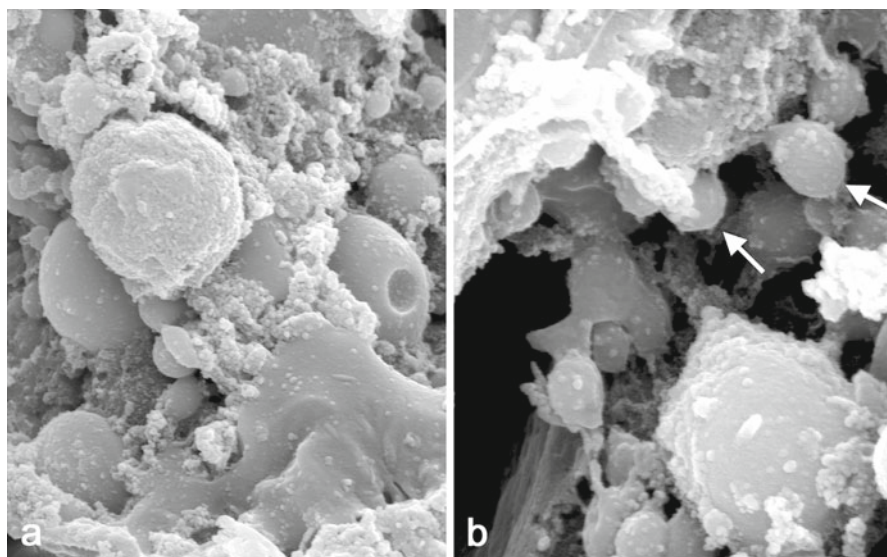


Fig. 15.10 Scanning electron micrographs of the apocrine process in the 9 h old prepupal SG. The gland, dissected under the stereomicroscope and having a lumen evidently filled with material, was fixed and processed to critical point drying, after which it was broken up to expose the inferior portion that included the luminal surface, and then sputter coated. The image reveals (a) numerous aposome-like spheres (*arrows*) and various material-bearing structures on the surface of apical membrane (10,000 \times). In addition, at higher magnification (b), some of these spheroid structures (*arrows*) displayed constrictions and show a decapitation of the aposome's stalk (*arrowheads*) (20,000 \times). (Reprinted with the permission of the publisher)

ubiquitously or strongly in the salivary glands, and assessed whether LacZ or GFP signal was present in the SG lumen of 8–10 h old prepupae. For the proteomic analysis, multiple samples each containing the secretion released into the lumen of prepupal glands from several hundreds gland pairs were collected. The pooled samples, whether separated by 1-dimensional electrophoresis or not, were reduced, alkylated, trypsin-digested, chromatographically separated and their proteins identified by MALDI-TOF/TOF or ESI-MS/MS mass spectrometry. The initial analysis by this approach identified 279 proteins (Farkaš et al. 2014). By pursuing this proteomic



Fig. 15.9 (continued) numerous microvilli (*m*), but the material inside the lumen becomes electron dense and almost evenly distributed (*arrows*), consisting of many small pieces (f); 4000 \times . At the mid-phase of apocrine secretion (+9 h APF), microvilli (*m*) are less abundant (*arrows*), and larger pieces and more electron dense material (*arrowheads*) start to appear in the lumen (g); 6700 \times . At later stages of apocrine secretion (+10 h APF), the microvilli are absent and the luminal material becomes flocculent; it stays electron-dense, and larger pieces of material (*arrows*) are irregularly scattered in the lumen. Some of these clearly contain structured material of the cytoplasm including ER, Golgi (*G*), mitochondria (*M*) or multivesiculated elements (*MVE*) (h, i, j); 2700 \times , 8000 \times and 14,000 \times , respectively. *L* in all images means lumen. (Reprinted with the permission of the publisher)

approach we found over 1000 proteins in the secretion from all sorts of categories including cytoskeletal proteins, cytoplasmic/cytosolic proteins, signaling molecules, membrane components, ER, mitochondria, Golgi and other organellar proteins, nuclear or chromosomal proteins including transcription factors and chromatin remodeling proteins, and even nucleolar proteins (Farkaš et al. 2014). Their ontological distribution shows that they include 41.2 % cytosolic proteins, 11.2 % ER chaperones + Golgi proteins, 6.9 % mitochondrial proteins, 15.9 % membrane proteins, and 11.6 % chromosomal, nucleolar and RNA/DNA binding/editing/modifying proteins (Fig. 15.11a). They also reflect a very wide range of biological processes: 11.7 % are transport and secretory proteins, 17 % are cytoskeletal proteins, 8.3 % are involved in signaling, 25.2 % are involved in basal metabolism, 7.3 % are nuclear proteins and transcription factors, 12.6 % are involved in protein synthesis and modification, 2.9 % are involved in storage, and 6.3 % have unknown functions (Fig. 15.11b). In addition, they also represent many cellular/molecular functions: *e.g.* enzymes 38 %, proteins associated with development 12 %, DNA and RNA binding proteins 10 %, cytoskeletal proteins 9 %, transport proteins 8 % *etc.* (Fig. 15.11c). Thus, the apocrine secretion is not selective for different protein categories.

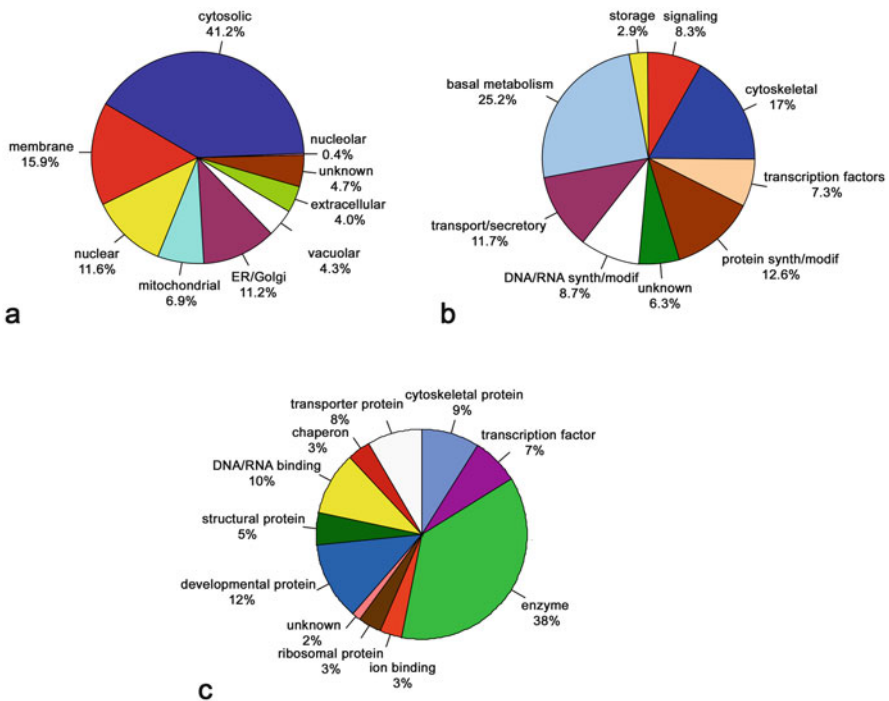


Fig. 15.11 Ontological classification of proteins released via apocrine secretion. The proteins were detected by a combination of immunohistochemistry, GFP-/EYFP-/RFP-fusions fluorescence, chromogenic staining of LacZ-insertions and mass spectrometry. The pies show (a) categories of proteins according to subcellular localization, (b) distribution by biological process, and (c) distribution by cellular/molecular function. (Reprinted with the permission of the publisher)

Nonetheless, our finding that some proteins in the *Drosophila* salivary glands are released by apocrine secretion earlier, while other proteins are released later, documents that this is not a random, but rather a highly regulated process. This also opens up a potentially new area for further research. We cannot unambiguously infer what categorical features of proteins determine their earlier versus later release. From an ultrastructural perspective, the early phases of secretion seem to be associated with the extrusion of more soluble proteins, whereas larger pieces of cytoplasm, which are harder to solubilize, are released at later stages. However, even at very early phases we documented release of larger pieces of the cytoplasm. Most likely, it is easier to detect the occurrence of such “less soluble” material at later stages because the released materials are being accumulated in the lumen over a secretory phase that lasts 2 h, which increases the chances for the detection of larger pieces (Farkaš et al. 2014). When we investigated the order of protein secretion during this two-hour time window using antibody staining, we found that it was highly reproducible in its regularity. To shed more light on the molecular mechanism that controls this gradual release of proteins, it will be helpful to identify the time-course of the secretion of individual proteins, using both microscopical as well as mass spectrometric approaches.

The temporal profile of the cytoplasmic accumulation of glue-containing granules, described above, demonstrates that the larval salivary glands are chiefly involved in the production and secretion of Sgs-glue. However, the typical exocytotic secretion that accomplishes this function is temporarily separated from the later apocrine secretion in the *Drosophila* salivary glands by a 14–16 h period. Although this interval may appear to be a relatively short time in the vertebrate world, it is a period of rapid and dramatic change in this insect. In response to a metamorphic pulse of ecdysterone, the relatively mobile and actively feeding larva stops feeding, enters a short wandering stage, become motionless, pupariates and then enters the early pupal stage where larval tissues initiate programmed histolysis and imaginal discs initiate metamorphosis. In this short interval, the larva undergoes dramatic morphogenetic changes that are associated with numerous and complex biochemical and cellular events. Therefore, the 14–16 h period between exocytosis and apocrine secretion can be considered as a substantial time interval. It is significant that the very same cells exercise these two apparently separate and independent processes. To answer the question of whether these two processes are truly separate and independent, the immense potential of *Drosophila* model system can be used for molecular genetic dissection of exocytosis vs. the apocrine secretion.

15.3.3 Postapocrine Fate of *Drosophila* SGs

As mentioned above, the apocrine secretion in the prepupal salivary glands takes place just a few hours prior to programmed cell death (PCD). Therefore, it was logical to ask whether the material released from the cells 4–6 h prior to their histolysis is already degraded, as this would link apocrine secretion with their temporally

close senescence. To address this issue, secretory material from 8–10 h old prepupal salivary glands was isolated, proteins extracted, and probed by western blotting with selected antibodies. The tested antigens (Rab11 membrane component, BR-C transcription factor, tumor suppressor protein p127, myosin II, Rop, β -tubulin, EcR, Scrib, Arm and several other proteins) remained as intact and undegraded in the prepupal secretion when compared to the total protein extracted from the late larval salivary glands when probed by western blotting (Farkaš et al. 2014). Thus, the proteins and associated complexes released by apocrine secretion are intact, and most probably also fully functional.

This raises yet another question with regard to the programmed cell death. Are salivary gland cells that are losing the majority of their cellular protein components able to retain basic vital functions? We experimentally documented that glands in the final phases of protein extrusion (+10 h APF), as well as glands several hours older (12–14 h APF) still incorporate radioactively labeled uridine ($[^{14}\text{C}]$ -uridine or $[^3\text{H}]$ -uridine) and amino acids ($[^{35}\text{S}]$ -methionine or $[^3\text{H}]$ -leucine) into newly synthesized RNA and proteins, respectively. Furthermore, the pattern of proteins synthesized is not static, but changes as the glands continue to age. These prepupal salivary glands also have viable cells as assessed by a dye exclusion test with trypan blue. Thus, even at time points past the massive, noncanonical apocrine secretion, these glands have cells that are fully alive and continue to maintain a pattern of transcriptional and protein synthetic activities (Farkaš et al. 2014). Indeed, this fits precisely with our understanding of the well-defined puffing pattern of salivary gland polytene chromosomes during this developmental period (Ashburner 1970, 1972; Richards 1976a, b; Ashburner and Berendes 1978). Therefore, this secretory cycle appears to be one of the vital and programmed functions of salivary gland prepupal development and appears to not be associated with PCD.

Interestingly, many of the proteins identified in our initial top-down proteomic analysis or immunodetected microscopically are encoded by genes recovered by Maybeck and Röper (2009) in their targeted gain-of-function screen for embryonic salivary gland morphogens. These include genes such as *chic*, *egl*, *btsz*, *Arp87C*, and others, and according to the modENCODE project and FlyAtlas tissue expression data (Chintapalli et al. 2007; Graveley et al. 2011; Robinson et al. 2013), such genes are known to be moderately to highly expressed in salivary glands. This indicates that these genes, which are important for the embryonic morphogenesis of this tissue remain active and are highly or increasingly expressed throughout the life of the gland, and so may be essential or vital for maintaining this organ's identity, structure or function until the realization of cell death. On the other hand, several polypeptides detected by mass spectrometry, such as transferrin, and the larval serum proteins (yolk proteins) are almost surely not endogenous products of salivary glands, but exemplary representatives of haemolymph or fat body proteins. This strongly indicates that these are transsudated, similar to previously observed transsudated proteins *e.g.* albumin in mammalian tears (Ng et al. 2000; Grus et al. 2005; Zhou et al. 2009; Versura et al. 2010). And indeed, we recently described that there is tremendous endocytosis and vacuolation in the early-to-mid prepupal salivary glands of *Drosophila*. This appears to be associated with complex endo-

somal trafficking that is able to bring in various cargoes from the circulating haemolymph. After consolidation of the numerous vacuoles with the salivary gland's ER and Golgi systems, these would easily be recruited into the apocrine pathway few hours later (Farkaš et al. 2015).

In this context, it should be also emphasized that we were unable to detect any low-molecular weight degradation products, even on overexposed X-ray films from western blots. As we detected only undegraded proteins in the released material by western blotting as well as morphologically “perfect” pieces of cellular structures in the lumen by electron microscopy, it implies that the apocrine secretion process is a real secretory activity with a different functional significance (Farkaš et al. 2014). Therefore, it can be concluded that apocrine secretion is a selective process; only undegraded proteins are released whereas those targeted for proteasomal degradation are retained in cells. This is a novel and important attribute of *Drosophila* apocrine secretion.

All the observations showed that only proteins, and not nuclear DNA, are released during apocrine secretion. To verify this result for all cells in the entire gland, which is composed of columnar, transitional and corpuscular cells, we detected DNA with Hoechst 33258 and various proteins with antibodies at 8, 9 and 10 h after pupariation. These experiments confirmed that during all of the three time points when various proteins are unambiguously secreted, nuclear DNA remains intact in all of the cells of the gland. This appears as one of the major hallmarks of the apocrine process (Farkaš et al. 2014; Farkaš 2015). The major outstanding question is what physiological purpose is served by the apocrine secretion in the prepupal glands, and also, whether it occurs in other *Drosophila* species or cyclorrhaphous dipterans.

15.3.4 Major Conclusions from Apocrine Secretion in the Drosophila SGs and Their Relevance to Vertebrates

Its identification in the prepupal SGs of *Drosophila* suggests that we should consider this type of a cell externalization mechanism in a wider context. Though it is a rarely investigated process, studying apocrine secretion has a very long history. The first identified paper on an apocrine secretory organ is that of Harder (1694) who described a special lachrymal gland in rodents. Then Purkyně (also known as Purkinje) (1833a, b) discovered the human sweat gland, currently the most intensely studied apocrine organ, which was then described in detail by his pupil Wendt (1833, 1834). Almost simultaneously, their findings were confirmed and extended by Breschet and Roussel de Vouzeme (1834), and by Gurlt (1835). The axillary armpit glands, which contain the highest known concentration of apocrine sweat glands in the human skin, were first recognized by Horner (1846). Independently, Velpeau (1839) and later Verneuil (1854) described a chronic acneiform infection of

the cutaneous sweat (apocrine) glands that later was named hidradenitis suppurativa (HS) (Richter 1932; Brunsting 1939; Lasko et al. 2008; Blok et al. 2013). This identifies a specific medical problem closely associated with the apocrine process. Talke (1903) then described the presence of two types of glandular cells, clear cells and dark cells, in the human sweat apocrine gland. Mislawsky (1909) suggested that these are transitional to each other and are fundamentally of the same cell type. Today investigators studying sweat glands believe that the glandular secretory cells of the apocrine sweat glands are only of one type, being different from those of the eccrine sweat glands.

Ranvier (1879) was the first to distinguish “holocrine” secretion in the sebaceous gland from “eccrine/merocrine” secretion in the sweat glands. But it was not until (1917) and (1921) when Schiefferdecker, based on Ranvier’s observations, suggested that the sweat gland cells be classified functionally according to how they secreted their contents, by an eccrine/merocrine, apocrine or holocrine mechanism. This contribution provided a conceptual breakthrough. It established a clear functional definition of three substantially different categories of secretion based on the mechanism underlying the externalization of cellular materials (Fig. 15.12). Since

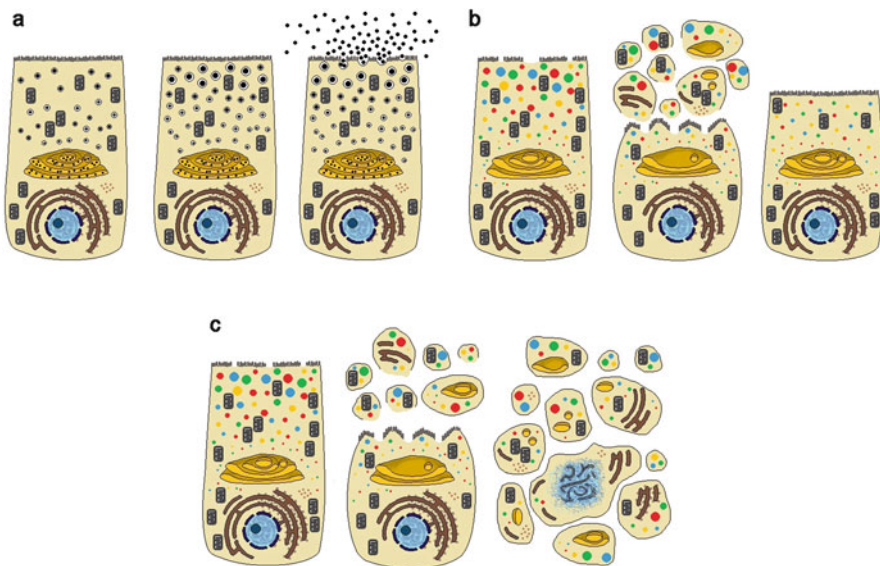


Fig. 15.12 Schematic illustration of the three major secretory mechanisms. (a) exocytosis (merocrine secretion) involves homotypic membrane fusion between vesicles and the cell membrane, thus allowing for only the externalization of the cargo present inside the secretory granules. (b) Apocrine secretion occurs by discharging a portion of the cell when intracellular components are freed into a lumen through the shedding of whole pieces of the cytoplasm. After release, the cytoplasm is reconstituted and a new cycle of secretion may occur. (c) Holocrine secretion means “complete secretion” of the cell’s entire contents and occurs when the cell becomes completely dissolved. All of its compartments, including the nucleus, can serve as secretory products. The cell never recuperates. (Reprinted with the permission of the publisher)

that time, apocrine secretion has been confirmed and studied by many authors (Herzenberg 1927; Richter and Schmidt 1934; Kuno 1938; Kato and Minamitani 1941; Iwashige 1951; Hibbs 1962; Schaumburg-Lever and Lever 1975).

In spite of the literature that accumulated over time, the mechanism and purpose of the apocrine secretion remains enigmatic. So, our puzzlement of its function in the dying SGs highlights a general lack of understanding. One of the reasons is the lack of suitable model organism or model tissue, as well as not having a set of clearly defined characteristics of the process, which currently stems from many controversial and incomplete observations made in various animals and human samples. The careful analysis of the apocrine process in *Drosophila* SGs has opened the door to comprehensive and synthetic comparison of many previous studies. Unfortunately, these often have misleading conclusions when compared to the current data that helped us to draw an elementary outline of the apocrine secretion process. First of all, observations in *Drosophila* clearly establish that apocrine secretion is a non-canonical and non-vesicular transport and secretory mechanism. It has been observed or unambiguously described in sweat glands, mammary glands, lacrimal tear glands as well as in many other tissues including the cerumenal glands, epididymis, and many others (Kawabata and Kurosumi 1976; Kurosumi and Kawabata 1977; Agnew et al. 1980; Gudeman et al. 1989; Morales and Cavicchia 1991; Paulsen 2003; Farkaš 2015). Though some of the glands (notably the pituitary and parathyroid glands) (Ream and Principato 1981; Schwarz et al. 1988) are typical endocrine glands, all of the other secretory organs are exocrine glands, many of which serve as barrier epithelia, just as do the *Drosophila* SGs. Therefore, in the majority of cases, apocrine secretion may serve a means to interface communication with the external environment.

It is very interesting that the *Drosophila* salivary gland cells have the capability to secrete jellyfish GFP- or bacterial lacZ-fusion proteins as well as lacZ-nonfusion reporters. This indicates that heterologous proteins can be recruited to the apocrine secretory machinery/pathway (Farkaš et al. 2014). This evokes the question of what mechanism is used to label and/or recruit proteins into the apocrine trafficking pathway? We can speculate about what potential complex posttranslational modification(s) would be able to recruit such a massive and diverse amount of varied proteins. However, there is also one additional and unexpected possibility we raise as a question: if the apocrine machinery is capable of recruiting such divergent categories of proteins from all cellular compartments and organelles, and such an enormous population of these proteins can be released, would it not be wise for a cell to coopt or invent an energetically less expensive summoning system? Using such a system would enable cells to devote much less effort towards labeling and modification if they marked the relatively fewer number of proteins that should be retained, and not mark those to be recruited for apocrine secretion. If this is the case, it opens research vistas towards a novel selection mechanism.

In contrast to previously published views, apocrine secretion is characterized by a massive protein release, rather than just devoted to the secretion of oily substances. Our current, albeit preliminary proteomic analyses of the apocrine secretory material, revealed that it is a very complex mixture consisting of hundreds or even

thousands proteins from different subcellular locations with highly variable functions. The ontological distribution of these protein categories strongly resembles that of various organellar proteomes (Farkaš et al. 2014). Making use of recent advances in mass spectrometry and improved peptidome prefractionation, in-depth proteomic analyses of human body fluids, although without any special attention to apocrine secretion, were documented in the last 3–4 years. Interestingly and fortunately, some of them have provided insights into the proteomic composition of milk, sweat, tears, cerumen, saliva, etc. (Bandhakavi et al. 2009; Gao et al. 2012; Raiszadeh et al. 2012; Zhou et al. 2012; Feig et al. 2013), all of which are produced by apocrine organs. In accordance with the expectations and conclusions on apocrine secretion from the larval *Drosophila* salivary glands, these fluids are also remarkably complex. Though none of the currently available proteomes can be considered definitive, they can be organized into mutually comparable ontological categories. This comparison revealed that the distribution of categories between various proteomes is quite similar (Fig. 15.13). Among these human fluid pro-

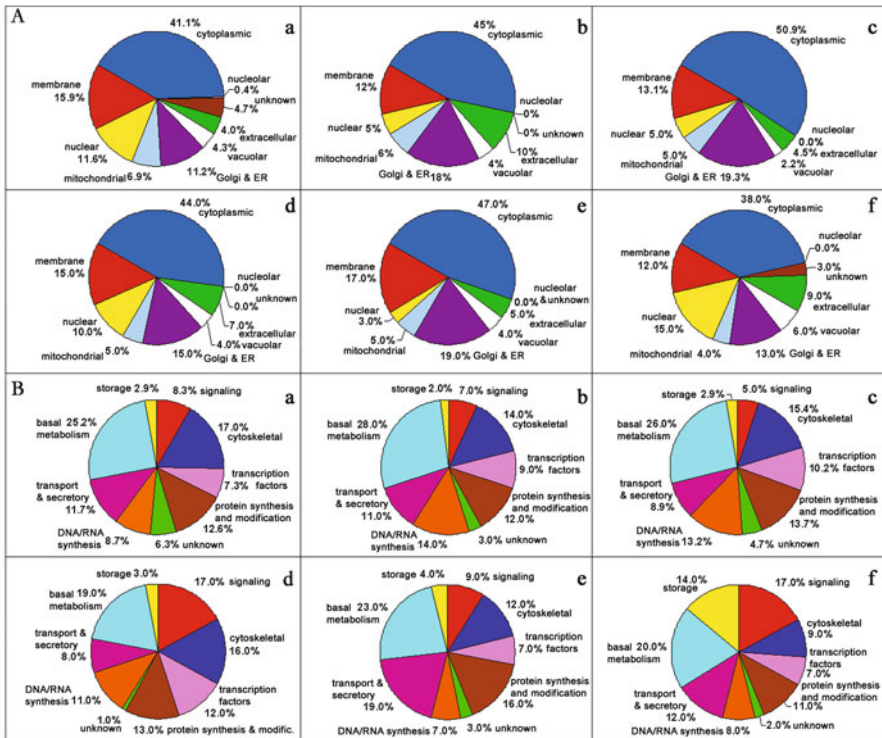


Fig. 15.13 Mass spectrometry analysis of the apocrine secretions. It contains a strikingly similar overall distribution of major ontological categories of proteins (A=subcellular localization, B=biological process). Secretions isolated from (a) *Drosophila* salivary glands; (b) human tears; (c) human sweat; (d) human cerumens; (e) human milk; (f) human bronchoalveolar fluid. (Reprinted with the permission of the publisher)

teomes, all of the same categories seen in the apocrine secretion from *Drosophila* SGs seem to be represented. This suggests that there must be a common purpose and function of apocrine secretion even among evolutionary distant metazoan groups, and that this could evolve from a common, fundamentally advantageous, ancestral trait. Comparison of five most complex proteomes identified to date (sweat, tears, cerumen, saliva and milk) reveal more than 300 shared entries. Put simply, between 30 and 65 % of apocrine fluids contain identical proteins regardless of their anatomical origin (Farkaš 2015).

Merocrine exocytosis appears to be common to all eukaryotic cells from microbial yeasts to humans (Alberts et al. 2007; Lodish et al. 2012), while apocrine secretion is observed only in cells organized into tissues or organs; it is not found in individual cells. As such, apocrine secretion represents one of the few mechanisms that demarcate an evolutionary signature which uniquely characterizes metazoan eukaryotes. As already mentioned, as a very important feature of metazoan eukaryotes, apocrine secretion should have evolved quite early during or just after the Cambrian radiation, probably not later than during the Devonian period. With a period of 470–500 MYA (Hedges and Kumar 2009), the identification of genes that control apocrine secretion would significantly contribute to our understanding of molecular determinants that comprise a metazoan signature.

Apocrine secretion serves a fundamentally different purpose than other types of secretion. Furthermore, exocytosis can release only soluble proteins, solubilized inside of vesicle and bound on a cargo receptor (Machado et al. 2010). In contrast, apocrine secretion can release any kind of protein including polypeptides that would be insoluble in canonical vesicles. From an energetic perspective, it is a quite efficient mechanism. It saves the energy that would have been required to pack individual proteins into a vesicle and make them soluble for vesicular release. In fact, during apocrine discharge, the majority of secreted proteins inside gland's lumen appear to be in their *in situ* location within their original subcellular compartments, which maintains them as both soluble and functional.

15.3.5 *Distinguishing Molecular, Cellular and Evolutionary Attributes of Apocrine Secretion*

The finding and comprehensive analysis of apocrine secretion in the *Drosophila* salivary glands (Farkaš et al. 2014) combined with a careful comparison of many historical and recent data in vertebrate models (Farkaš 2015), has made it clear that apocrine secretion has several specific characteristics and features that distinguish it from canonical exocytosis. (1) Apocrine secretion is non-canonical and non-vesicular trafficking and secretory pathway present exclusively in multicellular organisms. (2) It represents the *en masse* secretion of cellular components. (3) Apocrine secretion releases a secretory material that is a highly complex proteinaceous mixture with organellar components from all cellular compartments

including the nucleus and nucleolus - the nuclear DNA, however, itself remains intact. (4) This secretory process is tightly regulated and selective, as some proteins or components are always released earlier than others. (5) Phylogenetic comparison reveals that anatomically divergent apocrine glands secrete very similar components with a conserved ontological distribution, with different secretions sharing 30–65 % of their proteins in common. (6) The apocrine secretion is an attribute restricted to metazoan, organized and polarized epithelial tissues or glands and is not observed in unicellular organisms or individual cells. (7) Even after a massive apocrine secretion, the released cellular components are renewed in the secretory cell by continued transcription and protein synthesis.

15.4 Conclusions

The *Drosophila* larval SGs have two major excretory functions that have been unambiguously documented. The first is the production and secretion of Sgs glue proteins at the very end of larval development and their expectoration during pupariation. The second is associated with the production and release of a highly complex proteinaceous mixture at the end of prepupal period. This is accomplished by apocrine secretion. Thus, the first large secretory activity is associated with the widely-known and well-described classical ER-Golgi-linked vesicular secretory machinery and results in the exocytosis of targeted proteins, whereas the second secretory activity is associated with a much less understood non-canonical and non-vesicular apocrine secretion. A comparison of the secretory material and its properties between exocytotic Sgs proteins and apocrine secretion reveals unexpected capabilities of this organ – it can reprogram its function to achieve two distinctly different roles. In contrast to exocytosis which releases and delivers a single product or a very small group of proteins or peptides, apocrine secretion serves to deliver hundreds or thousands of membranous, cytoskeletal, cytosolic, microsomal, mitochondrial, ribosomal, Golgi, and even nuclear as well as nucleolar proteins across the interface with the external environment. Moreover, an in-depth proteomic analysis of apocrine secretion from the *Drosophila* SGs and comparison with secretory materials from human apocrine glands has shown that all major ontological groups of proteins and their mutual distribution, either categorized by their subcellular location or biological/molecular function, remains highly conserved among evolutionary distant apocrine glands.

Acknowledgements I appreciate the comments, critical reading of the manuscript and many helpful suggestions by Bruce A. Chase. The author also would like to thank Denisa Beňová-Liszeková, Milan Beňo, Ludmila Pečeňová, Lucia Mentelová, Magda Bardáčová and other members of the lab and close colleagues for help and continuous support during preparation of this manuscript. *Drosophila* Bloomington Stock Center, Indiana University and the Developmental Studies Hybridoma Bank, University of Iowa are acknowledged for making fly stocks and antibodies available to us during many previous years. This work was supported by an APVT-51-027402,

a VEGA 2/0170/10, 2/0109/13 grants, a MVTS-32060600/EC-INSTRUCT-FP7-211252 grant, and EEA-Norwegian FM SK-0086 grant to R.F.

References

- Abrams EW, Vining MS, Andrew DJ (2003) Constructing an organ: the *Drosophila* salivary gland as a model for tube formation. *Trends Cell Biol* 13:247–254
- Adams MD, Celniker SE, Holt RA, Evans CA, Gocayne JD, Amanatides PG, Scherer SE, Li PW, Hoskins RA, Galle RF, George RA, Lewis SE, Richards S, Ashburner M, Henderson SN, Sutton GG, Wortman JR, Yandell MD, Zhang Q, Chen LX, Brandon RC, Rogers YH, Blazej RG, Champe M, Pfeiffer BD, Wan KH, Doyle C, Baxter EG, Helt G, Nelson CR, Gabor GL, Abril JF, Agbayani A, An HJ, Andrews-Pfannkoch C, Baldwin D, Ballew RM, Basu A, Baxendale J, Bayraktaroglu L, Beasley EM, Beeson KY, Benos PV, Berman BP, Bhandari D, Bolshakov S, Borkova D, Botchan MR, Bouck J, Brokstein P, Brottier P, Burtis KC, Busam DA, Butler H, Cadieu E, Center A, Chandra I, Cherry JM, Cawley S, Dahlke C, Davenport LB, Davies P, de Pablos B, Delcher A, Deng Z, Mays AD, Dew I, Dietz SM, Dodson K, Doup LE, Downes M, Dugan-Rocha S, Dunkov BC, Dunn P, Durbin KJ, Evangelista CC, Ferraz C, Ferriera S, Fleischmann W, Fosler C, Gabrielian AE, Garg NS, Gelbart WM, Glasser K, Glodek A, Gong F, Gorrell JH, Gu Z, Guan P, Harris M, Harris NL, Harvey D, Heiman TJ, Hernandez JR, Houck J, Hostin D, Houston KA, Howland TJ, Wei MH, Ibegwam C, Jalali M, Kalush F, Karpen GH, Ke Z, Kennison JA, Ketchum KA, Kimmel BE, Kodira CD, Kraft C, Kravitz S, Kulp D, Lai Z, Lasko P, Lei Y, Levitsky AA, Li J, Li Z, Liang Y, Lin X, Liu X, Mattei B, McIntosh TC, McLeod MP, McPherson D, Merkulov G, Milshina NV, Mobarry C, Morris J, Moshrefi A, Mount SM, Moy M, Murphy B, Murphy L, Muzny DM, Nelson DL, Nelson DR, Nelson KA, Nixon K, Nusskern DR, Pacleb JM, Palazzolo M, Pittman GS, Pan S, Pollard J, Puri V, Reese MG, Reinert K, Remington K, Saunders RD, Scheeler F, Shen H, Shue BC, Sidén-Kiamos I, Simpson M, Skupski MP, Smith T, Spier E, Spradling AC, Stapleton M, Strong R, Sun E, Svirskas R, Tector C, Turner R, Venter E, Wang AH, Wang X, Wang ZY, Wassarman DA, Weinstock GM, Weissenbach J, Williams SM, Worley KC, Woodage T, Wu D, Yang S, Yao QA, Ye J, Yeh RF, Zaveri JS, Zhan M, Zhang G, Zhao Q, Zheng L, Zheng XH, Zhong FN, Zhong W, Zhou X, Zhu S, Zhu X, Smith HO, Gibbs RA, Myers EW, Rubin GM, Venter JC (2000) The genome sequence of *Drosophila melanogaster*. *Science* 287(5461):2185–2195
- Adams MD, Sutton GG, Smith HO, Myers EW, Venter JC (2003) The independence of our genome assemblies. *Proc Natl Acad Sci U S A* 100:3025–3026
- Agnew WF, Yuen TG, Achtyl TR (1980) Ultrastructural observations suggesting apocrine secretion in the choroid plexus: a comparative study. *Neurol Res* 1:313–332
- Alberts B, Johnson A, Lewis J, Raff M, Roberts K, Walter P (2007) *Molecular biology of the cell*, 5th edn. New York, Garland Science
- Andrew DJ, Horner MA, Pettitt MG, Smolik SM, Scott MP (1994) Setting limits on homeotic gene function: restraint of *Sex combs reduced* activity by *teashirt* and other homeotic genes. *EMBO J* 13:1132–1144
- Armbruster K, Luschnig S (2012) The *Drosophila* Sec7 domain guanine nucleotide exchange factor protein Gartenzweig localizes at the cis-Golgi and is essential for epithelial tube expansion. *J Cell Sci* 125:1318–1328
- Ashburner M (1970) Function and structure of polytene chromosomes during insect development. *Adv Insect Physiol* 7:1–95
- Ashburner M (1972) Puffing patterns in *Drosophila melanogaster* and related species. In: Beerman W (ed) *Developmental studies on giant chromosomes*. Springer, Berlin, pp 101–151

- Ashburner M, Berendes HD (1978) Puffing of polytene chromosomes. In: Ashburner M, Wright TRF (eds) *The genetics and biology of Drosophila*, vol 2b. Academic, London, pp 315–395
- Ashburner M, Bonner JJ (1979) The induction of gene activity in *Drosophila* by heat shock. *Cell* 17:241–254
- Ashburner M, Chihara C, Meltzer P, Richards G (1974) Temporal control of puffing activity in polytene chromosomes. *Cold Spring Harb Symp Quant Biol* 38:655–662
- Ashburner M, Golic KG, Hawley RS (2005) *Drosophila: a laboratory handbook*. CSHL Press, New York
- Baehrecke EH (2003) Autophagic programmed cell death in *Drosophila*. *Cell Death Differ* 10:940–945
- Bandhakavi S, Stone MD, Onsongo G, Van Riper SK, Griffin TJ (2009) A dynamic range compression and three-dimensional peptide fractionation analysis platform expands proteome coverage and the diagnostic potential of whole saliva. *J Proteome Res* 8:5590–5600
- Bardwell JCA, Jakob U (2012) Conditional disorder in chaperone action. *Trends Biochem Sci* 37:517–525
- Barker JSF, Starmer WT, MacIntyre RJ (1990) *Ecological and evolutionary genetics of Drosophila*. Springer, New York
- Beckendorf SK, Kafatos FC (1976) Differentiation in the salivary glands of *Drosophila melanogaster*: characterization of the glue proteins and their developmental appearance. *Cell* 9:365–373
- Becker HJ (1959) Die Puffs der Speicheldrüsenchromosomen von *Drosophila melanogaster*. I. Beobachtungen zum Verhalten des Puffmusters im Normalstamm und bei zwei Mutanten, *giant* und *lethal-giant-larvae*. *Chromosoma* 10:654–678
- Beermann W (1952) Chromomerkonstanz und spezifische Modifikation der Chromosomenstruktur in der Entwicklung und Organdifferenzierung von *Chironomus tentans*. *Chromosoma* 5:139–198
- Beermann W (1972) Chromomeres and genes. In: Beermann W (ed) *Developmental studies on giant chromosomes*. Springer, Berlin, pp 1–53
- Berendes HD (1965) Salivary gland function and chromosomal puffing patterns in *Drosophila hydei*. *Chromosoma* 17:35–77
- Berendes HD, Ashburner M (1978) The salivary glands. In: Ashburner M, Wright TRF (eds) *The genetics and biology of Drosophila*, vol 2b. Academic Press, London, pp 453–498
- Berendes HD, Holt TKH (1965) Differentiation of transplanted larval salivary glands of *Drosophila hydei* in adults of the same species. *J Exp Zool* 160:299–317
- Biyasheva A, Do TV, Lu Y, Vaskova M, Andres AJ (2001) Glue secretion in the *Drosophila* salivary gland: a model for steroid-regulated exocytosis. *Dev Biol* 231:234–251
- Blank U (2011) The mechanisms of exocytosis in mast cells. *Adv Exp Med Biol* 716:107–122
- Blok JL, van Hattem S, Jonkman MF, Horváth B (2013) Systemic therapy with immunosuppressive agents and retinoids in hidradenitis suppurativa: a systematic review. *Br J Dermatol* 168:243–252
- Bodenstein D (1950) The postembryonic development of *Drosophila*. In: Demerec K (ed) *Biology of Drosophila*. Wiley, New York, pp 1–35
- Boyd M, Ashburner M (1977) The hormonal control of salivary gland secretion in *Drosophila melanogaster*: studies *in vitro*. *J Insect Physiol* 23:517–523
- Bradley PL, Haberman AS, Andrew DJ (2001) Organ formation in *Drosophila*: specification and morphogenesis of the salivary gland. *Bioessays* 23:901–911
- Breschet G, De Vauzeme R (1834) Recherches anatomiques et physiologiques sur les appareils tegumentaires des animaux. *Ann des Sci Nat*, 2e ser., Zool II: 167–238, 321–370
- Bridges CB (1935) Salivary chromosome maps. *J Hered* 26:60–64
- Bridges CB (1938) A revised map of the salivary gland X-chromosome of *Drosophila melanogaster*. *J Hered* 29:11–13
- Bridges CB (1942) A new map of the salivary 2L chromosome of *Drosophila melanogaster*. *J Hered* 33:403–408
- Bridges CB, Bridges PN (1939) A new map of the second chromosome: a revised map of the right limb of the second chromosome of *Drosophila melanogaster*. *J Hered* 30:475–476

- Brunsting HA (1939) Hidradenitis suppurativa; abscess of apocrine sweat glands – a study of the clinical and pathologic features with a report of twenty-two cases and a review of the literature. *Arch Dermatol Syphilol* 39:108–120
- Burgess J, Jauregui M, Tan J, Rollins J, Lallet S, Leventis PA, Boulianne GL, Chang HC, Le Borgne R, Krämer H, Brill JA (2011) AP-1 and clathrin are essential for secretory granule biogenesis in *Drosophila*. *Mol Biol Cell* 22:2094–2105
- Burgess J, Del Bel LM, Ma CI, Barylko B, Polevoy G, Rollins J, Albanesi JP, Krämer H, Brill JA (2012) Type II phosphatidylinositol 4-kinase regulates trafficking of secretory granule proteins in *Drosophila*. *Development* 139:3040–3050
- Burtis KC, Thummel CS, Jones CW, Karim FD, Hogness DS (1990) The *Drosophila* 74EF early puff contains *E74*, a complex ecdysone-inducible gene that encodes two *ets*-related proteins. *Cell* 61:85–99
- Campos-Ortega JA, Hartenstein V (1997) The embryonic development of *Drosophila melanogaster*, 2nd edn. Springer, Berlin
- Celniker SE, Rubin GM (2003) The *Drosophila melanogaster* genome. *Annu Rev Genomics Hum Genet* 4:89–117
- Chen CN, Malone T, Beckendorf SK, Davis RL (1987) At least two genes reside within a large intron of the *dunce* gene of *Drosophila*. *Nature* 329:721–724
- Chiergatti E, Meldolesi J (2005) Regulated exocytosis: new organelles for non-secretory purposes. *Nat Rev Mol Cell Biol* 6:181–187
- Chintapalli VR, Wang J, Dow JAT (2007) Using FlyAtlas to identify better *Drosophila melanogaster* models of human disease. *Nat Genet* 39:715–720
- Crosby MA, Meyerowitz EM (1986) *Drosophila* glue gene *Sgs3*: sequences required for puffing and transcriptional regulation. *Dev Biol* 118:593–607
- Crowley TE, Meyerowitz EM (1984) Steroid regulation of RNAs transcribed from the *Drosophila* 68C polytene chromosome puff. *Dev Biol* 102:110–121
- Crowley TE, Bond MW, Meyerowitz EM (1983) The structural genes for three *Drosophila* glue proteins reside at a single polytene chromosome puff locus. *Mol Cell Biol* 3:623–634
- Crowley TE, Mathers PH, Meyerowitz EM (1984) A *trans*-acting regulatory product necessary for expression of the *Drosophila melanogaster* 68C glue gene cluster. *Cell* 39:149–156
- Dyson HJ, Wright PE (2005) Intrinsically unstructured proteins and their functions. *Nat Rev Mol Cell Biol* 6:197–208
- Engoer E, Kress H (1980) Glucosamine metabolism in *Drosophila virilis* salivary gland cells: ontogenic changes of enzyme activities and metabolic changes. *Dev Biol* 78:63–75
- Farkaš R (2015) Apocrine secretion: new insights into an old phenomenon. *Biochim Biophys Acta* 1850:1740–1750
- Farkaš R, Mechler BM (2000) The timing of *Drosophila* salivary gland apoptosis displays an *l(2) gl*-dose response. *Cell Death Differ* 7:89–101
- Farkaš R, Sláma K (1999) Effect of bisacylhydrazine ecdysteroid mimics (RH-5849 and RH-5922) on chromosomal puffing, imaginal discs proliferation and pupariation in larvae of *Drosophila melanogaster*. *Insect Biochem Mol Biol* 29:1015–1027
- Farkaš R, Sláma K (2015) Respiratory metabolism of salivary glands during the late larval and prepupal development of *Drosophila melanogaster*. *J Insect Physiol* 81:109–117
- Farkaš R, Šučáková G (1998) The ultrastructural changes of larval and prepupal salivary glands of *Drosophila* cultured *in vitro* with ecdysone. *In Vitro Cell Dev Biol* 34:813–823
- Farkaš R, Šučáková G (1999) Developmental regulation of granule size and numbers in larval salivary glands of *Drosophila* by steroid hormone ecdysone. *Cell Biol Int* 23:671–676
- Farkaš R, Ďatková Z, Mentelová L, Löw P, Beňová-Liszeková D, Beňo M, Sass M, Řehulka P, Řehulková H, Raška O, Kováčik L, Šmígová J, Raška I, Mechler BM (2014) Apocrine secretion in *Drosophila* salivary glands: subcellular origin, dynamics, and identification of secretory proteins. *PLoS One* 9:e94383
- Farkaš R, Beňová-Liszeková D, Mentelová L, Mahmood S, Ďatková Z, Beňo M, Pečeňová L, Raška O, Šmígová J, Chase BA, Raška I, Mechler BM (2015) Vacuole dynamics in the salivary

- glands of *Drosophila melanogaster* during prepupal development. *Dev Growth Differ* 57:74–96
- Feig MA, Hammer E, Völker U, Jehmlich N (2013) In-depth proteomic analysis of the human cerumen—a potential novel diagnostically relevant biofluid. *J Proteomics* 83:119–129
- Fraenkel G (1952) A function of the salivary glands of the larvae of *Drosophila* and other flies. *Biol Bull* 103:285–286
- Fraenkel G, Brookes VJ (1953) The process by which the puparia of many species of flies become fixed to a substrate. *Biol Bull Mar Lab Woods Hole* 105:442–449
- Furia M, D'Avino PP, Digilio FA, Crispi S, Giordano E, Polito LC (1992) Effect of *ecd'* mutation on the expression of genes mapped at the *Drosophila melanogaster* 3C11-12 intermoult puff. *Genet Res* 59:19–26
- Gao X, McMahon RJ, Woo JG, Davidson BS, Morrow AL, Zhang Q (2012) Temporal changes in milk proteomes reveal developing milk functions. *J Proteome Res* 11:3897–3907
- Garfinkel MD, Pruitt RE, Meyerowitz EM (1983) DNA sequences, gene regulation and modular protein evolution in the *Drosophila* 68C glue gene cluster. *J Mol Biol* 168:765–789
- Giangrande A, Mettling C, Richards GP (1987) *Sgs-3* transcript levels are determined by multiple remote sequence elements. *EMBO J* 6:3079–3084
- Giangrande A, Mettling C, Martin M, Ruiz C, Richards GP (1989) *Drosophila Sgs3* TATA: effects of point mutations on expression *in vivo* and protein binding *in vitro* with staged nuclear extracts. *EMBO J* 8:3459–3466
- Gloor RD (1962) Untersuchungen über die Wirkung der Letalfaktoren l 52 und l 8 von *Drosophila melanogaster*. *Revue Suisse Zool* 69:409–463
- Graveley BR, Brooks AN, Carlson JW, Duff MO, Landolin JM, Yang L, Artieri CG, van Baren MJ, Boley N, Booth BW, Brown JB, Cherbas L, Davis CA, Dobin A, Li R, Lin W, Malone JH, Mattiuzzo NR, Miller D, Sturgill D, Tuch BB, Zaleski C, Zhang D, Blanchette M, Dudoit S, Eads B, Green RE, Hammonds A, Jiang L, Kapranov P, Langton L, Perrimon N, Sandler JE, Wan KH, Willingham A, Zhang Y, Zou Y, Andrews J, Bickel PJ, Brenner SE, Brent MR, Cherbas P, Gingeras TR, Hoskins RA, Kaufman TC, Oliver B, Celniker SE (2011) The developmental transcriptome of *Drosophila melanogaster*. *Nature* 471(7339):473–479
- Gregg TG, McCrate A, Reveal G, Hall S, Rypstra AL (1990) Insectivory and social digestion in *Drosophila*. *Biochem Genet* 28:197–207
- Grob H (1952) Entwicklungsphysiologische Untersuchungen an den Speicheldrüsen dem Darmtraktus und den Imaginalscheiben einer Letalrasse (*lgl*) von *Drosophila melanogaster*. *Z Indukt Abstamm- u VererbLehre* 84:320–360
- Grus FH, Podust VN, Bruns K, Lackner K, Fu S, Dalmaso EA, Wirthlin A, Pfeiffer N (2005) SELDI-TOF-MS ProteinChip array profiling of tears from patients with dry eye. *Invest Ophthalmol Vis Sci* 46:863–876
- Gudeman DM, Brightman MW, Merisko EM, Merrill CR (1989) Release from live choroids plexus of apical fragments and electrophoretic characterization of their synthetic products. *J Neurosci Res* 24:184–191
- Guild GM (1984) Molecular analysis of a developmentally regulated gene which is expressed in the larval salivary gland of *Drosophila*. *Dev Biol* 102:462–470
- Guild GM, Shore EM (1984) Larval salivary gland secretion proteins in *Drosophila*. Identification and characterization of the *Sgs-5* structural gene. *J Mol Biol* 179:289–314
- Gunasekaran K, Tsai CJ, Nussinov R (2004) Analysis of ordered and disordered protein complexes reveals structural features discriminating between stable and unstable monomers. *J Mol Biol* 341:1327–1341
- Gurlt EF (1835) Vergleichende Untersuchungen über die Haut des Menschen und der Haus-Säugethiere, besonders in Beziehung auf die Absonderungs-Organen des Haut-Talg und des Schwitzes. *Archiv für Anatomie, Physiologie und wissenschaftliche Medicin*, pp 399–418
- Hadorn E, Faulhaber I (1962) Range of variability in cell number of larval salivaries. *Drosoph Inf Serv* 36:71

- Harder JJ (1694) Glandula nova lachrymalis una cum ductu excretorio in cervis et damis. Acta Eruditorum Lipsiae 43:49–52
- Harrod MJE, Kastriasis CD (1972a) Developmental studies in *Drosophila*. II. Ultrastructural analysis of the salivary glands of *Drosophila pseudoobscura* during some stages of development. J Ultrastruct Res 38:482–499
- Harrod MJE, Kastriasis CD (1972b) Developmental studies in *Drosophila*. VI. Ultrastructural analysis of the salivary glands of *Drosophila pseudoobscura* during the late larval period. J Ultrastruct Res 40:292–312
- Hedges SB, Kumar S (2009) The timetree of life. Oxford University Press, Oxford
- Henderson KD, Andrew DJ (2000) Regulation and function of Scr, exd, and hth in the *Drosophila* salivary gland. Dev Biol 217:362–374
- Herzenberg H (1927) Neue Beiträge zur Lehre von den apokrinen Schweißdrüsen. Virchows Arch Path Anat 266:422–455
- Hibbs RG (1962) Electron microscopy of human apocrine sweat glands. J Invest Dermatol 38:77–84
- Horner WE (1846) Special anatomy and histology, vol 1, 7th edn. Lea and Blanchard Press, Philadelphia
- Hsu WS (1948) The Golgi material and mitochondria in the salivary glands of the larva of *Drosophila melanogaster*. Q J Microsc Sci 89:401–414
- Iwashige K (1951) Beiträge zur Kenntnis der Eisenreaktion bei den apokrinen Schweißdrüsen der Achselhaut von Japanerern. Arch Histol Jap 2:367–374
- Jahn R (2004) Principles of exocytosis and membrane fusion. Ann N Y Acad Sci 1014:170–178
- Japrun D, Dogan J, Freedman KJ, Nadzeyka A, Bauerdick S, Albrecht T, Kim MJ, Jemth P, Edel JB (2013) Single-molecule studies of intrinsically disordered proteins using solid-state nanopores. Anal Chem 85:2449–2456
- Jayaram SA, Senti KA, Tiklová K, Tsarouhas V, Hemphälä J, Samakovlis C (2008) COPI vesicle transport is a common requirement for tube expansion in *Drosophila*. PLoS One 3:e1964
- Jiang C, Baehrecke EH, Thummel CS (1997) Steroid regulated programmed cell death during *Drosophila* metamorphosis. Development 124:4673–4683
- Jiang C, Lamblin A-FJ, Steller H, Thummel CS (2000) A steroid-triggered transcriptional hierarchy controls salivary gland cell death during *Drosophila* metamorphosis. Mol Cell 5:445–455
- Jochova J, Zakeri Z, Lockshin RA (1997) Rearrangement of the tubulin and actin cytoskeleton during programmed cell death in *Drosophila* salivary glands. Cell Death Differ 4:140–149
- Kaminker JS, Bergman CM, Kronmiller B, Carlson J, Svirskas R, Patel S, Frise E, Wheeler DA, Lewis SE, Rubin GM, Ashburner M, Celniker SE (2002) The transposable elements of the *Drosophila melanogaster* euchromatin: a genomics perspective. Genome Biol 3:0084
- Kasai H, Takahashi N, Tokumaru H (2012) Distinct initial SNARE configurations underlying the diversity of exocytosis. Physiol Rev 92:1915–1964
- Kato S, Minamitani K (1941) Kurze Mitteilung über die apokrinen Schweißdrüsen in der Aussenhaut des Nasenflügels bei den Chinesen. Okajimas Folia Anat Jap Bd 20:71–80
- Kawabata I, Kurosumi K (1976) Transmission and scanning electron microscopy of the human ceruminous apocrine gland. II. Myoepithelial cells. Arch Histol Jpn 39:231–255
- Kerman BE, Cheshire AM, Andrew DJ (2006) From fate to function: the *Drosophila* trachea and salivary gland as models for tubulogenesis. Differentiation 74:326–348
- Kodani M (1948) The protein of the salivary gland secretion in *Drosophila*. Proc Natl Acad Sci U S A 34:131–135
- Kolesnikov NN, Zhimulev IF (1975) Synthesis of mucoprotein secretory substance in salivary glands of the *Drosophila melanogaster* 3rd instar larvae. Ontogenез 6:171–182 (in Russian with English summary)
- Korge G (1975) Chromosome puff activity and protein synthesis in larval salivary glands of *Drosophila melanogaster*. Proc Natl Acad Sci U S A 72:4550–4554
- Korge G (1977a) Larval saliva in *Drosophila melanogaster*: production, composition, and relationship to chromosome puffs. Dev Biol 58:339–355

- Korge G (1977b) Direct correlation between a chromosome puff and the synthesis of a larval saliva protein in *Drosophila melanogaster*. *Chromosoma* 62:155–174
- Korge G (1981) Genetic analysis of the larval secretion gene *Sgs-4* and its regulatory chromosome sites in *Drosophila melanogaster*. *Chromosoma* 84:373–390
- Korol A, Rashkovetsky E, Iliadi K, Nevo E (2006) *Drosophila* flies in “Evolution Canyon” as a model for incipient sympatric speciation. *Proc Natl Acad Sci U S A* 103:18184–18189
- Kress H (1979) Ecdysone-induced changes in glycoprotein synthesis and puff activities in *Drosophila virilis* salivary glands. *Chromosoma* 72:53–66
- Kuno Y (1938) Variations in secretory activity of human sweat glands. *Lancet* 231:299–303
- Kurosumi K, Kawabata I (1977) Transmission and scanning electron microscopy of the human ceruminous apocrine gland. *Arch Histol Jpn* 40:203–244
- Lane NJ, Carter YR, Ashburner M (1972) Puffs and salivary gland function: the fine structure of the larval and prepupal salivary glands of *Drosophila melanogaster*. *Wilhelm Roux Arch Entwickl Mechanik Org* 169:216–238
- Lasko LA, Post C, Kathju S (2008) Hidradenitis suppurativa: a disease of apocrine gland physiology. *JAAPA* 21:23–25
- Lefevre G (1976) A photographic representation and interpretation of the polytene chromosomes of *Drosophila melanogaster* salivary glands. In: Ashburner M, Novitski E (eds) *The genetics and biology of Drosophila*, vol 1a. Academic, London, pp 31–66
- Lehmann M (1996) *Drosophila Sgs* genes: stage and tissue specificity of hormone responsiveness. *BioEssays* 18:47–54
- Lehmann M, Korge G (1995) Ecdysone regulation of the *Drosophila Sgs-4* gene is mediated by the synergistic action of ecdysone receptor and SEBP 3. *EMBO J* 14:716–726
- Leshner S (1951a) Studies on the larval salivary gland of *Drosophila*. I. The nucleic acids. *Exp Cell Res* 2:577–585
- Leshner S (1951b) Studies on the larval salivary gland of *Drosophila*. II. Changes in nuclear and nucleolar volumes and their possible significance. *Exp Cell Res* 2:586–588
- Leshner S (1952) Studies on the larval salivary gland of *Drosophila*. III. The histochemical localization and possible significance of ribonucleic acid, alkaline phosphatase and polysaccharide. *Anat Rec* 114:633–652
- Lindsley DL, Grell EH (1968) Genetic variations of *Drosophila melanogaster*. Carnegie Institution publication, no. 627. Carnegie Institution, Washington, DC
- Lindsley DL, Zimm GG (1992) *The genome of Drosophila melanogaster*. Academic, San Diego
- Lodish H, Berk A, Kaiser CA, Krieger M, Bretscher A, Ploegh H, Amon A, Scott MP (2012) *Molecular cell biology*, 7th edn. W. H. Freeman Publishers, San Francisco
- Machado JD, Díaz-Vera J, Domínguez N, Alvarez CM, Pardo MR, Borges R (2010) Chromogranins A and B as regulators of vesicle cargo and exocytosis. *Cell Mol Neurobiol* 30:1181–1187
- Makino S (1938) A morphological study of the nucleus in various kinds of somatic cell of *Drosophila virilis*. *Cytologia* 9:272–282
- Malsam J, Kreye S, Söllner TH (2008) Membrane fusion: SNAREs and regulation. *Cell Mol Life Sci* 65:2814–2832
- Martin DN, Baehrecke EH (2004) Caspases function in autophagic programmed cell death in *Drosophila*. *Development* 131:275–284
- Maximov A, Tang J, Yang X, Pang ZP, Südhof TC (2009) Complexin controls the force transfer from SNARE complexes to membranes in fusion. *Science* 323:516–521
- Maybeck V, Röper K (2009) A targeted gain-of-function screen identifies genes affecting salivary gland morphogenesis/tubulogenesis in *Drosophila*. *Genetics* 181:543–565
- McGuffin LJ, Bryson K, Jones DT (2000) The PSIPRED protein structure prediction server. *Bioinformatics* 16:404–405
- Meyerowitz EM, Hogness DS (1982) Molecular organization of a *Drosophila* puff site that responds to ecdysone. *Cell* 28:165–176
- Meyerowitz EM, Martin CH (1984) Adjacent chromosomal regions can evolve at very different rates: evolution of the *Drosophila* 68C glue gene cluster. *J Mol Evol* 20:251–264

- Mislawsky AN (1909) Zur Lehre von der sogenannten blasenformigen Sekretion. Arch Mikrosk Anat 73:681–698
- Misra S, Crosby MA, Mungall CJ, Matthews BB, Campbell KS, Hradecky P, Huang Y, Kaminker JS, Millburn GH, Prochnik SE, Smith CD, Tupy JL, Whitfield EJ, Bayraktaroglu L, Berman BP, Bettencourt BR, Celniker SE, de Grey AD, Drysdale RA, Harris NL, Richter J, Russo S, Schroeder AJ, Shu SQ, Stapleton M, Yamada C, Ashburner M, Gelbart WM, Rubin GM, Lewis SE (2002) Annotation of the *Drosophila melanogaster* euchromatic genome: a systematic review. Genome Biol 3: RESEARCH0083
- Mittal J, Yoo T, Georgiou G, Truskett T (2013) Structural ensemble of an intrinsically disordered polypeptide. J Phys Chem B 117:118–124
- Morales A, Cavicchia JC (1991) Release of cytoplasmic apical protrusions from principal cells of the cat epididymis, an electron microscopic study. Tissue Cell 23:505–513
- Munro S (2005) The Arf-like GTPase Arl1 and its role in membrane traffic. Biochem Soc Trans 33:601–605
- Muskavitch MA, Hogness DS (1980) Molecular analysis of a gene in a developmentally regulated puff of *Drosophila melanogaster*. Proc Natl Acad Sci U S A 77:7362–7366
- Muskavitch MA, Hogness DS (1982) An expandable gene that encodes a *Drosophila* glue protein is not expressed in variants lacking remote upstream sequences. Cell 29:1041–1051
- Myat MM (2005) Making tubes in the *Drosophila* embryo. Dev Dyn 232:617–632
- Myat MM, Andrew DJ (2002) Epithelial tube morphology is determined by the polarized growth and delivery of apical membrane. Cell 111:879–891
- Ng V, Cho P, To CH (2000) Tear proteins of normal young Hong Kong Chinese. Graefes Arch Clin Exp Ophthalmol 238:738–745
- Niemeyer BA, Schwarz TL (2000) SNAP-24, a *Drosophila* SNAP-25 homologue on granule membranes, is a putative mediator of secretion and granule-granule fusion in salivary glands. J Cell Sci 113:4055–4064
- Painter TS (1933) A new method for the study of chromosome rearrangements and the plotting of chromosome maps. Science 178:585–586
- Painter TS (1934) Salivary chromosomes and the attack on the gene. J Hered 25:464–476
- Painter TS (1945) Nuclear phenomena associated with secretion in certain gland cells with especial reference to the origin of cytoplasmic nucleic acid. J Exp Zool 100:523–544
- Pardue ML, Feramisco J, Lindquist S (1989) Stress induced proteins. In: UCLA symposia on molecular and cellular biology, vol 96. Alan R. Liss, New York
- Parsons PA (1978) Habitat selection and evolutionary strategies in *Drosophila*: an invited address. Behav Genet 8:511–526
- Parsons PA (1981) Habitat selection and speciation in *Drosophila*. In: Atchley WR, Woodruff DS (eds) Evolution and speciation. Essays in honor of MJD White. Cambridge University Press, London, pp 219–240
- Parsons PA (1994) Habitats, stress, and evolutionary rates. J Evol Biol 7:387–397
- Pasteur N, Kastritsis CD (1973) Developmental studies in *Drosophila*. V. Alkaline phosphatases, dehydrogenases, and oxidases in organs and whole fly homogenates during development of *D. pseudoobscura*. Wilhelm Roux Arch Entwickl Mech Org 173:346–354
- Paulsen F (2003) The human nasolacrimal ducts. Adv Anat Embryol Cell Biol 170:1–106
- Pelling C (1966) A replicative and synthetic chromosomal unit – the modern concept of the chromosome. Proc R Soc B 164:279–289
- Pelling C (1970) Puff-RNA in polytene chromosomes. Cold Spring Harb Symp Quant Biol 35:521–531
- Pfeiffer BD, Ngo TT, Hibbard KL, Murphy C, Jenett A, Truman JW, Rubin GM (2010) Refinement of tools for targeted gene expression in *Drosophila*. Genetics 186:735–755
- Poels CLM (1970) Time sequence in the expression of various developmental characters induced by ecdysterone in *Drosophila hydei*. Dev Biol 23:210–225
- Poels CLM, De Loof A, Berendes H (1971) Functional and structural changes in *Drosophila* salivary gland cells triggered by ecdysterone. J Insect Physiol 17:1717–1729

- Porat-Shliom N, Milberg O, Masedunskas A, Weigert R (2013) Multiple roles for the actin cytoskeleton during regulated exocytosis. *Cell Mol Life Sci* 70:2099–2121
- Poulson DF (1937) Chromosomal deficiencies and the embryonic development of *Drosophila melanogaster*. *Proc Natl Acad Sci U S A* 23:133–137
- Poulson DF (1950) Histogenesis, organogenesis and differentiation in the embryo of *Drosophila melanogaster* Meigen. In: Demerec M (ed) *Biology of Drosophila*. Wiley, New York, pp 168–274
- Purkinje JE (1833a) Beobachtungen der spiralen Schweisscanäle der menschlichen Epidermis. *Amtl Bericht über die Vers deutscher Naturf u Ärzte zu Breslau* 11:59
- Purkinje JE (1833b) Beobachtungen der spiralen Schweisscanäle der menschlichen Epidermis. *Notizen aus dem Gebiete der Natur- und Heilkunde (Froriep) Weimar* 38:152
- Raiszadeh MM, Ross MM, Russo PS, Schaepper MA, Zhou W, Deng J, Ng D, Dickson A, Dickson C, Strom M, Osorio C, Soeprono T, Wulfkuhle JD, Petricoin EF, Liotta LA, Kirsch WM (2012) Proteomic analysis of eccrine sweat: implications for the discovery of schizophrenia biomarker proteins. *J Proteome Res* 11:2127–2139
- Ranvier L (1879) Sur la structure des glandes sudoripares. *Compt Rend Acad Séanc Acad Sci (Paris)* 89:1120–1123
- Ream LJ, Principato R (1981) Ultrastructural observations on the mechanism of secretion in the rat parathyroid after fluoride ingestion. *Cell Tissue Res* 214:569–573
- Richards GP (1976a) The control of prepupal puffing patterns *in vitro*: implications for prepupal ecdysone titres in *Drosophila melanogaster*. *Dev Biol* 48:191–195
- Richards GP (1976b) Sequential gene activation by ecdysone in polytene chromosomes of *Drosophila melanogaster*. IV. The mid prepupal period. *Dev Biol* 54:256–263
- Richards G (1981) The radioimmune assay of ecdysteroid titres in *Drosophila melanogaster*. *Mol Cell Endocrinol* 21:181–197
- Richter W (1932) Beiträge zur normalen und pathologischen Anatomie der apokrinen Hautdrüsen des Menschen mit besonderer Berücksichtigung des Achselhöhlenorgans. *Virchows Arch Pathol Anat Physiol Klin Med* 287:277–296
- Richter W, Schmidt W (1934) Über das Vorkommen apokriner Drüsen in der Haut des Nasenflügels. *Z mikr anat Forsch* 35:529–532
- Ritossa FM (1962) A new puffing pattern induced by temperature shock and DNP in *Drosophila*. *Experientia* 18:571–573
- Ritossa FM (1963) New puffs induced by temperature shock, DNP and salicylate in salivary chromosomes of *D. melanogaster*. *Drosoph Inf Serv* 37:122–123
- Robinson SW, Herzyk P, Dow JAT, Leader DP (2013) FlyAtlas: database of gene expression in the tissues of *Drosophila melanogaster*. *Nucleic Acids Res* 41(Database issue):D744–D750
- Romero P, Obradovic Z, Dunker AK (1997) Sequence data analysis for long disordered regions prediction in the calcineurin family. *Genome Inform* 8:110–124
- Romero P, Obradovic Z, LiX GE, Brown C, Dunker AK (2001) Sequence complexity of disordered protein. *Proteins* 42:38–48
- Ross EB (1939) The postembryonic development of the salivary glands of *Drosophila melanogaster*. *J Morphol* 65:471–496
- Roth GE, Wattler S, Bornschein H, Lehmann M, Korge G (1999) Structure and regulation of the salivary gland secretion protein gene *Sgs-1* of *Drosophila melanogaster*. *Genetics* 153:753–762
- Saraste J, Dale HA, Bazzocco S, Marie M (2009) Emerging new roles of the pre-Golgi intermediate compartment in biosynthetic-secretory trafficking. *FEBS Lett* 583:3804–3810
- Schaumburg-Lever G, Lever WF (1975) Secretion from human apocrine glands: an electron microscopic study. *J Invest Dermatol* 64:38–41
- Schiefferdecker P (1917) Die Hautdrüsen des Menschen und der Säugetiere. *Biol Zentralbl* 37:11–12
- Schiefferdecker P (1921) Über morphologische Sekretionserscheinungen in den ekkrinen Hautdrüsen des Menschen. *Arch Dermatol Syph* 132:130–132

- Schnitter M (1961) Zur Genetic und Entwicklungsphysiologie des Faktors 'letal scheiben defekt' (Isd) bei *Drosophila melanogaster*. *Revue suisse Zool* 68:345–418
- Schwarz R, MR F e-B, Peukert-Adam I (1988) The mode of secretion in the anterior pituitary gland of the cow and the ewe. *Anat Anz* 167:183–189
- Segraves WA, Hogness DS (1990) The *E75* ecdysone-inducible gene responsible for the 75B early puff in *Drosophila* encodes two new members of the steroid receptor superfamily. *Genes Dev* 4:204–219
- Shen J, Tareste DC, Paumet F, Rothman JE, Melia TJ (2007) Selective activation of cognate SNAREpins by Sec1/Munc18 proteins. *Cell* 128:183–195
- Skaer H (1993) The alimentary canal. In: Bate M, Martinez Arias A (eds) *The development of Drosophila melanogaster*. Cold Spring Harbor Press, New York, pp 941–1012
- Sonnenblick BP (1940) The salivary glands in the embryo of *Drosophila melanogaster*. *Genetics* 25:137
- Sonnenblick BP (1950) The early embryology of *Drosophila melanogaster*. In: Demerec M (ed) *Biology of Drosophila*. Wiley, New York, pp 62–167
- Sorsa V (1989) Chromosome maps of *Drosophila melanogaster*. CRC Press, Boca Raton
- Stark A, Lin MF, Kheradpour P, Pedersen JS, Parts L, Carlson JW, Crosby MA, Rasmussen MD, Roy S, Deoras AN, Ruby JG, Brennecke J, Harvard FlyBase curators, Berkeley Drosophila Genome Project, Hodges E, Hinrichs AS, Caspi A, Paten B, Park SW, Han MV, Maeder ML, Polansky BJ, Robson BE, Aerts S, van Helden J, Hassan B, Gilbert DG, Eastman DA, Rice M, Weir M, Hahn MW, Park Y, Dewey CN, Pachter L, Kent WJ, Haussler D, Lai EC, Bartel DP, Hannon GJ, Kaufman TC, Eisen MB, Clark AG, Smith D, Celniker SE, Gelbart WM, Kellis M (2007) Discovery of functional elements in 12 *Drosophila* genomes using evolutionary signatures. *Nature* 450:219–232
- Südhof TC (2004) The synaptic vesicle cycle. *Annu Rev Neurosci* 27:509–547
- Südhof TC, Rothman JE (2009) Membrane fusion: grappling with SNARE and SM proteins. *Science* 323:474–477
- Syed ZA, Härd T, Uv A, van Dijk-Härd IF (2008) A potential role for *Drosophila* mucins in development and physiology. *PLoS One* 3:e3041
- Szul T, Burgess J, Jeon M, Zinn K, Marques G, Brill JA, Sztul E (2011) The Garz Sec7 domain guanine nucleotide exchange factor for Arf regulates salivary gland development in *Drosophila*. *Cell Logist* 1:69–76
- Talke L (1903) Über die grossen Drüsen der Achselhöhenhaut des Menschen. *Arch Mikrosk Anat* 61:537–555
- Thummel CS (1996) Flies on steroids – *Drosophila* metamorphosis and the mechanisms of steroid hormone action. *Trends Genet* 12:306–310
- Thummel CS (2002) Ecdysone-regulated puff genes 2000. *Insect Biochem Mol Biol* 32:113–120
- Tsarouhas V, Senti KA, Jayaram SA, Tiklová K, Hemphälä J, Adler J, Samakovlis C (2007) Sequential pulses of apical epithelial secretion and endocytosis drive airway maturation in *Drosophila*. *Dev Cell* 13:214–225
- Uversky VN, Oldfield CJ, Dunker AK (2008) Intrinsically disordered proteins in human diseases: introducing the D2Concept. *Annu Rev Biophys* 37:215–246
- Velissariou V, Ashburner M (1980) The secretory proteins of the larval salivary gland of *Drosophila melanogaster*: cytogenetic correlation of a protein and a puff. *Chromosoma* 77:13–27
- Velissariou V, Ashburner M (1981) Cytogenetic and genetic mapping of a salivary gland secretion protein in *Drosophila melanogaster*. *Chromosoma* 84:173–185
- Velpeau A (1839) Aiselle. In: *Dictionnaire de Médecine, un Répertoire Général des Sciences Médicales sous la Rapport Théorique et Practique* tome. 2, 2nd edn. Bechet Jeune Paris, pp 86–109
- Verneuil AS (1854) Études sur les tumeurs de la peau et quelques maladies de glandes sudoripares. *Arch Gén Méd* 4:447–468
- Versura P, Nanni P, Bavelloni A, Blalock WL, Piazza M, Roda A, Campos EC (2010) Tear proteomics in evaporative dry eye disease. *Eye* 24:1396–1402

- Vining MS, Bradley PL, Comeaux CA, Andrew DJ (2005) Organ positioning in *Drosophila* requires complex tissue-tissue interactions. *Dev Biol* 287:19–34
- von Gaudecker B (1972) Der Strukturwandel der larvalen Speicheldrüse von *Drosophila melanogaster*. Ein Beitrag zur Frage nach der steuernden Wirkung aktiver Gene auf das Cytoplasma. *Z Zellforsch Mikrosk Anat* 127:50–86
- von Gaudecker B, Schmale EM (1974) Substrate-histochemical investigations and ultrahistochemical demonstrations of acid phosphatase in larval and prepupal salivary glands of *Drosophila melanogaster*. *Cell Tissue Res* 155:75–89
- Walter AM, Wiederhold K, Bruns D, Fasshauer D, Sørensen JB (2010) Synaptobrevin N-terminally bound to syntaxin-SNAP-25 defines the primed vesicle state in regulated exocytosis. *J Cell Biol* 188:401–413
- Wang S, Tsarouhas V, Xylourgidis N, Sabri N, Tiklová K, Nautiyal N, Gallio M, Samakovlis C (2009) The tyrosine kinase Stitcher activates Grainy head and epidermal wound healing in *Drosophila*. *Nat Cell Biol* 11:890–895
- Wang S, Meyer H, Ochoa-Espinosa A, Buchwald U, Onel S, Altenhein B, Heinisch JJ, Affolter M, Paululat A (2012) GBF1 (Gartenzweig)-dependent secretion is required for *Drosophila* tubulogenesis. *J Cell Sci* 125:461–472
- Wendt A (1833) De epidermide humana. Dissertatio inauguralis anatomica 4. pag. VI+36. Accedit tabula aenea. Universitas Vratislaviae
- Wendt A (1834) Über die menschliche Epidermis. *Archiv für Anatomie, Physiologie und wissenschaftliche Medicin*. pp 278–291
- Wu M, Lu L, Hong W, Song H (2004) Structural basis for recruitment of GRIP domain golgin-245 by small GTPase Arl1. *Nat Struct Mol Biol* 11:86–94
- Zhimulev IF, Kolesnikov NN (1975) Synthesis and secretion of mucoprotein glue in the salivary gland of *Drosophila melanogaster*. *Wilhelm Rouxs Arch Dev Biol* 178:15–28
- Zhou L, Beuerman RW, Chan CM, Zhao SZ, Li XR, Yang H, Tong L, Liu S, Stern ME, Tan D (2009) Identification of tear fluid biomarkers in dry eye syndrome using iTRAQ quantitative proteomics. *J Proteome Res* 8:4889–4905
- Zhou L, Zhao SZ, Koh SK, Chen L, Vaz C, Tanavde V, Li XR, Beuerman RW (2012) In-depth analysis of the human tear proteome. *J Proteomics* 75:3877–3885

Chapter 16

Salivary Gland Secretions of Phytophagous Arthropods

Maria P. Celorio-Mancera and John M. Labavitch

Abstract Thousands of arthropod species use plants as their main food source. Plants in turn are not completely passive towards arthropod herbivory. Arthropod saliva constitutes an important point of contact which initiates phytophagy and mediates chemical communication. Here we present a summary of those communications studying the constituents of arthropod saliva and their effect on plants. Particular attention has been dedicated to those reports identifying salivary gland genes and proteins in their entirety (transcriptomes and proteomes). The anatomy of salivary glands is highly variable and much of its complexity remains unstudied in various groups of phytophagous arthropods. Some important factors dictating the function of saliva in herbivory are the feeding strategy used by the arthropod, the developmental stage of the animal and the ecological niche in question. The function of many salivary components, such as the chemosensory proteins identified in arthropods, is still largely unknown. We consider the use of heterologous expression of these genes, chemoinformatic, molecular modeling and immunohistochemical studies to be of substantial importance for the elucidation of the functions of these genes as well as the functions of many other unknown proteins in arthropod systems. Additionally, the role of hemolymph proteins such as apolipoporphins and storage proteins in saliva is unclear and therefore attention must be devoted to the understanding of protein movement in the arthropod body.

M.P. Celorio-Mancera (✉)
Department of Zoology, Ecology, Stockholm University,
Svante Arrheniusväg 18 B, 106 91 Stockholm, Sweden
e-mail: maria.celorio@zoologi.su.se

J.M. Labavitch
Plant Sciences Department, University of California, Mail stop 5, Davis, CA 95616, USA
e-mail: jmlabavitch@ucdavis.edu

16.1 Introduction

Arthropoda comprises approximately one million described species grouped in nine phylogenetic groups, namely Hexapoda, Crustacea, Pauropoda, Diplopoda, Chilopoda, Symphyla, Arachnida, Xiphosura and Pycnogonida (Tree of Life Web Project 1995; Thorp 2009). Most phytophagous arthropods are within Hexapoda, specifically Insecta, which dominate terrestrial habitats with over 750,000 species described (Wilson 1988). Therefore, it is not surprising that almost half of the living organisms on Earth are represented by plants and their insect parasites (Schoonhoven et al. 2005). Interactions between arthropods and plants which are ubiquitous and highly diversified have drawn the attention of evolutionary biologists for explanations of this biological diversity. Ehrlich and Raven in 1964, suggested that an “arms race” between plants and their insect herbivores has led to species diversification via “coevolution” (Ehrlich and Raven 1964). They conclude that the insect herbivore must overcome the plant’s chemical deterrence or defense posed in order to, “escape” and “diversify”.

The herbivore’s feeding strategy represents one of its most effective means of coping with plant-defense mechanisms and, when considered along with the chemical composition of the phytophagous arthropod’s saliva, plays a critical role in diversification. Salivary secretions function as a matrix for chemical communication between the herbivore and the plant (Felton and Tumlinson 2008; Weech et al. 2008; Schmelz et al. 2009). Our new ability to inspect the complete array of proteins (proteomes), expressed genes (transcriptomes) and the genomes in the interacting organisms has provided us with a holistic view of the biological response. Thanks to this ability we can discuss aspects of the “general saliva composition” and examine later issues related to “specific molecular functions” of the salivary components. Currently, there are several reports describing the arthropod-saliva proteome or transcriptome, but even now many salivary components have not been assigned a biological function. This task is not trivial; an objective of this chapter is to find patterns within the literature that can lead to the study of components of insect saliva that may mediate communication between the plant and its arthropod parasite.

First, we review how arthropods feed on a plant. In general terms, the prevalent mode of plant feeding among Arthropoda is by means of either powerful chelicerae or mandibles. Chewing mouthparts are used by larvae of the Lepidoptera, but also by plant-feeding species within Diplopoda, Crustacea, Pauropoda and Symphyla, many of which are detritivores that encounter plant material in the decomposing organic matter they feed on. The biting-chewing strategy for feeding on plants can be considered the ancestral state among Arthropoda since the mouthparts required for this way to food acquisition have retained the appearance of the ancestral appendages, paired and segmental (Chapman 1995). Xyphosurans are mostly predators, feeding on mollusks, crustaceans and worms on the ocean floor. Pycnogonida, Arachnida and Chilopoda are mostly predators, but within the Arachnida we

encounter phytophagous Acari using a piercing proboscis to feed on plant cellular contents. By convergent evolution, this strategy for plant-feeding using a suctorial proboscis is observed in other taxa within Hexapoda: Lepidoptera, Coleoptera, Hymenoptera and Diptera (Krenn et al. 2005). As mentioned above, Hexapoda contains most of the phytophagous arthropods and also the widest range of plant-feeding strategies, ranging from detritivory, to piercing the living plant to defoliation by chewing. A sort of combination between piercing and chewing strategies has also been described for hexapods; the minute mandible blades of the gall midge larvae, *Mayetiola destructor*, resemble a short stylet which injects saliva into the plant cells (Stuart et al. 2012).

Sharma and collaborators (2014) conducted an exhaustive analysis of the literature regarding feeding strategies among those hexapods which use their stylets to pierce the plant tissue and withdraw its nutrients. We encourage the reader to consult their very thorough analysis and complement that with the summary we are reporting here, which includes only a discussion of recent reports (the second half of 2014 and the first half of 2015).

The complexity of the feeding strategy of piercing-sucking insects (specifically hemipteroids) has been revealed through comprehensive ecological and behavioral studies. The withdrawal of plant nutrients may involve the creation of a salivary sheath upon penetration of vascular tissues, or the utilization of an osmotic-pump mechanism by sap-sucking insects. For those insects that rupture plant leaf or stem parenchyma cells, three main categories for feeding strategies have been established: lacerate-and-flush, lacerate-and-sip and macerate-and-flush (Sharma et al. 2014).

It is important to realize that the arthropod's mode of accessing food may change drastically depending on its developmental stage (Chapman 1995); this is particularly true for those species undergoing complete metamorphosis during their life cycle, because this involves a complete reconfiguration of both the anatomy and physiology of feeding.

16.2 Salivary Glands and Their Components

The salivary glands in phytophagous arthropods are highly diverse in their anatomy and composition, and this complexity has not been fully investigated. In general, salivary glands can be tubular, acinar (alveolar) or reservoir type (Ribeiro 1995). These types display particularities; for example the location of the openings of their ducts in the animal body, which can have enormous implications for the arthropod-plant interaction. Similarly, different kinds of saliva might be found in the arthropod system; whether their mixture takes place represents yet another level of complexity when elucidating the role(s) of saliva components during the feeding process. In the Endopterygota it is common to count at least two kinds of glands associated with the mouthparts, the mandibular and the labial glands (Akai et al. 2003; Vegliante

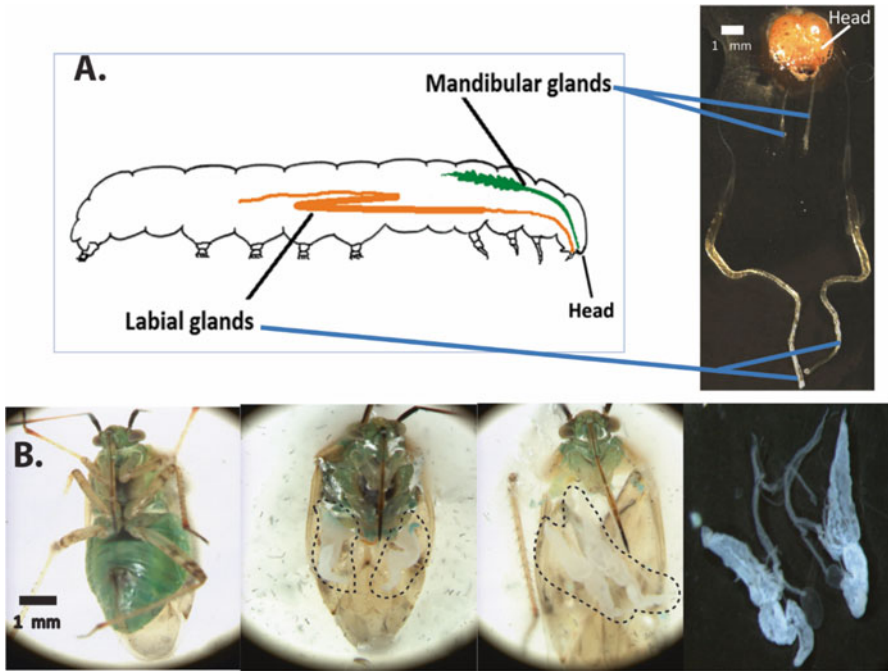


Fig. 16.1 Two examples of salivary glands in Neoptera. Drawing of a caterpillar's body (*side view*) indicating the position of the mandibular and the labial glands in relation to the head (**a**). The caterpillar drawing indicates also the corresponding position of the mandibular and labial glands in a dissected specimen of *Helicoverpa armigera* larva where the body has been removed except the head and the salivary glands. Four photographs depicting the ventral side of the mirid *Lygus hesperus* and the sequential exposure of its salivary glands (*inside dotted lines* and isolated from body at the furthest right photograph) after removal of the abdomen and thorax (**b**)

and Hasenfuss 2012). The labial pair is mostly dedicated to the production of silk (see Chapter 14) while the mandibular pair is associated with the production of saliva for the lubrication of the mandibles during the demanding task of biting and chewing abrasive plant material (Fig. 16.1 panel A). Other glands have been poorly studied and their general role(s) in the arthropod system are still unknown; e.g., the maxillary glands and De Filippi's glands observed in some lepidopterans (Vegliante and Hasenfuss 2012). However, perhaps the most studied salivary glands come from the order Diptera (see Chapter 15) because the fruit fly, *Drosophila melanogaster*, has been a model species for understanding biology for the last half century, and mosquitos are vectors of various tropical diseases in humans. The study of salivary glands and their contents in *Anopheles* spp has revealed invaluable knowledge about the dynamics of parasite and pathogen transmission (Dhar and Kumar 2003), hence open possibilities for the control of diseases such as malaria (James 2003; Maharaj et al. 2015).

16.2.1 *Hexapoda*

Most salivary transcriptomes and proteomes described up to date correspond to arthropod species in the group Pterygota (winged insects). Unfortunately, we lack knowledge about salivary gland composition for those saprophagous hexapods that are part of the soil fauna (Collembola, Protura and Diplura), insects which may feed on mosses and lichens in Archaeognatha (bristletails) and Embiidina (web-spinners) (Edgerly and Rooks 2004), and species in other groups within Neoptera such as Psocodea (bark lice), Plecoptera (stoneflies), Phasmida (stick/leaf insects) and Dermaptera (earwigs). We do know that certain plecopterans not only may use proteases and lipases for digestion but also amylase, since such activities were detected in whole body extracts of these insects confirming their ability to exploit plants for nutrient acquisition (de Figueroa et al. 2011; López-Rodríguez et al. 2012; but see 16.2.3). In another study, diet regimen affected the size of the salivary glands in the ring-legged earwig, *Euborellia annulipes* and juvenile hormone levels correlated positively with salivary gland size in this earwig species (Rankin et al. 1997), but the implications of these observations are still unclear.

16.2.1.1 Components of Saliva in Species Within the Hemipteroid Assemblage

As stated earlier, Sharma et al. (2014) provided in their review detailed information on salivary proteins detected in phytophagous hemipteroids. Thus, here we direct our attention to even more recent investigations in the literature and their conclusions. We also discussed, that the comprehensive description of the salivary transcriptome and proteome of a plant-feeding arthropod may be an important first step for the understanding of the arthropod-plant interaction; their “coherence” is equally valuable. Transcriptomic data “coherent” with proteomic data will simply mean that for a given number of predicted transcripts corresponds with the same number of predicted proteins. Experimentally, this is not the scenario observed; that is, many more transcripts (encoding secreted proteins) are predicted in relation to the number of secreted proteins that are actually detected (Chaudhary et al. 2015). This reflects our inability to capture all the biological plasticity at the protein level, partially due to the mere physical limitation of extracting saliva from small insects like aphids. Recently, the use of a neurostimulant seemed to increase aphid salivation, thus potentially improving the detection of secreted proteins (Chaudhary et al. 2015). Chaudhary and collaborators (2015) made additional observations which are important to highlight: (1) the salivary components of specialist and generalist aphid species are more similar to each other than expected, (2) protein movement may occur; i.e., from the hemocoel into the salivary glands, and (3) glucose dehydrogenases and trehalases were identified as common components of aphid saliva.

Other important components of aphid saliva characterized by means of functional genetic approaches are the so called “aphid effectors” (Bos et al. 2010). When

the genes encoding these effectors are expressed in plants using genetic engineering, they affect aphid fitness (either enhancing or, occasionally, suppressing it) suggesting a role in the regulation of plant defense responses (De Vos and Jander 2009; Elzinga et al. 2014; Rodriguez et al. 2014). Interestingly, one of these effectors, called Mp10 is highly similar in its amino acid sequence to chemosensory proteins (CSPs) from other insects (Bos et al. 2010). Transcripts encoding putative CSPs sharing high homology to Mp10 are differentially expressed in two populations of the brown planthopper, *Nilaparvata lugens* which display differences in their success as vectors of rice virus diseases (Ji et al. 2013). The amino acid composition of CSPs indicates that they may function as carriers of hydrophobic molecules (Pelosi et al. 2006). Understanding the macromolecular targets and physicochemical effects of aphid effectors and arthropod effectors, in general, may have great potential for the control of pest species. For example, plant-mediated RNAi down-regulating the expression of genes encoding salivary effectors in aphids is persistent across generations decreasing aphid population growth (Coleman et al. 2015). Research pioneering 3-D modeling strategies, heterologous expression and *in vitro* binding assays of CSPs are available for dipteran and lepidopteran species (Picimbon et al. 2000; Campanacci et al. 2003; Mosbah et al. 2003; Iovinella et al. 2013). Certainly, more of these studies and immunocytochemical localizations of odorant-binding proteins (OBPs) and CSPs in the arthropod body are necessary to reveal possible functions as effectors of plant defense responses.

We expect to see an increase in the number of comparative analyses of hemipteroid saliva at the genomic and proteomic level. Hattori and collaborators (2015) inspected the composition of the watery saliva of the green rice leafhopper, *Nephotettix cincticeps*, and concluded that its proteomic profile is consistent with that of other phloem feeders already characterized. Proteomic analysis of other hemipteran pests; e.g. mirids, will be fairly easy to conduct since the salivary glands are conspicuous in some species (Fig. 16.1 panel B) and techniques for collecting saliva when extruded into inert diets are well known (Habibi et al. 2001). Recently, high expression levels of polygalaturonase (PG)-encoding genes in salivary glands of another mirid, *Apolygus lucorum*, were reported (Zhang et al. 2015) and Celorio-Mancera et al. (2009) identified multiple endo- and exo-PGs in salivary glands isolated from the western tarnished plant bug, *Lygus hesperus*. Two of these PGs were extruded when the insect fed on an artificial diet (Celorio-Mancera et al. 2008). Several cell wall-digesting enzymes were identified in the salivary glands of the glassy-winged sharpshooter (*Homalodisca vitripennis*) the vector of Pierce's disease of grapevines. Antibodies were raised against a β -1,4-endoglucanase-enriched fraction from the vector's salivary glands and were used to demonstrate that the enzyme was extruded into grapevine xylem vessels when the sharpshooter fed from them (Backus et al. 2012).

The first study describing the sialotranscriptome of a thysanopteran was reported (Stafford-Banks et al. 2014). This study predicted that gene families in the Western flower thrip, *Frankliniella occidentalis*, are involved in detoxification and inhibition of plant defenses, sugar metabolism and general digestion as based on transcript sequence homology with other better characterized species. One of the main

conclusions was that the presence of transcripts encoding enzymes involved in the extra-oral digestion of plant cell wall components (β -glucosidases, endo- β -glucanases and pectin lyases) was coherent with the type of feeding damage that the thrips inflicted on plants (Stafford-Banks et al. 2014). Transcripts encoding putative CSPs and odorant receptors were also identified in this study.

16.2.1.2 Components of Saliva in Species Within Orthoptera

Interestingly, we could not find a similar description of the sialotranscriptome of an orthopteran. However, extensive transcriptomic and proteomic approaches have been used to understand the biology of migration in the migratory locust, *Locusta migratoria* (Chen et al. 2010; Tong et al. 2015; Tu et al. 2015). Information about what constitutes the saliva of orthopterans is scattered in the literature. A gene coding for a β -1,4-endoglucanase able to digest carboxymethyl-cellulose was detected in the cricket *Teleogryllus emma*, with the highest specific activity of this enzyme found in salivary glands (Kim et al. 2008). Lipase activity and disulfooxy fatty acids (caeliferins) were detected in oral secretions of grasshoppers and fatty acid amides in katydid and crickets (Alborn et al. 2007; Schafer et al. 2011).

16.2.1.3 Components of Saliva in Species Within Endopterygota

Different kinds of glands can be found in holometabolans depending on their ecology and developmental stage; e.g., mandibular, maxillary, hypopharyngeal and labial glands (Walker 2009). Labial glands are present in those groups of insects (Lepidoptera, Trichoptera, and Hymenoptera) where silk production is important for shelter and protection purposes (details in Chapter 14). The mandibular glands in lepidopterans have been associated with the lubrication of mouth parts and bolus formation. They are paired but not fused in the anterior region like the silk glands and they are not compartmentalized (Parthasarathy and Gopinathan 2005). Comparing the scientific reports on the salivary contents of labial and mandibular glands (Fig. 16.1. panel A) in lepidopteran larvae, the following conclusions are reached: (a) the primary function of the labial glands is the production of fibroin and sericin (silk proteins), (b) glucose oxidase, fructosidase, arylphorin, protease and oxidase/peroxidase are also important components of the labial glands, (c) proteins with high homology to CSPs are the main proteome component of mandibular glands, and levels of these proteins change in response to caterpillar diet (Celorio-Mancera et al. 2012, 2015) (Fig. 16.2), (d) both labial and mandibular glands contain proteins involved in digestion and immunity, (e) both types of glands harbor methionine-rich storage proteins, arylphorins and apoliphorins, all of which are proteins that may circulate through the larval body, (f) polygalacturonase or pectin lyase activities were not detected in caterpillars.

Extensive proteomic studies on salivary glands are now available for the larval stage of some lepidopterans. For example, lists of the proteins identified in the mid-

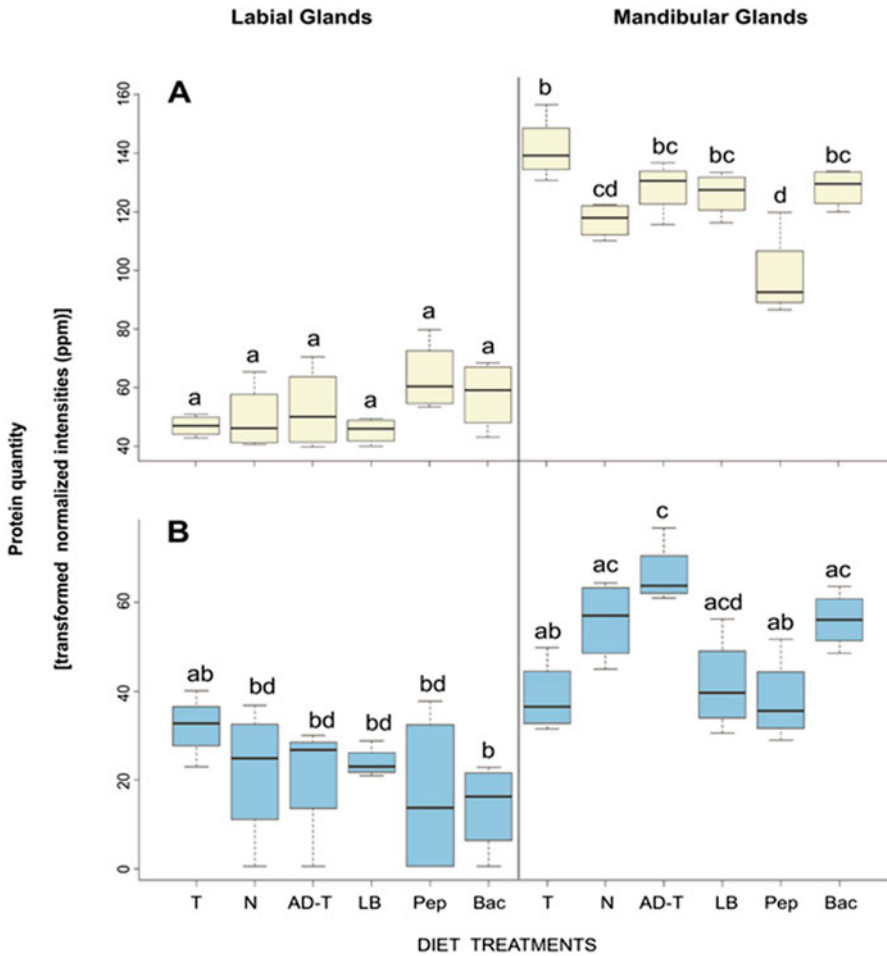


Fig. 16.2 Box-and-whisker plots of protein levels in salivary glands of caterpillars reared on different diets. (a) Chemosensory protein; (b) Odorant binding protein. Diet treatments: *Cirsium palustre* (T), *Urtica dioica* (N), artificial diet (AD), artificial diet and growth medium for bacteria (LB), LB containing peptidoglycan (Pep), LB containing living bacteria *Escherichia coli* (Bac). In treatment “AD-T”, the caterpillars were switched from feeding on artificial diet to plant material when molting into their fifth larval stage (Modified after Celorio-Mancera et al. 2015)

dle and posterior silk glands (labial glands) of silkworms in different stages of development have been generated by the Silkworm Genome Project and are accessible to the public through the Kaiko Proteome Database (<http://kaiko2ddb.dna.affrc.go.jp>) (Shimomura et al. 2009). Similarly, cDNA libraries are publicly available for the silk glands of the silkmoth, *Bombyx mori* (<http://silkbases.ab.a.u-tokyo.ac.jp> and <http://sgp.dna.affrc.go.jp/KAIKObase/>). The labial sialome of a generalist herbivore, the cotton bollworm *Helicoverpa armigera*, was inspected (Celorio-Mancera et al. 2011) and the labial and mandibular salivary gland proteomes were

compared in nymphalids (Celorio-Mancera et al. 2012, 2015). Important are those studies that have reported the activities (rather than just the presence of genes or proteins) of certain enzymes in the labial and/or mandibular glands in lepidopteran species. Reports have identified amylases, lysozymes and fructosidases (Burton et al. 1976; Mall et al. 1978; Liu et al. 2004; Asadi et al. 2010; Celorio-Mancera et al. 2012) and provided insights of the biological roles of glucose oxidase (Musser et al. 2005) and disaccharidases (Hirayama et al. 2007) in insects.

Akai and coauthors in 2003 pointed out that the labial glands of adult neolepidopterans were understudied, particularly those of pollen-feeding *Heliconius* butterflies. Currently, about 31 proteins have been identified in the extruded saliva of the common postman, *H. melpomene* (Harpel et al. 2015). Although most of the identified proteins are involved in proteolysis and carbohydrate hydrolysis, activities necessary for the consumption of pollen and nectar, many proteins found in this study have unknown roles and are obvious targets for functional genetic investigations. Indeed, pollen is protein rich, e.g. up to 32 % by weight in rapeseed (Rayner and Langridge 1985) but most pollen nutrients are inside the pollen grain and are only released following a slow digestive process (Dobson and Peng 1997).

In Mecoptera, the salivary glands are involved in mating behavior, producing the nuptial gift offered by the males during mating. Although some exceptions exist, the salivary glands of the mecopterans display sexual dimorphism and are highly diverse among species (Ma et al. 2011). Nevertheless, we know nothing about the composition of salivary glands in either larval or adult stages of these insects.

Although the salivary components of blood-feeding dipterans are well studied (see Chapter 17), the identification of transcripts and proteins in salivary glands of gall midges and *Toxorhynchites* mosquito species have been recently reported (Calvo et al. 2008; Stuart et al. 2012). Lipase-like, proteases and protease inhibitors were identified as components of the salivary glands of gall midge larvae (Stuart et al. 2012). Many salivary components are just referred to as “secreted salivary gland proteins” (SSGPs) since their sequences do not match significantly well to any known proteins. These investigations, although partially informative, revealed the high degree of specialization between these insects and their hosts, a relationship suggestive of the interaction between plants and their pathogens. The gene-for-gene model can be applied to understand the interaction between Cecidomyiidae and their hosts where avirulence genes were identified.

Due to their enormous impact on human economy, pest species such as the red flour beetle, *Tribolium castaneum*, are among the best studied hexapods so far. Although digestive enzymatic activities such as proteinase, amylase, xylanase and pectinase have been well characterized in coleopterans (Macedo and Freire 2011; Sami et al. 2011; Mika et al. 2013; Pauchet and Heckel 2013; Fabres et al. 2014; Kirsch et al. 2014; Pauchet et al. 2014), only a small number of studies have focused on the identification of genes or proteins in maxillary glands of beetle larvae (Srivastava 1959). Thus, although in the flour beetle putatively 19 genes code for CSPs and 49 for OBPs (Vieira and Rozas 2011), we do not know whether their expression is localized in specific tissues, such as the glands.

The anatomy and number of the salivary glands in Hymenoptera is highly variable (do Amaral and Machado-Santelli 2008; Elias-Santos et al. 2013). Besides the OBPs and CSPs detected in mandibular glands of all bee castes and stages, enzymes involved in quenching reactive oxygen species are present in the salivary glands of the honey bee, *Apis mellifera* (Iovinella et al. 2011). Arginine kinase is also found in both thorax and head salivary glands of a stingless bee species, *Melipona quadri-fasciata anthidioides* (Elias-Santos et al. 2013). Interestingly, the biological role of this kinase is still unclear, but it also was reported in the salivary glands of other species within Lepidoptera (Celorio-Mancera et al. 2011) and Hemiptera (Hattori et al. 2015).

16.2.2 *Diplopoda*

The activity of enzymes capable of degrading plant polysaccharides has been detected in salivary glands of some species of diplopods (Nunez and Crawford 1976). The salivary glands of this group of arthropods are arranged like those of vertebrates, with an acinal and a tubular portion (de Sousa and Fontanetti 2012) but the openings of their excretory ducts seem to vary substantially from species to species (El-Hifnawi and Seifert 1973). The ducts can open either into the oral cavity (El-Hifnawi 1974) or the foregut (de Sousa and Fontanetti 2012). Therefore, the degree of predigestion of the chewed food due to the action of salivary secretions may vary remarkably among species. Thus, it will be interesting to examine whether there is a correlation between the characteristics of the food source and the enzymatic activities, and salivary glandular anatomy in the different diplopods. It is also of interest to understand how dependent diplopods are on microorganisms for the acquisition of nutrients from food, as has been proposed (de Sousa and Fontanetti 2012). We have not found proteome or transcriptome-level studies conducted on saliva or salivary glands of Diplopoda. However, this type of study will be necessary to broaden our understanding of this group of arthropods, which is relevant due to their possible use as environmental indicators (Giuliano-Perez and Fontanetti 2011). Additionally, information about the salivary composition in Diplopoda would obviously aid the describing of evolutionary relationships of genes encoding salivary proteins in comparison with other arthropods that feed on living plants. For example, genes coding for CSPs was reported in Diplopoda (Iovinella et al. 2013) but still we lack information about their location(s) in the arthropod body.

16.2.3 *Other Arthropoda*

Crustacea represent a conspicuous group present in many habitats and with equally diverse feeding strategies. Salivary glands are not present in most crustaceans except for members of the Chephalocharida and Pentastomida (Hessler and Elofsson 2013;

Christoffersen and de Assis 2015). The antennal glands for osmoregulation and the digestive glands are more common features of the crustacean structural plan (Tsai and Lin 2014). Crustaceans are ubiquitous in marine and freshwater habitats but some groups have evolved into terrestrial habitats. One example is that of the Isopoda, which display extremely diverse feeding habits, including herbivory, which is considered to be the ancestral state of this group (Brusca 1997). Isopoda, commonly known as woodlice, have a digestive system consisting of a foregut, a pair of tubular midgut caeca (hepatopancreas) and a hindgut. The hepatopancreas is the site for secretion of digestive enzymes and absorption of nutrients. Although more investigations are needed to understand the digestive ability of these arthropods, there are indications that autochthonous microorganisms may be living in a mutualistic or commensal relationship with woodlice (Kostanjšek et al. 2002; Cragg 2003).

Most species in Chilopoda are predators and information about their salivary glands is scarce. However, a study on the common house centipede, *Scutigera coleoptrata*, indicated that maxillary glands and head glands deliver their secretions into the foregut and suggested that the ultrastructure of these glands is very different from those of Hexapoda (Hilken and Rosenberg 2006).

No proteomic or transcriptomic analyses have been conducted on salivary glands of species in the microarthropod groups Pauropoda and Symphyla. We consider the inspection of the saliva components in these groups to be a potential line of investigation, especially to further understanding of how the composition of microarthropods in the soil changes depending on biotic and abiotic factors (Menta et al. 2014).

Phytophagous mites within Arachnida can be considered to be among the most pervasive agricultural pests. One of the best studied species, for which the genome has been sequenced, is the two-spotted spider mite *Tetranychus urticae* (Grbić et al. 2011). Although there is no specific analysis of the salivary proteome of plant-feeding mites, investigations have been conducted on the feces and the whole-body of these parasites corroborating the presence of cysteine and aspartyl-type proteases (Santamaría et al. 2015). It has been suggested that “phytotoxins” in the saliva of Eriophyoid mites act as regulators of plant growth inducing galls (Royalty and Perring 1996). However, even with a protocol available for the possible collection of mite salivary secretions (De Lillo and Monfreda 2004), this speculation is still awaiting experimental evidence (Felton et al. 2014). We encountered contradictory evidence in relationship to the occurrence of genes encoding putative CSPs in Arachnida. Iovinella and coauthors (2013) mentioned that *csp* genes are not found in Chelicerata, but Vieira and Rozas (2011) reported *csp* genes in the deer tick, *Ixodes scapularis*.

16.3 Salivary Components and the Interaction Between Plants and Arthropods During Herbivory

Over the time-line of the co-evolution of phytophagous Arthropoda and flowering plants, many strategies have evolved for the adaptation to increasingly variable terrestrial habitats while enhancing the reproductive success of the interacting species. This “biological warfare” has influenced many aspects of the biology of animals and plants, including the impacts of the Arthropod’s need to obtain food from primary autotrophs, thus impacting plant adaptive and reproductive success. Aspects of this rivalry can be easily seen as we examine the role(s) of salivary secretions in the interaction.

We know that plants perceive pathogens, nematodes and arthropod herbivores (above and below ground) because transcriptional and even volatile emission changes occur in those attacked plants (Carroll et al. 2008; Robert et al. 2012 and references cited therein). The mechanisms of plant perception of lepidopteran herbivores have been extensively studied in *Arabidopsis* and *Nicotiana* and they mostly involve the effect of salivary or “regurgitant” components on these plants. Another well studied plant-insect interaction is that between the Hessian fly, *Mayetiola destructor*, and wheat, *Triticum* spp. This interaction is particularly interesting since its pattern is similar to those involving plant-pathogen interactions; that is, the gall midge produces proteins that are delivered in the saliva and the plant in turn, expresses resistance proteins (R) that prevent disease symptoms (Stuart et al. 2012).

The cues from bacteria, fungi and nematodes that are perceived by plants have been referred as pathogen-associated molecular patterns (PAMPs) or microbe-associated molecular patterns (MAMPs). The cues from phytophagous arthropods, most of salivary origin that are perceived by plants, have been named herbivore-associated molecular patterns (HAMPs). More recently, the term “effector” has been used (Bos et al. 2010) when reference is made only to those herbivore signals that interfere with plant defense responses (Felton et al. 2014). Upon damage, the plant produces or releases different amounts of molecules that may regulate defense against herbivory. These endogenous molecules in response to injury are called damage-associated molecular patterns (DAMPs). It has been pointed out that similar to the mammalian response towards hematophagous arthropods, the earliest response to plants towards arthropod herbivory involves the release of extracellular ATP, the elevation of cytosolic calcium and the production of reactive oxygen species (Guiguet et al. 2016). In turn, salivary apyrases, calcium-binding proteins and peroxiredoxins may modulate these early signaling in the plant to achieve successful plant parasitism, especially in gall-inducing and leaf-mining insects (Guiguet et al. 2016). The action of DAMPs, HAMPs and effectors on the plant system is very diverse and it is clear that we have not been able to understand completely the molecular dynamics underlying the outcome of the plant response. Moreover, in natural conditions, plants are attacked simultaneously by herbivores and pathogens below and above ground in addition to other biotic and abiotic factors, not even excluding endogenous developmental changes with reliance on hormones such as

jasmonates (Crozier et al. 2000). For a thorough discussion on the ecological implications and selection forces that may be shaping plant defense and arthropod offense in herbivory consult Schaefer and Ruxton (2011) and the references cited therein.

Aphids and whiteflies inflict a pathogen-like offense on the plant which is characteristic of local damage and thrips. Components in oral secretions including saliva in caterpillars also interfere with the plant defense response (Weech et al. 2008; Diezel et al. 2009). Lepidopteran larvae and beetles elicit the activation of jasmonic acid responses leading to the degradation of transcriptional regulators that allow for example, the release of volatiles attractive to egg parasitoids or predators (Walling 2000; Schaefer and Ruxton 2011). This is just an example of what has been observed in certain plant-arthropod interactions, because the picture is more complicated.

Among the many signaling events described for plants attacked by herbivores, wounding in plants induces plant polygalacturonase (PG), a hydrolase that digests the uronic acid-rich cell wall pectin polysaccharides producing oligogalacturonides (OGAs) which seem to be signals that elicit plant defense (Berger et al. 1999). Necrotrophic pathogens of plants also produce PGs. The activities of enzymes such as PGs open the wall polysaccharide network so that the pathogen can (1) grow within the host's tissues and (2) use the sugars released from wall structures to support their energy needs. In turn, PG-inhibiting proteins (PGIPs) are produced by many plants. Studies of plant PGIPs have shown that the PGIPs are selective inhibitors; they inhibit PGs produced by many fungal and bacterial pathogens (but not all pathogens) and inhibit some (but not all) PGs of pathogens that express several different PG-encoding genes (Sharrock and Labavitch 1994). The expression of a 'Bartlett' pear fruit PGIP-encoding gene in tomato fruit reduces the increase in fruit susceptibility to the grey mold (*Botrytis cinerea*) infection that normally accompanies fruit ripening (Powell et al. 2000). PGIPs in the plant tissue seem to elicit a defense response against the pathogen (Hammond-Kosack and Jones 2000). PG activity also has been identified in the salivary secretions of lygus bugs, *L. hesperus* and *L. lineolaris* (Shackel et al. 2005; D'Ovidio et al. 2004) and micro-injection of pure PG into alfalfa florets and cotton flowers causes tissue damage that is visibly like that caused by lygus bug feeding on these tissues (Celorio-Mancera et al. 2008). A detailed examination of the PGs in *L. hesperus* saliva (Celorio-Mancera et al. 2009) identified five different PG species, both *endo*- and *exo*-acting. At present, it is not clear which of these PGs is/are inhibited by PGIPs from different plant sources. This set of observations suggests the possibility that molecular or traditional breeding of crops to develop lines expressing increased levels of PGIPs that inhibit lygus bug salivary PGs may result in lines with reduced damage following lygus bug feeding. Although both feeding and salivary gland extracts from the hemipteran, *L. hesperus*, induce the emission of plant volatiles (Rodriguez-Saona et al. 2002), it is unclear which is the specific effect of lygus pectinases in the plant and whether plant inhibitors of pectinases actually protect the plant from herbivory (Fig. 16.3). *In vitro* tests of PG's ability to digest pectins have shown that PGIP alters the generation of OGA digestion products so that longer pectin-derived oligosaccharides are generated and that these OGAs are effective as elicitors of plant defense responses to pathogens (Cervone et al. 1989; Ridley et al. 2001). The

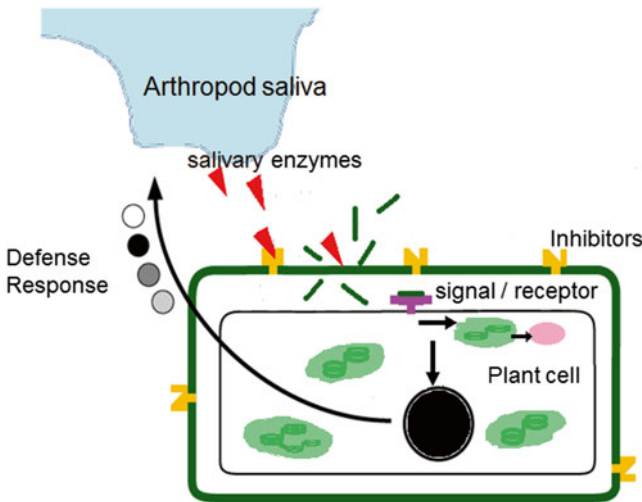


Fig. 16.3 Diagram illustrating a hypothesized plant–arthropod interaction, drawn after the polygalacturonase–polygalacturonase inhibiting–protein (PG–PGIP) model. The arthropod delivers plant cell wall–degrading enzymes produced in its salivary gland through piercing–sucking mouthparts into or in between cell walls. If inhibitors of these enzymes are present in the plant, oligosaccharides can be signals that bind to receptors initiating the cascade of events in signal transduction which may include processes located in chloroplasts and the peroxisomes. The signals induce gene regulatory changes in the nucleus that are translated in to plant defense responses deterring herbivory

possibility that this change in the size of pectin digestion products and expression of defenses occurs *in planta* has been indicated by tests of genetically modified *Arabidopsis thaliana* plants (Benedetti et al. 2015); whether PGIPs can reduce herbivore–caused crop damage in the field has not been tested.

Insect feeding on stored grains and seeds of many legumes can cause important postharvest losses of these dietary staples as well as reductions in the quality of the seeds needed for future crops. Insects target these plant products because they contain substantial amounts of fixed atmospheric CO₂, stored as starch, and amino acids that have been incorporated into seed storage proteins. These accumulated nutrients are the resources that germinating seeds require as they establish the “next generation” prior to the seedling’s acquisition of its autotrophic capability. Thus, the herbivorous animal and its plant “target” require the same resources. At the biochemical level, the insect makes use of α -amylase for harvesting the glucose that has been accumulated as starch polymers in seed amyloplasts. The adults often facilitate the biochemical interaction by depositing eggs directly on seeds so that larvae have easy access to the carbon- and energy-rich resource (e.g., the cowpea weevil, *Callosobruchus maculatus* and harvested mungbean seeds; Wisessing et al. 2010). The interaction is not one-sided in that many seeds, including those of mungbean and other common beans, include α -amylase inhibitors (α -AIs; Wisessing et al. 2010 and references cited therein) as part of the seed’s population of storage proteins.

The α -AIs of several bean species have been studied; the genes that encode these α -AIs have been identified and their inhibition of α -amylases from diverse insect sources has been described (e.g., Barbosa et al. 2010). These authors described the transgenic expression of the gene encoding the *Phaseolus vulgaris* α -AI-1 in *Coffea arabica* (coffee, an important crop plant with no natural resistance to the coffee berry borer, *Hypothenemus hampei*). Protein extracts from the transgenic lines gave substantial inhibition of the borer's α -amylase; tests to determine the ability of the transformed coffee plants to limit insect damage are underway.

The impact of α -AI proteins on seed longevity/quality can be seen as an example of a role played by a “pre-formed” plant defense strategy. An examination of the roles of insect proteinases in the “harvesting” of plant amino acids through digestion of seed storage proteins also involves a pre-formed defense strategy in that the seeds of several plant species accumulate storage proteins that are inhibitors of insect proteinases (Macedo et al. 2011). However, this aspect of defense is often reinforced by a wound-induced defensive response that involves regulatory roles for plant hormone systems and both local and system-wide induction of genes involved in “defense” responses to insects, including additional proteinase inhibitors (PIs) (Ryan 1990; Koiwa et al. 1997; Howe and Jander 2008). Plants with reduced ability to express PI genes in response to insect feeding, either because of mutations that impact PI structure or responses to hormonal or other plant signal networks, generally are impaired in their herbivore defense capability (Howe and Jander 2008). For example, tomato plants that are exposed to the tobacco hornworm, *Manduca sexta*, normally activate a wound-inducible set of defense genes, including those encoding PIs; however, a mutant tomato line with impaired synthesis of the octadecanoid-derived hormone jasmonic acid does not express the defense genes and suffers considerably more feeding damage. The authors (Howe et al. 1996) proposed the name “*defenseless1*” for this mutated tomato line.

16.4 Concluding Remarks and Future Perspectives

Based on the literature reviewed, we conclude that CSPs and OBPs are components of arthropod saliva that may mediate chemical communication between the organisms that participate in herbivory. These proteins may carry chemical cues of plant or epiphytic pathogen origin from the plant surface to the insect and have an effect on arthropod behavior and/or physiology. There is a great need for understanding the interactions between plant and arthropod macromolecules during feeding. We consider that the field of cheminformatics and molecular modeling can open new options for the discovery of chemical compounds that can target CSPs and OBPs. Finding molecules that interact and interfere with these proteins may elucidate their function *in vivo* and reveal whether they are involved in chemical communication or transport of plant molecules for their catabolism. We summarize in Table 16.1 the current knowledge about the occurrence of salivary CSPs at the transcript and protein levels in Arthropoda (Tree of Life Web Project 1995).

Table 16.1 Occurrence of chemosensory proteins (CSPs) and their coding genes in Arthropoda

Arthropoda				Salivary <i>csp</i> genes	Salivary CSPs		
Hexapoda	Collembola			?	?		
	Protura			?	?		
	Diplura			?	?		
	Insecta	Archaeognatha			?	?	
		Thysanura			?	?	
		Pterygota	Ephemeroptera			?	?
			Odonata			?	?
			Neoptera	Plecoptera		?	?
				Embiidina		?	?
				Phasmida		?	?
				Orthoptera		?	?
				Mantophasmatodea		?	?
				Zoraptera		?	?
				Dictyoptera		?	?
				Dermaptera		?	?
				Grylloblattodea		?	?
				Endopterygota	Hemipteroid assemblage	Psocodea	?!
		Thysanoptera	Yes			?	
		Hemiptera			Yes	Yes	
		Megaloptera			?	?	
		Raphidioptera			?	?	
		Neuroptera			?	?	
		Coleoptera			?!	?!	
	Strepsiptera		?		?		
	Diptera		Yes		Yes		
	Mecoptera		?		?		
	Siphonaptera		?	?			
	Trichoptera		?	?			
Lepidoptera		Yes	Yes				
Hymenoptera		Yes	Yes				
Crustacea				?!	?		
Paupoda				?	?		
Diplopoda				?!	?		
Chilopoda				?	?		
Symphyla				?	?		
Arachnida				No?	No?		
Xiphosura				?	?		
Pycnogonida				?	?		

Those groups highlighted in green indicate that phytophagy is present in one or more species in the group. ?=no information available; ?!=CSPs or their genes have been reported for the group but whether they are localized in salivary glands is unknown; No?=unclear assessment

Another topic that needs attention is the recurrent suggestion in the literature of protein passage from the hemocoel into salivary glands. Apolipoporphins and storage proteins have been considered hemolymph proteins reported in the soluble protein fraction of salivary glands or in saliva of several arthropod species (hemipteroids, lepidopterans). Chaudhary and collaborators (2015) have speculated that they may interfere with plant immune responses. However, the levels of these proteins were observed to be affected in immune-challenged insects (Freitak et al. 2007; Lourenço et al. 2009). Therefore, testing the role of apolipoporphins in either lipid transport or interference with plant lipoprotein metabolism is a plausible idea if indeed these proteins are moving from the hemocoel into the glands. Alternatively, are they transporting hydrophobic molecules from the plant to the insect for host detection/preference or relocating them in the animal body for detoxification?

The role of saliva during the interaction between gall-inducing arthropods and plants is unclear. Growth-inducing effectors or “auxin protectors” are claimed to be present in arthropod saliva but no evidence has been accumulated. Inspection of the sialotranscriptomes of gall-inducing arthropods other than the Cecidomyiids, e.g. the Cynipids and eriophyoid mites, will be of great value.

Finally, we consider that the study of the interaction between arthropod grazers and aquatic macrophytes is an interesting and virtually unexplored field. It would be intriguing to know how the profiles of the salivary proteomes of these aquatic or semiaquatic arthropods that feed on aquatic plants are in comparison to their terrestrial counterparts. Moreover, what is the defense response triggered in the aquatic plants? We have started to increase our knowledge on this matter; the total amount of phenolic compounds and plant toughness increase upon herbivory in the aquatic Eurasian water-milfoil, *Myriophyllum spicatum* (Fornoff and Gross 2014). Nevertheless, can we find homologues for CSPs and OBPs in aquatic lepidopterans that feed on aquatic plants?

There is a plethora of literature exploring how oral secretions from arthropods affect plant defense responses towards herbivory. We can conclude that there is no simple answer that allows us to summarize and understand whether plant responses are suppressed or induced by the phytophagous parasites. To a certain degree, the plant response towards pathogens and arthropods feeding on single-cells or vasculature displays similarities and differences when it is compared to plant responses to chewing herbivores. However, in natural conditions the plant is exposed to different biotic and abiotic stresses. We consider it important to study natural populations of phytophagous Arthropoda and the physiological stage of their host plants in the field.

References

- Akai H, Hakim RS, Kristensen NP (2003) Labial glands, silk and saliva. *Handb Zool* 4:377–388
- Alborn HT, Hansen TV, Jones TH, Bennett DC, Tumlinson JH, Schmelz EA, Teal PEA (2007) Disulfoxy fatty acids from the American bird grasshopper *Schistocerca Americana*, elicitors of plant volatiles. *Proc Natl Acad Sci U S A* 104:12976–12981

- Asadi A, Ghadamyari M, Sajedi RH, Sendi JJ, Tabari M (2010) Biochemical characterization of midgut, salivary glands and haemolymph α -amylases of *Naranga aenescens*. *B Insectol* 63:175–181
- Backus EA, Andrews KB, Shugart HJ, Greve LC, Labavitch JM, Alhaddad H (2012) Salivary enzymes are injected into xylem by the glassy-winged sharpshooter, a vector of *Xylella fastidiosa*. *J Insect Physiol* 58:949–959
- Barbosa AEAD, Albuquerque EVS, Silva MCM, Souza DSL, Oliviera-Neto OB, Valencia A, Rocha TL, Grossi-de-Sa MF (2010) α -Amylase inhibitor-1-gene from *Phaseolus vulgaris* expressed in *Coffea arabica* plants inhibits α -amylases from the coffee berry borer pest. *BMC Biotechnol* 10:44
- Benedetti M, Pontiggia D, Raggi S, Cheng Z, Scaloni F, Ferrari S, Ausubel FM, Cervone F, De Lorenzo G (2015) Plant immunity triggered by engineered in vivo release of oligogalacturonides, damage-associated molecular patterns. *Proc Natl Acad Sci U S A* 112:5533–5538
- Bergey DR, Orozco-Cardenas M, de Moura DS, Ryan CA (1999) A wound- and systemin-inducible polygalacturonase in tomato leaves. *Proc Natl Acad Sci U S A* 96:1756–1760
- Bos JIB, Prince D, Pitino M, Maffei ME, Win J, Hogenhout SA (2010) A functional genomics approach identifies candidate effectors from the aphid species *Myzus persicae* (green peach aphid). *PLoS Genet* 6(11)
- Brusca R (1997) Isopoda. Version 06 August 1997. <http://tolweb.org/Isopoda/6320/1997.08.06>. In: The Tree of Life Web Project, <http://tolweb.org/>
- Burton RL, Starks KJ, Sauer JR (1976) β -fructosidase activity in silk glands of *Heliothis zea*. *J Insect Physiol* 22:1045–1048
- Calvo E, Pham VM, Ribeiro JMC (2008) An insight into the sialotranscriptome of the non-blood feeding *Toxorhynchites amboinensis* mosquito. *Insect Biochem Mol Biol* 38:499–507
- Campanacci V, Lartigue A, Hallberg BM, Jones TA, Giudici-Orticoni MT, Tegoni M, Cambillau C (2003) Moth chemosensory protein exhibits drastic conformational changes and cooperativity on ligand binding. *Proc Natl Acad Sci U S A* 100:5069–5074
- Carroll MJ, Schmelz EA, Teal PEA (2008) The attraction of *Spodoptera frugiperda* neonates to cowpea seedlings is mediated by volatiles induced by conspecific herbivory and the elicitor inceptin. *J Chem Ecol* 34:291–300
- Celorio-Mancera MP, Powell AL, Allen ML, Ahmadi H, Salemi MR, Phinney BS, Shackel KA, Greve LC, Teuber LR, Labavitch JM (2008) Polygalacturonase causes lygus-like damage on plants: cloning and identification of western tarnished plant bug (*Lygus hesperus*) polygalacturonases secreted during feeding. *Arthropod Plant Interact* 2:215–225
- Celorio-Mancera MP, Greve LC, Teuber LR, Labavitch JM (2009) Identification of endo- and exopolygalacturonase activity in *Lygus hesperus* (Knight) salivary glands. *Arch Insect Biochem Physiol* 70:122–135
- Celorio-Mancera MP, Courtiade J, Muck A, Heckel DG, Musser RO, Vogel H (2011) Sialome of a generalist lepidopteran herbivore: identification of transcripts and proteins from *Helicoverpa armigera* labial salivary glands. *PLoS One* 6:e26676
- Celorio-Mancera MP, Sundmalm SM, Vogel H, Rutishauser D, Ytterberg AJ, Zubarev RA, Janz N (2012) Chemosensory proteins, major salivary factors in caterpillar mandibular glands. *Insect Biochem Mol Biol* 42:796–805
- Celorio-Mancera MP, Ytterberg AJ, Rutishauser D, Janz N, Zubarev RA (2015) Effect of host plant and immune challenge on the levels of chemosensory and odorant-binding proteins in caterpillar salivary glands. *Insect Biochem Mol Biol* 61:34–45
- Cervone F, Hahn M, De Lorenzo G, Darvill A, Albersheim P (1989) Host-pathogen interactions. XXXIII. A plant protein converts a fungal pathogenesis factor into an elicitor of defense responses. *Plant Physiol* 90:542–548
- Chapman RF (1995) Mechanisms of food handling by chewing insects. In: Chapman RF, de Boer G (eds) *Regulatory mechanisms in insect feeding*. Chapman and Hall, New York, pp 3–31

- Chaudhary R, Atamian HS, Shen ZX, Briggs SP, Kaloshian I (2015) Potato aphid salivary proteome: enhanced salivation using resorcinol and identification of aphid phosphoproteins. *J Proteome Res* 14:1762–1778
- Chen SA, Yang PC, Jiang F, Wei YY, Ma ZY, Kang L (2010) *De novo* analysis of transcriptome dynamics in the migratory locust during the development of phase traits. *PLoS One* 5:e15633
- Christoffersen ML, de Assis JE (2015) The crustacea volume 5 part A. In: Vaupel Klein C, Charmantier-Daures M, Schram F (eds) *Treatise on zoology – anatomy taxonomy biology*. Brill, Leiden, pp 5–75
- Coleman AD, Wouters RHM, Mugford ST, Hogenhout SA (2015) Persistence and transgenerational effect of plant-mediated RNAi in aphids. *J Exp Bot* 66:541–548
- Cragg SM (2003) Marine wood boring arthropods: ecology, functional anatomy, and control measures. In: Goodell B, Nicholas DD, Schultz TP (eds) *Wood deterioration and preservation: advances in our changing world*. American Chemical Society, Washington, pp 272–286
- Crozier A, Kamiya Y, Bishop G, Yokota T (2000) Biosynthesis of hormones and elicitor molecules. In: Buchanan BB, Gruissem W, Jones RL (eds) *Biochemistry and molecular biology of plants*. American Society of Plant Physiologists, Rockville, pp 915–919
- de Figueroa JMT, Trenzado CE, Lopez-Rodriguez MJ, Sanz A (2011) Digestive enzyme activity of two stonefly species (Insecta, Plecoptera) and their feeding habits. *Comp Biochem Physiol A* 160:426–430
- De Lillo E, Monfreda R (2004) ‘Salivary secretions’ of eriophyoids (Acari: Eriophyoidea): first results of an experimental model. *Exp Appl Acarol* 34:291–306
- de Sousa CM, Fontanetti CS (2012) Structure and function of the foregut and salivary glands of the synanthropic diplopod *Urostreptus atrobrunneus* (Spirostreptidae). *Anim Biol* 62:493–504
- De Vos M, Jander G (2009) *Myzus persicae* (green peach aphid) salivary components induce defence responses in *Arabidopsis thaliana*. *Plant Cell Environ* 32:1548–1560
- Dhar R, Kumar N (2003) Role of mosquito salivary glands. *Curr Sci* 85:1308–1313
- Diezel C, von Dahl CC, Gaquerel E, Baldwin IT (2009) Different lepidopteran elicitors account for cross-talk in herbivory-induced phytohormone signaling. *Plant Physiol* 150:1576–1586
- do Amaral JB, Machado-Santelli GM (2008) Salivary system in leaf-cutting ants (*Atta sexdens rubropilosa* Forel, 1908) castes: a confocal study. *Micron* 39:1222–1227
- Dobson HEM, Peng YS (1997) Digestion of pollen components by larvae of the flower-specialist bee *Chelostoma florissomne* (Hymenoptera: Megachilidae). *J Insect Physiol* 43:89–100
- D’Ovidio R, Raiola A, Capodicasa C, Devoto A, Pontiggia D, Roberti S, Galletti R, Conti E, O’Sullivan D, De Lorenzo G (2004) Characterization of the complex locus of bean encoding polygalacturonase-inhibiting proteins reveals subfunctionalization for defense against fungi and insects. *Plant Physiol* 135:2424–2435
- Edgerly JS, Rooks EC (2004) Lichens, sun, and fire: a search for an embiid-environment connection in Australia (Order Embiidina : Australembiidae and Notoligotomidae). *Environ Entomol* 33:907–920
- Ehrlich P, Raven P (1964) Butterflies and plants: a study in coevolution. *Evolution* 18:586–608
- El-Hifnawi E (1974) Salivary-glands of Diplopoda. 3. Anatomy and ultrastructure of diverting system. *Z Morphol Tiere* 77:221–233
- El-Hifnawi E, Seifert G (1973) Salivary-glands of diplopoda. 1. Topography and histology of salivary-glands in *Polyxenus lagurus*, *Craspedosoma rawlinsii* and *Schizophyllum sabulosum*. *Z Morphol Tiere* 74:323–348
- Elias-Santos D, Fialho MDQ, Vitorino R, Oliveira LL, Zanuncio JC, Serrao JE (2013) Proteome of the head and thorax salivary glands in the stingless bee *Melipona quadrifasciata anthidioides*. *Apidologie* 44:684–698
- Elzinga DA, De Vos M, Jander G (2014) Suppression of plant defenses by a *Myzus persicae* (Green Peach Aphid) salivary effector protein. *Mol Plant Microbe In* 27:747–756
- Fabres A, da Silva JDM, Fernandes KVS, Xavier J, Rezende GL, Oliveira AEA (2014) Comparative performance of the red flour beetle *Tribolium castaneum* (Coleoptera: Tenebrionidae) on different plant diets. *J Pest Sci* 87:495–506

- Felton GW, Tumlinson JH (2008) Plant-insect dialogs: complex interactions at the plant-insect interface. *Curr Opin Plant Biol* 11:457–463
- Felton GW, Chung SH, Gloria M, Hernandez E, Louis J, Peiffer M, Tian DL (2014) Herbivore oral secretions are the first line of protection against plant-induced defences. *Annu Plant Rev* 47:37–76
- Fornoff F, Gross EM (2014) Induced defense mechanisms in an aquatic angiosperm to insect herbivory. *Oecologia* 175:173–185
- Freitag D, Wheat CW, Heckel DG, Vogel H (2007) Immune system responses and fitness costs associated with consumption of bacteria in larvae of *Trichoplusia ni*. *BMC Biol* 5:56
- Giuliano-Perez D, Fontanetti C (2011) Assessment of the toxic potential of sewage sludge in the midgut of the diplopod *Rhinocricus padbergi*. *Water Air Soil Poll* 218:437–444
- Grbić M, Van Leeuwen T, Clark RM, Rombauts S, Rouzé P, Grbić V, Osborne EJ, Dermauw W, Ngoc PCT, Ortego F, Hernández-Crespo P, Diaz I, Martínez M, Navajas M, Sucena E, Magalhães S, Nagy L, Pace RM, Djuranović S, Smagghe G, Iga M, Christiaens O, Veenstra JA, Ewer J, Villalobos RM, Hutter JL, Hudson SD, Velez M, Yi SV, Zeng J, Pires-Da Silva A, Roch F, Cazaux M, Navarro M, Zhurov V, Acevedo G, Bjelica A, Fawcett JA, Bonnet E, Martens C, Baele G, Wissler L, Sanchez-Rodriguez A, Tirry L, Blais C, Demeestere K, Henz SR, Gregory TR, Mathieu J, Verdon L, Farinelli L, Schmutz J, Lindquist E, Feyereisen R, Van De Peer Y (2011) The genome of *Tetranychus urticae* reveals herbivorous pest adaptations. *Nature* 479:487–492
- Guiguet A, Dubreuil G, Harris MO, Appel HM, Schultz JC, Pereira MH, Giron D (2016) Shared weapons of blood- and plant-feeding insects: surprising commonalities for manipulating hosts. *J Insect Physiol* 84:4–21
- Habibi J, Backus EA, Coudron TA, Brandt SL (2001) Effect of different host substrates on hemipteran salivary protein profiles. *Entomol Exp Appl* 98:369–375
- Hammond-Kosack K, Jones JDG (2000) Responses to plant pathogens. In: Buchanan BB, Gruissem W, Jones RL (eds) *Biochemistry & molecular biology of plants*. American Society of Plant Physiologists, Rockville, pp 1135–1136
- Harpel D, Cullen DA, Ott SR, Jiggins CD, Walters JR (2015) Pollen feeding proteomics: salivary proteins of the passion flower butterfly, *Heliconius melpomene*. *Insect Biochem Mol Biol* 63:7–13
- Hattori M, Komatsu S, Noda H, Matsumoto Y (2015) Proteome analysis of watery saliva secreted by green rice leafhopper, *Nephotettix cincticeps*. *PLoS One* 10:e0123671
- Hessler RR, Elofsson R (2013) The crustacea volume 4 part A. In: Vaupel Klein C, Charmantier-Daures M, Schram F (eds) *Treatise on zoology – anatomy, taxonomy, biology*. Brill, Leiden, pp 91–97
- Hilken G, Rosenberg J (2006) Ultrastructural investigation of a salivary gland in a centipede: structure and origin of the maxilla I-gland of *Scutigera coleoptrata* (Chilopoda, Notostigmophora). *J Morphol* 267:375–381
- Hirayama C, Konno K, Wasano N, Nakamura M (2007) Differential effects of sugar-mimic alkaloids in mulberry latex on sugar metabolism and disaccharidases of Eri and domesticated silkworms: enzymatic adaptation of *Bombyx mori* to mulberry defense. *Insect Biochem Mol Biol* 37:1348–1358
- Howe GA, Jander G (2008) Plant immunity to insect herbivores. *Annu Rev Plant Biol* 59:41–66
- Howe GA, Lightner J, Browse J, Ryan CA (1996) An octadecanoid pathway mutant (JL5) of tomato is compromised in signaling for defense against insect attack. *Plant Cell* 8:2067–2077
- Iovinella I, Dani FR, Niccolini A, Sagona S, Michelucci E, Gazzano A, Turillazzi S, Felicioli A, Pelosi P (2011) Differential expression of odorant-binding proteins in the mandibular glands of the honey bee according to caste and age. *J Proteome Res* 10:3439–3449
- Iovinella I, Bozza F, Caputo B, Della Torre A, Pelosi P (2013) Ligand-binding study of *Anopheles gambiae* chemosensory proteins. *Chem Senses* 38:409–419
- James AA (2003) Blocking malaria parasite invasion of mosquito salivary glands. *J Exp Biol* 206:3817–3821

- Ji R, Yu HX, Fu Q, Chen HD, Ye WF, Li SH, Lou YG (2013) Comparative transcriptome analysis of salivary glands of two populations of rice brown planthopper, *Nilaparvata lugens*, that differ in virulence. PLoS One 8(11)
- Kim N, Choo YM, Lee KS, Hong SJ, Seol KY, Je YH, Sohn HD, Jin BR (2008) Molecular cloning and characterization of a glycosyl hydrolase family 9 cellulase distributed throughout the digestive tract of the cricket *Teleogryllus emma*. Comp Biochem Physiol B 150:368–376
- Kirsch R, Gramzow L, Theißen G, Siegfried BD, French-Constant RH, Heckel DG, Pauchet Y (2014) Horizontal gene transfer and functional diversification of plant cell wall degrading polygalacturonases: key events in the evolution of herbivory in beetles. Insect Biochem Mol Biol 52:33–50
- Koiwa H, Bressan RA, Hasegawa PM (1997) Regulation of protease inhibitors and plant defense. Trends Plant Sci 2:379–384
- Kostanjšek R, Štrus J, Avguštin G (2002) Genetic diversity of bacteria associated with the hindgut of the terrestrial crustacean *Porcellio scaber* (Crustacea: Isopoda). FEMS Microbiol Ecol 40:171–179
- Krenn HW, Plant JD, Szucsich NU (2005) Mouthparts of flower-visiting insects. Arthropod Struct Dev 34:1–40
- Liu F, Cui LW, Cox-Foster D, Felton GW (2004) Characterization of a salivary lysozyme in larval *Helicoverpa zea*. J Chem Ecol 30:2439–2457
- López-Rodríguez MJ, Trenzado CE, Tierno de Figueroa JM, Sanz A (2012) Digestive enzyme activity and trophic behavior in two predator aquatic insects (Plecoptera, Perlidae). A comparative study. Comp Biochem Physiol A 162:31–35
- Lourenço AP, Martins JR, Bitondi MMG, Simões ZLP (2009) Trade-off between immune stimulation and expression of storage protein genes. Arch Insect Biochem Physiol 71:70–87
- Ma N, Liu SY, Hua BZ (2011) Morphological diversity of male salivary glands in Panorpidae (Mecoptera). Eur J Entomol 108:493–499
- Macedo MLR, Freire MDM (2011) Insect digestive enzymes as a target for pest control. ISJ-Invertebrate Survival Journal 8:190–198
- Macedo MLR, Diz Filho EBS, Freire MCM, Oliva MLV, Sumikawa JT, Toyama MH, Marangoni S (2011) A trypsin inhibitor from *Sapindus saponaria* L. seeds: purification, characterization, and activity towards pest insect digestive enzyme. Protein J 30:9–19
- Maharaj PD, Widen SG, Huang J, Wood TG, Thangamani S (2015) Discovery of mosquito saliva microRNAs during CHIKV Infection. PLoS Neglect Trop D 9:19
- Mall SB, Singh AR, Dixit A (1978) Digestive enzymes of mature larva of *Atteva fabriciella* (Swed) (Lepidoptera, Yponomeutidae). J Anim Morphol Physiol 25:86–92
- Menta C, Garcia-Montero LG, Pinto S, Conti FD, Baroni G, Maresi M (2014) Does the natural microcosm created by *Tuber aestivum* affect soil microarthropods? A new hypothesis based on Collembola in truffle culture. Appl Soil Ecol 84:31–37
- Mika N, Zorn H, Ruhl M (2013) Insect-derived enzymes: a treasure for industrial biotechnology and food biotechnology. In: Vilcinskas A (ed) Yellow biotechnology II: insect biotechnology in plant protection and industry. Springer, Berlin, pp 1–17
- Mosbah A, Campanacci V, Lartigue A, Tegoni M, Cambillau C, Darbon H (2003) Solution structure of a chemosensory protein from the moth *Mamestra brassicae*. Biochem J 369:39–44
- Musser RO, Kwon HS, Williams SA, White CJ, Romano MA, Holt SM, Bradbury S, Brown JK, Felton GW (2005) Evidence that caterpillar labial saliva suppresses infectivity of potential bacterial pathogens. Arch Insect Biochem Physiol 58:138–144
- Nunez FS, Crawford CS (1976) Digestive enzymes of the desert millipede *Orthoporus ornatus* (Girard) (Diplopoda: Spirostreptidae). Comp Biochem Phys A 55:141–145
- Parthasarathy R, Gopinathan KP (2005) Comparative analysis of the development of the mandibular salivary glands and the labial silk glands in the mulberry silkworm, *Bombyx mori*. Gene Expr Patterns 5:323–339
- Pauchet Y, Heckel DG (2013) The genome of the mustard leaf beetle encodes two active xylanases originally acquired from bacteria through horizontal gene transfer. Proc R Soc Lond B: Biological Sciences 280(1763)

- Pauchet Y, Kirsch R, Giraud S, Vogel H, Heckel DG (2014) Identification and characterization of plant cell wall degrading enzymes from three glycoside hydrolase families in the cerambycid beetle *Apriona japonica*. *Insect Biochem Mol Biol* 49:1–13
- Pelosi P, Zhou JJ, Ban LP, Calvello M (2006) Soluble proteins in insect chemical communication. *Cell Mol Life Sci* 63:1658–1676
- Picimbon JF, Dietrich K, Angeli S, Scaloni A, Krieger J, Breer H, Pelosi P (2000) Purification and molecular cloning of chemosensory proteins from *Bombyx mori*. *Arch Insect Biochem Physiol* 44:120–129
- Powell ALT, van Kan J, ten Have A, Visser J, Greve LC, Bennett AB, Labavitch JM (2000) Transgenic expression of pear PGIP in tomato limits fungal colonization. *Mol Plant Microbe In* 13:942–950
- Rankin SM, Dossat HB, Garcia KM (1997) Effects of diet and mating status upon corpus allatum activity, oocyte growth, and salivary gland size in the ring-legged earwig. *Entomol Exp Appl* 83:31–40
- Rayner CJ, Langridge DF (1985) Amino-acids in bee-collected pollens from Australian indigenous and exotic plants. *Austral J Exp Agric* 25:722–726
- Ribeiro JMC (1995) Insect saliva: function, biochemistry and physiology. In: Chapman RF, De Boer G (eds) *Regulatory mechanism in insect feeding*. Chapman and Hall, New York, pp 74–97
- Ridley BL, O'Neill MA, Mohnen D (2001) Pectins: structure, biosynthesis and oligogalacturonide-related signaling. *Phytochemistry* 57:929–967
- Robert CAM, Erb M, Duployer M, Zwahlen C, Doyen GR, Turlings TCJ (2012) Herbivore-induced plant volatiles mediate host selection by a root herbivore. *New Phytol* 194:1061–1069
- Rodriguez PA, Stam R, Warbroek T, Bos JIB (2014) Mp10 and Mp42 from the aphid species *Myzus persicae* trigger plant defenses in *Nicotiana benthamiana* through different activities. *Mol Plant Microbe In* 27:30–39
- Rodriguez-Saona C, Crafts-Brandner SJ, Williams L, Pare PW (2002) *Lygus hesperus* feeding and salivary gland extracts induce volatile emissions in plants. *J Chem Ecol* 28:1733–1747
- Royalty RN, Perring TM (1996) Chapter 3.1 nature of damage and its assessment. In: Lindquist EE, Bruin J, Sabelis MW (eds) *Eriophyoid mites: their biology, natural enemies and control*. Elsevier, Amsterdam, pp 506–508
- Ryan CA (1990) Protease inhibitors in plants: genes or improving defenses against insects and pathogens. *Annu Rev Phytopathol* 28:425–449
- Sami AJ, Anwar MA, Rehman FU, Shakoori AR (2011) Digestive cellulose hydrolyzing enzyme activity (endo- β -1, 4-D-glucanase) in the gut and salivary glands of blister beetle, *Mylabris pustulata*. *Pak J Zool* 43:393–401
- Santamaría ME, González-Cabrera J, Martínez M, Grbic V, Castañera P, Díaz L, Ortego F (2015) Digestive proteases in bodies and faeces of the two-spotted spider mite, *Tetranychus urticae*. *J Insect Physiol* 78:69–77
- Schaefer HM, Ruxton GD (2011) Chemical communication by plants about herbivores. In: *Plant-animal communication*. Oxford University Press, Oxford, pp 187–204
- Schafer M, Fischer C, Meldau S, Seebald E, Oelmüller R, Baldwin IT (2011) Lipase activity in insect oral secretions mediates defense responses in *Arabidopsis*. *Plant Physiol* 156:1520–1534
- Schmelz EA, Engelberth J, Alborn HT, Tumlinson JH, Teal PEA (2009) Phytohormone-based activity mapping of insect herbivore-produced elicitors. *Proc Natl Acad Sci U S A* 106:653–657
- Schoonhoven LM, van Loon JJA, Dicke M (2005) *Insect-plant biology*. Oxford University Press, Oxford
- Shackel KA, Celorio-Mancera MP, Ahmadi H, Greve LC, Teuber LR, Backus EA, Labavitch JM (2005) Micro-injection of *Lygus* salivary gland proteins to simulate feeding damage in alfalfa and cotton flower. *Arch Insect Biochem Physiol* 58:69–83

- Sharma A, Khan AN, Subrahmanyam S, Raman A, Taylor GS, Fletcher MJ (2014) Salivary proteins of plant-feeding hemipteroids – implication in phytophagy. *Bull Entomol Res* 104:117–136
- Sharrock KR, Labavitch JM (1994) Polygalacturonase inhibitors of Bartlett pear fruits: differential effects on *Botrytis cinerea* polygalacturonase isozymes, and influence on products of fungal hydrolysis of pear cell walls and on ethylene induction in cell culture. *Physiol Mol Plant Pathol* 45:305–319
- Shimomura M, Minami H, Suetsugu Y, Ohyanagi H, Satoh C, Antonio B, Nagamura Y, Kadono-Okuda K, Kajiwara H, Sezutsu H, Nagaraju J, Goldsmith MR, Xia Q, Yamamoto K, Mita K (2009) KAIKObase: an integrated silkworm genome database and data mining tool. *BMC Genomics* 10:486
- Srivastava US (1959) The maxillary glands of some Coleoptera. *Proc Royal Entomol Soc Lond General Entomol A* 34:57–62
- Stafford-Banks CA, Rotenberg D, Johnson BR, Whitfield AE, Ullman DE (2014) Analysis of the salivary gland transcriptome of *Frankliniella occidentalis*. *PLoS One* 9:e94447
- Stuart JJ, Chen MS, Shukle R, Harris MO (2012) Gall midges (Hessian flies) as plant pathogens. *Annu Rev Phytopathol* 50:339–357
- Thorp JH (2009) Chapter 14 – Arthropoda and related groups. In: Resh VH, Cardé RT (eds) *Encyclopedia of insects*. Academic, San Diego, pp 50–56
- Tong XW, Chen B, Huang LH, Feng QL, Kang L (2015) Proteomic analysis reveals that COP9 signalosome complex subunit 7A (CSN7A) is essential for the phase transition of migratory locust. *Sci Rep* 5:12542
- Tree of Life Web Project (1995) Arthropoda. Version 01 January 1995 (temporary). <http://tolweb.org/Arthropoda/2469/1995.01.01> in The Tree of Life Web Project. <http://tolweb.org/>
- Tsai JR, Lin HC (2014) Functional anatomy and ion regulatory mechanisms of the antennal gland in a semi-terrestrial crab, *Ocypode stimpsoni*. *Biol Open* 3:409–417
- Tu XB, Wang J, Hao K, Whitman DW, Fan YL, Cao GC, Zhang ZH (2015) Transcriptomic and proteomic analysis of pre-diapause and non-diapause eggs of migratory locust, *Locusta migratoria* L (Orthoptera: Acridoidea). *Sci Rep* 5:11402
- Vegliante F, Hasenfuss I (2012) Morphology and diversity of exocrine glands in lepidopteran larvae. *Annu Rev Entomol* 57:187–204
- Vieira FG, Rozas J (2011) Comparative genomics of the odorant-binding and chemosensory protein gene families across the Arthropoda: origin and evolutionary history of the chemosensory system. *Genome Biol Evol* 3:476–490
- Walker GP (2009) Salivary glands. In: Resh VH, Cardé RT (eds) *Encyclopedia of insects*. Academic Press, Amsterdam, pp 897–901
- Walling LL (2000) The myriad plant responses to herbivores. *J Plant Growth Regul* 19:195–216
- Weech MH, Chapleau M, Pan L, Ide C, Bede JC (2008) Caterpillar saliva interferes with induced *Arabidopsis thaliana* defence responses via the systemic acquired resistance pathway. *J Exp Bot* 59:2437–2448
- Wilson EO (1988) The diversity of life. In: de Blij HJ (ed) *Earth '88: changing geographic perspectives*. National Geographic Society, Washington, pp 68–78
- Wisessing A, Engkagul A, Wongpiyasatid A, Choowongkamon K (2010) Biochemical characterization of the alpha-amylase inhibitor in mungbeans and its application in inhibiting the growth of *Callosobruchus maculatus*. *J Agric Food Chem* 58:2131–2137
- Zhang LL, Xu J, Xiao HJ, Lu YH, Liang GM, Zhang YJ, Wu KM (2015) Molecular characterization and expression profiles of polygalacturonase genes in *Apolygus lucorum* (Hemiptera: Miridae). *PLoS One* 10:11

Chapter 17

Glandular Matrices and Secretions: Blood-Feeding Arthropods

Ben J. Mans

Abstract Blood-feeding evolved independently in various arthropod lineages and this is evident in the compositions of the secretory component of their salivary gland transcriptomes (sialomes). Salivary gland-derived secretory proteins modulate the vertebrate host's defenses (hemostatic and immune responses) and assist the hematophagous arthropod to successfully obtain a blood meal. Salivary proteins not only modulate host defenses, but also assist in the creation of a feeding site, or hematoma, by secretion of enzymes that can remodel the host's dermis extracellular matrix. The host's extracellular matrix also plays an important role in the initiation of hemostatic and inflammatory responses and blood-feeding arthropods have evolved molecules that specifically interfere with these responses. As such, vector-host interaction may be seen as interplay between the vertebrate host's extracellular matrix and the salivary-derived "extra-cellular matrix" of the arthropod. Our understanding of this interplay is still rudimentary given the fact that we do not know the functions of the majority of secretory proteins in all sialomes. The rapid expansion of sialome diversity as discovered with next-generation technologies contributes towards this, but also holds the promise that we will be able to grasp the structure of the sialoverse in the future.

17.1 Introduction

Arthropods are one of the most diverse lineages in the Tree of Life and have occupied the majority of environmental and nutritional niches available to complex organisms. This includes being scavengers, predators, farmers, pollinators, soldiers and parasites. Arthropod parasites may be endo or ectoparasitic (parasitism occurs outside the host), the latter associated with blood-feeding arthropods. Hematophagy (blood-feeding) evolved at least 20 times independently within the Arthropoda and all lineages found similar but unique strategies to address the same problem,

B.J. Mans (✉)

Parasites, Vectors and Vector-borne Diseases, Onderstepoort Veterinary Institute,
Agricultural Research Council, Onderstepoort 0110, Pretoria, South Africa
e-mail: MansB@arc.agric.za

i.e. feeding at the vector-host interface while modulating host defenses (Ribeiro 1995; Carvalho et al. 2010; Mans 2011). In the light of multiple independent events for the evolution of blood-feeding behavior, it is prudent to review the history of various arthropod lineages to appreciate the sheer extent of convergence and the background from which each lineage adapted to blood-feeding (Fig. 17.1).

Arthropods are composed of four major lineages, the Chelicerata, Crustacea, Myriapoda and Hexapoda (Fig. 17.1), that shared a common ancestor ~550 million years ago (MYA), coinciding with the origins of the vertebrate circulatory system (Doolittle and Feng 1987; Edgecombe and Legg 2014). All lineages are considered monophyletic, except for the Crustacea which is paraphyletic, due the Hexapoda that seem to derive from a crustacean ancestor (Edgecombe and Legg 2014). Of these, the Myriapoda (centipedes and millipedes) is the only lineage in which blood-feeding behavior did not evolve, although centipedes can bite and secrete venom into vertebrates. Centipede venom possess several components that will affect the extracellular matrix (ECM) of the host, notably chitinase, hyaluronidase, metalloprotease and serine protease activity. The majority of the protein families observed are, however, unique attesting to the independent origins of the predatory lifestyle of centipedes (Undheim et al. 2014).

The Chelicerata are composed of Pycnogonida (sea spiders), Xiphosura (horseshoe crabs) and Arachnida (harvestmen, hooded tick spiders, microwhip scorpions, mites, pseudoscorpions, scorpions, spiders and sun spiders). Like centipedes, the venoms of arachnids such as spiders and scorpions possess hyaluronidases, metalloproteases and serine proteases that targets the ECM of the vertebrate host (Kuhn-Nentwig et al. 2011; Fry et al. 2009). However, these non-blood feeding chelicerates are outside the scope of the current review. Blood-feeding evolved at least three times in the Chelicerata, all in the Acari: Once within the trombidiform mites (Acariformes) (Bochkov et al. 2008), once within the ticks (Parasitiformes: Ixodida) (Mans et al. 2011, 2012) and once, but probably multiple times in the dermanyssid mites (Parasitiformes: Mesostigmata) (Radovsky 1969).

The Crustaceans are composed of a diverse array of organisms that include crabs, crayfish, krill, lobsters, shrimps, woodlice and tongue worms. Blood-feeding behavior evolved at least three times in the Crustacea, in copepods (Copepoda) and isopods (Malacostraca) that parasitize fishes, and tongue worms (Pentastomida) that parasitize mammals and reptiles (Klomp maker and Boxhall 2015). Very little is known regarding the blood-feeding biology and the molecular mechanisms underlying parasite-host interactions of these crustaceans (Eichner et al. 2008), and will not be further discussed.

The Hexapoda (Insecta) include the alder flies, bark lice, beetles, butterflies and moths, snake flies, fleas, lacewings, wasps, true flies, thrips, true bugs, true lice and twisted wings. Blood-feeding evolved several times in the insects, once in fleas (Siphonaptera), once in the true lice (Phthiraptera), once in the bedbugs (Hemiptera: Cimicidae), probably twice in the triatomines (Hemiptera: Reduviidae), at least five times in the Nematocera (Diptera) and five times in the Brachycera (Diptera) and once in moths (Lepidoptera: Calyptra) (Ribeiro et al. 2010a; Schofield and Galvão 2009; Grimaldi and Engel 2010; Mans 2011; Hwang and Weirauch 2012). The pos-

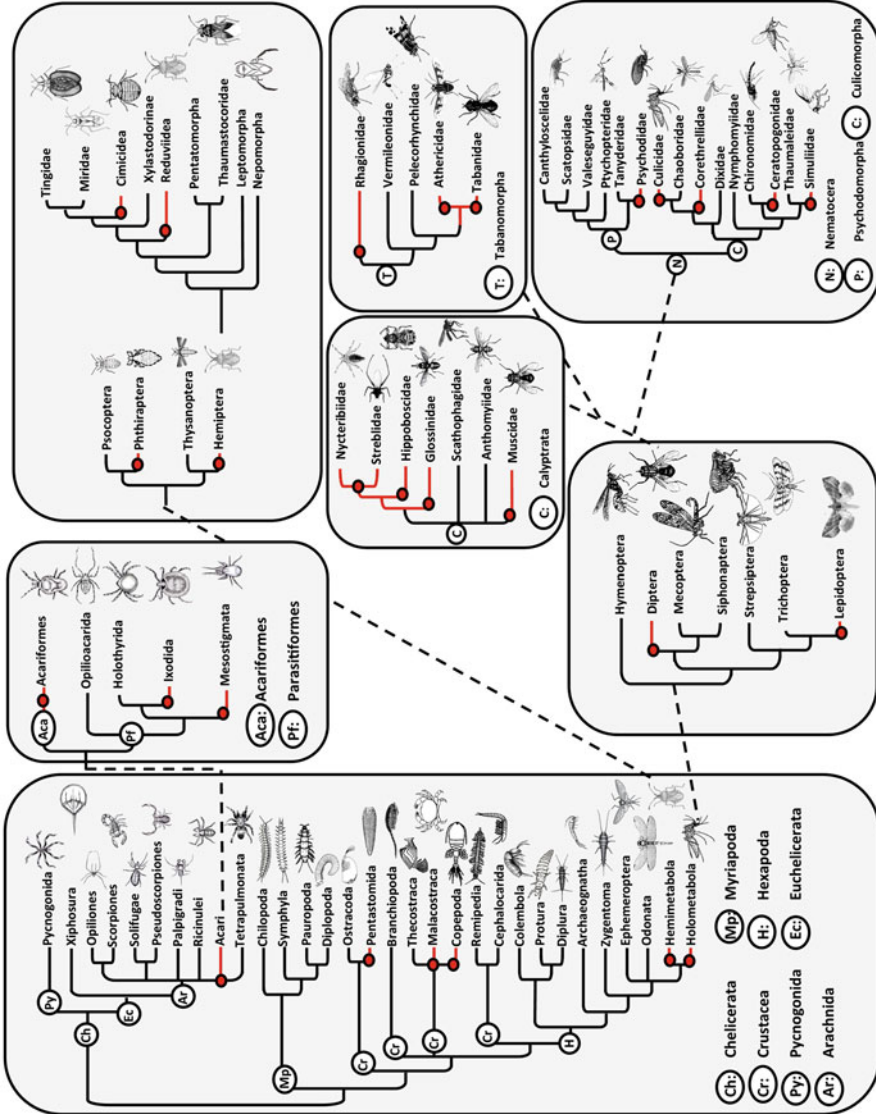


Fig. 17.1 Evolution of blood-feeding behavior in arthropods. Red branches indicate hematophagous lineages and red dots hypotheses regarding independent evolution of blood-feeding. Systematic relationships are indicated for arthropods (Giribet and Edgecombe 2012), Acari (Klompen et al. 2007) and the Hexapoda (Grimaldi and Engel 2010)

sibility that blood-feeding evolved only once in triatomines, nematocera and brachycera, respectively, has also been considered (Weirauch and Munro 2009; Grimaldi and Engel 2010; Patterson and Gaunt 2010; Ribeiro et al. 2010a; Hwang and Weirauch 2012).

Blood-feeding is estimated to have evolved at different periods for different lineages. Within the chelicerates (Acari) it has been estimated to have evolved ~320–290 MYA in ticks (Mans et al. 2011, 2012), ~37 MYA in trombiculid mites (Shatrov and Kudryashova 2006; Jeyaprakash and Hoy 2009) and <65 MYA in the *Dermanyssina* (Klompfen et al. 2007). Blood-feeding in the acariformes and mesostigmata therefore only evolved after radiation of the major extant mammalian lineages that occurred 65 MYA, while ticks evolved blood-feeding during the time of diversification of diapsid, synapsid reptiles and tetrapods that preceded modern reptiles, dinosaurs and mammals (Mans et al. 2012). The majority of insects including cimicid bugs, fleas, lice, nematoceran flies and some brachycerans (Rhagionidae, Tabanidae) evolved blood-feeding in the Late Jurassic–Early Cretaceous (250–150 MYA). The moths and some brachycerans (Calyptera) evolved blood-feeding much later in the Tertiary (<65 MYA) (Grimaldi and Engel 2010). While the Reduviidae are old with fossils and molecular clock analysis placing their origin at >175 MYA, the origin of blood-feeding lineages seem to have occurred only in the Oligocene or Miocene (~12–32 MYA) (Patterson and Gaunt 2010; Hwang and Weirauch 2012; Ibarra-Cerdeña et al. 2014).

The vertebrate circulatory system evolved at least 450 MYA and this was well established in its current form by the time that mammal and avian lineages had diverged by ~250 MYA (Doolittle and Feng 1987; Ribeiro et al. 2015c). The vertebrate blood system was therefore present at the times that major arthropod lineages originated and diverged. Blood-feeding evolved not because a new food niche was established, but perhaps as the inevitable consequence of the availability of an accessible diet in the form of the vertebrate blood system. This food source can replenish itself on a regular basis, providing a virtually unlimited source of nutrients there for the taking, if host defenses can be neutralized. Blood-feeding arthropods evolved extensive repertoires of salivary gland-derived molecules that can modulate host immune responses and the diversity observed in these sialomes (molecules secreted during feeding) are testament to the convergent evolution that occurred in the face of a common goal, to obtain a blood-meal (Mans 2011).

17.2 The Vector-Host Interphase

Interaction with the vertebrate host occur via the skin. To access a blood-meal, arthropods has to breach the vertebrate skin by cutting, piercing or biting. The manner in which the skin is broken determine the depth of penetration and the extent of damage caused by the arthropod as well as its interaction with the vertebrate ECM (Fig. 17.2). The mouthparts of all blood-feeding arthropods have evolved in unique

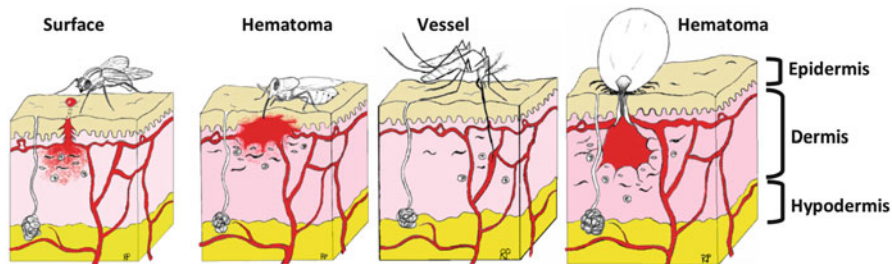


Fig. 17.2 Different modes of feeding and creation of the hematoma in insects and ticks. Indicated are surface feeders, insects that create a hematoma just beneath the epidermis, insects that feed from a blood vessel and ticks that create a larger hematoma in the dermis

ways to allow rupture of the host's skin. In insects all piercing–sucking mouthparts evolved from mandibles, maxillae and the laciniae, while in arachnids it evolved from the chelicerae and a unique organ in ticks, the hypostome (Krenn and Aspöck 2012).

The simplest and perhaps most primitive manner of feeding is biting, cutting or scraping of the host skin from which blood then oozes and is sucked up. This behavior is found in snipe flies (Rhagionidae) (Nagatomi and Soroida 1985). Arthropods may also cut, pierce or tear the skin and insert a proboscis in the case of insects or a hypostome in the case of ticks. During initial feeding, the arthropod may move the proboscis or hypostome up and down in a probing manner. This continued movement accompanied by cutting, ruptures cells and capillary vessels forming a site of injury into which cellular fluids and blood collect, called a hematoma (Ribeiro 1995). Some arthropods will expand this hematoma by secreting matrix modifying enzymes, anti-hemostatic and anti-inflammatory molecules to ensure a constant accumulation of blood. Secretion of saliva also reduce probing time allowing for shorter host interaction periods (Ribeiro and Garcia 1981; Ribeiro 2000).

For arthropods with short mouthparts, the hematoma forms under the epidermis and this is found in biting midges (Ceratopogonidae) (McKeever et al. 1988), black flies (Simuliidae), some mosquitoes (Culicidae), deer and horse flies (Tabanidae), some louse flies (Hippoboscidae), tsetse flies (Glossinidae), sand flies (Psychodidae) and stable flies (Stomoxinae) (Krenn and Aspöck 2012).

Some insects have long piercing proboscis or stylets that they use to probe, find and insert directly into a blood vessel to obtain blood. This feeding mechanism is observed in assassin bugs (Reduviidae), bed bugs (Cimicidae), fleas (Anoplura and Siphonaptera), lice (Phthiraptera), some louse flies (Hippoboscidae) and mosquitoes (Culicidae) (Krenn and Aspöck 2012).

In the case of ticks, their hypostomes may be short or long and the hematoma may be formed at different depths. All hypostomes have serrated teeth and cutting into the skin will cause significant damage to the tissues around it (Sonenshine 1991; Coons and Alberti 1999; Sonenshine and Roe 2014). The length of the hypostome depends on the life stage of the tick, with larvae generally having mouthparts ~50–100 μm , while nymphs may be similar or twice as long, and adults

ranging from 200 to 1200 μm (Kröber and Guerin 2007). Some genera (*Dermacentor*, *Rhipicephalus*, *Haemaphysalis*) have very short mouthparts and rarely penetrate below the epidermis. The average thickness of the epidermis may be 50 μm and the hypostome may only extend into the Malpighian layer (stratum basale) (Moorhouse and Tatchell 1966). Depth of penetration in this case does not depend on the length of the hypostome since all life stages reach the same depth. These ixodids secrete copious amounts of cement that encapsulate the hypostome and help to anchor it and may extend into the dermis, where the hematoma is formed. A significant part of the cement cone may form on the surface of the feeding site, which may explain the uniformity of penetration (Moorhouse and Tatchell 1966). For ticks with longer mouthparts, the hypostome may extend well into the dermis and for metastrates in this group (*Amblyomma*, *Hyalomma*) can form large cement cones deep in the skin, with little cement on the surface (Moorhouse and Tatchell 1966; Balashov 1972; Kemp et al. 1982). The cement binds tightly with components of the epidermis and dermis and are usually left behind after feeding is completed (Moorhouse and Tatchell 1966). Prostrates (*Ixodes*) may or may not secrete cement, depending on the species (Balashov 1972). Argasids and the Nuttalliellidae does not secrete cement during feeding, but it has been argued that the larvae may secrete cement (Mans et al. 2012).

17.3 The Host Skin and Defense Responses

The vertebrate skin serves as first line of defense to foreign invasion and is the primary site of interaction with ecto-parasites. Skin differs in thickness between species and body location, but all are composed of the epidermis (outer layer), the dermis and the hypodermis, the latter composed of a fat layer for body insulation. The epidermis may be a thick keratinized, stratified, squamous epithelium composed of five layers or may lack some of the layers and be thinner. The layers include at the bottom, the stratum basale that lies on a basement membrane that separate the epidermis and dermis, followed by the stratum spinosum, stratum granulosum, stratum lucidum and stratum corneum (the upper layer composed of dead keratinized cells) (Lai-Cheong and McGrath 2009). The dermis contains the blood and lymphatic vessels, nerves, sweat glands and connective tissue. The connective tissue may contain both loose and dense irregular connective tissue (Xue and Jackson 2015). Blood-feeding arthropods will predominantly interact with the epidermis and dermis, where blood vessels are located and lacerated, where the hematoma forms and where inflammation occurs as a response to feeding (Fig. 17.2). The dermis may be considered as an extensive ECM of connective tissue traversed by blood and lymphatic vessels. During inflammation, immune cells traverse the blood and lymphatic vessel walls and enter the ECM. Inflammatory reactions including edema, pain, itching and swelling also occurs within the ECM and it may therefore be considered that vector-host interactions are primarily an interplay between the

vertebrate ECM found in the dermis and the salivary gland derived “ECM” of the blood-feeding arthropod.

The connective tissue in the dermis ECM is composed of a variety of proteins including collagens, elastin, fibrillin, fibronectin, vitronectin, laminins, thrombospondins, tenascins, osteonectin, and a variety of proteoglycans and polysaccharides such as hyaluronic acid (Bosman and Stamenkovic 2003; Xue and Jackson 2015). Together these form a complex network that function as structural scaffold that supports blood and lymphatic vessels. Cells regularly found within the dermis includes adipocytes, fibroblasts and macrophages. The components of the ECM not only play a structural role, but function in wound healing, hemostasis, cell interaction and cell migration (Bosman and Stamenkovic 2003; Xue and Jackson 2015).

The feeding time of insects are short (seconds to minutes), while those of nymphal and adult soft ticks (*Argasidae*) are generally within minutes or rarely hours (Balashov 1972). *Argasid* larvae may not feed at all, or feed for short (minutes) or long periods (4–7 days) depending on the species (Balashov 1972; Sonenshine 1991). The life stages of all hard ticks (*Ixodidae*) feed for prolonged periods that may last from 4 to 12 days and is characterized by a slow feeding phase of several days, followed by a rapid engorgement phase that generally take 1–2 days (Balashov 1972; Sonenshine 1991). This imply that short and long feeders will interact with the ECM to different extents. Short feeders need to establish a hematoma as fast as possible, while long feeders such as ixodids, can progressively modify the hematoma in preparation for the fast feeding event. Because ixodids feed so long, they have to deal with the cutaneous wound healing responses of the host as well as cellular immune responses (Francischetti et al. 2005a, 2009). The wound healing process may be divided into three main phases: the inflammatory phase, the proliferative phase and the remodeling phase (Xue and Jackson 2015). Short feeders only deal with the inflammatory phase, while ixodids and *argasid* larvae have to face the proliferative and remodeling phases as well.

The inflammatory phase spans the first 5 days after injury and is initiated at the moment of injury or the start of feeding for arthropods. The peak of this response occurs within minutes to hours and includes the immediate arrest of blood-loss via the hemostatic system (blood clotting cascade, platelet aggregation and vasoconstriction) and innate immune responses facilitated by the infiltration of basophils, macrophages, monocytes and neutrophils into the site of injury (McCarty and Percival 2013; Xue and Jackson 2015). The proliferative phase follows and starts from day 2–3 and may last up to 10 days. This phase is characterized by intense proliferation of endothelial cells, fibroblast accumulation, collagen and matrix metalloprotease synthesis that leads to re-epithelialization, ECM formation, angiogenesis and removal of the blood clot and scab. Angiogenesis, the formation of new capillary blood vessels, play an important role by providing nutrients to the proliferating cells and for synthesis of the ECM components (McCarty and Percival 2013; Xue and Jackson 2015). The remodelling phase occurs from day eight and may last up to 14 days to months depending on the damage. This is characterized by collagen accumulation, remodelling of the ECM, wound contraction, cross-linking of collagen fibers and scar formation (McCarty and Percival 2013; Xue and Jackson 2015).

Most ixodids will complete feeding before the start of this phase and do not need to deal with this. However, one-host ticks such as members of the former genus *Boophilus* (syn. *Rhipicephalus*) and two-host ticks (some *Hyalomma* and *Rhipicephalus* species) that complete all or two life stages while attached to the host will need to deal with this phase, since they may feed up to 14–28 days (Balashov 1972; Sonenshine 1991).

17.4 Arthropod Modelling of the Host Matrix

One of the aims of the formation of the hematoma is the generation of a space into which blood can collect in sufficient volumes to satisfy the needs of the feeding arthropod. For some arthropods that feed directly from blood vessels, formation of the hematoma is not that important. However, for others that needs pooled blood, formation of the hematoma must be accompanied by changes in the vertebrate ECM. The probing phase of feeding is important, since this period allow arthropods to explore the dermis, find and rupture blood vessels and determine whether the site is suitable for the formation of the hematoma (Friend and Smith 1977). Probing accompanied by secretion of saliva also allows arthropods to dispense adequate quantities of bioactive components into the surrounding environment to attain a localized area in which the host's defense mechanisms can be modulated. In ticks this is taken even further by aggregation behavior during feeding, that allows multiple ticks to feed within the same vicinity, thereby contributing *en masse* to suppression of host defenses over a much larger area of feeding (Sonenshine 2004). Male ticks that do not in general feed to repletion, also show co-feeding and aggregation behavior aimed at the creation of a communal feeding foci, by secretion of saliva into the feeding site (Wang et al. 1998). It may not be surprising that several molecules secreted by blood-feeding arthropods can directly remodel the ECM of the dermis or interfere with ECM function. While no specific protease directed against collagen has been identified in saliva or salivary glands of any hematophagous arthropods (Francischetti et al. 2003), other enzymes such as hyaluronidases, metalloproteases and chitinases have been identified.

17.4.1 Hyaluronidases

Hyaluronidases are generally found in arthropod venoms where they act as spreading factors to increase dissemination of venom at the bite site (Kreil 1995). In blood-feeding they act to “spread” anti-hemostatic and immune-modulators and increase the feeding site since hyaluronic acid confers the majority of the permeability characteristics to the ECM of the dermis due its hydrodynamic properties (Toole 2000). Hyaluronidase is present in the saliva of the argasid *Ornithodoros savignyi* and the ixodid *Amblyomma hebraeum* (Neitz et al. 1978). It was found in

a number of blood-feeding insects (Charlab et al. 1999; Ribeiro et al. 2000, 2004a; Cerná et al. 2002; Campbell et al. 2005; Volfova et al. 2008). This includes biting midge (*Culicoides kibunensis*, *Cu. sonorensis*), blackflies (*Eusimilium latipes*, *Odagmia ornata* and *Simulium vittatum*), cat flea (*Ctenocephalides felis*), deer fly (*Chrysops viduatus*), horse fly (Xu et al. 2008), mosquito (*Culex quinquefasciatus*), frog biting midges and sand fly (*Lutzomyia longipalpis*, and *Phlebotomus duboscqi*, *Ph. halepensis*, *Ph. papatasi*, *Ph. perniciosus* and *Ph. sergenti*) (Ribeiro et al. 2014a). Substrate specificity indicate that sandfly hyaluronidases are similar to that of Hymenoptera venom and mammalian sperm that functions as endo-N-acetylhexosaminidases (Cerná et al. 2002). Interestingly, no activity was found in the kissing bug (*Rhodnius prolixus*), mosquitoes (*Aedes aegypti* and *Anopheles stephensi*), tsetse fly (*Glossina fuscipes*), stable fly (*Stomoxys calcitrans*) and human louse (*Pediculus humanus*) (Ribeiro et al. 2000; Volfova et al. 2008). The majority of these do not feed from hematomas but either cannulate blood vessels (kissing bugs and mosquitoes) or feed by cutting the skin and feeding from shallow hematomas (tsetse fly, stable fly). Not all blood-feeding arthropods may therefore need extensive ECM remodeling. It should be noted that hyaluronidase transcripts have been found in salivary gland transcriptomes of the tsetse fly *G. morsitans morsitans* (Alves-Silva et al. 2010), so the ability to remodel the ECM may be species dependent.

17.4.2 Proteases

A variety of proteases have been identified in salivary gland transcriptomes. These include serine proteases in assassin bugs (Amino et al. 2001; Santos et al. 2007; Assumpção et al. 2008, 2012a; Kato et al. 2010; Bussacos et al. 2011a; Schwarz et al. 2014), bed bugs (Francischetti et al. 2010), biting midges (Russell et al. 2009), black flies (Andersen et al. 2009; Chagas et al. 2011), horse flies (Ribeiro et al. 2015a), mosquitoes (Calvo et al. 2009a, 2010a), stable flies (Wang et al. 2009), tsetse flies (Alves-Silva et al. 2010) and ticks (Nene et al. 2002; Ribeiro et al. 2006, 2011; Batista et al. 2008; Francischetti et al. 2008a). While the molecular function of most of these proteases has not been elucidated yet, it is likely that they function in ECM remodeling. In some cases, serine proteases have been implicated in the activation of plasminogen or protein C that will result in anti-inflammatory or anticoagulant activity (Pichu et al. 2014). An interesting case of a non-trypsin-like serine protease is that of longistatin, a double-domain EF-hand protein from the hard tick *Haemaphysalis longicornis*, which activates plasminogen and exhibits serine protease activity (Anisuzzaman et al. 2010, 2011, 2012), with the implication that other protein families may also exhibit protease activity that can affect the ECM.

In both hard and soft tick sialomes extensive expansion of the metalloproteases have been observed, which is not seen in insect sialomes (Mans 2011; Mans et al. 2008a, 2016). The majority of tick metalloproteases have no known function. However, metalloproteases that acts as fibrin(ogen)lytic enzymes targeting both

fibrinogen and fibrin have been characterized in the ixodid *Ixodes scapularis* (Francischetti et al. 2003). Another metalloprotease was shown to degrade integrin $\alpha_5\beta_1$ but not $\alpha_v\beta_5$, $\alpha_v\beta_3$, $\alpha_9\beta_1$ and $\alpha_2\beta_1$ (Francischetti et al. 2005a). In this role it inhibits angiogenesis and endothelial cell proliferation and would directly affect the inflammatory and proliferative phase of wound healing, since $\alpha_5\beta_1$ is the receptor for fibronectin that plays a central role in angiogenesis (Kim et al. 2000).

17.4.3 Chitinases

Cement is secreted in soluble form, but hardens once secreted into the feeding site and interact strongly with the vertebrate ECM (Moorhouse and Tatchell 1966; Sonenshine 1991). Chitinase secreted during tick feeding, may play an important role in maintaining the integrity of cement or during its formation (Kim et al. 2014). Suppression of chitinase expression led to ticks that can easily detach, while the feeding site were prone to bleeding (Kim et al. 2014). The cement cone is composed of glycine and proline rich proteins, lipoproteins in the core of the sheath and glycoproteins on the outside (Moorhouse and Tatchell 1966; Maruyama et al. 2010). There is not much evidence for the presence of D-N-acetylglucosamine, the building block of chitin, in the cement cone. However, D-N-acetylglucosamine is one of the building blocks of hyaluronan in the vertebrate dermis. The chitin-binding domain of human chitinase can bind to hyaluronan (Ujita et al. 2003). The structure of bee venom hyaluronidase is also similar to that of bacterial chitinase (Marković-Housley et al. 2000). The probability that tick chitinase remove or remodel hyaluronan to allow tick cement to bind and interact with the connective tissue should be considered (Lee et al. 2011). Similarly, a large number of proteins with chitin-binding domains exist in tick salivary transcriptomes. These most probably play an important role in interacting with the vertebrate ECM. Similarly, chitinases are found in salivary transcriptomes from biting midges (Campbell et al. 2005), frog biting midges (Ribeiro et al. 2014a) and mosquitoes (Calvo et al. 2004, 2009a, 2010a; Ribeiro et al. 2004a).

17.5 Arthropod Modulation of Host Defenses

Beyond modeling of the vertebrate ECM contained in the dermis, arthropods secrete a variety of molecules that do not specifically interact with the ECM of the dermis itself, but targets vertebrate defense mechanisms such as the hemostatic and immune systems that do interact with the ECM (Fig. 17.3). This ensures that blood does not clot and platelets do not aggregate within the hematoma and ECM and impede blood-feeding. This also assists in shortening the probing time of blood-feeding insects before they find a blood vessel (Ribeiro et al. 1984a).

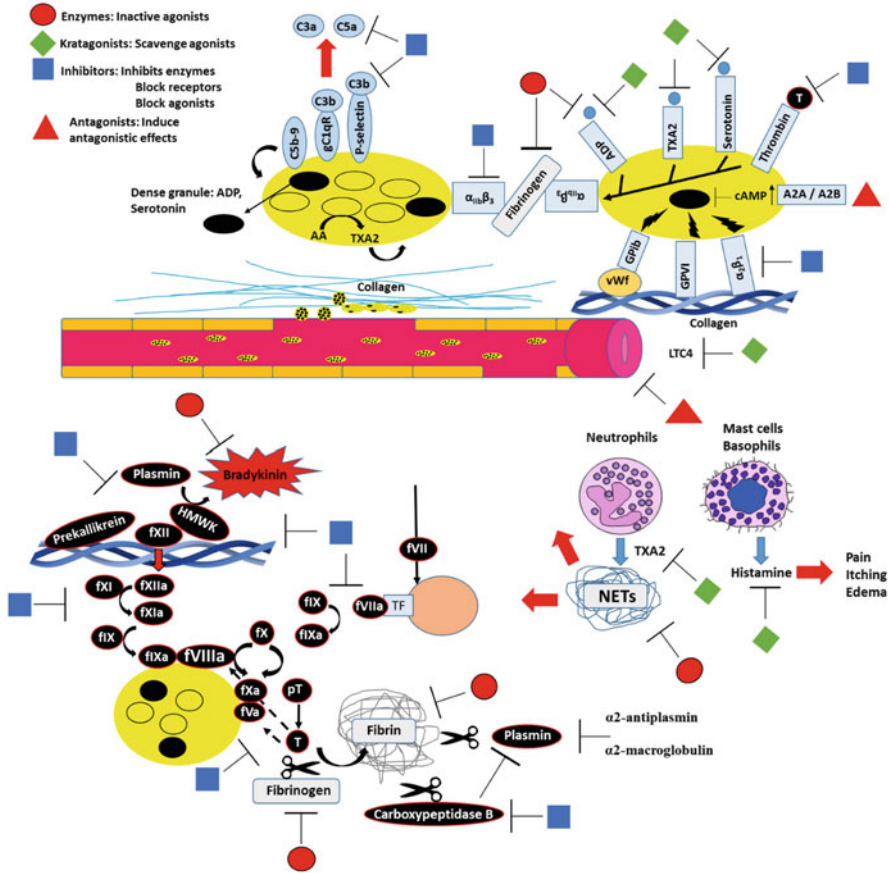


Fig. 17.3 Inhibition of the vertebrate host’s hemostatic and inflammatory responses by blood-feeding arthropods. Platelet aggregation mediated by various agonists are indicated at the *top*, while blood-coagulation and inflammatory responses are indicated at the *bottom*. Different classes of modulators are indicated to have an inhibitory effect and include enzymes that inactivate agonists, kratagonists that scavenge agonists, inhibitors that either inhibit enzymes, or block receptors, or block agonists and antagonists that induce antagonistic signals

17.5.1 Platelet Aggregation

When arthropods probe and lacerate capillary vessels and cells, collagen from the ECM is exposed and function to bind and activate platelets in mammals, or thrombocytes in birds and reptiles. Binding may occur via the von Willebrand’s receptor (GPIb-IX-IV) that binds to von Willebrand’s factor (vWf) bound to collagen, or via integrin $\alpha_2\beta_1$ or GPVI (Fig. 17.3). vWf rapidly binds to exposed collagen and binds platelets effectively under high shear conditions found close to the vessel wall and leads to outside-in signaling that results in platelet activation (Jurk and Kehrel 2005).

Integrin $\alpha_2\beta_1$ (GPIa/IIa) does not function explicitly under high shear conditions, but is important to assist in adhesion to collagen as well as platelet spreading. It functions in a secondary capacity, since it first needs to be activated via inside-outside signaling (Jurk and Kehrel 2005). GPVI binds directly to collagen via the Gly-Pro-Hyp ((GPO)n) repeats found in collagen and also leads to platelet activation via outside-in signaling. All three receptors are important for normal hemostasis and disruption of their functions will prevent platelet activation. Collagen-induced platelet activation results in release of platelet α -granules and dense granules and the synthesis and release of thromboxane A_2 (TXA $_2$) from membrane bound arachidonic acid (Fig. 17.3). α -Granules contain various proteins involved in hemostasis and inflammation, notably vWf, vitronectin, factor V, MIP-1 α (CCL3), platelet factor 4 (CXCL4), platelet-derived growth factor, P-selectin (CD62P), CD40L (CD154), RANTES (CCL5), insulin-like growth factor 1 and interleukin-1 (IL-1) (Thomas and Storey 2015). Dense granules contain adenosine diphosphate (ADP), adenosine triphosphate (ATP) and serotonin. Both ADP and serotonin bind to their own receptors on the platelet surface initiating their own signal transduction cascades that activate platelets resulting in an amplification cascade (Thomas and Storey 2015). Platelet activation is accompanied by shape change and pseudopod formation and the outside-in activation of integrin $\alpha_{IIb}\beta_3$ (GPIIb/IIIa) (Fig. 17.3). Integrin $\alpha_{IIb}\beta_3$ undergoes a conformation change that allows binding to soluble fibrinogen and this serves to cross-link activated platelets that results in the phenomenon of platelet aggregation (Jurk and Kehrel 2005). A variety of inhibitors of platelet aggregation from blood-feeding arthropods has been described (Tables 17.1A and 17.1B).

The secondary role that collagen play in platelet aggregation can be observed by the prolonged time it takes for collagen (~1 min) to induce platelet aggregation *in vitro* and the fact that scavengers of ADP and TXA $_2$ can completely abolish collagen mediated platelet aggregation (Mans et al. 1998a; Francischetti et al. 2000; Mans and Ribeiro 2008a; Assumpção et al. 2010; Ma et al. 2012). However, the important role that collagen play in the initiation of hemostasis is emphasized by the inhibitors that specifically or indirectly target this molecule. Aegyptin from the mosquito *Ae. aegypti*, binds directly to collagen and prevent interaction with vWf, GPVI and $\alpha_2\beta_1$ (Calvo et al. 2007a). Aegyptin knockout in transgenic mosquitoes significantly increase probing time and impaired efficient feeding and blood meal volumes (Chagas et al. 2014a). Aegyptin specifically binds to the vWf recognition site (RGQOGVMGF) in collagen and can prevent carotid thrombus formation and can also interact with the (GPO)n motif important for GPVI binding, and GFOGER important for recognition by $\alpha_2\beta_1$ (Calvo et al. 2009b). Targeting of the vWf interaction site may be expected for an arthropod that rupture and feeds from a blood vessel and would need to prevent binding of vWf to exposed collagen and adhesion of platelets under high shear conditions. Anopheline antiplatelet protein (AAPP), an abundant salivary molecule has been described from *An. stephensi* that is able to inhibit GPVI and $\alpha_2\beta_1$ interaction with collagen and inhibit collagen-induced platelet aggregation (Yoshida et al. 2008). The C-terminal region corresponding to exon 3–4 has been shown to be the active domain responsible for binding to collagen of

Table 17.1A Platelet aggregation inhibitors from ticks

Species	Name	Target	Family	Reference
<i>Ornithodoros moubata</i>	Apyrase	ATP, ADP	5'-NT	Ribeiro et al. (1991), Díaz-Martín et al. (2015)
<i>Ornithodoros savignyi</i>	Apyrase	ATP, ADP	5'-NT	Mans et al. (1998a, b), Stutzer et al. (2009)
<i>Argas monolakensis</i>	Apyrase	ATP, ADP	5'-NT	Mans et al. (2008b)
<i>Ixodes scapularis</i>	Apyrase	ATP, ADP	5'-NT	Ribeiro et al. (1985), Stutzer et al. (2009)
<i>Ornithodoros moubata</i>	Moubatin	TXA2	Lipocalin	Waxman and Connolly, (1993), Keller et al. (1993), Mans and Ribeiro (2008a)
<i>Ornithodoros savignyi</i>	TSGP2/3	TXA2	Lipocalin	Mans and Ribeiro, (2008a)
<i>Ornithodoros moubata</i>	TAI	$\alpha 2\beta 1$	ND	Karczewski et al. (1995)
<i>Ornithodoros moubata</i>	Disagregin	$\alpha \text{IIb}\beta 3$	BPTI	Karczewski et al. (1994)
<i>Ornithodoros savignyi</i>	Savignygrin	$\alpha \text{IIb}\beta 3$	BPTI	Mans et al. (2002a)
<i>Argas monolakensis</i>	Monogrin	$\alpha \text{IIb}\beta 3$	BPTI	Mans et al. (2008b)
<i>Dermacentor variabilis</i>	Variabilin	$\alpha \text{IIb}\beta 3$	Ixodegrins	Wang et al. (1996), Francischetti et al. (2005b)
<i>Amblyomma americanum</i>	AamS6	Plasmin	Serpin	Mulenga et al. (2013)
<i>Amblyomma americanum</i>	AAS19	Thrombin	Serpin	Kim et al. (2015)
<i>Haemaphysalis longicornis</i>	Longicornin	Collagen	ND	Cheng et al. (1999)
<i>Ixodes ricinus</i>	IRS-2	Cathepsin G	Serpin	Chmelar et al. (2011)
<i>Ixodes scapularis</i>	YY-39	$\alpha \text{IIb}\beta 3$	Ixodegrins	Francischetti et al. (2005b), Tang et al. (2015)
<i>Dermacentor reticulatus</i>	SHBP	Serotonin	Lipocalin	Sangamnatdej et al. (2002)
<i>Ornithodoros savignyi</i>	TSGP1	Serotonin	Lipocalin	Mans et al. (2008c)
<i>Argas monolakensis</i>	Monotonin	Serotonin	Lipocalin	Mans et al. (2008c)
<i>Ixodes scapularis</i>	IS-14	Serotonin	Lipocalin	Mans et al. (2008c)
	IS-15	Serotonin	Lipocalin	

Indicated are the common name for the platelet aggregation inhibitors, its molecular target and the protein family to which they belong. ND – not determined

Table 17.1B Platelet aggregation inhibitors from insects

Species	Name	Target	Family	Reference
<i>Aedes aegypti</i>	Aegyptin	Collagen	30 kDa	Calvo et al. (2007a)
<i>Anopheles stephensi</i>	AAPP	Collagen	30 kDa	Yoshida et al. (2008)
<i>Simulium nigritanum</i>	Simplagrin	Collagen	30 kDa	Chagas et al. (2014b)
<i>Aedes aegypti</i>	Apyrase	ATP, ADP	5'-NT	Champagne et al. (1995a)
<i>Aedes albopictus</i>	Apyrase	ATP, ADP	5'-NT	Dong et al. (2012)
<i>Anopheles gambiae</i>	Apyrase	ATP, ADP	5'-NT	Lombardo et al. (2000)
<i>Triatoma infestans</i>	Apyrase	ATP, ADP	5'-NT	Faudry et al. (2004)
<i>Tabanus yao</i>	Apyrase	ATP, ADP	5'-NT	An et al. (2011)
<i>Glossina morsitans</i>	Apyrase	ATP, ADP	5'-NT	Caljon et al. (2010)
<i>Cimex lectularius</i>	Apyrase	ATP, ADP	Cimex	Valenzuela et al. (1998)
<i>Phlebotomus papatasi</i>	Apyrase	ATP, ADP	Cimex	Valenzuela et al. (2001)
<i>Xenopsylla cheopis</i>	Apyrase	ATP, ADP	CD39	Andersen et al. (2007)
<i>Ctenocephalides felis</i>	Apyrase	ATP, ADP	CD39	Ribeiro et al. (2012a)
<i>Rhodnius prolixus</i>	PAI1, PAI2	ADP	Lipocalin	Francischetti et al. (2000)
<i>Dipetalogaster maxima</i>	DMAV	Superoxide	Antigen 5	Assumpção et al. (2013)
<i>Triatoma infestans</i>	TIAV	Superoxide	Antigen 5	Assumpção et al. (2013)
<i>Triatoma infestans</i>	Triplatin	TXA2	Lipocalin	Ma et al. (2012)
<i>Triatoma pallidipennis</i>	Pallidipin	TXA2	Lipocalin	Assumpção et al. (2010)
<i>Dipetalogaster maxima</i>	Dipetalodipin	TXA2	Lipocalin	Assumpção et al. (2010)
<i>Anopheles stephensi</i>	AnSt-D7L1	TXA2	D7	Alvarenga et al. (2010)
<i>Dipetalogaster maxima</i>	Dipetalodipin	HETE	Lipocalin	Assumpção et al. (2010)
<i>Rhodnius prolixus</i>	ABP	Biogenic amines	Lipocalin	Andersen et al. (2003)
<i>Anopheles gambiae</i>	D7r1-D7r4	Biogenic amines	D7/OBP	Calvo et al. (2006)

(continued)

Table 17.1B (continued)

Species	Name	Target	Family	Reference
<i>Aedes aegypti</i>	AeD71	Biogenic amines	D7/OBP	Calvo et al. (2006)
<i>Lutzomyia longipalpis</i>	LJM11	Biogenic amines	Yellow	Xu et al. (2011)
<i>Tabanus yao</i>	Tablysin-15	α IIb β 3	Antigen 5	Ma et al. (2011)
<i>Tabanus yao</i>	Vasotab TY	α IIb β 3	Kazal	Zhang et al. (2014)
<i>Lutzomyia ayacuchensis</i>	Ayadualin	α IIb β 3	Novel	Kato et al. (2015)
<i>Chrysops</i> spp.	Chrysoptin	α IIb β 3	5'-NT	Reddy et al. (2000)
<i>Simulium vittatum</i>	Simukunin	Cathepsin G	BPTI	Tsujimoto et al. (2012)
<i>Phlebotomus papatasi</i>	Adenosine, 5' AMP	A _{2A} , A _{2B}	Nucleotides	Ribeiro et al. (1999)
<i>Phlebotomus argentipes</i>	Adenosine, 5' AMP	A _{2A} , A _{2B}	Nucleotides	Ribeiro and Modi (2001)
<i>Culex quinquefasciatus</i>	PAF phosphorylcholine hydrolase	PAF	Phospholipase C	Ribeiro and Francischetti (2001)

Indicated are the common name for the platelet aggregation inhibitors, its molecular target and the protein family to which they belong

AAPP and is composed of two tightly packed anti-parallel α -helices, while the rest of the structure seems unordered (Hayashi et al. 2013; Sugiyama et al. 2014). AAPP and aegyptin belongs to the 30 kDa mosquito protein family and the same C-terminal region has been shown to be important for interaction of aegyptin and collagen (Ribeiro et al. 2007; Calvo et al. 2009b), and will probably have a similar structure as well. Surprisingly, targeting of vWf binding to collagen is also found in the black fly, *Si. nigrimanum* that secrete Simplagrin, that specifically binds to the vWf recognition site (RGQOGVMGF) and inhibit platelet adhesion under high shear conditions, but does not inhibit interaction of GPVI and $\alpha_2\beta_1$ with collagen (Chagas et al. 2014b). This may indicate that inhibition of vWf interaction with collagen may be important, even for arthropods that feed from hematomas, probably since the flow of blood from ruptured blood vessels still needs to be maintained to fill the hematoma. It has been proposed that Simplagrin and Aegyptin are orthologs that shared a common ancestry when hematophagy evolved in a common ancestor to mosquitoes and black flies (Chagas et al. 2014b). It was, however, acknowledged that the molecular mechanisms of collagen interaction between these inhibitors differ, while the modelled structure of Simplagrin is not the same as the AAPP structure, leaving the possibility of convergent evolution between these hematophagous families and functions open (Chagas et al. 2014b). However, submission of both Aegyptin and Simplagrin to the Phyre2 server (Kelley et al. 2015), returned as best hit the

C-terminal domain structure of AAPP with confidences of 96% and 87%, respectively (BJ Mans, personal observation), indicating that the region involved in collagen interaction has similar structures. Even so, pairwise sequence alignment indicate less than 25% sequence identity between Simplagrin and Aegyptin or AAPP. These proteins falls within the twilight zone of sequence identity, where orthology and even homology is problematic to establish with confidence (Rost 1999). Since interaction with the triple helix bundle of collagen probably require helical structures and the C-terminal domain of the mosquito proteins possess this, convergent evolution of these proteins towards collagen binding cannot be excluded. As yet, this specific case does not give convincing evidence for evolution of blood-feeding in the last common ancestor of the Culicomorpha.

In ticks at least one protein, tick adhesion inhibitor (TAI) from the soft tick *Or. moubata* inhibit adhesion of platelets to collagen. TAI has no effect on platelet aggregation, but do inhibit binding of a monoclonal antibody to integrin $\alpha_2\beta_1$ suggesting that this receptor is the target (Karczewski et al. 1995).

Inhibitors of collagen-induced platelet aggregation that does not specifically interact with collagen, but rather targets secondary activators such as adenosine diphosphate (ADP) and TXA2 also exist. ADP is targeted by apyrases (ATP diphosphohydrolases) found in ticks (Ribeiro et al. 1985, 1991; Mans et al. 1998a, 2008b), mosquitoes (Ribeiro et al. 1984b), biting midges (Pérez de León and Tabachnick 1996); black flies (Cupp et al. 1995), assassin bugs (Sarkis et al. 1986), bed bugs (Valenzuela et al. 1998) and fleas (Ribeiro et al. 1990; Cheeseman 1998; Andersen et al. 2007). Apyrase activity has evolved or has been exapted numerous times independently for the purpose of blood-feeding in different protein families (Stutzer et al. 2009; Hughes 2013). This includes the 5'-nucleotidase family for ticks (Stutzer et al. 2009), assassin bugs (Faudry et al. 2004), mosquitoes (Champagne et al. 1995a; Lombardo et al. 2000; Dong et al. 2012), horse flies (An et al. 2011) and tsetse flies (Caljon et al. 2010). Apyrases that belong to the *Cimex* family of apyrases include those from bed bugs (Valenzuela et al. 1998), and sand flies (Valenzuela et al. 2001). Apyrase that belong to the CD39 family was found in flea transcriptomes, but need to be experimentally confirmed (Andersen et al. 2007; Ribeiro et al. 2012a). Unique scavengers of ADP is found in the lipocalins from the assassin bug *R. prolixus* and this specific form of scavenging has not yet been observed in other hematophagous arthropods (Francischetti et al. 2000, 2002a). Collagen-induced platelet aggregation is also mediated by superoxide production and antigen 5 family members from the assassin bugs *Dipetalogaster maxima* and *Triatoma infestans* can inhibit low collagen dose induced platelet aggregation by scavenging superoxide (Assumpção et al. 2013).

Scavengers of TXA2 was initially misidentified as inhibitors specific for collagen, due to the high specificity for collagen-induced platelet aggregation, although none inhibited adhesion to collagen, or where the TXA2 mimetic U46619 or the precursor arachidonic acid was used at too high a molar ratio relative to the inhibitor to allow efficient scavenging. This included moubatin from the tick *Or. moubata* (Mans and Ribeiro 2008a; Waxman and Connolly 1993), triplatin from the assassin

bug *Tr. infestans* (Morita et al. 2006; Ma et al. 2012) and pallidipin from *Tr. pallidipennis* (Noeske-Jungblut et al. 1994; Assumpção et al. 2010). Scavengers confirmed as TXA2 scavengers include TSGP3 from the soft tick *Or. savignyi* (Mans and Ribeiro 2008a), Dipetalodipin from *D. maxima* (Assumpção et al. 2010) and AnSt-D7L1, a two-domain D7 protein from *An. stephensi*, of which the N-terminal domain is capable of binding both leukotriene C4 (LTC4) and TXA2 (Alvarenga et al. 2010).

Scavengers of biogenic amines (biogenic amine binding proteins, BABP), involved in platelet aggregation, such as serotonin and epinephrine as well as histamine involved in itch and inflammatory reactions are also secreted by hematophagous arthropods. This includes the lipocalins from assassin bugs (Andersen et al. 2003; Xu et al. 2013) and argasid and ixodid ticks (Paesen et al. 1999; Sangamnatdej et al. 2002; Mans et al. 2008c). The D7 proteins are related to the odorant-binding protein family and act as scavengers of serotonin, epinephrine, norepinephrine and histamine in mosquitoes (Calvo et al. 2006, 2009c; Mans et al. 2007). In the sand fly *L. longipalpis*, the “Yellow” protein family functions as biogenic amine scavengers (Xu et al. 2011). The nitrophorins from *R. prolixus* deserves special mention. Nitrophorins are lipocalins, but instead of just scavenging molecules inside the “cup-like” anti-parallel eight stranded β -barrel of the lipocalin fold, they bind a heme moiety capable of binding nitric oxide (NO), that is released when secreted into the host environment to act as a potent vasodilator (Ribeiro et al. 1993). Once NO is released, the nitrophorins scavenge histamine via the same heme moiety (Ribeiro and Walker 1994).

The last class of scavengers described to date include the cysteinyl leukotriene scavengers. Cysteinyl leukotrienes (LTC4, LTD4 and LTE4) are synthesized from leukotriene A4 in platelets, neutrophils, macrophages, basophils and mast cells during inflammation (Austen 2007). LTC4 is a potent skin vasodilator that leads to edema, wheal formation and occlusion of blood vessels within 10 min and may persist for more than 2 h (Soter et al. 1983). Cysteinyl leukotriene scavengers has been found in lipocalins from argasid ticks (Mans and Ribeiro 2008b), D7 proteins from mosquitoes (Calvo et al. 2009c; Alvarenga et al. 2010) and tablysin-15 from the CAP/AG5 family from the tabanid fly *Tabanus yao* (Xu et al. 2012).

In almost all cases, scavengers of bioactive molecules are some of the most abundant proteins present in the sialomes of hematophagous organisms, allowing them to exist within the feeding site at molar concentrations above 1 μ M. They also generally bind their ligands with affinities in the nM range and are therefore effective scavengers, leading them to be classified as “kratagonists” from the Greek word “to arrest or seize” (Ribeiro and Arca 2009).

Targeting of specific platelet receptors also occur. As such, TAI targets the collagen receptor integrin $\alpha_2\beta_1$ (Karczewski et al. 1995). The fibrinogen receptor $\alpha_{IIb}\beta_3$ are specifically targeted by proteins that present the integrin recognition motifs RGD, RED, KGD, VGD, MLD, KTS, RTS, or WGD (Assumpção et al. 2012b). Inhibitors of $\alpha_{IIb}\beta_3$ have been found in soft ticks: disagregin (Karczewski et al. 1994), savignygrins (Mans et al. 2002a) and the monogrins (Mans et al. 2008b),

hard ticks: variabilin (Wang et al. 1996) and the ixodegrins (Francischetti et al. 2005b; Tang et al. 2015), tabanid flies: tablysin-15 (Xu et al. 2008; Ma et al. 2011), sand flies (Kato et al. 2015) and chrysoptin from deer flies (Grevelink et al. 1993; Reddy et al. 2000). The sequence for chrysoptin belongs to the 5'-nucleotidase family and shows 96% similarity to the active apyrase from horse fly (An et al. 2011), but even though the active site residues are conserved (BJ Mans, personal observation), no apyrase activity was associated with chrysoptin (Reddy et al. 2000). However, the disaggregation effect observed in this latter study was also observed with tick apyrase (Mans et al. 1998b, 2000), with the implication that ADP removal from its receptor can induce outside-in signaling that leads to dissociation of fibrinogen from its receptor. A number of proteins with integrin recognition motifs has been identified from a variety of hematophagous arthropods using bioinformatics (Assumpção et al. 2012b). These predictions should be experimentally confirmed, since these RGD-like motifs needs to be presented on a restricted conformation to be biologically active. Other receptors found on platelets include the ADP (P2Y1, P2Y12), ATP (P2X1), epinephrine (α 2A), P-selectin, CD40L, serotonin, thrombin (PAR1, PAR4) and TXA2 (TP α) receptors (Jurk and Kehrel 2005; Thomas and Storey 2015). While scavengers or inhibitors of the receptor agonists have been discovered, no inhibitors that specifically interact with these receptors have yet been identified. Even so, there is a probability that apyrase may interact with the ADP receptors, since apyrase can disaggregate platelets already aggregated with ADP and reverse their shape change from a spherical back to a discoid form, even if they have already secreted their granule contents, suggesting that ADP may be leached or removed from the receptor (Mans et al. 2000). Another study implicated a potential heparin glycosylated protein from *Or. moubata* in P-selectin interaction, but this study is considered preliminary since no functional data was presented (García-Varas et al. 2010).

Secretion of chemical modulators is rare, but sand flies from the genus *Phlebotomus* secrete adenosine and 5'-AMP during feeding, which are potent platelet aggregation inhibitors (Ribeiro et al. 1999; Ribeiro and Modi 2001). The production of pro-inflammatory cytokines by dendritic cells is inhibited by adenosine and this immune-modulatory effect was linked with adenosine in the saliva of *Phlebotomus* sand flies and the hard tick *I. scapularis* (Oliveira et al. 2011; Carregaro et al. 2015).

17.5.2 The Clotting Cascade

The rupture of blood vessels during probing releases fVII from the blood stream into the ECM where it binds to tissue-factor (TF) expressed on stromal fibroblasts in the dermis. Binding to TF leads to an activated TF-fVIIa complex. This complex activates fIX and fX to fIXa and soluble fXa that then binds to fV. In activated platelets phosphatidylserine translocate to the outer membrane and serves as activator for the prothrombinase complex (fXa/fVa) that leads to activation of thrombin (Lentz 2003; Majumder et al. 2005). Platelets also shed small vesicles (50–100 nm) that

fulfill the same function (Lentz 2003). This pathway is called the extrinsic or tissue factor pathway. Formation of the prothrombinase complex increase the activity of fXa towards thrombin more than 150,000 fold. In a feedback loop, thrombin activates fV and fVIII that then activates fXI that activates fIX. Thrombin can also activate fXIa which can activate fV, both reactions using polyphosphate as cofactor (Choi et al. 2011, 2015). Polyphosphate is secreted by platelets and has become an important cofactor and accelerator of all key steps in coagulation (Morrissey et al. 2012).

An intrinsic pathway, also known as the contact activation pathway exist (Walsh 2001; Long et al. 2015). Exposed collagen binds high-molecular weight kininogen (HMWK), prekallikrein and fXII leading to formation of activated kallikrein and fXIIa. fXII can also autoactivate itself to fXIIa when binding to anionic surfaces such as activated platelets, heparin secreted by mast cells, polyphosphate secreted by platelets or DNA found in neutrophil extracellular traps (NETs) (Brunnée et al. 1997). fXIIa then activates fXIa, which activates fIXa that forms the tenase complex with fVIIIa. fVIIIa and fIXa forms the tenase complex that activates fX.

Thrombin cleaves fibrinogen that leaks from damaged capillaries and cleaved fibrinogen cross-links into a fibrin network (Lentz 2003). Binding of intact soluble fibrinogen by $\alpha_{\text{IIb}}\beta_3$ leads to platelet aggregation and with the fibrin network forms a plug that rapidly seals off the wound. Once blood loss has been stopped and as part of the wound healing process, plasminogen is activated to plasmin by urokinase, tissue plasminogen activator, fXIa, fXIIa or kallikrein. Plasmin degrades the fibrin clot and can be inhibited by α_2 -antiplasmin or α_2 -macroglobulin. Thrombin activatable fibrinolysis inhibitor (Carboxypeptidase B) is activated by thrombin and removes C-terminal lysine residues from fibrin, thereby preventing plasmin binding to fibrin and inhibits the fibrinolysis process (Draxler and Medcalf 2015).

Almost all points in the clotting cascade is targeted by hematophagous arthropods (Figure 17.3; Tables 17.2A and 17.2B). Inhibitors of the contact activation pathway that targets kallikrein, fXI or fXII has been found in ticks (Tanaka et al. 1999; Sasaki et al. 2004; Kato et al. 2005; Decrem et al. 2009; Kim et al. 2015), mosquitoes (Isawa et al. 2002, 2007a; Calvo et al. 2006), assassin bugs (Isawa et al. 2007b; Ishimaru et al. 2012) and sand flies (Alvarenga et al. 2013; Kato et al. 2015).

Inhibitors of TF-fVIIa, fVIIIa-fIXa, fXa-fV or fXa has been found in ticks (Waxman et al. 1990; Gordon and Allen 1991; Limo et al. 1991; Gaspar et al. 1995, 1996; Joubert et al. 1995, 1998; Zhu et al. 1997a; Ibrahim et al. 2001b; Ehebauer et al. 2002; Francischetti et al. 2002b, 2004; Narasimhan et al. 2002; Batista et al. 2010; Schuit et al. 2013; Pasqualoto et al. 2014; Kim et al. 2015), mosquitoes (Stark and James 1995, 1996, 1998; Calvo et al. 2011), assassin bugs (Hellmann and Hawkins 1965; Ribeiro et al. 1995; Sun et al. 1996; Zhang et al. 1998), black flies (Jacobs et al. 1990; Abebe et al. 1994, 1996; Tsujimoto et al. 2012), sand flies (Collin et al. 2012), biting midges (Pérez de León et al. 1998) and bed bugs (Valenzuela et al. 1996).

Thrombin inhibitors abound in hard and soft ticks (Hellman and Hawkins 1967; Anastopoulos et al. 1991; Hoffmann et al. 1991; Gaspar et al. 1995; van de Locht et al. 1996; Zhu et al. 1997a, 1997b; Nienaber et al. 1999; Horn et al. 2000; Ibrahim et al. 2001a; Kazimírová et al. 2002; Mans et al. 2002b, 2008b; Iwanaga et al. 2003;

Table 17.2A Blood clotting inhibitors from ticks

Species	Name	Target	Family	Reference
<i>Ornithodoros moubata</i>	ND	Thrombin	ND	Hellman and Hawkins (1967)
<i>Ornithodoros moubata</i>	Ornithodorin	Thrombin	BPTI	van de Loch et al. (1996)
<i>Ornithodoros savignyi</i>	Savignin	Thrombin	BPTI	Nienaber et al. (1999), Mans et al. (2002b)
<i>Argas monolakensis</i>	Monobin	Thrombin	BPTI	Mans et al. (2008b)
<i>Amblyomma americanum</i>	Americanin	Thrombin	ND	Zhu et al. (1997b)
<i>Ixodes ricinus</i>	Ixin	Thrombin	ND	Hoffmann et al. (1991)
<i>Ixodes holocyclus</i>	ND	Thrombin	ND	Anastopoulos et al. (1991)
<i>Rhipicephalus microplus</i>	BmAP	Thrombin	ND	Horn et al. (2000)
<i>Rhipicephalus microplus</i>	Microphilin	Thrombin	ND	Ciprandi et al. (2006)
<i>Rhipicephalus microplus</i>	RmS-15	Thrombin	Serpin	Rodriguez-Valle et al. (2015)
<i>Amblyomma variegatum</i>	Variegin	Thrombin	Hirudin-like	Kazimírová et al. (2002), Koh et al. (2007)
<i>Haemaphysalis longicornis</i>	Madanins	Thrombin	Madanin	Iwanaga et al. (2003)
<i>Haemaphysalis longicornis</i>	Chimadanin	Thrombin	Madanin	Nakajima et al. (2006)
<i>Hyalomma marginatum rufipes</i>	Hyalomin-1	Thrombin	Madanin	Jablonka et al. (2015)
<i>Rhipicephalus calcaratus</i>	Calcaratin	Thrombin	ND	Motoyashiki et al. (2003)
<i>Hyalomma dromedarii</i>	NTI-1	Thrombin	ND	Ibrahim et al. (2001a)
<i>Hyalomma dromedarii</i>	NTI-2	Thrombin	ND	Ibrahim et al. (2001a)
<i>Ornithodoros moubata</i>	TAP	fXa	BPTI	Waxman et al. (1990)
<i>Ornithodoros savignyi</i>	fXaI	fXa	BPTI	Gaspar et al. (1996), Joubert et al. (1998)
<i>Rhipicephalus appendiculatus</i>	fXaI	fXa	ND	Limo et al. (1991)
<i>Hyalomma truncatum</i>	fXaI	fXa	ND	Joubert et al. (1995)
<i>Hyalomma dromedarii</i>	fXaI	fXa	ND	Ibrahim et al. (2001b)
<i>Ixodes scapularis</i>	Salp14	fXa	BTSP	Narasimhan et al. (2002)

(continued)

Table 17.2A (continued)

Species	Name	Target	Family	Reference
<i>Amblyomma americanum</i>	AAS19	fXa, fXIa	Serpin	Kim et al. (2015)
<i>Amblyomma cajennense</i>	Amblyomin-X	fXa	BPTI	Batista et al. (2010)
<i>Haemaphysalis longicornis</i>	HLS2	Thrombin	Serpin	Imamura et al. (2005)
<i>Ixodes scapularis</i>	TIx-5	fXa-fV	PLUNC	Schuijt et al. (2013)
<i>Haemaphysalis longicornis</i>	Longistatin	Plasminogen	EF-hand	Anisuzzaman et al. (2011, 2012)
<i>Ornithodoros moubata</i>	rOmEno	Plasminogen	Enolase	Díaz-Martín et al. (2013)
<i>Ixodes scapularis</i>	MP1	Fibrin	Metalloprotease	Francischetti et al. (2003)
<i>Rhipicephalus bursa</i>	TCI	Carboxy-peptidase B	Beta-defensin	Arolas et al. (2005a, b)
<i>Haemaphysalis longicornis</i>	HITCI	Carboxy-peptidase B	Beta-defensin	Gong et al. (2007)
<i>Rhipicephalus microplus</i>	BmTI-A	Kallikrein	BPTI	Tanaka et al. (1999)
<i>Rhipicephalus microplus</i>	BmTI-D	Kallikrein	BPTI	Sasaki et al. (2004)
<i>Haemaphysalis longicornis</i>	Haemaphysalin	Kallikrein	BPTI	Kato et al. (2005)
<i>Ixodes ricinus</i>	Ir-CPI	Kallikrein-fXIIa-fXIa	BPTI	Decrem et al. (2009)
<i>Ixodes scapularis</i>	Ixolaris	fXa-TF-VIIa	BPTI	Francischetti et al. (2002b)
<i>Ixodes scapularis</i>	Penthalaris	fX, fXa	BPTI	Francischetti et al. (2004)
<i>Ornithodoros moubata</i>	TAM-a	Vasodilation	Calcitonin	Iwanaga et al. (2014)
<i>Ornithodoros savignyi</i>	BSAP1	PT pathway	ND	Ehebauer et al. (2002)
	BSAP2			

Indicated are the common name for the blood-clotting inhibitors, its molecular target and the protein family to which they belong. *ND* not determined

Motoyashiki et al. 2003; Imamura et al. 2005; Ciprandi et al. 2006; Nakajima et al. 2006; Koh et al. 2007; Jablonka et al. 2015; Rodriguez-Valle et al. 2015), assassin bugs (Noeske-Jungblut et al. 1995; Fuentes-Prior et al. 1997), mosquitoes (Stark and James 1996; Waidhet-Kouadio et al. 1998; Valenzuela et al. 1999), tsetse flies (Cappello et al. 1996; Cappello et al. 1998), black flies (Abebe et al. 1994; Chagas et al. 2010), horn flies (Cupp et al. 2000). Of interest is that fXa inhibitors was predominantly found in culicines, while anophelines have thrombin inhibitors (Stark and James 1996). More recently a thrombin inhibitor was characterized in *Ae. aegypti*, but only inhibited thrombin weakly (Watanabe et al 2010).

Table 17.2B Blood-clotting inhibitors from insects

Species	Name	Target	Family	Reference
<i>Anopheles stephensi</i>	Hamadarin	fXII, HMWK	D7/OBP	Isawa et al. (2002)
<i>Anopheles gambiae</i>	D7r1	fXII, HMWK	D7/OBP	Calvo et al. (2006)
<i>Anopheles stephensi</i>	Anophensin	fXII, HMWK	SG7	Isawa et al. (2007a)
<i>Triatoma infestans</i>	Triafestin-1/2	fXII, HMWK	Lipocalin	Isawa et al. (2007b)
<i>Triatoma dimidiata</i>	Dimiconin	fXII	Lipocalin	Ishimaru et al. (2012)
<i>Phlebotomus dubosci</i>	PdSP15a/b	Polyphosphate	OBP	Alvarenga et al. (2013)
<i>Lutzomyia ayacuchensi</i>	Ayadualin	fXII	Novel	Kato et al. (2015)
<i>Aedes aegypti</i>	AFXa	fXa	Serpin	Stark and James, (1998)
<i>Aedes albopictus</i>	Alboserpin	fXa	Serpin	Calvo et al. (2011)
<i>Rhodnius prolixus</i>	Prolixin S	fVIII	Lipocalin	Ribeiro et al. (1995), Sun et al. (1996)
<i>Simulium vittatum</i>	NA	fXa	ND	Jacobs et al. (1990);
<i>Simulium argus</i>	NA	fXa	ND	Abebe et al. (1994)
<i>Simulium metallicum</i>	NA	fXa	ND	Abebe et al. (1994)
<i>Simulium ochraceum</i>	NA	fXa	ND	Abebe et al. (1994)
<i>Simulium vittatum</i>	NA	fV	ND	Abebe et al. (1996)
<i>Simulium vittatum</i>	Simikunin	fXa	BPTI	Tsujimoto et al. (2012)
<i>Lutzomyia longipalpis</i>	Lufaxin	fXa	SP06	Collin et al. (2012)
<i>Culicoides variipennis sonorensis</i>	NA	fXa	ND	Pérez de León et al. (1998)
<i>Cimex lectularius</i>	NA	fVIIIa/FIXa	ND	Valenzuela et al. (1996)
<i>Triatoma pallidipennis</i>	Triabin	Thrombin	Lipocalin	Noeske-Jungblut et al. (1995), Fuentes-Prior et al. (1997)
<i>Anopheles stephensi</i>	NA	Thrombin	ND	Waidhet-Kouadio et al. (1998)
<i>Anopheles albimanus</i>	Anophelin	Thrombin	Anophelin	Valenzuela et al. (1999)
<i>Glossina morsitans morsitans</i>	Tsetse thrombin inhibitor	Thrombin	Novel	Cappello et al. (1996), (1998)

(continued)

Table 17.2B (continued)

Species	Name	Target	Family	Reference
<i>Simulium vittatum</i>	NA	Thrombin	ND	Abebe et al. (1994)
<i>Simulium argus</i>	NA	Thrombin	ND	Abebe et al. (1994)
<i>Thyrsopelma guianense</i>	NA	Thrombin	ND	Chagas et al. (2010)
<i>Hematobia irritans</i>	NA	Thrombin	ND	Cupp et al. (2000)
<i>Tabanus yao</i>	Tablysins 2-7	Fibrinogen	AG 5/SCP	Ma et al. (2009)
<i>Cimex lectularius</i>	Nitrophorin	Vasodilation	Inositol phosphatases	Valenzuela et al. (1995), Valenzuela and Ribeiro (1998)
<i>Rhodnius prolixus</i>	Nitrophorins	Vasodilation	Lipocalin	Ribeiro et al. (1993); Weichsel et al. (1998)
<i>Culicoides variipennis sonorensis</i>	NA	Vasodilation	ND	Pérez de León et al. (1997)
<i>Simulium vittatum</i>	SVEP	Vasodilation	Novel	Cupp et al. (1994), (1998)
<i>Lutzomyia longipalpis</i>	Maxadilan	Vasodilation	Novel	Ribeiro et al. (1989), Lerner and Shoemaker (1992)
<i>Phlebotomus papatasi</i>	Adenosine	Vasodilator	Nucleotides	Ribeiro et al. (1999)
<i>Phlebotomus argentipes</i>	Adenosine	Vasodilator	Nucleotides	Ribeiro and Modi (2001)
<i>Hybomitra bimaculata</i>	Vasotab	Vasodilator	Kazal	Takác et al. (2006)
<i>Tabanus yao</i>	Vasotab TY	Vasodilator	Kazal	Ma et al. (2009)
<i>Tabanus yao</i>	Peroxindase TY	Vasodilator	Peroxidase	Ma et al. (2009)
<i>Anopheles albimanus</i>	NA	Norepinephrine	Peroxidase	Ribeiro and Nussenzveig (1993), Ribeiro and Valenzuela (1999)
<i>Anopheles gambiae</i>	NA	Norepinephrine	Peroxidase	Ribeiro et al. (1994)
<i>Aedes aegypti</i>	Sialokinin	Vasodilator	Tachykinin	Ribeiro (1992), Champagne and Ribeiro (1994)
<i>Aedes triseriatus</i>	Sialokinin	Vasodilator	Tachykinin	Ribeiro et al. (1994)

Indicated are the common name for the blood-clotting inhibitors, its molecular target and the protein family to which they belong. *ND* not determined

Molecules capable of fibrinolysis has also been characterized. This includes metalloproteases from the ixodid *I. scapularis* (Francischetti et al. 2003). The horse fly *Ta. yao* possess several antigen 5/SCP family members named tablysin 2–7 that are fibrinogenolytic (Ma et al. 2009). Carboxypeptidase B inhibitors that will lead to increased rates of fibrinolysis has been characterized in the hard ticks *Ha. longicornis* and *Rhipicephalus bursa* (Arolas et al. 2005a, b; Gong et al. 2007). Plasminogen activators have been found in the soft tick *Or. moubata* which secrete a enolase that performs this function (Díaz-Martín et al. 2013), while the hard tick *Ha. longicornis* secrete longistatin, a two-domain EF-hand protein that can proteolytically activate plasmin (Anisuzzaman et al. 2011, 2012).

17.5.3 Pain Responses and Inflammation

Activation of the contact phase of coagulation leads to generation of kallikrein, while the fibrinolytic pathway leads to plasmin generation (Sharma 2005; del Rosso et al. 2008). Both of these enzymes can release bradykinin from high molecular weight kininogen (HMWK). Bradykinin causes pain responses, vascular permeability (edema) and is a vasodilator. Pain and edema at the feeding site leads to host grooming responses and vector neutralization and death (Allen 1989). Inhibitors of both the kallikrein and fibrinolytic systems has been described above. However, cathepsin L is a lysosomal enzyme that is released from cells into the extracellular fluid during acute inflammation. It can function as a kininogenase, i.e. releasing bradykinin from HMWK or low molecular weight kininogen (LMWK) (Desmazes et al. 2001; Puzer et al. 2004). Bradykinin also mediates carrageenan-induced inflammatory pain and edema in the rat paw edema model (Ikeda et al. 2001). Sialostatin L and L2 are cystatins specific for cathepsin L found in the saliva of *I. scapularis* and inhibit carrageenan-induced inflammation in rat paw (Kotsyfakis et al. 2006; Kotsyfakis et al. 2007). HISC-1, a cathepsin L specific inhibitor has also been described in the metastriate tick *Ha. longicornis* (Yamaji et al. 2009). The sialostatins may therefore be important mediators of bradykinin mediated inflammation, pain and edema. Vaccination with sialostatin L led to tick rejection within 24 h of attachment, indicating that sialostatin L functions in the inflammatory phase (Kotsyfakis et al. 2007), most probably to limit bradykinin mediated inflammation. Sialostatin L also impact on dendritic cell maturation and dendritic cell mediated T-cell proliferation and autoimmunity, based on its inhibitory activity against cathepsin S and minimized symptoms of experimental autoimmune encephalomyelitis in mice (Sá-Nunes et al. 2009). It should be noted that bradykinin also drive dendritic cell maturation, which may explain the effect of sialostatin L on these cells (Scharfstein et al. 2007). *Ixodes scapularis* also secrete a metallo dipeptidyl carboxypeptidase that acts as a kininase that degrade bradykinin and anaphylatoxin (Ribeiro et al. 1985; Ribeiro and Spielman 1986; Ribeiro and Mather 1998). *Phlebotomus dubosqi* salivary proteins 15a and 15b (PdSP15a, PdSP15b) belongs to the OBP family and binds to dextran, polyphosphate and heparin and inhibits activation of the contact phase pathway as well as bradykinin generation by preventing

the binding of coagulation factors to these surfaces (Alvarenga et al. 2013). Anophensin from *An. stephensi* interrupt interaction of fXII and HMWK, thereby inhibiting the generation of bradykinin, while hamadarin from the same mosquito associate with the fXII-HMWK complex and inhibit their association with the activating surface (Isawa et al. 2002, 2007a). Triafestin-1 and triafestin-2 from *Tr. infestans* binds to fXII and prekallikrein and prevent their activation, thereby inhibiting bradykinin release (Isawa et al. 2007b). Other inhibitors of the contact pathway will probably also inhibit bradykinin release, but this has not been experimentally confirmed.

17.5.4 Vasoconstriction

Nitric oxide (NO) is a potent vasodilator, but is also very labile. A number of blood-feeding arthropods evolved proteins capable of carrying NO, which is then released at the site of feeding including nitrophorin from the bed bug *Cimex lectularius* (Valenzuela et al. 1995) and the nitrophorins from *R. prolixus* (Ribeiro et al. 1993). While the *Rhodnius* nitrophorins belong to the lipocalin family, the *Cimex* nitrophorin belong to the inositol phosphatase family supporting convergent evolution of these functions and independent evolution of blood-feeding in assassin and bed bugs (Valenzuela and Ribeiro 1998). A vasodilator was also identified in the biting midge *Cu. variipennis* (Pérez de León et al. 1997). Vasodilatory proteins named SVEP (*Simulium vittatum* erythema protein) was characterized from the black fly *Si. vittatum* (Cupp et al. 1994, 1998). The sand fly *L. longipalpis* produce Maxadilan, a potent vasodilatory peptide (Ribeiro et al. 1989; Lerner et al. 1991; Lerner and Shoemaker 1992). *Phlebotomus* species produce adenosine as vasodilator (Ribeiro et al. 1999). Horse and deer flies also produce vasodilators (Rajská et al. 2003), and in the case of horse flies a peptide named vasotab belonging to the Kazal family was identified in the hairy-legged horsefly *Hybomitra bimaculata* (Takác et al. 2006). A homolog from the horse fly *Ta. yao* (Vasotab TY) is a vasodilator, but also inhibits platelet aggregation by targeting $\alpha_{IIIb}\beta_3$ (Ma et al. 2009; Xu et al. 2008; Zhang et al. 2014). *Tabanus yao* also possess a peroxidase (Peroxindase TY) capable of inhibiting vasoconstriction (Ma et al. 2009). The mosquito *An. albimanus* and *An. gambiae* use a catechol oxidase/peroxidase activity that belongs to the myeloperoxidase family as vasodilator, by oxidizing the vasoconstrictor norepinephrine (Ribeiro and Nussenzveig 1993; Ribeiro et al. 1994; Ribeiro and Valenzuela 1999). *Ae. aegypti* and *Ae. triseriatus* secrete vasodilatory peptides called sialokinins that is related to the tachykinins (Ribeiro 1992; Ribeiro et al. 1994; Champagne and Ribeiro 1994; Beerntsen et al. 1999).

Hard ticks synthesize and secrete prostaglandin E2, a potent vasodilator (Ribeiro et al. 1985; Ribeiro et al. 1992), while soft ticks from the genus *Ornithodoros* possess adrenomedullin peptides postulated to have originated from the vertebrate host via horizontal gene transfer (Francischetti et al. 2008a; Iwanaga et al. 2014).

The scavenging of leukotriene B4 (LTB4) which can act as an indirect vasoconstrictor (Bäck et al. 2004; Bäck et al. 2007) will also inhibit vasoconstriction.

Scavenging of LTB₄ has been observed in hard and soft ticks (Beaufays et al. 2008; Mans and Ribeiro 2008a), while LTB₄ production by neutrophils were inhibited by sand flies (Monteiro et al. 2005; Carregaro et al. 2008).

Vasodilation can also assist in the physical enlargement of the feeding site by induction of hyperemia (increased blood-flow) that leads to erythema at the feeding site. This is a common feature of blood-feeding arthropods that feed from the hematoma that forms close to the epidermis and are found in sand flies (Ribeiro et al. 1986). Excess erythema may, however, be counter-productive for hematoma formation when linked with edema due to increased endothelial permeability as caused by the vasodilator LTC₄. Wheal formation and erythema caused by LTC₄ can occur within 10 min and persists for up to 2 h, leading to occlusion of blood vessels and decreased blood volume (Soter et al. 1983). As indicated before, a number of LTC₄ scavengers has been found in blood-feeding arthropods. Hard ticks surprisingly, can induce vasoconstriction (slow-feeding) or vasodilation (rapid-feeding) depending on feeding phase and may use vasoconstriction to control blood-flow in the early slow-feeding phases when the quantity of blood needed is minimal (Pekáriková et al. 2015).

It has been shown that ixodids can inhibit endothelial cell proliferation and angiogenesis (Francischetti et al. 2005a; Fukumoto et al. 2006; Islam et al. 2009; Drewes et al. 2012). Dipetalopidin, inhibits angiogenesis by scavenging 15-hydroxyicosatetraenoic acid (HETE), a derivative of the 15-lipoxygenase pathway (Assumpção et al. 2010). TabRTS from tabanid flies belong to the antigen 5 family and possess the integrin recognition motif RTS in its C-terminal and inhibits angiogenesis, presumably targeting integrin $\alpha_1\beta_1$ (Ma et al. 2010). While the rationale behind the inhibition of angiogenesis seems clear for ixodids, the effects on angiogenesis from fast feeding insects is more obscure, given that this phenomenon only occurs in the advanced proliferation and remodeling stages of wound healing. Rather than angiogenesis *per se*, their effects may be more immediate aimed at the arrest of bleeding or inflammation. Angiogenesis may therefore be a secondary effect implicating the effectors of angiogenesis in early hemostasis or inflammatory responses. In this regard, factors involved in angiogenesis also play an important function in platelet activation, aggregation and coagulation. As such, HETE increase platelet aggregation and thrombin generation (Vijil et al. 2014). The control of platelet responses therefore seems to be a central theme in host defense control by blood-feeding arthropods. The integrins $\alpha_5\beta_1$ which is important in angiogenesis is also important for neutrophil migration via $\alpha_5\beta_1$ interaction with fibronectin and play a key role in the immediate infiltration of neutrophils into the site of injury (Everitt et al. 1996).

17.5.5 Inflammatory Responses

A large number of inflammatory mediators are targeted by hematophagous arthropods (Tables 17.3A and 17.3B). A strong link between the complement cascade, platelet aggregation and coagulation during vascular injury has emerged

Table 17.3A Immuno-modulators from ticks

Species	Compound	Target	Family	Reference
<i>Ixodes scapularis</i>	Isac	Complement C3	Isac	Valenzuela et al. (2000)
<i>Ornithodoros moubata</i>	OmCI	Complement C5	Lipocalin	Nunn et al. (2005)
<i>Ixodes ricinus</i>	Iris	Elastase	Serpin	Prevot et al. (2006)
<i>Rhipicephalus microplus</i>	BmTI-A	Elastase	BPTI	Tanaka et al. (1999)
<i>Rhipicephalus microplus</i>	RmS-3	Elastase	Serpin	Rodriguez-Valle et al. (2015)
<i>Amblyomma americanum</i>	AamS6	Elastase	Serpin	Mulenga et al. (2013)
<i>Ornithodoros savignyi</i>	TSGP4	LTC4	Lipocalin	Mans and Ribeiro (2008b)
<i>Argas monolakensis</i>	AM-33	LTC4	Lipocalin	Mans and Ribeiro (2008b)
<i>Ixodes ricinus</i>	IRS-2	Chymase	Serpin	Chmelar et al. (2011)
<i>Ixodes scapularis</i>	ISL929	Neutrophils	ADAMTS	Guo et al. (2009)
	ISL 1373			
<i>Rhipicephalus appendiculatus</i>	HBP1	Histamine	Lipocalin	Paesen et al. (1999)
	HBP2	Histamine		
	MS-HBP	Histamine		
<i>D. reticulatus</i>	SHBP	Histamine Serotonin	Lipocalin	Sangamnatdej et al. (2002)
<i>Ornithodoros savignyi</i>	TSGP1	Histamine Serotonin	Lipocalin	Mans et al. (2008c)
<i>Argas monolakensis</i>	Monomine	Histamine	Lipocalin	Mans et al. (2008c)
<i>Argas monolakensis</i>	Monotonin	Serotonin	Lipocalin	Mans et al. (2008c)
<i>Ixodes scapularis</i>	IS-14	Serotonin	Lipocalin	Mans et al. (2008c)
	IS-15			
<i>Rhipicephalus appendiculatus</i>	Japanin	DC modulation	Lipocalin	Preston et al. (2013)
<i>Ornithodoros moubata</i>	Moubatin	LTB4	Lipocalin	Mans et al. (2008a)
<i>Ornithodoros moubata</i>	OmCI	LTB4	Lipocalin	Roversi et al. (2013)
<i>Ornithodoros savignyi</i>	TSGP2/3	LTB4	Lipocalin	Mans et al. (2008a)
<i>Ixodes ricinus</i>	Ir-LBP	LTB4	Lipocalin	Beaufays et al. (2008)

(continued)

Table 17.3A (continued)

Species	Compound	Target	Family	Reference
<i>Ixodes ricinus</i>	Tryptogalinin	Tryptase	BPTI	Valdés et al. (2013)
<i>Rhipicephalus appendiculatus</i>	TdPI	Tryptase	BPTI	Paesen et al. (2007)
<i>Rhipicephalus appendiculatus</i>	Ra-KLP	maxiK channels	BPTI	Paesen et al. (2009)
<i>Rhipicephalus sanguineus</i>	Evasin-1	CCL3, CCL4, CCL18	Evasin-1	Frauensschuh et al. 2007
<i>Rhipicephalus sanguineus</i>	Evasin-3	CXCL1; CXCL8	Evasin-3	Déruaz et al. (2008)
<i>Rhipicephalus sanguineus</i>	Evasin-4	CCL5; CCL11	Evasin-1	Déruaz et al. (2008)
<i>Rhipicephalus microplus</i>	BmTI-2	Elastase	BPTI	Sasaki et al. (2004)
<i>Rhipicephalus microplus</i>	BmTI-3	Elastase	BPTI	Sasaki et al. (2004)
<i>Rhipicephalus microplus</i>	Boophilin	Elastase	BPTI	Soares et al. (2012)
<i>Rhipicephalus sanguineus</i>	RsTIQ2	Elastase	BPTI	Sant'Anna Azzolini et al. (2003)
<i>Ixodes scapularis</i>	Sialostatin L	Cathepsin L, V	Cystatin	Kotsyfakis et al. (2006)
<i>Ixodes scapularis</i>	Sialostatin L2	Cathepsin L, V	Cystatin	Kotsyfakis et al. (2007)
<i>Ornithodoros moubata</i>	OmC2	Cathepsin B, C, H, L, S	Cystatin	Salát et al. (2010)
<i>Amblyomma americanum</i>	MIF	Macrophages	MIF	Jaworski et al. (2001)
<i>Dermacentor variabilis</i>	HRF	Basophils	HRF	Mulenga et al. (2003)
<i>Rhipicephalus appendiculatus</i>	IGBPA	Immunoglobulins	IGBPA	Wang and Nuttall (1999)
	IGBPB		ML	
	IGBPC		ML	
<i>Ixodes scapularis</i>	Salp15	CD4+ T cells	Salp15	Anguita et al. (2002)
<i>Dermacentor andersoni</i>	p36	T lymphocytes	ETX_MTX2	Bergman et al. (1998, 2000)
<i>Ixodes scapularis</i>	Metallo Dipeptidyl Carboxypeptidase	Bradykinin	ND	Ribeiro and Mather (1998)
<i>Rhipicephalus microplus</i>	Bookase	Bradykinin	ND	Bastiani et al. (2002)
<i>Ixodes scapularis</i>	PGE2	Inflammation	ND	Ribeiro et al. (1985)

Indicated are the common name for the immuno-modulators, its molecular target and the protein family to which they belong. *ND* not determined

Table 17.3B Immuno-modulators from insects

Species	Name	Target	Family	Reference
<i>Lutzomyia longipalpis</i>	SALO	Complement C4	Novel	Cavalcante et al. (2003), Mendes-Sousa et al. (2013), Ferreira et al. (2016)
<i>Lutzomyia migonei</i>	NA	Complement	ND	Cavalcante et al. (2003)
<i>Panstrongylus megistus</i>	NA	Complement	ND	Cavalcante et al. (2003)
<i>Triatoma brasiliensis</i>	NA	Complement	ND	Cavalcante et al. (2003)
<i>Rhodnius prolixus</i>	NA	Complement	ND	Cavalcante et al. (2003)
<i>Rhodnius prolixus</i>	Nitrophorins	Histamine	Lipocalin	Ribeiro and Walker (1994), Weichsel et al. (1998);

Indicated are the common name for the immuno-modulators, its molecular target and the protein family to which they belong. *ND* not determined

(Markiewski et al. 2007; Peerschke et al. 2008, 2010). During platelet activation a number of platelet receptors can bind complement and activate the complement cascade via the classical or alternative pathways (del Conde et al. 2005; Peerschke et al. 2006). Phosphatidyl serine on activated platelet surfaces can activate C1 to C1q which can bind to the platelet receptor cC1qR leading to activation of $\alpha_{IIb}\beta_3$, platelet aggregation, P selectin expression, and platelet procoagulant activity (Peerschke and Ghebrehiwet 1997). P-selectin can bind C3b and thereby activate the alternative pathway leading to C3a generation (del Conde et al. 2005). Activation of the complement cascade is agonist dependent, with weaker responses for ADP and epinephrine (serotonin?) than for thrombin or arachidonic acid (collagen/ TXA2?) (Peerschke et al. 2006). Granule secretion by activated platelets and the release of chondroitin sulphate also further activates the classical complement pathway (Hamad et al. 2008). Complement activation leads to the generation of C3a, C4a and C5a. C3a, C4a and C5a can recruit inflammatory cells to the site of injury. C3a enhances platelet responses to agonists such as ADP and thrombin. C5a can activate endothelial cells to express tissue factor, while C5b-9 can induce platelet activation and procoagulant responses in platelets (Peerschke et al. 2008). Complement inhibitors specific for the alternative pathway and C3b have been identified in the hard ticks *I. scapularis* and *I. ricinus* and have been shown to belong to the Isac family (Ribeiro 1987a; Valenzuela et al. 2000; Daix et al. 2007; Couvreur et al. 2008). Members of the Isac family can also bind to properdin, thereby accelerating the decay of C3 convertase and inhibiting the alternative complement pathway (Tyson et al. 2007, 2008). Soft ticks from the genus *Ornithodoros* inhibits the classical pathway and specifically complement C5 using lipocalins from the moubatin-clade (Nunn et al. 2005; Roversi et al. 2007; Mans and Ribeiro 2008a). Saliva from the sand flies *L. longipalpis*, *L. migonei*, the assassin bugs *Panstrongylus megistus*, *Tr. brasiliensis* and *R. prolixus* could inhibit the classical complement pathway,

while the mosquito *Ae. aegypti* and the cat flea *Ct. felis* could not (Cavalcante et al. 2003; Mendes-Sousa et al. 2013). SALO, an 11 kDa protein with no known homology was recently identified as the inhibitor from *L. longipalpis* that targets the classical complement pathway and inhibits C4b deposition and C4 cleavage (Ferreira et al. 2016). Saliva from the sand fly, *L. longipalpis*, could also inhibit the alternative complement pathway (Mendes-Sousa et al. 2013). While inhibitors for the complement pathway from fast-feeders certainly aim to limit the inflammatory responses of C3 and C5, the major role in feeding may lie in neutralizing the impact that complement have on platelet aggregation and coagulation.

Neutrophils are recruited into sites of injury within minutes after injury where they secrete serine proteases involved in inflammatory responses. They also secrete neutrophil extracellular traps (NETs) that are composed of a web of chromatin fibers and serine proteases. NETs play an important role in inflammation and hemostasis (platelet activation and blood coagulation) (Massberg et al. 2010; Gould et al. 2014). Platelets can also contribute towards NET formation via secretion of thromboxane A2 (TXA2) (Caudrillier et al. 2012). The triatomine bugs *D. maxima* and *Tr. infestans* are able to scavenge TXA2 and inhibit platelet-mediated NET formation via the lipocalins, dipetalodipin and triplatin (Mizurini et al. 2015). Triplatin and dipetalodipin can also inhibit collagen-induced platelet aggregation due to their TXA2 scavenging properties (Morita et al. 2006; Assumpção et al. 2010; Ma et al. 2012). TXA2 scavenging by the soft tick lipocalins (moubatin and TSGP3) from *Or. moubata* and *Or. savignyi* has also been observed and functions to inhibit collagen-mediated platelet aggregation (Mans and Ribeiro 2008a), but probably also function to inhibit platelet mediated NET formation. Interestingly, saliva from *I. ricinus* did not inhibit NET formation, which may indicate that it lacks TXA2 scavenging capabilities, although platelet mediated NET formation was not tested (Menten-Dedoyart et al. 2012). TXA2 scavenging was also not determined, although it was shown that leukotriene B4 (LTB4) could be scavenged by the *I. ricinus* lipocalin Ir-LBP (Beaufays et al. 2008), a function that can also be performed by moubatin and TSGP3 (Mans and Ribeiro 2008a). This does not imply that Ir-LBP will also scavenge TXA2, since TSGP2 from *Or. savignyi* can bind LTB4, but not TXA2 (Mans and Ribeiro 2008a). The mosquito *An. stephensi* scavenge TXA2 via D7L1 (D7 odorant binding family) and inhibits collagen-mediated platelet aggregation (Alvarenga et al. 2010), but will presumably also inhibit platelet-mediated NET formation. An endonuclease is secreted by the mosquito *C. quinquefasciatus* (Calvo and Ribeiro 2006), which could presumably also function in NET degradation. Endonucleases has also been found in salivary gland transcriptomes of frog biting midges (Ribeiro et al. 2014a), horse flies (Ribeiro et al. 2015a), sand flies (Valenzuela et al. 2004; Anderson et al. 2006; Oliveira et al. 2006; Hostomská et al. 2009), stable flies (Wang et al. 2009) and tsetse flies (Alves-Silva et al. 2010). LTB4 is generated by activated innate immune cells such as neutrophils, macrophages and mast cells and is an important stimulus for neutrophil migration, aggregation and degranulation during inflammation (Bäck et al. 2004, 2007; Ohnishi et al. 2008). Other immune cells such as eosinophils, monocytes/macrophages, mast cells and dendritic cells are also recruited by LTB4 into the site of injury (Bäck et al. 2004, 2007;

Ohnishi et al. 2008). Scavenging of LTB₄ will prevent infiltration into the feeding site and has been discussed for ticks. The sand fly *L. longipalpis* could inhibit the production and effects of LTB₄ on neutrophil migration (Monteiro et al. 2005). *Phlebotomus papatasi* and *Ph. duboscqi* saliva also inhibited production of LTB₄ by neutrophils (Carregaro et al. 2008).

The serine proteases cathepsin G and elastase are secreted by neutrophils during NET formation (Gardiner and Andrews 2012). Cathepsin G function to activate platelets, while elastase potentiate the activity of cathepsin G on platelet aggregation (Selak et al. 1988; Renesto et al. 1992; Selak 1992). Inhibitors capable of inhibiting cathepsin G induced platelet aggregation have been characterized in the hard tick *I. ricinus*, named IRS2 – *I. ricinus*-serpin 2 (Chmelar et al. 2011). Iris can also inhibit chymase, which is produced by activated mast cells and function with cathepsin G to activate connective tissue-activating peptide-III (CTAP-III) secreted by activated platelets to neutrophil-2 (NAP-2), that activate neutrophils and serve as chemoattractant (Schiemann et al. 2006). A fXa, cathepsin G and chymase inhibitor named Simikunin were characterized from the black fly *Si. vittatum* (Tsujiimoto et al. 2012). A number of elastase inhibitors were characterized in hard ticks (Tanaka et al. 1999; Sant’Anna Azzolini et al. 2003; Sasaki et al. 2004; Prevot et al. 2006; Soares et al. 2012; Cao et al. 2013; Mulenga et al. 2013; Rodriguez-Valle et al. 2015). They either belong to the Kunitz/BPTI or the serpin families (Tables 17.3A).

Neutrophils also secrete the potent platelet activator, platelet activating factor (PAF) (Renesto et al. 1992). The mosquito *C. quinquefasciatus* secretes a phospholipase C enzyme capable of hydrolyzing PAF thereby inhibiting PAF-induced platelet aggregation, while *A. aegypti* and *An. gambiae* did not exhibit this activity (Ribeiro and Francischetti 2001).

Monocytes migrate into the site of injury within 2 hours after injury and mature to macrophages that ingest and remove cellular debris, secrete growth factors and cytokines that promote the proliferation phase, angiogenesis, proliferation of cells involved in ECM synthesis. Iris can also bind to monocytes and macrophages, inhibiting secretion of tumor necrosis factor- α (TNF α), acting in an anti-inflammatory manner (Prevot et al. 2009). TNF α acts as a recruitment factor during wound healing by inducing the secretion of cytokines such as macrophage inflammatory protein-2, cytokine-induced neutrophil chemoattractant and interleukin-8 that attract macrophages and neutrophils to the site of injury (Driscoll et al. 1997). Iris also inhibit the production of pro-inflammatory cytokines interferon- γ , interleukin-6 and interleukin-8 by T-cells and PBMCs, and inhibits elastase, prolongs the contact phase of the blood-clotting cascade and promote fibrinolysis (Leboulle et al. 2002; Prevot et al. 2006).

Mast cells carry a variety of components in their granules which include histamine, serotonin, heparin, PAF, LTC₄, TXA₂, prostaglandin D₂, cytokines, eosinophil chemotactic factor, chymase, cathepsin G and β -tryptase, the most abundant secretory serine protease in these cells (Ribatti and Ranieri 2015). Basophils also carry histamine and heparin. In both cell types, binding of allergens to receptor bound immunoglobulin E induces secretion of granules (Ribatti and Ranieri 2015). Inhibitors and scavengers of histamine, serotonin, PAF, LTC₄, TXA₂, heparin and

cathepsin G were described above. Trypsase induce fibroblast migration and proliferation, collagen synthesis, tissue wound repair and remodeling and angiogenesis (Ribatti and Ranieri 2015). The hard tick *Rhipicephalus appendiculatus* secrete a trypsin inhibitor (TdPI) that inhibit trypsin and plasmin. Injection of TdPI into mice ears resulted in the uptake of TdPI into mast cells and localization within the cytosolic granules, where it presumably inhibit trypsin (Paesen et al. 2007). Trypsinogen from the ixodid *I. scapularis* also inhibits trypsin, elastase and plasmin and seems to be evolutionary related to TdPI (Valdés et al. 2013).

17.6 The Sialoverse

The sialoverse describes all proteins secreted from the salivary glands of blood-feeding arthropods during feeding and may be seen as a systematic organization of these proteins into protein families, domains or folds (galaxies) in the larger sialome universe (Ribeiro and Arca 2009). Each galaxy expands or contracts as genes undergo duplication or are lost, species diverge or becomes extinct and members are separated by their evolutionary distance in time since divergence. Some galaxies (protein families) expand much faster than others due to gene duplication and preferential expansion of specific protein families in different blood-feeding lineages (Tables 17.4A and 17.4B). Galaxies may become sister-galaxies as lineage specific expansion occur in different lineages. The size of the sialoverse is therefore not fixed, but depends on lineage specific history (species divergence and adaptation to hematophagy), as well as environmental effects such as mass extinction events, and therefore also acknowledge historical events and is not purely a description of extant sialomes. Our own knowledge of the sialoverse also depends on taxonomic sampling as well as sequence coverage and is closely linked with historical progress in science and technology.

Our knowledge regarding the sialoverse in the twentieth century depended on physiological and biochemical assays that indicated that biologically active components were present in the saliva or salivary extracts of blood-feeding arthropods (Ribeiro 1987b, 1995). We also obtained glimpses of its complexity in the protein profiles observed in polyacrylamide gels or chromatograms that aimed to analyze salivary gland complexity. Prior to 1990 we had no specific knowledge regarding the molecular identities of these proteins and the sialoverse were a conceptualization of generalized functionalities with regard to vector-host interactions (Ribeiro 1987b; Titus and Ribeiro 1990; Law et al. 1992).

From 1990 to 2000, individual genes or proteins were sequenced and could be placed into known or novel protein families or folds (Waxman et al. 1990; Keller et al. 1993; Karczewski et al. 1994; Champagne et al. 1995a, 1995b; Cupp et al. 1998; Joubert et al. 1998; Valenzuela and Ribeiro 1998; Valenzuela et al. 1998, 1999; Charlab et al. 1999; Paesen et al. 1999). By the end of the millennium the total number of proteins and functions described for blood-feeding arthropods were in the low hundreds (Ribeiro and Francischetti 2003). The advent of conventional

Table 17.4A Salivary gland transcriptomes generated for ticks

Species	Library type	Secretory proteins	Most expanded	2n Most expanded	Reference
Argasidae					
<i>Argas monolakensis</i>	C	137	Lipocalin (32)	BTSP (21)	Mans et al. (2008a)
<i>Antricola delacruzii</i>	C	25	Mucin (6)	Metalloprotease (3)	Ribeiro et al. (2012b)
<i>Ornithodoros coriaceus</i>	C	123	Lipocalin (39)	BTSP (19)	Francischetti et al. (2008b)
<i>Ornithodoros parkeri</i>	C	132	Lipocalin (48)	BTSP (20)	Francischetti et al. (2008a)
Ixodidae					
<i>Ixodes pacificus</i>	C	66	BTSP (16)	Lipocalin (10)	Francischetti et al. (2005b)
<i>Ixodes ricinus</i>	C	129	BTSP (47)	BPTI (18)	Chmelar et al. (2008)
<i>Ixodes ricinus</i>	N	3882	Lipocalin (564)	Metalloprotease (564)	Schwarz et al. (2013)
<i>Ixodes ricinus</i>	N	3670	Lipocalin (568)	BPTI (478)	Kotsyfakis et al. (2015)
<i>Ixodes scapularis</i>	C	76	BPTI (26)	BTSP (22)	Valenzuela et al. (2002a)
<i>Ixodes scapularis</i>	C	274	BPTI (44)	BTSP (42)	Ribeiro et al. (2006)
<i>Amblyomma americanum</i>	C	193	Lipocalin (69)	BPTI (65)	Aljamali et al. (2009)
<i>Amblyomma americanum</i>	C	104	Lipocalin (31)	BTSP (9)	Gibson et al. (2013)
<i>Amblyomma americanum</i>	N	849	Lipocalin (213)	BPTI (110)	Karim and Ribeiro, (2015)
<i>Amblyomma maculatum</i>	N	886	Lipocalin (304)	Metalloprotease (147)	Karim et al. (2011)
<i>Amblyomma. variegatum</i>	C	140	Metalloprotease (18)	Lipocalin (12)	Ribeiro et al. (2011)
<i>Amblyomma cajennense</i>	N	1362	Lipocalin (275)	BPTI (187)	Garcia et al. (2014)
<i>Amblyomma parvum</i>	N	476	Lipocalin (109)	BPTI (61)	Garcia et al. (2014)
<i>Amblyomma triste</i>	N	1761	Lipocalin (589)	BPTI (135)	Garcia et al. (2014)
<i>Haemaphysalis flava</i>	N	–	–	–	Xu et al. (2015)
<i>Haemaphysalis longicornis</i>	N	–	–	–	Tirloni et al. (2015)
<i>Hyalomma marginatum rufipes</i>	C	43	Lipocalin (5)	BPTI (2)	Francischetti et al. (2011)

(continued)

Table 17.4A (continued)

Species	Library type	Secretory proteins	Most expanded	2n Most expanded	Reference
<i>Dermacentor andersoni</i>	C	139	Lipocalin (21)	BPTI (21)	Alarcon-Chaidez et al. (2007)
<i>Dermacentor andersoni</i>	N	–	–	–	Mudenda et al. (2014)
<i>Rhipicephalus appendiculatus</i>	C	107	Metalloprotease (24)	BTSP (6)	Nene et al. (2004)
<i>Rhipicephalus appendiculatus</i>	N	2134	Lipocalin (516)	BPTI (236)	de Castro et al. (2016)
<i>Rhipicephalus microplus</i>	N	93	Lipocalin (49)	BPTI (2)	Tirloni et al. (2014)
<i>Rhipicephalus pulchellus</i>	N	1414	Lipocalin (331)	BPTI (196)	Tan et al. (2015)
<i>Rhipicephalus sanguineus</i>	C	102	Lipocalin (31)	BPTI (10)	Anatriello et al. (2010)

Indicated is the library type (conventional or next-generation sequencing), the number of secretory proteins, the most expanded protein family and the number in parenthesis, the second most expanded and the number in parenthesis. Abbreviations are for the basic pancreatic trypsin inhibitor (BPTI) and basic tail secretory protein (BTSP) families. Where no data is available in the sequence database or the reference it is indicated with –

cDNA library sequencing resulted in an increase of those sialomes characterized to several hundred genes per sialome in 2002 (Francischetti et al. 2002c; Nene et al. 2002; Valenzuela et al. 2002a, 2002b). Our knowledge of sialome complexity for a specific lineage depended on the number of clones that were sequenced (several hundreds, to thousands or tens of thousands), whether the same sialome was characterized by different groups or whether cDNA libraries were normalized or sequenced directly (Tables 17.4A and 17.4B). Direct sequencing without normalization showed that it was useful to detect abundant transcripts which generally corresponded with secretory products, while normalization tended to enhance the detection of housekeeping proteins. Our roadmap seemed clear as more and more salivary gland transcriptomes were sequenced and with every sialome added to the sequence database, the underlying structure of each protein galaxy in each taxonomic lineage became clear.

The second decade of the twenty-first century virtually exploded with the maturation of next-generation sequencing technologies (Martin and Wang 2011). For ticks the total number of known proteins at the time (~9524) was almost matched in the sialome of a single tick species (Karim et al. 2011). Subsequent sialomes sequenced for ticks confirmed that secretory proteins range in the thousands (Gibson et al. 2013; Schwarz et al. 2013; Garcia et al. 2014; Karim and Ribeiro 2015; Kotsyfakis et al. 2015; de Castro et al. 2016). The same phenomenon was observed for the limited number of sialomes sequenced for insects using next-generation sequencing (Chagas et al. 2013; Ribeiro et al. 2014a, 2015b; Schwarz et al. 2014).

Table 17.4B Salivary gland transcriptomes generated for insects

Species	Library type	Secretory proteins	Most expanded	2nd Most expanded	Reference
Bed bug					
<i>Cimex lectularius</i>	C	68	OBP (14)	Inositol Polyphosphate Phosphatase (14)	Francischetti et al. (2010)
Biting midges					
<i>Culicoides nubeculosus</i>	C	32	OBP (9)	BPTI (7)	Russel et al. (2009)
<i>Culicoides sonorensis</i>	C	64	OBP (12)	BPTI (4)	Campbell et al. (2005)
Black flies					
<i>Simulium guianense</i>	C	428	D7 (72)	SVEP vasodilator (56)	Chagas et al. (2011)
<i>Simulium nigrimanum</i>	C	245	Aegyptin (10)	OBP (8)	Ribeiro et al. (2010b)
<i>Simulium vittatum</i>	C	124	Pro/Glu-rich (19)	SVEP (19)	Andersen et al. (2009)
Fleas					
<i>Ctenocephalides felis</i>	C	91	Acid phosphatase (21)	FS-H (19)	Ribeiro et al. (2012a)
<i>Xenopsylla cheopis</i>	C	84	FS-H (15)	Acid phosphatase (10)	Andersen et al. (2007)
Frog biting midges					
<i>Corethrella appendiculata</i>	N	819	Serine protease (64)	OBP (35)	Ribeiro et al. (2014a)
Horse fly					
<i>Tabanus bromius</i>	N	320	Antigen 5 (25)	Short peptide family 30/2 (18)	Ribeiro et al. (2015a)
Mosquitoes					
<i>Aedes aegypti</i>	C	38	Antigen 5 (4)	D7 (4)	Valenzuela et al. (2002b)
<i>Aedes aegypti</i>	C	136	D7 (6)	Antigen 5 (3)	Ribeiro et al. (2007)
<i>Aedes albopictus</i>	C	150	D7 (24)	Maltase (10)	Arcà et al. (2007)
<i>Anopheles darlingi</i>	C	93	D7 (9)	gSG7 (3)	Calvo et al. (2004)
<i>Anopheles darlingi</i>	C	114	D7 (12)	Aegyptin (8)	Calvo et al. (2009a)
<i>Anopheles funestus</i>	C	49	SG (1)	D7 (6)	Calvo et al. (2007b)
<i>Anopheles gambiae</i>	C	92	D7 (8)	Antigen 5 (3)	Francischetti et al. (2002c)

(continued)

Table 17.4B (continued)

Species	Library type	Secretory proteins	Most expanded	2nd Most expanded	Reference
<i>Anopheles gambiae</i>	C	155	D7 (8)	SG1 (6)	Arcà et al. (2005)
<i>Anopheles stephensi</i>	C	74	D7 (10)	SG1 (9)	Valenzuela et al. (2003)
<i>Culex pipiens quinquefasciatus</i>	C	103	D7 (11)	Maltase (6)	Ribeiro et al. (2004a)
<i>Culex tarsalis</i>	C	80	D7 (8)	Aegyptin (8)	Calvo et al. (2010a)
<i>Ochlerotatus triseriatus</i>	C	182	Aegyptin (5)	D7 (4)	Calvo et al. (2010b)
<i>Psorophora albipes</i>	N	802	Long-D7 (26)	Short-D7 (23)	Chagas et al. (2013)
Sand flies					
<i>Lutzomyia longipalpis</i>	C	28	C-type lectin (5)	Yellow (3)	Valenzuela et al. (2004)
<i>Phlebotomus arabicus</i>	C	74	27 kDa (6)	25 kDa (6)	Hostomská et al. (2009)
<i>Phlebotomus argentipes</i>	C	30	PpSP15 (5)	D7 (2)	Anderson et al. (2006)
<i>Phlebotomus ariasi</i>	C	24	D7 (3)	PpSP15 (2)	Oliveira et al. (2006)
<i>Phlebotomus duboscqi</i>	C	38	PpSP12 (9)	PpSP15 (3)	Kato et al. (2006)
<i>Phlebotomus orientalis</i>	C	26	PpSP15 (5)	D7 (4)	Vlkova et al. (2014)
<i>Phlebotomus papatasi</i>	C	53	PpSP14 (10)	PpSP28 (7)	Abdeladhim et al. (2012)
<i>Phlebotomus perniciosus</i>	C	30	PpSP15 (3)	D7 (3)	Anderson et al. (2006)
Stable fly					
<i>Stomoxys calcitrans</i>	C	27	Thrombostasin (3)	Antigen 5 (3)	Wang et al. (2009)
Triatomines					
<i>Panstrongylus megistus</i>	C	29	Lipocalin (19)	Serine protease (4)	Bussacos et al. (2011a)
<i>Panstrongylus megistus</i>	N	635	Lipocalin (87)	Kazal (13)	Ribeiro et al. (2015b)
<i>Rhodnius prolixus</i>	C	74	Lipocalin (62)	Antigen 5 (2)	Ribeiro et al. (2004b)
<i>Rhodnius brethesi</i>	C	24	Lipocalin (22)	MYS1 (1)	Bussacos et al. (2011b)
<i>Rhodnius robustus</i>	C	40	Lipocalin (36)	Antigen 5 (1)	Bussacos et al. (2011b)

(continued)

Table 17.4B (continued)

Species	Library type	Secretory proteins	Most expanded	2nd Most expanded	Reference
<i>Triatoma brasiliensis</i>	C	370	Lipocalin (341)	Kazal (9)	Santos et al. (2007)
<i>Triatoma dimidiata</i>	C	80	Lipocalin (58)	Antigen 5 (6)	Kato et al. (2010)
<i>Triatoma infestans</i>	C	118	Lipocalin (69)	Trialyisin (14)	Assumpção et al. (2008)
<i>Triatoma infestans</i>	N	2228	Lipocalin (109)	Antigen 5 (8)	Schwarz et al. (2014)
<i>Triatoma rubida</i>	C	93	Lipocalin (74)	Antigen 5 (10)	Ribeiro et al. (2012c)
Tsetse fly					
<i>Glossina morsitans morsitans</i>	C	550	Endonuclease (19)	Antigen 5 (4)	Alves-Silva et al. (2010)

Indicated is the library type (conventional or next-generation sequencing), the number of secretory proteins, the most expanded protein family and the number in parenthesis, the second most expanded and the number in parenthesis. Abbreviations are for the basic pancreatic trypsin inhibitor (BPTI) and basic tail secretory protein (BTSP) families. Where no data is available in the sequence database or the reference it is indicated with –

As such, conventional sequencing indicated that the numbers of secretory proteins range in the lower hundreds. The few salivary transcriptomes sequenced to date with next-generation sequencing technologies all indicate values for secretory proteins at least ten fold higher than their conventional sequencing partners. Whether this is an artefact of the next-generation sequencing technologies (Martin and Wang 2011), cannot yet be ascertained, since those sequenced with these technologies do not have completed genomes. For those insects for which genomes have been determined the number of protein family members in the genome corresponds with those obtained by conventional sequencing approaches for those genes which shows lineage specific expansion. For example, the sialome of *R. prolixus* indicated 62 lipocalins (Ribeiro et al. 2004b), while genome sequencing indicated the presence of 51 lipocalin genes (Mesquita et al. 2015). Next generation sequencing of the digestive tract (non-salivary) detected 88 lipocalins (Ribeiro et al. 2014b).

The sialome are a historical documentation of the adaptation to the vector-host interface and may be used to inform us regarding the evolutionary history of hematophagy in arthropods (Mans 2011). Hypotheses regarding the origins of blood-feeding in various lineages may be addressed, since comparative analysis should enable us to find orthologous genes with functions evolved specifically for adaptation to hematophagy and these would support the evolution of blood-feeding behavior in the last common ancestor. Comparative analysis may also allow us to discover the deeper generalities of adaptation to the blood-feeding interface, i.e. features common to sialomes that is not apparent by simple comparison of genes (Mans 2011). In this regard, the following features was previously identified:

17.6.1 Different Lineages Have Unique Salivary Gland Repertoires

A comparison of sialomes indicates that various lineages possess different dominant families (Tables 17.4A and 17.4B and references therein), implying that these lineages diverged before adaptation to a blood-feeding lifestyle. The salivary gland repertoires of assassin bugs, bed bugs and fleas differ completely from the hematophagous dipterans, while the bracyceran flies differ from the nematocerans. Ticks differ again from the insects in the majority of the protein families. During the evolution of blood-feeding, different lineages would utilize those families currently expressed in the salivary gland and these may have been preselected based on the specific environmental niche occupied by the parasite at that specific time. As such, some may have been phytophagous, scavengers, arthropod parasites, non-hematophagous vertebrate parasites or predators (Mans 2011). It can be expected that whenever a new sialome from a distant lineage is determined, it will certainly differ from those already known and we should expect interesting new results for hematophagous acariform and mesostigmatid mites, copepods, isopods, tongue worms, lice, snipe flies and moths. It would also be interesting to see whether hippoboscids and the bat flies will have salivary gland repertoires that is similar to the tsetse flies.

17.6.2 Similar Protein Family Repertoires Are Found in the Sialomes of Closely Related Lineages

Lineages that share a common ancestor and who may have had similar environmental niches before adaptation to a blood-feeding environment, would have had similar salivary gland repertoires before adapting to a blood-feeding environment. The same protein families may be found in the sialomes, but few orthologous genes may be present if these lineages adapted to blood-feeding independently (Mans 2011). In this regard, comparative analysis of sialomes may assist in interpreting the evolutionary history of blood-feeding, especially for lineages with contentious interpretations regarding the evolution of blood-feeding.

An hypothesis regarding a common hematophagous origin for all hemipterans could be falsified given the differences observed in sialomes of the Cimicidae and the Reduviidea. Within the Reduviidea, a common origin for blood-feeding has been proposed based on systematic analysis (Weirauch and Munro 2009; Patterson and Gaunt 2010). This may even be supported by the large expansion of lipocalins observed in all sialomes described to date for the Reduviidae that is absent in the Cimicidae (Ribeiro et al. 2012d). However, even though a significant number of lipocalins have been assigned functions, few orthologs can be found between *Rhodnius* and the other triatomine genera (*Triatoma*, *Dipetalogaster* and *Panstrongylus*) (Santos et al. 2007; Assumpção et al. 2008; Kato et al. 2010;

Assumpção et al. 2011; Mans 2011; Ribeiro et al. 2012d; Schwarz et al. 2014). Orthologs seem to be recovered between *Triatoma*, *Dipetalogaster* and *Panstrongylus* (Assumpção et al. 2011; Schwarz et al. 2014), but systematic analysis indicate that *Dipetalogaster* and *Panstrongylus* group within the *Triatoma* clade and it may thus be expected (Ibarra-Cerdeña et al. 2014). The Triatominae is not monophyletic with regard to hematophagous lineages, since *Rhodnius* group with predatory Reduviinae and independent evolution of blood-feeding behavior could not be excluded (Hwang and Weirauch 2012; Ibarra-Cerdeña et al. 2014). What may be more surprising is the recent evolution of blood-feeding behavior in the triatomines (~32–12 MYA), the extensive lineage specific expansion of lipocalins and the divergence among the various paralogs. Compared to soft ticks, where orthologs involved in anti-hemostatic and immune responses have been conserved more than 230 million years (Mans and Ribeiro 2008b; Mans et al. 2008b, 2008c, 2012), the divergence of the triatomine lipocalins, may suggest that the lineages diverged before adaptation to blood-feeding was fully attained. What would be of interest is the sequencing of a non-hematophagous triatomine to determine whether lipocalin expansions in the salivary glands is a common feature. The salivary transcriptome of the large milkweed bug, *Oncopeltus fasciatus* which belongs to the Pentatomorpha was sequenced (Francischetti et al. 2007). No lipocalins could be detected, probably since the Reduviidae diverged from other Heteroptera more than 200 MYA (Hwang and Weirauch 2012). The one “smoking gun” that point to a common origin for hematophagy in the Triatominae is the thrombin inhibitors found in the midguts of the assassin bugs. *Rhodnius* and the infestins are Kazal-type thrombin inhibitors that derive from *R. prolixus* and *Tr. infestans*, respectively (Friedrich et al. 1993; Campos et al. 2002). They retrieve each other using reciprocal best BLAST hit analysis suggesting that these Kazal inhibitors are orthologs. If these are indeed orthologs, it may indicate that larger diversification occurred in the salivary glands compared to midgut proteins, and that many more orthologs may be found in the midgut transcriptomes.

Ticks exhibit the same puzzling phenomenon as observed for the triatomines. Very few orthologs are conserved between the soft and hard tick families, even though they possess the same major protein families such as lipocalins, Kunitz/BPTI, metalloproteases and basic tail secretory protein (BTSP) (Mans and Neitz 2004; Mans et al. 2008a; Mans 2011). However, systematic relationships of the three families (Argasidae, Ixodidae and Nuttalliellidae) imply that blood-feeding must have evolved in the ancestral lineage (Mans et al. 2011, 2012). Even so, little conservation of characters involved in blood-feeding not related to tick-host interaction are observed between the soft and hard tick families (Mans 2014). Characters unique to the hard and soft tick families are found in the monotypic family, Nuttalliellidae (Mans et al. 2012), and it was suggested that these characters were present in the ancestral lineage. This argues for a common origin of a blood-feeding lifestyle, but independent evolution of salivary gland functions after divergence of the lineages (Mans et al. 2016). A possible reason for rapid speciation during adaptation to a blood-feeding lifestyle, may be the availability of numerous host species

with similar defense mechanisms and the vast opportunity this have for potential new niches and host specialization.

The other potential interesting case of evolution of hematophagy in a large group of blood-feeding lineages, are the Nematocera. Comparison of the sialomes of Psychodomorpha and Culicomorpha suggest that these lineages adapted independently to blood-feeding since they only share two main secretory families and most of their anti-hemostatic functions are performed by different protein families (Ribeiro et al. 2010a). The Culicomorpha is more interesting, since a variety of lineages with different biology are hematophagous. This includes mosquitoes, frog biting midges, biting midges and black flies. In the Culicomorpha an extensive number of families are unique to each lineage (Ribeiro et al. 2010a). While the odorant binding/D7 proteins are found in all lineages and also seem to be prone to gene duplication, even the functions as kratagonists are not conserved. Again, if blood-feeding originated in the ancestral Culicomorpha lineage, it would seem as if speciation occurred during adaptation to a blood-feeding lifestyle.

The argument has been made that the diversity observed in sialomes are indicative of host immune pressure that forces constant change in salivary repertoires, evolution of function and loss of orthologous genes, with the implication that a constant arms race between vector salivary repertoires and host immunity exist (Francischetti et al. 2009). This argument have some merit, but it does not explain why orthologous genes are indeed found within genera, where orthologous function has been conserved at least as long as the divergence from other sister genera (Mans and Ribeiro 2008b; Mans et al. 2008b; Mans 2014). Other explanations that could explain diverse salivary gland repertoires may be simple stochastic birth and death of genes and gene families (Eirín-López et al. 2012), and that lineages may have diverged while still adapting to blood-feeding.

17.6.3 The Same Protein Families Are Prone to Expansion in Closely Related Lineages

All lineages have specific protein families that show extensive gene duplication. This is observed for lipocalins in assassin bugs and ticks, the cimex nitrophorin/inositol polyphosphate 5 phosphatase family in bed bugs, the endonuclease family in tsetse flies, the acid phosphatase and FS1 antigen families in fleas, the odorant-binding/D7 family in bed bugs, mosquitoes, sand flies, and biting midges, the antigen 5 and thrombostasin family in stable flies (Tables 17.4A and 17.4B).

In general these families also constitute the most abundant proteins in the sialomes. Gene duplication is an important mechanism to increase the expression levels of proteins and may account for expansion (Rogozin 2014). Expansion may also be related to the genes expressed in the salivary glands at the time of blood-feeding evolution and therefore available for innovation. In many cases these families are involved in scavenging functions of the kratagonists and their specific functionality, i.e. tight binding of small bioactive molecules, will only allow proteins with

architectures compatible with this function to be used. The high diversity observed for these abundant families suggest that they have higher mutational rates than normal cellular proteins, i.e. indicative of positive selection. Duplication of highly expressed genes that is secreted into an extracellular environment, and would therefore not jeopardize existing cellular functions, could also be a mechanism to experiment with high mutation rates that would allow evolution of new function. Gene duplication and subfunctionalization could therefore be a self-propelling mechanism to generate diversity in sialomes (Mans 2011).

17.6.4 Different Blood-Feeding Lineages Target the Same Host Defense Mechanisms

From the discussions above regarding host defenses and vector counter-measures it is clear that the same key components of the host defenses are targeted by hematophagous arthropods (n). This might be expected or even seem logical (Ribeiro 1995), but has only been confirmed empirically over the last 20 years. It attests to the importance that the vertebrate targets play in vertebrate defenses but also make the argument that anti-defense mechanisms are very important in the acquisition of a blood-meal. The redundancy observed in sialomes only match the redundancy observed in host defense mechanisms. Whether this is evidence of an arms race is not certain. It has been speculated that hematophagous arthropods may have influenced the evolution of host defenses (Mans 2011), and if so, this would satisfy the demand of an arms race. However, the host defense system is redundant for effective control, since deficiencies have a significant impact on survival. If this redundant host defense system existed before adaptation to a blood-feeding lifestyle, which by most accounts seems valid, the redundancy observed in sialomes may simply reflect the fact that multiple targets needs to be neutralized to be effective for successful feeding and long term contribution to species fitness.

17.7 Future Perspectives

It has been estimated that if the sialome is composed of a 1000 proteins, that it would take 20 years of concerted effort from 100 scientists, or 2000 scientist years to delineate each protein function (Ribeiro and Arca 2009). The complexities revealed by next-generation sequencing have indicated that the sialome is potentially much larger, especially if we do not only consider a strict gene count, but take into account that different proteins may have multiple functions. A number of the salivary proteins have multiple functions involved in host interactions. This include nitrophorin 2 that can bind NO, histamine and inhibit coagulation (Andersen and Montfort 2000), the double domain D7 protein from *An. gambiae* which scavenge cysteinyl leukotrienes with the N-terminal domain and biogenic amines with the

C-terminal domain (Calvo et al. 2009c), the double D7 domain protein from *An. stephensi* which scavenges cysteinyl leukotrienes with the N-terminal domain and TXA2 with the C-terminal domain (Alvarenga et al. 2010), the single domain D7 protein, D7r1, that binds serotonin and inhibits fXIIa (Calvo et al. 2006), the moubatin-like lipocalins that can bind both LTB4 and TXA2, and OMCI that also targets complement C5 (Nunn et al. 2005; Mans and Ribeiro 2008a), tablysin-15 that binds cysteinyl leukotrienes and integrins $\alpha_{IIb}\beta_3$ and $\alpha_v\beta_3$ (Ma et al. 2011; Xu et al. 2012). Vasotab TY that is a vasodilator and binds $\alpha_{IIb}\beta_3$ (Ma et al. 2009; Zhang et al. 2014). Serpin 19 from *Am. americanum* that can inhibit fXa, fXIa, trypsin and plasmin (Kim et al. 2015). IRS-2 from *I. ricinus* targets cathepsin G and chymase (Chmelar et al. 2011). If this is the norm rather than the exception, our estimate of salivary function may be severely underestimated. Current estimates for the secretory proteins of different sialomes indicate that the numbers vary from several thousand for ticks, to hundreds for insects.

While many of these functions are performed by orthologs between various genera, many seem to be lineage specific. A conservative estimate of unique orthologous groups may still be in the thousands. The same function may appear multiple times in different lineages, but since these functions are performed by non-orthologous genes, cannot be transferred by simple homologous relationships. Using the 2 years per protein characterization estimate (Ribeiro and Arca 2009), we now approach 20,000 scientist years (or 200 years of concerted efforts by 100 scientists), to gain a complete functional understanding of the sialoverse and even then not all proteins would have been functionally characterized. Conversely, it is foreseen that we should have a fairly good description of the sialoverse that covers the taxonomic breadth of the blood-feeding arthropods as well as the total number of unique orthologous groups, within the next 50 years if funding continues. Once we have exhausted this avenue using bioinformatic and proteomic approaches to validate the transcriptomes, the focus will return to biochemistry, physiology, genetics, systems and structural biology to elucidate functions empirically.

Acknowledgements This work was funded by the incentive funding for rated researchers grant from the National Research Foundation of South Africa (NRF-Mans 76499), and the ARC Tick Vaccine project (30/01/V010). I thank Ronel Pienaar for the line drawings depicting various feeding modes.

References

- Abdeladhim M, Jochim RC, Ben Ahmed M, Zhioua E, Chelbi I, Cherni S, Louzir H, Ribeiro JM, Valenzuela JG (2012) Updating the salivary gland transcriptome of *Phlebotomus papatasi* (Tunisian strain): the search for sand fly-secreted immunogenic proteins for huMans. *PLoS One* 7:e47347
- Abebe M, Cupp MS, Ramberg FB, Cupp EW (1994) Anticoagulant activity in salivary gland extracts of black flies (Diptera: Simuliidae). *J Med Entomol* 31:908–911
- Abebe M, Ribeiro JM, Cupp MS, Cupp EW (1996) Novel anticoagulant from salivary glands of *Simulium vittatum* (Diptera: Simuliidae) inhibits activity of coagulation factor V. *J Med Entomol* 33:173–176

- Alarcon-Chaidez FJ, Sun J, Wikel SK (2007) Transcriptome analysis of the salivary glands of *Dermacentor andersoni* Stiles (Acari: Ixodidae). *Insect Biochem Mol Biol* 37:48–71
- Aljamali MN, Hern L, Kupfer D, Downard S, So S, Roe BA, Sauer JR, Essenberg RC (2009) Transcriptome analysis of the salivary glands of the female tick *Amblyomma americanum* (Acari: Ixodidae). *Insect Mol Biol* 18:129–154
- Allen JR (1989) Immunology of interactions between ticks and laboratory animals. *Exp Appl Acarol* 7:5–13
- Alvarenga PH, Francischetti IM, Calvo E, Sá-Nunes A, Ribeiro JM, Andersen JF (2010) The function and three-dimensional structure of a thromboxane A₂/cysteinyl leukotriene-binding protein from the saliva of a mosquito vector of the malaria parasite. *PLoS Biol* 8:e1000547
- Alvarenga PH, Xu X, Oliveira F, Chagas AC, Nascimento CR, Francischetti IM, Juliano MA, Juliano L, Scharfstein J, Valenzuela JG, Ribeiro JM, Andersen JF (2013) Novel family of insect salivary inhibitors blocks contact pathway activation by binding to polyphosphate, heparin, and dextran sulfate. *Arterioscler Thromb Vasc Biol* 33:2759–2770
- Alves-Silva J, Ribeiro JM, Van Den Abbeele J, Attardo G, Hao Z, Haines LR, Soares MB, Berriman M, Aksoy S, Lehane MJ (2010) An insight into the sialome of *Glossina morsitans morsitans*. *BMC Genomics* 11:213
- Amino R, Tanaka AS, Schenkman S (2001) Triapsin, an unusual activatable serine protease from the saliva of the hematophagous vector of Chagas' disease *Triatoma infestans* (Hemiptera: Reduviidae). *Insect Biochem Mol Biol* 31:465–472
- An S, Ma D, Wei JF, Yang X, Yang HW, Yang H, Xu X, He S, Lai R (2011) A novel allergen Tab y 1 with inhibitory activity of platelet aggregation from salivary glands of horseflies. *Allergy* 66:1420–1427
- Anastopoulos P, Thurn MJ, Broady KW (1991) Anticoagulant in the tick *Ixodes holocyclus*. *Aust Vet J* 68:366–367
- Anatriello E, Ribeiro JM, de Miranda-Santos IK, Brandão LG, Anderson JM, Valenzuela JG, Maruyama SR, Silva JS, Ferreira BR (2010) An insight into the sialotranscriptome of the brown dog tick *Rhipicephalus sanguineus*. *BMC Genomics* 11:450
- Andersen JF, Montfort WR (2000) The crystal structure of nitrophorin 2. A trifunctional antihemostatic protein from the saliva of *Rhodnius prolixus*. *J Biol Chem* 275:30496–30503
- Andersen JF, Francischetti IM, Valenzuela JG, Schuck P, Ribeiro JM (2003) Inhibition of hemostasis by a high affinity biogenic amine-binding protein from the saliva of a blood-feeding insect. *J Biol Chem* 278:4611–4617
- Andersen JF, Hinnebusch BJ, Lucas DA, Conrads TP, Veenstra TD, Pham VM, Ribeiro JM (2007) An insight into the sialome of the oriental rat flea, *Xenopsylla cheopis* (Rots). *BMC Genomics* 8:102
- Andersen JF, Pham VM, Meng Z, Champagne DE, Ribeiro JM (2009) Insight into the sialome of the Black Fly *Simulium vittatum*. *J Proteome Res* 8:1474–1488
- Anderson JM, Oliveira F, Kamhawi S, Mans BJ, Reynoso D, Seitz AE, Lawyer P, Garfield M, Pham M, Valenzuela JG (2006) Comparative salivary gland transcriptomics of sandfly vectors of visceral leishmaniasis. *BMC Genomics* 7:52
- Anguita J, Ramamoorthi N, Hovius JW, Das S, Thomas V, Persinski R, Conze D, Askenase PW, Rincón M, Kantor FS, Fikrig E (2002) Salp15, an *Ixodes scapularis* salivary protein, inhibits CD4(+) T cell activation. *Immunity* 16:849–859
- Anisuzzaman, Islam MK, Miyoshi T, Alim MA, Hatta T, Yamaji K, Matsumoto Y, Fujisaki K, Tsuji N (2010) Longistatin, a novel EF-hand protein from the ixodid tick *Haemaphysalis longicornis*, is required for acquisition of host blood-meals. *Int J Parasitol* 40:721–729
- Anisuzzaman, Islam MK, Alim MA, Miyoshi T, Hatta T, Yamaji K, Matsumoto Y, Fujisaki K, Tsuji N (2011) Longistatin, a plasminogen activator, is key to the availability of blood-meals for ixodid ticks. *PLoS Pathog* 7:e1001312
- Anisuzzaman, Islam MK, Alim MA, Miyoshi T, Hatta T, Yamaji K, Matsumoto Y, Fujisaki K, Tsuji N (2012) Longistatin is an unconventional serine protease and induces protective immunity against tick infestation. *Mol Biochem Parasitol* 182:45–53

- Arcà B, Lombardo F, Valenzuela JG, Francischetti IM, Marinotti O, Coluzzi M, Ribeiro JM (2005) An updated catalogue of salivary gland transcripts in the adult female mosquito *Anopheles gambiae*. *J Exp Biol* 208:3971–3986
- Arcà B, Lombardo F, Francischetti IM, Pham VM, Mestres-Simon M, Andersen JF, Ribeiro JM (2007) An insight into the sialome of the adult female mosquito *Aedes albopictus*. *Insect Biochem Mol Biol* 37:107–127
- Arolas JL, Lorenzo J, Rovira A, Castellà J, Aviles FX, Sommerhoff CP (2005a) A carboxypeptidase inhibitor from the tick *Rhipicephalus bursa*: isolation, cDNA cloning, recombinant expression, and characterization. *J Biol Chem* 280:3441–3448
- Arolas JL, Popowicz GM, Lorenzo J, Sommerhoff CP, Huber R, Aviles FX, Holak TA (2005b) The three-dimensional structures of tick carboxypeptidase inhibitor in complex with A/B carboxypeptidases reveal a novel double-headed binding mode. *J Mol Biol* 350:489–498
- Assumpção TC, Francischetti IM, Andersen JF, Schwarz A, Santana JM, Ribeiro JM (2008) An insight into the sialome of the blood-sucking bug *Triatoma infestans* a vector of Chagas' disease. *Insect Biochem Mol Biol* 38:213–232
- Assumpção TC, Alvarenga PH, Ribeiro JM, Andersen JF, Francischetti IM (2010) Dipetalodipin, a novel multifunctional salivary lipocalin that inhibits platelet aggregation, vasoconstriction, and angiogenesis through unique binding specificity for TXA₂, PGF₂α, and 15(S)-HETE. *J Biol Chem* 285:39001–39012
- Assumpção TC, Charneau S, Santiago PB, Francischetti IM, Meng Z, Araújo CN, Pham VM, Queiroz RM, de Castro CN, Ricart CA, Santana JM, Ribeiro JM (2011) Insight into the salivary transcriptome and proteome of *Dipetalogaster maxima*. *J Proteome Res* 10:669–679
- Assumpção TC, Eaton DP, Pham VM, Francischetti IM, Aoki V, Hans-Filho G, Rivitti EA, Valenzuela JG, Diaz LA, Ribeiro JM (2012a) An insight into the sialotranscriptome of *Triatoma matogrossensis* a kissing bug associated with fogo selvagem in South America. *Am J Trop Med Hyg* 86:1005–1014
- Assumpção TC, Ribeiro JM, Francischetti IM (2012b) Disintegrins from hematophagous sources. *Toxins (Basel)* 4:296–322
- Assumpção TC, Ma D, Schwarz A, Reiter K, Santana JM, Andersen JF, Ribeiro JM, Nardone G, Yu LL, Francischetti IM (2013) Salivary antigen-5/CAP family members are Cu²⁺-dependent antioxidant enzymes that scavenge O₂ and inhibit collagen-induced platelet aggregation and neutrophil oxidative burst. *J Biol Chem* 288:14341–14361
- Austen KF (2007) Additional functions for the cysteinyl leukotrienes recognized through studies of inflammatory processes in null strains. *Prostaglandins Other Lipid Mediat* 83:182–187
- Bäck M, Qiu H, Haeggström JZ, Sakata K (2004) Leukotriene B₄ is an indirectly acting vasoconstrictor in guinea pig aorta via an inducible type of BLT receptor. *Am J Physiol Heart Circ Physiol* 287:419–424
- Bäck M, Sakata K, Qiu H, Haeggström JZ, Dahlén SE (2007) Endothelium-dependent vascular responses induced by leukotriene B₄. *Prostaglandins Other Lipid Mediat* 83:209–212
- Balashov YS (1972) Bloodsucking ticks (Ixodidae)—vectors of disease of man and animals. *Misc Pub Entomol Soc Am* 8:161–376
- Bastiani M, Hillebrand S, Horn F, Kist TB, Guimarães JA, Termignoni C (2002) Cattle tick *Boophilus microplus* salivary gland contains a thiol-activated metalloendopeptidase displaying kininase activity. *Insect Biochem Mol Biol* 32:1439–1446
- Batista IF, Chudzinski-Tavassi AM, Faria F, Simons SM, Barros-Batesti DM, Labruna MB, Leão LI, Ho PL, Junqueira-de-Azevedo IL (2008) Expressed sequence tags (ESTs) from the salivary glands of the tick *Amblyomma cajennense* (Acari: Ixodidae). *Toxicon* 51:823–834
- Batista IF, Ramos OH, Ventura JS, Junqueira-de-Azevedo IL, Ho PL, Chudzinski-Tavassi AM (2010) A new Factor Xa inhibitor from *Amblyomma cajennense* with a unique domain composition. *Arch Biochem Biophys* 493:151–156
- Beaufays J, Adam B, Menten-Dedoyart C, Fievez L, Grosjean A, Decrem Y, Prévôt PP, Santini S, Brasseur R, Brossard M, Vanhaeverbeek M, Bureau F, Heinen E, Lins L, Vanhamme L, Godfroid E (2008) Ir-LBP, an *Ixodes ricinus* tick salivary LTB₄-binding lipocalin, interferes with host neutrophil function. *PLoS One* 3:e3987

- Beerntsen BT, Champagne DE, Coleman JL, Campos YA, James AA (1999) Characterization of the Sialokinin I gene encoding the salivary vasodilator of the yellow fever mosquito, *Aedes aegypti*. *Insect Mol Biol* 8:459–467
- Bergman DK, Ramachandra RN, Wikel SK (1998) Characterization of an immunosuppressant protein from *Dermacentor andersoni* (Acari: Ixodidae) salivary glands. *J Med Entomol* 35:505–509
- Bergman DK, Palmer MJ, Caimano MJ, Radolf JD, Wikel SK (2000) Isolation and molecular cloning of a secreted immunosuppressant protein from *Dermacentor andersoni* salivary gland. *J Parasitol* 86:516–525
- Bochkov AV, Connor BM, Wauthy G (2008) Phylogenetic position of the mite family Myobiidae within the infraorder Eleutherengona (Acariformes) and origins of parasitism in eleutherengone mites. *Zool Anz* 247:15–45
- Bosman FT, Stamenkovic I (2003) Functional structure and composition of the extracellular matrix. *J Pathol* 200:423–428
- Brunnée T, Reddigari SR, Shibayama Y, Kaplan AP, Silverberg M (1997) Mast cell derived heparin activates the contact system: a link to kinin generation in allergic reactions. *Clin Exp Allergy* 27:653–663
- Bussacos AC, Nakayasu ES, Hecht MM, Assumpção TC, Parente JA, Soares CM, Santana JM, Almeida IC, Teixeira AR (2011a) Redundancy of proteins in the salivary glands of *Panstrongylus megistus* secures prolonged procurement for blood meals. *J Proteomics* 74:1693–1700
- Bussacos AC, Nakayasu ES, Hecht MM, Parente JA, Soares CM, Teixeira AR, Almeida IC (2011b) Diversity of anti-haemostatic proteins in the salivary glands of *Rhodnius* species transmitters of Chagas disease in the greater Amazon. *J Proteomics* 74:1664–1672
- Caljon G, De Ridder K, De Baetselier P, Coosemans M, Van Den Abbeele J (2010) Identification of a tsetse fly salivary protein with dual inhibitory action on human platelet aggregation. *PLoS One* 5:e9671
- Calvo E, Ribeiro JM (2006) A novel secreted endonuclease from *Culex quinquefasciatus* salivary glands. *J Exp Biol* 209:2651–2659
- Calvo E, Andersen J, Francischetti IM, deL Capurro M, deBianchi AG, James AA, Ribeiro JM, Marinotti O (2004) The transcriptome of adult female *Anopheles darlingi* salivary glands. *Insect Mol Biol* 13:73–88
- Calvo E, Mans BJ, Andersen JF, Ribeiro JM (2006) Function and evolution of a mosquito salivary protein family. *J Biol Chem* 281:1935–1942
- Calvo E, Tokumasu F, Marinotti O, Villeval JL, Ribeiro JM, Francischetti IM (2007a) Aegyptin, a novel mosquito salivary gland protein, specifically binds to collagen and prevents its interaction with platelet glycoprotein VI, integrin alpha2beta1, and von Willebrand factor. *J Biol Chem* 282:26928–26938
- Calvo E, Dao A, Pham VM, Ribeiro JM (2007b) An insight into the sialome of *Anopheles funestus* reveals an emerging pattern in anopheline salivary protein families. *Insect Biochem Mol Biol* 37:164–175
- Calvo E, Pham VM, Marinotti O, Andersen JF, Ribeiro JM (2009a) The salivary gland transcriptome of the neotropical malaria vector *Anopheles darlingi* reveals accelerated evolution of genes relevant to hematophagy. *BMC Genomics* 10:57
- Calvo E, Tokumasu F, Mizurini DM, McPhie P, Narum DL, Ribeiro JM, Monteiro RQ, Francischetti IM (2009b) Aegyptin displays high-affinity for the von Willebrand factor binding site (RGQOGVMGF) in collagen and inhibits carotid thrombus formation in vivo. *FEBS J* 277:413–427
- Calvo E, Mans BJ, Ribeiro JM, Andersen JF (2009c) Multifunctionality and mechanism of ligand binding in a mosquito antiinflammatory protein. *Proc Natl Acad Sci U S A* 106:3728–3733
- Calvo E, Sanchez-Vargas I, Favreau AJ, Barbian KD, Pham VM, Olson KE, Ribeiro JM (2010a) An insight into the sialotranscriptome of the West Nile mosquito vector *Culex tarsalis*. *BMC Genomics* 11:51

- Calvo E, Sanchez-Vargas I, Kotsyfakis M, Favreau AJ, Barbian KD, Pham VM, Olson KE, Ribeiro JM (2010b) The salivary gland transcriptome of the eastern tree hole mosquito *Ochlerotatus triseriatus*. *J Med Entomol* 47:376–386
- Calvo E, Mizurini DM, Sá-Nunes A, Ribeiro JM, Andersen JF, Mans BJ, Monteiro RQ, Kotsyfakis M, Francischetti IM (2011) Alboferpin, a factor Xa inhibitor from the mosquito vector of yellow fever, binds heparin and membrane phospholipids and exhibits antithrombotic activity. *J Biol Chem* 286:27998–28010
- Campbell CL, Vandyke KA, Letchworth GJ, Drolet BS, Hanekamp T, Wilson WC (2005) Midgut and salivary gland transcriptomes of the arbovirus vector *Culicoides sonorensis*. (Diptera: Ceratopogonidae). *Insect Mol Biol* 14:121–136
- Campos IT, Amino R, Sampaio CA, Auerswald EA, Friedrich T, Lemaire HG, Schenkman S, Tanaka AS (2002) Infestin, a thrombin inhibitor presents in *Triatoma infestans* midgut, a Chagas' disease vector: gene cloning, expression and characterization of the inhibitor. *Insect Biochem Mol Biol* 32:991–997
- Cao J, Shi L, Zhou Y, Gao X, Zhang H, Gong H, Zhou J (2013) Characterization of a new Kunitz-type serine protease inhibitor from the hard tick *Rhipicephalus haemaphysaloides*. *Arch Insect Biochem Physiol* 84:104–113
- Cappello M, Bergum PW, Vlasuk GP, Furnidge BA, Pritchard DI, Aksoy S (1996) Isolation and characterization of the tsetse thrombin inhibitor: a potent antithrombotic peptide from the saliva of *Glossina morsitans morsitans*. *Am J Trop Med Hyg* 54:475–480
- Cappello M, Li S, Chen X, Li CB, Harrison L, Narashimhan S, Beard CB, Aksoy S (1998) Tsetse thrombin inhibitor: bloodmeal-induced expression of an anticoagulant in salivary glands and gut tissue of *Glossina morsitans morsitans*. *Proc Natl Acad Sci U S A* 95:14290–14295
- Carregaro V, Valenzuela JG, Cunha TM, Verri WA Jr, Grespan R, Matsumura G, Ribeiro JM, Elnaiem DE, Silva JS, Cunha FQ (2008) Phlebotomine salivas inhibit immune inflammation-induced neutrophil migration via an autocrine DC-derived PGE2/IL-10 sequential pathway. *J Leukoc Biol* 84:104–114
- Carregaro V, Ribeiro JM, Valenzuela JG, Souza-Júnior DL, Costa DL, Oliveira CJ, Sacramento LA, Nascimento MS, Milanezi CM, Cunha FQ, Silva JS (2015) Nucleosides present on phlebotomine saliva induce immunosuppression and promote the infection establishment. *PLoS Negl Trop Dis* 9:e0003600
- Carvalho WA, Maruyama SR, Franzin AM, Abatepaulo AR, Anderson JM, Ferreira BR, Ribeiro JM, Moré DD, Augusto Mendes Maia A, Valenzuela JG, Garcia GR, de Miranda Santos IK (2010) *Rhipicephalus (Boophilus) microplus*: clotting time in tick-infested skin varies according to local inflammation and gene expression patterns in tick salivary glands. *Exp Parasitol* 124:428–435
- Caudrillier A, Kessenbrock K, Gilliss BM, Nguyen JX, Marques MB, Monestier M, Toy P, Werb Z, Looney MR (2012) Platelets induce neutrophil extracellular traps in transfusion-related acute lung injury. *J Clin Invest* 122:2661–2671
- Cavalcante RR, Pereira MH, Gontijo NF (2003) Anti-complement activity in the saliva of phlebotomine sand flies and other haematophagous insects. *Parasitology* 127:87–93
- Cerná P, Mikes L, Volf P (2002) Salivary gland hyaluronidase in various species of phlebotomine sand flies (Diptera: psychodidae). *Insect Biochem Mol Biol* 32:1691–1697
- Chagas AC, Medeiros JF, Astolfi-Filho S, Py-Daniel V (2010) Anticoagulant activity in salivary gland homogenates of *Thysopelma guianense* (Diptera: Simuliidae), the primary vector of onchocerciasis in the Brazilian Amazon. *Mem Inst Oswaldo Cruz* 105:174–178
- Chagas AC, Calvo E, Pimenta PF, Ribeiro JM (2011) An insight into the sialome of *Simulium guianense* (Diptera: Simuliidae) the main vector of River Blindness Disease in Brazil. *BMC Genomics* 12:612
- Chagas AC, Calvo E, Rios-Velázquez CM, Pessoa FA, Medeiros JF, Ribeiro JM (2013) A deep insight into the sialotranscriptome of the mosquito *Psorophora albipes*. *BMC Genomics* 14:875

- Chagas AC, Ramirez JL, Jasinskiene N, James AA, Ribeiro JM, Marinotti O, Calvo E (2014a) Collagen-binding protein, Aegyptin, regulates probing time and blood feeding success in the dengue vector mosquito, *Aedes aegypti*. *Proc Natl Acad Sci U S A* 111:6946–6951
- Chagas AC, McPhie P, San H, Narum D, Reiter K, Tokomasu F, Brayner FA, Alves LC, Ribeiro JM, Calvo E (2014b) Simiplagrin, a platelet aggregation inhibitor from *Simulium nigrimanum* salivary glands specifically binds to the Von Willebrand factor receptor in collagen and inhibits carotid thrombus formation *in vivo*. *PLoS Negl Trop Dis* 8:e2947
- Champagne DE, Ribeiro JM (1994) Sialokinin I and II: vasodilatory tachykinins from the yellow fever mosquito *Aedes aegypti*. *Proc Natl Acad Sci U S A* 91:138–142
- Champagne DE, Smartt CT, Ribeiro JM, James AA (1995a) The salivary gland-specific apyrase of the mosquito *Aedes aegypti* is a member of the 5'-nucleotidase family. *Proc Natl Acad Sci U S A* 92:694–698
- Champagne DE, Nussenzveig RH, Ribeiro JM (1995b) Purification partial characterization and cloning of nitric oxide-carrying heme proteins (nitrophorins) from salivary glands of the blood-sucking insect *Rhodnius prolixus*. *J Biol Chem* 270:8691–8695
- Charlab R, Valenzuela JG, Rowton ED, Ribeiro JM (1999) Toward an understanding of the biochemical and pharmacological complexity of the saliva of a hematophagous sand fly *Lutzomyia longipalpis*. *Proc Natl Acad Sci U S A* 96:15155–15160
- Cheeseman MT (1998) Characterization of apyrase activity from the salivary glands of the cat flea *Ctenocephalides felis*. *Insect Biochem Mol Biol* 28:1025–1030
- Cheng Y, Wu H, Li D (1999) An inhibitor selective for collagen-stimulated platelet aggregation from the salivary glands of hard tick *Haemaphysalis longicornis* and its mechanism of action. *Sci China Ser C Life Sci* 42:457–464
- Chmelar J, Anderson JM, Mu J, Jochim RC, Valenzuela JG, Kopecký J (2008) Insight into the sialome of the castor bean tick *Ixodes ricinus*. *BMC Genomics* 9:233
- Chmelar J, Oliveira CJ, Rezacova P, Francischetti IM, Kovarova Z, Pejler G, Kopacek P, Ribeiro JM, Mares M, Kopecky J, Kotsyfakis M (2011) A tick salivary protein targets cathepsin G and chymase and inhibits host inflammation and platelet aggregation. *Blood* 117:736–744
- Choi SH, Smith SA, Morrissey JH (2011) Polyphosphate is a cofactor for the activation of factor XI by thrombin. *Blood* 118:6963–6970
- Choi SH, Smith SA, Morrissey JH (2015) Polyphosphate accelerates factor V activation by factor XIa. *Thromb Haemost* 113:599–604
- Ciprandi A, de Oliveira SK, Masuda A, Horn F, Termignoni C (2006) *Boophilus microplus*: its saliva contains microphilin, a small thrombin inhibitor. *Exp Parasitol* 114:40–46
- Collin N, Assumpção TC, Mizurini DM, Gilmore DC, Dutra-Oliveira A, Kotsyfakis M, Sá-Nunes A, Teixeira C, Ribeiro JM, Monteiro RQ, Valenzuela JG, Francischetti IM (2012) Lufaxin, a novel factor Xa inhibitor from the salivary gland of the sand fly *Lutzomyia longipalpis* blocks protease-activated receptor 2 activation and inhibits inflammation and thrombosis *in vivo*. *Arterioscler Thromb Vasc Biol* 32:2185–2198
- Coons LB, Alberti G (1999) Acari: ticks. In: Harrison FW, Foelix RF (eds) *Microscopic anatomy of invertebrates volume 8B: Chelicerate Arthropoda*. Wiley-Liss, New York, pp 267–514
- Couvreur B, Beaufays J, Charon C, Lahaye K, Gensale F, Denis V, Charlotiaux B, Decrem Y, Prévôt PP, Brossard M, Vanhamme L, Godfroid E (2008) Variability and action mechanism of a family of anticoagulant proteins in *Ixodes ricinus*. *PLoS One* 3:e1400
- Cupp MS, Ribeiro JM, Cupp EW (1994) Vasodilative activity in black fly salivary glands. *Am J Trop Med Hyg* 50:241–246
- Cupp MS, Cupp EW, Ochoa-A JO, Moulton JK (1995) Salivary apyrase in New World blackflies (Diptera: Simuliidae) and its relationship to onchocerciasis vector status. *Med Vet Entomol* 9:325–330
- Cupp MS, Ribeiro JM, Champagne DE, Cupp EW (1998) Analyses of cDNA and recombinant protein for a potent vasoactive protein in saliva of a blood-feeding black fly *Simulium vittatum*. *J Exp Biol* 201:1553–1561

- Cupp MS, Zhang D, Cupp EW (2000) Horn fly (Diptera: Muscidae) saliva targets thrombin action in hemostasis. *J Med Entomol* 37:416–421
- Daix V, Schroeder H, Praet N, Georgin JP, Chiappino I, Gillet L, de Fays K, Decrem Y, Lebouille G, Godfroid E, Bollen A, Pastoret PP, Gern L, Sharp PM, Vanderplasschen A (2007) *Ixodes* ticks belonging to the *Ixodes ricinus* complex encode a family of anticomplement proteins. *Insect Mol Biol* 16:155–166
- de Castro MH, de Klerk D, Pienaar R, Latif AA, Rees DJ, Mans BJ (2016) De novo assembly and annotation of the salivary gland transcriptome of *Rhipicephalus appendiculatus* male and female ticks during blood feeding. *Ticks Tick Borne Dis* 7:536–548
- Decrem Y, Rath G, Blasioli V, Cauchie P, Robert S, Beaufays J, Frère JM, Feron O, Dogné JM, Dessy C, Vanhamme L, Godfroid E (2009) Ir-CPI, a coagulation contact phase inhibitor from the tick *Ixodes ricinus*, inhibits thrombus formation without impairing hemostasis. *J Exp Med* 206:2381–2395
- Del Conde I, Cruz MA, Zhang H, López JA, Afshar-Kharghan V (2005) Platelet activation leads to activation and propagation of the complement system. *J Exp Med* 201:871–879
- Del Rosso M, Fibbi G, Pucci M, Margheri F, Serrati S (2008) The plasminogen activation system in inflammation. *Front Biosci* 13:4667–4686
- Déruaz M, Frauenschuh A, Alessandri AL, Dias JM, Coelho FM, Russo RC, Ferreira BR, Graham GJ, Shaw JP, Wells TN, Teixeira MM, Power CA, Proudfoot AE (2008) Ticks produce highly selective chemokine binding proteins with antiinflammatory activity. *J Exp Med* 205:2019–2031
- Desmazes C, Gauthier F, Lalmanach G (2001) Cathepsin L, but not cathepsin B, is a potential kininogenase. *Biol Chem* 382:811–815
- Díaz-Martín V, Manzano-Román R, Oleaga A, Encinas-Grandes A, Pérez-Sánchez R (2013) Cloning and characterization of a plasminogen-binding enolase from the saliva of the argasid tick *Ornithodoros moubata*. *Vet Parasitol* 191:301–314
- Díaz-Martín V, Manzano-Román R, Oleaga A, Pérez-Sánchez R (2015) New salivary anti-haemostatics containing protective epitopes from *Ornithodoros moubata* ticks: assessment of their individual and combined vaccine efficacy. *Vet Parasitol* 212:336–349
- Dong F, Fu Y, Li X, Jiang J, Sun J, Cheng X (2012) Cloning, expression, and characterization of salivary apyrase from *Aedes albopictus*. *Parasitol Res* 110:931–937
- Doolittle RF, Feng DF (1987) Reconstructing the evolution of vertebrate blood coagulation from a consideration of the amino acid sequences of clotting proteins. *Cold Spring Harb Symp Quant Biol* 52:869–874
- Draxler DF, Medcalf RL (2015) The fibrinolytic system—more than fibrinolysis? *Transfus Med Rev* 29:102–119
- Drewes CC, Dias RY, Hebeda CB, Simons SM, Barreto SA, Ferreira JM Jr, Chudzinski-Tavassi AM, Farsky SH (2012) Actions of the Kunitz-type serine protease inhibitor Amblyomin-X on VEGF-A-induced angiogenesis. *Toxicol* 60:333–340
- Driscoll KE, Carter JM, Hassenbein DG, Howard B (1997) Cytokines and particle-induced inflammatory cell recruitment. *Environ Health Perspect* 105:1159–1164
- Edgecombe GD, Legg DA (2014) Origins and early evolution of arthropods. *Palaeontology* 57:457–468
- Ehebauer MT, Mans BJ, Gaspar AR, Neitz AW (2002) Identification of extrinsic blood coagulation pathway inhibitors from the tick *Ornithodoros savignyi* (Acari: Argasidae). *Exp Parasitol* 101:138–148
- Eichner C, Frost P, Dysvik B, Jonassen I, Kristiansen B, Nilsen F (2008) Salmon louse (*Lepeophtheirus salmonis*) transcriptomes during post molting maturation and egg production revealed using EST-sequencing and microarray analysis. *BMC Genomics* 9:126
- Eirín-López JM, Rebordinos L, Rooney AP, Rozas J (2012) The birth-and-death evolution of multigene families revisited. *Genome Dyn* 7:170–196
- Everitt EA, Malik AB, Hendey B (1996) Fibronectin enhances the migration rate of human neutrophils *in vitro*. *J Leukoc Biol* 60:199–206

- Faudry E, Lozzi SP, Santana JM, D'Souza-Ault M, Kieffer S, Felix CR, Ricart CA, Sousa MV, Vernet T, Teixeira AR (2004) *Tritatoma infestans* apyrases belong to the 5'-nucleotidase family. *J Biol Chem* 279:19607–19613
- Ferreira VP, Fazito Vale V, Pangburn MK, Abdeladhim M, Ferreira Mendes-Sousa A, Coutinho-Abreu IV, Rasouli M, Brandt EA, Meneses C, Lima KF, Nascimento Araújo R, Horácio Pereira M, Kotsyfakis M, Oliveira F, Kamhawi S, Ribeiro JM, Gontijo NF, Collin N, Valenzuela JG (2016) SALO, a novel classical pathway complement inhibitor from saliva of the sand fly *Lutzomyia longipalpis*. *Sci Rep* 6:19300
- Francischetti IM, Ribeiro JM, Champagne D, Andersen J (2000) Purification, cloning, expression, and mechanism of action of a novel platelet aggregation inhibitor from the salivary gland of the blood-sucking bug, *Rhodnius prolixus*. *J Biol Chem* 275:12639–12650
- Francischetti IM, Andersen JF, Ribeiro JM (2002a) Biochemical and functional characterization of recombinant *Rhodnius prolixus* platelet aggregation inhibitor 1 as a novel lipocalin with high affinity for adenosine diphosphate and other adenine nucleotides. *Biochemistry* 41:3810–3818
- Francischetti IM, Valenzuela JG, Andersen JF, Mather TN, Ribeiro JM (2002b) Ixolaris, a novel recombinant tissue factor pathway inhibitor (TFPI) from the salivary gland of the tick, *Ixodes scapularis*: identification of factor X and factor Xa as scaffolds for the inhibition of factor VIIa/tissue factor complex. *Blood* 99:3602–3612
- Francischetti IM, Valenzuela JG, Pham VM, Garfield MK, Ribeiro JM (2002c) Toward a catalog for the transcripts and proteins (sialome) from the salivary gland of the malaria vector *Anopheles gambiae*. *J Exp Biol* 205:2429–2451
- Francischetti IM, Mather TN, Ribeiro JM (2003) Cloning of a salivary gland metalloprotease and characterization of gelatinase and fibrin(ogen)lytic activities in the saliva of the Lyme disease tick vector *Ixodes scapularis*. *Biochem Biophys Res Commun* 305:869–875
- Francischetti IM, Mather TN, Ribeiro JM (2004) Penthalaris, a novel recombinant five-Kunitz tissue factor pathway inhibitor (TFPI) from the salivary gland of the tick vector of Lyme disease, *Ixodes scapularis*. *Thromb Haemost* 91:886–898
- Francischetti IM, Mather TN, Ribeiro JM (2005a) Tick saliva is a potent inhibitor of endothelial cell proliferation and angiogenesis. *Thromb Haemost* 9:167–174
- Francischetti IM, My Pham V, Mans BJ, Andersen JF, Mather TN, Lane RS, Ribeiro JM (2005b) The transcriptome of the salivary glands of the female western black-legged tick *Ixodes pacificus* (Acari: Ixodidae). *Insect Biochem Mol Biol* 35:1142–1161
- Francischetti IM, Lopes AH, Dias FA, Pham VM, Ribeiro JM (2007) An insight into the sialotranscriptome of the seed-feeding bug, *Oncopeltus fasciatus*. *Insect Biochem Mol Biol* 37:903–910
- Francischetti IM, Mans BJ, Meng Z, Gudderra N, Veenstra TD, Pham VM, Ribeiro JM (2008a) An insight into the sialome of the soft tick *Ornithodoros parkeri*. *Insect Biochem Mol Biol* 38:1–21
- Francischetti IM, Meng Z, Mans BJ, Gudderra N, Hall M, Veenstra TD, Pham VM, Kotsyfakis M, Ribeiro JM (2008b) An insight into the salivary transcriptome and proteome of the soft tick and vector of epizootic bovine abortion *Ornithodoros coriaceus*. *J Proteomics* 71:493–512
- Francischetti IM, Sa-Nunes A, Mans BJ, Santos IM, Ribeiro JM (2009) The role of saliva in tick feeding. *Front Biosci* 14:2051–2088
- Francischetti IM, Calvo E, Andersen JF, Pham VM, Favreau AJ, Barbian KD, Romero A, Valenzuela JG, Ribeiro JM (2010) Insight into the sialome of the bed bug *Cimex lectularius*. *J Proteome Res* 9:3820–3831
- Francischetti IM, Anderson JM, Manoukis N, Pham VM, Ribeiro JM (2011) An insight into the sialotranscriptome and proteome of the coarse bontlegged tick *Hyalomma marginatum rufipes*. *J Proteomics* 74:2892–2908
- Frauenschuh A, Power CA, Déruaz M, Ferreira BR, Silva JS, Teixeira MM, Dias JM, Martin T, Wells TN, Proudfoot AE (2007) Molecular cloning and characterization of a highly selective chemokine-binding protein from the tick *Rhipicephalus sanguineus*. *J Biol Chem* 282:27250–27258

- Friedrich T, Kröger B, Bialojan S, Lemaire HG, Höffken HW, Reuschenbach P, Otte M, Dodt J (1993) A Kazal-type inhibitor with thrombin specificity from *Rhodnius prolixus*. *J Biol Chem* 268:16216–16222
- Friend WG, Smith JJ (1977) Factors affecting feeding by bloodsucking insects. *Annu Rev Entomol* 22:309–331
- Fry BG, Roelants K, Champagne DE, Scheib H, Tyndall JD, King GF, Nevalainen TJ, Norman JA, Lewis RJ, Norton RS, Renjifo C, de la Vega RC (2009) The toxicogenomic multiverse: convergent recruitment of proteins into animal venoms. *Annu Rev Genomics Hum Genet* 10:483–511
- Fuentes-Prior P, Noeske-Jungblut C, Donner P, Schlenning WD, Huber R, Bode W (1997) Structure of the thrombin complex with triabin, a lipocalin-like exosite-binding inhibitor derived from a triatomine bug. *Proc Natl Acad Sci U S A* 94:11845–11850
- Fukumoto S, Sakaguchi T, You M, Xuan X, Fujisaki K (2006) Tick troponin I-like molecule is a potent inhibitor for angiogenesis. *Microvasc Res* 71:218–221
- García GR, Gardinassi LG, Ribeiro JM, Anatriello E, Ferreira BR, Moreira HN, Mafra C, Martins MM, Szabó MP, de Miranda-Santos IK, Maruyama SR (2014) The sialotranscriptome of *Amblyomma triste*, *Amblyomma parvum* and *Amblyomma cajennense* ticks uncovered by 454-based RNA-seq. *Parasit Vectors* 7:430
- García-Varas S, Manzano-Román R, Fernández-Soto P, Encinas-Grandes A, Oleaga A, Pérez-Sánchez R (2010) Purification and characterisation of a P-selectin-binding molecule from the salivary glands of *Ornithodoros moubata* that induces protective anti-tick immune responses in pigs. *Int J Parasitol* 40:313–326
- Gardiner EE, Andrews RK (2012) Neutrophil extracellular traps (NETs) and infection-related vascular dysfunction. *Blood Rev* 26:255–259
- Gaspar AR, Crause JC, Neitz AW (1995) Identification of anticoagulant activities in the salivary glands of the soft tick, *Ornithodoros savignyi*. *Exp Appl Acarol* 19:117–127
- Gaspar AR, Joubert AM, Crause JC, Neitz AW (1996) Isolation and characterization of an anticoagulant from the salivary glands of the tick, *Ornithodoros savignyi* (Acari: Argasidae). *Exp Appl Acarol* 20:583–598
- Gibson AK, Smith Z, Fuqua C, Clay K, Colbourne JK (2013) Why so many unknown genes? Partitioning orphans from a representative transcriptome of the lone star tick *Amblyomma americanum*. *BMC Genomics* 14:135
- Giribet G, Edgecombe GD (2012) Reevaluating the arthropod tree of life. *Annu Rev Entomol* 57:167–186
- Gong H, Zhou J, Liao M, Hatta T, Harnnoi T, Umemiya R, Inoue N, Xuan X, Fujisaki K (2007) Characterization of a carboxypeptidase inhibitor from the tick *Haemaphysalis longicornis*. *J Insect Physiol* 53:1079–1087
- Gordon JR, Allen JR (1991) Factors V and VII anticoagulant activities in the salivary glands of feeding *Dermacentor andersoni* ticks. *J Parasitol* 77:167–170
- Gould TJ, Vu TT, Swystun LL, Dwivedi DJ, Mai SH, Weitz JI, Liaw PC (2014) Neutrophil extracellular traps promote thrombin generation through platelet-dependent and platelet-independent mechanisms. *Arterioscler Thromb Vasc Biol* 34:1977–1984
- Grevelink SA, Youssef DE, Loscalzo J, Lerner EA (1993) Salivary gland extracts from the deerfly contain a potent inhibitor of platelet aggregation. *Proc Natl Acad Sci U S A* 90:9155–9158
- Grimaldi D, Engel MS (2010) Evolution of the insects. Cambridge University Press, New York
- Guo X, Booth CJ, Paley MA, Wang X, DePonte K, Fikrig E, Narasimhan S, Montgomery RR (2009) Inhibition of neutrophil function by two tick salivary proteins. *Infect Immun* 77:2320–2329
- Hamad OA, Ekdahl KN, Nilsson PH, Andersson J, Magotti P, Lambris JD, Nilsson B (2008) Complement activation triggered by chondroitin sulfate released by thrombin receptor-activated platelets. *J Thromb Haemost* 6:1413–1421

- Hayashi H, Kyushiki H, Nagano K, Sudo T, Iyori M, Matsuoka H, Yoshida S (2013) Identification of the active region responsible for the anti-thrombotic activity of anopheline anti-platelet protein from a malaria vector mosquito. *Platelets* 24:324–332
- Hellman K, Hawkins RI (1967) The action of tick extracts on blood coagulation and fibrinolysis. *Thromb Diathes Haemorrh* 18:617–625
- Hellmann K, Hawkins RI (1965) Prolixins-S and prolixin-G; two anticoagulants from *Rhodnius prolixus* Stål. *Nature* 207:265–267
- Hoffmann A, Walsmann P, Riesener G, Paintz M, Markwardt F (1991) Isolation and characterization of a thrombin inhibitor from the tick *Ixodes ricinus*. *Pharmazie* 46:209–212
- Horn F, dos Santos PC, Termignoni C (2000) *Boophilus microplus* anticoagulant protein: an anti-thrombin inhibitor isolated from the cattle tick saliva. *Arch Biochem Biophys* 384:68–73
- Hostomská J, Volfová V, Mu J, Garfield M, Rohousová I, Volf P, Valenzuela JG, Jochim RC (2009) Analysis of salivary transcripts and antigens of the sand fly *Phlebotomus arabicus*. *BMC Genomics* 10:282
- Hughes AL (2013) Evolution of the salivary apyrases of blood-feeding arthropods. *Gene* 527:123–130
- Hwang WS, Weirauch C (2012) Evolutionary history of assassin bugs (insecta: hemiptera: Reduviidae): insights from divergence dating and ancestral state reconstruction. *PLoS One* 7:e45523
- Ibarra-Cerdeña CN, Zaldívar-Riverón A, Peterson AT, Sánchez-Cordero V, Ramsey JM (2014) Phylogeny and niche conservatism in North and Central American triatomine bugs (Hemiptera: Reduviidae: Triatominae), vectors of Chagas' disease. *PLoS Negl Trop Dis* 8:e3266
- Ibrahim MA, Ghazy AH, Maharem T, Khalil M (2001a) Isolation and properties of two forms of thrombin inhibitor from the nymphs of the camel tick *Hyalomma dromedarii* (Acari: Ixodidae). *Exp Appl Acarol* 25:675–698
- Ibrahim MA, Ghazy AH, Maharem TM, Khalil MI (2001b) Factor Xa (FXa) inhibitor from the nymphs of the camel tick *Hyalomma dromedarii*. *Comp Biochem Physiol B Biochem Mol Biol* 130:501–512
- Ikeda Y, Ueno A, Naraba H, Oh-ishi S (2001) Evidence for bradykinin mediation of carrageenin-induced inflammatory pain: a study using kininogen-deficient Brown Norway Katholiek rats. *Biochem Pharmacol* 61:911–914
- Imamura S, Da Silva Vaz I Jr, Sugino M, Ohashi K, Onuma M (2005) A serine protease inhibitor (serpin) from *Haemaphysalis longicornis* as an anti-tick vaccine. *Vaccine* 23:1301–1311
- Isawa H, Yuda M, Orito Y, Chinzei Y (2002) A mosquito salivary protein inhibits activation of the plasma contact system by binding to factor XII and high molecular weight kininogen. *J Biol Chem* 277:27651–27658
- Isawa H, Orito Y, Iwanaga S, Jingushi N, Morita A, Chinzei Y, Yuda M (2007a) Identification and characterization of a new kallikrein-kinin system inhibitor from the salivary glands of the malaria vector mosquito *Anopheles stephensi*. *Insect Biochem Mol Biol* 37:466–477
- Isawa H, Orito Y, Jingushi N, Iwanaga S, Morita A, Chinzei Y, Yuda M (2007b) Identification and characterization of plasma kallikrein-kinin system inhibitors from salivary glands of the blood-sucking insect *Triatoma infestans*. *FEBS J* 274:4271–4286
- Ishimaru Y, Gomez EA, Zhang F, Martini-Robles L, Iwata H, Sakurai T, Katakura K, Hashiguchi Y, Kato H (2012) Dimiconin, a novel coagulation inhibitor from the kissing bug, *Triatoma dimidiata*, a vector of Chagas disease. *J Exp Biol* 215:3597–3602
- Islam MK, Tsuji N, Miyoshi T, Alim MA, Huang X, Hata T, Fujisaki K (2009) The Kunitz-like modulatory protein haemangin is vital for hard tick blood-feeding success. *PLoS Pathog* 5:e1000497
- Iwanaga S, Okada M, Isawa H, Morita A, Yuda M, Chinzei Y (2003) Identification and characterization of novel salivary thrombin inhibitors from the ixodidae tick, *Haemaphysalis longicornis*. *Eur J Biochem* 270:1926–1934

- Iwanaga S, Isawa H, Yuda M (2014) Horizontal gene transfer of a vertebrate vasodilatory hormone into ticks. *Nat Commun* 5:3373
- Jablonka W, Kotsyfakis M, Mizurini DM, Monteiro RQ, Lukszo J, Drake SK, Ribeiro JM, Andersen JF (2015) Identification and mechanistic analysis of a novel tick-derived inhibitor of thrombin. *PLoS One* 10:e0133991
- Jacobs JW, Cupp EW, Sardana M, Friedman PA (1990) Isolation and characterization of a coagulation factor Xa inhibitor from black fly salivary glands. *Thromb Haemost* 64:235–238
- Jaworski DC, Jasinskas A, Metz CN, Bucala R, Barbour AG (2001) Identification and characterization of a homologue of the pro-inflammatory cytokine macrophage migration inhibitory factor in the tick, *Amblyomma americanum*. *Insect Mol Biol* 10:323–331
- Jeyaprakash A, Hoy MA (2009) First divergence time estimate of spiders, scorpions, mites and ticks (subphylum: Chelicerata) inferred from mitochondrial phylogeny. *Exp Appl Acarol* 47:1–18
- Joubert AM, Crause JC, Gaspar AR, Clarke FC, Spickett AM, Neitz AW (1995) Isolation and characterization of an anticoagulant present in the salivary glands of the bont-legged tick, *Hyalomma truncatum*. *Exp Appl Acarol* 19:79–92
- Joubert AM, Louw AI, Joubert F, Neitz AW (1998) Cloning, nucleotide sequence and expression of the gene encoding factor Xa inhibitor from the salivary glands of the tick, *Ornithodoros savignyi*. *Exp Appl Acarol* 22:603–619
- Jurk K, Kehrel BE (2005) Platelets: physiology and biochemistry. *Semin Thromb Hemost* 31:381–392
- Karczewski J, Endris R, Connolly TM (1994) Disagregin is a fibrinogen receptor antagonist lacking the Arg-Gly-Asp sequence from the tick, *Ornithodoros moubata*. *J Biol Chem* 269:6702–6708
- Karczewski J, Waxman L, Endris RG, Connolly TM (1995) An inhibitor from the argasid tick *Ornithodoros moubata* of cell adhesion to collagen. *Biochem Biophys Res Commun* 208:532–541
- Karim S, Ribeiro JM (2015) An insight into the sialome of the lone star tick *Amblyomma americanum* with a glimpse on its time dependent gene expression. *PLoS One* 10:e0131292
- Karim S, Singh P, Ribeiro JM (2011) A deep insight into the sialotranscriptome of the gulf coast tick *Amblyomma maculatum*. *PLoS One* 6:e28525
- Kato N, Iwanaga S, Okayama T, Isawa H, Yuda M, Chinzei Y (2005) Identification and characterization of the plasma kallikrein-kinin system inhibitor, haemaphysalin, from hard tick, *Haemaphysalis longicornis*. *Thromb Haemost* 93:359–367
- Kato H, Anderson JM, Kamhawi S, Oliveira F, Lawyer PG, Pham VM, Sangare CS, Samake S, Sissoko I, Garfield M, Sigutova L, Volf P, Doumbia S, Valenzuela JG (2006) High degree of conservancy among secreted salivary gland proteins from two geographically distant *Phlebotomus duboscqi* sandflies populations (Mali and Kenya). *BMC Genomics* 7:226
- Kato H, Jochim RC, Gomez EA, Sakoda R, Iwata H, Valenzuela JG, Hashiguchi Y (2010) A repertoire of the dominant transcripts from the salivary glands of the blood-sucking bug *Triatoma dimidiata* a vector of Chagas disease. *Infect Genet Evol* 10:184–191
- Kato H, Gomez EA, Fujita M, Ishimaru Y, Uezato H, Mimori T, Iwata H, Hashiguchi Y (2015) Ayadualin, a novel RGD peptide with dual antihemostatic activities from the sand fly *Lutzomyia ayacuchensis*, a vector of Andean-type cutaneous leishmaniasis. *Biochimie* 112:49–56
- Kazimirová M, Jancinová V, Petříková M, Takác P, Labuda M, Nosál R (2002) An inhibitor of thrombin-stimulated blood platelet aggregation from the salivary glands of the hard tick *Amblyomma variegatum* (Acari: Ixodidae). *Exp Appl Acarol* 28:97–105
- Keller PM, Waxman L, Arnold BA, Schultz LD, Condra C, Connolly TM (1993) Cloning of the cDNA and expression of moubatin, an inhibitor of platelet aggregation. *J Biol Chem* 268:5450–5456
- Kelley LA, Mezulis S, Yates CM, Wass MN, Sternberg MJ (2015) The Phyre2 web portal for protein modeling, prediction and analysis. *Nat Protoc* 10:845–858

- Kemp DH, Stone BF, Binnington KC (1982) Tick attachment and feeding: role of the mouthparts feeding apparatus salivary gland secretions and the host response. In: Obenchain FD, Galun R (eds) *Physiology of ticks*. Pergamon Press, Oxford, pp 119–167
- Kim S, Bell K, Mousa SA, Varner JA (2000) Regulation of angiogenesis *in vivo* by ligation of integrin alpha5beta1 with the central cell-binding domain of fibronectin. *Am J Pathol* 156:1345–1362
- Kim TK, Curran J, Mulenga A (2014) Dual silencing of long and short *Amblyomma americanum* acidic chitinase forms weakens the tick cement cone stability. *J Exp Biol* 217:3493–3503
- Kim TK, Tirloni L, Radulovic Z, Lewis L, Bakshi M, Hill C, da Silva Vaz I Jr, Logullo C, Termignoni C, Mulenga A (2015) Conserved *Amblyomma americanum* tick Serpin19, an inhibitor of blood clotting factors Xa and XIa, trypsin and plasmin, has anti-haemostatic functions. *Int J Parasitol* 45:613–627
- Klompfen H, Lekveishvili M, Black WC 4th (2007) Phylogeny of parasitiform mites (Acari) based on rRNA. *Mol Phylogenet Evol* 43:936–951
- Klompfen AA, Boxhall GA (2015) Fossil crustaceans as parasites and hosts. *Adv Parasitol* 90:233–289
- Koh CY, Kazimirova M, Trimmell A, Takac P, Labuda M, Nuttall PA, Kini RM (2007) Varieggin, a novel fast and tight binding thrombin inhibitor from the tropical bont tick. *J Biol Chem* 282:29101–29113
- Kotsyfakis M, Sá-Nunes A, Francischetti IM, Mather TN, Andersen JF, Ribeiro JM (2006) Antiinflammatory and immunosuppressive activity of sialostatin L, a salivary cystatin from the tick *Ixodes scapularis*. *J Biol Chem* 281:26298–26307
- Kotsyfakis M, Karim S, Andersen JF, Mather TN, Ribeiro JM (2007) Selective cysteine protease inhibition contributes to blood-feeding success of the tick *Ixodes scapularis*. *J Biol Chem* 282:29256–29263
- Kotsyfakis M, Schwarz A, Erhart J, Ribeiro JM (2015) Tissue- and time-dependent transcription in *Ixodes ricinus* salivary glands and midguts when blood feeding on the vertebrate host. *Sci Rep* 5:9103
- Kreil G (1995) Hyaluronidases – a group of neglected enzymes. *Protein Sci* 4:1666–1669
- Krenn HW, Aspöck H (2012) Form function and evolution of the mouthparts of blood-feeding Arthropoda. *Arthropod Struct Dev* 41:101–118
- Kröber T, Guerin PM (2007) *In vitro* feeding assays for hard ticks. *Trends Parasitol* 23:445–449
- Kuhn-Nentwig L, Stöcklin R, Nentwig W (2011) Venom composition and strategies in spiders: is everything possible? *Adv Insect Physiol* 40:1–86
- Lai-Cheong JE, McGrath JA (2009) Structure and function of skin, hair and nails. *Medicine* 37:223–226
- Law JH, Ribeiro JM, Wells MA (1992) Biochemical insights derived from insect diversity. *Annu Rev Biochem* 61:87–111
- Leboulle G, Crippa M, Decrem Y, Mejri N, Brossard M, Bollen A, Godfroid E (2002) Characterization of a novel salivary immunosuppressive protein from *Ixodes ricinus* ticks. *J Biol Chem* 277:10083–10089
- Lee CG, Da Silva CA, Dela Cruz CS, Ahangari F, Ma B, Kang MJ, He CH, Takyar S, Elias JA (2011) Role of chitin and chitinase/chitinase-like proteins in inflammation tissue remodeling and injury. *Annu Rev Physiol* 73:479–501
- Lentz BR (2003) Exposure of platelet membrane phosphatidylserine regulates blood coagulation. *Prog Lipid Res* 42:423–438
- Lerner EA, Shoemaker CB (1992) Maxadilan. Cloning and functional expression of the gene encoding this potent vasodilator peptide. *J Biol Chem* 267:1062–1066
- Lerner EA, Ribeiro JM, Nelson RJ, Lerner MR (1991) Isolation of maxadilan, a potent vasodilatory peptide from the salivary glands of the sand fly *Lutzomyia longipalpis*. *J Biol Chem* 266:11234–11236
- Limo MK, Voigt WP, Tumbo-Oeri AG, Njogu RM, ole-MoiYoi OK (1991) Purification and characterization of an anticoagulant from the salivary glands of the ixodid tick *Rhipicephalus appendiculatus*. *Exp Parasitol* 72:418–429

- Lombardo F, Di Cristina M, Spanos L, Louis C, Coluzzi M, Arcá B (2000) Promoter sequences of the putative *Anopheles gambiae* apyrase confer salivary gland expression in *Drosophila melanogaster*. *J Biol Chem* 275:23861–23868
- Long AT, Kenne E, Jung R, Fuchs TA, Renné T (2015) Contact system revisited: an interface between inflammation, coagulation, and innate immunity. *J Thromb Haemost* 14:427–437
- Ma D, Wang Y, Yang H, Wu J, An S, Gao L, Xu X, Lai R (2009) Anti-thrombosis repertoire of blood-feeding horsefly salivary glands. *Mol Cell Proteomics* 8:2071–2079
- Ma D, Gao L, An S, Song Y, Wu J, Xu X, Lai R (2010) A horsefly saliva antigen 5-like protein containing RTS motif is an angiogenesis inhibitor. *Toxicon* 55:45–51
- Ma D, Xu X, An S, Liu H, Yang X, Andersen JF, Wang Y, Tokumasu F, Ribeiro JM, Francischetti IM, Lai R (2011) A novel family of RGD-containing disintegrins (Tablysin-15) from the salivary gland of the horsefly *Tabanus yao* targets α IIb β 3 or α V β 3 and inhibits platelet aggregation and angiogenesis. *Thromb Haemost* 105:1032–1045
- Ma D, Assumpção TC, Li Y, Andersen JF, Ribeiro J, Francischetti IM (2012) Triplatin, a platelet aggregation inhibitor from the salivary gland of the triatomine vector of Chagas disease, binds to TXA(2) but does not interact with glycoprotein PVI. *Thromb Haemost* 107:111–123
- Majumder R, Weinreb G, Lentz BR (2005) Efficient thrombin generation requires molecular phosphatidylserine, not a membrane surface. *Biochemistry* 44:16998–17006
- Mans BJ (2011) Evolution of vertebrate hemostatic and inflammatory control mechanisms in blood-feeding arthropods. *J Innate Immun* 3:41–51
- Mans BJ (2014) Heme processing and the evolution of hematophagy. In: Sonenshine DE, Roe RM (eds) *Biology of ticks*, vol 1, 2nd edn. Oxford University Press, New York, pp 220–239
- Mans BJ, Neitz AW (2004) Adaptation of ticks to a blood-feeding environment: evolution from a functional perspective. *Insect Biochem Mol Biol* 34:1–17
- Mans BJ, Ribeiro JM (2008a) Function, mechanism and evolution of the moubatin-clade of soft tick lipocalins. *Insect Biochem Mol Biol* 38:841–852
- Mans BJ, Ribeiro JM (2008b) A novel clade of cysteinyl leukotriene scavengers in soft ticks. *Insect Biochem Mol Biol* 38:862–870
- Mans BJ, Gaspar AR, Louw AI, Neitz AW (1998a) Apyrase activity and platelet aggregation inhibitors in the tick *Ornithodoros savignyi* (Acari: Argasidae). *Exp Appl Acarol* 22:353–366
- Mans BJ, Gaspar AR, Louw AI, Neitz AW (1998b) Purification and characterization of apyrase from the tick, *Ornithodoros savignyi*. *Comp Biochem Physiol B Biochem Mol Biol* 120:617–624
- Mans BJ, Coetzee J, Louw AI, Gaspar AR, Neitz AW (2000) Disaggregation of aggregated platelets by apyrase from the tick, *Ornithodoros savignyi* (Acari: Argasidae). *Exp Appl Acarol* 24:271–182
- Mans BJ, Louw AI, Neitz AW (2002a) Savignygrin, a platelet aggregation inhibitor from the soft tick *Ornithodoros savignyi*, presents the RGD integrin recognition motif on the Kunitz-BPTI fold. *J Biol Chem* 277:21371–21378
- Mans BJ, Louw AI, Neitz AW (2002b) Amino acid sequence and structure modeling of savignin, a thrombin inhibitor from the tick, *Ornithodoros savignyi*. *Insect Biochem Mol Biol* 32:821–828
- Mans BJ, Calvo E, Ribeiro JM, Andersen JF (2007) The crystal structure of D7r4, a salivary biogenic amine-binding protein from the malaria mosquito *Anopheles gambiae*. *J Biol Chem* 282:36626–36633
- Mans BJ, Andersen JF, Francischetti IM, Valenzuela JG, Schwan TG, Pham VM, Garfield MK, Hammer CH, Ribeiro JM (2008a) Comparative sialomics between hard and soft ticks: implications for the evolution of blood-feeding behavior. *Insect Biochem Mol Biol* 38:42–58
- Mans BJ, Andersen JF, Schwan TG, Ribeiro JM (2008b) Characterization of anti-hemostatic factors in the argasid, *Argas monolakensis*: implications for the evolution of blood-feeding in the soft tick family. *Insect Biochem Mol Biol* 38:22–41
- Mans BJ, Ribeiro JM, Andersen JF (2008c) Structure, function, and evolution of biogenic amine-binding proteins in soft ticks. *J Biol Chem* 283:18721–18733

- Mans BJ, de Klerk D, Pienaar R, Latif AA (2011) *Nuttalliella namaqua*: a living fossil and closest relative to the ancestral tick lineage: implications for the evolution of blood-feeding in ticks. *PLoS One* 6:e23675
- Mans BJ, de Klerk D, Pienaar R, de Castro MH, Latif AA (2012) The mitochondrial genomes of *Nuttalliella namaqua* (Ixodoidea: Nuttalliellidae) and *Argas africanus* (Ixodoidea: Argasidae): estimation of divergence dates for the major tick lineages and reconstruction of ancestral blood-feeding characters. *PLoS One* 7:e49461
- Mans BJ, de Castro MH, Pienaar R, de Klerk D, Gaven P, Genu S, Latif AA (2016) Ancestral reconstruction of tick lineages. *Ticks Tick Borne Dis* 7:509–535
- Markiewski MM, Nilsson B, Ekdahl KN, Mollnes TE, Lambris JD (2007) Complement and coagulation: strangers or partners in crime? *Trends Immunol* 28:184–192
- Marković-Housley Z, Miglierini G, Soldatova L, Rizkallah PJ, Müller U, Schirmer T (2000) Crystal structure of hyaluronidase a major allergen of bee venom. *Structure* 8:1025–1035
- Martin JA, Wang Z (2011) Next-generation transcriptome assembly. *Nat Rev Genet* 12:671–682
- Maruyama SR, Anatriello E, Anderson JM, Ribeiro JM, Brandão LG, Valenzuela JG, Ferreira BR, Garcia GR, Szabó MP, Patel S, Bishop R, de Miranda-Santos IK (2010) The expression of genes coding for distinct types of glycine-rich proteins varies according to the biology of three metastrongyle ticks, *Rhipicephalus (Boophilus) microplus*, *Rhipicephalus sanguineus* and *Amblyomma cajennense*. *BMC Genomics* 11:363
- Massberg S, Grahl L, von Bruehl ML, Manukyan D, Pfeiler S, Goosmann C, Brinkmann V, Lorenz M, Bidzhakov K, Khandagale AB, Konrad I, Kennerknecht E, Reges K, Holdenrieder S, Braun S, Reinhardt C, Spannagl M, Preissner KT, Engelmann B (2010) Reciprocal coupling of coagulation and innate immunity via neutrophil serine proteases. *Nat Med* 16:887–896
- McCarty SM, Percival SL (2013) Proteases and Delayed Wound Healing. *Adv Wound Care (New Rochelle)* 2:438–447
- McKeever S, Wright MD, Hagan DV (1988) Mouthparts of females of four *Culicoides* species (Diptera: Ceratopogonidae). *Ann Entomol Soc Amer* 81:332–341
- Mendes-Sousa AF, Nascimento AA, Queiroz DC, Vale VF, Fujiwara RT, Araújo RN, Pereira MH, Gontijo NF (2013) Different host complement systems and their interactions with saliva from *Lutzomyia longipalpis* (Diptera, Psychodidae) and *Leishmania infantum* promastigotes. *PLoS One* 8:e79787
- Menten-Dedoyart C, Faccinnetto C, Golovchenko M, Dupiereux I, Van Lerberghe PB, Dubois S, Desmet C, Elmoulaj B, Baron F, Rudenko N, Oury C, Heinen E, Couvreur B (2012) Neutrophil extracellular traps entrap and kill *Borrelia burgdorferi sensu stricto* spirochetes and are not affected by *Ixodes ricinus* tick saliva. *J Immunol* 189:5393–53401
- Mesquita RD, Vionette-Amaral RJ, Lowenberger C, Rivera-Pomar R, Monteiro FA, Minx P, Spieth J, Carvalho AB, Panzera F, Lawson D, Torres AQ, Ribeiro JM, Sorgine MH, Waterhouse RM, Montague MJ, Abad-Franch F, Alves-Bezerra M, Amaral LR, Araujo HM, Araujo RN, Aravind L, Atella GC, Azambuja P, Berni M, Bittencourt-Cunha PR, Braz GR, Calderón-Fernández G, Carareto CM, Christensen MB, Costa IR, Costa SG, Dansa M, Daumas-Filho CR, De-Paula IF, Dias FA, Dimopoulos G, Emrich SJ, Esponda-Behrens N, Fampa P, Fernandez-Medina RD, da Fonseca RN, Fontenele M, Fronick C, Fulton LA, Gandara AC, Garcia ES, Genta FA, Giraldo-Calderón GI, Gomes B, Gondim KC, Granzotto A, Guarneri AA, Guigó R, Harry M, Hughes DS, Jablonka W, Jacquin-Joly E, Juárez MP, Koerich LB, Latorre-Estivalis JM, Lavore A, Lawrence GG, Lazoski C, Lazzari CR, Lopes RR, Lorenzo MG, Lugon MD, Majerowicz D, Marcet PL, Mariotti M, Masuda H, Megy K, Melo AC, Missirlis F, Mota T, Noriega FG, Nouzova M, Nunes RD, Oliveira RL, Oliveira-Silveira G, Ons S, Pagola L, Paiva-Silva GO, Pascual A, Pavan MG, Pedrini N, Peixoto AA, Pereira MH, Pike A, Polycarpo C, Prosdocimi F, Ribeiro-Rodrigues R, Robertson HM, Salerno AP, Salmon D, Santemas D, Schama R, Seabra-Junior ES, Silva-Cardoso L, Silva-Neto MA, Souza-Gomes M, Sterkel M, Taracena ML, Tojo M, Tu ZJ, Tubio JM, Ursic-Bedoya R, Venancio TM, Walter-Nuno AB, Wilson D, Warren WC, Wilson RK, Huebner E, Dotson EM, Oliveira PL (2015) Genome of *Rhodnius prolixus* an insect vector of Chagas disease reveals unique adaptations to hematophagy and parasite infection. *Proc Natl Acad Sci U S A* 112:14936–14941

- Mizurini DM, Aslan JS, Gomes T, Ma D, Francischetti IM, Monteiro RQ (2015) Salivary thromboxane A₂-binding proteins from triatomine vectors of Chagas disease inhibit platelet-mediated Neutrophil Extracellular Traps (NETs) formation and arterial thrombosis. *PLoS Negl Trop Dis* 9:e0003869
- Monteiro MC, Nogueira LG, Almeida Souza AA, Ribeiro JM, Silva JS, Cunha FQ (2005) Effect of salivary gland extract of *Leishmania* vector, *Lutzomyia longipalpis*, on leukocyte migration in OVA-induced immune peritonitis. *Eur J Immunol* 35:2424–2433
- Moorhouse DE, Tatchell RJ (1966) The feeding processes of the cattle-tick *Boophilus microplus* (Canestrini): a study in host-parasite relations. I. Attachment to the host. *Parasitology* 56:623–632
- Morita A, Isawa H, Orito Y, Iwanaga S, Chinzei Y, Yuda M (2006) Identification and characterization of a collagen-induced platelet aggregation inhibitor, triplatin, from salivary glands of the assassin bug, *Triatoma infestans*. *FEBS J* 273:2955–2962
- Morrissey JH, Choi SH, Smith SA (2012) Polyphosphate: an ancient molecule that links platelets, coagulation, and inflammation. *Blood* 119:5972–5979
- Motoyashiki T, Tu AT, Azimov DA, Ibragim K (2003) Isolation of anticoagulant from the venom of tick, *Boophilus calcaratus*, from Uzbekistan. *Thromb Res* 110:235–241
- Mudenda L, Pierlé SA, Turse JE, Scoles GA, Purvine SO, Nicora CD, Clauss TR, Ueti MW, Brown WC, Brayton KA (2014) Proteomics informed by transcriptomics identifies novel secreted proteins in *Dermacentor andersoni* saliva. *Int J Parasitol* 44:1029–1037
- Mulenga A, Macaluso KR, Simser JA, Azad AF (2003) The American dog tick, *Dermacentor variabilis*, encodes a functional histamine release factor homolog. *Insect Biochem Mol Biol* 33:911–919
- Mulenga A, Kim T, Ibelli AM (2013) *Amblyomma americanum* tick saliva serine protease inhibitor 6 is a cross-class inhibitor of serine proteases and papain-like cysteine proteases that delays plasma clotting and inhibits platelet aggregation. *Insect Mol Biol* 22:306–319
- Nagatomi A, Soroida K (1985) The structure of the mouthparts of the orthorrhaphous Brachycera (Diptera) with special reference to blood-sucking. *Beit zur Entomol Berlin* 35:263–368
- Nakajima C, Imamura S, Konnai S, Yamada S, Nishikado H, Ohashi K, Onuma M (2006) A novel gene encoding a thrombin inhibitory protein in a cDNA library from *Haemaphysalis longicornis* salivary gland. *J Vet Med Sci* 68:447–452
- Narasimhan S, Koski RA, Beaulieu B, Anderson JF, Ramamoorthi N, Kantor F, Cappello M, Fikrig E (2002) A novel family of anticoagulants from the saliva of *Ixodes scapularis*. *Insect Mol Biol* 11:641–650
- Neitz AW, Howell CJ, Potgieter DJ, Bezuidenhout JD (1978) Proteins and free amino acids in the salivary secretion and haemolymph of the tick *Amblyomma hebraeum*. *Onderstepoort J Vet Res* 45:235–240
- Nene V, Lee D, Quackenbush J, Skilton R, Mwaura S, Gardner MJ, Bishop R (2002) AvGI an index of genes transcribed in the salivary glands of the ixodid tick *Amblyomma variegatum*. *Int J Parasitol* 32:1447–1456
- Nene V, Lee D, Kang'a S, Skilton R, Shah T, de Villiers E, Mwaura S, Taylor D, Quackenbush J, Bishop R (2004) Genes transcribed in the salivary glands of female *Rhipicephalus appendiculatus* ticks infected with *Theileria parva*. *Insect Biochem Mol Biol* 34:1117–1128
- Nienaber J, Gaspar AR, Neitz AW (1999) Savignin, a potent thrombin inhibitor isolated from the salivary glands of the tick *Ornithodoros savignyi* (Acari: Argasidae). *Exp Parasitol* 93:82–91
- Noeske-Jungblut C, Krätzschar J, Haendler B, Alagon A, Possani L, Verhallen P, Donner P, Schleuning WD (1994) An inhibitor of collagen-induced platelet aggregation from the saliva of *Triatoma pallidipennis*. *J Biol Chem* 269:5050–5053
- Noeske-Jungblut C, Haendler B, Donner P, Alagon A, Possani L, Schleuning WD (1995) Triabin, a highly potent exosite inhibitor of thrombin. *J Biol Chem* 270:28629–28634
- Nunn MA, Sharma A, Paesen GC, Adamson S, Lissina O, Willis AC, Nuttall PA (2005) Complement inhibitor of C5 activation from the soft tick *Ornithodoros moubata*. *J Immunol* 174:2084–2091

- Ohnishi H, Miyahara N, Gelfand EW (2008) The role of leukotriene B(4) in allergic diseases. *Allergol Int* 57:291–298
- Oliveira F, Kamhawi S, Seitz AE, Pham VM, Guigal PM, Fischer L, Ward J, Valenzuela JG (2006) From transcriptome to immunome: identification of DTH inducing proteins from a *Phlebotomus arisai* salivary gland cDNA library. *Vaccine* 24:374–390
- Oliveira CJ, Sá-Nunes A, Francischetti IM, Carregaro V, Anatriello E, Silva JS, Santos IK, Ribeiro JM, Ferreira BR (2011) Deconstructing tick saliva: non-protein molecules with potent immunomodulatory properties. *J Biol Chem* 286:10960–10969
- Paesen GC, Adams PL, Harlos K, Nuttall PA, Stuart DI (1999) Tick histamine-binding proteins: isolation, cloning, and three-dimensional structure. *Mol Cell* 3:661–671
- Paesen GC, Siebold C, Harlos K, Peacey MF, Nuttall PA, Stuart DI (2007) A tick protein with a modified Kunitz fold inhibits human tryptase. *J Mol Biol* 368:1172–1186
- Paesen GC, Siebold C, Dallas ML, Peers C, Harlos K, Nuttall PA, Nunn MA, Stuart DI, Esnouf RM (2009) An ion-channel modulator from the saliva of the brown ear tick has a highly modified Kunitz/BPTI structure. *J Mol Biol* 389:734–747
- Pasqualoto KF, Balan A, Barreto SA, Simons SM, Chudzinski-Tavassi AM (2014) Structural findings and molecular modeling approach of a TFPI-like inhibitor. *Protein Pept Lett* 21:452–457
- Patterson JS, Gaunt MW (2010) Phylogenetic multi-locus codon models and molecular clocks reveal the monophyly of haematophagous reduviid bugs and their evolution at the formation of South America. *Mol Phylogenet Evol* 56:608–621
- Peerschke EI, Ghebrehwet B (1997) C1q augments platelet activation in response to aggregated Ig. *J Immunol* 159:5594–5598
- Peerschke EI, Yin W, Grigg SE, Ghebrehwet B (2006) Blood platelets activate the classical pathway of human complement. *J Thromb Haemost* 4:2035–2042
- Peerschke EI, Yin W, Ghebrehwet B (2008) Platelet mediated complement activation. *Adv Exp Med Biol* 632:81–91
- Peerschke EI, Yin W, Ghebrehwet B (2010) Complement activation on platelets: implications for vascular inflammation and thrombosis. *Mol Immunol* 47:2170–2175
- Pekáriková D, Rajská P, Kazimírová M, Pecháňová O, Takáč P, Nuttall PA (2015) Vasoconstriction induced by salivary gland extracts from ixodid ticks. *Int J Parasitol* 45:879–883
- Pérez de León AA, Tabachnick WJ (1996) Apyrase activity and adenosine diphosphate induced platelet aggregation inhibition by the salivary gland proteins of *Culicoides variipennis*, the North American vector of bluetongue viruses. *Vet Parasitol* 61:327–338
- Pérez de León AA, Ribeiro JM, Tabachnick WJ, Valenzuela JG (1997) Identification of a salivary vasodilator in the primary North American vector of bluetongue viruses, *Culicoides variipennis*. *Am J Trop Med Hyg* 57:375–381
- Pérez de León AA, Valenzuela JG, Tabachnick WJ (1998) Anticoagulant activity in salivary glands of the insect vector *Culicoides variipennis sonorensis* by an inhibitor of factor Xa. *Exp Parasitol* 88:121–130
- Pichu S, Ribeiro JM, Mather TN, Francischetti IM (2014) Purification of a serine protease and evidence for a protein C activator from the saliva of the tick, *Ixodes scapularis*. *Toxicon* 77:32–39
- Preston SG, Majtán J, Kouremenou C, Rysnik O, Burger LF, Cabezas Cruz A, Chiong Guzman M, Nunn MA, Paesen GC, Nuttall PA, Austyn JM (2013) Novel immunomodulators from hard ticks selectively reprogramme human dendritic cell responses. *PLoS Pathog* 9:e1003450
- Prevot PP, Adam B, Boudjeltia KZ, Brossard M, Lins L, Cauchie P, Brasseur R, Vanhaeverbeek M, Vanhamme L, Godfroid E (2006) Anti-hemostatic effects of a serpin from the saliva of the tick *Ixodes ricinus*. *J Biol Chem* 281:26361–26369
- Prevot PP, Beschin A, Lins L, Beaufays J, Grosjean A, Bruys L, Adam B, Brossard M, Brasseur R, Zouaoui Boudjeltia K, Vanhamme L, Godfroid E (2009) Exosites mediate the anti-inflammatory effects of a multifunctional serpin from the saliva of the tick *Ixodes ricinus*. *FEBS J* 276:3235–3246

- Puzer L, Cotrin SS, Alves MF, Egborge T, Araújo MS, Juliano MA, Juliano L, Brömme D, Carmona AK (2004) Comparative substrate specificity analysis of recombinant human cathepsin V and cathepsin L. *Arch Biochem Biophys* 430:274–283
- Radovsky FJ (1969) Adaptive radiation in the parasitic mesostigmata. *Acarologia* 11:450–483
- Rajská P, Pechánová O, Takác P, Kazimířová M, Roller L, Vidlicka L, Ciampor F, Labuda M, Nuttall PA (2003) Vasodilatory activity in horsefly and deerfly salivary glands. *Med Vet Entomol* 17:395–402
- Reddy VB, Kounga K, Mariano F, Lerner EA (2000) Chrysoptin is a potent glycoprotein IIb/IIIa fibrinogen receptor antagonist present in salivary gland extracts of the deerfly. *J Biol Chem* 275:15861–15867
- Renesto P, Kadiri C, Chignard M (1992) Combined activation of platelets by cathepsin G and platelet activating factor, two neutrophil-derived agonists. *Br J Haematol* 80:205–213
- Ribatti D, Ranieri G (2015) Tryptase, a novel angiogenic factor stored in mast cell granules. *Exp Cell Res* 332:157–162
- Ribeiro JM (1987a) *Ixodes dammini*: salivary anti-complement activity. *Exp Parasitol* 64:347–353
- Ribeiro JM (1987b) Role of saliva in blood-feeding by arthropods. *Annu Rev Entomol* 32:463–478
- Ribeiro JM (1992) Characterization of a vasodilator from the salivary glands of the yellow fever mosquito *Aedes aegypti*. *J Exp Biol* 165:61–71
- Ribeiro JM (1995) Blood-feeding arthropods: live syringes or invertebrate pharmacologists? *Infect Agents Dis* 4:143–152
- Ribeiro JM (2000) Blood-feeding in mosquitoes: probing time and salivary gland anti-haemostatic activities in representatives of three genera (*Aedes Anopheles Culex*). *Med Vet Entomol* 14:142–148
- Ribeiro JM, Arca B (2009) From Sialomes to the Sialoverse: an insight into salivary potion of blood-feeding insects. *Adv Insect Physiol* 37:59–118
- Ribeiro JM, Francischetti IM (2001) Platelet-activating-factor-hydrolyzing phospholipase C in the salivary glands and saliva of the mosquito *Culex quinquefasciatus*. *J Exp Biol* 204:3887–3894
- Ribeiro JM, Francischetti IM (2003) Role of arthropod saliva in blood feeding: sialome and post-sialome perspectives. *Annu Rev Entomol* 48:73–88
- Ribeiro JM, Garcia ES (1981) Platelet antiaggregating activity in the salivary secretion of the blood sucking bug *Rhodnius prolixus*. *Experientia* 37:384–386
- Ribeiro JM, Mather TN (1998) *Ixodes scapularis*: salivary kininase activity is a metallo dipeptidyl carboxypeptidase. *Exp Parasitol* 89:213–221
- Ribeiro JM, Modi G (2001) The salivary adenosine/AMP content of *Phlebotomus argentipes* Annandale and Brunetti, the main vector of human kala-azar. *J Parasitol* 87:915–917
- Ribeiro JM, Nussenzveig RH (1993) The salivary catechol oxidase/peroxidase activities of the mosquito *Anopheles albimanus*. *J Exp Biol* 179:273–287
- Ribeiro JM, Spielman A (1986) *Ixodes dammini*: salivary anaphylatoxin inactivating activity. *Exp Parasitol* 62:292–297
- Ribeiro JM, Valenzuela JG (1999) Purification and cloning of the salivary peroxidase/catechol oxidase of the mosquito *Anopheles albimanus*. *J Exp Biol* 202:809–816
- Ribeiro JM, Walker FA (1994) High affinity histamine-binding and antihistaminic activity of the salivary nitric oxide-carrying heme protein (nitrophorin) of *Rhodnius prolixus*. *J Exp Med* 180:2251–2257
- Ribeiro JM, Rossignol PA, Spielman A (1984a) Role of mosquito saliva in blood vessel location. *J Exp Biol* 108:1–7
- Ribeiro JM, Sarkis JJ, Rossignol PA, Spielman A (1984b) Salivary apyrase of *Aedes aegypti*: characterization and secretory fate. *Comp Biochem Physiol B* 79:81–86
- Ribeiro JM, Makoul GT, Levine J, Robinson DR, Spielman A (1985) Antihemostatic, antiinflammatory, and immunosuppressive properties of the saliva of a tick, *Ixodes dammini*. *J Exp Med* 161:332–344

- Ribeiro JM, Rossignol PA, Spielman A (1986) Blood-finding strategy of a capillary-feeding sandfly *Lutzomyia longipalpis*. *Comp Biochem Physiol A Comp Physiol* 83:683–686
- Ribeiro JM, Vachereau A, Modi GB, Tesh RB (1989) A novel vasodilatory peptide from the salivary glands of the sand fly *Lutzomyia longipalpis*. *Science* 243:212–214
- Ribeiro JM, Vaughan JA, Azad AF (1990) Characterization of the salivary apyrase activity of three rodent flea species. *Comp Biochem Physiol B* 95:215–219
- Ribeiro JM, Endris TM, Endris R (1991) Saliva of the soft tick, *Ornithodoros moubata*, contains anti-platelet and apyrase activities. *Comp Biochem Physiol A Comp Physiol* 100:109–112
- Ribeiro JM, Evans PM, MacSwain JL, Sauer J (1992) *Amblyomma americanum*: characterization of salivary prostaglandins E2 and F2 alpha by RP-HPLC/bioassay and gas chromatography-mass spectrometry. *Exp Parasitol* 74:112–116
- Ribeiro JM, Hazzard JM, Nussenzweig RH, Champagne DE, Walker FA (1993) Reversible binding of nitric oxide by a salivary heme protein from a bloodsucking insect. *Science* 260:539–541
- Ribeiro JM, Nussenzweig RH, Tortorella G (1994) Salivary vasodilators of *Aedes triseriatus* and *Anopheles gambiae* (Diptera: Culicidae). *J Med Entomol* 31:747–753
- Ribeiro JM, Schneider M, Guimarães JA (1995) Purification and characterization of prolixin S (nitrophorin 2), the salivary anticoagulant of the blood-sucking bug *Rhodnius prolixus*. *Biochem J* 308:243–249
- Ribeiro JM, Katz O, Pannell LK, Waitumbi J, Warburg A (1999) Salivary glands of the sand fly *Phlebotomus papatasi* contain pharmacologically active amounts of adenosine and 5'-AMP. *J Exp Biol* 202:1551–1559
- Ribeiro JM, Charlab R, Rowton ED, Cupp EW (2000) *Simulium vittatum* (Diptera: Simuliidae) and *Lutzomyia longipalpis* (Diptera: Psychodidae) salivary gland hyaluronidase activity. *J Med Entomol* 37:743–747
- Ribeiro JM, Charlab R, Pham VM, Garfield M, Valenzuela JG (2004a) An insight into the salivary transcriptome and proteome of the adult female mosquito *Culex pipiens quinquefasciatus*. *Insect Biochem Mol Biol* 34:543–563
- Ribeiro JM, Andersen JF, Silva-Neto MA, Pham VM, Garfield MK, Valenzuela JG (2004b) Exploring the sialome of the blood-sucking bug *Rhodnius prolixus*. *Insect Biochem Mol Biol* 34:61–79
- Ribeiro JM, Alarcon-Chaidez F, Francischetti IM, Mans BJ, Mather TN, Valenzuela JG, Wikel SK (2006) An annotated catalog of salivary gland transcripts from *Ixodes scapularis* ticks. *Insect Biochem Mol Biol* 36:111–129
- Ribeiro JM, Arcà B, Lombardo F, Calvo E, Phan VM, Chandra PK, Wikel SK (2007) An annotated catalogue of salivary gland transcripts in the adult female mosquito, *Aedes aegypti*. *BMC Genomics* 8:6
- Ribeiro JM, Mans BJ, Arcà B (2010a) An insight into the sialome of blood-feeding Nematocera. *Insect Biochem Mol Biol* 40:767–784
- Ribeiro JM, Valenzuela JG, Pham VM, Kleeman L, Barbian KD, Favreau AJ, Eaton DP, Aoki V, Hans-Filho G, Rivitti EA, Diaz LA (2010b) An insight into the sialotranscriptome of *Simulium nigrimanum* a black fly associated with fogo selvagem in South America. *Am J Trop Med Hyg* 82:1060–1075
- Ribeiro JM, Anderson JM, Manoukis NC, Meng Z, Francischetti IM (2011) A further insight into the sialome of the tropical bont tick *Amblyomma variegatum*. *BMC Genomics* 12:136
- Ribeiro JM, Assumpção TC, Ma D, Alvarenga PH, Pham VM, Andersen JF, Francischetti IM, Macaluso KR (2012a) An insight into the sialotranscriptome of the cat flea, *Ctenocephalides felis*. *PLoS One* 7:e44612
- Ribeiro JM, Labruna MB, Mans BJ, Maruyama SR, Francischetti IM, Barizon GC, de Miranda Santos IK (2012b) The sialotranscriptome of *Antricola delacruzi* female ticks is compatible with non-hematophagous behavior and an alternative source of food. *Insect Biochem Mol Biol* 42:332–342
- Ribeiro JM, Assumpção TC, Pham VM, Francischetti IM, Reisenman CE (2012c) An insight into the sialotranscriptome of *Triatoma rubida* (Hemiptera: Heteroptera). *J Med Entomol* 49:563–572

- Ribeiro JM, Assumpção TC, Francischetti IM (2012d) An insight into the Sialomes of bloodsucking Heteroptera. *Psyche* 2012:470436
- Ribeiro JM, Chagas AC, Pham VM, Lounibos LP, Calvo E (2014a) An insight into the sialome of the frog biting fly *Corethrella appendiculata*. *Insect Biochem Mol Biol* 44:23–32
- Ribeiro JM, Genta FA, Sorgine MH, Logullo R, Mesquita RD, Paiva-Silva GO, Majerowicz D, Medeiros M, Koerich L, Terra WR, Ferreira C, Pimentel AC, Bisch PM, Leite DC, Diniz MM, da S G V Junior JL, Da Silva ML, Araujo RN, Gandara AC, Brosson S, Salmon D, Bousbata S, González-Caballero N, Silber AM, Alves-Bezerra M, Gondim KC, Silva-Neto MA, Atella GC, Araujo H, Dias FA, Polycarpo C, Vionette-Amaral RJ, Fampa P, Melo AC, Tanaka AS, Balczun C, Oliveira JH, Gonçalves RL, Lazoski C, Rivera-Pomar R, Diambra L, Schaub GA, Garcia ES, Azambuja P, Braz GR, Oliveira PL (2014b) An insight into the transcriptome of the digestive tract of the bloodsucking bug *Rhodnius prolixus*. *PLoS Negl Trop Dis* 8:e2594
- Ribeiro JM, Kazimirova M, Takac P, Andersen JF, Francischetti IM (2015a) An insight into the sialome of the horse fly *Tabanus bromius*. *Insect Biochem Mol Biol* 65:83–90
- Ribeiro JM, Schwarz A, Francischetti IM (2015b) A deep insight into the sialotranscriptome of the Chagas disease vector *Panstrongylus megistus* (Hemiptera: Heteroptera). *J Med Entomol* 52:351–358
- Ribeiro JM, Zepeda-Mendoza ML, Bertelsen MF, Kristensen AT, Jarvis ED, Gilbert MT, da Fonseca RR (2015c) A refined model of the genomic basis for phenotypic variation in vertebrate hemostasis. *BMC Evol Biol* 15:124
- Rodriguez-Valle M, Xu T, Kurscheid S, Lew-Tabor AE (2015) *Rhipicephalus microplus* serine protease inhibitor family: annotation, expression and functional characterisation assessment. *Parasit Vectors* 8:7
- Rogozin IB (2014) Complexity of gene expression evolution after duplication: protein dosage rebalancing. *Genet Res Int* 2014:516508
- Rost B (1999) Twilight zone of protein sequence alignments. *Protein Eng* 12:85–94
- Roversi P, Lissina O, Johnson S, Ahmat N, Paesen GC, Ploss K, Boland W, Nunn MA, Lea SM (2007) The structure of OMCI, a novel lipocalin inhibitor of the complement system. *J Mol Biol* 369:784–793
- Roversi P, Ryffel B, Togbe D, Maillet I, Teixeira M, Ahmat N, Paesen GC, Lissina O, Boland W, Ploss K, Caesar JJ, Leonhartsberger S, Lea SM, Nunn MA (2013) Bifunctional lipocalin ameliorates murine immune complex-induced acute lung injury. *J Biol Chem* 288:18789–18802
- Russell CL, Heesom KJ, Arthur CJ, Helms CR, Mellor PS, Day MJ, Torsteinsdottir S, Björnsdóttir TS, Wilson AD (2009) Identification and isolation of cDNA clones encoding the abundant secreted proteins in the saliva proteome of *Culicoides nubeculosus*. *Insect Mol Biol* 18:383–393
- Salát J, Paesen GC, Rezáčová P, Kotsyfakis M, Kovárová Z, Sanda M, Majtán J, Grunclová L, Horká H, Andersen JF, Brynda J, Horn M, Nunn MA, Kopáček P, Kopecký J, Mares M (2010) Crystal structure and functional characterization of an immunomodulatory salivary cystatin from the soft tick *Ornithodoros moubata*. *Biochem J* 429:103–112
- Sangamnatdej S, Paesen GC, Slovak M, Nuttall PA (2002) A high affinity serotonin- and histamine-binding lipocalin from tick saliva. *Insect Mol Biol* 11:79–86
- Sant'Anna Azzolini S, Sasaki SD, Torquato RJ, Andreotti R, Andreotti E, Tanaka AS (2003) *Rhipicephalus sanguineus* trypsin inhibitors present in the tick larvae: isolation, characterization, and partial primary structure determination. *Arch Biochem Biophys* 417:176–182
- Santos A, Ribeiro JMC, Lehane MJ, Gontijo NF, Veloso AB, Sant'Anna MRV, Nascimento Araujo R, Grisard EC, Pereira MH (2007) The sialotranscriptome of the blood-sucking bug *Triatoma brasiliensis* (Hemiptera Triatominae). *Insect Biochem Mol Biol* 37:702–712
- Sá-Nunes A, Bafica A, Antonelli LR, Choi EY, Francischetti IM, Andersen JF, Shi GP, Chavakis T, Ribeiro JM, Kotsyfakis M (2009) The immunomodulatory action of sialostatin L on dendritic cells reveals its potential to interfere with autoimmunity. *J Immunol* 182:7422–7429
- Sarkis JJ, Guimarães JA, Ribeiro JM (1986) Salivary apyrase of *Rhodnius prolixus*. Kinetics and purification. *Biochem J* 233:885–891

- Sasaki SD, Azzolini SS, Hirata IY, Andreotti R, Tanaka AS (2004) *Boophilus microplus* tick larvae, a rich source of Kunitz type serine proteinase inhibitors. *Biochimie* 86:643–649
- Scharfstein J, Schmitz V, Svensjö E, Granato A, Monteiro AC (2007) Kininogens coordinate adaptive immunity through the proteolytic release of bradykinin, an endogenous danger signal driving dendritic cell maturation. *Scand J Immunol* 66:128–136
- Schiemann F, Grimm TA, Hoch J, Gross R, Lindner B, Petersen F, Bulfone-Paus S, Brandt E (2006) Mast cells and neutrophils proteolytically activate chemokine precursor CTAP-III and are subject to counterregulation by PF-4 through inhibition of chymase and cathepsin G. *Blood* 107:2234–2242
- Schofield CJ, Galvão C (2009) Classification evolution and species groups within the Triatominae. *Acta Trop* 110:88–100
- Schuit TJ, Bakhtiari K, Daffre S, Deponte K, Wielders SJ, Marquart JA, Hovius JW, van der Poll T, Fikrig E, Bunce MW, Camire RM, Nicolaes GA, Meijers JC, van 't Veer C (2013) Factor Xa activation of factor V is of paramount importance in initiating the coagulation system: lessons from a tick salivary protein. *Circulation* 128:254–266
- Schwarz A, von Reumont BM, Erhart J, Chagas AC, Ribeiro JM, Kotsyfakis M (2013) De novo *Ixodes ricinus* salivary gland transcriptome analysis using two next-generation sequencing methodologies. *FASEB J* 27:4745–4756
- Schwarz A, Medrano-Mercado N, Schaub GA, Struchiner CJ, Bargues MD, Levy MZ, Ribeiro JM (2014) An updated insight into the sialotranscriptome of *Triatoma infestans*: developmental stage and geographic variations. *PLoS Negl Trop Dis* 8:e3372
- Selak MA (1992) Neutrophil elastase potentiates cathepsin G-induced platelet activation. *Thromb Haemost* 68:570–576
- Selak MA, Chignard M, Smith JB (1988) Cathepsin G is a strong platelet agonist released by neutrophils. *Biochem J* 251:293–299
- Sharma JN (2005) The kallikrein-kinin system: from mediator of inflammation to modulator of cardioprotection. *Inflammopharmacology* 12:591–596
- Shatrov AB, Kudryashova NI (2006) Taxonomy life cycles and the origin of parasitism in trombiculid mites. In: Morand S, Krasnov BR, Poulin R (eds) *Micromammals and macroparasites: from evolutionary ecology to management*. Springer, Tokyo, pp 119–140
- Soares TS, Watanabe RM, Tanaka-Azevedo AM, Torquato RJ, Lu S, Figueiredo AC, Pereira PJ, Tanaka AS (2012) Expression and functional characterization of boophilin, a thrombin inhibitor from *Rhipicephalus (Boophilus) microplus* midgut. *Vet Parasitol* 187:521–528
- Sonenshine DE (1991) *Biology of ticks*, vol 1. Oxford University Press, Cambridge
- Sonenshine DE (2004) Pheromones and other semiochemicals of ticks and their use in tick control. *Parasitology* 129:S405–S425
- Sonenshine DE, Roe RM (2014) External and internal anatomy of ticks. In: Sonenshine DE, Roe RM (eds) *Biology of ticks*, vol 1, 2nd edn. Oxford University Press, New York, pp 74–98
- Soter NA, Lewis RA, Corey EJ, Austen KF (1983) Local effects of synthetic leukotrienes (LTC₄, LTD₄, LTE₄, and LTB₄) in human skin. *J Invest Dermatol* 80:115–119
- Stark KR, James AA (1995) A factor Xa-directed anticoagulant from the salivary glands of the yellow fever mosquito *Aedes aegypti*. *Exp Parasitol* 81:321–331
- Stark KR, James AA (1996) Salivary gland anticoagulants in culicine and anopheline mosquitoes (Diptera:Culicidae). *J Med Entomol* 33:645–650
- Stark KR, James AA (1998) Isolation and characterization of the gene encoding a novel factor Xa-directed anticoagulant from the yellow fever mosquito, *Aedes aegypti*. *J Biol Chem* 273:20802–20809
- Stutzer C, Mans BJ, Gaspar AR, Neitz AW, Maritz-Olivier C (2009) *Ornithodoros savignyi*: soft tick apyrase belongs to the 5'-nucleotidase family. *Exp Parasitol* 122:318–327
- Sugiyama K, Iyori M, Sawaguchi A, Akashi S, Tame JR, Park SY, Yoshida S (2014) The crystal structure of the active domain of *Anopheles* anti-platelet protein, a powerful anti-coagulant, in complex with an antibody. *J Biol Chem* 289:16303–16312

- Sun J, Yamaguchi M, Yuda M, Miura K, Takeya H, Hirai M, Matsuoka H, Ando K, Watanabe T, Suzuki K, Chinzei Y (1996) Purification, characterization and cDNA cloning of a novel anticoagulant of the intrinsic pathway, (prolixin-S) from salivary glands of the blood sucking bug, *Rhodnius prolixus*. *Thromb Haemost* 75:573–577
- Takác P, Nunn MA, Mészáros J, Pechánová O, Vrbjar N, Vlasáková P, Kozánek M, Kazimířová M, Hart G, Nuttall PA, Labuda M (2006) Vasotab, a vasoactive peptide from horse fly *Hybomitra bimaculata* (Diptera, Tabanidae) salivary glands. *J Exp Biol* 209:343–352
- Tan AW, Francischetti IM, Slovak M, Kini RM, Ribeiro JM (2015) Sexual differences in the sialomes of the zebra tick *Rhipicephalus pulchellus*. *J Proteomics* 117:120–144
- Tanaka AS, Andreotti R, Gomes A, Torquato RJ, Sampaio MU, Sampaio CA (1999) A double headed serine proteinase inhibitor – human plasma kallikrein and elastase inhibitor–from *Boophilus microplus* larvae. *Immunopharmacology* 45:171–177
- Tang J, Fang Y, Han Y, Bai X, Yan X, Zhang Y, Lai R, Zhang Z (2015) YY-39, a tick anti-thrombosis peptide containing RGD domain. *Peptides* 68:99–104
- Thomas MR, Storey RF (2015) The role of platelets in inflammation. *Thromb Haemost* 114:449–458
- Tirloni L, Reck J, Terra RM, Martins JR, Mulenga A, Sherman NE, Fox JW, Yates JR 3rd, Termignoni C, Pinto AF, Vaz Ida S Jr (2014) Proteomic analysis of cattle tick *Rhipicephalus (Boophilus) microplus* saliva: a comparison between partially and fully engorged females. *PLoS One* 9:e94831
- Tirloni L, Islam MS, Kim TK, Diedrich JK, Yates JR 3rd, Pinto AF, Mulenga A, You MJ, Da Silva Vaz I Jr (2015) Saliva from nymph and adult females of *Haemaphysalis longicornis*: a proteomic study. *Parasit Vectors* 8:338
- Titus RG, Ribeiro JM (1990) The role of vector saliva in transmission of arthropod-borne disease. *Parasitol Today* 6:157–160
- Toole BP (2000) Hyaluronan is not just a goo! *J Clin Invest* 106:335–336
- Tsujimoto H, Kotsyfakis M, Francischetti IM, Eum JH, Strand MR, Champagne DE (2012) Simukunin from the salivary glands of the black fly *Simulium vittatum* inhibits enzymes that regulate clotting and inflammatory responses. *PLoS One* 7:e29964
- Tyson K, Elkins C, Patterson H, Fikrig E, de Silva A (2007) Biochemical and functional characterization of Salp20, an *Ixodes scapularis* tick salivary protein that inhibits the complement pathway. *Insect Mol Biol* 16:469–479
- Tyson KR, Elkins C, de Silva AM (2008) A novel mechanism of complement inhibition unmasked by a tick salivary protein that binds to properdin. *J Immunol* 180:3964–3968
- Ujita M, Sakai K, Hamazaki K, Yoneda M, Isomura S, Hara A (2003) Carbohydrate binding specificity of the recombinant chitin-binding domain of human macrophage chitinase. *Biosci Biotechnol Biochem* 67:2402–2407
- Undheim EA, Jones A, Clauser KR, Holland JW, Pineda SS, King GF, Fry BG (2014) Clawing through evolution: toxin diversification and convergence in the ancient lineage Chilopoda (centipedes). *Mol Biol Evol* 31:2124–2148
- Valdés JJ, Schwarz A, Cabeza de Vaca I, Calvo E, Pedra JH, Guallar V, Kotsyfakis M (2013) Tryptogalinin is a tick Kunitz serine protease inhibitor with a unique intrinsic disorder. *PLoS One* 8:e62562
- Valenzuela JG, Ribeiro JM (1998) Purification and cloning of the salivary nitrophorin from the hemipteran *Cimex lectularius*. *J Exp Biol* 201:2659–2664
- Valenzuela JG, Walker FA, Ribeiro JM (1995) A salivary nitrophorin (nitric-oxide-carrying hemo-protein) in the bedbug *Cimex lectularius*. *J Exp Biol* 198:1519–1526
- Valenzuela JG, Guimaraes JA, Ribeiro JM (1996) A novel inhibitor of factor X activation from the salivary glands of the bed bug *Cimex lectularius*. *Exp Parasitol* 83:184–190
- Valenzuela JG, Charlab R, Galperin MY, Ribeiro JM (1998) Purification, cloning, and expression of an apyrase from the bed bug *Cimex lectularius*. A new type of nucleotide-binding enzyme. *J Biol Chem* 273:30583–30590

- Valenzuela JG, Francischetti IM, Ribeiro JM (1999) Purification cloning and synthesis of a novel salivary anti-thrombin from the mosquito *Anopheles albimanus*. *Biochemistry* 38:11209–11215
- Valenzuela JG, Charlab R, Mather TN, Ribeiro JM (2000) Purification, cloning, and expression of a novel salivary anticomplement protein from the tick, *Ixodes scapularis*. *J Biol Chem* 275:18717–18723
- Valenzuela JG, Belkaid Y, Rowton E, Ribeiro JM (2001) The salivary apyrase of the blood-sucking sand fly *Phlebotomus papatasi* belongs to the novel Cimex family of apyrases. *J Exp Biol* 204:229–237
- Valenzuela JG, Francischetti IM, Pham VM, Garfield MK, Mather TN, Ribeiro JM (2002a) Exploring the sialome of the tick *Ixodes scapularis*. *J Exp Biol* 205:2843–2864
- Valenzuela JG, Pham VM, Garfield MK, Francischetti IM, Ribeiro JM (2002b) Toward a description of the sialome of the adult female mosquito *Aedes aegypti*. *Insect Biochem Mol Biol* 32:1101–1122
- Valenzuela JG, Francischetti IM, Pham VM, Garfield MK, Ribeiro JM (2003) Exploring the salivary gland transcriptome and proteome of the *Anopheles stephensi* mosquito. *Insect Biochem Mol Biol* 33:717–732
- Valenzuela JG, Garfield M, Rowton ED, Pham VM (2004) Identification of the most abundant secreted proteins from the salivary glands of the sand fly *Lutzomyia longipalpis* vector of *Leishmania chagasi*. *J Exp Biol* 207:3717–3729
- van de Locht A, Stubbs MT, Bode W, Friedrich T, Bollschweiler C, Höffken W, Huber R (1996) The ornithodorin-thrombin crystal structure, a key to the TAP enigma? *EMBO J* 15:6011–6017
- Vijil C, HerMansson C, Jeppsson A, Bergström G, Hultén LM (2014) Arachidonate 15-lipoxygenase enzyme products increase platelet aggregation and thrombin generation. *PLoS One* 9:e88546
- Vlkova M, Sima M, Rohousova I, Kostalova T, Sumova P, Volfova V, Jaske EL, Barbian KD, Gebre-Michael T, Hailu A, Warburg A, Ribeiro JM, Valenzuela JG, Jochim RC, Volf P (2014) Comparative analysis of salivary gland transcriptomes of *Phlebotomus orientalis* sand flies from endemic and non-endemic foci of visceral leishmaniasis. *PLoS Negl Trop Dis* 8:e2709
- Volfova V, Hostomska J, Cerny M, Votypka J, Volf P (2008) Hyaluronidase of bloodsucking insects and its enhancing effect on *Leishmania* infection in mice. *PLoS Negl Trop Dis* 2:e294
- Waidhet-Kouadio P, Yuda M, Ando K, Chinzei Y (1998) Purification and characterization of a thrombin inhibitor from the salivary glands of a malarial vector mosquito, *Anopheles stephensi*. *Biochim Biophys Acta* 1381:227–233
- Walsh PN (2001) Roles of platelets and factor XI in the initiation of blood coagulation by thrombin. *Thromb Haemost* 86:75–82
- Wang H, Nuttall PA (1999) Immunoglobulin-binding proteins in ticks: new target for vaccine development against a blood-feeding parasite. *Cell Mol Life Sci* 56:286–295
- Wang X, Coons LB, Taylor DB, Stevens SE Jr, Gartner TK (1996) Variabilin, a novel RGD-containing antagonist of glycoprotein IIb-IIIa and platelet aggregation inhibitor from the hard tick *Dermacentor variabilis*. *J Biol Chem* 271:17785–17790
- Wang H, Paesen GC, Nuttall PA, Barbour AG (1998) Male ticks help their mates to feed. *Nature* 391:753–754
- Wang X, Ribeiro JM, Broce AB, Wilkerson MJ, Kanost MR (2009) An insight into the transcriptome and proteome of the salivary gland of the stable fly *Stomoxys calcitrans*. *Insect Biochem Mol Biol* 39:607–614
- Watanabe RM, Soares TS, Morais-Zani K, Tanaka-Azevedo AM, Maciel C, Capurro ML, Torquato RJ, Tanaka AS (2010) A novel trypsin Kazal-type inhibitor from *Aedes aegypti* with thrombin coagulant inhibitory activity. *Biochimie* 92:933–939
- Waxman L, Connolly TM (1993) Isolation of an inhibitor selective for collagen-stimulated platelet aggregation from the soft tick *Ornithodoros moubata*. *J Biol Chem* 268:5445–5449
- Waxman L, Smith DE, Arcuri KE, Vlasuk GP (1990) Tick anticoagulant peptide (TAP) is a novel inhibitor of blood coagulation factor Xa. *Science* 248:593–596

- Weichsel A, Andersen JF, Champagne DE, Walker FA, Montfort WR (1998) Crystal structures of a nitric oxide transport protein from a blood-sucking insect. *Nat Struct Biol* 5:304–309
- Weirauch C, Munro JB (2009) Molecular phylogeny of the assassin bugs (Hemiptera: Reduviidae), based on mitochondrial and nuclear ribosomal genes. *Mol Phylogenet Evol* 53:287–299
- Xu X, Yang H, Ma D, Wu J, Wang Y, Song Y, Wang X, Lu Y, Yang J, Lai R (2008) Toward an understanding of the molecular mechanism for successful blood feeding by coupling proteomics analysis with pharmacological testing of horsefly salivary glands. *Mol Cell Proteomics* 7:582–590
- Xu X, Oliveira F, Chang BW, Collin N, Gomes R, Teixeira C, Reynoso D, My Pham V, Elnaïem DE, Kamhawi S, Ribeiro JM, Valenzuela JG, Andersen JF (2011) Structure and function of a “yellow” protein from saliva of the sand fly *Lutzomyia longipalpis* that confers protective immunity against *Leishmania major* infection. *J Biol Chem* 286:32383–32393
- Xu X, Francischetti IM, Lai R, Ribeiro JM, Andersen JF (2012) Structure of protein having inhibitory disintegrin and leukotriene scavenging functions contained in single domain. *J Biol Chem* 287:10967–10976
- Xu X, Chang BW, Mans BJ, Ribeiro JM, Andersen JF (2013) Structure and ligand-binding properties of the biogenic amine-binding protein from the saliva of a blood-feeding insect vector of *Trypanosoma cruzi*. *Acta Crystallogr D Biol Crystallogr* 69:105–113
- Xu XL, Cheng TY, Yang H, Yan F, Yang Y (2015) De novo sequencing, assembly and analysis of salivary gland transcriptome of *Haemaphysalis flava* and identification of sialoprotein genes. *Infect Genet Evol* 32:135–142
- Xue M, Jackson CJ (2015) Extracellular matrix reorganization during wound healing and its impact on abnormal scarring. *Adv Wound Care (New Rochelle)* 4:119–136
- Yamaji K, Tsuji N, Miyoshi T, Islam MK, Hatta T, Alim MA, Anisuzzaman M, Kushibiki S, Fujisaki K (2009) A salivary cystatin, HISC-1, from the ixodid tick *Haemaphysalis longicornis* play roles in the blood-feeding processes. *Parasitol Res* 106:61–68
- Yoshida S, Sudo T, Niimi M, Tao L, Sun B, Kambayashi J, Watanabe H, Luo E, Matsuoka H (2008) Inhibition of collagen-induced platelet aggregation by anopheline antiplatelet protein, a saliva protein from a malaria vector mosquito. *Blood* 111:2007–2014
- Zhang Y, Ribeiro JM, Guimarães JA, Walsh PN (1998) Nitrophorin-2: a novel mixed-type reversible specific inhibitor of the intrinsic factor-X activating complex. *Biochemistry* 37:10681–10690
- Zhang Z, Gao L, Shen C, Rong M, Yan X, Lai R (2014) A potent anti-thrombosis peptide (vasotab TY) from horsefly salivary glands. *Int J Biochem Cell Biol* 54:83–88
- Zhu K, Sauer JR, Bowman AS, Dillwith JW (1997a) Identification and characterization of anticoagulant activities in the saliva of the lone star tick, *Amblyomma americanum* (L.). *J Parasitol* 83:38–43
- Zhu K, Bowman AS, Brigham DL, Essenberg RC, Dillwith JW, Sauer JR (1997b) Isolation and characterization of americanin, a specific inhibitor of thrombin, from the salivary glands of the lone star tick *Amblyomma americanum* (L.). *Exp Parasitol* 87:30–38

ERRATUM

Chapter 14 Insect Silks and Cocoons: Structural and Molecular Aspects

**Kenji Yukuhiro, Hideki Sezutsu, Takuya Tsubota, Yoko Takasu,
Tsunenori Kameda, and Naoyuki Yonemura**

© Springer International Publishing Switzerland 2016
E. Cohen, B. Moussian (eds.), *Extracellular Composite Matrices in Arthropods*,
DOI 10.1007/978-3-319-40740-1_14

DOI 10.1007/978-3-319-40740-1_18

The figure 14.7 in chapter 14 “Insect Silks and Cocoons: Structural and Molecular Aspects” was wrong. Below is the correct figure. The original chapter and the erratum chapter has been updated.

The updated original online version for this chapter can be found at
DOI [10.1007/978-3-319-40740-1_14](https://doi.org/10.1007/978-3-319-40740-1_14)

<i>Antheraea pernyi</i> & <i>A. yamamami</i>	Type1	GSGAGGAGGGYGWGDGGYGSDS
	Type2	-SGAGGS (GGY) _{1~3} GGYGSDS
	Type3	GSGAGG-----RGDGGYGS GSS
	Type4	-RRAGHDRAAGS
<i>A. assama</i>	TypeG _b	GGSG ^{AG} _G ^Y _G ^D _G GGYGWGDGGYGS ^D _S GR S G E G
	TypeG _c	GSGAGG ^R _V GGGY ^R _L GDGGYGS GSS
	TypeGa	GSGAGGAGDGGYGS GSSG E
	TypeR	RRAGHDRAAGS
<i>Rhodinia fugax</i>	Type1	GSGSRGLGGY YGKDGLLLDGEYGS GS
	Type2	GSGSRGLGGY YG-DG--LLDGGYGS GS
	Type3	GSSSDYTVYESSRRGSSSS
	Type4	GSSGVGYGRRYGS DS
<i>Saturnia japonica</i>	Type1LH	GSGAGGLGGHYGLHGGVYGS DS
	Type1LHL	GSGAGGLGGLYGLHGGVYGS SSSRRDSSSASS
	Type1W	GSSSRRVGGHYGW DGGVYGS DS
	Type2	GSSAASSERVYESES
<i>Samia ricini</i>	motif 1	GGAGSGYGGGAR ^R _G GYGHGYGSDGG
	motif 2	GGAGSGYGGGSWH ^G _S YGSDS ^G _S
	motif 3	GG ^G _S (GGYG) ^A _{1~3} DGG
	motif 4	GGAG ^G _D DGYGAGS

Index

- A**
ABC transporters. *See* ATP-binding cassette (ABC) transporters
Acari, 626–628
Acarus siro, 372
Accessory glands, 418–423, 431–432
Acheta domesticus, 70, 349, 351
Acid fuchsin staining, 529
Acid phosphatase, 659, 664
Aciniform spidroin 1 (AcSp1), 451, 459
ACP. *See* Amorphous calcium phosphate (ACP)
Actias selene, 524, 532, 534, 539
Aculeate insects, 542
Acyl-CoA reductases, 228–230
Acyrtosiphon pisum, 38, 39, 166, 182, 194, 348
Adalia bipunctata, 333
Adhesion, 565, 573
Adipocytes, 631
Adomerus triguttulus, 334
Adrenomedullin, 649
Aedes
 A. aegypti, 37, 39, 54, 77, 178, 180, 278, 280, 291, 300, 382, 392, 633, 638, 639, 659
 15-a1, 339
 15a2, 339
 15a3, 339
 AAEL0017501, 339
 AAEL006670, 339
 AAEL017471, 339
 A. albopictus, 342
 A. triseriatus, 647
Aegyptin, 636, 638–640, 659
Aeromonas dhkanesis 3K1C15, 392
Aeropyles, 332–335
 crown, 334
Affinity chromatography, 473, 476
Aggregate spider glue 2 (AgSG2), 456, 457
Aggregation pheromones, 242
Aglaspida, 149
Alanine, 493, 498–500
Aldehyde decarboxylases, 230–231
Aldehydes, 225, 228–232, 241
Alder flies, 626
Aldrichina grahami, 240
5,9-Alkadiene, 228
Allelochemicals, 290
Allenic hydrocarbons, 222
Allium sativum agglutinin (ASAL), 302
Allosamidin, 393
 α 2-antiplasmin, 643
 α -helix, 516, 532, 534
Alpha-2 macroglobulin (A2M), 457, 643
Alternate exons in *Chs-1*, 38
Alternative splicing, 530, 531, 534
Amblyomma
 A. americanum, 637, 644, 651, 657
 A. hebraeum, 70, 632
AmelF, 543, 545
American cockroach, 224, 226, 228
Aminolevulinate synthase, 78
Amnion, 327, 328, 344, 348
Amnioserosa, 348
Amorphous calcium carbonate (ACC)
 as dietary supplement, 155

- Amorphous calcium carbonate (ACC) (*cont.*)
 isotropic structure, 145
 phosphate incorporation, 146
 phosphoproteins, 150
 solubility, 145, 146, 151
 stabilization, 146, 151, 154, 156
- Amorphous calcium phosphate (ACP), 145,
 146, 148, 150, 151, 155–156
 bone grafts, bone cement, bone fillers, 155
 phosphate/calcium ratio, 140, 146, 151,
 156
 solid solution, 146, 156
- Amorphous domains, 520
- Amorphous region, 495–498
- Ampulla, 448, 464, 465
- Anagasta kuehniella*, 520
- Anaphe moloneyi*, 518
- Anaphylatoxin, 648
- Angiogenesis, 631, 634, 650, 655
- Annexin, 272
- Annulipalpia, 540, 541
- Anomala cuprea*, 298
- Anopheles* spp., 604
A. albimanus, 646
A. albitarsis, 342
A. gambiae, 3–4, 12, 13, 15, 39, 45, 49, 52,
 54, 70, 178, 180, 186, 188, 196,
 231, 262, 275, 278–280, 292, 300,
 638, 647, 660
 AGAP002134-RA, 339
 AGAP008696-RA, 339
A. shannoni, 333
A. stephensi, 633, 638, 646, 660
A. tessellatus, 295
- Anopheline antiplatelet protein (AAPP), 636
- Anophensin, 646, 649
- Anoplophora malasiaca*, 233
- Anoplura, 629
- Antennapedia, 536, 537
- Anterior silk glands (ASG), 517, 537
- Antheraea*
A. assama, 524, 532, 533, 539
A. mylitta, 518
A. pernyi, 517, 520, 523, 524, 527, 529,
 533, 539
A. polyphemus, 327, 328, 334
A. yanamai, 517, 520, 523, 524, 527, 529,
 533, 539, 542, 544
- Antibody-dependent cell-mediated
 cytotoxicity (ADCC), 547
- Anticarsia gemmatalis*, 294, 303
- Antigen 5, 638, 640, 648, 650, 660, 664
- Antimicrobial peptides, 273, 284, 412, 415,
 420, 424, 426, 431
- Apatite, 145, 148–151, 156
- Aphaenogaster cockerelli*, 238
- Aphid saliva, 605
- Aphis*
A. fabae, 239
A. glycines, 38
- Apical undulae, 73
- Apis mellifera*, 12, 13, 77, 190, 193, 196, 238,
 302, 543, 610
- Aplysia*, 337
- Apocrine secretion, 268, 271, 288, 562,
 576–590
- Apocrita, 542
- Apoidea, 516
- Apolygus lucorum*, 606
- Apolysis, 370, 382, 385
- Aposome, 579, 581
- Apyrase, 637, 638, 640, 642
- Aquaporins (AQPs), 433, 434
- Arabidopsis thaliana*, 304, 614
- Arachidonic acid, 636, 640, 653
- Arachnida, 602, 611, 626
- Arachnids, 446
- Aragonite, 145
- Araneus*
A. diadematus, 495
A. gemmoides, 460
A. ventricosus, 458, 547
- Arboviral vectors, 293
- Archaeognatha, 344, 347,
 348, 605
- Architecture, 68, 71, 73, 77, 82
- Arctiidae, 241
- Argadin, 393
- Argasids, 630
- Argifin, 393
- Arginine methyltransferase, 10
- Argiope*
A. aurantia, 460
A. bruennichi, 460
A. trifasciata, 457, 459, 497
- Arms race, 415, 416, 421
- Arrowhead (Awh), 537
- Arthropoda, 625
- Artificial silk fibers, 474–475
- Assassin bugs, 629, 633, 640, 641, 643,
 662–664
- ATP-binding cassette (ABC) transporters, 376,
 379, 381
- Attachment discs, 449, 451, 461, 462
- Attacini, 524
- Australian bulldog ant, 543, 545
- Autofluorescence, 91–93, 102, 103, 106–110,
 122–125

- Autographa californica* multicapsid nucleopolyhedrovirus (AcMNPV), 392
- Autoimmunity, 648
- Avians, 628
- Azinphosmethyl, 21
- B**
- Bacillus*
- B. subtilis*, 295
- B. thuringiensis*, 291, 295, 296
- Bactericera cockerelli*, 392
- Bactrocera oleae*, 342
- Baculentulus densus*, 347
- Baculoviruses, 293, 296, 297
- Bark lice, 626
- Barnacles, 138, 149
- Basic helix-loop-helix (bHLH), 456
- Basic tail secretory protein (BTSP), 658, 661, 663
- Basophils, 631, 641, 652, 655
- Beauveria bassiana*, 372–374, 393
- Bed bugs, 629, 633, 640, 643, 649, 659, 662, 664
- Bemisia tabaci*, 390
- Benzoylhydrazine
- chromafenozide, 384
- halofenozide, 383
- KU-106, 384
- methoxyfenozide, 383, 384
- RH-5849, 383
- tebufenozide, 383–386
- Benzoylphenyl urea (BPU)
- diflubenzuron, 375, 376, 379–381
- lufenuron, 378
- novaluron, 378
- triflumuron, 387
- β -1,3-Glucanases, 373
- β -sheet, 516, 531–534, 542, 544–546, 548
- β -tryptase, 655
- Bilin-binding protein (BBP), 201
- Biofactories, 446
- Biogenic amine binding proteins, 641
- Bio-inspired materials, 154
- Biological muscles, 497, 504
- Biomaterial, 446, 461, 479, 480
- Biomimetics, 496, 505
- application, 153–156
- rec1-resilin, 94, 97, 99, 104, 124–127
- Rec1/RSF, 127
- resilin-elastin-collagen (REC), 127
- resilin-like polypeptides (RLP), 124–128
- Biom mineralization
- dual mineral system, 151
- mechanical advantages, 146
- metabolic cost, 140, 141, 150, 151
- Biominerals, 502–504
- Biopolymers, 504
- Biting midges, 629, 633, 634, 640, 643, 649, 654, 659, 664
- Black bean aphid, 239
- Black flies, 629, 633, 639, 643, 659, 664
- BLAST searches, 532
- Blastoderm, 326, 344–347
- Blastodermal cuticle, 344–347, 355
- Blattella germanica*, 7, 8, 184, 380
- brownie*, 339, 340
- citrus*, 339, 340
- Block repeats, 451, 454, 458–462, 467–473, 479
- Blood clotting cascade, 631
- Blood-feeding, 625–688
- BmCpr2, 81
- BmCPT1, 77
- Bmsage, 535, 537
- Body armor, 466, 478, 480
- Bombycidae, 517, 539
- Bombycoidea, 517, 533, 539, 540
- Bombyx*
- B. mandarina*, 520, 538, 539
- B. mori*, 4–8, 11–13, 15–18, 20, 21, 40, 45–50, 54, 55, 72, 77, 80, 167, 171–176, 180–182, 185–192, 195, 196, 203, 285, 291, 298, 303, 384, 391, 393, 446, 516–518, 520, 521, 523, 525–527, 529–530, 532, 534–536, 538–540, 542, 544, 546, 548, 608
- BmEP80, 338
- BmVM30, 338
- BmVMP30, 338
- BmVMP90, 338
- ErA*, 338
- ErB*, 338
- HcA*, 338
- HcB*, 338
- Botrytis cinerea*, 613
- Brachiopods, 154
- Brachycera, 626
- Brachyura, 144
- Bradoriida, 149
- Bradykinin, 648, 652
- Breaking strain, 477, 499, 503
- Breaking stress, 457, 466, 473–474, 477
- Breeding strategy, 145
- Broad-horned flour beetle, 241
- Brugia pahangi*, 293

- Buprofezin, 390
 Burgess Shale, 149
 Bursicon, 200, 202, 203
 Butterflies, 626
- C**
- C/EBPs, 340
Cabrio, 37
 Caddisflies, 516, 540
Caenorhabditis elegans, 9, 38, 49
 Calcification, 138, 141, 145, 150, 153
 Calcite, 145, 146, 148, 151
 Calcium carbonate, 140, 146, 147, 149–151, 153, 154, 156
 Calcium chloride, 545
 Calcium phosphate, 140, 146–151, 153–156
 mandibular teeth, 149
 Calcofluor white, 291, 297, 299, 300
Callinectes sapidus, 168
 Callophorid fly, 240
Callosobruchus maculatus, 614
 Calmodulin, 272
Calpodes ethlius, 68, 71, 72, 81
 Calyptra, 626
 Cambrium explosion
 fossil records, 149
 shift from calcium phosphate to calcium carbonate, 150
Campodea fragilis, 347
Cancer pagurus, 142
 Captan, 390
 Cara mitad, 10
 Carbohydrate esterase, 44
 Carbonic anhydrase, 452
 Carboxylic ester hydrolase (CEH), 457
 Carboxymethyl-cellulose, 607
 Carboxypeptidase B, 643, 648
 Cardia, 264, 269–273
Carica papaya, 304
 CARM1, 10
Carpophilus, 242
 Carrageenan-induced rat paw edema
 model, 648
 Catecholamines, 70, 78
 Catechol oxidase, 649
 Cat flea, 633, 654
 Cathepsin G, 637, 639, 655, 666
 Cathepsin L, 648
 Cathepsin S, 648
 Cathepsins, 297
 Cecidomyiidae, 609
 Cement, 566, 573, 630, 634
- Centipedes, 626
 Central nervous system (CNS), 170, 177, 199, 202
 Cephalothorax, 456
 Cerambycid beetles, 235
 Ceratopogonidae, 629
Cerceris fumipennis, 241
 Chagas fever, 68
 CHCs. *See* Cuticular hydrocarbons (CHCs)
 Cheliceræ, 629
 Chelicerata, 344–346, 626
 Chelicerates, 71
 Chemical mimicry, 232, 238–239
 Chemoreception, 234–236
 Cephalocharida, 610
Cherax quadricarinatus, 139, 148, 149, 151–153
 molar teeth, 149
 Chilopoda, 602, 611
 Chilopods, 346
 Chimeric fusion proteins, 502, 504
 Chinese hamster ovary (CHO), 547
 Chiral, 223, 235–236, 238, 241, 242
 Chitin, 4–6, 68, 69, 71–78, 80–82
 α -chitin, 261
 β -chitin, 261
 binding domains, 343
 binding motifs, 353
 binding proteins (CBPs), 339, 343
 biocompatibility, 154
 biosynthetic pathway, 47
 Bouligand structure, 34
 chitin-binding domain, 152
 chitin-binding proteins, 152
 cross-ply laminae, 34
 deacetylation, 44
 degradation, 47, 53, 56
 γ -chitin, 261
 higher-order structure, 33, 34, 36
 molecular weight, 33–34
 nanofibers, 34
 precursors, 36–40
 protection, 56
 Chitinase, 343, 370, 371, 373, 375, 392–394, 626, 632, 634
 conserved motifs, 38, 40, 50
 crystal structure, 51
 domain organization, 48–51, 53
 gene family, 48, 52
 specialization in functions, 38, 52, 53
 tissue specificity, 38, 48, 52
 Chitin-binding, 70, 74–76, 80, 82
 Chitin-binding domain, 393

- Chitin binding domain 2 (ChtBD2), 76
 chitin-binding pocket, 263
 consensus sequence, 263
 conserved cysteine residues, 263
 intermolecular disulfide bridges, 262, 283
- Chitin deacetylase, 75, 80, 263, 288, 306
 domain organization, 45
 gene family, 45
 in vitro activity, 47
 loss of laminar organization, 46, 52
 role in cuticle assembly, 44
 tracheal cuticle development, 40
- Chitin nanofibers, 260, 261, 268, 270, 271, 276, 277, 279, 307
- Chitin synthase, 260, 270, 271, 276, 379, 381, 386, 387, 390–392
 oligomeric complex, 260
- Chitin synthase 1
 Chitin synthase A, 352
 Chs1, 352, 354
 Chs1a, 352
 Chs1b, 352
- Chitin synthase A
 alternate exons, 38, 39
 cuticular defects, 37
 loss of chitin, 36, 37, 39
 loss of laminae, 46, 52
 modeling, 41, 42
 mode of action, 40, 41
 molting defects, 36, 37, 40, 55, 56
 oligomeric complex, 38
 plasma membrane plaques, 43, 47
 promoter, 40, 44, 48
 proteolytic activation, 38
- Chitin synthase B
 alternative splicing, 40
 loss of PM integrity, 39
 promoter, 40, 44
- Chitosan, 154
- Chondroitin sulphate, 653
- Choriogenesis, 327, 329, 331, 337–340, 342
- Chorion, 169
- Chorionic layers, 326–355
- Choristoneura fumiferana*, 385–387
- Chromatin-remodeling, 9–11, 13
- Chromosome 22, 11, 13, 15, 17
- Chrysomya nigripes*, 335
- Chrysops viduatus*, 633
- Chrysoptin, 639, 642
- Chymase, 651, 655, 666
- Cicadas, 67
- Cimex lectularius*, 76, 638, 646, 649, 659
- Cimicidae, 626, 629, 662
- Circadian rhythms, 181, 182
- Cis-vaccenyl acetate*, 231
- Clofentazine, 389
- Clonostachys* sp. FO-7314, 393
- Clotting cascade, 642–648
- Coagulation baths, 476, 478
- Cob-weavers, 447, 449, 451, 456, 458, 461–464, 467
- Cocoon, 516–548
- Coffea arabica*, 615
- Coiled coil proteins, 543–545
- Coleoptera, 347, 348, 516
- Collagen, 154, 631, 632, 635–641, 643, 656
- Collembola, 344, 346, 605
- Colopterus*, 242
- Columnar cells, 260, 268, 270, 271, 559, 560
- Comb wax, 237
- Complement cascade
 alternative pathway, 653
 C1, 653
 C5, 653
 C3a, 653
 C4a, 653
 C5a, 653
 C3b, 653
 C5b-9, 653
 C3 convertase, 653
 classical pathway, 653
 C1q, 653
 platelet receptor cC1qR, 653
 properdin, 653
 P selectin, 653
- Complementary DNAs (cDNAs), 451, 454, 458–462, 467–471, 480
- Concanavalin A (ConA), 300
- Congo red, 299
- Connective tissue-activating peptide-III (CTAP-III), 655
- Conophthorus*, 233
- Consensus sequence, 456, 464
- Contact activation pathway, 643
 dextran, 648
 extrinsic pathway, 643
 factor V/Va (fVa), 636, 642
 factor VII/VIIa (fVIIa), 643
 factor VIII/VIIIa (fVIIIa), 643
 factor IX/IXa (fIXa), 642, 643
 factor X/Xa (fXa), 642–644, 646, 655, 666
 factor XI/XIa (fXIa), 643, 666
 factor XII/XIIa (fXIIa), 643, 666
 fibrin, 634, 643, 645
 heparin, 643, 648, 655
 intrinsic pathway, 643

- Contact activation pathway (*cont.*)
 phosphatidyl serine, 653
 polyphosphate, 643, 646, 648
 prothrombinase complex, 643
 tenase complex, 643
 TF-fVIIa complex, 642
 thrombin, 642, 643, 647, 653
 tissue-factor (TF), 642
 tissue plasminogen activator (TPA), 643
- Contact chemoreception, 234–236
- Contact phase pathway, 648
- Contact pheromones, 233–236, 240
- Convergent evolution, 531
- Convergent lady beetle, 242
- Copepoda, 626
- Copepods, 91–93, 118–120, 626, 662
- Corpuscular cells, 560, 561, 585
- Cosmophasis bitaeniata*, 239
- Countercurrent flow, 289
- Cowpea trypsin inhibitor, 301
- CPs. *See* Cuticular proteins (CPs)
- Crabs, 626
- Crayfish, 147, 149, 151–154, 156, 626
- CREB-binding, 10
- Cretaceous, 628
- Crosslinking, 330–332, 336, 338–342
 dityrosine, 90, 91, 94, 98, 102, 105, 126
 hydrogen peroxidase, 98
 peroxidase, 98
 trityrosine, 90, 91, 94, 98, 102, 105
- Crustacea, 138, 140–143, 145, 146, 344–346,
 602, 610, 626
- Crustaceans, 91–93, 117, 118
- Cry- δ -endotoxins, 291, 296, 300, 302–305
- Cryptolestes ferrugineus*, 374
- Crystallization
 degree of, 140
 inhibitors, 150
- csp* genes, 611
- Ctenocephalides felis*, 331, 334, 633, 638, 659
- C-terminal, 524, 527, 529, 542, 546
 domain, 451, 454, 458–461
- Cues in herbivory
 damage-associated molecular patterns
 (DAMPs), 612
 disulfooxy fatty acids, 607
 herbivore-associated molecular patterns
 (HAMPs), 612
 microbe-associated molecular patterns
 (MAMPs), 612
 oligogalacturonides (OGAs), 613
 pathogen-associated molecular patterns
 (PAMPs), 612
- Culex*
C. pipiens, 342
C. quinquefasciatus, 298, 633, 639
- Culicidae, 629
- Culicoides*
C. kibunensis, 633
C. nubeculosus, 295
C. sonorensis, 659
C. variipennis, 646, 647
- Culicomorpha, 640, 664
- Culiseta longiareolata*, 241
- Curly*, 79
- Cuticle protein
 CP30, 80
 CPR, 70, 76, 80
- Cuticular egg envelope, 326, 344, 346, 353
- Cuticular hydrocarbons (CHCs), 222–224,
 232–242, 374
- Cuticular plug, 346–348
- Cuticular proteins (CPs)
 ACP, 11, 17
 BmSIGRP, 21
 BR-C, 7, 9–12, 14–16, 19–21
 CPAP, 70
 CPF, 70
 CPF1, 4
 CPF3, 4
 CPF4, 4, 5, 13
 CPG, 4, 5, 17
 CPG11, 5
 CPG12, 5
 CPG24, 5
 CPH, 4, 5, 13
 CPH1, 5
 CPH33, 5
 CPLCA, 4
 CPLCG, 4
 CPLCP, 4
 CPLCW, 4
 cpr72Ec, 74, 76
 Cpr76Bd, 79
 Cpr97Eb, 79
 CPT, 4, 5
 genes
ACP65A, 17, 20
agcp2a, 13
agcp2b, 13
agcp2c, 13
agLCP12.3, 18
BhC4-1, 9
BMCCP4, 11
Bmor CPR46, 18
Bmor CPR53, 15, 20

- Bmor CPR96*, 15, 20
BmorCPR125, 15
BmorCPR21, 9, 16, 20, 21
BmorCPR92, 9, 16, 19
BmorCPR99, 9, 16
BMWCP1, 11
BMWCP2, 11, 16
BMWCP3, 11
BMWCP5, 11, 16
BR-C, 7, 9–12, 14–16, 19–21
DDC, 9
DEG78, 15
DGE84, 15
EDG78E, 9, 20
EDG84A, 9
GCPI, 6
LCP14, 6, 17
LCP16/17, 6, 18
LdGRP1, 21
LdGRP2, 21
LdGRP3, 21
TcCPR27, 5, 6
TcCPR4, 5, 6
 LCP, 11
 PCP, 11
 RR-1, 4–6, 13, 17, 18
 RR-2, 4–6, 13, 15, 17, 18
 RR-3, 4, 13
 TcCpr4, 5, 6, 80
 TcCpr18, 5, 6, 80
 TcCpr27, 5, 6, 80
 TcCP30, 5
 Tweedle, 6, 13
 Cuticular proteins analogous to peritrophins
 (CPAPs), 56
 Cuticulin, 4, 70, 371, 372
 CutProtFam-Pred, 4
Cycloa ginnaga, 495
Cyclosa mulmeinensis, 495, 501
 Cynipids, 617
 CYP4G1, 224, 231
 CYP4G2, 231
 CYP4G2-CPR fusion protein, 231
 CYP4G16, 231
 CYP4G55, 231
 Cystatins, 648
 Cysteine, 452, 453, 458, 468
 Cysteine protease inhibitor E, 304
 Cysteine-rich proteins (CRPs), 451, 457
 Cysteinyl leukotriene, 641, 665
 Cystic, 37
 Cytochrome P450, 373, 390
 Cytochrome P450 reductase (CPR), 230, 231
 Cytokine-induced neutrophil
 chemoattractant, 655
 Cytokines, 642, 655
- D**
Dacus oleae, 327
Dahlia triquetrella, 293
 Damsel flies, 91, 106, 113
Danaus plexippus, 298, 304
Daphnia magna, 343
 DDC. *See* Dopa decarboxylase (DDC)
 De Filippi's glands, 604
 Decapods, 144, 152, 153
 Decarbonylation, 225, 230, 231
 Deer flies, 642, 649
 Defective chorion-1 (*Dec-1*), 337, 341, 343
 Dendritic cells, 642, 648, 654
Dendroctonus, 233
 D. ponderosae, 231
Dendrolimus spectabilis, 522
 Denticle, 75, 80
 Dermanyssid mites, 626
 Dermanyssina, 628
Dermanyssus gallinae, 374
 Dermaptera, 347, 348, 605
Dermestes maculatus, 256, 271, 284
 Dermis, 629–632, 634, 642
desat2, 228
 Desaturase 1 (*desat1*), 228
 Desiccating conditions, 353, 354
 Desiccation, 221, 232, 236
 Desiccation resistance, 354
 Dextran, 648
D. frontalis, 233
 Di- and tri-tyrosine
 bonds, 331, 332
 covalent bonds, 340
 crosslinking, 330–332, 336, 340–342
Diabrotica virgifera virgifera, 305
 Diapsids, 628
 Diatomaceous earths (DE), 372
 Dichloroacetic acid (DCA), 545
 Dichlorodiphenyltrichlorethane (DDT), 291
 Dicondylia, 345
 Digitoxins, 290
 Dimethylaniline monooxygenase (FMO3), 457
 Dimethyldisulfide, 224
 (3R, 11S)-dimethylnonacosane, 222
 Dipetalodipin, 638, 641, 654
Dipetalogaster maxima, 638, 640
 Dipetalopidin, 650
 Diplopoda, 602, 610

- Diplopods, 345
 Diplura, 344, 346, 605
 Dipoles, 478
 Diptera, 333, 347, 517, 626
 Dipteran, 75, 76
 Disagregin, 637, 641
 Disulfide bonds, 521, 523, 529, 545
 Disulfide bridges, 330, 331, 336, 340
 Dityrosine, 78, 79, 94, 98, 331, 342
 Dopa, 342, 351
 Dopa decarboxylase (DDC), 342, 343, 352, 384
 Dopachrome, 78, 81, 342
 Dopachrome conversion enzymes, 339, 343
 Dopamine, 342, 343, 351
 Dopaminechrome, 342
 Dopamine-decarboxylase (Ddc), 78
 Dopamine-monooxygenase (DOMON), 74
 Dopaminequinone, 342
 Dopaquinone, 342
 Dope, 447, 448, 457, 465, 474–478, 480
 Dorso-ventral patterning, 343
 Dragline silk(s), 489, 490, 492–494, 503, 504
 Dragonflies, 90, 99, 101, 103, 104, 108, 110, 111, 113
 Draw rate, 475
 Drosocrystallin, 262, 278, 283, 291, 292
Drosophila
 D. ananassae, 574
 D. atripex, 574
 D. erecta, 574, 575
 D. grimshawi, 335
 D. hydei, 564
 D. mauritiana, 574
 D. melanogaster, 224, 558–590
 D. mojavensis, 574, 575
 D. parabiopectinata, 574
 D. persimilis, 574, 575
 D. pseudoobscura, 564, 574
 D. sechelia, 574, 575
 D. simulans, 574, 575
 D. virilis, 186, 331, 332, 342, 574
 D. willistoni, 574, 575
 D. yakuba, 574, 575
Drosophila melanogaster, 6–13, 15, 17, 20, 39, 45, 46, 49, 50, 54–56, 68, 69, 72–81, 167, 170–175, 177, 178, 180–185, 188, 190–192, 194–196, 199, 202, 203, 224, 225, 227–229, 231, 233, 240, 242, 262, 278, 291, 292, 305, 380, 395–397, 412, 435, 546, 604
 c106, 337
 Cad99C, 329, 330
 Closca, 336
 Crumbs, 329
 fc125, 337
 fc177, 332, 337
 femcoat, 337
 myosin VIIA (Myo7A), 329–330
 nasrat (fs(1)N), 336
 nudel, 343
 palisade, 336, 343
 peroxinectin-like (pxt), 337
 pipe, 343
 polehole (fs(1)ph), 336
 s15, 337
 s16, 337
 s18, 337
 s19, 337
 s36, 336, 337
 s38, 336, 337
 stardust, 329
 sV17, 336, 338, 343
 sV23, 336, 338, 343
 sVM23, 336
 VM26.A.1, 336
 VM26.A.2, 336
 VM32E, 332, 336, 337, 343
 VM34C, 336, 337
 dsRNA, 81, 297, 305–307
 dsRNase, 305
 Dual oxidase (Duox), 79, 341

E
 Ecdysial droplets, 71
 Ecdysis, 5–7, 11, 15, 17, 21, 146
 Ecdysone, 5–13, 15–18, 20, 77, 153, 352, 560, 561, 564
 Ecdysone oxidase genes, 539
 Ecdysone receptor (EcR), 7, 9, 10, 12, 14, 16, 20, 201, 384, 387
 Ecdysone signaling cascade (proteins, genes)
 ACP20, 17
 BR-C, 7, 9–12, 14–16, 19–21
 crq, 12
 DHR3, 7, 8, 14
 dronc, 8, 9, 12, 13, 15
 E74, 7–9, 14
 E74A, 7–9, 14, 18, 20
 E74B, 7, 8
 E75, 7–9, 14
 E75A, 7–10, 12, 14, 20
 E78B, 7
 E93, 7
 ECR, 7
 hid, 12

- HR3, 7–9, 14
 HR4, 7, 9, 14, 18
Rpr, 8, 12
Sgs4, 12
Sox14, 10
 USP, 7, 14, 16
 Ecdysone-inducible elements, 44
 Ecdysone-responsive transcription factors (ERTFs)
 BmBR-C, 12
 Ddc, 13, 15
 Eip28/28, 13
 Fbp1, 13
 hsp 22, 13
 L71-1, 9
 L71-6, 8, 9
 βFTZ-F1, 7–9, 14–20
 Ecdysteroid(s), 199–202, 340, 351, 352
 Echinoderms, 152
 Eclosion, 68
 Eclosion cascade
 bursicon, 396
 corazonin, 396
 crustacean cardioactive peptide (CCAP), 396
 ecdysis, 371, 387, 393, 395, 396
 ecdysis triggering hormone (ETH), 396
 eclosion hormone (EH), 396
 postecdysis, 395
 preecdysis, 395
 preecdysis triggering hormone (PETH), 396
 Ectoparasites, 630
 Ectoperitrophic space, 257, 263, 265, 270, 273, 284, 286, 288–291, 293, 294
 Edema, 630, 641, 648, 650
 Egg case protein-1 (ECP-1), 451, 455, 456, 460
 Egg case protein-2 (ECP-2), 451, 460
 Egg sacs, 449, 450, 459, 460, 462
 Egg water permeability, 353
 Egg-laying, 435
 Eggs, 413, 415, 417, 418, 420–425, 427–430, 432, 434
 Eggshell
 formation, 326, 328, 329, 331, 335, 337, 340, 355
 maternal layers, 344
 post-zygotic layers, 326
 radial organization, 327, 328
 structure, 326, 327, 342
 wax, 331
 Ejaculatory bulb (EB), 418, 423–424
 Ejaculatory duct, 417–419, 424–425
 Elastase, 651, 652, 655, 656
 Elastase inhibitors, 655
 Elastic energy storage, 111–114, 128
 Elastic modulus, 144, 457, 479
 Elastic recoil, 93, 94, 96–98, 112, 114
 Elasticity, 91, 93, 96, 97, 99, 100, 104, 105, 118, 121, 127, 128
 Elastin, 464, 466, 631
 Elastomeric proteins, 90, 93, 95, 96, 98, 105, 128
 Electric fields, 477
 Electrified fluid jet, 477
 Electron microscopy, 394
 SEM, 579
 TEM, 578, 579
 Electrophoretic mobility shift assay (EMSA), 16, 456
 Electrostatic interactions, 262, 265, 274, 288
Ellychnia corrusca, 233
eloF, 229
 Elongases, 228–229
 Elongation, 224–226, 228–229
 Elongation factor 1-alpha, 456
 Elongational flow, 465, 478
Elovl, 352
 Elytral cuticle, 79
 Embiidina, 605
 Embioptera, 347, 516
 Embryo, 72, 79–81, 412, 427, 430, 434, 435
 Embryogenesis, 326, 328, 338, 344, 346, 349, 352, 353
 Embryonic cuticle, 349
 Enamel (like), 149
 Encapsulation, 169
 ENCODE, 9
 Endochorion
 inner part (floor), 332
 outer part (roof), 332
 pillars, 329, 332, 337, 339
 Endocuticle, 5, 18, 69, 71, 79, 138, 139, 143, 144, 146, 156, 348–354, 374, 375, 394
 Endocytosis, 577, 578, 584
 Endonuclease, 654, 661, 664
 Endoparasites, 625
 Endoperitrophic space, 265, 266, 273, 284, 286–288, 290
 Endoplasmic reticulum, 78, 579
 Endopterygota, 603, 607–610
 Endosomal traffick, 562, 577, 584–585
 Endosulfan, 76
 Endothelial cell proliferation, 634, 650

- Enhancins, 278, 296, 297, 304, 305
 Entognatha, 344–346
 Entomopathogenic bacteria, 291, 292
 Entomopathogenic fungi (EF), 372–374
 Entomopathogenic viruses, 296, 304
 Entomopoxviruses (EPVs), 298
 Envelope, 68, 69, 71–73, 79, 81, 82
 Environmental factors
 aging, 498
 ambient temperature, 496–497
 humidity, 497
 solar radiation, 495, 504
 ultraviolet radiation, 498
 wind, 495–496
 Enzyme recycling, 289
 Eosinophil chemotactic factor, 655
 Eosinophils, 654
 Epembryonic membrane, 349, 351, 354
 Ephemeroptera, 347
Ephestia kuehniella, 301
 Epicuticle, 68–73, 79, 81, 82, 138, 139, 152,
 348–351, 353–355, 371–372, 374
 Epicuticular wax, 221
 Epidermis, 629, 630, 650
 Epinephrine, 641, 642, 653
 Equivalent Chain Length, 223
Erigone atra, 496
 Eriophyoid mites, 611, 617
 Erythema, 650
Escherichia coli, 468–470
 ESI-MS/MS, 581
 Etoxazole, 41, 387–389
 Eukaryotes, 589
Eurytoma amygdali, 333, 342
Eusimilium latipes, 633
 Evolution
 of blood-feeding, 626, 627, 640, 649,
 661, 662
 of *Drosophila* salivary glue secretions
 (Sgs), 574–576
 Exochorion, 326, 328, 329, 332, 333, 337, 339
 Exocuticle, 5, 18, 69–71, 79, 138, 139, 143,
 144, 146, 156, 371, 394–395
 Exocytosis, 560, 562, 563, 565, 566, 572, 573,
 576–578, 583, 586, 589, 590
 Exoskeleton, 68, 370, 372, 374, 375, 378,
 392–393, 396
 Expansion (Exp), 75
 Expectoration, 566, 573, 577, 590
 Extensibility, 495, 497–500
 Extracellular composite matrix (ECM), 78, 82
 Extracellular matrix, 68, 76, 77, 79, 81, 626
 Extracellular space, 72, 73, 75–78, 80
 Extradinticle (Exd), 536
 Extraembryonic
 cells, 328
 region, 344, 346
 Extrinsic pathway, 643
F
 Fasciclin, 456
 Fascin, 73
 FASTA, 574, 575
 Fatty acid synthase (FAS), 224–228, 231
 Fatty acyl-CoA reductases, 228, 230
 Feeding strategy
 chewing, 602
 piercing, 603
 Feline interferon (FeIFN), 547
 Female accessory glands, 417, 418, 431–432
 Fertilization, 412, 414, 417, 425, 427–429,
 432, 434, 435
 Fibers, 446, 447, 449–452, 454–457, 459–467,
 473–481
 Fibrilization
 at spinneret, 529, 533
 Fibrillin, 631
 Fibrin, 643, 645
 Fibrin(ogen)lytic enzyme, 633, 648
 Fibrinogen, 634, 636, 641–643, 647
 Fibrinolysis
 α 2-antiplasmin, 643
 α 2-macroglobulin, 643
 carboxypeptidase B, 643, 648
 fibrin(ogen)lytic, 633
 fXIa, 643
 fXIIa, 643
 kallikrein, 643, 648
 plasmin, 643, 648
 tissue plasminogen activator, 643
 urokinase, 643
 Fibroblasts, 631, 642
 Fibrohexamerin, 520–522, 537
 Fibroin, 446, 447, 459, 460, 465, 467, 471, 474
 heavy chain (H-fibroin), 520
 light chain (L-fibroin), 520–523
 modulator-binding protein-1 (FMBP-1),
 537, 539
 Fibronectin, 631, 634, 650
 Fibronectin-derived cell-adhesive
 sequence, 547
Ficus virgata, 304
 Flagelliform, 447, 449–451, 459, 462–463,
 466
 Fleas, 626, 629, 640, 659, 662, 664
 Flexibility, 91, 93, 95, 96, 99, 100, 104, 113,
 115, 118, 128

- Fluorapatite, 147–149
 Fluorescein isothiocyanate
 (FITC)-dextrans, 265
 Follicular epithelium cells, 329
 Forensic entomology, 232, 240
Forficula auricularia, 270
 Forkhead (Fkh), 536, 537
 Formic acid, 475
Formica exsecta, 237
Frankliniella occidentalis, 606
 Frog biting midges, 633, 634, 654, 659, 664
 Fructose-6-phosphate, 260, 306
 FS1 antigen, 664
 Fused lobes, 55
 Fushi tarazu transcription factor1 (FTZ-F1),
 384, 386
- G**
- Galanthus nivalis* agglutinin (GNA), 300, 301
Galleria mellonella, 520, 521, 526, 529,
 532, 534
 GAL4/UAS, 547
 Gametes, 412, 414, 415, 418, 425, 433–435
 Garnystan (Gny), 77
 Gas chromatography-mass spectrometry
 (GC-MS), 222, 234
 Gas exchange, 326, 332–334
 Gasp, 74, 76
 Gastric ceaca, 270
 Gastroliths, 145, 152–154
 GATA β , 340
 GC-MS. *See* Gas chromatography-mass
 spectrometry (GC-MS)
 Gelsolin, 272
 Gene amplification, 335, 337
 Gene Ontology (GO), 456
 Gene silencing, 327, 349, 351, 355
 Genital imaginal disc, 416
 Genome editing, 547, 548
 Geometridae, 241
 German cockroach, 222, 224, 227, 236
 Germline, 10
 Germline transformation, 546, 547
 GFP. *See* Green fluorescent protein (GFP)
 GGG family, 14
 Gilson's glands, 517
 GlcNAc, 75
Glilocladium sp. FTD-0668, 393
Glossina spp., 240
 G. fuscipes, 633
 G. morsitans morsitans, 646, 661
Glossinia morsitans morsitans, 265, 278, 300
 Glossinidae, 629
 Glucocorticoid, 10
 Glucosamine-6-phosphate
 N-acetyltransferase, 37
 Glucose-6-phosphate isomerase, 37
 Glue, 560, 562, 563, 565–567, 573,
 575–577, 590
 Glutamine, 495, 500
 Glutamine-fructose-6-phosphate, 37
 Glutamine-fructose-6-phosphate
 aminotransferase (GFAT), 37
 Glycine, 493, 495, 498–500
 Glycocalyx, 256, 286, 293, 300
 Glycomoieties
 N-glycosylation, 570
 O-glycosylation, 570
 Glycoprotein, 496, 497
 Glycosaminoglycans (GAGs), 265
O-glycosylation, 263, 264, 266, 283
 Glycosyltransferase, 74, 75, 82
 Glycosyltransferase-2 (GT-2), 40
Gnatocerus cornutus, 241
 Granular phenoloxidase (GPO), 187, 202
 Granule(s)
 densification, 572
 maturation, 564
 secretory, 559–561, 563–567, 573, 575, 586
 Granuloviruses, 303
 Green fluorescent protein (GFP), 474, 566,
 581, 582, 587
 Growth-blocking peptide (GBP), 202
 Grylloblattodea, 347
Gryllus bimaculatus, 333
 Guanidinium isothiocyanate (GdmSCN), 475
 Gumfoot lines, 447, 449, 451, 462, 463
- H**
- Haem, 78
Haemaphysalis longicornis, 37, 633, 637, 644,
 645, 657
 Hemolymph, 71, 77
 Hamadarin, 646, 649
Hanseniella agilis, 345
 Harvestmen, 626
 Hatching lines, 335
 Heavy chain promoter, 474
 HeLa cells, 480
Heliconius melpomene, 609
Helicoverpa
 H. armigera, 383, 394, 604, 608
 H. zea, 40, 276, 304
Heliothis virescens, 269, 293, 301, 303, 340,
 382, 392
 Hematoma, 629–634, 639, 650
 Hematophagy, 625, 639, 656, 661, 663, 664
 Heme protein, 341

- Hemiptera, 347, 626
 Hemipteroid assemblage, 605–607
 Hemolymph proteins
 apolipoporphins, 607, 617
 arylphorins, 607
 methionine-rich storage proteins, 607
 Hemozoin, 258, 292
n-heneicosane, 241
 9-Hentriacontene, 238
 Heparin, 642, 643, 648, 655
 Hepialoidea, 541
 7,11-Heptacosadiene, 233
 (*Z*, *Z*)-6,9-Heptacosadiene, 224
 (*Z*)-9-Heptacosene, 235
 Heteroptera, 663
 Hexafluoroisopropyl alcohol, 545
 Hexafluoro-2-propanol (HFIP), 474, 475,
 477, 478
 Hexapoda, 138, 141, 344, 602, 603, 605–611,
 626, 627
 Hexokinase, 37
 Hexythiazox, 389
 High-molecular weight kininogen, 643
 Hippoboscidae, 629
 Histamine, 641, 651, 653, 655, 665
 Histolysis, 561, 562, 583
 Histone methyltransferase, 10
 HISC-1, 648
 Holometabolous insects, 11
Homalodisca vitripennis, 606
Homarus americanus, 142, 144, 168
 Homologous recombination, 471
 Homothorax (Hth), 536
 Hooded tick spiders, 626
 Hormone receptor 3 (HR3), 384, 386
 Hornets, 516, 540, 543–546
 Horse flies, 629, 633, 640, 649, 654
 Horseshoe crabs, 626
 Host defense responses, 650
 Host dermis, 630, 632
 HR3/IE1, 547
 Human louse, 633
 Hyaluronic acid, 631, 632
 Hyaluronidase, 626, 632–634
Hybomitra bimaculata, 647, 649
 Hydrogen bonds, 493, 496, 503
 Hydrogen peroxide, 332, 341
 Hydrolytic enzymes, 258, 273, 283, 304, 306
 Hydrophobicity, 525
Hydropsyche angustipennis, 526, 541
 Hydrostatic interactions, 267
 Hydroxyapatite, 155
m-Hydroxybenzylhydrazine (HBHZ), 177
 20-hydroxyecdysone (20E), 340, 381, 384,
 386, 395, 396
 15-hydroxyicosatetraenoic acid, 650
 Hymenoptera, 516, 517, 542, 544
 Hyperemia, 650
 Hypodermis, 630
 Hypostome, 629, 630
Hypotheneumus hampei, 615
- I**
 Iblidae, 149
 Imaginal disc growth factors, 50
 Immobilized metal ion affinity
 chromatography, 473
 Immune response, 412, 419, 427, 429
Inachis io, 202
 Inclusion bodies, 471
 Infestins, 663
 Inflammatory inhibitors
 Ixodes ricinus immunosuppressant, 655
 Ixodes ricinus leukotriene binding protein
 (Ir-LBP), 651, 654
 Ornithodoros moubata complement
 inhibitor (OMCI), 666
 TdPI, 656
 tryptogalinin, 656
 Inflammatory phase, 631, 648
 Inflammatory responses
 autoimmunity, 648
 basophils, 655
 β -tryptase, 655
 carrageenan-induced rat paw edema
 model, 648
 connective tissue-activating peptide-III
 (CTAP-III), 655
 cysteinyl leukotriene, 641, 665
 cytokine-induced neutrophil
 chemoattractant, 655
 cytokines, 655
 dendritic cells, 654
 edema, 630, 648
 endonuclease, 654, 664
 eosinophil chemotactic factor, 655
 eosinophils, 654
 erythema, 650
 histamine, 641, 655, 665
 insulin-like growth factor 1, 636
 interferon- γ , 655
 interleukin-1, 636
 interleukin-6, 655
 interleukin-8, 655
 itching, 630
 leukotriene A4, 641
 leukotriene B4, 649, 654
 leukotriene C4 (LTC4), 641
 leukotriene E4 (LTE4), 641

- macrophage inflammatory protein (MIP-1 α), 636
- macrophage inflammatory protein-2 (MIP-2), 655
- macrophages, 654, 655
- mast cells, 654, 655
- monocytes, 654, 655
- neutrophil extracellular traps (NETs), 654
- neutrophils, 654, 655
- platelet factor 4, 636
- platelet-derived growth factor (PDGF), 636
- prostaglandin D2 (PGD2), 655
- RANTES, 636
- swelling, 630
- T-cell proliferation, 648
- Infrastructural elements, 564
- Inner epicuticle*, 69
- Innermost chorionic layer, 328, 329
- Inorganic–organic composite, 140
- Inositol polyphosphate 5 phosphatase, 664
- Insect cuticle
 - apical plasma membrane protrusions, 167, 197
 - chitin, 166, 167, 196, 204
 - elytron, 167, 183, 196, 197, 204
 - endocuticular layers, 166, 167
 - envelope, 166, 167
 - epicuticle, 166, 167
 - exocuticular layer, 166, 167
 - exoskeleton, 166, 168, 197, 200, 204
 - pore canal fibers, 167, 168, 197
 - procuticle, 166, 167, 187, 197
 - sclerotization, 166–205
 - tanning, 168–197, 200–204
 - trabeculae, 183, 204
- Insect growth regulators (IGRs), 375, 395
- Insecta, 344, 348, 602, 626
- insulin-like growth factor 1, 636
- Integripalpia, 540, 541
- Integument, 370, 374, 384
- Intermolt stage, 15, 18
- Internal factors
 - glandular proteins, 494, 495
 - phase conversion, 495
 - reeling speed, 493, 494, 504
 - spinning dope, 494, 501
 - spinning duct, 494, 499, 501, 502
- Intraperitrophic space, 286, 288
- Ions, 501–502
- Ips lecontei*, 234
- Iris, 651, 655
- IRS2, 655
- IRS-2, 637, 651, 666
- Isac, 651, 653
- Isaria fumosorosea*, 373
- Isoleucine (Ile), 225, 226, 543
- Isopoda, 611
- Isopods, 626, 662
- Isopropyl- β -D-1-thiogalactopyranoside, 471
- Isoptera, 347
- Itching, 630
- Ixodegrin, 637, 642
- Ixodes*, 630
 - I. ricinus*, 637, 644, 651, 655, 657
 - I. scapularis*, 611, 634, 637, 644, 648, 651, 652, 657
- Ixodida, 626
- J**
- Jalysus spinosus*, 355
- Japanese spider crab, 138
- JH. *See* Juvenile hormone (JH)
- Junonia orithya*, 199
- Jurassic, 628
- Juvenile hormone (JH), 8, 11, 12, 198–202, 340, 414, 415, 420, 422
- Juvenile hormone esterase, 539
- K**
- Kairomones, 232, 241
- Kallikrein, 643, 645, 648
- Kazal, 639, 647, 649, 660, 663
- Kininogen, 643
- Kininogenase, 648
- Kissing bug, 68, 70, 633
- Knickkopf (Knk), 74, 75
- Knickkopf (KNK), 56, 276, 352
- Kosmotropic salts, 479
- Kovats index, 223
- Kratagonists
 - biogenic amine binding proteins, 641
 - D7L1, 654
 - D7 proteins, 641, 664, 665
 - D7r1, 646, 666
 - dipetalopidin, 650
 - nitrophorin, 641, 649, 653
 - nitrophorin 2, 665
 - tablysin-15, 639, 641, 666
 - TSGP2, 637, 654
 - TSGP3, 641, 654
- Krill, 626
- Krotzkopf verkehrt (Kkv), 74
- Kunitz/BPTI, 655, 663
- Kyte and Doolittle hydropathy profile, 458

L

Labramin, 301
Lacanobia oleracea, 301–303
 Laccase, 339, 343
 Laccase2 (Lac2), 80, 342, 352, 354
 Lacewings, 542, 545, 626
 Lacinae, 629
 LacZ, 579, 582, 587
 Lamella, 349
 Laminae, 69, 73
 Laminins, 631
Laodelphax striatellus, 390
Lariophagus distinguendus, 235
 Larval hatching, 333, 335
Lasius niger, 239
Latrodectus hesperus, 446
 Leafroller, 68
 Lectins, 258, 284, 290, 292, 299–302, 456
Leishmania parasite, 295
Lepidocampa weberi, 347
 Lepidoptera, 333, 347, 348, 445, 516, 517, 522, 528, 529, 532, 533, 540, 541, 602, 603, 607, 610, 626
 Lepidopteran, 71, 72
Lepisma saccharina, 347
Leptestheria dahalacensis, 270
Leptinotarsa decemlineata, 21, 37, 38, 302
Leptothorax nylanderi, 237
 L-fibroin, 520–523, 525, 529, 537, 539, 541, 542, 546, 547
 Lice, 626, 628, 629, 662
 LIM domain-binding protein (Ldb), 537
 Limb(s), 464, 465
Limnephilus decipiens, 541
 Lineage specific expansion, 656, 661, 663
Linepithema humile, 237
 Lipid, 68–71, 78, 82, 331
 Lipocalins, 640, 641, 653, 654, 661–664, 666
 Lipophorin, 224
 15-lipoxygenase pathway, 650
 Lithium bromide (LiBr), 474, 477, 545
 locomotion, 474
 Lobsters, 626
Locusta migratoria, 37, 38, 54, 82, 182, 199, 268, 351, 607
 Longhorned beetles, 233, 234, 236
 Louse flies, 629
Lucilia cuprina, 261, 262, 264, 269, 272, 278, 284, 335, 376, 393
 Lumen, 464, 558, 559, 561, 563, 565–567, 573, 577–581, 583, 585, 586
Lutzomyia
 L. longipalpis, 633, 660
 L. migonei, 653

Lygus

L. hesperus, 604, 606, 613
 L. lineolaris, 331
Lymantria dispar, 279
 Lymantriidae, 241

M

Macrophage inflammatory protein-2, 655
 Macrophages, 631, 641, 652, 654, 655
Maculinea rebeli, 239
Magivicada, 67, 68
 Major ampullate silk proteins
 MaSp1, 498–503
 MaSp2, 498–500
 Major ampullate spidroin (MaSp)
 major ampullate spidroin 1 (MaSp1), 451, 452, 454–456, 458–460, 465, 468–471, 474, 480
 major ampullate spidroin 2 (MaSp2), 451, 452, 454–456, 458–460, 468, 469
 Major ampullate spidroin 1 (MaSp1), 471, 473
 Major royal jelly proteins (MRJPs), 190, 193
 Malacostraca, 149, 626
 Malaria parasite, 294, 295
 MALDI-TOF/TOF, 581
 Male accessory glands
 main cells, 417, 419, 420, 422
 secondary cells, 417, 419, 422
 Malpighian layer, 630
Mamestra
 M. brassicae, 391
 M. configurata, 45, 46, 266, 269, 279, 288, 297, 298
 Mammals, 626, 628, 635
 Mandibles, 142, 143, 149, 151, 156, 629
 Mandibulata, 344
Manduca quinque maculata, 199
Manduca sexta, 6–8, 12, 17, 18, 21, 72, 171, 176, 186–188, 199, 201, 202, 260, 269, 271, 272, 298, 301, 327, 334, 348, 354, 382, 384, 386, 395, 615
 Mantis shrimp, 149, 151
 Mantises, 542, 545
 Mantodea, 542
 MARCOIL, 544
 MaSp. *See* Major ampullate spidroin (MaSp)
 Mass extinction, 656
 Mass spectrometry, 70
 Massively parallel signature sequencing (MPSS), 456
 Mast cells, 641, 643, 654–656
 Mate recognition signals, 232
 Mating plug, 417, 419, 422, 423, 425

- Mats, 478
 Maxadilan, 647, 649
 Maxillae, 629
 Maximal draw ratio, 546
 Maximal tensile strength, 546
Mayetiola destructor, 603, 612
 Mechanical properties, 446, 447, 457, 460, 466, 473, 474, 476–478, 480, 489–505
 Meconium, 293
 Mecoptera, 609
Megacyllene
 M. caryae, 233, 234
 M. robinae, 233
 Melanisation
 N-acetyldopamine (NADA), 394
 N- β -alanyldopamine (NBAD), 394, 395
 Melanization, 340–343, 348, 351, 352
 Melanization and reddish coloration hormone (MRCH), 202
Melanoplus differentialis, 351
 Melatonin, 181, 182
Melipona quadrifasciata anthidioides, 610
Mesobuthus tamulus, 302
 Mesostigmata, 626, 628
Messor barbarus, 237
 Metallo dipeptidyl carboxypeptidase, 648, 652
 Metalloprotease, 626, 631–633, 645, 648, 657, 658, 663
Metarhizium anisopliae, 373, 393
 Methanol, 476
 Methionine, 226
 Methoxymercuration-demercuration, 224
 2-Methylalkanes, 223–225, 227
 Methyl-branched alkanes, 222, 233
 7-Methylheptacosane, 233
 (S)-11-Methylheptacosane, 235
 Methylmalonyl-CoA, 226, 227
 3-Methylpentacosane, 225, 226, 228
 (8Z,21S)-21-methyl-8-pentatriacontene, 236
 Micelles, 465
 Microapocrine secretion, 268, 270–272
 Microfibril, 73, 76
 Microfibrillar textures, 267
 Microfluidic devices, 474, 475, 477–478
 Micropylar canal, 333
 Micropyles, 332–335
 Microsurgery, 480
 Microvillar membrane
 α -mannosidase, 258
 β -glycosidase, 258
 Microvilli, 71, 73, 329, 330
 Microwhip scorpions, 626
 Middle silk gland secretory epithelium (MSG), 517, 547
 Midgut, 12, 76
 Millipedes, 626
 Mineral – organic composites, 138
 Mineralization, 139–145, 147, 149–154
 degree of, 140, 142–145
 Mineralized exoskeletons, 138–156
 Minor ampullate spidroin (MiSp), 451, 455, 458, 473
 Miocene, 628
 Mir-1 protein, 304
 MiSp1, 458
 Mites, 626, 628, 662
 MMTV promoter, 10
 Molecular orientation, 494, 497
 Mollusca, 148
 Molting, 138, 145, 153
 Monoclonal antibodies (mAbs), 547
 Monocytes, 631, 655
 Monogrins, 637, 641
 Monooxygenase, 456, 457
 Mosquitoes, 629, 633, 634, 636, 639–641, 643, 645, 659, 664
 Moths, 626, 628, 662
 Moubatin, 637, 640, 651, 654
 Moulting, 68, 70–72, 80, 81
 Mucin, 264–266, 280, 283, 285, 286, 296, 297, 304, 305, 575, 576
 Mucin domains, 33, 49, 264, 266, 277–279, 281, 299
 Mucus, 256, 264
 Multicapsid nucleopolyhedrovirus, 297, 303
Mummy, 37
Musca domestica, 180, 203, 231, 234, 294
 Mustard leaf beetle, 240
 Myeloperoxidase, 649
 Myosin 7a, 272
 Myriapoda, 138, 344–346, 626
Myriophyllum spicatum, 617
 Myristic, 228
 Myristoleic, 228
 Myrmecophilous salticid spider, 239
Myrmica schencki, 239
Mythimna separata, 389, 391, 393
Myzus persicae, 387, 393

N
N-acetyldopamine (NADA), 77, 342, 351
N-acetylglucosamine, 32, 37, 38, 41, 51, 53, 55, 71, 260, 265, 300, 374, 378, 379
N-acetylglucosaminidases, 295
 crystal structure, 53
 expression, 55
 gene family, 53, 56
 Nanocomposites, 140, 146, 152, 156

- Nanocrystals, 466, 477
 Nanofibers, 477, 478
 Nanoparticles, 459, 479
 Nanospring, 462
Nasonia jewel wasps, 233
Nasonia vitripennis, 180, 190, 194, 298
 Natural fiber, 489
 N- β -alanyldopamine (NBAD), 77, 342
 Necrophagous flies, 240
 Nematocera, 626, 664
Nemophora albi antennella, 353
Neocardina denticulate, 153
Neoclytus a. acuminatus, 233, 236
 Neoptera, 604, 605
Nephila
 N. antipodiana, 473
 N. clavata, 498
 N. clavipes, 454, 458–460, 463, 464
 N. edulis, 496
 N. inaurata, 457, 497
 N. pilipes, 493, 500
 N. senegalensis, 461
Nephotettix
 N. cincticeps, 606
 N. virescens, 390
 Nestmate recognition, 232, 237, 240
 Neuromodulators, 414, 432, 433
 Neuroptera, 516, 542
 Neutrophil, 631, 641, 643, 650, 651, 654, 655
 Neutrophil extracellular traps (NETs),
 643, 654
Nezara viridula, 241
 N-glycosylation, 298, 547
Nicotiana attenuata, 304
 Nikkomycin Z, 391
Nilaparvata lugens, 38, 46, 53, 54, 390, 606
 Nitidulidae, 242
 Nitric oxide, 641, 649
 Nitrophorins, 641, 649, 653, 664
 Noctuidae, 241
NodC, 41, 43
 (Z)-9-Nonacosene, 234
 Non-polyalanine block (NPAB),
 523–525, 528
 Nonsynonymous site/synonymous site, 538
 Norepinephrine, 641, 647, 649
 N-terminal domain (NTD), 451–453, 458,
 460, 465, 467, 468, 471, 479
 N-terminal sequencing, 532
 Nuclear magnetic resonance (NMR), 451,
 457–459, 477
 Nucleosome remodeling factor (NURF), 10
 Nutrient intake, 500–501
 Nuttalliellidae, 630, 663
- O**
 Obst-C, 74, 76
 Obstructor, 56, 152
 Obstructor-A (ObstA), 75
 Ocean acidification, 141
 Octopamine, 414, 433
Ocypus olens, 353
Odagmia ornata, 633
 Odorant binding proteins (OBPs), 339, 641, 664
Oecophylla smaragdina, 239
 Oenocytes, 224, 225, 228, 231, 372
 Oligocene, 628
Oncopeltus fasciatus, 171, 172, 174, 176, 178,
 348, 663
 Ontological, 582, 588, 590
 Oocyte, 412, 414, 417, 418, 425, 434
 Oogenesis, 328–330, 341, 349, 414
 Ootheca, 339, 355
 Operculum, 333, 335
 Orange pupa inducing factor orange pupa
 inducing factor (OPIF), 202
 Orb-weavers, 450, 458, 460–463
 Ordovician, 149
 Organellar, 582, 588, 589
 Organelles, 587
Ornithodoros
 O. moubata, 637, 644, 645, 651, 652
 O. savignyi, 632, 637, 644, 645, 651
Orthezia urticae, 334
 Orthologues, 574, 575
 Orthoptera, 347, 348, 607
Oryctes nasicornis, 270
Oryzaephilus surinamensis, 374
 Osteonectin, 631
Ostrinia
 O. furnacalis, 40, 44, 49, 53–55
 O. nubilalis, 240, 269, 275, 276, 290, 300,
 301, 304, 394
 Outer epicuticle, 69, 71
 Ovary, 335, 337, 339, 341, 355
 Oviductal fluid, 417, 426, 434
 Oviducts, 414, 417, 418, 420, 425–428,
 432–434
 Oviposition, 326, 332, 341, 342
 Ovulation, 414, 417, 418, 420, 421, 430,
 432–435
 Ovulin, 414, 420–422, 425, 433–435
 Oxidative decarboxylases, 231
 Oxidoreductases, 456
- P**
P. aenescens, 233
 Pain, 630, 648–649

- Pallidipin, 638, 641
Panarthropoda, 140
Pancrustacea, 138, 344
Panoistic ovaries, 335, 339, 355
Panonychus citri, 389
Panstrongylus megistus, 653, 660
Papilio
P. glaucus, 172, 173, 177
P. machaon, 177, 180, 194
P. polytes, 173, 177, 185, 194
P. xuthus, 171–177, 180, 185, 186, 190, 191, 193, 195, 198, 200–202, 522
Paragonia, 418
Parasites, 625, 662
Parental care, 326, 344
Parovaria, 417, 418, 427, 430–432
Particles, 476, 479–480
Pauropoda, 602, 611
Pauropods, 345
Pauropus silvaticus, 346
PCD. See Programmed cell death (PCD)
Pectinophora gossypiella, 302
Pedetontus unimaculatus, 348
Pediculus humanus, 633
P element, 546
Penaes semisulcatus, 343
Penetration (of sperms), 333
Pentastomida, 610, 626
Pentatomorpha, 663
Pentoxifyllin, 393
Peptidases, 456
Perimicrovillar compartment, 71
Perimicrovillar membrane
acidic phosphatase, 258
 α -glucosidase, 258, 288, 292
in blood-sucking bugs, 257, 258
in planthoppers, 257
in *Rhodnius prolyxus*, 258
in *Rickettsia prowazeki*, 259
in thrips, 258
Periodic acid-Schiff (PAS), 560
Periplaneta americana, 182, 199, 269, 274, 304
Peritrophic envelope, 268, 270
Peritrophic matrix, 32, 33, 36, 37, 47
chitin content, 260, 276
chitin degradation, 294–296
chitin nanofibers, 260, 261, 268, 270, 271, 276, 277, 279, 307
cross-hatch texture, 275
crosslinking by phenoloxidase, 262, 274, 282
crosslinking by transglutaminase, 262
delamination, 267–271, 283
effects of altered ion concentrations, 284, 287
effects of altered pH, 265
exclusion size, 265, 273, 276, 278, 280, 283, 284, 287–289, 291, 293
meconial, 293
permeability, 259, 263–266, 272–280, 283–288, 291, 296–298, 300, 301, 303, 304, 306
pore size, 272, 274, 275, 277, 279, 283, 284, 286, 292, 299
protein content, 276
semipermeable, 265, 277, 285
structure-function relations, 260, 273–277, 279–285, 307
thickness, 272, 273, 275, 276, 280, 284, 287, 288, 306
turgor pressure type I, 267–272, 288, 293
type II, 267, 269–272, 293
water-filled channels, 267
Peritrophic matrix associated proteins
class I proteins, 261
class II proteins, 261
class III proteins, 262
class IV proteins, 262
loosely associated proteins, 261, 262
secretion, 256, 262, 263, 268, 269, 271–273
tightly associated proteins, 262, 263, 278, 279
Peritrophic matrix function
barrier against pathogens and parasites, 285
heme detoxification, 258, 292
immobilization of digestive enzymes, 288
mechanical protection, 285
neutralization of toxins, 285
partitioning of digestion, 285
radical-scavenging antioxidant, 290
regulation of innate immunity, 285
resistance to osmotic swelling, 285
tannin detoxification, 290, 292
Peritrophic matrix proteins
chitin binding domains, 262, 277, 300
encoding genes, 262, 298
invertebrate intestinal mucins (IIMs), 264
mucin-like proteins, 305
non-mucin-like proteins, 263, 264
number of CBDs, 263, 275–278, 281–283, 299
Ser/Thr-rich linker domains, 263, 264
with multiple chitin binding domains, 271
with several chitin binding domains, 282
with single chitin binding domain, 283
Peritrophic membrane (PM), 391, 392, 394
Peritrophin(s), 56, 57, 263, 264, 343, 353
Peritrophin-A domain, 263
Peroxidase, 331, 332, 336, 339, 341–343, 647, 649

- Peroxiredoxins, 612
 pH, 494, 498, 499, 501–502, 504
Phaseolus vulgaris, 615
 Phasmatodea, 347
 Phasmida, 605
Pheadon cochleariae, 240
 Phenoloxidase, 332, 339, 342, 343
 Pheromones, 423, 424, 432
Phlebotomus
 P. duboscqi, 633, 648, 660
 P. halepensis, 633
 P. papatasi, 295, 302, 633, 638, 639, 647,
 655, 660
 P. perniciosus, 633
 P. sergenti, 633
 Phosphatidyl serine, 653
 Phosphatocopines, 149
 Phosphoamino acids, 154
 Phosphogenic events, 149
 Phosphoglucosamine mutase, 37
 Phospholipase C, 639, 655
 Phosphoproteins, 150
 Phosphorylated serine residues, 542
 Phosphothreonine, 155
 Phthiraptera, 626, 629
Phyllotreta flea beetles, 241
 Phylogenetic, 590
 Phylogenetic tree and phylogenetic analysis,
 45, 49, 54, 179, 191, 395
 Phylogeny, 345
Phymatopus californicus, 520, 541
 Phyre2 server, 639
Pichia pastoris, 468, 470
piggyBac transposon, 546
 Pigment
 ABC transporters, 166
 antraquinones, 166
 aphins, 166
 carotenoids, 166
 flavonoids/anthocyanins, 166
 3-hydroxykynurenine, 166
 melanins, 166, 169, 173, 177, 178, 181,
 186, 187, 190, 191, 195, 199–202
 melanogenesis, 166, 199
 ommochromes, 166
 papiliochromes, 166, 185
 pterins, 166, 170
 tertapyrroles, 166
 Plant inhibitors
 α -amylase inhibitors, 614
 polygalacturonase-inhibiting proteins
 (PGIPs), 613, 614
 Plaque, 71, 72
 Plasmin, 637, 643, 648, 656, 666
 Plasminogen, 633, 643, 645, 648
Plasmodium
 P. falciparum, 294, 295
 P. gallinaceum, 294, 295
 P. vivax, 295
 Plasticization, 70
 Plastron, 334, 335
 Platelet activating factor (PAF), 655
 Platelet activation, 635, 636, 650, 653, 654
 Platelet aggregation, 631, 635–643, 649, 650,
 653–655
 Platelet factor 4, 636
 Platelet receptor cC1qR, 653
 Platelet-derived growth factor, 636
 Plecoptera, 347
Plodia interpunctella, 520, 526
Plutella xylostella, 295, 387
P. maculicollis, 233
Pogonomyrmex barbatus, 238
Polistes
 P. dominulus, 239
 P. semenowi, 239
 Pollinators, 625
 Polyadenylation, 456
 Polyalanine block (PAB), 523–525
 Polyene hydrocarbons, 241
 Polyethylene glycol (PEG), 476
 Polymerization, 502
 Polymers, 470
 Polyoxins, 390, 391
Polyphagotarsonemus latus, 389
 Polyphosphate, 643, 646, 648
 Polyploid, 517
 Polysaccharide, 68
 Polytene chromosome, 560, 584
 Polytrophic meroistic ovaries, 335
 PONDR, 567, 572
 Pore canals, 138
 Posterior silk gland, 517, 536, 537, 546
 Post-mating responses, 420, 422–424
 Postpharyngeal glands, 237
 Post-spin draw, 476–477
 Posttranslational modification, 570, 587
 POU-M1, 536, 537
 Prawns, 149
 Precambrian-Cambrian boundary, 149
 Predators, 354, 625, 662
 Prekallikrein, 643, 649
 Prepupa, 539, 562, 573, 581
 Prepupal, 5, 7, 10–12, 17–21
 Proboscis, 629
Procambarus clarkii, 153
 Procuticle, 4, 5, 68, 69, 71–74, 76, 78–82,
 348, 349
 Programmed cell death (PCD), 561, 562, 576,
 583, 584

- Proliferative phase, 631, 634
 Properdin, 653
 Propionate, 224–226
 Pro-resilin, 90, 94, 98, 99, 101
 Prostaglandin, 649, 655
 Proteases, 415, 421, 422, 431, 456, 479, 626,
 633–634, 654, 655
 Proteomics, 480
 Prothorax, 517
 Prothrombinase complex, 642
 Protura, 344, 346, 347
 Proventriculus, 269, 278
Psacotheta hilaris, 236
 Psammaplin, 393
 P-selectin, 636, 642, 653
Pseudaletia
 P. separata, 171, 172, 176, 177, 180, 202
 P. unipuncta, 296
Pseudococcus sp., 390
 Pseudoscorpions, 626
 PsiPred, 567, 571
 Psocodea, 347
P. sulcifer, 239
 Psychodidae, 629
 Psychodomorpha, 664
 Pterygota, 345, 346
Ptinus tectus, 270
 Puff(s), 560, 563, 564, 574
 puffing pattern, 560, 584
 Pupa, 539, 548
 Pupal cuticle melanizing hormone
 (PCMH), 202
 Pupal melanization-reducing factor
 (PMRF), 202
 Pycnogonida, 626
 Pyralidae, 534, 539
 Pyraloidea, 521, 534
 Pyrethroid, 21
 Pyrethroid insecticides, 76
 Pyriform, 447, 449, 451, 461–462
Pyrrhalta, 233
- Q**
- Quinone
 based sclerotization, 340
 crosslinking, 332
- R**
- Raillietiella* sp., 346
 Random coil, 465, 479
 RANTES, 636
 Rebers & Riddiford (R&R), 57, 76
 consensus, 4, 13, 152
 consensus motif, 196, 197
 R&R-2 consensus domain, 101
 Rebuf (Reb), 75
 Receptivity, 416, 419, 420, 422
 Reduviidae, 628, 629, 662, 663
 Reduviinae, 663
 Regulation of chitin synthesis, 43, 44
 Remodeling phase, 631
 Reproduction, 412, 415, 425, 434, 435
 Reproductive glands, 416, 435
 Reproductive tract, 412–435
 Resilience, 94, 95, 98–100, 104, 105, 111,
 112, 124, 127, 128
 Resilin, 57, 90–128
 Resilin amino acids
 arginine, 97
 aspartic acid, 97, 125
 glutamic acid, 97, 100, 125
 glycine, 90, 95–97, 99, 100
 proline, 95–97, 99, 100
 Resilin composites
 chitin, 91, 105
 proteins, 91, 105, 106
 Resilin conformation
 α -helix, 95, 96
 β -sheet, 95, 96, 100
 β -turns, 95, 96, 99, 100
 hydrogen bonds, 95, 96, 99
 poly-L-proline II helix (PPII), 96, 99
 Resilin occurrence (arthropods)
 Aeshna sp., 90, 103, 108
 Astacus astacus, 91
 Calliphora vicina, 106, 114
 Centropages hamatus, 119, 120
 Cercopis vulnerata, 107, 111
 Cimex lectularius, 121, 122
 Coccinella septempunctata, 106, 109, 115
 Drosophila melanogaster, 94, 97, 99, 101,
 104, 124
 Eristalis tenax, 106, 110, 121, 123
 Forficula auricularia, 114
 Glossina morsitans, 110
 Labia minor, 114
 Libellula depressa, 106, 110
 Libellula luctuosa, 112
 Locusta migratoria, 92–93, 116, 117
 Palamnaeus swammerdami, 91
 Rhincalanus gigas, 119, 120
 Schistocerca gregaria, 90, 92–93, 97,
 99, 103
 Scolopendra morsitans, 91
 Stenus sp., 118
 Tettigonia viridissima, 116, 117
 Timomenus lugens, 114
 Tribolium castaneum, 99

- Resilin occurrence (structures)
 arthroal membranes, 106, 109, 110
 eyes, 101, 124
 legs, 110
 mechanoreceptors (sensillae), 119,
 121, 123
 mouthparts, 117–119, 121, 123
 reproductive organs, 119, 121, 123
 tarsal setae, 105, 106, 108, 109, 116
 wings, 90–93, 97, 103, 105, 108, 111–114
- Resorption, 145, 146, 151
- Respiration, 562
- Reticulitermes*, 238
R. flavipes, 239, 393
- Retroactive (Rtv), 74, 352
- Retrograde water flux, 289
- Rhagionidae, 628, 629
- Rhagoletis cerasi*, 327, 333
- Rhipicephalus*, 630, 632
R. appendiculatus, 656
R. bursa, 648
- Rhizoctonia solani* agglutinin, 274, 301
- Rhodinia*
R. fugax, 519, 524, 526, 527, 529
R. newara, 524, 532, 534, 539
- Rhodniin, 663
- Rhodnius prolixus*, 38, 39, 68–70, 81, 340,
 341, 343, 349, 351, 354, 633, 638,
 646, 653, 660
- Rhus vemicifera*, 186
- Rhyacophila obliterated*, 526, 541
- Rhyzopertha dominica*, 334, 372, 374
- Rickets, 202
- Rickettsiella*, 166
- RNA interference (RNAi), 8, 12, 36, 39, 57,
 222, 228, 242, 297, 306, 336,
 338–340, 352–354, 391, 392, 394,
 396, 397
- RNAi. *See* RNA interference (RNAi)
- RNA-sequencing, 535, 539, 540
- S**
- Saliva, 629, 632, 642, 648, 653–656
- Salivary gland(s), 517
 embryonic salivary gland, 584
 first instar, 559
 larval salivary gland, 558, 560, 561, 574,
 576, 583, 584
 prepupal, 562, 576–581, 583–585
 third instar, 559, 562
- Salmonella*, 468
- SALO, 653, 654
- Sambucus nigra* agglutinin II, 274, 301
- Samia*
S. pryeri, 517
S. ricini, 334, 335, 517–520, 524, 525,
 527–529, 534, 539, 548
- Sand flies, 629, 640, 642, 643, 650, 653, 654,
 660, 664
- Sap beetles, 242
- Saponins, 290
- Saturnia japonica*, 524, 526, 527
- Saturmiidae, 516, 517, 520, 522–525, 529,
 533–534, 539, 548
- Saturmiids, 522, 524, 525, 527, 529, 539, 541
- Savignygrins, 637, 641
- Sawflies, 542, 544
- Scar formation, 631
- Scavengers, 625, 636, 640–642, 650, 655, 662
- Sclerotin, 70, 78, 82
- Sclerotization, 78, 81, 340, 342, 343, 350–354,
 371, 394, 395, 397
- Scorpions, 71, 626
- SDS-PAGE, 529, 531, 532, 542, 545
- Sea spiders, 626
- Sealing, 121, 128
- Secondary metabolites, 290
- Secondary structure
 α -helices, 571, 573
 β -sheets, 571, 573
- Secretion
 holocrine, 419
 merocrine, 419
- Secretory cells, 417–420, 427, 428, 430–432
- Secretory pathway, 72, 73, 77, 82
- Seminal proteins, 417, 420, 421, 423, 425,
 431, 433–435
- Seminal receptacle, 417, 418, 427–431, 433
- Seminal vesicles, 417, 418
- Sequential gene activation, 560
- Ser1A, 530
- Ser1B, 530
- Ser1C, 530, 531
- Ser1D, 530, 531
- Sericine (ser)*
MG-1, 534
MG-2, 534
MG-3, 534
ser1, 530, 531, 535–537
ser2, 531, 535
ser3, 532, 535
- Sericins, 446
 repetitive motif, 531
 Ser1, 531, 533, 534
 Ser1A, 530
 Ser1B, 530
 Ser1C, 530

- Ser1D, 530
 Ser2, 531, 534
 Ser3, 532, 534
 sericin A, 531
 sericin M, 531
 sericin P, 531
 Sericulture, 516
 Serine proteases, 626, 633, 654, 655
 Serosa, 328, 344, 346–349, 351–354
 Serosal
 cells, 344, 347, 351, 352, 354, 355
 cuticle, 326, 328, 343, 344, 346–355
 endocuticle, 348, 350–353
 epicuticle, 349–351, 353–355
 membrane, 348, 355
 Serotonin, 182, 183, 199, 636, 637, 641, 642,
 651, 653, 655, 666
 Serpentine (Serp), 74, 75, 352
 Serpin 19, 666
Serratia marcescens, 51
 Sex peptide (SP), 414, 420
 Sex pheromones, 222, 228, 232, 234–236
 Shear force, 490, 494–496, 504
 Shear rate, 533
 Shrimps, 138, 144, 149, 151, 153, 626
 Sialokinins, 649
 Sialome, 628, 633, 641, 656, 658, 662–666
 Sialostatins, 648
 Sialoverse, 656–665
 Signal peptides, 152
 Silk, 516–548
 Silk assembly, 451, 457, 465, 475
 Silk fiber, 490, 494, 497–501, 503, 504
 Silk gland subset factor (SGSF), 456
 Silk Gland Subset Factor (SGSF), 456
 Silk gland(s), 516, 517, 533–541, 543, 544,
 546–548
 aciniform aggregate, 490, 491
 ampullate, 490–492, 495, 497, 498, 500
 factor-2 (SGF-2), 537
 flagelliform, 490, 491, 497
 piriform, 490, 491
 tubuliform, 490, 491
 Silk gland-specific transcripts (SSTs), 455,
 456
 Silk protein
 α -helical, 499
 β -crystallites, 492, 493
 β -sheet-rich structures, 495
 β -sheets, 492–495, 499, 503
 β -spiral, 493, 499
 random coils, 492, 493, 503
 secondary structures, 491, 492, 498
 Silkworms, 446, 465, 467, 473, 474, 516–518,
 524, 544–548
 genome database, 530, 532
 Simikunin, 646, 655
 Simiplagrin, 638, 639
Simulium
 S. nigrimanum, 638, 659
 S. vittatum, 633, 639, 646, 647, 649,
 655, 659
 Simuliidae, 629
 Siphonaptera, 517, 542, 626, 629
Sitophilus oryzae, 372
 Skin, 628–633, 641
 SMAD-like, 78, 82
 Snake flies, 626
 Snipe flies, 629, 662
 Sodium chloride, 476
 Sodium dodecyl sulfate (SDS), 452
 Sodium phosphate, 476
Sogatella furcifera, 390
 Solid phase microextraction (SPME), 235
 South African bont tick, 70
 Soya bean cysteine protease inhibitor, 301
 Sperm, 412–414, 416–425, 427–435
 competition, 414, 416, 419, 421
 storage, 417–419, 421, 422, 425, 427–433
 Spermathecae, 417, 418, 427–432
 Spermathecal secretory cells (SSC), 417, 418,
 420, 427, 430–432
 Spicipalpia, 540, 541
 Spider coating peptide (SCP), 451, 462, 463
 Spiders, 626
 Spidroins, 447, 451–456, 458, 460, 461, 464,
 465, 468, 475, 476, 478–480, 490,
 497–499, 501, 502, 504, 505
 Spigot, 461, 464
 Spinning dope, 447, 448, 457, 465,
 474–478, 480
 Spinning duct, 448, 464–466
Spodoptera
 S. exigua, 36, 39, 171, 172, 176, 180,
 383, 391
 S. frugiperda, 262, 271, 272, 291, 297,
 304, 387
 S. littoralis, 291, 295, 296, 301, 376
 S. litura, 298, 304, 383, 391
 Spreading factors, 632
 Stable flies, 629, 633, 654, 664
 Stearyl-CoA, 228, 229
Stenophyche marmorata, 542
 Stereochemistry, 222, 223, 235, 236
 Sternal deposits, 145
Stomaphis yanonis, 239

- Stomatopoda, 156
 Stomoxinae, 629
Stomoxys calcitrans, 633, 660
 Stratum basale, 630
 Stratum corneum, 630
 Stratum granulosum, 630
 Stratum lucidum, 630
 Stratum spinosum, 630
Streptomyces sp., 393
 S. cacaoui var. *asoensis*, 390
 S. tendae, 391
Stygotantulus stocki, 138
 Subcellular, 582, 588–590
 Sulfonylurea receptors (SUR), 379–381
 Sun spiders, 626
 Supercontraction, 497
Sylepta derogate, 539
 Symphyla, 345
 Symphyta, 542
 Synapsids, 628
 Syntaxin 1A (Syx1A), 74, 77
- T**
- Tabanidae, 628, 629
Tabanus yao, 638, 639, 641, 647, 649
 Tablysin-15, 639, 641, 666
 TabRTS, 650
 Tachykinins, 649
 Taenidia, 80
 Tail flipping, 138, 144
 Tandem repeats, 567, 570, 575
 Tanning, 339, 351
 Tannins, 290, 292
 Tantulocarida, 138
 Task-specific cues, 238
 T-cell proliferation, 648
 Tenascins, 631
 Tenase complex, 643
Tenebrio molitor, 272, 304
 Tensile strength, 495, 496, 499
 Terrestrial crustaceans, 138, 141
 Testis, 417, 418
 Tetraconata, 138, 344
Tetragonisca angustula, 334
Tetranychus
 T. cinnabarinus, 388, 389
 T. urticae, 387, 389
 Tetrapods, 628
Tetradontophora bielensis, 346
Tetropium
 T. cinnamopterum, 235
 T. fuscum, 235
 TF-fVIIa complex, 642
- Thrips, 626
 Thrombin, 642, 643, 650
 Thrombin inhibitors, 643, 663
 Thrombospondins, 631
 Thrombostasin, 660, 664
 Thromboxane A₂, 636, 654
 Thysanoptera, 347
 Thysanura, 516
 Tick adhesion inhibitor (TAI), 640
 Tissue plasminogen activator, 643
 Tissue-factor, 642
 Tobacco plants, 301, 303, 304
Tomocerus ishikashii, 347
 Tongue worms, 626, 662
 Toughness, 490, 495, 496, 498, 499, 503
 Trabecular layer, 329, 334
 Trace elements, 145, 146
 Transcription factor, 340, 353
 Transcriptome, 533
 Transgenic, 516, 536, 546–548
 Transglutaminase, 78, 79, 262, 283, 339
 Transitional cells, 559, 560
 Transmission electron microscopy, 167, 197
 Transparency, 123, 128
 Transposon, 546, 548
 Transsudation, 584
Trapezia spp., 143
 Trehalase, 36, 37
 Trehalose, 36, 38
 Triacylglycerol lipase (PTL), 457
 Triafestin-1, 646, 649
 Triafestin-2, 649
Trialeurodes vaporariorum, 390
Triatoma
 T. brasiliensis, 653, 661
 T. infestans, 374, 640
 T. pallidipennis, 638, 646
 Triatominae, 663
 Triatomines, 626, 660, 663
Tribolium
 T. castaneum, 5, 6, 12, 37–39, 45, 46, 49, 50, 52–56, 68, 75, 79–81, 167, 170–176, 178, 180, 181, 183, 184, 187, 188, 190–192, 195–197, 203, 256, 257, 264, 265, 273–276, 279–283, 285, 287–290, 298, 299, 301, 305, 334, 349, 351–354, 374, 376, 380, 391, 392, 394
 T. confusum, 372
Trichoplusia ni, 264, 279
Trichopsenius frosti, 239
 Trichoptera, 516, 517, 522, 527, 540–542
n-tricosane, 241
 (Z)-9-Tricosene, 228, 234

- Trioxys anelicae*, 239
 Triplatin, 638, 640, 654
Trissolcus basalus, 241
 Trityrosine, 79, 94, 98, 331, 341
 Trombiculid mites, 628
 Trombidiform mites, 626
 Trophallaxis, 237, 239
 Tropomyosin, 543
 True bugs, 626
 True flies, 626
 True lice, 626
Trypanosoma
 T. brucei rhodesiense, 295
 T. cruzi, 68
 Trypsin, 666
 Tryptase inhibitor (TdPI), 656
 Tryptogalinin, 652, 656
 Tsetse flies, 240, 629, 633, 640, 645, 654,
 662, 664
 t-SNARE, 77
Tubby (Tb), 74, 76
 Tubuliform spidroin (TuSp1), 451, 455–458,
 460, 469, 473
 Tumor necrosis factor–alpha, 655
Tweedle D (twlD), 76
Tylos europaeus, 168
 Tyrosine hydroxylase (TH), 78, 352
 Tyrosine metabolism
 arylalkylamine *N*-acetyltransferase, 169,
 181–183
 aspartate 1-decarboxylase (ADC), 169,
 172, 178–181, 183, 184
 β-alanine, 169, 178, 181, 183–185
 catechols, 166, 178, 204
 cuticular structural protein (CP), 166, 167,
 169, 183, 196–197
 dihydroxyindole (DHI), 169, 191
 5,6-dihydroxyindole-2-carboxylic acid
 (DHICA), 169, 191
 dihydroxyphenylalanine (DOPA), 169,
 177, 178, 188, 202
 dopachrome conversion enzyme (Yellow),
 169, 186, 190–195
 DOPA decarboxylase (DDC), 169, 172,
 177–178, 180, 199–202
 laccase, 186–190, 204
 N-acetyldopamine (NADA), 169, 182,
 183, 188
 NBAD hydrolase (Tan), 174, 185–186
 NBAD synthase (Ebony), 169, 173, 178,
 181, 183–185
 N-β-alanyldopamine (NBAD), 169, 178,
 181–186, 188
 6-pyruvoyl-tetrahydropterin synthase
 (PTS, Purple), 167
 tetrahydrobiopterin (BH₄), 167
 tyrosine hydroxylase (TH), 167, 169–177
- U**
 UDP-*N*-acetylglucosamine, 260
 UDP-*N*-acetylglucosamine pyrophosphorylase
 (UAP), 37, 306
 Ultrafiltration, 476
 Urea, 476
 Urokinase, 643
 Uronic acid, 265
 Uterus, 414, 417, 418, 421, 423, 425–428,
 430, 431, 434
- V**
 Vacuole(s)
 secretory, 561, 565, 577, 578
 vacuolation, 562, 584
 vacuolized vesicle, 577
 Valine, 225, 226
 Valvula cardiaca, 269, 272
 Variabilin, 637, 642
Varroa destructor, 239
 Vascular endothelial growth factor
 (VEGF), 547
 Vasoconstriction, 631, 649–650
 Vasodilation, 645, 647, 650
 Vasotab, 647, 649
 Vasotab TY, 639, 647, 649, 666
 Vector, 546, 548
 Vector-host interphase, 628–630
 Venom, 626, 632, 634
 Ventriculus, 271
 Vermiform (Verm), 74, 75
 Vesicle(s), 72, 74, 77, 412, 414, 417–419, 422
Vespa
 V. mandarinia japonica, 544
 V. simillima, 543
 Vespoidea, 516
 Vibronectin, 636
 Villin, 73
 Viral infectivity, 294, 296, 297, 305
 Viscoelasticity, 104, 105
 Vitelline membrane
 proteins, 328, 336, 339
 vitelline bodies, 328–330, 336
 Vitellogenesis, 328, 329, 338, 340
 Vitellogenin, 9, 12
 Vitronectin, 631
 Voltage, 477
 von Willebrand's factor, 635
 von Willebrand's receptor, 635
 Vssilk, 543

W

- Wasps, 626
- Water
 - uptake, 331, 353–354
 - waterproof, 330, 331, 355
 - waterproofing layers, 355
- Wax, 328–331, 350–352, 354, 355
 - layer, 328–331, 351, 354, 355
- Wet-spinning protocol, 476
- Wheat germ agglutinin (WGA),
 - 167, 300
- White cuticle, 349
- Wild silkmoth, 516, 520, 535, 538–540
- Windei*, 340
- Wing disc, 5, 12, 16–18
- Wollknäuel (Wol), 74, 77
- Woodlice, 626
- Wound contraction, 631
- Wound healing, 631, 634, 643, 650, 655

X

- Xanthotoxins, 290
- Xenobiotics, 290
- Xiphosura, 345, 626

X-ray

- analysis, 518
- diagrams, 518
- scattering, 544

Y

- Yellow, 77, 78, 81
- Yellow cuticle, 349
- Yellow proteins, 641
- Yellow-g*, 339, 340
- Yellow-related gene (YRG), 201
- Yield stress, 477
- Yolk, 327, 328, 346, 347
- Young's modulus, 104–106, 109, 116, 127,
 - 128, 493, 499
- Yponomeutoidea, 541

Z

- Zea mays*, 297, 304
- Zerknullt 1 (Zen1)*, 353
- Zootermopsis nevadensis*, 238
- Zoraptera, 347
- Zygentoma, 345–347